TECHNISCHE UNIVERSITÄT MÜNCHEN

WACKER-Institut für Siliciumchemie

Professur für Siliciumchemie

Unprecedented Silylenes and Silanones: Isolation, Characterization and Transition Metal-like Behavior

Dominik Reiter

Vollständiger Abdruck der von der Fakultät für Chemie der Technischen Universität München zur Erlangung des akademischen Grades eines

Doktors der Naturwissenschaften (Dr. rer. nat.)

genehmigten Dissertation.

Vorsitzender:	Prof. Dr. Klaus Köhler
Prüfer der Dissertation:	1. Prof. Dr. Shigeyoshi Inoue
	2. Prof. Dr. Tom Nilges
	3. Prof. Dr. Dr. h.c. mult. Herbert W. Roesky (schriftliche Beurteilung)
	Prof. Dr. Wolfgang Eisenreich (mündliche Prüfung)

Die Dissertation wurde am 20.04.2020 bei der Technischen Universität München eingereicht und durch die Fakultät für Chemie am 09.06.2020 angenommen.

»Immer erscheinen die entscheidenden Ideen nachträglich als einfache und selbstverständliche.«

Stefan Zweig (1881–1942)

Die vorliegende Arbeit wurde in der Zeit von Februar 2016 bis März 2020 im Rahmen der Professur für Siliciumchemie der Technischen Universität München unter Betreuung von Herrn Prof. Dr. Shigeyoshi Inoue angefertigt.

Acknowledgments

Mein besonderer Dank gilt Herrn *Prof. Dr. Shigeyoshi Inoue*, meinem Doktorvater, für die herzliche Aufnahme in seinen Arbeitskreis und das entgegengebrachte Vertrauen, ein faszinierendes Projekt am *WACKER-Institut für Siliciumchemie* bearbeiten zu können. Insbesondere bedanke ich mich für die vielen Freiheiten des eigenverantwortlichen Arbeitens und die Diskussionen und Anregungen, die sich aufgrund seiner fundierten Fachkenntnisse in der Hauptgruppenchemie ergaben.

Darüber hinaus bin ich dem gesamten *AK Inoue* für die stets entspannte Arbeitsatmosphäre und gute Zusammenarbeit sehr dankbar. Besonders hervorheben möchte ich meine direkten Laborkollegen und guten Freunde *Richard Holzner*, *Philipp Frisch* und *Franziska Hanusch*, die die Promotion zu einer äußerst angenehmen und unterhaltsamen Zeit, vor allem auch abseits der Chemie, gemacht haben. Gleiches gilt auch für die nächste Generation und die weiteren Teilnehmer der »Feierabendbier-Crew« *Ramona Baierl*, *Lisa Groll*, *Teresa Eisner*, *Florian Tschernuth*, *Martin Doleschal* und *Fabian Linsenmann*.

Der *WACKER Chemie AG* gilt mein Dank für die hervorragende Kooperation bei der gemeinsamen Projektarbeit. Insbesondere danke ich Herrn *Dr. Thomas Renner*, Herrn *Dr. Richard Weidner*, Frau *Dr. Elke Fritz-Langhals*, Herrn *Dr. Jan Tillmann* und Herrn *Dr. Niklas Wienkenhöver* für die konstruktiven Diskussionen und die produktive Atmosphäre bei den regelmäßigen Treffen.

Ferner möchte ich Herrn *Prof. Dr. Dr. h.c. Bernhard Rieger* und Herrn *Dr. Carsten Troll* vom *WACKER-Lehrstuhl für Makromolekulare Chemie* für die nicht selbstverständliche Unterstützung unserer zunächst überschaubaren Arbeitsgruppe danken. Die Nutzung der ausgezeichneten Ausstattung und der bestehenden Infrastruktur war eine große Hilfe. Meinen Doktorandenkollegen des *Silicium-Instituts* danke ich für die einmalige Laboratmosphäre und die zahlreichen wissenschaftlichen Diskussionen. Ein besonderes Wort des Dankes möchte ich an den »JACS-König« *Dr. Daniel Wendel* richten. Gemeinsam konnten wir bemerkenswerte Ergebnisse in der niedervalenten Siliciumchemie erzielen, insbesondere bei den Silanonen.

Ebenso gebührt mein Dank Amelie Porzelt und Dr. Tibor Szilvási für die ausgezeichnete und unkomplizierte Zusammenarbeit bei der Durchführung der unzähligen theoretischen Berechnungen und der Aufklärung der elektronischen Struktur meiner »kleinen« Moleküle. Im gleichen Sinne möchte ich mich beim Team der Röntgenstrukturanalyse um Dr. Alexander Pöthig, Dr. Philipp Altmann und Philipp Frisch für die Messung und Verfeinerung zahlreicher Einkristalle bedanken. Ein großes Dankeschön geht auch an Ulrike Ammari (Elementaranalyse), Maria Matthews (VT-NMR),

Dr. Oksana Storcheva (EPR), sowie an meine Doktorandenkollegen *Maximilian Muhr* (LIDFI-MS), *Fabian Hörmann* (Photochemie) und *Kathrin Kratzl* (IR Spektroskopie & CO-Sensoren).

Meinen sehr engagierten und interessierten Studenten, die ich während meiner Tätigkeit am Arbeitskreis betreuen durfte, danke ich für ihren Einsatz und die stets sehr angenehme und produktive Zusammenarbeit. Meine Forschungspraktikanten/innen *Philipp Holzmüller*, *Daniel Döllerer*, *Philipp Pfändner*, *Carolin Feyerabend*, *Sebastian Stigler*, *Alexandra Walter*, *Simone Hirmer*, *Brigita Bratić* und *Fiona Kiefer* und mein Masterand *Martin Doleschal* haben die vorliegende Arbeit zum Teil in hohem Maße mitgestaltet.

Abschließend möchte ich mich ganz herzlich bei meiner Familie und meinen Freunden für die bedingungslose und kontinuierliche Unterstützung während meines gesamten Studiums und meiner Promotion bedanken. Ohne euch und euren starken Rückhalt, trotz der erheblich verringerten gemeinsamen Zeit, würde die vorliegende Dissertation nicht existieren. Insbesondere geht der Dank an meine Eltern *Petra* und *Josef* für das entgegengebrachte Vertrauen und die Ermöglichung meines Chemiestudiums. Meinen ehemaligen Mitbewohnern und guten Freunden *Bernhard Mittermeier* und *Alexander Kunz* danke ich für die unterhaltsamen und großartigen gemeinsamen Jahre in unserer WG.

List of Abbreviations and Formulas

ΔE_{ST}	singlet-triplet energy gap [kcal/mol]
δ	chemical shift [ppm]
λ	wavelength [nm]
Ad	adamantyl | $C_{10}H_{15}$
Ar	aryl
BCF	tris(pentafluorophenyl)borane | $B(C_6F_5)_3$
Bu	butyl | C_4H_9
cf.	latin *confer/conferatur:* "compare"
CAAC	cyclic alkyl amino carbene
CGMT	"Carter-Goddard-Malrieu-Trinquier"
Ch	chalcogen | O, S, Se, Te, Po, Lv
cHex	cyclohexyl | C_6H_{11}
Cp*	pentamethylcyclopentadienyl | C_5Me_5
CVD	chemical vapor deposition
d	day(s)
DFT	density functional theory
Dipp	diisopropylphenyl | 2,6-^{i}Pr$_2$-C_6H_3
DMAP	4-*N,N*-dimethylaminopyridine | Me_2N-C_5H_4N
DME	1,2-dimethoxyethane | $MeOCH_2CH_2OMe$
E	element
e.g.	latin *exempli gratia:* "for example"
E_{Hybrid}	energy of hybridization [kcal/mol]
EPR	electron paramagnetic resonance
Et	ethyl | C_2H_5
et al.	latin *et alii:* "and others"
GIAO	gauge-including atomic orbitals
h	hour(s)
HOMO	highest occupied molecular orbital
HMPA	hexamethylphosphoric triamide | $(Me_2N)_3P=O$
hypersilyl	tris(trimethylsilyl)silyl | Si(TMS)$_3$
i	iso

IDipp	1,3-bis(2,6-diisopropylphenyl)imidazolin-2-ylidene
IDippN	1,3-bis(2,6-diisopropylphenyl)imidazolin-2-iminato
$I^iPr_2Me_2$	1,3-diisopropyl-4,5-dimethylimidazolin-2-ylidene
$I^iPr_2Me_2O$	1,3-diisopropyl-4,5-dimethylimidazolin-2-one
IMe_4	1,3,4,5-tetramethylimidazolin-2-ylidene
in situ	latin: "on site"
IR	infrared
LUMO	lowest unoccupied molecular orbital
M	alkali metal | Li, Na, K, Rb, Cs, Fr; or transition metal
m	*meta*
m-Tol	*meta*-tolyl | 3-Me-C_6H_4
m.p.	melting point
Me	methyl | CH_3
Mes	mesityl | 2,4,6-Me_3-C_6H_2
Mes*	supermesityl | 2,4-6-^{t}Bu$_3$-C_6H_2
ML_n	transition metal complex
NBO	natural bond order
NHBO	*N*-heterocyclic boryloxy
NHC	*N*-heterocyclic carbene
NHI	*N*-heterocyclic imine
NHO	*N*-heterocyclic olefin
NHSi	*N*-heterocyclic silylene
NMR	nuclear magnetic resonance
NRT	natural resonance theory
o	*ortho*
p	*para*
PDMS	poly(dimethylsiloxane) | $(Me_2SiO)_n$
Ph	phenyl | C_6H_5
ppm	parts per million
Pr	propyl | C_3H_7
R	substituent / functional group
r.t.	room temperature
SC-XRD	single-crystal X-ray diffractometry

supersilyl	tri-*tert*-butylsilyl | Si^tBu_3
t	*tert*
Tbt	2,6-tris[bis(trimethylsilyl)methyl]phenyl | 2,4,6-$[CH(SiMe_3)_2]_3$-C_6H_2
TEMPO	(2,2,6,6,-tetramethylpiperidin-1-yl)oxyl | $(CH_2)_3(CMe_2)_2NO$
THF	tetrahydrofuran | C_4H_8O
Tipp	triisopropylphenyl | 2,4,6-$^iPr_3$-C_6H_2
TMS	trimethylsilyl | $SiMe_3$
UV–vis	ultraviolet–visible
VT	variable temperature
WBI	*Wiberg* bond index
vide infra	latin: “see below”
vide supra	latin: “see above”
X	halogen | F, Cl, Br, I, At, Ts
XRD	X-ray diffractometry

Publication List

- D. Reiter, R. Holzner, A. Porzelt, P. Frisch, S. Inoue, Silylated silicon carbonyl complexes: Mimics of ubiquitous transition metal carbonyls. *Nat. Chem.* **2020**, *revised manuscript submitted*

- D. Reiter, P. Frisch, D. Wendel, F. M. Hörmann, S. Inoue, Oxidation reactions of a versatile, two-coordinate, acyclic iminosiloxysilylene. *Dalton Trans.* **2020**, *49*, 7060-7068; https://dx.doi.org/10.1039/D0DT01522A

- R. Holzner†, D. Reiter†, P. Frisch, S. Inoue, DMAP-stabilized bis(silyl)silylenes as versatile synthons for organosilicon compounds. *RSC Adv.* **2020**, *10*, 3402-3406; https://dx.doi.org/10.1039/C9RA10628F

- D. Reiter, P. Frisch, T. Szilvási, S. Inoue, Heavier Carbonyl Olefination: The Sila-Wittig Reaction. *J. Am. Chem. Soc.* **2019**, *141*, 16991-16996; https://dx.doi.org/10.1021/jacs.9b09379

- D. Reiter†, R. Holzner†, A. Porzelt†, P. J. Altmann, P. Frisch, S. Inoue, Disilene-Silylene Interconversion: A Synthetically Accessible Acyclic Bis(silyl)silylene. *J. Am. Chem. Soc.* **2019**, *141*, 13536-13546; https://dx.doi.org/10.1021/jacs.9b05318

- D. Wendel†, D. Reiter†, A. Porzelt, P. J. Altmann, S. Inoue, B. Rieger, Silicon and Oxygen's Bond of Affection: An Acyclic Three-Coordinate Silanone and Its Transformation to an Iminosiloxysilylene. *J. Am. Chem. Soc.* **2017**, *139*, 17193-17198; https://dx.doi.org/10.1021/jacs.7b10634

† = these authors contributed equally.

Publications beyond the scope of this thesis:

- V. Nesterov, D. Reiter, P. Bag, P. Frisch, R. Holzner, A. Porzelt, S. Inoue, NHCs in Main Group Chemistry. *Chem. Rev.* **2018**, *118*, 9678-9842. https://dx.doi.org/10.1021/acs.chemrev.8b00079

- A. Kronast†, D. Reiter†, P. T. Altenbuchner, S. I. Vagin, B. Rieger, 2-Methoxyethylamino-bis(phenolate)yttrium Catalysts for the Synthesis of Highly Isotactic Poly(2-vinylpyridine) by Rare-Earth Metal-Mediated Group Transfer Polymerization. *Macromolecules* **2016**, *49*, 6260-6267; https://dx.doi.org/10.1021/acs.macromol.6b01179

† = these authors contributed equally.

Conference Contributions

- D. Reiter, A. Porzelt, P. Frisch, S. Inoue, Reactivity Studies of an Acyclic Three-Coordinate Iminosilylsilanone and its Isomeric Two-Coordinate Iminosiloxysilylene, *9th European Silicon Days* **2018**, *Saarbrücken*, Germany; **Poster Presentation – Poster Price.**

- D. Reiter, S. Inoue, Isolation and Reactivity Studies of Acyclic Three-Coordinate Silanones, *The 15th International Symposium on Inorganic Ring Systems (IRIS-15)* **2018**, *Kyoto,* Japan. **Poster Presentation.**

Abstract

In times of climate change, the development of more sustainable chemical processes is becoming increasingly important. Particular attention is being paid to replacing ubiquitous transition metal catalysts with more environmentally friendly main group compounds, which are based on highly abundant and non-toxic elements such as silicon. This doctoral thesis is focused on the investigation of the emerging class of low-coordinate organosilicon compounds with the aim of further uncovering their potential for applications in metal-free catalysis. In addition, new insights are obtained into the relationship between carbon and its heavier homologue silicon.

First, the isolation of an equilibrium mixture consisting of an elusive acyclic bis(silyl)silylene and its isomeric tetrasilyldisilene is outlined. Initial studies revealed the striking activation of challenging small molecules such as ethylene, H_2 and NH_3 under mild conditions, a reactivity that is prototypical for transition metal complexes and a prerequisite to most catalytic transformations. Moreover, Lewis base-stabilized bis(silyl)silylenes and the first example of an NHC-stabilized, acyclic silanoic ester, a heavier carboxylate ester analogue, were synthesized. Detailed theoretical calculations supplemented the experimental results and provided a closer insight into the disilene-silylene interconversion.

Subsequently, the donor-stabilization of otherwise elusive bis(silyl)silylenes is examined more closely. Thus, unprecedented silylene-DMAP adducts were isolated and their respective thermally induced isomerization *via* dissociation was demonstrated. As their capability of small molecule activation at elevated temperatures was verified, DMAP-stabilized bis(silyl)silylenes proved to be suitable synthetic equivalents of the corresponding, extremely reactive, donor-free silylenes.

In addition, carbonylation of the synthesized bis(silyl)silylenes provides access to the first isolable silicon carbonyl complexes at ambient temperature. These unprecedented organosilicon compounds were characterized extensively by both experimental methods and theoretical calculations. Preliminary investigations revealed a conspicuous reactivity, reminiscent of transition metal carbonyl complexes. Thus a photochemically induced dissociation of the CO moiety and an exchange reaction with a stronger donating isocyanide ligand was achieved.

Furthermore, a detailed reactivity study of an acyclic iminosiloxysilylene reveals additional insights into this relatively unexplored class of compounds. The silylene served not only as a transition metal mimic *via* activating challenging small molecules, but also as a precursor for heavier carbon congeners by oxidation. Thus, a novel acyclic silaimine (heavier imine) was accessible, which underwent a rare 1,3-dipolar cycloaddition reaction with N_2O, resulting in the formation of a unique oxatriazasilole.

Next, the suitability of silylenes for the synthesis of remarkable silanones (heavier ketone homologues) is demonstrated. Oxygenation of "masked" iminosilylsilylenes with N_2O enabled the isolation of the first room temperature stable, neutral, three-coordinate, acyclic silanones. These unprecedented iminosilylsilanones are indefinitely stable in the solid-state, but undergo distinct rearrangement pathways in solution, depending on the nature of the silyl substituent. Thus, the above mentioned, remarkable iminosiloxysilylene is accessible *via* isomerization.

Finally, the successful application of the versatile *Wittig* reaction to an iminosilylsilanone is outlined, which represents the first example of a heavier carbonyl olefination method. Due to the differences in stability and reactivity between carbonyl compounds and silanones (the strongly polarized and thus zwitterionic Si=O moiety is much more reactive) both similarities and differences in reactivity toward *Wittig* reagents were observed. Whereas functionalized phosphorus ylides led to reactions deviating from the "classical" *Wittig* reaction, non-stabilized ylides afforded a series of silenes (heavier alkenes) *via* the sila-*Wittig* reaction.

In conclusion, this thesis reveals new aspects and a deeper understanding of low-coordinate organosilicon compounds at the interface between the versatile chemistry of carbon and transition metals. Thus, new avenues and opportunities to achieve the ultimate goal of a diverse silicon-based catalysis are disclosed.

Kurzfassung

Die Entwicklung nachhaltigerer chemischer Prozesse nimmt in Zeiten des Klimawandels eine immer wichtigere Rolle ein. Ein besonderes Augenmerk wird dabei auf den Ersatz der allgegenwärtigen Übergangsmetallkatalysatoren durch umweltfreundlichere Hauptgruppenverbindungen gelegt, die auf sehr reichhaltigen und ungiftigen Elementen wie Silicium basieren. Die vorliegende Doktorarbeit beschäftigt sich mit der Untersuchung der aufstrebenden Klasse der niedrigkoordinierten Organosiliciumverbindungen mit dem Ziel, ihr Potential für Anwendungen in der metallfreien Katalyse genauer zu erschließen. Darüber hinaus werden neue Erkenntnisse über die Verwandtschaft zwischen Kohlenstoff und seinem schwereren Homolog Silicium gewonnen.

Zunächst wird die Isolierung einer Gleichgewichtsmischung bestehend aus einem schwer zu isolierenden acyclischen Bis(silyl)silylene und seinem isomeren Tetrasilyldisilen dargestellt. Erste Studien zeigten die eindrucksvolle Aktivierung von anspruchsvollen kleinen Molekülen wie Ethylen, H_2 und NH_3 unter milden Bedingungen, eine Reaktivität, die typisch für Übergangsmetallkomplexe ist und eine Voraussetzung für die meisten katalytischen Umwandlungen bildet. Ferner wurden Lewis-Basen-stabilisierte Bis(silyl)silylene und das erste Exemplar eines NHC-stabilisierten, acyclischen Silanonsäureesters, ein schwereres Carbonsäureester-Analogon, synthetisiert. Detaillierte theoretische Berechnungen ergänzten die experimentellen Ergebnisse und lieferten einen tieferen Einblick in die Disilen-Silylen-Umwandlung.

Anschließend wird die Donorstabilisierung von ansonsten schwer zugänglichen Bis(silyl)silylenen genauer unter die Lupe genommen. Dabei wurden neuartige Silylen-DMAP-Addukte isoliert und ihre jeweilige, thermisch induzierte, Isomerisierung durch Dissoziation aufgezeigt. Da ihre Fähigkeit zur Aktivierung kleiner Moleküle bei erhöhten Temperaturen verifiziert wurde, erwiesen sich DMAP-stabilisierte Bis(silyl)silylene als geeignete synthetische Äquivalente der entsprechenden, extrem reaktiven, donorfreien Silylene.

Darüber hinaus ermöglicht die Carbonylierung der dargestellten Bis(silyl)silylene den Zugang zu den ersten isolierbaren Siliciumcarbonylkomplexen bei Raumtemperatur. Diese einzigartigen Organosiliciumverbindungen wurden sowohl durch experimentelle Methoden als auch durch theoretische Berechnungen umfassend charakterisiert. Erste Untersuchungen offenbarten eine bemerkenswerte Reaktivität, die an Übergangsmetallcarbonyle erinnert. So wurde neben einer photochemisch induzierten Dissoziation des CO Liganden eine Austauschreaktion mit einem stärker donierenden Isocyanid Liganden erreicht.

Ferner enthüllt eine eingehende Reaktivitätsstudie eines acyclischen Iminosiloxysilylens weitere Erkenntnisse über diese relativ unerforschte Verbindungsklasse. Das Silylen diente dabei nicht nur als Übergangsmetall-Imitator, indem es anspruchsvolle kleine Moleküle aktivierte, sondern auch als Vorstufe für schwerere Kohlenstoff-Kongenere durch Oxidation. So war ein neuartiges acyclisches Silaimin (schwereres Imin) zugänglich, das eine seltene 1,3-dipolare Cycloadditionsreaktion mit N_2O einging, die zur Bildung eines einzigartigen Oxatriazasilols führte.

Als nächstes wird die Eignung von Silylenen für die Synthese bemerkenswerter Silanone (schwerere Keton-Homologe) dargelegt. Die Oxygenierung von »maskierten« Iminosilylsilylenen mit N_2O ermöglichte die Isolierung der ersten raumtemperaturstabilen, neutralen, dreifachkoordinierten, acyclischen Silanone. Diese beispiellosen Iminosilylsilanone sind im Festkörper unbegrenzt stabil, durchlaufen jedoch unterschiedliche Umlagerungsreaktionen in Lösung, abhängig von der Art des Silyl-Substituenten. So ist das oben erwähnte, einzigartige Iminosiloxysilylene über eine Isomerisierung verfügbar.

Abschließend wird die erfolgreiche Anwendung der vielseitigen *Wittig*-Reaktion auf ein Iminosilylsilanon beschrieben, die das erste Beispiel für eine schwerere Carbonylolefinierung darstellt. Aufgrund der Unterschiede in Stabilität und Reaktivität zwischen Carbonylverbindungen und Silanonen (die stark polarisierte und damit zwitterionische Si=O Bindung ist wesentlich reaktiver) wurden sowohl Ähnlichkeiten als auch Unterschiede in der Reaktivität gegenüber *Wittig*-Reagenzien beobachtet. Während funktionalisierte Phosphorylide zu Reaktionen führten, die von der »klassischen« *Wittig*-Reaktion abweichen, lieferten nicht stabilisierte Ylide über die Sila-*Wittig*-Reaktion eine Reihe von Silenen (schwerere Alkene).

Insgesamt zeigt diese Arbeit neue Aspekte und ein tieferes Verständnis von niedrigkoordinierten Organosiliciumverbindungen an der Schnittstelle zwischen der vielseitigen Chemie von Kohlenstoff und Übergangsmetallen auf. Dadurch eröffnen sich neue Wege und Möglichkeiten, um das langfristige Ziel einer vielfältigen siliciumbasierten Katalyse zu erreichen.

Table of Contents

Acknowledgments I

List of Abbreviations and Formulas III

Publication List VI

Conference Contributions VIII

Abstract IX

Kurzfassung XI

1. Introduction 1

2. Low-coordinate Organosilicon Compounds 3

2.1 Silylenes 6

2.1.1 Historic Milestones and General Reactivity 10

2.1.2 Acyclic Two-Coordinate Silylenes 16

2.1.3 Acyclic Bis(silyl)silylenes 20

2.2 Silanones 25

2.2.1 Historic Milestones 27

2.2.2 General Reactivity 29

2.3 Catalytic Applications 31

3. Scope of this Work 34

4. Disilene–Silylene Interconversion: A Synthetically Accessible Acyclic Bis(silyl)silylene 38

5. DMAP-stabilized bis(silyl)silylenes as versatile synthons for organosilicon compounds 50

6. Silylated silicon carbonyl complexes: Mimics of ubiquitous transition metal carbonyls 56

7. Oxidation reactions of a versatile, two-coordinate, acyclic iminosiloxysilylene 63

8. Silicon and Oxygen's Bond of Affection: An Acyclic Three-Coordinate Silanone and Its Transformation to an Iminosiloxysilylene 73

9. Heavier Carbonyl Olefination: The Sila-Wittig Reaction 80

10. Summary and Outlook 87

10.1 Acyclic Two-Coordinate Silylenes 87
10.1.1 Investigations on Bis(silyl)silylenes 87
10.1.2 Investigations on a Iminosiloxysilylene 91
10.2 Acyclic Three-Coordinate Silanones 94
10.2.1 Investigations on Iminosilylsilanones 94
10.2.2 Investigations on the Sila-Wittig Reaction 95
10.3 Main Conclusion and Perspective 98
11. Zusammenfassung und Ausblick 99
11.1 Acyclische zweifachkoordinierte Silylene 99
11.1.1 Studien zu Bis(silyl)silylenen 99
11.1.2 Studien zu einem Iminosiloxysilylen 104
11.2 Acyclische dreifachkoordinierte Silanone 107
11.2.1 Studien zu Iminosilylsilanonen 107
11.2.2 Studien zur Sila-Wittig Reaktion 108
11.3 Fazit und Prognose 111
12. Bibliography 113
13. Appendix 139
13.1 Supporting Information Chapter 4 139
13.2 Supporting Information Chapter 5 231
13.3 Supporting Information Chapter 6 257
13.4 Supporting Information Chapter 7 322
13.5 Supporting Information Chapter 8 398
13.6 Supporting Information Chapter 9 463
13.7 Licenses for Copyrighted Content 577
13.7.1 License for Chapter 4 577
13.7.2 License for Chapter 5 578
13.7.3 License for Chapter 7 579
13.7.4 License for Chapter 8 580
13.7.5 License for Chapter 9 581
Oath of Compliance with the Principles of Scientific Integrity 582

1. Introduction

A catalyst is usually associated by the everyday person with a component of the automotive industry for the efficient reduction of pollutant emissions in the exhaust gas.[1] These catalysts successfully convert the toxic and environmentally harmful substances carbon monoxide (CO), nitrogen oxides (NO_x) and various hydrocarbons *via* redox reactions (oxidation and reduction processes) into the less polluting gases carbon dioxide (CO_2), nitrogen (N_2) and water vapor. However, the concept of catalysis encompasses a far more diverse range of applications that have become an integral part of everyday life.[1-3]

The term catalysis originates from the Greek word "κατάλυσις" – which can be translated as to annul, to pick up or to untie – and was introduced already in 1835 by the Swedish chemist *Jöns Jacob Berzelius*.[4-5] However, it took more than half a century until *Nobel* laureate *Wilhelm Ostwald* established a generally accepted definition of catalysis based on reaction kinetics:

> »*Katalyse ist die Beschleunigung eines langsam verlaufenden chemischen Vorganges durch die Gegenwart eines fremden Stoffes.*«[6-7] [*"Catalysts are substances which change the velocity of a reaction without modification of the energy factors of the reaction."*][5]
>
> *Wilhelm Ostwald* (1853–1932)

In a more modern perspective, catalysts are capable of changing the kinetic but not the thermodynamic parameters of various chemical reactions. As they significantly accelerate conversions by lowering the activation energy, product formation can occur under much milder conditions (lower temperatures and reduced pressures). Therefore, catalysts are key reagents for both scientists and engineers from an ecological and economic point of view in order to reduce costs and emissions in numerous processes.[2-3]

It is not surprising that catalysis has developed into a versatile and multidisciplinary field of research. Nowadays, the production of about 85–90% of all industrially manufactured chemical products is based on the use of catalytic processes.[2] The outstanding role of catalysis for our modern society and everyday life cannot be overstated, as it enabled and ensures access to fertilizers, fuels, pharmaceutical products, plastics and other important commodities.[8]

The vast majority (>80%) of all industrially relevant chemical and petrochemical processes use heterogeneous catalysis, in which the respective reagents and the catalyst are present in separate phases.[9] Despite the fact that the solid catalysts applied are highly active and product separation is

simple, fine tuning their structure and thus controlling the selectivity is difficult or almost impossible. In contrast, the subfield of homogeneous catalysis focuses on the use of soluble organometallic complexes, which enables a relatively facile variation of both their electronic and steric properties.[10] With a better understanding of the mechanistic details of the catalytic cycles, tailor-made homogenous catalysts can be designed for each specific problem and outstanding chemo- and stereoselectivities can be achieved.

Although both types of catalysts display significant differences, they have one thing in common, namely a strong dependence on the use of transition metals and their corresponding complexes.[3] Despite the extraordinary properties of transition metals and their almost unlimited range of applications, this circumstance results in some serious disadvantages. Transition metal-based catalysts are generally relatively expensive (low abundance), often rather toxic and ecologically harmful. Therefore, research to develop alternative catalysts, that provide comparable performance at lower cost and using less toxic materials, has received increased attention.

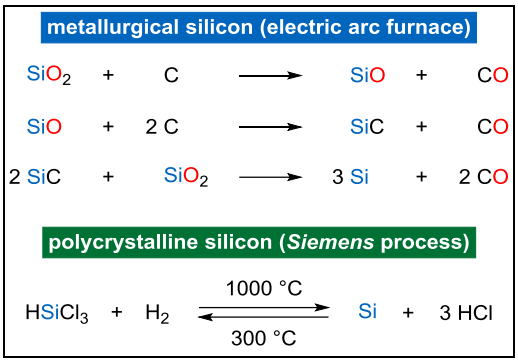
Over the past decades, main group chemistry has experienced a renaissance and the flourishing field of single-site, non-metallic compounds mimicking transition metal complexes has emerged.[11-14] Even though main group compounds are not as variable as transition metals, due to the lack of accessible d-orbitals, fascinating reactivity patterns have been found throughout the periodic table. Thus, the activation of challenging small molecules, such as H_2, CO, NH_3 and alkenes, a reactivity reminiscent of transition metal complexes and even first catalytic applications have been revealed.[15-19] Nevertheless, research into this particular chemistry and the development of more sustainable technologies are still in their infancy.

A very interesting or even the ideal main group element for the replacement of transition metals is silicon, as it is virtually infinitely available and non-toxic. Extensive research has unveiled the stabilization and isolation of previously unimaginable molecules and their striking reactivity.[16] Low-coordinate organosilicon compounds in particular are promising targets on the way to circumventing the ubiquitous use of transition metals and developing an even more advantageous catalysis. Unfortunately, reports on applications of silicon-based catalysis are still extremely scarce and further intensive research is required.

2. Low-coordinate Organosilicon Compounds

The semi-metal silicon is with a natural occurrence of about 26% the second most abundant element in the earth's crust after oxygen (about 49%) and is non-toxic to the human body.[20] The name silicon is derived from the Latin words "silex" or "silicis" (meaning flint or pebble) and implies the similarity to its adjacent elements in the periodic table boron and carbon. Despite its high availability, silicon is never found in elementary form, but only bound in minerals such as silicates or as silicon dioxide (SiO_2; *e.g.* see sand, quartz, amethyst).[21] The reason for this phenomenon is the high affinity of silicon to oxygen (oxophilicity), which also resulted in the relatively late isolation of elemental silicon in 1824 by *Jöns Jacob Berzelius*.[20]

Since the chemical industry is also dependent on the use of the oxygen-containing minerals, a highly energy consuming process is currently required for the production of silicon. Thus, the reduction of quartz with coke in an electric arc furnace at temperatures around 2000 °C affords metallurgical-grade silicon (98.5–99.7% purity) (Scheme 1).[20] In order to minimize the formation of undesired by-products such as silicon carbide (SiC), the ratio of the reactants must be precisely adjusted. The silicon obtained is of sufficiently high purity for use as an alloying material or in steel production.

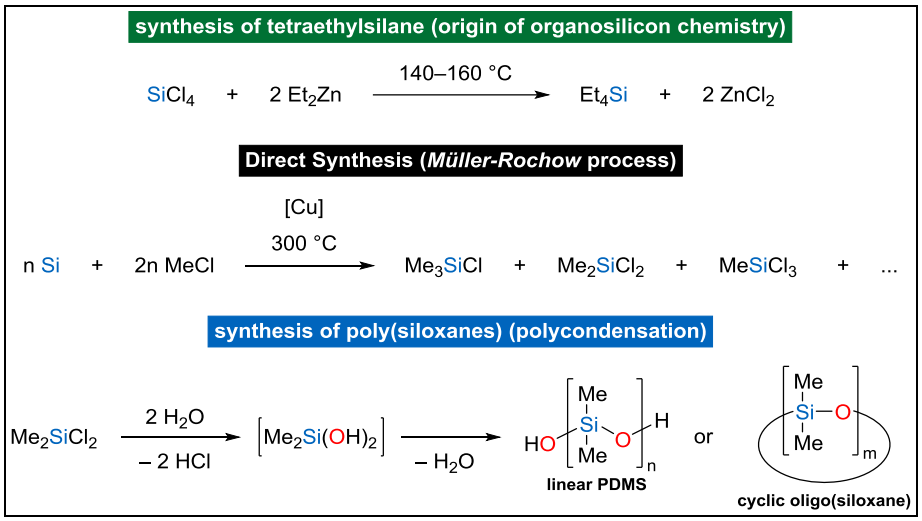


Scheme 1. Production of metallurgical silicon *via* reduction of quartz and polycrystalline silicon with the *Siemens* process.

For the production of solar cells and thus for applications in the photovoltaic industry, however, the purity of metallurgical silicon is not high enough. The therefore required polycrystalline silicon (solar-grade silicon; >99.99% purity) is available *via* the energy intensive *Siemens* process. First, the crude silicon is converted with gaseous hydrogen chloride in a fluidized bed reactor at 300–350 °C to trichlorosilane ($HSiCl_3$). After purification through complex distillations steps, polycrystalline silicon is obtained subsequent to the decomposition of $HSiCl_3$ at about 1000 °C and chemical vapor deposition (CVD) on hot polysilicon rods.[20]

Electronic-grade silicon, the purest silicon accessible (≥99.9999999%), is the base material for manufacturing microelectronic components for all modern electronic devices. Large cylindrical ingots of this monocrystalline silicon are obtained by the commonly employed *Czochralski* method. A monocrystalline silicon seed crystal is dipped into a crucible containing a 1425 °C hot polycrystalline silicon melt and pulled out under slow rotation, thereby depositing the high purity-silicon. Due to the better solubility, almost all impurities remain in the melt. A fine tuning of the electronic properties of the resulting semiconducting material is possible *via* addition of dopant impurity atoms, such as aluminum, arsenic, boron and phosphorus. The production of computer chips is finally initiated by cutting the monocrystalline silicon cylinders into wafers.[20]

Since the pioneering work of *Charles Friedel* and *James Mason Crafts* in 1863 on the synthesis of tetraethylsilane (Et_4Si) by reaction of silicon tetrachloride ($SiCl_4$) with diethylzinc (Et_2Zn) in a sealed tube (Scheme 2), organosilicon chemistry has developed into an incredibly versatile field.[16,22] *Frederic Stanley Kipping* is considered one of the founding fathers because of his many groundbreaking contributions to this branch of chemistry. He implemented the utilization of *Grignard* reagents for the synthesis of alkyl-/arylsilanes as early as in 1904.[23] *Kipping* also synthesized the first poly(siloxanes) $(R_2SiO)_n$ *via* hydrolysis of different dichlorosilanes.[24-25] Assuming that these new compounds are silicon analogues of ketones, the name "silicones" was erroneously given to poly(siloxanes) and has remained a trivial name until now.[26] Accordingly, the synthesis and isolation of the so-called "silanones" ($R_2Si{=}O$) is today referred to as "*Kipping's* dream".[26-27]



Scheme 2. Milestones in organosilicon chemistry: Synthesis of the first compound containing a silicon-carbon bond (tetraethylsilane), production of dimethyldichlorosilane *via* the *Müller-Rochow* process and preparation of poly(dimethylsiloxane) (PDMS) after hydrolysis of Me_2SiCl_2 and subsequent polycondensation.

Despite his outstanding results, *Kipping* did not yet recognize the potential of organosilicon compounds for future applications and announced the following toward the end of his career:

"We have considered all the known types of organic derivatives of silicon and we see how few are their number in comparison with the purely organic compounds. Since the few which are known are very limited in their reactions, the prospect of any immediate and important advance in this section of chemistry does not seem very hopeful."[23]

Frederic Stanley Kipping (1863–1949)

Nevertheless, his results paved the way for industrial applications of organosilicon chemistry and inspired *Richard Müller* and *Eugene George Rochow* to independently develop an alternative approach to the poly(siloxane) precursor dimethyldichlorosilane (Me_2SiCl_2) in the 1940s.[28-29] The thus discovered and now well-established "Direct Synthesis" is also known as the "*Müller-Rochow* process" in honor of the two pioneers. It directly converts metallurgical silicon with alkyl halides in the presence of a copper catalyst into a variety of alkylchlorosilanes, which can be separated by fractional distillation (Scheme 2). The alkylchlorosilanes obtained represent the monomers of poly(siloxanes) and can be hydrolyzed to linear or cyclic oligo(siloxanes). Subsequent ring opening polymerization or polycondensation affords high-molecular weight poly(siloxanes). Of particular interest is the synthesis of Me_2SiCl_2, which provides access to poly(dimethylsiloxane), the most commonly used representative for a broad variety of applications.[20]

The chemistry of silicon has always fascinated chemists because of its natural abundance, the intriguing properties and its proximity to carbon – the "carrier of life" – in the periodic table.[20] Today, organosilicon compounds are omnipresent and have become indispensable in everyday life and the chemical industry. All compounds mentioned so far are tetra-coordinate, with the silicon nuclei appearing in the most stable oxidation states +IV or 0. In sharp contrast to its lighter congener, however, silicon is capable of forming isolable hyper-coordinate molecules. For instance, penta- and hexa-coordinate silyl anions and *N*-heterocyclic carbene (NHC)-stabilized silicon(IV) halides are accessible (Figure 1).[16,30]

In addition, enormous progress has been made in recent decades in the development of the emerging class of low-coordinate organosilicon compounds, owing to the convenient availability of suitable halosilane precursors. As shown in various reports, the use of tailor-made ligand frameworks is necessary to sufficiently stabilize these electronically unfavorable and thus extremely reactive species.[16] Accordingly, a restoration of the preferred tetrahedral coordination sphere with four

substituents around the silicon atom (*via* intra- or intermolecular reactions) is suppressed due to appropriate kinetic and/or thermodynamic stabilization. After comprehensive investigations, a series of silicon analogues of important reactive organic intermediates, such as silylium ions (carbenium ions), silyl radicals (carbon radicals) and silanides (carbanions), have been successfully isolated.[16]

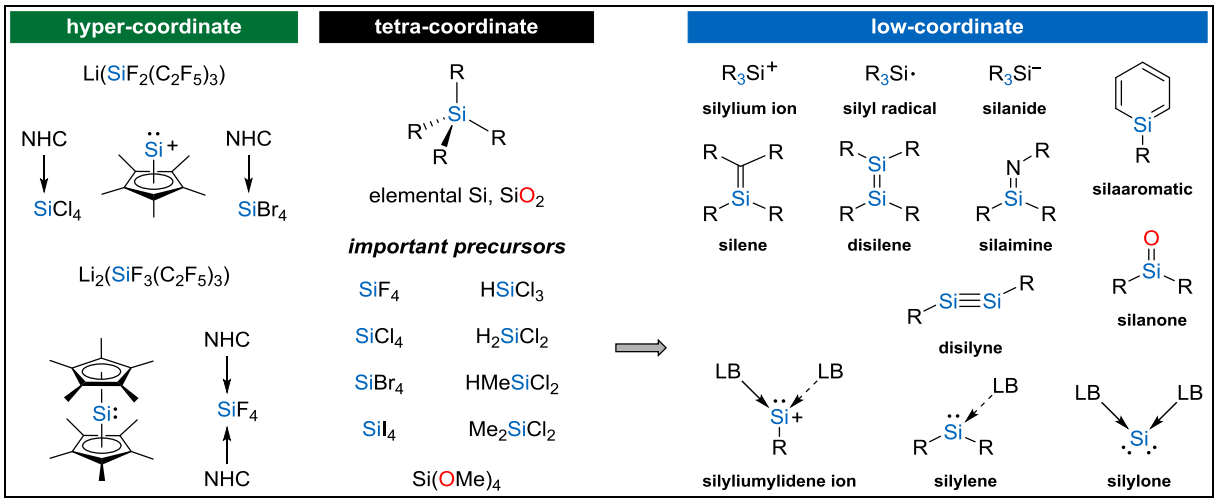


Figure 1. Overview of the coordination chemistry of silicon with selected example species. LB = Lewis base; such as NHC, cyclic (alkyl)(amino)carbene (CAAC) or 4-*N*,*N*-dimethylaminopyridine (DMAP).

The disproval of the empirically formulated "double bond rule" in 1976/1981 by the groundbreaking work of *Lappert*, *Brook*, *West* and *Yoshifuji* on the isolation of the first distannene ($R_2Sn{=}SnR_2$),[31] silene ($R_2Si{=}CR_2$),[32] disilene ($R_2Si{=}SiR_2$)[33] and diphosphene ($RP{=}PR$),[34] gave rise to the flourishing chemistry of multiply bonded main group compounds.[27,30,35-37] Not only heavier homologues of alkenes were synthesized, but also silicon analogues of alkynes, imines and aromatic molecules. As the main focus of this thesis is on silylenes (heavier carbenes; R_2Si:) and the above mentioned silanones (heavier ketones), these compound classes will be examined in more detail in the following sections.

2.1 Silylenes

Carbenes are neutral, divalent carbon compounds with the general formula R_2C:, where the σ- and/or π-donating substituents R are either monodentate (homo- or heteroleptic) or bidentate, chelating ligands. Due to their inherently high reactivity, carbenes often represent only intermediary species. However, since the seminal work of *Guy Bertrand* and *Anthony Joseph Arduengo III* on the isolation of the first stable carbenes, a plethora of isolable derivatives has been reported.[38-39] The ubiquitous NHCs in particular have become an indispensable part of modern chemistry and are used in a wide range of applications.[40-42] Due to the facile fine tuning of their electronic and steric parameters,[43-44] NHCs can be used effectively in organocatalysis,[45] f-block element chemistry[46] or as tailor-made

ligands for transition metal complexes and catalytic processes.[47-49] In addition, they are used very successfully in main group chemistry for the isolation of highly reactive and otherwise elusive compounds.[30,50]

Divalent silylenes, the heavier silicon congeners of carbenes, are one of the most important and intensively studied species among the low-coordinate organosilicon compounds.[16,30,51-67] In comparison to their lighter homologues, the properties and electronic structure of silylenes differ significantly. The example of the two parent species methylene (H_2C:) and silylene (H_2Si:) already reveals major discrepancies, taking into account their calculated molecular structures and electronic configuration.[68] Whereas H_2C: exhibits a triplet ground state and thus a diradical character with sp^2-type orbitals, H_2Si: favors the singlet ground state resulting in an ambiphilic nature with a filled 3s-orbital (lone pair of electrons) and a vacant $3p_z$-orbital (Figure 2). The corresponding theoretically calculated single-triplet energy gaps (ΔE_{ST}) are in line with the observed distinct multiplicities (H_2C: ΔE_{ST} = –10.8 kcal/mol; H_2Si: ΔE_{ST} = 18.2 kcal/mol).[68]

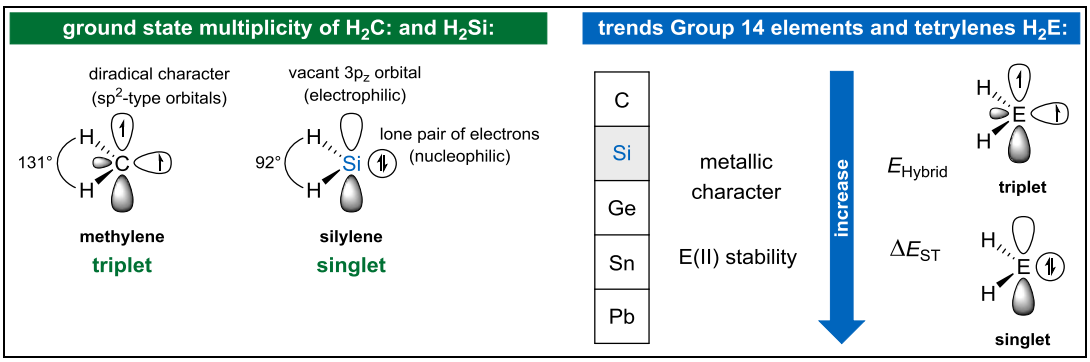


Figure 2. Ground state multiplicity of the parent tetrylenes methylene and silylene and general trends for key features of the Group 14 elements and their respective metallylenes (H_2E:).

In addition, the tendency to form hybrid orbitals generally decreases as one descends from carbon to lead in Group 14, due to a greater s-p-orbital separation (unfavorable overlap) with increasing effective nuclear charge.[60] These hybridization defects are reflected by the rising values for the energy of hybridization (E_{Hybrid}) within the carbon group (tetrels).[69] Since bonds of these hybrid orbitals are relatively weak, the heavier tetrel nuclei commonly prefer lower oxidation states and the stability of R_2E: metallylenes increases significantly. As a practical result of this so-called "inert pair effect", $SnCl_2$ and $PbCl_2$ are isolable compounds in contrast to their lighter, unstable analogues.

Consequently, the stereochemically active lone pairs of electrons of silylenes and heavier tetrylenes exhibit a more pronounced s-character in comparison to the lone pairs present in carbenes (high p-character). As the tetrylene lone pairs usually represent the highest occupied molecular orbitals

(HOMOs) and the empty np-orbitals the lowest unoccupied molecular orbitals (LUMOs), the singlet-triplet energy gap is generally correlated to the HOMO-LUMO gap. In addition, the H–E–H bond angles of the parent tetrylenes H_2E: decrease continuously within the tetrel group from top to bottom. Thus, the triplet ground state of H_2C: is closely associated with a significantly larger H–C–H bond angle (131°) compared to those observed for the heavier homologues (*cf.* H_2Si: 92° and H_2Ge: 91°).[68]

Despite or perhaps because of the differences to carbenes, the possibility of gaining access to a triplet ground state silylene and the search for the first isolable derivative and its corresponding reactivity has fascinated organosilicon chemists for a long time.[68,70-80] As indicated above, the R–Si–R angle is directly related to the respective ground state multiplicity of silylenes. Theoretical calculations by *Gordon* in 1985 revealed a "crossover angle" for the singlet and triplet energy curves of H_2Si: at ca. 130°.[81] Accordingly, for R–Si–R angles greater than the crossover angle, the triplet ground state of a silylene R_2Si: should be energetically favored, due to the increased p-character of the σ-orbital and the lowered σ→p promotion energy (Figure 3).[75,78] Moreover, the crossover angle is strongly dependent on the steric encumbrance and electronegativity of the substituents R, which is apparent from the calculated series of Me_2Si: (140°), H_2Si: (130°) and $(H_3Si)_2Si$: (115°).[75] Therefore, less electronegative and sterically crowded ligands should enable the generation of a triplet ground state silylene *via* opening the R–Si–R bond angle above the crossover angle.

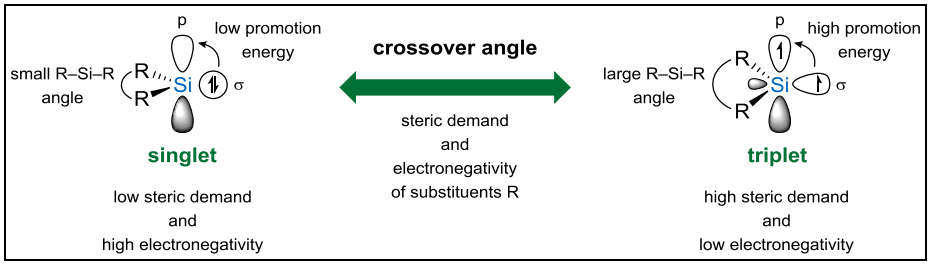


Figure 3. Influence of important parameters on the ground state multiplicity of silylenes (R_2Si:).

As predestinated electropositive substituents alkali metals and sterically demanding boryl and silyl groups were considered. Remarkably, the generation of transient triplet silylenes was indeed reported using such ligands and their electronic nature and multiplicity verified by electron paramagnetic resonance (EPR) spectroscopy and DFT calculations.[82-84] However, to this date, no isolable triplet ground state silylene is known and the reactivity of these elusive species remains unexplored. One of the most promising targets to finally achieve the isolation of unprecedented triplet silylenes are bis(silyl)silylenes, which will be discussed in more detail (*vide infra*).[85]

Silylenes are electron deficient compounds of an ambiphilic nature. They can function both as Lewis acids and as Lewis bases *via* their vacant $3p_z$-orbitals and their lone pairs of electrons, respectively. Whereas the lone pair is considered relatively inert (coordination chemistry), the high reactivity of silylenes is based on the unfulfilled octet rule caused by the empty $3p_z$-orbital. Stabilization is therefore indispensable for reducing the electrophilicity and thus enabling the isolation of silylenes. In principle, a distinction is made between kinetic (sterically encumbered substituents) and thermodynamic (electron-donating substituents) stabilization, but both concepts can also be applied simultaneously (Figure 4). On the one hand, utilization of electronegative substituents, such as amines, phosphines or alkoxides, results in an intramolecular thermodynamic stabilization of silylenes *via* π-electron-donation to the free $3p_z$-orbital (mesomeric effects). In addition, their σ-acceptor abilities (inductive effects) lead to an increase in the s-character of the HOMO and thus to a preferred singlet state. On the other hand, additional intermolecular coordination of Lewis bases is also a common method for reducing the extensive electrophilicity and accessing otherwise elusive silylenes. Nevertheless, this is accompanied by an increase in the coordination number and a relatively strong decrease in reactivity of the resulting three-coordinate derivatives.[60]

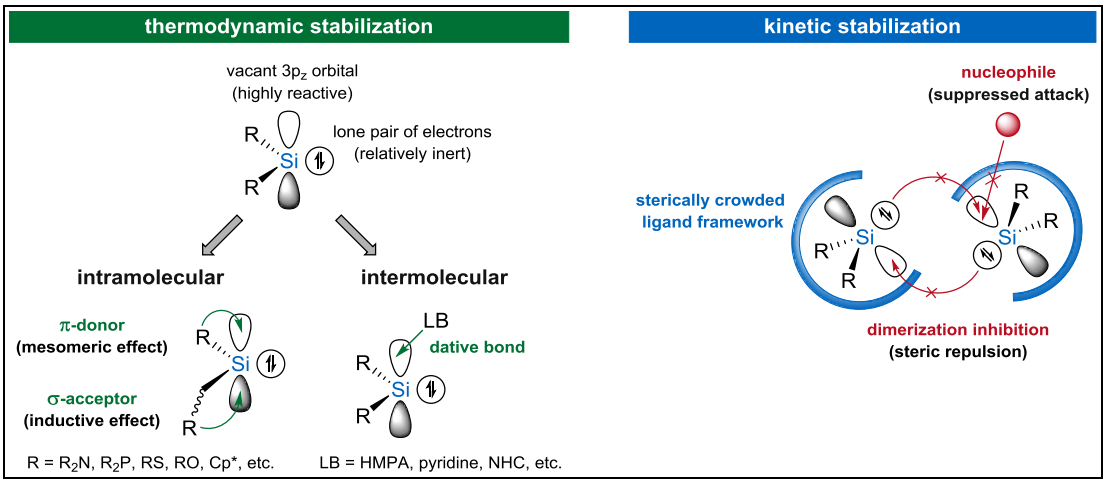


Figure 4. Thermodynamic and kinetic stabilization of divalent silylenes. HMPA = hexamethylphosphoric triamide.

Kinetic stabilization can be realized by the use of a sterically demanding ligand framework. By shielding the vacant $3p_z$-orbital, nucleophilic attacks on the reactive, low-valent silylene moiety are prevented. Furthermore, the frequently observed intermolecular dimerization reactions (providing disilenes) or oligomerizations can be bypassed by steric repulsion of the silylenes from each other.

2.1.1 Historic Milestones and General Reactivity

Silylenes have long been regarded as short-lived intermediates but not as stable and isolable species, which is not unexpected given the properties described above.[16] These divalent organosilicon compounds were already postulated by *Kipping* as reactive intermediates almost 100 years ago.[86] Reliable reports verifying the existence of dichlorosilylene (Cl_2Si:) have been available since the late 1930s.[87-88] A few decades later, *Skell* and *Goldstein* were able to demonstrate the formation of transient dimethylsilylene (Me_2Si:) *via* reductive debromination of Me_2SiCl_2 with sodium/potassium vapor at temperatures between 260–280 °C.[89] *Michl* and *West* later successfully characterized this organosilylene spectroscopically by photolysis of dodecamethylcyclohexasilane in an argon matrix under cryogenic conditions.[90] Due to a clever ligand design providing sufficient kinetic and/or thermodynamic stabilization, the chemistry of isolable silylenes has developed into a flourishing field with a plethora of reported derivatives.[16,30,51-67] In the following a brief overview of the most significant landmarks in the isolation of divalent silylenes is given.

The initial major pioneering step in silylene chemistry was achieved with the isolation of the first monomeric Si(II) compound decamethylsilicocene (**L1**) by *Jutzi et al.* in 1986 (Figure 5).[91-92] However, due to the two η^5-coordinating pentamethylcyclopentadienyl (Cp*) ligands, the ambient temperature stable Cp^*_2Si: (**L1**) is hyper-coordinate and thus not considered a typical divalent species with electron deficiency. As a result of the effective sterical shielding, the chemistry of **L1** is mainly based on the nucleophilicity of the silicon lone pair and the lability of the Cp* substituents.[93]

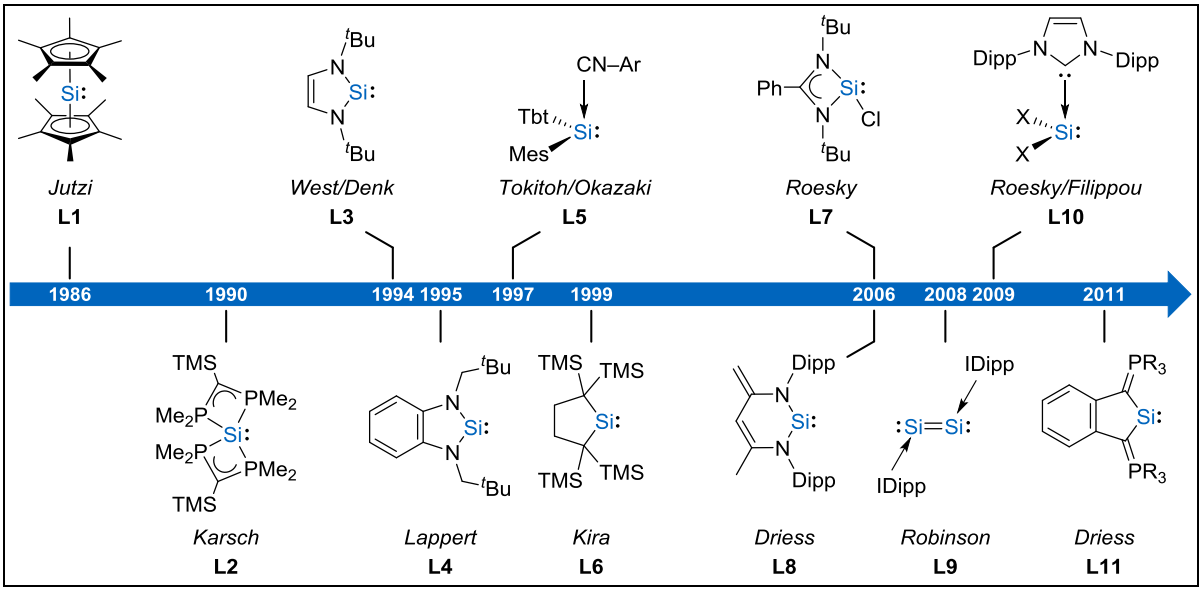


Figure 5. Timeline of historical milestones in the chemistry of divalent silicon species. Ar = Tipp (2,4,6-^{i}Pr$_3$-C$_6$H$_2$), Tbt (2,4,6-[CH(SiMe$_3$)$_2$]$_3$-C$_6$H$_2$), Mes* (2,4,6-^{t}Bu$_3$-C$_6$H$_2$); Mes = 2,4,6-Me$_3$-C$_6$H$_2$, Dipp = 2,6-^{i}Pr$_2$-C$_6$H$_3$; X = Cl, Br; TMS = SiMe$_3$; IDipp = 1,3-bis(2,6-diisopropylphenyl)imidazolin-2-ylidene; R = Ph, *m*-Tol (3-methylphenyl).

A few years later, *Karsch* and co-workers presented the tetra-coordinate silylene **L2**, thermodynamically stabilized by two chelating phosphine ligands.[94] As mentioned above, the versatile chemistry of NHCs started in 1991 with the first isolable representative 1,3-bis (1-adamantyl)imidazolin-2-ylidene, which was synthesized by *Arduengo* and colleagues *via* deprotonation of a corresponding imidazolium salt.[39] Only three years later, *Denk*, *West et al.* succeeded in the isolation of the first heavier homologue **L3**, an *N*-heterocyclic silylene (NHSi), representing the "genuine" stable silylene (two-coordinate).[95] The silylene moiety is thereby stabilized by two adjacent nitrogen nuclei that are embedded in an aromatic five-membered ring. The corresponding saturated analogue of **L3** is significantly less stable but more reactive, due to the lack of aromaticity.[52] Similar to NHCs, the nowadays well-explored class of NHSis comprises the most reported silylene derivatives and has been the subject of detailed investigations.[16,54,56] The group of *Lappert* reported with silylene **L4** the first NHSi containing a phenyl ring in the backbone (conjugated π-framework).[96] Later, they managed to isolate a unique donor-acceptor adduct of an NHC with its corresponding heavier NHSi congener.[97] Furthermore, the first example of two silylene moieties in a single molecule was accessible with the isolation of a spacer-separated biphenyl-bis(silylene).[98]

The concept of additional Lewis base-stabilization for the isolation of low-valent organosilicon compounds was initially introduced by *Tokitoh* and *Okazaki* in 1997 with the preparation of the silylene-isocyanide adducts **L5**.[99] This intermolecular coordination, which leads to an increase in the coordination number, has found widespread applications in modern organosilicon chemistry, especially using the diverse NHCs.[30,50] A milestone in the chemistry of carbocyclic silylenes was reached by *Kira et al.* with the isolation of the first dialkyl-substituted silylene **L6**.[100] Despite the adequate stabilization provided by the TMS groups adjacent to the carbon atoms (steric demand and β-silyl effect), **L6** slowly isomerizes in solution affording a cyclic silene *via* 1,2-silyl migration. Nevertheless, the reactivity of silylene **L6** was investigated thoroughly.[61] By modifying the ligand framework, an equilibrium mixture consisting of another dialkylsilylene and its disilene dimer was found later.[101]

The diversity of isolable silylenes was expanded with the preparation of the first monomeric chlorosilylene [PhC(N^{t}Bu)$_2$](Cl)Si: (**L7**) by *So*, *Roesky* and co-workers in 2006.[102] The initially applied low yielding reductive dechlorination of the respective trichlorosilane was later modified to a dehydrochlorination protocol that uses a dichlorosilane precursor and provides **L7** with drastically increased yield.[103] The intramolecular base-stabilized, three-coordinate NHSi **L7** has found widespread applications as a suitable starting compound for the synthesis of functionalized silylenes

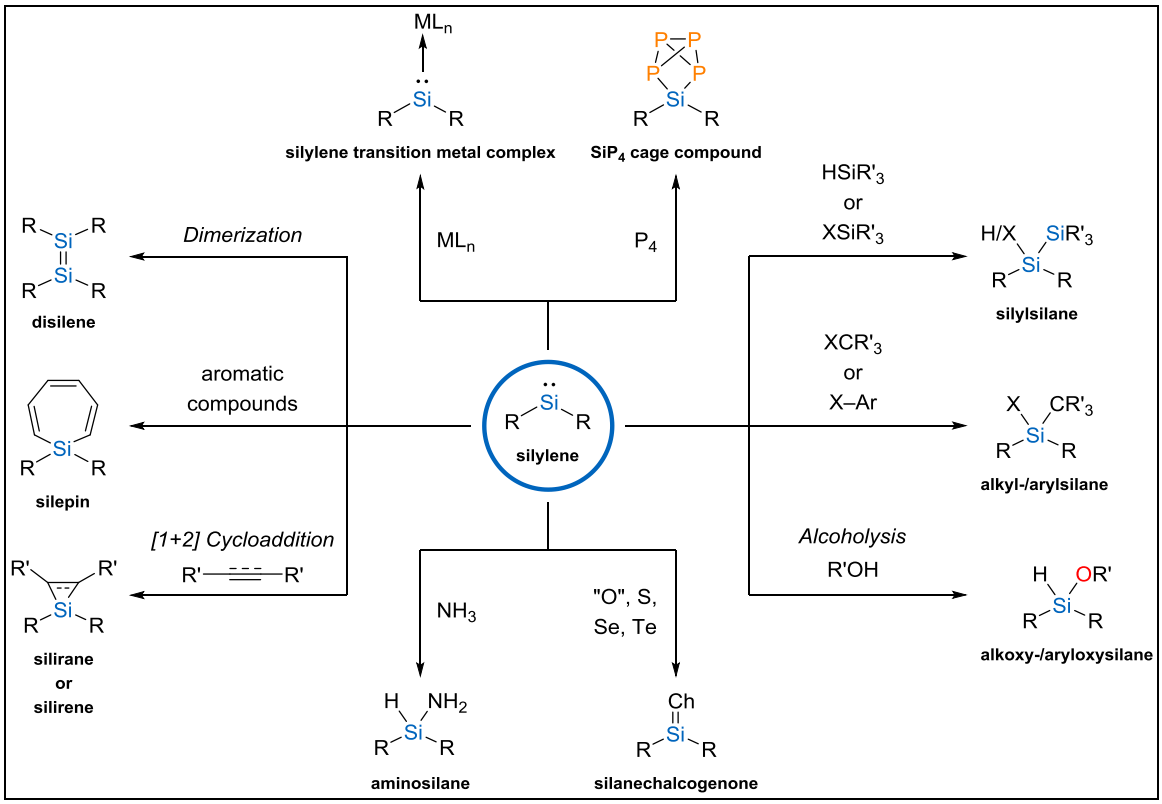
via salt metathesis reactions.[16,59,62-64] Furthermore, the first interconnected bis(silylene) containing a Si(I)–Si(I) bond was synthesized,[104] which paved the way for numerous other derivatives and a diverse reactivity.[64-65] *Driess* and co-workers utilized the bidentate *β*-diketiminate ligand HC[CMeN(Dipp)]$_2$ to synthesize the first six-membered NHSi HC[(C=CH$_2$)(CMe)(NDipp)$_2$]Si: (**L8**).[105] The zwitterionic, ylide-like diaminosilylene exhibits a particularly versatile reactivity, also due to its butadiene backbone.[16,63] Another milestone in low-valent silicon chemistry was set by *Robinson et al.* with the synthesis of the interconnected bis(chlorosilylene) [(IDipp)SiCl]$_2$ and the unique NHC-stabilized silicon "allotrope" [(IDipp)Si]$_2$ (**L9**) in 2008.[106] The NHC-supported diatomic Si(0) complex **L9** was subjected to a detailed reactivity study, such as transition metal coordination chemistry or oxidation reactions.[30,50,107-110] Very recently, even its successful application as a Si-Transfer agent was demonstrated.[111] In addition, *Roesky* and colleagues reported analog CAAC-stabilized Si(0) complexes and a related triatomic silicon(0) cluster.[112-114]

The simultaneous isolation of the first NHC-stabilized silicon(II) dihalides IDipp·SiX$_2$ (**L10**) (X = Cl, Br) by the groups of *Roesky* and *Filippou* in 2009 heralded the start of a very fruitful era in organosilicon chemistry.[115-116] A few years later, the iodine analogue IDipp·SiI$_2$ was also successfully synthesized.[117] Overall, these diverse divalent silicon compounds were utilized in a plethora of different reactions, in particular as valuable building blocks to gain access to novel silylene derivatives.[30,66,118] Other rare members of the small carbocyclic silylene family were isolated by Driess and co-workers. The new silylene representatives **L11** are uniquely stabilized by two phosphorus ylide functionalities in an aromatic framework.[119]

In addition to the cyclic and/or hyper-coordinate derivatives shown above, a large variety of interesting silylenes is known today.[16,30,51-67] Of particular interest are acyclic silylenes and bis(silyl)silylenes due to their exceptionally high reactivity, which will be discussed in more detail (*vide infra*). Nevertheless, despite intensive investigations, there are still no reports in the literature regarding isolable triplet ground state silylenes. Over the years, many different silylene reaction patterns have been discovered.[16,30,51-67] In the following, selected typical silylene reactivities are briefly presented, including the activation of industrially relevant small molecules.

Owing to their specific electron configuration and structure, divalent silylenes (R$_2$Si:) are ambiphilic and in general very reactive species. As already mentioned above, their Lewis base character is rather less pronounced, due to the relative inertness of the lone pair of electrons. Nevertheless, silylenes have been successfully applied in the coordination chemistry with transition metals. While early reports comprise complexes of transient and otherwise elusive silylenes stabilized by transition

metal fragments (*e.g.* $(Me)_2(HNEt_2)Si{:}\rightarrow Fe(CO)_4$, $(^tBuO)_2(HMPA)Si{=}Fe(CO)_4$ and $(Ph)_2(MeCN)Si{=}RuCp^*(PMe_3)_2$),[120-122] many silylene transition metal complexes derived from isolable derivatives are known today (Scheme 3).[16,30,50] *Jutzi* reported the first reaction of a stable divalent silicon compound in 1990 *via* treating Cp^*_2Si: (**L1**) with (CO)AuCl, which resulted in the formation of the *Fischer*-type silylene complex $Cp^*_2Si{:}\rightarrow AuCl$.[123] Although a few applications of silylene transition metal complexes for catalytic conversions have already been found, the potential of silylene ligands is still rather untapped.[124] A recent theoretical study indicated the capability of silylenes as powerful substitutes for commonly used phosphine (PR_3) or NHC ligands.[125] Due to their partially superior features (*e.g.* σ-donating and π-accepting properties) they could facilitate elementary catalytic steps, such as oxidative addition and reductive elimination. Overall, silylenes not only serve as ligands for transition metal complexes, but can also form various Lewis acid-base adducts with main group element compounds (*e.g.* $CaCp^*_2$, BR_3, GeR_2).[16,30]



Scheme 3. Overview of the most common reactions of silylenes including some intriguing examples.

Apart from the coordination chemistry caused by the lone pair of electrons, the high reactivity of silylenes is mainly attributable to the vacant $3p_z$-orbital (Lewis acidic nature). One of the most frequently observed types of reaction is the insertion of the silylene moiety into a plethora of non-polar and polar bonds.[16,30,51-67] This reactivity has been known for a long time and is often used to verify the existence of transient silylenes *via* formation of significantly more stable Si(IV) compounds. Thus,

Skell and *Goldstein* proved the generation of Me_2Si: by identifying pentamethyldisilane ($Me_2Si(H)(TMS)$) after trapping Me_2Si: with trimethylsilane (TMS–H) back in 1964.[89] Analogously, a wide range of alkyl-, aryl- and silylsilanes is available *via* insertion reactions of silylenes into alkyl halides, aryl halides, halosilanes and silanes. Apart from Si–H, Si–X and C–X bonds, the formal oxidative addition of other bonds such as H–X, B–H, B–X, P–H, P–X and X–X has been observed. Another popular method of trapping silylenes is alcoholysis, which leads to the formation of different alkoxy- and aryloxysilanes ($R_2Si(H)(OR')$).

The activation of white phosphorus (P_4) is an exciting but relatively unexplored area in modern main group chemistry with only rare examples of low-coordinate organosilicon compounds affording a series of rather distinct products.[126-127] Thus, the isolation of a unique SiP_4 cage compound was achieved by *Driess et al.* after exposure of the six-membered NHSi **L8** to P_4 (insertion of the silylene unit into a P–P bond of the P_4 tetrahedron).[128] Interestingly, *Roesky* and co-workers observed the formation of a four-membered Si_2P_4 ring using the three-coordinate NHSi **L7**.[129] Utilization of the amine-substituted derivative $[PhC(N^tBu)_2]((TMS)_2N)Si$: instead, provided a peculiar compound containing a Si=P–P=P–P=Si chain.[130] Of particular importance is also the activation of N–H bonds and above all the oxidative addition of ammonia (NH_3) by main group compounds.[11,13-15,17,131-134] However, research into this chemistry is still in its infancy, which is not surprising as even most transition metal complexes are not capable of conducting such a process.[135] The first report involving a divalent silylene was the synthesis of $HC[(C=CH_2)(CMe)(NDipp)_2]Si(H)(NH_2)$ *via* reaction of the zwitterionic, ylide-like diaminosilylene **L8** with NH_3.[136] In addition to NH_3, the insertion of R_2Si: into the N–H bonds of various amines was revealed.[16]

A prototypical reaction of insufficiently stabilized silylenes is the formation of disilenes *via* dimerization. The aforementioned isolation of the first disilene $Mes_2Si=SiMes_2$ by West *et al.* in 1981 is a prime example, since after photolysis of Mes_2SiTMS_2 a rapid dimerization of the intermediary generated silylene Mes_2Si: was observed.[33] Furthermore, less sterically shielded silylenes, such as H_2Si: and Cl_2Si:, even undergo oligomerization reactions yielding oligosilanes. In contrast to the planar alkenes, the bonding situation of the heavier disilene congeners is fundamentally different and the isolation of stable derivatives was long considered impossible ("double bond rule"). In order to understand the bonding situation of disilenes and their heavier homologues, the "Carter-Goddard-Malrieu-Trinquier" (CGMT) model was developed and later named after its creators.[137-139] Accordingly, a rotation of singlet tetrylenes is essential to circumvent the steric repulsion between the lone pairs of electrons and to establish a double donor-acceptor-interaction, which is necessary for the

formation of disilenes (indicated in Figure 4; *vide supra*). The resulting *trans*-bent structure of disilenes strongly correlates with the singlet-triplet energy gap of the corresponding monomeric silylenes (higher $\Delta E_{ST} \rightarrow$ more pronounced *trans*-bent structure). Today, disilenes represent an important class within the family of low-coordinate organosilicon compounds, with a large number of isolable derivatives and a versatile substitution pattern.[16,35-36,67,133,140-142] In addition, many interesting reactivities, including small molecule activation, have been revealed in recent decades.

In a similar way to carbenes providing cyclopropanes, silylenes undergo [1+2] cycloaddition reactions with alkenes affording silacyclopropanes (siliranes). This reactivity was already indicated more than 50 years ago.[143] Siliranes have emerged as suitable synthons in organosilicon chemistry, especially as silylene transfer reagents.[144-146] The use of alkynes instead leads to the formation of silacyclopropenes (silirenes), which display a source of silylenes themselves upon photochemically induced retro-cycloaddition reactions.[147] Remarkably, silylenes can also react with aromatic compounds, comparable to triplet ground state carbenes or specific singlet carbenes.[148] Thus, after thermally or photochemically induced promotion to excited singlet or triplet states, singlet silylenes form bycyclic silanorcaradienes ([1+2] cycloaddition products), which quickly isomerize to silacycloheptatrienes (silepins) *via* a *Büchner*-type ring expansion (insertion).[58,149-154] In addition to benzene derivatives, heteroaromatic compounds such as pyridine derivatives can also be applied, resulting in the synthesis of azasilepin species.[155-156]

Oxidation reactions of silylenes with various oxygenation agents (*e.g.* O_2, CO_2, N_2O, $R_3N^+–O^-$, $R_3P=O$), heavier elemental chalcogenes Ch (Ch = S, Se, Te) or chalcogen transfer reagents, such as $R_3P=Ch$, have been the subject of numerous studies.[16,30,51-67] In this manner, for example, access to silanechalcogenones $R_2Si=Ch$ is possible. Of particular interest for organosilicon chemists is the formation of silanones (Ch = O), which will be discussed in detail later. Apart from the isolation of monomeric silanethiones (Ch = S), silaneselones (Ch = Se) and silanetellones (Ch = Te), the corresponding dimeric species $(R_2SiCh)_2$ and various other heterocyclic organosilicon compounds including three-membered R_2SiCh_2 and five-membered R_2SiCh_4 rings were reported.

Overall, as already indicated, in addition to the rather concise presentation of selected silylene reactivities, an extensive series of further reactions has been found.[16,30,51-67] However, with regard to the results outlined in this work, the suitability of silylenes for the synthesis of silaimines ($R_2Si=NR'$) should also be briefly mentioned. Exposure of silylenes to organic azides results in the formation of silaimines *via* concomitant nitrogen evolution. Insufficiently stabilized derivatives can undergo subsequent reactions providing disilaaziridines, silatetrazolines or azido(amido)silanes.[157-158]

2.1.2 Acyclic Two-Coordinate Silylenes

The R–Si–R angles of silylenes R_2Si: are directly linked to the singlet-triplet energy gaps and the HOMO-LUMO gaps and thus correlate with the inherent reactivities (*vide supra*). Since most of the reported derivatives are embedded in small cyclic frameworks, they are forced to adopt rather acute R–Si–R angles (geometry reasons). Therefore, the development of acyclic silylenes has been considered as a promising approach to circumvent these limitations and enable the formation of significantly more obtuse angles. Due to their higher reactivity, however, acyclic silylenes are considerably more labile and consequently more challenging to isolate. Early attempts to access acyclic silylenes, such as $^tBu_2Si$:, Mes_2Si:, $Tipp_2Si$:, Ad_2Si: (diadamantylsilylene) and $(^iPr_2N)_2Si$:, were essentially limited to *in situ* formation and isolation of Si(IV) trapping products.[70-71,159-160] Remarkably, the first synthetically accessible representative, that is relatively stable at temperatures rather close to ambient conditions (–20 °C), was described by *Müller, West et al.* back in 2003.[161] However, the sterically demanding acyclic diaminosilylene $((TMS)_2N)_2Si$: (**L12**) (Figure 6) decomposes rapidly at room temperature and was therefore trapped with MeOH and PhOH to unambiguously verify its existence.

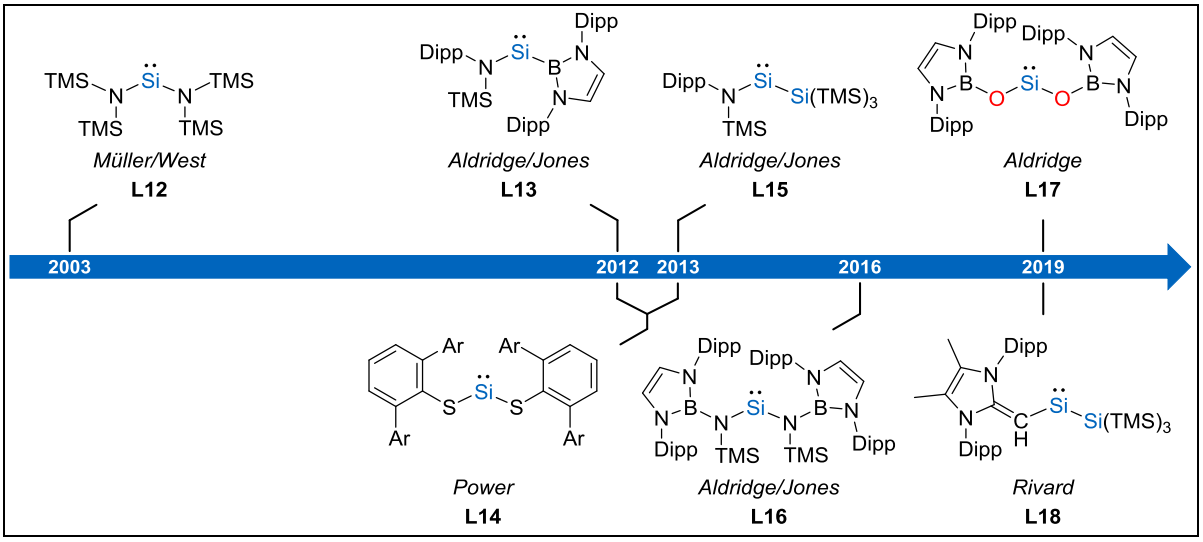


Figure 6. Timeline of historical milestones in the chemistry of two-coordinate acyclic silylenes. Ar = Mes, Dipp and Tipp.

Although decamethylsilicocene Cp^*_2Si: (**L1**) and its derivatives $Cp^*(R_5C_5)Si$: (*e.g.* $Cp^*(^iPr_5C_5)Si$:) can be regarded as acyclic silylenes, they are not "true" two-coordinate species, but rather "resting states" of silylenes bearing σ-bonded substituents, due to their η^5-coordinating aromatic ligands (π-bonded).[93,162] *Jutzi* and co-workers employed the unique and versatile silyliumylidene ion $[Cp^*Si:^+][B(C_6F_5)_4^-]$ to gain access to a number of other hyper-coordinate acyclic silylenes.[162-163] Thus, the arylsilylene $(2,6\text{-Tipp-}C_6H_3)(\eta^3\text{-}Cp^*)Si$:, the aminosilylene $((TMS)_2N)(\eta^2\text{-}Cp^*)Si$: and

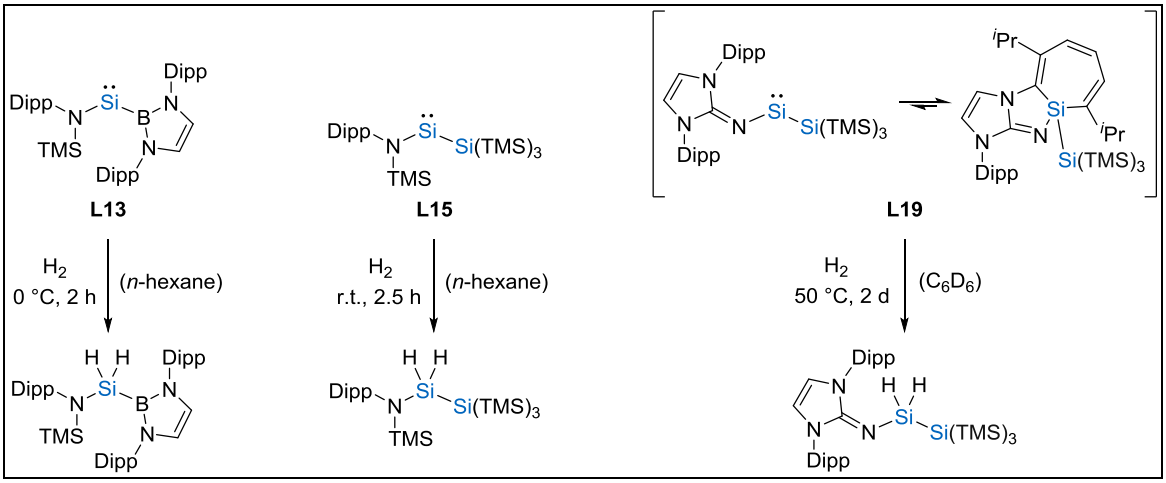
the ferriosilylene $(Cp^*(CO)_2Fe)(\eta^3\text{-}Cp^*)Si$: were obtained.[164-166] This series was extended *via* isolation of iminosilylene $(IDippN)(\eta^2\text{-}Cp^*)Si$: (IDippN = 1,3-bis(2,6-diisopropylphenyl)imidazolin-2-iminato) by our group.[167] This particular report already outlines the application of the nowadays widely used *N*-heterocyclic imines (NHIs) for the stabilization of elusive main group compounds.[168] NHIs are structurally derived from NHCs and are strong electron donors (2σ and/or $2\pi/4\pi$).

A major breakthrough in the chemistry of divalent silylenes was achieved simultaneously by *Aldridge/Jones et al.* and *Power* and colleagues with the isolation of the first stable acyclic two-coordinate derivatives in 2012. Whereas aminoborylsilylene **L13** was synthesized *via* ligation and reduction of the corresponding aminotribromosilane with the appropriate lithium boryl reagent, bis(arylthio)silylene **L14** (Ar = Mes) was obtained by reduction of the corresponding bis(arylthio)dibromosilane with *Jones'* magnesium(I) compound.[169-171] A combination of experimental data and theoretical calculations illustrated the correlation between the Si–R–Si bond angle and the HOMO-LUMO energy gap (**L13**: 109.7(1)°/2.04 eV and **L14**: 90.5(1)°/4.23 eV). Accordingly, **L13** should be more reactive than **L14**, which has been demonstrated and will be discussed below. This accomplished cornerstone led to broad resonance in the low-coordinate organosilicon community.[172-173] The pool of isolable acyclic silylenes was soon extended with the successful preparation of aminosilylsilylene **L15** and the bis(arylthio)silylene derivatives **L14** (Ar = Dipp and Tipp).[174-175] A few years later the first stable acyclic diaminosilylene was finally made available by *Aldridge/Jones* and co-workers. Silylene **L16** represents a sterically crowded version of **L12** and was prepared *via* salt metathesis reaction between *Roesky's* NHC-stabilized dichlorosilylene IDipp·$SiCl_2$ (**L10**) and the corresponding lithium amide.[176] In the course of this work, the small list of accessible acyclic two-coordinate silylenes was further expanded with the isolation of the first dioxy- and vinylsilyl-substituted derivatives **L17** and **L18**.[177-178] Remarkably, these accounts feature the introduction of the novel *N*-heterocyclic boryloxy (NHBO) ligand class and the application of the increasingly used *N*-heterocyclic olefins (NHOs).[179] Both ligand types are strongly related to NHCs and NHIs.

Noteworthy, in addition to stable acyclic silylenes, a series of "masked" species has been isolated, which are usually present in a more stable form (or in equilibrium), but still exhibit silylene reactivity. *Tokitoh et al.* reported on the thermally induced accessibility of the bis(aryl)silylene (Tbt)(Mes)Si: *via* dissociation of its corresponding disilene dimer.[58,150,180] Trapping of the reactive silylene led to the formation of the above mentioned silylene-isocyanide adducts **L5** (Figure 5). The existence of an equilibrium consisting of a cyclotrisilene and an acyclic disilenyl silylene was demonstrated by

Cowley/Scheschkewitz and colleagues.[181-182] Strikingly, a reversible silepin formation of the reactive iminosilylsilylene (IDippN)((TMS)$_3$Si)Si: (**L19**) *via* intramolecular aromatic C=C bond activation reaction of its flanking ligand framework was found in our laboratories.[183] Hence, the potential of divalent silylenes to undergo both oxidative addition and reductive elimination was demonstrated. Recently, *Cui et al.* managed to isolate the first silanorcaradiene derivative (intermediate of silepin formation) by intramolecular cyclopropanation of a transient triplet ground state boryl-lithiosilylene.[84,184]

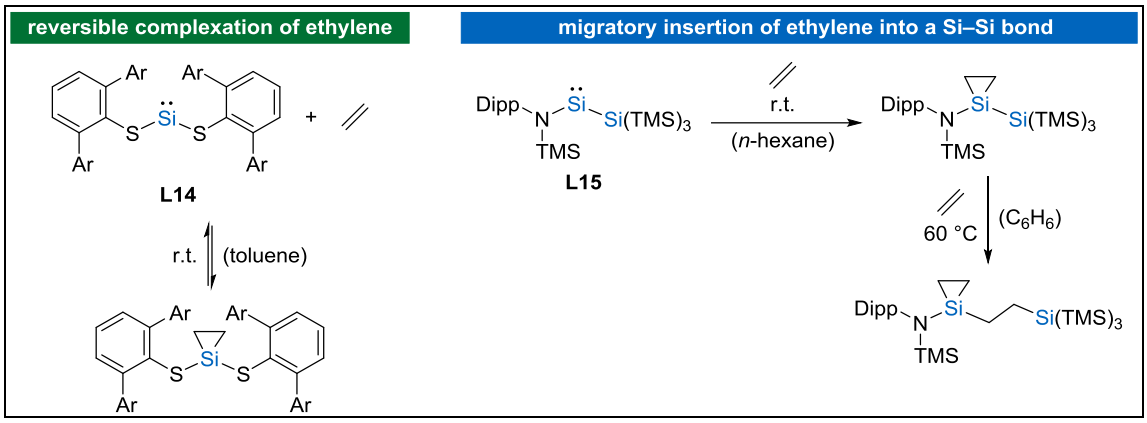
Despite the rather limited number of isolable (masked) acyclic two-coordinate silylenes, a remarkable reactivity of this low-valent organosilicon class has already been found. As a consequence of the potentially larger R–Si–R bond angles and the associated smaller ΔE_{ST} and HOMO-LUMO gaps, acyclic silylenes are indeed significantly more reactive than their cyclic counterparts. Thus a behavior reminiscent of traditional transition metal complexes was found *via* the activation of challenging and industrially relevant small molecules. Certainly the most striking reaction is the unprecedented single-site activation of molecular dihydrogen (H_2) with **L13**, **L15** and masked **L19**, selectively providing the corresponding dihydrosilanes by oxidative addition (Scheme 4). In sharp contrast, bis(arylthio)silylenes **L14** are not capable of a similar process due to their less advantageous key features (*vide supra*).



Scheme 4. Single-site activation of dihydrogen by divalent acyclic two-coordinate silylenes.

Nevertheless, **L14** reacts with alkynes and 2,3-dimethyl-1,3-butadiene under formation of novel silirene derivatives and a five-membered silacyclopent-3-ene *via* [1+2] and [1+4] cycloadditions, respectively.[185] Utilization of ethylene instead resulted in a remarkable reversible C=C bond activation and silirane formation (Scheme 5).[186] Such a reversible complexation represents a pivotal step for potential catalytic applications and is seldom observed among main group compounds.[187-188]

Another fascinating reactivity of acyclic two-coordinate silylenes mimicking transition metal complexes was found by *Rieger et al.* in 2016. Exposure of ethylene to aminosilylsilylene **L15** selectively afforded the novel silirane ((TMS)DippN)((TMS)$_3$Si)Si(CH$_2$CH$_2$).[189] Subjecting this silirane to elevated temperatures in the presence of ethylene resulted in the unique migratory insertion of the coordinated olefin moiety into the Si–Si bond and subsequent formation of an alkyl-substituted silirane. NMR experiments with deuterated ethylene verified the proposed mechanism.



Scheme 5. Transition metal-like reactivity of acyclic two-coordinate silylenes with ethylene. Ar = Mes and Dipp.

The outstanding importance of acyclic silylenes for small molecule activation was further demonstrated with carbonylation experiments. The reactivity of divalent silylenes toward carbon monoxide (CO) is limited to argon matrix isolation studies and DFT calculations, but there are no reports in the literature about isolable products at ambient temperature.[190-196] Recently, however, the unprecedented reaction of aminoborylsilylene **L13** with CO was disclosed. Nevertheless, the formation of silicon carbonyl complex ((TMS)DippN)([(CH)(NDipp)]$_2$B)Si⇆CO was not observed, but the isolation of a six-membered Si$_2$C$_2$O$_2$ heterocycle (reductive coupling of CO) was achieved.[197] In addition, a somewhat related coupling of CO was found for cyclic silylenes by employing reactive spacer-separated bis(NHSi) derivatives.[198-200]

Further investigations revealed the oxidative addition of NH$_3$ and P$_4$ to the acyclic silylenes **L15**, **L16** and **L18** under mild conditions.[176,178,201] Interestingly, exposure of carbon dioxide (CO$_2$) to **L13** and masked iminosilylsilylene **L19** provided different novel organosilicon compounds. Thus, the acyclic silaimine (TMSO)([(CH)(NDipp)]$_2$B)Si=NDipp and the first monomeric silicon carbonate complex (IDippN)((TMS)$_3$Si)Si(O$_2$C=O) were successfully isolated.[183,197] A characteristic result of the intrinsically high reactivity of acyclic silylenes is the intramolecular C–H bond activation of the flanking ligand frameworks, resulting in more stable tetra-coordinate organosilicon compounds.[169,174]

The first example of an intermolecular C–H bond activation was achieved *via* reaction of **L18** with ^{t}BuNC and formation of a silyl cyanide species.[178]

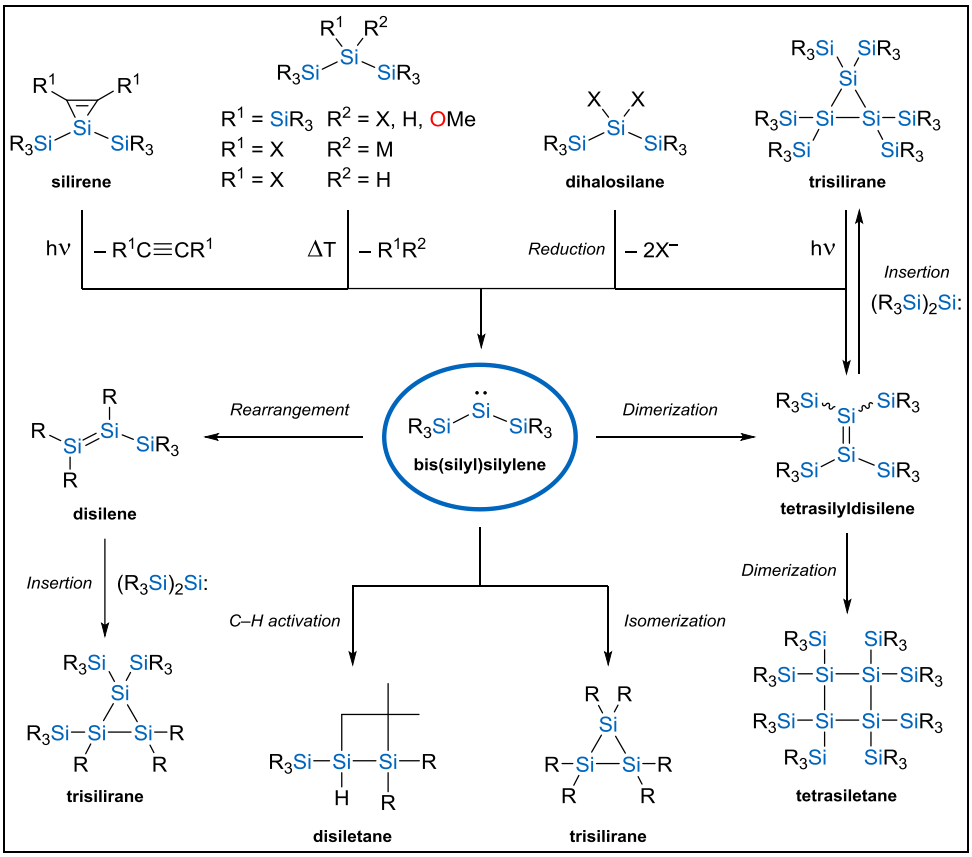
Overall, the chemistry of divalent acyclic silylenes is still in its infancy and their untapped potential for catalytic applications must be further exploited in order to possibly achieve a silylene-based metal-free catalysis in the future. Triplet ground state silylenes could also play a key role in this regard. However, there are still no isolable triplet silylenes known, as mentioned above.

2.1.3 Acyclic Bis(silyl)silylenes

The chemistry of bis(silyl)silylenes $(R_3Si)_2Si$: is strongly linked to the quest for stable triplet ground state silylenes.[73-80,85] The influence of the sterically easily tunable electropositive silyl groups on the electronic nature, multiplicity and structure of divalent silylenes (R–Si–R angle, ΔE_{ST} and HOMO-LUMO gap) can ultimately lead to a preference of the triplet over the singlet ground state (*vide supra*; Figure 3). Already monosilyl-substituted acyclic two-coordinate silylenes exhibit an extraordinarily high reactivity, as demonstrated *via* the successful single-site activation of H_2 by aminosilylsilylene ((TMS)DippN)((TMS)$_3$Si)Si: (**L15**) and masked iminosilylsilylene (IDippN)((TMS)$_3$Si)Si: (**L19**) (Scheme 4). Consequently, acyclic donor-free bis(silyl)silylenes can be considered as even more reactive species. In general, verification of the formation of these non-isolable species (at least until this work) is achieved by identifying stable trapping or decomposition products.

The first detailed experiments regarding bis(silyl)silylenes can be traced back to the end of the 1970s/beginning of the 1980s. The groups of *Sakurai* and *Gaspar* used different hypersilyl-substituted reagents $(TMS)_3SiR$ (R = H, Cl and OMe) to generate bis(trimethylsilyl)silylene $(TMS)_2Si$: *via* thermally induced elimination of TMS–R (Scheme 6).[202-203] The reactive silylene eventually leads to the formation of octakis(trimethylsilyl)cyclotetrasilane after intermediate dimerization to the transient disilene $(TMS)_2Si{=}Si(TMS)_2$. Some years later, the suitability of trisiliranes for gaining access to disilylated silylenes was demonstrated through photolysis of $((Et_3Si)_2Si)_3$, which provided $(Et_3Si)_2Si{=}Si(SiEt_3)_2$ both as photodissociation by-product and dimerization product of the corresponding bis(silyl)silylene.[204] Notably, the respective trisilirane itself is available after reductive debromination of $(Et_3Si)_2SiBr_2$ *via* insertion of $(Et_3Si)_2Si$: into its disilene dimer (formal trimerization). The pool of available tetrasilyldisilenes was extended by *Kira et al.* and *Sekiguchi* and colleagues with the isolation of $(R_3Si)_2Si{=}Si(SiR_3)_2$ (SiR_3 = Si^{i}Pr$_2$Me, Si^{t}BuMe$_2$, Si^{i}Pr$_3$ and Si^{t}Bu$_2$Me).[77,205-207] These disilenes were synthesized after immediate dimerization of $(R_3Si)_2Si$:, afforded either by reductive debromination of the corresponding dibromosilanes or by photolysis of

the respective cyclic trisilanes. Disilene $(^{i}Pr_3Si)_2Si{=}Si(Si^{i}Pr_3)_2$ is also available after dimerization of $(^{i}Pr_3Si)_2Si$:, generated *via* thermally or photochemically induced decomposition of $(^{i}Pr_3Si)_3SiH$.[75] Reduction of dibromosilane $(^{i}Pr_2MeSi)(^{t}BuMe_2Si)SiBr_2$ furnished the transient asymmetric silylene $(^{i}Pr_2MeSi)(^{t}BuMe_2Si)Si$: which dimerized to the corresponding stereogenic disilene.[208] Interestingly, besides (*E*)/(*Z*)-isomerization of the latter even the formation of $(^{i}Pr_2MeSi)_2Si{=}Si(Si^{i}BuMe_2)_2$ was revealed.



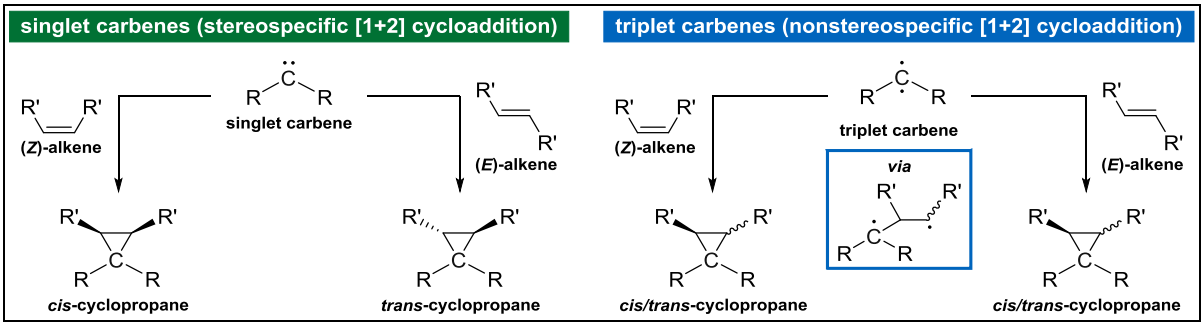
Scheme 6. Synthetic approaches to bis(silyl)silylenes and commonly observed decomposition/isomerization pathways.

Klinkhammer examined the preparation of the sterically crowded acyclic two-coordinate bis(hypersilyl)silylene $((TMS)_3Si)_2Si$: by treating $HSiCl_3$ with potassium hypersilanide ($KSi(TMS)_3$). However, the reaction provided trisilirane $((TMS)_2Si)_3$, presumably after initial formation of $((TMS)_3Si)_2SiHCl$, followed by reductive dehydrochlorination and subsequent rearrangement (1,2-silyl migration) and insertion reactions of the extremely reactive silylene.[209-210] After reductive debromination of the less sterically encumbered $((TMS)_2MeSi)_2SiBr_2$, a higher substituted trisilirane was isolated *via* insertion of transient $((TMS)_2MeSi)_2Si$: into the intermediary formed rearranged disilene $((TMS)_2MeSi)(TMS)Si{=}Si(Me)(TMS)$ (obtained by silylsilylene-disilene interconversion).[211] Even with a tremendously sterically demanding silyl substitution pattern, no isolable acyclic two-coordinate bis(silyl)silylene was accessible until now. Hence, *Sekiguchi* and co-

workers observed the selective and irreversible formation of the rearranged disilene ((ᵗBu₂MeSi)₂MeSi)(ᵗBu₂MeSi)Si=Si(Me)(Siᵗ Bu₂Me) by 1,2-silyl migration (Siᵗ Bu₂Me) of the reactive, extremely bulky silylene ((ᵗBu₂MeSi)₂MeSi)₂Si:.[212]

The generation of bis(supersilyl)silylene (ᵗBu₃Si)₂Si: was reported by *Wiberg* both *via* reductive dehalogenation of (ᵗBu₃Si)₂SiBr₂ and thermally induced LiX elimination of the silylenoids (ᵗBu₃Si)₂Si(X)(Li) (X = F, Cl, Br).[213-214] Its formation was identified by the characterization of 1,1-di-*tert*-butyl-4,4-dimethyl-2-(tri-*tert*-butylsilyl)-1,2-disiletane, resulting from an irreversible intramolecular C–H bond activation of the adjacent ligand framework. A triplet ground state was predicted for (ᵗBu₃Si)₂Si: and later supported by theoretical calculations.[74,79] *Gaspar et al.* obtained a similar disiletane by intermediary formation of (ᵗBu₃Si)(ⁱPr₃Si)Si: (photolysis of suitable heterocycles) and subsequent C–H bond activation.[76] They concluded such reactivity as proof for the triplet ground state multiplicity of divalent silylenes. However, thorough DFT calculations later indicated a singlet ground state for (ᵗBu₃Si)(ⁱPr₃Si)Si: and unveiled the singlet state being responsible for intramolecular C–H bond insertion reactions (even for triplet ground state silylenes).[79-80] The triplet nature of bis(supersilyl)silylene (ᵗBu₃Si)₂Si: was finally verified by *Sekiguchi* and colleagues in 2003. Irradiation of the silirenes (ᵗBu₃Si)₂Si(CRCR) (R = Me, Et) under argon matrix isolation conditions and subsequent EPR spectroscopy at 9 K disclosed the inherent diradical character and thus the triplet ground state.[82] Annealing of the matrix led to rapid decomposition of (ᵗBu₃Si)₂Si: to the above-mentioned disiletane and other by-products, due to the presence of the respective alkynes (RC≡CR).

As a presumably more reliable experimental reactivity for the determination of the ground state multiplicity of divalent silylenes, the stereochemistry of olefin addition was considered. In particular, the adaption of the so-called "*Skell* rule" originating from carbene chemistry was investigated in more detail.[215] Accordingly, singlet carbenes undergo a stereospecific addition with stereogenic alkenes (Scheme 7). In contrast, a nonstereospecific cycloaddition is observed for triplet carbenes, due to the formation of biradical intermediates that allow for facile rotation and loss of the initial stereochemistry.



Scheme 7. Stereochemistry of olefin addition to carbenes R_2C: according to the *Skell* rule (simplified representation).

However, in the case of divalent silylenes, the situation could be more complicated and a failure of the *Skell* rule cannot be excluded out, as even triplet silylenes could react *via* their respective singlet states.[75,78,80] In addition, the purity of the utilized stereogenic alkenes is absolutely decisive for the resulting silirane product ratio, since in general the respective (*Z*)-isomers react faster and therefore misinterpretations can occur. Hence, gas contaminations of the corresponding other isomer led to the initially erroneous assumption of a nonstereospecific addition of 2-butenes to dimesitylsilylene Mes_2Si:, which was refuted shortly afterwards [70,72] All other singlet silylenes investigated so far also reacted as expected under preservation of the stereochemistry.[71,75,77] Unfortunately, the transient triplet silylene $(^tBu_3Si)_2Si$: did not undergo [1+2] cycloaddition reactions with stereogenic olefins, most likely for steric reasons.[82] Further studies are therefore necessary in order to make a conclusive statement about the applicability of the *Skell* hypothesis to silylene chemistry. A promising starting point in this context could be the experimental and theoretical investigation of the other verified, but sterically significantly less congested triplet ground state silylenes $(^tBu_3Si)(M)Si$: (M = Li, K), as already indicated by Apeloig and co-workers.[80,83] However, to date, these studies have either never been conducted or at least have not been reported.

The only possibility to obtain isolable acyclic bis(silyl)silylene species so far is *via* additional coordination of strong Lewis bases, more precisely NHCs.[30,85] As mentioned earlier, the resulting formation of such three-coordinate organosilicon compounds is accompanied by a drastically reduced reactivity (Lewis acidity) and an exclusively singlet ground state multiplicity. The first examples were the NHC-stabilized derivatives **L20**, obtained by *Sekiguchi et al.* by reductive debromination of $(^tBu_3Si)_2SiBr_2$ and $(^tBu_2MeSi)_2SiBr_2$ with potassium graphite (KC_8) in the presence of 1,3,4,5-tetramethylimidazolin-2-ylidene (IMe_4) and 1,3-diisopropyl-4,5-dimethylimidazolin-2-ylidene ($I^iPr_2Me_2$) (Figure 7).[216] Interestingly, reversible one-electron oxidation of $IMe_4{\cdot}Si(Si^tBu_3)_2$ provided a unique silylene radical cation NHC adduct. During the course of this work, *Cowley, Holthausen* and colleagues successfully demonstrated the disilene-silylsilylene interconversion by preparing the NHC-stabilized bis(silyl)silylene **L21** from the corresponding disilene 4-(1-pyrrolidinyl)pyridine adduct.[217]

In view of the limited examples of isolable acyclic bis(silyl)silylenes, their cyclic counterparts are briefly discussed in the following. In analogy to donor-free acyclic derivatives, no stable two-coordinate cyclic bis(silyl)silylene has been reported so far. The first report concerning the generation of such a divalent species was provided by *Kira* and co-workers by synthesizing the transient four-membered silylene $Me_2Si[SiTMS]_2Si$:, which dimerized and subsequently rearranged to a fused bycyclic disilene.[218] All attempts to gain access to the five-membered homocyclic silylene

$[(Me_2Si)(Si(TMS)_2)]_2Si$: resulted in the intermediary formation of an endocyclic disilene (*via* 1,2-silyl migration), which subsequently dimerized. Nonetheless, generation of the transient cyclic bis(silyl)silylene was indicated by NMR spectroscopy and verified by a trapping reaction with Et_3SiH, affording $Me_2Si[SiTMS]_2Si(H)(SiEt_3)$.[211,219-221]

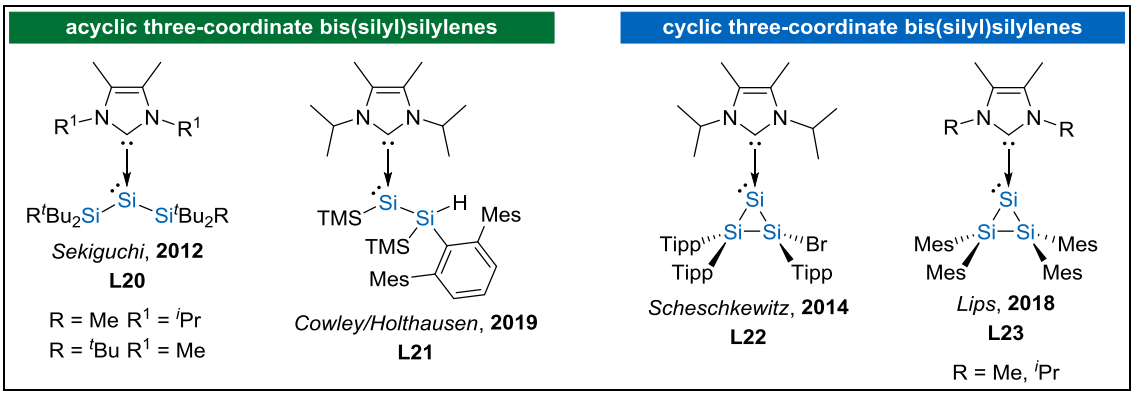


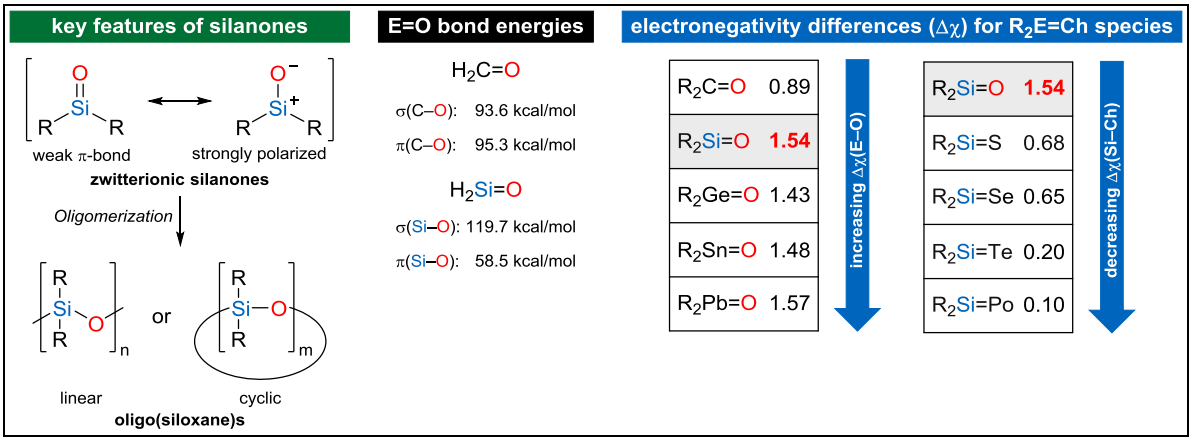
Figure 7. Ambient temperature stable three-coordinate bis(silyl)silylene derivatives.

Isolable cyclic bis(silyl)silylenes are restricted in the same manner as their acyclic analogues to NHC adducts. Thus *Scheschkewitz et al.* used their versatile reagent lithium disilenide $(Tipp)_2Si{=}Si(Tipp)(Li)$ to achieve the formation of the Si_3-cyclopropylidene **L22** *via* a substitution-reduction-rearrangement-cyclization cascade with NHC-stabilized silicon tetrabromide ($I^iPr_2Me_2{\cdot}SiBr_4$).[222-223] Recently, the similar cyclic bis(silyl)silylenes **L23** were obtained by *Lips* and colleagues.[224] Co-reduction of $I^iPr_2Me_2{\cdot}SiCl_4$ and Mes_2SiCl_2 with excessive amounts of lithium naphthalenide provided the $I^iPr_2Me_2$-stabilized derivative. Interestingly, the IMe_4 analogue was not accessible using the same approach, but only through an NHC exchange reaction of the $I^iPr_2Me_2$ congener.

As a consequence of the extremely high reactivity of bis(silyl)silylenes no isolable two-coordinate derivative has been found so far. Accordingly, the quest for the first stable representative, which could even exhibit a triplet ground state character, proceeds. Furthermore, the reactivity of bis(silyl)silylenes has only been scarcely investigated and a reaction typical for a triplet silylene is completely unknown. In this context, potential catalytic applications are of particular interest, but also the synthesis of novel, donor-stabilized bis(silyl)silylenes could provide deeper insights.

2.2 Silanones

In sharp contrast to the ubiquitous ketones, which are certainly among the most versatile and valuable building blocks of organic chemistry, the heavier silicon analogues, the so-called silanones ($R_2Si{=}O$), are still very elusive species.[16,27,30,225] Although *Kipping et al.* postulated the existence of silanones more than a century ago, all their synthetic attempts only afforded single-bonded oligo- or poly(siloxane)s $(R_2SiO)_n$.[24-26] Even nowadays, stable silanones are one of the most sought-after low-coordinate organosilicon compounds for main group chemists and their isolation is often referred to in the literature as "*Kipping's* dream".[27,225] Unlike their lighter ketone congeners, silanones are thermodynamically and kinetically unstable and therefore extremely reactive compounds that undergo a facile, barrierless head-to-tail oligomerization providing cyclic or linear oligo(siloxanes) *via* Si–O single bond formation (Scheme 8).[226-228] The origin of this instability lies on the one hand in the small HOMO-LUMO energy gaps and the inherently weak π-bonds, due to the unfavorable overlap of the p_π(Si) and p_π(O) orbitals.[229-230] A detailed theoretical investigation revealed an enormous energy difference for the σ(Si–O) (119.7 kcal/mol) and π(Si–O) (58.5 kcal/mol) bonds of $H_2Si{=}O$.[231] In contrast $H_2C{=}O$ features bonds of almost identical energy values (σ(C–O) = 93.6 kcal/mol and π(C–O) = 95.3 kcal/mol).



Scheme 8. Characteristic properties and reactivity of silanones in comparison to their lighter/heavier homologues.

On the other hand, silanones exhibit a highly zwitterionic, ylide-like character as a result of the strongly polarized $Si^{\delta+}$–$O^{\delta-}$ double bond.[232] This situation becomes apparent considering the high difference in electronegativity between silicon and oxygen ($\Delta\chi_{(Si-O)}$ = 1.54; *Pauling* scale), which is almost twice the value between carbon and oxygen ($\Delta\chi_{(C-O)}$ = 0.89).[233] Silanones occupy a somewhat special position within the homologous series of the carbonyl congeners $R_2E{=}O$ (E = group 14 element), since their $\Delta\chi_{(E-O)}$ is outside the trend of a steadily rising electronegativity difference with increasing atomic number. Hence, a series of germanones ($R_2Ge{=}O$; $\Delta\chi_{(Ge-O)}$ = 1.43) including a

stable three-coordinate, "genuine" derivative have been isolated.[27,234] Reports on stable stannanones ($R_2Sn{=}O$; $\Delta\chi_{(Sn-O)} = 1.48$) and plumbanones ($R_2Pb{=}O$; $\Delta\chi_{(Pb-O)} = 1.57$) are however essentially limited to the isolation of species bearing formal E=O moieties.[27,235] Due to the significantly reduced $\Delta\chi$ between silicon and the heavier chalcogenes, the isolation of silanechalcogenone homologues $R_2Si{=}Ch$ becomes much more feasible in comparison to silanones. Accordingly, a series of stable silanethiones ($R_2Si{=}S$; $\Delta\chi_{(Si-S)} = 0.68$), silaneselones ($R_2Si{=}Se$; $\Delta\chi_{(Si-Se)} = 0.65$) and silanetellones ($R_2Si{=}Te$; $\Delta\chi_{(Si-Te)} = 0.20$) have been described.[16,30,51-67]

As a consequence of the particular electronic nature of silanones, isolation of these extremely reactive organosilicon compounds is a rather challenging task.[16,27,30,225] It is generally necessary to reduce their intrinsically high reactivity in order to prevent decomposition reactions, such as intramolecular isomerization or oligo-/polymerization. For this purpose, tailor-made ligand frameworks have to be designed, which ensure sufficient kinetic and/or thermodynamic stabilization. Hence, analogous methods can be used as for the isolation of divalent silylenes (*vide supra*; Figure 4). Intramolecular stabilization of silanones can be achieved by reducing the strong polarization *via* electron-donating substituents, such as amines, imines or silyl groups (Figure 8). Another frequently applied method is the additional coordination of Lewis bases and Lewis acids, resulting in the formation of donor-stabilized or donor-acceptor-stabilized silanones. However, these tetra-coordinate organosilicon species exhibit a significantly decreased reactivity, similar to hyper-coordinate silylenes. The usually observed oligomerization reactions of silanones can be suppressed by the use of sterically encumbered substituents (kinetic stabilization).

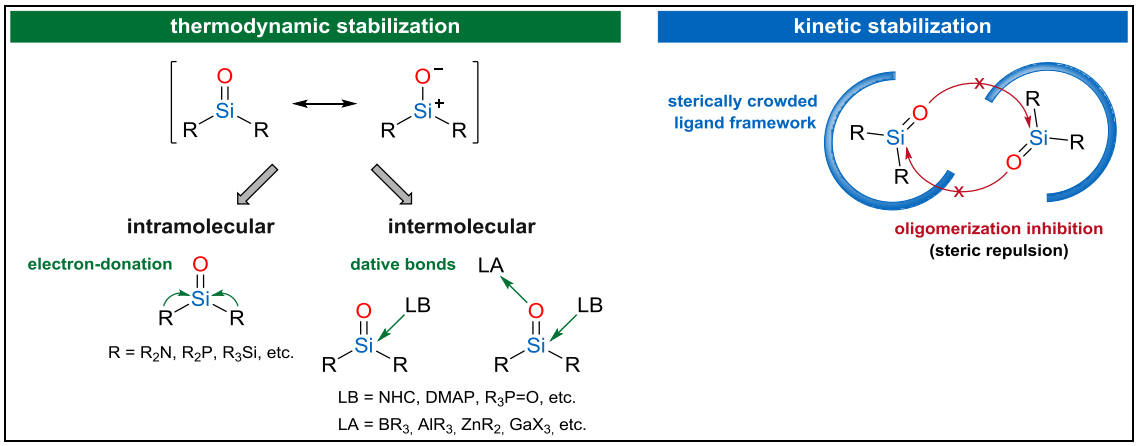


Figure 8. Thermodynamic and kinetic stabilization of silanones.

Over the last decades a series of isolable silanone derivatives have been isolated by a careful design of suitable substituents. A frequently used synthetic approach is the oxygenation of silylenes. The most important achievements in silanone chemistry are briefly discussed in the following.

2.2.1 Historic Milestones

Due to their characteristic properties and reactivity described above, silanones have for a long time only been the subject of gas phase, DFT and argon matrix isolation studies.[16,27,30,225] Early reports comprise the experimental detection and theoretical investigation of such *in-situ* generated fleeting intermediates *via* infrared (IR) spectroscopy.[236-246] Further evidence for the formation of these elusive transient organosilicon species in solution was obtained from the 1980s onwards with the characterization of dimerization or trapping products.[247-250] Nevertheless, it took until 2007 when *Driess et al.* achieved a major breakthrough in silanone chemistry with their seminal work on isolating the first ambient temperature stable silanone species. The unique donor-acceptor stabilized silaformamide (HC[(CMe)$_2$(NDipp)$_2$])(H)Si=O→BCF (**L24**) was accessible by treating the six-membered NHSi **L8** (*vide supra*; Figure 5) with an equimolar amount of the water-borane adduct H$_2$O·BCF (Figure 9).[251] Interestingly, controlled addition of water vapor led to the formation of a novel intramolecular donor-stabilized siloxysilylene. Subsequent oxygenation with N_2O or CO_2 selectively provided the four-coordinate silanoic ester derivative **L25** *via* concomitant liberation of gaseous N_2 or CO.[252] Due to its efficient stabilization, **L25** is stable both at high temperatures and in dry-air.

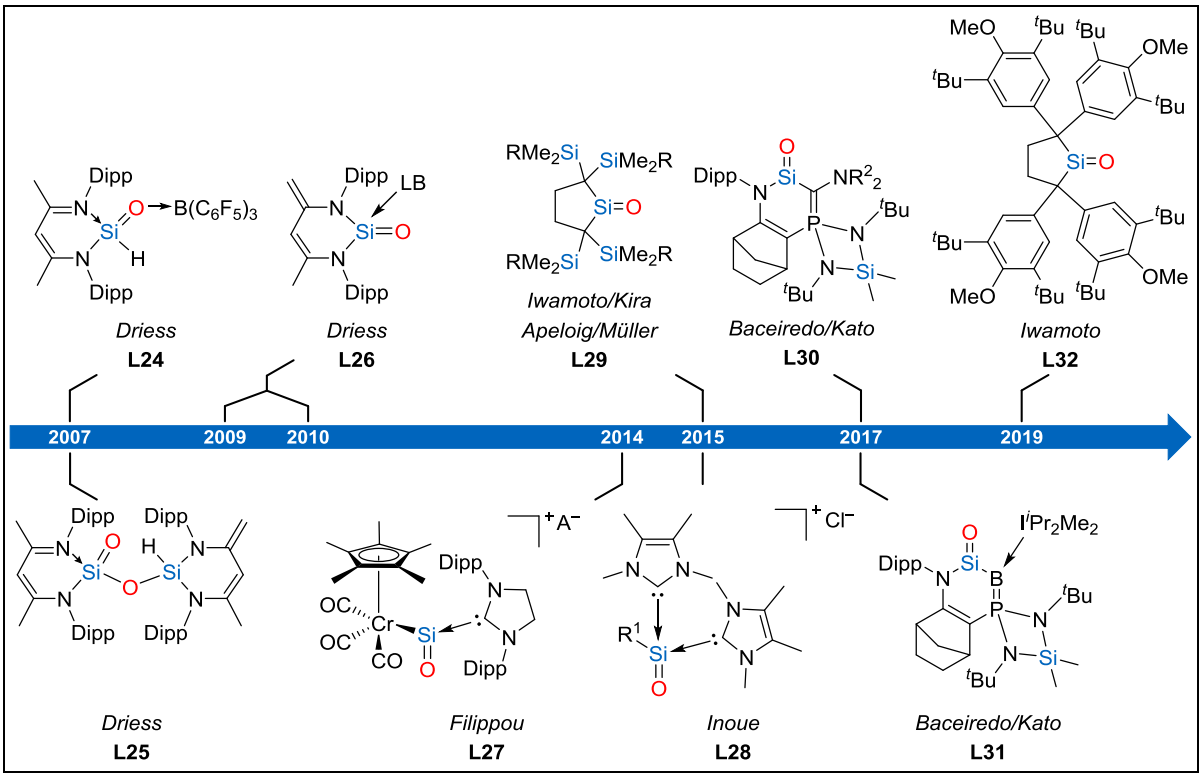


Figure 9. Timeline of historical milestones in the chemistry of three- and four-coordinate silanone species. LB = IMe$_4$, DMAP, I^{i}Pr$_2$Me$_2$O (1,3-diisopropyl-4,5-dimethylimidazolin-2-one); A = B(3,5-(CF$_3$)$_2$-C$_6$H$_3$)$_4$; R = ^{i}Pr, Me; R^1 = 2,6-Mes$_2$-C$_6$H$_3$, 2,4,6-^{i}Pr$_3$-C$_6$H$_2$; R^2 = ^{i}Pr, cHex (cyclohexyl).

The great versatility of the zwitterionic, ylide-like diaminosilylene **L8** was further employed by *Driess* and co-workers to gain access to the Lewis base-stabilized silanones **L26** (sila-urea species). Accordingly, exposure of the silylene NHC adduct HC[(C=CH_2)(CMe)(NDipp)$_2$]Si(IMe_4) to N_2O solely afforded the corresponding IMe_4-stabilized silanone.[253] The analogue DMAP-supported derivative was synthesized slightly later.[254-255] Remarkably, reaction of NHC-stabilized **L8** with molecular oxygen (O_2) resulted in the formation of unprecedented donor-stabilized dioxasiliranes.[256] Internal oxygen transfer of the $I^iPr_2Me_2$ adduct HC[(C=CH_2)(CMe)(NDipp)$_2$]SiO_2($I^iPr_2Me_2$) strikingly furnished the first and so far only example of a cyclourea-stabilized silanone representative HC[(C=CH_2)(CMe)(NDipp)$_2$]Si=O($I^iPr_2Me_2O$).

The stunning isolation of the NHC-stabilized cationic chromiosilanone **L27** bearing a three-coordinate silicon nucleus was presented by Filippou and colleagues in 2014.[225,257] Nevertheless, this room temperature stable, trigonal planar silanone complex can be regarded as NHC adduct of silicon monoxide that is stabilized *via* the coordination sphere of the organometallic chromium framework. Related cationic silanones, more precisely the NHC-stabilized sila-acylium ions **L28** were synthesized by our group.[258] Oxygenation of the corresponding NHC silyliumylidene ion adducts with CO_2 provided these tetra-coordinate, aryl-substituted complexes, which are the first isolable derivatives of heavier acylium ion congeners.[259]

Iwamoto, Kira et al. investigated the synthesis of cyclic extra-coordination free dialkylsilanone **L29** (R = Me) *via* oxidation of their unique carbocyclic silylene **L6** (*vide supra*; Figure 5) with TEMPO ((2,2,6,6,-tetramethylpiperidin-1-yl)oxyl).[260-261] However, due to insufficient kinetic and thermodynamic stabilization of the generated reactive silanone, only dimerization affording the corresponding 1,3-dioxadisiletane was observed. This transient silanone was later analyzed and characterized by IR spectroscopy in the course of a detailed argon matrix isolation and DFT study by *Apeloig, Müller* and co-workers.[262] Dehydrobromination of a sterically more demanding dibromosilanol with $KSiTMS_3$ led to the formation of the three-coordinate carbocyclic silanone **L29** (R = ^{i}Pr), which is persistent in solution at –80 °C.[263] Nevertheless, an irreversible silanone-silene isomerization affording the corresponding siloxysilene (silyl silenol ether) *via* facile 1,3-silyl migration was discovered at higher temperatures.

During the course of this work some further striking results in silanone chemistry were achieved. *Baceiredo, Kato* and colleagues isolated the first cyclic three-coordinate silanones **L30** which are stable at room-temperature in the solid-state in 2017.[264] Despite efficient stabilization of the Si=O moiety by the adjacent electron-donating substituents, these donor-free amino(phosphonium ylide)silanones

dimerize in solution with half-life times of 0.5 h (R = ^{i}Pr) and 5 h (R = cHex). Fine tuning of the ligand framework *via* implementation of an NHC-stabilized phosphonium-bora-ylide substituent provided silanone **L31** with a significantly prolonged lifetime in solution.[265] Thus full conversion of the dimerization reaction of amino(phosphonium-bora-ylide)silanone **L31** was observed only after 8 days at ambient temperature.

Just recently, a sterically crowded, carbon-based modification of **L29** finally enabled the unprecedented isolation of the first room temperature stable, three-coordinate dialkylsilanone **L32** bearing an unperturbed Si=O double bond.[266] *Iwamoto et al.* synthesized this special carbocyclic silanone by oxygenation of the corresponding silylene with N_2O in quantitative yield. Remarkably, **L32** is indefinitely stable at ambient temperature in both solid-state and solution, but still dimerizes in a head-to-tail process at elevated temperatures. This unique result can presumably be interpreted as the final fulfillment of *Kipping's* dream.

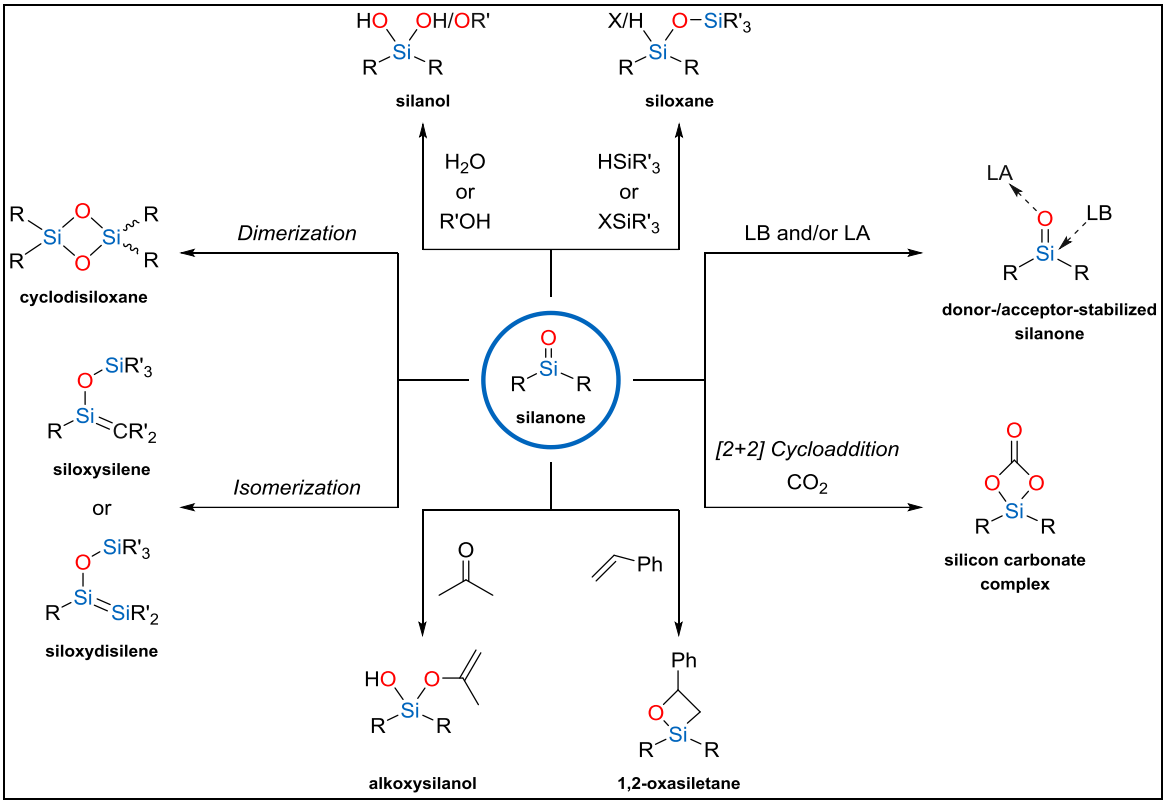
Apart from the silanones described in more detail above, extensive investigations over the last decade have revealed various other derivatives with differently applied stabilization methods and exceptional substitution patterns.[16,27,30,225] In analogy to silylenes, however, most of the reported stable species are embedded in cyclic frameworks and contributions comprising acyclic counterparts are seldom observed. One of these rare examples was described by *Driess* and co-workers with the isolation of NHC-stabilized acyclic aryl(phosphino)silanone (Tipp$_2$-C$_6$H$_3$)(Ph$_2$P)Si=O(IMe$_4$).[267] Nonetheless, there are still no reports in the literature about isolable acyclic, three-coordinate silanones. These low-coordinate organosilicon compounds could be more reactive and enable intriguing transformations, just like acyclic donor-free silylenes compared to their cyclic congeners.

2.2.2 General Reactivity

The overall reactivity of silanones $R_2Si=O$ has been scarcely explored due to the long absence of isolable representatives and is often limited to trapping reactions of *in situ* generated extremely reactive derivatives.[16,27,30,225] As indicated above, most stable species require additional intra- or intermolecular stabilization and are consequently significantly less reactive than their rare donor-free congeners. In the following, a short presentation of the most important silanone reactions revealed so far is given.

Like many other low-coordinate organosilicon compounds, silanones are highly sensitive to water. Therefore, hydrolysis leads to the formation of silanediols $R_2Si(OH)_2$ (Scheme 9). Similarly, alcoholysis of silanones with alcohols or phenols (R'OH) provides alkoxy- or aryloxysilanols $R_2Si(OH)(OR')$, respectively. Furthermore, silanones have been shown to react with a series of silanes

or halosilanes furnishing siloxanes (1,2-adducts). This reactivity, together with hydrolysis, represents a suitable method for verifying the formation of fleeting silanone intermediates.



Scheme 9. Overview of the most common reactions of silanones including some intriguing examples.

Since silanones are susceptible to the barrierless, rapid head-to tail oligomerization, which generally yields oligo(siloxane)s, dimerization to *cis*- or *trans*-cyclodisiloxanes is a frequently observed decomposition pathway. If accessible silyl groups are present in the ligand framework that tend to undergo silyl migration reactions (such as TMS), the isomerization of silanones is a commonly competing process for the oligomerization. In this manner interesting low-coordinate organosilicon species like siloxysilenes or siloxydisilenes are available. One of the most effective methods to achieve the isolation of otherwise elusive silanones is the additional coordination of strong Lewis acids (*e.g.* BR_3, AlR_3, ZnR_2 and GaX_3) and/or Lewis bases (*e.g.* NHCs, DMAP and $R_3P{=}O$) (*vide supra*; Figure 8). Interestingly, it is not only possible to utilize acceptor-/donor-stabilized silanone precursors, but also to add these reagents after silanone formation, in order to obtain hyper-coordinate silanone derivatives.

Another prototypical reactivity of silanones are [2+2] cycloaddition reactions with suitable reagents. Hence, conversion of silanones with the greenhouse gas CO_2 leads to the formation of silicon carbonate complexes. The same products are partially obtained when silylenes are exposed to excessive amounts of CO_2 (*via* generation of transient silanones under concomitant liberation of CO), which

frequently renders CO_2 an unsuitable oxygenation agent for accessing silanones from silylenes. Additionally, the capability of silanones to react with alkenes was recently demonstrated by *Iwamoto et al.* for the first time. Reaction of carbocyclic silanone **L32** with styrene provided the corresponding formal [2+2] cycloaddition product (1,2-oxasiletane). This observation is remarkably considering that the lighter carbonyl analogues usually react with alkenes *via* photochemical reactions (*Paternò–Büchi* reaction), but also quite expected since silanones are much more reactive than their congeners.[268-269] The high reactivity is also reflected in the activation of carbonyl compounds (ene-type reaction), such as acetone, under formation of corresponding alkoxysilanes.

All in all, investigations into the reactivity of silanones are still in their infancy. However, with increasing reports on isolable silanones over the last years, including the first three-coordinate derivatives, further contributions about specific and surprising reactions are expected in the future. Of particular interest is the discovery of differences and/or similarities with regard to the chemistry of the lighter carbonyl congeners. Potential applications of silanones in catalysis may also be conceivable.

2.3 Catalytic Applications

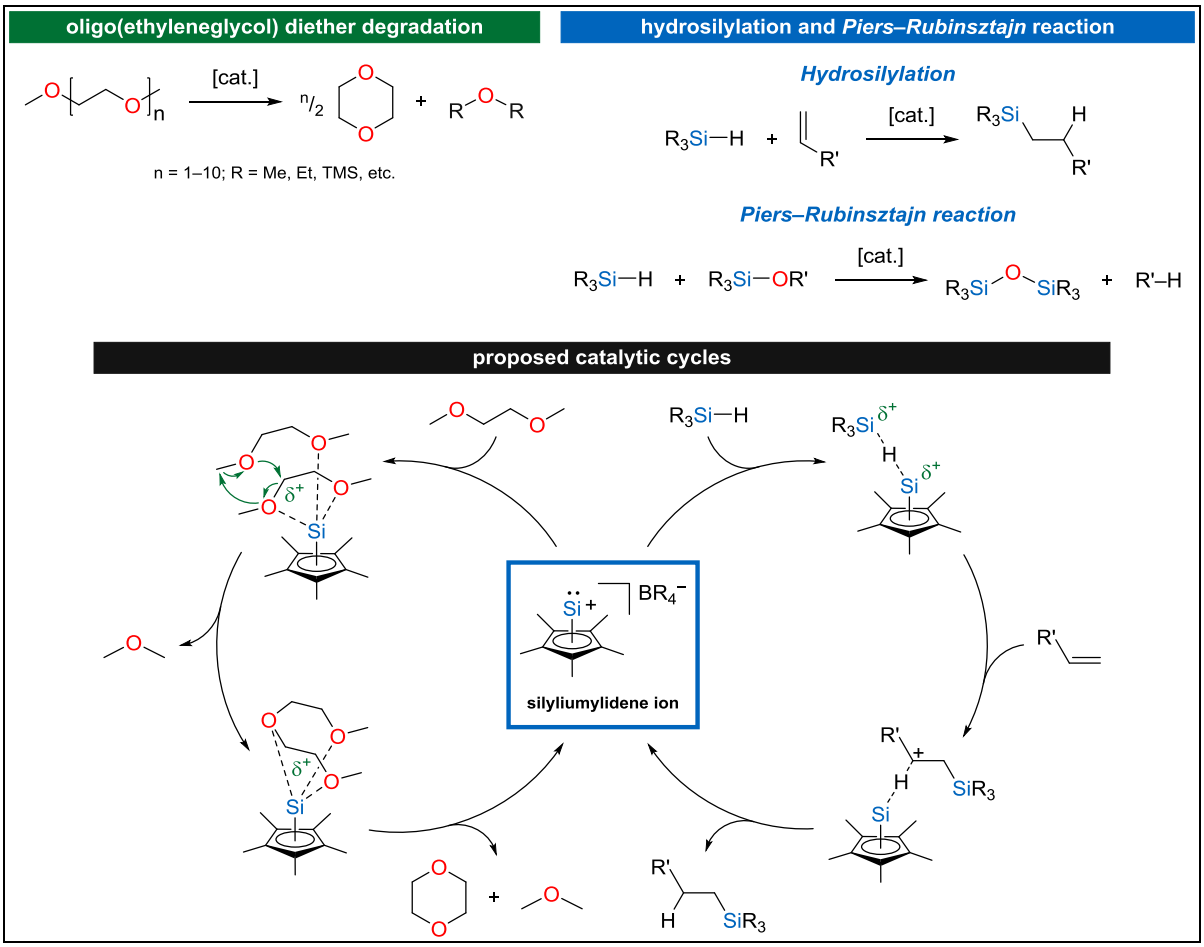
As mentioned in the introduction, the semi-metal silicon is an exceedingly attractive element for replacing the omnipresent, ecologically and economically rather unfavorable transition metals in catalysis, due to its outstanding properties (almost unlimited quantities and non-toxicity). Especially low-coordinate organosilicon compounds have been considered in recent years for applications in metal-free catalysis, owing to their exceptionally high reactivity and versatility. To date, however, only a few examples of catalytic conversions with these derivatives are known.[16]

One of the most advanced representatives is the class of silylium ions (R_3Si^+). Due to their extraordinary high electrophilicity, fluorophilicity and oxophilicity a series of catalytic transformations using these reactive organosilicon compounds has been reported.[270-272] Hence, these low-coordinate species have been successfully applied particularly in challenging *Diels-Alder* reactions, C–H alkylation, C–H arylation and *Friedel-Crafts* C–H silylation protocols.

An emerging group of low-valent organosilicon species are the extremely reactive silyliumylidene ions ($RSi:^+$).[16,30,162,273-274] Silyliumylidene ions can be regarded as a formal combination of silylium ions and silylenes and exhibit a unique electronic structure (two empty 3p-orbitals together with a lone pair of electrons). Accordingly, they are very reactive species and have already been successfully utilized in a few catalytic conversions. *Jutzi et al.* applied their seminal η^5-coordinated (π-bonded) silyliumylidene ion $[Cp^*Si:^+][B(C_6F_5)_4^-]$ for the selective degradation of oligo(ethyleneglycol)

diethers.[162-163,275] Thus, for example a high conversion of 1,2-dimethoxyethane (DME) into dimethyl ether and 1,4-dioxane was observed in the presence of catalytic amounts (~0.5 mol%) of $[Cp^*Si:^+][B(C_6F_5)_4^-]$ (Scheme 10). A prerequisite for the observed catalytic activity are the free coordination sites on the low-valent silicon nucleus, which are accessible *via* the open coordination sphere of the Cp* ligand.

Very recently, the *WACKER Chemie AG* reported on the utilization of *Jutzi's* silyliumylidene ion $[Cp^*Si:^+][B(C_6F_5)_4^-]$ and its derivatives (modified anions BR_4^-) in industrially important catalytic processes.[276] Thus, a highly efficient Si(II) catalysis was found for the hydrosilylation of various alkenes with selected silanes. Remarkably, the investigated silyliumylidene ions are even able to compete with current benchmark catalysts based on the precious transition metal platinum. The versatility of these unique hyper-coordinate silyliumylidene ions was further demonstrated by the conversion of silanes with alkoxysilanes under formation of siloxanes *via* the so-called *Piers–Rubinsztajn* reaction. Hence, these results could pave the way for an alternative and more sustainable, metal-free catalysis in this field.



Scheme 10. Application of the silyliumylidene ions $[Cp^*Si:^+][BR_4^-]$ in catalytic oligo(ethyleneglycol) diether degradation, hydrosilylation and *Piers–Rubinsztajn* reactions, including postulated catalytic cycles.

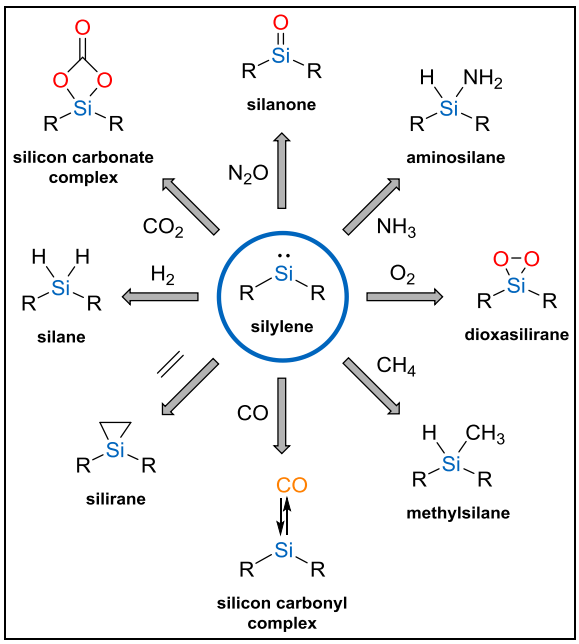
During the course of this work, catalytic hydroboration reactions were described by *So* and colleagues with their previously reported NHC-stabilized parent silyliumylidene ion.[277] In addition to a number of suitable substrates, such as aliphatic and aromatic carbonyl compounds and pyridine derivatives, even the catalytic reduction of CO_2 was demonstrated.[278]

Considering the potential of low-coordinate organosilicon compounds with respect to the activation of small molecules and the fascinating catalytic conversions already found, further research in this direction seems a very promising task, which may reveal the first applications of silylenes and silanones.

3. Scope of this Work

Modern main group chemistry has developed into a promising branch that is even capable of competing with the versatile d-block chemistry of transition metals. As pointed out in the introduction, a remarkable transition metal-like reactivity and even first catalytic cycles involving compounds based on main group elements were found. Despite extensive research and its extraordinary abilities, applications of organosilicon compounds are still severely limited. Low-coordinate derivatives and in particular acyclic, two-coordinate silylenes represent the most suitable candidates for fulfilling the demanding requirements on the way to a versatile silicon-based catalysis. Prior to his work, however, only very few isolable representatives of silylenes of this type were known in the literature.[169-170,174-176] In addition, reactivity studies concerning these highly reactive organosilicon species were not yet very advanced.[169,174,176,185-186]

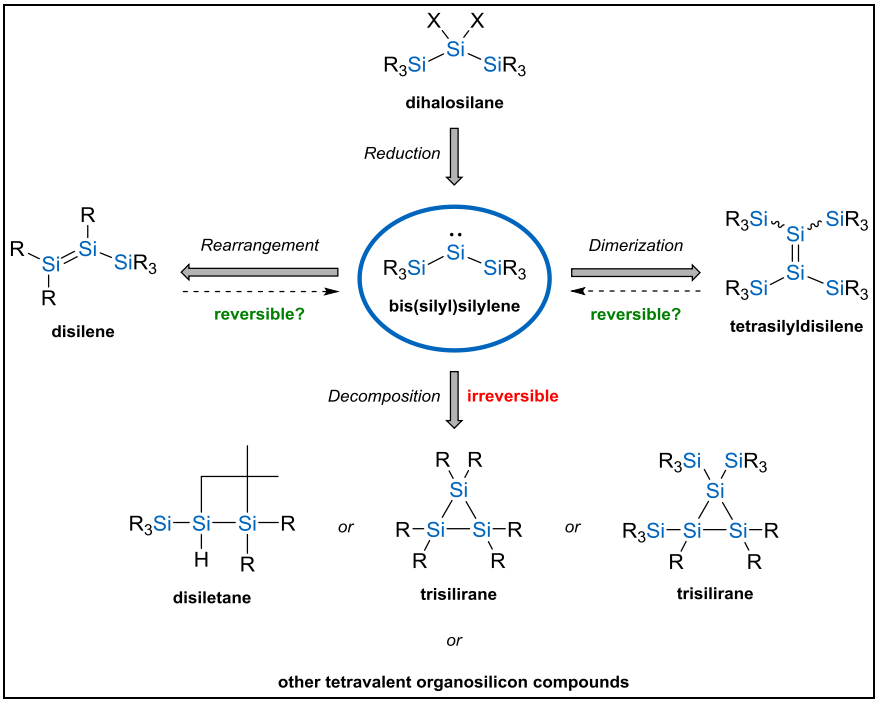
Accordingly, one focus of this PhD thesis is the synthesis and isolation of novel acyclic, donor-free silylenes to gain a deeper understanding of this unprecedented class of compounds. Subsequent to the potentially successful access, the synthesized divalent organosilicon compounds will be subjected to detailed reactivity studies in order to further reveal their true potential and suitability for applications in metal-free catalysis. Thus, the priority lies in the activation of industrially relevant and enthalpically strong small molecules, such as alkenes, carbon monoxide, dihydrogen, dinitrogen and methane, leading to the formation of unique organosilicon compounds (Scheme 11).



Scheme 11. Reported and plausible organosilicon compounds accessible *via* small molecule activation by divalent silylenes.

In general, an oxidative addition of the substrates to the silylene centers is frequently observed for the formation of tetra-coordinate organosilicon species *via* small molecule activation. Nevertheless, reductive elimination, a key step in catalytic cycles, resulting in the regeneration of the two-coordinate silylene is a major challenge, due to the extraordinary stability of tetravalent silicon compounds.[17] Therefore, investigations in this direction will also be carried out to detect a possible reversibility of the bond activations.

As mentioned above, acyclic, two-coordinate bis(silyl)silylenes are of particular interest, since they are considered as extremely reactive derivatives, due to their small HOMO-LUMO gaps and potential triplet ground state, but have never been isolated so far. In order to bypass the usually observed rapid decomposition pathways and to achieve the first isolation/synthetic accessibility, a clever ligand framework has to be chosen (Scheme 12).[85,211] A conceivable approach to access a unique bis(silyl) silylene might also be the potential reversibility of the isomerization reactions affording three-coordinate disilenes.



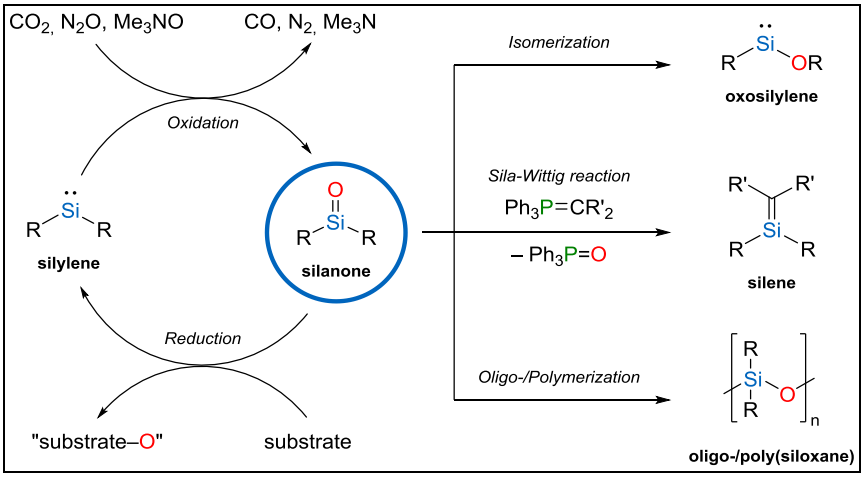
Scheme 12. Targeted approach to acyclic, donor-free bis(silyl)silylenes *via* reductive dehalogenation of corresponding dihalosilanes and commonly observed isomerization pathways.

Bis(silyl)silylenes could turn out to be key reagents for the activation of extremely challenging small molecules such as CO, CH_4 and N_2, which has not been possible with isolable low-coordinate silylenes prior to this work, even though a reactivity was indicated by DFT calculations and argon matrix isolation studies.[190-196] The easily tunable electropositive silyl groups adjacent to the silylene moiety could therefore provide sufficient electronic and kinetic stabilization for the resulting elusive products.

A very promising reaction is the carbonylation of bis(silyl)silylenes, which could ultimately lead to the isolation of unprecedented silicon carbonyl complexes (Scheme 11), since a reversible reaction of an acyclic aminosilylsilylene with CO has already been observed in our laboratories, but the structure of the product could not be identified so far (unpublished results).

Another ambitious major goal of this work is the isolation of the first ambient temperature stable, neutral, acyclic, three-coordinate silanone. In contrast to the ubiquitous lighter homologous carbonyl compounds, the synthesis and isolation of a donor-free silanone has still not been successful, despite more than 100 years of silicon chemistry. Particularly because of their high reactivity (favorable decomposition), silanones are still one of the most sought-after molecules for main group chemists, which are almost entirely unexplored but could provide a high potential for new applications.

A predestinated approach to gain access to these elusive species seems to be the oxygenation of the obtained novel acyclic silylenes with various oxidizing agents, such as CO_2, N_2O and Me_3NO (Scheme 13). Isolation should be feasible with a suitable ligand framework that ensures adequate stabilization. Following the successful synthesis, a detailed reactivity study of the unique silanones will be performed. The focus lies on typical reactions for carbonyl compounds, for instance an unprecedented approach to silenes *via* the *Wittig* reaction would be conceivable. Moreover, not only a selective polymerization, leading to the formation of novel poly(siloxanes), but also catalytic applications, through oxygen transfer and silylene regeneration, could be realized.



Scheme 13. Targeted synthetic approach for unprecedented acyclic, two-coordinate silanones, *via* oxygenation of divalent silylenes, with plausible isomerization pathways and planned reactivities including a potential catalytic cycle.

Overall, this work is intended to acquire a deeper understanding of the chemistry of low-coordinate organosilicon compounds. On the one hand, fundamental differences and/or similarities between silicon and its lighter congener carbon should be revealed, which could eventually facilitate the synthesis of novel compounds and applications in organo(metallic)catalysis. On the other hand, the potential of low-valent silicon compounds as possible substitutes for versatile transition metal complexes will be further investigated. The knowledge acquired in this project could open up new avenues, which ideally enable the development of novel catalytic processes with low-coordinate organosilicon compounds.

4. Disilene–Silylene Interconversion: A Synthetically Accessible Acyclic Bis(silyl)silylene

Title: "Disilene–Silylene Interconversion: A Synthetically Accessible Acyclic Bis(silyl)silylene"[279]

Status: Article; published online: July 28, 2019.

Journal: *Journal of the American Chemical Society* **2019**, *141* (34), 13536–13546.

Publisher: American Chemical Society (ACS)

DOI: 10.1021/jacs.9b05318

Authors: Dominik Reiter, Richard Holzner, Amelie Porzelt, Philipp J. Altmann, Philipp Frisch, and Shigeyoshi Inoue[a]

Reprinted with permission of the American Chemical Society. © 2019 American Chemical Society.

Content: Two-coordinate silylenes and especially acyclic derivatives have emerged as promising targets for possible applications in silicon-based catalysis, due to their transition metal-like behavior. Acyclic, sterically crowded bis(silyl)silylenes with their proposed small HOMO-LUMO gaps and potential triplet ground state are considered as very reactive representatives. However, no isolable silylene of this type has been reported so far.

This article outlines the unprecedented isolation of an equilibrium mixture consisting of the first acyclic bis(silyl)silylene ((TMS)$_3$Si)(^{t}Bu$_3$Si)Si: and its corresponding isomeric tetrasilyldisilene (TMS)(^{t}Bu$_3$Si)Si=Si(TMS)$_2$. Interestingly, the well-known propensity of the hypersilyl substituent ((TMS)$_3$Si) to silyl migrations was exploited to enable the successful isolation. Thorough DFT calculations provided a closer insight into the disilene-silylene interconversion *via* 1,2-silyl shifts and the nature of the equilibrium. The computational results for the novel silylene indicated a triplet ground state, but even with experimental studies using EPR/NMR spectroscopy and investigations on the Skell rule (stereospecificity of the [2+1] cycloaddition with stereogenic alkenes) no clear conclusions about the ground state multiplicity could be drawn so far.

Preliminary investigations displayed both extreme silylene and disilene reactivity in the facile oxidative addition of industrially relevant small molecules, such as ethylene, dihydrogen and ammonia, even under very mild conditions. Strikingly, a rapid activation of the enthalpically strong molecule H_2 was even possible at –40 °C. Thus, the enormous potential of acyclic silylenes mimicking transition metal complexes was successfully demonstrated. In the course of our studies, we further isolated different Lewis base-stabilized bis(silyl)silylenes and thereby gained a more profound insight into the disilene-silylene rearrangement. Remarkably, oxygenation of such a derivative with N_2O afforded the first acyclic example of an NHC-stabilized silanoic ester, a heavier carboxylate ester analogue, thus paving the way for further research.

[a]D. Reiter and R. Holzner planned and executed all experiments and co-wrote the manuscript. A Porzelt designed and performed the theoretical analyses and contributed to writing the article. P. J. Altmann and P. Frisch carried out the SC-XRD measurements and processed the corresponding data. All work was performed under the supervision of S. Inoue.

JACS
JOURNAL OF THE AMERICAN CHEMICAL SOCIETY
Cite This: J. Am. Chem. Soc. 2019, 141, 13536−13546
Article
pubs.acs.org/JACS

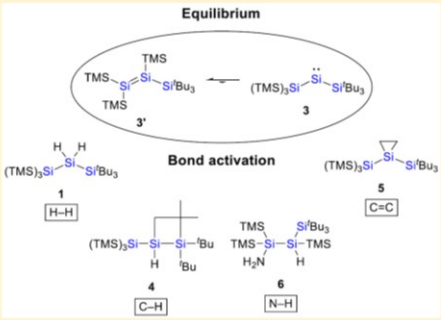
Disilene−Silylene Interconversion: A Synthetically Accessible Acyclic Bis(silyl)silylene

Dominik Reiter,[†] Richard Holzner,[†] Amelie Porzelt,[†] Philipp J. Altmann, Philipp Frisch, and Shigeyoshi Inoue*

Department of Chemistry, WACKER-Institute of Silicon Chemistry and Catalysis Research Center, Technische Universität München, Lichtenbergstraße 4, 85748 Garching bei München, Germany

Supporting Information

ABSTRACT: Silylenes have recently shown fascinating reactivity patterns, which are normally observed almost exclusively for transition-metal complexes. In particular, very reactive representatives are considered to be promising candidates, which may become powerful and economical alternatives for catalytic applications in the future. Here, we present the isolation of an equilibrium mixture consisting of a tetrasilyldisilene and its isomeric bis(silyl)silylene, the first isolable silylene of this type. Preliminary investigations demonstrate the extreme inherent reactivity via facile small-molecule activation even under very mild conditions. Thus, the oxidative addition of challenging targets such as H_2 and NH_3 was achieved. In addition, by synthesizing donor-stabilized bis(silyl)silylenes we gained further insights into the disilene−silylene rearrangement by 1,2-silyl migrations. Thorough theoretical calculations support the observed experimental results.



INTRODUCTION

Low-valent silicon compounds have attracted considerable attention and nowadays make an important contribution to modern main group chemistry.[1] In particular, two-coordinate silylenes (RR′Si:), the silicon analogues of carbenes (RR′C:), play an important role because of their ambiphilic nature, which is reflected in a wide variety of reactivity patterns. Silylenes have a free $3p_z$ orbital and a lone pair of electrons and, in contrast to carbenes, are almost exclusively in the singlet ground state.[2] To ensure the isolation of silylenes, sufficient kinetic and/or thermodynamic stabilization by adjacent, tailormade substituents is essential. Therefore, a vast majority of stable silylenes are embedded in cyclic frameworks, including the well-established group of *N*-heterocyclic silylenes (NHSis), the silicon version of *N*-heterocyclic carbenes (NHCs).[3]

In contrast to their diverse counterparts, there are only scarce examples of stable acyclic silylenes reported.[4] Their true potential is revealed by silylenes bearing nucleophilic boryl and/or electropositive silyl substituents, leading to wide RSiR′ angles and small HOMO−LUMO gaps. Thus, these highly reactive compounds are to a certain extent capable of mimicking transition-metal complexes in the activation of small molecules. Remarkably, acyclic silylenes can even undergo the oxidative addition of enthalpically strong molecules such as H_2.[4a,d,g] Very recently, the reductive coupling of CO by an isolable aminoborylsilylene was also reported.[5] Bis(silyl)silylenes with sterically demanding substituents are considered to be even more reactive species because of their wider RSiR′ angles, smaller HOMO−LUMO gaps, and potential triplet ground state.[2a−d,6] Lately, the intrinsic nature of triplet ground state silylenes was experimentally proven by in situ generated silylenes analyzed by low-temperature glass matrix EPR studies;[7] however, typical triplet silylene reactivity is still unexplored.[2f] Nevertheless, no isolable two-coordinate acyclic bis(silyl)silylene has been reported so far. In situ generated, extremely reactive $(R_3Si)_2Si$: species are verifiable only as stable tetravalent silicon compounds, formed as products of subsequent intra- and intermolecular reactions. The general decomposition pathways include dimerization to disilenes (heavier alkene congeners), 1,2-silyl migration, and/or intramolecular C−H/Si−Si bond activation affording disilenes or cyclic silanes (Scheme 1).

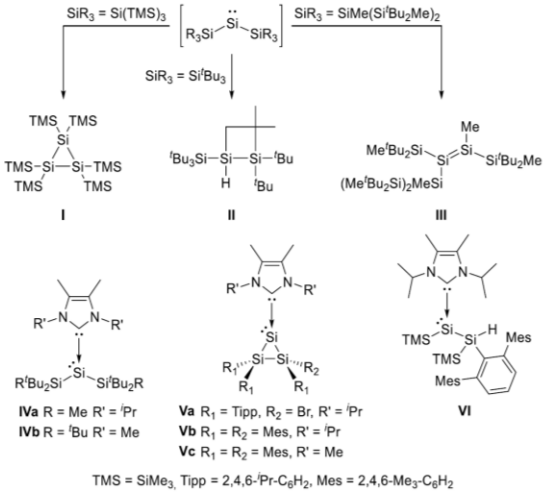
Klinkhammer, for example, observed the formation of hexakis(trimethylsilyl)cyclotrisilane **I** as the formal decomposition product of bis(hypersilyl)silylene $(((TMS)_3Si)_2Si$:) by treating $HSiCl_3$ with alkali metal hypersilanides (silyl anions).[8] The experimentally evidenced triplet ground state bis(supersilyl)silylene $((^tBu_3Si)_2Si$:) undergoes an intramolecular C−H activation reaction (occurring from the singlet state[2f]) even at very low temperatures, providing disiletane **II**.[7a] Sekiguchi et al. pursued the isolation of the sterically crowded bis(silyl)silylene $((^tBu_2MeSi)_2MeSi)_2Si$:, but irreversible formation of disilene **III** occurred via a 1,2-silyl migration.[9] To

Received: May 17, 2019
Published: July 28, 2019

ACS Publications © 2019 American Chemical Society

DOI: 10.1021/jacs.9b05318
J. Am. Chem. Soc. 2019, 141, 13536−13546

Scheme 1. Isomerization Reactions of Transient Bis(silyl)silylenes I–III and Reported Examples of Bis(silyl)silylene NHC Adducts IV–VI



date, isolable bis(silyl)silylenes are accessible only with the aid of additional σ-donor molecules such as NHCs.[10] The first examples of acyclic bis(silyl)silylene NHC adducts **IV** were obtained by reductive debromination of the corresponding dibromosilanes with KC_8 in the presence of NHCs.[11] Scheschkewitz et al. and the Lips group reported cyclic derivatives **V** with a Si_3 scaffold via the reaction of NHC·$SiBr_4$ with a disilenyllithium reagent and the coreduction of NHC·$SiCl_4$ and Mes_2SiCl_2 (Mes = 2,4,6-Me_3-C_6H_2), respectively.[12] Very recently, Cowley and colleagues experimentally demonstrated the disilene–silylsilylene equilibrium[13] for the first time by synthesizing and isolating NHC-stabilized bis(silyl)silylene **VI** from the corresponding donor-supported disilene.[14] Thus, the quest for isolable, acyclic two-coordinate bis(silyl)silylenes is ongoing.

Sterically demanding silyl groups are ideal candidates for the stabilization of otherwise elusive species because they are strong σ-donors and provide kinetic stabilization; however, they sometimes tend to migrate.[1] On the basis of the previous results achieved with the hypersilyl- and supersilyl groups, we envisioned a combination of both substituents as a promising approach to gaining access to unprecedented low-coordinate silicon compounds through controlled 1,2-silyl shifts. Herein, we present the isolation of a novel tetrasilyldisilene displaying bis(silyl)silylene reactivity.

RESULTS AND DISCUSSION

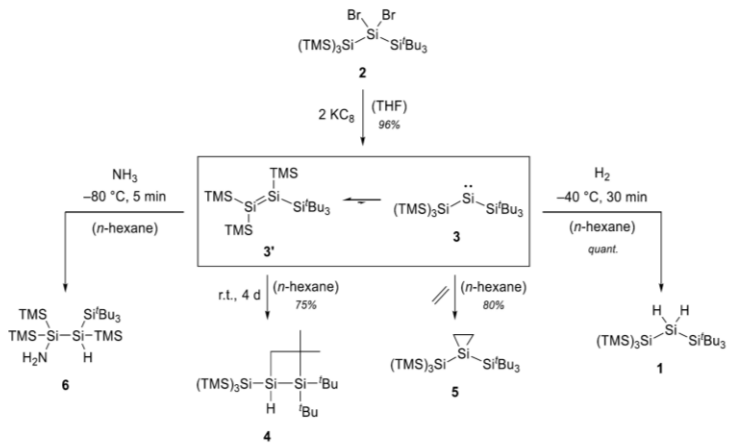
Bis(silyl)silylene–Tetrasilyldisilene Interconversion. The entry into this chemistry provided the isolation of the silane ((TMS)$_3$Si)(^{t}Bu$_3$Si)SiH$_2$ (**1**).[15] Bromination of **1** in *n*-pentane furnished the corresponding dibromosilane **2**, which was isolated as colorless crystals in high yield and fully characterized (Scheme 2).

Subsequent reductive debromination of **2** with 2 equiv of KC_8 at low temperatures resulted in a color change from colorless to blood red with the concomitant formation of black graphite. Multinuclear and 2D NMR analyses of the isolated product suggested the formation of tetrasilyldisilene **3′**, the isomer of (hypersilyl)(supersilyl)silylene **3**. The three-coordinate silicon nuclei of **3′** resonate at δ = 161.9 ppm (SiTMS$_2$) and δ = 132.4 ppm (Si(TMS)Si^{t}Bu$_3$) in the ^{29}Si NMR spectrum, which is in line with the signals for disilene **III** (δ = 158.9 and 103.8 ppm).[9] However, all attempts to crystallize the reaction product have been unsuccessful so far. Calculations performed at the M06-2X/6-31+g(d,p) level of density functional theory revealed a bent and twisted structure for tetrasilyldisilene **3′** (Figure 2)[16] comparable to that for disilene **III**.[9] The calculated ^{29}Si NMR resonances at δ = 162.5 and 140.5 ppm (gauge-independent atomic orbital (GIAO)/M06-L/6-311++(2d,2p); solvent model based on density (SMD): benzene)) are in good agreement with the experimental values. (For details see the Supporting Information[16]).

Variable-temperature (VT) UV–vis spectroscopy revealed only two characteristic absorption bands at λ_{max} = 352 and 469 nm. The calculated transitions, by means of time-dependent density functional theory (TD-DFT), at 335 and 467 nm are assigned to the HOMO−1 → LUMO and HOMO → LUMO transitions of disilene **3′**, respectively.

Keeping a product solution at room temperature results in a rather slow decomposition and the selective formation of disiletane **4**. Nevertheless, full conversion was not observed

Scheme 2. Synthesis and Reactivity of Bis(silyl)silylene 3 and Its More Stable Isomer Tetrasilyldisilene 3′



DOI: 10.1021/jacs.9b05318
J. Am. Chem. Soc. 2019, 141, 13536–13546

until after 4 days. Monitoring the decomposition reaction by NMR spectroscopy revealed no signals other than those assigned to **3′** and **4**. In addition, no signs of decomposition were observed when a product solution was stored at −35 °C in a glovebox for at least 1 year. Disiletane **4** was fully characterized, and its molecular structure was unambiguously confirmed by single-crystal X-ray diffraction (SC-XRD) (Figure 1). As already shown in the case of **II**,[7a] the formation

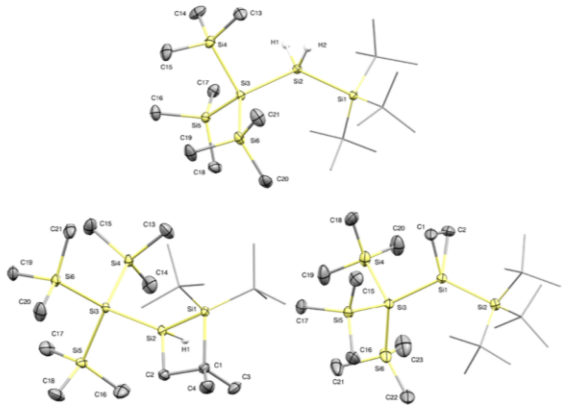


Figure 1. Molecular structures of **1** (top), **4** (bottom left), and **5** (bottom right). Ellipsoids are set at 50% probability. Hydrogen atoms are omitted for clarity, except for the respective Si−H nuclei of silane **1** and disiletane **4**. Selected bond lengths (Å) and angles (°): **1**: Si1−Si2 2.369(1), Si2−Si3 2.350(1); Si1−Si2−Si3 132.1(1). **4**: Si1−Si2 2.345(1), Si1−C1 1.957(2), C1−C2 1.572(2), Si2−C2 1.916(2), Si2−Si3 2.346(1); C1−Si1−Si2 76.3(1), Si1−Si2−C2 76.6(1), Si1−C1−C2 97.3(1), C1−C2−Si2 99.7(1). **5**: Si1−C1 1.885(2), Si1−C2 1.890(2), C1−C2 1.542(3), Si1−Si2 2.372(1), Si1−Si3 2.371(1); Si1−C1−C2 66.1(1), C1−C2−Si1 65.7(1), C2−Si1−C1 48.2(1), Si2−Si1−Si3 131.7(1).

of **4** quite likely originates from C−H bond activation of a *tert*-butyl group of bis(silyl)silylene **3**. Thus, the slow conversion of **3′** to **4** already indicates the existence of an equilibrium between bis(silyl)silylene **3** and disilene **3′** in solution. DFT calculations concerning **3** revealed the silylene located 5.7 kcal/mol in energy above its disilene isomer **3′** as well as its triplet state 2.5 kcal/mol lower in energy (Si−Si:−Si bond angles: 140.7° (triplet) and 116.2° (singlet)) (Figure 2).[16] Several theoretical studies concerning possible triplet ground state silylenes have been published in the last few decades. For different bis(silyl)silylenes, however, deviating values for the respective singlet−triplet energy gaps were found, depending on the methods and basis sets used.[2b,f,6a] Clearly, the singlet triplet gap of **3** with a value of 2.5 kcal/mol is not high enough to readily take it for granted and judge the ground state multiplicity of **3** at the moment.

Therefore, we intended to experimentally elucidate the ground state multiplicity of bis(silyl)silylene isomer **3**. Because NMR spectroscopy provided no further insights (possible resonances for the singlet silylene of **3** were not observed), we used EPR spectroscopy (X-band: 9.267 GHz), the method of choice for potential triplet ground state detection. However, all EPR spectra obtained from a solution containing the equilibrium mixture of **3**/**3′**, measured in the temperature range of 133−286 K, exhibited only a strong EPR signal at around 331 mT (g = 2.0067), corresponding to a typical silyl radical of still unknown structure. Sekiguchi et al. observed similar species (at around 340 mT, g = 2.0055) when measuring the in situ generated triplet silylenes.[7] Nonetheless, under our measurement conditions, no analogous weak, broad signal at around 800 mT, assignable to the triplet silylene of **3**, was observed. Thus, the combined results suggest the position of the equilibrium being either almost entirely shifted to disilene **3′** or the decomposition to disiletane **4** being too rapid and beyond the detection limit for both the singlet and triplet ground state bis(silyl)silylene **3**.

As further evidence for the equilibrium, we intended [2 + 1] or [2 + 2] cycloaddition reactions with unsaturated organic substrates under the formation of defined trapping products. Whereas the reaction of **3**/**3′** with phenylacetylene, diphenylacetylene, and anthracene led to complicated mixtures of products, exposure to ethylene resulted in the clean formation of silirane **5** as the sole product, clearly indicating silylene reactivity (Scheme 2). Interestingly, no [2 + 2] cycloaddition reaction of tetrasilyldisilene **3′** with ethylene was observed. Silirane **5** was fully characterized, including its solid-state structure (Figure 1). The ring silicon nucleus resonates at δ = −164.3 ppm in the ^{29}Si NMR spectrum and exhibits a large Si−Si−Si bond angle of 131.7(1)° due to the sterically congested electropositive silyl groups.

According to the ethylene addition selectivity, we pursued [2 + 1] cycloaddition reactions of (*E*)/(*Z*) alkenes with respect to the Skell rule to further investigate the ground state multiplicity of bis(silyl)silylene **3**.[17] The Skell rule originates

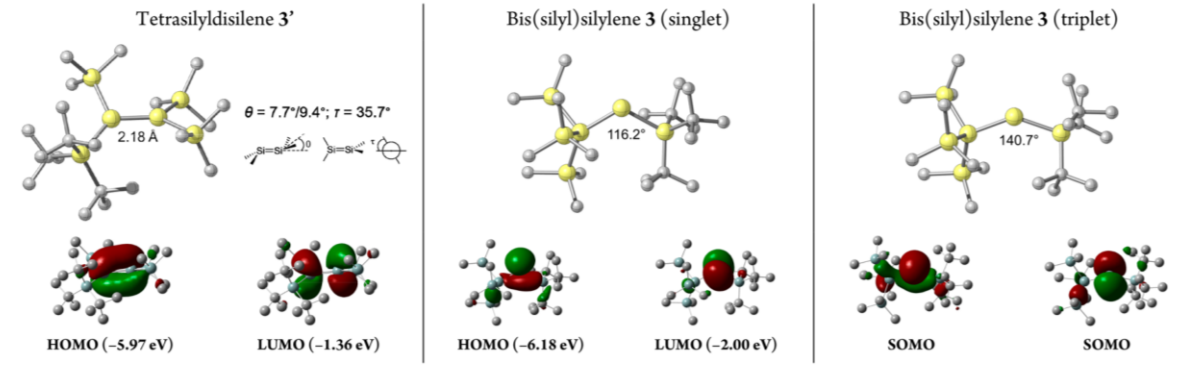
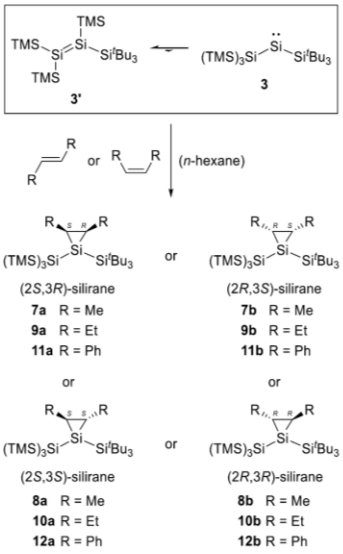


Figure 2. Calculated structures of tetrasilyldisilene **3′** and bis(silyl)silylene **3** (singlet/triplet state) with their corresponding frontier orbitals.

DOI: 10.1021/jacs.9b05318
J. Am. Chem. Soc. 2019, 141, 13536−13546

from carbene chemistry and predicts the stereospecific olefin addition of singlet carbenes. Triplet carbenes undergo a nonstereospecific cycloaddition via a diradical intermediate, allowing for facile rotation and a loss of initial stereochemistry. In the case of silylenes, however, the situation might be more complicated, and a failure of the Skell rule cannot be ruled out.[2c,f,6a] Nonetheless, investigated singlet silylenes react according to the rule, and intended cycloaddition reactions of the transient triplet silylene $(^tBu_3Si)_2Si$: did not furnish any corresponding silirane.[6a,7a,18] This prompted us to investigate the stereochemistry of olefin cycloaddition with the equilibrium mixture of **3**/**3′**. Because of the different silyl groups, not only two silirane isomers (cis and trans) but four different stereoisomers can be formed (Scheme 3). Therefore, we initially used the simplest isomers, (*E*)- and (*Z*)-2-butenes. The exposure of **3**/**3′** to (*Z*)-2-butene selectively afforded *cis*-silirane **7**. Compound **7** was sufficiently characterized by multinuclear and 2D NMR spectroscopy, albeit not being able to resolve its stereochemistry ((2*S*,3*R*)-silirane **7a** or (2*R*,3*S*)-silirane **7b**). The observed ^{29}Si NMR resonance at $\delta = -131.7$ ppm for the silirane silicon nucleus is shifted to slightly lower field compared to those observed for reported *cis*-bis(trialkylsilyl)siliranes ($\delta = -154.5$ to -159.1 ppm) and silirane **5**.[6a,18c] On the other hand, the reaction of **3**/**3′** with (*E*)-2-butene furnished approximately a 50:50 mixture of *cis*-silirane **7** and *trans*-silirane **8**. Again, the absolute configuration of **8** remains unclear, but the silirane silicon atom exhibits a similar downfield shift in the ^{29}Si NMR spectrum ($\delta = -123.3$ ppm) in comparison to reported bis(trialkylsilyl)siliranes ($\delta = -144.1$ to -149.6 ppm) and **5**.[6a,18c] The observed nonstereospecificity most likely originates from (*Z*)-2-butene contamination (~1.3%) because the purity of the utilized alkenes is crucial to the silirane product ratio. This was already recognized in the initially observed nonstereospecific cycloadditions of 2-butenes to dimesitylsilylene, in which gas contamination of the respective other isomer led to misinterpretations.[18b,19] Accordingly, the reaction of **3**/**3′** with an approximately 50:50 mixture of both stereogenic alkenes provided *cis*-silirane **7** as the sole product because of the higher reactivity of the (*Z*)-isomer.

Scheme 3. Plausible Silirane Stereoisomers Formed Upon [2 + 1] Cycloaddition Reaction of (Hypersilyl)(supersilyl)silylene 3 with (*E*)- and (*Z*)-Alkenes



To gain deeper insight, we turned to sterically more demanding alkenes with higher isomeric purity. However, the utilization of 3-hexenes and stilbenes (1,2-diphenylethylenes) led to significantly slower or even no (stilbene) cycloaddition reactions with the concomitant formation of disiletane **4**, especially with the respective (*E*)-isomer. The most satisfying result was obtained with (*Z*)-3-hexene, with ^{29}Si NMR analysis ($\delta = -133.2$ ppm) indicating the selective formation of *cis*-silirane **9**. The reaction of **3**/**3′** with (*E*)-3-hexene, on the contrary, led to the formation of a mixture of products. However, *trans*-silirane **10** was identified by ^{1}H and ^{29}Si NMR ($\delta = -127.1$ ppm; typical downfield shift compared to the cis isomer) spectroscopy. Interestingly, no resonances for *cis*-silirane **9** were observed. Therefore, we conclude that [2 + 1] cycloaddition reactions of bis(silyl)silylene **3** with stereogenic alkenes are most likely stereospecific.

Overall, the outcome of the cycloaddition reactions with stereogenic alkenes cannot yet reveal with certainty the ground state multiplicity of bis(silyl)silylene **3** because even triplet ground state silylenes could react via their singlet state.[2c,f,6a] Therefore, further examinations are essential and both a reliable method for determining the ground state multiplicity (besides EPR spectroscopy) and typical triplet silylene reactivity have yet to be found.

Surprisingly, the disilene/silylene equilibrium mixture is also capable of activating dihydrogen via oxidative addition. So far, only a few examples of low-coordinate silicon compounds are known to react similarly. This series consists of three acyclic silylenes and one disilene with small HOMO–LUMO gaps (2.0–3.0 eV), which undergo fast reactions under relatively mild conditions (from 2 h at 0 °C to up to 2 days at 50 °C).[4a,d,g,20] Recently, Iwamoto et al. reported hydrogen splitting reactions by boryldisilenes.[21] Although no observable sign of reaction was detectable at −80 °C (3 h), treating an *n*-hexane solution of **3**/**3′** at −40 °C with H_2 (1 bar) resulted in a color change from blood red to pale yellow within 30 min. The quantitative formation of silane **1** was detected by NMR spectroscopy (Scheme 2). Again, no formation of the respective disilene addition product was detected. The molecular structure of **1** revealed a large Si–Si–Si bond angle of 132.1(1)° comparable to that of silirane **5**, indicating a large Si–Si:–Si bond angle for bis(silyl)silylene **3** (Figure 1). Contrary to reported acyclic silylenes, which are able to activate H_2, singlet bis(silyl)silylene **3** exhibits a large HOMO–LUMO gap of 4.18 eV (Figure 2). Because acyclic silylenes with a comparable large HOMO–LUMO gap have shown no reaction toward H_2,[4b] the extreme reactivity of bis(silyl)silylene **3** is rather astonishing. Thus, we performed additional calculations concerning the bimolecular reaction of H_2 and singlet **3** and determined a very low effective barrier of 4.2 kcal/mol. The calculated barrier is significantly lower than that reported for Aldridge's acyclic aminoborylsilylene (23.2 kcal/mol),[4a] which therefore rationalizes the observed fast reaction of bis(silyl)silylene **3**. These results contrast with the generally assumed connectivity of a low HOMO–LUMO gap and the activation of dihydrogen for acyclic silylenes. Thus, this correlation presumably does not account for acyclic bis(silyl)silylenes. Additionally, this observation represents the first example of dihydrogen activation by a bis(silyl)silylene

DOI: 10.1021/jacs.9b05318
J. Am. Chem. Soc. 2019, 141, 13536–13546

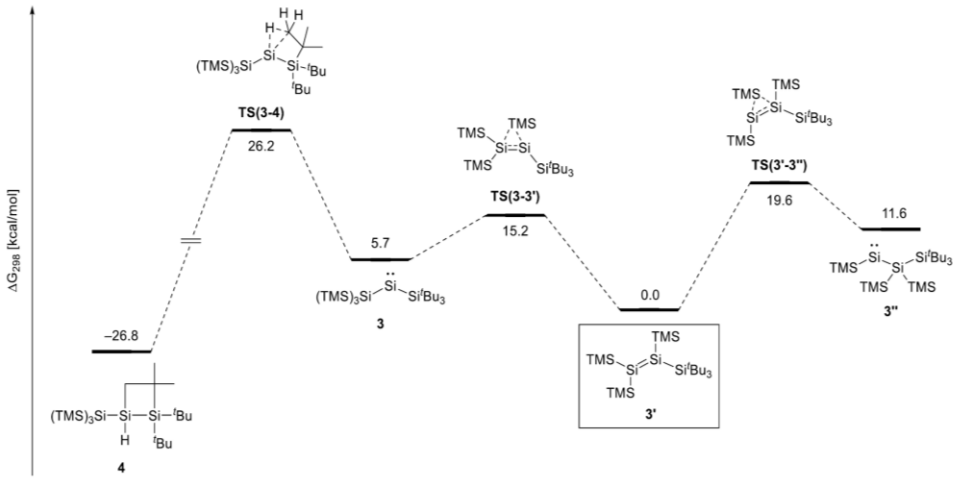


Figure 3. DFT-derived energy profile for the silylene–disilene–silylene equilibrium at the M06-2X/6-311+G(d,p)(SMD = benzene)//M06-2X/6-31+G(d,p) level of theory.

and the fastest reaction of a low-coordinate silicon compound toward H_2 to date.

DLPNO-CCSD(T)/cc-pVQZ single-point calculations based on the PBEh-3c optimized structures of **3** revealed the singlet state of **3** located 4.6 kcal/mol lower in energy than the triplet, thus supporting the assumed reactivity toward H_2.[22]

Besides dihydrogen, the activation of ammonia via oxidative addition is still a challenging target even for transition-metal complexes.[23] However, the rapid growth of main group chemistry in recent decades has revealed various reactive compounds capable of activating ammonia under mild conditions.[24] Among them are only a few silicon compounds, all of which bear low-coordinate centers, represented by their most prominent examples, silylenes[4f,25] and disilenes.[26] On the basis of the results so far, we envisaged the reaction of **3**/**3′** with ammonia as a promising target. Indeed, a facile reaction was observed even at −80 °C by treating an *n*-hexane solution of **3**/**3′** with an equimolar amount of NH_3 (0.4 M solution in 1,4-dioxane). The successful hydroamination reaction was clearly evident by the immediate color change from blood red to pale yellow. Multinuclear and 2D NMR spectroscopy identified the major product formed as aminosilane **6**, the addition product derived from tetrasilyldisilene **3′**. The reaction is completely regiospecific, with the preferred regioisomer bearing the amino group attached to the silicon nucleus with the two TMS groups, presumably for steric reasons. A similar observation was reported by Scheschkewitz and colleagues.[26b] The Si–NH_2 atom resonates at δ = −35.7 ppm in the ^{29}Si NMR spectrum, which agrees well with those observed for similar compounds (δ = −14.7 to −48.6 ppm)[26] and the theoretically calculated value (δ = −36.8 ppm). The Si–H nucleus exhibits a high-field shift in the ^{29}Si NMR spectrum at δ = −119.9 ppm compared to the reported ones (δ = −57.1 to −72.4 ppm) but is in good accordance with the calculated shift (δ = −116.6 ppm). Performing the reaction at elevated temperatures leads to less-selective product formation, presumably also affording the respective regioisomer and the adduct of bis(silyl)silylene **3**. Besides proving the existence of tetrasilyldisilene **3′**, these results further strengthen the assumption of an equilibrium between silylene **3** and disilene **3′**. Further calculations to obtain a conclusive mechanistic picture concerning ammonia activation are under current investigation.

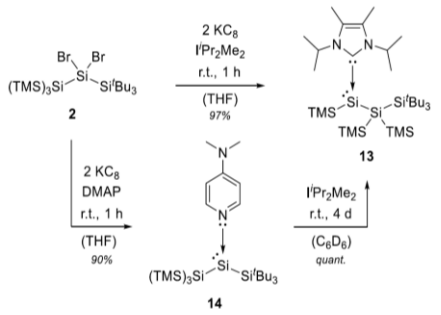
In addition, very fast reactions of **3**/**3′** with small molecules O_2, CO_2, and P_4 were observed, but in all cases, nonselective reactions occurred, leading to product mixtures. However, these observations underline the high reactivity of the equilibrium mixture containing bis(silyl)silylene **3** and tetrasilyldisilene **3′**.

As previously investigated theoretically for $((H_3Si)H_2Si)$-(H)Si: and $(H_3Si)HSi{=}SiH_2$,[13b] further verification of the experimentally observed equilibrium was provided by DFT calculations (Figure 3). Accordingly, disilene **3′** represents the most stable isomer, with an effective barrier of 15.2 kcal/mol for the TMS group migration affording bis(silyl)silylene **3**. Interestingly, another regioisomeric bis(silyl)silylene (TMS)-$((TMS)_2(^tBu_3Si)Si)$Si: **3′′** is accessible via a second 1,2-silyl shift with its formation connected to an effective barrier of 19.6 kcal/mol. Thus, the isomerization reactions between bis(silyl)-silylenes **3**/**3′′** and disilene **3′** via TMS group migrations represent an equilibrium, with disilene **3′** as the kinetic product. The decomposition of disilene **3′**/silylene **3** proceeds via C–H activation, connected to a substantially higher barrier of 26.2 kcal/mol, affording thermodynamic product **4** in an irreversible reaction.

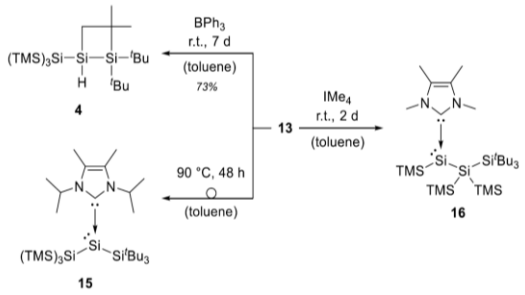
Lewis Base-Stabilized Bis(silyl)silylenes. To gain deeper insight into the disilene–silylene interconversion, we attempted to trap **3** and/or **3′** with additional Lewis bases such as phosphines and NHCs. However, treating the equilibrium mixture of **3**/**3′** with PMe_3 and NHCs with varying steric demand did not furnish a clean donor–acceptor product. The resulting mixtures of products contained several donor-stabilized species, presumably including both bis(silyl)silylene and disilene adducts. Instead, the reductive debromination of **2** with KC_8 in the presence of 1,3-diisopropyl-4,5-dimethyl-imidazolin-2-ylidene ($I^iPr_2Me_2$) selectively furnished NHC-stabilized bis(silyl)silylene **13** in excellent yield (Scheme 4). Interestingly, the formation of initially targeted bis(silyl)-silylene NHC adduct **15** (Scheme 5) was not observed, but two consecutive 1,2-silyl migrations from silylene **3** through disilene **3′** to silylene **3′′** occurred and finally NHC-stabilized regioisomeric silylene **13** was obtained. Presumably, **13** is

DOI: 10.1021/jacs.9b05318
J. Am. Chem. Soc. 2019, 141, 13536−13546

Scheme 4. Synthesis and Interconversion of Novel Donor-Stabilized Bis(silyl)silylenes



Scheme 5. Reactivity of NHC-Stabilized Bis(silyl)silylene 13



formed as the preferred product as a result of less steric congestion between $I^iPr_2Me_2$ and silylene **3′′** compared to silylene **3**. The divalent silicon nucleus of **13** exhibits a downfield-shifted resonance in the ^{29}Si NMR spectrum (δ = −104.7 ppm) relative to those observed for reported bis(silyl)silylenes **IV**–**VI** (δ = −110.5 to −136.6 ppm). The molecular structure of **13** was unambiguously confirmed by SC-XRD analysis (Figure 4). The $I^iPr_2Me_2$-stabilized divalent silicon center adopts a trigonal pyramidal geometry with the sum of bond angles amounting to 340.9° (**IVb**, 344.3°; **Va**, 302.7°, **Vb**, 293.4°, **Vc**, 255.5°; and **VI**, 317.3°). The low degree of pyramidalization indicates less-pronounced s character of the lone pair of electrons at the three-coordinate

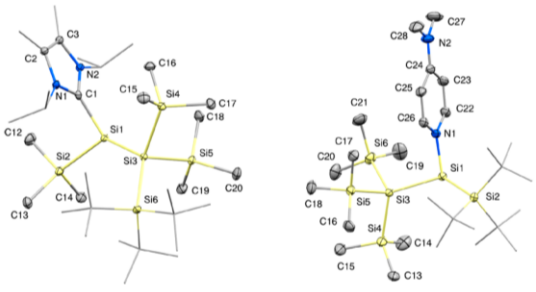


Figure 4. Molecular structures of **13** (left) and **14** (right). Ellipsoids are set at 50% probability. Hydrogen atoms and solvent molecules are omitted for clarity. Selected bond lengths (Å) and angles (°): **13**: Si1–Si2 2.360(1), Si1–Si3 2.437(1), Si1–C1 1.961(2); C1–Si1–Si2 99.3(1), C1–Si1–Si3 115.6(1), Si2–Si1–Si3 126.0(1). **14**: Si1–Si2 2.433(1), Si1–Si3 2.420(1), Si1–N1 1.942(2); N1–Si1–Si2 104.5(1), N1–Si1–Si3 98.1(1), Si2–Si1–Si3 116.1(1).

silicon atom. The C_{NHC}–Si bond length is 1.961(2) Å, which is in the typical range for C_{NHC}–Si bonds[10b] but elongated in comparison to **IV**–**VI** (1.933–1.960 Å) and thus displaying a weaker interaction between the NHC $I^iPr_2Me_2$ and the silylene moiety in complex **13**.

In contrast, the utilization of weaker Lewis base 4-*N*,*N*-dimethylaminopyridine (DMAP) afforded DMAP-coordinated silylene **14** in 90% yield. In this case, regioisomeric (hypersilyl)(supersilyl)silylene **3** was trapped as donor–acceptor complex **14**. The less-shielded three-coordinate silicon atom shows a significant downfield shift in the ^{29}Si NMR spectrum at δ = 68.8 ppm. A similar trend was observed for donor-stabilized β-diketiminato silylenes (δ = −12.0 to 37.4 ppm)[27] reported by Driess et al. However, that case is far less pronounced because the respective donor-free silylene resonates only at δ = 88.4 ppm.[28] The solid-state structure (Figure 4) revealed a higher degree of pyramidalization around the divalent silicon nucleus (sum of bond angles: 318.7°) and therefore illustrates the increased s character of base-stabilized silylene **14**. The N_{DMAP}–Si bond length of 1.942(2) Å agrees well with those observed for previously reported DMAP-stabilized low-valent silicon complexes ($d_{(N-Si)}$ = 1.85–2.01 Å).[27b,29] Surprisingly, the treatment of silylene **14** with an equimolar amount of $I^iPr_2Me_2$ does not afford corresponding NHC-stabilized silylene **15** but, selectively again, provides rearranged silylene NHC adduct **13**. This observation for the Lewis base exchange further indicates the presence of the silylene–disilene–silylene equilibrium discussed above. In addition, our results are an extension of the recent findings regarding the disilene–silylene rearrangement, reported by Cowley, Holthausen, and colleagues.[14]

To gain more profound knowledge concerning the accessibility of all isomers in equilibrium, we investigated the reactivity of silylene **13** with respect to Lewis base abstraction and exchange. The reaction of **13** with 1 equiv of Lewis acid BPh_3 provided disiletane **4** through NHC abstraction and the concomitant formation of the NHC–borane adduct $I^iPr_2Me_2{\cdot}BPh_3$ (Scheme 5). Full conversion, however, was observed only after a reaction time of 1 week at ambient temperature. Monitoring the reaction with ^1H and ^{29}Si NMR spectroscopy revealed the intermediary formation of tetrasilyldisilene **3′**. Therefore, NHC abstraction initially affords respective donor-free silylene **3′′** being in equilibrium with disilene **3′** and silylene **3**. As already mentioned, the irreversible decomposition of the equilibrium mixture is kinetically limited but thermodynamically preferred, thus accounting for the long reaction times.

Silylene **13** is completely stable as a solid and in solution at room temperature. However, heating a solution of **13** to 90 °C results again in a double TMS migration and the formation of initially targeted NHC-supported silylene **15** (Scheme 5) in 58% yield (NMR). Additional DFT calculations revealed that **15** is slightly more stable than **13** with an effective activation barrier of 30.0 kcal/mol for the interconversion, thus being in line with the required elevated temperature and prolonged reaction time for the isomerization. Nevertheless, silylene **15** could not be isolated in its pure form because of incomplete conversion and concomitant decomposition via the formation of disiletane **4** and free $I^iPr_2Me_2$. Neither prolonged heating (at different temperatures) nor solvent change to benzene, *n*-hexane, or THF affected the outcome of the reaction in favor of silylene **15**, thus further confirming the existence of the equilibrium. Nonetheless, **15** was unambiguously characterized

DOI: 10.1021/jacs.9b05318
J. Am. Chem. Soc. 2019, 141, 13536–13546

by a combination of multinuclear and 2D NMR studies, supported by the results obtained from DFT calculations. The ^{29}Si resonance of the three-coordinate Si nucleus is shifted to higher field (δ = −120.6 ppm) compared to that for donor-stabilized silylenes **13** and **14** and agrees well with its GIAO-predicted chemical shift (δ = −127.2 ppm). In particular, the huge difference from that observed for analogous DMAP-stabilized silylene **14** emphasizes the stronger interaction between bis(silyl)silylene **3** and the better σ-donor molecule.

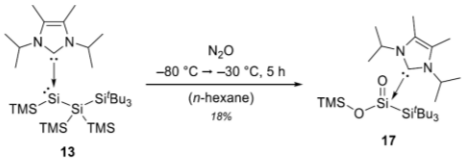
Furthermore, an even stronger donor−acceptor interaction was shown by the successful exchange of I^{i}Pr$_2$Me$_2$ with the stronger σ-donating NHC, 1,3,4,5-tetramethylimidazolin-2-ylidene (IMe$_4$). IMe$_4$-stabilized bis(silyl)silylene **16** was sufficiently characterized by multinuclear NMR spectroscopy (Scheme 5). The low-valent silicon nucleus exhibits a signal observed at δ = −117.1 ppm in the ^{29}Si NMR spectrum. The high-field-shifted resonance compared to that observed for **13** indicates a stronger interaction between NHC and bis(silyl)-silylene **3**. The theoretically determined resonance at δ = −115.2 ppm supports the formation of NHC adduct **16**. However, it was neither possible to remove free I^{i}Pr$_2$Me$_2$, nor to observe a rearrangement to the corresponding IMe$_4$-stabilized bis(silyl)silylene adduct of **3** because of an even more facile decomposition reaction.

Additional DFT calculations also reflect the trend observed for the σ-donor−silylene interactions by ^{29}Si NMR spectroscopy (details in Tables S9 and S11 in the Supporting Information), and thus the gas-phase Gibbs free bond-dissociation energy increases from 15.3 kcal/mol (**14**) to 16.3 kcal/mol (**15**) to 22.0 kcal/mol (**13**) and finally to 27.6 kcal/mol (**16**). These observations correlate well with the increasing donor strength of the Lewis base used and also confirm the inability to access ((TMS)$_3$Si)(^{t}Bu$_3$Si)Si:(IMe$_4$), the regioisomeric product of **16**. In addition to the higher gas-phase Gibbs free bond-dissociation energy, the reduced steric demand of IMe$_4$ makes **16** more susceptible for subsequent reactions. This is evidenced by the slow decomposition of 16 in solution. In the case of NHC-stabilized silylene **13**, rearrangement to **15** is still the preferred pathway, although decomposition and disiletane **4** formation occur during heating. For DMAP-stabilized silylene **14**, the isomerization equilibrium finally providing **13** appears to be the only accessible pathway subsequent to Lewis base dissociation.

NHC-Stabilized Silanoic Ester. Even though the oxygenation of **3**/**3′** led only to complicated mixtures with no isolable products, we investigated the reaction of **13** toward various oxidizing agents because the last decades have witnessed significant attention in the synthesis of heavier analogues of carbonyl compounds. However, in particular, the isolation of organosilicon compounds bearing a Si=O moiety is a rather demanding task because of their extreme reactivity. The origin of this reactivity lies in the kinetic and thermodynamic instability of the weak Si=O π-bond attributed to the unfavorable p$_\pi$-orbital overlap of silicon and oxygen.[30] In addition, the Pauling electronegativity difference between silicon and oxygen ($\Delta\chi_{(Si-O)}$ = 1.54) is much larger than that between carbon and oxygen ($\Delta\chi_{(C-O)}$ = 0.89).[31] Thus, the zwitterionic, ylide-like Si$^{\delta+}$−O$^{\delta-}$ resonance form makes a large contribution to the nature of the strongly polarized Si=O double bond.[32] As a consequence, the Si=O double bond is prone to barrierless, rapid head-to-tail oligomerization affording oligosiloxanes via Si−O σ-bond formation.[33] Despite this challenge, the Si=O moiety could be tamed[10b,34] and a series of donor-[27a,c,35] and donor−acceptor-stabilized[27b,36] heavier carbonyl compounds have been reported. Even a few examples of donor-free, three-coordinate silanones (silicon analogues of ketones) have been isolated.[4h,37] Nevertheless, silanoic esters, the heavier congeners of carboxylate esters, remain rather elusive compounds with scarcely any reported example species.[38]

Because we recently reported the isolation of a stable silyl-substituted silanone,[4h] we assumed that **13**, with two silyl groups, was a promising precursor for gaining access to silanone derivatives. However, the reaction of NHC-stabilized silylene **13** toward Me$_3$NO, CO$_2$, and O$_2$ resulted in either no reaction or the formation of a complicated mixture of products. Interestingly, the exposure of an *n*-hexane solution of **13** to N$_2$O results in a color change from purple-red to pale red with the concomitant formation of a white precipitate. After workup, unique NHC-supported silanoic ester **17** was isolated in 18% yield (Scheme 6). The exact mechanism of the formation of **17** is unclear but presumably includes the initial generation of a silanone. Subsequent silyl migration, further oxidation, and rearrangement might eventually lead to **17**. In ^{29}Si NMR, the Si=O silicon nucleus exhibits a resonance at δ = −50.8 ppm, which exactly matches the GIAO-DFT value and agrees with those reported for related species (δ = −49.1 to −91.5 ppm).[38] The ^{1}H NMR spectrum provided the most intriguing spectroscopic feature of **17**, an unusual broad splitting of the NHC wingtip methine protons ($\Delta\delta$ = 2.68 ppm). The reason for this observation is presumably hydrogen bonding of one isopropyl C−H proton to the oxygen atom of the Si=O bond. The solid-state structure of **17** (Figure 5) revealed a close O···H distance of 2.143 Å, being much shorter than the sum of the van der Waals radii of hydrogen and oxygen (2.72 Å) and thus supporting this assumption.[39] The

Scheme 6. Oxygenation of Silylene 13 Furnishing NHC-Stabilized Silanoic Ester 17



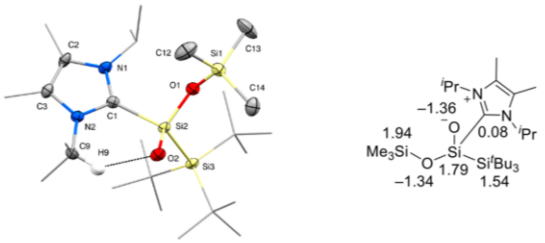


Figure 5. Molecular structure of **17** with ellipsoids set at 50% probability (left) and the results of NBO analysis of **17** (right). Hydrogen atoms, except for H9 involved in hydrogen bonding (visualized by the dashed line), are omitted for clarity. Selected bond lengths (Å) and angles (°): Si1−O1 1.641(2), Si2−O2 1.556(2), Si2−O1 1.655(3); Si2−Si3 2.415(1), Si2−C1 1.984(3); O2−Si2−O1 115.5(1), O2−Si2−C1 106.9(1), O1−Si2−C1 101.2(1), O2−Si2−Si3 111.7(1), O1−Si2−Si3 107.0(1), C1−Si2−Si3 114.3(1).

DOI: 10.1021/jacs.9b05318
J. Am. Chem. Soc. 2019, 141, 13536−13546

experimentally determined Si=O bond length of 1.556(2) Å is in the range observed for similar compounds ($d_{Si=O}$ = 1.52–1.59 Å) and much shorter than the measured Si–O single bonds (d_{Si-O} = 1.641(2) and 1.655(3) Å).[38] Interestingly, the TMS–O σ-bond is shorter than the Si2–O1 bond and the C_{NHC}–Si bond is elongated compared to that observed for the precursor, silylene NHC adduct **13** (d_{C-Si} = 1.961(2) Å).

Characteristic Si=O and Si–O–Si stretching vibrations at $\tilde{\nu}$ = 1069 and 971 cm^{-1}, respectively, were found in the IR spectrum of **17**. NHC-stabilized silanoic ester **17** is not a particularly stable compound because decomposition to an unidentified mixture of products was observed in solution at temperatures higher than −30 °C. Possible multiple bonding in four-coordinate silanoic esters and related thioesters has already been investigated in detail by Driess, Apeloig, and co-workers.[35a] Nevertheless, our entirely silyl-substituted silanoic ester is the first example of its kind. Natural bond orbital (NBO) analysis revealed strong polarization for both central silicon oxygen bonds (details in the Supporting Information). The Wiberg bond indices (WBIs) of the Si2–O1 (0.47) and Si2–O2 (0.91) bonds are relatively low, contradictory to the short Si2–O2 bond observed in the solid state. Natural resonance theory (NRT) revealed the zwitterionic formulation as the major resonance structure (Table S15). However, NBO analysis further features negative hyperconjugation of the lone pairs of O2 into the σ^* orbitals of Si2–C1 and Si2–O1, thus rationalizing the observed short Si2–O2 bond as well as the elongated O1–Si2 and Si2–C1 bonds (Figure S81). Moreover, both highly polarized Si–O bonds and the reduced C_{NHC}–Si interaction account for the limited thermal stability of **17**.

■ CONCLUSIONS

We used the novel dibromosilane $((TMS)_3Si)(^tBu_3Si)SiBr_2$ (**2**) to gain access to the equilibrium mixture of tetrasilyldisilene **3′** and the first example of an isolable bis(silyl)silylene **3**. The highly reactive nature of **3**/**3′** was demonstrated by the facile activation of small molecules under very mild conditions. In particular, the fastest reactions discovered for a low-valent silicon compound toward dihydrogen and ammonia via oxidative addition were observed. These results further demonstrate the potential of main group compounds as transition-metal mimics and possible catalysts for the future. In the course of our study, we further isolated unprecedented donor-stabilized bis(silyl)silylenes **13** and **14** and revealed deeper insights into the disilene–silylene rearrangement. In addition, the first acyclic NHC-stabilized silanoic ester, **17**, was isolated. Currently, the synthesis of bis(silyl)silylene transition-metal complexes to examine the inherent σ-donor strength and further studies regarding the ground state multiplicity of **3** are under active investigation in our laboratories.

■ ASSOCIATED CONTENT

Supporting Information

The Supporting Information is available free of charge on the ACS Publications website at DOI: 10.1021/jacs.9b05318.

Experimental details, including synthesis, spectroscopic, crystallographic, and computational data (PDF)

Crystallographic data (CCDC 1915625–1915631) (CIF)

■ AUTHOR INFORMATION

Corresponding Author

*s.inoue@tum.de

ORCID

Shigeyoshi Inoue: 0000-0001-6685-6352

Author Contributions

†D.R., R.H., and A.P. contributed equally to this work.

Notes

The authors declare no competing financial interest.

■ ACKNOWLEDGMENTS

We are exceptionally grateful to the WACKER Chemie AG and the European Research Council (SILION 637394) for continued financial support. We thank Dr. Daniel Wendel for revising the manuscript, Maria Matthews for the low-temperature NMR studies, and Dr. Oksana Storcheva for the EPR measurements. We also thank Prof. Dr. M. C. Holthausen (Goethe-Universität Frankfurt am Main) and J. I. Schweizer for fruitful discussions, computational resources, and advice. Quantum chemical calculations were performed in parts at the Leibniz Supercomputing Center of the Bavarian Academy of Science and Humanities.

■ REFERENCES

(1) Lee, V. Y. *Organosilicon Compounds: Theory and Experiment (Synthesis)*; Academic Press: New York, 2017.

(2) (a) Grev, R. S.; Schaefer, H. F., III; Gaspar, P. P. In search of triplet silylenes. *J. Am. Chem. Soc.* **1991**, *113*, 5638–5643. (b) Holthausen, M. C.; Koch, W.; Apeloig, Y. Theory Predicts Triplet Ground-State Organic Silylenes. *J. Am. Chem. Soc.* **1999**, *121*, 2623–2624. (c) Gaspar, P. P.; Xiao, M.; Pae, D. H.; Berger, D. J.; Haile, T.; Chen, T.; Lei, D.; Winchester, W. R.; Jiang, P. The quest for triplet ground state silylenes. *J. Organomet. Chem.* **2002**, *646*, 68–79. (d) Yoshida, M.; Tamaoki, N. DFT Study on Triplet Ground State Silylenes Revisited: The Quest for the Triplet Silylene Must Go On. *Organometallics* **2002**, *21*, 2587–2589. (e) Apeloig, Y.; Pauncz, R.; Karni, M.; West, R.; Steiner, W.; Chapman, D. Why Is Methylene a Ground State Triplet while Silylene Is a Ground State Singlet? *Organometallics* **2003**, *22*, 3250–3256. (f) Kosa, M.; Karni, M.; Apeloig, Y. Were Reactions of Triplet Silylenes Observed? *J. Am. Chem. Soc.* **2013**, *135*, 9032–9040.

(3) For recent reviews on silylenes, see (a) Haaf, M.; Schmedake, T. A.; West, R. Stable Silylenes. *Acc. Chem. Res.* **2000**, *33*, 704–714. (b) Gehrhus, B.; Lappert, M. F. Chemistry of thermally stable bis(amino)silylenes. *J. Organomet. Chem.* **2001**, *617–618*, 209–223. (c) Nagendran, S.; Roesky, H. W. The Chemistry of Aluminum(I), Silicon(II), and Germanium(II). *Organometallics* **2008**, *27*, 457–492. (d) Mizuhata, Y.; Sasamori, T.; Tokitoh, N. Stable Heavier Carbene Analogues. *Chem. Rev.* **2009**, *109*, 3479–3511. (e) Kira, M. An isolable dialkylsilylene and its derivatives. A step toward comprehension of heavy unsaturated bonds. *Chem. Commun.* **2010**, *46*, 2893–2903. (f) Asay, M.; Jones, C.; Driess, M. *N*-Heterocyclic Carbene Analogues with Low-Valent Group 13 and Group 14 Elements: Syntheses, Structures, and Reactivities of a New Generation of Multitalented Ligands. *Chem. Rev.* **2011**, *111*, 354–396. (g) Yao, S.; Xiong, Y.; Driess, M. Zwitterionic and Donor-Stabilized *N*-Heterocyclic Silylenes (NHSis) for Metal-Free Activation of Small Molecules. *Organometallics* **2011**, *30*, 1748–1767. (h) Sen, S. S.; Khan, S.; Samuel, P. P.; Roesky, H. W. Chemistry of functionalized silylenes. *Chem. Sci.* **2012**, *3*, 659–682. (i) Sen, S. S.; Khan, S.; Nagendran, S.; Roesky, H. W. Interconnected Bis-Silylenes: A New Dimension in Organosilicon Chemistry. *Acc. Chem. Res.* **2012**, *45*, 578–587.

(4) (a) Protchenko, A. V.; Birjkumar, K. H.; Dange, D.; Schwarz, A. D.; Vidovic, D.; Jones, C.; Kaltsoyannis, N.; Mountford, P.; Aldridge,

DOI: 10.1021/jacs.9b05318
J. Am. Chem. Soc. 2019, 141, 13536–13546

S. A Stable Two-Coordinate Acyclic Silylene. *J. Am. Chem. Soc.* **2012**, *134*, 6500−6503. (b) Rekken, B. D.; Brown, T. M.; Fettinger, J. C.; Tuononen, H. M.; Power, P. P. Isolation of a Stable, Acyclic, Two-Coordinate Silylene. *J. Am. Chem. Soc.* **2012**, *134*, 6504−6507. (c) Inoue, S.; Leszczyńska, K. An Acyclic Imino-Substituted Silylene: Synthesis, Isolation, and its Facile Conversion into a Zwitterionic Silaimine. *Angew. Chem., Int. Ed.* **2012**, *51*, 8589−8593. (d) Protchenko, A. V.; Schwarz, A. D.; Blake, M. P.; Jones, C.; Kaltsoyannis, N.; Mountford, P.; Aldridge, S. A Generic One-Pot Route to Acyclic Two-Coordinate Silylenes from Silicon(IV) Precursors: Synthesis and Structural Characterization of a Silylsilylene. *Angew. Chem., Int. Ed.* **2013**, *52*, 568−571. (e) Rekken, B. D.; Brown, T. M.; Fettinger, J. C.; Lips, F.; Tuononen, H. M.; Herber, R. H.; Power, P. P. Dispersion Forces and Counterintuitive Steric Effects in Main Group Molecules: Heavier Group 14 (Si−Pb) Dichalcogenolate Carbene Analogues with Sub-90° Interligand Bond Angles. *J. Am. Chem. Soc.* **2013**, *135*, 10134−10148. (f) Hadlington, T. J.; Abdalla, J. A. B.; Tirfoin, R.; Aldridge, S.; Jones, C. Stabilization of a two-coordinate, acyclic diaminosilylene (ADASi): completion of the series of isolable diaminotetrylenes,:$E(NR_2)_2$ (E = group 14 element). *Chem. Commun.* **2016**, *52*, 1717−1720. (g) Wendel, D.; Porzelt, A.; Herz, F. A. D.; Sarkar, D.; Jandl, C.; Inoue, S.; Rieger, B. From Si(II) to Si(IV) and Back: Reversible Intramolecular Carbon−Carbon Bond Activation by an Acyclic Iminosilylene. *J. Am. Chem. Soc.* **2017**, *139*, 8134−8137. (h) Wendel, D.; Reiter, D.; Porzelt, A.; Altmann, P. J.; Inoue, S.; Rieger, B. Silicon and Oxygen's Bond of Affection: An Acyclic Three-Coordinate Silanone and Its Transformation to an Iminosiloxysilylene. *J. Am. Chem. Soc.* **2017**, *139*, 17193−17198. (i) Loh, Y. K.; Ying, L.; Ángeles Fuentes, M.; Do, D. C. H.; Aldridge, S. An *N*-Heterocyclic Boryloxy Ligand Isoelectronic with *N*-Heterocyclic Imines: Access to an Acyclic Dioxysilylene and its Heavier Congeners. *Angew. Chem., Int. Ed.* **2019**, *58*, 4847−4851.

(5) Protchenko, A. V.; Vasko, P.; Do, D. C. H.; Hicks, J.; Ángeles Fuentes, M.; Jones, C.; Aldridge, S. Reduction of carbon oxides by an acyclic silylene: reductive coupling of CO. *Angew. Chem., Int. Ed.* **2019**, *58*, 1808−1812.

(6) (a) Gaspar, P. P.; Beatty, A. M.; Chen, T.; Haile, T.; Lei, D.; Winchester, W. R.; Braddock-Wilking, J.; Rath, N. P.; Klooster, W. T.; Koetzle, T. F.; Mason, S. A.; Albinati, A. Tris(triisopropylsilyl)silane and the Generation of Bis(triisopropylsilyl)silylene. *Organometallics* **1999**, *18*, 3921−3932. (b) Jiang, P.; Gaspar, P. P. Tri-*tert*-butylsilyl(triisopropylsilyl)silylene (^{t}Bu)$_3$Si−Si−Si(^{i}Pr)$_3$ and Chemical Evidence for Its Reactions from a Triplet Electronic State. *J. Am. Chem. Soc.* **2001**, *123*, 8622−8623.

(7) (a) Sekiguchi, A.; Tanaka, T.; Ichinohe, M.; Akiyama, K.; Tero-Kubota, S. Bis(tri-*tert*-butylsilyl)silylene: Triplet Ground State Silylene. *J. Am. Chem. Soc.* **2003**, *125*, 4962−4963. (b) Sekiguchi, A.; Tanaka, T.; Ichinohe, M.; Akiyama, K.; Gaspar, P. P. Tri-*tert*-butylsilylsilylenes with Alkali Metal Substituents (^{t}Bu$_3$Si)SiM (M = Li, K): Electronically and Sterically Accessible Triplet Ground States. *J. Am. Chem. Soc.* **2008**, *130*, 426−427.

(8) (a) Klinkhammer, K. W. Tris(trimethylsilyl)silanides of the Heavier Alkali Metals—A Structural Study. *Chem. - Eur. J.* **1997**, *3*, 1418−1431. (b) Klinkhammer, K. W. In *Organosilicon Chemistry III: From Molecules to Materials*; Auner, N., Weis, J., Eds.; Wiley-VCH: Weinheim, 1998.

(9) Ichinohe, M.; Kinjo, R.; Sekiguchi, A. The First Stable Methyl-Substituted Disilene: Synthesis, Crystal Structure, and Regiospecific MeLi Addition. *Organometallics* **2003**, *22*, 4621−4623.

(10) (a) Marschner, C. Silylated Group 14 Ylenes: An Emerging Class of Reactive Compounds. *Eur. J. Inorg. Chem.* **2015**, *2015*, 3805−3820. (b) Nesterov, V.; Reiter, D.; Bag, P.; Frisch, P.; Holzner, R.; Porzelt, A.; Inoue, S. NHCs in Main Group Chemistry. *Chem. Rev.* **2018**, *118*, 9678−9842.

(11) Tanaka, H.; Ichinohe, M.; Sekiguchi, A. An Isolable NHC-Stabilized Silylene Radical Cation: Synthesis and Structural Characterization. *J. Am. Chem. Soc.* **2012**, *134*, 5540−5543.

(12) (a) Jana, A.; Omlor, I.; Huch, V.; Rzepa, H. S.; Scheschkewitz, D. *N*-Heterocyclic Carbene Coordinated Neutral and Cationic Heavier Cyclopropylidenes. *Angew. Chem., Int. Ed.* **2014**, *53*, 9953−9956. (b) Guddorf, B. J.; Hepp, A.; Lips, F. Efficient Synthesis of a NHC-Coordinated Trisilacyclopropylidene and Its Coordination Behavior. *Chem. - Eur. J.* **2018**, *24*, 10334−10338.

(13) (a) Sakurai, H.; Nakadaira, Y.; Sakaba, H. Chemistry of organosilicon compounds. 181. Silylene-to-disilene and disilene-to-silylene rearrangements. *Organometallics* **1983**, *2*, 1484−1486. (b) Nagase, S.; Kudo, T. Silylene-disilene isomerizations. A theoretical study. *Organometallics* **1984**, *3*, 1320−1322.

(14) Stanford, M. W.; Schweizer, J. I.; Menche, M.; Nichol, G. S.; Holthausen, M. C.; Cowley, M. J. Intercepting the Disilene-Silylsilylene Equilibrium. *Angew. Chem., Int. Ed.* **2019**, *58*, 1329−1333.

(15) Detailed experimental and analytical data for the preparation of **1** and its precursors can be found in the Supporting Information.

(16) Geometry optimizations and harmonic frequency calculations were performed at the M06-2X/6-31+G(d,p) level of density functional theory. NMR chemical shift values were calculated using the gauge-independent atomic orbital (GIAO) method implemented in *Gaussian 09* and the M06-L functional along with the 6-311G(2,p) basis set and the SMD solvent model for the structures obtained at the M06-2X/6-31+G(d,p) level of theory. For detailed information, see the Supporting Information.

(17) Skell, P. S.; Woodworth, R. C. Structure of Carbene, CH_2. *J. Am. Chem. Soc.* **1956**, *78*, 4496−4497.

(18) (a) Pae, D. H.; Xiao, M.; Chiang, M. Y.; Gaspar, P. P. Diadamantylsilylene and its stereochemistry of addition. *J. Am. Chem. Soc.* **1991**, *113*, 1281−1288. (b) Zhang, S.; Wagenseller, P. E.; Conlin, R. T. Addition of dimesitylsilylene to olefins. A reinvestigation. *J. Am. Chem. Soc.* **1991**, *113*, 4278−4281. (c) Kira, M.; Iwamoto, T.; Maruyama, T.; Kuzuguchi, T.; Yin, D.; Kabuto, C.; Sakurai, H. Hexakis(trialkylsilyl)cyclotrisilanes and photochemical generation of bis(trialkylsilyl)silylenes. *J. Chem. Soc., Dalton Trans.* **2002**, 1539−1544.

(19) Ando, W.; Fujita, M.; Yoshida, H.; Sekiguchi, A. Stereochemistry of the addition of diarylsilylenes to *cis*- and *trans*-2-butenes. *J. Am. Chem. Soc.* **1988**, *110*, 3310−3311.

(20) Wendel, D.; Szilvási, T.; Jandl, C.; Inoue, S.; Rieger, B. Twist of a Silicon−Silicon Double Bond: Selective Anti-Addition of Hydrogen to an Iminodisilene. *J. Am. Chem. Soc.* **2017**, *139*, 9156−9159.

(21) (a) Kosai, T.; Iwamoto, T. Stable Push−Pull Disilene: Substantial Donor−Acceptor Interactions through the Si = Si Double Bond. *J. Am. Chem. Soc.* **2017**, *139*, 18146−18149. (b) Kosai, T.; Iwamoto, T. Cleavage of Two Hydrogen Molecules by Boryldisilenes. *Chem. - Eur. J.* **2018**, *24*, 7774−7780.

(22) Personal communication: Prof. M. C. Holthausen (Goethe-Universität Frankfurt am Main); References for the additional calculations: (a) Riplinger, C.; Neese, F. An efficient and near linear scaling pair natural orbital based local coupled cluster method. *J. Chem. Phys.* **2013**, *138*, 034106. (b) Riplinger, C.; Sandhoefer, B.; Hansen, A.; Neese, F. Natural triple excitations in local coupled cluster calculations with pair natural orbitals. *J. Chem. Phys.* **2013**, *139*, 134101. (c) Kendall, R. A.; Dunning, T. H., Jr. Electron affinities of the first-row atoms revisited. Systematic basis sets and wave functions. *J. Chem. Phys.* **1992**, *96*, 6796−6806. (d) Woon, D. E.; Dunning, T. H., Jr. Gaussian basis sets for use in correlated molecular calculations. III. The atoms aluminum through argon. *J. Chem. Phys.* **1993**, *98*, 1358−1371. (e) Grimme, S.; Brandenburg, J. G.; Bannwarth, C.; Hansen, A. Consistent structures and interactions by density functional theory with small atomic orbital basis sets. *J. Chem. Phys.* **2015**, *143*, 054107.

(23) Hoover, J. Ammonia activation at a metal. *Science* **2016**, *354*, 707−708.

(24) (a) Power, P. P. Interaction of Multiple Bonded and Unsaturated Heavier Main Group Compounds with Hydrogen, Ammonia, Olefins, and Related Molecules. *Acc. Chem. Res.* **2011**, *44*, 627−637. (b) Yadav, S.; Saha, S.; Sen, S. S. Compounds with Low-Valent p-Block Elements for Small Molecule Activation and Catalysis. *ChemCatChem* **2016**, *8*, 486−501.

DOI: 10.1021/jacs.9b05318
J. Am. Chem. Soc. 2019, 141, 13536−13546

(25) (a) Jana, A.; Schulzke, C.; Roesky, H. W. Oxidative Addition of Ammonia at a Silicon(II) Center and an Unprecedented Hydrogenation Reaction of Compounds with Low-Valent Group 14 Elements Using Ammonia Borane. *J. Am. Chem. Soc.* **2009**, *131*, 4600−4601. (b) Protchenko, A. V.; Bates, J. I.; Saleh, L. M. A.; Blake, M. P.; Schwarz, A. D.; Kolychev, E. L.; Thompson, A. L.; Jones, C.; Mountford, P.; Aldridge, S. Enabling and Probing Oxidative Addition and Reductive Elimination at a Group 14 Metal Center: Cleavage and Functionalization of E−H Bonds by a Bis(boryl)stannylene. *J. Am. Chem. Soc.* **2016**, *138*, 4555−4564.

(26) (a) Boomgaarden, S.; Saak, W.; Weidenbruch, M.; Marsmann, H. Ammonia and Chlorine Additions to a Tetrasilabuta-1,3-diene: Conglomerate versus Racemate Crystallization. *Z. Anorg. Allg. Chem.* **2001**, *627*, 349−352. (b) Meltzer, A.; Majumdar, M.; White, A. J. P.; Huch, V.; Scheschkewitz, D. Potential Protecting Group Strategy for Disila Analogues of Vinyllithiums: Synthesis and Reactivity of a 2,4,6-Trimethoxyphenyl-Substituted Disilene. *Organometallics* **2013**, *32*, 6844−6850. (c) Wendel, D.; Szilvási, T.; Henschel, D.; Altmann, P. J.; Jandl, C.; Inoue, S.; Rieger, B. Precise Activation of Ammonia and Carbon Dioxide by an Iminodisilene. *Angew. Chem., Int. Ed.* **2018**, *57*, 14575−14579.

(27) (a) Xiong, Y.; Yao, S.; Driess, M. An Isolable NHC-Supported Silanone. *J. Am. Chem. Soc.* **2009**, *131*, 7562−7563. (b) Xiong, Y.; Yao, S.; Müller, R.; Kaupp, M.; Driess, M. Activation of Ammonia by a Si = O Double Bond and Formation of a Unique Pair of Sila-Hemiaminal and Silanoic Amide Tautomers. *J. Am. Chem. Soc.* **2010**, *132*, 6912−6913. (c) Yao, S.; Xiong, Y.; Driess, M. *N*-Heterocyclic Carbene (NHC)-Stabilized Silanechalcogenones: NHC-Si(R_2)=E (E = O, S, Se, Te). *Chem. - Eur. J.* **2010**, *16*, 1281−1288.

(28) Driess, M.; Yao, S.; Brym, M.; Van Wüllen, C.; Lentz, D. A New Type of *N*-Heterocyclic Silylene with Ambivalent Reactivity. *J. Am. Chem. Soc.* **2006**, *128*, 9628−9629.

(29) Yeong, H.-X.; Xi, H.-W.; Li, Y.; Lim, K. H.; So, C.-W. A Silyliumylidene Cation Stabilized by an Amidinate Ligand and 4-Dimethylaminopyridine. *Chem. - Eur. J.* **2013**, *19*, 11786−11790.

(30) Avakyan, V. G.; Sidorkin, V. F.; Belogolova, E. F.; Guselnikov, S. L.; Gusel'nikov, L. E. AIM and ELF Electronic Structure/G2 and G3 π-Bond Energy Relationship for Doubly Bonded Silicon Species, H_2Si = X (X = $E^{14}H_2$, $E^{15}H$, E^{16}). *Organometallics* **2006**, *25*, 6007−6013.

(31) Allred, A. L. Electronegativity values from thermochemical data. *J. Inorg. Nucl. Chem.* **1961**, *17*, 215−221.

(32) Kapp, J.; Remko, M.; Schleyer, P. v. R. H_2XO and $(CH_3)_2XO$ Compounds (X = C, Si, Ge, Sn, Pb): Double Bonds vs Carbene-Like Structures−Can the Metal Compounds Exist at All? *J. Am. Chem. Soc.* **1996**, *118*, 5745−5751.

(33) (a) Kudo, T.; Nagase, S. Theoretical study on the dimerization of silanone and the properties of the polymeric products $(H_2SiO)_n$ (n = 2, 3, and 4). Comparison with dimers $(H_2SiS)_2$ and $(H_2CO)_2$. *J. Am. Chem. Soc.* **1985**, *107*, 2589−2595. (b) Kimura, M.; Nagase, S. The Quest of Stable Silanones: Substituent Effects. *Chem. Lett.* **2001**, *30*, 1098−1099.

(34) Xiong, Y.; Yao, S.; Driess, M. Chemical Tricks To Stabilize Silanones and Their Heavier Homologues with E = O Bonds (E = Si−Pb): From Elusive Species to Isolable Building Blocks. *Angew. Chem., Int. Ed.* **2013**, *52*, 4302−4311.

(35) (a) Epping, J. D.; Yao, S.; Karni, M.; Apeloig, Y.; Driess, M. Si = X Multiple Bonding with Four-Coordinate Silicon? Insights into the Nature of the Si = O and Si = S Double Bonds in Stable Silanoic Esters and Related Thioesters: A Combined NMR Spectroscopic and Computational Study. *J. Am. Chem. Soc.* **2010**, *132*, 5443−5455. (b) Xiong, Y.; Yao, S.; Müller, R.; Kaupp, M.; Driess, M. From silicon(II)-based dioxygen activation to adducts of elusive dioxasiliranes and sila-ureas stable at room temperature. *Nat. Chem.* **2010**, *2*, 577−580. (c) Ahmad, S. U.; Szilvási, T.; Irran, E.; Inoue, S. An NHC-Stabilized Silicon Analogue of Acylium Ion: Synthesis, Structure, Reactivity, and Theoretical Studies. *J. Am. Chem. Soc.* **2015**, *137*, 5828−5836. (d) Hansen, K.; Szilvási, T.; Blom, B.; Irran, E.; Driess, M. From an Isolable Acyclic Phosphinosilylene Adduct to Donor-Stabilized Si = E Compounds (E = O, S, Se). *Chem. - Eur. J.* **2015**, *21*, 18930−18933. (e) Troadec, T.; Lopez Reyes, M.; Rodriguez, R.; Baceiredo, A.; Saffon-Merceron, N.; Kato, T. Donor-Stabilized Silacyclobutanone: A Precursor of 1-Silaketene via Retro-[2 + 2]-Cycloaddition Reaction at Room Temperature. *J. Am. Chem. Soc.* **2016**, *138*, 2965−2968.

(36) (a) Yao, S.; Brym, M.; van Wüllen, C.; Driess, M. From a Stable Silylene to a Mixed-Valent Disiloxane and an Isolable Silaformamide−Borane Complex with Considerable Silicon−Oxygen Double-Bond Character. *Angew. Chem., Int. Ed.* **2007**, *46*, 4159−4162. (b) Xiong, Y.; Yao, S.; Driess, M. Silicon Analogues of Carboxylic Acids: Synthesis of Isolable Silanoic Acids by Donor−Acceptor Stabilization. *Angew. Chem., Int. Ed.* **2010**, *49*, 6642−6645. (c) Xiong, Y.; Yao, S.; Driess, M. Coordination of a Si = O subunit to metals: complexes of donor-stabilized silanone featuring a terminal Si = O→M coordination (M = Zn, Al). *Dalton Trans* **2010**, *39*, 9282−9287. (d) Gao, Y.; Hu, H.; Cui, C. The Reactivity of a Silacyclopentadienylidene towards Aldehydes: Silole Ring Expansion and the Formation of Base-Stabilized Silacyclohexadienones. *Chem. - Eur. J.* **2011**, *17*, 8803−8806. (e) Muraoka, T.; Abe, K.; Haga, Y.; Nakamura, T.; Ueno, K. Synthesis of a Base-Stabilized Silanone-Coordinated Complex by Oxygenation of a (Silyl)(silylene)tungsten Complex. *J. Am. Chem. Soc.* **2011**, *133*, 15365−15367. (f) Ghadwal, R. S.; Azhakar, R.; Roesky, H. W.; Pröpper, K.; Dittrich, B.; Goedecke, C.; Frenking, G. Donor−acceptor stabilized silaformyl chloride. *Chem. Commun.* **2012**, *48*, 8186−8188. (g) Muraoka, T.; Abe, K.; Kimura, H.; Haga, Y.; Ueno, K.; Sunada, Y. Synthesis, structures, and reactivity of the base-stabilized silanone molybdenum complexes. *Dalton Trans* **2014**, *43*, 16610−16613. (h) Fukuda, T.; Hashimoto, H.; Sakaki, S.; Tobita, H. Stabilization of a Silaaldehyde by its η_2 Coordination to Tungsten. *Angew. Chem., Int. Ed.* **2016**, *55*, 188−192. (i) Lopez Reyes, M.; Troadec, T.; Rodriguez, R.; Baceiredo, A.; Saffon-Merceron, N.; Branchadell, V.; Kato, T. Donor/Acceptor-Stabilized 1-Silaketene: Reversible [2 + 2] Cycloaddition with Pyridine and Evolution by an Olefin Metathesis Reaction. *Chem. - Eur. J.* **2016**, *22*, 10247−10253. (j) Muraoka, T.; Kimura, H.; Trigagema, G.; Nakagaki, M.; Sakaki, S.; Ueno, K. Reactions of Silanone(silyl)tungsten and -molybdenum Complexes with MesCNO, $(Me_2SiO)_3$, MeOH, and H_2O: Experimental and Theoretical Studies. *Organometallics* **2017**, *36*, 1009−1018.

(37) (a) Filippou, A. C.; Baars, B.; Chernov, O.; Lebedev, Y. N.; Schnakenburg, G. Silicon−Oxygen Double Bonds: A Stable Silanone with a Trigonal-Planar Coordinated Silicon Center. *Angew. Chem., Int. Ed.* **2014**, *53*, 565−570. (b) Ishida, S.; Abe, T.; Hirakawa, F.; Kosai, T.; Sato, K.; Kira, M.; Iwamoto, T. Persistent Dialkylsilanone Generated by Dehydrobromination of Dialkylbromosilanol. *Chem. - Eur. J.* **2015**, *21*, 15100−15103. (c) Alvarado-Beltran, I.; Rosas-Sánchez, A.; Baceiredo, A.; Saffon-Merceron, N.; Branchadell, V.; Kato, T. A Fairly Stable Crystalline Silanone. *Angew. Chem., Int. Ed.* **2017**, *56*, 10481−10485. (d) Rosas-Sánchez, A.; Alvarado-Beltran, I.; Baceiredo, A.; Saffon-Merceron, N.; Massou, S.; Hashizume, D.; Branchadell, V.; Kato, T. Cyclic (Amino)(Phosphonium-Bora-Ylide)-Silanone: A Remarkably Room Temperature Persistent Silanone. *Angew. Chem., Int. Ed.* **2017**, *56*, 15916−15920.

(38) (a) Yao, S.; Xiong, Y.; Brym, M.; Driess, M. An Isolable Silanoic Ester by Oxygenation of a Stable Silylene. *J. Am. Chem. Soc.* **2007**, *129*, 7268−7269. (b) Ghadwal, R. S.; Azhakar, R.; Roesky, H. W.; Pröpper, K.; Dittrich, B.; Klein, S.; Frenking, G. Donor—Acceptor-Stabilized Silicon Analogue of an Acid Anhydride. *J. Am. Chem. Soc.* **2011**, *133*, 17552−17555. (c) Rodriguez, R.; Gau, D.; Troadec, T.; Saffon-Merceron, N.; Branchadell, V.; Baceiredo, A.; Kato, T. A Base-Stabilized Sila-β-Lactone and a Donor/Acceptor-Stabilized Silanoic Acid. *Angew. Chem., Int. Ed.* **2013**, *52*, 8980−8983. (d) Rodriguez, R.; Troadec, T.; Gau, D.; Saffon-Merceron, N.; Hashizume, D.; Miqueu, K.; Sotiropoulos, J.-M.; Baceiredo, A.; Kato, T. Synthesis of a Donor-Stabilized Silacyclopropan-1-one. *Angew. Chem., Int. Ed.* **2013**, *52*, 4426−4430. (e) Wang, Y.; Chen, M.; Xie, Y.; Wei, P.; Schaefer, H. F., III; Robinson, G. H. Stabilization of Silicon−Carbon Mixed Oxides. *J. Am. Chem. Soc.* **2015**, *137*, 8396−8399. (f) Wang, Y.; Chen, M.; Xie,

DOI: 10.1021/jacs.9b05318
J. Am. Chem. Soc. 2019, 141, 13536−13546

Y.; Wei, P.; Schaefer, H. F., III; Schleyer, P. v. R.; Robinson, G. H. Stabilization of elusive silicon oxides. *Nat. Chem.* **2015**, *7*, 509−513. (g) Rodriguez, R.; Gau, D.; Saouli, J.; Baceiredo, A.; Saffon-Merceron, N.; Branchadell, V.; Kato, T. A Stable Monomeric SiO_2 Complex with Donor−Acceptor Ligands. *Angew. Chem., Int. Ed.* **2017**, *56*, 3935−3939. (h) Do, D. C. H.; Protchenko, A. V.; Ángeles Fuentes, M.; Hicks, J.; Kolychev, E. L.; Vasko, P.; Aldridge, S. A β-diketiminate stabilized sila-acyl chloride: systematic access to base-stabilised silicon analogues of classical carbonyl compounds. *Angew. Chem., Int. Ed.* **2018**, *57*, 13907−13911. (i) Rodriguez, R.; Alvarado-Beltran, I.; Saouli, J.; Saffon-Merceron, N.; Baceiredo, A.; Branchadell, V.; Kato, T. Reversible CO_2 Addition to a Si = O Bond and Synthesis of a Persistent SiO_2−CO_2 Cycloadduct Stabilized by a Lewis Donor−Acceptor Ligand. *Angew. Chem., Int. Ed.* **2018**, *57*, 2635−2638.
(39) Bondi, A. van der Waals Volumes and Radii. *J. Phys. Chem.* **1964**, *68*, 441−451.

DOI: 10.1021/jacs.9b05318
J. Am. Chem. Soc. 2019, 141, 13536−13546

5. DMAP-stabilized bis(silyl)silylenes as versatile synthons for organosilicon compounds

Title: "DMAP-stabilized bis(silyl)silylenes as versatile synthons for organosilicon compounds"[280]

Status: Paper; published online: January 21, 2020.

Journal: *RSC Advances* **2020**, *10*(6), 3402–3406.

Publisher: Royal Society of Chemistry (RSC)

DOI: 10.1039/C9RA10628F

Authors: Richard Holzner, Dominik Reiter, Philipp Frisch, and Shigeyoshi Inoue[a]

Reprinted with permission of the Royal Society of Chemistry. © Royal Society of Chemistry 2020.

Content: The concept of Lewis base-stabilization is a well-established method in modern main group chemistry and especially in organosilicon chemistry to achieve the isolation of otherwise elusive compounds. However, the resulting additional electron donation into the free $3p_z$ orbital of silylenes significantly reduces the electrophilicity and thus the overall reactivity of the respective donor-acceptor adducts.

This publication represents a continuation of the acyclic bis(silyl)silylene project and focuses on the isolation and reactivity investigations of novel DMAP-supported bis(silyl)silylenes, including the first bis(hypersilyl)silylene derivative. In sharp contrast to the more common NHC-silylene adducts, the inherently weaker donor-acceptor interaction of DMAP-stabilized bis(silyl)silylenes enabled a facile dissociation at elevated temperatures. Accordingly, the liberation of DMAP provided convenient access to the corresponding, extremely reactive donor-free silylenes. Interestingly, variation of the substitution pattern of the silyl ligand framework led to varying isomerization pathways and formation of different silylene decomposition products. In addition to the synthesis of a disiletane (C–H bond activation) and a trisilirane (1,2-silyl migrations followed by Si–Si bond insertion), the unique formation of a rare example of an azasilepin (dearomative *Buchner*-type ring expansion) was observed. Since the DMAP-stabilized bis(silyl)silylenes exhibited thermally induced selective activation of small molecules, such as H_2 and ethylene, these adducts can be considered as suitable synthetic equivalents of transient donor-free bis(silyl)silylenes. Moreover, the preparation of unknown DMAP-coordinated silaimines was achieved.

In the course of our studies on the unfortunately unsuccessful synthesis of $(^t\mathrm{Bu_3Si})_2\mathrm{Si(DMAP)}$, we isolated instead the novel silylene radical anion $[\mathrm{K(tol)_2}][(^t\mathrm{Bu_3Si})_2\mathrm{Si}]$ after over-reduction of $(^t\mathrm{Bu_3Si})_2\mathrm{SiBr_2}$ with excess $\mathrm{KC_8}$. Since, the reactivity of alkali metal-substituted silyl radicals is virtually unexplored, future research could provide access to functionalized new silyl radicals *via* salt metathesis reactions.

[a]R. Holzner and D. Reiter planned and executed all experiments and co-wrote the manuscript. P. Frisch carried out the SC-XRD measurements and processed the corresponding data. All work was performed under the supervision of S. Inoue.

RSC Advances

ROYAL SOCIETY OF CHEMISTRY

PAPER

View Article Online
View Journal | View Issue

Check for updates

Cite this: *RSC Adv.*, 2020, **10**, 3402

DMAP-stabilized bis(silyl)silylenes as versatile synthons for organosilicon compounds†

Richard Holzner,‡ Dominik Reiter,‡ Philipp Frisch and Shigeyoshi Inoue *

Received 17th December 2019
Accepted 6th January 2020

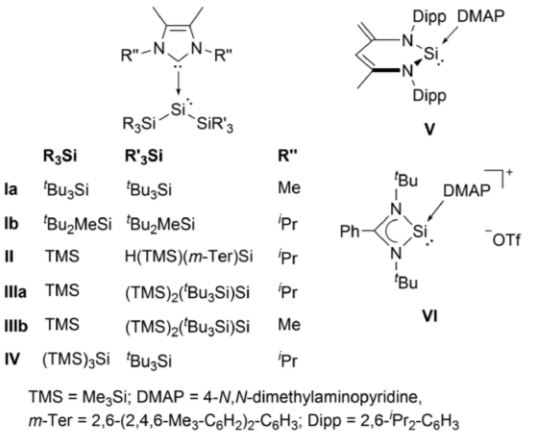
DOI: 10.1039/c9ra10628f

rsc.li/rsc-advances

DMAP-stabilized silylenes **1a–c** are obtained from the reductive debromination of the corresponding dibromosilanes in the presence of DMAP. Their distinctly different thermal isomerization reactions *via* C–H bond activation, dearomative ring expansion and silyl migration are discussed. Furthermore, complexes **1** dissociate at elevated temperatures, providing the corresponding free silylenes *in situ*, which are even capable of single-site activation of H_2. Additionally, a potassium-substituted silicon-centered radical **2** is isolated from overreduction of $(^tBu_3Si)_2SiBr_2$.

Introduction

Silylenes (R_2Si:), the heavier congeners of carbenes (R_2C:) have attracted much attention in modern main group chemistry in recent years.[1] The substituents R can either be monodentate, or cyclic, bidentate ligands, as in the case of the extensively studied class of *N*-heterocyclic silylenes (NHSis). In general, silylenes possess a lone pair of electrons and an empty $3p_z$ orbital and can therefore display ambiphilic reaction behaviour both as Lewis bases and Lewis acids. This particular reactivity profile even enables the facile activation of small molecules.[2] Thus, silylenes are considered to be promising candidates for metal-free catalysis.[2] In contrast to carbenes, however, the singlet ground state is energetically favoured for almost all reported silylenes. The two sole exceptions are transient silylenes bearing two bulky and strongly electropositive supersilyl ($^tBu_3Si$) substituents, or both supersilyl groups and alkali metal substituents. However, these species were only generated and analyzed *in situ* at temperatures below 15 K.[3] These reports already underline the peculiarity of bis(silyl)silylenes. In fact, no room temperature stable, two-coordinate derivative has been isolated to date. In all synthetic attempts the extremely reactive bis(silyl)silylene was not stable and either silyl migration[4] or C–H bond activation occurred, even at low temperatures.[3a] Very recently, we presented a bis(silyl)silylene that undergoes reversible isomerization to the corresponding tetra(silyl)disilene.[5] Although this compound is relatively stable, it eventually decomposes *via* insertion of the silylene moiety into a C–H bond of a substituent. A convenient method to stabilize silylenes is to control their excessive electrophilicity by coordination of a Lewis base, as already recognized by Tokitoh and co-workers in 1997.[6] In fact, electron donation from *N*-heterocyclic carbenes (NHCs) was the only way so far to isolate bis(silyl)silylenes.[7] Sekiguchi *et al.* successfully employed this approach and obtained the NHC-stabilized silylenes **I** (Fig. 1).[8] Lately, several additional examples of acyclic bis(silyl)silylene NHC complexes were reported by Cowley (**II**)[9] and by our group (**III** and **IV**).[5] Besides those acyclic representatives, the groups of Schesch-kewitz[10] and Lips[11] synthesized NHC-stabilized silylenes with the low-coordinate silicon center being embedded in a three-membered silicon cycle. Although electron-donation of NHCs to the vacant p-orbital of silylenes is an effective method to allow isolation of these compounds, it brings the downside of a significantly reduced reactivity. Accordingly, none of the



	R_3Si	R'_3Si	R"
Ia	$^tBu_3Si$	$^tBu_3Si$	Me
Ib	$^tBu_2MeSi$	$^tBu_2MeSi$	^{i}Pr
II	TMS	H(TMS)(*m*-Ter)Si	^{i}Pr
IIIa	TMS	$(TMS)_2(^tBu_3Si)Si$	^{i}Pr
IIIb	TMS	$(TMS)_2(^tBu_3Si)Si$	Me
IV	$(TMS)_3Si$	$^tBu_3Si$	^{i}Pr

TMS = Me_3Si; DMAP = 4-*N*,*N*-dimethylaminopyridine, *m*-Ter = 2,6-(2,4,6-Me_3-C_6H_2)$_2$-C_6H_3; Dipp = 2,6-^{i}Pr$_2$-C_6H_3

Fig. 1 Acyclic NHC-stabilized bis(silyl)silylenes **I–IV** and low-coordinate silicon DMAP complexes **V** and **VI**.

Department of Chemistry, WACKER-Institute of Silicon Chemistry and Catalysis Research Center, Lichtenbergstraße 4, 85748 Garching bei München, Germany. E-mail: s.inoue@tum.de

† Electronic supplementary information (ESI) available: Experimental details and crystallographic data. CCDC 1967942–1967945. For ESI and crystallographic data in CIF or other electronic format see DOI: 10.1039/c9ra10628f

‡ R. H. and D. R. contributed equally to this work.

This journal is © The Royal Society of Chemistry 2020

examples listed is capable of activating small molecules such as dihydrogen. Therefore, a weaker donor–acceptor interaction is necessary to achieve a balance between reactivity and stability of the respective bis(silyl)silylene compounds. 4-*N*,*N*-Dimethylaminopyridine (DMAP) is a much weaker Lewis base, compared to NHCs and was already applied by the groups of Driess[12] and So[13] to isolate the low-coordinate silicon donor–acceptor complexes **V** and **VI**. Thus, we envisioned DMAP to be a suitable Lewis base, strong enough to stabilize elusive bis(silyl)silylenes, yet weak enough to partially maintain their reactivity. Very recently, we reported the first acyclic bis(silyl)silylene–DMAP adduct **1a** (*cf.* Scheme 1).[5]

Herein, we extend this class of donor-stabilized, highly reactive bis(silyl)silylenes. Decomposition pathways and reactivity of these novel silylenes are presented and discussed in detail. Additionally, we report the synthesis and characterization of the potassium-substituted silyl radical **2**.

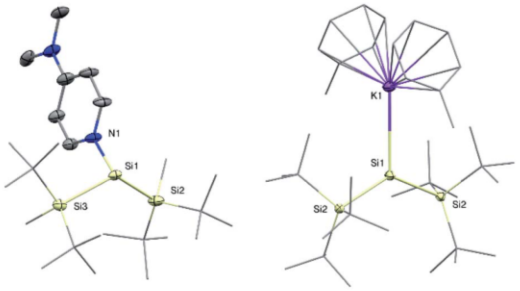


Fig. 2 Molecular structures of silylene **1b** (left) and silyl radical **2** (right) with thermal ellipsoids drawn at the 30% probability level. Hydrogen atoms are omitted for clarity. Selected bond lengths [Å] and angles [°]: **1b**: Si1–N1 1.937(5), Si1–Si2 2.390(3), Si1–Si3 2.378(3), Si2–Si1–Si3 123.1(1), Si2–Si1–N1 96.2(2), Si3–Si1–N1 98.8(2); **2**: Si1–Si2 2.3936(14), Si1–K1 3.315(2), K1–Si1–Si2 114.91(2), Si2–Si1–Si2* 130.19(3).

Results and discussion

Synthesis of novel DMAP–silylene complexes 1 and radical 2

In an approach analogue to the synthesis of **1a**, we obtained the donor-stabilized bis(silyl)silylene **1b** from the reductive debromination of the corresponding dibromosilane with KC_8 in presence of DMAP (Scheme 1). Silylene **1b** was obtained as red-brown crystals in excellent yield (92%) and fully characterized. Neither the formation of any decomposition products, nor of the disilene $(^tBu_2MeSi)_2Si{=}Si(Si^tBu_2Me)_2$ [14] was observed during the synthesis. Compared to compound **1a**, the ^{29}Si NMR signal of the silylene Si atom in **1b** is slightly upfield-shifted to 61.5 ppm (68.8 ppm in **1a**). Single crystal X-ray diffraction (SC-XRD) analysis revealed a Si:–N^{DMAP} bond length in compound **1b** of 1.937(5) Å (Fig. 2). This value is essentially identical to that in **1a** (1.942(2) Å)[5] and clearly within the range of previously reported low-coordinate silicon–DMAP donor–acceptor complexes (1.84–2.01 Å).[9,12,13,15] The high degree of pyramidalization around the silylene center in **1b** (sum of bond angles $\Sigma\theta = 318.1°$) results from the stereo-chemically active electron lone pair and also compares very well to **1a** ($\Sigma\theta = 318.7°$).[5]

Additionally, the steric hindrance of the silylene center was increased by introducing bulky hypersilyl groups ($(TMS)_3Si$), resulting in complex **1c**. Compound **1c**, which is the first stable bis(hypersilyl)silylene species, was identified by the characteristic ^{29}Si NMR signal of the low-coordinate silicon nucleus (72.5 ppm), similar to the resonances of **1a** and **1b**.[5] Remarkably, in this case, the facile TMS-migrations were prevented by the coordination of DMAP and the silylene could be stabilized successfully. In sharp contrast, we were not able to isolate the bis(hypersilyl)silylene moiety with NHCs. This result underlines the difference in reactivity between NHCs and the weaker Lewis base DMAP. Unfortunately, the reaction was accompanied by the by-product formation of hexakis(trimethylsilyl)trisilirane (**4**) and $Si(TMS)_4$, reflecting the high propensity of hypersilyl groups towards TMS-group migrations.

Despite several attempts, we were not able to isolate the DMAP-stabilized bis(supersilyl) silylene $(^tBu_3Si)_2Si{:}\leftarrow$ DMAP with the same approach used for the syntheses of **1**. Even at low temperatures, the reduction of the corresponding dibromosilane only afforded the decomposition product of the free silylene (disiletane from C–H bond activation).[3a] With an excess of 3.5 equivalents of KC_8, however the potassium-substituted silyl radical **2** was generated, even in the presence of DMAP. The solid state structure of **2** was unambiguously determined by SC-XRD analysis (Fig. 2). Silyl radical **2** exhibits a completely planar geometry (sum of bond angles $\Sigma\theta = 360.0°$) which is typical for alkali metal-substituted silyl radicals.[16] The Si–K bond distance (3.315(2) Å) is in the same range as observed in four-coordinate potassium silanides, such as hypersilyl potassium (3.352(4) Å).[4a] Thus compound **2** is clearly a contact ion pair in the solid state. Unfortunately, **2** is extremely sensitive and decomposes in toluene solution. Therefore, no satisfactory spectroscopic data was obtained. After synthesis in absence of DMAP and

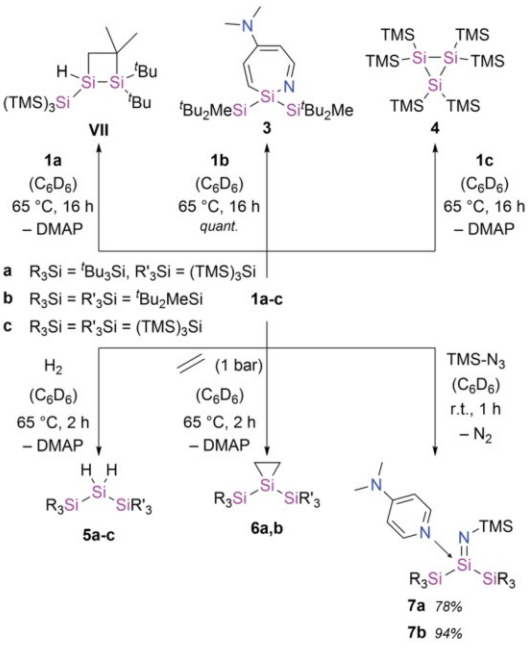


Scheme 1 Synthesis of DMAP-stabilized silylenes **1a–c** and silyl radical **2**.

stabilization by crown ether (18-C-6) however, we were able to obtain an EPR spectrum which contains a signal with a *g* value of 2.0056 and a hyperfine coupling $a(\alpha\text{-}^{29}\text{Si}) = 2.92$ mT (see ESI, Fig. S7†). Coupling with the β-^{29}Si nuclei was not observable. This *g* value is in the same range, as it was reported for other alkali metal-substituted silyl radicals.[16,17] Furthermore, no signal splitting from coupling of the unpaired electron with the K nucleus was observed. Presumably, in solution, compound **2** in presence of crown ether exists as solvent-separated ion pair. This observation is consistent with reports of a potassium substituted silyl radical.[16]

Thermally induced isomerization of 1

With the novel silylene complexes **1** in hand, we initially tested their thermal stability. Silylene **1a** isomerizes to the respective disiletane **VII** *via* DMAP dissociation and subsequent C–H bond activation at elevated temperatures (Scheme 2). The same product, that was observed for the decomposition of the donor-free disilene/silylene equilibrium mixture.[5] Surprisingly, upon heating compound **1b** to 65 °C, the silylene fragment inserts into the pyridine ring of DMAP, generating azasilepin **3** by dearomative ring expansion in quantitative yield. Silepin formation *via* insertion of a silylene into an aromatic ring system has previously been reported,[18] oftentimes either thermally[19] or photochemically[20] induced. After transformation from **1b** to **3** and thus increase of the coordination number, the ^{29}Si NMR signal of the central silicon atom is strongly upfield-shifted to −28.1 ppm. This value is comparable to that of a similar compound, reported by Tokitoh *et al.* from the reaction of a transient, *in situ* generated bis(aryl)silylene with DMAP (−20.8 ppm).[21] In comparison to **1b**, the Si–N bond distance in **3** is shortened by 10% to 1.750(1) Å, indicating a covalent bonding-type instead of the dative interaction in **1b**. This bond length is identical to that in Tokitoh's azasilepin.[21] Furthermore, the Si center adopts a tetrahedral coordination sphere within the boat-shaped, seven-membered heterocyclic ring (*cf.* Fig. 3). In sharp contrast to the related compounds **1a** and **1b** however, the thermal decomposition of silylene **1c** does not proceed *via* C–H, or C–N bond activation, but in fact by silyl migration. At 65 °C, **1c** isomerizes under liberation of DMAP to the cyclic silane **4**, which was already observed from rearrangement of $((TMS)_3Si)_2Si$: in the attempted synthesis of the free silylene.[4a,d]



Scheme 2 Thermally-induced decomposition of silylenes **1** and synthesis of hydrosilanes **5**, siliranes **6** and silaimines **7**.

Small molecule activation by silylenes 1

Single-site activation of the enthalpically strong, apolar dihydrogen molecule remains a challenging task for low-coordinate silicon compounds. So far, this was only achieved by few acyclic, donor-free silylenes and a masked iminosilyl silylene.[5,18a,22] In fact, to date, there are no reports of H_2 activation by a silylene base complex.

Although, the thermal decomposition reactions of **1a–c** strongly depend on the silyl substituents and proceed *via* three different mechanisms, they are all based on the extreme reactivity of the respective free silylene. Furthermore, the calculated Gibbs free bond-dissociation energy of **1a** (15.3 kcal mol^{-1}),[5] which is lower than for the analogous, NHC-coordinated (hypersilyl)(supersilyl)silylene **IV**[5] (16.3 kcal mol^{-1})[5] also suggests a higher reactivity of the DMAP–silylene complexes, compared to the NHC-stabilized bis(silyl)silylenes. Therefore, we conceived compounds **1a–c** to be easily accessible synthetic equivalents for these unstable, elusive, donor-free bis(silyl) silylenes and conducted a reactivity study towards activation of small molecules. Indeed, all three DMAP–silylenes underwent dihydrogen addition reactions upon heating to 65 °C, furnishing the reported corresponding dihydrosilanes **5a–c** in

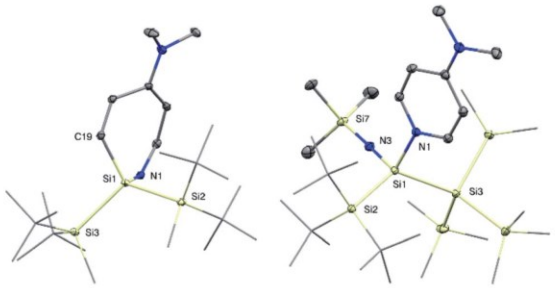


Fig. 3 Molecular structures of azasilepin **3** (left) and silaimine **7a** (right) with thermal ellipsoids drawn at the 30% probability level. Hydrogen atoms are omitted for clarity. Selected bond lengths [Å] and angles [°]: **3**: Si1–N1 1.750(1), Si1–C19 1.878(1), Si1–Si2 2.4144(6), Si2–Si1–Si3 113.74(2), Si2–Si1–N1 109.08(4), N1–Si1–C19 104.71(5); **7a**: Si1–Si2 2.453(1), Si1–N1 1.928(2), Si1–N3 1.616(2), N3–Si7 1.660(2), Si2–Si1–Si3 125.08(3), N1–Si1–N3 106.08(8), Si1–N3–Si7 177.1(1).

This journal is © The Royal Society of Chemistry 2020

quantitative yields. (Scheme 2).[5,23] Remarkably, the oxidative addition of dihydrogen to the DMAP–silylene complexes proceeds in a selective fashion, without the formation of the respective decomposition products. Free DMAP was simply removed from the product by precipitation with one equivalent of $SiBr_4$ and subsequent filtration. Notably, no reaction was observed upon exposure of NHC-stabilized bis(silyl)silylenes **Ia** and **IIIa** to H_2, even at elevated temperatures. This result underlines the inherently high reactivity of bis(silyl)silylene–DMAP complexes upon thermal dissociation of the stabilizing donor. Presumably, the H_2 addition to the silylene fragments of **1** proceeds *via* a bimolecular reaction similar to that proposed for the free silylene (^{t}Bu$_3$Si)((TMS)$_3$Si)Si:.[5]

Additional reactivity investigations were carried out with **1a** and **1b** due to their easier accessibility. Silirane formation – another classical silylene reactivity – was observed after treatment of **1a** and **1b** with ethylene, yielding compounds **6**. The ^{29}Si NMR shift of the central Si-atom in **6b** (−174.5 ppm) is similar to that of the earlier reported **6a** (−164.3 ppm).[5]

Since the isolation of the first silaimine by Wiberg *et al.* in 1985,[24] a number of these heavier imine analogues have been published. Besides donor free examples,[25] many silaimines need additional stabilization by a coordinating Lewis base, such as NHCs.[7] Interestingly, reaction of **1a** and **1b** with trimethylsilyl azide furnishes the DMAP-coordinated silaimines **7** under liberation of gaseous N_2. The ^{29}Si NMR signals of the central Si atoms in **7a** and **7b** were observed at −25.9 ppm and −25.5 ppm, respectively. Compared to a silaimine–pyridine adduct (δ^{29}Si = −12.6 ppm),[25b] these resonances are slightly upfield-shifted, presumably due to the electropositive silyl groups. In the solid state, compound **7a** displays a tetrahedral coordination sphere around the silicon center. Silaimine **7a** contains three unique Si–N bonds, distinguishable by their characteristic lengths: a short Si=N bond (1.616(2) Å), a significantly longer Si7–N3 single bond to the TMS group (1.660(2) Å) and an even further elongated, dative Si–N^{DMAP} bond (1.928(2) Å). The central Si=N distance is slightly longer, than in the donor-free silaimines, from the groups of Wiberg and Kira (1.57–1.59 Å)[25a,25c] and essentially identical to Klingebiel's silaimine–pyridine adduct (1.611(2) Å).[25b] Interestingly, the geometry of the imino group is almost linear (θ = 177.1(1)°). A similar observation was reported by Kira *et al.* and attributed to the electronic properties of the TMS group.[25c] Notably, compound **7a** slowly decomposes in solution under liberation of DMAP and probably formation of the donor-free silaimine, which decomposes further to a mixture of unidentified species. Complex **7b** instead is stable in solution.

Conclusions

In summary, we utilized our recently published method to synthesize two novel DMAP-stabilized silylenes **1b** and **1c**. Compound **1c** is the first stable bis(hypersilyl)silylene complex, which could be synthesized so far. Surprisingly, silyl radical **2** was obtained in a related fashion from the over-reduction of the corresponding dibromosilane. The silylene complexes **1a–c** turned out to undergo facile oxidative addition with dihydrogen and ethylene at relatively mild conditions. This remarkable reactivity originates from the respective free silylenes, which are generated *in situ* from dissociation of complexes **1**. Stabilization of transient bis(silyl)silylenes with DMAP is the only method so far to isolate these species and reactivate their extreme reactivity upon dissociation. Therefore, complexes **1** can be considered easily accessible, stable synthetic equivalents of otherwise elusive bis(silyl)silylenes. Additionally, the unprecedented, DMAP-coordinated silaimines **7** were isolated from the reactions of the silylene complexes with trimethylsilyl azide.

Conflicts of interest

The authors declare no conflict of interest.

Acknowledgements

We are exceptionally grateful to the WACKER Chemie AG and the European Research Council (SILION 637394) for continued financial support. We thank Dr Oksana Storcheva for the EPR measurements.

Notes and references

1 For selected reviews on silylenes see: (*a*) M. Haaf, T. A. Schmedake and R. West, *Acc. Chem. Res.*, 2000, **33**, 704–714; (*b*) B. Gehrhus and M. F. Lappert, *J. Organomet. Chem.*, 2001, **617–618**, 209–223; (*c*) S. Nagendran and H. W. Roesky, *Organometallics*, 2008, **27**, 457–492; (*d*) Y. Mizuhata, T. Sasamori and N. Tokitoh, *Chem. Rev.*, 2009, **109**, 3479–3511; (*e*) M. Kira, *Chem. Commun.*, 2010, **46**, 2893–2903; (*f*) M. Asay, C. Jones and M. Driess, *Chem. Rev.*, 2011, **111**, 354–396; (*g*) S. Yao, Y. Xiong and M. Driess, *Organometallics*, 2011, **30**, 1748–1767; (*h*) S. S. Sen, S. Khan, S. Nagendran and H. W. Roesky, *Acc. Chem. Res.*, 2012, **45**, 578–587; (*i*) S. S. Sen, S. Khan, P. P. Samuel and H. W. Roesky, *Chem. Sci.*, 2012, **3**, 659–682; (*j*) B. Blom and M. Driess, in *Functional Molecular Silicon Compounds II*, ed. D. Scheschkewitz, Springer, Cham, 2013, vol. 156, pp. 85–123.

2 (*a*) P. P. Power, *Nature*, 2010, **463**, 171–177; (*b*) C. Weetman and S. Inoue, *ChemCatChem*, 2018, **10**, 4213–4228.

3 (*a*) A. Sekiguchi, T. Tanaka, M. Ichinohe, K. Akiyama and S. Tero-Kubota, *J. Am. Chem. Soc.*, 2003, **125**, 4962–4963; (*b*) A. Sekiguchi, T. Tanaka, M. Ichinohe, K. Akiyama and P. P. Gaspar, *J. Am. Chem. Soc.*, 2008, **130**, 426–427.

4 (*a*) K. W. Klinkhammer, *Chem.–Eur. J.*, 1997, **3**, 1418–1431; (*b*) M. Ichinohe, R. Kinjo and A. Sekiguchi, *Organometallics*, 2003, **22**, 4621–4623; (*c*) K. Hassler, A. Dzambaski and J. Baumgartner, *Silicon Chem.*, 2008, **3**, 271–288; (*d*) C. Marschner, *Eur. J. Inorg. Chem.*, 2015, **2015**, 3805–3820; (*e*) S. K. Mueller, A. Dzambaski, N. Altenhuber, A. Torvisco, K. Hassler and M. Flock, *J. Mol. Struct.*, 2015, **1099**, 197–203; (*f*) M. Haas, A. Knoechl, T. Wiesner, A. Torvisco, R. Fischer and C. Jones, *Organometallics*, 2019, **38**, 4158–4170.

5 D. Reiter, R. Holzner, A. Porzelt, P. J. Altmann, P. Frisch and S. Inoue, *J. Am. Chem. Soc.*, 2019, **141**, 13536–13546.

6 N. Takeda, H. Suzuki, N. Tokitoh, R. Okazaki and S. Nagase, *J. Am. Chem. Soc.*, 1997, **119**, 1456–1457.

7 V. Nesterov, D. Reiter, P. Bag, P. Frisch, R. Holzner, A. Porzelt and S. Inoue, *Chem. Rev.*, 2018, **118**, 9678–9842.

8 H. Tanaka, M. Ichinohe and A. Sekiguchi, *J. Am. Chem. Soc.*, 2012, **134**, 5540–5543.

9 M. W. Stanford, J. I. Schweizer, M. Menche, G. S. Nichol, M. C. Holthausen and M. J. Cowley, *Angew. Chem., Int. Ed.*, 2019, **58**, 1329–1333.

10 A. Jana, I. Omlor, V. Huch, H. S. Rzepa and D. Scheschkewitz, *Angew. Chem., Int. Ed.*, 2014, **53**, 9953–9956.

11 B. J. Guddorf, A. Hepp and F. Lips, *Chem.–Eur. J.*, 2018, **24**, 10334–10338.

12 Y. Xiong, S. Yao, R. Müller, M. Kaupp and M. Driess, *J. Am. Chem. Soc.*, 2010, **132**, 6912–6913.

13 H.-X. Yeong, H.-W. Xi, Y. Li, K. H. Lim and C.-W. So, *Chem.–Eur. J.*, 2013, **19**, 11786–11790.

14 A. Sekiguchi, S. Inoue, M. Ichinohe and Y. Arai, *J. Am. Chem. Soc.*, 2004, **126**, 9626–9629.

15 T. Yamaguchi and A. Sekiguchi, *J. Am. Chem. Soc.*, 2011, **133**, 7352–7354.

16 S. Inoue, M. Ichinohe and A. Sekiguchi, *Organometallics*, 2008, **27**, 1358–1360.

17 (*a*) D. Bravo-Zhivotovskii, I. Ruderfer, S. Melamed, M. Botoshansky, B. Tumanskii and Y. Apeloig, *Angew. Chem., Int. Ed.*, 2005, **44**, 739–743; (*b*) S. Ishida, T. Iwamoto and M. Kira, *J. Am. Chem. Soc.*, 2003, **125**, 3212–3213; (*c*) G. Molev, D. Bravo-Zhivotovskii, M. Karni, B. Tumanskii, M. Botoshansky and Y. Apeloig, *J. Am. Chem. Soc.*, 2006, **128**, 2784–2785; (*d*) S. Inoue, M. Ichinohe and A. Sekiguchi, *J. Am. Chem. Soc.*, 2007, **129**, 6096–6097.

18 (*a*) D. Wendel, A. Porzelt, F. A. D. Herz, D. Sarkar, C. Jandl, S. Inoue and B. Rieger, *J. Am. Chem. Soc.*, 2017, **139**, 8134–8137; (*b*) S. Ishida, T. Tamura and T. Iwamoto, *Dalton Trans.*, 2018, **47**, 11317–11321.

19 (*a*) H. Suzuki, N. Tokitoh and R. Okazaki, *J. Am. Chem. Soc.*, 1994, **116**, 11572–11573; (*b*) H. Suzuki, N. Tokitoh and R. Okazaki, *Bull. Chem. Soc. Jpn.*, 1995, **68**, 2471–2481.

20 (*a*) M. Kira, S. Ishida, T. Iwamoto and C. Kabuto, *J. Am. Chem. Soc.*, 2002, **124**, 3830–3831; (*b*) M. Kira, S. Ishida, T. Iwamoto, A. de Meijere, M. Fujitsuka and O. Ito, *Angew. Chem., Int. Ed.*, 2004, **43**, 4510–4512; (*c*) T. Kosai, S. Ishida and T. Iwamoto, *Chem. Commun.*, 2015, **51**, 10707–10709.

21 Y. Mizuhata, T. Sato and N. Tokitoh, *Heterocycles*, 2012, **84**, 413–418.

22 (*a*) A. V. Protchenko, K. H. Birjkumar, D. Dange, A. D. Schwarz, D. Vidovic, C. Jones, N. Kaltsoyannis, P. Mountford and S. Aldridge, *J. Am. Chem. Soc.*, 2012, **134**, 6500–6503; (*b*) A. V. Protchenko, A. D. Schwarz, M. P. Blake, C. Jones, N. Kaltsoyannis, P. Mountford and S. Aldridge, *Angew. Chem., Int. Ed.*, 2013, **52**, 568–571.

23 (*a*) T. Gross, H. Reinke and H. Oehme, *Can. J. Chem.*, 2000, **78**, 1399–1404; (*b*) A. Sekiguchi, T. Fukawa, M. Nakamoto, V. Y. Lee and M. Ichinohe, *J. Am. Chem. Soc.*, 2002, **124**, 9865–9869.

24 N. Wiberg, K. Schurz and G. Fischer, *Angew. Chem., Int. Ed. Engl.*, 1985, **24**, 1053–1054.

25 (*a*) N. Wiberg, K. Schurz, G. Reber and G. Müller, *J. Chem. Soc., Chem. Commun.*, 1986, 591–592; (*b*) J. Niesmann, U. Klingebiel, M. Schäfer and R. Boese, *Organometallics*, 1998, **17**, 947–953; (*c*) T. Iwamoto, N. Ohnishi, Z. Gui, S. Ishida, H. Isobe, S. Maeda, K. Ohno and M. Kira, *New J. Chem.*, 2010, **34**, 1637–1645; (*d*) S. Inoue and K. Leszczyńska, *Angew. Chem., Int. Ed.*, 2012, **51**, 8589–8593; (*e*) J. Keuter, A. Hepp, C. Mück-Lichtenfeld and F. Lips, *Angew. Chem., Int. Ed.*, 2019, **58**, 4395–4399; (*f*) A. V. Protchenko, P. Vasko, D. C. H. Do, J. Hicks, M. Ángeles Fuentes, C. Jones and S. Aldridge, *Angew. Chem., Int. Ed.*, 2019, **58**, 1808–1812.

 This journal is © The Royal Society of Chemistry 2020

6. Silylated silicon carbonyl complexes: Mimics of ubiquitous transition metal carbonyls

Title: "Silylated silicon carbonyl complexes: Mimics of ubiquitous transition metal carbonyls"

Status: Article, revised Manuscript submitted

Journal: *Nature Chemistry* **2020**

Publisher: Nature Research

Authors: Dominik Reiter, Richard Holzner, Amelie Porzelt, Philipp Frisch, and Shigeyoshi Inoue[a]

Content: Transition metal carbonyls are ubiquitous and versatile complexes with a broad range of applications, especially in highly efficient industrial processes. Nevertheless, utilization of these key reagents still has significant disadvantages, such as the limited availability (high cost) and the frequently rather high toxicity of transition metals. Investigations on a possible replacement by more sustainable main group carbonyls are still in their infancy, as there is hardly any reported example. In particular, accounts of carbonyl complexes with the highly abundant and non-toxic element silicon have so far been limited to theoretical and argon-matrix isolation studies.

This contribution highlights the unprecedented preparation of the first isolable silicon carbonyl complexes. The novel silylene-CO adducts were accessible *via* selective carbonylation of the (donor-stabilized) bis(silyl)silylenes (*vide supra*) and were thoroughly analyzed both experimentally and computationally. Remarkably, these complexes feature a strong, transition metal-like CO-bonding motif with CO→Si σ donation and Si→CO π backbonding. The exceptional role of two sterically encumbered, electropositive silyl substituents proved to be elementarily important for the stabilization and isolation of the silicon carbonyl complexes, which partly explains the long absence of similar compounds due to the lack of suitable precursors. Despite their high thermal stability, the silylene-CO adducts still exhibit a preserved silylene reactivity similar to the related DMAP-stabilized bis(silyl)silylenes mentioned above. In contrast to the latter, however, significantly elevated temperatures are necessary to achieve dissociation and thus silylene isomerization or small molecule activation.

Moreover, the silicon carbonyl complexes displayed a conspicuous reactivity, reminiscent of transition metal carbonyls. Not only dissociation *via* photolysis was observed, but also CO substitution by a stronger donating isocyanide ligand. In addition, the CO moiety was successfully converted into a CN group upon reaction with $TMSN_3$. In view of the current discussion about low-coordinate organosilicon compounds mimicking transition metal complexes, these findings can be considered as further evidence of the untapped potential of acyclic silylenes.

[a]D. Reiter and R. Holzner planned and executed all experiments and analyzed the data. A Porzelt designed and conducted the computational investigations. P. Frisch performed the single-crystal X-ray diffraction measurements. S. Inoue designed and conceived the project. D. Reiter and S. Inoue wrote the manuscript with input and critical revision from all authors.

Silylated silicon carbonyl complexes: Mimics of ubiquitous transition metal carbonyls

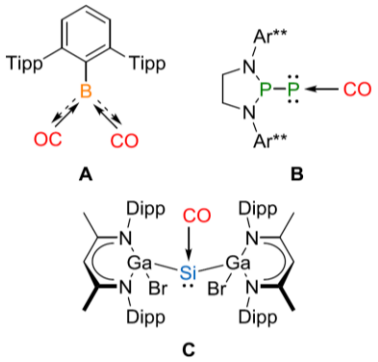
Dominik Reiter, Richard Holzner, Amelie Porzelt, Philipp Frisch, Shigeyoshi Inoue*

Silicon carbonyl complexes, compounds with silicon–CO (carbon monoxide) bonds, are long sought-after species that are largely unexplored. In fact, these elusive compounds have mainly been the subject of theoretical and/or low-temperature matrix isolation studies, but their instability has long precluded isolation under ambient conditions. Here we present the synthesis, unprecedented isolation and full characterization of stable silyl-substituted silicon carbonyl complexes, along with bonding analysis and initial reactivity investigations. Importantly, these complexes exhibit strong CO-bonding, with CO→Si σ donation and Si→CO π backbonding, which is reminiscent of transition metal carbonyls. This striking similarity between the abundant semi-metal silicon and rare transition metals provides new opportunities for the development of silicon-based catalysis.

Since the discovery of $PtCl_2(CO)_2$ by Schützenberger in 1868, transition metal carbonyl complexes (compounds with metal–CO bonds) have gained huge attention both in academia and industry[1-3]. In the following years, Hieber in particular played a pivotal role in the extensive development of transition metal carbonyls[4]. Today, these organometallic compounds are key reagents in numerous applications, including the Cativa process, hydroformylation, and the Pauson-Khand reaction[5]. Although these versatile processes are highly efficient, they still have considerable disadvantages. They often require expensive and rare transition metals, which raises questions of sustainability, and frequently use rather toxic metals, that have a negative impact on the environment. There has been a concerted effort in current chemical research to develop environmentally benign and sustainable processes that replace transition metals with ecologically and economically more advantageous main group elements[6-8]. However, despite intensive investigations, carbonyl complexes with elements other than transition metals remain rare.

Aside from several remarkable boron mono-carbonyl complexes[9], Braunschweig *et al.* have isolated borylene dicarbonyl complex **A**, a unique example of a multicarbonyl main group element adduct (Fig. 1)[10]. Apart from boron, phosphorus carbonyl compounds (including phosphaketene **B**)[11, 12] have been obtained and recently alkaline earth metal carbonyls[13] were observed in low-temperature matrix isolation studies. In addition, reports on carbonyl complexes with group 14 elements (carbon group) are also very rare. Thus, carbonylation of specific carbenes (R_2C:) led to the formation of ketenes (R_2C=C=O) instead of Lewis adducts (R_2C←CO)[14, 15].

Silicon, the heavier homologue of carbon and the second most abundant element in the earth's crust, has been demonstrated to participate in bonding situations, structures and reactivity patterns at the interface of transition metals and main group elements. Thus, not only the isolation of carbon analogous compounds, but also transition metal-like reactivity, such as the activation of small molecules, has already been demonstrated[16]. Together with its high availability and low toxicity, silicon therefore represents a very promising element for metal-free catalysis. Nevertheless, reports on silicon carbonyl complexes have so far been limited mainly to computational and matrix isolation studies[17-23]. It was found that linear silaketenes (R_2Si=C=O) are not even a minimum on the potential energy surface, but are merely the transition state for inversion of the Lewis adducts (R_2Si←CO). Recently, the reactivity of isolable silylenes (heavier carbenes; R_2Si:) toward CO has been investigated, but no silicon carbonyl complexes were obtained either[24-26]. Thus, the structural motif of these elusive compounds and their chemical behavior remained unclear. However, very recently, Schreiner/Schulz *et al.* isolated the first ambient temperature stable silicon carbonyl complex **C**, bearing a gallium-based ligand framework.[27]



Tipp = 2,4,6-^{i}Pr$_3$-C_6H_2, Dipp = 2,6-^{i}Pr$_2$-C_6H_3
Ar** = 2,6-[CH(4-^{t}Bu-C_6H_4)$_2$]$_2$-4-Me-C_6H_2

Fig. 1|Selected examples of isolable main group carbonyl complexes.

Department of Chemistry, WACKER-Institute of Silicon Chemistry and Catalysis Research Center, Technische Universität München, Lichtenbergstraße 4, 85748 Garching bei München, Germany. *E-Mail: s.inoue@tum.de

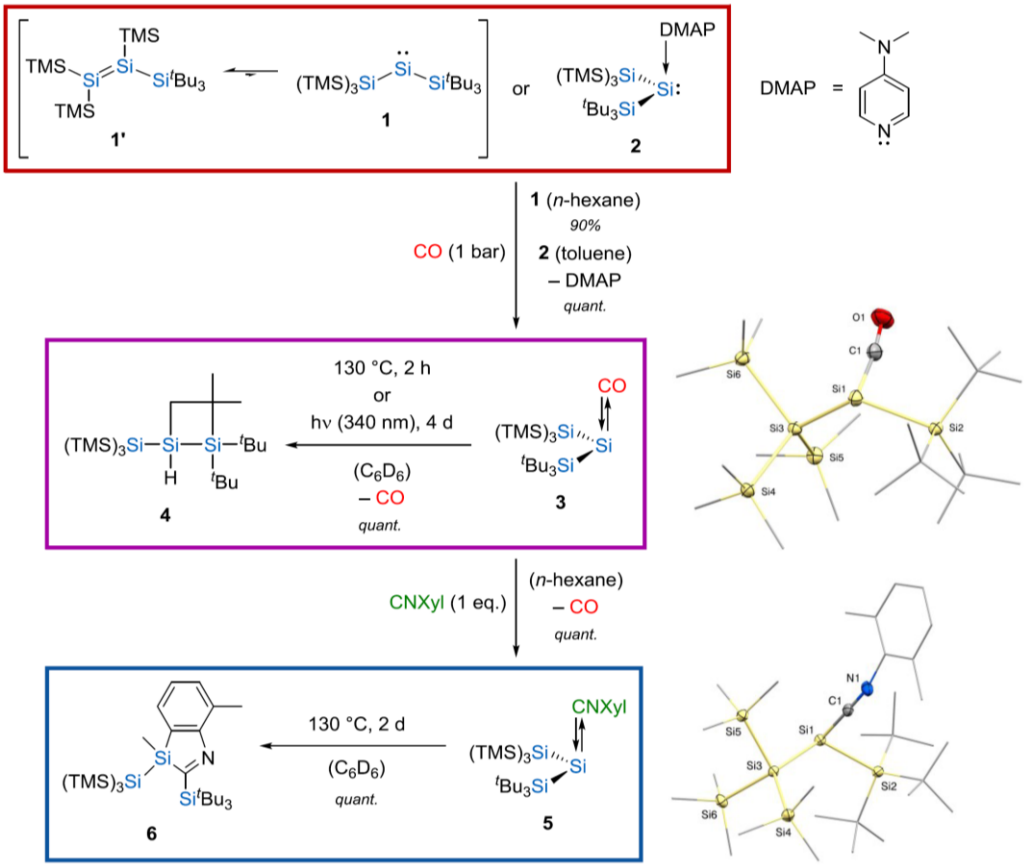


Fig. 2|Synthetic outlines. Synthesis and transition metal mimic chemistry of silicon carbonyl complex ((TMS)$_3$Si)(^{t}Bu$_3$Si)Si⇆CO (**3**) and silicon isocyanide complex ((TMS)$_3$Si)(^{t}Bu$_3$Si)Si⇆CNXyl (**5**), including the molecular structures of **3** and **5** with hydrogen atoms omitted for clarity. DMAP = 4-*N*,*N*-dimethylaminopyridine, CNXyl = 2,6-dimethylphenyl isocyanide.

Herein, we present the synthesis, isolation and initial reactivity investigations of the first structurally characterized metal-free silicon carbonyl complexes, which resemble classical transition metal carbonyls.

Exposure of an *n*-hexane solution of the recently reported equilibrium mixture containing bis(silyl)silylene **1** and its tetrasilyldisilene isomer **1'**[28] to CO (1 bar) at –30 °C resulted in a color change from blood-red to purple. Silicon carbonyl complex **3** was isolated as purple crystals in 90% yield after work-up and crystallization from *n*-hexane (Fig. 2). Alternatively, **3** can also be obtained by the reaction of 4-*N*,*N*-dimethylaminopyridine (DMAP)-stabilized bis(silyl)silylene **2**[28] with CO (1 bar) in quantitative yield. Bis(silyl)silylene carbonyl complex **3** exhibits a downfield-shifted signal in the ^{13}C nuclear magnetic resonance (NMR) spectrum at $\delta = 226.1$ ppm in comparison to the resonance observed for "free" carbon monoxide ($\delta = 184.5$ ppm) and compound **C** ($\delta = 206.5$ ppm)[27]. The silicon nucleus of the SiCO moiety resonates at $\delta = -228.5$ ppm in the ^{29}Si NMR spectrum, the typical region for silyl anions[16], but at lower field than that of complex **C** ($\delta = -256.5$ ppm). In addition, the observed signal is strongly upfield-shifted compared to Lewis adduct **2** ($\delta = 68.8$ ppm) and thus indicates a significantly stronger donor-acceptor interaction. Infrared (IR) spectroscopy revealed a substantial bathochromic shift (red shift) for the CO stretching mode at $\tilde{\nu} = 1908$ cm^{-1} with respect to that of free CO ($\tilde{\nu} = 2143$ cm^{-1})[29]. The absorption band is observed at even lower wavenumbers than those of the transient silicon carbonyl complexes studied by argon matrix isolation methods, the borylene dicarbonyl complex **A** and isolable silicon carbonyl complex **C** ($\tilde{\nu} = 2065$–1942 cm^{-1})[10, 18, 20, 21, 23, 27]. This remarkable red shift for the CO band is closely related to classical transition metal carbonyl complexes bearing π backbonding from the metal to the carbonyl moiety (terminal M–CO: $\tilde{\nu} = 2120$–1850 cm^{-1})[3].

The molecular structure of **3** was unambiguously confirmed by single-crystal X-ray diffraction (SC-XRD) analysis (Fig. 2), which revealed a strongly bent (trigonal pyramidal) structure with an angle between the Si2–Si1–Si3 plane and the Si1–C1 bond vector of $\theta = 103.7(1)°$ and an almost linear Si1–C1–O1 moiety (bond angle of 171.3(1)°). Furthermore, the C1–O1 distance (1.153(2) Å) is considerably elongated compared to those of gaseous CO (1.128 Å)[3] and **C** (1.136(7) Å)[27] and is essentially the same as that observed for typical transition metal carbonyls[3]. The short Si1–C1 bond length (1.794(2) Å) is significantly shorter than that of silicon carbonyl complex **C** (1.865(6) Å) and lies between the commonly observed Si=C double (1.70–1.76 Å) and Si–C single (1.87–1.93 Å) bonds[30].

Compound **3** is indefinitely stable at ambient temperature in the solid state and in solution under argon atmosphere. Silicon

carbonyl complex **3** shows a higher thermal stability than DMAP-stabilized bis(silyl)silylene **2** and only decomposes completely after 2 hours at 130 °C to disiletane **4** under liberation of CO. The formation of **4** originates from C–H bond activation of a *tert*-butyl group of bis(silyl)silylene **1** as reported previously[28].

Analogous to transition metal carbonyl complexes, photolysis of **3** (λ_{max} = 340 nm) resulted in the immediate liberation of CO with simultaneous color change from purple to blood-red and formation of **1**/**1′**. The photodissociation is partially reversible until disiletane **4** is irreversibly formed after 4 days of continuous irradiation. Since these results indicate a preserved silylene reactivity of **3**, we investigated the activation of the small molecules dihydrogen and ethylene. Although no reaction was observed at ambient temperature, silane ((TMS)$_3$Si)(^{t}Bu$_3$Si)SiH$_2$ and silirane (silacyclopropane) ((TMS)$_3$Si)(^{t}Bu$_3$Si)Si(CH$_2$CH$_2$) are formed selectively and rapidly upon irradiation[28]. These oxidative addition products can also be obtained *via* the thermally induced dissociation of **3**, but only with prolonged reaction times.

The combined analytical data suggest a bent donor-acceptor bonding motif (((TMS)$_3$Si)(^{t}Bu$_3$Si)Si⇆CO) with backdonation from the silylene moiety to the carbonyl group (strong Si1–C1 and weakened C1–O1 bond) for silicon carbonyl complex **3**.

To provide insight into the electronic structure of **3**, we performed calculations at the M06-2X/6-311+G(d,p)//M06-2X/6-31+G(d,p) level of density functional theory (DFT) including a variety of simplified model compounds (for details see Supplementary Information). This analysis revealed the bis(silyl)-substituted derivatives **3** and (TMS)$_2$SiCO (**I**), exhibiting the highest Si–C$_{CO}$ bond dissociation energies, as the energetically most preferred complexes with respect to complex formation (from the free silylenes), which is also reflected in the structural data of the complexes. Natural population analysis (NPA) charges of the model complexes clearly depict the silyl effect. The electropositive silyl groups with their strong σ donating nature increase the electron density at the central Si atom and thus change the polarization of the SiCO moiety (Fig. 3A) (*cf.* NPA charges of the central Si nuclei in (R)(R′)SiCO: **3**: –0.07; **I**: –0.02; **II** (R = CH$_3$ / R′ = Ph): 0.78; **III** (R = R′ = H): 0.23). In sharp contrast to **II** and **III**, both the central silicon atoms and the CO units in **I** and **3** have negative NPA charges, further highlighting π backdonation from the silylene centers to the carbonyl ligands being present. The calculated Wiberg bond indices (WBI; indication of the bond order) decrease going from **3** (1.31) to **I** (1.23), as an effect of the reduced steric demand of the silyl groups, and further upon exchange of the silyl groups in **II** (1.00) and **III** (0.97). Natural bond orbital (NBO) analysis of **3** revealed two bonds between the silylene and the CO moiety, bearing different polarization for the σ bond (27% Si1 sp$^{5.23}$/73% C1 sp$^{0.54}$) and the π bond (68% Si1 sp$^{7.02}$/32% C1 sp$^{17.11}$). Natural resonance theory (NRT) analysis unveiled a preference for the doubly bonded Si–C$_{CO}$ moiety even though second order perturbation theory revealed substantial electron donation from the oxygen lone pair into the π*(Si–C$_{CO}$) orbital. This is apparent in the natural localized molecular orbitals (NLMOs, Fig. 3B) with the oxygen lone pair bearing a contribution of the CO carbon atom (14%). In contrast, NBO and NRT analysis of the simplified model compound (TMS)$_2$SiCO (**I**) revealed only a singly bonded Si–C$_{CO}$ unit in line with the reduced WBI. While in the case of **II** electron donation from the silylene moiety to the CO solely occurs from the silylene lone pair, model compound **I** bears additional electron donation from the Si–Si bonds into the π*(CO) orbitals justifying the increased interaction.

Additional insights into the bonding situation of **3** were obtained using Bader's quantum theory of atoms in molecules (QTAIM)[31]. Accordingly, a strongly polar covalent interaction was found for the Si–C$_{CO}$ bond of **3**[32, 33] (see Supplementary Information, Table S12 and Figure S33) with the delocalization indices δ_{AB} (number of electron pairs shared between two atoms A and B) reflecting the elongated C–O bond and strong Si–C$_{CO}$ interaction with a decreased δ_{CO} (1.56; *cf.* free CO: δ_{CO} = 1.74) and a high δ_{SiC} (1.03), respectively. The 1D Laplacian profile along the Si–C$_{CO}$ bond path is rather indicative of a dative bonding situation[32, 34, 35]. The inherent π backbonding is consistent with a significant Si···O$_{CO}$ interaction present in **3** ($\delta_{Si\cdots O(CO)}$ = 0.17; model compounds **I**: $\delta_{Si\cdots O(CO)}$ = 0.17; **II**: $\delta_{Si\cdots O(CO)}$ = 0.13; **III**: $\delta_{Si\cdots O(CO)}$ = 0.12), reminiscent of the bonding situation in transition metal carbonyl complexes[32, 36].

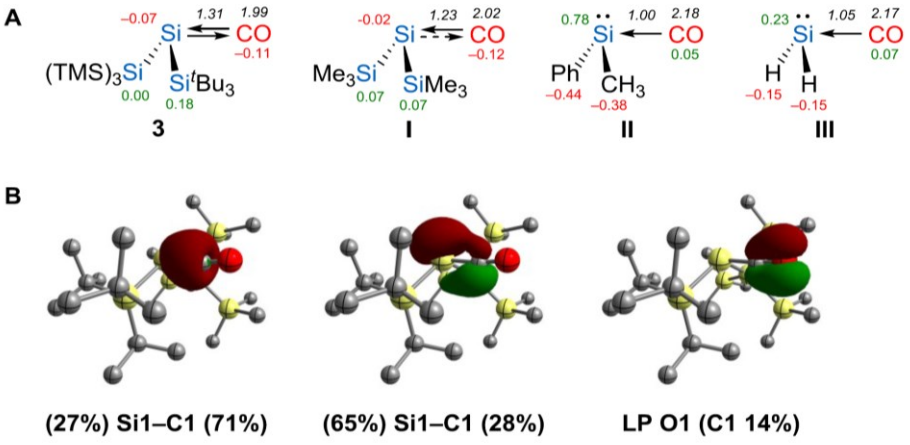


Fig. 3|Bonding analysis of ((TMS)$_3$Si)(^{t}Bu$_3$Si)SiCO (3). (A) Results from NBO analysis of **3** and the related simplified model compounds **I**, **II** and **III**. NPA charges (green and red) and WBIs (black). (**B**) NLMOs representing the Si1–C1 bonds and the electron pair at O1 in complex **3**.

To further investigate the decisive silyl effect experimentally, we exposed the recently reported acyclic iminosilyl- and iminosiloxysilylenes[37, 38] to CO and observed no reaction. However, reductive debromination of (^{t}Bu$_3$Si)$_2$SiBr$_2$ with potassium graphite (KC$_8$) in the presence of CO successfully provided the corresponding silicon carbonyl complex (^{t}Bu$_3$Si)$_2$Si⇆CO (**8**) (for details, see Supplementary Information).

To study the relationship of **3** to transition metal carbonyls in more detail, we turned to ligand exchange reactions. Upon treatment of **3** with 2,6-dimethylphenyl isocyanide (CNXyl) in *n*-hexane, an immediate color change from purple to dark blue was observable. The rare example of a silylene isocyanide complex **5** was obtained in quantitative yield after solvent removal (Fig. 2). The exchange reaction of these valence isoelectronic ligands is prototypical for transition metal carbonyl complexes and therefore another feature of silicon carbonyl complex **3** as a transition metal mimic[3, 39]. The driving force of the reaction is the stronger σ-donating nature of the isocyanide ligand compared to CO. ^{29}Si NMR spectroscopy revealed a downfield-shifted resonance for the SiCNXyl moiety at δ = –177.0 ppm compared to **3**, but a strong highfield shift with respect to other reported silicon isocyanide complexes (δ = 26 to –55.0 ppm)[40, 41]. IR spectroscopy unveiled a substantial red shift for the CN stretching mode at $\tilde{\nu}$ = 1966 cm^{-1} in comparison to that observed for free CNXyl ($\tilde{\nu}$ = 2119 cm^{-1}). SC-XRD analysis exposed a strongly bent molecular structure (θ = 107.3(1)°) with an almost linear Si1–C1–N1 bond angle (174.0(1)°) and a short Si1–C1 bond (1.819(2) Å).

Complex **5** is thermally more stable than compound **3** and isomerizes selectively and quantitatively to 1,3-azasilole **6** only after 2 days at 130 °C, analogous to an observation by Tokitoh *et al.* with a related complex[40]. Interestingly, intramolecular C–C bond activation and subsequent 1,2-silyl migration occurred, instead of Si–C$_{CNXyl}$ bond cleavage and formation of **4**, which is consistent with an increased bond dissociation energy of 40.8 kcal/mol for compound **5** in comparison to 29.8 kcal/mol for complex **3**. The combined experimental and theoretical data for complex **5** revealed a structural motif analogous to ((TMS)$_3$Si)(^{t}Bu$_3$Si)Si⇆CO (**3**) (see Supplementary Information for full analysis). Thus, **5** should be considered as a silicon isocyanide complex with π backbonding (((TMS)$_3$Si)(^{t}Bu$_3$Si)Si⇆CNXyl), reflecting the results of a recent theoretical study on metallylene isocyanide complexes[42].

Finally, we were interested in functionalizing the carbon monoxide moiety. Thus, we investigated the reactivity of silicon carbonyl complex **3** toward nucleophiles. Surprisingly, even at elevated temperatures, **3** does not react with water but is sensitive to oxygen under formation of an unidentified product mixture. Additionally, no reaction with MeOH, EtOH, MeLi and ^{t}BuLi was observed. Since transition metal carbonyls are known to react with azides to form isocyanato complexes (Fig. 4A)[43], we envisaged a similar reaction with **3**. Whereas no reaction of **3** with NaN$_3$ in THF was observed (even at elevated temperatures), treatment of **3** with trimethylsilyl azide (TMSN$_3$) resulted in a color change from purple to colorless with simultaneous conversion into a novel product. Multinuclear and 2D NMR studies, elemental analysis and mass spectrometry in combination with supportive DFT calculations identified the obtained compound as silyl cyanide ((TMS)$_3$Si)(^{t}Bu$_3$Si)Si(OTMS)(CN) (**7**) (Fig. 4B) (for details, see Supplementary Information). The experimentally observed NMR resonances are in good agreement with the calculated values ($\delta_{exp/cal}$(^{13}C$_{CN}$) = 131.4/133.2 ppm and $\delta_{exp/cal}$(^{29}Si$_{SiCN}$) = –27.6/–29.3 ppm). Despite the revealed similarity of **3** to transition metal carbonyls, silyl ether **7** is formed, not the silyl isocyanate analogous to the case of transition metals. However, this can be easily understood by considering the high oxophilicity of silicon, which provides alternative reaction pathways to favor Si–O bond formation.

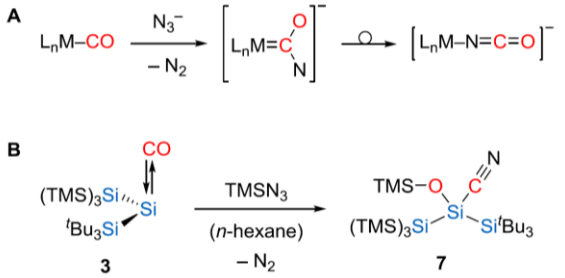


Fig. 4|Reactivity of carbonyl complexes with azides. (A) Formation of isocyanato complexes *via* reaction of transition metal carbonyls with azides. **(B)** Conversion of **3** with TMSN$_3$ to silyl cyanide **7**.

In conclusion, we have succeeded in synthesizing and fully characterizing the first isolable and room temperature stable silicon carbonyl complexes, which are reminiscent of traditional transition metal complexes in structure, bonding motif and reactivity. Besides photodissociation and exchange of the CO ligand by a stronger donor molecule, the CO moiety was successfully converted into a CN group. In addition to the close analogy to transition metal carbonyls, silicon carbonyl complexes showed novel reactivity profiles, which overall may enable new catalytic processes in the future.

1. Herrmann, W. A. 100 years of metal carbonyls: a serendipitous chemical discovery of major scientific and industrial impact. *J. Organomet. Chem.* **383**, 21-44 (1990).
2. Werner, H. Complexes of Carbon Monoxide and Its Relatives: An Organometallic Family Celebrates Its Birthday. *Angew. Chem. Int. Ed.* **29**, 1077-1089 (1990).
3. Holleman, A. F., Wiberg, E., Wiberg, N. *Lehrbuch der Anorganischen Chemie*. (de Gruyter, Berlin, 2007), vol. 102.
4. Behrens, H. The chemistry of metal carbonyls: "the life work of Walter Hieber". *J. Organomet. Chem.* **94**, 139-159 (1975).
5. Beller, M. *Catalytic Carbonylation Reactions*. Topics in Organometallic Chemistry (Springer-Verlag, Berlin Heidelberg, 2006), vol. 18.
6. Power, P. P. Main-group elements as transition metals. *Nature* **463**, 171-177 (2010).
7. Martin, D., Soleilhavoup, M., Bertrand, G. Stable singlet carbenes as mimics for transition metal centers. *Chem. Sci.* **2**, 389-399 (2011).
8. Weetman, C., Inoue, S. The Road Travelled: After Main-Group Elements as Transition Metals. *ChemCatChem* **10**, 4213-4228 (2018).
9. Légaré, M.-A., Pranckevicius, C., Braunschweig, H. Metallomimetic Chemistry of Boron. *Chem. Rev.* **119**, 8231-8261 (2019).
10. Braunschweig, H. *et al.* Multiple complexation of CO and related ligands to a main-group element. *Nature* **522**, 327-330 (2015).
11. Puschmann, F. F. *et al.* Phosphination of Carbon Monoxide: A Simple Synthesis of Sodium Phosphaethynolate (NaOCP). *Angew. Chem. Int. Ed.* **50**, 8420-8423 (2011).
12. Hansmann, M. M., Bertrand, G. Transition-Metal-like Behavior of Main Group Elements: Ligand Exchange at a Phosphinidene. *J. Am. Chem. Soc.* **138**, 15885-15888 (2016).
13. Wu, X. *et al.* Observation of alkaline earth complexes M(CO)$_8$ (M = Ca, Sr, or Ba) that mimic transition metals. *Science* **361**, 912-916 (2018).
14. Lavallo, V. *et al.* CO Fixation to Stable Acyclic and Cyclic Alkyl Amino Carbenes: Stable Amino Ketenes with a Small HOMO–LUMO Gap. *Angew. Chem. Int. Ed.* **45**, 3488-3491 (2006).
15. Hudnall, T. W., Bielawski, C. W. An *N,N'*-Diamidocarbene: Studies in C–H Insertion, Reversible Carbonylation, and Transition-Metal Coordination Chemistry. *J. Am. Chem. Soc.* **131**, 16039-16041 (2009).

16. Lee, V. Y. *Organosilicon Compounds: Theory and Experiment (Synthesis)*. (Academic Press, New York, 2017), vol. 1.
17. Pearsall, M. A., West, R. The reactions of diorganosilylenes with carbon monoxide. *J. Am. Chem. Soc.* **110**, 7228-7229 (1988).
18. Arrington, C. A., Petty, J. T., Payne, S. E., Haskins, W. C. K. The reaction of dimethylsilylene with carbon monoxide in low-temperature matrices. *J. Am. Chem. Soc.* **110**, 6240-6241 (1988).
19. Hamilton, T. P., Schaefer, H. F., III Silaketene: A product of the reaction between silylene and carbon monoxide? *J. Chem. Phys.* **90**, 1031-1035 (1989).
20. Tacke, M. *et al.* Complexes of decamethylsilicocene: $Cp_2^*Si(CO)$ and $Cp_2^*Si(N_2)$. *Z. Anorg. Allg. Chem.* **619**, 865-868 (1993).
21. Maier, G., Reisenauer, H. P., Egenolf, H. Quest for Silaketene: A Matrix-Spectroscopic and Theoretical Study. *Organometallics* **18**, 2155-2161 (1999).
22. Becerra, R., Cannady, J. P., Walsh, R. Silylene Does React with Carbon Monoxide: Some Gas-Phase Kinetic and Theoretical Studies. *J. Phys. Chem. A* **105**, 1897-1903 (2001).
23. Bornemann, H., Sander, W. Reactions of methyl(phenyl)silylene with CO and PH_3—the formation of acid–base complexes. *J. Organomet. Chem.* **641**, 156-164 (2002).
24. Protchenko, A. V. *et al.* Reduction of carbon oxides by an acyclic silylene: reductive coupling of CO. *Angew. Chem. Int. Ed.* **58**, 1808-1812 (2019).
25. Wang, Y. *et al.* Silicon-Mediated Selective Homo- and Heterocoupling of Carbon Monoxide. *J. Am. Chem. Soc.* **141**, 626-634 (2019).
26. Xiong, Y. *et al.* Homocoupling of CO and isocyanide mediated by a C,C′-bis(silylenyl)-substituted ortho-carborane. *Chem. Commun.* **56**, 747-750 (2020).
27. Ganesamoorthy, C. *et al.* A silicon–carbonyl complex stable at room temperature. *Nat. Chem.*, (2020; DOI: 10.1038/s41557-020-0456-x).
28. Reiter, D. *et al.* Disilene-Silylene Interconversion: A Synthetically Accessible Acyclic Bis(silyl)silylene. *J. Am. Chem. Soc.* **141**, 13536-13546 (2019).
29. Huber, K. P., Herzberg, G. *Molecular Spectra and Molecular Structure IV. Constants of Diatomic Molecules*. (Van Nostrand Reinhold Company, New York, 1979), vol. 4.
30. Fischer, R. C., Power, P. P. π-Bonding and the Lone Pair Effect in Multiple Bonds Involving Heavier Main Group Elements: Developments in the New Millennium. *Chem. Rev.* **110**, 3877-3923 (2010).
31. Bader, R. F. W. *Atoms in Molecules: A Quantum Theory*. (Oxford University Press, Oxford, 1990).
32. Macchi, P., Sironi, A. Chemical bonding in transition metal carbonyl clusters: complementary analysis of theoretical and experimental electron densities. *Coord. Chem. Rev.* **238-239**, 383-412 (2003).
33. Macchi, P., Sironi, A. *Interactions Involving Metals: From "Chemical Categories" to QTAIM and Backwards*. C. F. Matta, R. J. Boyd, Eds., The Quantum Theory of Atoms in Molecules: From Solid State to DNA and Drug Design (Wiley-VCH, Weinheim, 2007).
34. Schweizer, J. I. *et al.* A Disilene Base Adduct with a Dative Si–Si Single Bond. *Angew. Chem. Int. Ed.* **55**, 1782-1786 (2016).
35. Stanford, M. W. *et al.* Intercepting the Disilene-Silylsilylene Equilibrium. *Angew. Chem. Int. Ed.* **58**, 1329–1333 (2019).
36. Cabeza, J. A., Van der Maelen, J. F., García-Granda, S. Topological Analysis of the Electron Density in the N-Heterocyclic Carbene Triruthenium Cluster $[Ru_3(\mu\text{-}H)_2(\mu_3\text{-}MeImCH)(CO)_9]$ (Me_2Im = 1,3-dimethylimidazol-2-ylidene). *Organometallics* **28**, 3666-3672 (2009).
37. Wendel, D. *et al.* From Si(II) to Si(IV) and Back: Reversible Intramolecular Carbon–Carbon Bond Activation by an Acyclic Iminosilylene. *J. Am. Chem. Soc.* **139**, 8134-8137 (2017).
38. Wendel, D. *et al.* Silicon and Oxygen's Bond of Affection: An Acyclic Three-Coordinate Silanone and Its Transformation to an Iminosiloxysilylene. *J. Am. Chem. Soc.* **139**, 17193-17198 (2017).
39. Boyarskiy, V. P., Bokach, N. A., Luzyanin, K. V., Kukushkin, V. Y. Metal-Mediated and Metal-Catalyzed Reactions of Isocyanides. *Chem. Rev.* **115**, 2698-2779 (2015).
40. Takeda, N. *et al.* Synthesis and Properties of the First Stable Silylene–Isocyanide Complexes. *Chem. Eur. J.* **9**, 3530-3543 (2003).
41. Abe, T., Iwamoto, T., Kabuto, C., Kira, M. Synthesis, Structure, and Bonding of Stable Dialkylsilaketenimines. *J. Am. Chem. Soc.* **128**, 4228-4229 (2006).
42. Mansikkamäki, A., Power, P. P., Tuononen, H. M. Computational Analysis of n→π* Back-Bonding in Metallylene–Isocyanide Complexes R_2MCNR' (M = Si, Ge, Sn; R = ^{t}Bu, Ph; R′ = Me, ^{t}Bu, Ph). *Organometallics* **32**, 6690-6700 (2013).
43. Beck, W., Fehlhammer, W. P. Reactions of Metal Carbonyls with the Azide Ion and – vice versa – Reactions of Azido Complexes with Carbon Monoxide: Isocyanato Complexes. Analogous Reactions in NO^+/N_3^- Transition Metal Chemistry. *Z. Anorg. Allg. Chem.* **636**, 157-162 (2010).

Methods

Synthesis of ((TMS)$_3$Si)(^{t}Bu$_3$Si)Si⇆CO (3)

Silicon carbonyl complex **3** was obtained by two different methods, either by direct carbonylation of **1**/**1′** (Method A) or more conveniently by exposure of **2** to CO *via* a Lewis base exchange reaction (Method B):

Method A. A solution of **1**/**1′** (100 mg, 210 µmol) in *n*-hexane (3 mL) was cooled to –30 °C, degassed and exposed to CO (1 bar). Subsequently, the reaction mixture was warmed to ambient temperature, whereby a color change from blood-red to purple was observed. After stirring for 1 h, all volatiles were removed *in vacuo*. Purple crystals of **3** (95.0 mg, 189 µmol, 90%), which were suitable for single-crystal X-ray diffraction (SC-XRD) analysis, were obtained by cooling a concentrated *n*-hexane solution of **3** to –35 °C for several days.

Method B. A solution of **2** (600 mg, 1.00 mmol) in toluene (15 mL) was degassed and subsequently exposed to CO (1 bar) at room temperature. The reaction mixture was stirred for 5 h, whereby a color change from red-brown to purple was observed. After removal of all volatiles *in vacuo*, the residue was extracted with cold *n*-hexane (3 × 5 mL, –35 °C). DMAP was separated from the mixture *via* filtration. Removal of the solvent *in vacuo* provided **3** as a purple solid (505 mg, 1.00 mmol, quantitative yield).

Note: Removal of free DMAP is also possible by addition of an equimolar amount of silicon tetrabromide ($SiBr_4$) to the reaction mixture and subsequent filtration (DMAP forms an unidentified Lewis acid/base adduct with $SiBr_4$, which is insoluble in common organic solvents; no reaction of **3** with $SiBr_4$ in solution was detected at least within 1 day).

Silicon carbonyl complex **3** is indefinitely stable as a solid and in solution under argon atmosphere at ambient temperature, but slowly decomposes in solution at elevated temperatures (≥ 90 °C) to free, gaseous CO and disiletane **4**. **m.p.:** 76-77 °C (decomposition; color change from purple to black). **^{1}H NMR (500 MHz, C$_6$D$_6$, 300 K):** δ [ppm] = 1.23 (s, 27H, C(C*H*$_3$)$_3$), 0.39 (s, 27H, *TMS*). **^{13}C{^{1}H} NMR (126 MHz, C$_6$D$_6$, 300 K):** δ [ppm] = 226.1 (*C*O), 32.0 (C(*C*H$_3$)$_3$), 25.5 (*C*(CH$_3$)$_3$), 3.0 (*TMS*). **^{29}Si{^{1}H} NMR (99 MHz, C$_6$D$_6$, 300 K):** δ [ppm] = 42.8 (*Si*^{t}Bu$_3$), –6.9 (*TMS*), –119.0 (*Si*(TMS)$_3$), –228.5 (*Si*CO). **IR (solid):** $\tilde{\nu}$ [cm^{-1}] = 2950 (w), 2857 (m), 1908 (s) ($\tilde{\nu}_{CO}$), 1477 (w), 1388 (w), 1244 (m), 1011 (w), 826 (s), 684 (m), 622 (m), 468 (m). **Anal. Calcd. [%] for C$_{22}$H$_{54}$OSi$_6$:** C, 52.51; H, 10.82. Found [%]: C, 52.76; H, 10.54. **UV-Vis (*n*-hexane, 298 K):** λ_{max} [nm] = 373 (theo.: 351; HOMO→LUMO+1). **LIFDI-MS:** calculated for **3** ($C_{22}H_{54}OSi_6$): 502.2790; observed: 502.3820.

The full experimental details and characterization of the new compounds can be found in the Supplementary Information.

Data availability

X-ray crystallographic data are available free of charge from the *Cambridge Crystallographic Data Centre* under the reference numbers CCDC 1976834 (**3**) and CCDC 1976835 (**5**) *via* https://www.ccdc.cam.ac.uk/structures/. All additional data are contained in the main text or the Supplementary Information.

Acknowledgments We thank Prof. Dr. M. C. Holthausen and Dr. J. I. Schweizer for fruitful discussions, computational resources, and advice. Quantum chemical calculations were performed in parts at the Leibniz Supercomputing Center of the Bavarian Academy of Science and Humanities. We acknowledge Maximilian Muhr (Prof. R. A. Fischer) for the LIFDI-MS measurement.

Funding We are exceptionally grateful to the WACKER Chemie AG and the European Research Council (SILION 637394) for continued financial support.

Author contributions: D.R. and R.H. planned and executed all experiments and analyzed the data. A.P. designed and conducted the computational investigations. P.F. performed the single-crystal X-ray diffraction measurements. S.I. designed and conceived the project. D.R. and S.I. wrote the manuscript with input and critical revision from all authors.

Competing interests: The authors declare no competing financial interest.

Additional information
Correspondence and requests for materials should be addressed to S.I.

7. Oxidation reactions of a versatile, two-coordinate, acyclic iminosiloxysilylene

Title: "Oxidation reactions of a versatile, two-coordinate, acyclic iminosiloxysilylene"[281]

Status: Paper, published online: April 30, 2020.

Journal: *Dalton Transactions* **2020**, *49* (21), 7060-7068.

Publisher: Royal Society of Chemistry (RSC)

DOI: 10.1039/D0DT01522A

Authors: Dominik Reiter, Philipp Frisch, Daniel Wendel, Fabian M. Hörmann, and Shigeyoshi Inoue[a]

Reprinted with permission of the Royal Society of Chemistry. © Royal Society of Chemistry 2020.

Content: Low-valent organosilicon compounds exhibit characteristics and a reactivity at the interface between carbon and transition metals. Two-coordinate silylenes and in particular their most reactive acyclic derivatives have been successfully applied in the activation of small molecules, a typical feature of transition metal complexes and generally a prerequisite for catalytic processes. Nevertheless, in addition to the small number of isolated representatives and the limited knowledge about their reactivity, catalytic applications involving acyclic silylenes have not yet been found.

This manuscript comprises a detailed investigation of the reactivity of a unique acyclic iminosiloxysilylene. The silylene was accessible *via* isomerization of the first isolable acyclic, neutral, three-coordinate iminosilylsilanone (*vide infra*). On the one hand, iminosiloxysilylene served as a transition metal mimic, since the formal oxidative addition of various challenging small molecules, such as white phosphorus and ammonia, was achieved under mild conditions. Moreover, a photochemically induced dearomative *Buchner*-type ring expansion of the flanking ligand framework, leading to the formation of a novel iminosiloxysilepin, was observed.

On the other hand, oxidation of the silylene represented a suitable platform to gain access to heavier carbon homologues. Direct oxygenation with O_2, N_2O and CO_2 resulted in the intermediary formation of novel siloxysilanones, which underwent subsequent reactions. Thus, both dimerization provided new cyclodisiloxanes and a [2+2] cycloaddition afforded a silicon carbonate complex. Interestingly, exposure of iminosiloxysilylene to N_2O in the presence of Lewis bases furnished rare examples of donor-stabilized silanoic ester derivatives.

On a final note, the synthesis of a novel acyclic silaimine was achieved *via* reaction of the silylene with an organosilyl azide. Remarkably, the silaimine served as an excellent reagent for small molecule activation, which was particularly highlighted in the formation of a unique oxatriazasilole. This striking 1,3-dipolar cycloaddition product with N_2O is unprecedented, even in the well-explored organic chemistry and offers new avenues for future research.

[a]D. Reiter planned and executed all experiments and wrote the manuscript. P. Frisch carried out the SC-XRD measurements and processed the corresponding data. D. Wendel and F. M. Hörmann contributed to several experiments and provided valuable mental input. All work was performed under the supervision of S. Inoue.

Dalton Transactions

ROYAL SOCIETY OF CHEMISTRY

PAPER

View Article Online
View Journal | View Issue



Cite this: *Dalton Trans.*, 2020, **49**, 7060

Oxidation reactions of a versatile, two-coordinate, acyclic iminosiloxysilylene†

Dominik Reiter, Philipp Frisch, Daniel Wendel, Fabian M. Hörmann and Shigeyoshi Inoue *

Received 26th April 2020,
Accepted 29th April 2020

DOI: 10.1039/d0dt01522a

rsc.li/dalton

Due to their outstanding reactivity, acyclic silylenes have emerged as attractive organosilicon alternatives for transition metal complexes on the way to metal-free catalysis. However, exploration of their reactivity is still in its infancy, as only a few derivatives of this unique compound class have been isolated so far. Here, we present the results of an extensive reactivity investigation of the previously reported acyclic iminosiloxysilylene **1**. Divalent silylene **1** proved to be a versatile building block for a plethora of novel organosilicon compounds. Thus, not only the activation of the rather challenging targets NH_3 and P_4 could be achieved, but also the conversion into a reactive donor-free silaimine, which itself turned out to be a useful reagent for small molecule activation. In addition, **1** served as an excellent precursor for gaining access to donor-stabilized heavier carbonyl compounds. Our results thus provide further insights into the chemistry of low-valent silicon at the interface between carbon and transition metals.

Introduction

The vast majority of all catalytic processes are based on the use of transition metal complexes. Despite their almost unlimited range of applications, the utilization of transition metals also has disadvantages. For example, many of them are of limited availability and are therefore relatively expensive. Additionally, transition metal catalysts are often rather toxic and frequently remain in the end product. Modern main group chemistry tries to address these problems and pave the way for a more advantageous and sustainable catalysis.[1] The semi-metal silicon with its high availability (second most abundant element in the earth's crust) and non-toxicity seems to be an ideal candidate for the replacement of transition metals. Particularly low-coordinate organosilicon compounds are considered for metal-free catalysis due to their exceptionally high reactivity. So far, however, only a few examples of catalytic conversions using these derivatives are known.[2] Nevertheless, industry interest has already been raised and the WACKER Chemie AG recently even reported on the development of a highly efficient Si(II) catalysis.[3] Among low-valent silicon compounds, divalent silylenes (heavier carbene congeners; R_2Si:) and especially acyclic derivatives emerged as promising targets, due to their high potential in the activation of small molecules, such as hydrogen.[4] Compared to their cyclic counterparts, acyclic silylenes have more obtuse R–Si–R angles and hence smaller HOMO–LUMO and singlet–triplet energy gaps. Consequently, they are even more reactive than cyclic silylenes.

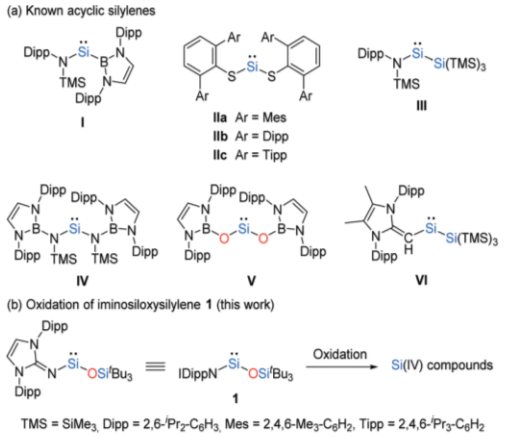
Small molecule activation is prototypical for transition metal complexes and usually represents the first step toward catalysis.[5] Therefore, knowledge about the reactivity of acyclic silylenes is essential for the development of possible future catalysts. Nevertheless, there is only a small number of acyclic, two-coordinate silylenes reported whose reactivity has been scarcely investigated.[6] Only in 2012 did Aldridge/Jones *et al.* and Power and colleagues simultaneously report on the first examples of acyclic silylenes with the isolation of aminoborylsilylene **I** and bis(arylthio)silylene **IIa** (Scheme 1).[6a,b] The pool of available compounds was later extended with **IIb,c**, aminosilylsilylene **III** and diaminosilylene **IV**.[6c–e]

Very recently, even the first dioxy- and vinylsilyl-substituted derivatives **V** and **VI** were synthesized.[6g,h] Apart from isolable, acyclic silylenes, several "masked" species were also isolated, which are generally present in a more stable form, but exhibit silylene reactivity. Tokitoh and colleagues reported a bis(aryl)silylene, accessible *via* thermal dissociation of its corresponding disilene dimer.[7] The remarkable equilibrium between a cyclotrisilene and a disilenyl silylene was demonstrated by Scheschkewitz and co-workers.[8] We have recently isolated a tetrasilyldisilene that serves as a source for its extremely reactive

Department of Chemistry, WACKER-Institute of Silicon Chemistry and Catalysis Research Center, Technische Universität München, Lichtenbergstraße 4, 85748 Garching bei München, Germany. E-mail: s.inoue@tum.de

†Electronic supplementary information (ESI) available: Experimental details including synthetic, spectroscopic and crystallographic. CCDC 1983560 (**13a**), 1983561 (**3**), 1983562 (**12a**), 1983563 (**11**), 1983564 (**7**), 1983565 (**6**) and 1983579 (**9**). For ESI and crystallographic data in CIF or other electronic format see DOI: 10.1039/d0dt01522a

This journal is © The Royal Society of Chemistry 2020



Scheme 1 (a) Reported isolable, acyclic, two-coordinate silylenes. (b) Structure and reactivity of iminosiloxysilylene **1**.

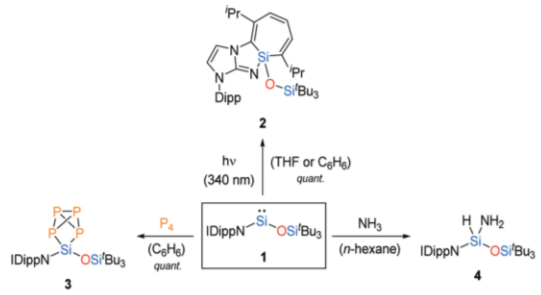
bis(silyl)silylene isomer through a 1,2-silyl migration.[9] Furthermore, reactive iminosilylsilylenes undergo reversible intramolecular, aromatic C=C bond activation reactions of their flanking ligand framework, providing stable silacycloheptatrienes (silepins).[6f,10] Lately, Cui *et al.* were able to isolate the first silanorcaradiene derivative, the intermediate of silepin formation, by intramolecular cyclopropanation of a transient triplet ground state boryllithiosilylene.[11] These known (masked) acyclic silylenes exhibit a reactivity reminiscent of traditional transition metal complexes, thus oxidative addition of challenging small molecules such as NH_3, CO_2, CO, H_2 and alkenes was achieved. Nevertheless, the chemistry of divalent acyclic silylenes is still largely unexplored. Here, we extend the reactivity studies of our recently reported two-coordinate iminosiloxysilylene (IDippN)(^{t}Bu$_3$SiO)Si: (**1**) (Scheme 1).[6f]

Results and discussion

Reactivity toward group 15 reagents

As reported previously, (IDippN)(^{t}Bu$_3$SiO)Si: (**1**) has a relatively small N–Si–O bond angle (103.7(1)°) and a high HOMO–LUMO energy gap (4.33 eV).[6f] Accordingly, no reaction toward H_2 was observed, even at elevated temperatures. However, exposure to ethylene selectively provided the respective silirane (IDippN)(^{t}Bu$_3$SiO)Si(CH$_2$CH$_2$).[6f] Only recently, we observed the activation of a ylidic C–H bond of a Wittig reagent affording a novel silyl-substituted phosphorus ylide.[12]

As a starting point for our further investigations, we have taken a closer look at the thermal stability of **1**. Iminosiloxysilylene **1** is completely stable as a solid and in solution at room temperature, but formation of an unknown product was observed at elevated temperatures in benzene. However, the reaction is extremely slow and only about 10% conversion was detected after 10 days at 130 °C. ^{1}H NMR spectroscopy indicated formation of iminosiloxysilepin **2**



Scheme 2 Photochemically induced isomerization of silylene **1** and reactivity toward ammonia and white phosphorus.

(Scheme 2). Silepin formation occurs either intramolecularly with reactive silylenes or intermolecularly thermally or photochemically induced *via* excited singlet or triplet states.[7b,c,10,11,13] Consequently, we switched to photochemistry and irradiation (λ_{max} = 340 nm) of a benzene or THF solution of **1** indeed led to selective formation of iminosiloxysilepin **2** within 4 hours. Compound **2** was isolated as a pale yellow solid in quantitative yield and fully characterized. The more shielded central silicon nucleus resonates at δ = −15.5 ppm in the ^{29}Si NMR spectrum and is highfield-shifted compared to silylene **1** (δ = 58.9 ppm) and its related iminosilylsilepins (δ = 16.3 and 11.6 ppm).[6f,10] In sharp contrast to our earlier reported iminosilylsilepins, neither reversible C=C bond activation nor reactivity toward small molecules was possible.

Activation of white phosphorus (P_4) is an interesting and relatively unexplored field in modern main group chemistry with only limited examples of low-coordinate silicon compounds including cyclic silylenes.[14] In fact, the first example of a reaction between an acyclic silylene and P_4 was only recently reported with the activation and functionalization by vinyl silylsilylene **VI**.[6h] Motivated by the structural relationship between **VI** and silylene **1**, we pursued the reaction with P_4.

After stirring an equimolar amount of **1** and P_4 in toluene for 3 hours, a color change from colorless to pale orange was observed. Quantitative formation of a novel product, different from that observed for **VI**, was detected. ^{31}P NMR spectroscopy revealed three distinct resonances at δ = 152.1 ppm (doublet of doublets; $^1J(P_2P_1)$ = 157.6 Hz, $^1J(P_3P_1)$ = 149.6 Hz), δ = −327.7 ppm (doublet of triplets; $^1J(P_2P_3)$ = 181.6 Hz, $^1J(P_1P_3)$ = 149.6 Hz) and δ = −337.0 ppm (doublet of triplets; $^1J(P_3P_2)$ = 181.6 Hz, $^1J(P_1P_2)$ = 157.6 Hz) for non-chemically equivalent phosphorus nuclei. The observed chemical shifts and the splitting pattern are very similar to a 1 : 1 adduct of P_4 and the β-diketiminato silylene HC[(C=CH$_2$)(CMe)(NDipp)$_2$]Si: (δ(^{31}P) = 131.9, −342.4 and −348.0 ppm) reported by Driess and colleagues.[15] In the ^{29}Si NMR spectrum a highfield-shifted resonance at δ = −87.9 ppm compared to HC[(C=CH$_2$)(CMe)(NDipp)$_2$]Si(P_4) (δ = −40.4 ppm) was observed. The structural relationship was unambiguously confirmed by single-crystal X-ray diffraction (SC-XRD) analysis (Fig. 1). The molecular structure of **3** contains both elongated Si–P (av. 2.263 Å) and

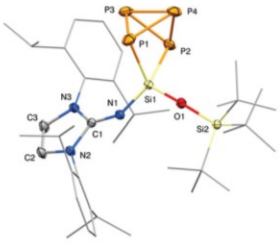


Fig. 1 Molecular structure of **3** with ellipsoids set at 50% probability. Hydrogen atoms are omitted for clarity. Selected bond lengths [Å] and angles [°]: Si1–O1 1.617(1), Si1–P1 2.256(1), Si1–P2 2.270(1), Si1–N1 1.657(1), N1–C1 1.280(2), P3–P4 2.162(1); N1–Si1–O1 109.1(1), Si1–N1–C1 149.0(1), Si1–O1–Si2 166.7(1), P1–Si1–P2 86.7(1).

P–P (av. 2.263 Å) bonds and a similar short P3–P4 bridgehead bond (2.162(1) Å) compared to Driess's SiP_4 cage compound (*cf.* $d_{Si-P(av.)}$ = 2.247, $d_{P-P(av.)}$ = 2.229 and $d_{P-P(bridgehead)}$ = 2.159(2) Å).[15]

Since HC[(C=CH_2)(CMe)(NDipp)$_2$]Si(P_4) reacts slowly with a silylene equivalent to (HC[(C=CH_2)(CMe)(NDipp)$_2$]Si)$_2$(P_4), we investigated the reactivity of **3** toward **1**.[15] The formation of a comparable product was indicated, but not feasible, because in our case an even slower reaction was observed (only ~10% conversion after 10 days at 110 °C in benzene), presumably due to the increased steric encumbrance of acyclic silylene **1**.

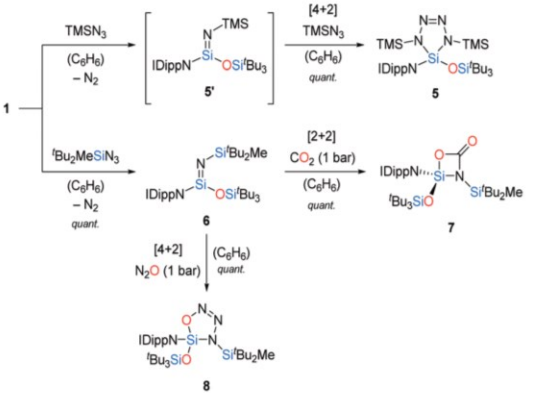
The exploration of ammonia activation is still in its infancy for main group compounds,[1a–c,1e,5,9,16] which is not surprising as even most transition metal complexes are not capable of the oxidative addition of NH_3.[17] Thus, there are only less than a handful of silylenes reported that activate ammonia *via* cleavage of the N–H bond.[6e,18] Accordingly, we envisioned iminosiloxysilylene **1** as an attractive reagent for this demanding purpose. And indeed, the treatment of **1** with an equimolar amount of NH_3 (0.4 m solution in 1,4-dioxane) resulted in the formation of the hydroamination product **4** (Scheme 2). Aminosilane **4** was clearly characterized by multinuclear and 2D NMR analysis. ^{1}H NMR spectroscopy unambiguously identified the SiH (δ = 4.81 ppm; $^1J_{SiH}$ = 243.8 Hz) and $SiNH_2$ (broad signal at δ = −0.14 ppm) moieties. The tetra-coordinate central silicon nucleus resonates at δ = −66.5 ppm in the ^{29}Si NMR spectrum. The spectroscopic data are in good accordance with those observed for related aminosilanes ($\delta(^1H_{SiH})$ = 5.22–4.72 ppm ($^1J_{SiH}$ = 214.4–251.7 Hz), $\delta(^1H_{SiNH_2})$ = 0.99 to −0.05 ppm and $\delta(^{29}Si)$ = −35.7 to −45.0 ppm).[6e,18] Interestingly, compound **4** even reacts with excessive amounts of ammonia to an unidentified mixture of products, presumably also including the elimination of the imino ligand under formation of IDippNH and (H_2N)(^{t}Bu$_3$SiO)Si(H)(NH_2). A similar σ-bond metathesis reaction between an Si–N bond and NH_3 was previously reported.[6e]

Furthermore, we were interested in the preparation of a novel silaimine (R_2Si=NR), as these species are generally much more reactive than their lighter imine congeners (highly polarized $Si^{\delta+}$–$N^{\delta-}$ double bond) and thus interesting compounds. Since the pioneering work of Wiberg *et al.* in 1985 on isolable silaimines (isolation of ^{t}Bu$_2$Si=NSi^{t}Bu$_3$),[19] a broad variety of three- and four-coordinate derivatives have been reported.[20] However, acyclic, three-coordinate derivatives are still quite rare and their reactivity rather unexplored. Additionally, to the best of our knowledge, there is no example of an isolable, acyclic silaimine obtained directly from the corresponding silylene. A recent report by Aldridge/Jones *et al.* nevertheless describes such a synthesis, which however involves isomerization *via* a 1,3-silyl migration.[20l]

We initiated our studies with the commercially available trimethylsilyl azide. The reaction of **1** with one equivalent of $TMSN_3$ led to an immediate gas evolution (N_2). Subsequent ^{1}H NMR spectroscopy detected remaining **1** together with the concomitant formation of a novel product. Repetition of the reaction with a starting material ratio of 1 : 2 selectively and quantitatively provided silatetrazoline **5** (Scheme 3).

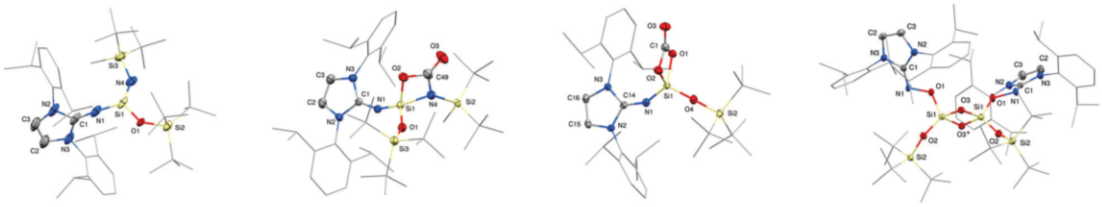
Heterocycle **5** is formed *via* an immediate 1,3-dipolar [4 + 2] cycloaddition reaction of the intermediary formed silaimine **5′** with $TMSN_3$. This reactivity has already been observed previously.[20e,21] Compound **5** was fully characterized and exhibits a strongly upfield-shifted resonance for the cyclic Si atom in the ^{29}Si NMR spectrum (δ = −90.6 ppm), due to the increased coordination number (*cf.* **1**: δ = 58.9 ppm).

Since the steric congestion was obviously not sufficient for the isolation of silaimine **5′** and thus a subsequent reaction was favored, we synthesized the bulkier azide derivative ^{t}Bu$_2$MeSiN_3. Treatment of **1** with an equimolar amount of ^{t}Bu$_2$MeSiN_3 led again to N_2 evolution, but in this case full conversion was detected. Formation of the three-coordinate silaimine **6** was indicated by a downfield-shifted ^{29}Si NMR resonance at δ = −50.1 ppm, with respect to that observed for **5**. The molecular structure of **6** was unambiguously determined by SC-XRD analysis and confirmed the assumption (Fig. 2). The central silicon atom adopts a trigonal planar geometry (sum of bond angles: 359.9°) with a short Si=N double bond (1.573(2) Å) and a long Si3–N4 bond (1.693(2) Å). These charac-



Scheme 3 Reaction of 1 with organosilyl azides: formation of silaimines and subsequent cycloaddition reactions.

This journal is © The Royal Society of Chemistry 2020



6 7 9 11

Fig. 2 Molecular structures of **6**, **7**, **9** (one out of two independent molecules in the asymmetric unit) and *cis*-**11** with ellipsoids set at 50% probability. Hydrogen atoms are omitted for clarity. Selected bond lengths [Å] and angles [°]: **6**: Si1–O1 1.618(3), Si1–N1 1.623(2), Si1–N4 1.573(2), N1–C1 1.275(4); N1–Si1–O1 107.0(1), N1–Si1–N4 130.7(1), N4–Si1–O1 122.2(1). **7**: Si1–O1 1.613(1), Si1–O2 1.699(1), Si1–N1 1.620(1), Si1–N4 1.764(2), N1–C1 1.286(2); N1–Si1–O1 112.7(1), O2–Si1–N4 78.6(1). **9**: Si1–O1 1.712(2), Si1–O2 1.712(2), Si1–O4 1.585(2), Si1–N1 1.609(2), N1–C14 1.299(3); N1–Si1–O4 112.5(1), O1–Si1–O2 78.0(1). *cis*-**11**: Si1–O1 1.623(2), Si1–O2 1.601(2), Si1–O3 1.659(2), Si1–O3* 1.673(2), N1–C1 1.305(2); O1–Si1–O2 114.5(1), O3–Si1–O3* 88.8(1).

teristic structural features are essentially the same as those observed for Wiberg's seminal silaimine.[20b] However, the determined Si–N–Si bond angle is significantly more acute (139.4(1)°) than the one found for $^{t}Bu_2Si{=}NSi^{t}Bu_3$, which bears an almost linear Si–N–Si bond (177.8(2)°). In addition, the short Si1–N1 bond length (1.623(2) Å) clearly reflects the strong electron donation from the N-heterocyclic imino (NHI) ligand to the central silicon nucleus (resonance stabilization; *cf.* iminosilylsilanone (IDippN)($^{t}Bu_3Si$)Si=O[6f]).

Inspired by a reactivity study regarding small molecule activation by N-heterocyclic silaimines reported by Jones *et al.*, we envisaged acyclic silaimine **6** as a similarly suitable reagent.[20m] Whereas analogously no reaction toward H_2 (even at elevated temperatures) was observed, exposure of **6** to CO_2 (1 bar) selectively provided the [2 + 2] cycloaddition product azaoxasiletane **7** in quantitative yield (Scheme 3). The observed ^{29}Si NMR resonance for the silicon atom embedded in the four-membered ring (δ = −89.6 ppm) is in line with those observed for related compounds(δ = −49.2 to −120.0 ppm).[20j,m,22]

The solid-state structure of **7** is in close analogy to the previously reported planar SiOCN heterocycles and features similar long Si–O (1.699(1) Å) and Si–N (1.764(2) Å) single bonds (*cf.* d_{Si-O} = 1.693(2)–1.788(2) Å and d_{Si-N} = 1.755(3)–1.808 (2) Å) and an exocyclic C=O double bond (1.195(2) Å; *cf.* $d_{C=O}$ = 1.191(4)–1.222(3) Å). Additionally, the absolute configuration for the synthesized chiral molecule was revealed.

Next, we aimed at a possible 1,3-dipolar cycloaddition reaction of silaimine **6** with dinitrogen monoxide (N_2O), a 1,3-dipole closely related to azides (diazonium betaine type) but substantially less reactive. Such reactions with N_2O are extremely rare and usually require relatively harsh conditions (high pressure and/or temperatures).[23] Furthermore, the incorporation of all three atoms of N_2O into the end product is seldom observed.[24] Wiberg and colleagues already observed a reaction between $^{t}Bu_2Si{=}NSi^{t}Bu_3$ and N_2O and proposed the intermediate formation of an unstable [4 + 2] cycloaddition product, but unfortunately could not verify the assumed structure.[19]

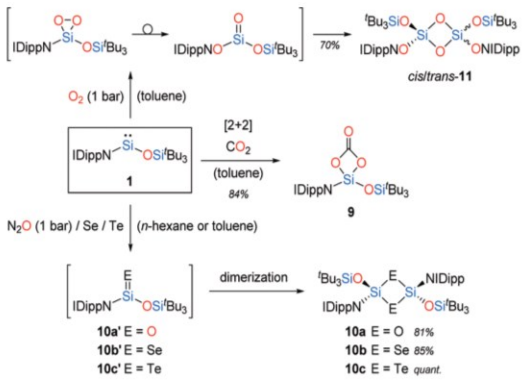
And indeed, exposure of a benzene solution of **6** to N_2O (1 bar) selectively afforded oxatriazasilole **8** as the [4 + 2] cycloaddition product, after stirring for one hour at ambient temperature. Heterocycle **8** was fully characterized and the cyclic silicon atom exhibits a resonance in the ^{29}Si NMR spectrum at δ = −103.7 ppm. To the best of our knowledge, such unprecedented compounds are elusive and have not yet been isolated. Our results thus confirmed the structure of Wiberg's postulated intermediate and are in line with the results of a recent density functional theory (DFT) study.[25] In addition, oxatriazasilole **8** is thermally very stable and no subsequent isomerization or decomposition in solution at temperatures up to 130 °C was observed.

Oxygenation reactions

Silylenes are attractive and versatile precursors for gaining access to fascinating, oxygen-containing organosilicon compounds, due to their inherent high reactivity. Important driving forces for the formation of these species are the high oxophilicity and stability of silicon in the oxidation state +4. In recent decades, a plethora of reactions of various silylenes with commonly used oxygenation agents, such as CO_2, N_2O, Me_3NO and even O_2 have been reported.[26] Consequently, we were interested in the oxidation of iminosiloxysilylene **1**, which could provide otherwise elusive compounds.

The entry to this particular investigation was made with carbon monoxide. The reactivity of isolable silylenes toward CO is an almost unexplored but highly relevant field in modern main group chemistry, as promising compounds could be formed *via* carbonylation. Thus, three recent reports describe the silylene-induced coupling of CO.[20l,27] It is not surprising that no reaction of **1** with CO was observed, since **1** is less reactive compared to certain other acyclic silylenes. We then continued our studies with the greenhouse gas carbon dioxide. Exposure of a toluene solution of **1** to carbon dioxide (1 bar) selectively afforded silicon carbonate complex **9** in high yield (Scheme 4). Compound **9** represents the formal [2 + 2] cycloaddition product of the intermediary formed, highly reactive iminosiloxysilanone (IDippN)($^{t}Bu_3SiO$)Si=O (**10a′**) (*via*

This journal is © The Royal Society of Chemistry 2020



Scheme 4 Oxygenation of silylene **1** with small, gaseous molecules and reactions toward heavier chalcogenes.

reduction of CO_2 to CO) with another equivalent of CO_2. The $SiO_2C{=}O$ silicon nucleus of the fully characterized, rare four-coordinate, monomeric complex resonates at $\delta = -90.9$ ppm in the ^{29}Si NMR spectrum, which is highfield-shifted compared to the previously reported, strongly related complexes (IDippN)$(R_3Si)Si(O_2C{=}O)$ (R = TMS, ^{t}Bu; $\delta = -35.0$ and -43.0 ppm).[6f,10] SC-XRD analysis clearly provided the molecular structure of **9** (Fig. 2). The structural parameters are very similar to those observed for (IDippN) $((TMS)_3Si)Si(O_2C{=}O)$, however the Si–O1/O2 (1.712(2) Å) and Si–N (1.609(2) Å) bonds are shortened (*cf.* $d_{Si-O} = 1.740(2)$–$1.741(2)$ Å and $d_{Si-N} = 1.628(2)$ Å), presumably due to the reduced steric demand around the tetrahedral silicon center.[10]

Interestingly, silicon carbonate complex **9** reacts with another equivalent of CO_2 in a slow equilibrium reaction to **9′**. Unfortunately, complete conversion and isolation of **9′** was not possible, as heating of the reaction mixture or removal of CO_2 selectively regenerates **9**. Compound **9′** was clearly identified by multinuclear and 2D NMR analysis, however its structure remains unclear (presumably CO_2 inserts into the Si–N bond; for details, see ESI†).

Besides CO_2, N_2O has proven to be a useful and mild reagent for the oxygenation of silylenes.[26] Accordingly, we treated acyclic silylene **1** with N_2O (1 bar) and observed the selective synthesis of a sole product isolated in 81% yield. NMR spectroscopy indicated formation of cyclodisiloxane **10a** ($\delta(^{29}Si) = -83.5$ ppm), the dimer of the above mentioned (IDippN)(^{t}Bu$_3$SiO)Si=O (**10a′**) (Scheme 4). Silanones ($R_2Si{=}O$; heavier ketone congeners) are extremely reactive compounds, due to the strongly polarized $Si^{\delta+}$–$O^{\delta-}$ double bond.[28] Thus, the additionally weak Si=O π-bond (unfavorable p_π-orbital overlap between Si and O) is susceptible for the usually observed barrier-free, fast head-to-tail oligomerization yielding oligosiloxanes.[29] The molecular structure obtained by SC-XRD analysis unambiguously confirmed the formation of **10a** and revealed a *trans*-configuration (see ESI†).

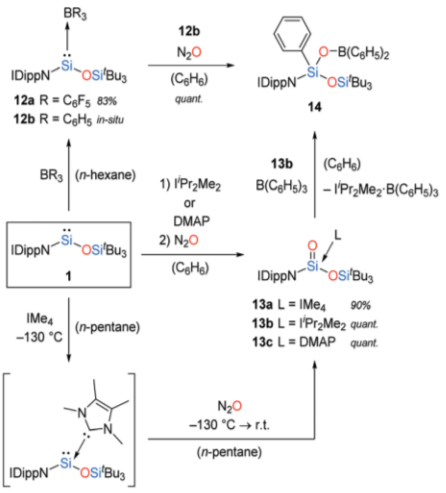
Because of the smaller difference in electronegativity between silicon and the heavier chalcogens E (E = S, Se and Te; $\Delta\chi_{(Si-O)} = 1.54$, $\Delta\chi_{(Si-S)} = 0.68$, $\Delta\chi_{(Si-Se)} = 0.65$ and $\Delta\chi_{(Si-Te)} = 0.20$), resulting Si–E double bonds are significantly less polarized and the isolation of monomeric (IDippN)(^{t}Bu$_3$SiO)Si=E compounds becomes more feasible.[30] Therefore, we conducted the reaction of **1** with elemental sulfur, selenium and tellurium. Unfortunately, treatment of **1** with an equimolar amount of S_8 in toluene led to the formation of a complicated mixture of products. In addition to the desired Si=S moiety, the formation of five-membered SiS_4 or three-membered SiS_2 species is conceivable as previously reported.[26] In contrast, reaction of **1** with one equivalent of elemental selenium or tellurium selectively provided the novel compounds silicon diselenide **10b** and silicon ditelluride **10c** in up to quantitative yield (Scheme 4). Multinuclear and 2D NMR spectroscopy indicated the existence of monomeric silaneselone (IDippN)(^{t}Bu$_3$SiO)Si=Se (**10b′**) and silanetellone (IDippN)(^{t}Bu$_3$SiO)Si=Te (**10c′**) in solution. The substantially downfield-shifted ^{29}Si NMR resonances for the respective SiE nuclei (**10b**: $\delta(^{29}Si) = 6.2$ ppm and **10c**: $\delta(^{29}Si) = -14.6$ ppm) compared to that observed for the SiO atom in **10a** ($\delta(^{29}Si) = -83.5$ ppm) support this assumption, as much less pronounced low field shifts are expected for the analogous dimers. Nevertheless, the molecular structure of **10b** revealed a dimeric form in the solid-state (see ESI†).

Finally, we utilized molecular oxygen as a relatively harsh oxidizing agent for silylene **1**. Exposure of O_2 (1 bar) to a cooled (−80 °C) toluene solution of **1** led to a rather controlled formation of cyclodisiloxane **11** (mixture of *cis* (~71%) and *trans* (~29%)) (Scheme 4). Compound **11** represents the dimer of the *in situ* generated dioxosilanone (sila-carbonate) (IDippNO) (^{t}Bu$_3$SiO)Si=O (formed *via* rearrangement of the extremely reactive dioxasilirane (IDippN)(^{t}Bu$_3$SiO)SiO_2) and was isolated in 70% yield after crystallization. The solid-state structure of the *cis*-isomer was clearly confirmed by SC-XRD analysis (Fig. 2). The ^{29}Si NMR resonance for the SiO_4 moiety of **11** ($\delta = -84.5$ ppm) is almost the same as that observed for *trans*-cyclodisiloxane **10a**.

Because the synthesized Si=O double bonded species proved to be to reactive and subsequent dimerization took place, we targeted the isolation of the respective monomeric compounds with the aid of additional Lewis acid/base-stabilization. This method is widely used in modern main group chemistry and especially in organosilicon chemistry.[26] In particular, the strong σ-donating N-heterocyclic carbenes (NHCs) are frequently applied as Lewis bases for the isolation of otherwise elusive compounds.[31] Nonetheless, the cyclo-disiloxanes **10a** and **11** are too stable and no reaction with the strong Lewis acid tris(pentafluorophenyl)borane $B(C_6F_5)_3$ (BCF) or NHCs was observed. Therefore, we intended the preparation of donor- or acceptor-stabilized derivatives of iminosiloxysilylene **1** with subsequent exploration of oxygenation reactions.

Initially, the reaction of silylene **1** toward the commercially available reagent BCF was performed and the selective formation of a sole product was observed. Silylene-BCF adduct **12a** was isolated in 83% yield after crystallization from *n*-hexane (Scheme 5). The analytical data obtained (*e.g.* $\delta(^{11}B) = -20.3$ ppm) largely resemble those of related NHI-substituted

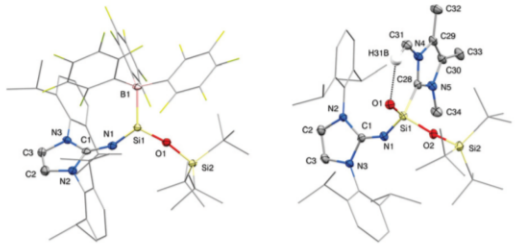
 This journal is © The Royal Society of Chemistry 2020



Scheme 5 Synthesis of acceptor-/donor-stabilized derivatives of iminosiloxysilylene **1** and subsequent oxygenation reactions. IMe_4 = 1,3,4,5-tetramethylimidazolin-2-ylidene.

silylene-BCF complexes (*cf.* $\delta(^{11}B)$ = −15.1 to −21.5 ppm).[10,16f,32] In contrast to the reported compounds, the resonance for the low-valent silicon nucleus (estimated quartet due to $^{1}J_{BSi}$ coupling; spin ^{11}B = 3/2) was not found in the ^{29}Si NMR spectrum, presumably because of the high quadrupole moment of the adjacent ^{11}B atom. The molecular structure of **12a** was unambiguously determined by SC-XRD analysis (Fig. 3).

The low-coordinate silicon atom adopts a trigonal planar geometry (sum of bond angles: 359.6°) with comparable long Si–B (2.086(3) Å) and Si–N (1.621(2) Å) bonds (*cf.* d_{Si-B} = 2.080(5)–2.117(2) Å and d_{Si-N} = 1.605(3)–1.635(2) Å).[10,16f,32] According to the rather obtuse Si–N–C bond angle (150.8(3)°; *cf.* $\angle_{Si-N-C}$ = 151.1(1)–167.5(1)°), a less pronounced 1-sila-2-azaallene (Si=N^{+}=C) character can be assumed for **12a**.



12a **13a**

Fig. 3 Molecular structures of **12a** and **13a** with ellipsoids set at 50% probability. Hydrogen atoms, except for H31B involved in hydrogen bonding (visualized by the dashed line), and cocrystallized toluene are omitted for clarity. Selected bond lengths [Å] and angles [°]: **12a**: Si1–B1 2.086(3), Si1–O1 1.598(2), Si1–N1 1.621(2), N1–C1 1.296(4); B1–Si1–O1 116.5(1), B1–Si1–N1 128.9(1), N1–Si1–O1 114.2(1). **13a**: Si1–O1 1.554(2), Si1–O2 1.653(2), Si1–C28 1.935(3), Si1–N1 1.684(2), N1–C1 1.271(3); N1–Si1–O2 104.2(1), O1–Si1–O2 115.5(1).

With silylene-BCF adduct **12a** in hand we carried out the targeted oxygenation reactions. Unfortunately, complex **12a** did not undergo any reaction toward N_2O and even O_2, which is probably due to the strong donor–acceptor interaction. Therefore, we turned to possible donor-stabilization of **1** with strong Lewis bases, such as 4-*N*,*N*-dimethylaminopyridine (DMAP) and NHCs. Whereas no reaction of **1** with 1,3-diisopropyl-4,5-dimethylimidazolin-2-ylidene ($I^iPr_2Me_2$) and DMAP was observed, treatment of **1** with the less sterically crowded NHCs 1,3-diethyl-4,5-dimethylimidazolin-2-ylidene (IEt_2Me_2) and 1,3,4,5-tetramethylimidazolin-2-ylidene (IMe_4) at ambient temperature resulted in the formation of complicated product mixtures. To increase the selectivity, the reaction of **1** with IMe_4 was studied in more detail at low temperatures. Addition of IMe_4 to silylene **1** at −130 °C led to a color change from colorless to yellow with assumed formation of the desired NHC-stabilized silylene. However, upon warming to room-temperature, the color changed to red and again a mixture of products was detected *via* ^{1}H NMR spectroscopy. Consequently, *in situ* formation of donor-stabilized **1** and oxygenation without isolation seemed promising. And indeed, performing the former reaction at −130 °C and carefully exposing the yellow solution to N_2O (1 bar) resulted in the selective formation of a novel NHC-stabilized product. The IMe_4-stabilized silanoic ester derivative **13a** was identified by multinuclear and 2D NMR analysis (Scheme 5).

Due to the above mentioned high tendency of the Si=O moiety to undergo subsequent reactions, tailor-made ligand frameworks providing sufficient kinetic and/or thermodynamic stabilization are necessary for the isolation of such species. Thus, with the rather weakly donating nature of electronegative oxygen-substituents, only a few examples have been reported, all of which are four-coordinate, because of necessary additional intra- or intermolecular stabilization.[33] Recently, our group isolated the first example of an acyclic, four-coordinate, NHC-stabilized silanoic ester ($^{t}Bu_3Si$)(TMSO)Si=O ($I^iPr_2Me_2$), which is rather unstable (decomposition above −30 °C in solution).[9] In sharp contrast, NHC adduct **13a** is thermally very stable in solution up to 130 °C without any detectable signs of decomposition. The Si=O silicon nucleus exhibits a resonance at δ = −88.5 ppm in the ^{29}Si NMR spectrum, which is in good accordance with those observed for related, but almost exclusively cyclic, silanoic ester species (δ = −49.1 to −91.5 ppm).[9,33] Comparable to ($^{t}Bu_3Si$)(TMSO)Si=O ($I^iPr_2Me_2$), complex **13a** features hydrogen bonding of one NHC methyl C–H proton to the Si=O oxygen atom (unusual broad splitting of the wingtip methyl protons: $\Delta\delta$ = 1.03 ppm), which is also reflected in the solid-state structure of complex **13a** (Fig. 3). Thus, a close O···H distance of 2.153 Å (H31B in calculated position), being much shorter than the sum of the van der Waals radii of hydrogen and oxygen (2.72 Å) was revealed.[34]

Furthermore, the Si=O bond (1.554(2) Å) is essentially the same as that observed for ($^{t}Bu_3Si$)(TMSO)Si=O($I^iPr_2Me_2$)

(1.556(2) Å) and lies in the range of the mentioned previously reported base-stabilized silanoic esters (*cf.* $d_{Si=O}$ = 1.52–1.59 Å).[9,33] Significantly elongated Si1–O2 (1.653(2) Å) and Si2–O2 (1.626(2) Å) single bonds emphasize the double bond character. The C_{NHC}–Si bond (1.935(3) Å) is characteristic for a dative donor–acceptor interaction.[31]

Out of curiosity about the possible formation of the $I^iPr_2Me_2$/DMAP-stabilized derivatives of **13a**, we exposed the unreacted reaction mixtures of silylene **1** and the respective Lewis base to N_2O (1 bar) at room-temperature. Surprisingly, the donor-stabilized silanoic ester derivatives **13b** and **13c** were afforded in quantitative yield (Scheme 5). Therefore, these reactions proceed *via* an initial oxygenation of **1** to (IDippN)(^{t}Bu$_3$SiO)Si=O (**10a′**), followed by an immediate coordination of the respective donor molecule. The Lewis base-stabilization is even energetically preferred over the dimerization of **10a′** to *trans*-cyclodisiloxane **10a**. The complexes **13b** and **13c** are closely analogous to the IMe_4-stabilized derivative **13a** and exhibit slightly downfield-shifted resonances in the ^{29}Si NMR spectra at δ = −86.7 and −87.8 ppm, respectively.

After the successful synthesis of donor-stabilized complexes of **10a′**, a subsequent reactivity investigation was targeted. Because of the more convenient access to (IDippN)(^{t}Bu$_3$SiO)Si=O($I^iPr_2Me_2$) **13b**, this NHC-stabilized silanoic ester derivative was subjected to some follow-up reactions. As substitution reactions of weaker σ-donors by stronger Lewis bases are often observed for NHC-supported organosilicon compounds, we investigated a possible ligand exchange reaction to support the dative interaction.[31] The treatment of **13b** with the more nucleophilic IMe_4 resulted in clean formation of **13a** and simultaneous liberation of $I^iPr_2Me_2$, but due to the relatively strong donor–acceptor interaction (with additional hydrogen bonding) elevated temperatures were necessary (full conversion only after 1 d at 110 °C; see ESI†).

To verify the intermediary formation of **10a′** during the synthesis of *trans*-cyclodisiloxane **10a**, we pursued an abstraction of the coordinating NHC to achieve the subsequent dimerization to **10a**. For this purpose, we studied the reaction of **13b** toward common NHC abstraction reagents such as CO_2 or Lewis acidic BR_3 compounds. Thus, exposure of (IDippN)(^{t}Bu$_3$SiO)Si=O($I^iPr_2Me_2$) **13b** to CO_2 (1 bar) led to an immediate full conversion to the above described silicon carbonate complex (IDippN)(^{t}Bu$_3$SiO)Si(O_2C=O) (**9**) with concomitant formation of the insoluble NHC-CO_2 adduct $I^iPr_2Me_2$·CO_2.[35] Since NHC abstraction with CO_2 occurred, but the faster [2 + 2] cycloaddition reaction of **10a′** with another equivalent of CO_2 providing **9** instead of dimerization to **10a** was observed, we turned to the Lewis acids $B(C_6F_5)_3$ and BPh_3.

Interestingly, addition of an equimolar amount of BCF to **13b** at room temperature resulted in the unselective formation of novel silicon-containing products, but only a conversion of 50% was detected. The addition of a second equivalent of BCF then led to full conversion. The formation of a mixture of products, containing the desired NHC-borane adduct $I^iPr_2Me_2$·$B(C_6F_5)_3$ and a compound bearing a Si–F bond, was identified by multinuclear and 2D NMR spectroscopy. However, purification and isolation was not possible so far. The reaction most likely proceeds *via* NHC-abstraction and simultaneous formation of $I^iPr_2Me_2$·$B(C_6F_5)_3$ and the Lewis acid-stabilized silanoic ester derivative (IDippN)(^{t}Bu$_3$SiO)Si=O($B(C_6F_5)_3$), which undergoes subsequent bond activation and rearrangement reactions. To the best of our knowledge, all isolable acceptor-stabilized Si=O species require additional strong inter-/intramolecular stabilization to prevent these follow-up reactions.[33c,i,36] Iwamoto *et al.* recently isolated an aryl(boryloxy)silane *via* isomerization of an unstable acceptor-stabilized silanone, due to the lack of sufficient stabilization of the strong electron-deficient Si nucleus.[37]

On the other hand, reaction of **13b** with two equivalents of BPh_3 led to the selective formation of the analogous aryl(boryloxy)silane **14** (Scheme 5), however, due to the weaker Lewis acidic nature of BPh_3 compared to BCF, a significantly increased temperature was necessary (full conversion after 2 h at 130 °C; see ESI†). Nevertheless, separation of the simultaneously formed borane NHC adduct $I^iPr_2Me_2$·BPh_3 and isolation of **14** turned out to be difficult. Fortunately, the silylene-borane adduct **12b** was also accessible and, in sharp contrast to the BCF analogue **12a**, susceptible to a subsequent oxygenation reaction. Thus, exposure of the *in situ* synthesized (IDippN)(^{t}Bu$_3$SiO)Si(BPh_3) (**12b**) to N_2O (1 bar) successfully afforded adduct **14** in quantitative yield. Compound **14** was fully characterized and exhibits a characteristic resonance in the ^{29}Si NMR spectrum (δ = −81.4 ppm) reflecting its central, four-coordinate silicon nucleus. In addition, silane **14** is thermally very stable in solution (no signs of decomposition up to 130 °C) and in the solid-state.

On a final note, trapping of the reactive intermediates during the formation of cyclodisiloxane **11** appeared to be rather difficult. All performed reactions of the different donor/acceptor-stabilized derivatives of iminosiloxysilylene **1** toward molecular O_2 resulted in the unselective formation of a mixture of products. These mixtures most likely include Lewis acid/base-stabilized derivatives of the extremely reactive dioxasilirane (IDippN)(^{t}Bu$_3$SiO)SiO_2 and the acyclic sila-carbonate (IDippNO)(^{t}Bu$_3$SiO)Si=O, however the isolation of these species was not possible so far.

Conclusions

An in depth reactivity study of the recently reported iminosiloxysilylene **1**, a rare member of the small acyclic silylene family, was presented. Over the last decade, these highly reactive silylenes have shown fascinating reactivity trends that are promising for the ultimate goal of implementing the highly abundant silicon into metal-free catalysis. Our results extend the knowledge about these still rather unexplored compounds and highlights their capability as versatile organosilicon reagents. Thus, not only their enormous potential as transition metal mimics *via* the activation of challenging small molecules (P_4, NH_3, CO_2 and N_2O), but also their role as important precursors for unique heavier carbon homologues has been further demon-

 This journal is © The Royal Society of Chemistry 2020

strated. With the striking formation of the elusive, neutral oxatriazasilole **8** we were able to isolate the initial product of a 1,3-dipolar cycloaddition reaction with N_2O for the first time, which is unprecedented even in organic chemistry. In addition, the isolation of rare examples of silanoic esters was achieved. The suitability of these diverse organosilicon complexes for catalytic applications is currently under active investigation in our laboratories.

Conflicts of interest

There are no conflicts to declare.

Acknowledgements

We are exceptionally grateful to the WACKER Chemie AG and the European Research Council (SILION 637394) for continued financial support. We thank Prof. T. Nilges and colleagues for the generous gift of white phosphorus and Maximilian Muhr (Prof. R. A. Fischer) for the LIFDI-MS measurements.

Notes and references

1 (*a*) P. P. Power, *Nature*, 2010, **463**, 171–177; (*b*) D. Martin, M. Soleilhavoup and G. Bertrand, *Chem. Sci.*, 2011, **2**, 389–399; (*c*) C. Weetman and S. Inoue, *ChemCatChem*, 2018, **10**, 4213–4228; (*d*) M.-A. Légaré, C. Pranckevicius and H. Braunschweig, *Chem. Rev.*, 2019, **119**, 8231–8261; (*e*) R. L. Melen, *Science*, 2019, **363**, 479–484.

2 (*a*) H. F. T. Klare and M. Oestreich, *Dalton Trans.*, 2010, **39**, 9176–9184; (*b*) A. Schulz and A. Villinger, *Angew. Chem., Int. Ed.*, 2012, **51**, 4526–4528; (*c*) P. Jutzi, *Chem. – Eur. J.*, 2014, **20**, 9192–9207; (*d*) J. C. L. Walker, H. F. T. Klare and M. Oestreich, *Nat. Rev. Chem.*, 2020, **4**, 54–62; (*e*) B.-X. Leong, J. Lee, Y. Li, M.-C. Yang, C.-K. Siu, M.-D. Su and C.-W. So, *J. Am. Chem. Soc.*, 2019, **141**, 17629–17636.

3 E. Fritz-Langhals, *Org. Process Res. Dev.*, 2019, **23**, 2369–2377.

4 (*a*) R. West, *Nature*, 2012, **485**, 49–50; (*b*) M. Driess, *Nat. Chem.*, 2012, **4**, 525–526.

5 T. Chu and G. I. Nikonov, *Chem. Rev.*, 2018, **118**, 3608–3680.

6 For acyclic, two-coordinate silylenes, see. (*a*) A. V. Protchenko, K. H. Birjkumar, D. Dange, A. D. Schwarz, D. Vidovic, C. Jones, N. Kaltsoyannis, P. Mountford and S. Aldridge, *J. Am. Chem. Soc.*, 2012, **134**, 6500–6503; (*b*) B. D. Rekken, T. M. Brown, J. C. Fettinger, H. M. Tuononen and P. P. Power, *J. Am. Chem. Soc.*, 2012, **134**, 6504–6507; (*c*) A. V. Protchenko, A. D. Schwarz, M. P. Blake, C. Jones, N. Kaltsoyannis, P. Mountford and S. Aldridge, *Angew. Chem., Int. Ed.*, 2013, **52**, 568–571; (*d*) B. D. Rekken, T. M. Brown, J. C. Fettinger, F. Lips, H. M. Tuononen, R. H. Herber and P. P. Power, *J. Am. Chem. Soc.*, 2013, **135**, 10134–10148; (*e*) T. J. Hadlington, J. A. B. Abdalla, R. Tirfoin, S. Aldridge and C. Jones, *Chem. Commun.*, 2016, **52**, 1717–1720; (*f*) D. Wendel, D. Reiter, A. Porzelt, P. J. Altmann, S. Inoue and B. Rieger, *J. Am. Chem. Soc.*, 2017, **139**, 17193–17198; (*g*) Y. K. Loh, L. Ying, M. Á. Fuentes, D. C. H. Do and S. Aldridge, *Angew. Chem., Int. Ed.*, 2019, **58**, 4847–4851; (*h*) M. M. D. Roy, M. J. Ferguson, R. McDonald, Y. Zhou and E. Rivard, *Chem. Sci.*, 2019, **10**, 6476–6481.

7 (*a*) N. Tokitoh, H. Suzuki, R. Okazaki and K. Ogawa, *J. Am. Chem. Soc.*, 1993, **115**, 10428–10429; (*b*) H. Suzuki, N. Tokitoh and R. Okazaki, *Bull. Chem. Soc. Jpn.*, 1995, **68**, 2471–2481; (*c*) N. Takeda and N. Tokitoh, *Synlett*, 2007, 2483–2491.

8 (*a*) M. J. Cowley, V. Huch, H. S. Rzepa and D. Scheschkewitz, *Nat. Chem.*, 2013, **5**, 876–879; (*b*) H. Zhao, K. Leszczyńska, L. Klemmer, V. Huch, M. Zimmer and D. Scheschkewitz, *Angew. Chem., Int. Ed.*, 2018, **57**, 2445–2449.

9 D. Reiter, R. Holzner, A. Porzelt, P. J. Altmann, P. Frisch and S. Inoue, *J. Am. Chem. Soc.*, 2019, **141**, 13536–13546.

10 D. Wendel, A. Porzelt, F. A. D. Herz, D. Sarkar, C. Jandl, S. Inoue and B. Rieger, *J. Am. Chem. Soc.*, 2017, **139**, 8134–8137.

11 L. Zhu, J. Zhang and C. Cui, *Inorg. Chem.*, 2019, **58**, 12007–12010.

12 D. Reiter, P. Frisch, T. Szilvási and S. Inoue, *J. Am. Chem. Soc.*, 2019, **141**, 16991–16996.

13 (*a*) H. Suzuki, N. Tokitoh and R. Okazaki, *J. Am. Chem. Soc.*, 1994, **116**, 11572–11573; (*b*) M. Kira, S. Ishida, T. Iwamoto and C. Kabuto, *J. Am. Chem. Soc.*, 2002, **124**, 3830–3831; (*c*) M. Kira, S. Ishida, T. Iwamoto, A. de Meijere, M. Fujitsuka and O. Ito, *Angew. Chem., Int. Ed.*, 2004, **43**, 4510–4512; (*d*) T. Kosai, S. Ishida and T. Iwamoto, *Chem. Commun.*, 2015, **51**, 10707–10709; (*e*) T. Kosai, S. Ishida and T. Iwamoto, *Angew. Chem., Int. Ed.*, 2016, **55**, 15554–15558.

14 (*a*) M. Scheer, G. Balázs and A. Seitz, *Chem. Rev.*, 2010, **110**, 4236–4256; (*b*) N. A. Giffin and J. D. Masuda, *Coord. Chem. Rev.*, 2011, **255**, 1342–1359; (*c*) S. S. Sen, S. Khan, H. W. Roesky, D. Kratzert, K. Meindl, J. Henn, D. Stalke, J.-P. Demers and A. Lange, *Angew. Chem., Int. Ed.*, 2011, **50**, 2322–2325; (*d*) S. Khan, R. Michel, S. S. Sen and H. W. Roesky, *Angew. Chem., Int. Ed.*, 2011, **50**, 11786–11789; (*e*) S. Khan, S. S. Sen and H. W. Roesky, *Chem. Commun.*, 2012, **48**, 2169–2179.

15 Y. Xiong, S. Yao, M. Brym and M. Driess, *Angew. Chem., Int. Ed.*, 2007, **46**, 4511–4513.

16 (*a*) S. Boomgaarden, W. Saak, M. Weidenbruch and H. Marsmann, *Z. Anorg. Allg. Chem.*, 2001, **627**, 349–352; (*b*) P. P. Power, *Acc. Chem. Res.*, 2011, **44**, 627–637; (*c*) A. Meltzer, M. Majumdar, A. J. P. White, V. Huch and D. Scheschkewitz, *Organometallics*, 2013, **32**, 6844–6850; (*d*) S. Yadav, S. Saha and S. S. Sen, *ChemCatChem*, 2016, **8**, 486–501; (*e*) A. Rammo and D. Scheschkewitz, *Chem. – Eur. J.*, 2017, **24**, 6866–6885; (*f*) D. Wendel, T. Szilvási, D. Henschel, P. J. Altmann, C. Jandl, S. Inoue and

B. Rieger, *Angew. Chem., Int. Ed.*, 2018, **57**, 14575–14579; (*g*) D. C. H. Do, A. V. Protchenko, M. Á. Fuentes, J. Hicks, P. Vasko and S. Aldridge, *Chem. Commun.*, 2020, **56**, 4684–4687.
17 J. Hoover, *Science*, 2016, **354**, 707–708.
18 (*a*) A. Jana, C. Schulzke and H. W. Roesky, *J. Am. Chem. Soc.*, 2009, **131**, 4600–4601; (*b*) A. V. Protchenko, J. I. Bates, L. M. A. Saleh, M. P. Blake, A. D. Schwarz, E. L. Kolychev, A. L. Thompson, C. Jones, P. Mountford and S. Aldridge, *J. Am. Chem. Soc.*, 2016, **138**, 4555–4564.
19 N. Wiberg, K. Schurz and G. Fischer, *Angew. Chem., Int. Ed. Engl.*, 1985, **24**, 1053–1054.
20 For selected examples of silaimines, see. (*a*) M. Hesse and U. Klingebiel, *Angew. Chem., Int. Ed. Engl.*, 1986, **25**, 649–650; (*b*) N. Wiberg, K. Schurz, G. Reber and G. Müller, *J. Chem. Soc., Chem. Commun.*, 1986, 591–592; (*c*) M. Denk, R. Hayashi and R. West, *J. Am. Chem. Soc.*, 1994, **116**, 10813–10814; (*d*) J. Niesmann, U. Klingebiel, M. Schäfer and R. Boese, *Organometallics*, 1998, **17**, 947–953; (*e*) B. Gehrhus, P. B. Hitchcock and M. F. Lappert, *Z. Anorg. Allg. Chem.*, 2001, **627**, 1048–1054; (*f*) T. Iwamoto, N. Ohnishi, Z. Gui, S. Ishida, H. Isobe, S. Maeda, K. Ohno and M. Kira, *New J. Chem.*, 2010, **34**, 1637–1645; (*g*) L. Kong and C. Cui, *Organometallics*, 2010, **29**, 5738–5740; (*h*) R. S. Ghadwal, H. W. Roesky, K. Pröpper, B. Dittrich, S. Klein and G. Frenking, *Angew. Chem., Int. Ed.*, 2011, **50**, 5374–5378; (*i*) H. Cui and C. Cui, *Dalton Trans.*, 2015, **44**, 20326–20329; (*j*) F. M. Mück, J. A. Baus, A. Ulmer, C. Burschka and R. Tacke, *Eur. J. Inorg. Chem.*, 2016, 1660–1670; (*k*) T. J. Hadlington, T. Szilvási and M. Driess, *Angew. Chem., Int. Ed.*, 2017, **56**, 14282–14286; (*l*) A. V. Protchenko, P. Vasko, D. C. H. Do, J. Hicks, M. Á. Fuentes, C. Jones and S. Aldridge, *Angew. Chem., Int. Ed.*, 2019, **58**, 1808–1812; (*m*) K. Yuvaraj and C. Jones, *Dalton Trans.*, 2019, **48**, 11961–11965.
21 For selected examples of [4 + 2] cycloaddition reactions between silaimines and azides, see. (*a*) R. West and M. Denk, *Pure Appl. Chem.*, 1996, **68**, 785–788; (*b*) N. J. Hill, D. F. Moser, I. A. Guzei and R. West, *Organometallics*, 2005, **24**, 3346–3349; (*c*) A. C. Tomasik, A. Mitra and R. West, *Organometallics*, 2009, **28**, 378–381; (*d*) Y. Xiong, S. Yao and M. Driess, *Chem. – Eur. J.*, 2009, **15**, 8542–8547.
22 T. J. Hadlington, T. Szilvási and M. Driess, *Chem. Commun.*, 2018, **54**, 9352–9355.
23 K. Severin, *Chem. Soc. Rev.*, 2015, **44**, 6375–6386.
24 (*a*) K. Banert and O. Plefka, *Angew. Chem., Int. Ed.*, 2011, **50**, 6171–6174; (*b*) N. J. Hartmann, G. Wu and T. W. Hayton, *Angew. Chem., Int. Ed.*, 2015, **54**, 14956–14959; (*c*) J. Hicks, A. Heilmann, P. Vasko, J. M. Goicoechea and S. Aldridge, *Angew. Chem., Int. Ed.*, 2019, **58**, 17265–17268; (*d*) M. D. Anker and M. P. Coles, *Angew. Chem., Int. Ed.*, 2019, **58**, 18261–18265.
25 C. B. Yildiz, *Comput. Theor. Chem.*, 2018, **1134**, 47–53.
26 V. Y. Lee, *Organosilicon Compounds: Theory and Experiment (Synthesis)*, Academic Press, New York, 2017.
27 (*a*) Y. Wang, A. Kostenko, T. J. Hadlington, M.-P. Luecke, S. Yao and M. Driess, *J. Am. Chem. Soc.*, 2019, **141**, 626–634; (*b*) Y. Xiong, S. Yao, T. Szilvási, A. Růžička and M. Driess, *Chem. Commun.*, 2020, **56**, 747–750.
28 (*a*) J. Kapp, M. Remko and P. v. R. Schleyer, *J. Am. Chem. Soc.*, 1996, **118**, 5745–5751; (*b*) Y. Xiong, S. Yao and M. Driess, *Angew. Chem., Int. Ed.*, 2013, **52**, 4302–4311.
29 (*a*) T. Kudo and S. Nagase, *J. Phys. Chem.*, 1984, **88**, 2833–2840; (*b*) T. Kudo and S. Nagase, *J. Am. Chem. Soc.*, 1985, **107**, 2589–2595; (*c*) M. Kimura and S. Nagase, *Chem. Lett.*, 2001, **30**, 1098–1099; (*d*) V. G. Avakyan, V. F. Sidorkin, E. F. Belogolova, S. L. Guselnikov and L. E. Gusel'nikov, *Organometallics*, 2006, **25**, 6007–6013.
30 A. L. Allred, *J. Inorg. Nucl. Chem.*, 1961, **17**, 215–221.
31 V. Nesterov, D. Reiter, P. Bag, P. Frisch, R. Holzner, A. Porzelt and S. Inoue, *Chem. Rev.*, 2018, **118**, 9678–9842.
32 S. Inoue and K. Leszczyńska, *Angew. Chem., Int. Ed.*, 2012, **51**, 8589–8593.
33 For selected examples of donor/acceptor-stabilized oxygen-substituted silanones, see. (*a*) S. Yao, Y. Xiong, M. Brym and M. Driess, *J. Am. Chem. Soc.*, 2007, **129**, 7268–7269; (*b*) J. D. Epping, S. Yao, M. Karni, Y. Apeloig and M. Driess, *J. Am. Chem. Soc.*, 2010, **132**, 5443–5455; (*c*) R. S. Ghadwal, R. Azhakar, H. W. Roesky, K. Pröpper, B. Dittrich, S. Klein and G. Frenking, *J. Am. Chem. Soc.*, 2011, **133**, 17552–17555; (*d*) R. Rodriguez, D. Gau, T. Troadec, N. Saffon-Merceron, V. Branchadell, A. Baceiredo and T. Kato, *Angew. Chem., Int. Ed.*, 2013, **52**, 8980–8983; (*e*) R. Rodriguez, T. Troadec, D. Gau, N. Saffon-Merceron, D. Hashizume, K. Miqueu, J.-M. Sotiropoulos, A. Baceiredo and T. Kato, *Angew. Chem., Int. Ed.*, 2013, **52**, 4426–4430; (*f*) Y. Wang, M. Chen, Y. Xie, P. Wei, H. F. Schaefer III and G. H. Robinson, *J. Am. Chem. Soc.*, 2015, **137**, 8396–8399; (*g*) Y. Wang, M. Chen, Y. Xie, P. Wei, H. F. Schaefer III, P. v. R. Schleyer and G. H. Robinson, *Nat. Chem.*, 2015, **7**, 509–513; (*h*) R. Rodriguez, D. Gau, J. Saouli, A. Baceiredo, N. Saffon-Merceron, V. Branchadell and T. Kato, *Angew. Chem., Int. Ed.*, 2017, **56**, 3935–3939; (*i*) D. C. H. Do, A. V. Protchenko, M. Á. Fuentes, J. Hicks, E. L. Kolychev, P. Vasko and S. Aldridge, *Angew. Chem., Int. Ed.*, 2018, **57**, 13907–13911; (*j*) R. Rodriguez, I. Alvarado-Beltran, J. Saouli, N. Saffon-Merceron, A. Baceiredo, V. Branchadell and T. Kato, *Angew. Chem., Int. Ed.*, 2018, **57**, 2635–2638.
34 A. Bondi, *J. Phys. Chem.*, 1964, **68**, 441–451.
35 B. R. Van Ausdall, J. L. Glass, K. M. Wiggins, A. M. Aarif and J. Louie, *J. Org. Chem.*, 2009, **74**, 7935–7942.
36 (*a*) S. Yao, M. Brym, C. van Wüllen and M. Driess, *Angew. Chem., Int. Ed.*, 2007, **46**, 4159–4162; (*b*) Y. Xiong, S. Yao and M. Driess, *Angew. Chem., Int. Ed.*, 2010, **49**, 6642–6645; (*c*) R. S. Ghadwal, R. Azhakar, H. W. Roesky, K. Pröpper, B. Dittrich, C. Goedecke and G. Frenking, *Chem. Commun.*, 2012, **48**, 8186–8188; (*d*) A. Rosas-Sánchez, I. Alvarado-Beltran, A. Baceiredo, N. Saffon-Merceron, S. Massou, D. Hashizume, V. Branchadell and T. Kato, *Angew. Chem., Int. Ed.*, 2017, **56**, 15916–15920.
37 R. Kobayashi, S. Ishida and T. Iwamoto, *Angew. Chem., Int. Ed.*, 2019, **58**, 9425–9428.

 This journal is © The Royal Society of Chemistry 2020

8. Silicon and Oxygen's Bond of Affection: An Acyclic Three-Coordinate Silanone and Its Transformation to an Iminosiloxysilylene

Title: "Silicon and Oxygen's Bond of Affection: An Acyclic Three-Coordinate Silanone and Its Transformation to an Iminosiloxysilylene"[282]

Status: Article; published online: November 3, 2017.

Journal: *Journal of the American Chemical Society* **2017**, *139*(47), 17193–17198.

Publisher: American Chemical Society (ACS)

DOI: 10.1021/jacs.7b10634

Authors: Daniel Wendel, Dominik Reiter, Amelie Porzelt, Philipp J. Altmann, Shigeyoshi Inoue, and Bernhard Rieger[a]

Reprinted with permission of the American Chemical Society. © 2017 American Chemical Society.

Content: In sharp contrast to the pervasive and versatile ketones, silanones, the heavier silicon congeners, are still rather elusive and largely unexplored species. Despite the impressive progress made over the last decades in isolating a number of unique silanone derivatives, including even three-coordinate ones, reports of isolable acyclic, donor-free silanones are practically unknown.

This publication outlines the capability of silylenes for the remarkable isolation of the first ambient temperature stable, three-coordinate acyclic iminosilylsilanones. These elusive species, which have ever since fascinated many generations of organosilicon chemists, were synthesized *via* simple oxygenation of "masked" iminosilylsilylenes with N_2O. The fully characterized novel silanones are indefinitely stable in the solid-state and exhibit lifetimes of up to 2 days in solution. SC-XRD analysis and supportive DFT calculations provided deeper insights into the nature of the Si=O double bond and unveiled the combination of the σ-donating electropositive silyl groups and the π-donating NHI ligand as crucial for the stabilization.

Preliminary reactivity investigations toward MeOH and CO_2 resulted in the formation of novel methoxysilanols and silicon carbonate complexes, respectively. Interestingly, distinct rearrangement pathways were revealed, depending on the type of silyl ligand used. Whereas a 1,3-silyl migration of the hypersilyl-substituted derivative led to a transient disilene, the supersilyl (^{t}Bu$_3$Si)-supported iminosilylsilanone isomerized to the first isolable acyclic, two-coordinate iminosiloxysilylene (*vide supra*). Furthermore, a transition metal-like reactivity for the silylene was found by the formation of a novel silirane *via* a selective [2+1] cycloaddition reaction with ethylene. In summary, our results represent another fascinating advance in the field of low-coordinate organosilicon compounds and pave the way for further promising studies on acyclic silanones.

[a]D. Wendel and D. Reiter planned and executed all experiments and co-wrote the manuscript. A Porzelt designed and performed the theoretical analyses and provided valuable mental input. P. J. Altmann carried out the SC-XRD measurements and processed the corresponding data. All work was performed under the supervision of S. Inoue and B. Rieger.

JACS
JOURNAL OF THE AMERICAN CHEMICAL SOCIETY
Article
Cite This: J. Am. Chem. Soc. 2017, 139, 17193-17198
pubs.acs.org/JACS

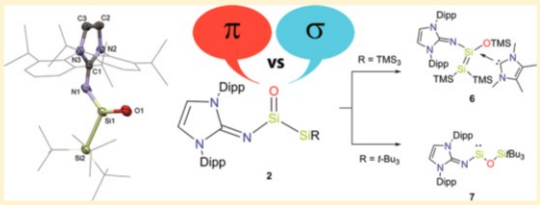
Silicon and Oxygen's Bond of Affection: An Acyclic Three-Coordinate Silanone and Its Transformation to an Iminosiloxysilylene

Daniel Wendel,[†,‡] Dominik Reiter,[†,§] Amelie Porzelt,[§] Philipp J. Altmann,[⊥] Shigeyoshi Inoue,[*,§] and Bernhard Rieger[*,‡]

[‡]WACKER-Chair of Macromolecular Chemistry, [§]WACKER-Institute of Silicon Chemistry, [⊥]Catalysis Research Center, Technische Universität München, Lichtenbergstraße 4, 85748 Garching bei München, Germany

Supporting Information

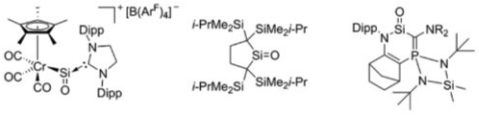
ABSTRACT: A long-term dream comes true: An acyclic, neutrally charged silanone at last! Here, we report on the first examples of isolable acyclic, neutral, three-coordinate silanones **2** with indefinite stability as solids and lifetimes in solution of up to 2 days. The electronic properties of the Si=O bond were investigated via DFT calculations and revealed the π-donating *N*-heterocyclic imino (NHI) and σ-donating silyl groups as key factors for their enhanced stability. Besides initial reactivity studies of **2** toward CO_2 and methanol, different isomerization pathways depending on the silyl substitution pattern were found. For **2a** (R = TMS), a 1,3-silyl shift gave an intermediary disilene, which was trapped as unique NHC-disilene adduct **6**. For the more stable silanone **2b** (R = *t*-Bu), a selective transformation to the first reported room temperature stable, acyclic, two-coordinate *N*,*O*-silylene **7** exhibiting a fascinating siloxy ligand was observed. Both compounds were fully characterized experimentally and their bonding features were analyzed by theoretical calculations.



INTRODUCTION

Poly(siloxanes) are some of the most important and widely used inorganic polymers with a broad spectrum of applications ranging from industrial purposes to custom-designed materials of our daily life.[1] Considering today's widespread success, it is quite peculiar that poly(siloxanes) $(R_2SiO)_n$ were discovered by mere accident, when about one century ago organosilicon pioneer Frederic S. Kipping had actually been seeking silicon analogs of ketones ($R_2Si{=}O$).[2] Since then, the truly monomeric $R_2Si{=}O$ unit, generally referred to as silanone, has been one of the most sought-after compounds in modern main group chemistry ("Kipping's dream").[3] Unlike their lighter congeners, silanones possess a highly reactive Si=O double bond, which tends to undergo rapid head-to-tail polymerization to form stable Si−O σ-bonds.[4] This extreme reactivity is mainly attributed to the strong $Si^{\delta+}{-}O^{\delta-}$ polarization as a result of the large difference in electronegativity between both elements and an unfavorable overlap of the interacting silicon and oxygen p_π-orbitals.[5] Therefore, until a few years ago, silanones have been observed only in the gas phase or in argon matrices at low temperatures.[6] However, the recent decade has witnessed several attempts to tame the polarized Si=O double bond by additional coordination to Lewis acids or bases,[7] giving rise to a variety of isolable donor−acceptor[8] or donor-stabilized[9] complexes. A more recent approach abstains from this external perturbation and relies on the basic idea of kinetic and thermodynamic stabilization of the Si=O moiety by only two adjacent ligands (Chart 1).[10] The first impressive breakthrough toward three-coordinate silanones was achieved by Filippou et al., who isolated stable

Chart 1. Literature Known Examples of Three-Coordinate Silanones I−III



cationic metallosilanone **I**, which may partly be considered as an NHC-adduct of silicon monoxide.[11] Iwamoto and co-workers followed shortly after by reporting transient dialkylsilanone **II** stable at −80 °C.[12] Even more spectacular is the recent success of the group of Kato, who took advantage of two strong π-donors and isolated the first crystalline cyclic silanone **III** with half-life times in solution of up to 5 h at room temperature.[13]

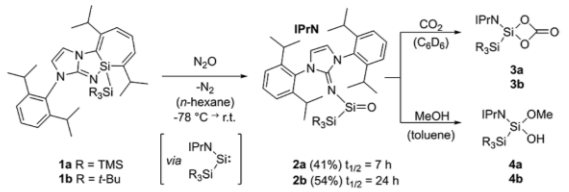
We have previously reported an acyclic iminosilylsilylene, which reversibly inserts into a C=C double bond of its aromatic ligand framework to form silepin **1a** (Scheme 1).[14] This tendency to undergo reductive elimination has been exploited to use **1a** as direct synthetic equivalent of silylene in the activation of small molecules. Continuing this study, we were interested to see whether the *N*-heterocyclic imino (NHI) ligand[15] as single π-donor of the silepin-silylene system may sufficiently stabilize a highly polarized Si=O moiety.

Received: October 6, 2017
Published: November 3, 2017

ACS Publications © 2017 American Chemical Society

DOI: 10.1021/jacs.7b10634
J. Am. Chem. Soc. 2017, 139, 17193−17198

Scheme 1. Preparation and Reactivity of Acyclic Three-Coordinate Silanones 2



Herein, we present the first examples of acyclic and neutrally charged silanones **2** with a planar three-coordinate Si atom. Furthermore, chemical lifetimes, isomerization pathways, and initial reactivity studies of **2** are discussed in detail.

RESULTS AND DISCUSSIONS

Exposure of an *n*-hexane solution of silepin **1** at −78 °C to an atmosphere of N_2O followed by warming to room temperature instantly gave a white precipitate, which was separated by filtration, washed with *n*-hexane and dried in vacuo to give pure silanone **2** in moderate yield (**2a** 41%, **2b** 54%) (Scheme 1). The ^{29}Si NMR spectra of both compounds displayed signals for the central silicon atom at 33.7 ppm for **2a** and 28.8 ppm for **2b** (calc. 33.3 ppm at SMD-B3LYP/6-311+G(2d,2p) level of theory), respectively. Both NMR shifts are in the typical region for three-coordinate silicon compounds, but are considerably high-field shifted in comparison to **I** (169.6 ppm)[11] and **II** (128.4 ppm).[12] They even fall in the same range as cyclic silanone **III** (38.4 ppm)[13] with two π-donating substituents, illustrating the strong donor qualities of a single NHI ligand. The characteristic Si═O stretching vibration was found at 1144 cm^{-1} for both compounds, which is in good agreement with the calculated value ($\nu_{Si=O}$ = 1155 cm^{-1}) and comparable to other Si═O containing structures.[12,16] The UV−vis spectrum of **2b** in toluene revealed an broad absorption peak at 282 nm in the same region as related acyclic three-coordinate germanone (297 nm).[10] Colorless crystals of **2b** were obtained by slow diffusion of Et_2O into a saturated THF solution at −35 °C over several days. Single-crystal X-ray analysis confirmed the monomeric structure of **2b** and exposed the position of the Si═O moiety in a well-protected steric pocket between the two bulky ligands (Figure 1).

The crystal structure revealed a trigonal planar silicon center (sum of bonding angles: 360°) and a Si1−O1 bond length of **2b** (1.537(3) Å), which is slightly longer than that of metallosilanone **I** (1.526 Å)[11] and cyclic silanone **III** (1.533 Å),[13] but generally shorter than those of tetra-coordinate base-stabilized silanones.[8,9] The potent electron donation from the exocyclic nitrogen atom of the NHI ligand to the electron deficient silicon atom is clearly evidenced by a short Si1−N1 bond (1.646(3) Å), for which reason resonance form **2b′** should be denoted (Chart 2). Further, the N1−C1 bond (1.319(4)Å) is elongated and the endocyclic C−N bonds (C1−N2 1.364(5) Å/ C1−N3 1.368(5) Å) are slightly shortened.[17] Combined with a small Si1−N1−C1 angle of merely 131.7(3)° one can assume that the positive charge may be delocalized over the iminato ring as illustrated in structure **2b″**. However, according to the X-ray data, the almost perpendicular assembly of the planar NHC fragment to the N1Si1O1 plane (dihedral angle 89.9(4)°) seems to limit this conjugative effect. To obtain further insights into the bonding properties of **2b**, we performed density functional theory (DFT) calculations at

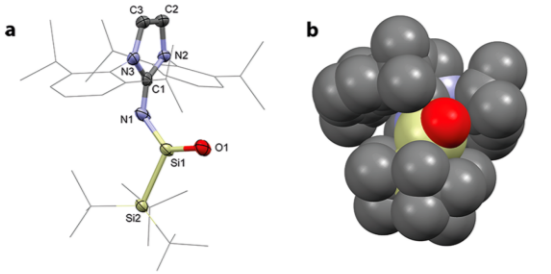
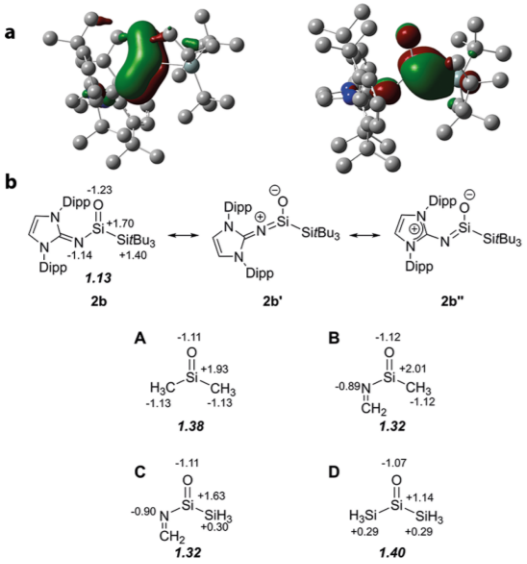


Figure 1. (a) Molecular structure and (b) space filling representation of silanone **2b** in the solid state with ellipsoids set at the 50% probability level (one out of two independent molecules in the asymmetric unit). For clarity, hydrogen atoms are omitted and *t*-Bu as well as Dipp groups are simplified as wireframes. Selected bond lengths (Å) and angles (deg): Si1−O1 1.537(3), Si1−N1 1.646(3), N1−C1 1.319(4), C1−N2 1.364(5), C1−N3 1.368(5), Si1−Si2 2.358(2), N1−Si1−Si2 112.6(1), C1−N1−Si1 131.7(3).

Chart 2. (a) DFT-Calculated HOMO−10 *E* = −7.78 eV and LUMO+4 *E* = −0.41 eV of 2b, (b) Plausible Resonance Forms of 2b and Calculated Smaller Silanones A, B, C, and D Including NPA Charges and Bond Orders (in bold and italics)



the B3LYP/6-311+G(d) level of theory. The analysis of the Kohn−Sham orbitals (Chart 2a) showed that HOMO−10 represents the Si═O π-bond, which obviously mixes with the nonbonding orbital of the exocyclic nitrogen atom, explaining the observed short Si1−N1 distance. As already extracted from the X-ray data, an expansion of the conjugation to the NHC ring fragment could not be found. Interestingly, the LUMO+4 reveals significant hyperconjugation from the Si−C σ-bond of the silyl group to the π^*-bonding orbital of Si═O moiety. Moreover, from NBO analysis (Chart 2b) a decreased Si═O bond order (1.13) and an increased negative charge on the oxygen center (−1.23) compared to those of dimethylsilanone **A** (1.38 and −1.11) were found, illustrating the strong polarization of the Si═O double bond. However, the positive character at Si1 decreases. To explain this effect, we calculated

DOI: 10.1021/jacs.7b10634
J. Am. Chem. Soc. 2017, 139, 17193−17198

the smaller iminoalkyl- **B**, iminosilyl- **C** and disilylsilanone **D** analogs. Here too the trend is visible, that the positive charge at the silicon center is effectively reduced by presumable σ-donation and hyperconjugation of the silyl group.[4b] In compound **2b** this effect fully sets in and Si1 has only a slightly higher positive charge (1.70) than Si2 attached to *t*-Bu groups (1.40). Our analysis proves that besides the kinetical stabilization due to steric encumbrance, especially the π-donor qualities of NHI ligand but as well σ-donor properties of silyl group are key to stabilize acyclic silanone **2b**.

In terms of reactivity, both silanones **2** were directly and quantitatively converted by CO_2 to the respective silicon carbonate complexes **3**, similarly to the reaction of silepin **1a** with carbon dioxide (Scheme 1).[14] Moreover, the reaction of silanones **2** toward methanol was tested. As in carbonyl chemistry, where ketones form hemiketals with alcohols, the corresponding silanol **4** was isolated in good yield (**4a** 71%, **4b** 69%). The ^{29}Si NMR shift of the silicon center of **4a** at −38.6 ppm and **4b** at −46.6 ppm, respectively, clearly displayed the change in coordination number from three to four. The X-ray diffraction analysis of **4a** (Figure 2) verified the presence of a

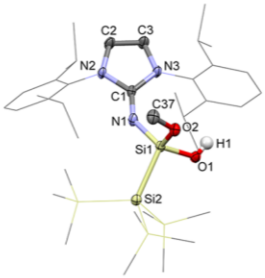
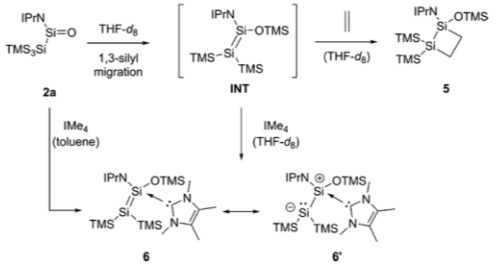


Figure 2. Molecular structure of silanol **4a** in the solid state with ellipsoids set at the 50% probability level. For clarity, hydrogen atoms and cocrystallized solvent molecules are omitted and TMS as well as Dipp groups are simplified as wireframes. Selected bond lengths (Å) and angles (deg): Si1−O1 1.642(2), Si1−O2 1.660(2), Si1−N1 1.680(2), N1−C1 1.278(3), C1−N2 1.394(3), C1−N3 1.396(3), N1−Si1−O1 118.7(1), C1−N1−Si1 142.4(2).

tetra-coordinate silicon center attached to one methoxy and one hydroxyl group. The Si1−O1 bond length of **4a** (1.642(2) Å) is unambiguously distinguishable from the original Si=O bond of **2b**. Interestingly, in this structure, the Si1−N1 bond (1.680(2) Å) is elongated and the N1−C1 bond (1.278(3) Å) slightly shortened in comparison to **2b**, which underlines the disappearance of the former Si=N double-bond character.

A key criterion for storage, handling and reaction design of silanones is their lifetime. Monitoring a C_6D_6 solution of silanone **2a** via ^{1}H NMR spectroscopy showed the full decomposition to an unspecific product mixture within 14 h ($t_{1/2}$ = 7 h). ^{1}H, ^{29}Si and ^{1}H/^{29}Si HMBC NMR data pointed to one major asymmetric product, presumably formed by TMS migration from the hypersilyl group to the Si=O center and subsequent activation of the NHI ligand (see the Supporting Information). Further experiments revealed that its half-life can be extended considerably by using **2a** in CD_3CN solutions ($t_{1/2}$ = 4 days). Consistent with additional Lewis base coordination, the ^{29}Si NMR signal of the Si=O center is shifted from +33.7 ppm to −48.3 ppm. Crystals of tetra-coordinate acetonitrile-silanone adduct **2a** × CD_3CN were isolated and verified the additional solvent coordination (see SI). Still, we were interested to pin down the reactive intermediate in the decomposition process of **2a**. According to literature, a 1,3-silyl migration has been reported for transient cyclic dialkylsilanone **II** to form an intermediary silene.[12] Indeed, we figured out that the same TMS migration can be instantly induced by addition of THF-d_8 to solid **2a**, resulting in a strongly yellow colored solution (Scheme 2). Subsequent NMR

Scheme 2. Isomerization Pathway of Silanone 2a and Trapping of Intermediary Disilene INT



analysis indicated the quantitative formation of the proposed transient disilene **INT**. Strikingly, the different electronic environment at both silicon centers of **INT** due to the asymmetric substitution pattern is already noticeable in the ^{29}Si NMR shifts (−8.0 ppm (*Si*OTMS), − 196.6 ppm (*Si*TMS$_2$)), which suggest a polarized Si=Si double bond with high zwitterionic character. Because of the short lifetime of this species, isolation and full characterization was not possible and so trapping experiments were performed. Exposure of a THF-d_8 solution of **2a**, in situ forming **INT**, to ethylene immediately gave the colorless [2 + 2]-cycloaddition product **5**. 1,2-Disiletane **5** was sufficiently characterized via 2D NMR experiments and matching theoretical NMR shifts. Further, we tried to stabilize **INT** with a strong NHC donor. Reaction of **INT** in THF-d_8 or alternatively directly silanone **2a** in toluene with IMe_4 exclusively gave room-temperature-stable NHC-stabilized disilene adduct **6**. The ^{29}Si NMR shifts of **6** (−35.2 ppm (*Si*OTMS), − 174.6 ppm (*Si*TMS$_2$)) are similar to those of intermediary disilene **INT**, especially the latter, illustrating the presence of a highly negatively charged silicon atom, consistent with typical silyl anions.[18]

Orange-red crystals of **6** were isolated from an *n*-hexane solution at −35 °C. Subsequent X-ray analysis confirmed the coordination of the NHC donor to the distorted tetrahedral Si1 center (Figure 3a). The Si1−C28 bond length (1.958(2) Å) is in the range of typical dative NHC-Si bonds,[19] the assumed Si1−Si2 double bond is extremely elongated (2.3297(9) Å), slightly shorter than Si2−Si3 (2.3397(9) Å) and Si2−Si4 (2.3445(9) Å) bond, but beyond the range of classical Si=Si double bonds (2.13−2.31 Å).[20]

Still, compound **6** possesses a typical trans-bent geometry and shows significant pyramidalization, especially at the Si2 center (bent angles θ(Si1) = 42.7° and θ(Si2) = 57.8°). This strong bending underpins the assumption of zwitterionic resonance structure **6′** with a lone pair at Si2, but is distinguishable from a potential Si1−Si2 dative bond as recently discovered for base-stabilized disilene adduct $Me_2EtN \rightarrow SiCl_2 \rightarrow Si(SiCl_3)_2$ with an even larger bent angle ($\theta(Si(SiCl_3)_2$ = 79.1°).[21] Because NHC adducts of multiply bonded silicon compounds are rarely found in literature,[22] we were further interested in the electronic

DOI: 10.1021/jacs.7b10634
J. Am. Chem. Soc. 2017, 139, 17193−17198

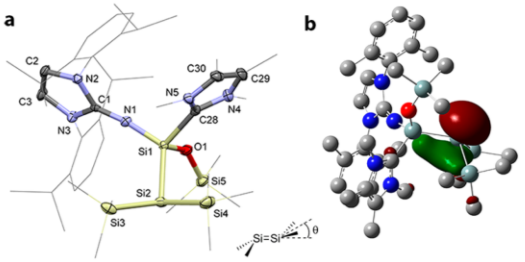
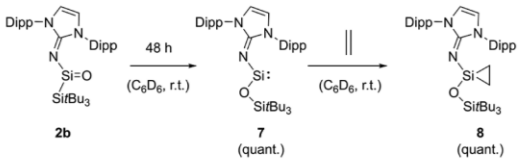


Figure 3. (a) Molecular structure of IMe_4 stabilized disilene adduct **6** in the solid state with ellipsoids set at the 50% probability level (one out of two independent molecules in the asymmetric unit). For clarity, hydrogen atoms and TMS as well as Dipp groups are simplified as wireframes. Selected bond lengths (Å) and angles (deg): Si1−Si2 2.3297(7), Si2−Si3 2.3397(9), Si2−Si4 2.3445(9), Si1−C28 1.958(2), Si1−O1 1.656(2), Si1−N1 1.659(2), N1−C1 1.263(3), C1−N2 1.407(3), C1−N3 1.400(3), C1−N1−Si1 168.9(2). b) DFT-calculated HOMO (−3.54 eV) of **6**.

properties of **6**. DFT calculations indicated that the HOMO (Figure 3b) mainly represents the lone pair at the Si2 atom with only short extensions not only to Si1 but to all surrounding silicon centers. The bond indices (see the Supporting Information) follow the same trend, with a WBI of Si1−Si2 (1.04) only slightly insinuating double bond character compared to Si2−Si3 (0.99) and Si2−Si4 (0.98). Regarding NPA charges, the polarization of Si1 (1.61) and Si2 (−0.60) in comparison to Si3 and Si4 (1.18) come to the same conclusion that the proposed zwitterionic canonical form **6′** is the most fitting representation to describe the electronic nature of this compound.

In strong contrast to the 1,3-silyl migration of **2a**, silanone **2b** shows almost no variations in the ^{29}Si NMR shifts during the solvent change from C_6D_6 to THF-d_8, indicating no observable donor−acceptor interaction between solvent and silanone. Because of replacement of TMS by *t*-Bu groups, silanone **2b** is indefinitely stable as a solid at room temperature, but remarkably forms mixed *N,O*-silylene **7** in C_6D_6 or THF-d_8 solution at ambient conditions within 48 h ($t_{1/2}$ = 24 h) in quantitative yield. This transformation can be accelerated by heating the solution to 60 °C, where full conversion was detected by NMR spectroscopy in less than 1 h (Scheme 3).

Scheme 3. Selective Transformation of Silanone 2b to Acyclic *N,O*-Silylene 7 and Formation of Silirane 8



The facile thermal rearrangement is supported by theoretical calculations, which determined that *N,O*-silylene **7** is in fact 28.8 kJ/mol more stable than silanone **2b**. We believe that most likely the oxophilicity of silicon, promoting formation of stable Si−O single bonds, is the driving force of this reaction, which even overcomes the counteracting change of oxidation state from Si(IV) back to less stable Si(II). The ^{29}Si NMR signal of the central silicon atom of silylene **7** at 58.9 ppm (C_6D_6) is high-field shifted compared to other room-temperature-stable two-coordinate diamino (204.6 ppm)[23] and dithiolato silylenes (285.5 ppm).[24]

In particular, the upfield shift in comparison to strongly related in situ generated iminosilylsilylene IPrNSi(II)SiTMS$_3$ (300.0 ppm)[14] suggests additional π-donation by the siloxy ligand. A band for the characteristic $Si_n \rightarrow Si_{3p}$ transition of **7** was observed at 328 nm, which is very close to the theoretically predicted data (HOMO → LUMO 341 nm). X-ray analysis of colorless crystals of **7** revealed a two-coordinate silicon center exhibiting an N1−Si1−O1 angle of 103.56(8)° (Figure 4a).

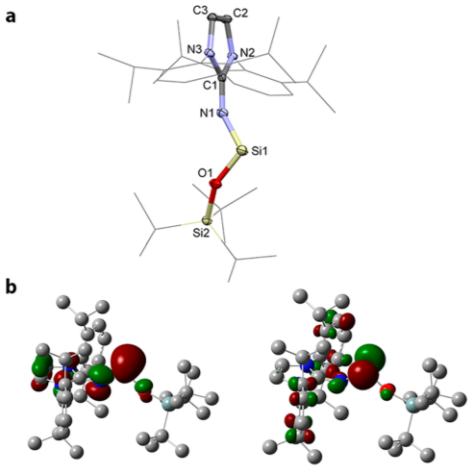


Figure 4. (a) Molecular structure of *N,O*-silylene **7** in the solid state with ellipsoids set at the 50% probability level (one out of two independent molecules in the asymmetric unit). For clarity, hydrogen atoms and *t*-Bu as well as Dipp groups are simplified as wireframes. Selected bond lengths (Å) and angles (deg): Si1−O1 1.643(1), O1−Si2 1.637(1), Si1−N1 1.661(2), N1−C1 1.281(2), C1−N2 1.380(3), C1−N3 1.386(2), N1−Si1−O1 103.56(8), C1−N1−Si1 147.7(2), Si1−O1−Si2 153.2(1). b) DFT-calculated HOMO (left, −5.04 eV) and LUMO (right, −0.71 eV) of **7**.

This angle is clearly wider than for cyclic NHSis (e.g., (CH(*t*-Bu)N)$_2$Si(II) 88.6°),[25] but considerably more compressed than for acyclic DippNTMSSi(II)SiTMS$_3$ (116.91°).[26] The Si1−N1 bond length (1.661(2) Å) is marginally longer than in the parent silanone structure **2b**, illustrating again a partial Si=N double bond character. Surprisingly, regarding potential π-donation by the siloxy group, both Si−O bonds have nearly the same length (Si1−O1 1.643(1) Å, O1−Si2 1.637(1) Å). Therefore, only a minor Si=O double bond character may be suggested. DFT calculations are in line with these findings, the HOMO of *N,O*-silylene **7** exhibits mainly lone pair character (Si_n), the LUMO resembles the empty Si_{3p} orbital with a HOMO−LUMO gap of 4.33 eV (Figure 4b). Both orbitals show only minor contributions from donating N or O atoms. For orbitals lower in energy, some interactions of silicon with nitrogen (HOMO−6), and even lower, minor interactions with oxygen can be found (see SI). The HOMO−LUMO gap is close to that of the acyclic dithiolato silylene by Power et al. (4.23 eV),[24] indicating a similar level of reactivity toward small molecules. Indeed, both silylenes show no sign of reactivity with molecular hydrogen, even if a reaction solution of **7** in H_2 atmosphere (1 bar) is heated to 60 °C for several days.[24] Regarding the activation of ethylene, it is reported that dithiolato silylene reversibly binds the olefin in a dissociation

DOI: 10.1021/jacs.7b10634
J. Am. Chem. Soc. 2017, 139, 17193−17198

equilibrium.[27] In contrast, *N,O*-silylene **7** quantitatively forms the corresponding silirane **8** within 20 min at room temperature with no observable reverse reaction. We believe that this disparity in reactivity is likely caused by reduced steric shielding at the Si(II) center of **7**.[28]

CONCLUSIONS

In summary, we have successfully isolated and fully characterized the first examples of acyclic, neutral, three-coordinate silanones **2** with indefinite stability as solids and lifetimes in solution up to 2 days. DFT calculations provided insight into the Si═O bonding and verified π-donating NHI and σ-donating silyl groups as important factors for their enhanced stability. First reactivity of silanones **2** toward CO_2 and methanol was tested and potential isomerization pathways were discovered. Here, a 1,3-silyl migration of **2a**, gave an intermediary disilene **INT**, which was trapped as 1,2-disiletane **5** in a [2 + 2]-cycloaddition with ethylene. Further, the NHC-disilene adduct **6** was isolated and analyzed by quantum chemical methods. Interestingly, for **2b**, the selective transformation to the first acyclic, two-coordinate *N,O*-silylene **7** was observed. Here, the enormous potential of acyclic silylene **7** to act as transition-metal mimic was demonstrated by successful activation of ethylene under ambient conditions. In total, our work not only continues the fulfillment of Kipping's dream of isolable silanones, but gives first insights into similarities and differences between this novel compound class and well-known carbonyl compounds.

ASSOCIATED CONTENT

Supporting Information

The Supporting Information is available free of charge on the ACS Publications website at DOI: 10.1021/jacs.7b10634.

Experimental details (PDF)

Crystallographic data (CCDC 1577580−1577584) (CIF)

AUTHOR INFORMATION

Corresponding Authors

*E-mail.: rieger@tum.de (B.R.).

*E-mail: s.inoue@tum.de (S.I.).

ORCID

Shigeyoshi Inoue: 0000-0001-6685-6352

Bernhard Rieger: 0000-0002-0023-884X

Author Contributions

†D.W. and D.R. contributed equally.

Notes

The authors declare no competing financial interest.

ACKNOWLEDGMENTS

We are exceptionally grateful to the WACKER Chemie AG and European Research Council (SILION 63794) for financial support. We thank Dr. Samuel Powley, Philipp Pahl, and Martin Machat for revising the manuscript and Dr. Alexander Pöthig for crystallographic advice. We also express our appreciation to the Leibniz Supercomputing Center of the Bavarian Academy of Science and Humanities for provision of computing time.

REFERENCES

(1) Jones, R. G.; Ando, W.; Chojnowski, J. *Silicon-Containing Polymers*; Springer: Dordrecht, The Netherlands, 2000.

(2) Kipping, F. S.; Lloyd, L. L. *J. Chem. Soc., Trans.* **1901**, *79*, 449−459.

(3) Sen, S. S. *Angew. Chem., Int. Ed.* **2014**, *53*, 8820−8822.

(4) (a) Kudo, T.; Nagase, S. *J. Am. Chem. Soc.* **1985**, *107*, 2589−2595. (b) Kimura, M.; Nagase, S. *Chem. Lett.* **2001**, *30*, 1098−1099.

(5) Avakyan, V. G.; Sidorkin, V. F.; Belogolova, E. F.; Guselnikov, S. L.; Gusel'nikov, L. E. *Organometallics* **2006**, *25*, 6007−6013.

(6) Examples of gas-phase and matrix-isolation experiments: (a) Glinski, R. J.; Gole, J. L.; Dixon, D. A. *J. Am. Chem. Soc.* **1985**, *107*, 5891−5894. (b) Withnall, R.; Andrews, L. *J. Am. Chem. Soc.* **1985**, *107*, 2567−2568. (c) Maier, G.; Meudt, A.; Jung, J.; Pacl, H., Matrix Isolation Studies of Silicon Compounds. In *The Chemistry of Organic Silicon Compounds*; John Wiley & Sons: Chichester, U.K., 1998; pp 1143−1185.

(7) Review on silanones and their heavier homologues: Xiong, Y.; Yao, S.; Driess, M. *Angew. Chem., Int. Ed.* **2013**, *52*, 4302−4311.

(8) (a) Yao, S.; Brym, M.; van Wuellen, C.; Driess, M. *Angew. Chem., Int. Ed.* **2007**, *46*, 4159−4162. (b) Xiong, Y.; Yao, S.; Driess, M. *Angew. Chem., Int. Ed.* **2010**, *49*, 6642−6645. (c) Xiong, Y.; Yao, S.; Driess, M. *Dalton Trans.* **2010**, *39*, 9282−9287. (d) Xiong, Y.; Yao, S.; Müller, R.; Kaupp, M.; Driess, M. *J. Am. Chem. Soc.* **2010**, *132*, 6912−6913. (e) Ghadwal, R. S.; Azhakar, R.; Roesky, H. W.; Pröpper, K.; Dittrich, B.; Klein, S.; Frenking, G. *J. Am. Chem. Soc.* **2011**, *133*, 17552−17555. (f) Muraoka, T.; Abe, K.; Haga, Y.; Nakamura, T.; Ueno, K. *J. Am. Chem. Soc.* **2011**, *133*, 15365−15367. (g) Ghadwal, R. S.; Azhakar, R.; Roesky, H. W.; Propper, K.; Dittrich, B.; Goedecke, C.; Frenking, G. *Chem. Commun.* **2012**, *48*, 8186−8188. (h) Rodriguez, R.; Gau, D.; Troadec, T.; Saffon-Merceron, N.; Branchadell, V.; Baceiredo, A.; Kato, T. *Angew. Chem., Int. Ed.* **2013**, *52*, 8980−8983. (i) Muraoka, T.; Abe, K.; Kimura, H.; Haga, Y.; Ueno, K.; Sunada, Y. *Dalton Trans.* **2014**, *43*, 16610−16613. (j) Reyes, M. L.; Troadec, T.; Rodriguez, R.; Baceiredo, A.; Saffon-Merceron, N.; Branchadell, V.; Kato, T. *Chem. - Eur. J.* **2016**, *22*, 10247−10253. (k) Rodriguez, R.; Gau, D.; Saouli, J.; Baceiredo, A.; Saffon-Merceron, N.; Branchadell, V.; Kato, T. *Angew. Chem., Int. Ed.* **2017**, *56*, 3935−3939.

(9) (a) Yao, S.; Xiong, Y.; Brym, M.; Driess, M. *J. Am. Chem. Soc.* **2007**, *129*, 7268−7269. (b) Xiong, Y.; Yao, S.; Driess, M. *J. Am. Chem. Soc.* **2009**, *131*, 7562−7563. (c) Yao, S.; Xiong, Y.; Driess, M. *Chem. - Eur. J.* **2010**, *16*, 1281−1288. (d) Xiong, Y.; Yao, S.; Müller, R.; Kaupp, M.; Driess, M. *Nat. Chem.* **2010**, *2*, 577−580. (e) Epping, J. D.; Yao, S.; Karni, M.; Apeloig, Y.; Driess, M. *J. Am. Chem. Soc.* **2010**, *132*, 5443−5455. (f) Rodriguez, R.; Troadec, T.; Gau, D.; Saffon-Merceron, N.; Hashizume, D.; Miqueu, K.; Sotiropoulos, J.-M.; Baceiredo, A.; Kato, T. *Angew. Chem., Int. Ed.* **2013**, *52*, 4426−4430. (g) Hansen, K.; Szilvási, T.; Blom, B.; Irran, E.; Driess, M. *Chem. - Eur. J.* **2015**, *21*, 18930−18933. (h) Troadec, T.; Lopez Reyes, M.; Rodriguez, R.; Baceiredo, A.; Saffon-Merceron, N.; Branchadell, V.; Kato, T. *J. Am. Chem. Soc.* **2016**, *138*, 2965−2968.

(10) Analog strategy for isolation of acyclic three-coordinate germanone: Li, L.; Fukawa, T.; Matsuo, T.; Hashizume, D.; Fueno, H.; Tanaka, K.; Tamao, K. *Nat. Chem.* **2012**, *4*, 361−365.

(11) Filippou, A. C.; Baars, B.; Chernov, O.; Lebedev, Y. N.; Schnakenburg, G. *Angew. Chem., Int. Ed.* **2014**, *53*, 565−570.

(12) Ishida, S.; Abe, T.; Hirakawa, F.; Kosai, T.; Sato, K.; Kira, M.; Iwamoto, T. *Chem. - Eur. J.* **2015**, *21*, 15100−15103.

(13) Alvarado-Beltran, I.; Rosas-Sánchez, A.; Baceiredo, A.; Saffon-Merceron, N.; Branchadell, V.; Kato, T. *Angew. Chem., Int. Ed.* **2017**, *56*, 10481−10485.

(14) Wendel, D.; Porzelt, A.; Herz, F. A. D.; Sarkar, D.; Jandl, C.; Inoue, S.; Rieger, B. *J. Am. Chem. Soc.* **2017**, *139*, 8134−8137.

(15) Ochiai, T.; Franz, D.; Inoue, S. *Chem. Soc. Rev.* **2016**, *45*, 6327−6344.

(16) Linden, M. M.; Reisenauer, H. P.; Gerbig, D.; Karni, M.; Schäfer, A.; Müller, T.; Apeloig, Y.; Schreiner, P. R. *Angew. Chem., Int. Ed.* **2015**, *54*, 12404−12409.

DOI: 10.1021/jacs.7b10634
J. Am. Chem. Soc. 2017, 139, 17193−17198

(17) Inoue, S.; Leszczynska, K. *Angew. Chem., Int. Ed.* **2012**, *51*, 8589−8593.
(18) Marschner, C. *Eur. J. Inorg. Chem.* **1998**, *1998*, 221−226.
(19) Ahmad, S. U.; Szilvasi, T.; Irran, E.; Inoue, S. *J. Am. Chem. Soc.* **2015**, *137*, 5828−5836.
(20) (a) Weidenbruch, M., In *The Chemistry of Organic Silicon Compounds*, Rappoport, Z., Apeloig, Y., Eds.; John Wiley & Sons: Chichester, U.K., 2001; Vol. 3, pp 391−428. (b) Wendel, D.; Szilvási, T.; Jandl, C.; Inoue, S.; Rieger, B. *J. Am. Chem. Soc.* **2017**, *139*, 9156−9159.
(21) Schweizer, J. I.; Scheibel, M. G.; Diefenbach, M.; Neumeyer, F.; Würtele, C.; Kulminskaya, N.; Linser, R.; Auner, N.; Schneider, S.; Holthausen, M. C. *Angew. Chem., Int. Ed.* **2016**, *55*, 1782−1786.
(22) (a) Yamaguchi, T.; Sekiguchi, A.; Driess, M. *J. Am. Chem. Soc.* **2010**, *132*, 14061−14063. (b) Leszczynska, K.; Abersfelder, K.; Mix, A.; Neumann, B.; Stammler, H.-G.; Cowley, M. J.; Jutzi, P.; Scheschkewitz, D. *Angew. Chem., Int. Ed.* **2012**, *51*, 6785−6788. (c) Yamaguchi, T.; Asay, M.; Sekiguchi, A. *J. Am. Chem. Soc.* **2012**, *134*, 886−889. (d) Cowley, M. J.; Huch, V.; Rzepa, H. S.; Scheschkewitz, D. *Nat. Chem.* **2013**, *5*, 876−879.
(23) Hadlington, T. J.; Abdalla, J. A. B.; Tirfoin, R.; Aldridge, S.; Jones, C. *Chem. Commun.* **2016**, *52*, 1717−1720.
(24) Rekken, B. D.; Brown, T. M.; Fettinger, J. C.; Tuononen, H. M.; Power, P. P. *J. Am. Chem. Soc.* **2012**, *134*, 6504−6507.
(25) Moser, D. F.; Guzei, I. A.; West, R. *Main Group Met. Chem.* **2001**, *24*, 811−812.
(26) Protchenko, A. V.; Schwarz, A. D.; Blake, M. P.; Jones, C.; Kaltsoyannis, N.; Mountford, P.; Aldridge, S. *Angew. Chem., Int. Ed.* **2013**, *52*, 568−571.
(27) Lips, F.; Fettinger, J. C.; Mansikkamaki, A.; Tuononen, H. M.; Power, P. P. *J. Am. Chem. Soc.* **2014**, *136*, 634−637.
(28) Kato, T.; Rosas-Sánchez, A.; Alvarado-Beltran, I.; Baceiredo, A.; Saffon-Merceron, N.; Massou, S.; Hashizume, D.; Branchadell, V. *Angew. Chem.* **2017**, DOI: 10.1002/ange.201710358.

DOI: 10.1021/jacs.7b10634
J. Am. Chem. Soc. 2017, 139, 17193−17198

9. Heavier Carbonyl Olefination: The Sila-Wittig Reaction

Title: "Heavier Carbonyl Olefination: The Sila-Wittig Reaction"[283]

Status: Article; published online: September 27, 2019.

Journal: *Journal of the American Chemical Society* **2019**, *141* (42), 16991–16996.

Publisher: American Chemical Society (ACS)

DOI: 10.1021/jacs.9b09379

Authors: Dominik Reiter, Philipp Frisch, Tibor Szilvási, and Shigeyoshi Inoue[a]

Reprinted with permission of the American Chemical Society. © 2019 American Chemical Society.

Content: The *Wittig* reaction, which converts a huge variety of carbonyl compounds with phosphorus ylides into tailor-made alkenes, is without any doubt one of the most important reactions in organic chemistry. Today, this reaction, which was developed and named after *Nobel* laureate *Georg Wittig*, has a wide range of applications in both academia and industry. Despite extensive research and the development of advanced modifications and even catalytic variants, *Wittig's* olefination has not yet been adapted to heavier carbonyl homologues.

This article demonstrates the successful application of the *Wittig* reaction to the above mentioned iminosilylsilanone (IDippN)(^{t}Bu$_3$Si)Si=O and thus represents the first report on a heavier carbonyl olefination method. In sharp contrast to the "classical" *Wittig* reaction, the phosphorus ylides used were not synthesized *in situ* but isolated, in order to prevent reactions of the much more reactive silanones with the bases applied for deprotonation of the respective phosphonium salts or the deprotonation byproducts. Initially, commercially available stabilized ylides were investigated, but due to the significant differences in stability and reactivity between silanones and their lighter carbonyl congeners (silanones bear a strongly polarized and thus zwitterionic Si=O double bond), a reactivity deviating from the *Wittig* olefination was observed.

With semi-stabilized ylides, the formation of a silanoyl-substituted ylide was accomplished *via* a nucleophilic attack of the utilized phosphorus ylide to the Si=O moiety. Additionally, a successful sila-*Wittig* reaction was indicated with the synthesis of a silacyclobutene, which represents the formal 4π-electron electrocyclization product of an intermediary generated transient silene.

Remarkably, exposure of (IDippN)(^{t}Bu$_3$Si)Si=O to a series of non-stabilized ylides provided the selective formation of various silenes *via* the unprecedented sila-*Wittig* reaction under mild conditions. Analogous to the classical Wittig reaction, a high preference for the respective (*Z*)-isomers was generally observed. Unfortunately, the synthesized iminosilylsilenes proved to be too reactive and decomposed during isolation attempts. Nevertheless, the sila-*Wittig* reaction represents an unprecedented method to gain access to otherwise elusive compounds.

[a]D. Reiter planned and executed all experiments and wrote the manuscript. P. Frisch carried out the SC-XRD measurements and processed the corresponding data. T. Szilvási designed and performed the theoretical analyses and provided valuable mental input. All work was performed under the supervision of S. Inoue.

JACS JOURNAL OF THE AMERICAN CHEMICAL SOCIETY
Article
Cite This: J. Am. Chem. Soc. 2019, 141, 16991−16996
pubs.acs.org/JACS

Heavier Carbonyl Olefination: The Sila-Wittig Reaction

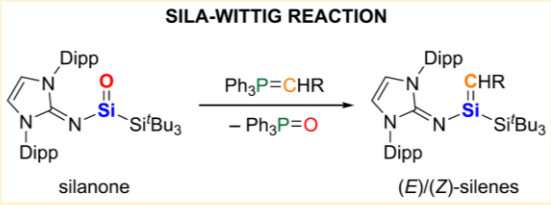
Dominik Reiter,[†] Philipp Frisch,[†] Tibor Szilvási,[‡] and Shigeyoshi Inoue*[,†]

[†]Department of Chemistry, WACKER-Institute of Silicon Chemistry and Catalysis Research Center, Technische Universität München, Lichtenbergstraße 4, 85748 Garching bei München, Germany

[‡]Department of Chemical and Biological Engineering, University of Wisconsin—Madison, 1415 Engineering Drive, Madison, Wisconsin 53706-1607, United States

Supporting Information

ABSTRACT: The Wittig reaction is one of the most versatile tools in the repertoire of organic chemists. Thus, a broad variety of carbonyl compounds can be converted to tailor-made alkenes with phosphorus ylides under mild conditions. However, no comparable reaction has been reported for silanones, the silicon congeners of ketones. Here, we demonstrate for the first time the successful application of the Wittig olefination to iminosilylsilanone **1**. The selective formation of a series of silenes ($R_2Si{=}CR_2$) via the sila-Wittig reaction revealed an unprecedented approach to otherwise elusive compounds. In addition, the highly reactive and zwitterionic nature of **1** was also susceptible to nucleophilic attacks and cycloaddition reactions by and with the phosphorus ylides. Our results therefore make another important contribution to discovering the differences and similarities between carbon and silicon.

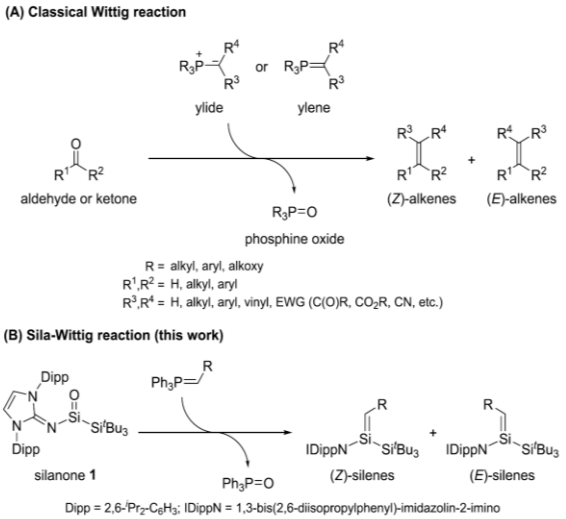


INTRODUCTION

Since the discovery of alkene synthesis from carbonyl compounds with phosphorus ylides by Staudinger[1] and further intense developments by Wittig,[2] this versatile chemo- and regioselective reaction has become indispensable and surpasses all other known olefination methods.[3] Therefore, the now widely known Wittig reaction has emerged as a powerful synthetic tool with applications both in academia and industry.[3] The "classical" Wittig reaction occurs either between an aldehyde or ketone and a phosphorus ylide (or ylene; for convenience, the ylene form is used throughout this Article), providing a mixture of (*E*)- and (*Z*)-alkenes and the respective phosphine oxide byproduct (Scheme 1). Over the years, various protocols have been developed to fine-tune the stereoselectivity and thus the olefin product ratio. In general, the nature of the ylide plays a pivotal role and strongly determines the stereoselectivity of the reaction.[4] While non-stabilized ylides (alkyl substituents) mainly lead to (*Z*)-alkenes and stabilized ylides (electron-withdrawing groups (EWGs)) to (*E*)-alkenes, utilization of semi-stabilized ylides (aryl or alkenyl substituents) results in a rather low stereoselective outcome.

A major limitation of the traditional Wittig reaction is the partially reduced overall efficiency caused by the sometimes challenging removal of the phosphine oxide byproduct.[5] Recent investigations addressed this issue and targeted the development of catalytic Wittig reactions with reduced phosphine oxide formation.[6] Despite its discovery a long time ago, the mechanism of the Wittig reaction is not fully elucidated and is still controversially discussed.[4a] For the lithium-salt free Wittig reaction, however, the mechanism generally accepted today involves an irreversible [2+2] cycloaddition affording a four-membered oxaphosphetane as the only intermediate under kinetic control.[4a]

Scheme 1. (A) Conversion of an Aldehyde or a Ketone into Alkenes via the Wittig Reaction, and (B) Syntheses of Silenes from Iminosilylsilanone 1 via the Sila-Wittig Reaction



Received: August 29, 2019
Published: September 27, 2019

ACS Publications © 2019 American Chemical Society

DOI: 10.1021/jacs.9b09379
J. Am. Chem. Soc. 2019, 141, 16991−16996

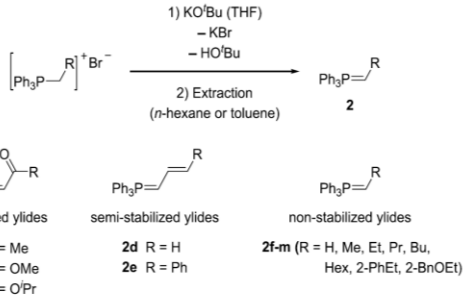
In marked contrast to carbonyl compounds, the formation of heavier alkene homologues $R_2E{=}CR_2$ (E = Si (silenes), Ge, Sn, Pb) from carbonyl congeners $R_2E{=}O$ (silanones: E = Si) via the Wittig reaction is not known. Nevertheless, a sila-Wittig-type reaction by formation of a Lewis base-stabilized silene was observed when mesitylaldehyde was exposed to a stable phosphonium sila-ylide.[7] The absence of further reports is not surprising when one considers the lack of suitable precursors. It was not until 1976/1981 that Lappert, Brook, West, and Yoshifuji disproved the well-known "double bond rule" with their seminal work on the isolation of the first distannene[8] ($R_2Sn{=}SnR_2$), silene,[9] disilene[10] ($R_2Si{=}SiR_2$), and diphosphene[11] (RP=PR), respectively. Despite the rapid growth in multiply bonded main group compounds,[12] including the isolation of the first silanones,[13] this area of chemistry remains challenging to this day.[14]

We recently achieved the isolation of the unprecedented, acyclic and three-coordinate iminosilylsilanone **1**.[13e] Here, we report for the first time about the conversion of a silanone into silenes via the sila-Wittig reaction (Scheme 1). Because of the distinct nature of carbonyl compounds and silanones (the higher polarity and weaker π-bond of the Si=O moiety leads to a zwitterionic character and hence to instability),[12d] both similarities and differences in reactivity toward Wittig reagents were observed.

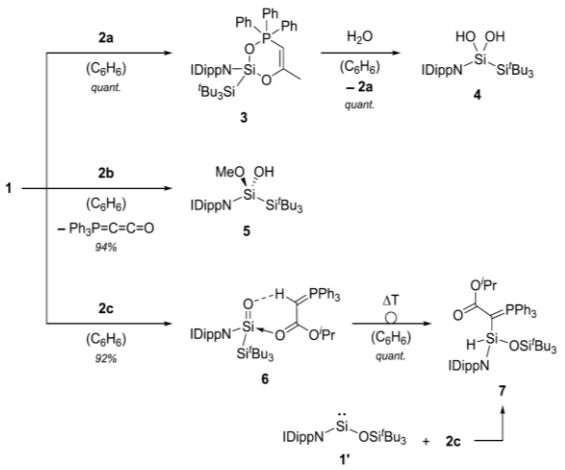
RESULTS AND DISCUSSION

Reactivity Studies with Stabilized Ylides. The classical Wittig reaction typically consists of two steps. First, a suitable phosphorus ylide is synthesized, usually by *in situ* deprotonation of the respective phosphonium salt with strong bases, such as organolithium compounds, NaH, or KO^{t}Bu.[3b] The carbonyl compound is then added directly to the reaction mixture and the olefination takes place. In our case, however, the general method was not applicable since silanones can react with the bases used or the byproducts of deprotonation itself. Thus, we pursued a modified approach and isolated the phosphorus ylides **2** by reaction of the corresponding phosphonium bromides with KO^{t}Bu in THF, followed by subsequent extraction with either *n*-hexane or toluene (Scheme 2; for details see the Supporting Information). We then treated the isolated ylides **2** with iminosilylsilanone **1** in benzene at room temperature. It is worth mentioning that for a successful sila-Wittig olefination, the reactions generally have to be relatively fast, as otherwise **1** slowly and irreversibly rearranges to its more stable iminosiloxysilylene isomer (IDippN)(^{t}Bu$_3$SiO)Si: (**1′**) (Scheme 3).[13e]

Scheme 2. Synthesis and Structures of Selected Phosphorus Ylides



Scheme 3. Reactivity of Silanone 1 toward Stabilized Ylides



We started our investigations with stabilized ylides, as some of them are commercially available. Reaction of silanone **1** with the ketone-substituted ylide **2a** selectively provided a novel product. However, ^{31}P NMR spectroscopy did not confirm $Ph_3P{=}O$ formation, thus not indicating a successful sila-Wittig reaction. Instead a resonance at δ = −86.9 ppm, characteristic for a penta-coordinate phosphorus nucleus, was observed.[3b] Additional multinuclear/2D NMR spectroscopy and mass spectrometry identified dioxaphosphasiline **3** as formal hetero-Diels–Alder reaction product (Scheme 3). The ring silicon atom exhibits a signal at δ = −61.0 ppm with a $^2J_{PSi}$ coupling constant of 20.4 Hz in the ^{29}Si NMR spectrum. Although we were not able to crystallize **3** and confirm its molecular structure by single-crystal X-ray diffraction (SC-XRD), exposure to H_2O selectively afforded silanediol **4** and ylide **2a** and thus further verified the assumed structure. The change in coordination number around the central silicon nucleus of **4** was clearly evident by the corresponding high-field shift (δ = −44.7 ppm) in the ^{29}Si NMR spectrum compared to that observed for **1** (δ = 28.8 ppm).[13e] Furthermore, **4** was also obtained by direct treatment of **1** with H_2O.

As additional confirmation of dioxaphosphasiline **3**, we calculated its structure and NMR chemical shifts using density functional theory (DFT).[15] Accordingly, the computed ^{29}Si and ^{31}P NMR resonances at $\delta(^{29}Si)$ = −55.9 ppm and $\delta(^{31}P)$ = −80.5 ppm are in good agreement with the experimentally observed values.

In contrast, reaction of **1** with the ester-substituted ylide **2b** led to the unexpected simultaneous formation of methoxysilanol **5** ($\delta(^{29}Si_{central})$ = −46.6 ppm) and the Bestmann ylide $Ph_3P{=}C{=}C{=}O$. While **5** is also accessible via methanolysis of **1**,[13e] the Bestmann ylide is usually prepared by deprotonation of **2b** with strong bases such as NaHMDS.[16] Hence, silanone **1** formally served as a base in this particular reaction.

Astonished at this result, we investigated ester-substituted ylides with increased steric encumbrance. Whereas treatment of **1** with $Ph_3P{=}CHCOO^tBu$ resulted in almost no conversion and mainly silanone isomerization, reaction with **2c** selectively

DOI: 10.1021/jacs.9b09379
J. Am. Chem. Soc. 2019, 141, 16991−16996

afforded **6** as the sole product in 92% yield. The molecular structure of ylide-stabilized silanone **6** was unambiguously confirmed by SC-XRD, which revealed a short Si=O double bond (1.548(3) Å) being essentially identical to that observed for donor-free silanone **1** (1.537(3) Å) (Figure 1). The short

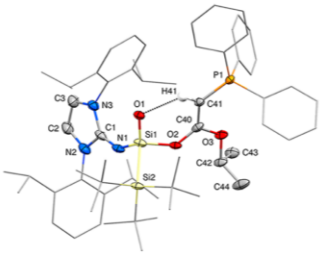


Figure 1. Molecular structure of **6** with ellipsoids set at 30% probability. Hydrogen atoms, except for H41 involved in hydrogen bonding (visualized by the dashed line), are omitted for clarity. Selected bond lengths [Å] and angles [°]: Si1–O1 1.548(3), Si1–O2 1.806(3), Si1–Si2 2.360(5), Si1–N1 1.707(5), O2–C40 1.299(6); Si2–Si1–O1 109.9(2), Si1–O2–C40 128.5(3).

O2–C40 (1.299(6) Å) and very long Si1–O2 (1.806(3) Å) distances support a donor–acceptor interaction. The dative Si1–O2 bond is even significantly longer compared to that observed for a cyclourea-stabilized silanone (d_{Si-O} = 1.727(2) Å) reported by Driess and colleagues.[17] Additionally, a close O1···H41 distance of 2.186 Å (H41 in calculated position), being much shorter than the sum of the van der Waals radii of hydrogen and oxygen (2.72 Å),[18] indicates hydrogen bonding. The pronounced downfield shift of the ylidic α-hydrogen from δ = 3.32 ppm (**2c**, $^2J_{PH}$ = 24.3 Hz) to δ = 7.55 ppm (**6**, $^2J_{PH}$ = 21.7 Hz) in the ^{1}H NMR spectrum is in line with this observation. High-field-shifted resonances in the ^{29}Si (δ = −50.2 ppm) and ^{31}P (δ = 12.9 ppm; **2c**: δ = 18.3 ppm) NMR spectra agree well with the Lewis base stabilization. Rivard et al. recently reported on the utilization of Wittig reagents as electron donors for low-valent group 14 elements.[19] Our results revealed donor abilities apart from the ylidic α-carbon atoms and thus extend the knowledge of this underdeveloped ligand class.

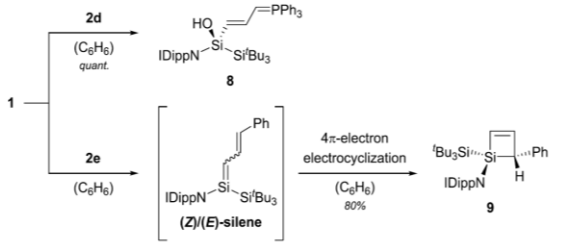
Comparable to silanone **1**, adduct **6** is not thermally stable and quantitatively isomerizes slowly in solution. Multinuclear and 2D NMR spectroscopy indicated formation of the silyl-substituted phosphorus ylide **7** (Scheme 3). The central silicon nucleus exhibits a doublet resonance at δ = −58.6 ppm with a coupling constant $^2J_{PSi}$ of 38.6 Hz in the ^{29}Si{^{1}H} NMR spectrum. The observed ^{31}P NMR shift at δ = 19.9 ppm is characteristic for a four-coordinate phosphorus ylide (cf. **2c**: δ = 18.3 ppm). Additionally, the Si–H moiety was clearly observed in the ^{1}H NMR spectrum at δ = 4.50 ppm with coupling constants $^1J_{SiH}$ = 229.8 Hz and $^3J_{PH}$ = 3.1 Hz.

Furthermore, the theoretically calculated ^{29}Si and ^{31}P NMR chemical shifts of **7** at $\delta(^{29}Si)$ = −57.5 ppm and $\delta(^{31}P)$ = 17.2 ppm agree well with the experimentally observed results and thus support the formation of **7**.

The reaction most likely proceeds via the isomerization of ylide-stabilized silanone **6** to iminosiloxysilylene **1′** under dissociation of phosphorus ylide **2c**. The subsequent insertion of **1′** into the ylidic C–H bond of **2c** provides silyl-substituted phosphorus ylide **7**. To support this assumption, we treated **1′** with **2c** at ambient temperature and in fact obtained the same product **7** in quantitative yield. However, the exact mechanism remains unclear, since also a concerted reaction pathway is plausible.

Reactivity Studies with Semi-stabilized Ylides. We then continued our studies with semi-stabilized ylides (Scheme 2). Whereas reaction of **1** toward Ph_3P=CHPh resulted in a slow and unselective formation of a complicated mixture of products, including starting materials, silylene **1′**[13e] and other unknown products, utilization of the vinyl-substituted ylide **2d** afforded a sole product. Multinuclear and 2D NMR analyses and mass spectrometry identified the silanoyl-substituted phosphorus ylide **8** as the product formed (Scheme 4).

Scheme 4. Reactivity of Silanone 1 toward Semi-stabilized Ylides



The central silicon atom exhibiting a resonance in the ^{29}Si NMR spectrum at δ = −30.4 ppm with a $^4J_{PSi}$ coupling constant of 3.4 Hz, clearly indicates the change in the coordination number from three to four. The slight high-field shift observed in the ^{31}P NMR at δ = 9.6 ppm compared to ylide **2d** (δ = 11.4 ppm) supports the proposed structure. SC-XRD unambiguously confirmed the molecular structure of **8** (Figure 2) and revealed short C=C (1.362(1) Å) and P=C (1.695(1) Å) bonds together with its absolute configuration. The mechanism of the reaction presumably involves a nucleophilic attack of the vinylogous Wittig ylide to the Si=O moiety of **1**. Subsequent hydrogen migration to the oxygen atom and double bond formation finally provides **8**.

In contrast, utilization of the phenyl-substituted derivative **2e** did not lead to similar product formation, probably for steric reasons. Instead, a successful sila-Wittig reaction was indicated via detection of Ph_3P=O formation by ^{31}P NMR spectroscopy (δ = 24.8 ppm). However, further spectroscopic analyses revealed no resonances for the corresponding silenes, but pointed out the formation of silacyclobutene **9** as formal 4π-electron electrocyclization product of the transient silene. ^{29}Si NMR spectroscopy showed a change in coordination number with an observed upfield-shifted resonance at δ = −30.2 ppm (cf. **1**: δ = 28.8 ppm).[13e] Since initially two different silenes and subsequently two stereogenic centers are formed upon cycloaddition, there are up to four different stereoisomers plausible. Nevertheless, the solid-state structure determined by SC-XRD revealed the absolute configuration of **9**. In addition, the silacyclobutene moiety was clearly identified with a sum of bond angles of 359.6° and a short C=C double bond (1.333(2) Å).

Reactivity Studies with Non-stabilized Ylides. Motivated by the above-mentioned results, we investigated non-stabilized ylides and initially used the simplest, hydrogen-substituted ylide **2f**. Immediate full conversion of silanone **1** and **2f** to a mixture of products was detected by multinuclear

DOI: 10.1021/jacs.9b09379
J. Am. Chem. Soc. 2019, 141, 16991–16996

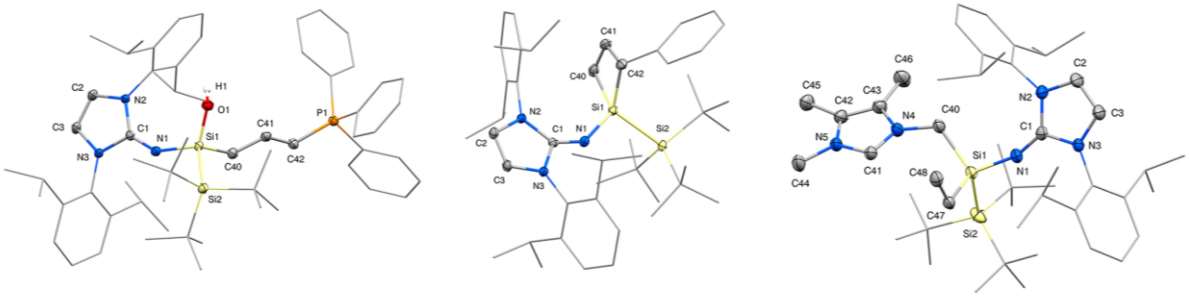
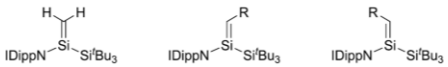


Figure 2. Molecular structures of **8** (left), **9** (middle), and **11** (right). Ellipsoids are set at 50% probability. Hydrogen atoms, except for the respective O−H nucleus of ylide **8**, and cocrystallized benzene (**8**) are omitted for clarity. Selected bond lengths [Å] and angles [°]: **8**: Si1−O1 1.668(1), Si1−Si2 2.373(1), Si1−N1 1.698(2), Si1−C40 1.838(2), P1−C42 1.695(2); Si2−Si1−O1 103.4(1), Si1−C40−C41 126.0(1). **9**: Si1−Si2 2.393(1), Si1−N1 1.697(1), Si1−C40 1.874(1), Si1−C42 1.943(1), C40−C41 1.333(2); C40−Si1−C42 74.9(1), Si1−C40−C41 91.8(1), C40−C41−C42 109.0(1), Si1−C42−C41 83.9(1). **11**: Si1−Si2 2.421(1), Si1−N1 1.692(1), Si1−C40 1.917(1), Si1−C47 1.888(1), C47−C48 1.528(2); Si2−Si1−N1 109.8(1), Si2−Si1−C40 115.9(1), Si2−Si1−C47 108.0(1).

NMR spectroscopy. In the ^{29}Si NMR spectrum a signal observed at δ = 68.1 ppm indicated formation of the half-parent silene **10a**; however, it disappeared completely within 3 h. A comparison to other silenes turned out to be difficult, because none of this type (iminosilylsilene) have been reported so far. Nevertheless, the detected ^{29}Si NMR resonance is characteristic for a three-coordinate silene.[12a−c] In addition, concomitant formation of $Ph_3P{=}O$ was clearly evidenced by its significant ^{31}P NMR resonance at δ = 24.8 ppm, once again confirming a successful sila-Wittig reaction. Presumably, the steric demand of **10a** is not sufficient and fast subsequent decomposition reactions, such as head-to-tail dimerization are thermodynamically favored.

Consequently, the increase in the steric encumbrance of the phosphorus ylides used (**2g−m**) resulted in instantaneous, quantitative silene and $Ph_3P{=}O$ formation (Table 1). In general, a high selectivity for the corresponding (*Z*)-silenes (**10b−g**) was observed, in analogy to the classical Wittig reaction, in which the utilization of triphenylphosphine-derived non-stabilized phosphorus ylides usually leads to very high *Z*-selectivities.[4a] The stereochemistry assignment was determined with nuclear Overhauser enhancement spectroscopy (NOESY) experiments. Interestingly, conversion of **1** with the 2-benzyloxyethyl-substituted ylide **2m** provided an approximately 45/55 mixture of (*Z*)- and (*E*)-silene **10h**/**10h′**. The silenes formed were sufficiently characterized by multinuclear and 2D NMR spectroscopy and mass spectrometry. Additionally, they are significantly more stable in solution than **10a**. In contrast to the classical Wittig reaction, however, a removal of the phosphine oxide byproduct was not possible at all, as decomposition to unidentified product mixtures occurred upon workup (solvent removal and subsequent extraction with diethyl ether and/or *n*-hexane).

Table 1. ^{29}Si NMR Resonances for the Respective Si=C Moieties of the Sila-Wittig Reaction Products with Non-stabilized Ylides



ylide		δ(^{29}Si) [ppm]		
no.	R	(*Z*)-silene	(*E*)-silene	stereoselectivity(*Z*)/(*E*) [%]
2f	H	68.1		–
2g	Me	55.9	50.5	~92/8
2h	Et	51.3	43.1	~94/6
2i	Pr	52.3	42.8	~94/6
2j	Bu	52.0	42.6	~89/11
2k	Hex	52.0	42.6	~85/15
2l	2-PhEt	53.0	43.3	~76/24
2m	2-BnOEt	56.3	46.5	~45/55

Very recently, Apeloig et al. reported on the synthesis and isomerization of (*E*)/(*Z*)-(^{t}Bu$_2$MeSi)(^{t}BuMe$_2$Si)Si=CH(1-Ad), the first-ever isolable silene stereoisomers.[20] Thus, we conducted further DFT calculations to support the formation of the silenes and especially the assignment of the (*E*)/(*Z*)-isomers. First, we calculated the structure and the central ^{29}Si NMR chemical shift of **10a**. The calculated resonance at δ = 68.9 ppm is in excellent agreement with the experimentally measured value (δ = 68.1 ppm) and therefore confirms the accuracy of the computational method. Furthermore, the calculated central ^{29}Si NMR chemical shifts of **10b** at δ = 56.5 ppm and **10b′** at δ = 51.2 ppm (for calculated structures, see Figure 3) agree well with the spectroscopically observed resonances (Table 1). These results verify our assignments for the respective (*E*)/(*Z*)-silenes.

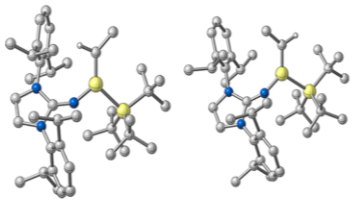


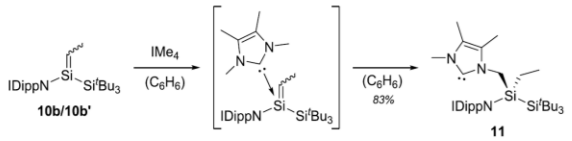
Figure 3. Calculated structures of (*Z*)-silene **10b** (left) and (*E*)-silene **10b′** (right) at the HCTH407/6-311+G(d)//B97-D/def2-SVP level of theory.

A limitation of the sila-Wittig reaction is the steric encumbrance of silanone **1** itself, which is necessary for its isolation. Therefore, no reaction other than silanone isomerization was observed with $Ph_3P{=}CMe_2$.[13e] Accordingly, formation and isolation of a stable iminosilylsilene derived from **1** seemed to be rather challenging.

DOI: 10.1021/jacs.9b09379
J. Am. Chem. Soc. 2019, 141, 16991−16996

N-Heterocyclic carbenes (NHCs) are frequently used as Lewis bases for the stabilization and isolation of reactive main group compounds.[12e] Hence we tried to isolate silenes **10** as NHC adducts. However, reaction of *in situ*-formed **10b**/**10b′** with 1,3,4,5-tetramethylimidazolin-2-ylidene (IMe_4) did not afford the corresponding NHC-stabilized silene, but an intramolecular C−H activation of a wingtip methyl group occurred and finally silyl-substituted NHC **11** formed (Scheme 5). Compound **11** was fully characterized and the now

Scheme 5. Synthesis of Silyl-Substituted NHC 11



tetravalent silicon moiety exhibits a resonance in the ^{29}Si NMR spectrum at δ = −21.0 ppm. The divalent carbon atom was clearly identified in the ^{13}C NMR with a characteristic downfield shift at δ = 213.2 ppm. SC-XRD analysis confirmed the molecular structure of the asymmetric silylcarbene **11** and revealed both a planar NHC skeleton and the absolute configuration (Figure 2). To the best of our knowledge, there is only one example of NHC C−H activation by a low-coordinate silicon compound reported so far. Driess et al. observed the formation of a comparable silyl-substituted NHC via reaction of their β-diketiminato silylene {HC[CMeN(Dipp)]$_2$}Si:) with IMe_4.[21] Our observation therefore underlines the high reactivity of iminosilylsilenes **10**. Nevertheless, the application of the Wittig reaction to a carbonyl homologue has been further demonstrated with the isolation of NHC **11**, because the former Si=O double bond was clearly converted into a Si−CH_2CH_3 bond via an intermediate Si=$CHCH_3$ double bond.

CONCLUSION

We presented the possibilities and limitations of the application of the Wittig reaction to iminosilylsilanone **1**, a heavier carbonyl congener. Utilization of stabilized phosphorus ylides selectively afforded several unprecedented silicon compounds, due to the zwitterionic character of **1** and the inherent functional groups of the ylides used. With semi-stabilized ylides, however, not only a nucleophilic attack at the Si=O moiety affording silanoyl-substituted ylide **8** was observed, but also a successful sila-Wittig reaction was indicated with the isolation of silacyclobutene **9**, the formal electrocyclic reaction product of the corresponding transient silene. Similar to the classical Wittig reaction yielding alkenes, exposure of **1** toward non-stabilized ylides finally provided a series of iminosilylsilenes **10**. The sila-Wittig reaction represents an extension of the limited synthesis methods for heavier alkenes and could therefore open new avenues for the isolation of otherwise elusive silenes.

ASSOCIATED CONTENT

Supporting Information

The Supporting Information is available free of charge on the ACS Publications website at DOI: 10.1021/jacs.9b09379.

Experimental details including synthetic, spectroscopic, crystallographic, and computational data (PDF)

Crystallographic data for **2h**, **2m**, **5**, **5a**, **6**, **8**, **9**, and **11** (CCDC 1949650−1949657) (CIF)

AUTHOR INFORMATION

Corresponding Author

*s.inoue@tum.de

ORCID

Tibor Szilvási: 0000-0002-4218-1570

Shigeyoshi Inoue: 0000-0001-6685-6352

Notes

The authors declare no competing financial interest.

ACKNOWLEDGMENTS

We are exceptionally grateful to the WACKER Chemie AG and the European Research Council (SILION 637394) for continued financial support. We thank Dr. Daniel Wendel for revising the manuscript and Maximilian Muhr (Prof. R. A. Fischer) for the LIFDI-MS measurements.

REFERENCES

(1) (a) Staudinger, H.; Meyer, J. Über neue organische Phosphorverbindungen III. Phosphinmethylenderivate und Phosphinimine. *Helv. Chim. Acta* **1919**, *2*, 635−646. (b) Staudinger, H.; Braunholtz, W. Über organische Phosphorverbindungen, V. Mitteilung über die Einwirkung von Carbonylenderivaten auf Phosphazine. *Helv. Chim. Acta* **1921**, *4*, 897−900.

(2) (a) Wittig, G.; Geissler, G. Zur Reaktionsweise des Pentaphenylphosphors und einiger Derivate. *Liebigs Ann. Chem.* **1953**, *580*, 44−57. (b) Wittig, G.; Schöllkopf, U. Über Triphenylphosphinmethylene als olefinbildende Reagenzien (1. Mitteil.). *Chem. Ber.* **1954**, *87*, 1318−1330. (c) Wittig, G. From Diyls to Ylides to My Idyll. *Science* **1980**, *210*, 600−604.

(3) (a) Takeda, T. *Modern Carbonyl Olefination: Methods and Applications*; Wiley-VCH Verlag GmbH & Co. KGaA: Weinheim, 2004. (b) Iaroshenko, V. *Organophosphorus Chemistry: From Molecules to Applications*; Wiley-VCH Verlag GmbH & Co. KGaA: Weinheim, 2019.

(4) (a) Byrne, P. A.; Gilheany, D. G. The modern interpretation of the Wittig reaction mechanism. *Chem. Soc. Rev.* **2013**, *42*, 6670−6696. (b) Farfán, P.; Gómez, S.; Restrepo, A. On the origins of stereoselectivity in the Wittig reaction. *Chem. Phys. Lett.* **2019**, *728*, 153−155.

(5) (a) Byrne, P. A.; Rajendran, K. V.; Muldoon, J.; Gilheany, D. G. A convenient and mild chromatography-free method for the purification of the products of Wittig and Appel reactions. *Org. Biomol. Chem.* **2012**, *10*, 3531−3537. (b) Lukin, K.; Kishore, V.; Gordon, T. Development of a Scalable Synthesis of Oxadiazole Based $S1P_1$ Receptor Agonists. *Org. Process Res. Dev.* **2013**, *17*, 666−671. (c) Batesky, D. C.; Goldfogel, M. J.; Weix, D. J. Removal of Triphenylphosphine Oxide by Precipitation with Zinc Chloride in Polar Solvents. *J. Org. Chem.* **2017**, *82*, 9931−9936.

(6) (a) O'Brien, C. J.; Tellez, J. L.; Nixon, Z. S.; Kang, L. J.; Carter, A. L.; Kunkel, S. R.; Przeworski, K. C.; Chass, G. A. Recycling the Waste: The Development of a Catalytic Wittig Reaction. *Angew. Chem., Int. Ed.* **2009**, *48*, 6836−6839. (b) Coyle, E. E.; Doonan, B. J.; Holohan, A. J.; Walsh, K. A.; Lavigne, F.; Krenske, E. H.; O'Brien, C. J. Catalytic Wittig Reactions of Semi- and Nonstabilized Ylides Enabled by Ylide Tuning. *Angew. Chem., Int. Ed.* **2014**, *53*, 12907−12911. (c) Longwitz, L.; Werner, T. Recent advances in catalytic Wittig-type reactions based on P(III)/P(V) redox cycling. *Pure Appl. Chem.* **2019**, *91*, 95−102.

(7) Gau, D.; Kato, T.; Saffon-Merceron, N.; Cossío, F. P.; Baceiredo, A. Stable Phosphonium Sila-ylide with Reactivity as a Sila-Wittig Reagent. *J. Am. Chem. Soc.* **2009**, *131*, 8762−8763.

(8) Goldberg, D. E.; Harris, D. H.; Lappert, M. F.; Thomas, K. M. A New Synthesis of Divalent Group 4B Alkyls M[$CH(SiMe_3)_2$]$_2$ (M =

DOI: 10.1021/jacs.9b09379
J. Am. Chem. Soc. 2019, 141, 16991−16996

Ge or Sn), and the Crystal and Molecular Strcuture of the Tin Compound. *J. Chem. Soc., Chem. Commun.* **1976**, 261−262.
(9) Brook, A. G.; Abdesaken, F.; Gutekunst, B.; Gutekunst, G.; Kallury, R. K. A solid silaethene: isolation and characterization. *J. Chem. Soc., Chem. Commun.* **1981**, 191−192.
(10) West, R.; Fink, M. J.; Michl, J. Tetramesityldisilene, a Stable Compound Containing a Silicon-Silicon Double Bond. *Science* **1981**, *214*, 1343−1344.
(11) Yoshifuji, M.; Shima, I.; Inamoto, N.; Hirotsu, K.; Higuchi, T. Synthesis and structure of bis(2,4,6-tri-*tert*-butylphenyl)diphosphene: isolation of a true phosphobenzene. *J. Am. Chem. Soc.* **1981**, *103*, 4587−4589.
(12) For recent reviews on multiply bonded main group compounds, see: (a) Power, P. P. π-Bonding and the Lone Pair Effect in Multiple Bonds between Heavier Main Group Elements. *Chem. Rev.* **1999**, *99*, 3463−3504. (b) Ottosson, H.; Eklof, A. M. Silenes: Connectors between classical alkenes and nonclassical heavy alkenes. *Coord. Chem. Rev.* **2008**, *252*, 1287−1314. (c) Fischer, R. C.; Power, P. P. π-Bonding and the Lone Pair Effect in Multiple Bonds Involving Heavier Main Group Elements: Developments in the New Millennium. *Chem. Rev.* **2010**, *110*, 3877−3923. (d) Xiong, Y.; Yao, S.; Driess, M. Chemical Tricks To Stabilize Silanones and Their Heavier Homologues with E═O Bonds (E═Si−Pb): From Elusive Species to Isolable Building Blocks. *Angew. Chem., Int. Ed.* **2013**, *52*, 4302−4311. (e) Nesterov, V.; Reiter, D.; Bag, P.; Frisch, P.; Holzner, R.; Porzelt, A.; Inoue, S. NHCs in Main Group Chemistry. *Chem. Rev.* **2018**, *118*, 9678−9842.
(13) For selected examples of isolable silanones, see: (a) Xiong, Y.; Yao, S.; Driess, M. An Isolable NHC-Supported Silanone. *J. Am. Chem. Soc.* **2009**, *131*, 7562−7563. (b) Filippou, A. C.; Baars, B.; Chernov, O.; Lebedev, Y. N.; Schnakenburg, G. Silicon−Oxygen Double Bonds: A Stable Silanone with a Trigonal-Planar Coordinated Silicon Center. *Angew. Chem., Int. Ed.* **2014**, *53*, 565−570. (c) Ishida, S.; Abe, T.; Hirakawa, F.; Kosai, T.; Sato, K.; Kira, M.; Iwamoto, T. Persistent Dialkylsilanone Generated by Dehydrobromination of Dialkylbromosilanol. *Chem. - Eur. J.* **2015**, *21*, 15100−15103. (d) Alvarado-Beltran, I.; Rosas-Sánchez, A.; Baceiredo, A.; Saffon-Merceron, N.; Branchadell, V.; Kato, T. A Fairly Stable Crystalline Silanone. *Angew. Chem., Int. Ed.* **2017**, *56*, 10481−10485. (e) Wendel, D.; Reiter, D.; Porzelt, A.; Altmann, P. J.; Inoue, S.; Rieger, B. Silicon and Oxygen's Bond of Affection: An Acyclic Three-Coordinate Silanone and Its Transformation to an Iminosiloxysilylene. *J. Am. Chem. Soc.* **2017**, *139*, 17193−17198. (f) Rosas-Sánchez, A.; Alvarado-Beltran, I.; Baceiredo, A.; Saffon-Merceron, N.; Massou, S.; Hashizume, D.; Branchadell, V.; Kato, T. Cyclic (Amino)-(Phosphonium-Bora-Ylide)Silanone: A Remarkably Room Temperature Persistent Silanone. *Angew. Chem., Int. Ed.* **2017**, *56*, 15916−15920. (g) Kobayashi, R.; Ishida, S.; Iwamoto, T. An Isolable Silicon Analogue of a Ketone that Contains an Unperturbed Si═O Double Bond. *Angew. Chem., Int. Ed.* **2019**, *58*, 9425−9428.
(14) Lee, V. Y. *Organosilicon Compounds: Theory and Experiment (Synthesis)*; Academic Press: New York, 2017.
(15) Geometry optimizations and harmonic frequency calculations were performed at the B97-D/def2-SVP level of density functional theory. NMR chemical shift values were calculated using the optimized geometries at the HCTH407/6-311+G(d)//B97-D/def2-SVP level of theory. All calculations were executed using Gaussian 09. For detailed information, see the Supporting Information.
(16) Bartlett, M. (Triphenylphosphoranylidene)ketene: The Bestmann Ylide. *Synlett* **2013**, *24*, 773−774.
(17) Xiong, Y.; Yao, S.; Müller, R.; Kaupp, M.; Driess, M. From silicon(II)-based dioxygen activation to adducts of elusive dioxasiliranes and sila-ureas stable at room temperature. *Nat. Chem.* **2010**, *2*, 577−580.
(18) Bondi, A. van der Waals Volumes and Radii. *J. Phys. Chem.* **1964**, *68*, 441−451.
(19) Swarnakar, A. K.; McDonald, S. M.; Deutsch, K. C.; Choi, P.; Ferguson, M. J.; McDonald, R.; Rivard, E. Application of the Donor−Acceptor Concept to Intercept Low Oxidation State Group 14 Element Hydrides using a Wittig Reagent as a Lewis Base. *Inorg. Chem.* **2014**, *53*, 8662−8671.
(20) Zborovsky, L.; Kostenko, A.; Bravo-Zhivotovskii, D.; Apeloig, Y. Mechanism of the Thermal Z⇌E Isomerization of a Stable Silene; Experiment and Theory. *Angew. Chem., Int. Ed.* **2019**, *58*, 14524−14528.
(21) Xiong, Y.; Yao, S.; Driess, M. Synthesis and Rearrangement of Stable NHC-Silylene Adducts and Their Unique Reactivity towards Cyclohexylisocyanide. *Chem. - Asian J.* **2010**, *5*, 322−327.

DOI: 10.1021/jacs.9b09379
J. Am. Chem. Soc. 2019, 141, 16991−16996

10. Summary and Outlook

Given the extraordinary importance and impact of the thriving field of main group compounds mimicking transition metal complexes, further studies in this area are an ambitious goal for the current generation of modern chemists. Despite intensive research, however, in particular the development and application of sustainable catalysts based on main group elements is still in its infancy.[11-14] An exceptionally promising class of compounds to achieve the high goal of a versatile metal-free catalysis are low-coordinate organosilicon compounds, due to their high reactivity and the excellent ecological and economical properties of silicon.[16] Therefore, deeper investigations in this direction are of great interest and potentially of significant benefit for the future.

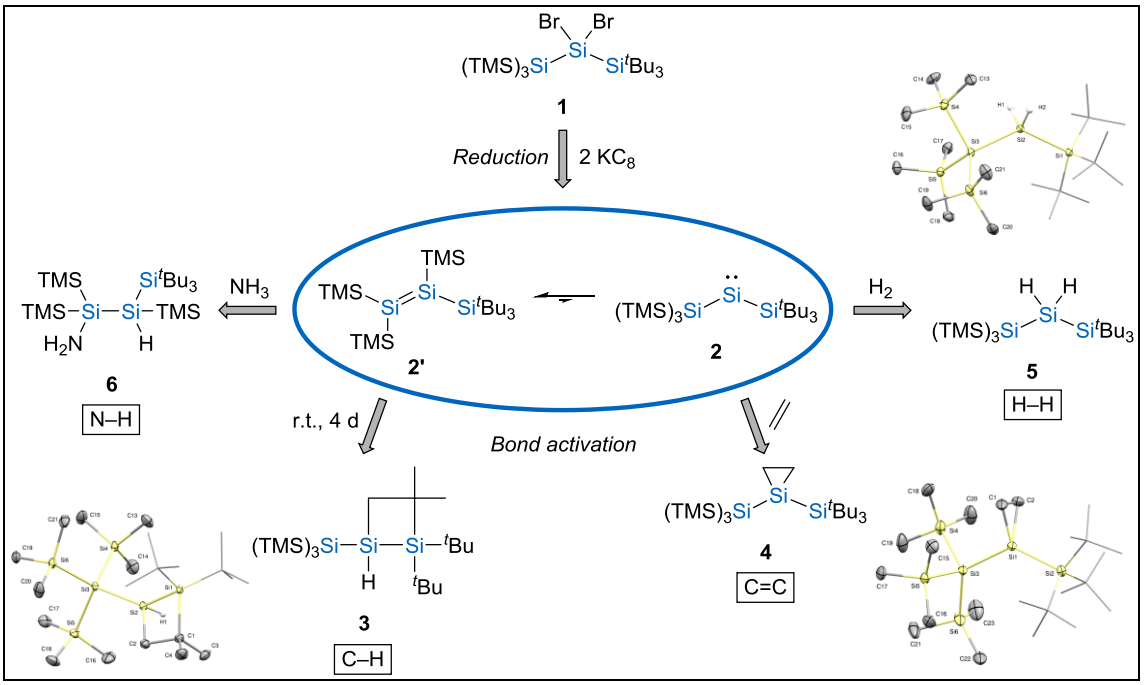
10.1 Acyclic Two-Coordinate Silylenes

Within the versatile class of low-coordinate organosilicon compounds, acyclic donor-free silylenes in particular represent one of the most suitable compounds to circumvent the use of transition metal complexes in catalysis. A major breakthrough was achieved with the seminal work of *Aldridge*, *Jones et al.* and *Power's* group on simultaneous reports of the first isolable acyclic, two-coordinate silylenes in 2012.[169-170] However, prior to this PhD thesis, almost no additional representative was known and the overall reactivity only slightly explored.[169-170,174-176,185-186] Thus, a main objective of the present work was to expand the number of isolable acyclic silylenes and to further investigate their reactivity with respect to eventual applications in catalysis.

10.1.1 Investigations on Bis(silyl)silylenes

Due to their inherent high reactivity and their potential triplet ground state, bis(silyl)silylenes are particularly sought-after, however, rapid decomposition reactions have so far prevented a successful isolation.[85,211] Therefore initial investigations concentrated on the first isolation of such an elusive species using a suitable ligand scaffold. In particular, the unique combination of sterically crowded hyper- and supersilyl groups was envisaged in order to achieve sufficient stabilization and possibly induce a reversible disilene-silylene interconversion *via* 1,2-silyl migration.

Subsequent to the successful isolation of novel dibromosilane **1**, reductive debromination of **1** indeed led to the formation of an unprecedented equilibrium mixture containing the first isolable two-coordinate bis(silyl)silylene ((TMS)$_3$Si)(^{t}Bu$_3$Si)Si: (**2**) and its isomeric tetrasilyldisilene (TMS)(^{t}Bu$_3$Si)Si=Si(TMS)$_2$ (**2'**) (Scheme 14).[279] Supportive DFT calculations revealed a closer insight into the nature of the equilibrium and the bonding situation of **2**. However, the assumed triplet ground state has neither experimentally nor theoretically been unambiguously proven.

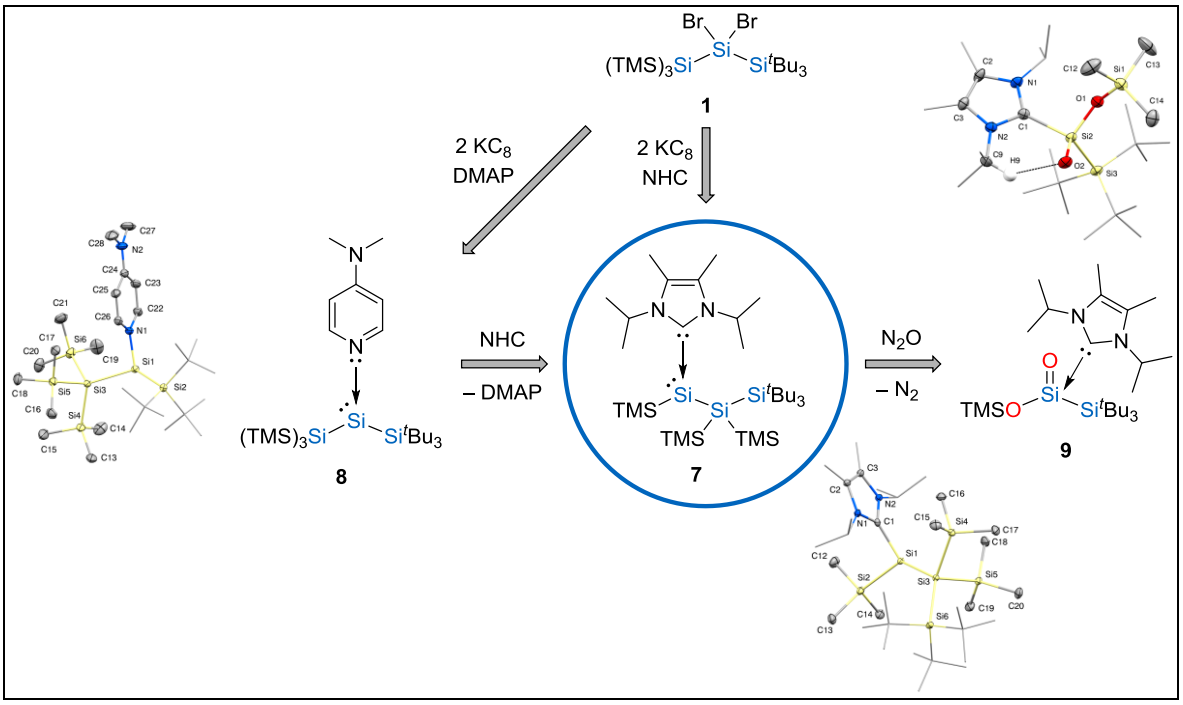


Scheme 14. Synthesis and reactivity of the first isolable two-coordinate bis(silyl)silylene ((TMS)$_3$Si)(^{t}Bu$_3$Si)Si: (**2**).

Although the mixture is indefinitely stable at –35 °C, it finally decomposes slowly in solution at ambient temperature under formation of disiletane **3**, *via* intramolecular C–H bond activation of the extremely reactive bis(silyl)silylene **2**. The existence of the equilibrium and the potential for catalytic applications was successfully demonstrated by facile oxidative addition of the industrially relevant small molecules NH_3, H_2 and ethylene under very mild conditions. Thus both tetrasilyldisilene and bis(silyl)silylene addition products were obtained.

Further details of the disilene-silylene rearrangement were acquired by isolating different Lewis base-stabilized bis(silyl)silylenes. Reductive debromination of dibromosilane **1** in the presence of the respective donor provided NHC-silylene adduct **7** and DMAP-silylene adduct **8** (Scheme 15). Interestingly, a selective interconversion was observed *via* reaction of DMAP-stabilized bis(silyl)silylene **8** with an equimolar amount of I^{i}Pr$_2$Me$_2$ with concomitant liberation of DMAP.

All attempts to gain access to a bis(silyl)silanone by oxidizing the various (donor-stabilized) bis(silyl)silylene only led to the observation of complicated mixtures of products, presumably induced by silyl migrations, insertion reactions and dimerization/oligomerization of highly reactive transient silanones. Nevertheless, oxygenation of NHC-stabilized bis(silyl)silylene **7** with N_2O resulted in the striking formation and isolation of the unprecedented donor-supported, acyclic silanoic ester **9**, a heavier carboxylate ester analogue, thus providing new avenues for further research.

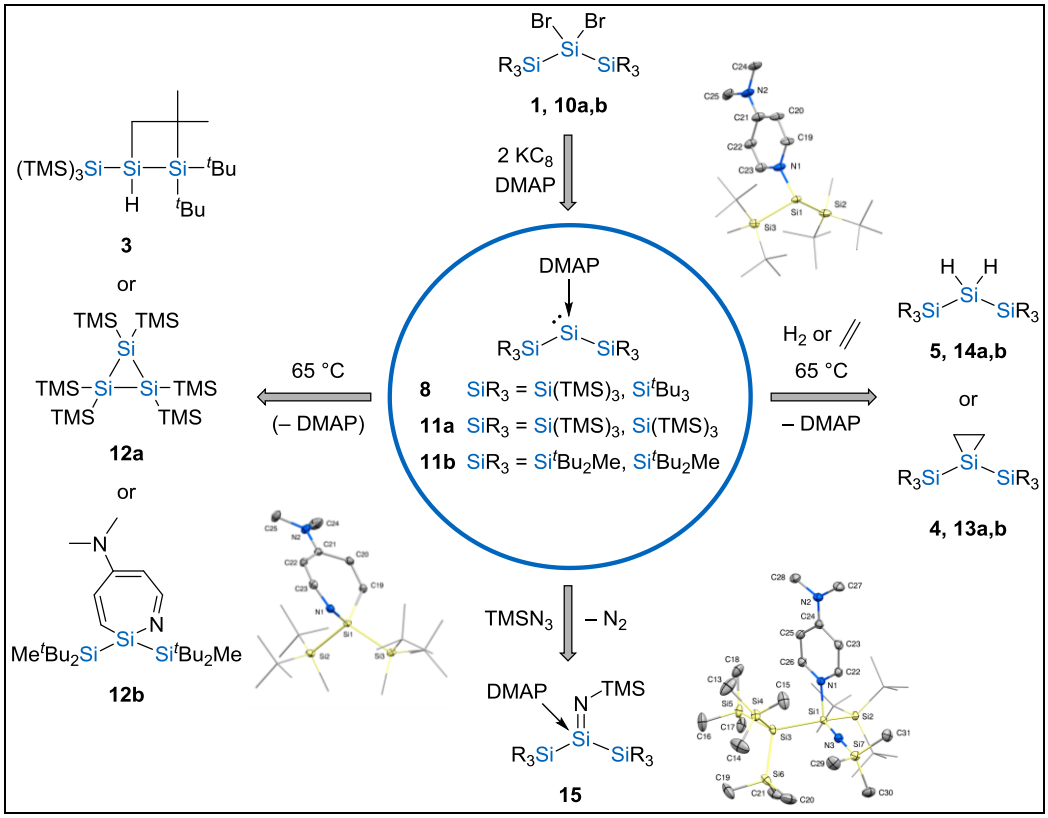


Scheme 15. Synthesis and interconversion of Lewis base-stabilized bis(silyl)silylenes **7** and **8** including the oxygenation reaction of **7**, which affords the unique NHC-stabilized silanoic ester **9**.

Motivated by the facile access to DMAP-stabilized bis(silyl)silylene **8** and the assumed relatively weak donor-acceptor interaction, indicated by the selective Lewis base exchange reaction and DFT calculations, further investigations were carried out. Due to the convenient availability of DMAP and various silyl-substituted dibromosilanes, additional DMAP-silylene adducts **11** were synthesized, including the first isolable bis(hypersilyl)silylene (Scheme 16).[280] Interestingly, deviating decomposition/isomerization reactions were observed at elevated temperatures, depending on the substitution pattern of the silyl ligand scaffold. Thus, not only the aforementioned disiletane **3** (C–H bond activation), but also trisilirane **12a** (1,2-silyl shifts followed by Si–Si bond insertion) and novel azasilepin **12b** (dearomative *Buchner*-type ring expansion) were afforded.

Since a retained reactivity of the respective donor-free bis(silyl)silylenes was observed upon dissociation of DMAP at elevated temperatures, the suitability of the DMAP-supported silylenes for small molecule activation was studied. Remarkably, the thermally induced formation of siliranes $(R_3Si)_2Si(CH_2CH_2)$ and silanes $(R_3Si)_2SiH_2$ was detected after exposure to ethylene and H_2, respectively. Accordingly, DMAP-stabilized bis(silyl)silylenes were found to be convenient equivalents of the corresponding two-coordinate silylenes. Additionally, novel donor-stabilized silaimines **15** were obtained.

During the planned synthesis of $(^tBu_3Si)_2Si(DMAP)$, only disiletane **3** and the novel silylene radical anion $[K(tol)_2][(^tBu_3Si)_2Si]$ were accessible after over-reduction of $(^tBu_3Si)_2SiBr_2$ with excess KC_8.

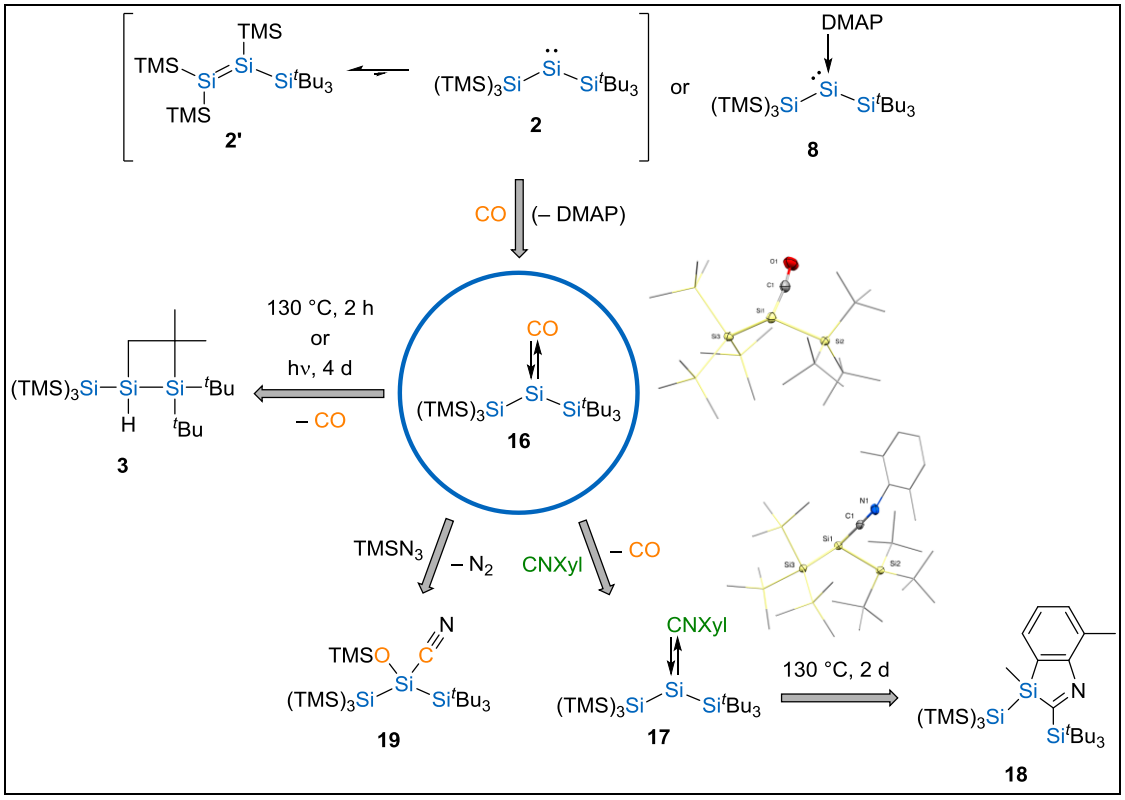


Scheme 16. Isolation, decomposition/isomerization pathways and reactivity of DMAP-stabilized bis(silyl)silylenes.

Silicon carbonyl complexes have only been the subject of computational and argon-matrix isolation studies prior to this work, but their instability has precluded isolation so far. Thus, carbonylation of the synthesized (donor-stabilized) bis(silyl)silylenes seemed to be an encouraging attempt to gain access to these long sought-after species.

And indeed, exposure of the three- or two-coordinate acyclic bis(silyl)silylenes **2** and **8** to carbon monoxide provided the first silicon carbonyl complex ((TMS)$_3$Si)(^{t}Bu$_3$Si)Si⇆CO (**16**) isolated at ambient temperature (Scheme 17). This unique organosilicon compound was thoroughly investigated by both experimental analyses and computational methods. Accordingly, a striking similarity to transition metal carbonyl complexes was revealed with a strong Si–CO bonding motif involving CO→Si σ donation and Si→CO π backbonding. Furthermore, the provided stabilization of the adjacent sterically encumbered, electropositive silyl groups is of utmost importance for the successful isolation of silicon carbonyl complex **16**. The long absence of this compound class is thus not further surprising, considering the lack of suitable precursors.

CO-silylene adduct **16** is thermally remarkably stable, but still shows a preserved silylene reactivity in analogy to the DMAP-stabilized bis(silyl)silylenes (*vide supra*), however only at much higher temperatures.



Scheme 17. Synthesis and transition metal-like reactivity of the unprecedented silicon carbonyl complex (**16**).

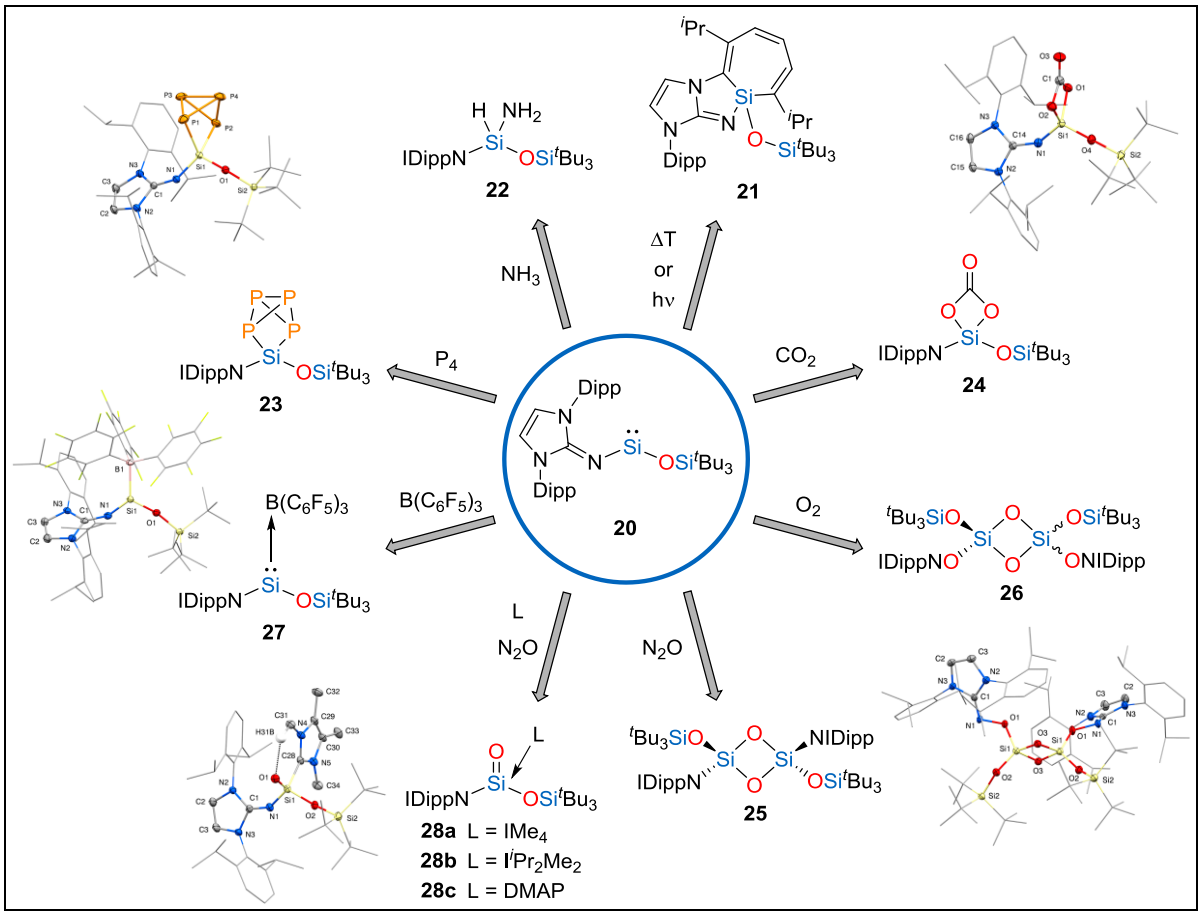
Initial investigations unveiled a transition metal-like reactivity. Thus, photodissociation *via* irradiation of **16** resulted in the liberation of CO under simultaneous formation of disiletane **3**. Additionally, an exchange reaction by substitution of CO with a more strongly donating isocyanide ligand was observed. Silicon isocyanide complex **17** exhibits even higher thermal stability, but eventually isomerized to 1,3-azasilole **18** (C–C bond activation followed by an 1,2-silyl migration).

Motivated by the formation of isocyanato complexes *via* treatment of transition metal carbonyls with azides, a similar reactivity was envisaged with silicon carbonyl complex **16**. Interestingly, conversion of **16** with $TMSN_3$ provided silyl cyanide **19** instead of a silyl isocyanate analogous to the case of transition metals. The origin of the deviating reactivity presumably lies in the high oxophilicity of silicon, which induces the observed silyl migration.

10.1.2 Investigations on a Iminosiloxysilylene

Apart from the results obtained regarding the bis(silyl)silylene project, a novel acyclic silylene was successfully isolated during the course of this work. The first acyclic, two-coordinate iminosiloxysilylene **20** was obtained *via* isomerization of the unique iminosilylsilanone **33a** (*vide infra*; Scheme 20), thus extending the limited number of derivatives of this compound class.[282] With silylene **20** in hand, a comprehensive reactivity study was conducted.[281] Whereas exposure of **20** to ethylene led to the formation of silirane (IDippN)(^{t}Bu$_3$SiO)Si(CH_2CH_2),[282] a novel silyl-substituted

phosphorus ylide was obtained by insertion of the silylene into the ylidic C–H bond of the ester-functionalized *Wittig* reagent $Ph_3P{=}CH(COO^iPr)$.[283] Iminosiloxysilylene **20** is thermally very stable, but isomerizes extremely slowly to iminosiloxysilepin **21** at elevated temperatures (Scheme 18).[281] The selective reaction can be considerably accelerated by a photochemical approach using irradiation.



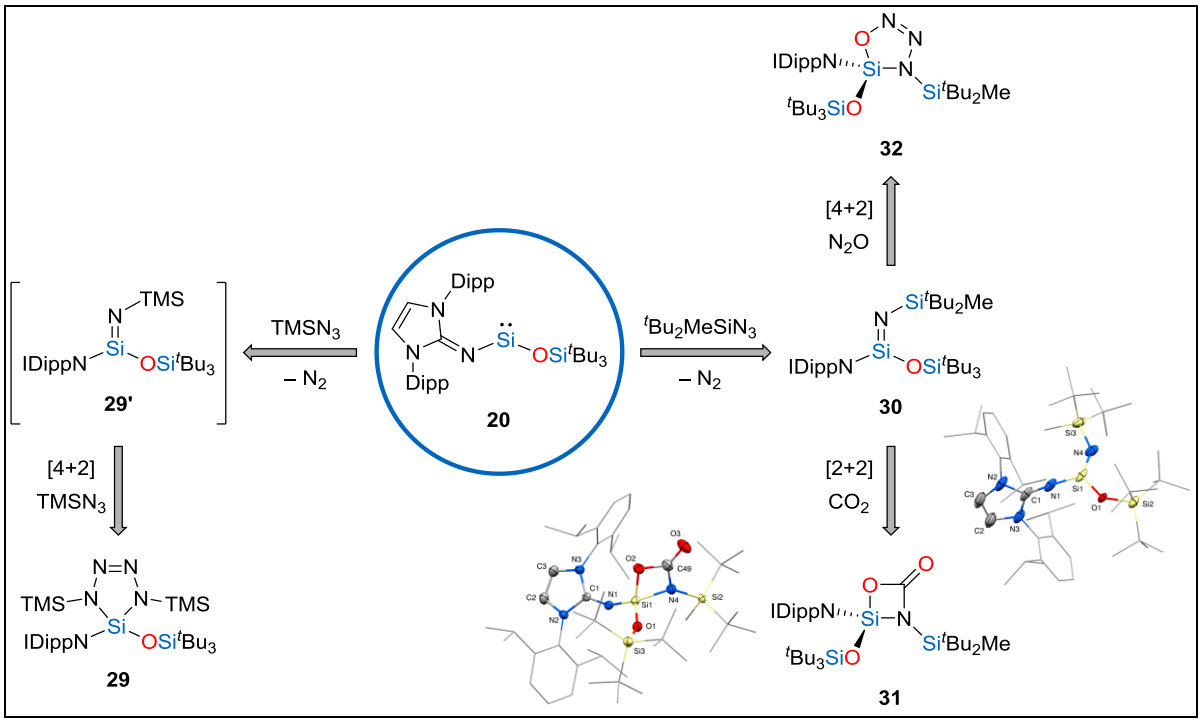
Scheme 18. Thorough oxidation reactions of iminosiloxysilylene **20** and formation of silylene-BCF adduct **27**.

Interestingly, a transition metal-like reactivity was revealed *via* small molecule activation of ammonia and white phosphorus under mild conditions. Accordingly, aminosilane $(IDippN)(^tBu_3SiO)Si(H)(NH_2)$ (**22**) and the SiP_4 cage compound **23** were accessible. The stable silicon carbonate complex **24** was afforded as the sole product of the reaction of iminosiloxysilylene **20** and excessive amounts of CO_2. Since compound **24** represents the formal [2+2] cycloaddition product of the transient silanone $(IDippN)(^tBu_3SiO)Si{=}O$, oxygenation of **20** with the milder oxidizing agent N_2O was performed. Nevertheless, *trans*-cyclodisiloxane **25** was isolated after rapid head-to-tail dimerization of $(IDippN)(^tBu_3SiO)Si{=}O$. Additionally, the relatively harsh oxidation with molecular oxygen provided cyclodisiloxane **26** after rearrangement of the intermediary formed, extremely reactive dioxasilirane $(IDippN)(^tBu_3SiO)SiO_2$ to transient sila-carbonate $(IDippNO)(^tBu_3SiO)Si{=}O$ and subsequent dimerization of the latter.

Due to the high propensity of the siloxysilanone intermediates to undergo follow-up reactions, an additional Lewis acid/base-stabilization was pursued to possibly enable the isolation of these reactive species. Although treatment of iminosiloxysilylene **20** with BCF selectively afforded novel silylene-BCF adduct **27**, the inherent strong donor-acceptor interaction prevented subsequent oxygenation reactions. Serendipitously, exposure of **20** to N_2O in the presence of various Lewis bases selectively formed the donor-stabilized silanoic ester derivatives **28**.

Motivated by the significantly higher reactivity of silaimines compared to their lighter imine congeners, the synthesis of novel acyclic derivatives was targeted. The initial reaction of iminosiloxysilylene **20** toward commercially available trimethylsilyl azide resulted in the formation of silatetrazoline **29** (Scheme 19). The need for a molar excess of $TMSN_3$ is unavoidable due to the apparently higher reactivity of the intermediary formed silaimine **29'**, which undergoes a rapid [4+2] cycloaddition reaction with $TMSN_3$ affording heterocycle **29**.

Exposure of silylene **20** to an equimolar amount of the more sterically encumbered $^tBu_2MeSiN_3$ on the other hand, successfully provided access to acyclic, three-coordinate silaimine **30**. Thus, the increased steric demand of the adjacent silyl group inhibited the subsequent cyclization. Nevertheless, a [2+2] cycloaddition reaction of **30** with CO_2 was possible and isolation of azaoxasiletane **31** achieved.



Scheme 19. Reactivity of silylene **20** toward organosilyl azides: formation of iminosiloxysilaimines and subsequent cycloaddition reactions.

On a final note, a seldom observed 1,3-dipolar cycloaddition reaction with N_2O under mild conditions was found. This striking formation of the unique oxatriazasilole **32**, which represents the initial product of such [4+2] cycloaddition reactions, is unprecedented, even in the well-explored organic chemistry. Besides the avoidance of the relatively harsh conditions generally required, there are scarcely any reports of all three N_2O atoms being incorporated into the product.[284-288]

10.2 Acyclic Three-Coordinate Silanones

Silanones, the heavier analogues of the ubiquitous ketones, are other highly sought-after species within the class of low-coordinate organosilicon compounds. The last decades have witnessed impressive progress regarding the isolation of these extremely reactive, phantom species.[27,252-253,257-258,263] However, prior to this work, no isolable neutral, acyclic, three-coordinate silanone was known and the overall reactivity of these elusive compounds was only insufficiently understood. Therefore, another focus of this work was the accessibility of an unprecedented silanone and exploration of its reactivity, especially with respect to the pronounced chemistry of carbonyl compounds.

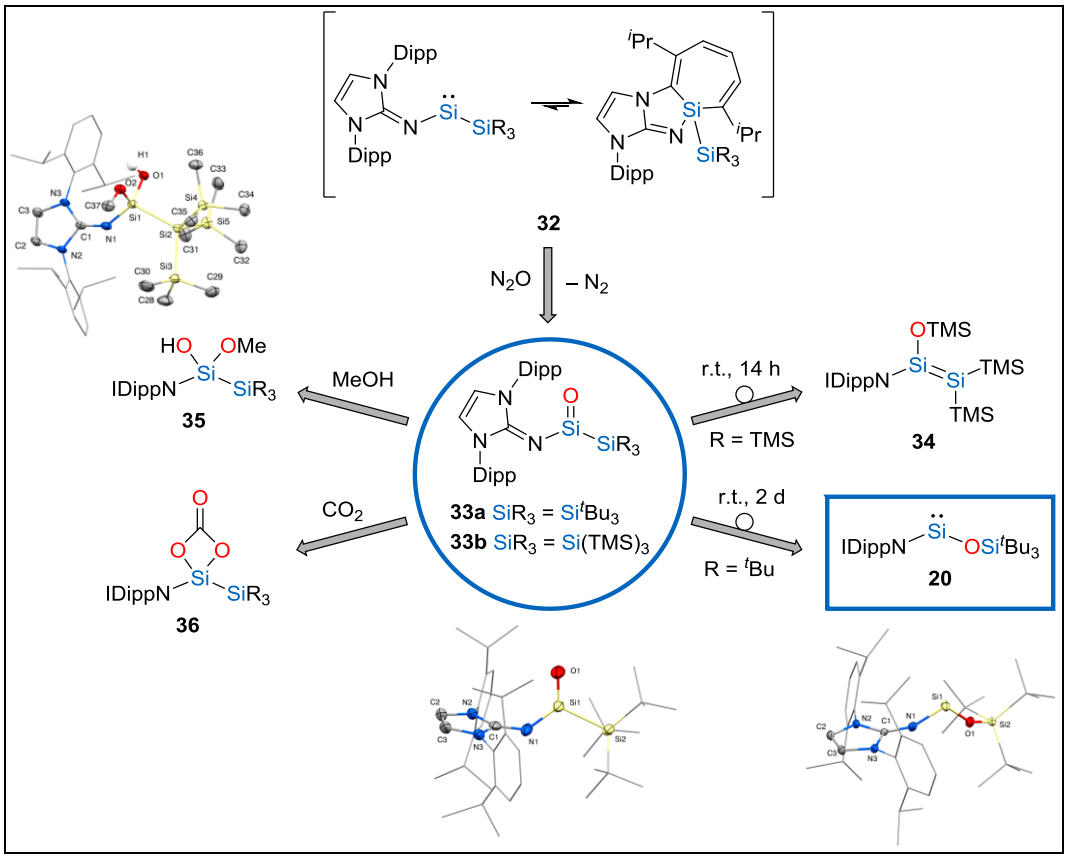
10.2.1 Investigations on Iminosilylsilanones

As a predestined strategy for the isolation of such an elusive derivative, oxygenation of the obtained novel acyclic silylenes was pursued. However, almost all attempts to gain access to the first acyclic, donor-free, neutral silanone *via* exposure of the (donor-stabilized) silylenes to various oxidizing agents only led to the formation of complicated products mixtures or novel cyclodisiloxanes (*vide supra*). Fortunately, the unique examples of Lewis base-stabilized silanoic ester derivatives **9** and **28** outlined above have been obtained. In order to still achieve the isolation of new silanones, other precursor compounds had to be used.

Interestingly, in the course of this work the synthesis of remarkable iminosilylsilepins was achieved in our laboratories, which act as "masked" acyclic silylenes.[183] The high suitability of silylenes for the generation of silanones was demonstrated *via* oxidation of the silepins **32** with N_2O, providing the striking iminosilylsilanones **33** (Scheme 20).[282] These seminal examples of acyclic, donor-free, neutral silanones were fully characterized and more profound insights into the nature of the Si=O double bond were revealed by SC-XRD analysis and detailed computational studies. The combination of the σ-donating electropositive silyl groups and the π-donating NHI ligand was found to be crucial in ensuring adequate stabilization and preventing subsequent reactions.

The synthesized iminosilylsilanones **32** exhibit infinite stability in the solid-state, but isomerize to different products in solution, depending on the type of silyl substituent. Thus, the aforementioned

unique iminosiloxysilylene **20** is accessible *via* rearrangement of the supersilyl-substituted silanone **33a**. In contrast, the high tendency of the hypersilyl group to silyl migrations results in a faster isomerization of derivative **33b** to transient siloxydisilene **34**, which decomposes in solution but can be isolated in the form of an NHC-disilene adduct.



Scheme 20. Synthesis and initial reactivity studies of the first acyclic, neutral, three-coordinate silanones **33**.

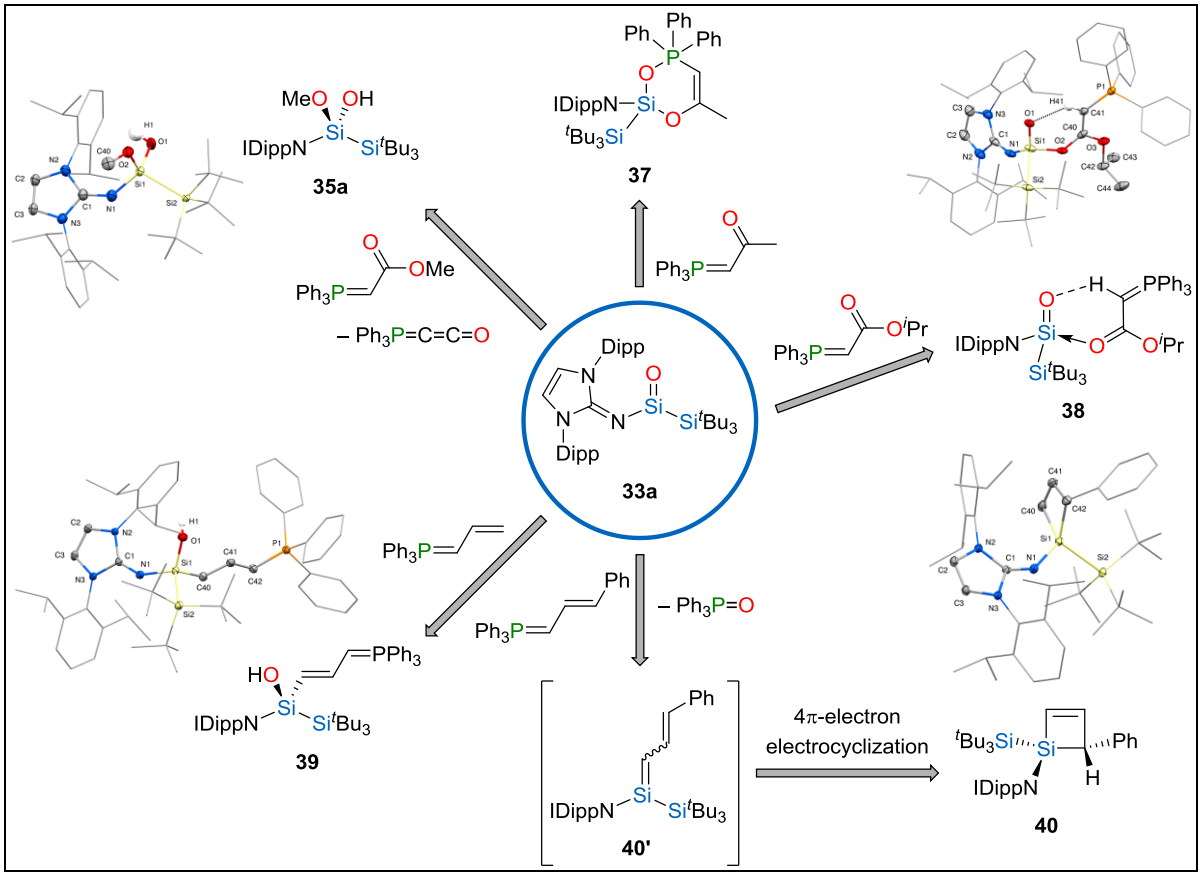
Moreover, preliminary reactivity investigations were conducted with the novel silanones **33**. As expected, alcoholysis of **33** with methanol led to oxidation and formation of methoxysilanols **35**. The inherent Si=O double bond was further experimentally proven via [2+2] cycloaddition reactions with CO_2 and generation of the unknown monomeric silicon carbonate complexes **36**. The obtained results represent a next step forward in organosilicon chemistry and should induce further investigations.

10.2.2 Investigations on the Sila-Wittig Reaction

With iminosilylsilanones **33** in hand, reactivity investigations with respect to classical carbonyl compounds were carried out. One of the most important and versatile reactions of carbonyl compounds is the conversion to a broad range of alkenes *via* the *Wittig* olefination. In sharp contrast, no olefination method for heavier carbonyl congeners was known in advance of this work. Thus, the potential application of the *Wittig* reaction to silanones **33** was studied. Due to the higher stability and

the lower propensity for silyl migrations, only the $^{t}Bu_3Si$-substituted derivative **33a** was used. To prevent possible side reactions with the much more reactive silanone, only isolable phosphorus ylides were employed.

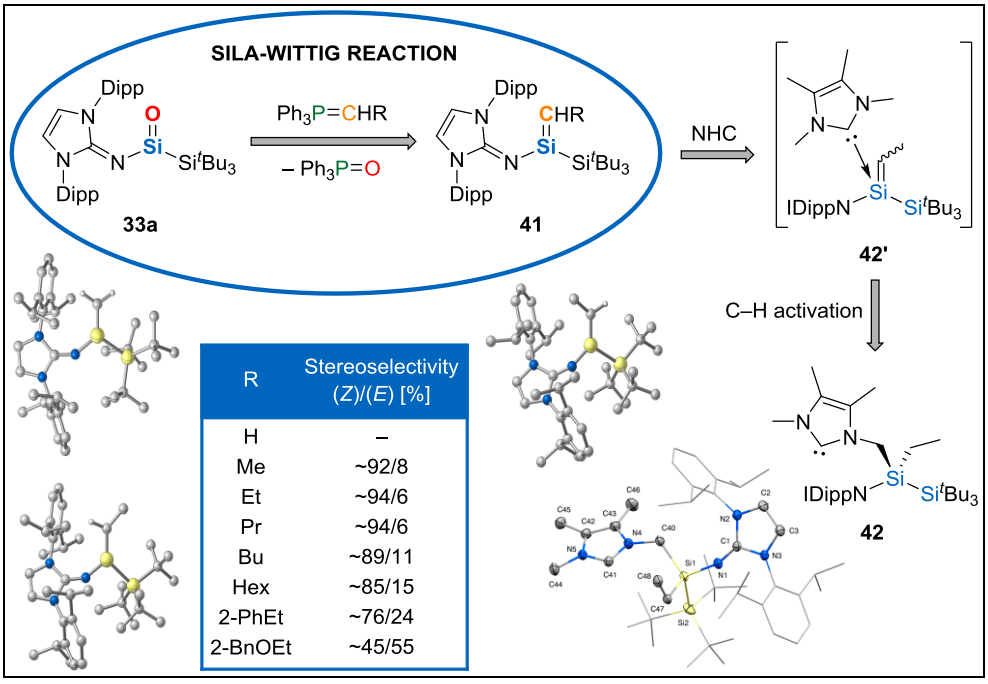
At first, reactions toward stabilized *Wittig* reagents were investigated, due to their convenient access and in some cases even commercial availability. As carbonyl compounds and silanones differ significantly in terms of stability and reactivity (silanones exhibit a strongly polarized, zwitterionic and therefore much more reactive Si=O double bond), no *Wittig* olefination was observed at all. Interestingly, reaction of silanone **33a** with a ketone-substituted ylide resulted in a formal Hetero-*Diels-Alder* reaction providing dioxaphosphasiline **37** (Scheme 21).[283] The outcome of the exposure to ester-substituted *Wittig* reagents was strongly dependent on the steric encumbrance, thus conversion of **33a** with $Ph_3P{=}CH(COOMe)$ simultaneously provided methoxysilanol **35a** and the Bestmann ylide $Ph_3P{=}C{=}C{=}O$ *via* formal methanol transfer. In contrast, reaction with the sterically demanding derivative $Ph_3P{=}CH(COO^{i}Pr)$ selectively afforded ylide-stabilized silanone **38**. Interestingly, adduct **38** quantitatively isomerizes to silyl-substituted phosphorus ylide $(IDippN)(^{t}Bu_3SiO)Si(H)(C{=}PPh_3(COO^{i}Pr))$ at elevated temperatures. The same product is also accessible *via* reaction of iminosiloxysilylene **20** with $Ph_3P{=}CH(COO^{i}Pr)$ (*vide supra*).



Scheme 21. Reactivity of iminosilylsilanone **33a** toward stabilized and semi-stabilized *Wittig* reagents.

Continuation of the reactivity studies of silanone **33a** with semi-stabilized ylides initially revealed the formation of the novel silanoyl-substituted phosphorus ylide **39**, presumably induced *via* nucleophilic attack of the vinylogous ylide to the silanone moiety. In contrast, conversion of **33a** with the sterically crowded phenyl-substituted derivative Ph_3P=CHCHCHPh afforded transient silene **40'**, which selectively isomerized rapidly to silacyclobutene **40** (*via* a 4π-electron electrocyclization reaction), thus indicating a successful sila-*Wittig* reaction.

Inspired by these results, non-stabilized ylides were finally tested, as they should allow less side reactions due to the lack of additional functional groups. Strikingly, treatment of iminosilylsilanone **33a** with a variety of non-stabilized *Wittig* reagents resulted in the selective formation of the novel silenes **41** (Scheme 22). Accordingly, the unprecedented sila-*Wittig* reaction converts silanones into silenes under mild conditions, similar to the classical *Wittig* olefination. In addition, an analogously high preference for the corresponding (*Z*)-isomers was generally observed. As a consequence of the significantly increased reactivity of silenes compared to their lighter alkene homologues, the synthesized three-coordinate silenes **41** decomposed during isolation attempts. Even Lewis base-stabilization does not prevent subsequent reactions, since silyl-substituted NHC **42** was isolated from transient NHC-stabilized silene **42'** after intramolecular C–H bond activation.

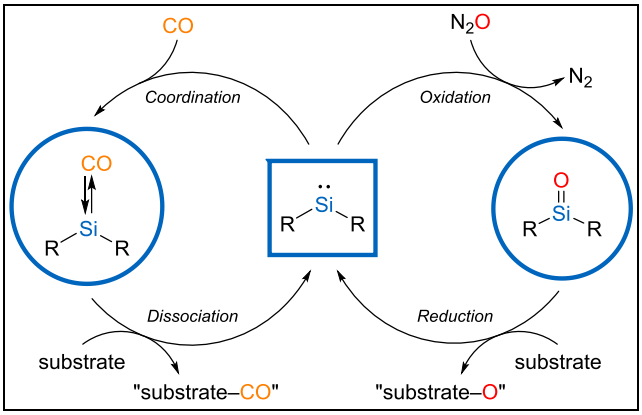


Scheme 22. Synthesis of iminosilylsilenes **41** *via* sila-*Wittig* reaction of silanone **33a** with non-stabilized phosphorus ylides.

Nonetheless, the sila-*Wittig* reaction represents the first successful application of the versatile carbonyl olefination to heavier congeners and provides a novel platform to gain access to otherwise elusive compounds.

10.3 Main Conclusion and Perspective

The overall objective of this PhD thesis was the deeper investigation of the evolving class of low-coordinate organosilicon compounds with respect to further uncovering their potential for applications in metal-free catalysis. Accordingly, novel acyclic, two-coordinate silylenes were successfully isolated, including the first synthetically accessible, extremely reactive bis(silyl)silylene. Remarkably, unprecedented silicon carbonyl complexes could be synthesized *via* selective carbonylation of bis(silyl)silylene derivatives. All of these unique compounds exhibit a reactivity that is reminiscent of transition metal complexes, such as the activation of industrially important small molecules under mild conditions. Therefore, these results can be seen as further proof of the untapped potential of low-coordinate organosilicon compounds and brings scientists working in this field one step closer to a versatile silicon-based catalysis. In addition, new insights were revealed into the relationship between silicon and its lighter homologue carbon. Most impressively, the first acyclic, neutral, three-coordinate silanone was isolated and its application in the versatile *Wittig* reaction was successfully demonstrated, thus providing new avenues for future research.



Scheme 23. Postulated catalytic cycles involving acyclic silylenes, silanones and silicon carbonyl complexes.

Very recently, the limited number of catalytic conversions using low-valent organosilicon compounds has been extended. Fascinating results were achieved by the *WACKER Chemie AG* with the development of a highly efficient Si(II) catalysis.[276] In particular the reported hydrosilylation of alkenes with silyliumylidene ions $[Cp^*Si:^+][BR_4^-]$ is comparable in activity to the currently applied platinum catalysis and could thus pave the way for the development of more sustainable processes. Accordingly, the unique compounds isolated in this work could also become key reagents for future catalytic conversions. For example, oxygen transfer from silanones to suitable reagents under formation of silylenes would be conceivable, as oxygen transfer was already verified with the sila-*Wittig* reaction (Scheme 23). Moreover, carbonylation reactions using silicon carbonyl complexes could be a promising target, since the reversibility of CO coordination has been experimentally proven.

11. Zusammenfassung und Ausblick

Angesichts des Einflusses und der außerordentlichen Bedeutung des florierenden Gebiets der Hauptgruppenverbindungen, die Übergangsmetallkomplexe nachahmen, sind weiterführende Studien in diesem Bereich ein ehrgeiziges Ziel für die heutige Generation moderner Chemiker. Trotz intensiver Forschung steckt jedoch insbesondere die Entwicklung und Anwendung nachhaltiger Katalysatoren, die auf Hauptgruppenelementen basieren, noch in den Kinderschuhen.[11-14] Eine besonders vielversprechende Verbindungsklasse, um das hohe Ziel einer vielseitigen metallfreien Katalyse zu erreichen, sind niedrigkoordinierte Organosiliciumverbindungen, aufgrund ihrer hohen Reaktivität und der hervorragenden ökologischen und ökonomischen Eigenschaften von Silicium.[16] Daher sind tiefergehende Untersuchungen in dieser Hinsicht von großem Interesse und potentiell von bedeutendem Nutzen für die Zukunft.

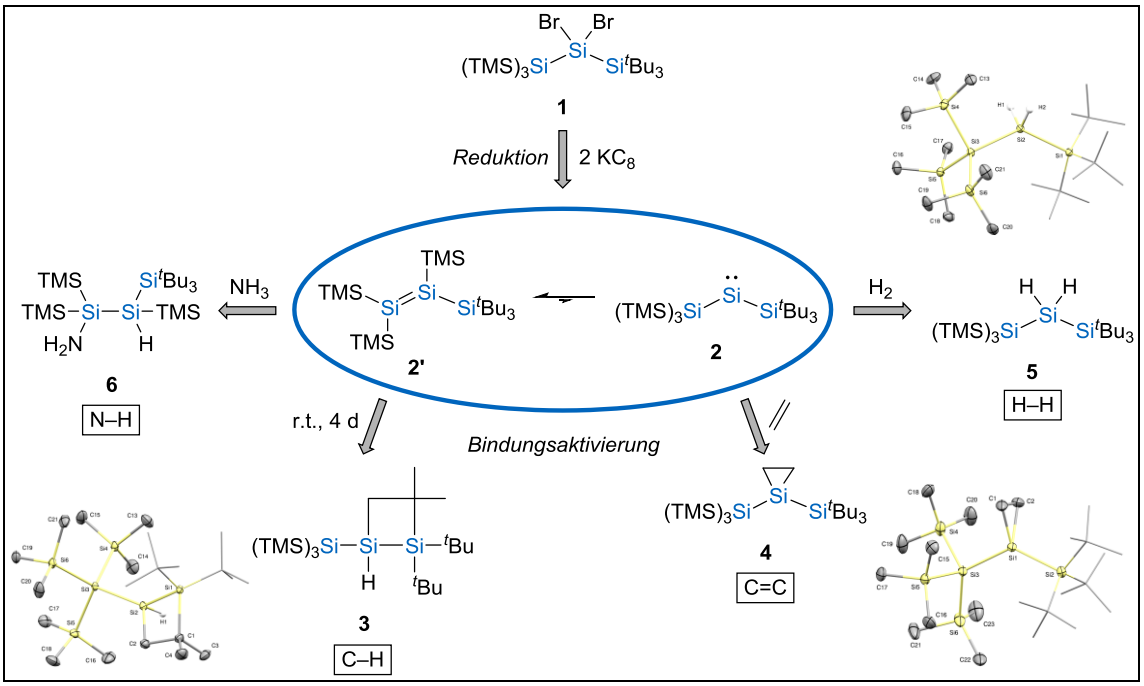
11.1 Acyclische zweifachkoordinierte Silylene

Innerhalb der vielseitigen Klasse der niedrigkoordinierten Organosiliciumverbindungen stellen speziell acyclische donor-freie Silylene eine der vielversprechendsten Verbindungen dar, um den Einsatz von Übergangsmetallkomplexen in der Katalyse zu umgehen. Ein wichtiger Durchbruch wurde mit den bahnbrechenden, gleichzeitigen Veröffentlichungen von *Aldridge, Jones et al.* und der Gruppe um *Power* zu den ersten isolierbaren acyclischen, zweifachkoordinierten Silylenen im Jahr 2012 erzielt.[169-170] Vor dieser Doktorarbeit war jedoch fast kein zusätzliches Derivat bekannt und ihre Reaktivität insgesamt nur marginal untersucht.[169-170,174-176,185-186] Ein Hauptziel der vorliegenden Arbeit war es folglich, die Anzahl der isolierbaren acyclischen Silylene zu erweitern und ihre Reaktivität im Hinblick auf mögliche Anwendungen in der Katalyse weiter zu erforschen.

11.1.1 Studien zu Bis(silyl)silylenen

Aufgrund ihrer intrinsisch hohen Reaktivität und ihres potentiellen Triplett-Grundzustands sind Bis(silyl)silylene besonders begehrt, jedoch haben schnelle Zersetzungsreaktionen bisher eine erfolgreiche Isolierung verhindert.[85,211] Daher konzentrierten sich die anfänglichen Untersuchungen auf die erstmalige Isolierung einer derartig schwer zugänglichen Spezies unter Verwendung eines geeigneten Ligandengerüsts. Insbesondere wurde die einzigartige Kombination von sterisch überfrachteten Hyper- und Supersilylgruppen ins Auge gefasst, um eine ausreichende Stabilisierung zu erreichen und möglicherweise eine reversible Disilen-Silylen-Umwandlung *via* 1,2-Silylmigrationen zu induzieren.

Nach der erfolgreichen Isolierung des neuen Dibromsilans **1** führte die reduktive Debromierung von **1** tatsächlich zur Bildung einer beispiellosen Gleichgewichtsmischung, bestehend aus dem ersten isolierbaren zweifachkoordinierten Bis(silyl)silylen ((TMS)$_3$Si)(^{t}Bu$_3$Si)Si: (**2**) und seinem isomeren Tetrasilyldisilene (TMS)(^{t}Bu$_3$Si)Si=Si(TMS)$_2$ (**2'**) (Schema 24).[279] Ergänzende DFT-Berechnungen offenbarten einen näheren Einblick in die Natur des Gleichgewichts und die Bindungssituation von **2**. Der vermeintliche Triplett-Grundzustand konnte jedoch weder experimentell noch theoretisch eindeutig nachgewiesen werden.



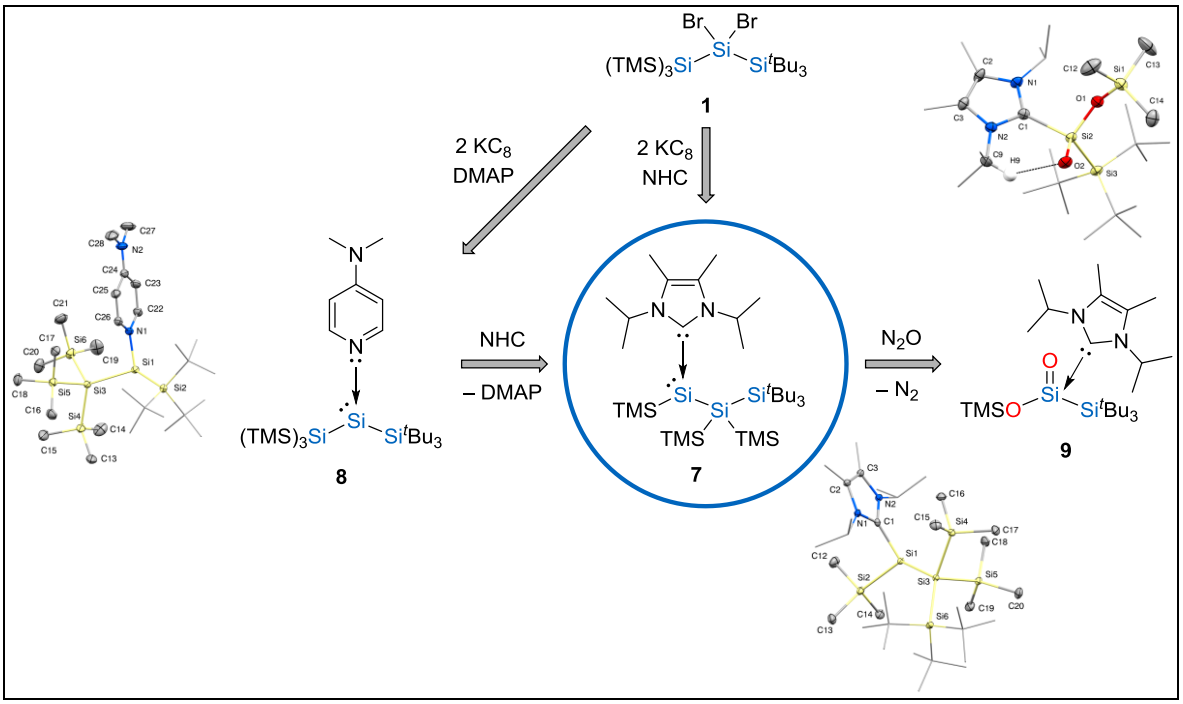
Schema 24. Synthese und Reaktivität des ersten isolierbaren acyclischen, zweifachkoordinierten Bis(silyl)silylens ((TMS)$_3$Si)(^{t}Bu$_3$Si)Si: (**2**).

Obwohl die Mischung bei –35 °C unbegrenzt stabil ist, zersetzt sie sich schließlich langsam in Lösung bei Raumtemperatur unter Bildung von Disiletan **3** *via* intramolekularer C–H-Aktivierung des extrem reaktiven Bis(silyl)silylens **2**. Die Existenz des Gleichgewichts und das Potential für katalytische Anwendungen konnten durch einfache oxidative Addition der industriell relevanten kleinen Moleküle NH_3, H_2 und Ethen unter sehr milden Bedingungen erfolgreich demonstriert werden. So wurden sowohl Tetrasilyldisilen- als auch Bis(silyl)silylen-Additionsprodukte erhalten.

Weitere Details zur Disilen-Silylen-Umlagerung wurden durch die Isolierung verschiedener Lewis-Basen-stabilisierter Bis(silyl)silylene gewonnen. Reduktive Debromierung von Dibromsilan **1** in Gegenwart der jeweiligen Donoren lieferte das NHC-Silylen-Addukt **7** und das DMAP-Silylen-Addukt **8** (Schema 25). Interessanterweise wurde eine selektive Interkonversion durch Reaktion von

DMAP-stabilisiertem Bis(silyl)silylen **8** mit einer äquimolaren Menge $I^tPr_2Me_2$ unter simultaner Freisetzung von DMAP beobachtet.

Alle Versuche, Zugang zu einem Bis(silyl)silanon durch Oxidation der verschiedenen (donorstabilisierten) Bis(silyl)silylene zu erhalten, führten lediglich zur Bildung komplizierter Produktgemische, vermutlich induziert durch Silylmigrationen, Insertionsreaktion und Di-/Oligomerisierung hochreaktiver transienter Silanone. Dennoch führte die Oxygenierung des NHC-stabilisierten Bis(silyl)silylens **7** mit N_2O zur erstaunlichen Bildung und Isolierung des präzedenzlosen donorstabilisierten, acyclischen Silanonsäureesters **9**, einem schwereren Carbonsäureester, womit sich neue Wege für die weitere Forschung eröffnen.



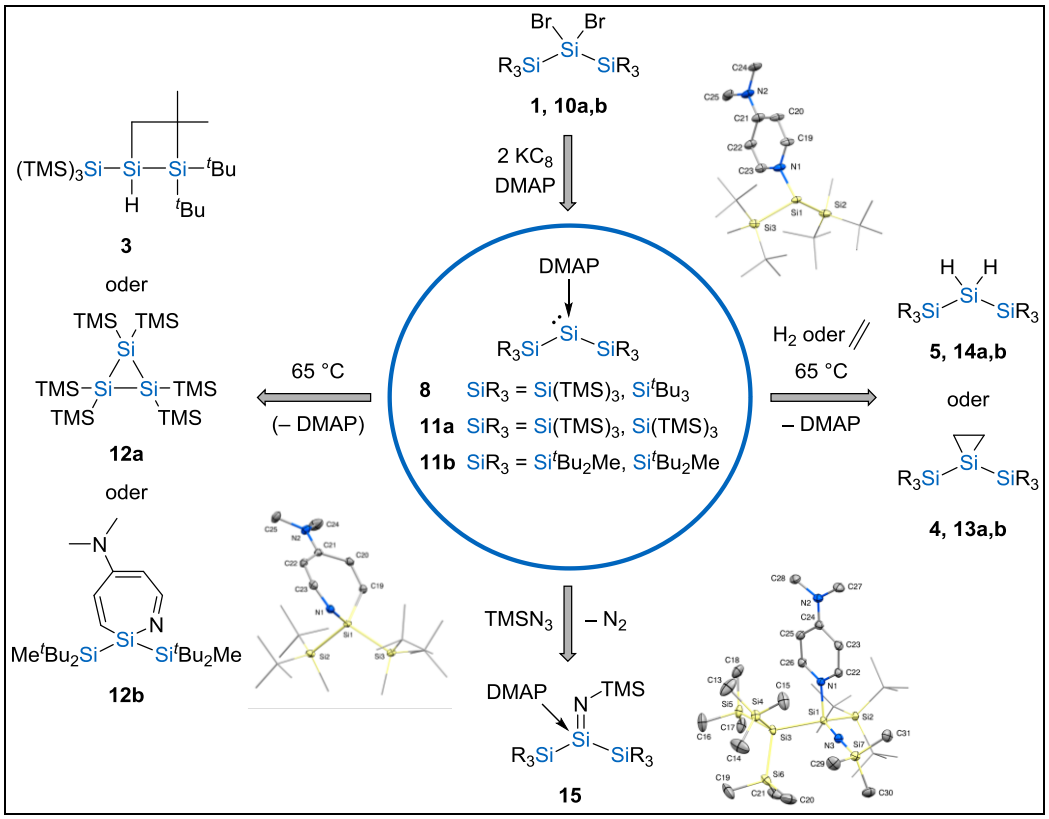
Schema 25. Synthese und Interkonversion von Lewis-Basen-stabilisierten Bis(silyl)silylenen **7** und **8** inklusive der Oxygenierung von **7**, die den einzigartigen NHC-stabilisierten Silanonsäureester **9** ergibt.

Motiviert durch den einfachen Zugang zu DMAP-stabilisiertem Bis(silyl)silylen **8** und der mutmaßlich relativ schwachen Donor-Akzeptor-Wechselwirkung, angedeutet durch die selektive Lewis-Basen-Austauschreaktion und DFT-Berechnungen, wurden weitere Untersuchungen durchgeführt. Aufgrund der komfortablen Verfügbarkeit von DMAP und verschiedenen silylsubstituierten Dibromsilanen wurden weitere DMAP-Silylene-Addukte **11** synthetisiert, darunter das erste isolierbare Bis(hypersilyl)silylen (Schema 26).[280] Interessanterweise wurden bei erhöhten Temperaturen abweichende Zersetzungs-/Isomerisierungsreaktionen beobachtet, die vom Substitutionsmuster des Silylligandengerüsts abhängig sind. So wurden nicht nur das bereits erwähnte Disiletan **3** (C–H-Aktivierung), sondern auch das Trisiliran **12a** (1,2-Silylmigration, gefolgt von

Si–Si-Bindungsinsertion) und das neuartige Azasilepin **12b** (dearomative *Buchner*-Ringerweiterung) erhalten.

Nachdem bei der Dissoziation von DMAP bei erhöhten Temperaturen eine erhaltene Reaktivität der jeweiligen donorfreien Bis(silyl)silylene beobachtet wurde, wurde die Eignung der DMAP-stabilisierten Silylene für die Aktivierung kleiner Moleküle erforscht. Bemerkenswerterweise konnte die thermisch induzierte Bildung von Siliranen $(R_3Si)_2Si(CH_2CH_2)$ und Silanen $(R_3Si)_2SiH_2$ nach Exposition gegenüber Ethen bzw. H_2 nachgewiesen werden. Dementsprechend erwiesen sich DMAP-stabilisierte Bis(silyl)silylene als komfortable Pendants zu den entsprechenden zweifachkoordinierten Silylenen. Zusätzlich wurden die neuen donor-stabilisierten Silaimine **15** hergestellt.

Bei der geplanten Synthese von $(^tBu_3Si)_2Si(DMAP)$ waren nur Disiletan **3** und nach einer Überreduktion von $(^tBu_3Si)_2SiBr_2$ mit überschüssigem KC_8 das neue Silylenradikal-Anion $[K(tol)_2][(^tBu_3Si)_2Si]$ zugänglich.



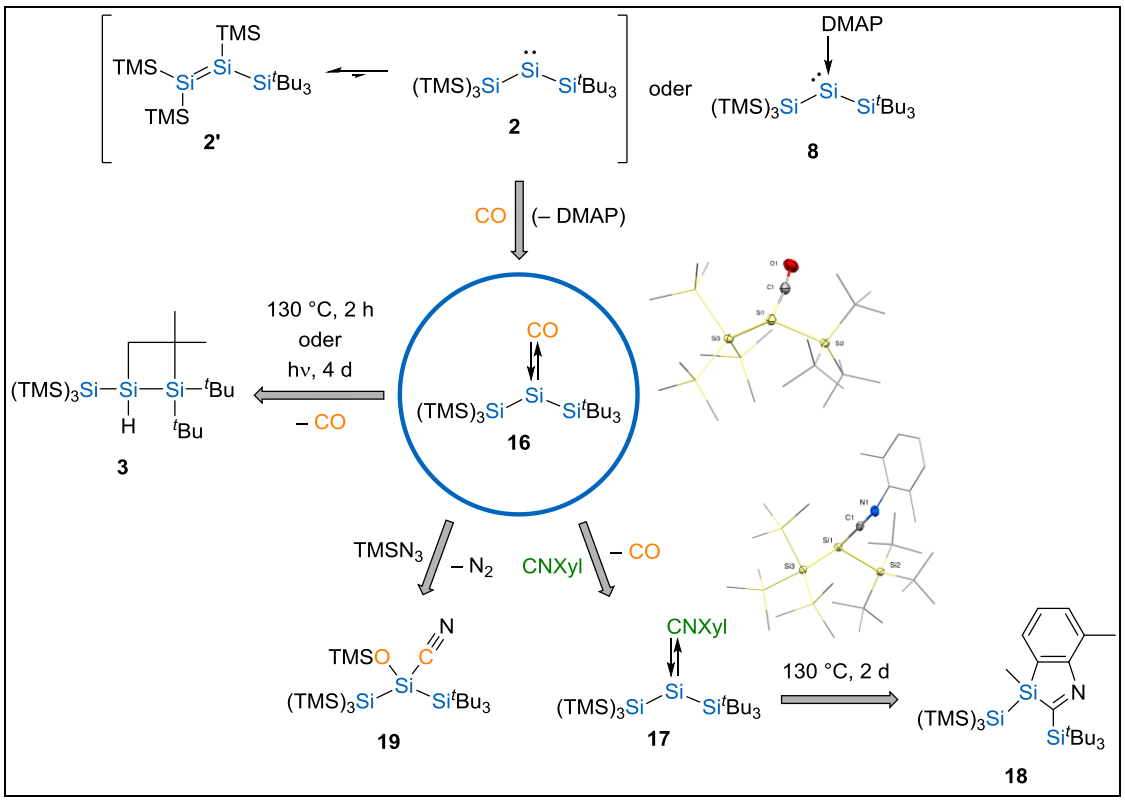
Schema 26. Isolierung, Abbau-/Isomerisierungswege und Reaktivität von einzigartigen DMAP-stabilisierten Bis(silyl)silylenen.

Siliciumcarbonylkomplexe waren im Vorfeld dieser Arbeit nur Gegenstand theoretischer und Argon-Matrix-Isolationsstudien, da deren Instabilität eine Isolierung bisher verhinderte. Folglich

schien die Carbonylierung der synthetisierten (donorstabilisierten) Bis(silyl)silylene ein vielversprechender Ansatz zu sein, um Zugang zu diesen lang ersehnten Spezies zu erlangen.

In der Tat lieferte die Exposition der drei- oder zweifachkoordinierten acyclischen Bis(silyl)silylene **2** und **8** gegenüber Kohlenstoffmonoxid den ersten Siliciumcarbonylkomplex ((TMS)$_3$Si)(^{t}Bu$_3$Si) Si⇆CO (**16**), der bei Umgebungstemperatur isoliert wurde (Schema 27). Diese einzigartige Organosiliciumverbindung wurde sowohl durch experimentelle Analysen als auch durch theoretische Methoden umfassend untersucht. Dementsprechend zeigte sich eine erstaunliche Ähnlichkeit mit Übergangsmetall-Carbonylkomplexen in Form eines starken Si–CO-Bindungsmotivs mit CO→Si σ-Donierung und Si→CO π-Rückbindung. Darüber hinaus ist die gewährleistete Stabilisierung der angrenzenden sterisch anspruchsvollen, elektropositiven Silylgruppen von größter Bedeutung für die erfolgreiche Isolierung des Siliciumcarbonylkomplexes **16**. Die lange Abwesenheit dieser Verbindungsklasse ist daher nicht weiter verwunderlich, wenn man den Mangel an geeigneten Vorläufern bedenkt.

CO-Silylen-Addukt **16** ist thermisch außerordentlich stabil, weist aber dennoch eine erhaltene Silylen-Reaktivität in Analogie zu den DMAP-stabilisierten Bis(silyl)silylenen auf (*vide supra*), allerdings erst bei wesentlich höheren Temperaturen.



Schema 27. Synthese und übergangsmetallartige Reaktivität des beispiellosen Siliciumcarbonylkomplexes (**16**).

Erste Untersuchungen ergaben eine übergangsmetallartige Reaktivität. So führte die Photodissoziation durch Bestrahlung von **16** zur Freisetzung von CO unter gleichzeitiger Bildung von Disiletan **3**. Zusätzlich wurde eine Austauschreaktion *via* Substitution von CO durch einen stärker donierenden Isocyanid-Liganden beobachtet. Siliciumisocyanidkomplex **17** weist eine noch höhere thermische Stabilität auf, isomerisiert aber letztendlich zu 1,3-Azasilol **18** (C–C-Aktivierung, gefolgt von einer 1,2-Silylmigration).

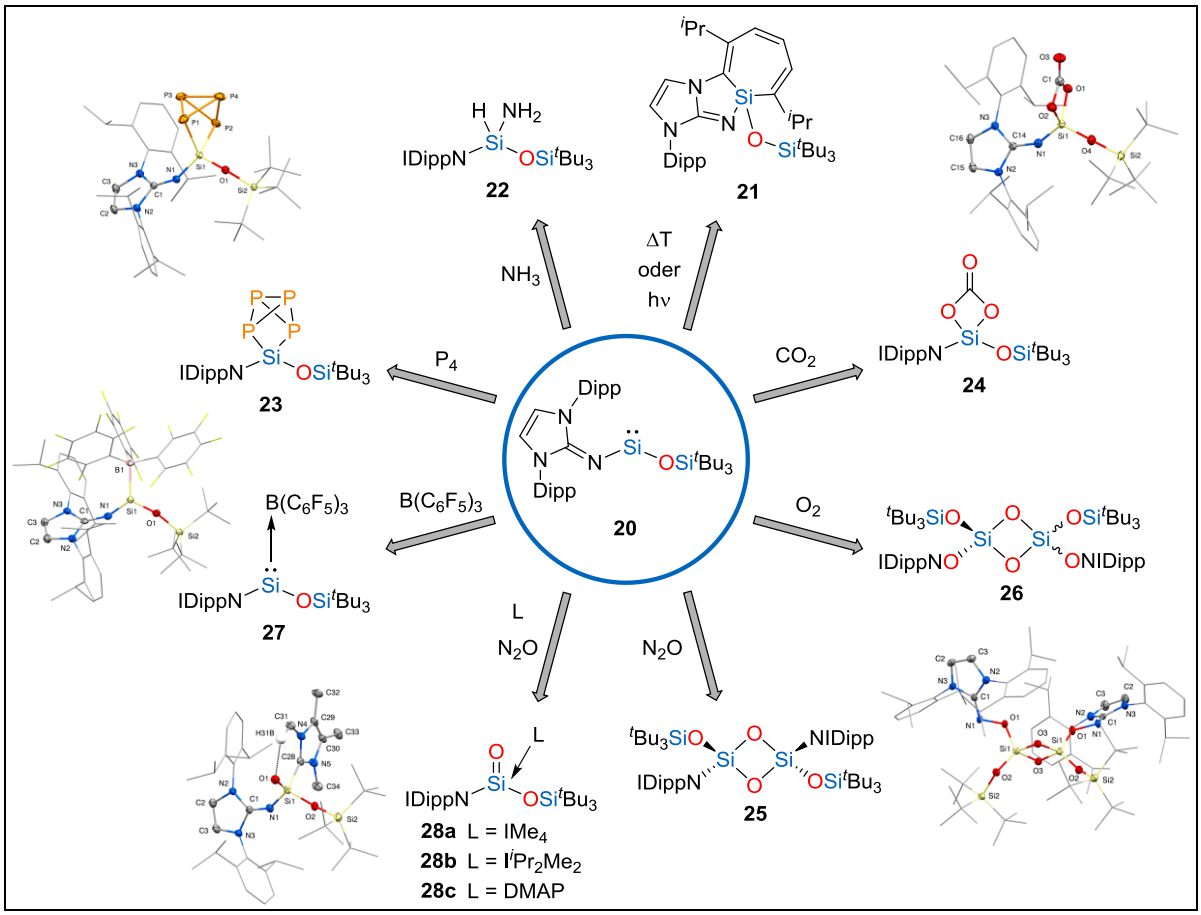
Motiviert durch die Bildung von Isocyanatokomplexen *via* Behandlung von Übergangsmetallcarbonylen mit Aziden, wurde eine ähnliche Reaktivität des Siliciumcarbonylkomplexes **16** angestrebt. Interessanterweise lieferte die Reaktion von **16** mit $TMSN_3$ Silylcyanid **19** anstelle eines Silylisocyanats analog zur Chemie der Übergangsmetalle. Der Ursprung der abweichenden Reaktivität lässt sich vermutlich auf die hohe Oxophilie des Siliciums zurückführen, die die beobachtete Silylmigration induziert.

11.1.2 Studien zu einem Iminosiloxysilylen

Abgesehen von den Ergebnissen, die im Rahmen des Bis(silyl)silylen-Projekts erzielt wurden, gelang es im Laufe dieser Arbeit, ein neuartiges acyclisches Silylen zu isolieren. Das erste acyclische, zweifachkoordinierte Iminosiloxysilylen **20** wurde durch Isomerisierung des einzigartigen Iminosilylsilanons **33a** (*vide infra*; Schema 30) erhalten, wodurch die limitierte Anzahl von Derivaten dieser Verbindungsklasse erweitert wurde.[282] Mit Silylen **20** in der Hand wurde eine umfassende Reaktivitätsstudie durchgeführt.[281] Während die Umsetzung von **20** mit Ethen zur Bildung von Siliran (IDippN)(^{t}Bu$_3$SiO)Si(CH_2CH_2) führte,[282] wurde ein neuartiges silylsubstituiertes Phosphorylid durch Insertion des Silylens in die ylidische C–H Bindung des esterfunktionalisierten Wittig Reagenz Ph_3P=CH(COO^{i}Pr) gewonnen.[283] Iminosiloxysilylen **20** ist thermisch sehr stabil, isomerisiert aber bei erhöhten Temperaturen extrem langsam zu Iminosiloxysilepin **21** (Schema 28).[281] Die selektive Reaktion kann durch einen photochemischen Ansatz mittels Bestrahlung erheblich beschleunigt werden.

Interessanterweise wurde eine übergangsmetallartige Reaktivität *via* Aktivierung der kleinen Moleküle Ammoniak und weißem Phosphor unter milden Bedingungen festgestellt. Demzufolge waren Aminosilan (IDippN)(^{t}Bu$_3$SiO)Si(H)(NH_2) (**22**) und die SiP_4-Käfigverbindung **23** zugänglich. Der stabile Siliciumcarbonatkomplex **24** wurde als einziges Produkt der Reaktion von Iminosiloxysilylen **20** und überschüssigen Mengen an CO_2 gebildet. Da Verbindung **24** das formale [2+2] Cycloadditionsprodukt des transienten Silanons (IDippN)(^{t}Bu$_3$SiO)Si=O darstellt, wurde eine

Oxygenierung von **20** mit dem milderen Oxidationsmittel N_2O durchgeführt. Allerdings wurde das *trans*-Cyclodisiloxan **25** nach schneller Kopf-Schwanz-Dimerisierung von (IDippN)(^{t}Bu$_3$SiO)Si=O isoliert. Zusätzlich lieferte die relativ harsche Oxidation mit molekularem Sauerstoff Cyclodisiloxan **26** nach Umlagerung des intermediär gebildeten, extrem reaktiven Dioxasilirans (IDippN)(^{t}Bu$_3$SiO)SiO_2 zum transienten Silacarbonat (IDippNO)(^{t}Bu$_3$SiO)Si=O und anschließender Dimerisierung der letztgenannten Verbindung.



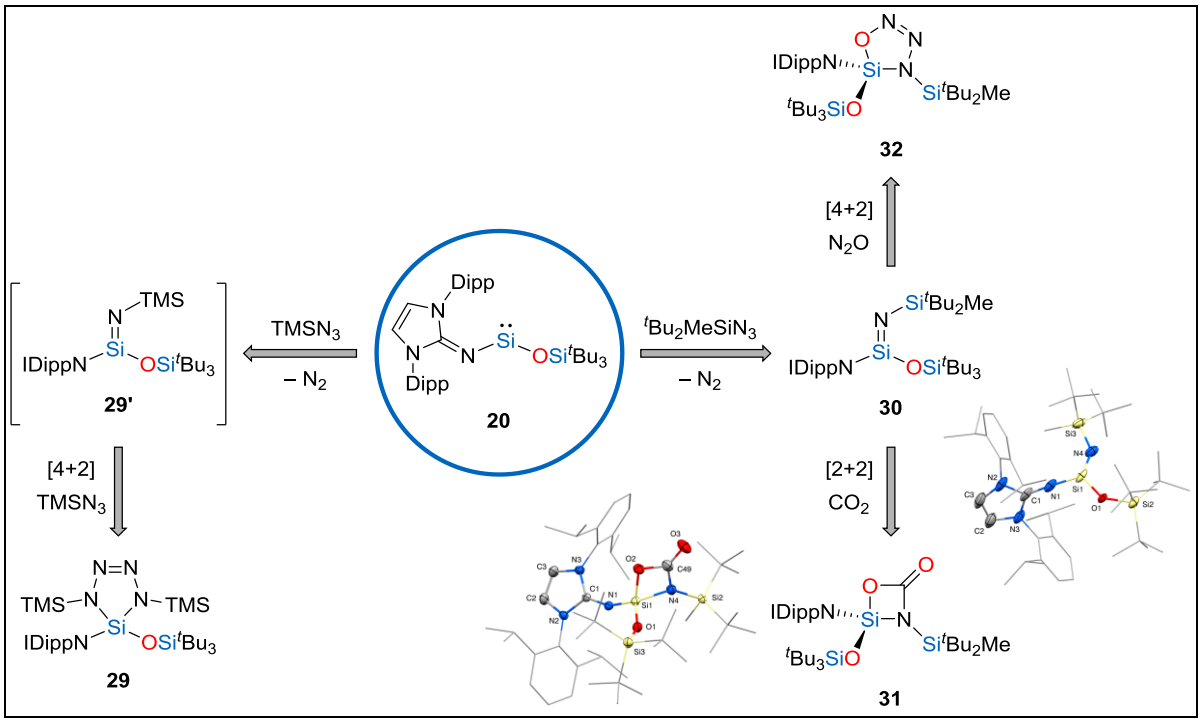
Schema 28. Umfassende Oxidationsreaktionen von Iminosiloxysilylen **20** und Bildung des Silylen-BCF-Addukts **27**.

Angesichts der hohen Neigung der Siloxysilanon Intermediate zu Folgereaktionen wurde eine zusätzliche Lewis-Säuren/Basen-Stabilisierung angestrebt, um möglicherweise die Isolierung dieser reaktiven Spezies zu ermöglichen. Obwohl die Reaktion von Iminosiloxysilylene **20** mit BCF selektiv das neue Silylen-BCF Addukt **27** hervorbrachte, verhinderte die inhärent starke Donor-Akzeptor-Wechselwirkung nachfolgende Oxidationsreaktionen. Erfreulicherweise wurden durch Exposition von **20** gegenüber N_2O in Gegenwart verschiedener Lewis-Basen selektiv die donorstabilisierten Silanonsäureester-Derivate **28** gebildet.

Motiviert durch die signifikant höhere Reaktivität der Silaimine im Vergleich zu ihren leichteren Imin-Kongeneren, wurde die Synthese neuartiger acyclischer Derivate anvisiert. Die Initialreaktion

von Iminosiloxysilylen **20** mit kommerziell erhältlichem Trimethylsilylazid führte zur Bildung von Silatetrazolin **29** (Schema 29). Die Notwendigkeit eines molaren Überschusses von $TMSN_3$ ist aufgrund der augenscheinlich höheren Reaktivität des intermediär gebildeten Silaimins **29'**, das eine schnelle [4+2] Cycloadditionsreaktion mit $TMSN_3$ eingeht und zur Bildung des Heterozyklus **29** führt, unumgänglich.

Die Behandlung von Silylen **20** mit einer äquimolaren Menge des sterisch anspruchsvolleren Azids $^tBu_2MeSiN_3$ hingegen ermöglichte den Zugang zu dem acyclischen, dreifachkoordinierten Silaimin **30**. Demzufolge hemmte die erhöhte sterische Hinderung der anliegenden Silylgruppe eine anschließende Cyclisierung. Dennoch war eine [2+2]-Cycloaddition von **30** mit CO_2 möglich und die Isolierung von Azaoxasiletan **31** wurde erreicht.



Schema 29. Reaktivität von Silylen **20** gegenüber Organosilylaziden: Bildung von Iminosiloxysilaiminen und nachfolgende Cycloadditionsreaktionen.

Zu guter Letzt wurde eine selten beobachtete 1,3-dipolare Cycloaddition mit N_2O unter milden Bedingungen entdeckt. Die erstaunliche Bildung des einzigartigen Oxatriazasilols **32**, das das Startprodukt derartiger [4+2]-Cycloadditionsreaktionen darstellt, ist selbst in der umfassend erforschten organischen Chemie ohnegleichen. Abgesehen von der Vermeidung der allgemein notwendigen relativ harschen Bedingungen gibt es nahezu keine Berichte über den Einbau aller drei N_2O-Atome in das Produkt.[284-288]

11.2 Acyclische dreifachkoordinierte Silanone

Silanone, die schwereren Analoga der ubiquitären Ketone, sind weitere sehr begehrte Spezies innerhalb der Klasse der niedrigkoordinierten Organosiliciumverbindungen. In den letzten Jahrzehnten wurden beeindruckende Fortschritte hinsichtlich der Isolierung dieser extrem reaktiven Phantomspezies erzielt.[27,252-253,257-258,263] Vor dieser Arbeit war jedoch kein isolierbares neutrales, acyclisches, dreifachkoordiniertes Silanon bekannt und die Reaktivität dieser schwer zugänglichen Verbindungen war nur unzureichend erfasst. Daher lag ein weiterer Fokus dieser Arbeit auf der Erschließung eines beispiellosen Silanons und der Erforschung dessen Reaktivität, insbesondere im Hinblick auf die ausgeprägte Chemie der Carbonylverbindungen.

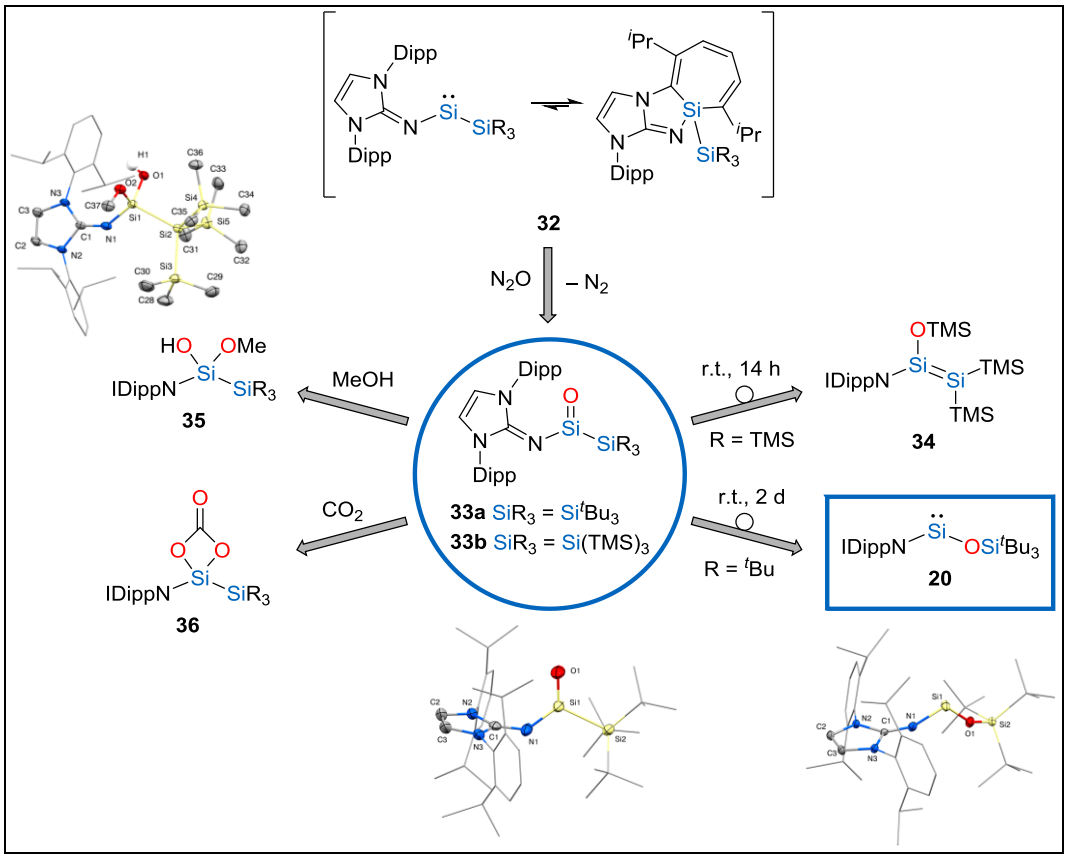
11.2.1 Studien zu Iminosilylsilanonen

Als prädestinierte Strategie zur Isolierung einer solch schwer erreichbaren Verbindung wurde die Oxygenierung der erhaltenen neuartigen acyclischen Silylene verfolgt. Fast alle Versuche, über die Exposition der (donorstabilisierten) Silylene gegenüber verschiedenen Oxidationsmitteln Zugang zum ersten acyclischen, donorfreien, neutralen Silanon zu erhalten, führten jedoch nur zur Bildung komplizierter Produktgemische oder neuartiger Cyclodisiloxane (*vide supra*). Erfreulicherweise wurden die oben aufgeführten einzigartigen Exemplare von Lewis-Basen-stabilisierten Silanonsäureester-Derivaten **9** und **29** gewonnen. Um dennoch die Isolierung neuer Silanone zu erreichen, war es notwendig, alternative Vorläuferverbindungen zu verwenden.

Interessanterweise wurde im Laufe dieser Arbeit die Synthese bemerkenswerter Iminosilylsilepine in unseren Laboren erreicht, die als »maskierte« acyclische Silylene fungieren.[183] Die hervorragende Eignung von Silylenen für die Generierung von Silanonen wurde *via* Oxidation der Silepine **32** mit N_2O aufgezeigt, wodurch die Iminosilylsilanone **33** gebildet wurden (Schema 30).[282] Diese wegweisenden Vertreter acyclischer, donorfreier, neutraler Silanone wurden vollständig charakterisiert und tiefere Einblicke in die Natur der Si=O Doppelbindung wurden durch Röntgenstrukturanalyse und detaillierte theoretische Berechnungen enthüllt. Die Kombination aus den σ-donierenden elektropositiven Silylgruppen und dem π-donierenden NHI-Liganden erwies sich als entscheidend, um eine adäquate Stabilisierung zu gewährleisten und Folgereaktionen zu verhindern.

Die synthetisierten Iminosilylsilanone **32** weisen eine unbegrenzte Stabilität im Festkörper auf, isomerisieren aber abhängig von der Art des Silylsubstituenten zu verschiedenen Produkten in Lösung. So ist das oben erwähnte einzigartige Iminosiloxysilylen **20** durch Umlagerung des

supersilylsubstituierten Silanons **33a** zugänglich. Im Gegensatz dazu führt die ausgeprägte Tendenz der Hypersilylgruppe zu Silylmigrationen zu einer schnelleren Isomerisierung von Derivat **33b** zu dem transienten Siloxydisilen **34**, das sich zwar in Lösung zersetzt, aber in Form eines NHC-Disilen Addukts isoliert werden kann.



Schema 30. Synthese und initiale Reaktivitätsstudien der ersten acyclischen, neutralen, dreifachkoordinierten Silanone **33**.

Darüber hinaus wurden vorläufige Reaktivitätsuntersuchungen mit den neuartigen Silanonen **33** durchgeführt. Wie erwartet führte die Alkoholyse von **33** mit Methanol zur Oxidation und Bildung von Methoxysilanolen **35**. Die intrinsische Si=O Doppelbindung wurde ferner experimentell über [2+2]-Cycloadditionsreaktionen mit CO_2 unter Darstellung der neuartigen monomeren Siliciumcarbonat-komplexe **36** verifiziert. Die erzielten Ergebnisse bringen die siliciumorganische Chemie einen weiteren Schritt nach vorne und sollten zu tiefergehenden Untersuchungen anregen.

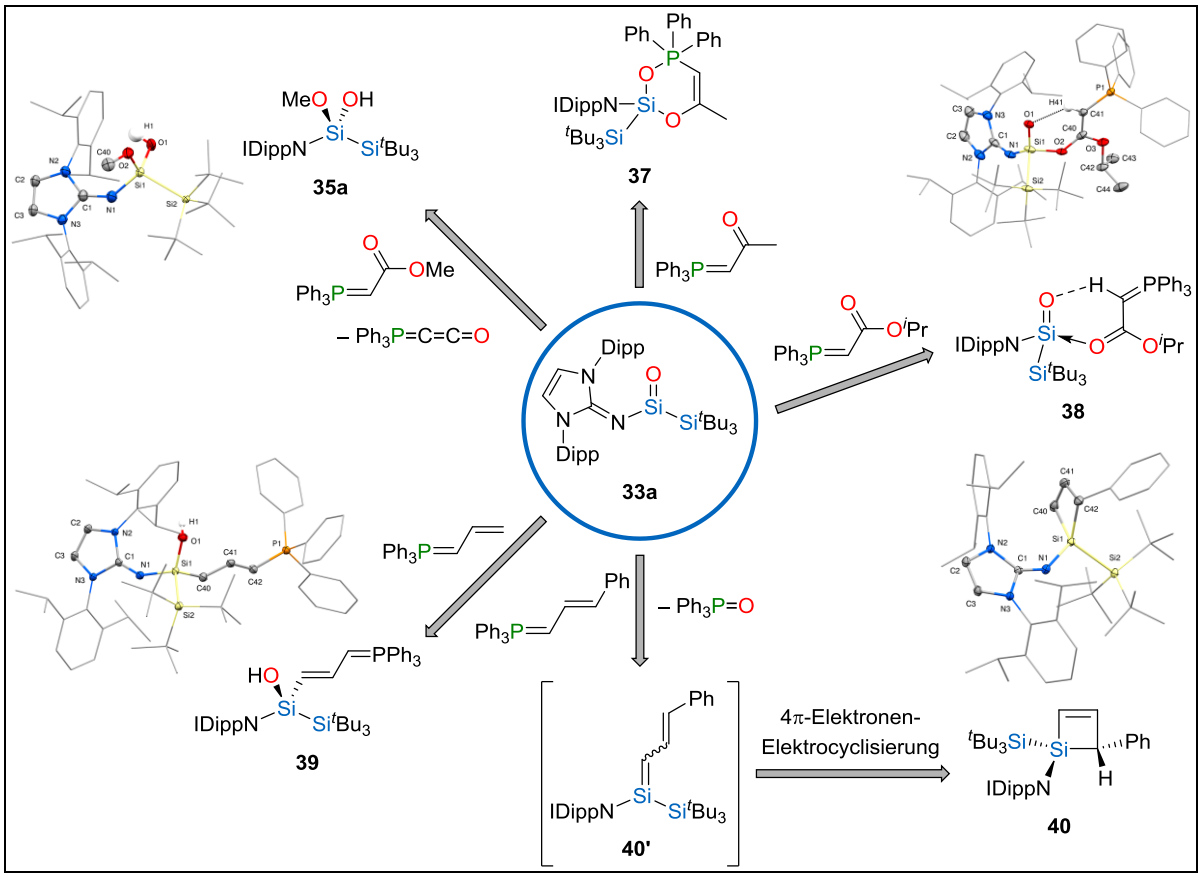
11.2.2 Studien zur Sila-Wittig Reaktion

Mit den Iminosilylsilanonen **33** in der Hand wurden Reaktivitätsstudien in Bezug auf klassische Carbonylverbindungen durchgeführt. Eine der wichtigsten und vielseitigsten Reaktionen von Carbonylverbindungen ist die Umwandlung in ein breites Spektrum von Alkenen über die *Wittig*-Olefinierung. In starkem Kontrast dazu war im Vorfeld dieser Arbeit keine Olefinierungsmethode für

schwerere Carbonylkongenere bekannt. Folglich wurde die mögliche Anwendung der *Wittig*-Reaktion auf die Silanone **33** untersucht. Aufgrund der höheren Stabilität und der geringeren Neigung zu Silylmigrationen wurde ausschließlich das $^{t}Bu_3Si$-substituierte Derivat **33a** eingesetzt. Um potentielle Nebenreaktionen mit dem wesentlich reaktiveren Silanon zu verhindern, wurden nur isolierbare Phosphorylide genutzt.

Zunächst wurden Reaktionen gegenüber stabilisierten *Wittig*-Reagenzien erforscht, da diese leicht zugänglich und teilweise sogar kommerziell erhältlich sind. Da sich Carbonylverbindungen und Silanone hinsichtlich Stabilität und Reaktivität deutlich unterscheiden (Silanone weisen eine stark polarisierte, zwitterionische und damit wesentlich reaktivere Si=O Doppelbindung auf), wurde überhaupt keine *Wittig*-Olefinierung registriert. Interessanterweise führte die Reaktion von Silanon **33a** mit einem ketonsubstituierten Ylid über eine formale Hetero-*Diels-Alder*-Reaktion zur Bildung von Dioxaphosphasilin **37** (Schema 31).[283] Das Resultat der Exposition mit estersubstituierten *Wittig*-Reagenzien war stark von der sterischen Hinderung abhängig, so dass die Umsetzung von **33a** mit $Ph_3P{=}CH(COOMe)$ simultan Methoxysilanol **35a** und das Bestmann Ylid $Ph_3P{=}C{=}C{=}O$ *via* einen formalen Methanoltransfer lieferte. Im Gegensatz dazu wurde bei der Reaktion mit dem sterisch anspruchsvolleren Derivat $Ph_3P{=}CH(COO^{i}Pr)$ selektiv das ylidstabilisierte Silanon **38** erhalten. Interessanterweise isomerisiert Addukt **38** quantitativ zu dem silylsubstituierten Phosphorylid $(IDippN)(^{t}Bu_3SiO)Si(H)(C{=}PPh_3(COO^{i}Pr))$ bei erhöhten Temperaturen. Das gleiche Produkt ist auch über die Reaktion von Iminosiloxysilylen **20** mit $Ph_3P{=}CH(COO^{i}Pr)$ erhältlich (*vide supra*).

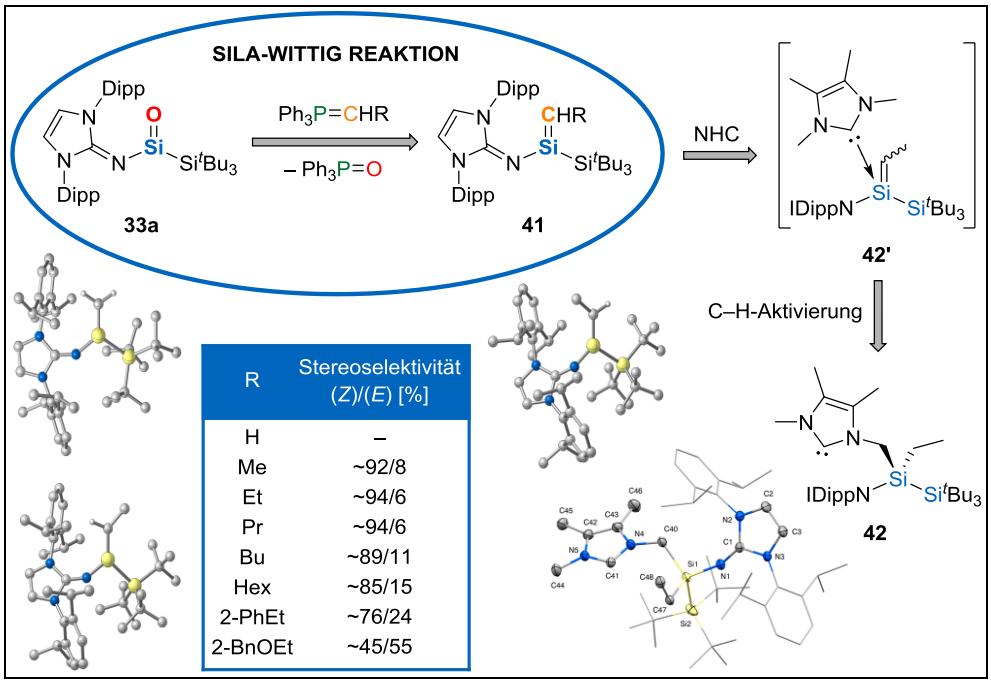
Die Fortsetzung der Reaktivitätsstudien von Silanon **33a** mit semi-stabilisierten Yliden resultierte zunächst in der Bildung des neuartigen silanoylsubstituierten Phosphorylids **39**, die vermutlich durch einen nukleophilen Angriff des vinylogischen Ylids auf die Silanonkomponente induziert wurde. Im Gegensatz dazu lieferte die Umsetzung von **33a** mit dem sterisch überfrachteten phenylsubstituierten Derivat $Ph_3P{=}CHCHCHPh$ das transiente Silene **40'**, das schnell und selektiv zu Silacyclobuten **40** isomerisierte (über eine 4π-Elektronen-Elektrocyclisierung) und damit auf eine erfolgreiche sila-*Wittig*-Reaktion hinweist.



Schema 31. Reaktivität von Iminosilylsilanone **33a** gegenüber stabilisierten und semi-stabilisierten *Wittig*-Reagenzien.

Inspiriert von diesen Ergebnissen wurden schließlich nicht-stabilisierte Ylide getestet, da diese aufgrund des Nichtvorhandenseins zusätzlicher funktioneller Gruppen weniger Nebenreaktionen zulassen sollten. Erstaunlicherweise führte die Umsetzung von Iminosilylsilanone **33a** mit einer Vielzahl von nicht-stabilisierten *Wittig*-Reagenzien zur selektiven Bildung der neuartigen Silene **41** (Schema 32). Dementsprechend wandelt die beispiellose sila-*Wittig*-Reaktion Silanone unter milden Bedingungen in Silene um, ähnlich der klassischen *Wittig*-Olefinierung. Darüber hinaus wurde allgemein eine analog hohe Präferenz für die entsprechenden (*Z*)-Isomere beobachtet. Als Konsequenz der deutlich höheren Reaktivität der Silene im Vergleich zu ihren leichteren Alken-Homologen zersetzten sich die synthetisierten dreifachkoordinierten Silene **41** während Isolierungsversuchen. Auch eine Lewis-Basen-Stabilisierung verhindert keine Folgereaktionen, da das silylsubstituierte NHC **42** nach intramolekularer C–H-Aktivierung des transienten NHC-stabilisierten Silens **42'** isoliert wurde.

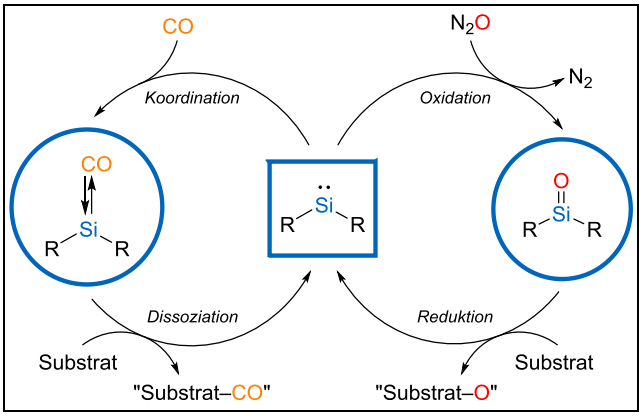
Nichtsdestotrotz stellt die sila-*Wittig*-Reaktion die erste erfolgreiche Anwendung der vielseitigen Carbonylolefinierung auf schwerere Kongenere dar und bietet eine neuartige Plattform, um Zugang zu sonst schwer erreichbaren Verbindungen zu erhalten.



Schema 32. Synthese von Iminosilylsilenen **41** über die sila-*Wittig*-Reaktion von Silanon **33a** mit nicht-stabilisierten Phosphoryliden.

11.3 Fazit und Prognose

Das Gesamtziel dieser Doktorarbeit war die tiefergehende Untersuchung der sich entfaltenden Klasse von niedrigkoordinierten Organosiliciumverbindungen im Hinblick auf der weiteren Erschließung ihres Potentials für Anwendungen in der metallfreien Katalyse. So wurden erfolgreich neue acyclische, zweifachkoordinierte Silylene isoliert, darunter das erste synthetisch zugängliche, extrem reaktive Bis(silyl)silylen. Erstaunlicherweise konnten beispiellose Siliciumcarbonylkomplexe durch selektive Carbonylierung von Bis(silyl)silylenderivaten synthetisiert werden. All diese einzigartigen Verbindungen weise eine Reaktivität auf, die an Übergangsmetallkomplexe erinnert, wie z.B. die Aktivierung von industriell relevanten kleinen Molekülen unter milden Bedingungen. Daher können diese Resultate als weiterer Beweis für das ungenutzte Potential niedrigkoordinierter Organosiliciumverbindungen angesehen werden und bringen die auf diesem Gebiet tätigen Wissenschaftler einer vielseitigen Katalyse auf Siliciumbasis einen Schritt näher. Darüber hinaus wurden neue Erkenntnisse über die Verwandtschaft zwischen Silicium und seinem leichteren Homologen Kohlenstoff gewonnen. Am eindrucksvollsten war dabei die Isolierung des ersten acyclischen, neutralen, dreifachkoordinierten Silanons, dessen Anwendung in der vielfältigen *Wittig*-Reaktion erfolgreich demonstriert wurde und damit neue Wege für die zukünftige Forschung eröffnet.



Schema 33. Postulierte katalytische Zyklen mit acyclischen Silylenen, Silanonen und Siliciumcarbonylkomplexen.

In jüngster Zeit wurde die begrenzte Anzahl von katalytischen Umsetzungen, bei denen niedervalente Organosiliciumverbindungen eingesetzt werden, erweitert. Faszinierende Ergebnisse wurden dabei von der *WACKER Chemie AG* mit der Entwicklung einer hocheffizienten Si(II)-Katalyse erzielt.[276] Insbesondere die beschriebene Hydrosilylierung von Alkenen mit Silyliumyliden-Ionen $[Cp^*Si:^+][BR_4^-]$ ist in ihrer Aktivität vergleichbar mit der derzeit angewandten Platin-Katalyse und könnte somit den Weg für die Entwicklung nachhaltigerer Prozesse ebnen. Dementsprechend könnten die in dieser Arbeit isolierten einzigartigen Verbindungen auch zu Schlüsselreagenzien für zukünftige katalytische Reaktionen werden. Denkbar wäre z.B. ein Sauerstofftransfer von Silanonen auf geeignete Substrate unter Bildung von Silylenen, da ein erfolgreicher Sauerstofftransfer bereits mit Hilfe der sila-*Wittig*-Reaktion verifiziert wurde (Schema 33). Außerdem könnten Carbonylierungsreaktionen unter Verwendung von Siliciumcarbonylkomplexen ein vielversprechendes Ziel sein, da die Reversibilität der CO-Koordination experimentell nachgewiesen wurde.

12. Bibliography

[1] B. Lindström, L. J. Petterson, A Brief History of Catalysis. *CATTECH* **2003,** *7,* 130-138.

[2] I. Chorkendorff, J. W. Niemantsverdriet, *Concepts of Modern Catalysis and Kinetics*. Wiley-VCH Verlag GmbH & Co. KGaA, Weinheim, **2017**.

[3] B. Cornils, W. A. Herrmann, J. Xu, H.-W. Zanthoff, *Catalysis from A to Z: A Concise Encyclopedia*. Wiley-VCH Verlag GmbH & Co. KGaA, Weinheim, **2019**.

[4] J. J. Berzelius, *Årsberättelsen om framsteg i fysik och kemi [Annual report on progress in physics and chemistry]*. Royal Swedish Academy of Sciences, **1835**.

[5] M. W. Roberts, Birth of the catalytic concept (1800-1900). *Catal. Lett.* **2000,** *67,* 1-4.

[6] W. Ostwald, *Z. Phys. Chem.* **1894,** *15*, 705-706.

[7] G. Ertl, T. Gloyna, Katalyse: Vom Stein der Weisen zu Wilhelm Ostwald. *Z. Phys. Chem.* **2003,** *217*, 1207-1220.

[8] J. M. Thomas, The societal significance of catalysis and the growing practical importance of single-site heterogeneous catalysts. *Proc. R. Soc. A* **2012,** *468*, 1884-1903.

[9] R. A. van Santen, *Modern Heterogeneous Catalysis: An Introduction*. Wiley-VCH Verlag GmbH & Co. KGaA, Weinheim, **2017**.

[10] B. Cornils, W. A. Herrmann, M. Beller, R. Paciello, *Applied Homogeneous Catalysis with Organometallic Compounds: A Comprehensive Handbook in Four Volumes*. Wiley-VCH Verlag GmbH & Co. KGaA, Weinheim, **2017**.

[11] P. P. Power, Main-group elements as transition metals. *Nature* **2010,** *463,* 171-177.

[12] L. C. Wilkins, R. L. Melen, Enantioselective Main Group Catalysis: Modern Catalysts for Organic Transformations. *Coord. Chem. Rev.* **2016,** *324*, 123-139.

[13] C. Weetman, S. Inoue, The Road Travelled: After Main-Group Elements as Transition Metals. *ChemCatChem* **2018,** *10,* 4213-4228.

[14] R. L. Melen, Frontiers in molecular p-block chemistry: From structure to reactivity. *Science* **2019,** *363*, 479-484.

[15] D. Martin, M. Soleilhavoup, G. Bertrand, Stable singlet carbenes as mimics for transition metal centers. *Chem. Sci.* **2011,** *2*, 389-399.

[16] V. Y. Lee, *Organosilicon Compounds: Theory and Experiment (Synthesis)*. Academic Press, New York, **2017**.

[17] T. Chu, G. I. Nikonov, Oxidative Addition and Reductive Elimination at Main-Group Element Centers. *Chem. Rev.* **2018,** *118*, 3608-3680.

[18] T. J. Hadlington, M. Driess, C. Jones, Low-valent group 14 element hydride chemistry: towards catalysis. *Chem. Soc. Rev.* **2018,** *47*, 4176-4197.

[19] M.-A. Légaré, C. Pranckevicius, H. Braunschweig, Metallomimetic Chemistry of Boron. *Chem. Rev.* **2019,** *119*, 8231-8261.

[20] A. F. Holleman, E. Wiberg, N. Wiberg, *Lehrbuch der Anorganischen Chemie*. de Gruyter, Berlin, **2007**.

[21] H. W. Roesky, *Efficient Methods for Preparing Silicon Compounds*. Elsevier, Amsterdam, **2016**.

[22] C. Friedel, J. M. Crafts, Ueber einige neue organische Verbindungen des Siliciums und das Atomgewicht dieses Elementes. *Justus Liebigs Ann. Chem.* **1863,** *127*, 28-32.

[23] N. R. Thomas, Frederic Stanley Kipping—Pioneer in Silicon Chemistry: His Life & Legacy. *Silicon* **2010,** *2*, 187-193.

[24] G. Martin, F. S. Kipping, XXXVIII.—Benzyl and ethyl derivatives of silicon tetrachloride. *J. Chem. Soc., Trans* **1909,** *95*, 302-314.

[25] R. Robison, F. S. Kipping, XLIII.—Organic derivatives of silicon. Part V. Benzylethylsilicone, dibenzylsilicone, and other benzyl and benzylethyl derivatives of silicane. *J. Chem. Soc., Trans.* **1908,** *93*, 439-456.

[26] F. S. Kipping, L. L. Lloyd, XLVII.—Organic derivatives of silicon. Triphenylsilicol and alkyloxysilicon chlorides. *J. Chem. Soc., Trans.* **1901,** *79*, 449-459.

[27] Y. Xiong, S. Yao, M. Driess, Chemical Tricks To Stabilize Silanones and Their Heavier Homologues with E=O Bonds (E=Si–Pb): From Elusive Species to Isolable Building Blocks. *Angew. Chem. Int. Ed.* **2013,** *52*, 4302-4311.

[28] E. G. Rochow, The Direct Synthesis of Organosilicon Compounds. *J. Am. Chem. Soc.* **1945,** *67*, 963-965.

[29] R. Müller, One hundred years of organosilicon chemistry. *J. Chem. Educ.* **1965,** *42*, 41-47.

[30] V. Nesterov, D. Reiter, P. Bag, P. Frisch, R. Holzner, A. Porzelt, S. Inoue, NHCs in Main Group Chemistry. *Chem. Rev.* **2018,** *118*, 9678-9842.

[31] D. E. Goldberg, D. H. Harris, M. F. Lappert, K. M. Thomas, A New Synthesis of Divalent Group 4B Alkyls $M[CH(SiMe_3)_2]_2$ (M = Ge or Sn), and the Crystal and Molecular Strcuture of the Tin Compound. *J. Chem. Soc., Chem. Commun.* **1976**, 261-262.

[32] A. G. Brook, F. Abdesaken, B. Gutekunst, G. Gutekunst, R. K. Kallury, A solid silaethene: isolation and characterization. *Chem. Commun.* **1981**, 191-192.

[33] R. West, M. J. Fink, J. Michl, Tetramesityldisilene, a Stable Compound Containing a Silicon-Silicon Double Bond. *Science* **1981,** *214*, 1343-1344.

[34] M. Yoshifuji, I. Shima, N. Inamoto, K. Hirotsu, T. Higuchi, Synthesis and structure of bis(2,4,6-tri-*tert*-butylphenyl)diphosphene: isolation of a true phosphobenzene. *J. Am. Chem. Soc.* **1981,** *103*, 4587-4589.

[35] P. P. Power, π-Bonding and the Lone Pair Effect in Multiple Bonds between Heavier Main Group Elements. *Chem. Rev.* **1999,** *99*, 3463-3504.

[36] R. C. Fischer, P. P. Power, π-Bonding and the Lone Pair Effect in Multiple Bonds Involving Heavier Main Group Elements: Developments in the New Millennium. *Chem. Rev.* **2010,** *110*, 3877-3923.

[37] H. Ottosson, Silenes: Connectors between classical alkenes and nonclassical heavy alkenes. *Coord. Chem. Rev.* **2008,** *252*, 1287-1314.

[38] A. Igau, H. Grützmacher, A. Baceiredo, G. Bertrand, Analogous *α,α'*-Bis-Carbenoid, Triply Bonded Species: Synthesis of a Stable λ³-Phosphino Carbene-λ⁵-Phosphaacetylene. *J. Am. Chem. Soc.* **1988,** *110,* 6463-6466.

[39] A. J. Arduengo, III, R. L. Harlow, M. Kline, A stable crystalline carbene. *J. Am. Chem. Soc.* **1991,** *113,* 361-363.

[40] M. N. Hopkinson, C. Richter, M. Schedler, F. Glorius, An overview of N-heterocyclic carbenes. *Nature* **2014,** *510,* 485-496.

[41] S. P. Nolan, *N-Heterocyclic Carbenes: Effective Tools for Organometallic Synthesis*. Wiley-VCH Verlag GmbH & Co. KGaA, Weinheim, **2014**.

[42] S. Díez-González, *N-Heterocyclic Carbenes : From Laboratory Curiosities to Efficient Synthetic Tools: Edition 2*. Royal Society of Chemistry, Cambridge, **2016**.

[43] H. V. Huynh, Electronic Properties of N-Heterocyclic Carbenes and Their Experimental Determination. *Chem. Rev.* **2018,** *118,* 9457-9492.

[44] D. Munz, Pushing Electrons—Which Carbene Ligand for Which Application? *Organometallics* **2018,** *37,* 275-289.

[45] D. M. Flanigan, F. Romanov-Michailidis, N. A. White, T. Rovis, Organocatalytic Reactions Enabled by N-Heterocyclic Carbenes. *Chem. Rev.* **2015,** *115,* 9307-9387.

[46] P. L. Arnold, I. J. Casely, F-Block N-Heterocyclic Carbene Complexes. *Chem. Rev.* **2009,** *109,* 3599-3611.

[47] S. Díez-González, N. Marion, S. P. Nolan, N-Heterocyclic Carbenes in Late Transition Metal Catalysis. *Chem. Rev.* **2009,** *109,* 3612-3676.

[48] M. G. Gardiner, C. C. Ho, Recent advances in bidentate bis(N-heterocyclic carbene) transition metal complexes and their applications in metal-mediated reactions. *Coord. Chem. Rev.* **2018,** *375,* 373-388.

[49] E. Peris, Smart N-Heterocyclic Carbene Ligands in Catalysis. *Chem. Rev.* **2018,** *118,* 9988-10031.

[50] A. Doddi, M. Peters, M. Tamm, N-Heterocyclic Carbene Adducts of Main Group Elements and Their Use as Ligands in Transition Metal Chemistry. *Chem. Rev.* **2019,** *119*, 6994-7112.

[51] M. Weidenbruch, Silylenes and disilenes: examples of low coordinated silicon compounds. *Coord. Chem. Rev.* **1994,** *130*, 275-300.

[52] R. West, M. Denk, Stable silylenes: synthesis, structure, reactions. *Pure Appl. Chem.* **1996,** *68*, 785-788.

[53] Z. Rappoport, Y. Apeloig, *The Chemistry of Organic Silicon Compounds. Volume 2*. John Wiley & Sons, Ltd., Chichester, **1998**.

[54] M. Haaf, T. A. Schmedake, R. West, Stable Silylenes. *Acc. Chem. Res.* **2000,** *33*, 704-714.

[55] N. Tokitoh, R. Okazaki, Recent topics in the chemistry of heavier congeners of carbenes. *Coord. Chem. Rev.* **2000,** *210*, 251-277.

[56] B. Gehrhus, M. F. Lappert, Chemistry of thermally stable bis(amino)silylenes. *J. Organomet. Chem.* **2001,** *617-618*, 209-223.

[57] N. J. Hill, R. West, Recent developments in the chemistry of stable silylenes. *J. Organomet. Chem.* **2004,** *689*, 4165-4183.

[58] N. Takeda, N. Tokitoh, A Bulky Silylene Generated under Mild Conditions: Its Application to the Synthesis of Organosilicon Compounds. *Synlett* **2007,** *16*, 2483-2491.

[59] S. Nagendran, H. W. Roesky, The Chemistry of Aluminum(I), Silicon(II), and Germanium(II). *Organometallics* **2008,** *27*, 457-492.

[60] Y. Mizuhata, T. Sasamori, N. Tokitoh, Stable Heavier Carbene Analogues. *Chem. Rev.* **2009,** *109*, 3479-3511.

[61] M. Kira, An isolable dialkylsilylene and its derivatives. A step toward comprehension of heavy unsaturated bonds. *Chem. Commun.* **2010,** *46*, 2893-2903.

[62] M. Asay, C. Jones, M. Driess, N-Heterocyclic Carbene Analogues with Low-Valent Group 13 and Group 14 Elements: Syntheses, Structures, and Reactivities of a New Generation of Multitalented Ligands. *Chem. Rev.* **2011,** *111*, 354-396.

[63] S. Yao, Y. Xiong, M. Driess, Zwitterionic and Donor-Stabilized N-Heterocyclic Silylenes (NHSis) for Metal-Free Activation of Small Molecules. *Organometallics* **2011,** *30*, 1748-1767.

[64] S. S. Sen, S. Khan, P. P. Samuel, H. W. Roesky, Chemistry of functionalized silylenes. *Chem. Sci.* **2012,** *3*, 659-682.

[65] S. S. Sen, S. Khan, S. Nagendran, H. W. Roesky, Interconnected Bis-Silylenes: A New Dimension in Organosilicon Chemistry. *Acc. Chem. Res.* **2012,** *45*, 578-587.

[66] H. W. Roesky, Chemistry of low valent silicon *J. Organomet. Chem.* **2013,** *730*, 57-62.

[67] D. Scheschkewitz, *Functional Molecular Silicon Compounds II: Low Oxidation States*. Springer International Publishing AG, Basel, **2014**.

[68] Y. Apeloig, R. Pauncz, M. Karni, R. West, W. Steiner, D. Chapman, Why Is Methylene a Ground State Triplet while Silylene Is a Ground State Singlet? *Organometallics* **2003,** *22*, 3250-3256.

[69] W. Kutzelnigg, Orthogonal and non-orthogonal hybrids. *J. Mol. Struct.: THEOCHEM* **1988,** *169*, 403-419.

[70] W. Ando, M. Fujita, H. Yoshida, A. Sekiguchi, Stereochemistry of the addition of diarylsilylenes to *cis*- and *trans*-2-butenes. *J. Am. Chem. Soc.* **1988,** *110*, 3310-3311.

[71] D. H. Pae, M. Xiao, M. Y. Chiang, P. P. Gaspar, Diadamantylsilylene and its stereochemistry of addition. *J. Am. Chem. Soc.* **1991,** *113*, 1281-1288.

[72] S. Zhang, P. E. Wagenseller, R. T. Conlin, Addition of dimesitylsilylene to olefins. A reinvestigation. *J. Am. Chem. Soc.* **1991,** *113*, 4278-4281.

[73] R. S. Grev, H. F. Schaefer, III, P. P. Gaspar, In search of triplet silylenes. *J. Am. Chem. Soc.* **1991,** *113*, 5638-5643.

[74] M. C. Holthausen, W. Koch, Y. Apeloig, Theory Predicts Triplet Ground-State Organic Silylenes. *J. Am. Chem. Soc.* **1999,** *121*, 2623-2624.

[75] P. P. Gaspar, A. M. Beatty, T. Chen, T. Haile, D. Lei, W. R. Winchester, J. Braddock-Wilking, N. P. Rath, W. T. Klooster, T. F. Koetzle, S. A. Mason, A. Albinati, Tris(triisopropylsilyl)silane and the Generation of Bis(triisopropylsilyl)silylene. *Organometallics* **1999,** *18*, 3921-3932.

[76] P. Jiang, P. P. Gaspar, Tri-*tert*-butylsilyl(triisopropylsilyl)silylene (tBu)$_3$Si–Si–Si(iPr)$_3$ and Chemical Evidence for Its Reactions from a Triplet Electronic State. *J. Am. Chem. Soc.* **2001,** *123*, 8622-8623.

[77] M. Kira, T. Iwamoto, T. Maruyama, T. Kuzuguchi, D. Yin, C. Kabuto, H. Sakurai, Hexakis(trialkylsilyl)cyclotrisilanes and photochemical generation of bis(trialkylsilyl)silylenes. *J. Chem. Soc., Dalton Trans.* **2002**, 1539-1544.

[78] P. P. Gaspar, M. Xiao, D. H. Pae, D. J. Berger, T. Haile, T. Chen, D. Lei, W. R. Winchester, P. Jiang, The quest for triplet ground state silylenes. *J. Organomet. Chem.* **2002,** *646*, 68-79.

[79] M. Yoshida, N. Tamaoki, DFT Study on Triplet Ground State Silylenes Revisited: The Quest for the Triplet Silylene Must Go On. *Organometallics* **2002,** *21*, 2587-2589.

[80] M. Kosa, M. Karni, Y. Apeloig, Were Reactions of Triplet Silylenes Observed? *J. Am. Chem. Soc.* **2013,** *135*, 9032-9040.

[81] M. S. Gordon, Potential-energy surfaces in singlet and triplet silylene. *Chem. Phys. Lett.* **1985,** *114*, 348-352.

[82] A. Sekiguchi, T. Tanaka, M. Ichinohe, K. Akiyama, S. Tero-Kubota, Bis(tri-*tert*-butylsilyl)silylene: Triplet Ground State Silylene. *J. Am. Chem. Soc.* **2003,** *125*, 4962-4963.

[83] A. Sekiguchi, T. Tanaka, M. Ichinohe, K. Akiyama, P. P. Gaspar, Tri-*tert*-butylsilylsilylenes with Alkali Metal Substituents (^{t}Bu$_3$Si)SiM (M = Li, K): Electronically and Sterically Accessible Triplet Ground States. *J. Am. Chem. Soc.* **2008,** *130*, 426-427.

[84] L. Zhu, J. Zhang, C. Cui, Intramolecular Cyclopropanation of Alkali-Metal-Substituted Silylene with the Aryl Substituent of an N-Heterocyclic Framework. *Inorg. Chem.* **2019,** *58*, 12007-12010.

[85] C. Marschner, Silylated Group 14 Ylenes: An Emerging Class of Reactive Compounds. *Eur. J. Inorg. Chem.* **2015**, 3805-3820.

[86] F. S. Kipping, J. E. Sands, XCIII.—Organic derivatives of silicon. Part XXV. Saturated and unsaturated silicohydrocarbons, Si_4Ph_8. *J. Chem. Soc., Trans* **1921,** *119*, 830-847.

[87] R. Schwarz, G. Pietsoh, Versuche zur Darstellung des Siliciumdichlorides. *Z. Anorg. Allg. Chem.* **1937,** *232*, 249-256.

[88] R. K. Asundi, M. Karim, R. Samuel, Emission bands of $SiCl_2$ and $SnCl_2$. *Proc. Phys. Soc.* **1938,** *50*, 581-598.

[89] P. S. Skell, E. J. Goldstein, Dimethylsilene: CH_3SiCH_3. *J. Am. Chem. Soc.* **1964,** *86*, 1442-1443.

[90] T. J. Drahnak, J. Michl, R. West, Dimethylsilylene, $(CH_3)_2Si$. *J. Am. Chem. Soc.* **1979,** *101*, 5427-5428.

[91] P. Jutzi, D. Kanne, C. Krüger, Decamethylsilicocene—Synthesis and Structure. *Angew. Chem. Int. Ed. Engl.* **1986,** *25*, 164.

[92] P. Jutzi, U. Holtmann, D. Kanne, C. Krüger, R. Blom, R. Gleiter, I. Hyla-Kryspin, Decamethylsilicocene — The first stable silicon(II) compound: Synthesis, structure, and bonding. *Eur. J. Inorg. Chem.* **1989,** *112*, 1629-1639.

[93] T. Kühler, P. Jutzi, Decamethylsilicocene: Synthesis, Structure, Bonding and Chemistry. *Adv. Organomet. Chem.* **2003,** *49*, 1-34.

[94] H. H. Karsch, U. Keller, S. Gamper, G. Müller, $Si[(Me_2P)_2C(SiMe_3)]_2$, a Stable σ-Bonded Compound Containing Divalent Silicon. *Angew. Chem. Int. Ed. Engl.* **1990,** *29*, 295-296.

[95] M. Denk, R. Lennon, R. Hayashi, R. West, A. V. Belyakov, H. P. Verne, A. Haaland, M. Wagner, N. Metzler, Synthesis and Structure of a Stable Silylene. *J. Am. Chem. Soc.* **1994,** *116*, 2691-2692.

[96] B. Gehrhus, M. F. Lappert, J. Heinicke, R. Boese, D. Bläser, Synthesis, structures and reactions of new thermally stable silylenes. *J. Chem. Soc., Chem. Commun.* **1995**, 1931-1932.

[97] W. M. Boesveld, B. Gehrhus, P. B. Hitchcock, M. F. Lappert, P. v. R. Schleyer, A crystalline carbene–silylene adduct $1,2\text{-}C_6H_4[N(R)]_2C\text{-}Si[N(R)]_2C_6H_4\text{-}1,2$ ($R = CH_2Bu^t$); synthesis, structure and bonding in model compounds. *Chem. Commun.* **1999**, 755-756.

[98] B. Gehrhus, P. B. Hitchcock, M. F. Lappert, Synthesis of a Stable Biphenyl-Bis(carbene) and -Bis(silylene) [M{(NCH$_2$Bu^t)$_2$C$_6$H$_3$-3,4}]$_2$ (M = C or Si). *Z. Anorg. Allg. Chem.* **2005,** *631*, 1383-1386.

[99] N. Takeda, H. Suzuki, N. Tokitoh, R. Okazaki, S. Nagase, Reaction of a Sterically Hindered Silylene with Isocyanides: The First Stable Silylene–Lewis Base Complexes. *J. Am. Chem. Soc.* **1997,** *119*, 1456-1457.

[100] M. Kira, S. Ishida, T. Iwamoto, C. Kabuto, The First Isolable Dialkylsilylene. *J. Am. Chem. Soc.* **1999,** *121*, 9722-9723.

[101] T. Abe, R. Tanaka, S. Ishida, M. Kira, T. Iwamoto, New Isolable Dialkylsilylene and Its Isolable Dimer That Equilibrate in Solution. *J. Am. Chem. Soc.* **2012,** *134*, 20029-20032.

[102] C.-W. So, H. W. Roesky, J. Magull, R. B. Oswald, Synthesis and Characterization of [PhC(N*t*Bu)$_2$]SiCl: A Stable Monomeric Chlorosilylene. *Angew. Chem. Int. Ed.* **2006,** *45*, 3948-3950.

[103] S. S. Sen, H. W. Roesky, D. Stern, J. Henn, D. Stalke, High Yield Access to Silylene RSiCl (R = PhC(N*t*Bu)$_2$) and Its Reactivity toward Alkyne: Synthesis of Stable Disilacyclobutene. *J. Am. Chem. Soc.* **2010,** *132*, 1123-1126.

[104] S. S. Sen, A. Jana, H. W. Roesky, C. Schulzke, A Remarkable Base-Stabilized Bis(silylene) with a Silicon(I)–Silicon(I) Bond. *Angew. Chem. Int. Ed.* **2009,** *48*, 8536-8538.

[105] M. Driess, S. Yao, M. Brym, C. Van Wüllen, D. Lentz, A New Type of N-Heterocyclic Silylene with Ambivalent Reactivity. *J. Am. Chem. Soc.* **2006,** *128*, 9628-9629.

[106] Y. Wang, Y. Xie, P. Wei, R. B. King, H. F. Schaefer, III, P. v. R. Schleyer, G. H. Robinson, A Stable Silicon(0) Compound with a Si=Si Double Bond. *Science* **2008,** *321*, 1069-1071.

[107] Y. Wang, G. H. Robinson, Unique homonuclear multiple bonding in main group compounds. *Chem. Commun.* **2009**, 5201-5213.

[108] Y. Wang, G. H. Robinson, Carbene Stabilization of Highly Reactive Main-Group Molecules. *Inorg. Chem.* **2011,** *50*, 12326–12337.

[109] Y. Wang, G. H. Robinson, Carbene-stabilized main group diatomic allotropes. *Dalton Trans.* **2012,** *41*, 337-345.

[110] Y. Wang, G. H. Robinson, N-Heterocyclic Carbene—Main-Group Chemistry: A Rapidly Evolving Field. *Inorg. Chem.* **2014,** *53*, 11815–11832.

[111] Y. Wang, C. A. Tope, Y. Xie, P. Wei, J. Urbauer, H. F. Schaefer, III, G. H. Robinson, Carbene-Stabilized Disilicon as a Si-Transfer Agent: Synthesis of a Dianionic Silicon Tris(dithiolene) Complex. *Angew. Chem. Int. Ed.* **2020**, DOI: 10.1002/anie.201916395.

[112] K. C. Mondal, P. P. Samuel, H. W. Roesky, R. R. Aysin, L. A. Leites, S. Neudeck, J. Lübben, B. Dittrich, N. Holzmann, M. Hermann, G. Frenking, One-Electron-Mediated Rearrangements of 2,3-Disiladicarbene. *J. Am. Chem. Soc.* **2014,** *136*, 8919-8922.

[113] K. C. Mondal, S. Roy, B. Dittrich, B. Maity, S. Dutta, D. Koley, S. K. Vasa, R. Linser, S. Dechert, H. W. Roesky, A soluble molecular variant of the semiconducting silicondiselenide. *Chem. Sci.* **2015,** *6*, 5230-5234.

[114] K. C. Mondal, S. Roy, B. Dittrich, D. M. Andrada, G. Frenking, H. W. Roesky, A Triatomic Silicon(0) Cluster Stabilized by a Cyclic Alkyl(amino) Carbene. *Angew. Chem. Int. Ed.* **2016,** *55*, 3158-3161.

[115] R. S. Ghadwal, H. W. Roesky, S. Merkel, J. Henn, D. Stalke, Lewis Base Stabilized Dichlorosilylene. *Angew. Chem. Int. Ed.* **2009,** *48*, 5683-5686.

[116] A. C. Filippou, O. Chernov, G. Schnakenburg, $SiBr_2$(Idipp): A Stable N-Heterocyclic Carbene Adduct of Dibromosilylene. *Angew. Chem. Int. Ed.* **2009,** *48*, 5687-5690.

[117] A. C. Filippou, Y. N. Lebedev, O. Chernov, M. Straßmann, G. Schnakenburg, Silicon(II) Coordination Chemistry: N-Heterocyclic Carbene Complexes of Si^{2+} and SiI^{+}. *Angew. Chem. Int. Ed.* **2013,** *52*, 6974-6978.

[118] R. S. Ghadwal, R. Azhakar, H. W. Roesky, Dichlorosilylene: A High Temperature Transient Species to an Indispensable Building Block. *Acc. Chem. Res.* **2013,** *46*, 444-456.

[119] M. Asay, S. Inoue, M. Driess, Aromatic Ylide-Stabilized Carbocyclic Silylene. *Angew. Chem. Int. Ed.* **2011,** *50*, 9589-9592.

[120] G. Schmid, E. Welz, Base-Stabilized Silyleneiron Complexes. *Angew. Chem. Int. Ed. Engl.* **1977,** *16*, 785-786.

[121] C. Zybill, G. Müller, Synthesis and Structure of [$(OC)_4Fe{=}Si(O\mathit{t}Bu)_2{\cdot}$HMPT], a Donor-Stabilized Silanediyl ("Silylene") Complex. *Angew. Chem. Int. Ed. Engl.* **1987,** *26*, 669-670.

[122] D. A. Straus, T. D. Tilley, A. L. Rheingold, S. J. Geib, Preparation, characterization, and x-ray crystal structure of an acetonitrile-complexed ruthenium silylene. *J. Am. Chem. Soc.* **1987,** *109*, 5872-5873.

[123] P. Jutzi, A. Möhrke, Bis(pentamethylcyclopentadienyl)silylene as Ligand in Gold(I) Chloride Complexes. *Angew. Chem. Int. Ed. Engl.* **1990,** *29*, 893-894.

[124] B. Blom, D. Gallego, M. Driess, N-heterocyclic silylene complexes in catalysis: new frontiers in an emerging field. *Inorg. Chem. Front.* **2014,** *1*, 134-148.

[125] Z. Benedek, T. Szilvási, Can low-valent silicon compounds be better transition metal ligands than phosphines and NHCs? *RSC Adv.* **2015,** *5*, 5077-5086.

[126] M. Scheer, G. Balázs, A. Seitz, P_4 Activation by Main Group Elements and Compounds. *Chem. Rev.* **2010,** *110*, 4236-4256.

[127] S. Khan, S. S. Sen, H. W. Roesky, Activation of phosphorus by group 14 elements in low oxidation states. *Chem. Commun.* **2012,** *48*, 2169-2179.

[128] Y. Xiong, S. Yao, M. Brym, M. Driess, Consecutive Insertion of a Silylene into the P_4 Tetrahedron: Facile Access to Strained SiP_4 and Si_2P_4 Cage Compounds. *Angew. Chem. Int. Ed.* **2007,** *46*, 4511-4513.

[129] S. S. Sen, S. Khan, H. W. Roesky, D. Kratzert, K. Meindl, J. Henn, D. Stalke, J.-P. Demers, A. Lange, Zwitterionic Si-C-Si-P and Si-P-Si-P Four-Membered Rings with Two-Coordinate Phosphorus Atoms. *Angew. Chem. Int. Ed.* **2011,** *50*, 2322-2325.

[130] S. Khan, R. Michel, S. S. Sen, H. W. Roesky, A P_4 Chain and Cage from Silylene-Activated White Phosphorus. *Angew. Chem. Int. Ed.* **2011,** *50*, 11786-11789.

[131] P. P. Power, Interaction of Multiple Bonded and Unsaturated Heavier Main Group Compounds with Hydrogen, Ammonia, Olefins, and Related Molecules. *Acc. Chem. Res.* **2011,** *44*, 627-637.

[132] S. Yadav, S. Saha, S. S. Sen, Compounds with Low-Valent p-Block Elements for Small Molecule Activation and Catalysis. *ChemCatChem* **2016,** *8*, 486-501.

[133] A. Rammo, D. Scheschkewitz, Functional Disilenes in Synthesis. *Chem. Eur. J.* **2017,** *24*, 6866-6885.

[134] D. Wendel, T. Szilvási, D. Henschel, P. J. Altmann, C. Jandl, S. Inoue, B. Rieger, Precise Activation of Ammonia and Carbon Dioxide by an Iminodisilene. *Angew. Chem. Int. Ed.* **2018,** *57*, 14575-14579.

[135] J. Hoover, Ammonia activation at a metal. *Science* **2016,** *354*, 707-708.

[136] A. Jana, C. Schulzke, H. W. Roesky, Oxidative Addition of Ammonia at a Silicon(II) Center and an Unprecedented Hydrogenation Reaction of Compounds with Low-Valent Group 14 Elements Using Ammonia Borane. *J. Am. Chem. Soc.* **2009,** *131*, 4600-4601.

[137] E. A. Carter, W. A. Goddard, III, Relation between singlet-triplet gaps and bond energies. *J. Phys. Chem.* **1986,** *90*, 998-1001.

[138] G. Trinquier, J. P. Malrieu, Nonclassical distortions at multiple bonds. *J. Am. Chem. Soc.* **1987,** *109*, 5303-5315.

[139] G. Trinquier, Double bonds and bridged structures in the heavier analogs of ethylene. *J. Am. Chem. Soc.* **1990,** *112*, 2130-2137.

[140] M. Kira, Bonding and structure of disilenes and related unsaturated group-14 element compounds. *Proc. Jpn. Acad. Ser. B* **2012,** *88*, 167-191.

[141] K. K. Milnes, L. C. Pavelka, K. M. Baines, Cycloaddition of carbonyl compounds and alkynes to (di)silenes and (di)germenes: reactivity and mechanism. *Chem. Soc. Rev.* **2016,** *45*, 1019-1035.

[142] C. Präsang, D. Scheschkewitz, Reactivity in the periphery of functionalised multiple bonds of heavier group 14 elements. *Chem. Soc. Rev.* **2016,** *45*, 900-921.

[143] P. S. Skell, E. J. Goldstein, Silacyclopropanes. *J. Am. Chem. Soc.* **1964,** *86*, 1442-1442.

[144] A. K. Franz, K. A. Woerpel, Development of Reactions of Silacyclopropanes as New Methods for Stereoselective Organic Synthesis. *Acc. Chem. Res.* **2000,** *33*, 813-820.

[145] T. G. Driver, K. A. Woerpel, Mechanism of Silver-Mediated Di-tert-butylsilylene Transfer from a Silacyclopropane to an Alkene. *J. Am. Chem. Soc.* **2004,** *126*, 9993-10002.

[146] C. C. Ventocilla, K. A. Woerpel, Synthesis of Silyloxy Dienes by Silylene Transfer to Divinyl Ketones: Application to the Asymmetric Synthesis of Substituted Cyclohexanes. *J. Org. Chem.* **2012,** *77*, 3277-3283.

[147] M. Ishikawa, A. Naka, J. Ohshita, The Chemistry of Silacyclopropenes. *Asian J. Org. Chem.* **2015,** *4*, 1192-1209.

[148] T. A. Perera, E. W. Reinheimer, T. W. Hudnall, Photochemically Switching Diamidocarbene Spin States Leads to Reversible Büchner Ring Expansions. *J. Am. Chem. Soc.* **2017,** *139*, 14807-14814.

[149] H. Suzuki, N. Tokitoh, R. Okazaki, A Novel Reactivity of a Silylene: The First Examples of [1 + 2] Cycloaddition with Aromatic Compounds. *J. Am. Chem. Soc.* **1994,** *116*, 11572-11573.

[150] H. Suzuki, N. Tokitoh, R. Okazaki, Thermal Dissociation of Disilenes into Silylenes. *Bull. Chem. Soc. Jpn.* **1995,** *68*, 2471-2481.

[151] M. Kira, S. Ishida, T. Iwamoto, C. Kabuto, Excited-State Reactions of an Isolable Silylene with Aromatic Compounds. *J. Am. Chem. Soc.* **2002,** *124*, 3830-3831.

[152] M. Kira, S. Ishida, T. Iwamoto, A. de Meijere, M. Fujitsuka, O. Ito, The Singlet Excited State of a Stable Dialkylsilylene Is Responsible for Its Photoreactions. *Angew. Chem. Int. Ed.* **2004,** *43*, 4510-4512.

[153] T. Kosai, S. Ishida, T. Iwamoto, Transformation of azulenes to bicyclic [4]dendralene and heptafulvene derivatives *via* photochemical cycloaddition of dialkylsilylene. *Chem. Commun.* **2015,** *51*, 10707-10709.

[154] T. Kosai, S. Ishida, T. Iwamoto, A Two-Coordinate Cyclic (Alkyl)(amino)silylene: Balancing Thermal Stability and Reactivity. *Angew. Chem. Int. Ed.* **2016,** *55*, 15554-15558.

[155] Y. Mizuhata, T. Sato, N. Tokitoh, Reactions of an Overcrowded Silylene with Pyridines: Formation of a Novel 2*H*-1,2-Azasilepine and Its Further Cycloaddition. *Heterocycles* **2012,** *84*, 413-418.

[156] S. Ishida, T. Tamura, T. Iwamoto, Dearomative cycloadditions of a silylene with pyrazine and quinoxaline. *Dalton Trans.* **2018,** *47*, 11317-11321.

[157] B. Gehrhus, P. B. Hitchcock, M. F. Lappert, The Thermally Stable Silylene Si[$(NCH_2Bu^t)_2C_6H_4$-1,2]: Reactions with Bu^tCN, AdCN, Bu^tNC, AdN_3, and Me_3SiN_3 (Ad = 1-Adamantyl). *Z. Anorg. Allg. Chem.* **2001,** *627*, 1048-1054.

[158] Y. Xiong, S. Yao, M. Driess, Striking Reactivity of a Stable, Zwitterionic Silylene Towards Substituted Diazomethanes, Azides, and Isocyanides. *Chem. Eur. J.* **2009,** *15*, 8542-8547.

[159] P. Boudjouk, U. Samaraweera, R. Sooriyakumaran, J. Chrusciel, K. R. Anderson, Convenient Routes to Di-*tert*-butylsilanediyl: Chemical, Thermal and Photochemical Generation. *Angew. Chem. Int. Ed. Engl.* **1988,** *27*, 1355-1356.

[160] K. Sakamoto, S. Tsutsui, H. Sakurai, M. Kira, Generation and Trapping of Bis(dialkylamino)silylenes: Experimental Evidence for Bridged Structure of Diaminosilylene Dimers. *Bull. Chem. Soc. Joc.* **1997,** *70*, 253-260.

[161] G.-H. Lee, R. West, T. Müller, Bis[bis(trimethylsilyl)amino]silylene, an Unstable Divalent Silicon Compound. *J. Am. Chem. Soc.* **2003,** *125*, 8114-8115.

[162] P. Jutzi, The Pentamethylcyclopentadienylsilicon(II) Cation: Synthesis, Characterization, and Reactivity. *Chem. Eur. J.* **2014,** *20*, 9192-9207.

[163] P. Jutzi, A. Mix, B. Rummel, W. Schoeller, B. Neumann, H.-G. Stammler, The $(Me_5C_5)Si^+$ Cation: A Stable Derivative of HSi^+. *Science* **2004,** *305*, 849-851.

[164] P. Jutzi, K. Leszczyńska, B. Neumann, W. W. Schoeller, H.-G. Stammler, [2,6-$(Trip)_2H_3C_6$](Cp*)Si: A Stable Monomeric Arylsilicon(II) Compound. *Angew. Chem. Int. Ed.* **2009,** *48*, 2596-2599.

[165] P. Jutzi, A. Mix, B. Neumann, B. Rummel, W. Schoeller, H.-G. Stammler, A. B. Rozhenko, Reversible Transformation of a Stable Monomeric Silicon(II) Compound into a Stable

Disilene by Phase Transfer: Experimental and Theoretical Studies of the System $\{[(Me_3Si)_2N](Me_5C_5)Si\}_n$ with n = 1,2. *J. Am. Chem. Soc.* **2009,** *131*, 12137-12143.

[166] P. Jutzi, K. Leszczyńska, A. Mix, B. Neumann, B. Rummel, W. Schoeller, H.-G. Stammler, Synthesis and Characterization of the Ferrio-Substituted Silicon(II) Compound $Me_5C_5(CO)_2FeSiC_5Me_5$. *Organometallics* **2010,** *29*, 4759-4761.

[167] S. Inoue, K. Leszczyńska, An Acyclic Imino-Substituted Silylene: Synthesis, Isolation, and its Facile Conversion into a Zwitterionic Silaimine. *Angew. Chem. Int. Ed.* **2012,** *51*, 8589-8593.

[168] T. Ochiai, D. Franz, S. Inoue, Applications of N-heterocyclic imines in main group chemistry. *Chem. Soc. Rev.* **2016,** *45*, 6327-6344.

[169] A. V. Protchenko, K. H. Birjkumar, D. Dange, A. D. Schwarz, D. Vidovic, C. Jones, N. Kaltsoyannis, P. Mountford, S. Aldridge, A Stable Two-Coordinate Acyclic Silylene. *J. Am. Chem. Soc.* **2012,** *134*, 6500-6503.

[170] B. D. Rekken, T. M. Brown, J. C. Fettinger, H. M. Tuononen, P. P. Power, Isolation of a Stable, Acyclic, Two-Coordinate Silylene. *J. Am. Chem. Soc.* **2012,** *134*, 6504-6507.

[171] S. P. Green, C. Jones, A. Stasch, Stable Magnesium(I) Compounds with Mg-Mg Bonds. *Science* **2007,** *318*, 1754-1757.

[172] R. West, Two-armed silicon. *Nature* **2012,** *485*, 49-50.

[173] M. Driess, Breaking the limits with silylenes. *Nat. Chem.* **2012,** *4*, 525-526.

[174] A. V. Protchenko, A. D. Schwarz, M. P. Blake, C. Jones, N. Kaltsoyannis, P. Mountford, S. Aldridge, A Generic One-Pot Route to Acyclic Two-Coordinate Silylenes from Silicon(IV) Precursors: Synthesis and Structural Characterization of a Silylsilylene. *Angew. Chem. Int. Ed.* **2013,** *52*, 568-571.

[175] B. D. Rekken, T. M. Brown, J. C. Fettinger, F. Lips, H. M. Tuononen, R. H. Herber, P. P. Power, Dispersion Forces and Counterintuitive Steric Effects in Main Group Molecules: Heavier Group 14 (Si–Pb) Dichalcogenolate Carbene Analogues with Sub-90° Interligand Bond Angles. *J. Am. Chem. Soc.* **2013,** *135*, 10134-10148.

[176] T. J. Hadlington, J. A. B. Abdalla, R. Tirfoin, S. Aldridge, C. Jones, Stabilization of a two-coordinate, acyclic diaminosilylene (ADASi): completion of the series of isolable diaminotetrylenes, :$E(NR_2)_2$ (E = group 14 element). *Chem. Commun.* **2016,** *52*, 1717-1720.

[177] Y. K. Loh, L. Ying, M. Ángeles Fuentes, D. C. H. Do, S. Aldridge, An N-Heterocyclic Boryloxy Ligand Isoelectronic with N-Heterocyclic Imines: Access to an Acyclic Dioxysilylene and its Heavier Congeners. *Angew. Chem. Int. Ed.* **2019,** *58*, 4847-4851.

[178] M. M. D. Roy, M. J. Ferguson, R. McDonald, Y. Zhou, E. Rivard, A Vinyl Silylsilylene and its Activation of Strong Homo- and Heteroatomic Bonds *Chem. Sci.* **2019,** *10*, 6476-6481.

[179] M. M. D. Roy, E. Rivard, Pushing Chemical Boundaries with *N*-Heterocyclic Olefins (NHOs): From Catalysis to Main Group Element Chemistry. *Acc. Chem. Res.* **2017,** *50*, 2017-2025.

[180] N. Tokitoh, H. Suzuki, R. Okazaki, K. Ogawa, Synthesis, structure, and reactivity of extremely hindered disilenes: the first example of thermal dissociation of a disilene into a silylene. *J. Am. Chem. Soc.* **1993,** *115*, 10428-10429.

[181] M. J. Cowley, V. Huch, H. S. Rzepa, D. Scheschkewitz, Equilibrium between a cyclotrisilene and an isolable base adduct of a disilenyl silylene. *Nat. Chem.* **2013,** *5*, 876-879.

[182] H. Zhao, K. Leszczyńska, L. Klemmer, V. Huch, M. Zimmer, D. Scheschkewitz, Disilenyl Silylene Reactivity of a Cyclotrisilene. *Angew. Chem. Int. Ed.* **2018,** *57*, 2445-2449.

[183] D. Wendel, A. Porzelt, F. A. D. Herz, D. Sarkar, C. Jandl, S. Inoue, B. Rieger, From Si(II) to Si(IV) and Back: Reversible Intramolecular Carbon–Carbon Bond Activation by an Acyclic Iminosilylene. *J. Am. Chem. Soc.* **2017,** *139*, 8134-8137.

[184] L. Zhu, J. Zhang, H. Yang, C. Cui, Synthesis of Silaketenimine Anion and Its Coupling with Isocyanide. *J. Am. Chem. Soc.* **2019,** *141*, 19600-19604.

[185] F. Lips, A. Mansikkamäki, J. C. Fettinger, H. M. Tuononen, P. P. Power, Reactions of Alkenes and Alkynes with an Acyclic Silylene and Heavier Tetrylenes under Ambient Conditions. *Organometallics* **2014,** *33*, 6253-6258.

[186] F. Lips, J. C. Fettinger, A. Mansikkamäki, H. M. Tuononen, P. P. Power, Reversible Complexation of Ethylene by a Silylene under Ambient Conditions. *J. Am. Chem. Soc.* **2014,** *136*, 634-637.

[187] Y. Peng, B. D. Ellis, X. Wang, J. C. Fettinger, P. P. Power, Reversible Reactions of Ethylene with Distannynes Under Ambient Conditions. *Science* **2009,** *325*, 1668-1670.

[188] R. Rodriguez, D. Gau, T. Kato, N. Saffon-Merceron, A. De Cózar, F. P. Cossío, A. Baceiredo, Reversible Binding of Ethylene to Silylene–Phosphine Complexes at Room Temperature. *Angew. Chem. Int. Ed.* **2011,** *50*, 10414-10416.

[189] D. Wendel, W. Eisenreich, C. Jandl, A. Pöthig, B. Rieger, Reactivity of an Acyclic Silylsilylene toward Ethylene: Migratory Insertion into the Si–Si Bond. *Organometallics* **2016,** *35*, 1-4.

[190] M. A. Pearsall, R. West, The reactions of diorganosilylenes with carbon monoxide. *J. Am. Chem. Soc.* **1988,** *110*, 7228-7229.

[191] C. A. Arrington, J. T. Petty, S. E. Payne, W. C. K. Haskins, The reaction of dimethylsilylene with carbon monoxide in low-temperature matrices. *J. Am. Chem. Soc.* **1988,** *110*, 6240-6241.

[192] T. P. Hamilton, H. F. Schaefer, III, Silaketene: A product of the reaction between silylene and carbon monoxide? *J. Chem. Phys.* **1989,** *90*, 1031-1035.

[193] M. Tacke, C. Klein, D. J. Stufkens, A. Oskam, P. Jutzi, A. Bunte, Complexes of decamethylsilicocene: $Cp_2^*Si(CO)$ and $Cp_2^*Si(N_2)$. *Z. Anorg. Allg. Chem.* **1993,** *619*, 865-868.

[194] G. Maier, H. P. Reisenauer, H. Egenolf, Quest for Silaketene: A Matrix-Spectroscopic and Theoretical Study. *Organometallics* **1999,** *18*, 2155-2161.

[195] R. Becerra, J. P. Cannady, R. Walsh, Silylene Does React with Carbon Monoxide: Some Gas-Phase Kinetic and Theoretical Studies. *J. Phys. Chem. A* **2001,** *105*, 1897-1903.

[196] H. Bornemann, W. Sander, Reactions of methyl(phenyl)silylene with CO and PH_3—the formation of acid–base complexes. *J. Organomet. Chem.* **2002,** *641*, 156-164.

[197] A. V. Protchenko, P. Vasko, D. C. H. Do, J. Hicks, M. Ángeles Fuentes, C. Jones, S. Aldridge, Reduction of carbon oxides by an acyclic silylene: reductive coupling of CO. *Angew. Chem. Int. Ed.* **2019,** *58*, 1808-1812.

[198] Y. Wang, A. Kostenko, T. J. Hadlington, M.-P. Luecke, S. Yao, M. Driess, Silicon-Mediated Selective Homo- and Heterocoupling of Carbon Monoxide. *J. Am. Chem. Soc.* **2019,** *141*, 626-634.

[199] M.-P. Luecke, A. Kostenko, Y. Wang, S. Yao, M. Driess, Silicon-Mediated Coupling of Carbon Monoxide, Ammonia, and Primary Amines to Form Acetamides. *Angew. Chem. Int. Ed.* **2019,** *58*, 12940-12944.

[200] Y. Xiong, S. Yao, T. Szilvási, A. Růžička, M. Driess, Homocoupling of CO and isocyanide mediated by a C,C′-bis(silylenyl)-substituted ortho-carborane. *Chem. Commun.* **2020,** *56*, 747-750.

[201] A. V. Protchenko, J. I. Bates, L. M. A. Saleh, M. P. Blake, A. D. Schwarz, E. L. Kolychev, A. L. Thompson, C. Jones, P. Mountford, S. Aldridge, Enabling and Probing Oxidative Addition and Reductive Elimination at a Group 14 Metal Center: Cleavage and Functionalization of E–H Bonds by a Bis(boryl)stannylene. *J. Am. Chem. Soc.* **2016,** *138*, 4555-4564.

[202] Y. Nakadaira, T. Kobayashi, T. Otsuka, H. Sakurai, Chemistry of organosilicon compounds. 108. Efficient trapping of silylenes through disilene intermediates. *J. Am. Chem. Soc.* **1979,** *101*, 486-487.

[203] Y. S. Chen, P. P. Gaspar, Octakis(trimethylsilyl)cyclotetrasilane. A stable cyclotetrasilane from a silylene precursor. *Organometallics* **1982,** *1*, 1410-1412.

[204] H. Matsumoto, A. Sakamoto, Y. Nagai, The persilylcyclotrisilane $[(Et_3Si)_2Si]_3$. *J. Chem. Soc., Chem. Commun.* **1986**, 1768-1769.

[205] M. Kira, T. Maruyama, C. Kabuto, K. Ebata, H. Sakurai, Stable Tetrakis(trialkylsilyl)disilenes; Synthesis, X-Ray Structures, and UV/VIS Spectra. *Angew. Chem. Int. Ed. Engl.* **1994,** *33*, 1489-1491.

[206] A. Sekiguchi, S. Inoue, M. Ichinohe, Y. Arai, Isolable Anion Radical of Blue Disilene $(^{t}Bu_2MeSi)_2Si=Si(SiMe^{t}Bu_2)_2$ Formed upon One-Electron Reduction: Synthesis and Characterization. *J. Am. Chem. Soc.* **2004,** *126*, 9626-9629.

[207] M. Kira, Isolable silylene, disilenes, trisilaallene, and related compounds. *J. Organomet. Chem.* **2004,** *689*, 4475-4488.

[208] M. Kira, S. Ohya, T. Iwamoto, M. Ichinohe, C. Kabuto, Facile Rotation around Si=Si Double Bonds in Tetrakis(trialkylsilyl)disilenes. *Organometallics* **2000,** *19*, 1817-1819.

[209] K. W. Klinkhammer, Tris(trimethylsilyl)silanides of the Heavier Alkali Metals—A Structural Study. *Chem. Eur. J.* **1997,** *3*, 1418-1431.

[210] K. W. Klinkhammer in:, *Organosilicon Chemistry III: From Molecules to Materials*. Wiley-VCH, Weinheim, **1998**.

[211] K. Hassler, A. Dzambaski, J. Baumgartner, Dihaloheptasilanes $X_2Si[SiMe(SiMe_3)_2]_2$ as potential precursors for silylenes, disilenes and cyclotrisilanes. *Silicon Chem.* **2008,** *3*, 271-288.

[212] M. Ichinohe, R. Kinjo, A. Sekiguchi, The First Stable Methyl-Substituted Disilene: Synthesis, Crystal Structure, and Regiospecific MeLi Addition. *Organometallics* **2003,** *22*, 4621-4623.

[213] N. Wiberg, Sterically overloaded supersilylated main group elements and main group element clusters. *Coord. Chem. Rev.* **1997,** *163*, 217-252.

[214] N. Wiberg, W. Niedermayer, Silylene R*XSi (R*=Si^{t}Bu$_3$; X=H, Me, Ph, Hal, R*): Bildung und Reaktionen. *J. Organomet. Chem.* **2001,** *628*, 57-64.

[215] P. S. Skell, R. C. Woodworth, STRUCTURE OF CARBENE, CH_2. *J. Am. Chem. Soc.* **1956,** *78*, 4496-4497.

[216] H. Tanaka, M. Ichinohe, A. Sekiguchi, An Isolable NHC-Stabilized Silylene Radical Cation: Synthesis and Structural Characterization. *J. Am. Chem. Soc.* **2012,** *134*, 5540-5543.

[217] M. W. Stanford, J. I. Schweizer, M. Menche, G. S. Nichol, M. C. Holthausen, M. J. Cowley, Intercepting the Disilene-Silylsilylene Equilibrium. *Angew. Chem. Int. Ed.* **2019,** *58*, 1329–1333.

[218] H. Kobayashi, T. Iwamoto, M. Kira, A Stable Fused Bicyclic Disilene as a Model for Silicon Surface. *J. Am. Chem. Soc.* **2005,** *127*, 15376-15377.

[219] X.-Q. Xiao, H. Zhao, Z. Xu, G. Lai, X.-L. He, Z. Li, Reduction of the dihalocyclopentasilanes. A quest for a homocyclic silylene. *Chem. Commun.* **2013,** *49*, 2706-2708.

[220] S. K. Mueller, A. Dzambaski, N. Altenhuber, A. Torvisco, K. Hassler, M. Flock, Synthesis and characterization of 1,1-dihalogenated cyclopentasilanes. *J. Mol. Struct.* **2015,** *1099*, 197-203.

[221] M. Haas, A. Knoechl, T. Wiesner, A. Torvisco, R. Fischer, C. Jones, Attempted Synthesis of a Homocyclic Bis(silyl)silylene Leads to the Formation of a Tricyclo[3,1,1,$1^{2,4}$]octasilane. *Organometallics* **2019,** *38*, 4158-4170.

[222] D. Scheschkewitz, A Silicon Analogue of Vinyllithium: Structural Characterization of a Disilenide. *Angew. Chem. Int. Ed.* **2004,** *43*, 2965-2967.

[223] A. Jana, I. Omlor, V. Huch, H. S. Rzepa, D. Scheschkewitz, N-Heterocyclic Carbene Coordinated Neutral and Cationic Heavier Cyclopropylidenes. *Angew. Chem. Int. Ed.* **2014,** *53*, 9953-9956.

[224] B. J. Guddorf, A. Hepp, F. Lips, Efficient Synthesis of a NHC-Coordinated Trisilacyclopropylidene and Its Coordination Behavior. *Chem. Eur. J.* **2018,** *24*, 10334-10338.

[225] S. S. Sen, A Stable Silanone with a Three-Coordinate Silicon Atom: A Century-Long Wait is Over. *Angew. Chem. Int. Ed.* **2014,** *53*, 8820-8822.

[226] T. Kudo, S. Nagase, Theoretical study of silanone. Thermodynamic and kinetic stability. *J. Phys. Chem.* **1984,** *88*, 2833-2840.

[227] T. Kudo, S. Nagase, Theoretical study on the dimerization of silanone and the properties of the polymeric products $(H_2SiO)_n$ (n = 2, 3, and 4). Comparison with dimers $(H_2SiS)_2$ and $(H_2CO)_2$. *J. Am. Chem. Soc.* **1985,** *107*, 2589-2595.

[228] M. Kimura, S. Nagase, The Quest of Stable Silanones: Substituent Effects. *Chem. Lett.* **2001,** *30*, 1098-1099.

[229] V. G. Avakyan, V. F. Sidorkin, E. F. Belogolova, S. L. Guselnikov, L. E. Gusel'nikov, AIM and ELF Electronic Structure/G2 and G3 π-Bond Energy Relationship for Doubly Bonded Silicon Species, H_2SiX (X = $E^{14}H_2$, $E^{15}H$, E^{16}). *Organometallics* **2006,** *25*, 6007-6013.

[230] J. D. Epping, S. Yao, M. Karni, Y. Apeloig, M. Driess, Si═X Multiple Bonding with Four-Coordinate Silicon? Insights into the Nature of the Si═O and Si═S Double Bonds in Stable Silanoic Esters and Related Thioesters: A Combined NMR Spectroscopic and Computational Study. *J. Am. Chem. Soc.* **2010,** *132*, 5443-5455.

[231] H. Suzuki, N. Tokitoh, R. Okazaki, S. Nagase, M. Goto, Synthesis, Structure, and Reactivity of the First Kinetically Stabilized Silanethione. *J. Am. Chem. Soc.* **1998,** *120*, 11096-11105.

[232] J. Kapp, M. Remko, P. v. R. Schleyer, H_2XO and $(CH_3)_2XO$ Compounds (X = C, Si, Ge, Sn, Pb): Double Bonds vs Carbene-Like Structures – Can the Metal Compounds Exist at All? *J. Am. Chem. Soc.* **1996,** *118*, 5745-5751.

[233] A. L. Allred, Electronegativity values from thermochemical data. *J. Inorg. Nucl. Chem.* **1961,** *17*, 215-221.

[234] L. Li, T. Fukawa, T. Matsuo, D. Hashizume, H. Fueno, K. Tanaka, K. Tamao, A stable germanone as the first isolated heavy ketone with a terminal oxygen atom. *Nat. Chem.* **2012,** *4*, 361-365.

[235] A. V. Zabula, T. Pape, A. Hepp, F. M. Schappacher, U. C. Rodewald, R. Pöttgen, F. E. Hahn, Trapping of Tin(II) and Lead(II) Homologues of Carbon Monoxide by a Benzannulated Lutidine-Bridged Bisstannylene. *J. Am. Chem. Soc.* **2008,** *130*, 5648-5649.

[236] J. S. Anderson, J. S. Ogden, Matrix Isolation Studies of Group-IV Oxides. I. Infrared Spectra and Structures of SiO, Si_2O_2, and Si_3O_3. *J. Chem. Phys.* **1969,** *51*, 4189-4196.

[237] J. W. Hastie, R. H. Hauge, J. L. Margrave, Reactions and structures of matrix-isolated SiO species at low temperatures from infrared spectra. *Inorg. Chim. Acta* **1969,** *3*, 601-606.

[238] H. Schnöckel, Matrixreaktionen von SiO. IR-spektroskopischer Nachweis der Molekeln SiO_2 und $OSiCl_2$. *Z. Anorg. Allg. Chem.* **1980,** *460*, 37-50.

[239] C. A. Arrington, R. West, J. Michl, On the proposed thermal interconversion of matrix-isolated dimethylsilylene and 1-methylsilene: their reactions with oxygen atom donors. *J. Am. Chem. Soc.* **1983,** *105*, 6176-6177.

[240] R. J. Glinski, J. L. Gole, D. A. Dixon, Oxidation processes in the gas-phase silane-ozone system. Chemiluminescent emission and the molecular structure of H_2SiO. *J. Am. Chem. Soc.* **1985,** *107*, 5891-5894.

[241] R. Withnall, L. Andrews, Infrared spectroscopic evidence for silicon-oxygen double bonds: silanone and the silanoic and silicic acid molecules. *J. Am. Chem. Soc.* **1985,** *107*, 2567-2568.

[242] V. N. Khabashesku, Z. A. Kerzina, E. G. Baskir, A. K. Maltsev, O. M. Nefedov, Direct spectroscopic study of unstable molecules with silicon–oxygen multiple bonds: low temperature matrix stabilization of $(CH_3)_2Si{=}O$ and $(CD_3)_2Si{=}O$ in the gas phase. *J. Organomet. Chem.* **1988,** *347*, 277-293.

[243] R. Withnall, L. Andrews, Matrix reactions of methylsilanes and oxygen atoms. *J. Phys. Chem.* **1988,** *92*, 594-602.

[244] M. Bogey, B. Delcroix, A. Walters, J.-C. Guillemin, Experimentally Determined Structure of H_2SiO by Rotational Spectroscopy and Isotopic Substitution. *J. Mol. Spectrosc.* **1996,** *175*, 421-428.

[245] V. N. Khabashesku, Z. A. Kerzina, K. N. Kudin, O. M. Nefedov, Matrix isolation infrared and density functional theoretical studies of organic silanones, $(CH_3O)_2Si{=}O$ and $(C_6H_5)_2Si{=}O$. *J. Organomet. Chem.* **1998,** *566*, 45-59.

[246] H. Bornemann, W. Sander, Oxidation of Methyl(phenyl)silylene-Synthesis of a Dioxasilirane. *J. Am. Chem. Soc.* **2000,** *122*, 6727-6734.

[247] W. Ando, M. Ikeno, Y. Hamada, Reaction of dimesitylsilylene with epoxides. Silanone–epoxide adducts. *J. Chem. Soc., Chem. Commun.* **1981**, 621-622.

[248] N. Wiberg, G. Preiner, K. Schurz, Zur Frage der intermediären Bildung von Silanonen $R_2Si{=}O$ bei Reaktionen von Silenen mit Distickstoffoxid. *Chem. Ber.* **1988,** *121*, 1407-1412.

[249] J. Belzner, H. Ihmels, B. O. Kneisel, R. Herbst-Irmer, Chalcogen Transfer to Bis[2-(dimethylaminomethyl)phenyl]silanediyl by Isocyanates and Isothiocyanates. *Chem. Ber.* **1996,** *129*, 125-130.

[250] N. Takeda, N. Tokitoh, R. Okazaki, Reaction of a Stable Silylene–Isocyanide Complex with Nitrile Oxides: A New Approach to the Generation of a Silanone. *Chem. Lett.* **2000,** *29*, 244-245.

[251] S. Yao, M. Brym, C. van Wüllen, M. Driess, From a Stable Silylene to a Mixed-Valent Disiloxane and an Isolable Silaformamide–Borane Complex with Considerable Silicon–Oxygen Double-Bond Character. *Angew. Chem. Int. Ed.* **2007,** *46*, 4159-4162.

[252] S. Yao, Y. Xiong, M. Brym, M. Driess, An Isolable Silanoic Ester by Oxygenation of a Stable Silylene. *J. Am. Chem. Soc.* **2007,** *129*, 7268-7269.

[253] Y. Xiong, S. Yao, M. Driess, An Isolable NHC-Supported Silanone. *J. Am. Chem. Soc.* **2009,** *131*, 7562-7563.

[254] Y. Xiong, S. Yao, R. Müller, M. Kaupp, M. Driess, Activation of Ammonia by a Si=O Double Bond and Formation of a Unique Pair of Sila-Hemiaminal and Silanoic Amide Tautomers. *J. Am. Chem. Soc.* **2010,** *132*, 6912-6913.

[255] Y. Xiong, S. Yao, E. Irran, M. Driess, From a Stable Silanone Complex to Isolable, Donor-Supported Silicoxonium Halides [LSi(dmap)=O–SiMe3]+X–. *Chem. Eur. J.* **2011,** *17*, 11274-11279.

[256] Y. Xiong, S. Yao, R. Müller, M. Kaupp, M. Driess, From silicon(II)-based dioxygen activation to adducts of elusive dioxasiliranes and sila-ureas stable at room temperature. *Nat. Chem.* **2010,** *2*, 577-580.

[257] A. C. Filippou, B. Baars, O. Chernov, Y. N. Lebedev, G. Schnakenburg, Silicon–Oxygen Double Bonds: A Stable Silanone with a Trigonal-Planar Coordinated Silicon Center. *Angew. Chem. Int. Ed.* **2014,** *53*, 565-570.

[258] S. U. Ahmad, T. Szilvási, E. Irran, S. Inoue, An NHC-Stabilized Silicon Analogue of Acylium Ion: Synthesis, Structure, Reactivity, and Theoretical Studies. *J. Am. Chem. Soc.* **2015,** *137*, 5828-5836.

[259] S. U. Ahmad, T. Szilvási, S. Inoue, A facile access to a novel NHC-stabilized silyliumylidene ion and C-H activation of phenylacetylene. *Chem. Commun.* **2014,** *50*, 12619-12622.

[260] T. Iwamoto, H. Masuda, S. Ishida, C. Kabuto, M. Kira, Addition of Stable Nitroxide Radical to Stable Divalent Compounds of Heavier Group 14 Elements. *J. Am. Chem. Soc.* **2003,** *125*, 9300-9301.

[261] T. Iwamoto, H. Masuda, S. Ishida, C. Kabuto, M. Kira, Diverse reactions of nitroxide-radical adducts of silylene, germylene, and stannylene. *J. Organomet. Chem.* **2004,** *689*, 1337-1341.

[262] M. M. Linden, H. P. Reisenauer, D. Gerbig, M. Karni, A. Schäfer, T. Müller, Y. Apeloig, P. R. Schreiner, Preparation of a Silanone through Oxygen Atom Transfer to a Stable Cyclic Silylene. *Angew. Chem. Int. Ed.* **2015,** *54*, 12404-12409.

[263] S. Ishida, T. Abe, F. Hirakawa, T. Kosai, K. Sato, M. Kira, T. Iwamoto, Persistent Dialkylsilanone Generated by Dehydrobromination of Dialkylbromosilanol. *Chem. Eur. J.* **2015,** *21*, 15100-15103.

[264] I. Alvarado-Beltran, A. Rosas-Sánchez, A. Baceiredo, N. Saffon-Merceron, V. Branchadell, T. Kato, A Fairly Stable Crystalline Silanone. *Angew. Chem. Int. Ed.* **2017,** *56*, 10481-10485.

[265] A. Rosas-Sánchez, I. Alvarado-Beltran, A. Baceiredo, N. Saffon-Merceron, S. Massou, D. Hashizume, V. Branchadell, T. Kato, Cyclic (Amino)(Phosphonium-Bora-Ylide)Silanone: A Remarkably Room Temperature Persistent Silanone. *Angew. Chem. Int. Ed.* **2017,** *56*, 15916-15920.

[266] R. Kobayashi, S. Ishida, T. Iwamoto, An Isolable Silicon Analogue of a Ketone that Contains an Unperturbed Si=O Double Bond. *Angew. Chem. Int. Ed.* **2019,** *58*, 9425-9428.

[267] K. Hansen, T. Szilvási, B. Blom, E. Irran, M. Driess, From an Isolable Acyclic Phosphinosilylene Adduct to Donor-Stabilized Si=E Compounds (E=O, S, Se). *Chem. Eur. J.* **2015,** *21*, 18930-18933.

[268] T. Bach, Stereoselective Intermolecular [2 + 2]-Photocycloaddition Reactions and Their Application in Synthesis. *Synthesis* **1998**, 683-703.

[269] M. D'Auria, The Paternò–Büchi reaction – a comprehensive review. *Photochem. Photobiol. Sci.* **2019,** *18*, 2297-2362.

[270] H. F. T. Klare, M. Oestreich, Silylium ions in catalysis. *Dalton Trans.* **2010,** *39*, 9176-9184.

[271] A. Schulz, A. Villinger, "Tamed" Silylium Ions: Versatile in Catalysis. *Angew. Chem. Int. Ed.* **2012,** *51*, 4526-4528.

[272] J. C. L. Walker, H. F. T. Klare, M. Oestreich, Cationic silicon Lewis acids in catalysis. *Nat. Rev. Chem.* **2020,** *4*, 54-62.

[273] S. L. Powley, S. Inoue, NHC-Stabilised Silyliumylidene Ions. *Chem. Rec.* **2019,** *19*, 2179-2188.

[274] P. Frisch, S. Inoue, Lewis base-stabilized silyliumylidene ions in transition metal coordination chemistry. *Dalton Trans.* **2020**, DOI: 10.1039/D0DT00659A.

[275] K. Leszczyńska, A. Mix, R. J. F. Berger, B. Rummel, B. Neumann, H.-G. Stammler, P. Jutzi, The Pentamethylcyclopentadienylsilicon(II) Cation as a Catalyst for the Specific Degradation of Oligo(ethyleneglycol) Diethers. *Angew. Chem. Int. Ed.* **2011,** *50*, 6843-6846.

[276] E. Fritz-Langhals, Silicon(II) Cation $Cp^*Si:^+$ X^-: A New Class of Efficient Catalysts in Organosilicon Chemistry. *Org. Process Res. Dev.* **2019,** *23*, 2369-2377.

[277] Y. Li, Y.-C. Chan, B.-X. Leong, Y. Li, E. Richards, I. Purushothaman, S. De, P. Parameswaran, C.-W. So, Trapping a Silicon(I) Radical with Carbenes: A Cationic cAAC–Silicon(I) Radical and an NHC–Parent-Silyliumylidene Cation. *Angew. Chem. Int. Ed.* **2017,** *56*, 7573-7578.

[278] B.-X. Leong, J. Lee, Y. Li, M.-C. Yang, C.-K. Siu, M.-D. Su, C.-W. So, A Versatile NHC-Parent Silyliumylidene Cation for Catalytic Chemo- and Regioselective Hydroboration. *J. Am. Chem. Soc.* **2019,** *141*, 17629-17636.

[279] D. Reiter, R. Holzner, A. Porzelt, P. J. Altmann, P. Frisch, S. Inoue, Disilene-Silylene Interconversion: A Synthetically Accessible Acyclic Bis(silyl)silylene. *J. Am. Chem. Soc.* **2019,** *141*, 13536-13546.

[280] R. Holzner, D. Reiter, P. Frisch, S. Inoue, DMAP-stabilized bis(silyl)silylenes as versatile synthons for organosilicon compounds. *RSC Adv.* **2020,** *10*, 3402-3406.

[281] D. Reiter, P. Frisch, D. Wendel, F. M. Hörmann, S. Inoue, Oxidation reactions of a versatile, two-coordinate, acyclic iminosiloxysilylene. *Dalton Trans.* **2020,** *49*, 7060-7068.

[282] D. Wendel, D. Reiter, A. Porzelt, P. J. Altmann, S. Inoue, B. Rieger, Silicon and Oxygen's Bond of Affection: An Acyclic Three-Coordinate Silanone and Its Transformation to an Iminosiloxysilylene. *J. Am. Chem. Soc.* **2017,** *139*, 17193-17198.

[283] D. Reiter, P. Frisch, T. Szilvási, S. Inoue, Heavier Carbonyl Olefination: The Sila-Wittig Reaction. *J. Am. Chem. Soc.* **2019,** *141*, 16991-16996.

[284] K. Banert, O. Plefka, Synthesis with Perfect Atom Economy: Generation of Diazo Ketones by 1,3-Dipolar Cycloaddition of Nitrous Oxide at Cyclic Alkynes under Mild Conditions. *Angew. Chem. Int. Ed.* **2011,** *50*, 6171-6174.

[285] K. Severin, Synthetic chemistry with nitrous oxide. *Chem. Soc. Rev.* **2015,** *44*, 6375-6386.

[286] N. J. Hartmann, G. Wu, T. W. Hayton, Synthesis of a "Masked" Terminal Nickel(II) Sulfide by Reductive Deprotection and its Reaction with Nitrous Oxide. *Angew. Chem. Int. Ed.* **2015,** *54*, 14956-14959.

[287] J. Hicks, A. Heilmann, P. Vasko, J. M. Goicoechea, S. Aldridge, Trapping and Reactivity of a Molecular Aluminium Oxide Ion. *Angew. Chem. Int. Ed.* **2019,** *58*, 17265-17268.

[288] M. D. Anker, M. P. Coles, Aluminium-Mediated Carbon Dioxide Reduction by an Isolated Monoalumoxane Anion. *Angew. Chem. Int. Ed.* **2019,** *58*, 18261-18265.

13. Appendix

13.1 Supporting Information Chapter 4

Supporting Information

Disilene-Silylene Interconversion: A Synthetically Accessible Acyclic Bis(silyl)silylene

Dominik Reiter,[†] Richard Holzner,[†] Amelie Porzelt,[†] Philipp J. Altmann, Philipp Frisch, and Shigeyoshi Inoue[*]

Table of Contents

1. Experimental Section S2
1.1 General Methods and Instrumentation S2
1.2 Synthesis of ((TMS)$_3$Si)SiH$_2$Cl (**18**) S3
1.3 Synthesis of ((TMS)$_3$Si)(^{t}Bu$_3$Si)SiH$_2$ (**1**) S5
1.4 Synthesis of ((TMS)$_3$Si)(^{t}Bu$_3$Si)SiBr$_2$ (**2**) S7
1.5 Synthesis and reactivity of bis(silyl)silylene **3**/tetrasilyldisilene **3'** S9
1.6 Synthesis of disiletane **4** S13
1.7 Synthesis of ((TMS)$_3$Si)(^{t}Bu$_3$Si)Si(CH$_2$CH$_2$) (**5**) S18
1.8 [2+1] cycloaddition reactions of **3**/**3'** with (*E*)-/(*Z*)-alkenes S20
1.9 Synthesis of aminosilane **6** S35
1.10 Synthesis of (TMS)((TMS)$_2$(^{t}Bu$_3$Si)Si)Si(^{i}Pr$_2$Me$_2$) (**13**) S37
1.11 Synthesis and reactivity of ((TMS)$_3$Si)(^{t}Bu$_3$Si)Si(DMAP) (**14**) S41
1.12 Synthesis of ((TMS)$_3$Si)(^{t}Bu$_3$Si)Si(^{i}Pr$_2$Me$_2$) (**15**) S44
1.13 Synthesis of (TMS)((TMS)$_2$(^{t}Bu$_3$Si)Si)Si(IMe$_4$) (**16**) S47
1.14 Synthesis of (TMSO)(^{t}Bu$_3$Si)Si=O(^{i}Pr$_2$Me$_2$) (**17**) S49
2. X-ray Crystallographic Data S52
3. DFT Calculations S67
4. References S91

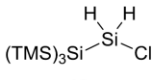
1. Experimental Section

1.1 General Methods and Instrumentation

All manipulations were carried out under exclusion of H_2O and O_2 under an atmosphere of argon 4.6 (≥99.996%; *Westfalen AG*) using standard *Schlenk* techniques or in a *LABstar* glovebox from *MBraun Inertgas-Systeme GmbH* with H_2O and O_2 levels below 0.5 ppm. The glassware used was heat dried under fine vacuum prior to use with *Triboflon III* grease (mixture of polytetrafluoroethylene (PTFE) and perfluoropolyether (PFPE)) from *Freudenberg & Co. KG* as sealant. All solvents were refluxed over sodium/benzophenone, freshly distilled under argon and deoxygenated before use. The deuterated solvents benzene (C_6D_6), THF (THF-d_8) and toluene (toluene-d_8) were obtained from *Sigma-Aldrich Chemie GmbH*, dried over Na/K alloy, flask-to-flask condensed, deoxygenated by three freeze-pump-thaw cycles and stored over 3 Å molecular sieves in the glovebox. All NMR samples were prepared under argon in *J. Young* PTFE valve NMR tubes. The NMR spectra were recorded on *Bruker AV400US* (^{1}H: 400.13 MHz) *AV500* (^{1}H: 500.13 MHz) or *AV500C* (^{1}H: 500.36 MHz, ^{13}C: 125.83 MHz, ^{29}Si: 99.41 MHz) spectrometers at ambient temperature (300 K). Low temperature NMR spectra were recorded on a *Bruker DRX400* (^{1}H: 400.13 MHz, ^{13}C: 100.62 MHz, ^{29}Si: 79.49 MHz) spectrometer. The ^{1}H, ^{13}C{^{1}H} and ^{29}Si{^{1}H} NMR spectroscopic chemical shifts δ are reported in ppm relative to tetramethylsilane. ^{1}H and ^{13}C{^{1}H} NMR spectra are calibrated against the residual proton and natural abundance carbon resonances of the respective deuterated solvent as internal standard (C_6D_6: δ(^{1}H) = 7.16 ppm and δ(^{13}C) = 128.1 ppm, THF-d_8: δ(^{1}H) = 1.73 ppm and δ(^{13}C) = 25.4 ppm, toluene-d_8: δ(^{1}H) = 2.09 ppm and δ(^{13}C) = 20.4 ppm).[S1] The following abbreviations are used to describe signal multiplicities: s = singlet, d = doublet, dd = doublet of doublets, dq = doublet of quartets, t = triplet, sept = septet, m = multiplet, br = broad. Some NMR spectra include resonances for silicone grease (C_6D_6: δ(^{1}H) = 0.29 ppm, δ(^{13}C) = 1.4 ppm and δ(^{29}Si) = –21.8 ppm) derived from *B. Braun Melsungen AG Sterican*® cannulas. EPR spectra were recorded on a *Jeol jes-Fa200 esr* spectrometer with a spectrometer frequency of 9.267 GHz (X-band). Quantitative elemental analyses (EA) were carried out using a *EURO EA* (*HEKAtech*) instrument equipped with a CHNS combustion analyzer at the *Laboratory for Microanalysis* at the *TUM Catalysis Research Center*. IR spectra were recorded on a *Perkin Elmer* FT-IR spectrometer (diamond ATR, Spectrum Two) in a range of 400–4000 cm^{-1} at room temperature inside an argon-filled glovebox. The intensities of the IR bands are abbreviated as following: s = strong, m = medium, w = weak. The UV-Vis spectrum was taken on a *Varian, Inc. Cary 50* spectrophotometer with a *Schlenk* quartz cuvette.

Melting Points (m.p.) were determined in sealed glass capillaries under inert gas by a *Büchi M-565* melting point apparatus. Unless otherwise stated, all commercially available chemicals were purchased from *abcr GmbH*, *Sigma-Aldrich Chemie GmbH* or *Tokyo Chemical Industry Co., Ltd.* and used without further purification. Dinitrogen monoxide (N_2O) 5.0 (≥99.999%), ethylene 3.5 (≥99.95%) and hydrogen 5.0 (≥99.999%) were purchased from *Westfalen AG* and used as received. *(E)*-2-butene and *(Z)*-2-butene (technical grade, estimated purity between 2.0 (≥99%) and 3.5 (≥99.5%) with lower isomeric purity) were obtained from *GHC Gerling, Holz & Co. Handels GmbH* and degassed by three freeze-pump-thaw cycles to remove ethylene contamination. The compounds tris(trimethylsilyl)silyl potassium ($KSi(TMS)_3$)[S2], tri(*tert*-butyl)silyl sodium ($NaSi^tBu_3(THF)_2$)[S3], 1,3,4,5-tetramethylimidazol-2-ylidene (IMe_4) and 1,3-diisopropyl-4,5-dimethylimidazol-2-ylidene ($I^iPr_2Me_2$)[S4] were prepared as described in the corresponding references. Potassium graphite (KC_8) was synthesized following a literature reported procedure upon heating a 1:8 mixture of potassium and graphite in a thick-walled, PTFE-capped pressurizeable Schlenk flask to 500 °C until a homogenous bronze powder was obtained.[S5]

1.2 Synthesis of $((TMS)_3Si)SiH_2Cl$ (18)



18
$C_9H_{29}ClSi_5$
313.21 g/mol

A solution of dichlorosilane in toluene (38.9 wt%, 7.63 g, 75.5 mmol, 2.5 eq.) was diluted with toluene (200 mL) and cooled to –78 °C. Solvent-free $KSi(TMS)_3$ (8.66 g, 30.2 mmol, 1.0 eq.) in toluene (400 mL) was slowly added over a period of 7 hours. Subsequently, the reaction mixture was stirred for 16 hours and thereby gradually warmed to room temperature. KCl was separated from the mixture by filtration and the solvent removed *in vacuo*. The crude product, containing ~3% of the di-substituted compound bis[tris(trimethylsilyl)silyl]silane ($(((TMS)_3Si)_2SiH_2)$[S6], was purified by sublimation (90 °C / 5.0×10^{-3} mbar) providing **18** as a colorless, waxy solid (8.51 g, 27.2 mmol, 90%).

m.p.: 207-208 °C.

^{1}H NMR (500 MHz, C_6D_6, 300 K): δ [ppm] = 5.21 (s, 2H, Si*H*), 0.24 (s, 27H, *TMS*).

^{13}C{^{1}H} NMR (126 MHz, C_6D_6, 300 K): δ [ppm] = 2.1 (*TMS*).

^{29}Si{^{1}H} NMR (99 MHz, C_6D_6, 300 K): δ [ppm] = –9.1 (*TMS*), –17.0 (*Si*H_2Cl), –133.2 (*Si*$(TMS)_3$).

Anal. Calcd. [%] for $C_9H_{29}ClSi_5$: C, 34.51; H, 9.33. Found [%]: C, 33.95; H, 9.34.

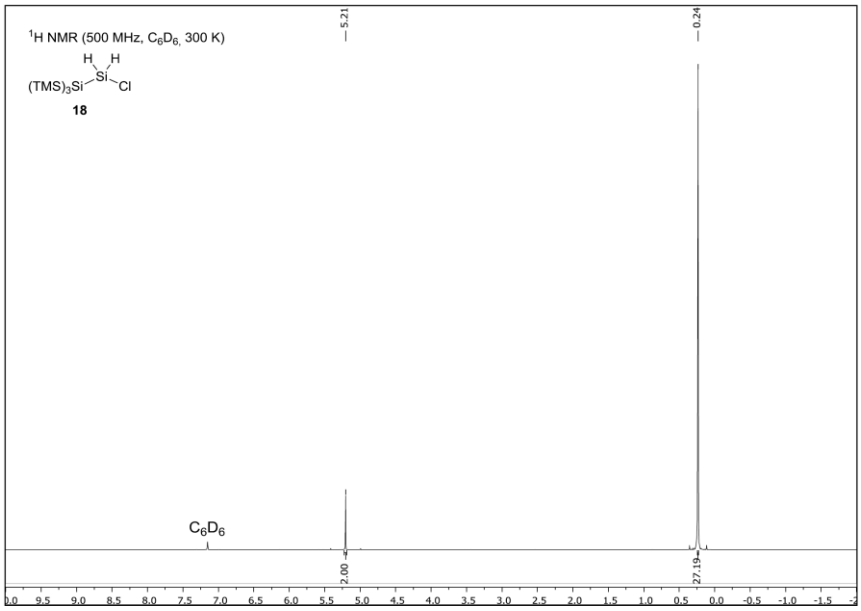


Figure S1. ^{1}H NMR spectrum of ((TMS)$_3$Si)SiH$_2$Cl (**18**) in C_6D_6 at 300 K.

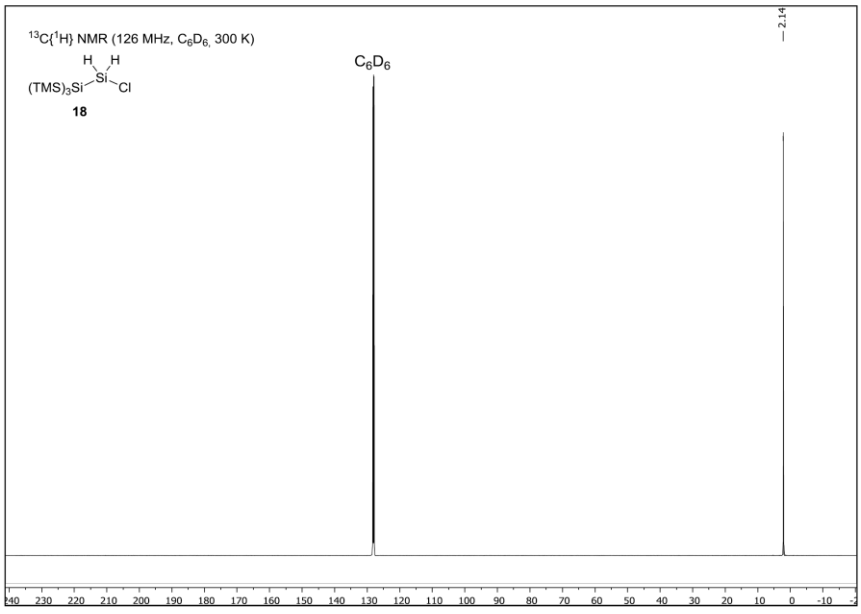


Figure S2. ^{13}C{^{1}H} NMR spectrum of ((TMS)$_3$Si)SiH$_2$Cl (**18**) in C_6D_6 at 300 K.

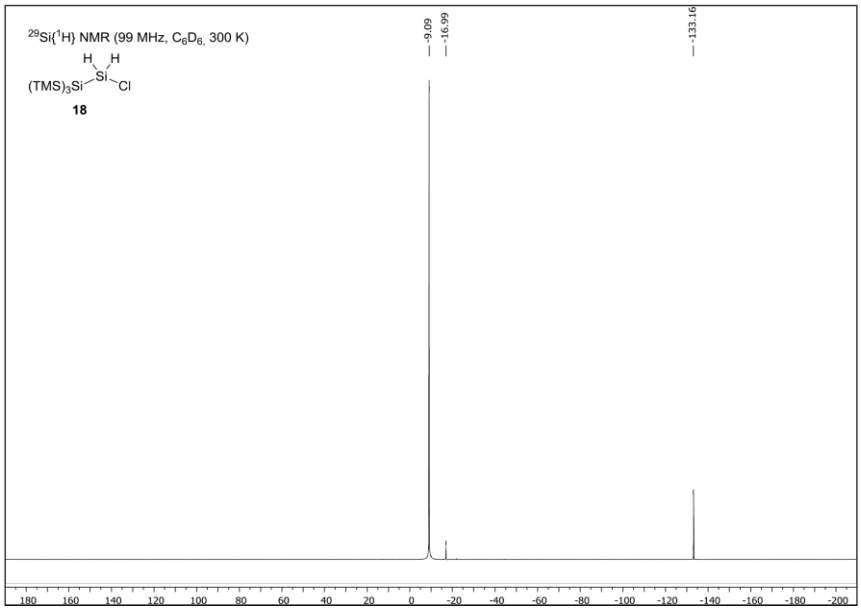
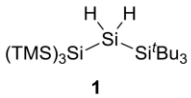


Figure S3. $^{29}Si\{^{1}H\}$ NMR spectrum of $((TMS)_3Si)SiH_2Cl$ (**18**) in C_6D_6 at 300 K.

1.3 Synthesis of $((TMS)_3Si)(^tBu_3Si)SiH_2$ (1)



1

$C_{21}H_{56}Si_6$

477.19 g/mol

A solution of $NaSi^tBu_3(THF)_2$ (7.98 g, 21.8 mmol, 1.0 eq.) in THF (45 mL) was slowly added to a solution of **18** (6.82 g, 21.8 mmol, 1.0 eq.) in THF (60 mL) at –78 °C. The reaction mixture was warmed to room temperature and subsequently stirred for one hour. The solvent was removed *in vacuo* and the residue extracted with *n*-pentane (60 mL). NaCl was separated from the mixture by filtration and the solvent removed under high vacuum, yielding **1** as a colorless solid (10.2 g, 21.3 mmol, 98%). The product was of sufficient purity and used in following reactions without further purification. Block-shaped crystals, suitable for single-crystal X-ray diffraction (SC-XRD) analysis, were obtained by storing a saturated *n*-hexane solution of **1** at –35 ° C overnight.

m.p.: 163-164 °C.

^{1}H NMR (500 MHz, C_6D_6, 300 K): δ [ppm] = 3.39 (s, 2H, Si*H*$_2$), 1.23 (s, 27H, C(C*H*$_3$)$_3$), 0.36 (s, 27H, *TMS*).

^{13}C{^{1}H} NMR (126 MHz, C_6D_6, 300 K): δ [ppm] = 31.8 (C(*C*H$_3$)$_3$), 23.8 (*C*(CH$_3$)$_3$), 2.9 (*TMS*).

^{29}Si{^{1}H} NMR (99 MHz, C_6D_6, 300 K): δ [ppm] = 21.2 (*Si*^{t}Bu$_3$), –8.6 (*TMS*), –114.1 (*Si*H$_2$), –132.9 (*Si*(TMS)$_3$).

Anal. Calcd. [%] for $C_{21}H_{56}Si_6$: C, 52.86; H, 11.83. Found [%]: C, 52.73; H, 11.89.

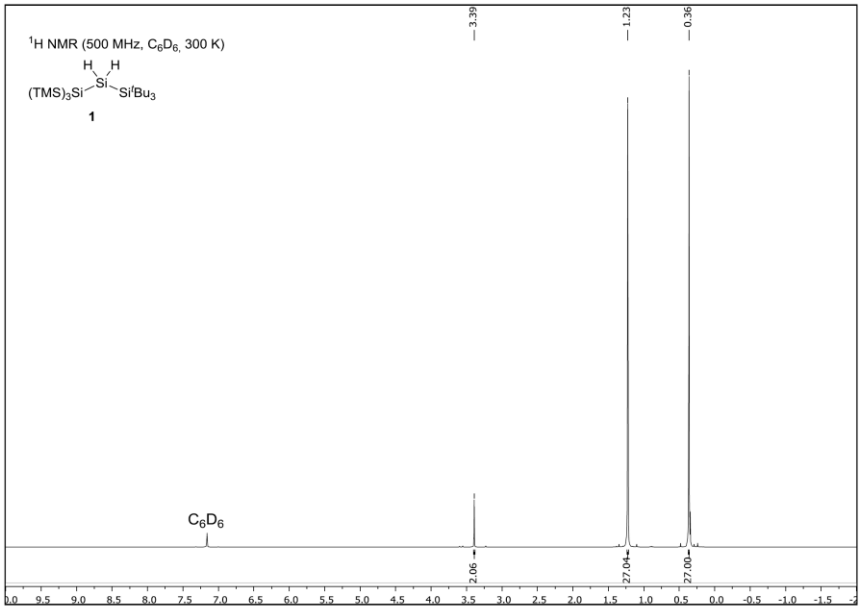


Figure S4. ^{1}H NMR spectrum of ((TMS)$_3$Si)(^{t}Bu$_3$Si)SiH$_2$ (**1**) in C_6D_6 at 300 K.

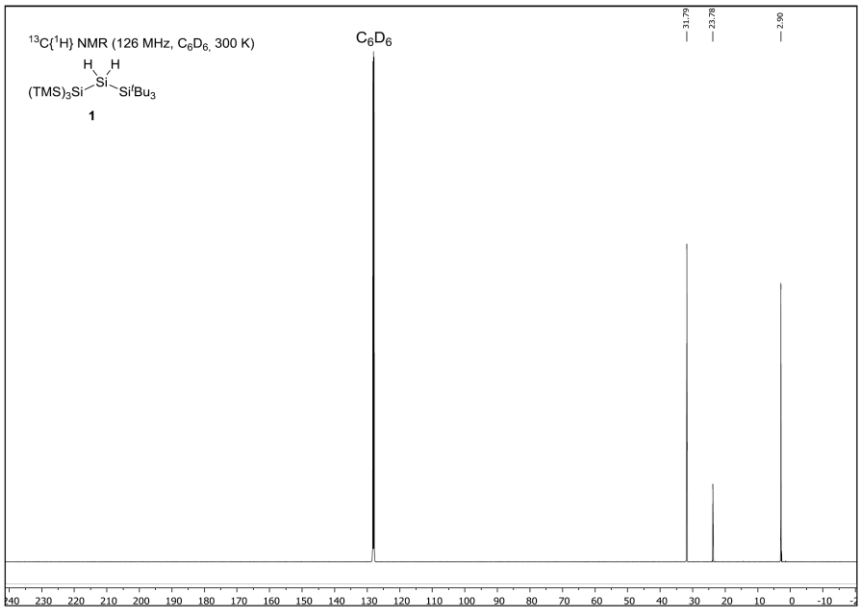


Figure S5. ^{13}C{^{1}H} NMR spectrum of ((TMS)$_3$Si)(^{t}Bu$_3$Si)SiH$_2$ (**1**) in C_6D_6 at 300 K.

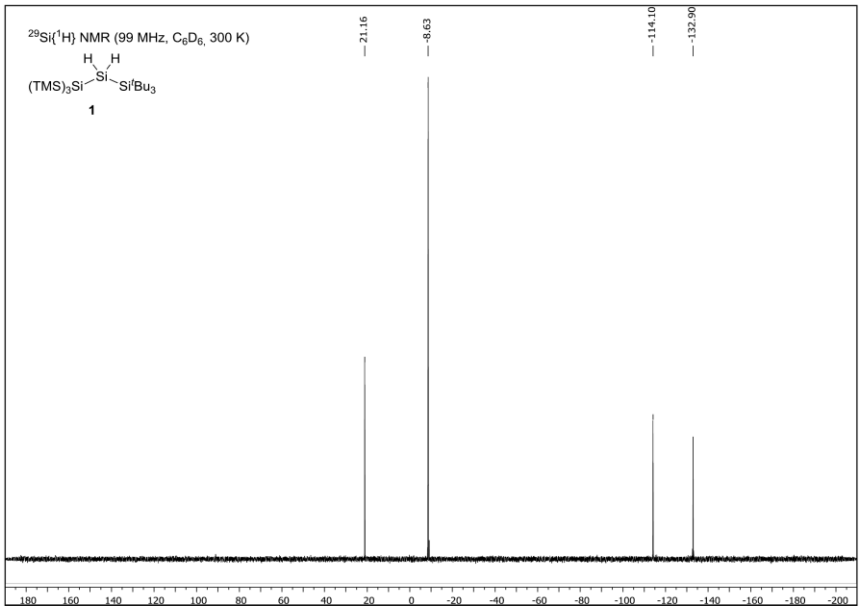
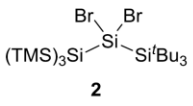


Figure S6. $^{29}Si\{^1H\}$ NMR spectrum of $((TMS)_3Si)(^tBu_3Si)SiH_2$ (**1**) in C_6D_6 at 300 K.

1.4 Synthesis of $((TMS)_3Si)(^tBu_3Si)SiBr_2$ (2)



2

$C_{21}H_{54}Br_2Si_6$

634.98 g/mol

To a cooled (0 °C) solution of **1** (9.86 g, 20.7 mmol, 1.0 eq.) in *n*-pentane (100 mL) was added bromine (2.12 mL, 6.61 g, 41.3 mmol, 2.0 eq.) dropwise *via* a syringe. Subsequently, the reaction mixture was warmed to room temperature and stirred for 15 minutes. All volatiles were removed *in vacuo*. Recrystallization of the residue from *n*-hexane afforded colorless crystals of **2** (11.2 g, 17.7 mmol, 86%). The molecular structure of **2** could not be obtained *via* X-ray crystallography, since all suitable crystals revealed highly disordered structures or crystal twinning.

m.p.: 186-187 °C.

^{1}H NMR (500 MHz, C_6D_6, 300 K): δ [ppm] = 1.35 (s, 27H, C(C<u>*H*</u>$_3$)$_3$), 0.45 (s, 27H, <u>*TMS*</u>).

^{13}C{^{1}H} NMR (126 MHz, C_6D_6, 300 K): δ [ppm] = 32.3 (C(<u>*C*</u>H$_3$)$_3$), 26.1 (<u>*C*</u>(CH$_3$)$_3$), 4.4 (<u>*TMS*</u>).

^{29}Si{^{1}H} NMR (99 MHz, C_6D_6, 300 K): δ [ppm] = 27.9 (<u>*Si*</u>^{t}Bu$_3$), 16.3 (<u>*Si*</u>Br$_2$), –7.2 (<u>*TMS*</u>), –88.5 (<u>*Si*</u>(TMS)$_3$).

Anal. Calcd. [%] for $C_{21}H_{54}Br_2Si_6$: C, 39.72; H, 8.57; Br, 25.17. Found [%]: C, 39.55; H, 8.67; Br, 25.40.

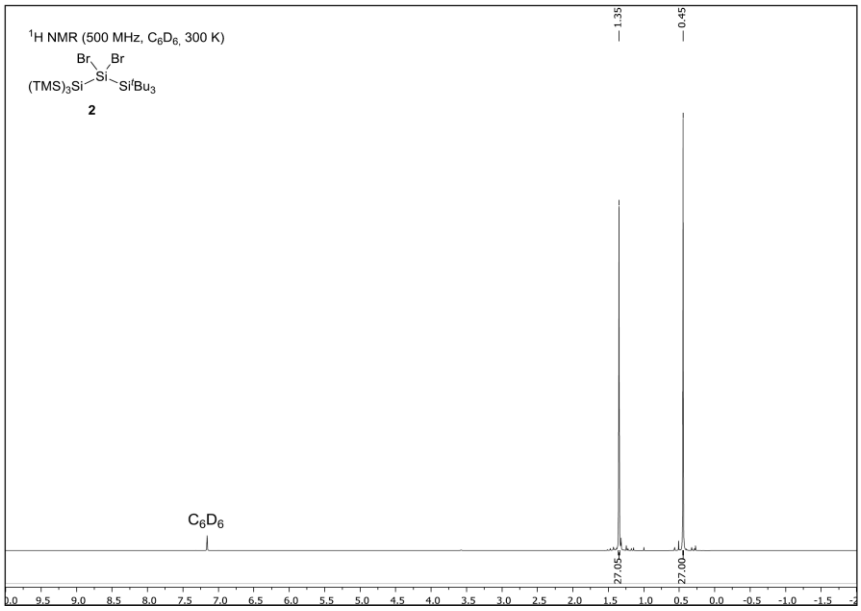


Figure S7. ^{1}H NMR spectrum of ((TMS)$_3$Si)(^{t}Bu$_3$Si)SiBr$_2$ (**2**) in C_6D_6 at 300 K.

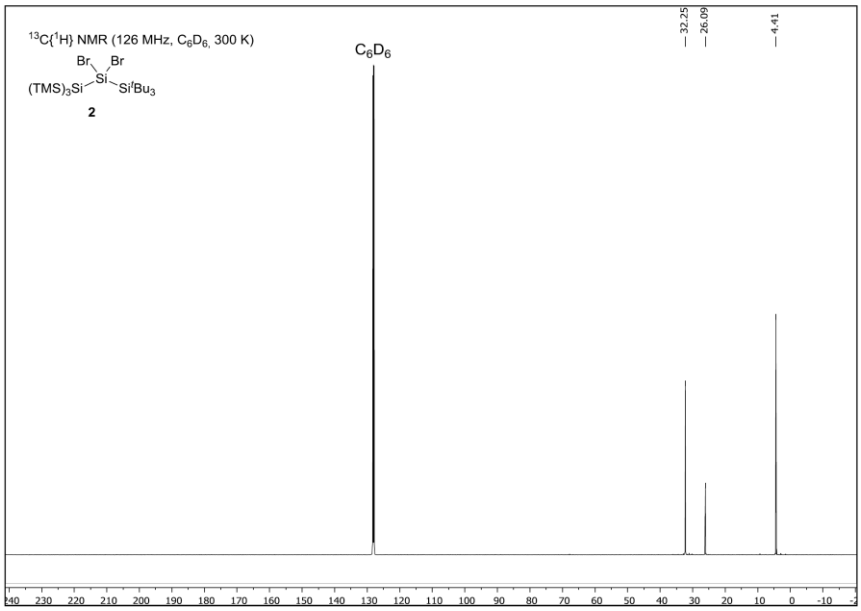


Figure S8. ^{13}C{^{1}H} NMR spectrum of ((TMS)$_3$Si)(^{t}Bu$_3$Si)SiBr$_2$ (**2**) in C_6D_6 at 300 K.

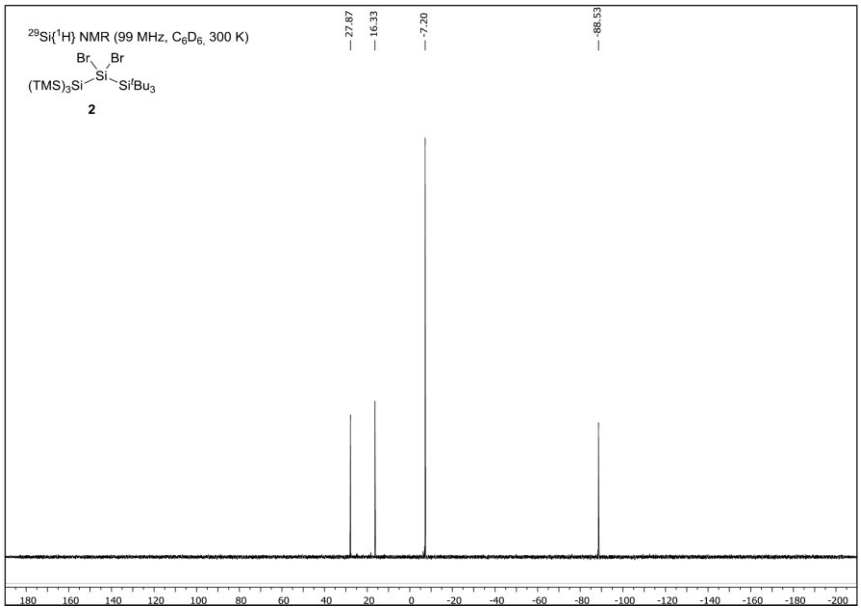
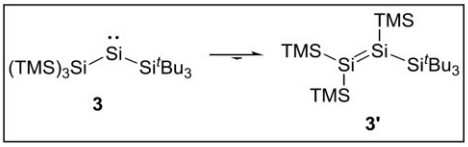


Figure S9. ^{29}Si{^{1}H} NMR spectrum of ((TMS)$_3$Si)(^{t}Bu$_3$Si)SiBr$_2$ (**2**) in C_6D_6 at 300 K.

1.5 Synthesis and reactivity of bis(silyl)silylene 3/tetrasilyldisilene 3'



$C_{21}H_{54}Si_6$
475.15 g/mol

Precooled THF (35 mL, –78 °C) was added to a mixture of **2** (3.00 g, 4.72 mmol, 1.0 eq.) and KC_8 (1.28 g, 9.45 mmol, 2.0 eq.) at –78 °C. The reaction mixture was stirred for 16 hours and thereby gradually warmed to –15 °C using a cryostat. Subsequently, the solvent was removed *in vacuo* and the residue extracted with precooled *n*-pentane (3 × 15 mL, –78 °C) at –78 °C. Graphite and KBr were separated from the mixture by filtration. Removal of the solvent *in vacuo* at –15 °C furnished the equilibrium mixture of bis(silyl)silylene **3** and tetrasilyldisilene **3'** as a blood red waxy solid (2.15 g, 4.52 mmol, 96%). **3**/**3'** is stable as a solid and in solution at –35 °C for at least 1 year, however slowly decomposes in solution at room temperature to disiletane **4** (*vide infra*). By using variable temperature (VT) NMR and UV-Vis spectroscopic studies, only tetrasilyldisilene **3'** and disiletane **4** were detected. Performed EPR spectroscopy, to possibly observe the triplet ground state of bis(silyl)silylene **3**, revealed solely a strong signal around 331 mT (g = 2.0067), corresponding to a typical silyl radical

of unknown structure. Sekiguchi *et al.* observed comparable EPR signals in the measurement of *in situ* generated triplet silylenes.[S7]

^{1}H NMR (400 MHz, toluene-*d*$_8$, 258 K): δ [ppm] = 1.31 (s, 27H, C(C$\underline{H}_3$)$_3$), 0.59 (s, 9H, *TMS*), 0.51 (s, 9H, *TMS*), 0.46 (s, 9H, *TMS*).

^{13}C{^{1}H} NMR (101 MHz, toluene-*d*$_8$, 258 K): δ [ppm] = 32.4 (C($\underline{C}$H$_3$)$_3$), 24.3 ($\underline{C}$(CH$_3$)$_3$), 5.8 (*TMS*), 4.1 (*TMS*), 3.5 (*TMS*).

^{29}Si{^{1}H} NMR (79 MHz, toluene-*d*$_8$, 258 K): δ [ppm] = 161.3 ($\underline{Si}$TMS$_2$), 131.3 ($\underline{Si}$(TMS)Si^{t}Bu$_3$), 31.1 ($\underline{Si}^t$Bu$_3$), –6.3 (*TMS*), –6.7 (*TMS*), –7.0 (*TMS*).

^{29}Si{^{1}H} NMR (99 MHz, C$_6$D$_6$, 300 K): δ [ppm] = 161.9 ($\underline{Si}$TMS$_2$), 132.4 ($\underline{Si}$(TMS)Si^{t}Bu$_3$), 31.7 ($\underline{Si}^t$Bu$_3$), –6.8 (*TMS*), –7.7 (*TMS*).

Anal. Calcd. [%] for C$_{21}$H$_{54}$Si$_6$: C, 53.08; H, 11.46. Found [%]: C, 52.25; H, 11.54.

UV-Vis (*n*-hexane, 273 K): λ_{max} [nm] = 352 (theo.: 335; HOMO–1→LUMO), 469 (theo.: 467; HOMO→LUMO).

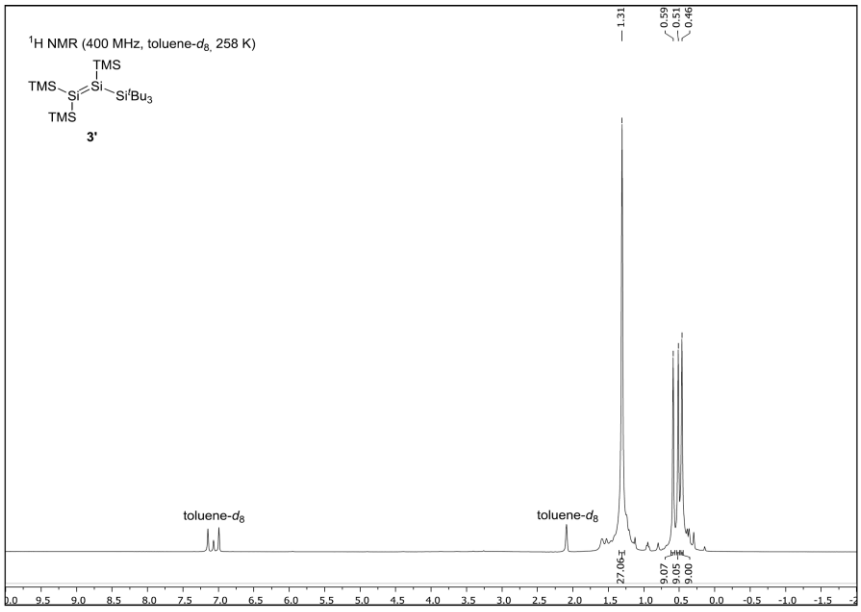


Figure S10. ^{1}H NMR spectrum of bis(silyl)silylene **3**/tetrasilyldisilene **3'** in toluene-d_8 at 258 K.

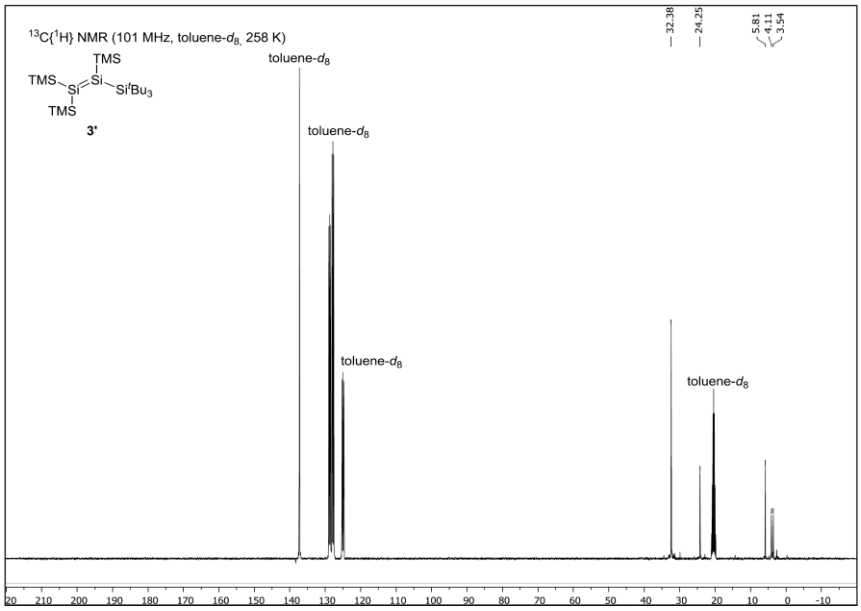


Figure S11. $^{13}C\{^1H\}$ NMR spectrum of bis(silyl)silylene **3**/tetrasilyldisilene **3'** in toluene-d_8 at 258 K.

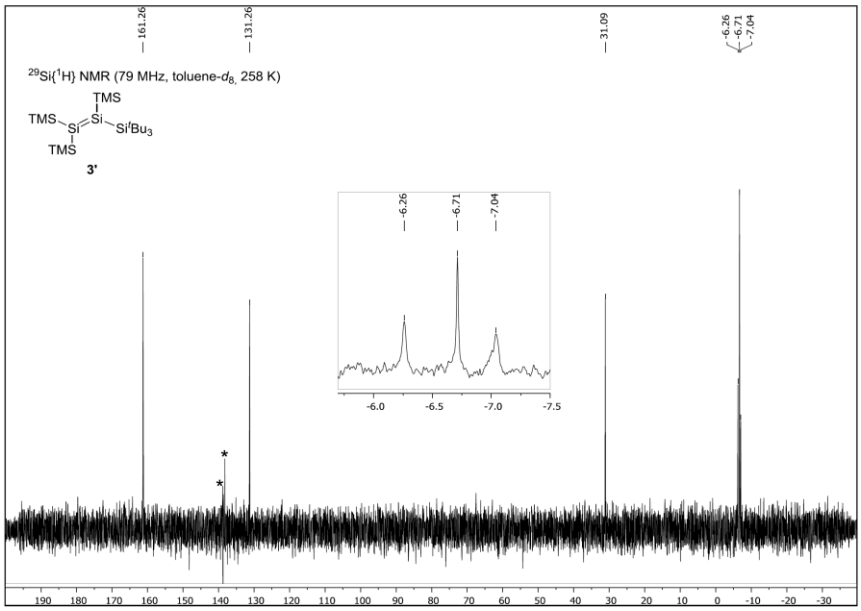


Figure S12. $^{29}Si\{^1H\}$ NMR spectrum of bis(silyl)silylene **3**/tetrasilyldisilene **3'** in toluene-d_8 at 258 K. Spectrometer related artefacts are marked with asterisks *.

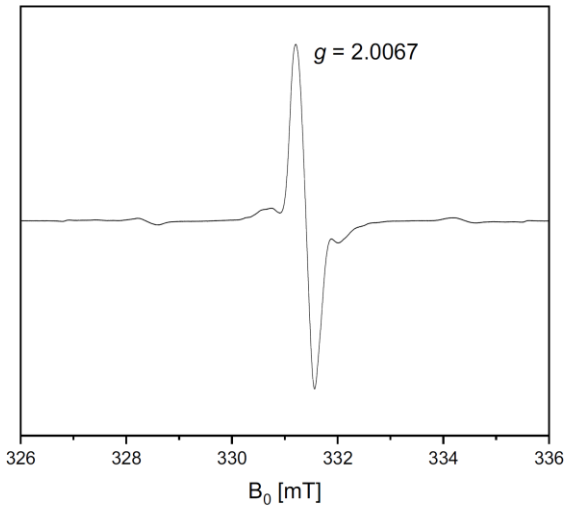


Figure S13. EPR spectrum of bis(silyl)silylene **3**/tetrasilyldisilene **3'** in *n*-pentane at 258 K measured with a spectrometer frequency of 9.267 GHz (X-band). The detected signal originates from a silyl radical with unknown structure.

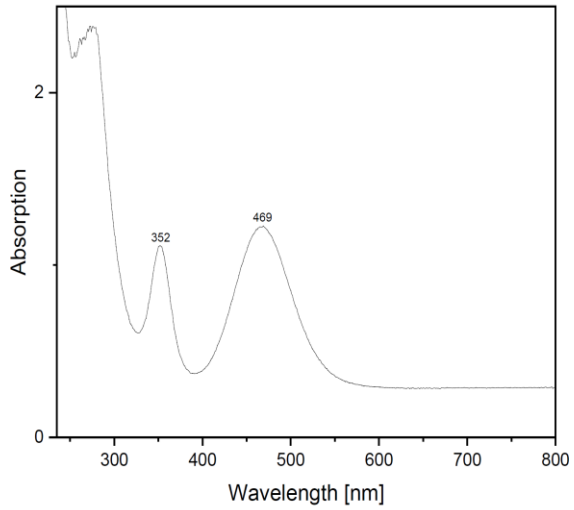
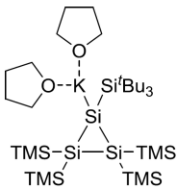


Figure S14. UV-Vis spectrum of bis(silyl)silylene **3**/tetrasilyldisilene **3'** in *n*-hexane ($c = 3.0 \times 10^{-4}$ M). The two characteristic disilene absorption bands at $\lambda_{max} = 352$ and 469 nm are presumably based on the HOMO–1→LUMO (theo.: 335 nm) and HOMO→LUMO (theo.: 467 nm) transitions.

Reduction of bis(silyl)silylene 3/tetrasilyldisilene 3'



19
$C_{32}H_{79}KO_2Si_8$
759.76 g/mol

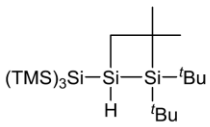
Utilization of excessive amounts of KC_8 for the reductive debromination of $((TMS)_3Si)(^tBu_3Si)SiBr_2$ (**2**) led to formation of a mixture of products, presumably also including radical species. Comparable results were obtained by reduction of bis(silyl)silylene **3**/tetrasilyldisilene **3'** with different equivalents of KC_8. The only product identified so far was the novel cyclic potassium silanide **19** by SC-XRD analysis (*vide infra*). However, selective formation and further characterization was not possible.

Oxidative addition of H_2 to bis(silyl)silylene 3/tetrasilyldisilene 3' providing 1

A solution of **3/3'** (50 mg, 105 µmol) in *n*-hexane (5 mL) was frozen in liquid nitrogen, degassed and warmed to –40 °C. Subsequently, the solution was exposed to H_2 (1 bar) under vigorous stirring. The observed color change from blood red to colorless within 30 min indicated successful dihydrogen activation. All volatiles were removed *in vacuo* and ^{1}H NMR spectroscopy revealed quantitative conversion of **3**/**3'** to $((TMS)_3Si)(^tBu_3Si)SiH_2$ (**1**).

Note: At least within 3 hours, no sign of reaction was observed at –80 °C, however, dihydrogen activation could still work at temperatures below –40 °C.

1.6 Synthesis of disiletane 4



4
$C_{21}H_{54}Si_6$
475.17 g/mol

The 1,3-disilacyclobutane **4** was obtained by two different methods, either by slow decomposition of bis(silyl)silylene **3**/tetrasilyldisilene **3'** in solution (Method A) or by NHC abstraction from the NHC-stabilized bis(silyl)silylene **13** (*vide infra*) (Method B). The long reaction time for the formation of **4** originates from the thermal stability of the equilibrium mixture of **3**/**3'**, which isomerizes to bis(silyl)silylene **3** and subsequently undergoes a C–H activation finally affording disiletane **4**. The even longer reaction time observed for Method B results from the NHC abstraction and the additional isomerization step from the corresponding donor-free silylene **3''** of **13** to **3**/**3**'.

Method A:

A solution of **3/3'** (150 mg, 316 µmol) in *n*-hexane (5 mL) was stirred for 4 days at room temperature. The observed color change from blood red to colorless indicated complete conversion.

Subsequently, the solution was concentrated and stored at –35 °C furnishing **4** as colorless crystals (112 mg, 236 µmol, 75%), which were suitable for SC-XRD analysis. A comparable long reaction time was observed in benzene, THF or toluene.

Method B:

To a mixture of **13** (100 mg, 153 µmol, 1.0 eq.) and BPh_3 (36.9 mg, 153 µmol, 1.0 eq.) was added toluene (3 mL). The reaction mixture was stirred for 7 days, whereby the color of the solution changed from purple-red to colorless. The solvent was removed *in vacuo*. Treatment of the residue with *n*-hexane resulted in the formation of a colorless precipitate (byproduct carbene-borane adduct $I^iPr_2Me_2 \cdot BPh_3$[S8]) which was removed by filtration. Cooling the concentrated filtrate to –35 °C for several days afforded colorless crystals of **4** (53.1 mg, 112 µmol, 73%).

m.p.: 141-142 °C.

^{1}H NMR (500 MHz, C_6D_6, 300 K): δ [ppm] = 4.37 (dd, ^3J = 7.8 Hz, ^3J = 5.9 Hz, 1H, Si*H*), 1.45 (s, 3H, C(C*H*$_3$)$_2$), 1.36 (s, 3H, C(C*H*$_3$)$_2$), 1.33–1.30 (m, 2H, C*H*$_2$), 1.29 (s, 9H, C(C*H*$_3$)$_3$), 1.23 (s, 9H, C(C*H*$_3$)$_3$), 0.34 (s, 27H, *TMS*).

^{13}C{^{1}H} NMR (126 MHz, C_6D_6, 300 K): δ [ppm] = 37.4 (*C*(CH$_3$)$_2$), 31.9 (C(*C*H$_3$)$_2$), 31.9 (C(*C*H$_3$)$_2$), 31.5 (C(*C*H$_3$)$_3$), 31.0 (C(*C*H$_3$)$_3$), 29.5 (*C*H$_2$), 23.6 (*C*(CH$_3$)$_3$), 22.9 (*C*(CH$_3$)$_3$), 2.8 (*TMS*).

^{29}Si{^{1}H} NMR (99 MHz, C_6D_6, 300 K): δ [ppm] = 35.6 (*Si*^{t}Bu$_2$), –9.2 (*TMS*), –60.4 (*Si*H), –133.8 (*Si*(TMS)$_3$).

Anal. Calcd. [%] for $C_{21}H_{54}Si_6$: C, 53.08; H, 11.46. Found [%]: C, 53.11; H, 11.55.

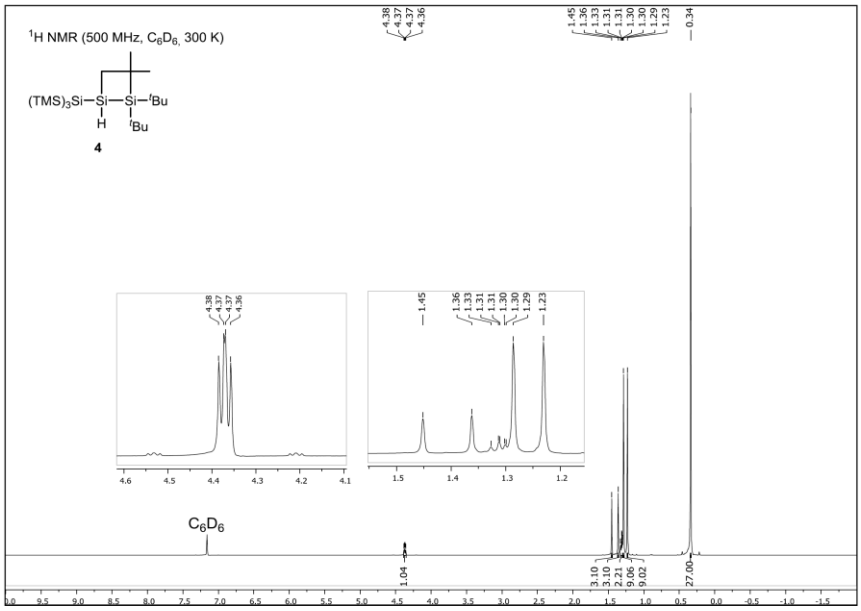


Figure S15. ^{1}H NMR spectrum of disiletane **4** in C_6D_6 at 300 K.

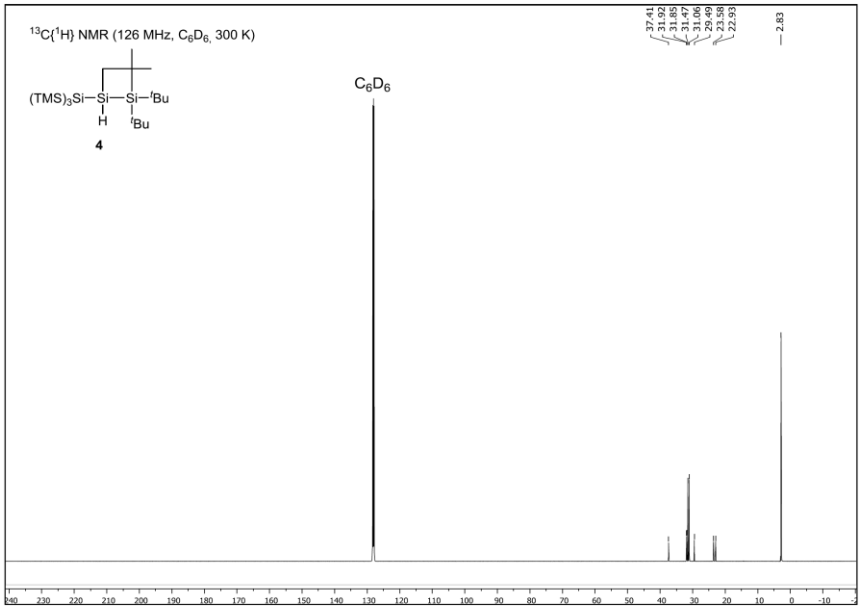


Figure S16. $^{13}C\{^1H\}$ NMR spectrum of disiletane **4** in C_6D_6 at 300 K.

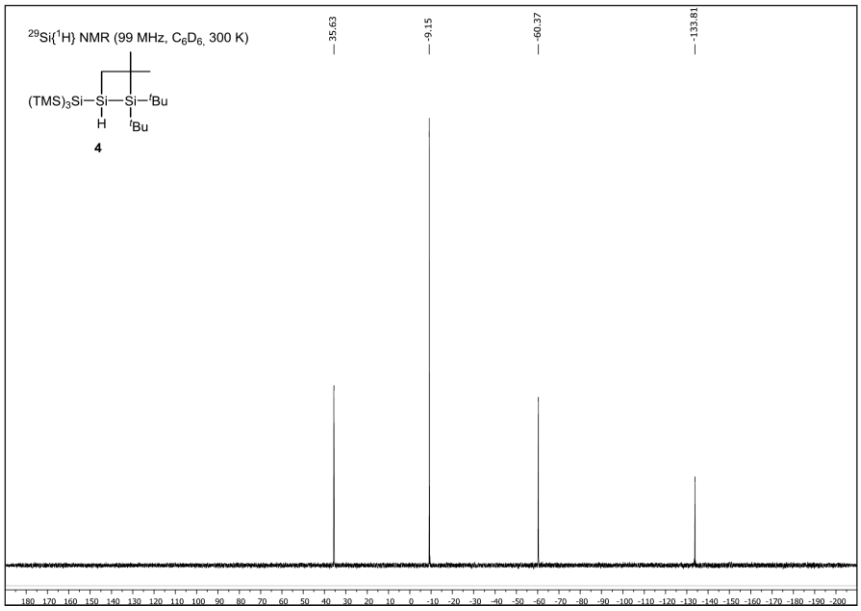


Figure S17. ^{29}Si{^{1}H} NMR spectrum of disiletane **4** in C_6D_6 at 300 K.

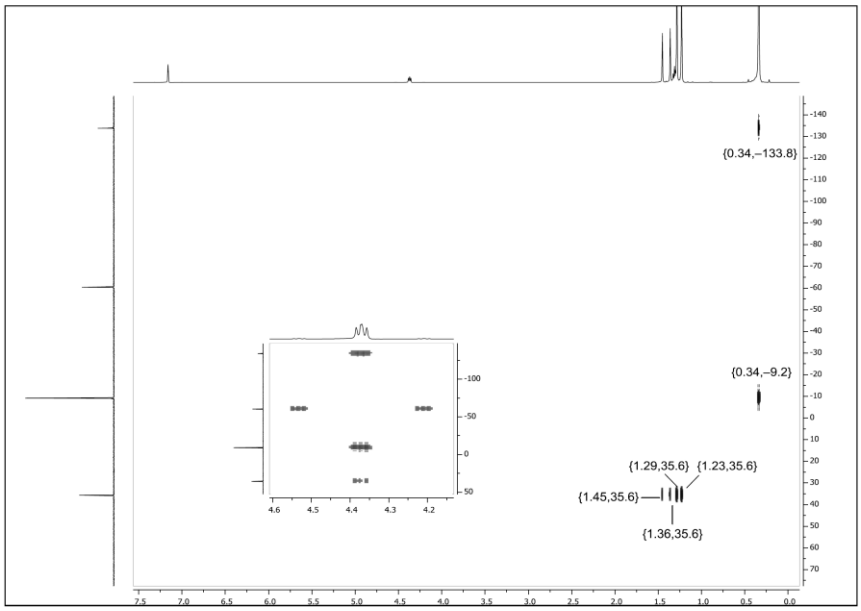
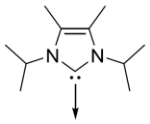


Figure S18. ^{1}H/^{29}Si HMBC NMR spectrum of disiletane **4** in C_6D_6 at 300 K.

Byproduct NHC-borane adduct I^{i}Pr$_2$Me$_2$·BPh$_3$ (Method B):



I^{i}Pr$_2$Me$_2$·BPh$_3$
$C_{29}H_{35}BN_2$
422.42 g/mol

^{1}H NMR (400 MHz, C$_6$D$_6$, 300 K): δ [ppm] = 7.68 (d, ^3J = 7.0 Hz, 6H, C$_{ar}$*H*), 7.32 (t, ^3J = 7.5 Hz, 6H, C$_{ar}$*H*), 7.19 (d, ^3J = 7.3 Hz, 3H, C$_{ar}$*H*), 5.04 (sept, ^3J = 7.1 Hz, 2H, NC*H*(CH$_3$)$_2$), 1.52 (s, 6H, CC*H*$_3$), 0.70 (d, ^3J = 7.0 Hz, 12H, NCH(C*H*$_3$)$_2$).

The spectroscopic data match those previously reported.[S8]

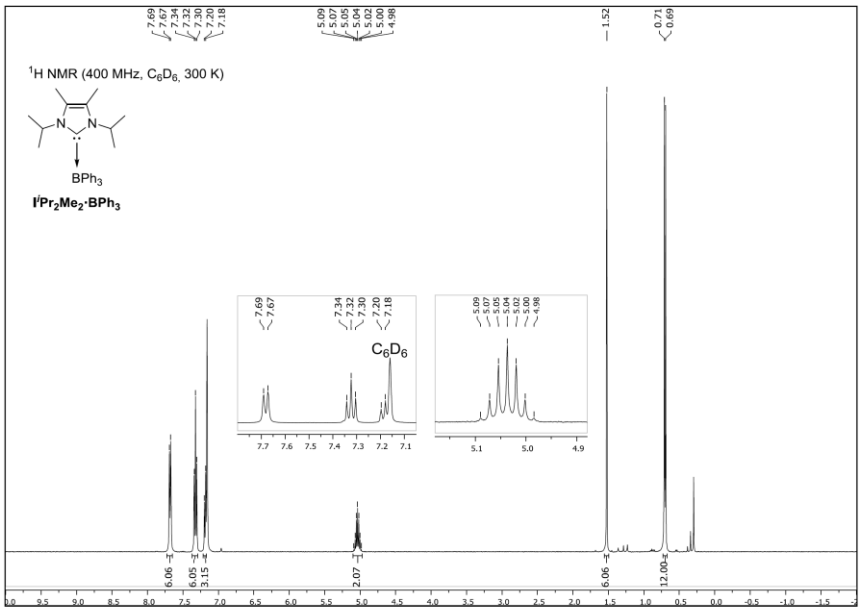
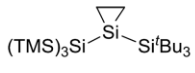


Figure S19. ^{1}H NMR spectrum of the byproduct NHC-borane adduct **I^{i}Pr$_2$Me$_2$·BPh$_3$** in C_6D_6 at 300 K.

1.7 Synthesis of ((TMS)$_3$Si)(^{t}Bu$_3$Si)Si(CH$_2$CH$_2$) (5)



5

$C_{23}H_{58}Si_6$

503.23 g/mol

A solution of **3/3'** (150 mg, 316 µmol) in *n*-hexane (5 mL) was frozen in liquid nitrogen, degassed and warmed to –80 °C. Subsequently, the solution was exposed to ethylene (1 bar) under vigorous stirring. The reaction mixture was warmed to ambient temperature, whereby the color changed from blood red to pale yellow. The solvent was removed *in vacuo* and the residue recrystallized from a saturated Et_2O solution at –35 °C. Silirane **5** was obtained as colorless crystals (127 mg, 252 mmol, 80%), which were suitable for single-crystal X-ray diffraction analysis.

m.p.: 142-143 °C (gas formation, sticky colorless oil).

^{1}H NMR (500 MHz, C_6D_6, 300 K): δ [ppm] = 1.21 (s, 27H, C(C$\underline{H}_3$)$_3$), 0.96–0.93 (m, 2H, C$\underline{H}_2$CH$_2$), 0.78–0.75 (m, 2H, CH$_2$C$\underline{H}_2$), 0.37 (s, 27H, *TMS*).

^{13}C{^{1}H} NMR (126 MHz, C_6D_6, 300 K): δ [ppm] = 32.4 (C($\underline{C}$H$_3$)$_3$), 24.9 ($\underline{C}$(CH$_3$)$_3$), 4.1 (*TMS*), 1.2 ($\underline{C}$H$_2$CH$_2$).

^{29}Si{^{1}H} NMR (99 MHz, C_6D_6, 300 K): δ [ppm] = 20.2 ($\underline{Si}$^{t}Bu$_3$), –8.3 (*TMS*), –113.7 ($\underline{Si}$(TMS)$_3$), –164.3 ($\underline{Si}$CH$_2$CH$_2$).

Anal. Calcd. [%] for $C_{23}H_{58}Si_6$: C, 54.90; H, 11.62. Found [%]: C, 54.73; H, 11.39.

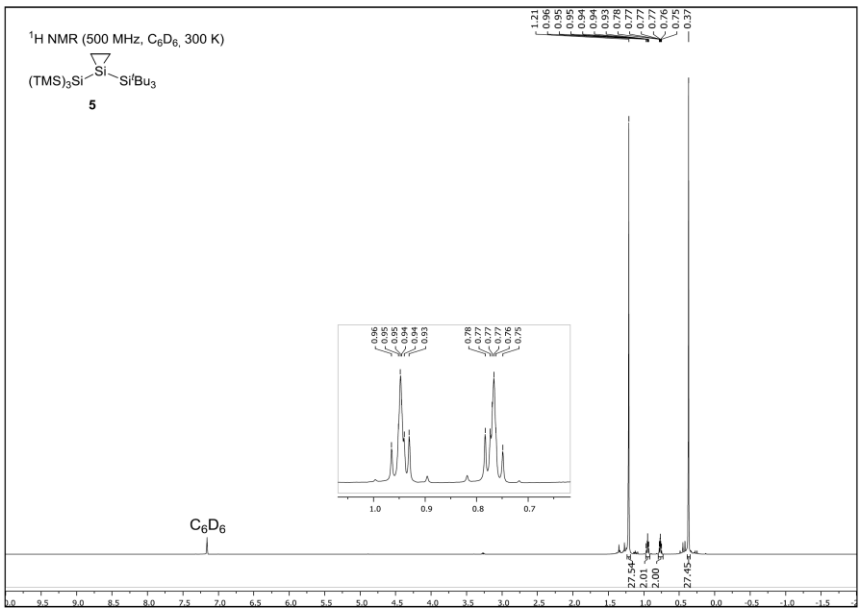


Figure S20. ^{1}H NMR spectrum of ((TMS)$_3$Si)(^{t}Bu$_3$Si)Si(CH$_2$CH$_2$) (**5**) in C_6D_6 at 300 K.

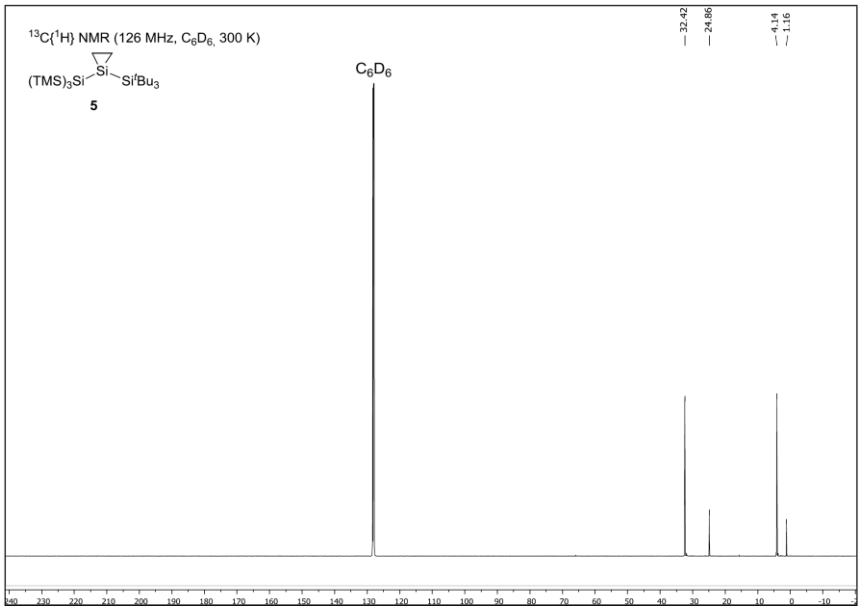


Figure S21. $^{13}C\{^{1}H\}$ NMR spectrum of $((TMS)_3Si)(^tBu_3Si)Si(CH_2CH_2)$ (**5**) in C_6D_6 at 300 K.

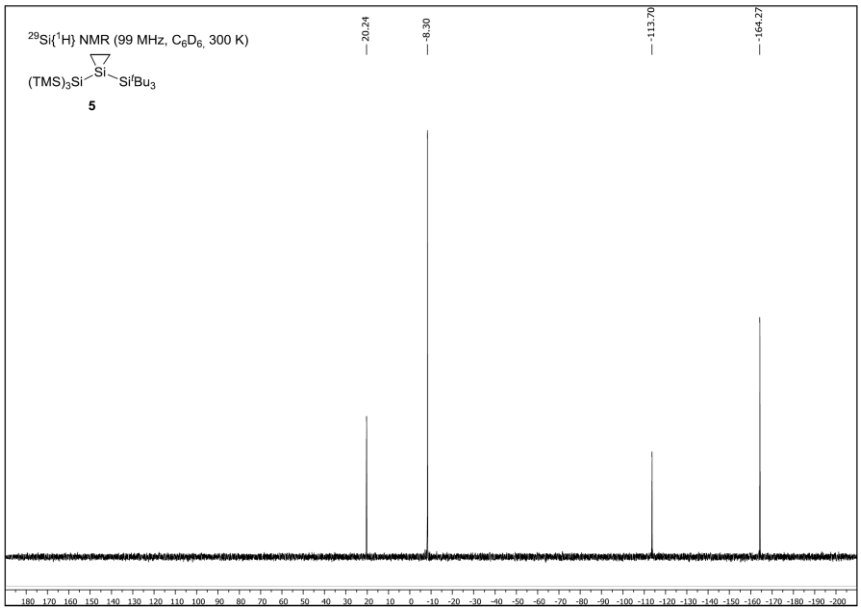


Figure S22. $^{29}Si\{^{1}H\}$ NMR spectrum of $((TMS)_3Si)(^tBu_3Si)Si(CH_2CH_2)$ (**5**) in C_6D_6 at 300 K.

1.8 [2+1] cycloaddition reactions of 3/3' with (*E*)-/(*Z*)-alkenes

General information:

As observed previously, the purity of stereogenic alkenes investigated for [2+1] cycloaddition reactions with silylenes is decisive for the resulting silirane product ratio.[S9] However, high purity alkenes, especially with respect to contamination with other stereoisomers, are often difficult to obtain due to their similar physical data and thus associated separation issues. For our studies we purchased *(E)*-2-butene and *(Z)*-2-butene (technical grade, estimated purity between 2.0 (≥99%) and 3.5 (≥99.5%) with lower isomeric purity) from *GHC Gerling, Holz & Co. Handels GmbH*. The corresponding approximate amounts of contamination with the other stereoisomers were determined via ^{1}H and ^{13}C NMR (1 bar in 0.5 mL C_6D_6; *vide infra*): *(E)*-2-butene (~1.3% *(Z)*-2-butene) and *(Z)*-2-butene (~0.7% *(E)*-2-butene). Utilized (*E*)-3-hexene (>99.0%) and (*Z*)-3-hexene (>97.0%) were obtained from *Tokyo Chemical Industry Co., Ltd.* and dried over 4 Å molecular sieves.

Spectroscopic data for (*E*)-2-butene:



C_4H_8
56.11 g/mol

^{1}H NMR (500 MHz, C_6D_6, 300 K): δ [ppm] = 5.43–5.33 (m, 2H, C*H*), 1.57–1.56 (m, 6H, CH_3).

^{13}C{^{1}H} NMR (126 MHz, C_6D_6, 300 K): δ [ppm] = 126.1 (*C*H), 18.1 (*C*H_3).

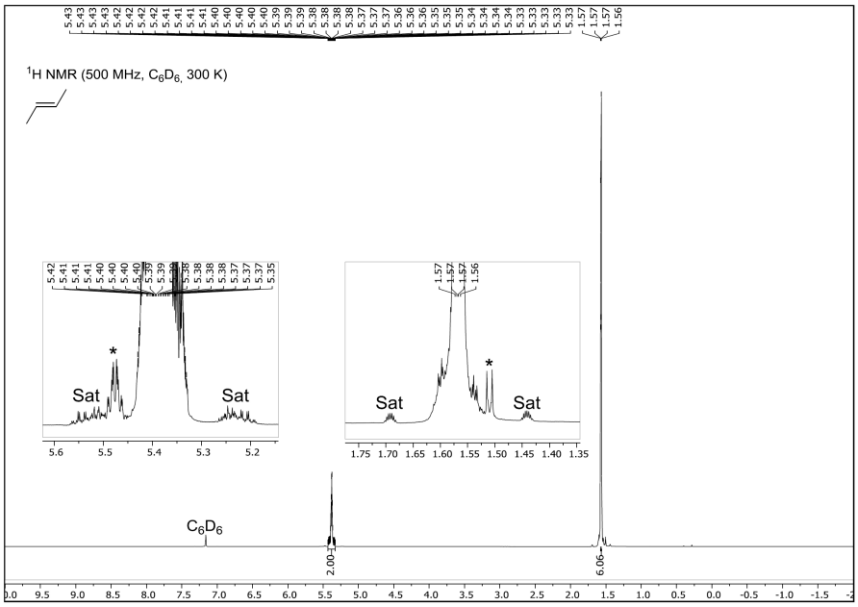


Figure S23. ^{1}H NMR spectrum of (*E*)-2-butene in C_6D_6 at 300 K. The respective resonances of the (*Z*)-2-butene contamination are marked with asterisks * and ^{13}C satellites with Sat.

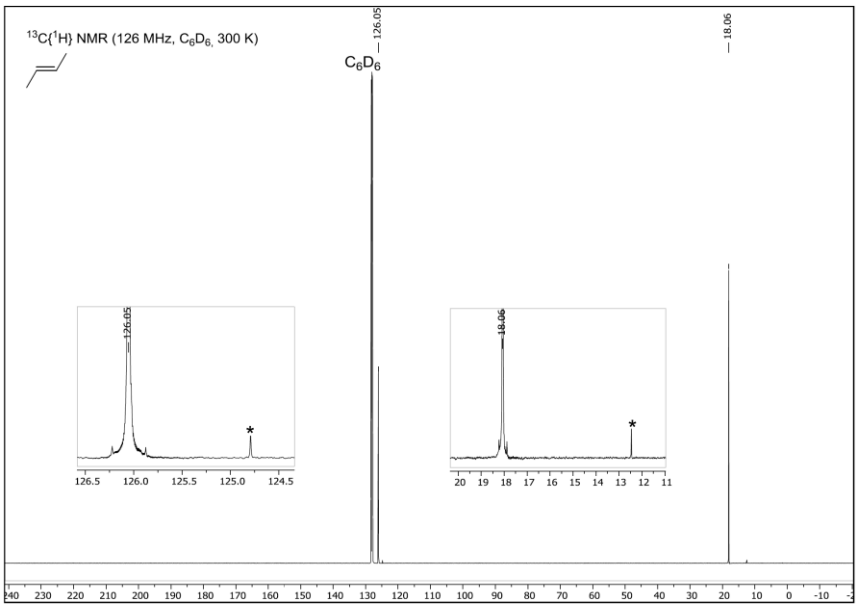


Figure S24. ^{13}C{^{1}H} NMR spectrum of (*E*)-2-butene in C_6D_6 at 300 K. The respective resonances of the (*Z*)-2-butene contamination are marked with asterisks *.

Spectroscopic data for (*Z*)-2-butene:



C_4H_8
56.11 g/mol

^{1}H NMR (500 MHz, C_6D_6, 300 K): δ [ppm] = 5.52–5.44 (m, 2H, C*H*), 1.52–1.50 (m, 6H, C*H*$_3$).

^{13}C{^{1}H} NMR (126 MHz, C_6D_6, 300 K): δ [ppm] = 124.8 (*C*H), 12.5 (*C*H$_3$).

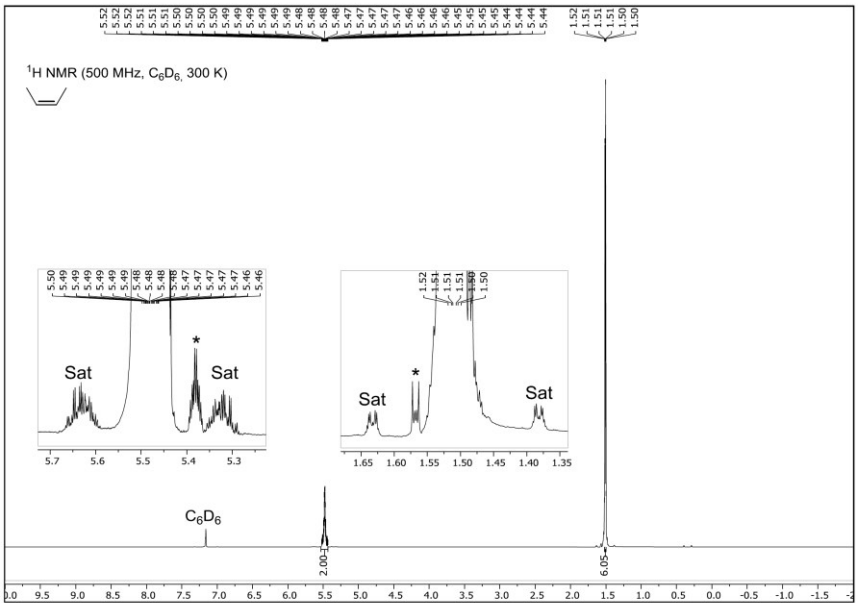


Figure S25. ^{1}H NMR spectrum of (*Z*)-2-butene in C_6D_6 at 300 K. The respective resonances of the (*E*)-2-butene contamination are marked with asterisks * and ^{13}C satellites with Sat.

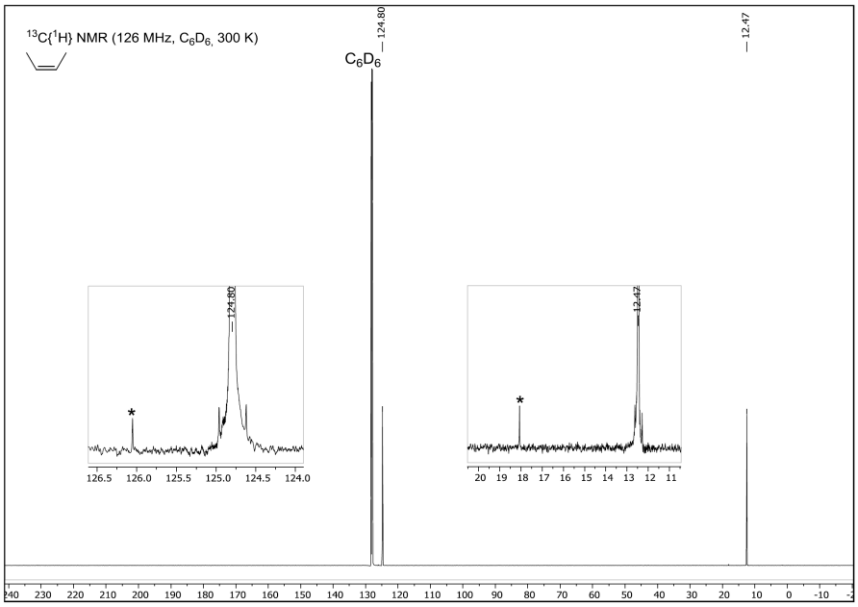
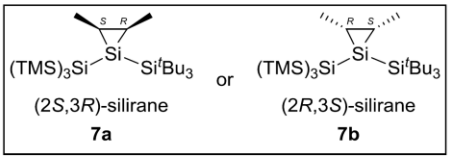


Figure S26. $^{13}C\{^1H\}$ NMR spectrum of (*Z*)-2-butene in C_6D_6 at 300 K. The respective resonances of the (*E*)-2-butene contamination are marked with asterisks *.

Reaction with (*Z*)-2-butene: synthesis of *cis*-silirane 7



$C_{25}H_{62}Si_6$
531.28 g/mol

A solution of **3/3'** (150 mg, 316 µmol) in *n*-hexane (5 mL) was frozen in liquid nitrogen, degassed and warmed to –30 °C. Subsequently, the solution was exposed to (*Z*)-2-butene (1 bar) under vigorous stirring. The reaction mixture was warmed to ambient temperature, whereby the color changed from blood red to pale yellow. Removal of all volatiles *in vacuo* furnished *cis*-silirane **7** as an off-white solid (168 mg, 316 µmol, quantitative yield).

^{1}H NMR (500 MHz, C_6D_6, 300 K): δ [ppm] = 1.57 (d, ^3J = 2.3 Hz, 3H, CHC*H*$_3$), 1.56 (d, ^3J = 2.3 Hz, 3H, CHC*H*$_3$), 1.34–1.31 (m, 2H, C*H*CH$_3$), 1.26 (s, 27H, C(C*H*$_3$)$_3$), 0.39 (s, 27H, *TMS*).

$^{13}C\{^1H\}$ NMR (101 MHz, C_6D_6, 300 K): δ [ppm] = 32.9 (C(*C*H$_3$)$_3$), 24.3 (*C*(CH$_3$)$_3$), 17.7 (*C*HCH$_3$), 13.7 (CH*C*H$_3$), 4.5 (*TMS*).

$^{29}Si\{^1H\}$ NMR (79 MHz, C_6D_6, 300 K): δ [ppm] = 27.3 (*Si*^{t}Bu$_3$), –8.4 (*TMS*), –100.5 (*Si*(TMS)$_3$), –131.7 (*central Si*).

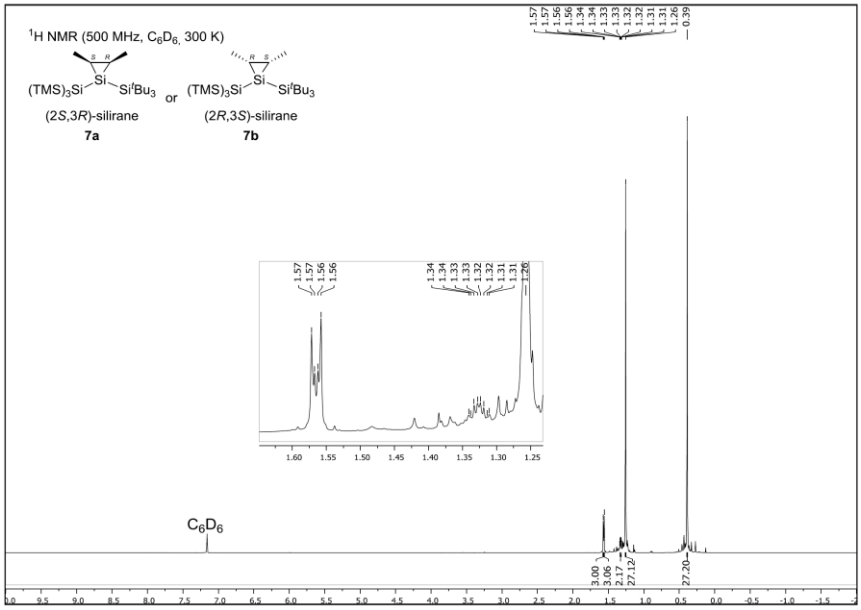


Figure S27. ^{1}H NMR spectrum of *cis*-silirane **7** in C_6D_6 at 300 K.

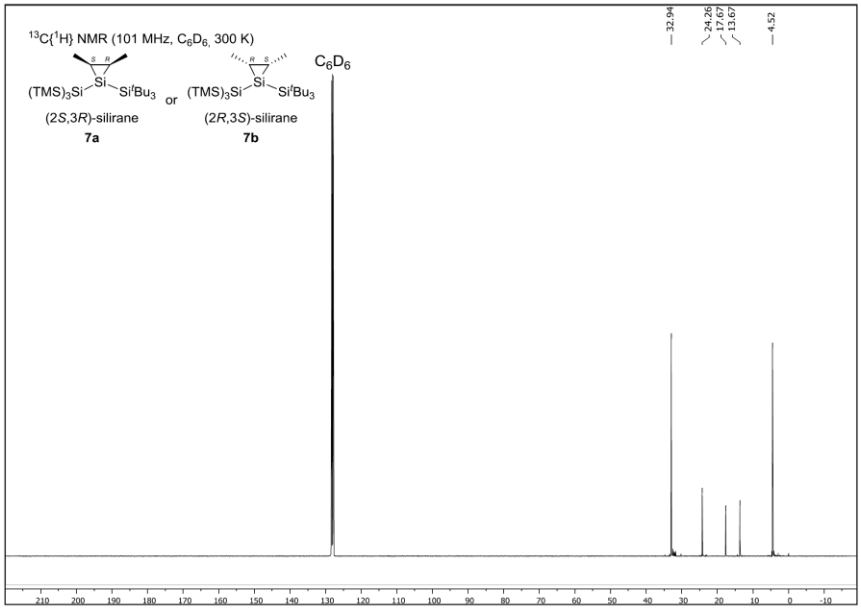


Figure S28. $^{13}C\{^1H\}$ NMR spectrum of *cis*-silirane **7** in C_6D_6 at 300 K.

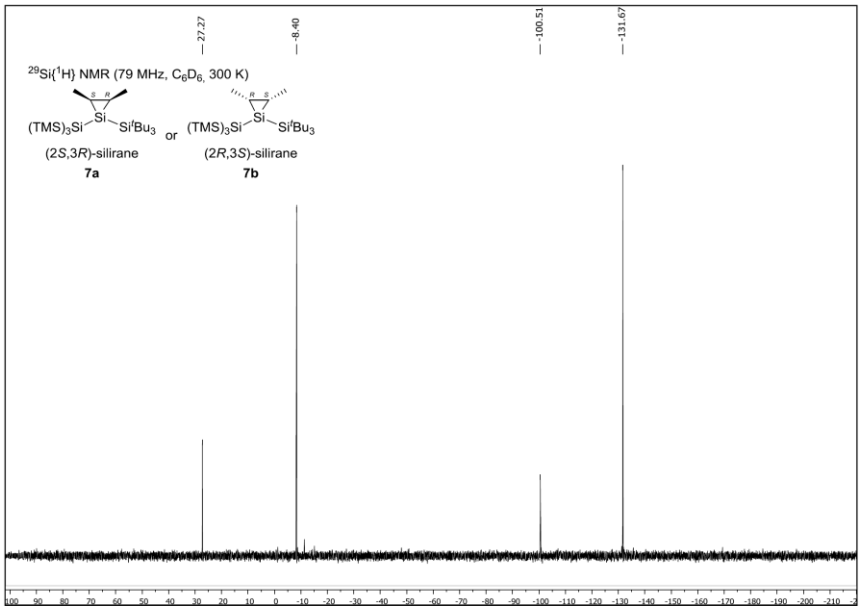


Figure S29. $^{29}Si\{^{1}H\}$ NMR spectrum of *cis*-silirane **7** in C_6D_6 at 300 K.

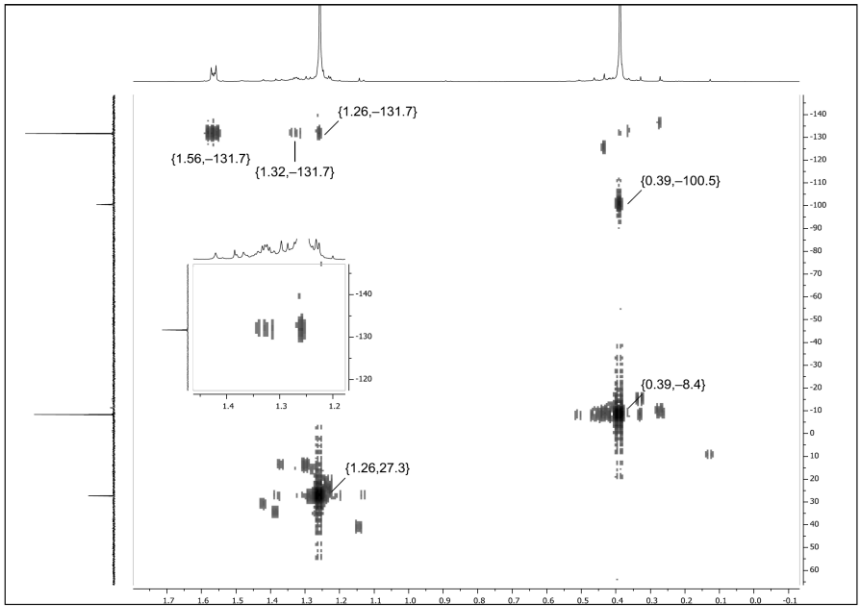
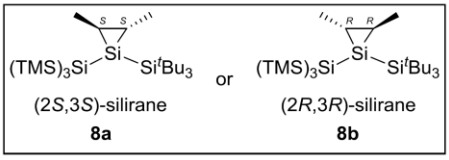


Figure S30. $^{1}H/^{29}Si$ HMBC NMR spectrum of *cis*-silirane **7** in C_6D_6 at 300 K.

Reaction with (*E*)-2-butene: synthesis of *trans*-silirane 8 (& *cis*-silirane 7)



$C_{25}H_{62}Si_6$
531.28 g/mol

A solution of **3/3'** (150 mg, 316 µmol) in *n*-hexane (5 mL) was frozen in liquid nitrogen, degassed and warmed to –30 °C. Subsequently, the solution was exposed to (*E*)-2-butene (1 bar) under vigorous stirring. The reaction mixture was warmed to ambient temperature, whereby the color changed from blood red to pale yellow. Removal of all volatiles *in vacuo* provided a ~50:50 mixture of *trans*-silirane **8** and *cis*-silirane **7** as an off-white oil (168 mg, 316 µmol, quantitative yield).

NMR characterization of *trans*-silirane 8:

^{1}H NMR (500 MHz, C_6D_6, 300 K): δ [ppm] = 1.68 (d, ^{3}J = 6.9 Hz, 3H, CHC$\underline{H}_3$), 1.60 (d, ^{3}J = 6.9 Hz, 3H, CHC$\underline{H}_3$), 1.24 (s, 27H, C(C$\underline{H}_3$)$_3$), 1.05 (dq, ^{3}J = 12.1 Hz, ^{3}J = 6.9 Hz, 1H, C$\underline{H}$CH$_3$), 0.79 (dq, ^{3}J = 12.1 Hz, ^{3}J = 6.9 Hz, 1H, C$\underline{H}$CH$_3$), 0.40 (s, 27H, $\underline{TMS}$).

^{13}C{^{1}H} NMR (101 MHz, C_6D_6, 300 K): δ [ppm] = 33.0 (C($\underline{C}$H$_3$)$_3$), 24.5 ($\underline{C}$(CH$_3$)$_3$), 23.8 ($\underline{C}$HCH$_3$), 20.5 (CH$\underline{C}$H$_3$), 19.7 ($\underline{C}$HCH$_3$), 18.3 (CH$\underline{C}$H$_3$), 5.0 ($\underline{TMS}$).

^{29}Si{^{1}H} NMR (79 MHz, C_6D_6, 300 K): δ [ppm] = 25.2 ($\underline{Si}$^{t}Bu$_3$), –8.5 ($\underline{TMS}$), –109.2 ($\underline{Si}$(TMS)$_3$), –123.3 ($\underline{central\ Si}$).

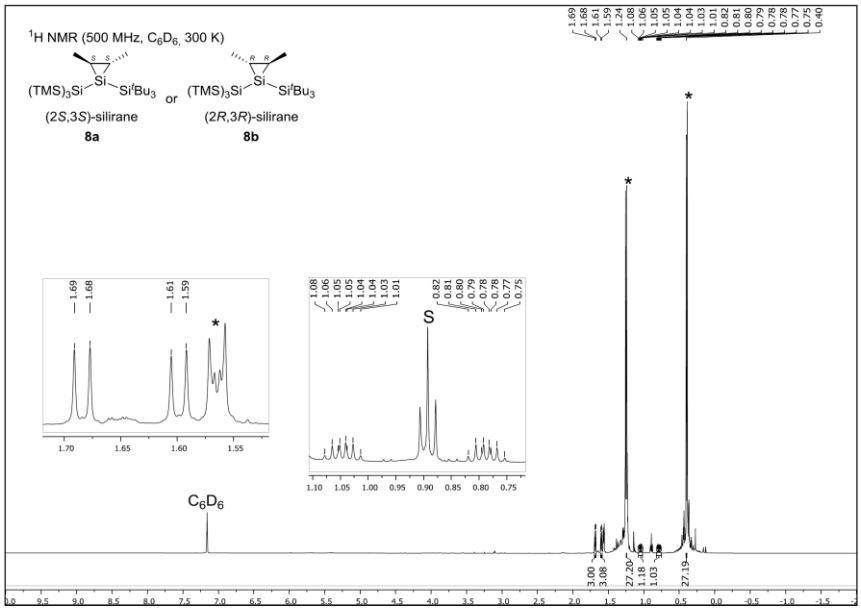


Figure S31. ^{1}H NMR spectrum of *trans*-silirane **8** and **7** in C_6D_6 at 300 K. The respective resonances of *cis*-silirane **7** are marked with asterisks * and residual *n*-hexane with an S.

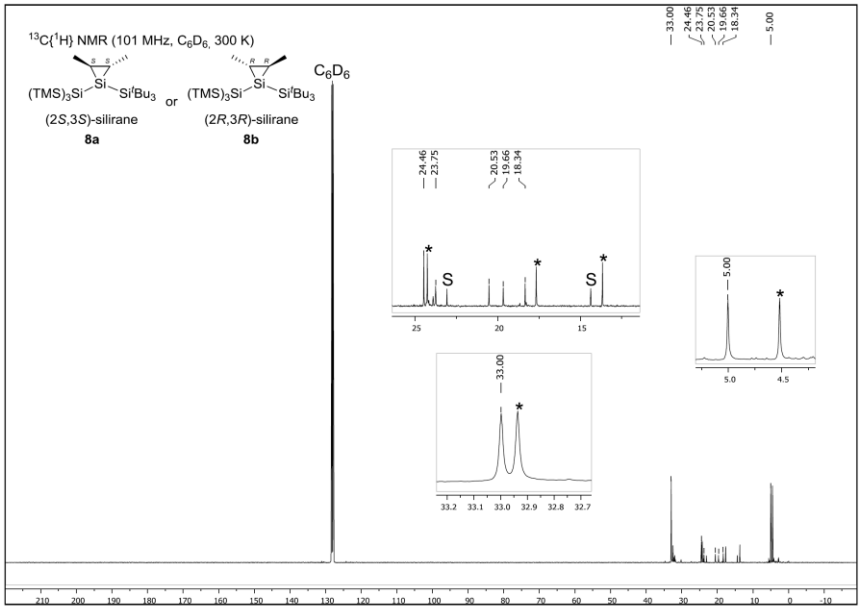


Figure S32. ^{13}C{^{1}H} NMR spectrum of *trans*-silirane **8** and **7** in C_6D_6 at 300 K. The respective resonances of *cis*-silirane **7** are marked with asterisks * and residual *n*-hexane with an S.

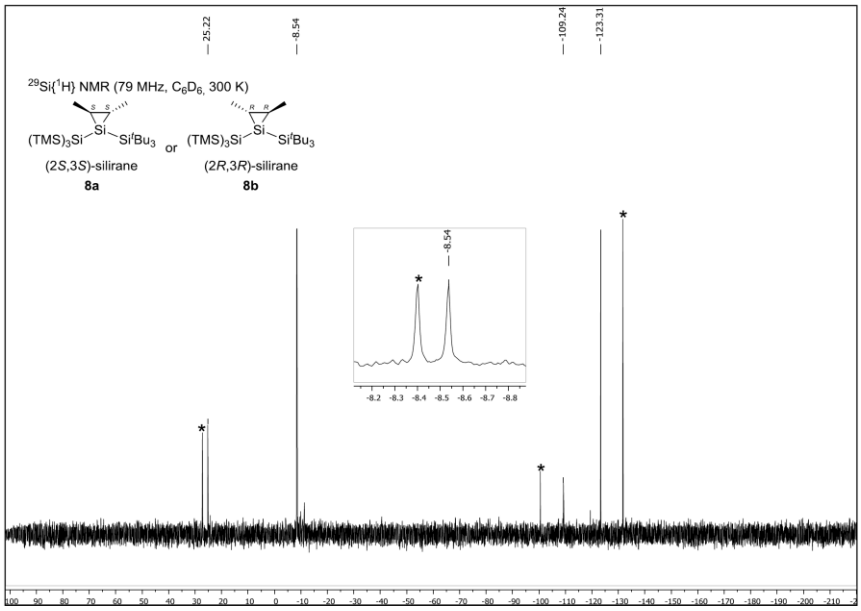


Figure S33. $^{29}Si\{^{1}H\}$ NMR spectrum of *trans*-silirane **8** and **7** in C_6D_6 at 300 K. The respective resonances of *cis*-silirane **7** are marked with asterisks *.

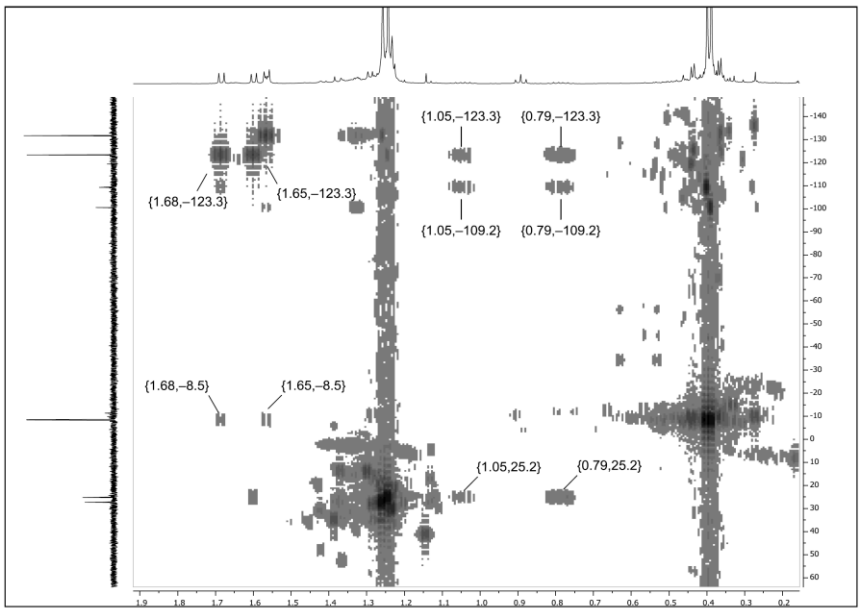


Figure S34. $^{1}H/^{29}Si$ HMBC NMR spectrum of *trans*-silirane **8** and **7** in C_6D_6 at 300 K.

Reaction with an approx. 50/50 mixture of (*E*)-2-butene and (*Z*)-2-butene:

Two thick-walled, PTFE-capped pressurizeable Schlenk flasks were evacuated and subsequently filled with (*E*)-2-butene and (*Z*)-2-butene, respectively (1 bar each). Both gases were transferred *via* vacuum to another thick-walled, PTFE-capped pressurizeable, cooled (–30 °C) *Schlenk* flask. The liquefied gases were vigorously stirred and vacuum transferred to a cooled (–30 °C) *J. Young* PTFE valve NMR tube containing frozen C_6D_6 (0.5 mL). The thus prepared gas mixture was analyzed by ^{1}H and ^{13}C NMR spectroscopy (*vide infra*).

In a second experiment, the prepared gas mixture was vacuum transferred to a cooled (–30 °C) *J. Young* PTFE valve NMR tube containing a solution of **3/3'** (10.0 mg, 21.0 µmol) in *n*-hexane (0.5 mL). Subsequently, the reaction mixture was warmed to ambient temperature under shaking, whereby the color changed from blood red to pale yellow. All volatiles were removed *in vacuo* and the resulting off-white solid dissolved in C_6D_6. NMR spectroscopy revealed quantitative formation of *cis*-silirane **7**.

According to this result, the non-stereospecific addition of **3**/**3'** to (*E*)-2-butene (formation of both *trans*-silirane **8** and *cis*-silirane **7**) presumably stems from the (*Z*)-2-butene contamination, since the reactivity of the (*Z*)-isomer is expected to be significantly higher. Similar conclusions were already drawn during the reinvestigation of [2+1] cycloaddition reactions of dimesitylsilylene to stereogenic alkenes.[S9b] In addition, it was assumed that smaller alkene substituents lead to a higher preference of the respective (*Z*)-isomer by sterically demanding silylenes. Therefore, further experiments with (*E*)/(*Z*)-3-hexene and (*E*)/(*Z*)-stilbene (1,2-diphenylethylene) were performed to prove the contamination assumption as a potential source for the loss of stereochemistry (*vide infra*).

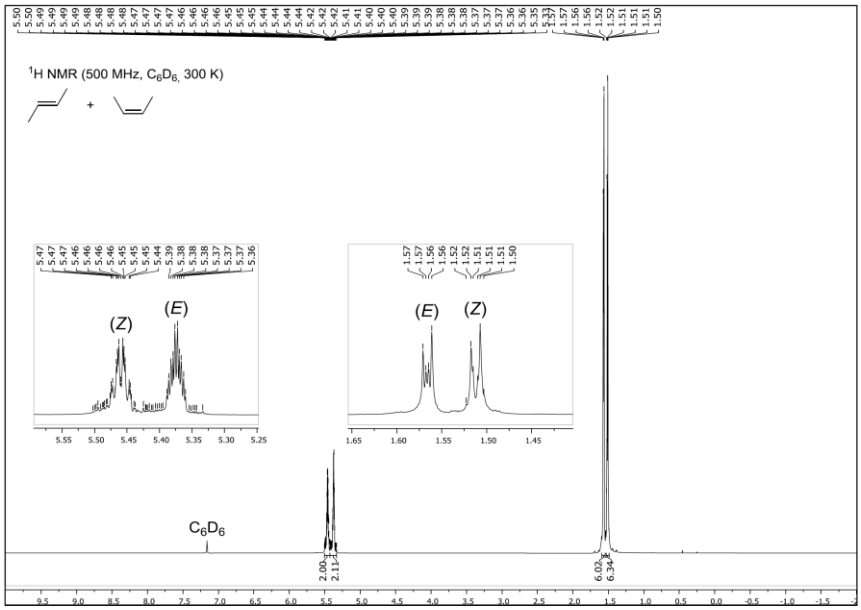


Figure S35. ^{1}H NMR spectrum of an approx. 50/50 mixture of (*E*)-2-butene and (*Z*)-2-butene in C_6D_6 at 300 K.

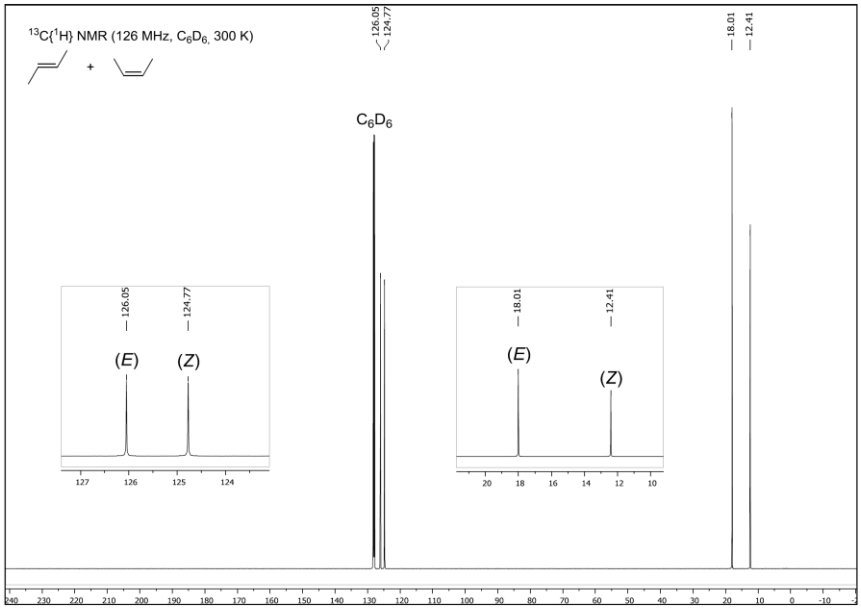
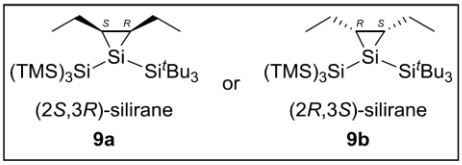


Figure S36. ^{13}C{^{1}H} NMR spectrum of an approx. 50/50 mixture of (*E*)-2-butene and (*Z*)-2-butene in C_6D_6 at 300 K.

Reaction with (*Z*)-3-hexene: synthesis of *cis*-silirane 9



$C_{27}H_{66}Si_6$
559.34 g/mol

To a cooled (–30 °C) solution of **3/3'** (30.0 mg, 63.1 µmol, 1.0 eq.) in *n*-hexane (1 mL) was added (*Z*)-3-hexene (5.31 mg, 63.1 µmol, 1.0 eq.) under vigorous stirring. Subsequently, the reaction mixture was warmed to ambient temperature, whereby the color changed from blood red to pale yellow. Removal of all volatiles *in vacuo* furnished *cis*-silirane **9** as an off-white solid (35.1 mg, 63.1 µmol, quantitative yield).

^{1}H NMR (500 MHz, C_6D_6, 300 K): δ [ppm] = 1.92–1.86 (m, 4H, C*H*$_2$CH$_3$), 1.26 (s, 27H, C(C*H*$_3$)$_3$), 0.40 (s, 27H, *TMS*). The resonances for the C*H*CH$_2$ and CH$_2$C*H*$_3$ protons could not be clearly assigned due to overlapping signals.

^{29}Si{^{1}H} NMR (99 MHz, C_6D_6, 300 K): δ [ppm] = 27.3 (*Si*^{t}Bu$_3$), –8.6 (*TMS*), –100.3 (*Si*(TMS)$_3$), –133.2 (*central Si*).

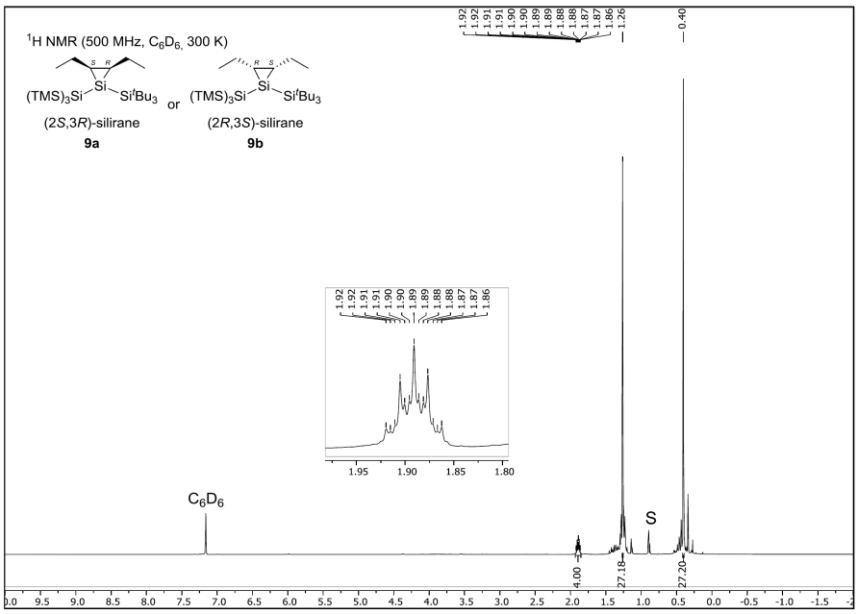


Figure S37. ^{1}H NMR spectrum of *cis*-silirane **9** in C_6D_6 at 300 K. Residual *n*-hexane is marked with an S.

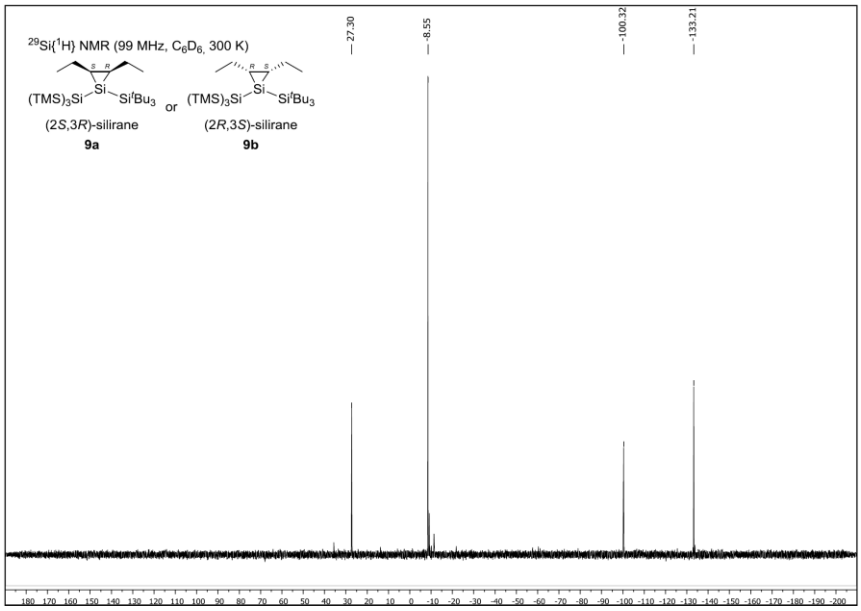


Figure S38. $^{29}Si\{^1H\}$ NMR spectrum of *cis*-silirane **9** in C_6D_6 at 300 K.

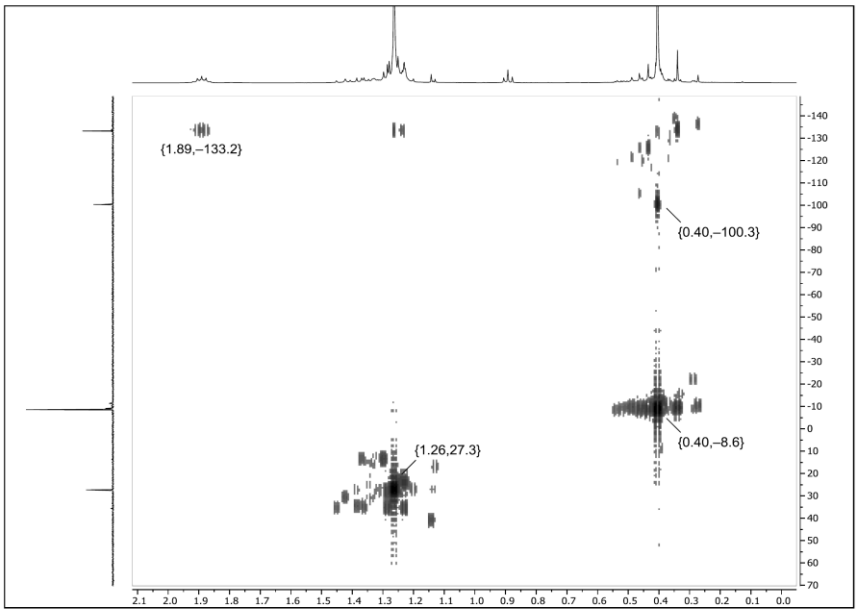
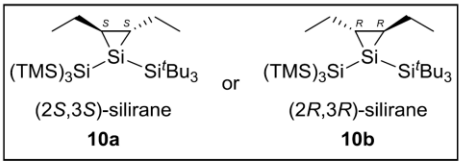


Figure S39. $^1H/^{29}Si$ HMBC NMR spectrum of *cis*-silirane **9** in C_6D_6 at 300 K.

Reaction with (*E*)-3-hexene: synthesis of *trans*-silirane 10



(2*S*,3*S*)-silirane **10a** or (2*R*,3*R*)-silirane **10b**

$C_{27}H_{66}Si_6$
559.34 g/mol

To a cooled (–30 °C) solution of **3/3'** (30.0 mg, 63.1 µmol, 1.0 eq.) in *n*-hexane (1 mL) was added (*E*)-3-hexene (5.31 mg, 63.1 µmol, 1.0 eq.) under vigorous stirring. Subsequently, the reaction mixture was warmed to ambient temperature, whereby the color changed from blood red to pale yellow. Removal of all volatiles *in vacuo* provided a mixture of *trans*-silirane **10**, disiletane **4** and other impurities as an off-white oil.

NMR characterization of *trans*-silirane 10:

^{1}H NMR (500 MHz, C_6D_6, 300 K): δ [ppm] = 1.27 (s, 27H, C(C<u>*H*</u>$_3$)$_3$), 0.41 (s, 27H, <u>*TMS*</u>). The resonances for the C<u>*H*</u>CH$_2$, C<u>*H*</u>$_2$CH$_3$ and CH$_2$C<u>*H*</u>$_3$ protons could not be clearly assigned due to overlapping signals.

^{29}Si{^{1}H} NMR (99 MHz, C_6D_6, 300 K): δ [ppm] = 26.2 (<u>*Si*</u>^{t}Bu$_3$), –8.4 (<u>*TMS*</u>), –108.5 (<u>*Si*</u>(TMS)$_3$), –127.1 (<u>*central Si*</u>).

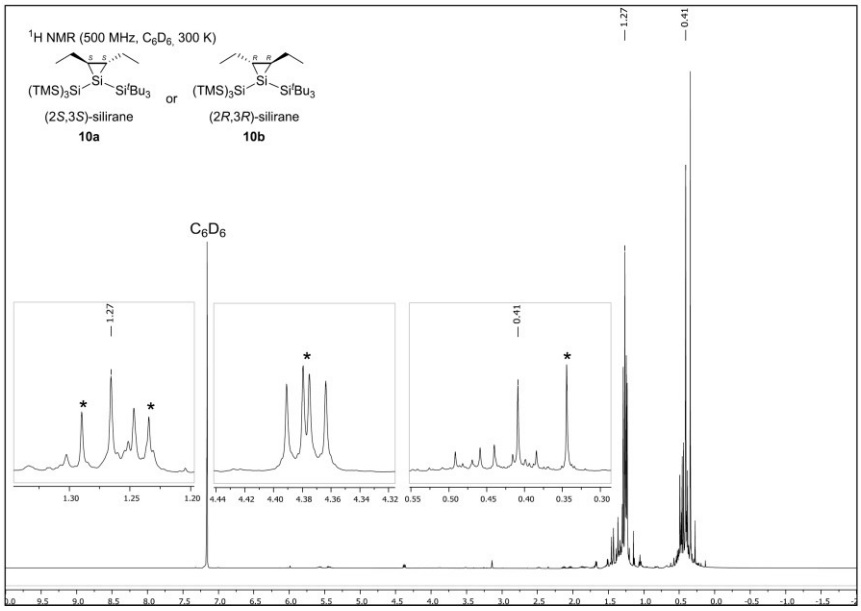


Figure S40. ^{1}H NMR spectrum of *trans*-silirane **10** and **4** in C_6D_6 at 300 K. The respective resonances of disiletane **4** are marked with asterisks *.

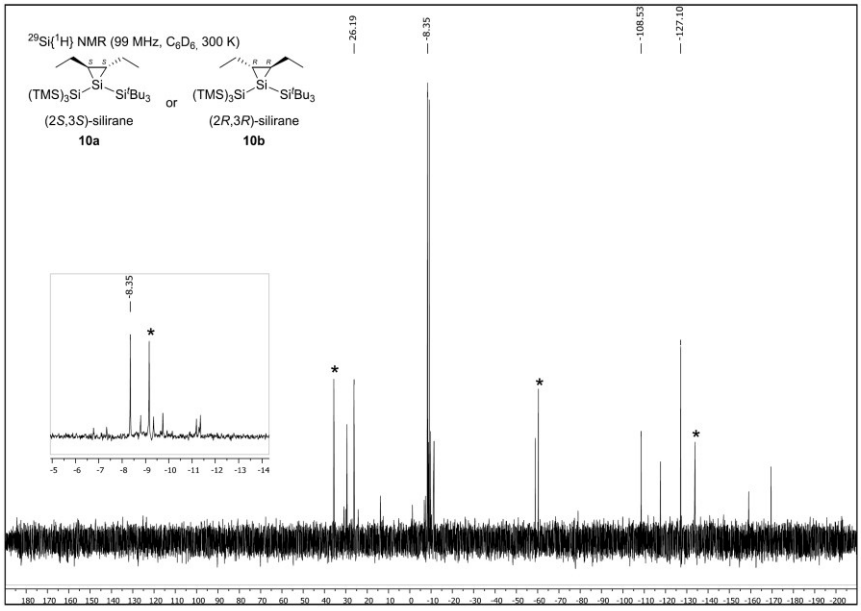
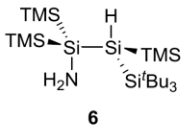


Figure S41. ^{29}Si{^{1}H} NMR spectrum of *trans*-silirane **10** and **4** in C_6D_6 at 300 K. The respective resonances of disiletane **4** are marked with asterisks *.

Reaction with (*E*)-stilbene and (*Z*)-stilbene:

Exposure of **3**/**3'** to (*E*)-stilbene and (*Z*)-stilbene resulted in no reaction but disiletane **4** formation, presumably due to steric reasons.

1.9 Synthesis of aminosilane 6



6

$C_{21}H_{57}NSi_6$

492.20 g/mol

To a cooled (–80 °C) solution of **3**/**3'** (375 mg, 789 µmol, 1.0 eq.) in *n*-hexane (60 mL) was added a 0.4 M NH_3 solution in 1,4-dioxane (1.97 mL, 13.4 mg, 789 µmol, 1.0 eq.) under vigorous stirring. An immediate color change from blood red to pale yellow with concomitant precipitation (1,4-dioxane) was observed. Stirring was continued at –80 °C for one hour and subsequently the solution was warmed to ambient temperature. All volatiles were removed *in vacuo*, providing crude aminosilane **6** as an orange oil. Multinuclear and 2D NMR analysis clearly revealed **6** as the major product. However, all further purification attempts *via* crystallization, distillation or washing were unsuccessful so far.

^{1}H NMR (500 MHz, C_6D_6, 300 K): δ [ppm] = 3.08 (s, 1H, Si*H*), 1.24 (s, 27H, C(C*H*$_3$)$_3$), 0.37 (s, 9H, *TMS*), 0.32 (s, 18H, *TMS*), –0.17 (br s, 2H, SiN*H*$_2$).

^{13}C{^{1}H} NMR (126 MHz, C_6D_6, 300 K): δ [ppm] = 32.1 (C(*C*H$_3$)$_3$), 23.6 (*C*(CH$_3$)$_3$), 4.6 (*TMS*), 1.2 (*TMS*), 0.5 (*TMS*).

^{29}Si{^{1}H} NMR (99 MHz, C_6D_6, 300 K): δ [ppm] = 29.6 (*Si*^{t}Bu$_3$), –11.5 (*TMS*), –12.2 (*TMS*), –12.9 (*TMS*), –35.7 (*Si*NH$_2$), –119.9 (*Si*H).

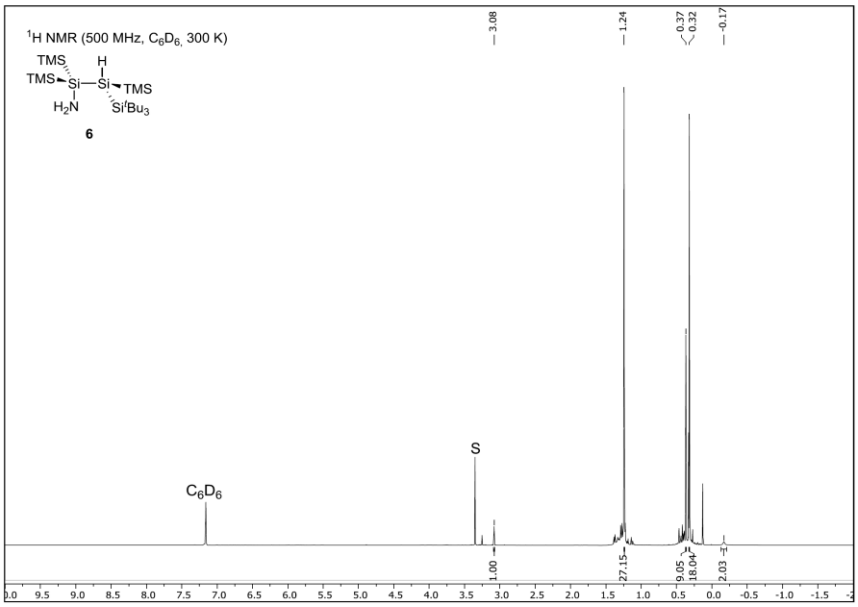


Figure S42. ^{1}H NMR spectrum of aminosilane **6** in C_6D_6 at 300 K. Residual 1,4-dioxane is marked with an S.

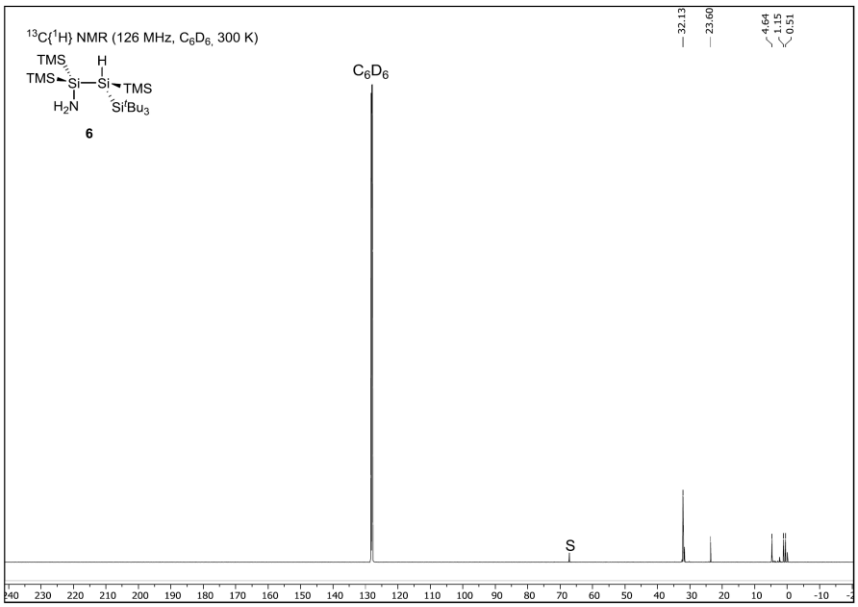


Figure S43. $^{13}C\{^1H\}$ NMR spectrum of aminosilane **6** in C_6D_6 at 300 K. Residual 1,4-dioxane is marked with an S.

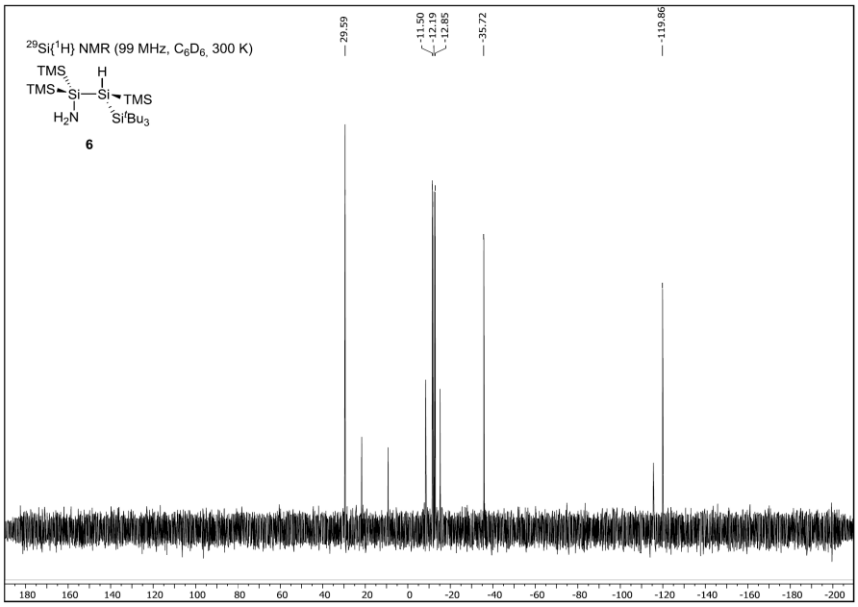
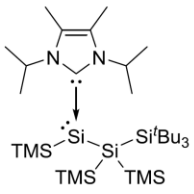


Figure S44. $^{29}Si\{^{1}H\}$ NMR spectrum of aminosilane **6** in C_6D_6 at 300 K.

1.10 Synthesis of (TMS)((TMS)$_2$(^{t}Bu$_3$Si)Si)Si(I^{i}Pr$_2$Me$_2$) (13)



13
$C_{32}H_{74}N_2Si_6$
655.47 g/mol

THF (60 mL) was added to a mixture of **2** (3.00 g, 4.72 mmol, 1.0 eq.), I^{i}Pr$_2$Me$_2$ (852 mg, 4.72 mmol, 1.0 eq.) and KC_8 (1.28 g, 9.45 mmol, 2.0 eq.) at ambient temperature. After stirring the reaction mixture for 1 h, the solvent was removed *in vacuo* and the residue was extracted with toluene (3 × 20 mL). Graphite and KBr were separated from the mixture by filtration and the solvent was removed under high vacuum to furnish **13** as a purple-red solid (3.01 g, 4.59 mmol, 97%). Crystals suitable for SC-XRD analysis were obtained by cooling a concentrated THF solution of **13** to –35 °C for several days. The NHC-stabilized bis(silyl)silylene **13** is completely stable as a solid and in solution at room temperature, but partially isomerizes to ((TMS)$_3$Si)(^{t}Bu$_3$Si)Si(I^{i}Pr$_2$Me$_2$) (**15**) (*vide infra*) at elevated temperatures.

m.p.: 160-161 °C (decomposition; color change from purple-red to orange).

^{1}H NMR (500 MHz, C$_6$D$_6$, 300 K): δ [ppm] = 6.58 (sept, ^3J = 7.1 Hz, 2H, NC*H*(CH$_3$)$_2$), 1.57 (s, 6H, CC*H*$_3$), 1.42 (s, 27H, C(C*H*$_3$)$_3$), 1.28 (d, ^3J = 7.1 Hz, 6H, NCH(C*H*$_3$)$_2$), 1.24 (d, ^3J = 7.1 Hz, 6H, NCH(C*H*$_3$)$_2$), 0.63 (s, 18H, *TMS*), 0.37 (s, 9H, *TMS*).

$^{13}C\{^1H\}$ NMR (126 MHz, C_6D_6, 300 K): δ [ppm] = 171.9 (*carbene C*), 126.5 ($\underline{C}CH_3$), 53.3 ($N\underline{C}H(CH_3)_2$), 33.7 ($C(\underline{C}H_3)_3$), 25.0 ($\underline{C}(CH_3)_3$), 22.5 ($NCH(\underline{C}H_3)_2$), 22.2 ($NCH(\underline{C}H_3)_2$), 10.5 ($C\underline{C}H_3$), 7.2 (*TMS*), 6.3 (*TMS*).

$^{29}Si\{^1H\}$ NMR (99 MHz, C_6D_6, 300 K): δ [ppm] = 29.4 ($\underline{Si}^t Bu_3$), –9.1 (*TMS*), –11.9 (*TMS*), –104.7 (*silylene Si*), –117.4 ($\underline{Si}(TMS)_2$).

IR (solid): $\tilde{\nu}$ [cm^{-1}] = 2949 (m), 2884 (m), 2851 (m), 1632 (w), 1477 (w), 1352 (m), 1238 (m), 1103 (w), 1014 (w), 828 (s), 749 (m), 673 (m), 618 (m), 492 (m).

Anal. Calcd. [%] for $C_{32}H_{74}N_2Si_6$: C, 58.64; H, 11.38; N, 4.27. Found [%]: C, 58.41; H, 11.49; N, 4.36.

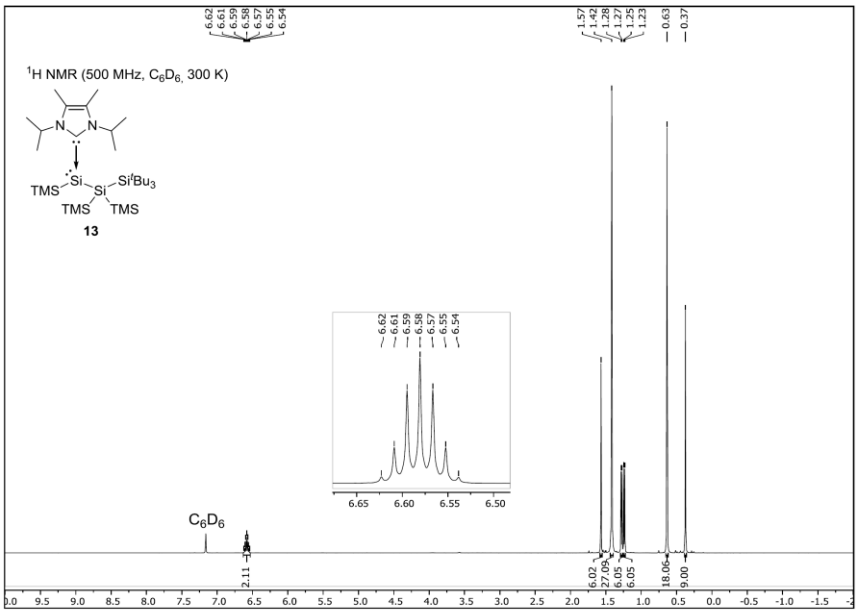


Figure S45. ^{1}H NMR spectrum of (TMS)((TMS)$_2$(^{t}Bu$_3$Si)Si(I^{i}Pr$_2$Me$_2$) (**13**) in C_6D_6 at 300 K.

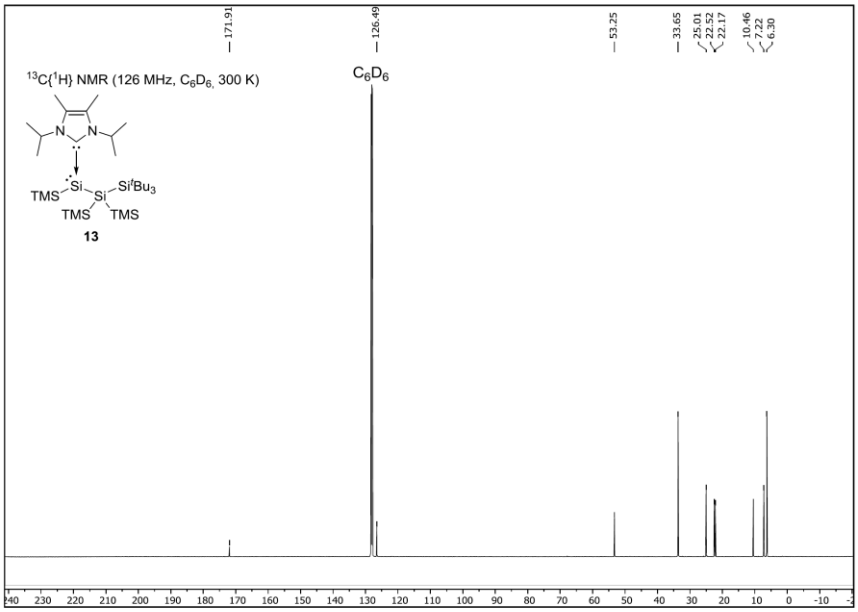


Figure S46. $^{13}C\{^{1}H\}$ NMR spectrum of (TMS)((TMS)$_2$(^{t}Bu$_3$Si)Si)Si(I^{i}Pr$_2$Me$_2$) (**13**) in C_6D_6 at 300 K.

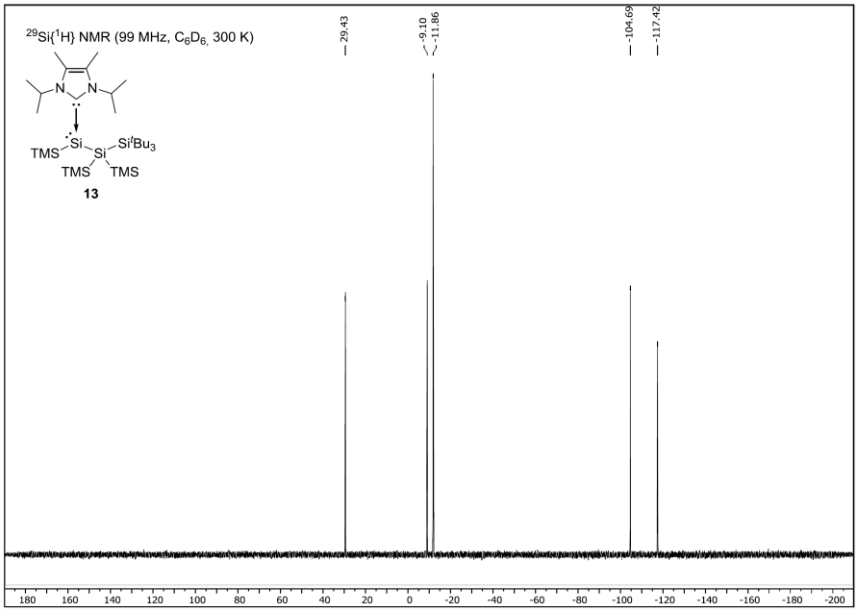


Figure S47. $^{29}Si\{^{1}H\}$ NMR spectrum of (TMS)((TMS)$_2$(^{t}Bu$_3$Si)Si)Si(I^{i}Pr$_2$Me$_2$) (**13**) in C_6D_6 at 300 K.

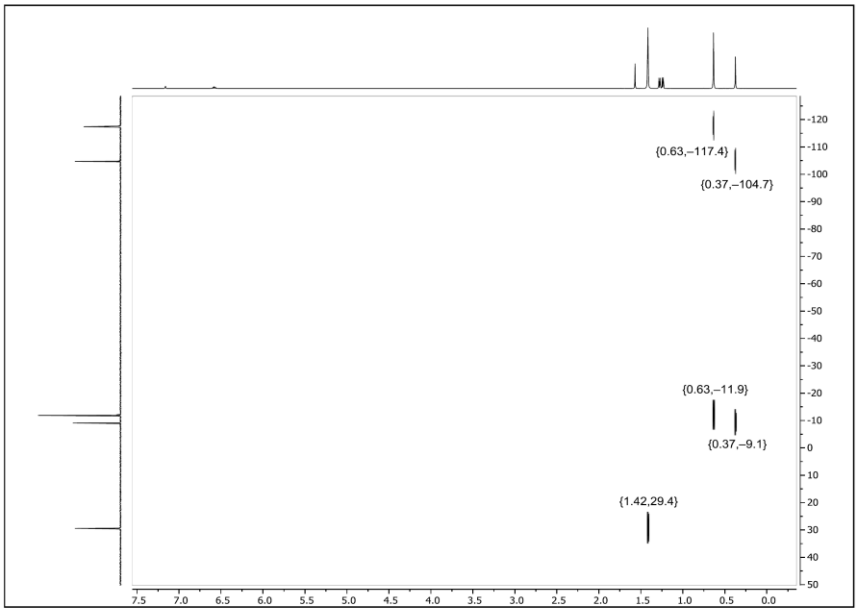


Figure S48. $^{1}H/^{29}Si$ HMBC NMR spectrum of (TMS)((TMS)$_2$(^{t}Bu$_3$Si)Si)Si(I^{i}Pr$_2$Me$_2$) (**13**) in C_6D_6 at 300 K.

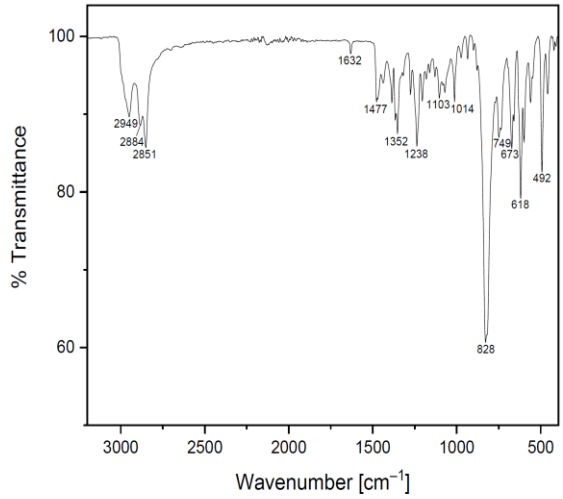
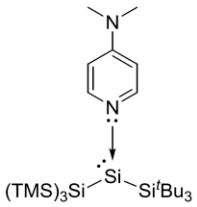


Figure S49. Solid-state FT-IR spectrum of (TMS)((TMS)$_2$(^{t}Bu$_3$Si)Si)Si(I^{i}Pr$_2$Me$_2$) (**13**).

1.11 Synthesis and reactivity of ((TMS)$_3$Si)(^{t}Bu$_3$Si)Si(DMAP) (14)



14
$C_{28}H_{64}N_2Si_6$
597.34 g/mol

THF (10 mL) was added to a mixture of **2** (200 mg, 315 µmol, 1.0 eq.), DMAP (38.5 mg, 315 µmol) and KC_8 (85.2 mg, 630 µmol, 1.0 eq.) at ambient temperature. After stirring the reaction mixture for 1 h, the solvent was removed *in vacuo* and the residue extracted with toluene (3 × 3 mL). Graphite and KBr were separated from the mixture by filtration and the solvent was removed under high vacuum to furnish **14** as a red-brown solid (170 mg, 285 µmol, 90%). Crystals suitable for SC-XRD analysis were obtained by cooling a concentrated THF solution to –35 °C for several days.

m.p.: 59-60 °C (decomposition; color change from red-brown to black)

^{1}H NMR (500 MHz, C_6D_6, 300 K): δ [ppm] = 8.79 (d, ^3J = 7.1 Hz, 2H, *o*-C_{DMAP}*H*), 5.62 (br s, 2H, *m*-C_{DMAP}*H*), 1.72 (s, 6H, N(CH_3)$_2$), 1.47 (s, 27H, C(CH_3)$_3$), 0.51 (s, 27H, *TMS*).

^{13}C{^{1}H} NMR (126 MHz, C_6D_6, 300 K): δ [ppm] = 154.7 (*p*-C_{DMAP}), 105.3 (*m*-C_{DMAP}), 38.1 (N(CH_3)$_2$), 33.2 (C(CH_3)$_3$), 25.5 (C(CH_3)$_3$), 4.9 (*TMS*). Due to a presumable overlap with the solvent signal, the resonance for the *o*-C_{DMAP} nuclei was not directly observed.

^{29}Si{^{1}H} NMR (99 MHz, C_6D_6, 300 K): δ [ppm] = 68.8 (*silylene Si*), 20.4 (*Si*^{t}Bu$_3$), –9.3 (*TMS*), –121.6 (*Si*(TMS)$_3$).

Anal. Calcd. [%] for $C_{28}H_{64}N_2Si_6$: C, 56.30; H, 10.80; N, 4.69. Found [%]: C, 55.98; H, 10.77; N, 4.40.

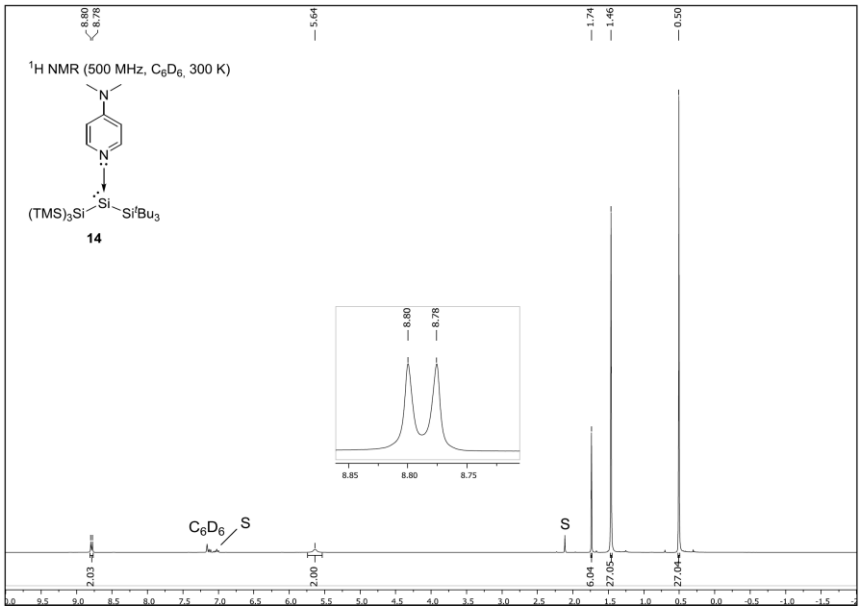


Figure S50. ^{1}H NMR spectrum of $((TMS)_3Si)(^tBu_3Si)Si(DMAP)$ (**14**) in C_6D_6 at 300 K. Residual toluene is labeled with an S.

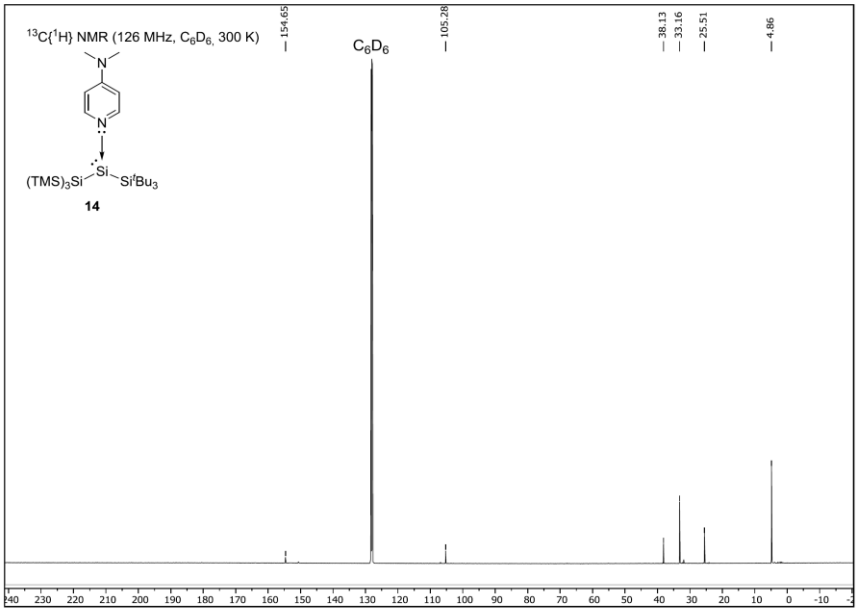


Figure S51. $^{13}C\{^1H\}$ NMR spectrum of $((TMS)_3Si)(^tBu_3Si)Si(DMAP)$ (**14**) in C_6D_6 at 300 K.

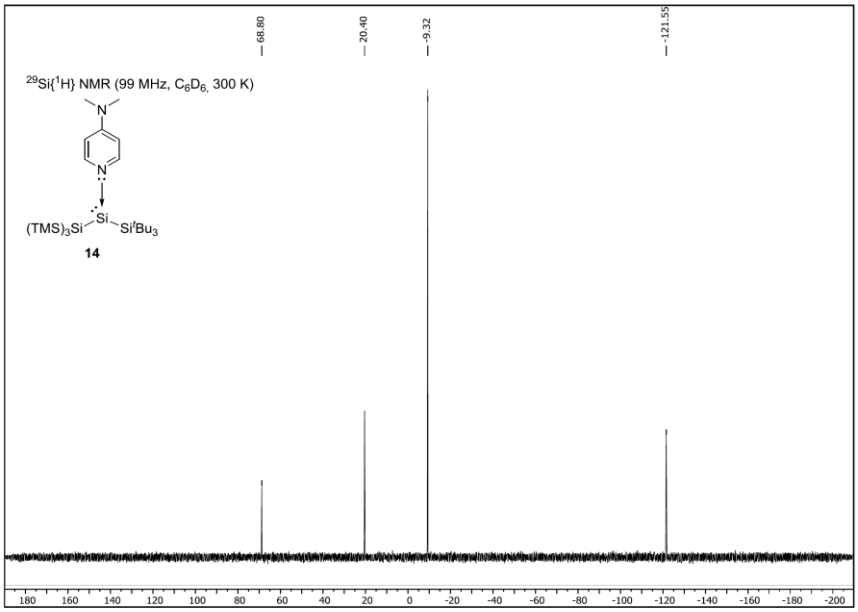


Figure S52. $^{29}Si\{^{1}H\}$ NMR spectrum of ((TMS)$_3$Si)(^{t}Bu$_3$Si)Si(DMAP) (**14**) in C_6D_6 at 300 K.

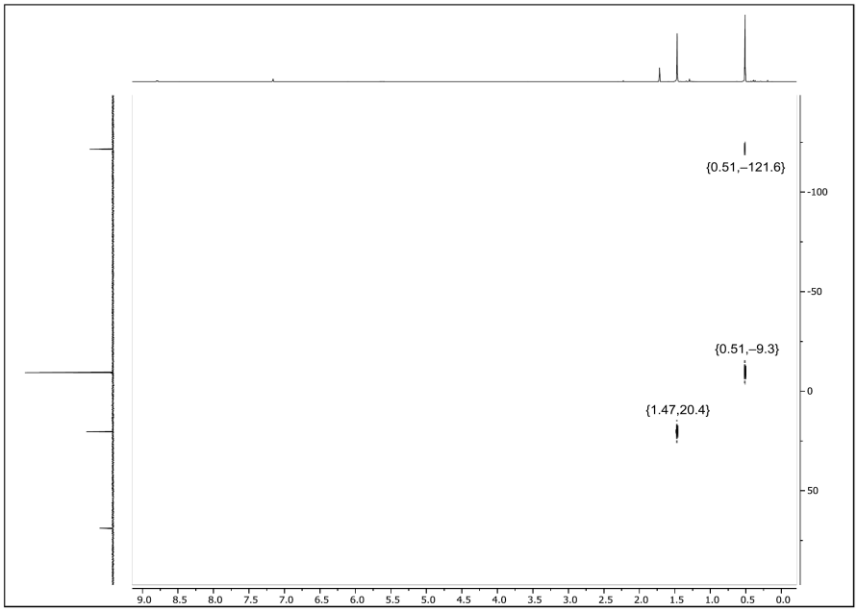
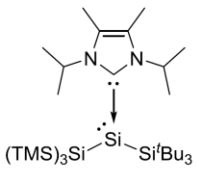


Figure S53. $^{1}H/^{29}Si$ HMBC NMR spectrum of ((TMS)$_3$Si)(^{t}Bu$_3$Si)Si(DMAP) (**14**) in C_6D_6 at 300 K.

Lewis base exchange reaction: synthesis of (TMS)((TMS)$_2$(^{t}Bu$_3$Si)Si)Si(I^{i}Pr$_2$Me$_2$) (13)

A *J. Young* PTFE valve NMR tube was filled with a solution of **14** (20.0 mg, 33.5 µmol, 1.0 eq.) and I^{i}Pr$_2$Me$_2$ (6.04 mg, 33.5 µmol, 1.0 eq.) in C_6D_6 (0.5 mL). Monitoring of the reaction mixture by ^{1}H NMR spectroscopy revealed quantitative conversion of **14** to the NHC-stabilized bis(silyl)silylene **13** with concomitant release of DMAP after 4 days.

1.12 Synthesis of ((TMS)$_3$Si)(^{t}Bu$_3$Si)Si(I^{i}Pr$_2$Me$_2$) (15)



15

$C_{32}H_{74}N_2Si_6$

655.47 g/mol

A solution of **13** (500 mg, 763 µmol) in toluene (10 mL) was heated to 90 °C for 48 h. Subsequently, the solvent was removed *in vacuo*. Multinuclear and 2D NMR spectroscopic analysis of the residue revealed the NHC-stabilized bis(silyl)silylene **15** as the major product (58%). In addition to remaining starting material **13** (16%), the simultaneous formation of disiletane **4** (13%) and free I^{i}Pr$_2$Me$_2$ (13%) was detected. Neither prolonged heating (at different temperatures), nor solvent change to THF, benzene or *n*-hexane affected the outcome of the reaction in favour of **15**. Therefore, the isomerization is presumably an equilibrium reaction, with initial NHC dissociation ultimately competing with re-coordination providing **15** or NHC release and disiletane **4** formation. DFT calculations support this assumption (*vide infra*). Nevertheless, all attempts to purify the residue and isolate **15** *via* crystallization, washing, or sublimation were unsuccessful so far.

^{1}H NMR (500 MHz, C_6D_6, 300 K): δ [ppm] = 6.70 (sept, ^3J = 7.0 Hz, 2H, NC*H*(CH$_3$)$_2$), 1.59 (s, 6H, CC*H*$_3$), 1.41 (s, 27H, C(C*H*$_3$)$_3$), 0.45 (s, 27H, *TMS*). The resonances for the NCH(C*H*$_3$)$_2$) protons could not be clearly assigned due to overlapping signals.

^{13}C{^{1}H} NMR (126 MHz, C_6D_6, 300 K): δ [ppm] = 171.9 (*carbene C*), 127.1 (*C*CH$_3$), 53.4 (N*C*H(CH$_3$)$_2$), 33.8 (C(*C*H$_3$)$_3$), 25.7 (*C*(CH$_3$)$_3$), 23.0 (NCH(*C*H$_3$)$_2$), 22.2 (NCH(*C*H$_3$)$_2$), 10.4 (C*C*H$_3$), 6.0 (*TMS*).

^{29}Si{^{1}H} NMR (99 MHz, C_6D_6, 300 K): δ [ppm] = 31.2 (*Si*^{t}Bu$_3$), –9.9 (*TMS*), –115.2 (*Si*(TMS)$_3$), –120.6 (*silylene Si*).

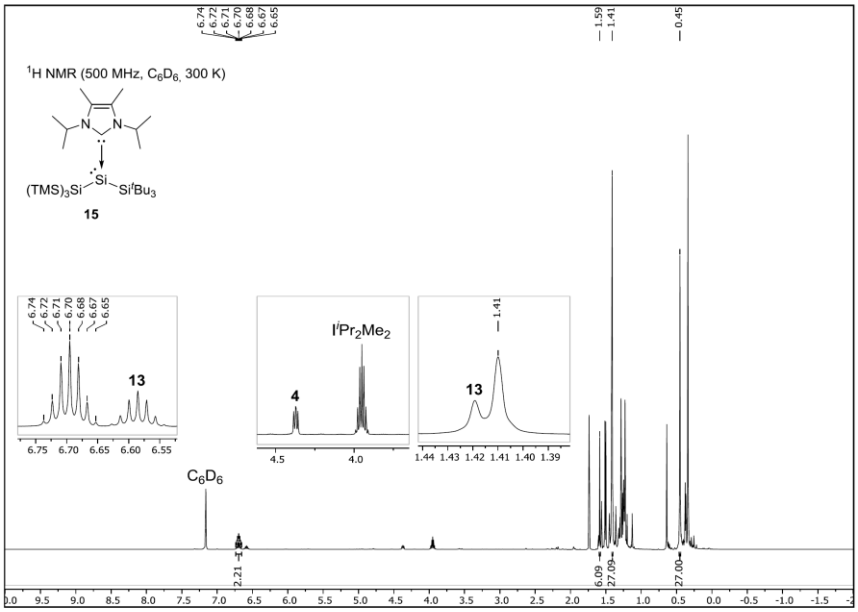


Figure S54. ^{1}H NMR spectrum of ((TMS)$_3$Si)(^{t}Bu$_3$Si)Si(I^{i}Pr$_2$Me$_2$) (**15**) in C_6D_6 at 300 K. Significant resonances for the side products (TMS)((TMS)$_2$(^{t}Bu$_3$Si)Si)Si(I^{i}Pr$_2$Me$_2$) (**13**), disiletane **4** and I^{i}Pr$_2$Me$_2$ are labeled accordingly.

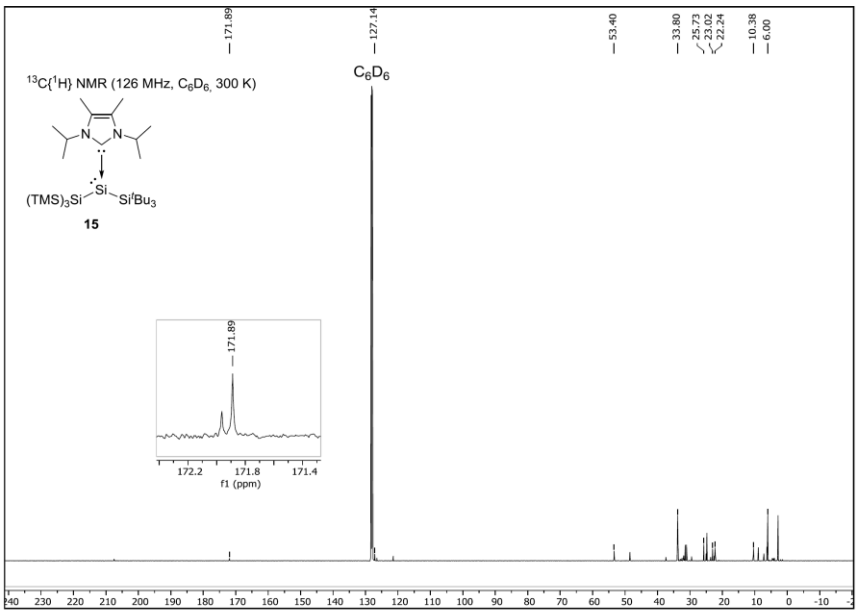


Figure S55. ^{13}C{^{1}H} NMR spectrum of ((TMS)$_3$Si)(^{t}Bu$_3$Si)Si(I^{i}Pr$_2$Me$_2$) (**15**) in C_6D_6 at 300 K. Here, only the resonances for **15** are assigned.

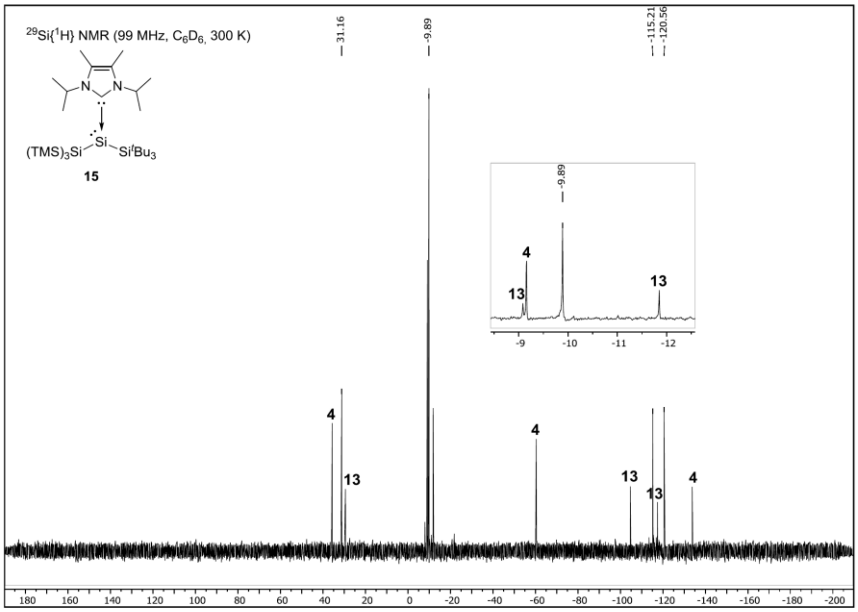


Figure S56. $^{29}Si\{^{1}H\}$ spectrum of $((TMS)_3Si)(^{t}Bu_3Si)Si(I^{i}Pr_2Me_2)$ (**15**) in C_6D_6 at 300 K. The resonances for the side products $(TMS)((TMS)_2(^{t}Bu_3Si)Si)Si(I^{i}Pr_2Me_2)$ (**13**) and disiletane **4** are labeled accordingly.

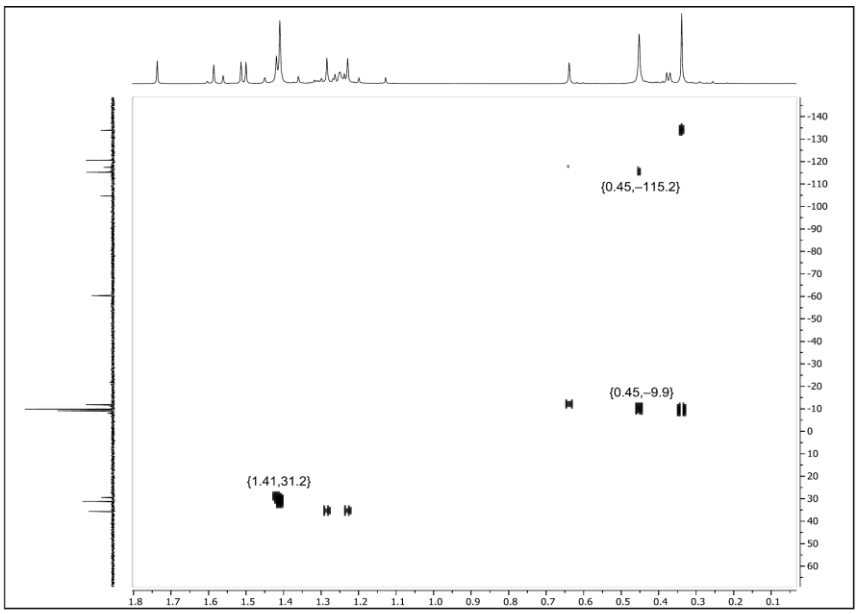
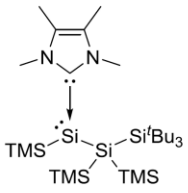


Figure S57. $^{1}H/^{29}Si$ HMBC NMR spectrum of $((TMS)_3Si)(^{t}Bu_3Si)Si(I^{i}Pr_2Me_2)$ (**15**) in C_6D_6 at 300 K. Here, only the correlations for **15** are assigned.

1.13 Synthesis of (TMS)((TMS)$_2$(^{t}Bu$_3$Si)Si)Si(IMe$_4$) (16)



16
$C_{28}H_{66}N_2Si_6$
599.36 g/mol

Toluene (10 mL) was added to a mixture of **13** (300 mg, 458 µmol, 1.0 eq.) and IMe$_4$ (56.8 g, 458 µmol, 1.0 eq.) at ambient temperature. After stirring the reaction mixture for 2 days, the solvent was removed *in vacuo*. Multinuclear and 2D NMR spectroscopic analysis of the residue revealed formation of the NHC-stabilized bis(silyl)silylene **16** and I^{i}Pr$_2$Me$_2$. Nevertheless, all attempts to purify the residue and isolate **16** *via* crystallization, washing, or sublimation were unsuccessful so far. NHC adduct **16** even slowly decomposes in solution to an unidentified product mixture.

^{1}H NMR (500 MHz, C$_6$D$_6$, 300 K): δ [ppm] = 3.68 (s, 6H, NC*H*$_3$), 1.43 (s, 27H, C(C*H*$_3$)$_3$), 1.31 (s, 6H, CC*H*$_3$), 0.53 (s, 18H, *TMS*), 0.39 (s, 9H, *TMS*).

^{13}C{^{1}H} NMR (126 MHz, C$_6$D$_6$, 300 K): δ [ppm] = 172.1 (*carbene C*), 125.4 (*C*CH$_3$), 36.8 (N*C*H$_3$), 33.3 (C(*C*H$_3$)$_3$), 25.1 (*C*(CH$_3$)$_3$), 8.6 (C*C*H$_3$), 6.3 (*TMS*), 5.9 (*TMS*).

^{29}Si{^{1}H} NMR (99 MHz, C$_6$D$_6$, 300 K): δ [ppm] = 30.6 (*Si*^{t}Bu$_3$), –9.2 (*TMS*), –11.4 (*TMS*), –117.1 (*silylene Si*), –118.9 (*Si*(TMS)$_2$).

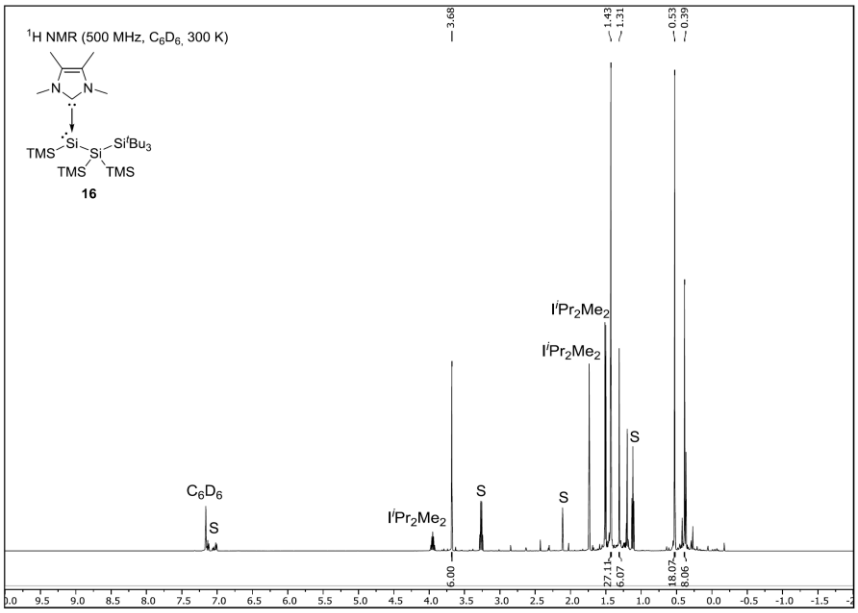


Figure S58. ^{1}H NMR spectrum of (TMS)((TMS)$_2$(^{t}Bu$_3$Si)Si)Si(IMe$_4$) (**16**) in C$_6$D$_6$ at 300 K. Residual solvents (S; toluene and Et$_2$O from a crystallization attempt) and I^{i}Pr$_2$Me$_2$ are labeled accordingly.

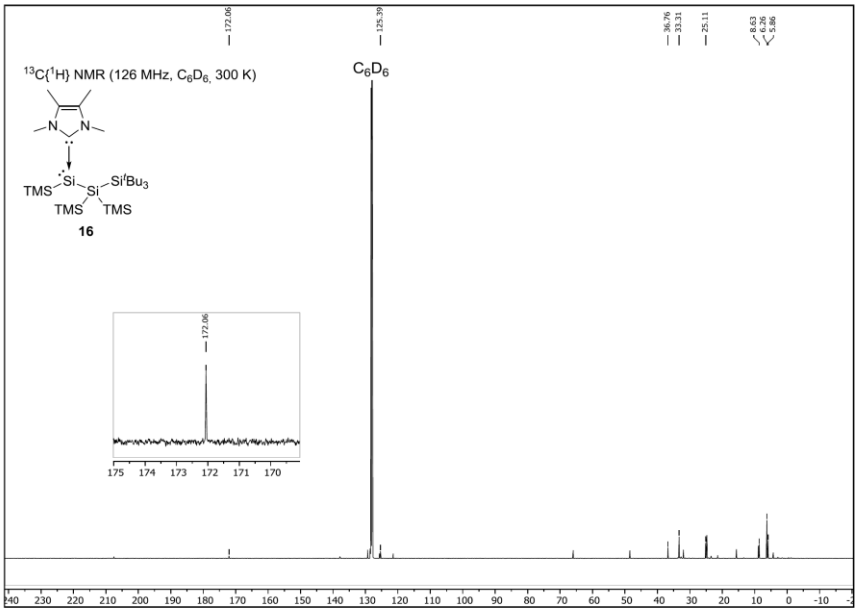


Figure S59. $^{13}C\{^{1}H\}$ NMR spectrum of (TMS)((TMS)$_2$(^{t}Bu$_3$Si)Si)Si(IMe$_4$) (**16**) in C_6D_6 at 300 K. Here, only the resonances for **16** are assigned.

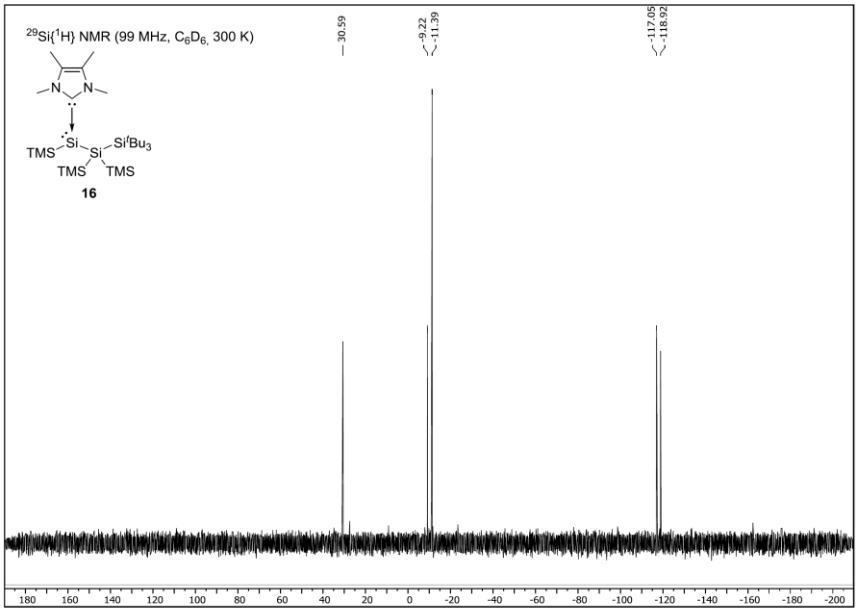


Figure S60. $^{29}Si\{^{1}H\}$ NMR spectrum of (TMS)((TMS)$_2$(^{t}Bu$_3$Si)Si)Si(IMe$_4$) (**16**) in C_6D_6 at 300 K.

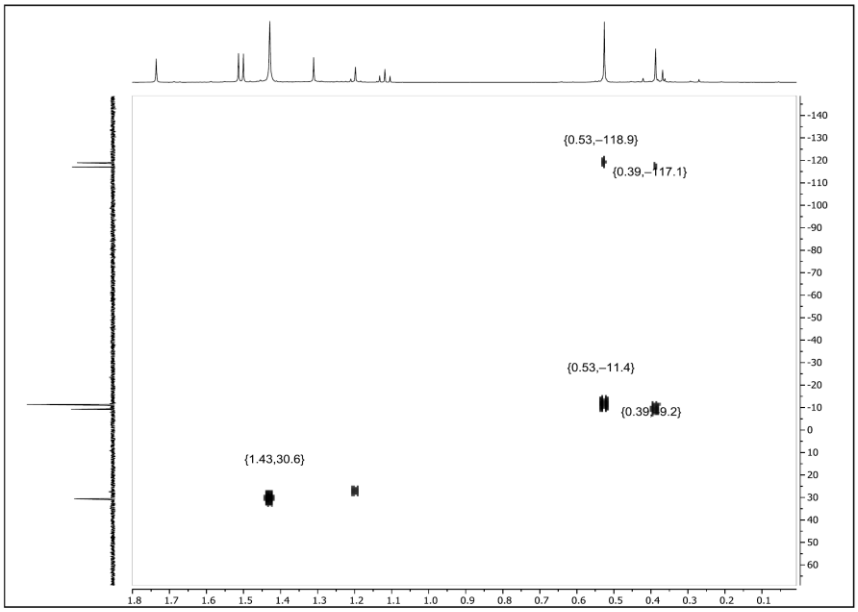
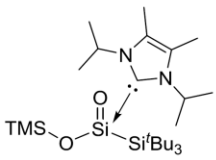


Figure S61. $^{1}H/^{29}Si$ HMBC NMR spectrum of (TMS)((TMS)$_2$(^{t}Bu$_3$Si)Si(IMe$_4$) (**16**) in C_6D_6 at 300 K.

1.14 Synthesis of (TMSO)(^{t}Bu$_3$Si)Si=O(I^{i}Pr$_2$Me$_2$) (17)



17
$C_{26}H_{56}N_2O_2Si_3$
513.00 g/mol

A solution of **13** (300 mg, 458 µmol) in *n*-hexane (15 mL) was frozen in liquid nitrogen and degassed. The solution was warmed to –80 °C and exposed to N_2O (1 bar) under vigorous stirring. Subsequently, the reaction mixture was allowed to warm to –30 °C over a period of 5 h, whereby the color changed from purple-red to pale red and a fine white precipitate formed. The solid was immediately separated *via* filtration, washed with cold *n*-hexane and dried *in vacuo* to provide the NHC-stabilized silanoic silylester **17** as a colorless powder (41.5 mg, 80.9 µmol, 18%). Suitable crystals for SC-XRD analysis were obtained by slow diffusion of *n*-hexane into a saturated THF solution at –35 °C for several days. The NHC-stabilized silanoic silylester **17** decomposes in solution at temperatures higher than –30 °C to an unidentified mixture of products. Thus, NMR characterization was performed at –30 °C. The observed unusual broad splitting of the NHC wingtip methine protons ($\Delta\delta$ = 2.68 ppm) in the ^{1}H NMR spectrum might originate from hydrogen bonding of one isopropyl C–H proton to the oxygen atom of the Si=O bond. This assumption is supported by the solid-state

structure of **17** (*vide infra*), which revealed a close O···H distance of 2.143 Å, being much shorter than the sum of the van der Waals radii of hydrogen and oxygen (2.72 Å).

m.p.: 97 °C (decomposition, color change from colorless to red).

^{1}H NMR (400 MHz, THF-d_8, 243 K): δ [ppm] = 8.23 (sept, ^{3}J = 7.0 Hz, 1H, NC$\underline{H}$(CH$_3$)$_2$), 5.55 (sept, ^{3}J = 6.9 Hz, 1H, NC$\underline{H}$(CH$_3$)$_2$), 2.35 (s, 3H, CC$\underline{H}_3$), 2.33 (s, 3H, CC$\underline{H}_3$), 1.55 (d, ^{3}J = 6.9 Hz, 3H, NCH(C$\underline{H}_3$)$_2$), 1.51 (d, ^{3}J = 6.5 Hz, 3H, NCH(C$\underline{H}_3$)$_2$), 1.43 (d, ^{3}J = 6.4 Hz, 3H, NCH(C$\underline{H}_3$)$_2$), 1.39 (d, ^{3}J = 7.2 Hz, 3H, NCH(C$\underline{H}_3$)$_2$), 1.22 (s, 27H, C(C$\underline{H}_3$)$_3$), 0.12 (s, 9H, O*TMS*).

^{13}C{^{1}H} NMR (101 MHz, THF-d_8, 243 K): δ [ppm] = 156.8 (*carbene C*), 129.1 (*C*CH$_3$), 127.0 (*C*CH$_3$), 51.6 (N*C*H(CH$_3$)$_2$), 50.2 (N*C*H(CH$_3$)$_2$), 32.5 (C(*C*H$_3$)$_3$), 24.6 (*C*(CH$_3$)$_3$), 23.4 (NCH(*C*H$_3$)$_2$), 23.2 (NCH(*C*H$_3$)$_2$), 21.8 (NCH(*C*H$_3$)$_2$), 20.6 (NCH(*C*H$_3$)$_2$), 11.0 (C*C*H$_3$), 10.7 (C*C*H$_3$), 3.3 (*TMS*).

^{29}Si{^{1}H} NMR (79 MHz, THF-d_8, 243 K): δ [ppm] = 6.6 (*Si*^{t}Bu$_3$), –3.4 (*TMS*), –50.8 (*Si*=O).

IR (solid): $\tilde{\nu}$ [cm^{-1}] = 2957 (w), 2847 (m), 1626 (w), 1469 (w), 1371 (m), 1244 (m), 1069 (m) ($\tilde{\nu}_{Si=O}$), 971 (s) ($\tilde{\nu}_{Si-O}$), 840 (s), 755 (m), 598 (w), 453 (m), 428 (m).

Anal. Calcd. [%] for C$_{26}$H$_{56}$N$_2$O$_2$Si$_3$: C, 60.87; H, 11.00; N, 5.46. Found [%]: C, 60.04; H, 10.92; N, 5.36.

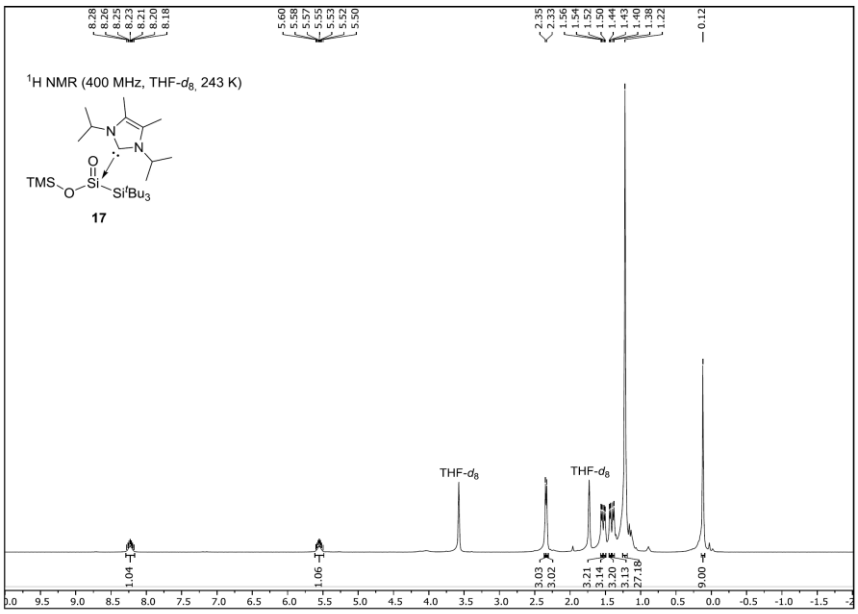


Figure S62. ^{1}H NMR spectrum of (TMSO)(^{t}Bu$_3$Si)Si=O(I^{i}Pr$_2$Me$_2$) (**17**) in THF-d_8 at 243 K.

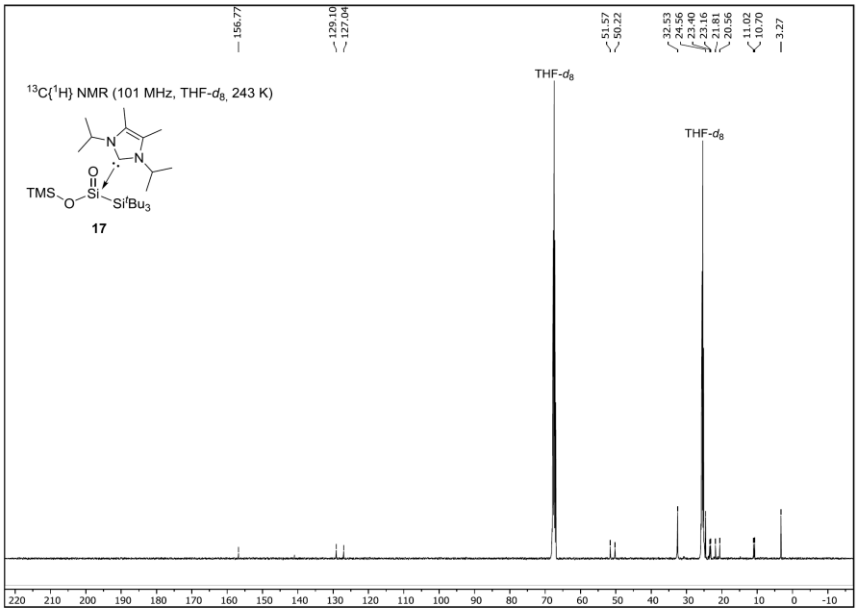


Figure S63. $^{13}C\{^1H\}$ NMR spectrum of (TMSO)(^{t}Bu$_3$Si)Si=O(I^{i}Pr$_2$Me$_2$) (**17**) in THF-d_8 at 243 K.

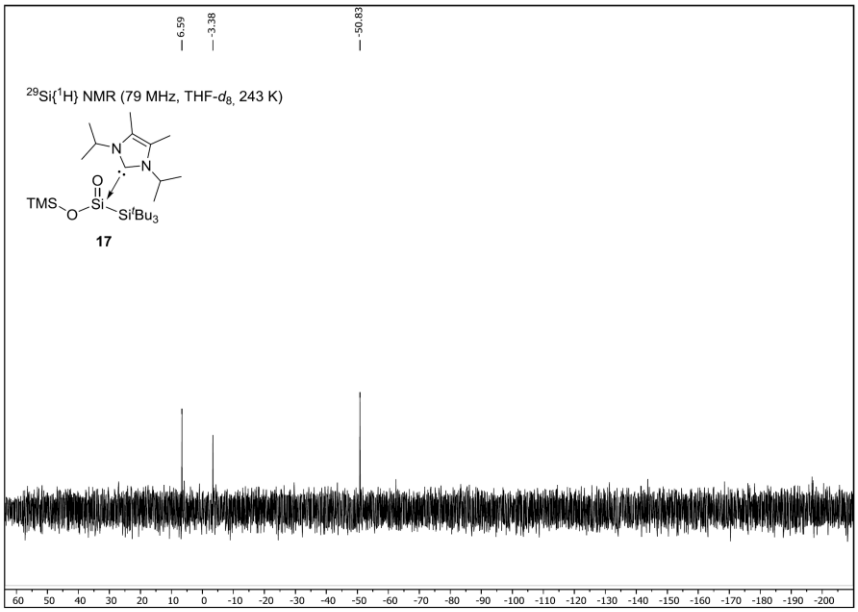


Figure S64. $^{29}Si\{^1H\}$ NMR spectrum of (TMSO)(^{t}Bu$_3$Si)Si=O(I^{i}Pr$_2$Me$_2$) (**17**) in THF-d_8 at 243 K.

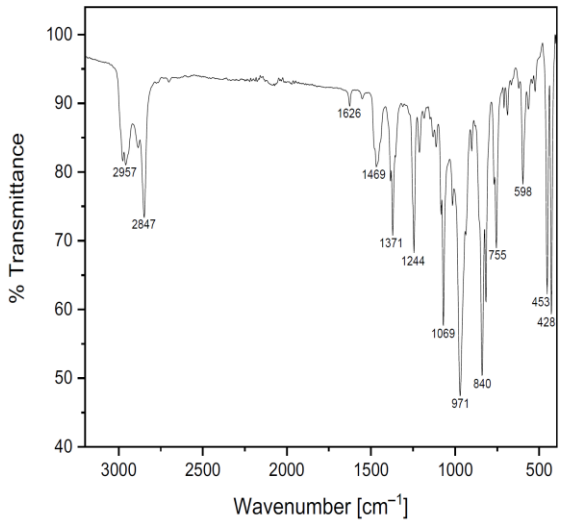


Figure S65. Solid-state FT-IR spectrum of (TMSO)(^{t}Bu$_3$Si)Si=O(I^{i}Pr$_2$Me$_2$) (**17**).

2. X-ray Crystallographic Data

General Information

The X-ray intensity data of **1**, **5**, **17** and **19** were collected on an X-ray single crystal diffractometer equipped with a CMOS detector (Bruker Photon-100), an IMS microsource with MoKα radiation (λ = 0.71073 Å) and a Helios mirror optic by using the APEX III software package.[S10] The X-ray intensity data of **2**, **13** and **14** were collected on an X-ray single crystal diffractometer equipped with a CMOS detector (Bruker Photon-100), a rotating anode (Bruker TXS) with MoKα radiation (λ = 0.71073 Å) and a Helios mirror optic by using the APEX III software package.[S10] The measurements were performed on single crystals coated with the perfluorinated ether Fomblin® Y. The crystals were fixed on the top of a microsampler, transferred to the diffractometer and frozen under a stream of cold nitrogen. A matrix scan was used to determine the initial lattice parameters. Reflections were merged and corrected for Lorenz and polarization effects, scan speed, and background using SAINT.[S11] Absorption corrections, including odd and even ordered spherical harmonics were performed using SADABS.[S11] Space group assignments were based upon systematic absences, E statistics, and successful refinement of the structures. Structures were solved by direct methods with the aid of successive difference Fourier maps, and were refined against all data using the APEX III software in conjunction with SHELXL-2014[S12] and

SHELXLE.[S13] All H atoms were placed in calculated positions and refined using a riding model, with methylene and aromatic C–H distances of 0.99 and 0.95 Å, respectively, and $U_{iso}(H) = 1.2 \cdot U_{eq}(C)$. Full-matrix least-squares refinements were carried out by minimizing $\Delta w(F_o^2 - F_c^2)^2$ with SHELXL-97[S14] weighting scheme. Neutral atom scattering factors for all atoms and anomalous dispersion corrections for the non-hydrogen atoms were taken from International Tables for Crystallography.[S15] The images of the crystal structures were generated by Mercury.[S16] The CCDC numbers CCDC-1915626 (**1**), CCDC-1915627 (**4**), CCDC-1915631 (**5**), CCDC-1915629 (**13**), CCDC-1915628 (**14**), CCDC-1915630 (**17**) and CCDC-1915625 (**19**) contain the supplementary crystallographic data for the structures. These data can be obtained free of charge from the Cambridge Crystallographic Data Centre *via* https://www.ccdc.cam.ac.uk/structures/.

Single Crystal X-ray Structure Determinations

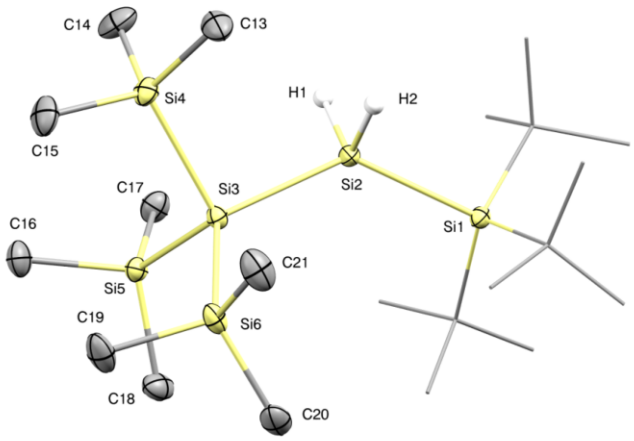


Figure S66. Molecular structure of **1** with ellipsoids set at 50% probability. Hydrogen atoms are omitted for clarity, except for the Si–H nuclei. Selected bond lengths [Å] and angles [°]: Si1–Si2 2.369(1), Si2–Si3 2.350(1), Si3–Si4 2.364(1), Si3–Si5 2.356(1), Si3–Si6 2.351(1); Si1–Si2–Si3 132.1(1), Si2–Si3–Si4 99.0(1), Si2–Si3–Si5 113.6(1), Si2–Si3–Si6 118.9(1), Si4–Si3–Si5 106.3(1), Si4–Si3–Si6 108.2(1), Si5–Si3–Si6 109.5(1).

Table S1. Crystal data and structure refinement for compound **1**.

Chemical formula	$C_{21}H_{56}Si_6$	
Formula weight	477.19 g/mol	
Temperature	100(2) K	
Wavelength	0.71073 Å	
Crystal size	0.231 × 0.278 × 0.384 mm	
Crystal habit	clear colourless fragment	
Crystal system	orthorhombic	
Space group	P 21 21 21	
Unit cell dimensions	a = 9.4966(3) Å	α = 90°
	b = 13.7852(5) Å	β = 90°
	c = 24.0165(9) Å	γ = 90°
Volume	3144.06(19) $Å^3$	
Z	4	
Density (calculated)	1.008 g/cm^3	
Absorption coefficient	0.272 mm^{-1}	
F(000)	1064	
Diffractometer	Bruker D8 Venture Duo IMS	
Radiation source	IMS microsource, Mo	
Theta range for data collection	2.25 to 25.02°	
Index ranges	–11<=h<=11, –16<=k<=16, –28<=l<=28	
Reflections collected	72550	
Independent reflections	5546 [R(int) = 0.0601]	
Coverage of independent reflections	99.9%	
Absorption correction	Multi-Scan	
Max. and min. transmission	0.9400 and 0.9030	
Refinement method	Full-matrix least-squares on F^2	
Refinement program	SHELXL-2014/7 (Sheldrick, 2014)	
Function minimized	$\Sigma\, w(F_o^2 - F_c^2)^2$	
Data / restraints / parameters	5546 / 0 / 271	
Goodness-of-fit on F^2	1.046	
Δ/σ_{max}	0.001	
Final R indices	5293 data; I>2σ(I)	R1 = 0.0236, wR2 = 0.0572
	all data	R1 = 0.0259, wR2 = 0.0581
Weighting scheme	$w = 1/[\sigma^2(F_o^2) + (0.0328P)^2 + 0.5764P]$	
	where $P = (F_o^2 + 2F_c^2)/3$	
Largest diff. peak and hole	0.266 and –0.188 $eÅ^{-3}$	
R.M.S. deviation from mean	0.036 $eÅ^{-3}$	

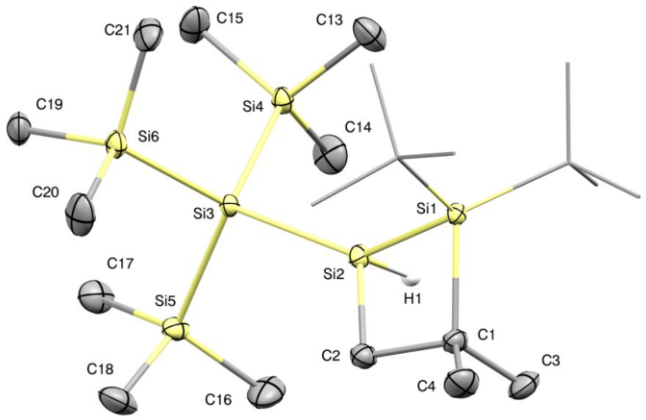


Figure S67. Molecular structure of **4** with ellipsoids set at 50% probability. Hydrogen atoms are omitted for clarity, except for the Si–H nucleus. Selected bond lengths [Å] and angles [°]: Si1–Si2 2.345(1), Si1–C1 1.957(2), C1–C2 1.572(2), Si2–C2 1.916(2), Si2–Si3 2.346(1); C1–Si1–Si2 76.3(1), Si1–Si2–C2 76.6(1), Si1–C1–C2 97.3(1), C1–C2–Si2 99.7(1).

Table S2. Crystal data and structure refinement for compound **4**.

Chemical formula	$C_{21}H_{54}Si_6$	
Formula weight	475.17 g/mol	
Temperature	100(2) K	
Wavelength	0.71073 Å	
Crystal size	0.116 × 0.157 × 0.166 mm	
Crystal habit	clear colourless fragment	
Crystal system	monoclinic	
Space group	P 1 21/n 1	
Unit cell dimensions	a = 12.4962(10) Å	α = 90°
	b = 14.8445(10) Å	β = 108.895(3)°
	c = 17.5284(14) Å	γ = 90°
Volume	3076.3(4) $Å^3$	
Z	4	
Density (calculated)	1.026 g/cm^3	
Absorption coefficient	0.278 mm^{-1}	
F(000)	1056	
Diffractometer	Bruker D8 Venture	
Radiation source	TXS rotating anode, Mo	
Theta range for data collection	2.42 to 25.03°	
Index ranges	–14<=h<=14, –17<=k<=17, –20<=l<=20	
Reflections collected	55818	
Independent reflections	5430 [R(int) = 0.0490]	
Coverage of independent reflections	99.9%	
Absorption correction	Multi-Scan	
Max. and min. transmission	0.9690 and 0.9550	
Refinement method	Full-matrix least-squares on F^2	
Refinement program	SHELXL-2014/7 (Sheldrick, 2014)	
Function minimized	$\Sigma\, w(F_o^2 - F_c^2)^2$	
Data / restraints / parameters	5430 / 0 / 265	
Goodness-of-fit on F^2	1.037	
Δ/σ_{max}	0.001	
Final R indices	4777 data; I>2σ(I)	R1 = 0.0282, wR2 = 0.0661
	all data	R1 = 0.0348, wR2 = 0.0692
Weighting scheme	$w = 1/[\sigma^2(F_o^2) + (0.0267P)^2 + 2.0069P]$	
	where $P = (F_o^2 + 2F_c^2)/3$	
Largest diff. peak and hole	0.732 and –0.272 $eÅ^{-3}$	
R.M.S. deviation from mean	0.043 $eÅ^{-3}$	

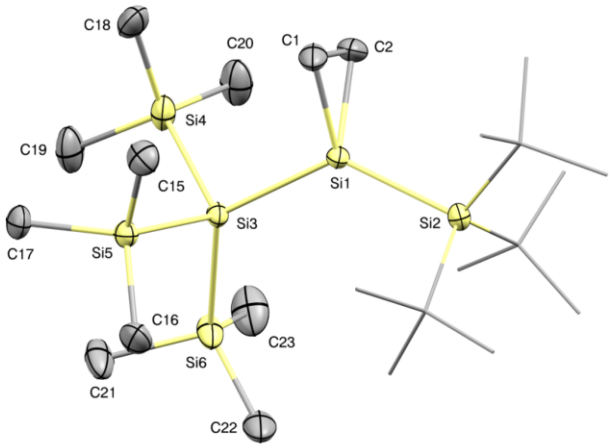


Figure S68. Molecular structure of **5** with ellipsoids set at 50% probability. Hydrogen atoms are omitted for clarity. Selected bond lengths [Å] and angles [°]: Si1–C1 1.885(2), Si1–C2 1.890(2), C1–C2 1.542(3), Si1–Si2 2.372(1), Si1–Si3 2.371(1); Si1–C1–C2 66.1(1), C1–C2–Si1 65.7(1), C2–Si1–C1 48.2(1).

Table S3. Crystal data and structure refinement for compound **5**.

Chemical formula	$C_{23}H_{58}Si_6$	
Formula weight	503.23 g/mol	
Temperature	100(2) K	
Wavelength	0.71073 Å	
Crystal size	0.108 × 0.204 × 0.288 mm	
Crystal habit	clear colourless fragment	
Crystal system	orthorhombic	
Space group	F d d 2	
Unit cell dimensions	a = 31.226(4) Å	α = 90°
	b = 33.796(4) Å	β = 90°
	c = 12.2692(14) Å	γ = 90°
Volume	12948(3) $Å^3$	
Z	16	
Density (calculated)	1.033 g/cm^3	
Absorption coefficient	0.267 mm^{-1}	
F(000)	4480	
Diffractometer	Bruker D8 Venture Duo IMS	
Radiation source	IMS microsource, Mo	
Theta range for data collection	2.41 to 25.35°	
Index ranges	–37<=h<=37, –40<=k<=40, –14<=l<=14	
Reflections collected	40402	
Independent reflections	5919 [R(int) = 0.0269]	
Coverage of independent reflections	99.9%	
Absorption correction	Multi-Scan	
Max. and min. transmission	0.9720 and 0.9370	
Refinement method	Full-matrix least-squares on F^2	
Refinement program	SHELXL-2014/7 (Sheldrick, 2014)	
Function minimized	$\Sigma\, w(F_o^2 - F_c^2)^2$	
Data / restraints / parameters	5919 / 1 / 280	
Goodness-of-fit on F^2	1.072	
Δ/σ_{max}	0.002	
Final R indices	5870 data; I>2σ(I)	R1 = 0.0180, wR2 = 0.0484
	all data	R1 = 0.0182, wR2 = 0.0485
Weighting scheme	$w = 1/[\sigma^2(F_o^2) + (0.0283P)^2 + 6.4105P]$	
	where $P = (F_o^2 + 2F_c^2)/3$	
Largest diff. peak and hole	0.226 and –0.135 $eÅ^{-3}$	
R.M.S. deviation from mean	0.035 $eÅ^{-3}$	

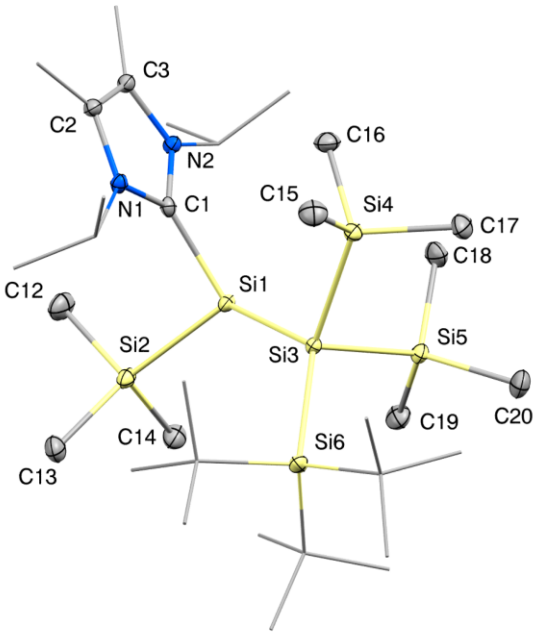


Figure S69. Molecular structure of **13** with ellipsoids set at 50% probability. Hydrogen atoms are omitted for clarity. Selected bond lengths [Å] and angles [°]: Si1–Si2 2.360(1), Si1–Si3 2.437(1), Si1–C1 1.961(2); C1–Si1–Si2 99.3(1), C1–Si1–Si3 115.6(1), Si2–Si1–Si3 126.0(1).

Table S4. Crystal data and structure refinement for compound **13**.

Chemical formula	$C_{32}H_{74}N_2Si_6$	
Formula weight	655.47 g/mol	
Temperature	100(2) K	
Wavelength	0.71073 Å	
Crystal size	0.096 × 0.139 × 0.162 mm	
Crystal habit	purple-red fragment	
Crystal system	triclinic	
Space group	P -1	
Unit cell dimensions	a = 11.3385(4) Å	α = 90.739(2)°
	b = 12.1541(4) Å	β = 97.371(2)°
	c = 16.6351(6) Å	γ = 116.9890(10)°
Volume	2019.35(12) $Å^3$	
Z	2	
Density (calculated)	1.078 g/cm^3	
Absorption coefficient	0.229 mm^{-1}	
F(000)	728	
Diffractometer	Bruker D8 Venture	
Radiation source	TXS rotating anode, Mo	
Theta range for data collection	2.22 to 25.03°	
Index ranges	–13<=h<=13, –14<=k<=14, –19<=l<=19	
Reflections collected	43501	
Independent reflections	7143 [R(int) = 0.0466]	
Coverage of independent reflections	99.9%	
Absorption correction	Multi-Scan	
Max. and min. transmission	0.9780 and 0.9640	
Refinement method	Full-matrix least-squares on F^2	
Refinement program	SHELXL-2014/7 (Sheldrick, 2014)	
Function minimized	$\Sigma\, w(F_o^2 - F_c^2)^2$	
Data / restraints / parameters	7143 / 0 / 385	
Goodness-of-fit on F^2	1.044	
Δ/σ_{max}	0.001	
Final R indices	6168 data; I>2σ(I)	R1 = 0.0306, wR2 = 0.0678
	all data	R1 = 0.0393, wR2 = 0.0711
Weighting scheme	$w = 1/[\sigma^2(F_o^2) + (0.0220P)^2 + 1.3289P]$	
	where $P = (F_o^2 + 2F_c^2)/3$	
Largest diff. peak and hole	0.328 and –0.271 $eÅ^{-3}$	
R.M.S. deviation from mean	0.045 $eÅ^{-3}$	

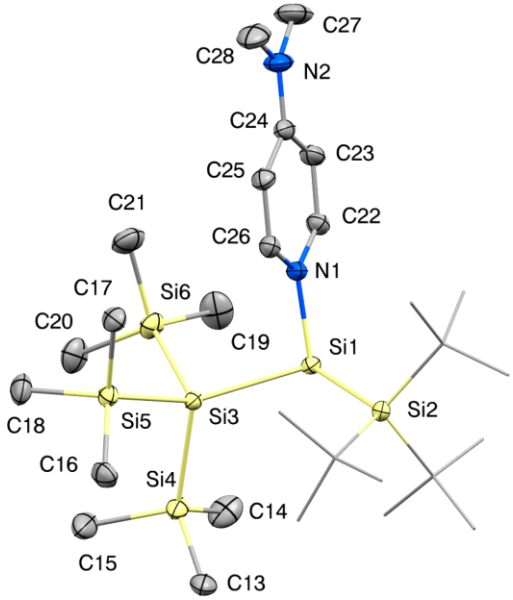


Figure S70. Molecular structure of **14** with ellipsoids set at 50% probability. Hydrogen atoms and solvent molecules are omitted for clarity. Selected bond lengths [Å] and angles [°]: Si1–Si2 2.433(1), Si1–Si3 2.420(1), Si1–N1 1.942(2); N1–Si1–Si2 104.5(1), N1–Si1–Si3 98.1(1), Si2–Si1–Si3 116.1(1).

Table S5. Crystal data and structure refinement for compound **14**.

Chemical formula	$C_{28}H_{64}N_2Si_6$	
Formula weight	597.34 g/mol	
Temperature	100(2) K	
Wavelength	0.71073 Å	
Crystal size	0.188 × 0.261 × 0.306 mm	
Crystal habit	clear orange-red fragment	
Crystal system	triclinic	
Space group	P -1	
Unit cell dimensions	a = 11.8830(19) Å	α = 94.596(6)°
	b = 12.9036(19) Å	β = 105.116(5)°
	c = 15.496(3) Å	γ = 110.563(5)°
Volume	2108.6(6) Å^3	
Z	2	
Density (calculated)	1.054 g/cm^3	
Absorption coefficient	0.222 mm^{-1}	
F(000)	740	
Diffractometer	Bruker D8 Venture	
Radiation source	TXS rotating anode, Mo	
Theta range for data collection	2.30 to 25.66°	
Index ranges	–14<=h<=14, –15<=k<=15, –18<=l<=18	
Reflections collected	82436	
Independent reflections	7972 [R(int) = 0.0755]	
Coverage of independent reflections	99.6%	
Absorption correction	Multi-Scan	
Max. and min. transmission	0.9590 and 0.9340	
Refinement method	Full-matrix least-squares on F^2	
Refinement program	SHELXL-2014/7 (Sheldrick, 2014)	
Function minimized	$\Sigma\, w(F_o^2 - F_c^2)^2$	
Data / restraints / parameters	7972 / 180 / 436	
Goodness-of-fit on F^2	1.038	
Δ/σ_{max}	0.005	
Final R indices	7075 data; I>2σ(I)	R1 = 0.0358, wR2 = 0.0920
	all data	R1 = 0.0407, wR2 = 0.0950
Weighting scheme	$w = 1/[\sigma^2(F_o^2) + (0.0391P)^2 + 1.4350P]$	
	where $P = (F_o^2 + 2F_c^2)/3$	
Largest diff. peak and hole	0.335 and –0.380 eÅ^{-3}	
R.M.S. deviation from mean	0.051 eÅ^{-3}	

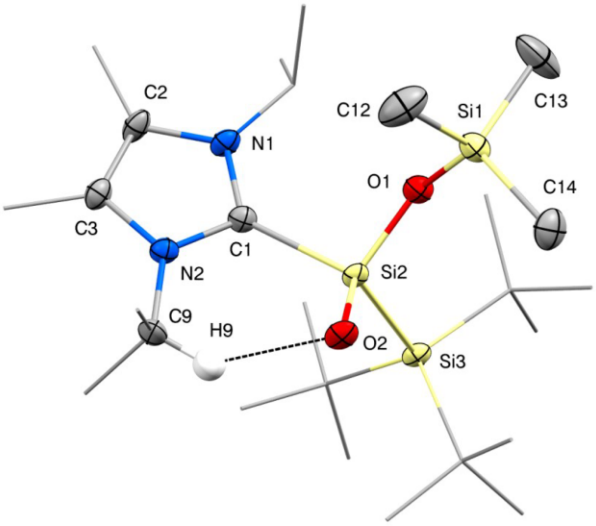


Figure S71. Molecular structure of **17** with ellipsoids set at 50% probability. Hydrogen atoms, except for H9 involved in hydrogen bonding (visualized by the dashed line), are omitted for clarity. Selected bond lengths [Å] and angles [°]: Si1–O1 1.641(2), Si2–O2 1.556(2), Si2–O1 1.655(3), Si2–Si3 2.415(1), Si2–C1 1.984(3); O2–Si2–O1 115.5(1), O2–Si2–C1 106.9(1), O1–Si2–C1 101.2(1), O2–Si2–Si3 111.7(1), O1–Si2–Si3 107.0(1), C1–Si2–Si3 114.3(1).

Table S6. Crystal data and structure refinement for compound **17**.

Chemical formula	$C_{26}H_{56}N_2O_2Si_3$	
Formula weight	513.00 g/mol	
Temperature	100(2) K	
Wavelength	0.71073 Å	
Crystal size	0.334 × 0.458 × 0.527 mm	
Crystal habit	clear pale brown fragment	
Crystal system	orthorhombic	
Space group	P n a 21	
Unit cell dimensions	a = 17.0644(9) Å	α = 90°
	b = 10.4534(6) Å	β = 90°
	c = 18.0274(9) Å	γ = 90°
Volume	3215.7(3) $Å^3$	
Z	4	
Density (calculated)	1.060 g/cm^3	
Absorption coefficient	0.170 mm^{-1}	
F(000)	1136	
Diffractometer	Bruker D8 Venture Duo IMS	
Radiation source	IMS microsource, Mo	
Theta range for data collection	2.25 to 25.02°	
Index ranges	–20<=h<=20, –12<=k<=12, –21<=l<=20	
Reflections collected	90131	
Independent reflections	5615 [R(int) = 0.0660]	
Coverage of independent reflections	100.0%	
Absorption correction	Multi-Scan	
Max. and min. transmission	0.9450 and 0.9160	
Refinement method	Full-matrix least-squares on F^2	
Refinement program	SHELXL-2014/7 (Sheldrick, 2014)	
Function minimized	$\Sigma\, w(F_o^2 - F_c^2)^2$	
Data / restraints / parameters	5615 / 1 / 317	
Goodness-of-fit on F^2	1.085	
Final R indices	5362 data; I>2σ(I)	R1 = 0.0352, wR2 = 0.0860
	all data	R1 = 0.0376, wR2 = 0.0877
Weighting scheme	$w = 1/[\sigma^2(F_o^2) + (0.0388P)^2 + 2.1487P]$	
	where $P = (F_o^2 + 2F_c^2)/3$	
Largest diff. peak and hole	0.404 and –0.222 $eÅ^{-3}$	
R.M.S. deviation from mean	0.048 $eÅ^{-3}$	

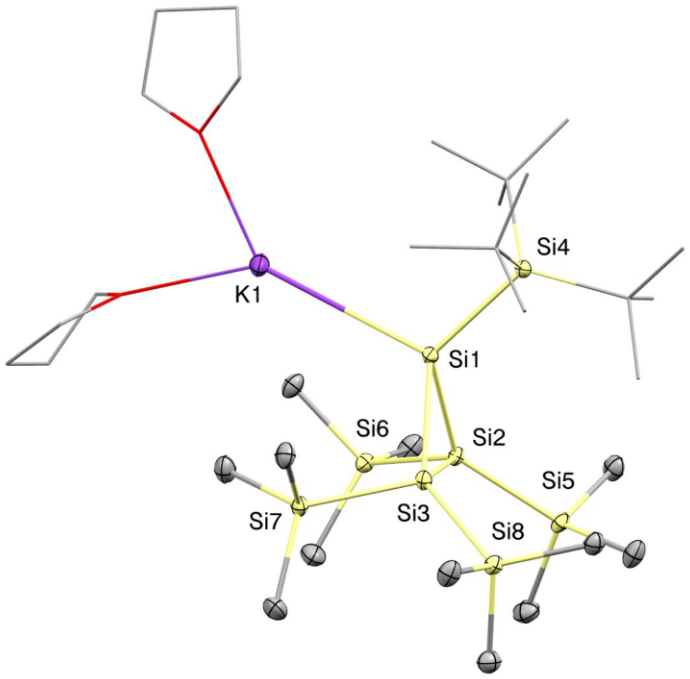


Figure S72. Molecular structure of **19** with ellipsoids set at 50% probability. Hydrogen atoms are omitted for clarity. Selected bond lengths [Å] and angles [°]: K1–Si1 3.465(1), Si1–Si2 2.364(1), Si1–Si3 2.364(1), Si1–Si4 2.378(1), Si2–Si3 2.358(1), Si2–Si5 2.357(1), Si2–Si6 2.348(1), Si3–Si7 2.342(1), Si3–Si8 2.367(1); Si2–Si1–Si3 59.8(1), Si2–Si1–Si4 123.6(1), Si2–Si1–K1 116.4(1), Si3–Si1–Si4 122.3(1), Si3–Si1–K1 115.6(1), Si4–Si1–K1 110.7(1).

Table S7. Crystal data and structure refinement for compound **19**.

Chemical formula	$C_{32}H_{79}KO_2Si_8$	
Formula weight	759.76 g/mol	
Temperature	100(2) K	
Wavelength	0.71073 Å	
Crystal size	0.217 × 0.286 × 0.293 mm	
Crystal habit	clear colourless fragment	
Crystal system	monoclinic	
Space group	P 21/n	
Unit cell dimensions	a = 14.4278(13) Å	α = 90°
	b = 21.935(2) Å	β = 91.076(3)°
	c = 14.7814(14) Å	γ = 90°
Volume	4677.1(7) $Å^3$	
Z	4	
Density (calculated)	1.079 g/cm^3	
Absorption coefficient	0.343 mm^{-1}	
F(000)	1672	
Diffractometer	Bruker D8 Venture Duo IMS	
Radiation source	IMS microsource, Mo	
Theta range for data collection	2.20 to 25.03°	
Index ranges	–17<=h<=17, –26<=k<=26, –17<=l<=17	
Reflections collected	184640	
Independent reflections	8263 [R(int) = 0.0510]	
Coverage of independent reflections	99.9%	
Absorption correction	Multi-Scan	
Max. and min. transmission	0.9290 and 0.9060	
Refinement method	Full-matrix least-squares on F^2	
Refinement program	SHELXL-2014/7 (Sheldrick, 2014)	
Function minimized	$\Sigma\, w(F_o^2 - F_c^2)^2$	
Data / restraints / parameters	8263 / 0 / 409	
Goodness-of-fit on F^2	1.039	
Final R indices	7411 data; I>2σ(I)	R1 = 0.0242, wR2 = 0.0552
	all data	R1 = 0.0296, wR2 = 0.0575
Weighting scheme	$w = 1/[\sigma^2(F_o^2) + (0.0236P)^2 + 2.5040P]$	
	where $P = (F_o^2 + 2F_c^2)/3$	
Largest diff. peak and hole	0.284 and –0.200 $eÅ^{-3}$	
R.M.S. deviation from mean	0.039 $eÅ^{-3}$	

3. DFT Calculations

General Information

Geometry optimizations and harmonic frequency calculations were performed using *Gaussian09*[S17] employing the M06-2X/6-31+G(d,p)[S18] level of density functional theory. The SMD polarizable continuum model was used to account for solvent effects of benzene.[S19] The "ultrafine" grid option was used for numerical integrations.[S20] Stationary points are characterized as minima by analysis of computed Hessians. The connectivity between minima and transition states was validated by IRC calculations[S21] or displacing the geometry along the transition mode, followed by unconstrained optimization. For improved energies, single point calculations were conducted at the SMD-M06-2X/6-311+G(d,p)[S22] level of theory; wave functions used for bonding analysis were obtained at the M06-2X/6-311++G(2d,2p) level.[S22] Natural Bond Orbital (NBO) and Natural Resonance Theory (NRT) analyses were performed using the *NBO 6.0* program[S23], interfaced with *Gaussian09*[S24]. NMR chemical shift values were calculated using the Gauge-Independent Atomic Orbital (GIAO) method implemented in *Gaussian09* and the M06-L[S25] functional along with the 6-311G(2d,p) basis set and the SMD solvent model for the structures obtained at the M06-2X/6-31+G(d,p) level of theory. $^{29}Si\{^{1}H\}$ NMR spectroscopic chemical shifts δ are reported in ppm relative to tetramethylsilane ($\delta(^{29}Si(SiMe_4)) = 0$ ppm). Pictures of molecular structures were generated with the ChemCraft[S26], Cylview[S27] or GaussView[S28] programs.

Comparison of calculated and experimental structures

Table S8. Comparison of selected bond lengths [Å] and angles [°] for the computed and experimental structures of **4**, **5**, **13**, **14** and **17**. Geometries are calculated at the M06-2X/6-31+G(d,p) level of theory. Experimental data are taken from SC-XRD analyses.

Compound	bond/angle	exp.	calc.	Δ(calc.-exp.)
4	Si1–Si2	2.345(1)	2.35	0.01
	Si1–C1	1.957(2)	1.96	0.00
	C1–C2	1.572(2)	1.57	0.00
	Si2–C2	1.916(2)	1.93	0.01
	Si2–Si3	2.346(1)	2.34	0.01
	C1–Si1–Si2	76.3(1)	76.5	0.20
	Si1–Si2–C2	76.6(1)	76.3	0.30
	Si1–C1–C2	97.3(1)	97.3	0.00
	C1–C2–Si2	99.7(1)	99.8	0.10
5	Si1–C1	1.885(2)	1.89	0.01
	Si1–C2	1.890(2)	1.90	0.01
	C1–C2	1.542(3)	1.53	0.01
	Si1–Si2	2.372(1)	2.36	0.01
	Si1–Si3	2.371(1)	2.36	0.01
	Si1–C1–C2	66.1(1)	66.3	0.20
	C1–C2–Si1	65.7(1)	66.1	0.40
	C2–Si1–C1	48.2(1)	47.5	0.70
13	Si1–Si2	2.360(1)	2.36	0.00
	Si1–Si3	2.437(1)	2.42	0.02
	Si1–C1	1.961(2)	1.99	0.03
	C1–Si1–Si2	99.3(1)	99.1	0.20
	C1–Si1–Si3	115.6(1)	112.6	3.00
	Si2–Si1–Si3	126.0(1)	125.4	0.60
14	Si1–Si2	2.433(1)	2.43	0.00
	Si1–Si3	2.420(1)	2.42	0.00
	Si1–N1	1.942(2)	1.99	0.05
	N1–Si1–Si2	104.5(1)	101.8	2.70
	N1–Si1–Si3	98.1(1)	93.3	4.80
	Si2–Si1–Si3	116.1(1)	116.0	0.10
17	Si1–O1	1.641(2)	1.68	0.04
	Si2–O2	1.556(2)	1.57	0.01
	Si2–O1	1.655(3)	1.68	0.03
	Si2–Si3	2.415(1)	2.39	0.02
	Si2–C1	1.984(3)	2.01	0.02
	O2–Si2–O1	115.5(1)	115.7	0.20
	O2–Si2–C1	106.9(1)	105.1	1.80
	O1–Si2–C1	101.2(1)	99.7	1.50
	O2–Si2–Si3	111.7(1)	114.4	2.70
	O1–Si2–Si3	107.0(1)	107.4	0.40
	C1–Si2–Si3	114.3(1)	113.8	0.50

Calculated $^{29}Si\{^{1}H\}$ NMR Resonances

Table S9. Comparison of experimental and calculated NMR chemical shifts.

Compound	Si	Exp. δ(^{29}Si) [ppm]	Calc. δ(^{29}Si) [ppm]	Δδ [ppm]
3'	*Si*TMS_2	161.9	162.5	0.6
	Si(TMS)Si^tBu_3	132.4	140.5	8.1
	Si^tBu_3	31.7	22.4	9.3
	TMS	–6.8	–6.3	0.5
	TMS	–7.7	–7.2	0.5
4	*Si*^{t}Bu_2	35.6	21.8	13.8
	TMS	–9.2	–10.2	1.0
	*Si*H	–60.4	–59.8	0.6
	Si$(TMS)_3$	–133.8	–143.9	10.1
5	*Si*^{t}Bu_3	20.2	7.4	12.8
	TMS	–8.3	–9.4	1.1
	Si$(TMS)_3$	–113.7	–124.8	11.1
	SiCH_2CH_2	–164.3	–162.1	2.2
6	*Si*^{t}Bu_3	29.6	23.2	6.4
	TMS	–11.5	–11.0	0.5
	TMS	–12.2	–13.9	1.7
	TMS	–12.9	–14.5	1.6
	SiNH_2	–35.7	–36.8	0.9
	*Si*H	–119.9	–116.6	3.3
13	*Si*^{t}Bu_3	29.4	18.2	11.2
	TMS	–9.1	–11.6	2.5
	TMS	–11.9	–12.6	0.7
	silylene Si	–104.7	–109.6	4.9
	Si$(TMS)_2$	–117.4	–128.8	11.4
14	*silylene Si*	68.8	75.0	6.2
	Si^tBu_3	20.4	9.7	10.7
	TMS	–9.3	–9.5	0.2
	Si$(TMS)_3$	–121.6	–126.9	5.3
15	*Si*^{t}Bu_3	31.2	23.5	7.7
	TMS	–9.9	–9.3	0.6
	Si$(TMS)_3$	–115.2	–117.5	2.3
	silylene Si	–120.6	–127.4	6.8
16	*Si*^{t}Bu_3	30.6	22.1	8.5
	TMS	–9.2	–9.6	0.4
	TMS	–11.4	–10.5	0.9
	silylene Si	–117.1	–115.2	1.8
	Si$(TMS)_2$	–118.9	–132.7	13.8
17	*Si*^{t}Bu_3	6.6	8.0	1.4
	TMS	–3.4	–10.6	7.2
	Si=O	–50.8	–50.8	0.0

Tetrasilyldisilene 3': Calculated structure, comparison and NMR shifts

A huge number of stable disilenes has already been reported up to date[S29], but to the best of our knowledge none of the type ABSi=SiA_2 (A,B = different silyl groups) is known. The calculated structure of **3'** has Si=Si bond length of 2.18 Å, located on the lower limit for silyl-substituted disilenes: $d_{(Si=Si)}$ = 2.19–2.26 Å.[S30] It further exhibits a bent and twisted structure (Figure S73). Reported disilenes have shown to have either a bent or a twisted geometry, with the distortion mode being mainly determined by the size and shape of the silyl substituents. There are only two examples with both distortions reported: (*E*)-[(^{t}Bu_2MeSi)$_2$MeSi](^{t}Bu_2MeSi)Si=SiMe(SiMe^tBu_2) and (*Z*)-(I^{t}BuN)(TMS_3Si)Si=Si(SiTMS_3)(I^{t}BuN).[S31] With regard to a comparable huge difference in the steric demand of the silyl groups in **3'**, we assume the calculated structure to be reasonable. The calculated NMR shifts are in good agreement with other tetrasilyl-substituted disilenes[S30] as well as with the measured experimental values (Table S9). The splitting of the NMR signals between the two sp^2 hybridized Si atoms is only slightly higher than in known A_2Si=SiB_2 disilenes (A,B = different silylgroups).[S30] For completion, relaxed potential energy scans of the dihedral angle revealed **3'** as the global minimum with several other local minima located at least 2.5 kcal/mol higher in energy in addition to non-matching NMR shifts.

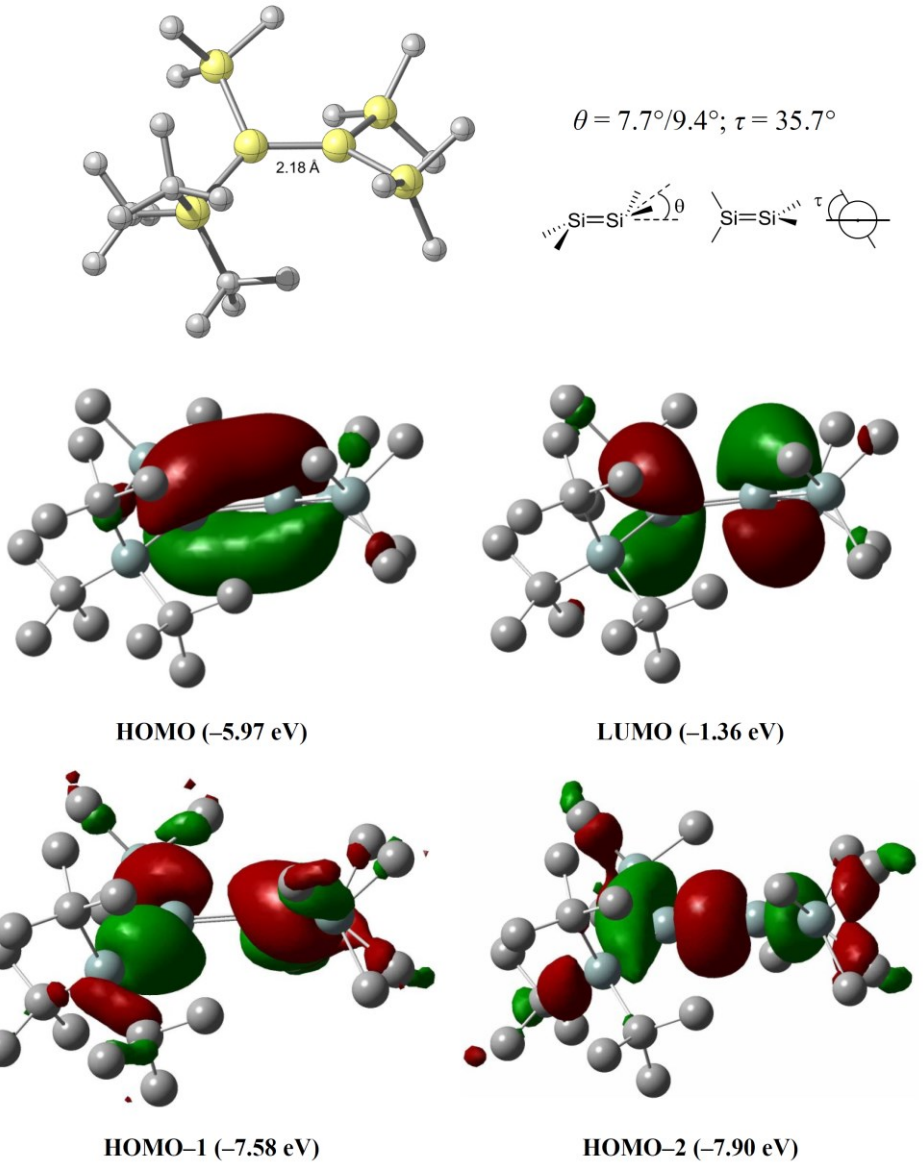


Figure S73. Caluclated molecular structure of tetrasilyldisilene **3'** with its frontier orbitals and their corresponding energy values; *trans*-bent angle θ and twist angle τ.

Table S10. Calculated transitions and UV-Vis absorption bands using TD-DFT (time-dependent-DFT).

Wavelength [nm]	MO contributions	Transition	f	Contribution
467.3	HOMO→LUMO	π→π*	0.1109	95.7%
334.9	HOMO–1→LUMO	σ(silyl)→π*	0.0571	86.5%
332.9	HOMO–2→LUMO	σ(silyl)→π*	0.0030	90.5%

Bis(silyl)silylenes 3/3'': calculated structures

The donor-free silylene **3** has a singlet-triplet energy gap ΔE_{S-T} of 2.5 kcal/mol, higher than the value calculated for silylene **3''** (0.6 kcal/mol). This is also reflected in an increase of the Si–Si:–Si bond angle at the silylene center. Only the most stable conformer is reported in each case.

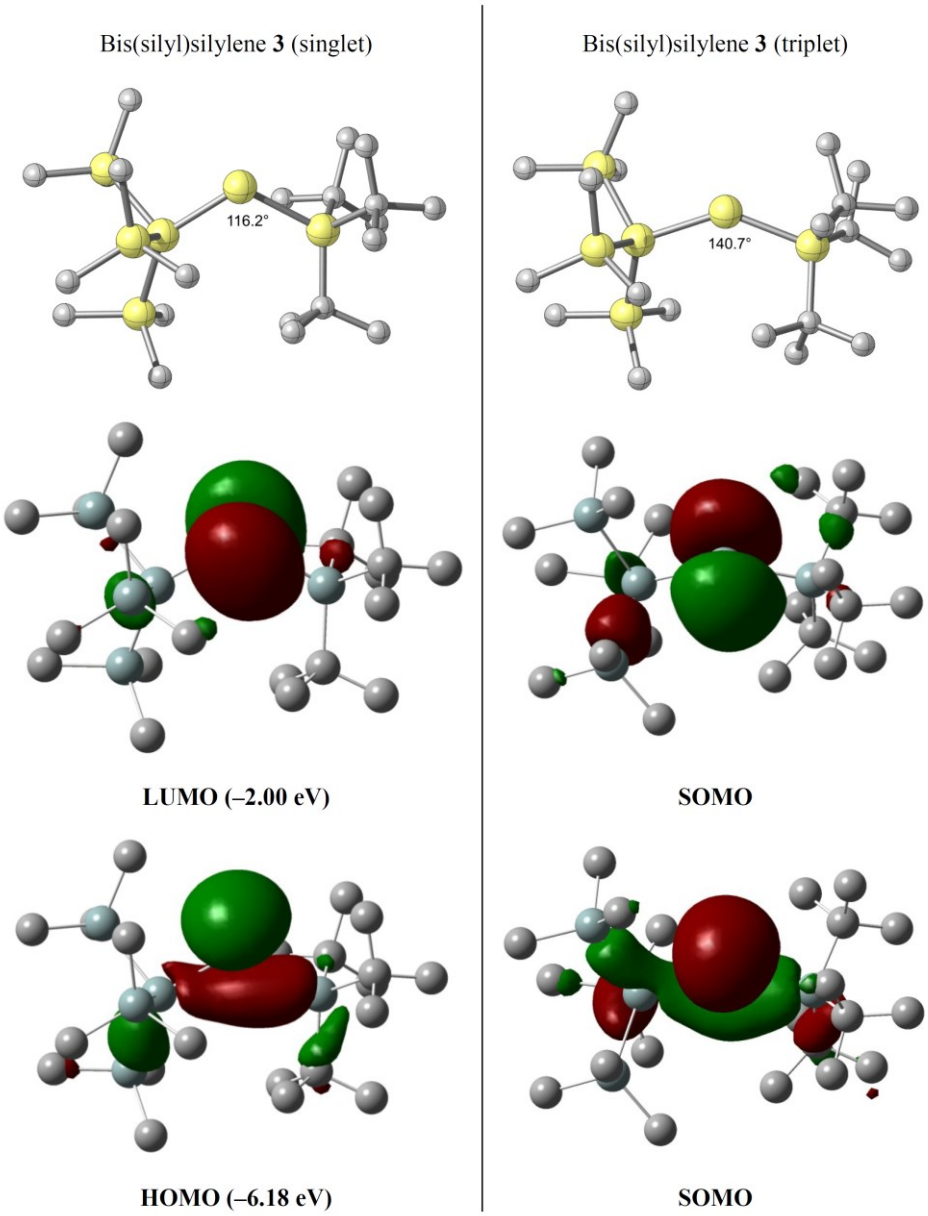


Figure S74. Caluclated molecular structures of bis(silyl)silylenes **3** with their corresponding frontier orbitals.

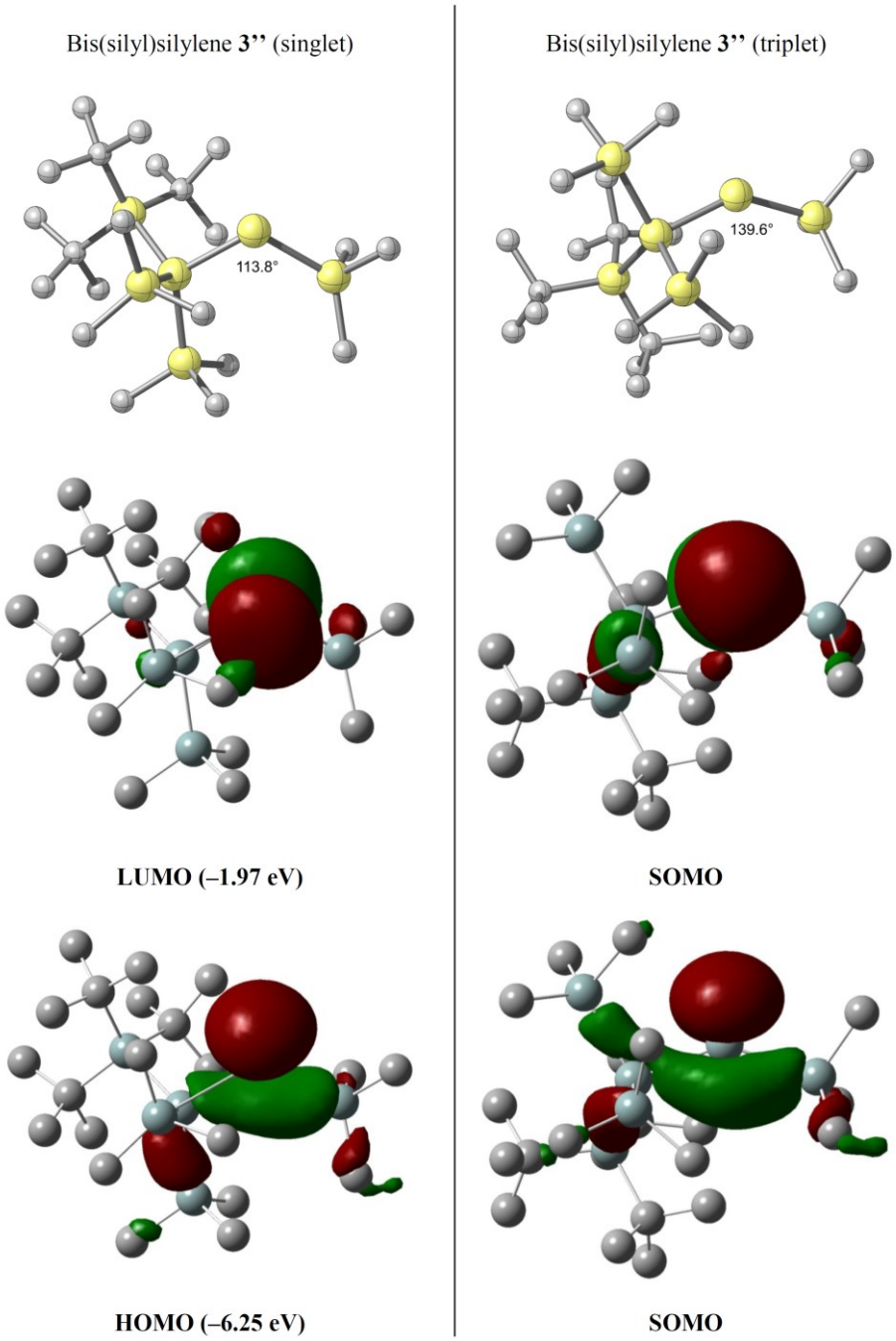


Figure S75. Caluclated molecular structures of bis(silyl)silylenes **3''** with their corresponding frontier orbitals.

Mechanism for the interconversion between the silylenes 3 and 3'', disilene 3' and the C–H activation product (disiletane 4) at 298 K

Based on recent reports on reactions of silyl-substituted silylenes occurring on the singlet potential energy surface[S32], only pathways occurring from the singlet silylenes have been investigated. As shown in Figure S68, rearrangement of **3'** (the most stable isomer) to **3** is accompanied with a barrier of 15.2 kcal/mol to yield **3** located 5.7 kcal/mol higher in energy. The effective barrier for the migration of the second TMS group to give **3''** is slightly higher with 19.6 kcal/mol. Thus, all isomerization reactions can be described as reactions in equilibrium with **3'** being the kinetic product. Decomposition of **3** *via* C–H activation, providing the thermodynamic product **4**, possesses an effective barrier of 26.2 kcal/mol, thus being in line with the experimentally observed reaction time of 4 days at r.t. for full conversion to **4**. Accordingly, we have proven the intermediacy of disilene **3'** as the kinetic product, which gives access to the very reactive bis(silyl)silyene **3**.

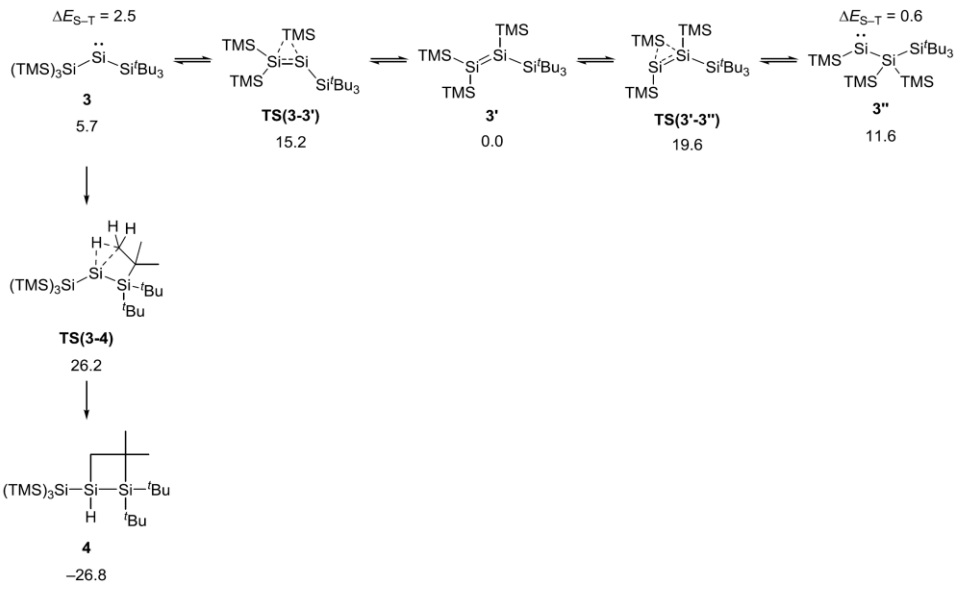


Figure S76. Computed pathway for the silylene-disilene-silylene interconversion at 298 K; the Gibbs Free energies ΔG_{298} and the singlet-triplet energy gap ΔE_{S-T} are reported in kcal/mol.

Mechanism for the interconversion between the silylenes 3 and 3'', disilene 3' and the C–H activation product (disiletane 4) at 133 K

In addition to the computed pathway for the silylene-disilene-silylene interconversion at 298 K, we calculated the same at 133 K, since we also performed EPR spectroscopy at this temperature. Here, we obtained comparable results with only slightly different energy values and effective barriers.

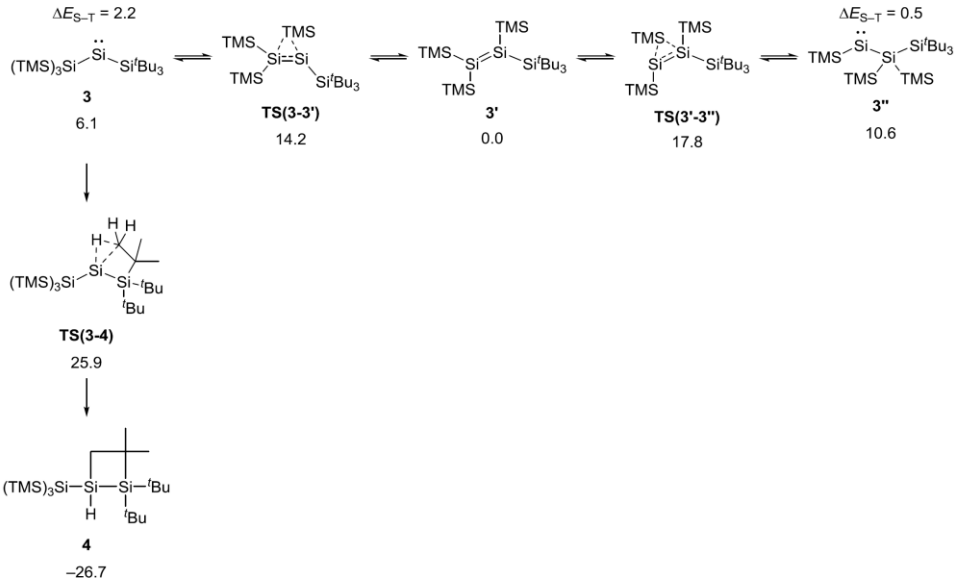


Figure S77. Computed pathway for the silylene-disilene-silylene interconversion at 133 K; the Gibbs Free energies ΔG_{133} and the singlet-triplet energy gap ΔE_{S-T} are reported in kcal/mol.

Bond dissociation energies for all Lewis base-stabilized silylenes

Table S11. Calculated bond dissociation energies for all plausible donor-stabilized bis(silyl)silylenes.

Compound	ΔG_{298} [kcal/mol]*	$D^0(0)$ [kcal/mol]*	ΔG_{298}^{iso} [kcal/mol]	ΔG_{298}^{base} [kcal/mol]
15 (**3**·I^{i}Pr$_2$Me$_2$)	16.3	44.6	0.0	0.0
13 (**3''**·I^{i}Pr$_2$Me$_2$)	22.0	47.4	0.3	0.3
3·IMe$_4$	22.5	47.6	0.0	–6.2
16 (**3''**·IMe$_4$)	27.6	50.7	0.9	–5.4
14 (**3**·DMAP)	15.3	33.5	0.0	1.0
3''·DMAP	17.4	33.1	3.8	4.9

* all dissociation energies are referenced to the singlet ground state of the corresponding donor-free silylene;
ΔG_{298}^{iso} relative energy between the respective two isomeric Lewis base-stabilized silylenes;
ΔG_{298}^{base} relative energy between all donor-stabilized silylenes, referenced to **15**.

Rearrangement of I^{i}Pr$_2$Me$_2$-stabilized bis(silyl)silylene 13

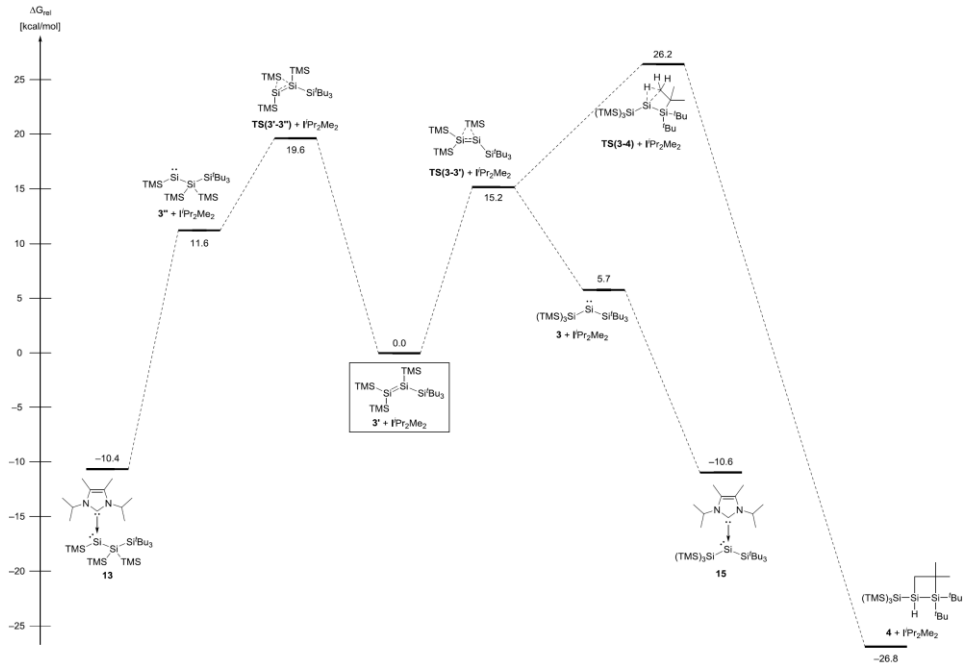


Figure S78. Computed pathway for the interconversion of the I^{i}Pr$_2$Me$_2$-stabilized silylenes **13** and **15** at 298 K.

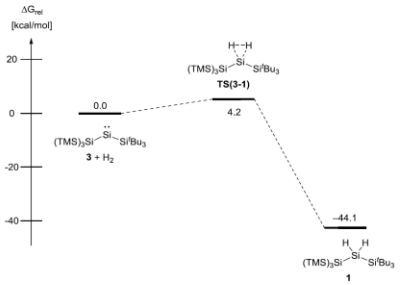


Figure S79. Computed pathway for the dihydrogen activation by singlet bis(silyl)silylene **3**.

Calculated IR Stretching Frequencies

Table S12. Selected experimentally determined and theoretically calculated IR frequencies.

Compound	Mode	Exp. $\tilde{\nu}$ [cm^{-1}]	Calc. $\tilde{\nu}$ [cm^{-1}]
17	*Si=O sym. stretch*	1069	1118
	Si–O–Si asym. stretch	971	948

Bonding analysis of the NHC-stabilized silanoic ester 17

There had been a lot of discussion in the community recently, concerning the formulation of Lewis structures with dative bonds or with a zwitterionic representation.[S33] We know that this is also the case for **17**, but for consistency, all structural representations in this report are given with dative C_{NHC}–Si bonds. Possible multiple bonding in four-coordinate silanoic esters and related thioesters has already been discussed in detail by Driess, Apeloig and co-workers in a combined theoretical and solid state NMR study.[S34] In contrast to their study, our silanoic ester **17** bears solely silyl substituents and one coordinating NHC. Thus, the NHC-stabilized silanoic ester **17** is prone for a more detailed investigation of its bonding situation.

Table S13. Selected results of the NBO analysis of the NHC-stabilized silanoic ester **17**.

Bond in **17**	NBO analysis (NLMOs)[a] pol.	hybr.	WBI
Si^2–Si^3	49% (Si^2) 51% (Si^3)	$sp^{1.74}$(Si^2) $sp^{2.44}$(Si^3)	0.85
Si^2–O^2	16% (Si^2) 84% (O^2)	$sp^{2.75}$(Si^2) $sp^{1.02}$(O^2)	0.91
Si^2–O^1	12% (Si^2) 88% (O^1)	$sp^{3.85}$(Si^2) $sp^{1.40}$(O^1)	0.47
Si^2–C^1	19% (Si^2) 81% (C^1)	$sp^{4.60}$(Si^2) $sp^{1.34}$(C^1)	0.54

Comparison to calculated less sterically encumbered silanoic ester derivatives

We calculated a collection of model systems with (**E-H**) and without (**A-D**) coordination of a stabilizing NHC as well as varying the number and position of silyl substituents. All model systems, as well as **17**, contain highly polarized Si–O bonds, whereas the WBIs of the Si^2–O^2 bond within the series **A-D** and **E-H** show only minor dependency on the substituents. Nevertheless, within **A-D** a less pronounced polarization of the Si^2–O^2 bond upon R^3 bearing a silyl group can be identified,

clearly evident by decrease of the difference of NPA charges $\Delta q(Si^2O^2)$. Furthermore, silyl groups at R^1 clearly increase the polarization of the $Si^2–O^1$ bond. Coordination of a NHC in **E-H** decreases the WBI of both Si–O bonds as expected, however polarizations of the $Si^2–O^2$ bond remain unchanged and only slightly reduced for $Si^2–O^1$. Comparison of model **A** to its NHC-stabilized congener **E** revealed quite similar polarization ($\Delta q(Si^2O^2)$ and $\Delta q(Si^2O^1)$) for both Si–O bonds upon NHC coordination.

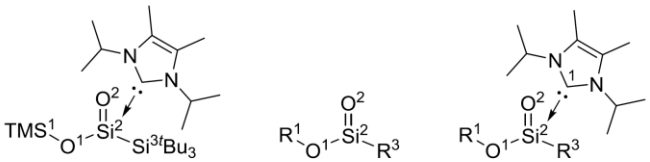


Figure S80. NHC-stabilized silanoic ester **17** and investigated simple donor-free and NHC-supported derivatives.

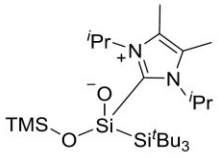
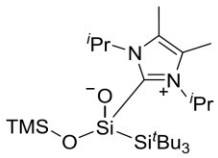
Table S14. Calculated structural parameters for the comparison of **17** with the smaller model systems **A-H**.

Compound	R^1/R^3	$q(Si^2)$	$q(O^2)$	$q(O^1)$	$\Delta q(Si^2O^2)$	$\Delta q(Si^2O^1)$	$WBI(Si^2O^2)$	$WBI(Si^2O^1)$
17	TMS/Si^{t}Bu$_3$	1.79	–1.36	–1.34	3.15	3.13	0.91	0.47
A	SiH_3/SiH_3	1.83	–1.17	–1.28	3.00	3.11	1.30	0.61
B	CH_3/CH_3	2.19	–1.19	–0.94	3.38	3.13	1.27	0.65
C	CH_3/SiH_3	1.81	–1.18	–0.94	2.99	2.75	1.28	0.65
D	SiH_3/CH_3	2.21	–1.18	–1.27	3.39	3.48	1.29	0.62
E	SiH_3/SiH_3	1.74	–1.28	–1.29	3.02	3.03	1.04	0.52
F	CH_3/CH_3	2.09	–1.30	–0.95	3.39	3.04	1.04	0.53
G	CH_3/SiH_3	1.74	–1.29	–0.96	3.03	2.70	1.04	0.54
H	SiH_3/CH_3	2.09	–1.29	–1.28	3.38	3.37	1.04	0.52

The same situation is also present in our silanoic ester **17**, although both WBIs are further decreased to 0.47 and 0.91 for the two Si–O bonds. Aiming on an explanation for the differences in the Si–O bond lengths for **17**, we used NBO analysis. Accordingly, the natural localized molecular orbitals (NLMOs, Figure S71), corresponding to the $\sigma(Si^2–Si^3)$, $\sigma(Si^2–O^1)$, $\sigma(Si^2–O^2)$ and $\sigma(Si^2–C^1)$ bonds, as well as three NLMOs, representing the electron lone pairs at O^2, are consistent with the zwitterionic representation as the major resonance structure within NRT analysis (Table S15). This analysis further revealed negative hyperconjugation of the lone pairs at O^2 into the $\sigma^*(Si^2–C^1)$ and $\sigma^*(Si^2–O^1)$. Both antibonding orbitals are partly populated ($Si^2–C^1$: 0.12 e, $Si^2–O^4$: 0.13 e) with decreased occupancy of the $LP(O^2)$ NBOs (1.83 e, 1.87 e). These results clearly rationalize the results found within SC-XRD structure: a short $Si^2–O^2$ bond length, being in the range of a Si=O double bond, and an elongated $Si^2–O^1$ bond, located on the upper end of reported Si–O single

bonds, together with an elongated C_{NHC}–Si bond. All in all, the bonding situation of our silanoic ester can be summarized as following: **17** possesses a zwitterionic representation with two highly polarized Si–O bonds and additional weakened Si^2–O^1 and Si^2–C^1 σ bonds by negative hyperconjugation. Thus, it is not astonishing that **17** possesses only limited thermal stability and is prone for the occurrence of side reactions.

Table S15. Results of NRT analysis of **17**.

Lewis structure		
Resonance weight	31.9 %	31.0 %

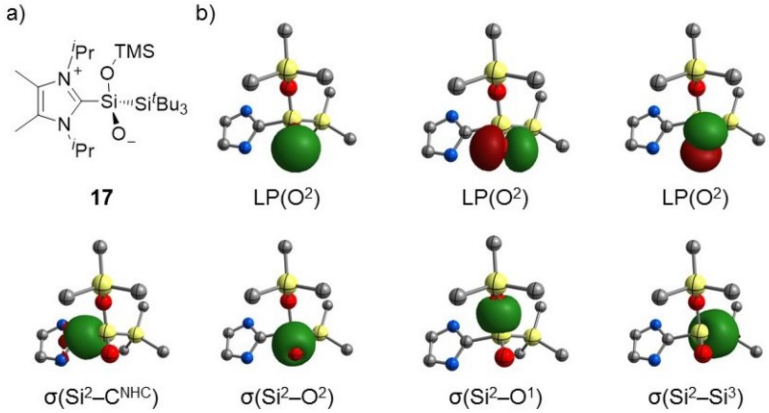


Figure S81. Results of the bonding analysis of **17**. (a) Dominant Lewis resonance structure according to NRT analysis; (b) NLMOs representing the electron lone pairs at O^2 and the C_{NHC}–Si^2, Si^2–O^1, Si^2–O^2, Si^2–Si^3 bonds.

Calculated energies at the M06-2X/6-311+G(d,p)(SMD: benzene) level of theory

Table S16. DFT-derived energies for the respective analyzed compounds.

Structure	E(SCF) [H/particle]
1	-2570.803718
TS(3-1)	-2570.722088
3 (singlet)	-2568.908465
3 (triplet)	-2568.912373
TS(3-4)	-2568.875705
TS(3-3')	-2568.893194
3'	-2568.917479
TS(3'-3'')	-2568.886242
3'' (singlet)	-2568.899001
3'' (triplet)	-2568.899965
4	-2568.960237
5	-2647.494162
6	-2625.496807
13	-3109.279400
14	-2951.000770
15	-3109.279819
16	-2952.175198
3''·DMAP	-2950.994669
3''·IMe$_4$	-2952.176611
17	-2152.162045
IMe$_4$	-383.232221
I^{i}Pr$_2$Me$_2$	-540.345382
DMAP	-382.067974

Cartesian coordinates (x,y,z) for the optimized structures

1

Si	2.56893	-0.01769	0.12410
H	0.41078	1.34809	2.00641
Si	0.46790	0.09189	1.19642
H	0.47762	-1.00674	2.20927
Si	-1.64474	0.00353	0.14058
Si	-2.96190	-0.69425	1.97177
Si	-2.33456	2.18854	-0.40498
Si	-2.24383	-1.39956	-1.66160
C	3.88807	0.61779	1.40737
C	3.84731	2.15068	1.53688
H	4.18092	2.65781	0.62737
H	4.52399	2.45855	2.34593
H	2.84573	2.51638	1.79079
C	3.59509	0.06101	2.81404
H	3.60077	-1.02958	2.85714
H	2.62642	0.40810	3.19044
H	4.36435	0.42223	3.51085
C	5.31895	0.21802	1.00420
H	5.58712	0.58147	0.00669
H	5.46923	-0.86504	1.01735
H	6.03431	0.65345	1.71614
C	2.82679	-1.89863	-0.31289
C	3.21719	-2.72588	0.92518
H	3.24386	-3.78898	0.64812
H	2.48875	-2.61812	1.73630
H	4.20570	-2.46887	1.31387
C	3.90974	-2.11037	-1.38502
H	3.63719	-1.66638	-2.34676
H	4.05452	-3.18680	-1.55340

TS(3-1)

Si	-2.55727	0.00360	0.14027
H	-0.48522	-1.49944	1.18760
Si	-0.43396	0.18045	1.20696
H	-0.38356	-1.16962	2.07720
Si	1.67450	-0.01175	0.12703
Si	3.05226	0.17605	2.03741
Si	2.27617	-2.01908	-0.94146
Si	2.31223	1.77550	-1.26713
C	-3.74763	-0.94601	1.36517
C	-3.58954	-2.47173	1.23671
H	-3.93719	-2.84928	0.27140
H	-4.19449	-2.95994	2.01306
H	-2.55256	-2.79893	1.37798
C	-3.45520	-0.60231	2.83862
H	-3.49876	0.46750	3.04998
H	-2.46919	-0.95774	3.15345
H	-4.20121	-1.09867	3.47507
C	-5.22464	-0.61078	1.08067
H	-5.50953	-0.80958	0.04287
H	-5.46379	0.43296	1.30134
H	-5.86570	-1.23181	1.72217
C	-3.04026	1.89266	-0.00482
C	-3.37910	2.48103	1.37649
H	-3.52529	3.56550	1.27720
H	-2.56895	2.32290	2.09758
H	-4.29950	2.06920	1.79796
C	-4.23695	2.14251	-0.93978
H	-4.00790	1.89068	-1.97948
H	-4.50255	3.20869	-0.91609

3 (singlet)

Si	2.47938	-0.05132	0.09767
Si	0.42074	-1.10324	0.75962
Si	-1.55478	-0.04566	0.06096
Si	-2.94912	-0.24307	1.96382
Si	-2.21260	1.95823	-1.00816
Si	-2.22928	-1.89831	-1.26928
C	2.80727	0.97019	1.73859
C	3.91811	2.02178	1.57850
H	4.86827	1.57014	1.27499
H	4.08636	2.52666	2.54080
H	3.66680	2.79437	0.84744
C	1.50688	1.67707	2.17466
H	0.72580	0.95142	2.45366
H	1.08530	2.33434	1.41048
H	1.69824	2.28305	3.07162
C	3.20643	0.05285	2.90944
H	4.17877	-0.42243	2.75740
H	2.46764	-0.73611	3.09200
H	3.27870	0.65516	3.82602
C	3.78726	-1.48657	-0.12196
C	3.54971	-2.64083	0.87102
H	4.33900	-3.39389	0.73635
H	2.58862	-3.13518	0.69764
H	3.57117	-2.32661	1.91621
C	5.23231	-0.98724	0.06139
H	5.47906	-0.15296	-0.60206
H	5.93268	-1.80447	-0.16282
H	5.43018	-0.66788	1.08887
C	3.67223	-2.10859	-1.52525

H 4.87650 -1.69270 -1.08418
C 1.50020 -2.49977 -0.81532
H 1.07871 -1.96253 -1.66734
H 0.74441 -2.51163 -0.01977
H 1.66094 -3.54222 -1.12549
C 2.48652 1.11557 -1.45242
C 3.86445 1.41022 -2.06717
H 4.40817 0.49722 -2.33019
H 4.49843 1.99735 -1.39607
H 3.73772 1.99566 -2.98872
C 1.80404 2.45165 -1.10464
H 2.35080 3.04341 -0.36878
H 0.79059 2.28883 -0.71966
H 1.70954 3.06095 -2.01505
C 1.59770 0.46275 -2.52194
H 1.45840 1.16011 -3.36086
H 0.60318 0.23049 -2.12329
H 2.02367 -0.45714 -2.93282
C -2.28318 -2.29230 2.72458
H -2.11694 -3.06359 1.96558
H -2.99927 -2.68595 3.45531
H -1.33459 -2.11873 3.23985
C -2.91432 0.65105 3.30175
H -1.88313 0.89522 3.57877
H -3.43652 0.31164 4.20362
H -3.39822 1.57202 2.96009
C -4.76964 -1.02121 1.51374
H -5.23563 -0.16703 1.01323
H -5.33764 -1.22908 2.42818
H -4.86323 -1.89461 0.85972
C -4.21063 2.35238 -0.20472
H -4.52686 3.35282 -0.52263
H -4.51059 2.22495 0.84080
H -4.75679 1.61880 -0.80538
C -1.55008 3.46726 0.74660
H -0.46335 3.52642 0.63770
H -1.76536 3.22880 1.79361
H -1.96696 4.45812 0.53176
C -1.91338 2.59740 -2.20533
H -0.85270 2.44476 -2.42819
H -2.15932 3.64276 -2.42478
H -2.49300 1.96826 -2.88972
C -4.01931 -0.90369 -2.10588
H -4.04281 0.08593 -2.57486
H -4.68745 -0.88451 -1.24087
H -4.42177 -1.62240 -2.82966
C -1.29383 -1.24480 -3.29145
H -0.29276 -1.68120 -3.26238
H -1.20372 -0.20245 -3.61383
H -1.86930 -1.78234 -4.05504
C -2.26347 -3.21734 -1.14216
H -2.59449 -3.83794 -1.98287
H -2.95906 -3.38028 -0.31211
H -1.27514 -3.56881 -0.83076

3 (triplet)

Si -2.58012 0.03072 0.12361
Si -0.35244 0.19389 0.86002
Si 1.81936 0.02655 0.06243
Si 3.00954 -0.39703 2.04603
Si 2.19524 -1.75010 -1.42446
Si 2.54285 2.09079 -0.78935
C -3.32436 -1.54936 0.99225
C -4.68500 -1.94715 0.38996
H -5.41488 -1.13234 0.42299
H -5.10416 -2.78708 0.96140
H -4.59616 -2.27738 -0.64910
C -2.37554 -2.75787 0.87797
H -1.41511 -2.56685 1.37044
H -2.17082 -3.04746 -0.15484
H -2.83683 -3.62240 1.37526
C -3.52201 -1.30199 2.49822
H -4.29036 -0.55255 2.70571
H -2.59122 -0.98787 2.98626
H -3.84337 -2.23776 2.97585

H -5.12578 1.57679 -0.64379
C -1.84781 2.71193 -0.53385
H -1.53173 2.40348 -1.53102
H -0.97813 2.65087 0.13397
H -2.12897 3.77280 -0.59008
C -2.50568 -0.85739 -1.60783
C -3.90468 -1.14938 -2.17933
H -4.53819 -0.25898 -2.22942
H -4.43567 -1.90839 -1.59697
H -3.80434 -1.53961 -3.20191
C -1.72508 -2.17999 -1.54926
H -2.16652 -2.91890 -0.87740
H -0.69563 -2.00470 -1.22760
H -1.68923 -2.62665 -2.55340
C -1.74291 0.03170 -2.60342
H -1.59294 -0.51729 -3.54431
H -0.75046 0.29949 -2.21995
H -2.27791 0.95322 -2.84994
C 2.42004 1.53865 3.18517
H 2.30695 2.49249 2.65970
H 3.12852 1.68635 4.00862
H 1.44682 1.27552 3.60902
C 3.00288 -1.45861 2.99428
H 1.97342 -1.74299 3.23973
H 3.55459 -1.36119 3.93632
H 3.45388 -2.27755 2.42440
C 4.86053 0.57172 1.63564
H 5.29677 -0.13412 0.92246
H 5.45178 0.52988 2.55794
H 4.96197 1.58113 1.22276
C 4.15319 -2.24828 -0.81751
H 4.44994 -3.14599 -1.37266
H 4.47292 -2.37816 0.22166
H 4.69978 -1.39738 -1.23564
C 1.49928 -3.51511 -0.07999
H 0.40762 -3.53041 -0.14417
H 1.77566 -3.52833 0.98018
H 1.87548 -4.43906 -0.53439
C 1.83993 -2.00079 -2.78401
H 0.79045 -1.75463 -2.96900
H 2.04443 -2.97976 -3.23276
H 2.45493 -1.26013 -3.30741
C 4.05882 1.39680 -1.89665
H 4.04713 0.55571 -2.59830
H 4.75907 1.15772 -1.09184
H 4.44512 2.27074 -2.43452
C 1.27351 2.03904 -2.82513
H 0.27541 2.42810 -2.61027
H 1.16443 1.11310 -3.39951
H 1.78814 2.76986 -3.46057
C 2.36842 3.39243 -0.28851
H 2.63319 4.22508 -0.95012
H 3.12069 3.34206 0.50580
H 1.40392 3.62223 0.17591

TS(3-4)

Si 2.60661 0.10179 0.02442
H 0.65283 2.27272 -0.33511
Si 0.48122 0.98013 0.48466
Si -1.63815 0.06589 0.06817
Si -2.19516 -0.87035 2.15395
Si -3.02153 1.96233 -0.15868
Si -2.26504 -1.42351 -1.64901
C 2.74949 1.53711 -1.28107
C 1.24875 1.64671 -1.60108
H 0.83827 0.83782 -2.20454
H 0.96385 2.60244 -2.06234
C 3.19102 2.88627 -0.68588
H 2.59184 3.18355 0.17906
H 3.07446 3.66452 -1.45383
H 4.24256 2.88072 -0.38587
C 3.60399 1.29464 -2.53233
H 4.66632 1.24243 -2.26349
H 3.48152 2.12690 -3.23952
H 3.35030 0.37383 -3.06012

H 3.96736 -1.41966 -2.32074
H 2.65391 -2.45879 -1.73694
H 4.33537 -2.98250 -1.58842
C 2.42645 1.08725 -1.48022
C 3.81433 1.49185 -2.00356
H 4.38502 0.63699 -2.37642
H 4.41739 1.99235 -1.23859
H 3.69702 2.19342 -2.84173
C 1.63777 2.36559 -1.16848
H 2.14041 3.01886 -0.45023
H 0.64821 2.11880 -0.77358
H 1.49474 2.94638 -2.09153
C 1.65158 0.37898 -2.60673
H 1.58959 1.04140 -3.48262
H 0.62535 0.15488 -2.29203
H 2.11459 -0.55397 -2.93508
C -2.29183 -1.53901 3.17110
H -2.12853 -2.50562 2.68522
H -3.00878 -1.67751 3.98896
H -1.33548 -1.22687 3.60389
C -2.99476 1.42016 2.86982
H -1.98552 1.76146 3.12495
H -3.56423 1.32313 3.80146
H -3.47147 2.20005 2.26713
C -4.73158 -0.70596 1.52031
H -5.17259 -0.00783 0.80297
H -5.34586 -0.69008 2.42846
H -4.79544 -1.71211 1.09437
C -1.70329 2.03876 -2.82773
H -2.20471 2.88546 -3.31077
H -1.99436 1.12723 -3.36125
H -0.62520 2.16843 -2.94994
C -4.10732 2.01173 -0.95493
H -4.45378 2.87986 -1.52853
H -4.47422 2.12535 0.07034
H -4.56816 1.11753 -1.38418
C -1.64298 3.52568 -0.10748
H -1.76638 3.42641 0.97568
H -2.26537 4.36564 -0.43820
H -0.60056 3.78494 -0.30725
C -3.84763 -1.52991 -2.17571
H -3.74968 -0.67329 -2.85040
H -4.66232 -1.32188 -1.47497
H -4.13140 -2.40155 -2.77739
C -0.91686 -2.30331 -2.57414
H 0.05670 -2.52340 -2.11778
H -0.77368 -1.47478 -3.27531
H -1.22040 -3.18559 -3.14968
C -2.47492 -3.44739 -0.21379
H -2.77660 -4.28212 -0.85759
H -3.25249 -3.31079 0.54371
H -1.55071 -3.72727 0.30146

TS(3-3')

Si -0.24192 -1.07655 0.69185
Si 1.19206 -2.05129 -1.22810
Si 1.55670 0.15262 0.22067
Si 3.40794 -0.70999 1.41593
C 3.94858 0.71567 2.54653
H 4.75952 0.37242 3.19995
H 4.30805 1.59263 2.00104
H 3.11765 1.03201 3.18668
C 4.89361 -1.21790 0.35574
H 5.69099 -1.59459 1.00711
H 4.65243 -2.00342 -0.36612
H 5.29302 -0.36471 -0.20040
C 2.89048 -2.11611 2.56545
H 2.24781 -2.85534 2.08314
H 3.77824 -2.62560 2.95804
H 2.33110 -1.70277 3.41102
Si 2.32264 2.17914 -0.78708
C 4.20121 2.12455 -1.01891
H 4.49337 1.34401 -1.72880
H 4.52187 3.08736 -1.43510
H 4.75123 1.96531 -0.08820

C	-3.42130	1.67570	0.75261
C	-2.96200	2.03587	2.17933
H	-3.49122	2.94186	2.50595
H	-1.88852	2.25448	2.21202
H	-3.16665	1.25361	2.91272
C	-4.95829	1.57634	0.75228
H	-5.36308	1.30288	-0.22738
H	-5.38562	2.55171	1.02371
H	-5.32493	0.84983	1.48325
C	-3.01907	2.86820	-0.13379
H	-3.41561	2.79547	-1.14989
H	-1.92955	2.98058	-0.19397
H	-3.42030	3.79155	0.30603
C	-2.61812	-0.11618	-1.82077
C	-4.00907	0.20066	-2.40011
H	-4.30047	1.24176	-2.23622
H	-4.79293	-0.43916	-1.98195
H	-3.99505	0.03555	-3.48664
C	-2.22940	-1.53298	-2.27562
H	-2.96859	-2.28678	-1.99218
H	-1.25620	-1.83766	-1.87451
H	-2.15179	-1.54919	-3.37197
C	-1.59199	0.83691	-2.45823
H	-1.62070	0.72521	-3.55188
H	-0.57254	0.60405	-2.13049
H	-1.77995	1.88819	-2.23028
C	2.31506	0.65581	3.45362
H	2.30221	1.71995	3.19719
H	2.91991	0.52873	4.35879
H	1.28695	0.35617	3.68598
C	2.82243	-2.21654	2.52569
H	1.76349	-2.49347	2.58392
H	3.27593	-2.40162	3.50602
H	3.30704	-2.87868	1.80065
C	4.84666	0.00013	1.82424
H	5.27868	-0.55154	0.98278
H	5.40485	-0.26904	2.72815
H	5.00180	1.06868	1.64132
C	1.67425	-1.29892	-3.18511
H	1.92392	-2.11488	-3.87307
H	2.19683	-0.39898	-3.52777
H	0.59880	-1.11162	-3.26002
C	4.05145	-2.12405	-1.43725
H	4.27672	-2.90512	-2.17246
H	4.38985	-2.47853	-0.45779
H	4.63899	-1.23680	-1.69569
C	1.27832	-3.29975	-0.85425
H	1.60752	-3.59912	0.14611
H	1.47081	-4.13277	-1.53997
H	0.19700	-3.13881	-0.80858
C	4.23586	1.87542	-1.60802
H	4.16223	1.23548	-2.49420
H	4.96070	1.42185	-0.92420
H	4.63216	2.84577	-1.92806
C	1.34595	2.81008	-2.06062
H	0.36769	3.00208	-1.60679
H	1.19652	2.13908	-2.91291
H	1.73632	3.76140	-2.44023
C	2.67921	3.32183	0.63899
H	2.94781	4.31590	0.26412
H	3.43984	3.01832	1.36569
H	1.72177	3.40507	1.16642

3'

Si	-0.08770	0.64733	0.13933
Si	0.05441	2.94401	0.72126
Si	1.89926	-0.25231	0.11257
Si	3.70451	0.97158	-0.76992
C	4.63637	-0.26330	-1.86929
H	5.43926	0.26401	-2.39860
H	5.09198	-1.08246	-1.30568
H	3.96886	-0.69765	-2.62089
C	4.95031	1.65459	0.47695
H	5.77891	2.13404	-0.05724
H	4.51187	2.38741	1.15789
C	3.90841	0.19420	1.45624
C	3.62960	1.40407	2.36461
H	2.63528	1.34810	2.82006
H	3.69813	2.35586	1.83375
H	4.37193	1.42514	3.17446
C	5.32327	0.33897	0.86455
H	6.05844	0.40705	1.67876
H	5.42510	1.24403	0.25771
H	5.60432	-0.51454	0.24018
C	3.88215	-1.05158	2.35600
H	4.19538	-1.95741	1.82949
H	2.88782	-1.22812	2.78331
H	4.57733	-0.90608	3.19428
C	2.51644	-1.65826	-0.78307
C	1.63310	-1.64709	-2.03883
H	1.51283	-2.67522	-2.40996
H	2.04378	-1.05468	-2.85986
H	0.63565	-1.26637	-1.80069
C	3.90220	-2.20444	-1.16265
H	4.53312	-2.37927	-0.28614
H	4.44028	-1.52923	-1.83806
H	3.78943	-3.16830	-1.67856
C	1.82858	-2.63135	0.19284
H	1.74549	-3.62202	-0.27713
H	0.81203	-2.29289	0.42728
H	2.36538	-2.76058	1.13427
C	-0.86676	-2.08504	2.73884
H	-1.11528	-2.45847	3.73903
H	0.11685	-1.60407	2.79476
H	-0.78167	-2.94641	2.06806
C	-2.32178	0.50540	3.44594
H	-2.50230	0.07624	4.43822
H	-3.14235	1.19528	3.22377
H	-1.39581	1.08893	3.49000
C	-3.84345	-1.79692	2.08633
H	-3.79323	-2.65276	1.40468
H	-4.65908	-1.14647	1.75422
H	-4.09760	-2.17690	3.08256
C	-2.36422	3.42325	0.84188
H	-2.19502	3.15221	1.88857
H	-3.08690	4.24711	0.81073
H	-1.41227	3.78403	0.44099
C	-4.78414	1.60235	0.43457
H	-5.22457	0.73925	-0.07337
H	-5.42343	2.47187	0.24193
H	-4.80523	1.40629	1.51175
C	-3.09805	2.48782	-1.97704
H	-2.09285	2.65286	-2.38072
H	-3.66074	3.42284	-2.07886
H	-3.58953	1.73182	-2.59822
C	-4.16001	-1.42917	-1.70458
H	-4.49868	-2.19582	-2.41166
H	-4.55245	-0.46569	-2.04625
H	-4.60396	-1.64968	-0.72895
C	-1.69653	-0.89021	-3.37578
H	-1.92099	0.16669	-3.55212
H	-2.23967	-1.47635	-4.12661
H	-0.62752	-1.04252	-3.54457
C	-1.71557	-3.20030	-1.30258
H	-2.09403	-3.53805	-0.33134
H	-0.62773	-3.30790	-1.29410
H	-2.11803	-3.87118	-2.07046

TS(3'-3'')

Si	-0.20080	-0.25697	-0.11440
Si	-1.00502	-2.25855	-1.15555
Si	-1.63794	1.05039	1.00004
Si	-1.40162	1.95361	-1.37017
C	-0.80219	3.74459	-1.23316
H	-1.19565	4.28088	-2.10645
H	-1.19360	4.21905	-0.32902
H	0.28383	3.85474	-1.23585
C	-3.26918	2.08423	-1.68419
H	-3.41248	2.56852	-2.65852
H	-3.78675	1.12210	-1.70393
C	1.93741	3.58921	0.41675
H	2.39469	4.51473	0.04704
H	0.86361	3.76516	0.52708
H	2.34928	3.38587	1.41099
C	1.64280	2.57392	-2.50411
H	2.02925	1.86304	-3.24152
H	0.55379	2.57662	-2.56528
H	2.00278	3.57113	-2.78676
C	-0.24374	-2.74724	-2.25189
H	-0.80180	-1.97330	-2.78314
H	0.21299	-3.40673	-3.00196
H	-0.93685	-3.34318	-1.65229
C	2.08525	-3.57766	-0.56097
H	1.40974	-4.15900	0.07396
H	2.36571	-4.19623	-1.42291
H	2.99125	-3.36770	0.00894
C	2.29802	-1.24703	-2.55785
H	1.75148	-0.44528	-3.06607
H	3.23163	-0.83311	-2.16384
H	2.55108	-2.00770	-3.30728
Si	-2.32113	0.05534	0.20231
C	-3.67983	-1.33359	-0.06158
C	-2.36356	1.34768	-1.25858
C	-2.59078	0.94511	1.93619
C	-3.77382	1.93103	1.91501
H	-3.94033	2.31737	2.93089
H	-3.58150	2.79472	1.27219
H	-4.70718	1.46776	1.58372
C	-1.33873	1.72575	2.38836
H	-0.99177	2.45725	1.65518
H	-1.57461	2.27101	3.31320
H	-0.50040	1.05740	2.60961
C	-2.85866	-0.08967	3.04634
H	-2.06050	-0.83843	3.11348
H	-2.90310	0.42851	4.01463
H	-3.80753	-0.61568	2.91737
C	-3.78684	1.79279	-1.64109
H	-4.32951	2.22208	-0.79326
H	-3.72713	2.56743	-2.41929
H	-4.38938	0.97633	-2.04628
C	-1.57703	2.60839	-0.87150
H	-2.06561	3.18041	-0.07850
H	-0.56477	2.36007	-0.53833
H	-1.49110	3.27181	-1.74440
C	-1.68217	0.76163	-2.50782
H	-2.20398	-0.11594	-2.89824
H	-1.66480	1.51597	-3.30820
H	-0.64342	0.47539	-2.29881
C	-3.33565	-2.59697	0.75132
H	-4.14484	-3.33208	0.63633
H	-2.41133	-3.06458	0.39551
H	-3.21174	-2.40567	1.81986
C	-3.75086	-1.78299	-1.53197
H	-4.12914	-1.00347	-2.19782
H	-2.78041	-2.11276	-1.90947
H	-4.43834	-2.63696	-1.61152
C	-5.09431	-0.87355	0.33746
H	-5.18806	-0.68427	1.40980
H	-5.40507	0.03186	-0.19390
H	-5.81458	-1.66501	0.08556

3'' (singlet)

Si	0.24862	0.57217	-0.03316
Si	1.18092	1.09319	2.09349
Si	1.67620	-0.56867	-1.54414
Si	0.46931	2.60670	-1.26761
C	-0.26896	2.72524	-3.00706
H	-0.00488	3.71941	-3.38907
H	0.18071	1.98413	-3.67566
H	-1.35400	2.62160	-3.06063
C	2.32722	2.84452	-1.59658
H	2.46990	3.75248	-2.19506
H	2.92657	2.94116	-0.69051
H	2.73360	2.01237	-2.18975
C	-0.16650	4.07249	-0.25590

H	5.36581	0.84072	1.07977
C	3.09422	2.30601	-1.96608
H	2.62370	1.81710	-2.82556
H	2.36102	2.99293	-1.53863
H	3.94254	2.89574	-2.33315
Si	2.63668	-2.42325	0.64743
C	4.31273	-2.13370	1.48480
H	4.20059	-1.49497	2.36726
H	4.72506	-3.09459	1.81470
H	5.04567	-1.66618	0.82144
C	2.89527	-3.56954	-0.83134
H	1.95242	-3.80486	-1.33256
H	3.56896	-3.11988	-1.56671
H	3.34373	-4.50999	-0.49048
C	1.56246	-3.27689	1.94466
H	1.34300	-2.59890	2.77545
H	0.61649	-3.64283	1.54104
H	2.11219	-4.13693	2.34511
C	-0.43993	4.16826	-0.63587
H	-1.51637	4.14952	-0.83212
H	-0.17606	5.18107	-0.30936
H	0.07767	3.96977	-1.57952
C	1.80692	3.36720	1.29595
H	2.54267	3.39944	0.49145
H	1.77748	4.36168	1.75770
H	2.15103	2.65288	2.05057
C	-0.98937	3.32947	2.25705
H	-2.06677	3.21488	2.12510
H	-0.68156	2.70598	3.10242
H	-0.79549	4.37523	2.52582
Si	-2.20021	-0.43239	-0.17257
C	-3.28349	0.89551	-1.11408
C	-2.93362	-0.87358	1.57770
C	-1.97226	-2.02004	-1.28274
C	-3.22953	-2.91046	-1.27991
H	-3.08138	-3.74112	-1.98414
H	-3.41758	-3.35223	-0.29697
H	-4.13321	-2.37738	-1.58814
C	-0.79515	-2.87773	-0.79879
H	-0.94261	-3.26127	0.21071
H	-0.67708	-3.74353	-1.46631
H	0.14207	-2.31257	-0.82508
C	-1.65495	-1.63936	-2.73993
H	-0.79105	-0.96813	-2.80862
H	-1.41031	-2.55231	-3.30014
H	-2.50219	-1.17034	-3.24615
C	-4.44928	-1.14041	1.53955
H	-4.72245	-1.92709	0.82977
H	-4.78540	-1.46439	2.53450
H	-5.02054	-0.24313	1.28370
C	-2.23770	-2.12012	2.15170
H	-2.49399	-3.03398	1.60862
H	-1.14624	-2.01146	2.15518
H	-2.55708	-2.26240	3.19327
C	-2.67067	0.26122	2.58290
H	-3.12542	1.20889	2.28805
H	-3.09227	-0.01581	3.55918
H	-1.59709	0.43019	2.72326
C	-2.48995	1.56837	-2.25158
H	-3.11196	2.35211	-2.70711
H	-1.57505	2.04785	-1.89035
H	-2.20631	0.87470	-3.04396
C	-3.71242	2.02058	-0.15807
H	-4.40016	1.67596	0.61896
H	-2.85375	2.49052	0.33056
H	-4.23071	2.80338	-0.72943
C	-4.56227	0.29176	-1.72350
H	-4.34466	-0.41206	-2.53142
H	-5.18123	-0.22351	-0.98229
H	-5.17042	1.09932	-2.15489

3'' (triplet)

Si	2.11636	0.42605	-0.87163
Si	3.95248	-0.94775	-0.38431
Si	-0.04350	0.85544	-0.08735
H	-3.73574	2.70948	-0.91738
C	-0.64889	1.30697	-2.99712
H	0.44384	1.34514	-2.99544
H	-0.95312	0.28664	-3.24235
H	-1.00356	1.96532	-3.80092
Si	-3.76634	0.00553	1.26514
C	-4.66018	-1.24006	0.14693
H	-4.08179	-2.14307	-0.05984
H	-5.57740	-1.53913	0.66955
H	-4.95773	-0.79748	-0.80874
C	-5.02233	1.40152	1.53822
H	-4.60415	2.20297	2.15547
H	-5.35260	1.83909	0.59094
H	-5.90836	1.00579	2.04890
C	-3.52655	-0.82392	2.96004
H	-2.78219	-1.62651	2.93704
H	-3.19856	-0.09052	3.70455
H	-4.47547	-1.25074	3.30545
C	0.05529	-3.39781	-2.24107
H	0.69090	-4.07171	-1.66165
H	-0.64743	-4.01696	-2.81259
H	0.68439	-2.86346	-2.95887
C	-2.43609	-1.76175	-2.29383
H	-2.06533	-1.61585	-3.31351
H	-3.17488	-2.57087	-2.32420
H	-2.94704	-0.85066	-1.97743
C	-1.61147	-3.32693	0.28569
H	-0.76058	-3.80053	0.78678
H	-2.16583	-2.75242	1.03251
H	-2.26532	-4.12304	-0.08998
Si	2.15063	0.08675	0.32757
C	3.17612	-0.85012	-1.04121
C	2.30325	-0.79453	2.06780
C	2.65998	1.95999	0.42621
C	4.01619	2.15384	1.13154
H	4.29990	3.21389	1.07068
H	3.96605	1.89642	2.19336
H	4.82406	1.57229	0.67852
C	1.61989	2.80552	1.18138
H	1.51941	2.52084	2.22980
H	1.92930	3.86034	1.15279
H	0.62598	2.74173	0.73549
C	2.77709	2.54668	-0.99201
H	1.87397	2.37344	-1.58716
H	2.92184	3.63382	-0.92318
H	3.62845	2.14147	-1.54497
C	3.76231	-1.15823	2.40272
H	4.42569	-0.28843	2.37470
H	3.80529	-1.56916	3.42109
H	4.17477	-1.91625	1.73228
C	1.78091	0.11056	3.19807
H	2.42791	0.97472	3.37051
H	0.76408	0.47198	3.00686
H	1.75795	-0.46719	4.13242
C	1.45296	-2.07960	2.12194
H	1.70039	-2.80138	1.33941
H	1.61150	-2.57690	3.08896
H	0.38044	-1.85440	2.05736
C	2.63013	-0.51457	-2.44145
H	3.17373	-1.10097	-3.19559
H	1.56764	-0.76711	-2.53345
H	2.74598	0.53985	-2.70246
C	3.03596	-2.37095	-0.86671
H	3.55332	-2.74199	0.02116
H	1.99033	-2.67680	-0.80262
H	3.47211	-2.88050	-1.73743
C	4.67988	-0.52223	-1.01596
H	4.88814	0.51841	-1.27760
H	5.13415	-0.72392	-0.04045
H	5.19678	-1.15075	-1.75467

4

Si	-2.61188	-0.07367	-0.07455
H	-0.37107	-2.29044	-0.46696
Si	-0.44030	-0.80124	-0.58293
H	-1.24117	3.98708	-0.06263
H	0.34388	4.14763	0.70960
H	0.00746	5.00647	-0.80268
Si	3.64330	-1.47499	-0.51781
C	4.68208	-0.66471	0.84246
H	4.12297	-0.44688	1.75499
H	5.49404	-1.35691	1.09751
H	5.14077	0.26488	0.49090
C	4.82895	-1.74561	-1.97153
H	4.35139	-2.32913	-2.76481
H	5.15112	-0.79393	-2.40754
H	5.72461	-2.28377	-1.63984
C	3.10870	-3.19583	0.09463
H	2.66481	-3.15370	1.09366
H	2.38722	-3.67874	-0.57378
H	3.99561	-3.83851	0.14521
C	0.16604	2.18946	3.26624
H	-0.73486	1.71251	3.65866
H	0.81268	2.43859	4.11692
H	-0.13045	3.13032	2.79151
C	2.76042	2.10611	1.82054
H	2.51185	3.13841	1.55108
H	3.32789	2.13593	2.75861
H	3.41142	1.69547	1.04652
C	1.64440	-0.46493	3.07057
H	0.76988	-0.92561	3.54001
H	2.12510	-1.22435	2.44697
H	2.34400	-0.18868	3.86859
Si	-1.87360	-0.58616	-0.05016
C	-2.92206	0.11136	1.44155
C	-1.46558	-2.48261	0.19982
C	-2.79006	-0.28651	-1.74010
C	-3.95300	-1.26830	-1.97614
H	-4.48459	-0.97996	-2.89403
H	-3.60400	-2.29508	-2.11829
H	-4.68309	-1.26869	-1.16128
C	-1.82073	-0.41286	-2.92828
H	-1.42083	-1.42179	-3.04709
H	-2.35087	-0.15727	-3.85695
H	-0.96965	0.26431	-2.83832
C	-3.36910	1.13975	-1.77338
H	-2.62988	1.89697	-1.49053
H	-3.70727	1.37118	-2.79311
H	-4.23329	1.25157	-1.11320
C	-2.69907	-3.30013	0.63019
H	-3.53331	-3.20428	-0.07092
H	-2.42938	-4.36450	0.67693
H	-3.05915	-3.01668	1.62268
C	-0.92802	-3.11113	-1.09628
H	-1.68627	-3.17993	-1.88023
H	-0.07436	-2.55807	-1.51487
H	-0.57834	-4.13137	-0.88645
C	-0.36876	-2.67785	1.25928
H	-0.66171	-2.32718	2.25060
H	-0.12705	-3.74683	1.34486
H	0.55432	-2.15702	0.98069
C	-2.83717	1.64912	1.49376
H	-3.32950	2.01070	2.40772
H	-1.80271	2.00508	1.51838
H	-3.33414	2.12568	0.64633
C	-2.36904	-0.42028	2.77554
H	-2.56453	-1.48735	2.90994
H	-1.29134	-0.26149	2.87307
H	-2.85603	0.10707	3.60790
C	-4.41025	-0.27851	1.37566
H	-4.92281	0.17768	0.52473
H	-4.55971	-1.36108	1.31945
H	-4.91611	0.07601	2.28490

5

Si	-0.47225	-1.05292	-0.02451
C	-0.39963	-2.75728	0.79492
H	0.53107	-3.04492	1.27958
H	-1.27226	-3.13929	1.32025
Si	-2.58063	0.01757	-0.04846

Si -0.64512 2.58123 -1.62010	Si 1.70161 -0.07065 0.01609	C -0.41925 -2.81143 -0.73071
Si 0.40137 2.04571 1.93410	Si 1.99579 -0.77619 2.23650	H -1.31159 -3.21472 -1.20189
Si -1.39803 -1.12671 0.03955	Si 3.15503 -1.35906 -1.31590	H 0.48983 -3.15528 -1.21703
C 5.39723 -0.14811 -1.30068	Si 2.32920 2.17776 -0.25675	C -2.76356 0.70630 -1.86295
H 5.56418 0.87615 -0.95352	C -2.70862 -0.50083 -1.98968	Si 1.67039 -0.05737 0.02288
H 5.21072 -0.11352 -2.37849	C -1.18276 -0.34233 -2.30578	C -1.39985 1.20573 -2.37712
H 6.31561 -0.72198 -1.13154	H -0.93050 0.69723 -2.54338	H -1.52625 1.66671 -3.36717
C 3.76962 -2.72059 -1.01363	H -0.87057 -0.95894 -3.15947	H -0.69298 0.37485 -2.49232
H 4.73470 -3.23168 -0.91304	C -3.06219 -1.97500 -2.25567	H -0.93639 1.94819 -1.72388
H 3.47976 -2.74565 -2.06858	H -2.39875 -2.66775 -1.72931	Si 3.05283 -1.66849 -1.02375
H 3.02865 -3.28825 -0.44309	H -2.94778 -2.17311 -3.33070	Si 2.36046 0.17935 2.26402
C 4.36272 -1.00481 1.45815	H -4.09433 -2.21950 -1.98745	C -3.18925 -0.40776 -2.83648
H 4.58284 -0.00472 1.84437	C -3.61527 0.35663 -2.87888	H -4.20555 -0.76683 -2.65564
H 5.25095 -1.62970 1.61047	H -4.67245 0.19619 -2.63232	H -2.50582 -1.26416 -2.79486
H 3.54493 -1.42992 2.04834	H -3.47630 0.08242 -3.93417	H -3.16115 -0.01546 -3.86262
C -1.31025 2.08188 -3.32136	H -3.41361 1.42682 -2.79010	C -3.78061 1.85573 -1.96998
H -2.28029 1.58045 -3.30402	C -3.84102 -1.05530 1.05096	H -4.77263 1.57098 -1.60547
H -0.60182 1.44297 -3.85714	C -3.41359 -2.53167 1.12204	H -3.88935 2.15192 -3.02279
H -1.42385 3.00789 -3.89872	H -2.41103 -2.63799 1.55218	H -3.46219 2.74390 -1.41620
C 0.90917 3.57804 -2.04497	H -3.41154 -3.01817 0.14419	Si 2.26416 1.94885 -1.08805
H 0.61028 4.49015 -2.57581	H -4.11384 -3.08413 1.76392	C -4.02146 -1.21947 0.39603
H 1.55030 2.99468 -2.71570	C -5.26221 -0.96824 0.46411	C -5.39004 -0.62312 0.01220
H 1.50853 3.86492 -1.17931	H -5.95666 -1.54611 1.09030	H -5.56110 0.36308 0.45426
C -1.92312 3.73610 -0.83145	H -5.31875 -1.37562 -0.54929	H -6.18627 -1.28838 0.37475
H -1.58232 4.12805 0.13222	H -5.63112 0.06216 0.43023	H -5.51459 -0.53229 -1.07034
H -2.88232 3.23241 -0.67122	C -3.88885 -0.53169 2.49473	C -3.88028 -2.57986 -0.31226
H -2.10077 4.58948 -1.49614	H -4.29838 0.48053 2.55830	H -4.78174 -3.17716 -0.11623
C 1.35508 3.62256 1.49726	H -2.90134 -0.53323 2.96974	H -3.03064 -3.14749 0.07624
H 1.63675 4.12251 2.43162	H -4.54134 -1.18408 3.09155	H -3.76968 -2.50012 -1.39539
H 0.76075 4.32749 0.90815	C -2.61082 1.83047 0.27896	C -4.05129 -1.52523 1.90437
H 2.27369 3.39678 0.94477	C -1.72471 2.56927 -0.73610	H -4.33731 -0.65613 2.50235
C 1.53441 1.10464 3.12441	H -1.66900 3.63377 -0.46576	H -3.08632 -1.89216 2.27140
H 1.83968 1.79725 3.91797	H -2.09700 2.51168 -1.76175	H -4.79801 -2.30857 2.09452
H 2.44129 0.75908 2.61737	H -0.70158 2.17728 -0.72317	C -2.45038 1.43481 1.28245
H 1.05774 0.24233 3.59826	C -4.02482 2.43000 0.22984	C -1.84341 0.89387 2.59113
C -1.11307 2.61058 2.92429	H -4.66762 2.03108 1.02092	H -1.71734 1.72388 3.30113
H -0.75997 3.26710 3.72869	H -4.51691 2.24279 -0.73153	H -0.85284 0.45581 2.42271
H -1.65451 1.78049 3.38597	H -3.97375 3.51895 0.37041	H -2.46082 0.13747 3.07767
H -1.82360 3.17884 2.31644	C -1.98197 2.10200 1.65786	C -3.79500 2.10643 1.60922
C -3.25365 -0.54168 0.20530	H -1.91322 3.18743 1.82072	H -4.49193 1.42264 2.10213
C -3.78301 -0.01033 -1.13736	H -0.96482 1.69543 1.71243	H -4.28958 2.50926 0.71950
H -4.78988 0.40429 -0.98917	H -2.55542 1.68387 2.48673	H -3.62379 2.94544 2.29826
H -3.86028 -0.78371 -1.90575	C 0.56446 -0.20156 3.33019	C -1.48031 2.51733 0.78781
H -3.15319 0.79685 -1.52649	H 0.67761 -0.60336 4.34367	H -1.85172 3.05689 -0.08817
C -3.36363 0.63126 1.19514	H -0.39606 -0.54913 2.93255	H -0.50102 2.09374 0.53716
H -3.07772 0.35967 2.21269	H 0.52199 0.89013 3.40184	H -1.31861 3.25977 1.58303
H -4.40473 0.98242 1.22967	C 2.03371 -2.66681 2.28173	C 3.15257 -3.25968 0.00116
H -2.74340 1.48083 0.88866	H 2.10947 -3.02078 3.31618	H 3.47099 -3.04958 1.02817
C -4.19809 -1.65873 0.68446	H 2.88642 -3.06906 1.72534	H 3.89751 -3.92762 -0.44736
H -3.96727 -1.98610 1.70211	H 1.12065 -3.08662 1.84552	H 2.20311 -3.79989 0.04628
H -4.17738 -2.53849 0.03489	C 3.60866 -0.10221 2.95817	C 4.23964 -0.00949 2.40074
H -5.23030 -1.28094 0.69381	H 3.58338 0.99092 3.02426	H 4.77430 0.72123 1.78672
C -0.82238 -2.11637 1.61787	H 4.47255 -0.38432 2.34762	H 4.55900 -1.01078 2.09226
C 0.71539 -2.15011 1.69705	H 3.76436 -0.49552 3.96919	H 4.54858 0.13293 3.44294
H 1.13611 -1.14250 1.76917	C 2.42049 -3.07175 -1.62934	C 1.90250 1.89558 2.92093
H 1.17676 -2.64088 0.83658	H 2.16396 -3.58220 -0.69560	H 0.83035 2.09778 2.83513
H 1.02373 -2.70058 2.59795	H 3.14094 -3.69347 -2.17328	H 2.43582 2.67843 2.37088
C -1.31391 -1.43540 2.90688	H 1.50796 -3.00283 -2.23080	H 2.18009 1.98164 3.97785
H -0.84552 -1.92074 3.77483	C 4.83727 -1.57065 -0.47362	C 1.59570 -1.14849 3.37193
H -2.39668 -1.51689 3.03582	H 5.29306 -0.60583 -0.22954	H 1.86608 -0.95821 4.41704
H -1.04693 -0.37431 2.94288	H 5.52273 -2.11152 -1.13624	H 1.97733 -2.13916 3.10177
C -1.34048 -3.56639 1.63597	H 4.74776 -2.14475 0.45455	H 0.50476 -1.18368 3.29742
H -1.04102 -4.04526 2.57899	C 3.42113 -0.52826 -2.99529	C 4.84064 -1.07531 -1.22966
H -0.92662 -4.16897 0.82347	H 2.46423 -0.33496 -3.49238	H 4.91348 -0.22990 -1.92086
H -2.43174 -3.62214 1.57365	H 4.01640 -1.17755 -3.64744	H 5.43039 -1.89883 -1.65003
C -1.13024 -2.18793 -1.57707	H 3.95073 0.42511 -2.89864	H 5.29931 -0.78401 -0.27975
C 0.20629 -2.94917 -1.55475	C 4.21688 2.22362 -0.10488	C 2.40757 -2.06304 -2.76753
H 1.05566 -2.27452 -1.40908	H 4.56702 3.26197 -0.13460	H 1.35183 -1.80399 -2.89249
H 0.34997 -3.44589 -2.52477	H 4.69633 1.68665 -0.93007	H 2.52081 -3.13113 -2.98590
H 0.24632 -3.72586 -0.78635	H 4.56144 1.77704 0.83350	H 2.98094 -1.50924 -3.51776
C -1.07708 -1.28072 -2.81773	C 1.88779 2.86616 -1.96226	C 2.32561 1.67878 -2.95868
H -1.97282 -0.66988 -2.94320	H 0.80859 2.95635 -2.11359	H 1.34914 1.39379 -3.36238
H -0.97118 -1.90169 -3.71848	H 2.28744 2.23010 -2.75794	H 3.03993 0.89261 -3.22311
H -0.21134 -0.60972 -2.78047	H 2.32706 3.86416 -2.07627	H 2.64261 2.60276 -3.45596
C -2.25265 -3.22300 -1.78091	C 1.62038 3.30783 1.08301	C 1.29833 3.54345 -0.75381
H -2.36398 -3.89762 -0.92611	H 1.82974 2.91651 2.08466	H 0.31095 3.57407 -1.21954

H -2.01577 -3.84126 -2.65810
H -3.22270 -2.75564 -1.97025

6

Si -0.18427 0.49074 0.60395
Si 0.17194 2.83076 0.68409
Si 1.79778 -0.39555 -0.39409
Si 3.79438 0.87781 -0.52817
H -0.04746 0.07549 2.03964
N 1.40847 -0.91697 -2.04937
H 1.11048 -0.19806 -2.70128
H 2.09516 -1.50689 -2.50893
C 4.80622 -0.09589 -1.80938
H 5.84802 0.24472 -1.80551
H 4.80548 -1.17605 -1.63475
H 4.40192 0.08006 -2.81221
C 4.73819 0.93813 1.12498
H 5.08646 1.95714 1.32499
H 4.12763 0.62480 1.97815
H 5.61514 0.28415 1.08711
C 3.74929 2.63822 -1.22605
H 3.28581 2.67365 -2.21694
H 3.22871 3.34753 -0.57785
H 4.78671 2.97775 -1.33502
Si 2.47107 -2.37504 0.74466
C 4.33290 -2.49172 1.08767
H 4.64225 -1.79288 1.86963
H 4.54180 -3.50603 1.44921
H 4.95966 -2.31878 0.20900
C 2.04349 -3.85343 -0.36084
H 1.05099 -3.78056 -0.81295
H 2.77594 -3.92560 -1.17336
H 2.09567 -4.78509 0.21402
C 1.68544 -2.50552 2.46188
H 2.01980 -1.66702 3.08323
H 0.59351 -2.49791 2.45658
H 2.02176 -3.43127 2.94326
C 0.45209 3.51229 -1.06233
H -0.50509 3.67558 -1.56873
H 0.97295 4.47556 -1.01387
H 1.05067 2.84043 -1.68442
C 1.71008 3.05829 1.76862
H 2.53210 2.38337 1.52071
H 2.08204 4.08737 1.69619
H 1.43756 2.87351 2.81361
C -1.11585 3.96015 1.49346
H -2.05262 4.03488 0.93578
H -1.34973 3.65290 2.51676
H -0.67658 4.96446 1.53958
Si -2.33180 -0.33121 -0.10284
C -2.84016 0.70015 -1.67292
C -3.52217 0.00613 1.41142
C -2.26904 -2.23725 -0.50424
C -3.66371 -2.88955 -0.50179
H -3.56304 -3.94503 -0.79122
H -4.13957 -2.86985 0.48188
H -4.34668 -2.41969 -1.21708
C -1.39041 -2.94791 0.53688
H -1.75453 -2.84483 1.56134
H -1.33820 -4.02238 0.30863
H -0.36924 -2.55851 0.50144
C -1.62318 -2.52433 -1.87146
H -0.62337 -2.08629 -1.95795
H -1.52299 -3.61353 -1.98860
H -2.23407 -2.17212 -2.70757
C -5.00704 -0.03657 1.00534
H -5.29181 -0.98052 0.53209
H -5.63136 0.08363 1.90204
H -5.26950 0.77521 0.32053
C -3.30314 -1.01629 2.54163
H -3.60876 -2.02854 2.26691
H -2.25705 -1.04838 2.86760
H -3.90761 -0.72039 3.41032
C -3.24297 1.38433 2.03383
H -3.35848 2.20623 1.32521
H 0.53767 3.42863 0.98815
H 2.07936 4.30047 1.00797

13

Si 1.10519 0.14246 1.12423
Si 1.37654 -1.79212 2.45020
C 2.62986 -0.11464 -0.12275
Si -0.93422 0.78782 -0.01560
Si -0.29365 1.99669 -1.96362
Si -1.30228 2.60708 1.51559
Si -2.88886 -0.61552 -0.30585
N 2.97818 -1.07561 -1.02196
N 3.71256 0.71341 -0.05874
C 4.26137 -0.85925 -1.50609
C 4.72642 0.26574 -0.88800
C 2.14724 -2.26278 -1.30710
H 1.19219 -2.03012 -0.82664
C 2.73609 -3.51070 -0.65068
H 2.91095 -3.35385 0.41494
H 3.67847 -3.80874 -1.11760
H 2.03082 -4.33924 -0.76649
C 1.91287 -2.47242 -2.80081
H 1.60861 -1.54647 -3.29476
H 1.10740 -3.20008 -2.92336
H 2.79428 -2.87181 -3.30605
C 4.95208 -1.67090 -2.55518
H 4.53609 -1.47906 -3.54843
H 4.89555 -2.74321 -2.36397
H 6.00800 -1.39886 -2.58246
C 6.06175 0.91915 -1.04614
H 6.00865 1.82197 -1.66034
H 6.75071 0.22472 -1.52850
H 6.49290 1.19057 -0.08047
C 3.78989 1.90405 0.82096
H 2.74379 2.08768 1.07940
C 4.52051 1.56207 2.11403
H 5.53434 1.19402 1.92612
H 3.96374 0.79913 2.66348
H 4.59025 2.45785 2.73821
C 4.35425 3.14324 0.12388
H 3.96829 4.02602 0.64209
H 4.03218 3.20506 -0.91841
H 5.44496 3.19069 0.16609
C 3.28025 -1.95828 2.63423
H 3.62302 -1.31315 3.45019
H 3.84973 -1.68582 1.73782
H 3.54607 -2.98830 2.90056
C 0.72209 -3.57180 2.18583
H 1.30152 -4.23434 2.84163
H 0.80150 -3.95436 1.16653
H -0.32596 -3.65386 2.48925
C 0.77193 -1.36432 4.19884
H 1.22288 -0.42650 4.53931
H 1.06330 -2.16031 4.89514
H -0.31549 -1.25377 4.25230
C -0.16690 1.09373 -3.63029
H -1.11827 0.73724 -4.03059
H 0.51688 0.24192 -3.57462
H 0.25291 1.80843 -4.34940
C 1.46746 2.66564 -1.73440
H 1.64461 3.48135 -2.44663
H 2.19724 1.87404 -1.94072
H 1.65138 3.04459 -0.72692
C -1.41348 3.49583 -2.28554
H -1.53866 4.11930 -1.39475
H -2.40856 3.20225 -2.63412
H -0.95597 4.11458 -3.06708
C 0.10232 3.87445 1.32595
H -0.03969 4.65165 2.08663
H 0.10416 4.36302 0.34621
H 1.07883 3.41150 1.49413
C -1.23313 2.04680 3.32789
H -1.12610 2.94003 3.95552
H -0.37042 1.39922 3.51554
H -2.13962 1.52338 3.64708
H 1.89083 4.36433 -1.17644
H 1.17937 3.73562 0.31717
C 4.01528 2.36825 -0.48896
H 4.41686 3.17545 -1.11342
H 4.71043 1.52730 -0.53610
H 3.99338 2.73197 0.54418

14

Si -0.37732 -0.40628 -1.18161
N 1.50459 -0.79129 -0.64954
C -3.16486 -2.31376 -1.20631
Si -1.58611 -2.17831 -0.04416
N 5.54426 -1.49442 0.17861
C -2.79235 -2.88347 -2.58758
H -3.66860 -2.81813 -3.24843
H -2.50211 -3.93688 -2.54503
H -1.98108 -2.31541 -3.05604
Si -0.39051 1.74944 -0.09233
C -3.73870 -0.90856 -1.46138
H -4.56248 -0.97165 -2.18726
H -2.99159 -0.22334 -1.88409
H -4.13982 -0.46179 -0.55199
Si -2.28698 3.03263 -0.68344
C -4.30349 -3.17573 -0.63249
H -5.12074 -3.23281 -1.36641
H -4.72499 -2.74925 0.28231
H -3.99085 -4.20029 -0.41172
Si 0.06316 2.43450 2.13937
C -0.56213 -3.85489 -0.14965
Si 1.33359 2.80799 -1.33490
C 0.23494 -3.94739 -1.46438
H -0.38290 -3.82594 -2.35569
H 0.71967 -4.93328 -1.52458
H 1.02764 -3.19649 -1.50399
C 6.46096 -1.81773 -0.90239
H 6.15930 -2.73891 -1.41325
H 7.45695 -1.96785 -0.48936
H 6.51067 -1.00614 -1.63753
C 1.99083 -0.71136 0.60490
H 1.27083 -0.45248 1.37047
C 3.30841 -0.94043 0.92919
H 3.60311 -0.84570 1.96623
C 4.23530 -1.27489 -0.08889
C 3.71385 -1.35691 -1.40392
H 4.34014 -1.60063 -2.25139
C 2.37717 -1.10875 -1.62695
H 1.95207 -1.16305 -2.62527
C 3.04392 2.47133 -0.57220
H 3.32878 1.42071 -0.69174
H 3.08174 2.71047 0.49599
H 3.80018 3.08150 -1.08091
C 1.18115 4.69387 -1.48921
H 2.05904 5.06814 -2.03004
H 1.13725 5.20331 -0.52280
H 0.29337 4.97598 -2.06475
C -1.46211 -5.10209 -0.06735
H -2.10968 -5.20063 -0.94241
H -2.09671 -5.10925 0.82342
H -0.83075 -6.00232 -0.02996
C 0.47081 -3.96341 0.98620
H 1.07964 -4.86703 0.83496
H 0.00622 -4.04911 1.97215
H 1.15700 -3.10967 1.00545
C -2.14723 -1.86161 1.80775
C -3.21612 -0.75674 1.85492
H -2.89181 0.14315 1.31634
H -3.39826 -0.46824 2.90090
H -4.17536 -1.07825 1.44090
C -0.96246 -1.32141 2.62387
H -0.10476 -2.00052 2.65176
H -1.27450 -1.13844 3.66335
H -0.63468 -0.36414 2.20734
C -2.70871 -3.09885 2.52879
H -3.54852 -3.55146 1.99346
H -3.07228 -2.80692 3.52509

H	-3.94810	1.55960	2.85871
H	-2.23272	1.43723	2.45356
C	-1.64512	0.78158	-2.64163
H	-1.92837	1.37182	-3.52476
H	-0.78974	1.28678	-2.17566
H	-1.31078	-0.19953	-2.98611
C	-3.20481	2.14652	-1.30173
H	-4.13001	2.21213	-0.72237
H	-2.41035	2.63403	-0.72819
H	-3.35181	2.73183	-2.22055
C	-4.03925	0.09557	-2.42479
H	-3.81907	-0.89228	-2.83684
H	-4.92522	0.00468	-1.78858
H	-4.30610	0.74775	-3.26845

15

Si	1.67558	1.98198	0.06229
Si	0.34632	0.11555	-0.73843
Si	-1.94902	-0.06990	-0.12454
Si	-2.51620	-2.14518	-1.15790
Si	-3.12278	0.20229	1.95491
Si	-3.10835	1.41039	-1.58763
C	3.56432	1.46357	0.27663
C	4.41203	2.57761	0.92077
H	4.31064	3.53818	0.40961
H	5.47347	2.29189	0.87745
H	4.16438	2.72884	1.97507
C	3.75673	0.19926	1.13583
H	3.41939	-0.70255	0.61797
H	3.23561	0.25260	2.09409
H	4.82831	0.06882	1.34808
C	4.18672	1.15361	-1.09516
H	4.32855	2.05329	-1.69935
H	3.57463	0.45408	-1.67450
H	5.17804	0.69678	-0.95372
C	1.53756	3.24822	-1.44077
C	1.65854	2.56514	-2.81821
H	1.54143	3.32848	-3.60146
H	0.88891	1.80317	-2.96503
H	2.62811	2.08610	-2.97409
C	2.56970	4.39065	-1.41207
H	2.59150	4.92832	-0.46049
H	2.31988	5.12079	-2.19566
H	3.58305	4.03465	-1.62134
C	0.13487	3.87906	-1.40030
H	0.02424	4.60076	-0.58598
H	-0.64935	3.12118	-1.28980
H	-0.06092	4.41645	-2.33977
C	1.05532	2.86833	1.71130
C	1.58403	4.29855	1.92398
H	1.19030	4.99531	1.17873
H	2.67509	4.36114	1.90252
H	1.25326	4.66176	2.90826
C	1.47878	2.02887	2.92850
H	2.55855	2.05005	3.10085
H	1.17557	0.98256	2.82091
H	0.99418	2.42019	3.83493
C	-0.48033	2.94772	1.74887
H	-0.80762	3.29960	2.73843
H	-0.93858	1.97074	1.57275
H	-0.87889	3.64366	1.00895
C	-2.37038	-1.96749	-3.04273
H	-3.19461	-1.37737	-3.45514
H	-2.41052	-2.96319	-3.50147
H	-1.43379	-1.48460	-3.33635
C	-1.42529	-3.64297	-0.70156
H	-0.35310	-3.42869	-0.67495
H	-1.59093	-4.41881	-1.45981
H	-1.70873	-4.06858	0.26613
C	-4.28184	-2.75939	-0.82610
H	-4.37873	-3.17847	0.17964
H	-4.51267	-3.55586	-1.54438
H	-5.03491	-1.97471	-0.94019
C	-4.25101	1.72512	1.90399
H	-4.81230	1.76732	2.84568
C	-2.86384	3.69012	1.39237
H	-2.73146	4.50877	2.11084
H	-3.78593	3.16749	1.65759
H	-3.00308	4.13717	0.40367
C	-4.29081	0.30177	-1.31861
C	-3.93378	0.39304	-2.81109
H	-4.67841	1.01931	-3.32266
H	-3.93484	-0.58079	-3.30795
H	-2.95498	0.85821	-2.96656
C	-4.45106	1.74900	-0.82812
H	-4.80992	1.80869	0.20024
H	-5.18185	2.27302	-1.46142
H	-3.50860	2.30120	-0.88437
C	-5.66162	-0.39084	-1.20932
H	-6.05733	-0.36956	-0.19046
H	-5.63737	-1.43366	-1.53875
H	-6.38461	0.13858	-1.84676
C	-3.53492	-1.06789	1.48144
C	-2.34067	-1.32942	2.41316
H	-1.70851	-0.44177	2.51925
H	-1.70535	-2.14569	2.06607
H	-2.70536	-1.59378	3.41711
C	-4.32253	0.09539	2.10735
H	-4.52229	-0.13197	3.16433
H	-5.28892	0.26102	1.62395
H	-3.76110	1.03390	2.07734
C	-4.44247	-2.31095	1.50513
H	-4.82160	-2.46222	2.52603
H	-3.90710	-3.22173	1.22336
H	-5.30980	-2.21214	0.84510
C	-2.32553	-2.22513	-1.25775
C	-1.45390	-3.10177	-0.34563
H	-0.65863	-2.51758	0.12858
H	-0.98014	-3.89810	-0.94249
H	-2.02404	-3.59426	0.44752
C	-1.43801	-1.83819	-2.44991
H	-1.94944	-1.21588	-3.18514
H	-1.10903	-2.75042	-2.96833
H	-0.54522	-1.29516	-2.11952
C	-3.48610	-3.08265	-1.78966
H	-4.18991	-3.37497	-1.00506
H	-3.08141	-4.00594	-2.22965
H	-4.05035	-2.57296	-2.57601

16

Si	-1.36567	0.56683	1.19160
Si	-1.73036	2.89403	1.09407
C	-2.85039	0.08767	-0.01025
Si	0.58221	-0.62661	0.39959
Si	-0.25957	-2.59158	-0.64706
Si	1.03529	-1.46165	2.61090
Si	2.52098	0.37075	-0.66688
N	-3.08080	0.28565	-1.33284
N	-3.97059	-0.54321	0.42885
C	-4.30735	-0.22797	-1.72195
C	-4.87250	-0.75591	-0.60034
C	-2.24021	1.06901	-2.22132
H	-1.32716	1.31864	-1.68487
C	-4.79091	-0.15530	-3.13015
H	-4.11954	-0.69196	-3.80836
H	-4.86369	0.88051	-3.47620
H	-5.78073	-0.60673	-3.21062
C	-6.16908	-1.46125	-0.39391
H	-6.01195	-2.48913	-0.05131
H	-6.72697	-1.50035	-1.33057
H	-6.78956	-0.94857	0.34744
C	-4.22775	-0.98811	1.79177
H	-3.35734	-0.72954	2.39718
C	-3.63621	2.98167	1.16040
H	-4.03696	2.32219	1.93837
H	-4.08612	2.68677	0.20375
H	-3.96259	4.00452	1.38192
C	-1.25886	4.15597	-0.25716
H	-1.80385	5.08374	-0.04180
H	-1.52749	3.83863	-1.26967
H	-1.95022	-3.87276	2.67801
C	6.03694	-1.36341	1.54063
H	5.54413	-2.07756	2.20971
H	5.87451	-0.34982	1.92462
H	7.10630	-1.56724	1.55143
C	-3.94406	2.45817	0.03291
H	-4.68716	3.24143	-0.16086
H	-3.89525	2.30434	1.11581
H	-4.30327	1.53655	-0.42788
C	-2.43975	3.06856	-2.57034
H	-2.44259	2.05681	-2.98956
H	-1.60325	3.61306	-3.02168
H	-3.36816	3.56925	-2.86870
C	-2.14496	4.82489	-0.07313
H	-1.21095	5.31365	-0.35880
H	-2.23981	4.87709	1.01712
H	-2.97438	5.40019	-0.50269
C	-1.49876	2.42955	3.21118
H	-2.26483	3.08715	2.78654
H	-1.26181	2.79620	4.21706
H	-1.93142	1.42935	3.30589
C	0.71454	4.21817	2.13098
H	1.69392	4.28558	1.64540
H	0.83118	4.55774	3.16751
H	0.03741	4.90959	1.62292
C	1.40835	1.48774	3.10211
H	1.12541	0.46519	3.37192
H	1.59274	2.03285	4.03586
H	2.35183	1.45826	2.54556
C	1.40779	2.17665	-3.11973
H	0.43495	2.25783	-3.61434
H	1.70287	1.12495	-3.16945
H	2.13744	2.76807	-3.68643

3''·DMAP

Si	-0.83138	1.65282	1.03042
Si	-1.05285	3.41088	-0.54796
Si	0.85960	-0.06326	0.81931
Si	-0.22082	-1.85468	1.96583
Si	2.19680	0.85549	2.58128
Si	2.10810	-0.68956	-1.15831
C	-3.85071	-0.35293	-1.23760
C	-4.57546	-0.24777	1.05155
C	-2.79223	4.05211	-0.10486
H	-2.88394	4.24109	0.96933
H	-3.56667	3.32754	-0.38608
H	-3.00247	4.98642	-0.63881
C	-1.09365	3.34465	-2.45571
H	-1.45189	4.32228	-2.80194
H	-1.78395	2.58871	-2.84627
H	-0.11284	3.17308	-2.90668
C	0.18040	4.77987	-0.10178
H	0.14892	4.99917	0.97048
H	-0.07398	5.69849	-0.64338
H	1.20900	4.50945	-0.36255
C	-1.42444	-2.89825	0.92576
H	-0.94175	-3.47744	0.13455
H	-2.20066	-2.27460	0.46439
H	-1.92236	-3.60202	1.60447
C	-1.31298	-1.18973	3.38607
H	-0.94736	-1.56813	4.34689
H	-2.34006	-1.55133	3.25638
H	-1.33204	-0.09910	3.44538
C	0.97421	-3.07595	2.79524
H	1.67587	-2.55314	3.45554
H	1.55746	-3.66899	2.08569
H	0.38929	-3.76784	3.41365
C	1.20416	0.86349	4.19557
H	1.80407	1.37970	4.95513
H	1.00156	-0.14799	4.56212
H	0.25501	1.39468	4.08601
C	2.61812	2.67359	2.23462
H	3.00173	3.12587	3.15705
H	1.72732	3.23814	1.93498
H	3.37882	2.79921	1.45817

H -4.97336 1.69342 1.08308
H -3.67304 2.65018 1.81376
C -4.29547 -1.24934 2.30494
H -4.79500 -1.07641 3.26598
H -3.78832 -2.21788 2.35652
H -5.06800 -1.31564 1.53249
C -2.07918 0.47257 3.53786
H -0.99862 0.39058 3.40347
H -2.38435 -0.23372 4.31829
H -2.27140 1.48330 3.91364
C -4.86303 0.74389 -1.89144
H -5.38755 0.52921 -0.95349
H -4.86036 -0.17222 -2.48970
H -5.44466 1.49758 -2.43577
C -3.35107 3.19130 -0.95002
H -2.64660 3.48333 -0.16837
H -4.36180 3.32615 -0.55359
H -3.22163 3.88497 -1.78930
C -2.27930 1.58722 -3.28209
H -2.97932 2.09489 -3.95782
H -1.99991 0.63159 -3.72876
H -1.37484 2.19855 -3.21576
C 1.21776 -1.50631 -0.02061
N 1.18146 -2.14637 1.17856
N 2.01261 -2.28830 -0.80907
C 2.45648 -3.40123 -0.11265
C 1.93160 -3.31235 1.14405
C 2.28088 -2.01708 -2.23990
H 1.95197 -0.98224 -2.37242
C 0.41861 -1.65626 2.33942
H 0.12658 -0.64805 2.03338
C 2.14595 -4.24347 2.29408
H 1.22127 -4.45902 2.83103
H 2.53741 -5.19190 1.92385
H 2.86866 -3.84071 3.00956
C 3.35815 -4.46164 -0.65764
H 3.34887 -5.32232 0.01222
H 3.03625 -4.80809 -1.64139
H 4.39144 -4.11375 -0.74023
C 3.76522 -2.11507 -2.59538
H 4.07411 -3.13694 -2.82714
H 3.94858 -1.50711 -3.48592
H 4.39681 -1.72709 -1.79104
C 1.39158 -2.89108 -3.11785
H 0.33968 -2.70443 -2.88894
H 1.56595 -2.64582 -4.16958
H 1.59490 -3.95706 -2.97656
C 1.26316 -1.56523 3.61103
H 0.77107 -0.87598 4.30405
H 1.35149 -2.52804 4.11902
H 2.26489 -1.18002 3.40284
C -0.84765 -2.48182 2.54684
H -1.36684 -2.13633 3.44437
H -1.51759 -2.37030 1.69237
H -0.62521 -3.54550 2.66943

3''·IMe4

Si -2.31866 -1.05271 0.01871
Si -0.37642 0.10575 -0.83920
Si 1.81044 -0.37362 -0.02410
Si 3.04726 1.43252 -0.94156
Si 2.68830 -0.87365 2.14389
Si 2.50520 -2.15485 -1.43077
C -3.84294 0.17586 0.23522
C -5.06068 -0.51684 0.87888
H -5.34311 -1.44108 0.36856
H -5.92542 0.16159 0.83403
H -4.89470 -0.75237 1.93360
C -3.51689 1.41835 1.09142
H -2.94540 2.15652 0.52288
H -2.95987 1.19242 2.00450
H -4.45710 1.90532 1.38849
C -4.29727 0.71176 -1.13389
H -4.76795 -0.06106 -1.74731
H -3.46132 1.13215 -1.70501
H -0.19077 4.39294 -0.25210
C -1.08489 3.64456 2.71081
H -1.47518 3.09159 3.57102
H -1.39854 4.69146 2.79919
H 0.00854 3.61491 2.76324
C -0.60193 -2.53750 -2.51689
H 0.28447 -2.39250 -3.13893
H -1.32467 -1.74966 -2.76104
H -1.05698 -3.49743 -2.79167
C -1.96965 -3.05892 0.05526
H -2.07257 -4.15082 0.05037
H -2.75854 -2.64619 -0.58541
H -2.13371 -2.70622 1.07527
C 0.86432 -4.09477 -0.36015
H 1.07913 -4.24213 0.70378
H 1.81968 -4.01195 -0.88697
H 0.35596 -4.99464 -0.72706
C -0.40072 -2.58776 3.14042
H -0.22645 -2.88988 4.18020
H -0.46944 -3.49782 2.53512
H -1.35724 -2.05925 3.09563
C 1.08924 -0.06977 3.90078
H 1.03381 -0.52880 4.89553
H 0.23476 0.60674 3.79504
H 2.00969 0.51994 3.85784
C 2.56632 -2.53501 2.96840
H 2.46373 -2.88836 4.00203
H 3.51256 -1.99306 2.89923
H 2.63369 -3.41589 2.32277
C 3.84352 -0.99340 -1.12662
C 3.38784 -1.78438 -2.36508
H 4.04668 -2.65341 -2.50292
H 3.44096 -1.19128 -3.28176
H 2.36438 -2.16222 -2.26041
C 3.99566 -2.01472 0.00984
H 4.40839 -1.57366 0.91834
H 4.67863 -2.81722 -0.30500
H 3.03875 -2.47659 0.26873
C 5.23609 -0.41130 -1.43041
H 5.69452 0.04632 -0.54943
H 5.21872 0.33793 -2.22722
H 5.90339 -1.22250 -1.75614
C 3.24829 1.64292 0.62763
C 2.11398 2.39843 1.34588
H 1.45875 1.71899 1.90185
H 1.48537 2.97918 0.66554
H 2.54778 3.09944 2.07424
C 4.04076 0.90573 1.72126
H 4.29960 1.61357 2.52164
H 4.97715 0.48337 1.34676
H 3.46204 0.09697 2.17637
C 4.19404 2.68181 -0.00174
H 4.63580 3.29786 0.79458
H 3.67457 3.36191 -0.68211
H 5.01868 2.21816 -0.55241
C 1.95691 1.30027 -2.29182
C 1.14728 2.54259 -1.89374
H 0.37730 2.30324 -1.15431
H 0.64912 2.96708 -2.77877
H 1.77406 3.33257 -1.47030
C 1.02218 0.40709 -3.12356
H 1.54777 -0.41709 -3.60893
H 0.55043 1.00570 -3.91799
H 0.22797 -0.02584 -2.51094
C 3.10756 1.75283 -3.20660
H 3.83841 2.38051 -2.68894
H 2.69569 2.34451 -4.03737
H 3.64159 0.90707 -3.64913
H -2.76125 1.98855 -2.50520
H -1.99555 0.49488 -3.11786
H -5.11231 -0.47891 2.18255
H -4.38732 -2.06957 1.80048

17

Si 0.01326 3.38173 -0.89553
C 3.81971 0.00183 3.08294
H 4.19844 0.53729 3.96252
H 4.60147 0.02245 2.32073
H 3.66146 -1.04128 3.37492
C 3.14155 -2.31337 -0.82622
C 2.21328 -3.54067 -0.82540
H 2.76872 -4.41661 -0.46092
H 1.84496 -3.78524 -1.82538
H 1.34748 -3.40495 -0.16792
C 3.80386 -2.26026 0.55958
H 4.55671 -1.47370 0.63518
H 4.30614 -3.21696 0.76479
H 3.07018 -2.09458 1.35371
C 4.24369 -2.56162 -1.87133
H 5.02669 -1.79899 -1.83528
H 3.85608 -2.59711 -2.89385
H 4.72566 -3.52896 -1.66785
C 3.28373 0.81309 -1.59396
C 2.55066 2.15382 -1.40350
H 2.15971 2.26291 -0.38730
H 1.71357 2.28472 -2.09188
H 3.25280 2.98258 -1.57780
C 4.49047 0.84287 -0.64047
H 5.06432 1.76495 -0.81068
H 5.17267 0.00304 -0.79762
H 4.18285 0.84037 0.40896
C 3.83395 0.76763 -3.03088
H 4.54821 1.59185 -3.17049
H 3.04986 0.89328 -3.78245
H 4.36390 -0.16479 -3.24907
C 0.84766 -1.00043 -2.62301
C 0.27276 0.35033 -3.07264
H -0.05764 0.95091 -2.21959
H -0.59058 0.18948 -3.73733
H 0.99642 0.94925 -3.63244
C -0.34136 -1.84882 -2.14360
H -0.06534 -2.88496 -1.93912
H -1.11976 -1.86690 -2.92250
H -0.79088 -1.44352 -1.23254
C 1.45442 -1.69368 -3.85483
H 2.32375 -1.16250 -4.25292
H 0.70000 -1.73487 -4.65449
H 1.75623 -2.72390 -3.64534
C -4.83862 -0.67288 -0.27316
C -3.40104 0.41308 1.33879
C -2.70614 0.30718 -0.85217
H -3.96110 -0.62050 -2.28011
H -1.94128 0.55262 -1.57915
H -3.18019 0.75664 2.34390
H -5.27454 -0.42650 1.85738
N -2.45292 0.68185 0.41887
N -5.97004 -1.34103 -0.60188
C -6.19118 -1.76085 -1.97623
H -7.13961 -2.29206 -2.03600
H -6.23636 -0.89937 -2.65224
H -5.39696 -2.43503 -2.31615
C -6.95454 -1.64618 0.42325
H -7.35197 -0.73088 0.87650
H -7.78167 -2.18960 -0.03036
H -6.52286 -2.27203 1.21258

IMe4

C -0.00001 1.56948 -0.00008
N -1.05666 0.70877 -0.00007
N 1.05666 0.70879 -0.00004
C -0.67982 -0.63285 -0.00001
C 0.67984 -0.63285 -0.00002
C -2.43479 1.15630 0.00015
H -2.42088 2.24530 -0.00106
C -1.66694 -1.75075 -0.00013
H -2.31176 -1.71953 -0.88499
H -2.31316 -1.71843 0.88367
H -1.14952 -2.71231 0.00089
C 1.66695 -1.75075 0.00015
H 2.31324 -1.71842 -0.88360

H -5.04003 1.50995 -0.98590
C -2.69404 -2.29871 -1.46131
C -2.54942 -1.64270 -2.84989
H -2.78978 -2.39124 -3.61894
H -1.53147 -1.28628 -3.02594
H -3.22394 -0.79560 -2.99740
C -4.09094 -2.94496 -1.41576
H -4.32189 -3.41126 -0.45462
H -4.15141 -3.72932 -2.18419
H -4.88168 -2.22133 -1.63799
C -1.64410 -3.42421 -1.41842
H -1.80314 -4.11649 -0.58693
H -0.62375 -3.02736 -1.34122
H -1.69401 -4.01274 -2.34586
C -2.07974 -2.08097 1.68394
C -3.10859 -3.20597 1.90130
H -3.01161 -4.00118 1.15732
H -4.14206 -2.84944 1.88266
H -2.93714 -3.66501 2.88611
C -2.16896 -1.14010 2.89809
H -3.17489 -0.73888 3.04690
H -1.47850 -0.29481 2.81434
H -1.90074 -1.69304 3.81011
C -0.68531 -2.72934 1.72885
H -0.50719 -3.16067 2.72549
H 0.10671 -2.00097 1.53193
H -0.57990 -3.53789 1.00287
C 2.80084 1.49656 -2.82017
H 3.32037 0.67269 -3.32059
H 3.21056 2.43665 -3.20940
H 1.73978 1.43635 -3.08541
C 2.52563 3.14914 -0.30398
H 1.55174 3.45804 -0.69747
H 3.26921 3.88179 -0.64112
H 2.48684 3.19908 0.79022
C 4.92294 1.37336 -0.64569
H 5.18239 1.77210 0.33901
H 5.40880 2.00437 -1.40017
H 5.34483 0.36839 -0.72619
C 3.13914 -2.70993 2.25193
H 3.55017 -2.92359 3.24584
H 3.89814 -2.97803 1.50987
H 2.26980 -3.35638 2.09451
C 4.28759 0.08879 2.47677
H 4.65622 -0.16039 3.47919
H 4.12786 1.17225 2.43565
H 5.07016 -0.16297 1.75490
C 1.59799 -0.53321 3.66596
H 0.58016 -0.92136 3.57463
H 1.54523 0.53169 3.91336
H 2.06753 -1.03871 4.51862
C 4.38397 -2.11104 -1.70018
H 4.93410 -2.08931 -0.75249
H 4.68709 -1.23738 -2.28670
H 4.69457 -3.00816 -2.24887
C 2.11100 -3.90132 -0.79057
H 1.18671 -3.95182 -0.20947
H 2.92018 -4.28798 -0.16483
H 2.00102 -4.57127 -1.65189
C 1.69589 -2.02048 -3.13800
H 2.20745 -2.70166 -3.82954
H 1.74039 -1.00769 -3.54605
H 0.64061 -2.30733 -3.09743
C -0.62748 1.94687 -0.23820
N -0.40163 2.57669 0.94084
N -1.05989 2.93873 -1.06526
C -1.11759 4.15771 -0.40759
C -0.69171 3.92716 0.86599
C -1.38434 2.79684 -2.47882
H -1.17846 1.76421 -2.76854
C 0.07546 1.93411 2.14826
H 0.09021 0.86059 1.97077
C -0.49916 4.84752 2.02160
H 0.54359 4.84249 2.35593
H -0.75544 5.86861 1.73588
H -1.12994 4.56547 2.87044
Si -0.10969 0.40665 -0.69858
Si -1.99122 -0.75625 0.20818
O -0.09999 1.95071 -0.02691
O -0.00092 0.34465 -2.26106
N 2.29900 0.02142 1.13046
N 2.51876 -1.01409 -0.75158
C 1.65738 -0.26379 -0.02610
C 3.57397 -0.52140 1.12712
C 3.71190 -1.17688 -0.06439
C 1.69702 0.85877 2.18885
H 0.64407 0.90154 1.91855
C 1.80901 0.23788 3.58100
H 2.78353 0.41778 4.04046
H 1.62007 -0.83884 3.56222
H 1.05318 0.70099 4.22183
C 2.24426 2.28068 2.13446
H 2.12233 2.68986 1.13035
H 3.30119 2.32224 2.41485
H 1.68122 2.90794 2.83228
C 4.55997 -0.40547 2.24395
H 4.63736 0.61828 2.61600
H 5.54769 -0.70142 1.88761
H 4.30079 -1.05512 3.08472
C 4.89657 -1.94045 -0.56198
H 5.10949 -1.71922 -1.60922
H 4.75614 -3.02033 -0.46350
H 5.77685 -1.66287 0.01993
C 2.20311 -1.55980 -2.09984
H 1.12658 -1.41914 -2.20127
C 2.84460 -0.69782 -3.18051
H 2.43578 0.31237 -3.11588
H 2.58210 -1.10533 -4.16094
H 3.93628 -0.67169 -3.10049
C 2.53437 -3.04706 -2.21791
H 2.25082 -3.59724 -1.31554
H 3.58884 -3.23486 -2.43281
H 1.95472 -3.45427 -3.05073
C 1.66656 3.43810 -1.78412
H 1.81113 4.39386 -2.29936
H 1.67815 2.63551 -2.52935
H 2.51322 3.28987 -1.10486
C -0.13169 4.75607 0.37768
H -0.15724 5.73718 -0.10834
H 0.70552 4.75190 1.08283
H -1.05726 4.64029 0.95237
C -1.36405 3.51858 -2.15456
H -2.35219 3.43722 -1.68929
H -1.26076 2.71135 -2.88653
H -1.31526 4.48023 -2.67763
C -1.42228 -2.49944 0.89037
C -0.74343 -2.33529 2.26009
H 0.07183 -1.60247 2.21153
H -0.30469 -3.29478 2.57159
H -1.43724 -2.02228 3.04498
C -0.35613 -3.12815 -0.02764
H -0.66713 -3.21314 -1.07103
H -0.11632 -4.13981 0.33280
H 0.57227 -2.55016 0.00099
C -2.57494 -3.50629 1.04208
H -3.39069 -3.12258 1.66192
H -2.20018 -4.42391 1.51904
H -2.99597 -3.79364 0.07446
C -2.86034 0.29121 1.61574
C -1.84740 0.88033 2.61659
H -1.21838 1.63166 2.12755
H -1.20644 0.12512 3.08112
H -2.39553 1.38364 3.42646
C -3.58238 1.50682 1.00608
H -3.95487 2.14760 1.81843
H -4.44322 1.22413 0.39530
H -2.90379 2.11151 0.39263
C -3.89404 -0.52743 2.41002
H -4.42950 0.13695 3.10376
H -3.42584 -1.31157 3.01312
H -4.64147 -1.00091 1.76639
C -3.17630 -0.96617 -1.32986
H 1.14953 -2.71231 -0.00096
H 2.31171 -1.71957 0.88505
C 2.43477 1.15632 -0.00004
H 2.42086 2.24531 0.00012
H -2.96030 0.80043 0.89160
H -2.96118 0.79838 -0.88994
H 2.96075 0.79929 0.89067
H 2.96070 0.79956 -0.89088

$I^iPr_2Me_2$

C 0.00002 -1.23722 -0.32495
N 1.06479 -0.40314 -0.16304
N -1.06478 -0.40314 -0.16324
C 0.68163 0.91113 0.10850
C -0.68168 0.91114 0.10827
C 2.42663 -0.94655 -0.20393
H 2.27099 -1.95910 -0.58512
C 3.02439 -1.05210 1.19835
H 2.35951 -1.62855 1.84644
H 3.17900 -0.06692 1.64869
H 3.99463 -1.55626 1.15404
C 3.33721 -0.20100 -1.17853
H 2.83105 -0.04209 -2.13475
H 4.23545 -0.79808 -1.36027
H 3.66113 0.76643 -0.78623
C 1.61154 2.06769 0.29230
H 2.05181 2.39358 -0.65566
H 2.42988 1.83461 0.97820
H 1.06627 2.91582 0.71146
C -1.61162 2.06769 0.29187
H -2.05284 2.39261 -0.65597
H -1.06603 2.91633 0.70958
H -2.42925 1.83515 0.97882
C -2.42661 -0.94662 -0.20390
H -2.27102 -1.95916 -0.58513
C -3.02400 -1.05217 1.19852
H -3.17850 -0.06697 1.64886
H -2.35896 -1.62864 1.84642
H -3.99427 -1.55632 1.15447
C -3.33752 -0.20107 -1.17817
H -4.23550 -0.79848 -1.36011
H -2.83149 -0.04152 -2.13434
H -3.66191 0.76603 -0.78541

DMAP

C -1.95018 -1.12991 0.01301
C -0.56378 -1.19658 -0.02258
C 0.18286 0.00001 -0.05137
C -0.56379 1.19660 -0.02239
C -1.95019 1.12990 0.01318
N -2.66335 -0.00001 0.02958
H -2.52346 -2.05434 0.03259
H -0.08365 -2.16685 -0.02668
H -0.08368 2.16688 -0.02626
H -2.52348 2.05433 0.03294
N 1.55377 -0.00001 -0.10669
C 2.26982 1.25150 0.04183
H 1.99555 1.95367 -0.75240
H 2.07179 1.72990 1.01149
H 3.33969 1.06008 -0.03769
C 2.26981 -1.25150 0.04216
H 3.33970 -1.06012 -0.03722
H 2.07159 -1.72964 1.01189
H 1.99569 -1.95389 -0.75193

A

Si -2.49638 -0.42362 0.00007
Si 0.42252 0.52760 -0.00005
Si 2.41838 -0.67989 0.00005
O -0.81526 -0.53474 -0.00026
O 0.26856 2.04481 0.00003
H -2.93650 0.29138 -1.21352
H -2.93601 0.29073 1.21423

C -1.55780 5.41110 -1.08327
H -1.56535 6.23658 -0.37018
H -0.88631 5.68142 -1.90444
H -2.56793 5.30923 -1.49184
H -2.43844 3.03103 -2.64701
H -0.75911 3.47627 -3.06401
H -0.59042 2.16451 2.98490
H 1.09075 2.27204 2.38013

B

Si -0.44944 0.20942 0.00000
O 0.86077 -0.76051 -0.00000
O -0.39056 1.73278 0.00000
C -1.93582 -0.88862 -0.00000
H -1.92178 -1.53491 0.88153
H -2.84699 -0.29023 -0.00020
H -1.92156 -1.53519 -0.88132
C 2.20117 -0.26199 0.00000
H 2.21356 0.83121 0.00001
H 2.70758 -0.63866 0.89060
H 2.70757 -0.63864 -0.89061

E

Si 2.66457 -1.75975 0.55812
Si 0.85262 0.29644 -0.60324
Si 1.02862 2.61624 -0.30417
O 1.71286 -0.39501 0.66773
O 1.02505 -0.31340 -2.02310
N -1.49965 0.04627 1.25325
N -2.00596 -0.52190 -0.75772
C -0.98448 -0.09657 0.01271
C -2.83592 -0.28399 1.26228
C -3.15416 -0.64401 -0.00885
C -0.76253 0.51632 2.42600
H 0.30268 0.36897 2.25051
C -1.93098 -0.83121 -2.19187
H -0.88495 -0.73977 -2.50335
H -2.28881 -1.85070 -2.34440
H -2.56443 -0.12850 -2.73641
H -3.43252 -0.24231 2.15985
H -0.97425 1.57332 2.59748
H -1.07391 -0.07123 3.29076
H 3.81096 -1.55184 -0.34968
H 1.86772 -2.92388 0.10633
H 3.16518 -2.02939 1.92657
H 0.64988 3.03015 1.07885
H 2.40584 3.10977 -0.55067
H 0.10358 3.32963 -1.22407
H -4.08382 -0.98160 -0.43910

H

Si 2.67069 -0.32480 -1.46306
Si 0.91372 0.49166 0.77062
O 1.80793 -0.65717 -0.07992
O 1.14996 1.98472 0.40970
N -1.42968 -1.22195 -0.00331
N -1.83067 0.86136 -0.34266
C -0.88796 0.01054 0.10930
C -2.70560 -1.14648 -0.51557
C -2.95700 0.17135 -0.73066
C -0.76872 -2.46530 0.38781
H 0.31001 -2.31662 0.33464
C -1.69559 2.32116 -0.43346
H -0.66280 2.57886 -0.17134
H -1.92078 2.62511 -1.45705
H -2.40379 2.78396 0.25658
H -3.30985 -2.02296 -0.68852
H -1.06547 -2.74240 1.40164
H -1.06343 -3.25057 -0.30945
H 3.81714 0.56944 -1.20364
H 1.79159 0.27223 -2.49818
H 3.17251 -1.62498 -1.96984
H -3.82432 0.67205 -1.13103
C -2.60075 -2.01512 -2.29984
H -3.22361 -2.03825 -3.20540
H -2.60523 -3.02625 -1.88156
H -1.58306 -1.74807 -2.60803
C -4.60238 -1.39734 -0.94509
H -5.13118 -0.62240 -0.38185
H -4.62615 -2.31854 -0.35392
H -5.18192 -1.58012 -1.86145
C -3.26529 0.34203 -2.14245
H -3.65668 1.18337 -1.56654
H -3.94859 0.18430 -2.98985
H -2.28457 0.61301 -2.54453

C

Si -0.05998 0.42979 -0.00554
O -1.08280 -0.84303 -0.00632
O -0.48967 1.89453 0.00307
C -2.50918 -0.72290 0.00521
H -2.81440 0.32659 0.02337
H -2.90105 -1.20787 -0.89059
H -2.88832 -1.23540 0.89109
Si 2.10528 -0.43759 0.00158
H 2.21064 -1.45098 -1.06969
H 3.05405 0.67045 -0.22286
H 2.33977 -1.06812 1.31888

F

Si 1.30750 0.42869 0.37914
O 1.97886 -0.75963 -0.60523
O 1.48966 1.92393 -0.00490
N -1.21464 -1.19497 0.07278
N -1.61156 0.90917 -0.09636
C -0.61902 0.01814 0.10363
C -2.56972 -1.06710 -0.13656
C -2.81878 0.26425 -0.24438
C -0.52738 -2.47044 0.26730
H 0.52172 -2.34173 -0.00251
C -1.45200 2.36773 -0.15794
H -0.37767 2.58669 -0.13493
H -1.90057 2.72532 -1.08635
H -1.96278 2.81474 0.69728
H -3.22631 -1.92055 -0.19834
H -0.61608 -2.78530 1.30941
H -0.98733 -3.21659 -0.38208
H -3.73671 0.80231 -0.42105
C 1.64245 -0.21250 2.10537
H 2.70132 -0.06603 2.34044
H 1.05608 0.34023 2.84547
H 1.42406 -1.28065 2.20848
C 2.09018 -0.50536 -1.99441
H 2.43805 0.51579 -2.18052
H 2.80202 -1.21792 -2.41915
H 1.11993 -0.64018 -2.49606
H -3.00431 -1.80834 -0.00019
H 2.43906 -1.53011 1.20999
H 2.43950 -1.53007 -1.20992
H 3.54863 0.26861 0.00023

D

Si -2.12513 -0.11918 -0.00009
Si 0.88946 0.20200 -0.00005
O -0.51718 -0.62054 0.00032
O 0.98526 1.72223 0.00006
H -2.38411 0.69418 -1.20394
H -2.39402 0.66084 1.22353
H -2.94034 -1.34848 -0.02014
C 2.27296 -1.02313 -0.00012
H 2.19873 -1.66862 -0.87942
H 3.23376 -0.50841 -0.00360
H 2.20291 -1.66375 0.88309

G

Si -1.15233 0.54403 0.05872
O -1.70628 -0.52367 1.23381
O -1.18230 2.07716 0.31757
N 1.29041 -1.23247 0.03460
N 1.81722 0.84372 -0.14485
C 0.76439 0.01261 0.00052
C 2.66023 -1.18373 -0.09277
C 2.99174 0.12924 -0.20520
C 0.52414 -2.47304 0.15465
H -0.45660 -2.23654 0.56782
C 1.75022 2.30880 -0.22455
H 0.71240 2.60825 -0.04157
H 2.41208 2.72683 0.53576
H 2.07924 2.62251 -1.21712
H 3.27066 -2.07293 -0.08495
H 0.41592 -2.93727 -0.82749
H 1.05642 -3.14691 0.82762
H 3.95003 0.61250 -0.31272
C -1.52076 -0.18777 2.60043
H -1.78257 0.85841 2.78658
H -2.16086 -0.83773 3.20173
H -0.47486 -0.34658 2.90274
Si -2.00133 -0.36278 -1.92871
H -3.47055 -0.19920 -2.04970
H -1.36207 0.28813 -3.10353
H -1.70245 -1.82032 -2.04292

C	0.90929	-0.10964	2.54328
H	1.89601	0.07149	2.98138
H	0.17518	0.44300	3.13736
H	0.69900	-1.18067	2.63094

4. References

[S1] G. R. Fulmer, A. J. M. Miller, N. H. Sherden, H. E. Gottlieb, A. Nudelman, B. M. Stoltz, J. E. Bercaw, K. I. Goldberg, *Organometallics* **2010**, *29*, 2176-2179.

[S2] C. Kayser, R. Fischer, J. Baumgartner, C. Marschner, *Organometallics* **2002**, *21*, 1023-1030.

[S3] N. Wiberg, K. Amelunxen, H.-W. Lerner, H. Schuster, H. Nöth, I. Krossing, M. Schmidt-Amelunxen, T. Seifert, *J. Organomet. Chem.* **1997**, *542*, 1-18.

[S4] N. Kuhn, T. Kratz, *Synthesis* **1993**, 561-562.

[S5] K. Fredenhagen, G. Cadenbach, *Z. Anorg. Allg. Chem.* **1926**, *158*, 249-263.

[S6] T. Gross, H. Reinke, H. Oehme, *Can. J. Chem.* **2000**, *78*, 1399-1404.

[S7] a) A. Sekiguchi, T. Tanaka, M. Ichinohe, K. Akiyama, S. Tero-Kubota, *J. Am. Chem. Soc.* **2003**, *125*, 4962-4963; b) A. Sekiguchi, T. Tanaka, M. Ichinohe, K. Akiyama, P. P. Gaspar, *J. Am. Chem. Soc.* **2008**, *130*, 426-427.

[S8] H. Cui, J. Zhang, C. Cui, *Organometallics* **2013**, *32*, 1-4.

[S9] a) W. Ando, M. Fujita, H. Yoshida, A. Sekiguchi, *J. Am. Chem. Soc.* **1988**, *110*, 3310-3311; b) S. Zhang, P. E. Wagenseller, R. T. Conlin, *J. Am. Chem. Soc.* **1991**, *113*, 4278-4281.

[S10] *APEX suite of crystallographic software*, APEX 3 version 2015.5-2; Bruker AXS Inc.: Madison, Wisconsin, USA, **2015**.

[S11] *SAINT*, Version 7.56a and SADABS Version 2008/1; Bruker AXS Inc.: Madison, Wisconsin, USA, **2008**.

[S12] G. M. Sheldrick, *SHELXL-2014*, University of Göttingen, Göttingen, Germany, **2014**.

[S13] C. B. Hübschle, G. M. Sheldrick, B. Dittrich, *J. Appl. Cryst.* **2011**, *44*, 1281-1284.

[S14] G. M. Sheldrick, *SHELXL-97*, University of Göttingen, Göttingen, Germany, **1998**.

[S15] A. J. C. Wilson, *International Tables for Crystallography*, Vol. C, Tables 6.1.1.4 (pp. 500-502), 4.2.6.8 (pp. 219-222), and 4.2.4.2 (pp. 193-199); Kluwer Academic Publishers: Dordrecht, The Netherlands, **1992**.

[S16] C. F. Macrae, I. J. Bruno, J. A. Chisholm, P. R. Edgington, P. McCabe, E. Pidcock, L. Rodriguez-Monge, R. Taylor, J. van de Streek, P. A. Wood, *J. Appl. Cryst.* **2008**, *41*, 466-470.

[S17] M. J. Frisch, G. W. Trucks, H. B. Schlegel, G. E. Scuseria, M. A. Robb, J. R. Cheeseman, G. Scalmani, V. Barone, B. Mennucci, G. A. Petersson, H. Nakatsuji, M. Caricato, X. Li, H. P. Hratchian, A. F. Izmaylov, J. Bloino, G. Zheng, J. L. Sonnenberg, M. Hada, M. Ehara, K. Toyota, R. Fukuda, J. Hasegawa, M. Ishida, T. Nakajima, Y. Honda, O. Kitao, H. Nakai, T. Vreven, J. A. Montgomery, Jr., J. E. Peralta, F. Ogliaro, M. Bearpark, J. J. Heyd, E. Brothers, K. N. Kudin, V. N. Staroverov, R. Kobayashi, J. Normand, K. Raghavachari, A. Rendell, J. C. Burant, S. S. Iyengar, J. Tomasi, M. Cossi, N. Rega, J. M. Millam, M. Klene, J. E. Knox, J. B. Cross, V. Bakken, C. Adamo, J. Jaramillo, R. Gomperts, R. E. Stratmann, O. Yazyev, A. J. Austin, R. Cammi, C. Pomelli, J. W. Ochterski, R. L. Martin, K. Morokuma, V. G. Zakrzewski, G. A. Voth, P. Salvador, J. J. Dannenberg, S. Dapprich, A. D. Daniels, Ö. Farkas, J. B. Foresman, J. V. Ortiz, J. Cioslowski, D. J. Fox, *Gaussian 09, Revision E.01*, Gaussian, Inc., Wallingford CT, **2009**.

[S18] a) R. Ditchfield, W. J. Hehre, J. A. Pople, *J. Chem. Phys.* **1971**, *54*, 724-728; b) W. J. Hehre, R. Ditchfield, J. A. Pople, *J. Chem. Phys.* **1972**, *56*, 2257-2261; c) Y. Zhao, D. G. Truhlar, *Theor. Chem. Acc.* **2008**, *120*, 215-241.
[S19] A. V. Marenich, C. J. Cramer, D. G. Truhlar, *J. Phys. Chem. B* **2009**, *113*, 6378-6396.
[S20] S. E. Wheeler, K. N. Houk, *J. Chem. Theory Comput.* **2010**, *6*, 395-404.
[S21] K. Fukui, *Acc. Chem. Res.* **1981**, *14*, 363-368.
[S22] a) R. Krishnan, J. S. Binkley, R. Seeger, J. A. Pople, *J. Chem. Phys.* **1980**, *72*, 650-654; b) A. D. McLean, G. S. Chandler, *J. Chem. Phys.* **1980**, *72*, 5639-5648.
[S23] E. D. Glendening, J. K. Badenhoop, A. E. Reed, J. E. Carpenter, J. A. Bohmann, C. M. Morales, C. R. Landis, F. Weinhold, *Vol. 34* **2013**, *Theoretical Chemistry Institute, University of Wisconsin, Madison*, 1429-1437.
[S24] a) E. D. Glendening, C. R. Landis, F. Weinhold, *Wiley Interdiscip. Rev. Comput. Mol. Sci.* **2011**, *2*, 1-42; b) E. D. Glendening, C. R. Landis, F. Weinhold, *J. Comput. Chem.* **2013**, *34*, 1429-1437.
[S25] Y. Zhao, D. G. Truhlar, *J. Chem. Phys.* **2006**, *125*, 194101.
[S26] G. A. Andrienko, http://www.chemcraftprog.com, **2015**.
[S27] C. Y. Legault, *Université de Sherbrooke*, http://www.cylview.org, **2009**.
[S28] R. Dennington, T. A. Keith, J. M. Millam, Version 5 ed., Semichem Inc., Shawnee Mission, KS, **2009**.
[S29] V. Y. Lee, *Organosilicon Compounds: Theory and Experiment (Synthesis), Vol. 1*, 1st ed., Academic Press, New York, **2017**; and references therein.
[S30] M. Kira, *Proc. Jpn. Acad. Ser. B* **201**, *88*, 167-191.
[S31] a) M. Ichinohe, R. Kinjo, A. Sekiguchi, *Organometallics* **2003**, *22*, 4621-4623. b) D. Wendel, T. Szilvási, C. Jandl, S. Inoue, B. Rieger, *J. Am. Chem. Soc.* **2017**, *139*, 9156-9159.
[S32] M. Kosa, M. Karni, Y. Apeloig, *J. Am. Chem. Soc.* **2013**, *135*, 9032-9040.
[S33] a) D. Himmel, I. Krossing, A. Schnepf, *Angew. Chem. Int. Ed.* **2014**, *53*, 370-374; b) G. Frenking, *Angew. Chem. Int. Ed.* **2014**, *53*, 6040-6046; c) D. Himmel, I. Krossing, A. Schnepf, *Angew. Chem. Int. Ed.* **214**, *53*, 6047-6048.
[S34] J. D. Epping, S. Yao, M. Karni, Y. Apeloig, M. Driess, *J. Am. Chem. Soc.* **2010**, *132*, 5443-5455.

13.2 Supporting Information Chapter 5

Supporting Information

DMAP-stabilized bis(silyl)silylenes as versatile synthons for organosilicon compounds

*Richard Holzner,[†] Dominik Reiter,[†] Philipp Frisch, and Shigeyoshi Inoue**

Department of Chemistry, WACKER-Institute of Silicon Chemistry, Technische Universität München, Lichtenbergstraße 4, 85748 Garching bei München (Germany) *E-mail: s.inoue@tum.de

Table of Contents

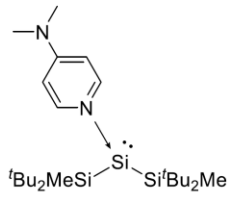
1. Experimental Section 3
1.1. General Methods and Instrumentation 3
1.2. (^{t}Bu$_2$MeSi)$_2$Si:←DMAP (**1b**) 4
1.3. Bis(hypersilyl)silylene DMAP complex (**1c**) 7
1.4. Silyl Radical **2** 9
1.5. Azasilepin **3** 10
1.6. Hexakis(trimethylsilyl)trisilirane (**4**) 14
1.7. Hydrosilanes **5a-c** 16
1.8. Siliranes **6** 17
1.9. Silaimine **7a** 18
1.10. Silaimine **7b** 19
2. X-ray Crystallographic Data 22
2.1. General Information 22
2.2 SC-XRD structures 23
2.3 Crystal data and structural refinement parameters 25
3. References 26

1. Experimental Section

1.1. General Methods and Instrumentation

All manipulations were carried out under exclusion of water and oxygen under an atmosphere of argon 4.6 (≥99.996%) using standard Schlenk and glovebox techniques. The glassware used was heat dried under fine vacuum prior to use. All solvents were refluxed over sodium/benzophenone, freshly distilled under argon and deoxygenated prior to use. PTFE-based grease (*Triboflon III* from *Freudenberg & Co. KG*) was used as sealant. Deuterated benzene (C_6D_6) was obtained from Sigma-Aldrich, dried over Na/K alloy, flask-to-flask condensed, deoxygenated by three freeze-pump-thaw cycles and stored over 3 Å molecular sieves in a glovebox. All NMR samples were prepared under argon in *J. Young* PTFE valve NMR tubes. The NMR spectra were recorded on a *Bruker DRX400* (^{1}H: 400.13 MHz, ^{13}C: 100.62 MHz, ^{29}Si: 79.49 MHz), AV500 (^{1}H: 500.13 MHz) or *AV500C* (^{1}H: 500.36 MHz, ^{13}C: 125.83 MHz, ^{29}Si: 99.41 MHz) spectrometer at ambient temperature (300 K), unless otherwise stated. The ^{1}H, ^{13}C{^{1}H} and ^{29}Si{^{1}H} NMR spectroscopic chemical shifts δ are reported in ppm relative to tetramethylsilane. ^{1}H and ^{13}C{^{1}H} NMR spectra are calibrated against the residual proton and natural abundance carbon resonances of the respective deuterated solvent as internal standard (C_6D_6: δ(^{1}H) = 7.16 ppm and δ(^{13}C) = 128.1 ppm).[S1] The following abbreviations are used to describe signal multiplicities: s = singlet, d = doublet, dd = doublet of doublets, m = multiplet, br = broad. In some NMR spectra, signals from silicone oil (C_6D_6: δ(^{1}H) = 0.29 ppm, δ(^{13}C) = 1.4 ppm and δ(^{29}Si) = -21.8 ppm), originating from the cannulas used (*B. Braun Melsungen AG Sterican®)*, can be observed. EPR spectra were recorded on a *Jeol* jes-Fa200 esr spectrometer with a spectrometer frequency of 9.267 GHz (X-band). Quantitative elemental analyses (EA) were measured with a *EURO EA (HEKAtech)* instrument equipped with a CHNS combustion analyzer at the *Laboratory for Microanalysis* at the *TUM Catalysis Research Center*. Melting Points (m.p.) were determined in sealed glass capillaries under inert gas by a *Büchi M-565* melting point apparatus. Unless otherwise stated, all commercially available chemicals were purchased from *abcr GmbH* or *Sigma-Aldrich* and used without further purification. Hydrogen (H_2) 5.0 (≥99.999%) and ethylene 3.5 (≥99.95%) were purchased from *Westfalen AG* and used as received. The compounds $((TMS)_3Si)_2SiBr_2$,[S2] $(^tBu_2MeSi)_2SiBr_2$,[S3] $(^tBu_3Si)_2SiBr_2$[S4] and $((TMS)_3Si)(^tBu_3Si)Si$←DMAP (**1a**)[S5] were prepared as described in the corresponding references. Potassium graphite (KC_8) was synthesized following a literature reported procedure upon heating a 1:8 mixture of potassium and graphite in a thick-walled, PTFE-capped pressurize-able Schlenk flask to 500 °C until a homogenous bronze powder was obtained.[S6]

1.2. (^{t}Bu$_2$MeSi)$_2$Si:←DMAP (1b)



1b

$Si_3C_{25}H_{52}N_2$

464.96 g/mol

THF (10 mL) was added to a mixture of (^{t}Bu$_2$MeSi)$_2$SiBr$_2$ (300 mg, 597 µmol, 1.0 eq.), KC_8 (169 mg, 1.25 mmol, 2.1 eq.) and DMAP (72.9 mg, 597 µmol, 1.0 eq.) at ambient temperature. After stirring for 3 hours, the solvent was removed under reduced pressure and the residue was extracted with toluene (3 × 2 mL) to remove KBr and graphite. The solvent was evaporated *in vacuo* and compound **1b** was obtained as red-brown, crystalline solid (233 mg, 551 µmol, 92%). Crystals suitable for SC-XRD analysis were obtained from a cooled (-35 °C) toluene solution of **1b**.

m.p. = 140 °C (decomposition; color change from red-brown to black)

^{1}H NMR (500 MHz, C_6D_6, 300 K): δ [ppm] = 8.66 (d, ^3J = 7.5 Hz, 2H, *o*-C^{DMAP}H), 5.42 (d, ^3J = 7.5 Hz, 2H, *m*-C^{DMAP}H), 1.76 (s, 6H, N(CH$_3$)$_2$), 1.41 (s, 36H, C(CH$_3$)$_3$), 0.42 (s, 6H, Si(CH$_3$)).
^{13}C{^{1}H} NMR (126 MHz, C_6D_6, 300 K): δ [ppm] = 154.3 (*p*-C^{DMAP}), 153.0 (*o*-C^{DMAP}), 105.2 (*m*-C^{DMAP}), 38.1 (N(CH$_3$)$_2$), 31.2 (C(CH$_3$)$_3$), 22.9 (C(CH$_3$)$_3$), -3.7 (Si(CH$_3$)).
^{29}Si{^{1}H} NMR (99 MHz, C_6D_6, 300 K): δ [ppm] = 61.5 (Si:), 11.8 (^{t}Bu$_2$MeSi).

Note: The chemical shifts of DMAP-stabilized silylenes **1** and silaimines **7** are dependent on the concentration of the NMR sample.

EA:	$Si_3C_{25}H_{52}N_2$	Calculated [%]:	C (64.58), H (11.27), N (6.03)
		Experimental [%]:	C (64.34), H (11.33), N (5.98)

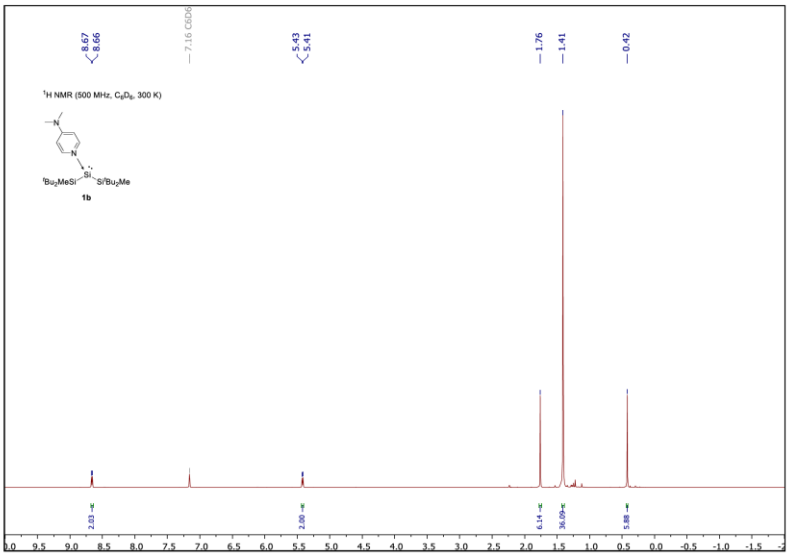


Fig. S1: ^{1}H NMR spectrum (500 MHz) of compound **1b** in C_6D_6 at 300 K.

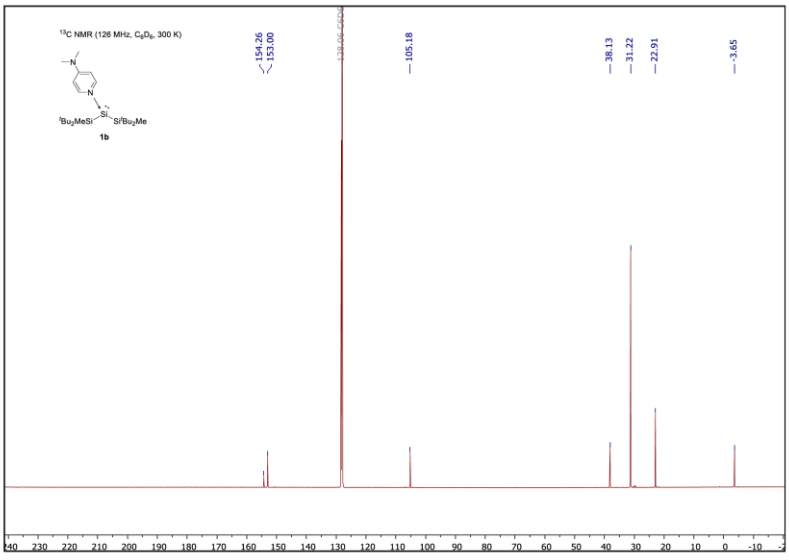


Fig. S2: ^{13}C NMR spectrum (126 MHz) of compound **1b** in C_6D_6 at 300 K.

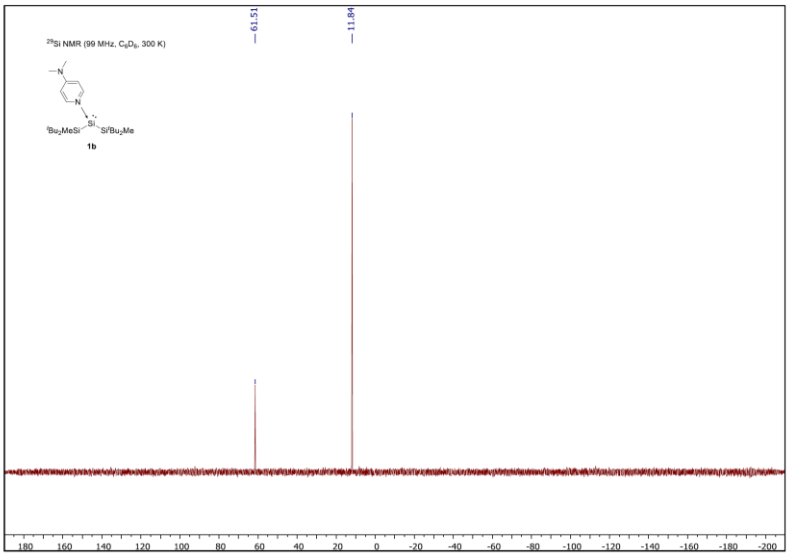


Fig. S3: ^{29}Si NMR spectrum (99 MHz) of compound **1b** in C_6D_6 at 300 K.

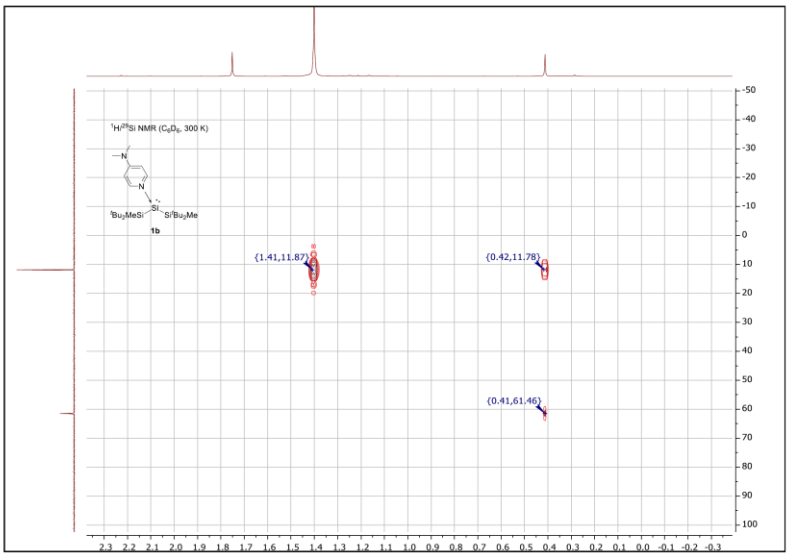
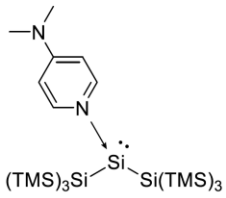


Fig. S4: ^{1}H/^{29}Si HMBC NMR spectrum of compound **1b** in C_6D_6 at 300 K.

1.3. Bis(hypersilyl)silylene DMAP complex (1c)



1c

$Si_9C_{25}H_{64}N_2$

645.57 g/mol

THF (10 mL) was added to a mixture of $((TMS)_3Si)_2SiBr_2$ (300 mg, 439 µmol, 1.0 eq.), KC_8 (125 mg, 922 µmol, 2.1 eq.) and DMAP (53.7 mg, 439 µmol, 1.0 eq.) at ambient temperature. After stirring for 3 hours, the solvent was removed under reduced pressure and the residue was extracted with toluene (3 × 2 mL) to remove KBr and graphite. The solvent was evaporated *in vacuo* and compound **1c** was obtained as dark-brown solid.

Note: During the synthesis of **1c**, the concomitant formation of hexakis(trimethylsilyl)trisilirane (**4**) and $Si(TMS)_4$ was observed. Therefore, no sample of **1c** with sufficient purity for elemental analysis was obtained and the yield was not determined.

^{1}H NMR (500 MHz, C_6D_6, 300 K): δ [ppm] = 8.65 (d, ^3J = 7.1 Hz, 2H, *o*-$C^{DMAP}\underline{H}$), 5.67 (d, ^3J = 6.6 Hz, 2H, *m*-$C^{DMAP}\underline{H}$), 1.73 (s, 6H, $N(C\underline{H}_3)_2$), 0.48 (s, 54H, $Si(C\underline{H}_3)_3$).
^{29}Si{^{1}H}(NMR (99 MHz, C_6D_6, 300 K): δ [ppm] = 72.5 (*Si*:), -9.7 ($\underline{Si}(CH_3)_3$), -121.8 ($\underline{Si}(TMS)_3$).

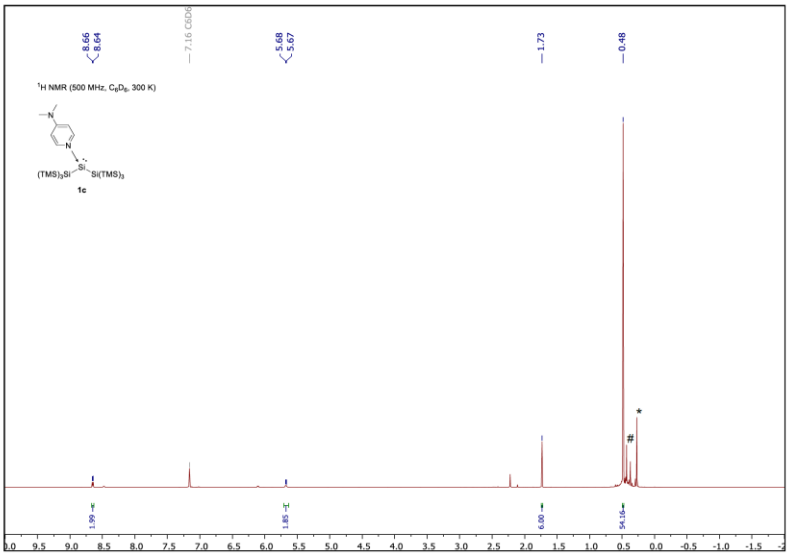


Fig. S5: ^{1}H NMR spectrum (500 MHz) of compound **1c** in C_6D_6 at 300 K. Signals labeled with * and # belong to $Si(TMS)_4$ and hexakis(trimethylsilyl)trisilirane (**4**), respectively.

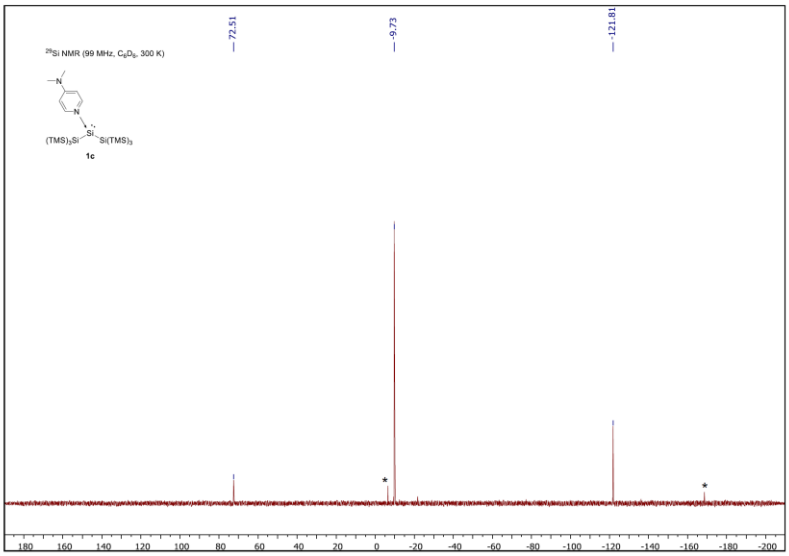
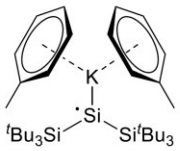


Fig. S6: ^{29}Si NMR spectrum (99 MHz) of compound **1c** in C_6D_6 at 300 K. Signals labeled with * belong to hexakis(trimethylsilyl)trisilirane (**4**).

1.4. Silyl Radical 2



2

$Si_3C_{38}H_{70}K$

650.33 g/mol

Precooled THF (10 mL, -78 °C) was added to a mixture of (^{t}Bu$_3$Si)$_2$SiBr$_2$ (100 mg, 170 µmol, 1.0 eq.) and KC_8 (92.2 mg, 682 µmol, 3.5 eq.). The reaction mixture was allowed to warm to room temperature over 16 hours and the solvent was subsequently removed under reduced pressure. Concomitantly formed KBr and graphite were separated by extracting the residue with toluene (3 × 4 mL). Evaporation of the solvent *in vacuo* and subsequent washing of the residue with *n*-hexane (3 × 2 mL) afforded compound **2** as orange-brown solid (54.1 mg, 88.5 µmol, 52%). Crystals suitable for SC-XRD analysis were obtained from a cooled (-35 °C) solution of **2** in toluene.

m.p. = 60 °C (decomposition; color change to dark red)

EPR (toluene, 286 K) g = 2.0056, a(α-^{29}Si) = 2.92 mT

Note: Compound **2** is completely NMR silent. Elemental analysis was not matching, presumably because an unquantifiable amount of coordinating toluene was removed during drying compound **2** in fine vacuum. Due to its extreme air and moisture sensitivity and the fact, that it is not stable in toluene, no satisfactory spectroscopic data of **2** was obtained before addition of crown ether (18-C-6). With crown ether however, one signal in the EPR spectrum was observed (Fig. **S7**). Hyperfine coupling with the β-^{29}Si nuclei was not visible.

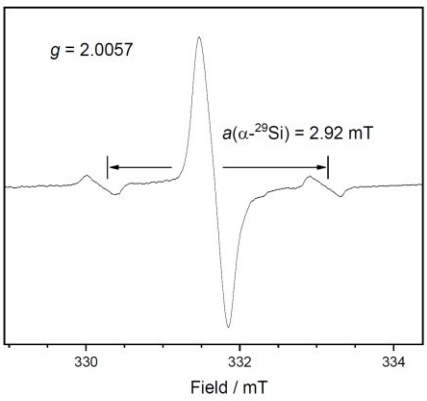
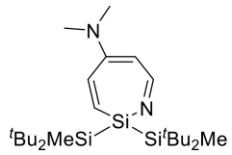


Fig. S7: X-band EPR spectrum of compound **2** + crown ether (18-C-6) in toluene (1×10^{-4}M, 286 K).

1.5. Azasilepin 3



3

$Si_3C_{25}H_{52}N_2$

464.96 g/mol

A solution of DMAP-stabilized silylene **1b** (36.0 mg, 85.1 µmol) in benzene (2 mL) was heated to 65 °C for 16 h. The color changed from deep-brown to yellow. Evaporation of the solvent, afforded compound **3** as yellow solid (36.0 mg, 85.1 µmol, quant.). Crystals suitable for SC-XRD analysis were obtained from a cooled (-35 °C) solution of **3** in *n*-hexane.

^{1}H NMR (500 MHz, C_6D_6, 300 K): δ [ppm] = 8.34 (d, ^{3}J = 4.7 Hz, 1H, NC*H*), 6.27 (dd, ^{3}J = 15.5 Hz, ^{4}J = 2.5 Hz, 1H, SiCHC*H*), 6.01 (d, ^{3}J = 15.5 Hz, 1H, SiC*H*), 4.68 (dd, ^{3}J = 4.7 Hz, ^{4}J = 2.5 Hz, 1H, NCHC*H*), 2.27 (s, 6H, N(CH_3)$_2$), 1.29 (s, 18H, C(CH_3)$_3$), 1.19 (s, 18H, C(CH_3)$_3$), 0.37 (s, 6H, Si(CH_3)).

^{13}C{^{1}H} NMR (126 MHz, C_6D_6, 300 K): δ [ppm] = 165.4 (SiNCH), 156.2 (*C*NMe$_2$), 138.2 (NCH*C*H), 137.4 (Si*C*HCH), 105.8 (SiCH*C*H), 40.3 (N(*C*H$_3$)$_2$), 30.4 (Si(C(*C*H$_3$)$_3$), 30.1 (Si(C(*C*H$_3$)$_3$), 22.5 (Si(*C*(CH$_3$)$_3$), 21.6 (Si(*C*(CH$_3$)$_3$), -4.9 (Si(*C*H$_3$)).

^{29}Si{^{1}H} NMR (99 MHz, C_6D_6, 300 K): δ [ppm] = 2.0 (*Si*^{t}Bu$_2$Me), -28.1 (*Si*N).

EA: $Si_3C_{25}H_{52}N_2$ Calculated [%]: C (64.58), H (11.27), N (6.03)
Experimental [%]: C (64.62), H (11.47), N (5.99)

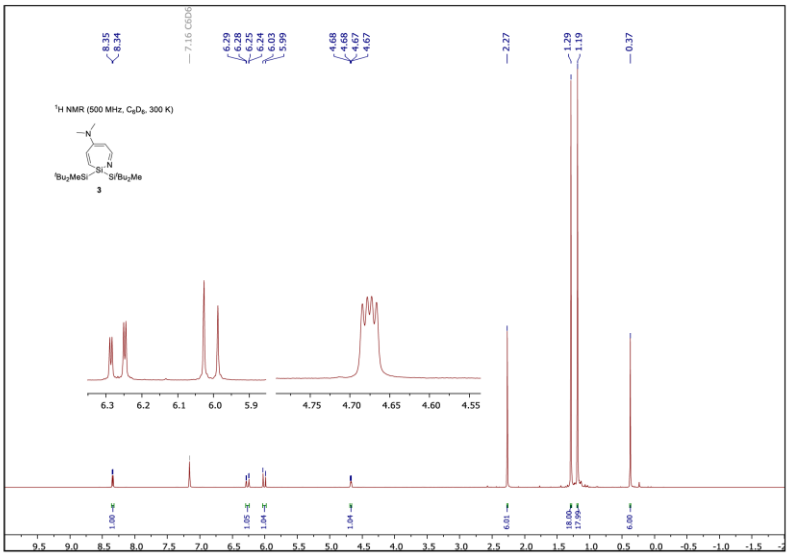


Fig. S8: ^{1}H NMR spectrum (500 MHz) of compound **3** in C_6D_6 at 300 K.

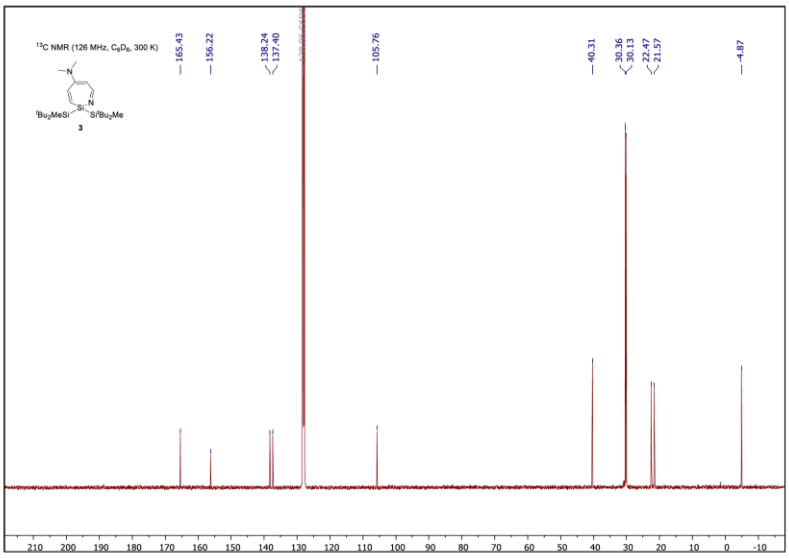


Fig. S9: ^{13}C NMR spectrum (126 MHz) of compound **3** in C_6D_6 at 300 K.

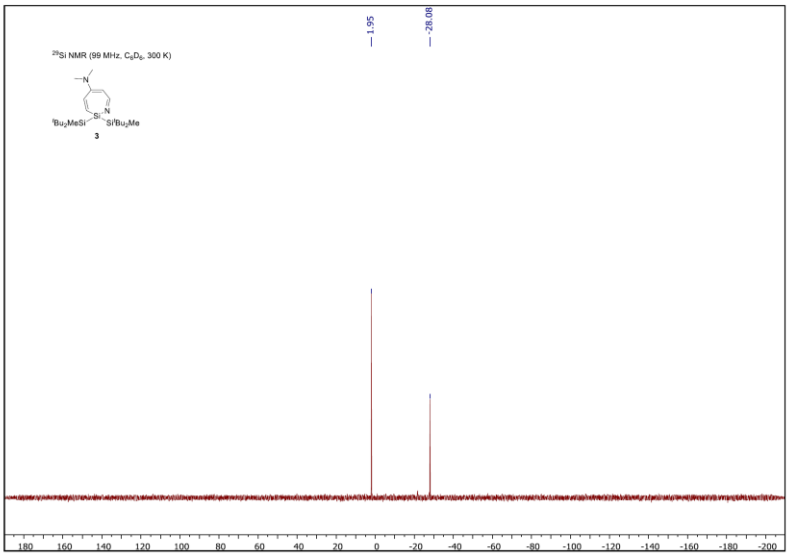


Fig. S10: ^{29}Si NMR spectrum (99 MHz) of compound **3** in C_6D_6 at 300 K.

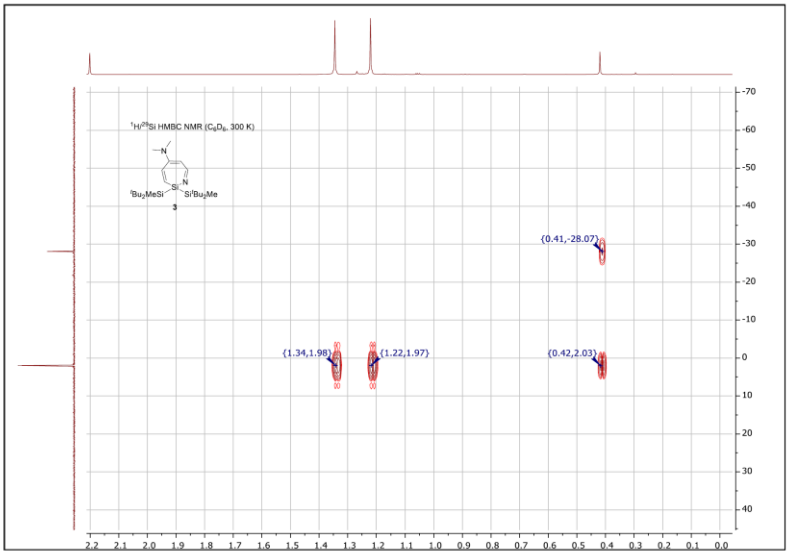


Fig. S11: ^{1}H/^{29}Si HMBC NMR spectrum of compound **3** in C_6D_6 at 300 K.

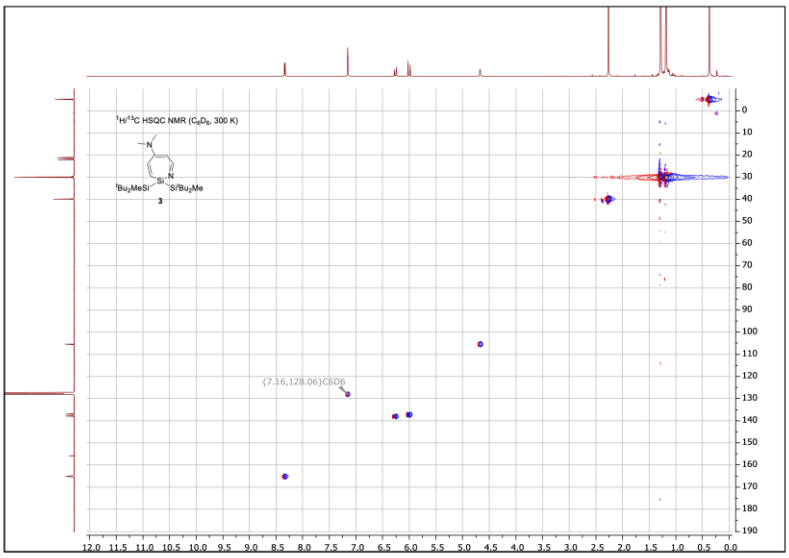
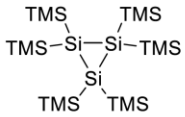


Fig. S12: ^{1}H/^{13}C HSQC NMR spectrum of compound **3** in C_6D_6 at 300 K.

1.6. Hexakis(trimethylsilyl)trisilirane (4)



4

$Si_9C_{18}H_{54}$

523.40 g/mol

A toluene solution of crude silylene **1c** (50 mg) was heated to 65 °C for 16 hours. After cooling down to ambient temperature, liberated DMAP was separated by precipitation with $SiBr_4$ (26.9 mg, 77.5 µmol, 1.0 eq.) and subsequent filtration. The resulting solution was concentrated under reduced pressure and compound **4** was obtained by crystallization at -35 °C as colorless solid (30.1 mg).

Note: Compound **4** has already been reported by Klinkhammer *et al.* from the attempted synthesis of the free silylene $((TMS)_3Si)_2Si:$.[S7] Therefore, we did not analyze it further. DMAP forms an unidentified adduct with $SiBr_4$ which is insoluble in common organic solvents. Thus, this adduct was not further analyzed.

^{1}H NMR (500 MHz, C_6D_6, 300 K): δ [ppm] = 0.43 (s, 54H, Si(C$\underline{H}_3$)$_3$).
^{13}C{^{1}H} NMR (126 MHz, C_6D_6, 300 K): δ [ppm] = 4.7 (Si($\underline{C}$H$_3$)$_3$).
^{29}Si{^{1}H} NMR (99 MHz, C_6D_6, 300 K): δ [ppm] = -6.5 ($\underline{Si}$(CH$_3$)$_3$), -168.6 ($\underline{Si}$(TMS)$_2$).

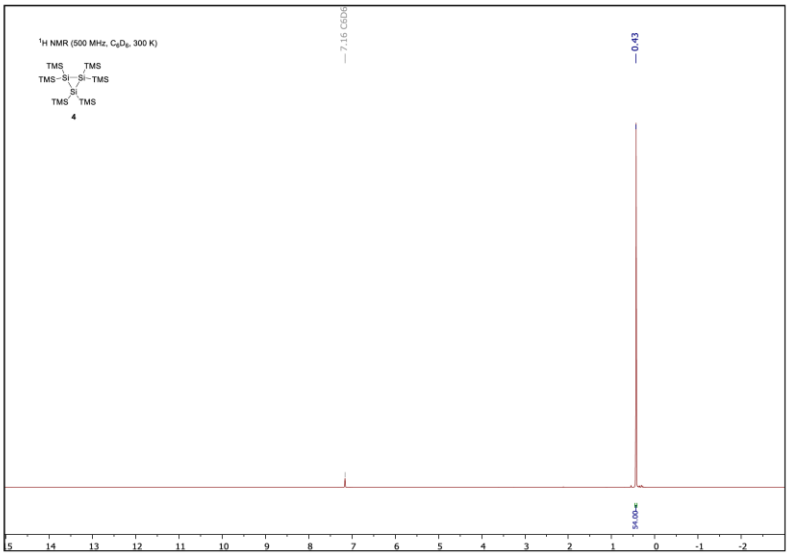


Fig. S13: ^{1}H NMR spectrum (500 MHz) of compound **4** in C_6D_6 at 300 K.

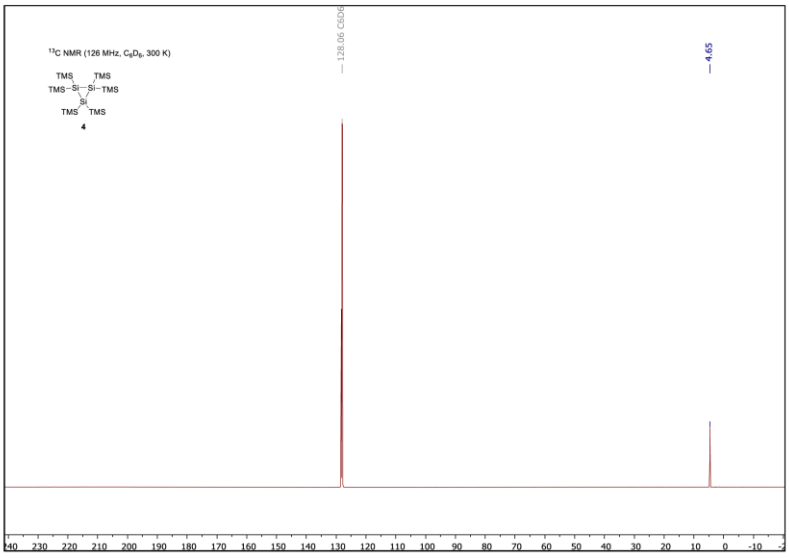


Fig. S14: ^{13}C NMR spectrum (126 MHz) of compound **4** in C_6D_6 at 300 K.

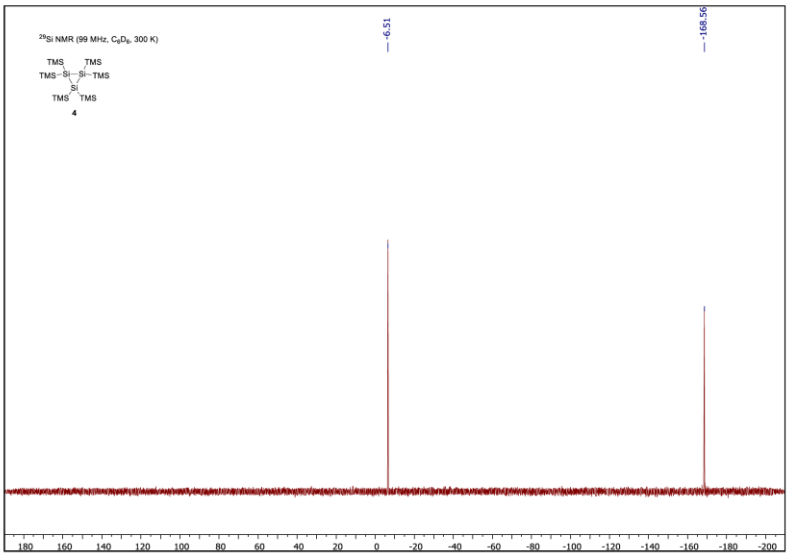
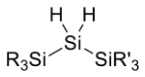


Fig. S15: ^{29}Si NMR spectrum (99 MHz) of compound **4** in C_6D_6 at 300 K.

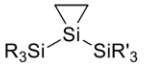
1.7. Hydrosilanes 5a-c



5a R = Si^{t}Bu$_3$, R' = Si(TMS)$_3$
5b R = R' = Si(TMS)$_3$
5c R = R' = Si^{t}Bu$_2$Me

In a pressurizable Schlenk flask, a solution of the respective DMAP-stabilized silylenes **1a-c** (100 µmol, 1.0 eq.) in toluene (5 mL) was frozen in liquid nitrogen, degassed and exposed to dihydrogen (1 bar). The reaction mixture was subsequently heated to 65 °C for 2 hours. Decolorization indicated full conversion. Concomitantly formed free DMAP was separated by precipitation with $SiBr_4$ (100 µmol, 1.0 eq.) and filtration. The solvent was removed under reduced pressure to afford hydrosilanes **5** as colorless solids in quantitative yields. Compounds **5a-c** were identified by comparison of NMR spectral data with corresponding literature reports (**5a**,[S5] **5b**,[S2] **5c**[S3]).

1.8. Siliranes 6



6a R = Si^{t}Bu$_3$, R' = Si(TMS)$_3$
6b R = R' = Si^{t}Bu$_2$Me

The synthesis of siliranes **6** was conducted by a similar procedure than than that for hydrosilanes **5** (*vide supra*). Instead of H_2, the DMAP-silylene complexes **1a** and **1b** were exposed to ethylene (1 bar). The compounds **6** were obtained as colorless solids. Silirane **6a** was identified by comparison of NMR spectral data with literature reports.[S5] Compound **6b** was identified by multinuclear NMR spectroscopy.

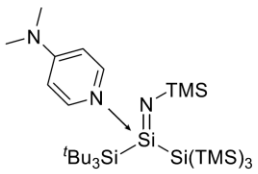
6b

^{1}H NMR (500 MHz, C_6D_6, 300 K): δ [ppm] = 1.10 (s, 36H, C(C$\underline{H}_3$)$_3$), 0.81 (s, 4H, C$\underline{H}_2$), 0.10 (s, 6H, Si(C$\underline{H}_3$)).

^{13}C NMR (126 MHz, C_6D_6, 300 K): δ [ppm] = 29.9 (C($\underline{C}$H$_3$)$_3$), 21.8 ($\underline{C}$(CH$_3$)$_3$), -0.7 ($\underline{C}$H$_2$), -6.3 (Si$\underline{C}$H$_3$)

^{29}Si{^{1}H} NMR (99 MHz, C_6D_6, 300 K): δ [ppm] = 11.2 ($\underline{Si}$^{t}Bu$_2$Me), -174.5 ($\underline{Si}$CH$_2$).

1.9. Silaimine 7a



7a

$Si_7C_{31}H_{73}N_3$

684.54 g/mol

Trimethylsilyl azide (11.6 mg, 100 µmol, 1.0 eq.) was added to a solution of silylene **1a** (60.0 mg, 100 µmol, 1.0 eq.) in benzene (2 mL) at ambient temperature. Decolorization from dark-brown to yellow and concomitant N_2 evolution was observed. After stirring the mixture for 1 hour, evaporation of the solvent under reduced pressure afforded compound **7a** as yellow solid (53.8 mg, 78.6 µmol, 78%). Crystals suitable for SC-XRD analysis were obtained from a cooled (-35 °C) *n*-hexane solution of **7a**.

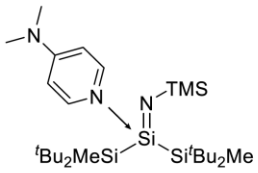
Note: Compound **7a** decomposes is solution under liberation of DMAP. Presumably, the donor-free silaimine is formed that decomposes further to an unidentified mixture of products.

^{1}H NMR (500 MHz, C_6D_6, 300 K): δ [ppm] = 9.42 (br. s, 1H, *o*-$C^{DMAP}\underline{H}$), 8.50 (br. s, 1H, *o*-$C^{DMAP}\underline{H}$), 6.06 (d, ^3J = 6.9 Hz, 2H, *m*-C^{DMAP}H), 1.83 (s, 6H, N(C$\underline{H}_3$)$_2$), 1.41 (s, 27H, Si(C(C$\underline{H}_3$)$_3$)), 0.69 (s, 9H, NSi(C$\underline{H}_3$)$_3$), 0.47 (s, 27H, Si(Si(C$\underline{H}_3$)$_3$)$_3$).

^{13}C NMR (126 MHz, C_6D_6, 300 K): δ [ppm] = 155.9 (*p*-C^{DMAP}), 150.6 (*o*-C^{DMAP}), 106.9 (*m*-C^{DMAP}), 38.3 (N(C$\underline{H}_3$)$_2$), 33.3 (C(C$\underline{H}_3$)$_3$), 25.1 (C(CH$_3$)$_3$), 7.7 (NSi(C$\underline{H}_3$), 5.3 (Si(Si(C$\underline{H}_3$)$_3$)$_3$).

^{29}Si{^{1}H} NMR (99 MHz, C_6D_6, 300 K): δ [ppm] = 2.0 (*Si*^{t}Bu$_3$), -9.4 (Si(*Si*Me$_3$)$_3$), -25.1 (N(*Si*Me$_3$), -25.9 (*Si*=N), -121.3 (*Si*(SiMe$_3$)$_3$).

1.10. Silaimine 7b



7b

$Si_4C_{28}H_{61}N_3$

552.16 g/mol

Analog to the synthesis of **7a** (*vide supra*) silylene **1b** (25 mg, 53.8 µmol, 1.0 eq.) was treated with trimethylsilyl azide (6.19 mg, 53.8 µmol, 1.0 eq.) to afford silaimine **7b** as yellow, crystalline solid (28.4 mg, 51.4 mmol, 96%).

^{1}H NMR (500 MHz, C_6D_6, 300 K): δ [ppm] = 8.82-8.81 (m, 2H, *o*-$C^{DMAP}\underline{H}$), 5.79 (d, ^{3}J = 7.3 Hz, 2H, *m*-$C^{DMAP}\underline{H}$), 1.80 (s, 6H, N($C\underline{H}_3$)$_2$), 1.34 (s, 18H, C($C\underline{H}_3$)$_3$), 1.16 (s, 18H, C($C\underline{H}_3$)$_3$), 0.72 (s, 9H, Si(CH_3)$_3$), 0.42 (s, 6H, Si($C\underline{H}_3$)).

^{13}C{^{1}H} NMR (126 MHz, C_6D_6, 300 K): δ [ppm] = 155.8 (*p*-C^{DMAP}), 145.7 (*o*-C^{DMAP}), 106.3 (*m*-C^{DMAP}), 38.3 (N($\underline{C}H_3$)$_2$), 31.1 (C($\underline{C}H_3$)$_3$), 31.1 (C($\underline{C}H_3$)$_3$), 22.5 ($\underline{C}$(CH_3)$_3$), 22.3 ($\underline{C}$(CH_3)$_3$), -4.5 (Si($\underline{C}H_3$)).

^{29}Si{^{1}H} NMR (99 MHz, C_6D_6, 300 K): δ [ppm] = -8.8 ($\underline{Si}$^{t}Bu$_2$Me), -24.9 ($\underline{Si}$Me$_3$), -25.5 ($\underline{Si}$=N).

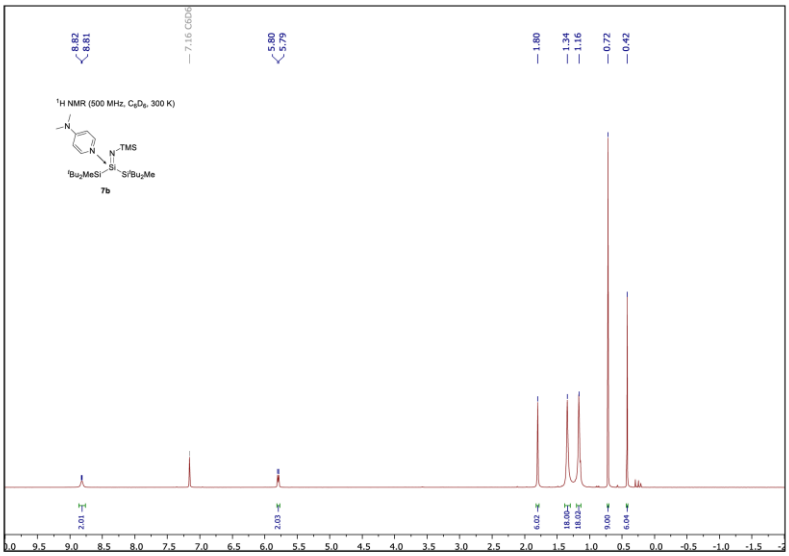


Fig. S16: ^{1}H NMR spectrum (500 MHz) of compound **7b** in C_6D_6 at 300 K.

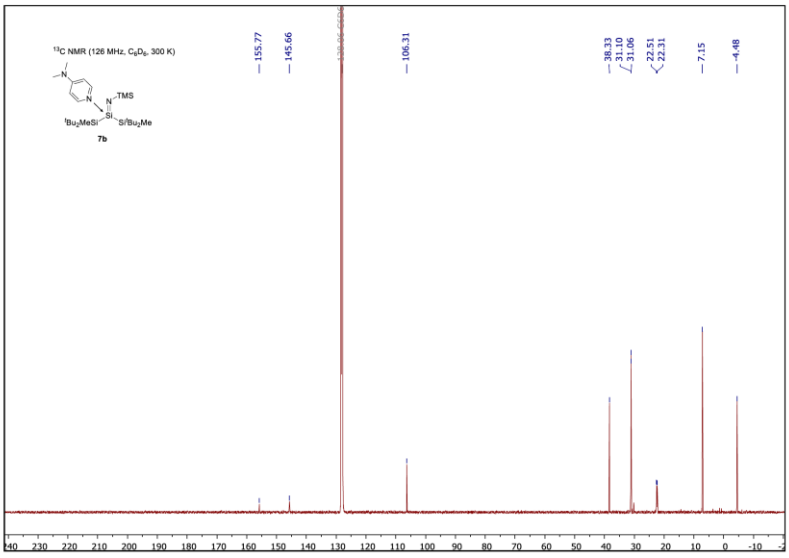


Fig. S17: ^{13}C NMR spectrum (126 MHz) of compound **7b** in C_6D_6 at 300 K.

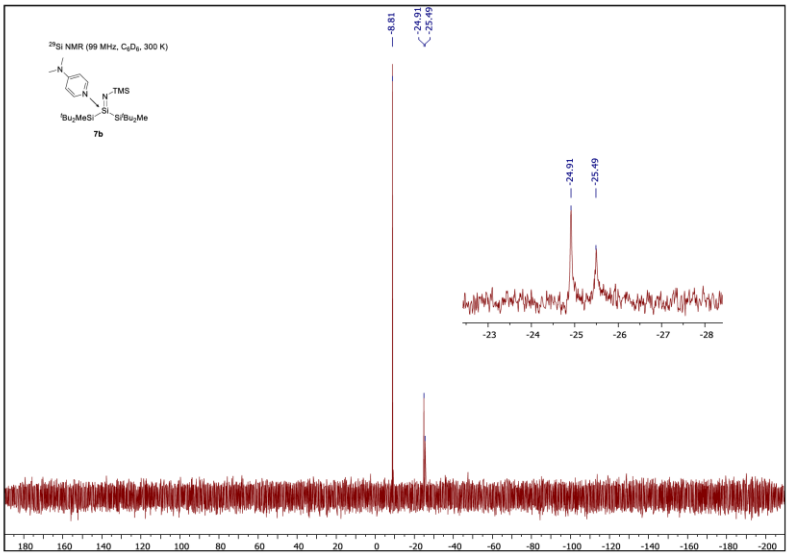


Fig. S18: ^{29}Si NMR spectrum (99 MHz) of compound **7b** in C_6D_6 at 300 K.

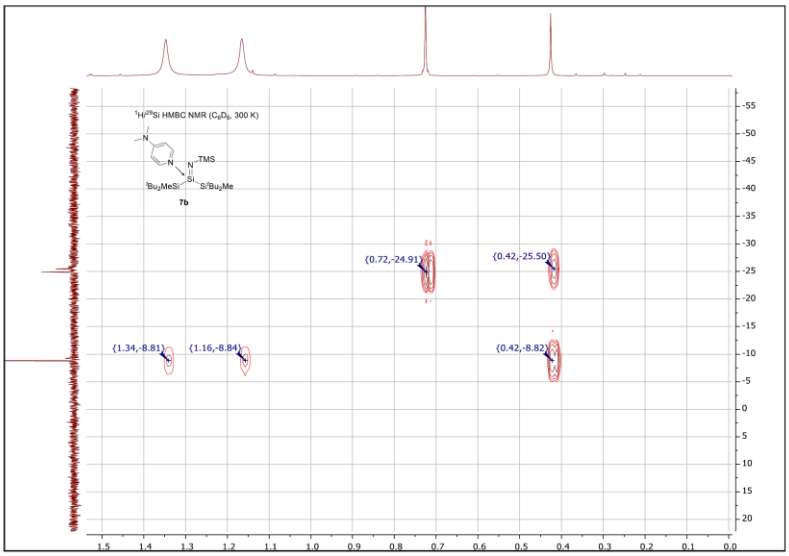


Fig. S19: $^{1}H/^{29}Si$ HMBC NMR spectrum of compound **7b** in C_6D_6 at 300 K.

2. X-ray Crystallographic Data

2.1. General Information

The X-ray intensity data of **2** were collected on an X-ray single crystal diffractometer equipped with a CMOS detector (*Bruker Photon-100*), a rotating anode (*Bruker TXS*) with MoKα radiation (λ = 0.71073 Å) and a *Helios* mirror optic by using the *APEX III* software package.[S8] The X-ray intensity data of **1b** and **7a** were collected on an X-ray single crystal diffractometer equipped with a CMOS detector (*Bruker Photon-100*), an IMS microsource with MoKα radiation (λ = 0.71073 Å) and a *Helios* mirror optic by using the *APEX III* software package.[S8] The X-ray intensity data of **3** was collected on an X-ray single crystal diffractometer equipped with a CCD detector (*Apex II CCD*), a fine-focus sealed tube with MoKα radiation (λ = 0.71073 Å) and a *Triumph* monochromator by using the *APEX II/III* software package.[S8] The measurements were performed on single crystals coated with the perfluorinated ether *Fomblin® Y*. The crystal was fixed on the top of a micro sampler, transferred to the diffractometer and frozen under a stream of cold nitrogen. A matrix scan was used to determine the initial lattice parameters. Reflections were merged and corrected for Lorenz and polarization effects, scan speed, and background using *SAINT*.[S9] Absorption corrections, including odd and even ordered spherical harmonics were performed using *SADABS*.[S9] Space group assignments were based upon systematic absences, E statistics, and successful refinement of the structures. Structures were solved by direct methods with the aid of successive difference Fourier maps, and were refined against all data using the *APEX III* software in conjunction with *SHELXL-2014*[S10] and *SHELXLE*.[S11] All H atoms were placed in calculated positions and refined using a riding model, with methylene and aromatic C–H distances of 0.99 and 0.95 Å, respectively, and $U_{iso}(H) = 1.2 \cdot U_{eq}(C)$. Full-matrix least-squares refinements were carried out by minimizing $\Delta w(F_o^2 – F_c^2)$[S9] with *SHELXL-97* weighting scheme.[S12] Neutral atom scattering factors for all atoms and anomalous dispersion corrections for the non-hydrogen atoms were taken from International Tables for Crystallography.[S13] The images of the crystal structures were generated by *Mercury*.[S14] The CCDC numbers CCDC-1967942 (**1b**), CCDC-1967943 (**2**), CCDC-1967944 (**3**) and CCDC-1967945 (**7a**) contain the supplementary crystallographic data for the structures. These data can be obtained free of charge from the Cambridge Crystallographic Data Centre *via* https://www.ccdc.cam.ac.uk/structures/.

2.2 SC-XRD structures

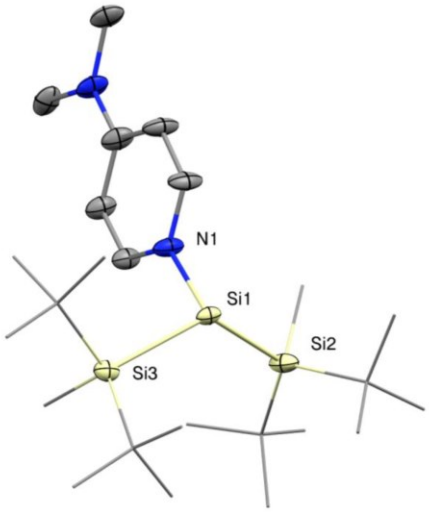


Fig. S20: SC-XRD structure of silylene **1b** with thermal ellipsoids drawn at the 30% probability level. Hydrogen atoms are omitted for clarity, ^{t}Bu- and Me-groups are simplified as wireframes. Selected bond lengths [Å] and angles [°]: Si1–N1 1.937(5), Si1–Si2 2.390(3), Si1–Si3 2.378(3), Si2–Si1–Si3 123.1(1), Si2–Si1–N1 96.2(2), Si3–Si1–N1 98.8(2).

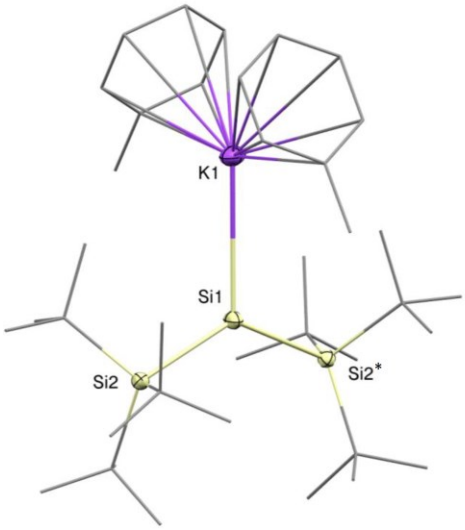


Fig. S21: SC-XRD structure of silyl radical **2** with thermal ellipsoids drawn at the 30% probability level. Hydrogen atoms are omitted for clarity, ^{t}Bu-groups and toluene molecules are simplified as wireframes. Selected bond lengths [Å] and angles [°]: Si1–Si2 2.3936(14), Si1–K1 3.315(2), K1–Si1–Si2 114.91(2), Si2–Si1–Si2* 130.19(3).

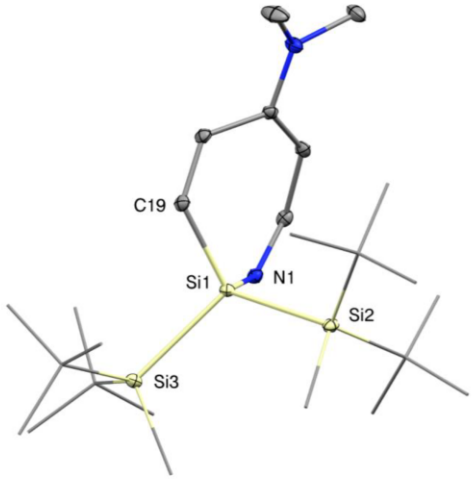


Fig. S22: SC-XRD structure of azasilepin **3** with thermal ellipsoids drawn at the 30% probability level. Hydrogen atoms are omitted for clarity, ^{t}Bu- and Me-groups are simplified as wireframes. Selected bond lengths [Å] and angles [°]: Si1–N1 1.750(1), Si1–C19 1.878(1), Si1–Si2 2.4144(6), Si2–Si1–Si3 113.74(2), Si2–Si1–N1 109.08(4), N1–Si1–C19 104.71(5).

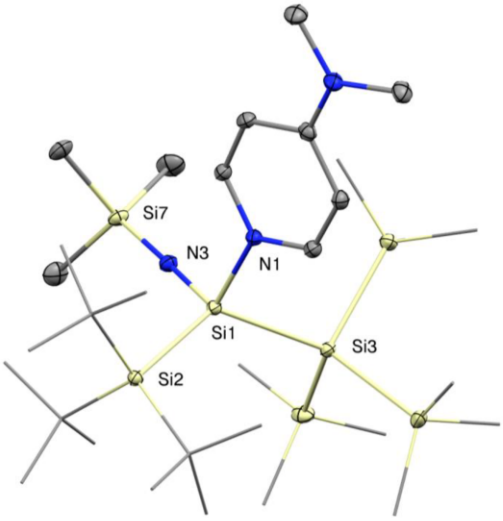


Fig. S23: SC-XRD structure of silaimine **7a** with thermal ellipsoids drawn at the 30% probability level. Hydrogen atoms are omitted for clarity, ^{t}Bu- and Me-groups are simplified as wireframes. Selected bond lengths [Å] and angles [°]: Si1–Si2 2.453(1), Si1–N1 1.928(2), Si1–N3 1.616(2), N3–Si7 1.660(2), Si2–Si1–Si3 125.08(3), N1–Si1–N3 106.08(8), Si1–N3–Si7 177.1(1).

2.3 Crystal data and structural refinement parameters

Table S1: Crystal data and structural refinement parameters for compounds **1**, **3**, **4** and **7a**.

Compound #	1b	2	3	7a
CCDC #	1967942	1967943	1967944	1967945
Chemical formula	$C_{25}H_{52}N_2Si_3$	$C_{38}H_{70}KSi_3$	$C_{25}H_{52}N_2Si_3$	$C_{31}H_{73}N_3Si_7$
Formula weight	464.96	650.31	464.96	684.55
Temperature	100(2) K	100(2) K	100(2) K	100(2) K
Wavelength	0.71073 Å	0.71073 Å	0.71073 Å	0.71073 Å
Crystal size	0.209 × 0.235 × 0.373 mm	0.176 × 0.299 × 0.302 mm	0.268 × 0.342 × 0.398 mm	0.059 × 0.153 × 0.213 mm
Crystal habit	clear dark red-brown fragment	clear yellow fragment	clear yellow fragment	clear yellow fragment
Crystal system	monoclinic	monoclinic	orthorhombic	triclinic
Space group	C 2/c	C 2/c	P b c a	P -1
Unit cell dimensions	a = 28.128(4) Å, α = 90° b = 15.312(2) Å, β = 110.180(4)° c = 14.6773(19) Å, γ = 90°	a = 20.678(7) Å, α = 90° b = 12.877(5) Å, β = 120.067(10)° c = 17.566(10) Å, γ = 90°	a = 11.9770(13) Å, α = 90° b = 16.9418(17) Å, α = 90° c = 28.631(3) Å, α = 90°	a = 11.515(9) Å, α = 97.728(17)° b = 11.940(9) Å, β = 92.844(18)° c = 16.100(7) Å, γ = 104.175(19)°
Volume	5933.4(14) $Å^3$	4048(3) $Å^3$	5809.6(11) $Å^3$	2119(2) $Å^3$
Z	8	4	8	2
Density (calculated)	1.041 g/cm^3	1.067 g/cm^3	1.063 g/cm^3	1.073 g/cm^3
Absorption coefficient	0.174 mm^{-1}	0.243 mm^{-1}	0.178 mm^{-1}	0.248 mm^{-1}
F(000)	2064	1436	2064	756
Diffractometer	Bruker D8 Venture Duo IMS	Bruker D8 Venture	Bruker D8 Kappa Apex II	Bruker D8 Venture Duo IMS
Radiation source	IMS microsource, Mo	TXS rotating anode, Mo	fine-focus sealed tube, Mo	IMS microsource, Mo
Theta range for data collection	1.94 to 25.35°	2.28 to 25.68°	2.20 to 26.37°	2.03 to 25.35°
Index ranges	-33<=h<=33, -18<=k<=18, -17<=l<=17	-25<=h<=25, -15<=k<=15, -21<=l<=20	-14<=h<=14, -21<=k<=21, -35<=l<=35	-13<=h<=13, -14<=k<=14, -18<=l<=19
Reflections collected	36869	68970	188411	89033
Independent reflections	5424 [R(int) = 0.0913]	3797 [R(int) = 0.0742]	5931 [R(int) = 0.0304]	7757 [R(int) = 0.0458]
Coverage of independent reflections	99.8%	98.6%	99.8%	99.9%
Absorption correction	Multi-Scan	Multi-Scan	Multi-Scan	Multi-Scan
Refinement method	Full-matrix least-squares on F^2	Full-matrix least-squares on F^2	Full-matrix least-squares on F^2	Full-matrix least-squares on F^2
Refinement program	SHELXL-2017/1 (Sheldrick, 2017)	SHELXL-2016/6 (Sheldrick, 2016)	SHELXL-2016/6 (Sheldrick, 2016)	SHELXL-2016/6 (Sheldrick, 2016)
Function minimized	$\Sigma w(F_o^2 - F_c^2)^2$	$\Sigma w(F_o^2 - F_c^2)^2$	$\Sigma w(F_o^2 - F_c^2)^2$	$\Sigma w(F_o^2 - F_c^2)^2$
Data / restraints / parameters	5424 / 6 / 328	3797 / 0 / 202	5931 / 0 / 287	7757 / 0 / 393
Goodness-of-fit on F^2	1.172	1.040	1.045	1.123
Final R indices	4238 data; I>2σ(I): R1 = 0.1217, wR2 = 0.2651 all data: R1 = 0.1445, wR2 = 0.2780	3472 data; I>2σ(I): R1 = 0.0305, wR2 = 0.0855 all data: R1 = 0.0341, wR2 = 0.0886	5356 data; I>2σ(I): R1 = 0.0289, wR2 = 0.0771 all data: R1 = 0.0334, wR2 = 0.0802	7180 data; I>2σ(I): R1 = 0.0402, wR2 = 0.0992 all data: R1 = 0.0439, wR2 = 0.1016
Weighting scheme	w=1/[$\sigma^2(F_o^2)$+108.1245P] where P=(F_o^2+2F_c^2)/3	w=1/[$\sigma^2(F_o^2)$+(0.0477P)^2+2.4242P] where P=(F_o^2+2F_c^2)/3	w=1/[$\sigma^2(F_o^2)$+(0.0388P)^2+3.2781P] where P=(F_o^2+2F_c^2)/3	w=1/[$\sigma^2(F_o^2)$+(0.0445P)^2+1.7142P] where P=(F_o^2+2F_c^2)/3
Largest diff. peak and hole	0.560 and -0.742 $eÅ^{-3}$	0.263 and -0.218 $eÅ^{-3}$	0.366 and -0.261 $eÅ^{-3}$	0.634 and -0.258 $eÅ^{-3}$
R.M.S. deviation from mean	0.104 $eÅ^{-3}$	0.040 $eÅ^{-3}$	0.042 $eÅ^{-3}$	0.058 $eÅ^{-3}$

3. References

[S1] G. R. Fulmer, A. J. M. Miller, N. H. Sherden, H. E. Gottlieb, A. Nudelman, B. M. Stoltz, J. E. Bercaw, K. I. Goldberg, *Organometallics* **2010**, *29*, 2176-2179.

[S2] T. Gross, H. Reinke, H. Oehme, *Can. J. Chem.* **2000**, *78*, 1399-1404.

[S3] A. Sekiguchi, T. Fukawa, M. Nakamoto, V. Y. Lee, M. Ichinohe, *J. Am. Chem. Soc.* **2002**, *124*, 9865-9869.

[S4] N. Wiberg, W. Niedermayer, H. Nöth, J. Knizek, W. Ponikwar, K. Polborn, D. Fenske, G. Baum, *Z. Anorg. Allg. Chem.* **2001**, *627*, 594-606.

[S5] D. Reiter, R. Holzner, A. Porzelt, P. J. Altmann, P. Frisch, S. Inoue, *J. Am. Chem. Soc.* **2019**, *141*, 13536-13546.

[S6] K. Fredenhagen, G. Cadenbach, *Z. Anorg. Allg. Chem.* **1926**, *158*, 249-263.

[S7] a) K. W. Klinkhammer, *Chem. Eur. J.* **1997**, *3*, 1418-1431. ; b) K. W. Klinkhammer, *Organosilicon Chemistry III - From Molecules to Materials* (Eds.: N. Auner, J. Weis), Wiley-VCH, **1997**.

[S8] *APEX suite of crystallographic software*, APEX 3 version 2015.5-2; Bruker AXS Inc.: Madison, Wisconsin, USA, 2015.

[S9] *SAINT*, Version 7.56a and SADABS Version 2008/1; Bruker AXS Inc.: Madison, Wisconsin, USA, 2008.

[S10] G. M. Sheldrick, SHELXL-2014, University of Göttingen, Göttingen, Germany, 2014.

[S11] C. B. Hübschle, G. M. Sheldrick, B. Dittrich, *J. Appl. Cryst.* **2011**, *44*, 1281-1284.

[S12] G. M. Sheldrick, SHELXL-97, University of Göttingen, Göttingen, Germany, 1998.

[S13] A. J. C. Wilson, *International Tables for Crystallography,* Volume C, Tables 6.1.1.4 (pp. 500-502), 4.2.6.8 (pp. 219-222), and 4.2.4.2 (pp. 193-199), Kluwer Academic Publishers: Dordrecht, The Netherlands, **1992**.

[S14] C. F. Macrae, I. J. Bruno, J. A. Chisholm, P. R. Edgington, P. McCabe, E. Pidcock, L. Rodriguez-Monge, R. Taylor, J. van de Streek, P. A. Wood, *J. Appl. Cryst.* **2008**, *41*, 466-470.

13.3 Supporting Information Chapter 6

Supplementary Information

Silylated silicon carbonyl complexes: Mimics of ubiquitous transition metal carbonyls

Dominik Reiter, Richard Holzner, Amelie Porzelt, Philipp Frisch, Shigeyoshi Inoue*

Table of Contents

1. Experimental Section S2
1.1 General Methods and Instrumentation S2
1.2 Synthesis of ((TMS)$_3$Si)(^{t}Bu$_3$Si)Si⇆CO (**3**) S3
1.3 Synthesis of Disiletane **4** S9
1.4 Small Molecule Activation S10
1.5 Synthesis of ((TMS)$_3$Si)(^{t}Bu$_3$Si)Si⇆CNXyl (**5**) S11
1.6 Synthesis of 1,3-Azasilole **6** S15
1.7 Synthesis of ((TMS)$_3$Si)(^{t}Bu$_3$Si)Si(OTMS)(CN) (**7**) S18
1.8 Synthesis of (^{t}Bu$_3$Si)$_2$Si⇆CO (**8**) S23
2. X-ray Crystallographic Data S27
3. DFT Calculations S32
4. References S64

1. Experimental Section

1.1 General Methods and Instrumentation

All manipulations were carried out under exclusion of H_2O and O_2 under an atmosphere of argon 4.6 (≥99.996%; *Westfalen AG*) using standard *Schlenk* techniques or in a *LABstar* glovebox from *MBraun Inertgas-Systeme GmbH* with H_2O and O_2 levels below 0.5 ppm. The glassware used was heat dried under fine vacuum prior to use with *Triboflon III* grease (mixture of polytetrafluoroethylene (PTFE) and perfluoropolyether (PFPE)) from *Freudenberg & Co. KG* as sealant. All solvents were refluxed over sodium/benzophenone, freshly distilled under argon and deoxygenated before use. Deuterated benzene was obtained from *Sigma-Aldrich Chemie GmbH*, dried over Na/K alloy, flask-to-flask condensed, deoxygenated by three freeze-pump-thaw cycles and stored over 3 Å molecular sieves in the glovebox. All NMR samples were prepared under argon in *J. Young* PTFE valve NMR tubes. The NMR spectra were recorded on *Bruker Avance Neo 400* (^{1}H: 400.23 MHz, ^{13}C: 100.65 MHz), or *AV500C* (^{1}H: 500.36 MHz, ^{13}C: 125.83 MHz, ^{29}Si: 99.41 MHz) spectrometers at ambient temperature (300 K). The ^{1}H, ^{13}C{^{1}H} and ^{29}Si{^{1}H} NMR spectroscopic chemical shifts δ are reported in ppm relative to tetramethylsilane. ^{1}H and ^{13}C{^{1}H} NMR spectra are calibrated against the residual proton and natural abundance carbon resonances of the deuterated solvent as internal standard (C_6D_6: δ(^{1}H) = 7.16 ppm and δ(^{13}C) = 128.1 ppm) (*1*). The following abbreviations are used to describe signal multiplicities: s = singlet, d = doublet, t = triplet, m = multiplet and combinations thereof (*e.g.* dd = doublet of doublets). Some NMR spectra include resonances for silicone grease (C_6D_6: δ(^{1}H) = 0.29 ppm, δ(^{13}C) = 1.4 ppm and δ(^{29}Si) = –21.8 ppm) derived from *B. Braun Melsungen AG Sterican®* cannulas. Quantitative elemental analyses (EA) were carried out using a *EURO EA* (*HEKAtech*) instrument equipped with a CHNS combustion analyzer at the *Laboratory for Microanalysis* at the *TUM Catalysis Research Center*. Elemental analyses provided partially and reproducibly low carbon percentages (~1% deviation), presumably due to the formation of incombustible SiC compounds. Infrared (IR) spectra were recorded on a *Perkin Elmer* FT-IR spectrometer (*diamond ATR, Spectrum Two*) in a range of 400–4000 cm^{-1} at room temperature inside an argon-filled glovebox. The intensities of the IR bands are abbreviated as following: s = strong, m = medium, w = weak. The UV-Vis spectra were taken on a *Varian, Inc. Cary 50* spectrophotometer with a *Schlenk* quartz cuvette. Melting Points (m.p.) were determined in sealed glass capillaries under inert gas by a *Büchi M-565* melting point apparatus. Liquid Injection Field Desorption Ionization

mass spectra (LIFDI-MS) were recorded on a *Waters Micromass LCT TOF* mass spectrometer equipped with a LIFDI-ion source (*LIFDI-700*) from *Linden CMS GmbH*. The samples were provided as filtered solution in toluene. Electrospray ionization mass spectra (ESI-MS) were acquired using an *LTQ FT Ultra* mass spectrometer from *Thermo Fisher Scientific Inc*. Photochemical experiments were carried out using an *Asahi Spectra Co., Ltd. MAX-302* Xenon Light Source at λ_{max} = 340 nm. Unless otherwise stated, all commercially available reagents were purchased from *abcr GmbH* or *Sigma-Aldrich Chemie GmbH* and used without further purification. Carbon monoxide (CO) 4.7 (≥99.997%), ethylene 3.5 (≥99.95%) and hydrogen 5.0 (≥99.999%) were purchased from *Air Liquide S.A.* or *Westfalen AG* and used as received. ^{13}C-labeled CO was obtained from *Sigma-Aldrich Chemie GmbH*. The compounds bis(silyl)silylene ((TMS)$_3$Si)(^{t}Bu$_3$Si)Si: (**1**)/tetrasilyldisilene (TMS)$_2$Si=Si(TMS)(Si^{t}Bu$_3$) (**1′**) (*2*), DMAP-stabilized bis(silyl)silylene ((TMS)$_3$Si)(^{t}Bu$_3$Si)Si (DMAP) (**2**) (*2*), KC_8 (*2*) and (^{t}Bu$_3$Si)$_2$SiBr$_2$ (*3*) were prepared as described in the corresponding references.

1.2 Synthesis of ((TMS)$_3$Si)(^{t}Bu$_3$Si)Si⇆CO (3)



3

$C_{22}H_{54}OSi_6$

503.18 g/mol

Silicon carbonyl complex **3** was obtained by two different methods, either by direct carbonylation of **1**/**1′** (Method A) or more conveniently by exposure of **2** to CO *via* a Lewis base exchange reaction (Method B).



Method A:

A solution of **1**/**1′** (100 mg, 210 µmol) in *n*-hexane (3 mL) was cooled to –30 °C, degassed and exposed to CO (1 bar). Subsequently, the reaction mixture was warmed to ambient temperature, whereby a color change from blood-red to purple was observed. After stirring for 1 h, all volatiles were removed *in vacuo*. Purple crystals of **3** (95.0 mg, 189 µmol, 90%), which were suitable for single-crystal X-ray diffraction (SC-XRD) analysis, were obtained by cooling a concentrated *n*-hexane solution of **3** to –35 °C for several days.

Method B:

A solution of **2** (600 mg, 1.00 mmol) in toluene (15 mL) was degassed and subsequently exposed to CO (1 bar) at room temperature. The reaction mixture was stirred for 5 h, whereby a color change from red-brown to purple was observed. After removal of all volatiles *in vacuo*, the residue was

extracted with cold *n*-hexane (3 × 5 mL, –35 °C). DMAP was separated from the mixture *via* filtration. Removal of the solvent *in vacuo* provided **3** as a purple solid (505 mg, 1.00 mmol, quantitative yield).

Note: Removal of free DMAP is also possible by addition of an equimolar amount of silicon tetrabromide ($SiBr_4$) to the reaction mixture and subsequent filtration (DMAP forms an unidentified Lewis acid/base adduct with $SiBr_4$, which is insoluble in common organic solvents; no reaction of **3** with $SiBr_4$ in solution was detected at least within 1 day).

Silicon carbonyl complex **3** is indefinitely stable as a solid and in solution under argon atmosphere at ambient temperature, but slowly decomposes in solution at elevated temperatures (≥ 90 °C) to free, gaseous CO and disiletane **4** (*vide infra*).

m.p.: 76-77 °C (decomposition; color change from purple to black).

^{1}H NMR (500 MHz, C_6D_6, 300 K): δ [ppm] = 1.23 (s, 27H, C(C*H*$_3$)$_3$), 0.39 (s, 27H, *TMS*).

^{13}C{^{1}H} NMR (126 MHz, C_6D_6, 300 K): δ [ppm] = 226.1 (*C*O), 32.0 (C(*C*H$_3$)$_3$), 25.5 (*C*(CH$_3$)$_3$), 3.0 (*TMS*).

^{29}Si{^{1}H} NMR (99 MHz, C_6D_6, 300 K): δ [ppm] = 42.8 (*Si*^{t}Bu$_3$), –6.9 (*TMS*), –119.0 (*Si*(TMS)$_3$), –228.5 (*Si*CO).

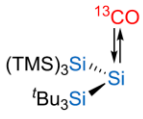
IR (solid): $\tilde{\nu}$ [cm^{-1}] = 2950 (w), 2857 (m), 1908 (s) ($\tilde{\nu}_{CO}$), 1477 (w), 1388 (w), 1244 (m), 1011 (w), 826 (s), 684 (m), 622 (m), 468 (m).

Anal. Calcd. [%] for $C_{22}H_{54}OSi_6$: C, 52.51; H, 10.82. Found [%]: C, 52.76; H, 10.54.

UV-Vis (*n*-hexane, 298 K): λ_{max} [nm] = 373 (theo.: 351; HOMO→LUMO+1).

LIFDI-MS: calculated for **3** ($C_{22}H_{54}OSi_6$): 502.2790
observed: 502.3820

Synthesis of ^{13}C-labeled Silicon Carbonyl Complex ((TMS)$_3$Si)(^{t}Bu$_3$Si)Si⇆^{13}CO (3′)



3'
$C_{21}{}^{13}CH_{54}OSi_6$
504.18 g/mol

For additional characteristic analytical data, the ^{13}C-labeled isotopomer ((TMS)$_3$Si)(^{t}Bu$_3$Si)Si⇆^{13}CO (**3′**) was synthesized using Method B and ^{13}CO. Thus, **3′** (84.4 mg, 167 µmol, quantitative yield) was afforded as a purple solid from **2** (100 mg, 167 µmol) and ^{13}CO. In the following only spectroscopic data with difference to the ^{12}C analogue are given.

^{29}Si{^{1}H} NMR (99 MHz, C_6D_6, 300 K): δ [ppm] = 42.8 (d, ^2J = 3.0 Hz, *Si*^{t}Bu$_3$), –6.9 (d, ^3J = 2.7 Hz, *TMS*), –118.9 (d, ^2J = 2.4 Hz, *Si*(TMS)$_3$), –228.5 (d, ^1J = 2.5 Hz, *Si*CO).

Doublet resonances for each ^{29}Si nucleus were observed in the ^{29}Si NMR spectrum due to coupling with the ^{13}C atom.

IR (solid): $\tilde{\nu}$ [cm^{-1}] = 2948 (w), 2857 (m), 1864 (s) ($\tilde{\nu}_{CO}$), 1477 (w), 1388 (w), 1244 (m), 1011 (w), 826 (s), 684 (m), 622 (m), 466 (m).

The CO stretching mode is red-shifted by 44 cm^{-1} in comparison to the ^{12}C isotopomer.

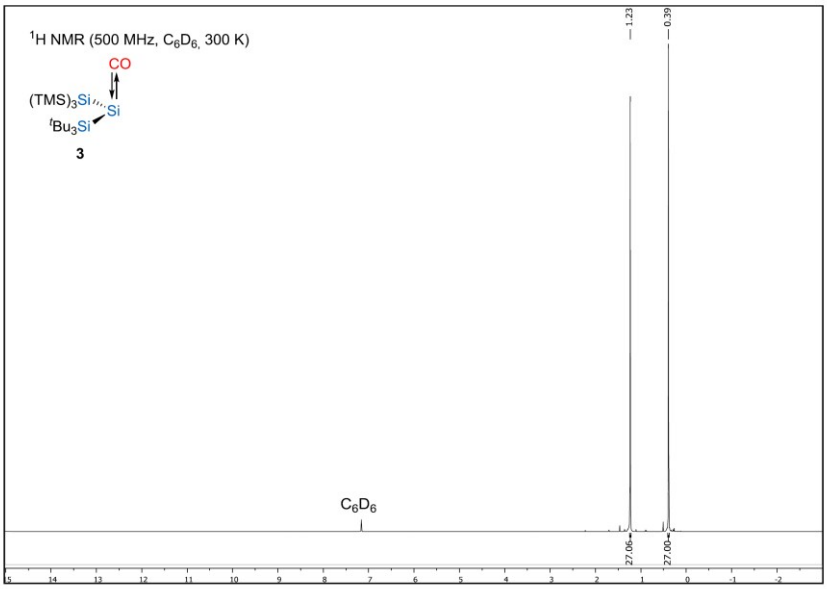


Figure S1. ^{1}H NMR spectrum of ((TMS)$_3$Si)(^{t}Bu$_3$Si)Si⇆CO (**3**) in C_6D_6 at 300 K.

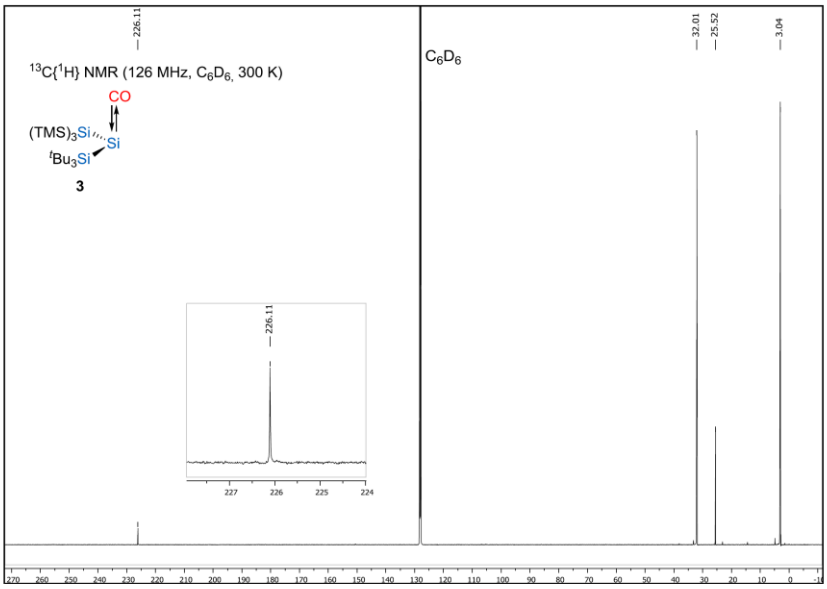


Figure S2. $^{13}C\{^1H\}$ NMR spectrum of $((TMS)_3Si)(^tBu_3Si)Si{\leftrightarrows}CO$ (**3**) in C_6D_6 at 300 K.

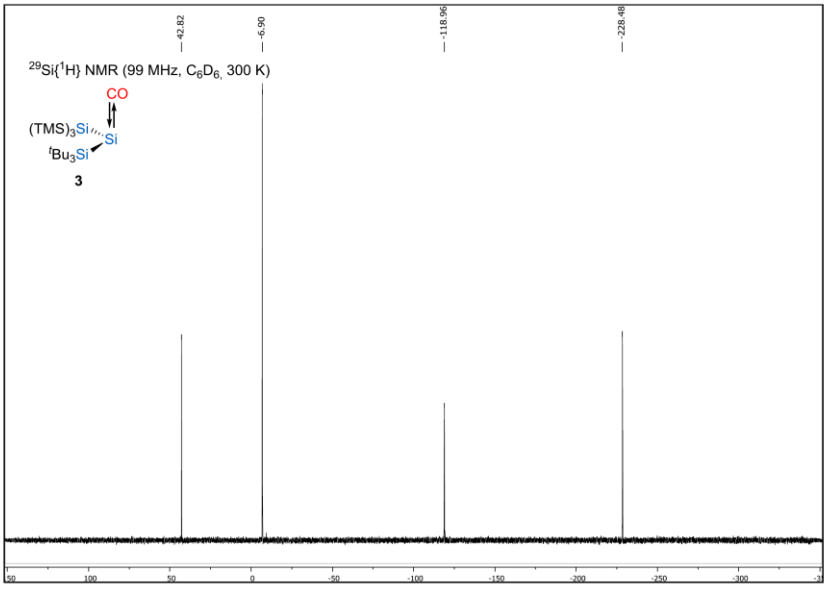


Figure S3. $^{29}Si\{^1H\}$ NMR spectrum of $((TMS)_3Si)(^tBu_3Si)Si{\leftrightarrows}CO$ (**3**) in C_6D_6 at 300 K.

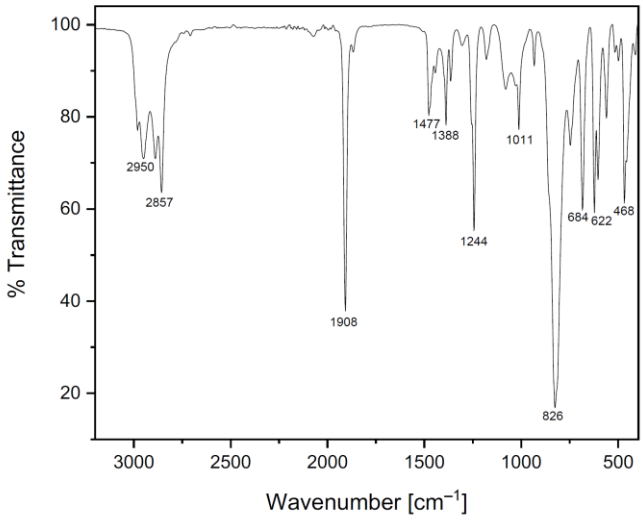


Figure S4. Solid-state FT-IR spectrum of ((TMS)$_3$Si)(^{t}Bu$_3$Si)Si⇆CO (**3**).

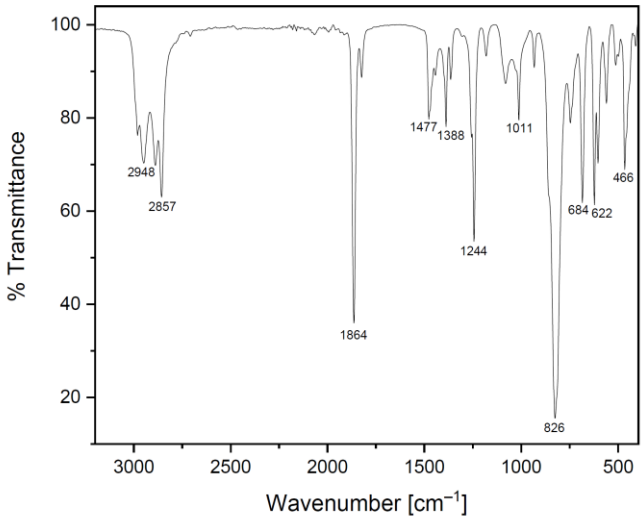


Figure S5. Solid-state FT-IR spectrum of ^{13}C-labeled ((TMS)$_3$Si)(^{t}Bu$_3$Si)Si⇆^{13}CO (**3′**).

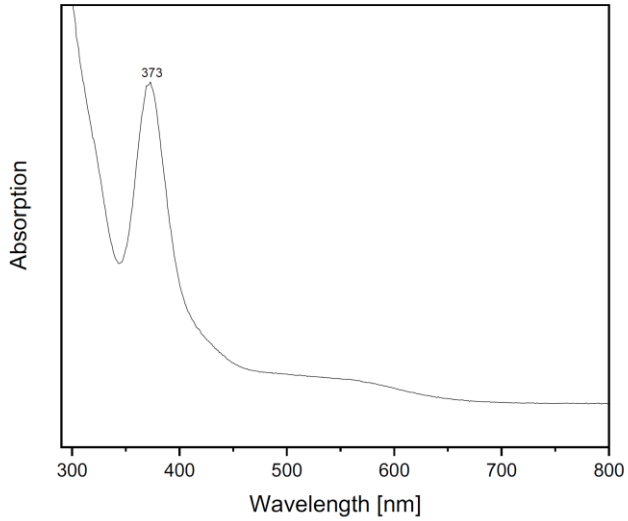


Figure S6. UV-Vis spectrum of ((TMS)$_3$Si)(^{t}Bu$_3$Si)Si⇆CO (**3**) in *n*-hexane (c = 3.0 × 10^{-4} M).

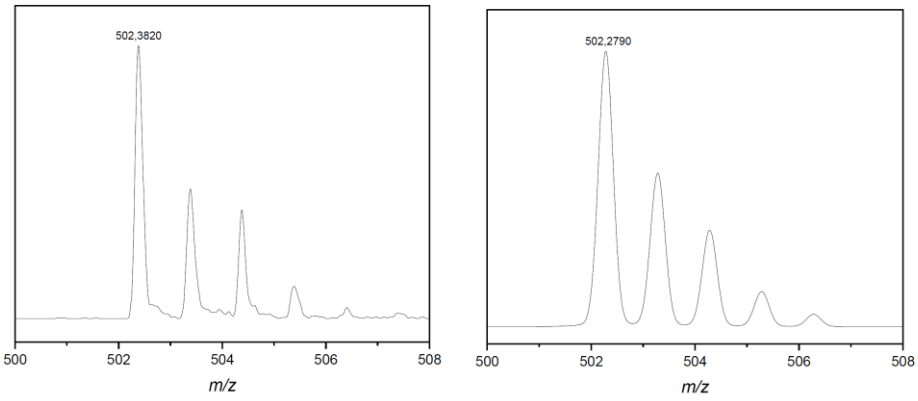
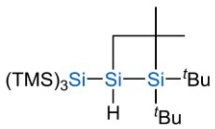


Figure S7. LIFDI-MS spectrometry (detail view with isotope pattern) of ((TMS)$_3$Si)(^{t}Bu$_3$Si)Si⇆CO (**3**). Measured (left; m/z = 502.3820) and simulated (right; m/z = 502.2790) mass spectrum.

1.3 Synthesis of Disiletane 4



4

$C_{21}H_{54}Si_6$

475.17 g/mol

Disiletane **4** was obtained *via* two distinct methods, either by thermal decomposition of silicon carbonyl complex ((TMS)$_3$Si)(^{t}Bu$_3$Si)Si⇆CO (**3**) (Method A) or upon irradiation of **3** (Method B). In both cases a C–H bond activation of a *tert*-butyl group by the silylene moiety takes place after the dissociation of CO.

Method A (thermally):

A solution of silicon carbonyl complex **3** (30.0 mg, 59.6 µmol) in C_6D_6 (0.5 mL) was heated to 130 °C for 2 h. A color change from purple to colorless indicated quantitative conversion, which was verified by ^{1}H NMR spectroscopy. Removal of all volatiles *in vacuo* provided disiletane **4** as a colorless solid (28.3 mg, 59.6 µmol, quantitative yield).

Method B (photochemically):

A *J. Young* PTFE valve NMR tube was charged with a solution of **3** (30.0 mg, 59.6 µmol) in C_6D_6 (0.5 mL). Photolysis of **3** (λ_{max} = 340 nm) resulted in an immediate color change from purple to blood-red with concomitant gas evolution (CO) and formation of bis(silyl)silylene ((TMS)$_3$Si)(^{t}Bu$_3$Si)Si:) (**1**) and its tetrasilyldisilene isomer (TMS)$_2$Si=Si(TMS)(Si^{t}Bu$_3$) (**1′**) (*2*). The photodissociation is partially reversible (observable color change from blood-red to purple after interruption of irradiation) until after irradiation at room temperature for 4 days, quantitative conversion to 1,2-disilacyclobutane **4** was detected by ^{1}H NMR spectroscopy. Removal of all volatiles *in vacuo* afforded **4** as a colorless solid (28.3 mg, 59.6 µmol, quantitative yield).

^{1}H NMR (500 MHz, C_6D_6, 300 K): δ [ppm] = 4.37 (dd, ^3J = 7.8 Hz, ^3J = 5.9 Hz, 1H, Si*H*), 1.45 (s, 3H, C(C*H*$_3$)$_2$), 1.36 (s, 3H, C(C*H*$_3$)$_2$), 1.33–1.30 (m, 2H, C*H*$_2$), 1.29 (s, 9H, C(C*H*$_3$)$_3$), 1.23 (s, 9H, C(C*H*$_3$)$_3$), 0.34 (s, 27H, *TMS*).

^{13}C{^{1}H} NMR (126 MHz, C_6D_6, 300 K): δ [ppm] = 37.4 (*C*(CH$_3$)$_2$), 31.9 (C(*C*H$_3$)$_2$), 31.9 (C(*C*H$_3$)$_2$), 31.5 (C(*C*H$_3$)$_3$), 31.0 (C(*C*H$_3$)$_3$), 29.5 (*C*H$_2$), 23.6 (*C*(CH$_3$)$_3$), 22.9 (*C*(CH$_3$)$_3$), 2.8 (*TMS*).

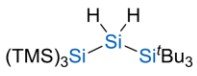
^{29}Si{^{1}H} NMR (99 MHz, C_6D_6, 300 K): δ [ppm] = 35.6 (*Si*^{t}Bu$_2$), –9.2 (*TMS*), –60.4 (Si*H*), –133.8 (*Si*(TMS)$_3$).

The spectroscopic data match those recently reported (*2*).

1.4 Small Molecule Activation

Similar to the synthesis of disiletane **4** (*vide supra*), both thermal decomposition (≥ 90 °C) or photolysis of **3** in the presence of small molecules are suitable for obtaining the products of oxidative addition to the silylene moiety. Due to the faster reaction times, however, only the photodissociation experiments are described in more detail below.

Synthesis of ((TMS)$_3$Si)(^{t}Bu$_3$Si)SiH$_2$



$C_{21}H_{56}Si_6$
477.19 g/mol

A *J. Young* PTFE valve NMR tube was charged with a solution of silicon carbonyl complex **3** (30.0 mg, 59.6 µmol) in C_6D_6 (0.5 mL), degassed and exposed to H_2 (1 bar). Photolysis of **3** (λ_{max} = 340 nm) resulted in an immediate color change from purple to colorless. Removal of all volatiles *in vacuo* afforded ((TMS)$_3$Si)(^{t}Bu$_3$Si)SiH$_2$ as a colorless solid (28.5 mg, 59.6 µmol, quantitative yield).

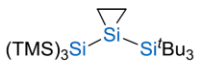
^{1}H NMR (500 MHz, C$_6$D$_6$, 300 K): δ [ppm] = 3.39 (s, 2H, Si*H*$_2$), 1.23 (s, 27H, C(C*H*$_3$)$_3$), 0.36 (s, 27H, *TMS*).

^{13}C{^{1}H} NMR (126 MHz, C$_6$D$_6$, 300 K): δ [ppm] = 31.8 (C(*C*H$_3$)$_3$), 23.8 (*C*(CH$_3$)$_3$), 2.9 (*TMS*).

^{29}Si{^{1}H} NMR (99 MHz, C$_6$D$_6$, 300 K): δ [ppm] = 21.2 (*Si*^{t}Bu$_3$), –8.6 (*TMS*), –114.1 (*Si*H$_2$), –132.9 (*Si*(TMS)$_3$).

The spectroscopic data match those recently reported (*2*).

Synthesis of ((TMS)$_3$Si)(^{t}Bu$_3$Si)Si(CH$_2$CH$_2$)



$C_{23}H_{58}Si_6$
503.23 g/mol

A *J. Young* PTFE valve NMR tube was charged with a solution of silicon carbonyl complex **3** (30.0 mg, 59.6 µmol) in C_6D_6 (0.5 mL), degassed and exposed to ethylene (1 bar). Photolysis of **3** (λ_{max} = 340 nm) resulted in an immediate color change from purple to colorless. Removal of all volatiles *in vacuo* afforded ((TMS)$_3$Si)(^{t}Bu$_3$Si)Si(CH$_2$CH$_2$) as a colorless solid (30.0 mg, 59.6 µmol, quantitative yield).

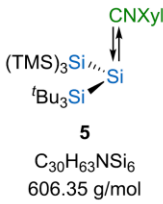
^{1}H NMR (500 MHz, C$_6$D$_6$, 300 K): δ [ppm] = 1.21 (s, 27H, C(C*H*$_3$)$_3$), 0.96–0.93 (m, 2H, C*H*$_2$CH$_2$), 0.78–0.75 (m, 2H, CH$_2$C*H*$_2$), 0.37 (s, 27H, *TMS*).

$^{13}C\{^1H\}$ NMR (126 MHz, C_6D_6, 300 K): δ [ppm] = 32.4 ($C(\underline{C}H_3)_3$), 24.9 ($\underline{C}(CH_3)_3$), 4.1 (*TMS*), 1.2 ($\underline{C}H_2CH_2$).

$^{29}Si\{^1H\}$ NMR (99 MHz, C_6D_6, 300 K): δ [ppm] = 20.2 ($\underline{Si}^tBu_3$), –8.3 (*TMS*), –113.7 ($\underline{Si}(TMS)_3$), –164.3 ($\underline{Si}CH_2CH_2$).

The spectroscopic data match those recently reported (*2*).

1.5 Synthesis of $((TMS)_3Si)(^tBu_3Si)Si{\leftrightarrows}CNXyl$ (5)



5
$C_{30}H_{63}NSi_6$
606.35 g/mol

To a mixture of silicon carbonyl complex **3** (100 mg, 199 µmol, 1.0 eq.) and 2,6-dimethylphenyl isocyanide (CNXyl) (26.1 mg, 199 µmol, 1.0 eq.) was added *n*-hexane (3 mL). An immediate color change from purple to deep blue with concomitant gas evolution (CO) was observed. The reaction mixture was stirred for an additional hour. Subsequent removal of the solvent *in vacuo* afforded silicon isocyanide complex **5** as a deep blue solid (121 mg, 199 µmol, quantitative yield). Crystals, suitable for SC-XRD analysis were obtained by cooling a saturated *n*-hexane solution to –35 °C for several days. Silicon isocyanide complex **5** is indefinitely stable as a solid and in solution at ambient temperature, but very slowly isomerizes in solution at elevated temperatures (≥ 130 °C) to 1,3-azasilole **6** (*vide infra*).



m.p.: 79-80 °C (decomposition; color change from deep blue to black).

^1H NMR (500 MHz, C_6D_6, 300 K): δ [ppm] = 6.78–6.75 (m, 1H, *p*-$C_{ar}\underline{H}$), 6.70–6.69 (m, 2H, *m*-$C_{ar}\underline{H}$), 2.49 (s, 6H, *o*-$C_{ar}C\underline{H}_3$), 1.36 (s, 27H, $C(C\underline{H}_3)_3$), 0.44 (s, 27H, *TMS*).

$^{13}C\{^1H\}$ NMR (126 MHz, C_6D_6, 300 K): δ [ppm] = 192.1 ($\underline{C}N$), 138.2 (*o*-$\underline{C}_{ar}$), 130.1 (*ipso*-$\underline{C}_{ar}$), 129.3 (*p*-$\underline{C}_{ar}H$), 128.9 (*m*-$\underline{C}_{ar}H$), 32.4 ($C(\underline{C}H_3)_3$), 25.5 ($\underline{C}(CH_3)_3$), 19.3 (*o*-$C_{ar}\underline{C}H_3$), 3.6 (*TMS*).

$^{29}Si\{^1H\}$ NMR (99 MHz, C_6D_6, 300 K): δ [ppm] = 37.6 ($\underline{Si}^tBu_3$), –8.1 (*TMS*), –119.1 ($\underline{Si}(TMS)_3$), –177.0 ($\underline{Si}CN$).

IR (solid): $\tilde{\nu}$ [cm^{-1}] = 2950 (w), 2856 (m), 1966 (w) ($\tilde{\nu}_{CN}$), 1471 (w), 1387 (w), 1244 (m), 1012 (m), 826 (s), 683 (m), 622 (m), 465 (m).

Anal. Calcd. [%] for $C_{30}H_{63}NSi_6$: C, 59.43; H, 10.47; N, 2.31. Found [%]: C, 58.17; H, 10.54; N, 2.34.

UV-Vis (*n*-hexane, 298 K): λ_{max} [nm] = 389 (theo.: 366; HOMO→LUMO+1).

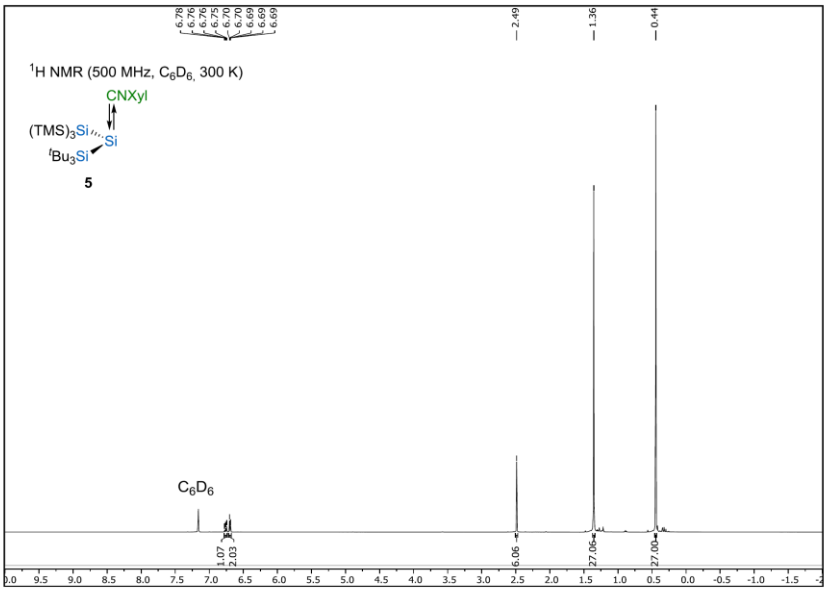


Figure S8. ^{1}H NMR spectrum of ((TMS)$_3$Si)(^{t}Bu$_3$Si)Si⇆CNXyl (**5**) in C_6D_6 at 300 K.

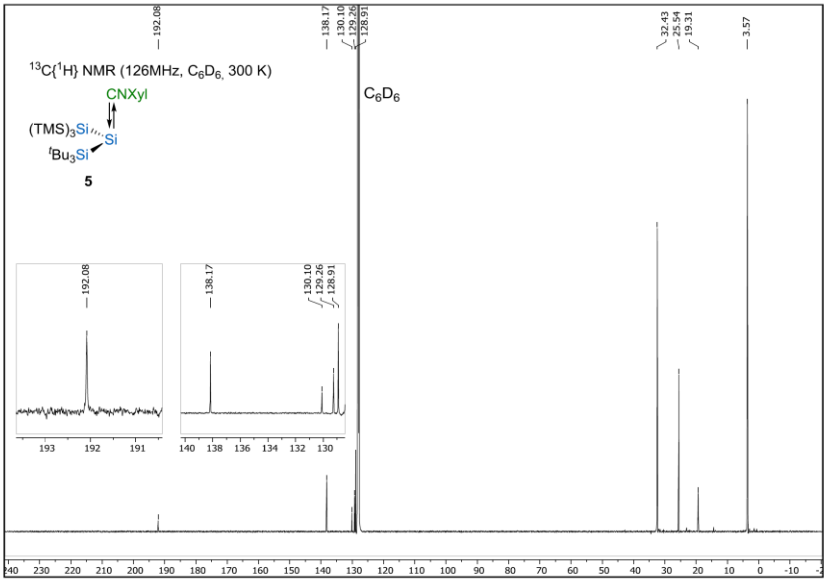


Figure S9. ^{13}C{^{1}H} NMR spectrum of ((TMS)$_3$Si)(^{t}Bu$_3$Si)Si⇆CNXyl (**5**) in C_6D_6 at 300 K.

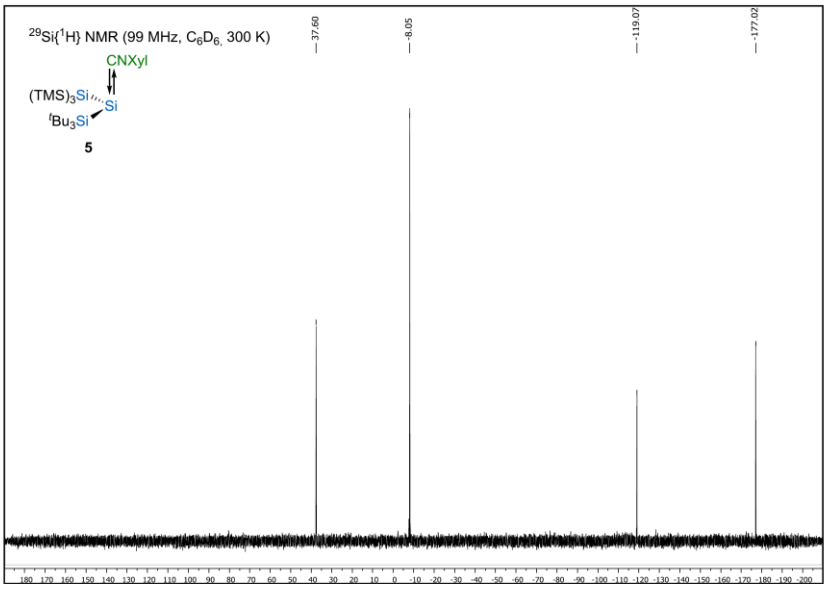


Figure S10. ^{29}Si{^{1}H} NMR spectrum of ((TMS)$_3$Si)(^{t}Bu$_3$Si)Si⇆CNXyl (**5**) in C_6D_6 at 300 K.

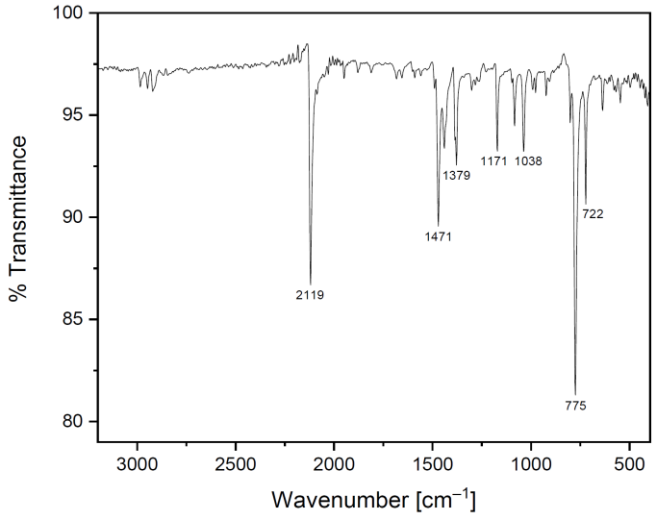


Figure S11. Solid-state FT-IR spectrum of 2,6-dimethylphenyl isocyanide (CNXyl).

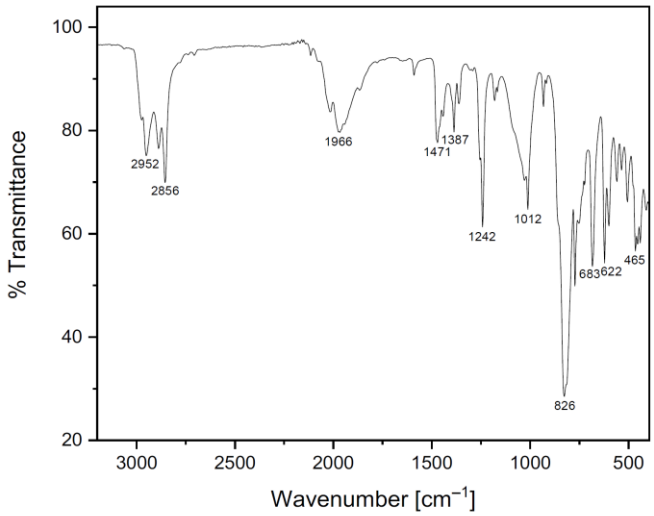


Figure S12. Solid-state FT-IR spectrum of ((TMS)$_3$Si)(^{t}Bu$_3$Si)Si⇆CNXyl (**5**).

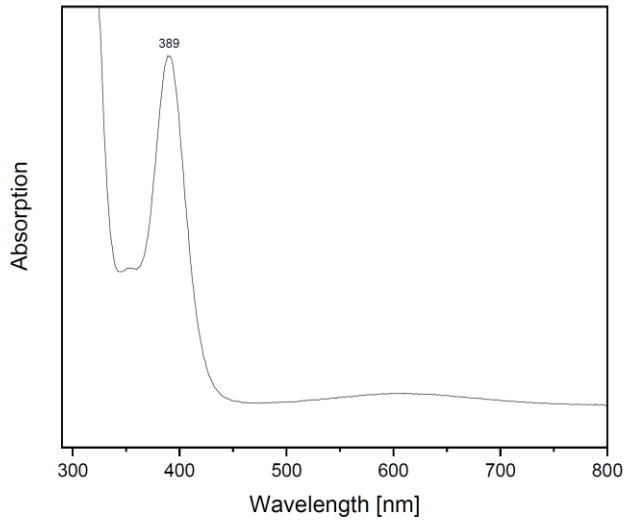
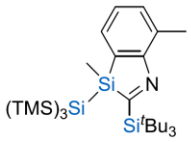


Figure S13. UV-Vis spectrum of ((TMS)$_3$Si)(^{t}Bu$_3$Si)Si⇆CNXyl (**5**) in *n*-hexane (c = 3.0 × 10^{-4} M).

1.6 Synthesis of 1,3-Azasilole 6



6
$C_{30}H_{63}NSi_6$
606.35 g/mol

A solution of silicon isocyanide complex **5** (50.0 mg, 82.5 µmol) in C_6D_6 (0.5 mL) was heated to 130 °C for 2 days. A color change from deep blue to deep green and finally to yellow was observed during the reaction. ^{1}H NMR spectroscopy indicated quantitative conversion to 1,3-azasilole **6**. Removal of the solvent *in vacuo* provided **6** as yellow solid (50.0 mg, 82.5 µmol, quantitative yield).

m.p.: 163-164 °C (decomposition; color change from yellow to orange).

^{1}H NMR (500 MHz, C_6D_6, 300 K): δ [ppm] = 7.71 (d, ^3J = 7.0 Hz, 1H, SiCC*H*), 7.15 (d, ^3J = 7.0 Hz, 1H, NCCCH$_3$C*H*, overlapping with solvent signal), 7.09 (pseudo t, ^3J = 7.0 Hz, 1H, SiCCHC*H*), 2.76 (s, 3H, $C_{ar}CH_3$), 1.36 (s, 27H, C(C*H*$_3$)$_3$), 0.68 (s, 3H, SiC*H*$_3$), 0.24 (s, 27H, *TMS*).

^{13}C{^{1}H} NMR (126 MHz, C_6D_6, 300 K): δ [ppm] = 212.8 (Si*C*=N), 158.4 (N*C*CCH$_3$), 134.4 (NC*C*CH$_3$), 132.9 (NCCCH$_3$*C*H), 131.4 (Si*C*CH), 130.6 (SiC*C*H), 127.4 (SiCCH*C*H), 32.1 (C(*C*H$_3$)$_3$), 23.1 (*C*(CH$_3$)$_3$), 19.2 (NCC*C*H$_3$), 4.0 (*TMS*), –0.3 (Si*C*H$_3$).

^{29}Si{^{1}H} NMR (99 MHz, C_6D_6, 300 K): δ [ppm] = 2.4 (*Si*CH$_3$), 0.8 (*Si*^{t}Bu$_3$), –8.8 (*TMS*), –126.7 (*Si*(TMS)$_3$).

Anal. Calcd. [%] for $C_{30}H_{63}NSi_6$: C, 59.43; H, 10.47; N, 2.31. Found [%]: C, 58.11; H, 10.59; N, 2.28.

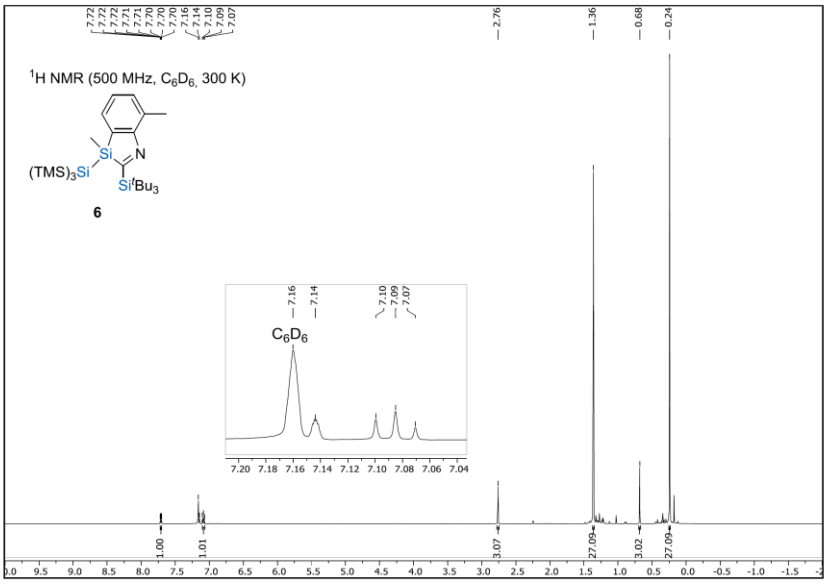


Figure S14. ^{1}H NMR spectrum of 1,3-azasilole **6** in C_6D_6 at 300 K.

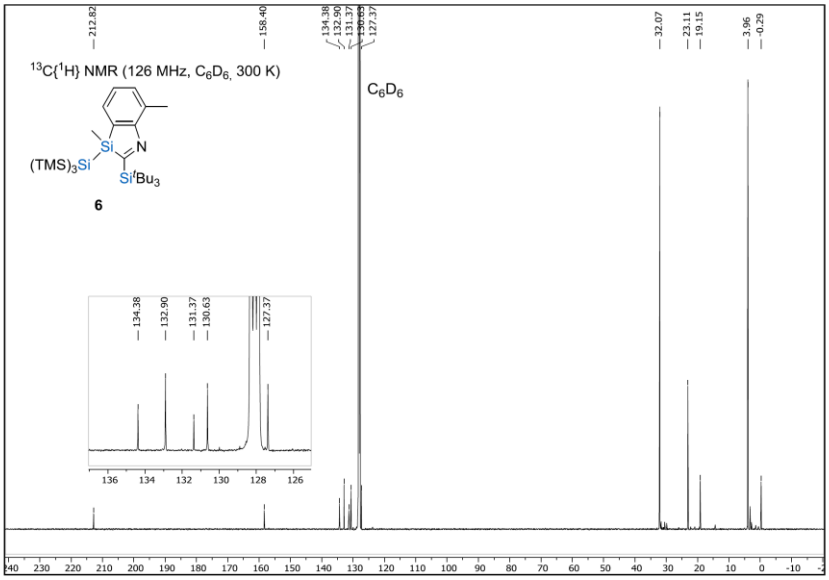


Figure S15. $^{13}C\{^1H\}$ NMR spectrum of 1,3-azasilole **6** in C_6D_6 at 300 K.

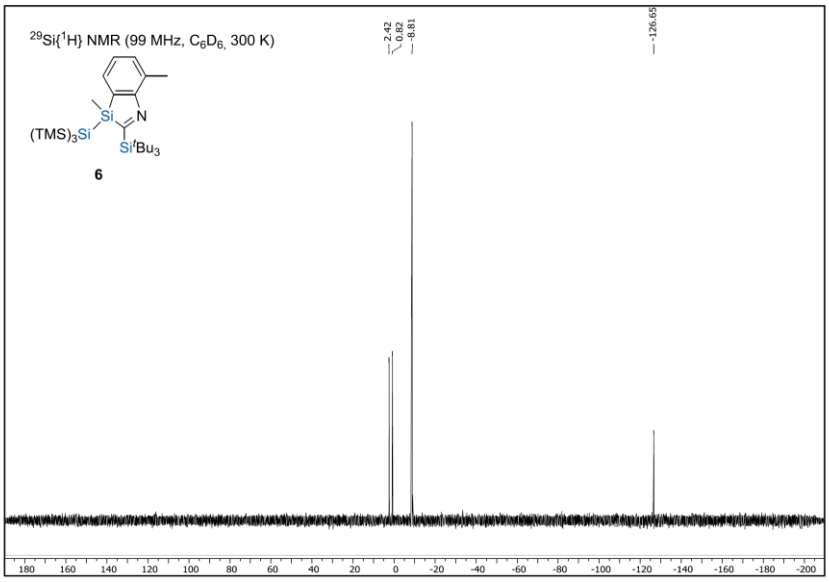


Figure S16. ^{29}Si{^{1}H} NMR spectrum of 1,3-azasilole **6** in C_6D_6 at 300 K.

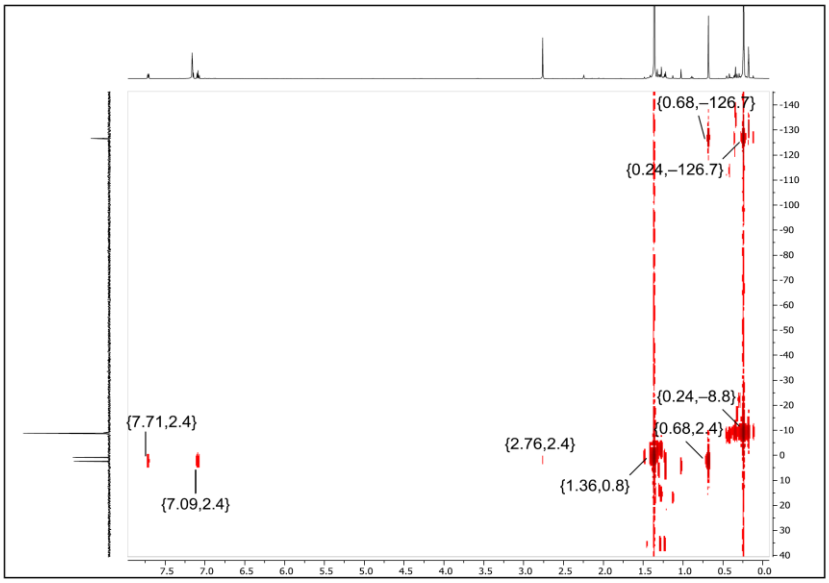
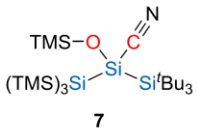


Figure S17. ^{1}H/^{29}Si HMBC NMR spectrum of 1,3-azasilole **6** in C_6D_6 at 300 K.

1.7 Synthesis of ((TMS)$_3$Si)(^{t}Bu$_3$Si)Si(OTMS)(CN) (7)



7

$C_{25}H_{63}NOSi_7$

590.38 g/mol

To a solution of silicon carbonyl complex **3** (100 mg, 199 µmol, 1.0 eq.) in *n*-hexane (3 mL) was added $TMSN_3$ (26.4 µL, 22.9 mg, 199 µmol, 1.0 eq.). Subsequently, the reaction mixture was stirred for 1 h, whereby a color change from purple to colorless was observed. Removal of all volatiles *in vacuo* provided crude silyl cyanide **7** as a colorless, waxy solid. Compound **7** is highly thermally (no sign of decomposition was observed upon heating **7** to 130 °C in C_6D_6) and photochemically stable and resistant to air and moisture. Silyl cyanide **7** is soluble in *n*-hexane, benzene, toluene, THF, Et_2O and CH_2Cl_2, but sparingly soluble in acetonitrile, ethanol, methanol and water.

Note: Compound **7** contains a minor by-product, most likely the isomeric silyl isocyanide ((TMS)$_3$Si)(^{t}Bu$_3$Si)Si(OTMS)(NC) (identified by IR, ^{13}C NMR and DFT calculations, *vide infra*). However, all further purification attempts *via* crystallization, distillation/sublimation, washing or flash chromatography were unsuccessful so far. In addition, the molecular structure of **7** could not be obtained by SC-XRD analysis because all grown "crystals" from a saturated acetonitrile solution did not diffract sufficiently.

m.p.: 132-133 °C.

^{1}H NMR (500 MHz, C_6D_6, 300 K): δ [ppm] = 1.29 (s, 27H, C(C*H*$_3$)$_3$), 0.45 (s, 27H, *TMS*), 0.31 (s, 9H, O*TMS*).

^{13}C{^{1}H} NMR (126 MHz, C_6D_6, 300 K): δ [ppm] = 131.4 (Si*C*N), 32.4 (C(*C*H$_3$)$_3$), 24.8 (*C*(CH$_3$)$_3$), 5.0 (*TMS*), 4.2 (O*TMS*).

^{29}Si{^{1}H} NMR (99 MHz, C_6D_6, 300 K): δ [ppm] = 14.4 (*Si*^{t}Bu$_3$), 11.9 (O*TMS*), –8.2 (*TMS*), –27.6 (*Si*CN), –111.6 (*Si*(TMS)$_3$).

IR (solid): $\tilde{\nu}$ [cm^{-1}] = 2952 (m), 2856 (m), 2129 (w) ($\tilde{\nu}_{NC}$), 1659 (w), 1477 (w), 1389 (w), 1245 (m), 1023 (m), 829 (s).

The observed NC stretching mode at $\tilde{\nu}$= 2129 cm^{-1} most likely originates from the presence of a minor amount of the corresponding silyl isocyanide isomer ((TMS)$_3$Si)(^{t}Bu$_3$Si)Si(OTMS)(NC). The respective CN stretching mode of silyl cyanide **7** is not observable (estimated low intensity); These observations are in good agreement with those for other silyl cyanides and the results of our DFT calculations (*vide infra*) (*4*).

Anal. Calcd. [%] for $C_{25}H_{63}NOSi_7$: C, 50.86; H, 10.76; N, 2.37. Found [%]: C, 50.72; H, 10.63; N, 2.68.

ESI-MS:	calculated for **7** ($C_{25}H_{63}NOSi_7$):	589.33
	calculated for [**7** – CN]$^+$ ($C_{24}H_{63}OSi_7$):	563.33
	observed:	563.33

Synthesis of ^{13}C-labeled Silyl Cyanide 7′



7'

$C_{24}{}^{13}CH_{63}NOSi_7$

591.37 g/mol

For additional characteristic analytical data, the ^{13}C-labeled isotopomer **7′** was synthesized using ((TMS)$_3$Si)(^{t}Bu$_3$Si)Si⇆^{13}CO (**3′**) and an equimolar amount of TMSN$_3$. Thus, crude silyl cyanide **7′** was afforded as a colorless, waxy solid using the above mentioned procedure. In the following only spectroscopic data with difference to the ^{12}C analogue are given.

^{13}C{^{1}H} NMR (126 MHz, C$_6$D$_6$, 300 K): δ [ppm] = 131.0 (Si*C*N), 32.1 (C(*C*H$_3$)$_3$), 24.4 (*C*(CH$_3$)$_3$), 4.6 (*TMS*), 3.9 (O*TMS*).

A strong resonance for the ^{13}C-labeled nucleus with ^{29}Si satellites ($^1J_{SiC}$ = 26.7 Hz) was clearly observed in the ^{13}C NMR spectrum. In addition, a weak resonance was found at δ = 195.6 ppm, which agrees well with the theoretically calculated shift for the corresponding isocyanide isomer (*vide infra*).

^{29}Si{^{1}H} NMR (99 MHz, C$_6$D$_6$, 300 K): δ [ppm] = 14.4 (d, $^2J_{CSi}$ = 6.0 Hz, *Si*^{t}Bu$_3$), 11.9 (O*TMS*), –8.2 (d, $^3J_{CSi}$ = 1.7 Hz, *TMS*), –27.7 (d, $^1J_{CSi}$ = 26.7 Hz, *Si*CN), –111.6 (d, $^2J_{CSi}$ = 5.6 Hz, *Si*(TMS)$_3$).

Doublet resonances for each ^{29}Si nucleus were observed in the ^{29}Si NMR spectrum due to coupling with the ^{13}C atom.

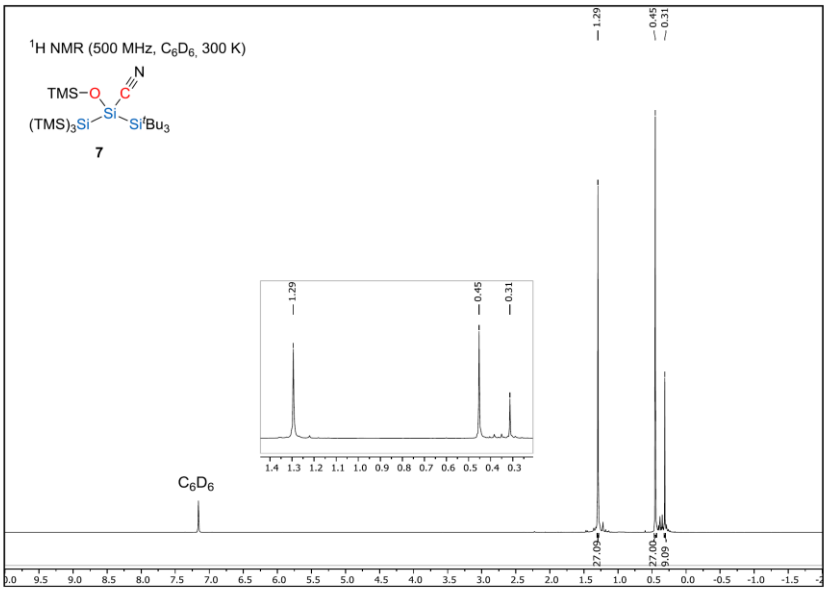


Figure S18. ^{1}H NMR spectrum of silyl cyanide **7** in C_6D_6 at 300 K.

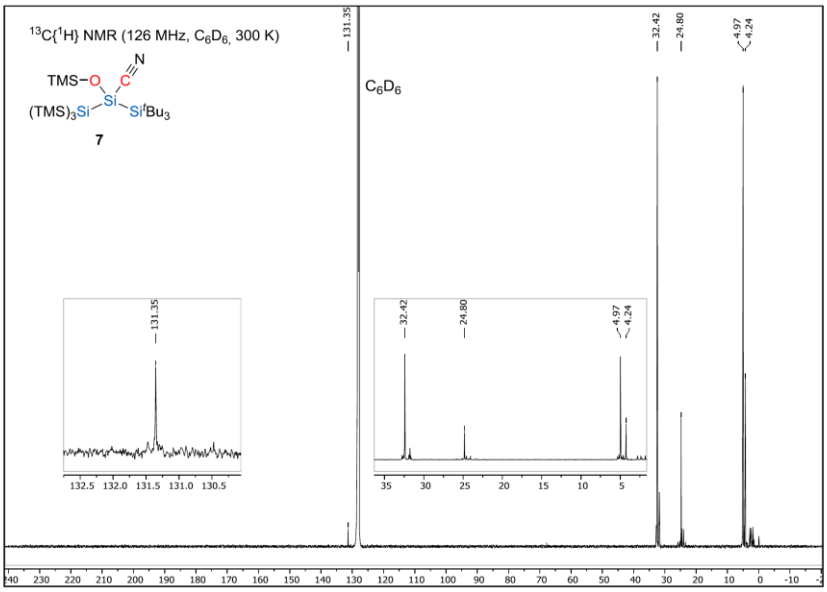


Figure S19. ^{13}C{^{1}H} NMR spectrum of silyl cyanide **7** in C_6D_6 at 300 K.

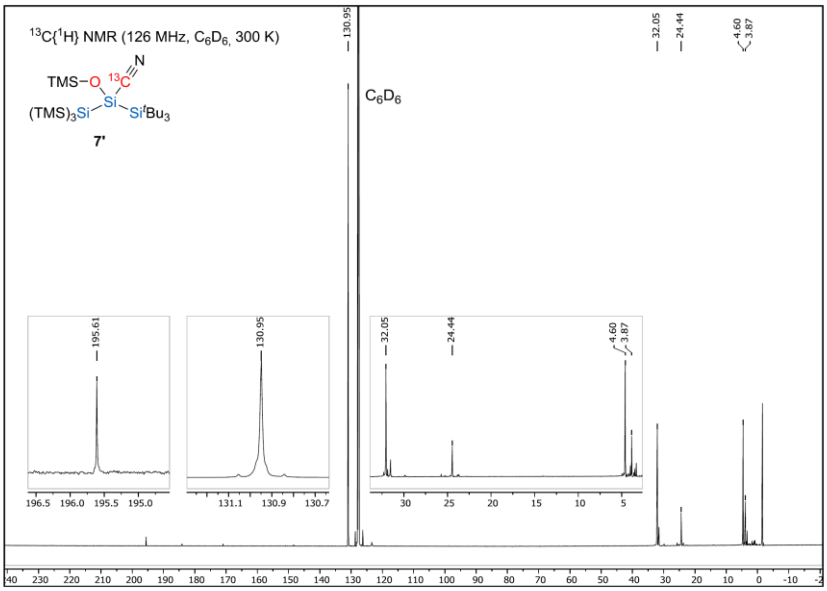


Figure S20. $^{13}C\{^1H\}$ NMR spectrum of ^{13}C-labeled silyl cyanide **7′** in C_6D_6 at 300 K.

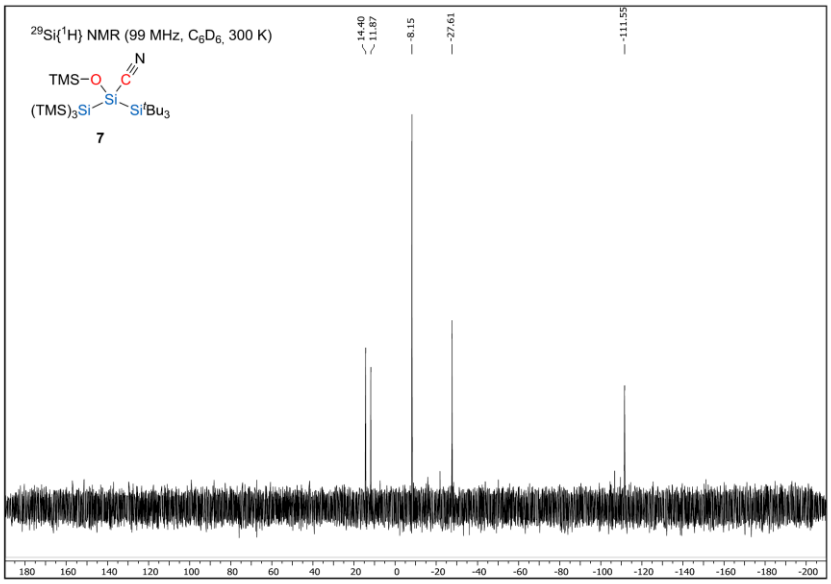


Figure S21. $^{29}Si\{^1H\}$ NMR spectrum of silyl cyanide **7** in C_6D_6 at 300 K.

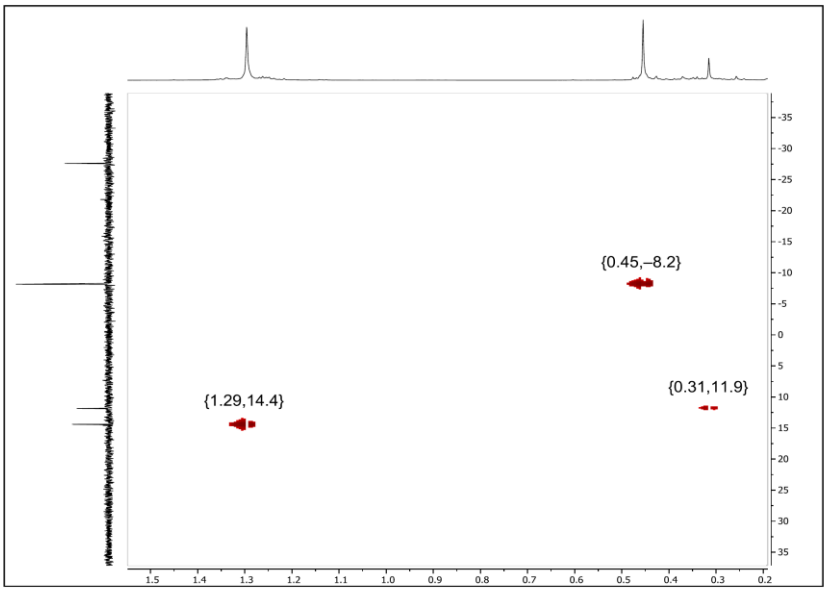


Figure S22. $^{1}H/^{29}Si$ HMBC NMR spectrum of silyl cyanide **7** in C_6D_6 at 300 K.

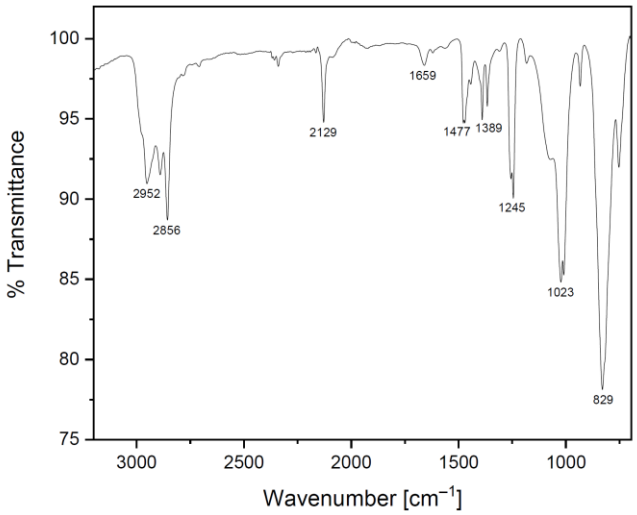


Figure S23. Solid-state FT-IR spectrum of silyl cyanide **7**.

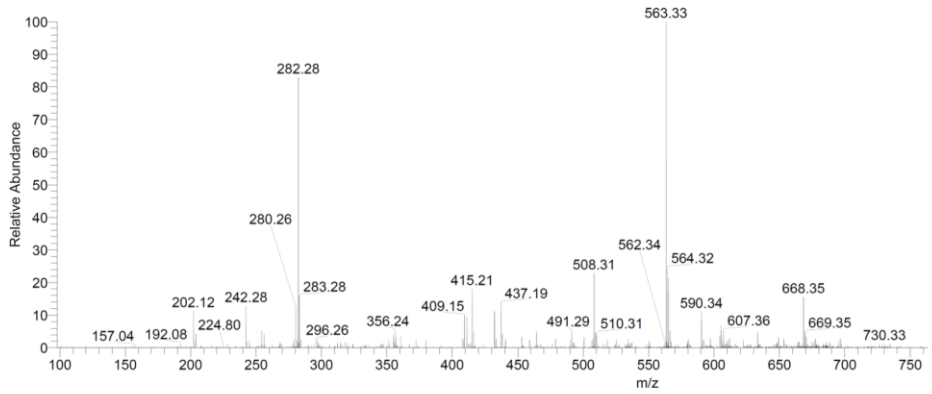


Figure S24. ESI-MS spectrometry of silyl cyanide **7** (acetonitrile solution). The observed peak at m/z = 563.33 corresponds to the $[\mathbf{7} - CN]^+$ fragment (calculated: m/z = 563.33).

1.8 Synthesis of (^{t}Bu$_3$Si)$_2$Si⇆CO (8)



8
$C_{25}H_{54}OSi_3$
454.96 g/mol



A thick-walled, pressurizeable Schlenk flask with a rubber septum, containing (^{t}Bu$_3$Si)$_2$SiBr$_2$ (2.00 g, 3.41 mmol, 1.0 eq.) and KC_8 (922 mg, 6.82 mmol, 2.0 eq.), was evacuated and subsequently exposed to CO (0.5 bar). The mixture was then cooled to –130 °C and precooled THF (25 mL, –80 °C) was added. As soon as the reaction mixture was frozen, the rubber septum was replaced by a PTFE-sealed screw cap and the Schlenk flask was filled with CO (1.5 bar). The reaction mixture was warmed to –80 °C and vigorously stirred for 6 h and then warmed to ambient temperature over a period of 16 h. Subsequently, all volatiles were removed *in vacuo* and the residue extracted with *n*-hexane (3 × 10 mL). Graphite and KBr were separated from the mixture by filtration. Removal of the solvent *in vacuo* provided a mixture of silicon carbonyl complex (^{t}Bu$_3$Si)$_2$Si⇆CO **8** (blue/purple) and 1,1-di-*tert*-butyl-4,4-dimethyl-2-(tri-*tert*-butylsilyl)-1,2-disiletane (analogous product to disiletane **4** (*vide supra*): formed *via* C–H bond activation of a *tert*-butyl group by the *in-situ* generated, extremely reactive, triplet ground state silylene (^{t}Bu$_3$Si)$_2$Si:) (*5*)). All attempts to purify the residue and isolate **8** *via* crystallization, washing, or sublimation were unsuccessful so far. Compound **8** is presumably even more thermally stable than ((TMS)$_3$Si)(^{t}Bu$_3$Si)Si⇆CO (**3**), since sublimation (130 °C / 5.0 × 10^{-3} mbar) did not lead to decomposition; however, neither to purification. Nevertheless, complex **8** was unambiguously characterized by multinuclear and 2D NMR spectroscopy (The detected resonances are in good agreement with those observed for complex **3**). In addition, photolysis of **8** resulted in an immediate

color change from purple to colorless with concomitant CO liberation and formation of the above mentioned disiletane by-product. In sharp contrast to ((TMS)$_3$Si)(^{t}Bu$_3$Si)Si⇆CO (**3**), the photodissociation of (^{t}Bu$_3$Si)$_2$Si⇆CO **8** is irreversible, as (^{t}Bu$_3$Si)$_2$Si: isomerizes extremely rapid.

^{1}H NMR (500 MHz, C$_6$D$_6$, 300 K): δ [ppm] = 1.30 (s, 54H, C(C*H*$_3$)$_3$).

^{13}C{^{1}H} NMR (126 MHz, C$_6$D$_6$, 300 K): δ [ppm] = 238.8 (*C*O), 32.2 (C(*C*H$_3$)$_3$), 26.4 (*C*(CH$_3$)$_3$).

^{29}Si{^{1}H} NMR (99 MHz, C$_6$D$_6$, 300 K): δ [ppm] = 46.5 (*Si*^{t}Bu$_3$), –232.1 (*Si*CO).

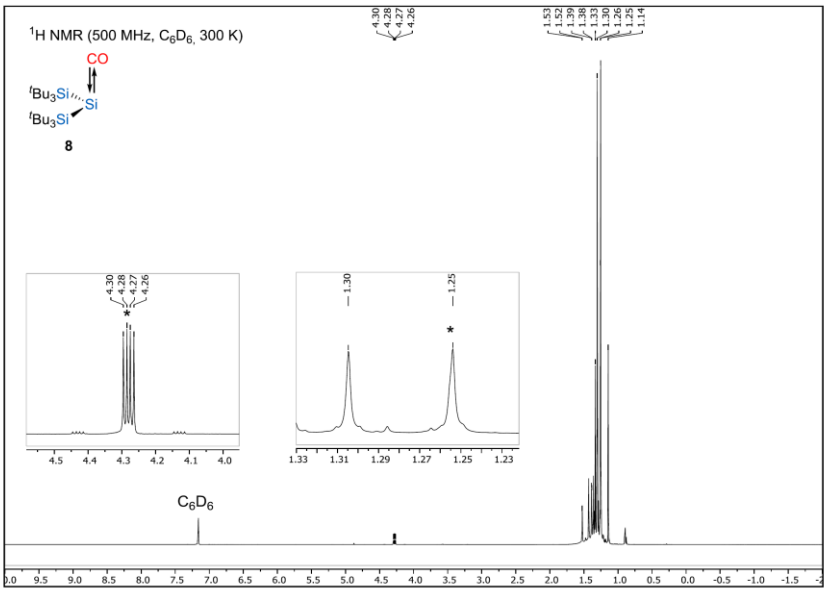


Figure S25. ^{1}H NMR spectrum of (^{t}Bu$_3$Si)$_2$Si⇆CO (**8**) in C$_6$D$_6$ at 300 K. Characteristic resonances of the disiletane by-product are marked with asterisks *.

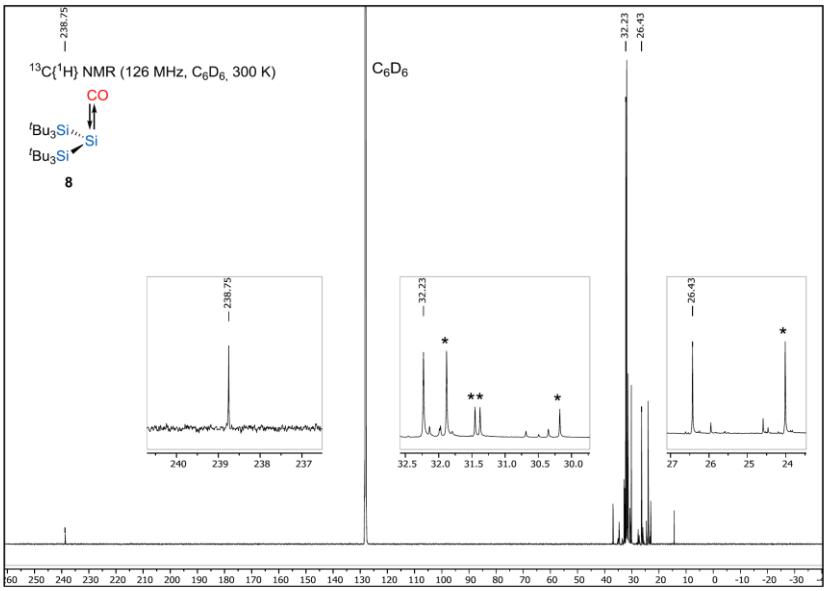


Figure S26. $^{13}C\{^1H\}$ NMR spectrum of (^{t}Bu$_3$Si)$_2$Si⇆CO (**8**) in C_6D_6 at 300 K. Characteristic resonances of the disiletane by-product are marked with asterisks *.

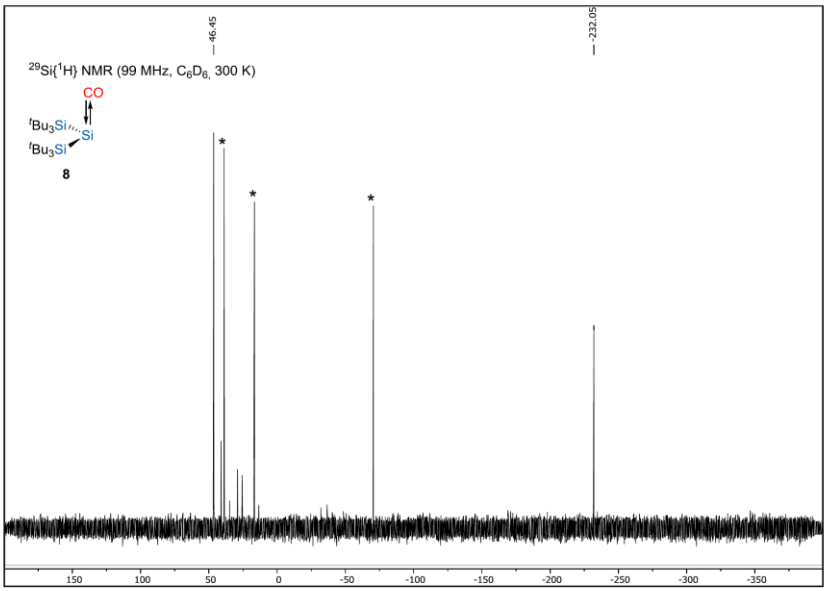


Figure S27. $^{29}Si\{^1H\}$ NMR spectrum of (^{t}Bu$_3$Si)$_2$Si⇆CO (**8**) in C_6D_6 at 300 K. The resonances of the disiletane by-product are marked with asterisks *.

Photolysis of (^{t}Bu$_3$Si)$_2$Si⇆CO (8) (Disiletane Formation)

A *J. Young* PTFE valve NMR tube was charged with a solution of crude (^{t}Bu$_3$Si)$_2$Si⇆CO (**8**) in C_6D_6 (0.5 mL). Irradiation of **8** (λ_{max} = 340 nm) resulted in an immediate color change from blue/purple to colorless with concomitant gas evolution (CO) and formation of 1,1-di-*tert*-butyl-4,4-dimethyl-2-(tri-*tert*-butylsilyl)-1,2-disiletane (*5*). Quantitative conversion was detected by ^{1}H NMR spectroscopy (*vide infra*).

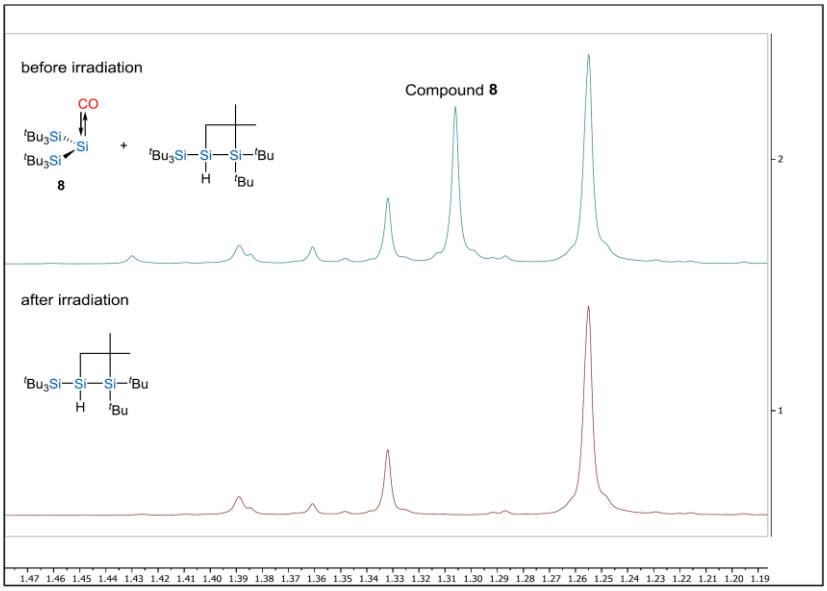


Figure S 28. Excerpt of the ^{1}H NMR spectra for the photolysis experiment of (^{t}Bu$_3$Si)$_2$Si⇆CO (**8**) in C_6D_6 at 300 K.

2. X-ray Crystallographic Data

General Information

The X-ray intensity data of **3** and **5** were collected on an X-ray single crystal diffractometer equipped with a CMOS detector (*Bruker Photon-100*), an IMS microsource with MoKα radiation (λ = 0.71073 Å) and a *Helios* mirror optic by using the *APEX III* software package (*6*). The measurements were performed on single crystals coated with the perfluorinated ether *Fomblin® Y*. The crystals were fixed on the top of a microsampler, transferred to the diffractometer and frozen under a stream of cold nitrogen. A matrix scan was used to determine the initial lattice parameters. Reflections were merged and corrected for Lorenz and polarization effects, scan speed, and background using *SAINT* (*7*). Absorption corrections, including odd and even ordered spherical harmonics were performed using *SADABS* (*7*). Space group assignments were based upon systematic absences, E statistics, and successful refinement of the structures. Structures were solved by direct methods with the aid of successive difference Fourier maps, and were refined against all data using the *APEX III* software in conjunction with *SHELXL-2014* (*8*) and *SHELXLE* (*9*). All H atoms were placed in calculated positions and refined using a riding model, with methylene and aromatic C–H distances of 0.99 and 0.95 Å, respectively, and $U_{iso}(H) = 1.2 \cdot U_{eq}(C)$. Full-matrix least-squares refinements were carried out by minimizing $\Delta w(F_o^2 – F_c^2)^2$ with *SHELXL-97* (*10*) weighting scheme. Neutral atom scattering factors for all atoms and anomalous dispersion corrections for the non-hydrogen atoms were taken from International Tables for Crystallography (*11*). The images of the crystal structures were generated by *Mercury* (*12*). The CCDC numbers CCDC-1976834 (**3**) and CCDC-1976835 (**5**) contain the supplementary crystallographic data for the structures. These data can be obtained free of charge from the *Cambridge Crystallographic Data Centre via* https://www.ccdc.cam.ac.uk/structures/.

Single Crystal X-ray Structure Determinations

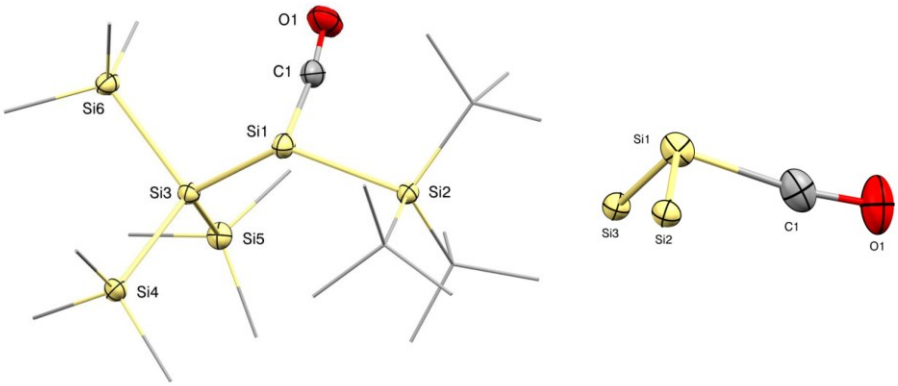


Figure S29. Molecular structure of **3** with ellipsoids set at 50% probability. Full view (left) and excerpt reflecting the trigonal pyramidal structure (right). Hydrogen atoms are omitted for clarity. Selected bond lengths [Å] and angles [°]: Si1–C1 1.794(2), C1–O1 1.153(2), Si1–Si2 2.398(1), Si1–Si3 2.382(1); Si2–Si1–Si3 132.4(1), Si2–Si1–C1 99.5(1), Si3–Si1–C1 90.9(1), Si1–C1–O1 171.3(1).

Table S1. Crystal data and structure refinement for compound **3**.

Chemical formula	$C_{22}H_{54}OSi_6$	
Formula weight	503.18 g/mol	
Temperature	100(2) K	
Wavelength	0.71073 Å	
Crystal size	0.221 × 0.283 × 0.297 mm	
Crystal habit	clear purple fragment	
Crystal system	orthorhombic	
Space group	P b c a	
Unit cell dimensions	a = 17.837(2) Å	α = 90°
	b = 17.019(2) Å	β = 90°
	c = 20.871(2) Å	γ = 90°
Volume	6335.8(12) $Å^3$	
Z	8	
Density (calculated)	1.055 g/cm^3	
Absorption coefficient	0.275 mm^{-1}	
F(000)	2224	
Diffractometer	Bruker D8 Venture Duo IMS	
Radiation source	IMS microsource, Mo	
Theta range for data collection	1.92 to 25.34°	
Index ranges	–21<=h<=21, –20<=k<=20, –25<=l<=25	
Reflections collected	200746	
Independent reflections	5811 [R(int) = 0.0501]	
Coverage of independent reflections	100.0%	
Absorption correction	Multi-Scan	
Refinement method	Full-matrix least-squares on F^2	
Refinement program	SHELXL-2016/6 (Sheldrick, 2016)	
Function minimized	$\Sigma\, w(F_o^2 - F_c^2)^2$	
Data / restraints / parameters	5811 / 0 / 280	
Goodness-of-fit on F^2	1.126	
Final R indices	5099 data; I>2σ(I)	R1 = 0.0273, wR2 = 0.0605
	all data	R1 = 0.0353, wR2 = 0.0680
Weighting scheme	$w = 1/[\sigma^2(F_o^2) + (0.0210P)^2 + 4.6359P]$	
	where $P = (F_o^2 + 2F_c^2)/3$	
Largest diff. peak and hole	0.272 and –0.221 $eÅ^{-3}$	
R.M.S. deviation from mean	0.044 $eÅ^{-3}$	

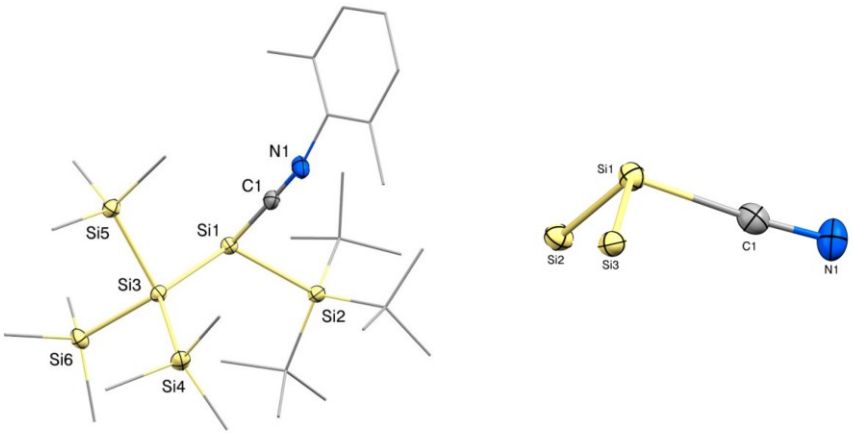


Figure S30. Molecular structure of **5** with ellipsoids set at 50% probability. Full view (left) and excerpt reflecting the trigonal pyramidal structure (right). Hydrogen atoms are omitted for clarity. Selected bond lengths [Å] and angles [°]: Si1–C1 1.819(2), C1–N1 1.177(2), N1–C2 1.400(2), Si1–Si2 2.406(1), Si1–Si3 2.380(1); Si2–Si1–Si3 125.5(1), Si2–Si1–C1 96.0(1), Si3–Si1–C1 99.5(1), Si1–C1–N1 174.0(1), C1–N1–C2 161.5(2).

Table S2. Crystal data and structure refinement for compound **5**.

Chemical formula	$C_{30}H_{63}NSi_6$	
Formula weight	606.35 g/mol	
Temperature	100(2) K	
Wavelength	0.71073 Å	
Crystal size	0.104 × 0.127 × 0.331 mm	
Crystal habit	clear intense blue fragment	
Crystal system	monoclinic	
Space group	P 21/c	
Unit cell dimensions	a = 19.5668(15) Å	α = 90°
	b = 8.9528(7) Å	β = 92.679(3)°
	c = 21.7330(17) Å	γ = 90°
Volume	3803.0(5) $Å^3$	
Z	4	
Density (calculated)	1.059 g/cm^3	
Absorption coefficient	0.238 mm^{-1}	
F(000)	1336	
Diffractometer	Bruker D8 Venture Duo IMS	
Radiation source	IMS microsource, Mo	
Theta range for data collection	2.08 to 25.35°	
Index ranges	–23<=h<=23, –10<=k<=10, –26<=l<=26	
Reflections collected	86591	
Independent reflections	6952 [R(int) = 0.0881]	
Coverage of independent reflections	100.0%	
Absorption correction	Multi-Scan	
Refinement method	Full-matrix least-squares on F^2	
Refinement program	SHELXL-2017/1 (Sheldrick, 2017)	
Function minimized	$\Sigma\, w(F_o^2 - F_c^2)^2$	
Data / restraints / parameters	6952 / 0 / 354	
Goodness-of-fit on F^2	1.054	
Final R indices	5880 data; I>2σ(I)	R1 = 0.0308, wR2 = 0.0708
	all data	R1 = 0.0414, wR2 = 0.0779
Weighting scheme	$w = 1/[\sigma^2(F_o^2) + (0.0245P)^2 + 2.3311P]$	
	where $P = (F_o^2 + 2F_c^2)/3$	
Largest diff. peak and hole	0.265 and –0.221 $eÅ^{-3}$	
R.M.S. deviation from mean	0.047 $eÅ^{-3}$	

3. DFT Calculations

General Information

Geometry optimizations and harmonic frequency calculations were performed using *Gaussian09* (*13*) employing the M06-2X/6-31+G(d,p) (*14-16*) level of density functional theory. The SMD polarizable continuum model was used to account for solvent effects of benzene (*17*). The "ultrafine" grid option was used for numerical integrations (*18*). Stationary points are characterized as minima by analysis of computed Hessians. The connectivity between minima and transition states was validated by IRC calculations (*19*) or displacing the geometry along the transition mode, followed by unconstrained optimization. For improved energies, single point calculations were conducted at the SMD-M06-2X/6-311+G(d,p) (*20, 21*) level of theory; wave functions used for bonding analysis were obtained at the M06-2X/6-311++G(2d,2p) level (*20, 21*). Natural Bond Orbital (NBO) and Natural Resonance Theory (NRT) analyses were performed using the *NBO 6.0* program (*22*), interfaced with *Gaussian09* (*23, 24*). The AIMAll (*25*) and multiwfn (*26, 27*) programs were used for QTAIM analyses (*28, 29*). NMR chemical shift values were calculated using the Gauge-Independent Atomic Orbital (GIAO) method implemented in *Gaussian09* and the M06-L(*30*) functional along with the 6-311G(2d,p) basis set and the SMD solvent model for the structures obtained at the M06-2X/6-31+G(d,p) level of theory. $^{13}C\{^{1}H\}$ and $^{29}Si\{^{1}H\}$ NMR spectroscopic chemical shifts δ are reported in ppm relative to tetramethylsilane ($\delta(^{13}C/^{29}Si(SiMe_4))$ = 0 ppm). Pictures of molecular structures were generated with the *ChemCraft* (*31*), *Cylview* (*32*) or *GaussView* (*33*) programs.

Comparison of Calculated and Experimental Structures

Table S3. Comparison of selected bond lengths [Å] and angles [°] for the computed and experimental structures of **3** and **5**. Geometries are calculated at the M06-2X/6-31+G(d,p) level of theory. Experimental data are taken from SC-XRD analyses; θ represents the angle between the Si2–Si1–Si3 plane and the Si1–C1 bond vector.

Compound	Bond/Angle	Exp.	Calc.	Δ(Calc.-Exp.)
3	Si1–C1	1.794(2)	1.82	0.03
	C1–O1	1.153(2)	1.15	0.00
	Si1–Si2	2.398(1)	2.40	0.00
	Si1–Si3	2.382(1)	2.40	0.02
	Si2–Si1–Si3	132.4(1)	125.0	7.4
	Si2–Si1–C1	99.5(1)	96.1	3.4
	Si3–Si1–C1	90.9(1)	91.5	0.6
	Si1–C1–O1	171.3(1)	172.0	0.7
	θ	103.7(1)	98.6	5.1
5	Si1–C1	1.819(2)	1.83	0.01
	C1–N1	1.177(2)	1.19	0.01
	N1–C2	1.400(2)	1.39	0.01
	Si1–Si2	2.406(1)	2.39	0.02
	Si1–Si3	2.380(1)	2.39	0.01
	Si2–Si1–Si3	125.5(1)	125.0	0.5
	Si2–Si1–C1	96.0(1)	95.0	1.0
	Si3–Si1–C1	99.5(1)	98.8	0.7
	Si1–C1–N1	174.0(1)	173.8	0.2
	C1–N1–C2	161.5(2)	155.3	6.2
	θ	107.3(1)	105.2	2.1

Calculated $^{29}Si\{^{1}H\}$ NMR Resonances

Table S4. Comparison of experimental and calculated NMR chemical shifts.

Compound	Si	Exp. δ(^{29}Si) [ppm]	Calc. δ(^{29}Si) [ppm]	Δδ [ppm]
3	*Si*^{t}Bu$_3$	42.8	37.2	5.6
	TMS	–6.9	–5.9	1.0
	Si(TMS)$_3$	–119.0	–126.9	7.9
	*Si*CO	–228.5	–238.3	9.8
5	*Si*^{t}Bu$_3$	37.6	29.2	8.4
	TMS	–8.1	–7.1	1.0
	Si(TMS)$_3$	–119.1	–127.2	8.1
	*Si*CN	–177.0	–187.9	10.9
7	*Si*^{t}Bu$_3$	14.4	8.1	6.3
	O*TMS*	11.9	9.2	2.7
	TMS	–8.2	–8.9	0.7
	*Si*CN	–27.6	–29.3	1.7
	Si(TMS)$_3$	–111.6	–117.3	5.7

Computed Ultraviolet-visible (UV-Vis) Spectroscopic Data

Table S5. Calculated transitions and UV-Vis absorption bands using TD-DFT (time-dependent-DFT).

Compound	Wavelength [nm]	MO contributions	f	Contribution
3	510.0	HOMO→LUMO	0.0042	94.2%
	351.1	HOMO→LUMO+1	0.0156	79.1%
		HOMO–1→LUMO		8.6%
5	556.7	HOMO→LUMO	0.0026	92.5%
	365.6	HOMO→LUMO+1	0.0834	81.1%
		HOMO–1→LUMO		5.7%

Bond Dissociation Energies for Lewis Base-Stabilized Silylenes ((TMS)$_3$Si)(^{t}Bu$_3$Si)Si(L)

Table S6. Calculated bond dissociation energies for donor-stabilized bis(silyl)silylenes ((TMS)$_3$Si)(^{t}Bu$_3$Si)Si(L). L = Lewis base; I^{i}Pr$_2$Me$_2$ = 1,3-diisopropyl-4,5-dimethylimidazolin-2-ylidene, IMe$_4$ = 1,3,4,5-tetramethylimidazolin-2-ylidene, CNXyl = 2,6-dimethylphenyl isocyanide.

L	ΔG_{298} [kcal/mol]*	$D^0(0)$ [kcal/mol]*	ΔG_{298}^{base} [kcal/mol]
DMAP (**2**)	15.3	33.5	0.0
I^{i}Pr$_2$Me$_2$	16.3	44.6	–1.0
CO (**3**)	21.2	29.8	–6.0
IMe$_4$	22.5	47.6	–7.3
CNXyl (**5**)	23.4	40.8	–8.2

* all dissociation energies are referenced to the singlet ground state of the donor-free silylene ((TMS)$_3$Si)(^{t}Bu$_3$Si)Si: (**1**); ΔG_{298}^{base} relative energy between all donor-stabilized silylenes, referenced to ((TMS)$_3$Si)(^{t}Bu$_3$Si)Si(DMAP) (**2**).

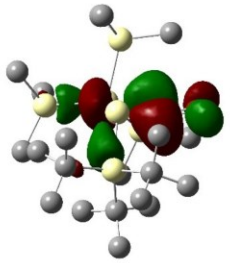
Calculated IR Stretching Frequencies

Table S7. Selected experimentally determined and theoretically calculated IR frequencies.

Compound	Mode	Exp. $\tilde{\nu}$ [cm^{-1}]	Calc. $\tilde{\nu}$ [cm^{-1}]
3	$^{12}C{\equiv}O$	1908	1949
	$^{13}C{\equiv}O$	1864	1902
	$\Delta^{12/13}$CO	44	47
5	$^{12}C{\equiv}N$	1966	1985

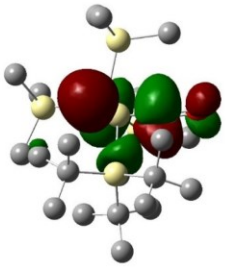
* calculated wavenumbers for the CO/CN stretching mode are scaled by a factor of 0.941/0.938, representing the ratio of the calculated stretching mode of free CO (2278 cm^{-1})/CNXyl (2260 cm^{-1}) to the experimental value (2143 cm^{-1}/2119 cm^{-1}) (*34*).

Frontier Orbitals of Silicon Carbonyl Complex ((TMS)$_3$Si)(^{t}Bu$_3$Si)Si⇆CO (3)



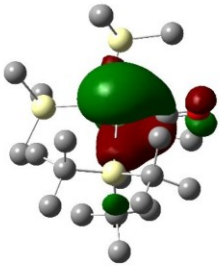
C1 (p) 0.49
Si3 (p) 0.28
O1 (p) 0.16
Si2 (s) –0.10
Si2 (p) 0.09
C3 (s) –0.09
Si5 (s) –0.07
C13 (s) –0.07
C10 (s) 0.07

LUMO (–0.71 eV)



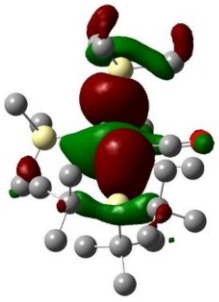
C8 (p) 0.32
Si3 (s) –0.27
Si1 (s) 0.26
Si5 (s) 0.22
Si3 (p) 0.20
C4 (s) –0.18
Si1 (p) 0.18
Si6 (s) 0.17
Si2 (p) 0.16…

LUMO+1 (–0.50 eV)



Si1 (p) 0.60
Si1 (s) –0.22
C1 (p) 0.14
Si2 (p) 0.13
O7 (p) 0.08
Si3 (p) 0.06

HOMO (–6.39 eV)



Si3 (p) 0.34
Si1 (p) 0.17
Si6 (p) 0.16
Si2 (p) 0.08

HOMO–1 (–7.60 eV)

Figure S31. Frontier orbitals (isovalue 0.04) of silicon carbonyl complex **3** including the corresponding orbital coefficients.

NBO Analysis of Silicon Carbonyl Complex ((TMS)$_3$Si)(^{t}Bu$_3$Si)Si⇆CO (3)

Table S8. Selected results of the NBO analysis of silicon carbonyl complex **3**.

Bond	NBO analysis (NLMOs)				
	NPA charge	Occupancy	Pol.	Hybr.	WBI
σ(Si1–C1)	–0.07 (Si1)	1.94	27% (Si1) 73% (C1)	$sp^{5.23}$ (Si1) $sp^{0.54}$ (C1)	1.31
π(Si1–C1)	0.43 (C1)	1.85	68% (Si1) 32% (C1)	$sp^{7.02}$ (Si1) $sp^{17.11}$ (C1)	1.31
σ(Si1–Si2)	1.83(Si2)	1.83	62% (Si1) 38% (Si2)	$sp^{1.41}$ (Si1) $sp^{3.37}$ (Si2)	0.83
σ(Si1–Si3)	–0.29(Si3)	1.87	49% (Si1) 51% (Si3)	$sp^{2.25}$ (Si1) $sp^{2.92}$ (Si3)	0.88
LP(O1)	–0.54 (O1)	1.97	–	$sp^{0.99}$ (O1)	–
LP(O1)	–	1.62	–	$sp^{99.99}$ (O1)	–
σ(C1–O1)	–	1.99	71% (O1) 29% (C1)	$sp^{1.04}$ (O1) $sp^{2.21}$ (C1)	1.99
π(C1–O1)	–	2.00	73% (O1) 27% (C1)	$sp^{90.98}$ (O1) $sp^{99.99}$ (C1)	1.99

Pol. = polarization, Hybr. = hybridization, WBI = Wiberg bond index.

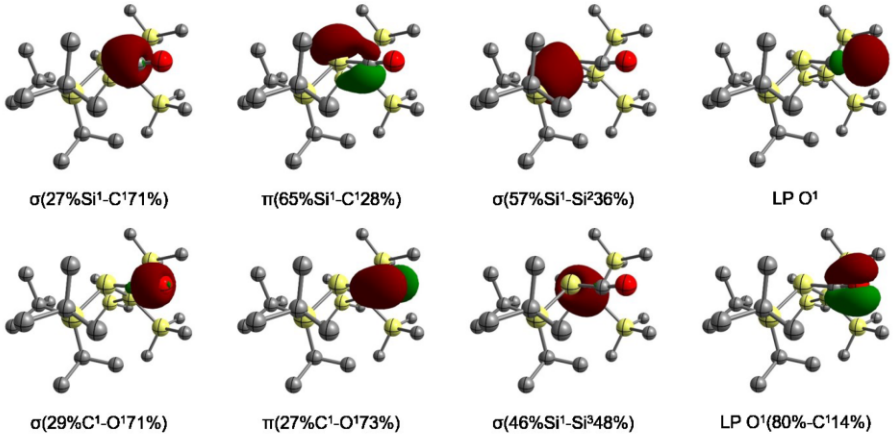


Figure S32. Selected natural localized molecular orbitals (NLMOs) of silicon carbonyl complex **3**.

Table S9. Fragment charges obtained from NPA analysis and results of NRT analysis of **3**.

Compound	Fragment charges			WBI			
	Central Si	R	R′	CO	Si–C	C–O	NRT[a]
3	–0.07	$(TMS)_3Si$ 0.00	$^tBu_3Si$ 0.18	–0.11	1.31	1.99	Si=C 54.0% Si–C 20.6%

[a]Only resonance structures that bear a weight higher than 1% are considered for NRT calculations. NRT analysis of **3** revealed 74 low-weighted resonance structures (<1%). Evaluation of all structures results in a SiC single/double/triple bond contribution of 43.2%/54.0%/2.8%.

Table S10. Selected results of the NBO second order perturbation theory analysis of silicon carbonyl complex **3**.

Donor NBO (Occupancy)	Acceptor NBO (Occupancy)	ΔE_{ij} [kcal/mol]
LP(O1) (1.62)	**π*(Si1–C1)** (0.39)	151
σ(Si1–Si2) (1.83)	**π*(Si1–C1)** (0.39)	10
σ(Si1–Si3) (1.87)	**π*(C1–O1)** (0.14)	18

Table 11. Selected results of the second order perturbation theory of silicon carbonyl complex **3**, for no bonds between the central silicon and carbon, as suggested by a referee during revision to estimate donation and backdonation.

Donor NBO (Occupancy)	Acceptor NBO (Occupancy)	ΔE_{ij} [kcal/mol]
LP Si1 (1.57)	**σ*(C1–O1)** (0.09)	15
LP Si1 (1.57)	**π*(C1–O1)** (0.39)	10
σ(Si1–Si2) (1.74)	**π*(C1–O1)** (0.39)	22
σ(Si1–Si2) (1.74)	**π*⊥(C1–O1)** (0.14)	7
σ(Si1–Si3) (1.83)	**π*(C1–O1)** (0.39)	5
σ(Si1–Si3) (1.83)	**π*⊥(C1–O1)** (0.14)	21
LP C1 (1.44)	**LV Si1** (0.53)	425

QTAIM Analysis of Silicon Carbonyl Complex ((TMS)$_3$Si)(^{t}Bu$_3$Si)Si⇆CO (3)

Table S12. Selected properties of the electron density distribution of the Si–O, C–O and Si–Si bonds in **3**: Bond path lengths d_{A-B}, and distances to bcps d_{A-bcp} and d_{bcp-B}, the electron density ρ_{bcp}, the Laplacian of the electron density $\nabla^2\rho_{bcp}$, the total energy density H_{bcp}, the bond ellipticity $\varepsilon_{bcp} = \lambda_1/\lambda_2 - 1$ (derived from the two negative eigenvalues of the Hessian matrix of the electron density at the bcp with $\lambda_1 \geq \lambda_2$), delocalization index $\delta_{A,B}$, atomic partial charges q_i from integration of the electron density over the corresponding atomic basins.

Bond	d_{A-B} [Å]	q_A[e]	q_B[e]	ρ_{bcp} [eÅ^{-3}]	$\nabla^2\rho_{bcp}$ [eÅ^{-5}]	H_{bcp} [E$_h$Å^{-3}]	ε_{bcp}	$\delta_{A,B}$	$\delta_{Si,O}$
Si1C1	1.83	0.36	0.54	0.68	8.81	–0.33	0.26	1.03	0.17
C1O1	1.15	0.54	–1.14	3.13	6.43	–5.74	0.00	1.56	-
Si1Si2	2.40	0.36	2.09	0.52	-2.19	–0.21	0.08	0.65	-
Si1Si3	2.40	0.36	–0.14	0.49	-1.79	–0.19	0.07	0.80	-

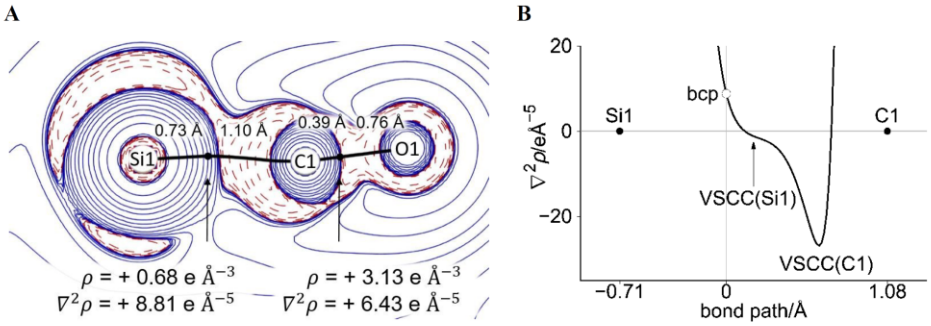


Figure S33. QTAIM Analysis of **3**. (**A**) 2D plot of $\nabla^2\rho$(r); charge concentration (red) and depletion (blue), bond paths (black lines) and bond-critical points (bcps; black dots) with characteristic properties of the Si1–C1 and C1–O1 bonds. (**B**) 1D Laplacian profile along the Si1–C1 bond path.

Calculations on Simplified Model Compounds (R)(R′)SiCO I–XI

Table S13. Comparison of calculated selected structural parameters of **3** and various related model compounds (R)(R′)Si(CO) **I-XI**. θ represents the angle between the R–Si–R′ plane and the Si–C bond vector.

Compound	R/ R′	d_{SiC} [Å]	d_{CO} [Å]	θ [°]	∠SiCO [°]	∠RSiR [°]
3	$(TMS)_3Si/^tBu_3Si$	1.82	1.15	98.6	172.0	125.0
I	TMS/TMS	1.82	1.15	81.5	177.8	100.3
IV	H_3Si/H_3Si	1.85	1.15	81.9	175.5	93.6
V	$H_2C{=}CH/H_3Si$	1.88	1.14	95.0	170.6	102.4
VI	^{t}Bu/^{t}Bu	1.89	1.14	104.0	165.4	114.1
VII	H_2B/H_2N	1.89	1.14	108.3	171.4	121.4
III	H/H	1.91	1.14	83.6	170.2	97.1
VIII	H_3C/H_3C	1.91	1.14	102.7	162.0	104.8
IX	$H_2C{=}N/H_3Si$	1.92	1.14	92.7	168.2	104.9
X	Ph/Ph	1.93	1.14	96.5	165.1	105.7
II	Ph/H_3C	1.93	1.14	99.3	163.5	105.7
XI	H_3Si/H_2N	2.00	1.14	100.2	162.6	102.2

Table S14. Comparison of calculated stabilization energies and IR stretching frequencies of **3** and various related model compounds (R)(R′)Si(CO) **I-XI**.

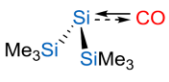
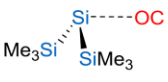
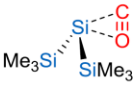
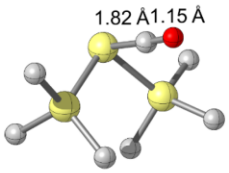
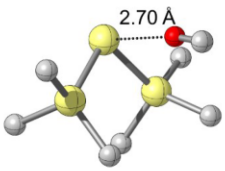
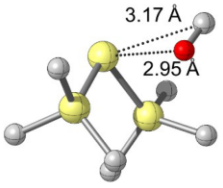
Compound	R/ R′	ΔG_{298}(A)[a]	$D^0(0)$[a]	ΔG_{298}(B)[b]	$\tilde{\nu}_{CO}$ [cm^{-1}][c]
3	$(TMS)_3Si/^tBu_3Si$	21.2	29.8	16.8	1949 (1908)
I	TMS/TMS	26.4	34.5	18.1	1967
IV	H_3Si/H_3Si	22.8	29.2	10.3	2009
III	H/H	15.2	22.2	1.1	2078 (2043 (*35*))
V	$H_2C{=}CH/H_3Si$	10.8	18.9	–1.7	2033
VI	^{t}Bu/^{t}Bu	7.4	15.5	–1.9	2008
VIII	H_3C/H_3C	3.0	11.6	–8.5	2027 (1962 (*36*))
X	Ph/Ph	3.0	10.6	–10.5	2056
II	Ph/H_3C	2.7	10.7	–9.4	2042 (1992 (*37*))
VII	H_2B/H_2N	1.5	9.5	–1.1	2031
XI	H_3Si/H_2N	–4.4	3.4	–18.2	2043
IX	$H_2C{=}N/H_3Si$	–7.4	0.5	–21.2	2058

[a]all dissociation energies of silicon carbonyl complexes **A** are referenced to the singlet ground state of the respective donor-free silylenes (R)(R′)Si:; [b]ΔG_{298}(B): energy for the silaketene transition state **B**; [c]scaled by a factor of 0.941 (experimental values); all calculated energy values are given in [kcal/mol].

Formation of other possible isomers of silicon carbonyl complexes (R)(R′)SiCO

In principle, other bonding modes between the CO ligand and the silylene moiety than *via* the carbon atom are conceivable, especially with regard to the high oxophilicity of silicon. However, no isomerization of silicon carbonyl complex ((TMS)$_3$Si)(^{t}Bu$_3$Si)Si⇆CO (**3**) or by-product formation was observed experimentally. To support this observation, further DFT calculations concerning the simplified model compound (TMS)$_2$SiCO (**I**) and its plausible isomers were performed. Accordingly, the (TMS)$_2$SiOC adduct (**Ia**) (binding *via* the oxygen atom of CO) is located 5.3 kcal/mol higher in energy than the donor-free silylene (TMS)$_2$Si: and free CO. We attribute the energetic discrimination to the charge distribution in the silylene: the free silylene has only a slight positive NPA charge in line with accumulation of charge at the silicon center. Hence, interaction with the negatively polarized oxygen is not favorable. These findings are in line with the results of earlier reports (*35, 36*). The potentially bridged species **Ib** is located even higher in energy (6.4 kcal/mol) and thus further supporting the explanation given before. On the other hand, bonding of the carbon monoxide *via* the carbon atom in silicon carbonyl complex (TMS)$_2$SiCO (**I**) is with an energy gain of 26.4 kcal/mol the most favorable isomer with respect to complex formation.

Table S15. Selected results for other plausible isomers of silicon carbonyl complex (TMS)$_2$SiCO (**I**).

Compound	I	Ia	Ib
			
Calc. Structure			
ΔG_{298}[a]	26.4	–5.3	–6.4

[a]referenced to the donor-free silylene TMS$_2$Si: and CO.

NBO Analysis of Simplified Model Compounds I–XI

Table S16. Fragment charges obtained from NPA analysis, WBIs and results of NRT analysis of all model compounds and CO.

Compound	Fragment charge				WBI		NRT[a]	
	Central Si	R	R′	CO	Si–C	C–O	Si=C	Si-C
I	–0.02	TMS 0.07	TMS 0.07	–0.12	1.23	2.02	30.7%	68.4%
IV	0.01	H_3Si 0.03	H_3Si 0.03	–0.07	1.14	2.09	28.4%	69.7%
V	0.37	H_2C=CH –0.37	H_3Si –0.02	0.01	1.06	2.15	21.9%	71.4%
VI	0.85	^{t}Bu –0.43	^{t}Bu –0.43	0.01	1.11	2.14	44.0%	45.9%
VII	0.73	H_2B –0.24	H_2N –0.49	0.00	1.02	2.15	38.9%	61.1%
III	0.23	H –0.15	H –0.15	0.07	1.05	2.17	36.3%	58.3%
VIII	0.75	H_3C –0.38	H_3C –0.38	0.02	1.05	2.16	21.2%	78.8%
X	0.80	Ph –0.44	Ph –0.43	0.07	0.97	2.19	29.6%	45.1%
II	0.78	Ph –0.44	H_3C –0.38	0.05	1.00	2.18	22.5%	68.8%
XI	0.58	H_3Si –0.08	H_2N –0.51	0.02	0.89	2.18	15.8%	74.0%
IX	0.56	H_2C=N –0.56	H_3Si –0.05	0.05	0.99	2.19	18.9%	73.4%
CO	–	C 0.51	O –0.51	–	–	2.25	–	–

[a]Only resonance structures that bear a weight higher than 1% are considered for NRT calculations.

Table S17. Selected results of the NBO analysis of silicon carbonyl complex **I**.

Bond	NBO analysis (NLMOs)				
	NPA charge	Occupancy	Pol.	Hybr.	WBI
LP Si1	–0.02 (Si1)	1.74	–	$sp^{0.33}$ (Si1)	–
Si1–C1	0.38 (C1)	1.96	25% (Si1) 75% (C1)	$sp^{8.86}$ (Si1) $sp^{0.46}$ (C1)	1.23
Si1–Si2	1.28 (Si2)	1.73	49% (Si1) 51% (Si2)	$sp^{12.72}$ (Si1) $sp^{2.70}$ (Si2)	0.80
Si1–Si3	1.28 (Si3)	1.75	50% (Si1) 50% (Si3)	$sp^{11.95}$ (Si1) $sp^{2.71}$ (Si3)	0.81
C1–O1	–0.50 (O1)	2.00	30% (C1) 70% (O1)	$sp^{2.02}$ (C1) $sp^{1.02}$ (O1)	2.02
C1–O1	–	2.00	26% (C1) 74% (O1)	$sp^{99.99}$ (C1) $sp^{99.99}$ (O1)	2.02
C1–O1	–	2.00	27% (C1) 73% (O1)	$sp^{99.99}$ (O1) $sp^{99.99}$ (C1)	2.02
LP O1	–	1.98	–	$sp^{0.99}$ (O1)	–

Pol. = polarization, Hybr. = hybridization, WBI = Wiberg bond index.

Table S18. Selected results of the second order perturbation theory analysis of silicon carbonyl complex **I**.

Donor NBO (Occupancy)	Acceptor NBO (Occupancy)	ΔE_{ij} [kcal/mol]
LP Si1 (1.74)	**σ*(C1–O1)** (0.03)	11
LP Si1 (1.74)	**π*(C1–O1)** (0.35)	8
σ(Si1–Si2) (1.73)	**π*(C1–O1)** (0.35)	10
σ(Si1–Si2) (1.73)	**π*⊥(C1–O1)** (0.22)	30
σ(Si1–Si3) (1.75)	**π*(C1–O1)** (0.35)	26
σ(Si1–Si3) (1.75)	**π*⊥(C1–O1)** (0.22)	11

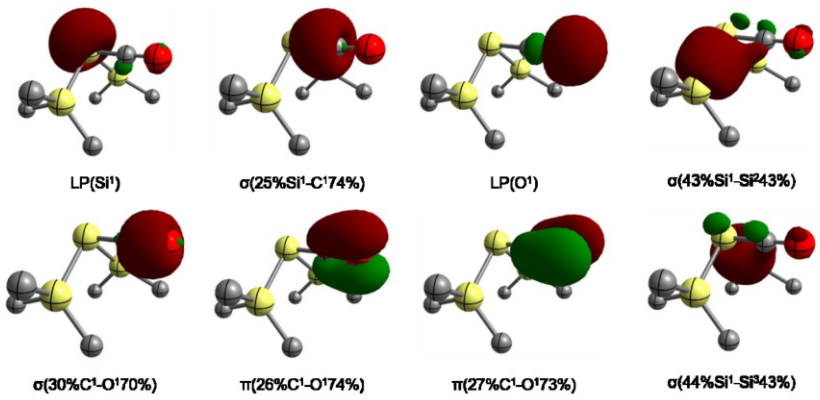


Figure S34. Selected NLMOs of silicon carbonyl complex **I**.

Table S19. Selected results of the NBO analysis of silicon carbonyl complex **II**.

Bond	NBO analysis (NLMOs)				
	NPA charge	Occupancy	Pol.	Hybr.	WBI
LP Si1	0.78 (Si1)	1.68	–	$sp^{0.63}$ (Si1)	–
Si1–C1	0.48 (C1)	1.97	21% (Si1) 79% (C1)	$sp^{12.39}$ (Si1) $sp^{0.48}$ (C1)	1.00
Si1–C2$_{Aryl}$	–0.47 (C2)	1.92	27% (Si1) 73% (C2)	$sp^{5.43}$ (Si1) $sp^{2.43}$ (C2)	0.76
Si1–C3$_{CH3}$	–1.07 (C3)	1.94	29% (Si1) 71% (C3)	$sp^{5.16}$ (Si1) $sp^{2.58}$ (C3)	0.81
C1–O1	–0.43 (O1)	2.00	30% (C1) 70% (O1)	$sp^{1.96}$ (C1) $sp^{1.11}$ (O1)	2.18
C1–O1	–	2.00	27% (C1) 73% (O1)	$sp^{99.99}$ (C1) $sp^{99.99}$ (O1)	2.18
C1–O1	–	2.00	25% (C1) 75% (O1)	$sp^{99.99}$ (O1) $sp^{99.99}$ (C1)	2.18
LP O1	–	1.98	–	$sp^{0.92}$ (O1)	–

Pol. = polarization, Hybr. = hybridization, WBI = Wiberg bond index.

Table S20. Selected results of the second order perturbation theory analysis of silicon carbonyl complex **II**.

Donor NBO (Occupancy)	Acceptor NBO (Occupancy)	ΔE_{ij} [kcal/mol]
LP Si1 (1.68)	**π*⊥(C1–O1)** (0.29)	29

QTAIM Analysis of Simplified Model Compounds I-III and Reference Compound H₃B⇆CO

Table S21. Selected results of QTAIM analyses of **I**, **II**, **III**, **VII**, **X**, **XI**, **CO** and **H₃B⇆CO**. Selected properties of the electron density distribution of the Si/B–C and C–O bonds: Bond path lengths $d_{A–B}$, and distances to bcps $d_{A–bcp}$ and $d_{bcp–B}$, the electron density ρ_{bcp}, the Laplacian of the electron density $\nabla^2\rho_{bcp}$, the total energy density H_{bcp}, the bond ellipticity $\varepsilon_{bcp} = \lambda_1/\lambda_2 - 1$ (derived from the two negative eigenvalues of the Hessian matrix of the electron density at the bcp with $\lambda_1 \geq \lambda_2$), delocalization index $\delta_{A,B}$, atomic partial charges q_i from integration of the electron density over the corresponding atomic basins.

Compound	Bond	$d_{A–B}$ [Å]	q_A [e]	q_B [e]	ρ_{bcp} [eÅ^{-3}]	$\nabla^2\rho_{bcp}$ [eÅ^{-5}]	H_{bcp} [E$_h$Å^{-3}]	ε_{bcp}	$\delta_{A,B}$	$\delta_{Si,O}$
I	SiC	1.82	0.34	0.56	0.67	9.24	–0.32	0.11	1.03	0.17
	CO	1.15	0.56	–1.14	3.14	6.47	–5.79	0.00	1.56	–
II	SiC	1.93	1.63	0.81	0.57	4.77	–0.28	0.47	0.70	0.13
	CO	1.14	0.81	–1.12	3.23	9.57	–6.00	0.00	1.65	–
IV	SiC	1.85	0.43	0.63	0.64	8.14	–0.31	0.11	0.95	0.15
	CO	1.15	0.63	–1.12	3.19	8.07	–5.91	0.00	1.60	–
III	SiC	1.91	1.49	0.83	0.57	5.88	–0.27	0.30	0.70	0.12
	CO	1.14	0.83	–1.12	3.26	10.16	–6.07	0.00	1.65	–
XI	SiC	2.00	1.12	0.86	0.50	2.65	–0.25	0.53	0.70	0.12
	CO	1.14	0.86	–1.13	3.24	9.92	–6.04	0.00	1.66	–
IX	SiC	1.92	1.13	0.80	0.58	5.30	–0.29	0.47	0.75	0.12
	CO	1.14	0.80	–1.11	3.24	10.28	–6.04	0.00	1.66	–
CO	CO	1.13	1.18	–1.18	3.31	10.76	–6.24	0.00	1.78	–
H₃B⇆CO	BC	1.55	1.73	0.95	0.91	11.09	–0.72	0.00	0.44	0.04
	CO	1.13	0.95	–1.13	3.30	10.08	–6.17	0.00	1.62	–

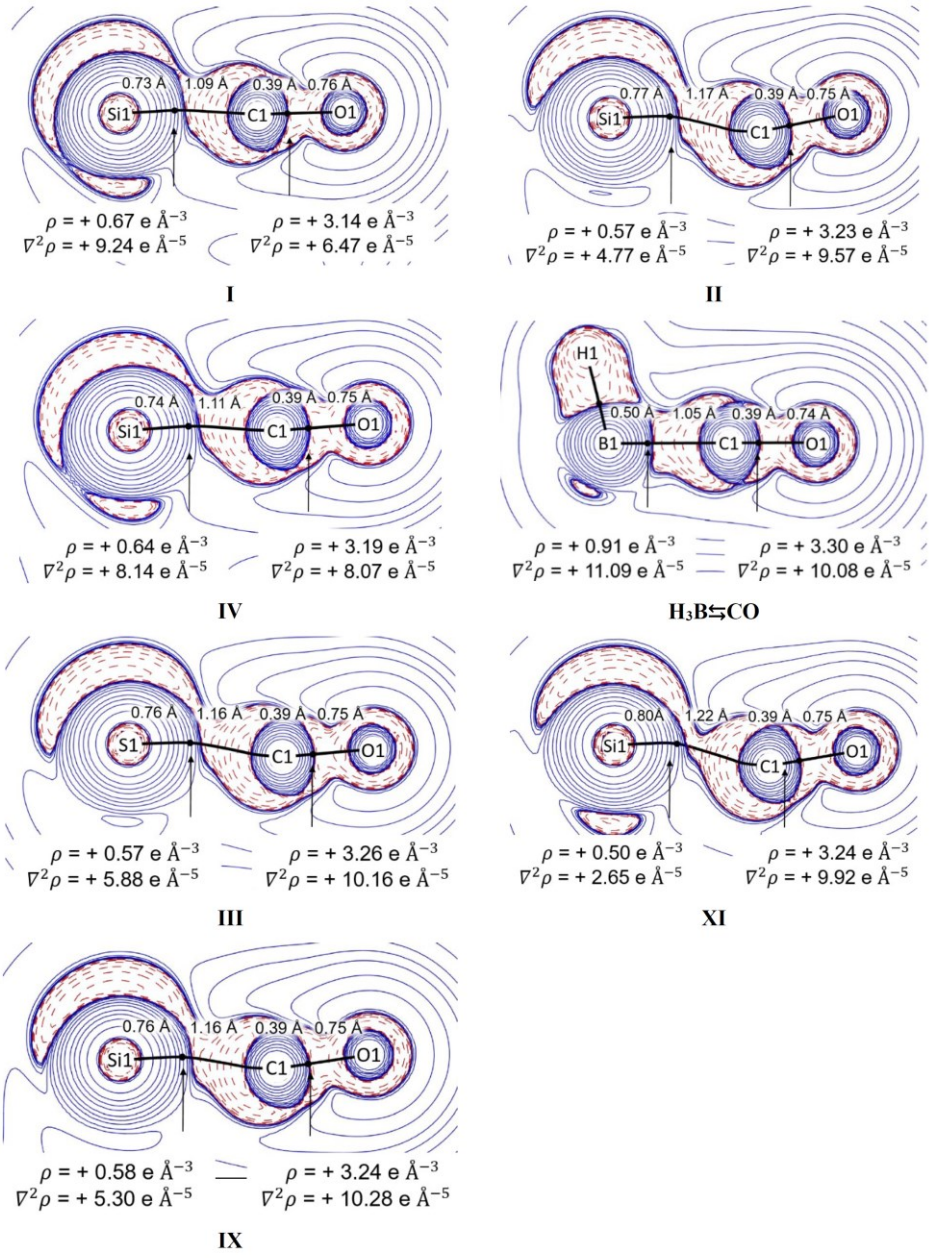
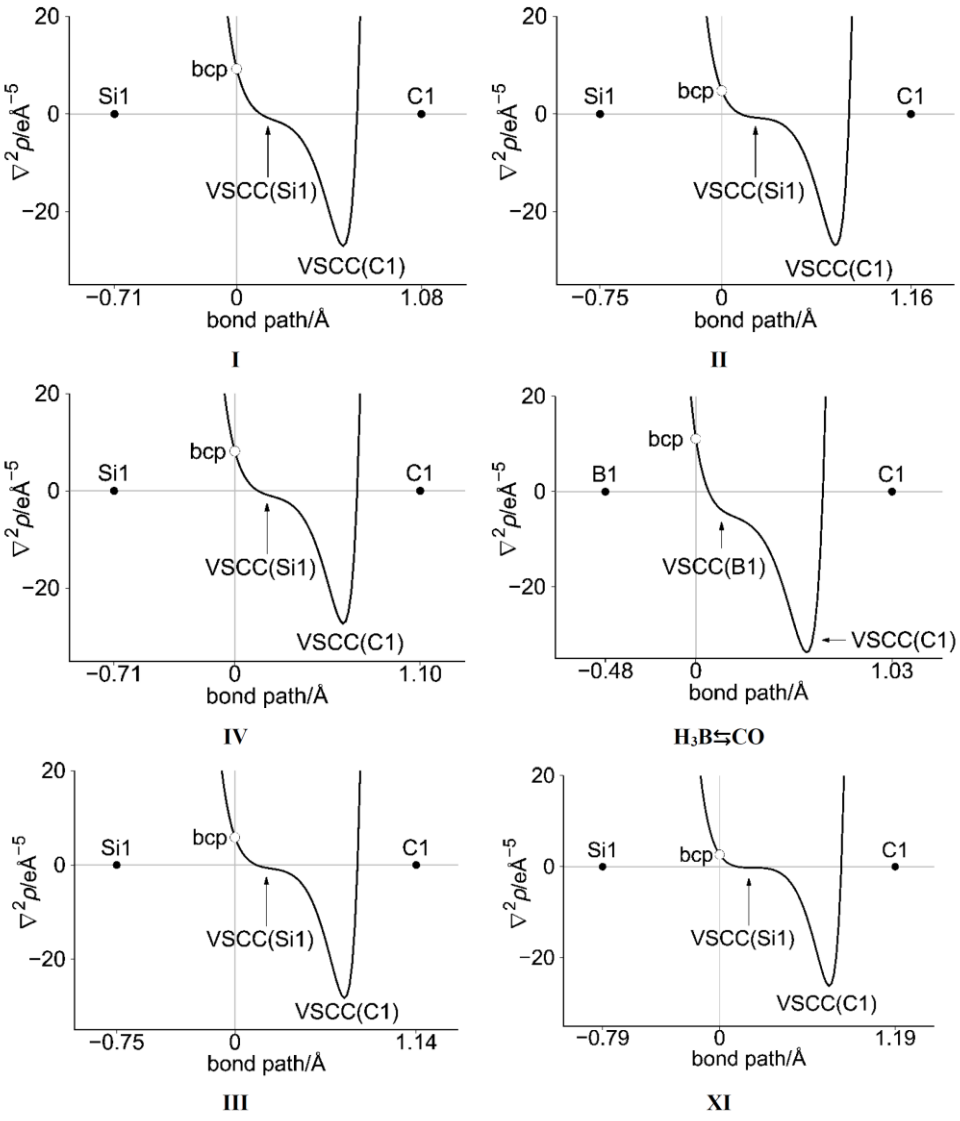
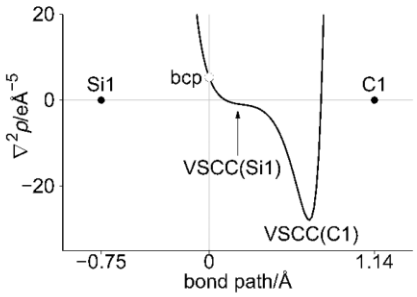


Figure S35. 2D plots of $\nabla^2\rho$(r); charge concentration (red) and depletion (blue), bond paths (black lines) and bond-critical points (bcps; black dots) with characteristic properties of the Si1–C1, C1–O1 and B1–O1 bonds for compounds **I–IV**, **IX**, **XI** and **H₃B⇆CO**.


20
0
−20
$\nabla^2\rho$/eÅ^{-5}
Si1
C1
bcp
VSCC(Si1)
VSCC(C1)
−0.71
0
1.08
bond path/Å
I
20
0
−20
$\nabla^2\rho$/eÅ^{-5}
Si1
C1
bcp
VSCC(Si1)
VSCC(C1)
−0.75
0
1.16
bond path/Å
II
20
0
−20
$\nabla^2\rho$/eÅ^{-5}
Si1
C1
bcp
VSCC(Si1)
VSCC(C1)
−0.71
0
1.10
bond path/Å
IV
20
0
−20
$\nabla^2\rho$/eÅ^{-5}
B1
C1
bcp
VSCC(B1)
VSCC(C1)
−0.48
0
1.03
bond path/Å
H3B⇆CO
20
0
−20
$\nabla^2\rho$/eÅ^{-5}
Si1
C1
bcp
VSCC(Si1)
VSCC(C1)
−0.75
0
1.14
bond path/Å
III
20
0
−20
$\nabla^2\rho$/eÅ^{-5}
Si1
C1
bcp
VSCC(Si1)
VSCC(C1)
−0.79
0
1.19
bond path/Å
XI



IX

Figure S36. 1D Laplacian profile along the Si1–C1 and B1–C1 bond paths for compounds **I–IV**, **IX**, **XI** and **$H_3B{\leftrightarrows}CO$**.

Frontier Orbitals of Silicon Isocyanide Complex ((TMS)$_3$Si)(^{t}Bu$_3$Si)Si⇆CNXyl (5)

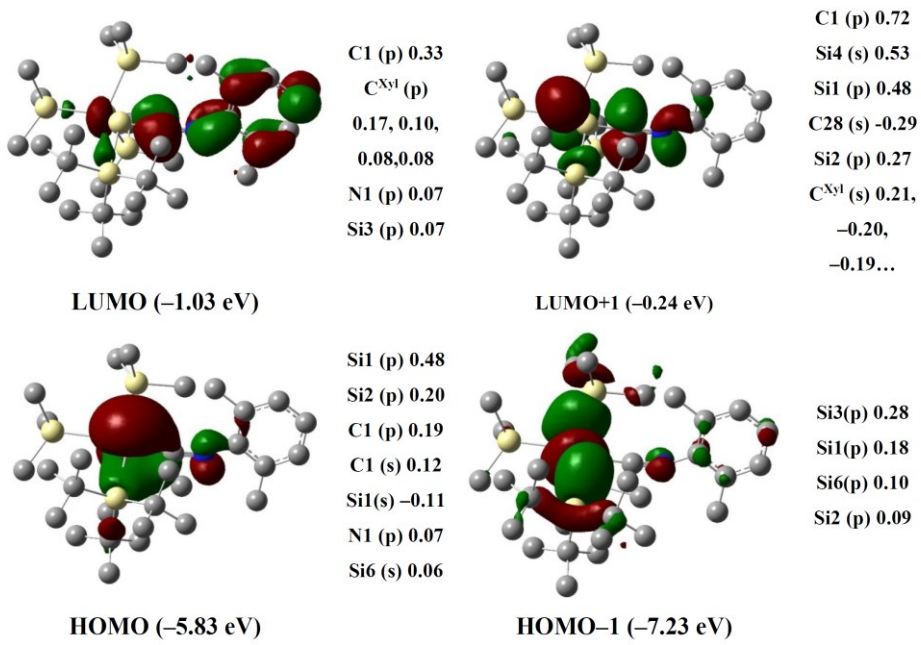


Figure S37. Frontier orbitals (isovalue 0.04) of silicon isocyanide complex **5** including the corresponding orbital coefficients.

NBO Analysis of Silicon Isocyanide Complex ((TMS)$_3$Si)(^{t}Bu$_3$Si)Si⇆CNXyl (5)

Table S22. Selected results of the NBO analysis of silicon isocyanide complex **5**.

Bond	NBO analysis (NLMOs)				
	NPA charge	Occupancy	Pol.	Hybr.	WBI
Si1–C1	–0.06 (Si1)	1.94	29% (Si1) 71% (C1)	$sp^{4.14}$ (Si1) $sp^{0.64}$ (C1)	1.30
Si1–C1	0.29 (C1)	1.85	69% (Si1) 31% (C1)	$sp^{7.04}$ (Si1) $sp^{24.47}$ (C1)	1.30
Si1–Si2	1.82 (Si2)	1.83	60% (Si1) 40% (Si2)	$sp^{1.52}$ (Si1) $sp^{3.01}$ (Si2)	0.85
Si1–Si3	–0.29 (Si3)	1.89	47% (Si1) 53% (C1)	$sp^{2.43}$ (Si1) $sp^{2.64}$ (Si3)	0.90
C1–N1	–0.60 (N1)	1.99	32% (C1) 68% (N1)	$sp^{1.79}$ (C1) $sp^{0.95}$ (N1)	2.00
C1–N1	–	1.95	32% (C1) 68% (N1)	$sp^{99.99}$ (C1) $sp^{99.99}$ (N1)	2.00
LP N1	–	1.58	–	$sp^{13.69}$ (N1)	–

Pol. = polarization, Hybr. = hybridization, WBI = Wiberg bond index.

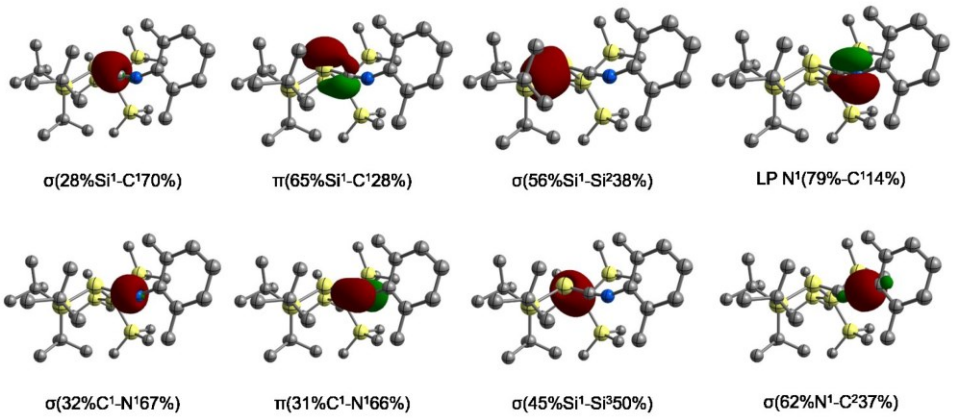


Figure S38. Selected NLMOs of silicon isocyanide complex **5**.

Table S23. Fragment charges obtained from NPA analysis and results of NRT analysis of silicon isocyanide complex **5** and **CNXyl**.

Compound	Fragment charges				WBI		
	Central Si	R	R′	CNXyl	Si–C	C–N	NRT[a]
5	–0.06	$(TMS)_3Si$ –0.05	$^tBu_3Si$ 0.15	–0.04	1.30	2.00	Si=C 77.0% Si–C 22.5%
CNXyl	–	C 0.30	N –0.56	0.27	–	2.34	–

[a]Only resonance structures that bear a weight higher than 1% are considered for NRT calculations.

Table S24. Selected results of the second order perturbation theory analysis of silicon isocyanide complex **5**.

Donor NBO (Occupancy)	Acceptor NBO (Occupancy)	ΔE_{ij} [kcal/mol]
LP N1 (1.58)	**π*(Si1–C1)** (0.41)	146
σ(Si1–Si2) (1.84)	**σ*(C1–N1)** (0.05)	11
σ(Si1–Si2) (1.84)	**π*(C1–N1)** (0.17)	10
σ(Si1–Si3) (1.89)	**π*(C1–N1)** (0.17)	13

QTAIM Analysis of 5 and Reference Compound $H_3B{\leftrightarrows}CNXyl$

Table S25. Selected properties of the electron density distribution of the Si/B–C, C–N and Si–Si bonds of **5**, **$H_3B{\leftrightarrows}CNXyl$** and **CNXyl**: Bond path lengths $d_{A–B}$, and distances to bcps $d_{A–bcp}$ and $d_{bcp–B}$, the electron density ρ_{bcp}, the Laplacian of the electron density $\nabla^2\rho_{bcp}$, the total energy density H_{bcp}, the bond ellipticity $\varepsilon_{bcp} = \lambda_1/\lambda_2 - 1$ (derived from the two negative eigenvalues of the Hessian matrix of the electron density at the bcp with $\lambda_1 \geq \lambda_2$), delocalization index $\delta_{A,B}$, atomic partial charges q_i from integration of the electron density over the corresponding atomic basins.

Compound	Bond	$d_{A–B}$ [Å]	q_A [e]	q_B [e]	ρ_{bcp} [eÅ^{-3}]	$\nabla^2\rho_{bcp}$ [eÅ^{-5}]	H_{bcp} [E_hÅ^{-3}]	ε_{bcp}	$\delta_{A,B}$	$\delta_{A,N}$
5	SiC	1.83	0.42	0.31	0.70	8.48	–0.35	0.25	0.97	0.15
	CN	1.19	0.31	–1.41	2.89	–8.51	–5.13	0.06	1.74	–
	Si1Si2	2.39	0.42	2.04	0.54	–2.34	–0.22	0.09	0.69	–
	Si1Si3	2.39	0.42	–1.14	0.51	–1.92	–0.20	0.09	0.83	–
$H_3B{\leftrightarrows}CNXyl$	BC	1.56	1.75	0.71	0.91	9.16	–0.74	0.00	0.44	0.03
	CN	1.16	0.71	–1.47	3.01	–2.77	–5.41	0.00	1.82	–
CNXyl	CN	1.17	0.89	–1.51	2.94	–3.86	–5.27	0.00	1.90	–

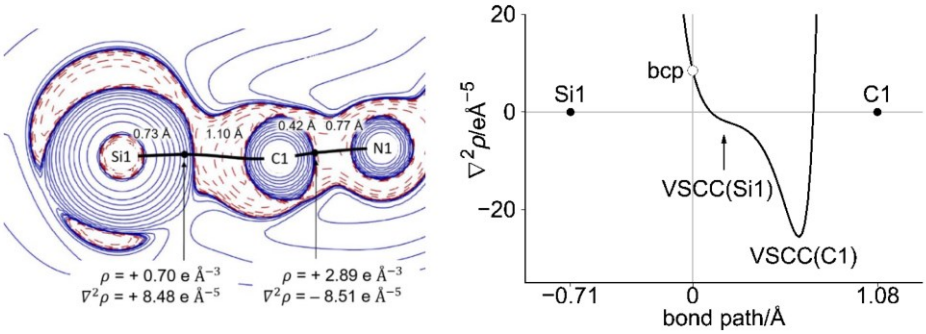


Figure S39. Left: 2D plot of $\nabla^2\rho$(r); charge concentration (red) and depletion (blue), bond paths (black lines) and bond-critical points (bcps; black dots) with characteristic properties of the corresponding Si–C and C–N bonds of **5**. **Right:** 1D Laplacian profile along the Si–C bond path of **5**.

Reactivity of ((TMS)$_3$Si)(^{t}Bu$_3$Si)Si⇆CO (3) toward TMSN$_3$

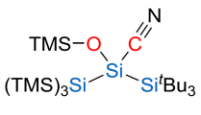
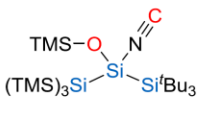
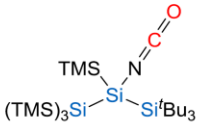
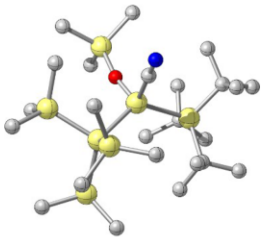
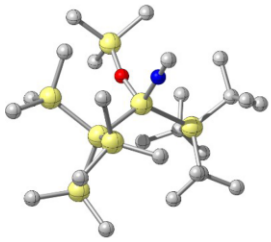
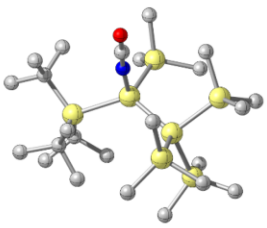
Since no molecular structure of the reaction product of **3** with TMSN$_3$ could be obtained, we calculated several different conceivable products based on the experimental data:

- Elemental analysis revealed a composition corresponding to the molecular formula $C_{25}H_{63}NOSi_7$ and thus verified the liberation of N_2 during the reaction.
- The observed main peak in the ESI-MS spectrum (m/z = 563.33) corresponds to the fragment [**7** – CN]$^+$ ($C_{24}H_{63}OSi_7$).
- ^{13}C NMR spectroscopy: δ [ppm] = 131.4 (Si*C*N), 4.2 (O*TMS*);
  Comparable cyanide shift reported for TMSCN: δ($^{13}C_{SiCN}$) = 127.3 ppm (*38*).
- Additional weak resonance for the ^{13}C-labeled isotopomer **7′** at δ = 195.6 ppm (SiN*C*).
- ^{29}Si NMR spectroscopy: δ [ppm] = 14.4 (*Si*^{t}Bu$_3$), 11.9 (N/O–*TMS*), –8.2 (*TMS*), –27.6 (*central Si*), –111.6 (*Si*(TMS)$_3$).

The three most relevant product isomers of this particular reaction with their calculated properties are given in Table S26. Silyl isocyanate **7b**, the analogue product for the reaction of transition metal carbonyl complexes with azides, exhibits calculated highfield-shifted resonances in the ^{29}Si NMR spectrum at δ = –10.4 (*additional TMS*) and –32.9 ppm (*central Si*) compared to the experimentally observed data. In particular, the significant difference for the additional TMS signal rather implies an O-bound TMS group present in the product. Moreover, the calculated IR spectrum shows an intense band for the NCO stretch at 2412 cm^{-1}, which does not match to the experimental spectrum. In contrast, the theoretically determined NMR resonances for silyl cyanide **7** match the experimental data perfectly (see also Table S4). The main peak obtained in the ESI-MS spectrum can also be clearly explained *via* dissociation of the CN moiety. Nevertheless, the calculated IR-active mode for compound **7** in the expected region (2300–2100 cm^{-1}) is only negligible. The isomeric product silyl isocyanide **7a** exhibits a N≡C stretching mode at 2206 cm^{-1}, which is in good agreement with the experimental spectrum. In addition, the weak resonance observed for the ^{13}C-labeled isotopomer at δ = 195.6 ppm in the ^{13}C NMR spectrum is in line with the calculated resonance for the SiN*C* moiety. In accordance with other silyl cyanides, we therefore conclude silyl cyanide **7** as the main product with a minor amount of silyl isocyanide **7a** as the by-product of the reaction of silicon carbonyl complex **3** with TMSN$_3$. Although **7a** is only 2.6 kcal/mol higher in energy compared to **7**, the interconversion of **7**/**7a** is associated with a

calculated barrier of 29.0 kcal/mol (**TS77a**). We thus do not assume an equilibrium of these two species, but two competing pathways for the formation of **7** and **7a**.

Table S26. Comparison of the calculated different conceivable isomers for the reaction product of silicon carbonyl complex ((TMS)$_3$Si)(^{t}Bu$_3$Si)Si⇆CO (**3**) with TMSN$_3$.

Compound	**7**	**7a**	**7b**
			
Calc. Structure			
ΔG_{298}[a]	–115.7	–113.2	–87.4
calculated ^{29}Si Shifts [ppm]			
central Si	–29.3	–15.6	–32.9
Si/O–*TMS*	9.2	8.8	–10.4
calculated ^{13}C Shifts [ppm]			
SiCN/SiNC	133.2	195.1	125.1
Si/O–*TMS*	5.5	5.4	6.8
IR [cm^{-1}]			
distinct IR modes	C≡N 2340 (negligible intensity)	N≡C 2206 (w)	N=C=O 2412(s)

[a] Gibbs free energies of formation are referenced to the energy of silylene carbonyl complex **3** and TMSN$_3$; all calculated energy values are given in [kcal/mol], frequencies are unscaled.

Calculated Energies

Table S27. Calculated Energies at the M06-2X/6-311+G(d,p)(SMD: benzene) level of density functional theory.

Structure	E(SCF) [H/particle]
$(TMS)_2Si{=}Si(TMS)(Si^tBu_3)$ (1′)	–2569.557739
$((TMS)_3Si)(^tBu_3Si)Si$: (1)	–2569.545564
$((TMS)_3Si)(^tBu_3Si)Si$(DMAP) (2)	–2951.797934
DMAP	–382.1979203
$((TMS)_3Si)(^tBu_3Si)Si{\leftrightarrows}CO$ (3)	–2682.906766
$((TMS)_3Si)(^tBu_3Si)Si{\leftrightarrows}CO$ ($TS3^B$)	–2682.898041
CO	–113.3053255
$((TMS)_3Si)(^tBu_3Si)Si{\leftrightarrows}CNXyl$ (5)	–2972.645396
CNXyl	–403.0346742
$((TMS)_3Si)(^tBu_3Si)Si(I^iPr_2Me_2)$	–3110.213262
$I^iPr_2Me_2$	–540.603328
$((TMS)_3Si)(^tBu_3Si)Si(IMe_4)$	–2952.995903
IMe_4	–383.381516
$((TMS)_3Si)(^tBu_3Si)Si(OTMS)(CN)$ 7	–3147.014008
$((TMS)_3Si)(^tBu_3Si)Si(OTMS)(NC)$ 7a	–3147.009726
$((TMS)_3Si)(^tBu_3Si)Si(TMS)(NCO)$ 7b	–3146.971391
$TMSN_3$	–573.4278384
N_2	–109.5164037
TS77a	–3146.968203

Cartesian Coordinates (x,y,z) for the Optimized Structures

1′

Si -0.08770 0.64733 0.13933
Si 0.05441 2.94401 0.72126
Si 1.89926 -0.25231 0.11257
Si 3.70451 0.97158 -0.76992
C 4.63637 -0.26330 -1.86929
H 5.43926 0.26401 -2.39860
H 5.09198 -1.08246 -1.30568
H 3.96886 -0.69765 -2.62089
C 4.95031 1.65459 0.47695
H 5.77891 2.13404 -0.05724
H 4.51187 2.38741 1.15789
H 5.36581 0.84072 1.07977
C 3.09422 2.30601 -1.96608
H 2.62370 1.81710 -2.82556
H 2.36102 2.99293 -1.53863
H 3.94254 2.89574 -2.33315
Si 2.63668 -2.42325 0.64743
C 4.31273 -2.13370 1.48480
H 4.20059 -1.49497 2.36726
H 4.72506 -3.09459 1.81470
H 5.04567 -1.66618 0.82144
C 2.89527 -3.56954 -0.83134
H 1.95242 -3.80486 -1.33256
H 3.56896 -3.11988 -1.56671
H 3.34373 -4.50999 -0.49048
C 1.56246 -3.27689 1.94466
H 1.34300 -2.59890 2.77545
H 0.61649 -3.64283 1.54104
H 2.11219 -4.13693 2.34511
C -0.43993 4.16826 -0.63587
H -1.51637 4.14952 -0.83212
H -0.17606 5.18107 -0.30936
H 0.07767 3.96977 -1.57952
C 1.80692 3.36720 1.29595
H 2.54267 3.39944 0.49145
H 1.77748 4.36168 1.75770
H 2.15103 2.65288 2.05057
C -0.98937 3.32947 2.25705
H -2.06677 3.21488 2.12510
H -0.68156 2.70598 3.10242
H -0.79549 4.37523 2.52582
Si -2.20021 -0.43239 -0.17257
C -3.28349 0.89551 -1.11408
C -2.93362 -0.87358 1.57770
C -1.97226 -2.02004 -1.28274
C -3.22953 -2.91046 -1.27991
H -3.08138 -3.74112 -1.98414
H -3.41758 -3.35223 -0.29697
H -4.13321 -2.37738 -1.58814
C -0.79515 -2.87773 -0.79879
H -0.94261 -3.26127 0.21071
H -0.67708 -3.74353 -1.46631
H 0.14207 -2.31257 -0.82508
C -1.65495 -1.63936 -2.73993
H -0.79105 -0.96813 -2.80862
H -1.41031 -2.55231 -3.30014
H -2.50219 -1.17034 -3.24615
C -4.44928 -1.14041 1.53955
H -4.72245 -1.92709 0.82977
H -4.78540 -1.46439 2.53450
H -5.02054 -0.24313 1.28370
C -2.23770 -2.12012 2.15170
H -2.49399 -3.03398 1.60862
H -1.14624 -2.01146 2.15518
H -2.55708 -2.26240 3.19327
C -2.67067 0.26122 2.58290
H -3.12542 1.20889 2.28805
H -3.09227 -0.01581 3.55918
H -1.59709 0.43019 2.72326
C -2.48995 1.56837 -2.25158
H -3.11196 2.35211 -2.70711
H -1.57505 2.04785 -1.89035
H -2.20631 0.87470 -3.04396
C -3.71242 2.02058 -0.15807
H -4.40016 1.67596 0.61896
H -2.85375 2.49052 0.33056
H -4.23071 2.80338 -0.72943
C -4.56227 0.29176 -1.72350
H -4.34466 -0.41206 -2.53142
H -5.18123 -0.22351 -0.98229
H -5.17042 1.09932 -2.15489

1

Si 2.47938 -0.05132 0.09767
Si 0.42074 -1.10324 0.75962
Si -1.55478 -0.04566 0.06096
Si -2.94912 -0.24307 1.96382
Si -2.21260 1.95823 -1.00816
Si -2.22928 -1.89831 -1.26928
C 2.80727 0.97019 1.73859
C 3.91811 2.02178 1.57850
H 4.86827 1.57014 1.27499
H 4.08636 2.52666 2.54080
H 3.66680 2.79437 0.84744
C 1.50688 1.67707 2.17466
H 0.72580 0.95142 2.45366
H 1.08530 2.33434 1.41048
H 1.69824 2.28305 3.07162
C 3.20643 0.05285 2.90944
H 4.17877 -0.42243 2.75740
H 2.46764 -0.73611 3.09200
H 3.27870 0.65516 3.82602
C 3.78726 -1.48657 -0.12196
C 3.54971 -2.64083 0.87102
H 4.33900 -3.39389 0.73635
H 2.58862 -3.13518 0.69764
H 3.57117 -2.32661 1.91621
C 5.23231 -0.98724 0.06139
H 5.47906 -0.15296 -0.60206
H 5.93268 -1.80447 -0.16282
H 5.43018 -0.66788 1.08887
C 3.67223 -2.10859 -1.52525
H 3.96736 -1.41966 -2.32074
H 2.65391 -2.45879 -1.73694
H 4.33537 -2.98250 -1.58842
C 2.42645 1.08725 -1.48022
C 3.81433 1.49185 -2.00356
H 4.38502 0.63699 -2.37642
H 4.41739 1.99235 -1.23859
H 3.69702 2.19342 -2.84173
C 1.63777 2.36559 -1.16848
H 2.14041 3.01886 -0.45023
H 0.64821 2.11880 -0.77358
H 1.49474 2.94638 -2.09153
C 1.65158 0.37898 -2.60673
H 1.58959 1.04140 -3.48262
H 0.62535 0.15488 -2.29203
H 2.11459 -0.55397 -2.93508
C -2.29183 -1.53901 3.17110
H -2.12853 -2.50562 2.68522
H -3.00878 -1.67751 3.98896
H -1.33548 -1.22687 3.60389
C -2.99476 1.42016 2.86982
H -1.98552 1.76146 3.12495
H -3.56423 1.32313 3.80146
H -3.47147 2.20005 2.26713
C -4.73158 -0.70596 1.52031
H -5.17259 -0.00783 0.80297
H -5.34586 -0.69008 2.42846
H -4.79544 -1.71211 1.09437
C -1.70329 2.03876 -2.82773
H -2.20471 2.88546 -3.31077
H -1.99436 1.12723 -3.36125
H -0.62520 2.16843 -2.94994
C -4.10732 2.01173 -0.95493
H -4.45378 2.87986 -1.52853
H -4.47422 2.12535 0.07034
H -4.56816 1.11753 -1.38418
C -1.64298 3.52568 -0.10748
H -1.76638 3.42641 0.97568
H -2.26537 4.36564 -0.43820
H -0.60056 3.78494 -0.30725
C -3.84763 -1.52991 -2.17571
H -3.74968 -0.67329 -2.85040
H -4.66232 -1.32188 -1.47497
H -4.13140 -2.40155 -2.77739
C -0.91686 -2.30331 -2.57414
H 0.05670 -2.52340 -2.11778
H -0.77368 -1.47478 -3.27531
H -1.22040 -3.18559 -3.14968
C -2.47492 -3.44739 -0.21379
H -2.77660 -4.28212 -0.85759
H -3.25249 -3.31079 0.54371
H -1.55071 -3.72727 0.30146

2

Si -0.37732 -0.40628 -1.18161
N 1.50459 -0.79129 -0.64954
C -3.16486 -2.31376 -1.20631
Si -1.58611 -2.17831 -0.04416
N 5.54426 -1.49442 0.17861
C -2.79235 -2.88347 -2.58758
H -3.66860 -2.81813 -3.24843
H -2.50211 -3.93688 -2.54503
H -1.98108 -2.31541 -3.05604
Si -0.39051 1.74944 -0.09233
C -3.73870 -0.90856 -1.46138
H -4.56248 -0.97165 -2.18726
H -2.99159 -0.22334 -1.88409
H -4.13982 -0.46179 -0.55199
Si -2.28698 3.03263 -0.68344
C -4.30349 -3.17573 -0.63249
H -5.12074 -3.23281 -1.36641
H -4.72499 -2.74925 0.28231
H -3.99085 -4.20029 -0.41172
Si 0.06316 2.43450 2.13937
C -0.56213 -3.85489 -0.14965
Si 1.33359 2.80799 -1.33490
C 0.23494 -3.94739 -1.46438
H -0.38290 -3.82594 -2.35569
H 0.71967 -4.93328 -1.52458
H 1.02764 -3.19649 -1.50399
C 6.46096 -1.81773 -0.90239
H 6.15930 -2.73891 -1.41325
H 7.45695 -1.96785 -0.48936
H 6.51067 -1.00614 -1.63753
C 1.99083 -0.71136 0.60490
H 1.27083 -0.45248 1.37047
C 3.30841 -0.94043 0.92919
H 3.60311 -0.84570 1.96623
C 4.23530 -1.27489 -0.08889
C 3.71385 -1.35691 -1.40392
H 4.34014 -1.60063 -2.25139
C 2.37717 -1.10875 -1.62695
H 1.95207 -1.16305 -2.62527
C 3.04392 2.47133 -0.57220
H 3.32878 1.42071 -0.69174
H 3.08174 2.71047 0.49599
H 3.80018 3.08150 -1.08091
C 1.18115 4.69387 -1.48921
H 2.05904 5.06814 -2.03004
H 1.13725 5.20331 -0.52280

H 0.29337 4.97598 -2.06475
C -1.46211 -5.10209 -0.06735
H -2.10968 -5.20063 -0.94241
H -2.09671 -5.10925 0.82342
H -0.83075 -6.00232 -0.02996
C 0.47081 -3.96341 0.98620
H 1.07964 -4.86703 0.83496
H 0.00622 -4.04911 1.97215
H 1.15700 -3.10967 1.00545
C -2.14723 -1.86161 1.80775
C -3.21612 -0.75674 1.85492
H -2.89181 0.14315 1.31634
H -3.39826 -0.46824 2.90090
H -4.17536 -1.07825 1.44090
C -0.96246 -1.32141 2.62387
H -0.10476 -2.00052 2.65176
H -1.27450 -1.13844 3.66335
H -0.63468 -0.36414 2.20734
C -2.70871 -3.09885 2.52879
H -3.54852 -3.55146 1.99346
H -3.07228 -2.80692 3.52509
H -1.95022 -3.87276 2.67801
C 6.03694 -1.36341 1.54063
H 5.54413 -2.07756 2.20971
H 5.87451 -0.34982 1.92462
H 7.10630 -1.56724 1.55143
C -3.94406 2.45817 0.03291
H -4.68716 3.24143 -0.16086
H -3.89525 2.30434 1.11581
H -4.30327 1.53655 -0.42788
C -2.43975 3.06856 -2.57034
H -2.44259 2.05681 -2.98956
H -1.60325 3.61306 -3.02168
H -3.36816 3.56925 -2.86870
C -2.14496 4.82489 -0.07313
H -1.21095 5.31365 -0.35880
H -2.23981 4.87709 1.01712
H -2.97438 5.40019 -0.50269
C -1.49876 2.42955 3.21118
H -2.26483 3.08715 2.78654
H -1.26181 2.79620 4.21706
H -1.93142 1.42935 3.30589
C 0.71454 4.21817 2.13098
H 1.69392 4.28558 1.64540
H 0.83118 4.55774 3.16751
H 0.03741 4.90959 1.62292
C 1.40835 1.48774 3.10211
H 1.12541 0.46519 3.37192
H 1.59274 2.03285 4.03586
H 2.35183 1.45826 2.54556
C 1.40779 2.17665 -3.11973
H 0.43495 2.25783 -3.61434
H 1.70287 1.12495 -3.16945
H 2.13744 2.76807 -3.68643

DMAP

C -1.95018 -1.12991 0.01301
C -0.56378 -1.19658 -0.02258
C 0.18286 0.00001 -0.05137
C -0.56379 1.19660 -0.02239
C -1.95019 1.12990 0.01318
N -2.66335 -0.00001 0.02958
H -2.52346 -2.05434 0.03259
H -0.08365 -2.16685 -0.02668
H -0.08368 2.16688 -0.02626
H -2.52348 2.05433 0.03294
N 1.55377 -0.00001 -0.10669
C 2.26982 1.25150 0.04183
H 1.99555 1.95367 -0.75240
H 2.07179 1.72990 1.01149
H 3.33969 1.06008 -0.03769
C 2.26981 -1.25150 0.04216
H 3.33970 -1.06012 -0.03722
H 2.07159 -1.72964 1.01189
H 1.99569 -1.95389 -0.75193

3

Si 0.43876 -0.37447 -1.11027
Si 2.56614 0.06429 -0.08460
Si -1.69039 0.01442 -0.08121
Si -2.30331 2.28634 0.10135
Si -2.32502 -1.05673 1.92156
Si -3.07535 -0.84659 -1.79686
O 0.31831 -3.28954 -0.56193
C 0.37733 -2.14338 -0.67761
C 3.00758 1.76797 -0.93662
C 4.18568 2.48744 -0.25392
C 1.80171 2.72360 -0.90295
C 3.35293 1.56840 -2.42323
C 2.45700 0.21892 1.85095
C 3.83877 0.30081 2.52449
C 1.65401 1.47153 2.23585
C 1.69210 -0.97604 2.44285
C 3.81409 -1.33819 -0.62474
C 5.26909 -0.83233 -0.56356
C 3.73193 -2.57697 0.28690
C 3.53614 -1.83102 -2.05861
C -2.33576 3.09289 -1.60815
C -4.05525 2.33682 0.82196
C -1.27878 3.36147 1.27140
C -1.85838 -0.02571 3.43848
C -1.62651 -2.80628 2.08007
C -4.21109 -1.24110 1.92202
C -4.86071 -0.22337 -1.69050
C -2.41161 -0.36367 -3.49930
C -3.11489 -2.73674 -1.69752
H 4.42991 3.39867 -0.81754
H 5.09126 1.87549 -0.21305
H 3.94033 2.79674 0.76663
H 2.06105 3.65614 -1.42304
H 1.50743 2.98673 0.11301
H 0.92611 2.30554 -1.41572
H 4.27887 1.00844 -2.57377
H 3.48913 2.55208 -2.89317
H 2.54862 1.05507 -2.96281
H 4.44877 1.12294 2.13822
H 4.41054 -0.62446 2.41129
H 3.70604 0.46854 3.60250
H 2.17955 2.40110 1.99848
H 1.47298 1.47050 3.32039
H 0.67549 1.49074 1.74001
H 2.16830 -1.93915 2.24712
H 0.67483 -1.01626 2.04369
H 1.61857 -0.85908 3.53367
H 5.47345 -0.05077 -1.29942
H 5.94798 -1.66820 -0.78269
H 5.53676 -0.44496 0.42489
H 4.06674 -2.37018 1.30675
H 4.39273 -3.35559 -0.11817
H 2.72587 -3.00307 0.33718
H 4.32246 -2.54107 -2.35009
H 3.52448 -1.02774 -2.79765
H 2.58103 -2.36065 -2.13258
H -1.37024 3.01337 -2.11800
H -2.58506 4.15631 -1.51759
H -3.09196 2.62387 -2.24651
H -4.42874 3.36664 0.77136
H -4.05053 2.03934 1.87614
H -4.76091 1.69422 0.28974
H -1.80633 4.31430 1.40078
H -0.28119 3.58277 0.88709
H -1.17273 2.90086 2.25892
H -2.39812 0.92770 3.43471
H -0.78778 0.19437 3.48139
H -2.13294 -0.56076 4.35500
H -0.53641 -2.83606 2.15487
H -1.91907 -3.42352 1.22423
H -2.03920 -3.26979 2.98403
H -4.54607 -1.91217 1.12417
H -4.72483 -0.28337 1.79736
H -4.53140 -1.67426 2.87707
H -4.92208 0.85235 -1.88552
H -5.31712 -0.42124 -0.71597
H -5.45986 -0.73388 -2.45372
H -1.45376 -0.85116 -3.70223
H -2.25755 0.71691 -3.58431
H -3.12618 -0.66785 -4.27307
H -2.11549 -3.17124 -1.80000
H -3.73610 -3.13558 -2.50793
H -3.53787 -3.08540 -0.74969

TS3^{B}

Si 0.39247 -0.62838 0.08547
Si 2.64437 0.06292 0.02379
Si -1.86130 -0.01698 -0.01027
Si -2.65345 -0.68507 -2.11385
Si -2.34836 2.27081 0.28637
Si -2.95167 -1.17296 1.72685
O 0.37044 -3.56283 0.07719
C 0.37352 -2.39904 0.08285
C 3.77725 -1.40337 -0.57476
C 5.17099 -0.86653 -0.96133
C 3.20698 -2.15203 -1.79454
C 3.97347 -2.44944 0.53773
C 2.66498 1.55993 -1.22294
C 3.89113 2.47118 -1.03289
C 2.65299 1.06988 -2.68155
C 1.39208 2.40866 -1.06141
C 3.06419 0.61633 1.84701
C 4.56802 0.87679 2.05384
C 2.29426 1.90266 2.19241
C 2.61527 -0.43105 2.88426
C -2.71644 -2.57194 -2.17786
C -4.39195 -0.00313 -2.42580
C -1.47564 -0.05676 -3.44915
C -2.15058 3.28494 -1.29750
C -1.38270 3.09539 1.68463
C -4.18840 2.34221 0.73191
C -4.80409 -1.28509 1.35193
C -2.30906 -2.93499 1.93133
C -2.67164 -0.25632 3.35679
H 5.82862 -1.71613 -1.19127
H 5.64486 -0.29552 -0.15739
H 5.13989 -0.23341 -1.85239
H 3.94130 -2.90247 -2.11841
H 3.00766 -1.49891 -2.64518
H 2.28189 -2.68346 -1.55966
H 4.54799 -2.05629 1.38084
H 4.53607 -3.30008 0.12987
H 3.02460 -2.84000 0.92116
H 4.83597 1.92562 -1.12201
H 3.88579 2.98003 -0.06493
H 3.88708 3.24926 -1.80866
H 3.57818 0.56354 -2.96771
H 2.53753 1.93649 -3.34701
H 1.81268 0.39348 -2.87408
H 1.25168 2.79860 -0.05058
H 0.50110 1.82895 -1.33187
H 1.43791 3.26910 -1.74423
H 5.15562 -0.04397 1.98939
H 4.72805 1.29041 3.05908
H 4.98036 1.59272 1.33627
H 2.61744 2.76742 1.60607
H 2.45708 2.14759 3.25083
H 1.21391 1.77098 2.05387
H 2.86843 -0.06328 3.88823
H 3.10113 -1.40016 2.75899
H 1.53334 -0.59276 2.84841
H -1.73493 -3.00757 -1.96246

H	-3.02602	-2.91306	-3.17219
H	-3.43077	-2.96976	-1.44896
H	-4.77934	-0.37779	-3.38009
H	-4.39393	1.09093	-2.47137
H	-5.08767	-0.30883	-1.63709
H	-1.85139	-0.30302	-4.44851
H	-0.49318	-0.52520	-3.32740
H	-1.34199	1.02920	-3.39297
H	-2.73241	2.85291	-2.11845
H	-1.11110	3.36623	-1.62445
H	-2.52845	4.29885	-1.12045
H	-0.35678	3.32866	1.38667
H	-1.34169	2.46334	2.57730
H	-1.87290	4.03717	1.95751
H	-4.39398	1.88675	1.70556
H	-4.80731	1.83738	-0.01743
H	-4.50631	3.39041	0.77881
H	-4.97881	-1.90456	0.46528
H	-5.26023	-0.30683	1.17599
H	-5.32542	-1.75631	2.19317
H	-1.27320	-2.94648	2.28373
H	-2.35462	-3.50541	0.99814
H	-2.92561	-3.45427	2.67453
H	-1.59896	-0.14383	3.55043
H	-3.10743	-0.81987	4.18946
H	-3.12176	0.74142	3.35305

CO

C	0.00000	0.00000	-0.64619
O	0.00000	0.00000	0.48465

5

Si	-0.17663	0.45763	-0.93545
Si	-0.14930	2.70348	-0.11632
Si	-1.50860	-1.30779	-0.04108
Si	-3.82170	-1.18969	-0.47376
Si	-1.24342	-2.04822	2.17825
Si	-0.73420	-3.09361	-1.38618
C	1.38524	-0.12890	-0.19408
C	-1.37154	3.59049	-1.36069
C	-1.80049	4.99411	-0.89656
C	-2.65064	2.75442	-1.54249
C	-0.73888	3.71143	-2.75872
C	-0.76341	2.84958	1.72717
C	-0.53664	4.24147	2.34287
C	-2.26394	2.52422	1.80748
C	-0.05441	1.80297	2.60256
C	1.66559	3.41459	-0.31167
C	1.65712	4.95350	-0.39464
C	2.57126	3.03313	0.87422
C	2.36080	2.87109	-1.57549
C	-4.13652	-1.14557	-2.33838
C	-4.63470	-2.74860	0.23597
C	-4.75619	0.23695	0.34441
C	-2.35931	-1.11093	3.38652
C	0.56411	-1.93862	2.72932
C	-1.72209	-3.87931	2.30004
C	-1.91832	-4.57200	-1.44877
C	-0.48488	-2.53203	-3.17555
C	0.91297	-3.75598	-0.71017
H	-2.43299	5.45543	-1.66823
H	-0.95212	5.66276	-0.72560
H	-2.39132	4.95763	0.02372
H	-3.29616	3.23131	-2.29348
H	-3.22642	2.67542	-0.62035
H	-2.43538	1.73971	-1.90088
H	0.11527	4.39272	-2.78245
H	-1.48854	4.10769	-3.45772
H	-0.41378	2.73702	-3.14136
H	-1.00632	5.04092	1.76175
H	0.52553	4.48109	2.44607
H	-0.97341	4.26829	3.35141
H	-2.88840	3.29356	1.34402
H	-2.56727	2.45422	2.86228
H	-2.49448	1.56096	1.33474
H	1.02996	1.93166	2.64205
H	-0.25766	0.79479	2.23179
H	-0.43373	1.86716	3.63296
H	1.17693	5.32073	-1.30509
H	2.69389	5.31880	-0.40575
H	1.15632	5.41666	0.46164
H	2.25974	3.50439	1.81018
H	3.59447	3.37507	0.66334
H	2.61329	1.95136	1.03159
H	3.32496	3.38362	-1.70268
H	1.78141	3.01894	-2.48886
H	2.57225	1.80097	-1.48670
H	-3.60539	-0.31889	-2.82118
H	-5.20717	-1.02793	-2.54094
H	-3.80555	-2.07690	-2.81031
H	-5.68116	-2.78441	-0.09009
H	-4.63156	-2.71984	1.33125
H	-4.14844	-3.67433	-0.08172
H	-5.83096	0.05746	0.21975
H	-4.52585	1.20731	-0.09931
H	-4.54829	0.29235	1.41811
H	-3.41291	-1.30203	3.15318
H	-2.19893	-0.02969	3.35347
H	-2.17741	-1.45259	4.41218
H	0.94256	-0.91285	2.72165
H	1.19815	-2.53261	2.06061
H	0.67054	-2.33848	3.74498
H	-1.04442	-4.51081	1.71659
H	-2.74207	-4.06646	1.95137
H	-1.65851	-4.20110	3.34650
H	-2.85874	-4.31308	-1.94650
H	-2.15427	-4.95865	-0.45253
H	-1.44979	-5.38055	-2.02254
H	0.20519	-1.68693	-3.25015
H	-1.43633	-2.21169	-3.61378
H	-0.09602	-3.36186	-3.77784
H	1.63279	-2.96490	-0.47797
H	1.37552	-4.42990	-1.44150
H	0.74904	-4.32786	0.20963
N	2.45029	-0.50881	0.16989
C	3.74114	-0.99940	0.00424
C	4.56760	-1.08725	1.13657
C	4.16820	-1.37933	-1.28313
C	5.86148	-1.57417	0.95547
C	5.46844	-1.86699	-1.41060
C	6.30888	-1.96380	-0.30439
H	6.52199	-1.64710	1.81438
H	5.82261	-2.16821	-2.39209
H	7.31907	-2.34184	-0.42579
C	4.06287	-0.67842	2.49337
H	3.56951	0.29737	2.45812
H	3.32699	-1.39768	2.86589
H	4.88697	-0.62686	3.20759
C	3.24920	-1.26260	-2.46619
H	2.35836	-1.88723	-2.33749
H	2.89366	-0.23566	-2.60097
H	3.75918	-1.57616	-3.37888

XylNC

C	0.23942	-1.23340	-0.00003
C	1.63381	-1.20818	-0.00013
C	2.32681	-0.00007	-0.00019
C	1.63389	1.20807	-0.00013
C	0.23949	1.23338	-0.00003
C	-0.42805	0.00001	0.00002
H	2.17749	-2.14829	-0.00017
H	3.41212	-0.00011	-0.00027
H	2.17762	2.14815	-0.00017
N	-1.81831	0.00006	0.00015
C	-2.99240	0.00009	0.00027
C	-0.53955	2.51907	0.00005
H	-1.18752	2.58401	-0.87976
H	-1.18740	2.58399	0.87994
H	0.13456	3.37756	0.00001
C	-0.53971	-2.51904	0.00004
H	-1.18757	-2.58391	0.87993
H	-1.18769	-2.58393	-0.87976
H	0.13434	-3.37757	0.00000

((TMS)$_3$Si)(^{t}Bu$_3$Si)Si(I^{i}Pr$_2$Me$_2$)

Si	1.67558	1.98198	0.06229
Si	0.34632	0.11555	-0.73843
Si	-1.94902	-0.06990	-0.12454
Si	-2.51620	-2.14518	-1.15790
Si	-3.12278	0.20229	1.95491
Si	-3.10835	1.41039	-1.58763
C	3.56432	1.46357	0.27663
C	4.41203	2.57761	0.92077
H	4.31064	3.53818	0.40961
H	5.47347	2.29189	0.87745
H	4.16438	2.72884	1.97507
C	3.75673	0.19926	1.13583
H	3.41939	-0.70255	0.61797
H	3.23561	0.25260	2.09409
H	4.82831	0.06882	1.34808
C	4.18672	1.15361	-1.09516
H	4.32855	2.05329	-1.69935
H	3.57463	0.45408	-1.67450
H	5.17804	0.69678	-0.95372
C	1.53756	3.24822	-1.44077
C	1.65854	2.56514	-2.81821
H	1.54143	3.32848	-3.60146
H	0.88891	1.80317	-2.96503
H	2.62811	2.08610	-2.97409
C	2.56970	4.39065	-1.41207
H	2.59150	4.92832	-0.46049
H	2.31988	5.12079	-2.19566
H	3.58305	4.03465	-1.62134
C	0.13487	3.87906	-1.40030
H	0.02424	4.60076	-0.58598
H	-0.64935	3.12118	-1.28980
H	-0.06092	4.41645	-2.33977
C	1.05532	2.86833	1.71130
C	1.58403	4.29855	1.92398
H	1.19030	4.99531	1.17873
H	2.67509	4.36114	1.90252
H	1.25326	4.66176	2.90826
C	1.47878	2.02887	2.92850
H	2.55855	2.05005	3.10085
H	1.17557	0.98256	2.82091
H	0.99418	2.42019	3.83493
C	-0.48033	2.94772	1.74887
H	-0.80762	3.29960	2.73843
H	-0.93858	1.97074	1.57275
H	-0.87889	3.64366	1.00895
C	-2.37038	-1.96749	-3.04273
H	-3.19461	-1.37737	-3.45514
H	-2.41052	-2.96319	-3.50147
H	-1.43379	-1.48460	-3.33635
C	-1.42529	-3.64297	-0.70156
H	-0.35310	-3.42869	-0.67495
H	-1.59093	-4.41881	-1.45981
H	-1.70873	-4.06858	0.26613
C	-4.28184	-2.75939	-0.82610
H	-4.37873	-3.17847	0.17964
H	-4.51267	-3.55586	-1.54438
H	-5.03491	-1.97471	-0.94019
C	-4.25101	1.72512	1.90399
H	-4.81230	1.76732	2.84568
H	-4.97336	1.69342	1.08308
H	-3.67304	2.65018	1.81376
C	-4.29547	-1.24934	2.30494

H	-4.79500	-1.07641	3.26598
H	-3.78832	-2.21788	2.35652
H	-5.06800	-1.31564	1.53249
C	-2.07918	0.47257	3.53786
H	-0.99862	0.39058	3.40347
H	-2.38435	-0.23372	4.31829
H	-2.27140	1.48330	3.91364
C	-4.86303	0.74389	-1.89144
H	-5.38755	0.52921	-0.95349
H	-4.86036	-0.17222	-2.48970
H	-5.44466	1.49758	-2.43577
C	-3.35107	3.19130	-0.95002
H	-2.64660	3.48333	-0.16837
H	-4.36180	3.32615	-0.55359
H	-3.22163	3.88497	-1.78930
C	-2.27930	1.58722	-3.28209
H	-2.97932	2.09489	-3.95782
H	-1.99991	0.63159	-3.72876
H	-1.37484	2.19855	-3.21576
C	1.21776	-1.50631	-0.02061
N	1.18146	-2.14637	1.17856
N	2.01261	-2.28830	-0.80907
C	2.45648	-3.40123	-0.11265
C	1.93160	-3.31235	1.14405
C	2.28088	-2.01708	-2.23990
H	1.95197	-0.98224	-2.37242
C	0.41861	-1.65626	2.33942
H	0.12658	-0.64805	2.03338
C	2.14595	-4.24347	2.29408
H	1.22127	-4.45902	2.83103
H	2.53741	-5.19190	1.92385
H	2.86866	-3.84071	3.00956
C	3.35815	-4.46164	-0.65764
H	3.34887	-5.32232	0.01222
H	3.03625	-4.80809	-1.64139
H	4.39144	-4.11375	-0.74023
C	3.76522	-2.11507	-2.59538
H	4.07411	-3.13694	-2.82714
H	3.94858	-1.50711	-3.48592
H	4.39681	-1.72709	-1.79104
C	1.39158	-2.89108	-3.11785
H	0.33968	-2.70443	-2.88894
H	1.56595	-2.64582	-4.16958
H	1.59490	-3.95706	-2.97656
C	1.26316	-1.56523	3.61103
H	0.77107	-0.87598	4.30405
H	1.35149	-2.52804	4.11902
H	2.26489	-1.18002	3.40284
C	-0.84765	-2.48182	2.54684
H	-1.36684	-2.13633	3.44437
H	-1.51759	-2.37030	1.69237
H	-0.62521	-3.54550	2.66943

((TMS)$_3$Si)(^{t}Bu$_3$Si)Si(IMe$_4$)

Si	-2.31866	-1.05271	0.01871
Si	-0.37642	0.10575	-0.83920
Si	1.81044	-0.37362	-0.02410
Si	3.04726	1.43252	-0.94156
Si	2.68830	-0.87365	2.14389
Si	2.50520	-2.15485	-1.43077
C	-3.84294	0.17586	0.23522
C	-5.06068	-0.51684	0.87888
H	-5.34311	-1.44108	0.36856
H	-5.92542	0.16159	0.83403
H	-4.89470	-0.75237	1.93360
C	-3.51689	1.41835	1.09142
H	-2.94540	2.15652	0.52288
H	-2.95987	1.19242	2.00450
H	-4.45710	1.90532	1.38849
C	-4.29727	0.71176	-1.13389
H	-4.76795	-0.06106	-1.74731
H	-3.46132	1.13215	-1.70501
H	-5.04003	1.50995	-0.98590
C	-2.69404	-2.29871	-1.46131
C	-2.54942	-1.64270	-2.84989
H	-2.78978	-2.39124	-3.61894
H	-1.53147	-1.28628	-3.02594
H	-3.22394	-0.79560	-2.99740
C	-4.09094	-2.94496	-1.41576
H	-4.32189	-3.41126	-0.45462
H	-4.15141	-3.72932	-2.18419
H	-4.88168	-2.22133	-1.63799
C	-1.64410	-3.42421	-1.41842
H	-1.80314	-4.11649	-0.58693
H	-0.62375	-3.02736	-1.34122
H	-1.69401	-4.01274	-2.34586
C	-2.07974	-2.08097	1.68394
C	-3.10859	-3.20597	1.90130
H	-3.01161	-4.00118	1.15732
H	-4.14206	-2.84944	1.88266
H	-2.93714	-3.66501	2.88611
C	-2.16896	-1.14010	2.89809
H	-3.17489	-0.73888	3.04690
H	-1.47850	-0.29481	2.81434
H	-1.90074	-1.69304	3.81011
C	-0.68531	-2.72934	1.72885
H	-0.50719	-3.16067	2.72549
H	0.10671	-2.00097	1.53193
H	-0.57990	-3.53789	1.00287
C	2.80084	1.49656	-2.82017
H	3.32037	0.67269	-3.32059
H	3.21056	2.43665	-3.20940
H	1.73978	1.43635	-3.08541
C	2.52563	3.14914	-0.30398
H	1.55174	3.45804	-0.69747
H	3.26921	3.88179	-0.64112
H	2.48684	3.19908	0.79022
C	4.92294	1.37336	-0.64569
H	5.18239	1.77210	0.33901
H	5.40880	2.00437	-1.40017
H	5.34483	0.36839	-0.72619
C	3.13914	-2.70993	2.25193
H	3.55017	-2.92359	3.24584
H	3.89814	-2.97803	1.50987
H	2.26980	-3.35638	2.09451
C	4.28759	0.08879	2.47677
H	4.65622	-0.16039	3.47919
H	4.12786	1.17225	2.43565
H	5.07016	-0.16297	1.75490
C	1.59799	-0.53321	3.66596
H	0.58016	-0.92136	3.57463
H	1.54523	0.53169	3.91336
H	2.06753	-1.03871	4.51862
C	4.38397	-2.11104	-1.70018
H	4.93410	-2.08931	-0.75249
H	4.68709	-1.23738	-2.28670
H	4.69457	-3.00816	-2.24887
C	2.11100	-3.90132	-0.79057
H	1.18671	-3.95182	-0.20947
H	2.92018	-4.28798	-0.16483
H	2.00102	-4.57127	-1.65189
C	1.69589	-2.02048	-3.13800
H	2.20745	-2.70166	-3.82954
H	1.74039	-1.00769	-3.54605
H	0.64061	-2.30733	-3.09743
C	-0.62748	1.94687	-0.23820
N	-0.40163	2.57669	0.94084
N	-1.05989	2.93873	-1.06526
C	-1.11759	4.15771	-0.40759
C	-0.69171	3.92716	0.86599
C	-1.38434	2.79684	-2.47882
H	-1.17846	1.76421	-2.76854
C	0.07546	1.93411	2.14826
H	0.09021	0.86059	1.97077
C	-0.49916	4.84752	2.02160
H	0.54359	4.84249	2.35593
H	-0.75544	5.86861	1.73588
H	-1.12994	4.56547	2.87044
C	-1.55780	5.41110	-1.08327
H	-1.56535	6.23658	-0.37018
H	-0.88631	5.68142	-1.90444
H	-2.56793	5.30923	-1.49184
H	-2.43844	3.03103	-2.64701
H	-0.75911	3.47627	-3.06401
H	-0.59042	2.16451	2.98490
H	1.09075	2.27204	2.38013

I^{i}Pr$_2$Me$_2$

C	0.00002	-1.23722	-0.32495
N	1.06479	-0.40314	-0.16304
N	-1.06478	-0.40314	-0.16324
C	0.68163	0.91113	0.10850
C	-0.68168	0.91114	0.10827
C	2.42663	-0.94655	-0.20393
H	2.27099	-1.95910	-0.58512
C	3.02439	-1.05210	1.19835
H	2.35951	-1.62855	1.84644
H	3.17900	-0.06692	1.64869
H	3.99463	-1.55626	1.15404
C	3.33721	-0.20100	-1.17853
H	2.83105	-0.04209	-2.13475
H	4.23545	-0.79808	-1.36027
H	3.66113	0.76643	-0.78623
C	1.61154	2.06769	0.29230
H	2.05181	2.39358	-0.65566
H	2.42988	1.83461	0.97820
H	1.06627	2.91582	0.71146
C	-1.61162	2.06769	0.29187
H	-2.05284	2.39261	-0.65597
H	-1.06603	2.91633	0.70958
H	-2.42925	1.83515	0.97882
C	-2.42661	-0.94662	-0.20390
H	-2.27102	-1.95916	-0.58513
C	-3.02400	-1.05217	1.19852
H	-3.17850	-0.06697	1.64886
H	-2.35896	-1.62864	1.84642
H	-3.99427	-1.55632	1.15447
C	-3.33752	-0.20107	-1.17817
H	-4.23550	-0.79848	-1.36011
H	-2.83149	-0.04152	-2.13434
H	-3.66191	0.76603	-0.78541

IMe$_4$

C	-0.00001	1.56948	-0.00008
N	-1.05666	0.70877	-0.00007
N	1.05666	0.70879	-0.00004
C	-0.67982	-0.63285	-0.00001
C	0.67984	-0.63285	-0.00002
C	-2.43479	1.15630	0.00015
H	-2.42088	2.24530	-0.00106
C	-1.66694	-1.75075	-0.00013
H	-2.31176	-1.71953	-0.88499
H	-2.31316	-1.71843	0.88367
H	-1.14952	-2.71231	0.00089
C	1.66695	-1.75075	0.00015
H	2.31324	-1.71842	-0.88360
H	1.14953	-2.71231	-0.00096
H	2.31171	-1.71957	0.88505
C	2.43477	1.15632	-0.00004
H	2.42086	2.24531	0.00012
H	-2.96030	0.80043	0.89160
H	-2.96118	0.79838	-0.88994
H	2.96075	0.79929	0.89067
H	2.96070	0.79956	-0.89088

7

Si	-0.38816	0.36155	-0.43908
Si	-2.40345	-0.91032	0.01654
Si	1.85566	-0.29418	0.05347
Si	2.37558	-1.31496	2.11837
Si	2.90630	-1.52666	-1.68787
Si	2.98250	1.77361	0.00940
Si	-1.09270	3.55208	0.10126
O	-0.61429	1.95846	-0.04983
C	-1.87054	-2.74361	0.36533
C	-3.20677	-0.09864	1.59311
C	-3.56955	-0.78973	-1.53895
C	-0.80963	-3.17236	-0.65909
H	0.08722	-2.54757	-0.58310
H	-0.49626	-4.20739	-0.45726
H	-1.15670	-3.13097	-1.69350
C	-1.20454	-2.86942	1.74441
H	-0.78977	-3.88093	1.85542
H	-0.37303	-2.16502	1.85407
H	-1.89941	-2.70952	2.57268
C	-3.04212	-3.73945	0.31052
H	-2.67750	-4.73808	0.58889
H	-3.84788	-3.47945	1.00419
H	-3.47175	-3.82140	-0.69127
C	-3.62964	0.65013	-2.08214
H	-4.28768	0.67383	-2.96177
H	-4.03109	1.35968	-1.35738
H	-2.64983	1.01135	-2.40856
C	-3.07317	-1.68126	-2.69308
H	-2.04855	-1.44731	-2.99644
H	-3.13285	-2.74622	-2.45354
H	-3.71474	-1.51129	-3.56839
C	-5.00692	-1.23009	-1.19851
H	-5.49442	-0.55629	-0.48883
H	-5.60960	-1.22149	-2.11726
H	-5.05250	-2.24317	-0.78770
C	-2.11822	0.26544	2.62005
H	-1.36522	0.94579	2.20386
H	-2.57910	0.77870	3.47622
H	-1.60329	-0.61342	3.00928
C	-3.93405	1.20536	1.23289
H	-4.82850	1.03661	0.62801
H	-4.25568	1.70789	2.15626
H	-3.28263	1.89366	0.69105
C	-4.23112	-1.02266	2.27734
H	-3.77609	-1.92931	2.68380
H	-4.69209	-0.48670	3.11891
H	-5.03714	-1.32447	1.60113
C	1.93874	-2.95784	-2.44947
H	1.00558	-2.61692	-2.90837
H	2.56212	-3.39218	-3.24010
H	1.70996	-3.74811	-1.72897
C	3.43059	-0.41340	-3.12016
H	2.57572	0.09540	-3.57424
H	4.16754	0.33505	-2.81549
H	3.89646	-1.04445	-3.88660
C	4.48524	-2.24716	-0.92734
H	4.26834	-2.93944	-0.10718
H	5.03544	-2.80069	-1.69733
H	5.14447	-1.46010	-0.54669
C	4.86601	1.57644	-0.00948
H	5.32198	2.57332	-0.04389
H	5.24675	1.06391	0.87750
H	5.20842	1.02797	-0.89239
C	2.52609	2.71141	-1.56496
H	2.87752	3.74823	-1.51469
H	2.99992	2.23564	-2.42791
H	1.44875	2.72218	-1.74672
C	2.52539	2.72577	1.58124
H	1.43979	2.77846	1.71222
H	2.94245	2.21802	2.45837
H	2.92451	3.74656	1.56722
C	1.35156	-0.64817	3.56590
H	1.89454	-0.84023	4.49876
H	1.19389	0.43264	3.48544
H	0.37327	-1.12676	3.64866
C	4.17315	-0.91568	2.55955
H	4.87310	-1.18529	1.76388
H	4.30577	0.14573	2.79220
H	4.44322	-1.48842	3.45504
C	2.23368	-3.21008	2.02383
H	1.71861	-3.60388	2.90695
H	1.68619	-3.55250	1.13994
H	3.23301	-3.65661	1.99358
C	0.25112	4.76031	-0.40033
H	0.42488	4.76359	-1.47991
H	-0.09573	5.76150	-0.11692
H	1.20431	4.58222	0.10208
C	-1.49390	3.87214	1.90724
H	-2.33634	3.27990	2.27249
H	-0.62882	3.65536	2.54344
H	-1.74355	4.93088	2.03954
C	-2.55416	3.91883	-1.02006
H	-2.37098	3.52867	-2.02715
H	-3.50731	3.51768	-0.66796
H	-2.66276	5.00634	-1.10311
C	-0.19483	0.35731	-2.33024
N	-0.02218	0.31339	-3.47813

7a

Si	-0.38637	0.36409	-0.45808
Si	-2.40164	-0.90424	0.00930
Si	1.85259	-0.29664	0.04173
Si	2.37562	-1.32761	2.10092
Si	2.89768	-1.52642	-1.70145
Si	2.99188	1.76426	0.00997
Si	-1.08087	3.54694	0.10315
O	-0.60604	1.95119	-0.04221
C	-1.87233	-2.74025	0.35650
C	-3.20137	-0.09810	1.59099
C	-3.57585	-0.78311	-1.54002
C	-0.81349	-3.17329	-0.66816
H	0.08457	-2.55023	-0.59492
H	-0.50252	-4.20882	-0.46487
H	-1.16201	-3.13302	-1.70209
C	-1.20430	-2.86665	1.73462
H	-0.79131	-3.87891	1.84570
H	-0.37107	-2.16400	1.84263
H	-1.89720	-2.70465	2.56401
C	-3.04509	-3.73471	0.30430
H	-2.68198	-4.73316	0.58553
H	-3.85101	-3.47183	0.99664
H	-3.47420	-3.81886	-0.69760
C	-3.64487	0.65901	-2.07676
H	-4.28305	0.67836	-2.97108
H	-4.07642	1.35557	-1.35663
H	-2.66346	1.03858	-2.37378
C	-3.07396	-1.66921	-2.69586
H	-2.04613	-1.43647	-2.98850
H	-3.13571	-2.73512	-2.46082
H	-3.70912	-1.49534	-3.57506
C	-5.01099	-1.23147	-1.20190
H	-5.50000	-0.56348	-0.48766
H	-5.61448	-1.21888	-2.12023
H	-5.05301	-2.24705	-0.79724
C	-2.11053	0.26505	2.61606
H	-1.35793	0.94496	2.19872
H	-2.56937	0.77836	3.47337
H	-1.59552	-0.61421	3.00424
C	-3.93031	1.20589	1.23393
H	-4.82909	1.03546	0.63584
H	-4.24583	1.71006	2.15853
H	-3.28298	1.89339	0.68600
C	-4.22472	-1.02202	2.27669
H	-3.76971	-1.92908	2.68218
H	-4.68439	-0.48627	3.11918
H	-5.03184	-1.32336	1.60149
C	1.92070	-2.94444	-2.47727
H	0.98335	-2.59860	-2.92402
H	2.53670	-3.37069	-3.27796
H	1.69522	-3.74281	-1.76462
C	3.43440	-0.40689	-3.12590
H	2.59069	0.12335	-3.57641
H	4.18240	0.32743	-2.81365
H	3.88982	-1.03557	-3.90044
C	4.47375	-2.26527	-0.95323
H	4.25474	-2.96209	-0.13752
H	5.01766	-2.81667	-1.72920
H	5.13960	-1.48574	-0.56853
C	4.87532	1.56259	-0.00617
H	5.33314	2.55842	-0.04640
H	5.25463	1.05470	0.88399
H	5.21753	1.00822	-0.88549
C	2.54515	2.71141	-1.56231
H	2.88442	3.75146	-1.49960
H	3.03692	2.24790	-2.42204
H	1.47007	2.70997	-1.75763
C	2.53579	2.71313	1.58432
H	1.45031	2.76746	1.71559
H	2.95185	2.20201	2.46000
H	2.93699	3.73314	1.57319
C	1.35946	-0.66399	3.55573
H	1.90608	-0.86152	4.48532
H	1.20469	0.41761	3.48047
H	0.38008	-1.13990	3.64101
C	4.17564	-0.93674	2.54007
H	4.87312	-1.20258	1.74096
H	4.31159	0.12264	2.77993
H	4.44602	-1.51650	3.43093
C	2.22885	-3.22225	2.00050
H	1.71554	-3.61776	2.88389
H	1.67794	-3.56063	1.11719
H	3.22711	-3.67087	1.96605
C	0.26702	4.75233	-0.39396
H	0.44521	4.75415	-1.47278
H	-0.07986	5.75424	-0.11311
H	1.21778	4.57380	0.11282
C	-1.48735	3.86874	1.90743
H	-2.33201	3.27830	2.27038
H	-0.62436	3.64972	2.54578
H	-1.73480	4.92802	2.03925
C	-2.53577	3.91633	-1.02540
H	-2.34130	3.53751	-2.03471
H	-3.48918	3.50528	-0.68598
H	-2.65035	5.00396	-1.09821
C	-0.06969	0.39577	-3.41301
N	-0.23048	0.40065	-2.24700

7b

Si	0.48720	0.70801	-0.19878
Si	2.56004	-0.52869	0.07490
Si	-1.69789	-0.26844	0.17735
Si	-2.31026	-0.80858	2.39561
Si	-2.34484	-2.13308	-1.15779
Si	-3.31563	1.31608	-0.64099
C	3.02982	-0.51812	1.96850
C	3.95567	-1.67915	2.37448
C	1.72061	-0.59785	2.77326
C	3.72282	0.77631	2.42013
C	2.23292	-2.33711	-0.54531
C	3.52806	-3.14270	-0.75593
C	1.34415	-3.10379	0.44918
C	1.47831	-2.29948	-1.88668
C	3.92859	0.34093	-1.00995
C	5.34115	-0.11842	-0.59733
C	3.79087	0.05984	-2.51758
C	3.83498	1.86716	-0.84428
C	-1.78497	0.48141	3.67934
C	-4.19715	-0.92847	2.52260

C	-1.66806	-2.51667	2.90176
C	-1.55866	-3.84769	-0.98839
C	-2.20691	-1.64872	-2.98519
C	-4.14019	-2.51548	-0.66214
C	-4.18590	2.29121	0.74890
C	-2.52077	2.49526	-1.89512
C	-4.77696	0.57946	-1.60947
H	4.19602	-1.58814	3.44295
H	4.90264	-1.65512	1.82463
H	3.50747	-2.66362	2.22789
H	1.93587	-0.67366	3.84856
H	1.09651	-1.45000	2.49634
H	1.12445	0.31266	2.62744
H	4.72369	0.89896	2.00069
H	3.83048	0.75958	3.51404
H	3.13695	1.65766	2.16710
H	4.15092	-3.19413	0.14147
H	4.13741	-2.73573	-1.56758
H	3.26724	-4.17328	-1.03473
H	1.81754	-3.24715	1.42311
H	1.12529	-4.10201	0.04810
H	0.38222	-2.59941	0.60812
H	2.00709	-1.74506	-2.66348
H	0.48827	-1.84731	-1.77385
H	1.33734	-3.32495	-2.25571
H	5.59542	0.15259	0.42927
H	6.07995	0.36493	-1.25185
H	5.47340	-1.19959	-0.70067
H	3.97889	-0.98721	-2.76924
H	4.53950	0.65826	-3.05482
H	2.80852	0.33978	-2.90676
H	4.63973	2.35017	-1.41590
H	3.93326	2.18844	0.19543
H	2.88512	2.24734	-1.23780
H	-0.74138	0.79481	3.59211
H	-1.92743	0.06358	4.68296
H	-2.41579	1.37350	3.60387
H	-4.47332	-0.97523	3.58297
H	-4.57711	-1.83187	2.03863
H	-4.70575	-0.06513	2.08400
H	-2.06181	-2.76846	3.89361
H	-0.57870	-2.58739	2.94558
H	-2.02633	-3.27816	2.20006
H	-1.46156	-4.16499	0.05417
H	-0.58637	-3.94192	-1.46971
H	-2.24860	-4.54296	-1.48330
H	-1.18080	-1.79040	-3.34156
H	-2.47659	-0.60710	-3.18306
H	-2.85754	-2.28721	-3.59447
H	-4.66533	-2.95779	-1.51744
H	-4.72131	-1.66347	-0.31231
H	-4.12488	-3.26538	0.13749
H	-4.30642	3.34016	0.45539
H	-3.66565	2.27383	1.70894
H	-5.18805	1.87738	0.90070
H	-2.33671	1.96686	-2.83786
H	-1.57566	2.93680	-1.57416
H	-3.22285	3.31050	-2.10832
H	-4.50957	-0.17365	-2.35437
H	-5.24299	1.42083	-2.13805
H	-5.53481	0.15319	-0.94683
Si	0.51074	3.01447	0.52477
C	1.74304	3.60005	1.83921
H	1.49566	4.65459	2.01351
H	1.63906	3.07818	2.79538
H	2.78686	3.56027	1.52144
C	0.83305	4.10350	-0.99514
H	0.28234	5.04434	-0.88130
H	1.89752	4.34730	-1.06873
H	0.52824	3.64403	-1.93892
C	-1.14794	3.49526	1.29029
H	-1.03621	4.47885	1.76130
H	-1.95177	3.56912	0.55761
H	-1.45278	2.78732	2.06724
N	0.42035	0.91335	-1.95535
C	0.18785	0.96014	-3.12409
O	-0.02208	1.01376	-4.28490

$TMSN_3$

N	-2.99686	-0.00012	-0.02587
N	-1.94670	0.00097	0.39664
N	-0.84652	0.00226	0.93024
Si	0.65902	-0.00004	-0.02140
C	0.68545	-1.54308	-1.08517
H	-0.17318	-1.56839	-1.76447
H	1.59334	-1.57823	-1.69629
H	0.65550	-2.44538	-0.46748
C	2.01126	0.00434	1.26181
H	2.99864	0.00339	0.78998
H	1.93595	0.89131	1.89741
H	1.93674	-0.87893	1.90264
C	0.68427	1.53653	-1.09451
H	0.65327	2.44254	-0.48232
H	1.59230	1.56885	-1.70557
H	-0.17418	1.55690	-1.77420

N_2

N	0.00000	0.00000	0.54919
N	0.00000	0.00000	-0.54919

TS77a

Si	-0.38715	0.37504	-0.49897
Si	-2.41953	-0.88016	0.00109
Si	1.86205	-0.27278	0.01496
Si	2.39091	-1.38119	2.04268
Si	2.89956	-1.50243	-1.73378
Si	3.04354	1.77110	0.03051
Si	-1.08006	3.56778	0.03226
O	-0.66765	1.95112	-0.08442
C	-1.88910	-2.71806	0.30700
C	-3.09471	-0.05927	1.63928
C	-3.73005	-0.75581	-1.44009
C	-0.92496	-3.14229	-0.81141
H	-0.01264	-2.53517	-0.79028
H	-0.62004	-4.18864	-0.66247
H	-1.35124	-3.05557	-1.81352
C	-1.11137	-2.86284	1.62289
H	-0.70113	-3.87988	1.69201
H	-0.26639	-2.16816	1.66667
H	-1.73223	-2.69990	2.50794
C	-3.07307	-3.69953	0.35380
H	-2.69403	-4.70597	0.58044
H	-3.80005	-3.44109	1.13018
H	-3.60463	-3.76262	-0.59827
C	-3.76992	0.67328	-2.01113
H	-4.54164	0.72999	-2.79152
H	-4.01563	1.42249	-1.25630
H	-2.81827	0.95109	-2.47401
C	-3.45320	-1.70666	-2.62155
H	-2.47883	-1.53523	-3.07770
H	-3.52898	-2.75990	-2.33895
H	-4.21842	-1.52794	-3.38975
C	-5.13934	-1.11047	-0.92059
H	-5.51148	-0.40738	-0.17288
H	-5.84161	-1.08410	-1.76512
H	-5.18542	-2.11658	-0.49163
C	-1.92766	0.28410	2.58446
H	-1.22671	0.99812	2.13673
H	-2.32276	0.75193	3.49785
H	-1.36537	-0.59791	2.89113
C	-3.82786	1.26012	1.35012
H	-4.76942	1.11900	0.81498
H	-4.06697	1.75644	2.30164
H	-3.20786	1.94315	0.76703
C	-4.06833	-0.97650	2.40319
H	-3.58340	-1.88127	2.77877
H	-4.46068	-0.43487	3.27549
H	-4.92480	-1.28165	1.79521
C	1.93877	-2.93904	-2.49341
H	0.99331	-2.61389	-2.93693
H	2.56128	-3.36566	-3.28908
H	1.73069	-3.73219	-1.76929
C	3.42385	-0.36893	-3.15307
H	2.58994	0.21500	-3.55164
H	4.21225	0.32301	-2.84121
H	3.82774	-0.98905	-3.96211
C	4.49114	-2.22685	-1.00252
H	4.28835	-2.93778	-0.19532
H	5.03342	-2.76179	-1.79122
H	5.15250	-1.44599	-0.61366
C	4.92228	1.53007	0.08244
H	5.39233	2.52080	0.05372
H	5.27599	1.01610	0.97844
H	5.27685	0.97627	-0.79298
C	2.72716	2.77107	-1.53891
H	3.07536	3.80181	-1.40512
H	3.28887	2.33141	-2.36808
H	1.67581	2.78612	-1.82804
C	2.52910	2.70992	1.59252
H	1.43914	2.77966	1.66805
H	2.88974	2.18263	2.48313
H	2.94419	3.72428	1.61216
C	1.38434	-0.82478	3.54988
H	1.98428	-1.00550	4.44949
H	1.14455	0.24306	3.51605
H	0.45004	-1.38025	3.66056
C	4.18628	-0.98708	2.49818
H	4.89002	-1.20025	1.68931
H	4.30451	0.05981	2.79556
H	4.46070	-1.61010	3.35818
C	2.27309	-3.27119	1.84482
H	1.72928	-3.71325	2.68668
H	1.76090	-3.57193	0.92489
H	3.27700	-3.70794	1.82990
C	0.27900	4.72035	-0.54590
H	0.45028	4.66083	-1.62408
H	-0.04946	5.74148	-0.31649
H	1.22952	4.55266	-0.03435
C	-1.40514	3.95087	1.84129
H	-2.22376	3.36466	2.26523
H	-0.51151	3.77133	2.44840
H	-1.66257	5.01149	1.94117
C	-2.57707	3.93734	-1.03902
H	-2.45371	3.49953	-2.03539
H	-3.52243	3.57893	-0.62431
H	-2.65926	5.02318	-1.16251
C	0.10102	0.66985	-2.49553
N	-0.56717	-0.28214	-2.68288

I

Si	0.00583	0.34037	-1.37868
Si	-1.82325	-0.34488	0.01306
Si	1.85848	-0.29000	0.00933
O	-0.13468	2.83352	0.23570
C	-0.06770	1.85564	-0.36906
C	3.42182	-0.11717	-1.03435
H	3.58498	0.92322	-1.33246
H	4.29835	-0.44862	-0.46590
H	3.35512	-0.71965	-1.94528
C	2.10600	0.69679	1.60042
H	2.95860	0.28480	2.15263
H	2.32192	1.74922	1.39084
H	1.22841	0.65651	2.25222
C	1.62697	-2.11559	0.44336
H	1.46804	-2.72046	-0.45524
H	2.52597	-2.49027	0.94613
H	0.77733	-2.27452	1.11437

C -2.15737 -2.14766 -0.44059
H -1.30018 -2.78942 -0.21596
H -3.01785 -2.52161 0.12571
H -2.38331 -2.24393 -1.50691
C -3.33095 0.69512 -0.44255
H -4.21267 0.33853 0.10198
H -3.18360 1.74932 -0.18612
H -3.54368 0.63394 -1.51394
C -1.56542 -0.21672 1.88075
H -0.73492 -0.83948 2.22695
H -1.36777 0.81601 2.18711
H -2.47207 -0.55107 2.39864

I^{S}

Si 0.00007 -1.59642 0.00008
Si -1.78572 -0.01766 -0.00829
Si 1.78585 -0.01767 0.00835
C 1.60103 1.51500 1.10818
H 0.72593 2.11796 0.85157
H 1.52341 1.23765 2.16455
H 2.49115 2.14561 0.99818
C 3.39982 -0.86442 0.51518
H 3.59847 -1.73752 -0.11427
H 4.24555 -0.17396 0.41844
H 3.36238 -1.20589 1.55462
C 1.97391 0.53111 -1.80089
H 2.85171 1.18239 -1.88525
H 2.13345 -0.32201 -2.46823
H 1.10422 1.08918 -2.15896
C -1.60163 1.51429 -1.10925
H -0.72670 2.11783 -0.85341
H -1.52420 1.23609 -2.16544
H -2.49197 2.14463 -0.99953
C -1.97364 0.53214 1.80069
H -1.10420 1.09082 2.15836
H -2.85177 1.18300 1.88480
H -2.13268 -0.32077 2.46842
C -3.39973 -0.86499 -0.51406
H -3.59795 -1.73784 0.11586
H -4.24554 -0.17463 -0.41727
H -3.36266 -1.20690 -1.55337

TSI^{B}

Si 0.00000 0.27326 -0.00002
Si -2.22862 -0.39521 -0.00001
Si 2.22863 -0.39521 -0.00001
O 0.00000 3.20628 -0.00000
C 0.00000 2.04560 -0.00001
C -3.26644 1.17751 0.00030
H -3.06929 1.78657 0.88737
H -3.06938 1.78686 -0.88659
H -4.32993 0.91339 0.00031
C -2.60365 -1.42338 1.53431
H -3.65066 -1.74725 1.52683
H -1.97482 -2.31813 1.57656
H -2.42738 -0.84343 2.44451
C -2.60388 -1.42291 -1.53457
H -1.97508 -2.31765 -1.57718
H -3.65090 -1.74676 -1.52705
H -2.42773 -0.84268 -2.44462
C 2.60369 -1.42324 1.53439
H 1.97486 -2.31797 1.57675
H 3.65070 -1.74712 1.52691
H 2.42746 -0.84319 2.44454
C 2.60384 -1.42305 -1.53449
H 3.65085 -1.74690 -1.52697
H 1.97504 -2.31781 -1.57699
H 2.42765 -0.84292 -2.44459
C 3.26644 1.17751 0.00013
H 3.06936 1.78677 -0.88682
H 3.06931 1.78665 0.88714
H 4.32993 0.91339 0.00014

Ia

Si 0.01993 0.10161 -1.49837
Si -1.73504 -0.48023 0.00205
Si 1.85033 -0.29105 -0.00773
C 3.47987 -0.20380 -0.96626
H 3.62380 0.78602 -1.41128
H 4.33077 -0.40601 -0.30554
H 3.50017 -0.93749 -1.77852
C 1.98459 0.95513 1.41543
H 2.80041 0.64846 2.08039
H 2.22493 1.95494 1.04016
H 1.06925 1.01947 2.00991
C 1.73022 -2.04122 0.71831
H 1.64172 -2.80004 -0.06652
H 2.64158 -2.26173 1.28639
H 0.87631 -2.15260 1.39292
C -1.98966 -2.34527 -0.24686
H -1.12079 -2.92925 0.07161
H -2.85031 -2.67494 0.34645
H -2.19705 -2.58449 -1.29470
C -3.32707 0.39553 -0.53089
H -4.17479 0.05197 0.07293
H -3.25097 1.48136 -0.40971
H -3.55108 0.19294 -1.58271
C -1.52880 -0.14922 1.85791
H -0.66475 -0.66807 2.28302
H -1.41656 0.92006 2.06777
H -2.42403 -0.49450 2.38859
C -0.49692 3.41673 0.31796
O -0.25814 2.50774 -0.31601

Ib

Si 0.00487 0.28697 -1.43245
Si -1.77840 -0.40009 -0.01288
Si 1.81258 -0.37426 -0.01028
O -0.42606 2.64267 0.29831
C 0.36718 3.21562 -0.27588
C 3.44317 -0.25473 -0.96179
H 3.62018 0.76899 -1.30743
H 4.28669 -0.55017 -0.32732
H 3.43864 -0.90513 -1.84235
C 1.99009 0.72452 1.52602
H 2.74209 0.28238 2.18998
H 2.34190 1.72534 1.25501
H 1.05817 0.82766 2.08794
C 1.61813 -2.18046 0.53854
H 1.51457 -2.85404 -0.31870
H 2.51451 -2.48723 1.09028
H 0.75256 -2.32786 1.19072
C -2.08260 -2.21179 -0.49757
H -1.23257 -2.85631 -0.25386
H -2.95472 -2.58736 0.05013
H -2.29418 -2.31288 -1.56679
C -3.33569 0.58573 -0.43796
H -4.19782 0.19825 0.11688
H -3.21920 1.64327 -0.17974
H -3.56039 0.52341 -1.50713
C -1.55967 -0.30485 1.86582
H -0.70259 -0.88341 2.22204
H -1.43093 0.73143 2.19481
H -2.45887 -0.69862 2.35435

II

Si -1.47825 0.27243 0.84114
O -2.57634 -1.87122 -1.00682
C -2.11319 -0.96779 -0.48759
C 0.35452 0.10956 0.30982
C 1.08647 -1.01922 0.71086
C 1.03450 1.11602 -0.39111
C 2.43663 -1.15680 0.39428
H 0.59494 -1.80210 1.28599
C 2.39091 0.99440 -0.69233
H 0.50451 2.00998 -0.71018
C 3.09327 -0.14611 -0.30678
H 2.97882 -2.04456 0.70585
H 2.89806 1.78847 -1.23249
H 4.14792 -0.24374 -0.54510
C -2.12302 1.87141 -0.00452
H -3.21640 1.89005 0.00092
H -1.78903 2.71776 0.60501
H -1.77303 2.03099 -1.02718

II^{S}

Si 1.95525 -0.83094 -0.00005
C 0.14360 -0.25479 -0.00020
C -0.83384 -1.26793 -0.00003
C -0.30717 1.07929 -0.00018
C -2.19629 -0.97174 0.00012
H -0.51629 -2.30942 -0.00007
C -1.66444 1.38598 -0.00005
H 0.41243 1.89417 -0.00031
C -2.61052 0.35836 0.00012
H -2.93026 -1.77174 0.00026
H -1.98966 2.42208 -0.00008
H -3.66988 0.59756 0.00027
C 2.84476 0.86200 0.00021
H 3.93075 0.74548 0.00035
H 2.56663 1.45409 -0.88198
H 2.56628 1.45388 0.88241

TSII^{B}

Si -1.36296 0.42713 0.00007
O -3.12731 -1.88803 -0.00012
C -2.42243 -0.95613 -0.00010
C 0.45288 0.08817 0.00002
C 1.34275 1.17370 -0.00009
C 0.98453 -1.21224 0.00012
C 2.72128 0.96628 -0.00012
H 0.96293 2.19310 -0.00015
C 2.35970 -1.41648 0.00009
H 0.32067 -2.07336 0.00021
C 3.23446 -0.32823 -0.00003
H 3.39294 1.81926 -0.00022
H 2.75155 -2.42895 0.00016
H 4.30745 -0.49060 -0.00005
C -2.12929 2.13268 0.00008
H -1.84098 2.69593 0.89032
H -1.84091 2.69591 -0.89015
H -3.21700 2.02664 0.00002

III

Si 1.19144 -0.00063 -0.13230
O -1.84569 -0.00075 -0.02707
C -0.71180 0.00214 0.05558
H 1.17527 -1.13115 0.86926
H 1.18090 1.13303 0.86603

III^{S}

Si 0.00000 0.00000 0.13260
H 0.00000 -1.08771 -0.92821
H 0.00000 1.08771 -0.92821

TSIII^{B}

Si	1.08436	0.00001	-0.00003
O	-1.82513	0.00003	0.00002
C	-0.66454	-0.00006	0.00003
H	1.70371	-1.32104	0.00003
H	1.70362	1.32110	0.00003

IV

Si	-0.00762	-0.05309	1.14115
Si	1.71193	-0.82993	-0.32134
Si	-1.76707	-0.73216	-0.32364
O	0.09212	2.45875	-0.47905
C	0.05003	1.46804	0.09409
H	1.36027	-0.79932	-1.76420
H	1.96141	-2.23994	0.06402
H	2.95959	-0.05397	-0.12102
H	-3.08662	-0.31856	0.21060
H	-1.64504	-0.23917	-1.71859
H	-1.70813	-2.21483	-0.34944

IV^{S}

Si	0.00014	1.25100	-0.00009
Si	1.66454	-0.44844	-0.00738
Si	-1.66461	-0.44836	0.00736
H	1.28524	-1.69920	-0.71610
H	1.79792	-0.77192	1.44259
H	2.99247	-0.00860	-0.50140
H	-2.99189	-0.00687	0.50170
H	-1.79855	-0.77330	-1.44216
H	-1.28619	-1.69891	0.71695

TSIV^{B}

Si	0.00000	-0.13853	-0.00010
Si	-2.18814	-0.86451	0.00004
Si	2.18815	-0.86448	0.00004
O	-0.00004	2.78958	0.00002
C	-0.00000	1.63239	0.00004
H	3.01099	0.36678	-0.00085
H	2.49116	-1.67548	-1.20095
H	2.49186	-1.67415	1.20175
H	-2.49180	-1.67424	1.20172
H	-2.49116	-1.67546	-1.20098
H	-3.01099	0.36674	-0.00077

V

Si	-0.23302	-0.10171	0.80460
Si	1.62281	-1.21699	-0.17854
O	0.85868	2.49229	-0.28186
C	0.44608	1.47137	0.01946
H	1.55768	-1.30700	-1.66073
H	1.66548	-2.59782	0.36082
H	2.88548	-0.53167	0.19801
C	-1.59860	-0.33648	-0.51552
H	-1.36063	-0.48175	-1.56990
C	-2.88222	-0.41274	-0.14734
H	-3.67644	-0.60033	-0.86746
H	-3.18968	-0.29080	0.88975

V^{S}

Si	-0.16313	0.96929	-0.03430
Si	1.86282	-0.30490	0.02582
H	1.85249	-1.41224	-0.96968
H	1.94962	-0.92949	1.37667
H	3.10043	0.48895	-0.17878
C	-1.29014	-0.54611	-0.10421
H	-0.95466	-1.57667	-0.23545
C	-2.60964	-0.34759	0.07421
H	-3.01559	0.65522	0.20428
H	-3.32928	-1.16500	0.10169

TSV^{B}

Si	-0.01146	0.20486	-0.10507
Si	-2.27644	0.51308	0.09856
H	-2.85156	1.18418	-1.08953
H	-2.62893	1.30369	1.29976
H	-2.82072	-0.85925	0.21724
C	1.48066	1.29018	-0.30642
H	1.41124	2.10385	-1.02726
C	2.64445	1.09717	0.32688
H	2.77344	0.31747	1.07305
H	3.51289	1.71401	0.10856
C	0.41505	-1.50674	-0.05715
O	0.67415	-2.63734	-0.03383

VI

Si	-0.00368	0.22471	-0.82701
O	0.10123	3.08319	0.11391
C	0.04064	1.95481	-0.06858
C	-1.65082	-0.40211	0.01970
C	-1.57572	-0.70851	1.51895
C	-2.74135	0.65347	-0.21991
C	-2.05596	-1.68572	-0.72877
H	-0.85237	-1.49949	1.74079
H	-1.30104	0.17623	2.10336
H	-2.55614	-1.05629	1.87604
H	-2.81514	0.93438	-1.27627
H	-3.71773	0.25424	0.08740
H	-2.56706	1.56445	0.36504
H	-3.00986	-2.06006	-0.33233
H	-2.18616	-1.50353	-1.80086
H	-1.31552	-2.48460	-0.60985
C	1.63245	-0.44931	0.01264
C	1.86509	-0.09722	1.48820
C	1.60128	-1.97985	-0.13759
C	2.81054	0.09879	-0.80853
H	1.98096	0.98302	1.63183
H	1.05130	-0.43661	2.13313
H	2.79060	-0.57457	1.84245
H	1.43201	-2.28911	-1.17609
H	2.56524	-2.40135	0.17921
H	0.82452	-2.43745	0.48467
H	3.75706	-0.29762	-0.41525
H	2.73599	-0.18234	-1.86387
H	2.86809	1.19305	-0.75927

VI^{S}

Si	0.00004	1.13226	-0.00073
C	-1.56716	-0.01434	0.01164
C	-1.72255	-0.40542	-1.47312
C	-1.58392	-1.26722	0.89187
C	-2.76311	0.86993	0.40275
H	-1.63670	0.45967	-2.14751
H	-0.98843	-1.15310	-1.78579
H	-2.72336	-0.82805	-1.63992
H	-1.47300	-1.01567	1.95304
H	-2.54708	-1.78651	0.78182
H	-0.79819	-1.98065	0.63123
H	-3.70349	0.31341	0.28383
H	-2.69839	1.19629	1.44705
H	-2.82482	1.77004	-0.21929
C	1.56717	-0.01443	-0.01170
C	1.72200	-0.40391	1.47355
C	1.58431	-1.26811	-0.89072
C	2.76323	0.86955	-0.40326
H	1.63447	0.46167	2.14713
H	0.98869	-1.15230	1.78637
H	2.72329	-0.82495	1.64152
H	1.47400	-1.01748	-1.95218
H	2.54729	-1.78751	-0.77971
H	0.79827	-1.98118	-0.62997
H	3.70355	0.31309	-0.28371
H	2.69870	1.19512	-1.44781
H	2.82481	1.77013	0.21812

TSVI^{B}

Si	-0.00000	0.36380	-0.00007
O	-0.00003	3.28027	-0.00059
C	-0.00002	2.11039	-0.00038
C	-1.71326	-0.46801	-0.00199
C	-2.02636	-1.07845	1.37482
C	-2.77385	0.58983	-0.33836
C	-1.74071	-1.58066	-1.06305
H	-1.28314	-1.82660	1.66993
H	-2.05923	-0.30996	2.15240
H	-3.00494	-1.57721	1.34223
H	-2.62217	1.01340	-1.33563
H	-3.76863	0.12566	-0.31289
H	-2.77394	1.40910	0.38905
H	-2.73026	-2.05734	-1.06896
H	-1.54426	-1.18891	-2.06600
H	-1.00342	-2.36370	-0.85066
C	1.71327	-0.46799	0.00216
C	1.74073	-1.58028	1.06360
C	2.02639	-1.07890	-1.37444
C	2.77384	0.58998	0.33818
H	1.54424	-1.18820	2.06641
H	1.00348	-2.36342	0.85146
H	2.73030	-2.05691	1.06969
H	2.05927	-0.31068	-2.15229
H	3.00498	-1.57763	-1.34166
H	1.28319	-1.82717	-1.66931
H	3.76862	0.12583	0.31286
H	2.77390	1.40902	-0.38950
H	2.62215	1.01388	1.33531

VII

Si	0.58786	0.09462	-0.46909
O	-2.33863	-0.36413	0.14472
C	-1.21886	-0.17723	0.01801
N	1.42033	-1.21677	0.29302
H	1.75165	-2.01077	-0.23204
H	1.71827	-1.22946	1.25684
B	0.62366	1.88977	0.27871
H	1.60104	2.38903	0.74556
H	-0.33948	2.57150	0.08631

VII^{S}

Si	0.03723	0.67214	-0.00008
N	1.25214	-0.55101	0.00003
H	1.12638	-1.55411	-0.00022
H	2.23198	-0.30077	0.00032
B	-1.64222	-0.45128	-0.00003
H	-2.21728	-0.72135	-1.01556
H	-2.21619	-0.72020	1.01648

TSVII^{B}

Si	-0.56511	0.10539	-0.00002
O	2.39124	-0.22975	0.00006
C	1.24934	-0.12104	0.00003
N	-1.31794	-1.43204	0.00002

H -1.61468 -1.89954 0.84269
H -1.61465 -1.89959 -0.84263
B -0.88305 1.96522 -0.00008
H -1.96046 2.46718 -0.00012
H 0.11615 2.61891 -0.00009

VIII

Si -0.45744 0.00001 -0.63076
O 2.45907 0.00015 0.16054
C 1.31888 -0.00006 0.08341
C -1.12299 1.52236 0.33481
C -1.12279 -1.52246 0.33477
H -0.54167 -2.42406 0.12174
H -1.17111 -1.37443 1.41678
H -2.14005 -1.71040 -0.02426
H -2.14009 1.71007 -0.02490
H -1.17198 1.37438 1.41680
H -0.54198 2.42408 0.12210

VIII^{S}

Si -0.00000 -0.76667 -0.00000
C 1.42659 0.50439 -0.01002
C -1.42660 0.50438 0.01001
H -2.39902 0.07496 0.26127
H -1.23115 1.36703 0.65863
H -1.49879 0.89846 -1.01638
H 1.23105 1.36730 -0.65825
H 1.49915 0.89804 1.01651
H 2.39890 0.07496 -0.26169

TSVIII^{B}

Si 0.38309 -0.00000 0.00006
O -2.52624 0.00002 -0.00004
C -1.35616 0.00005 0.00003
H 0.45560 2.45098 0.00047
H 1.84436 1.80827 -0.88913
H 1.84515 1.80793 0.88855
H 1.84506 -1.80800 0.88855
H 1.84427 -1.80836 -0.88913
H 0.45548 -2.45098 0.00048
C 1.22452 1.67419 -0.00004
C 1.22443 -1.67424 -0.00004

IX

Si 0.11224 -0.24257 0.87390
Si -0.12200 1.87510 -0.18821
O -2.45136 -1.24447 -0.41384
C -1.44616 -0.83792 -0.06806
H 0.14675 1.84917 -1.64810
H 0.84198 2.81464 0.43589
H -1.49290 2.39767 0.04650
N 1.20623 -1.16898 -0.18682
C 2.41973 -0.87376 -0.39808
H 2.92113 0.03212 -0.01855
H 3.04551 -1.54043 -1.00004

IX^{S}

Si -0.07930 1.19120 -0.00130
Si 1.62081 -0.50735 -0.00380
H 1.11823 -1.81295 -0.50459
H 2.10715 -0.69754 1.38980
H 2.79597 -0.10728 -0.82187
N -1.26615 0.01347 0.00092
C -2.23389 -0.79024 0.00030
H -2.68412 -1.13420 -0.93511
H -2.65195 -1.17468 0.93487

TSIX^{B}

Si -0.00971 -0.16032 0.00001
Si -2.28518 -0.36740 0.00000
O 1.00494 2.59246 -0.00001
C 0.59078 1.50899 0.00001
H -2.75903 1.03625 -0.00027
H -2.77565 -1.07130 1.20492
H -2.77554 -1.07174 -1.20471
N 1.17083 -1.40301 -0.00001
C 2.43811 -1.42616 0.00000
H 3.07503 -0.53120 0.00003
H 2.95515 -2.38949 -0.00002

X

Si 0.02444 1.08868 -0.96008
O 0.18882 3.16388 1.26594
C 0.11346 2.26404 0.57276
C 1.51723 0.02868 -0.39478
C 2.80125 0.59682 -0.38677
C 1.40167 -1.33686 -0.09961
C 3.92454 -0.15838 -0.05799
H 2.93039 1.64644 -0.64789
C 2.52692 -2.10326 0.20704
H 0.42420 -1.81269 -0.10824
C 3.78928 -1.51481 0.23777
H 4.90558 0.30706 -0.04565
H 2.41455 -3.16086 0.42685
H 4.66368 -2.10968 0.48288
C -1.53297 0.16732 -0.33374
C -2.61760 0.04825 -1.21550
C -1.66343 -0.40639 0.94372
C -3.78523 -0.62132 -0.84502
H -2.55205 0.48713 -2.20862
C -2.82922 -1.06651 1.32397
H -0.83730 -0.34361 1.64933
C -3.89299 -1.17650 0.42700
H -4.60853 -0.70430 -1.54796
H -2.90914 -1.49525 2.31847
H -4.80145 -1.69314 0.72138

X^{S}

Si -0.00005 1.73589 0.00005
C 1.46663 0.53085 -0.03878
C 2.68554 0.98596 0.49913
C 1.46299 -0.73294 -0.66117
C 3.83582 0.20002 0.46764
H 2.73345 1.97510 0.95191
C 2.61722 -1.50922 -0.72786
H 0.54587 -1.11119 -1.10616
C 3.80181 -1.04856 -0.15140
H 4.75887 0.56503 0.90762
H 2.59431 -2.47553 -1.22285
H 4.69929 -1.65846 -0.19395
C -1.46666 0.53073 0.03799
C -2.68594 0.98584 -0.49910
C -1.46259 -0.73310 0.66027
C -3.83617 0.19991 -0.46688
H -2.73413 1.97498 -0.95186
C -2.61680 -1.50938 0.72773
H -0.54516 -1.11147 1.10452
C -3.80178 -1.04869 0.15214
H -4.75951 0.56494 -0.90624
H -2.59352 -2.47574 1.22262
H -4.69926 -1.65854 0.19535

TSX^{B}

Si 0.00000 0.84947 -0.00006
O -0.00004 3.76264 0.00001
C 0.00001 2.59574 0.00008
C -1.64091 -0.00197 -0.03326
C -1.75562 -1.25550 -0.65700
C -2.78550 0.56580 0.54966
C -2.97907 -1.92028 -0.69535
H -0.88633 -1.71304 -1.12376
C -4.01232 -0.08885 0.48608
H -2.71630 1.52103 1.06319
C -4.11170 -1.33583 -0.13075
H -3.04901 -2.89036 -1.17760
H -4.88926 0.36850 0.93366
H -5.06651 -1.85055 -0.16799
C 1.64091 -0.00198 0.03322
C 1.75561 -1.25549 0.65698
C 2.78552 0.56580 -0.54968
C 2.97906 -1.92026 0.69537
H 0.88631 -1.71302 1.12373
C 4.01234 -0.08885 -0.48605
H 2.71632 1.52102 -1.06322
C 4.11170 -1.33581 0.13080
H 3.04899 -2.89034 1.17765
H 4.88929 0.36850 -0.93361
H 5.06652 -1.85054 0.16807

XI

Si -0.02413 0.65398 0.70176
Si 1.61138 -0.84728 -0.12236
O -2.42728 -1.08843 -0.20691
C -1.44981 -0.52379 -0.05727
H 1.25373 -2.24879 0.22080
H 1.80458 -0.76334 -1.59642
H 2.91593 -0.53887 0.51357
N -0.00143 1.92033 -0.49883
H -0.47434 2.79744 -0.33671
H 0.40565 1.86763 -1.42213

XI^{S}

Si 0.79767 -0.77710 -0.00002
Si -1.42879 0.13927 -0.00000
H -2.20015 -0.29632 1.19504
H -1.40261 1.63207 -0.00044
H -2.20099 -0.29713 -1.19419
N 1.56414 0.76685 -0.00007
H 2.57397 0.84680 0.00050
H 1.11647 1.67619 -0.00015

TSXI^{B}

Si -0.10566 0.46128 -0.00000
Si 1.93646 -0.56490 -0.00000
O -2.30028 -1.47894 -0.00002
C -1.43815 -0.70175 -0.00001
H 2.74070 -0.23543 1.19953
H 2.74072 -0.23539 -1.19950
H 1.60098 -2.00899 -0.00003
N -0.58804 2.10443 0.00002
H -0.78314 2.62077 0.84363
H -0.78314 2.62080 -0.84357

4. References

1. G. R. Fulmer *et al.*, NMR Chemical Shifts of Trace Impurities: Common Laboratory Solvents, Organics, and Gases in Deuterated Solvents Relevant to the Organometallic Chemist. *Organometallics* **29**, 2176-2179 (2010).
2. D. Reiter *et al.*, Disilene-Silylene Interconversion: A Synthetically Accessible Acyclic Bis(silyl)silylene. *J. Am. Chem. Soc.* **141**, 13536-13546 (2019).
3. N. Wiberg *et al.*, Disupersilylsilane R*$_2$SiX$_2$, Disupersilyldisilane R*$_2$XSi–SiX$_3$ und Tetrasupersilyltetrasilane R*$_2$XSi–SiX$_2$–SiX$_2$–SiXR*$_2$. *Z. Anorg. Allg. Chem.* **627**, 594-606 (2001).
4. M. R. Booth, S. G. Frankiss, The constitution, vibrational spectra and proton resonance spectra of trimethylsilyl cyanide and isocyanide. *Spectrochim. Acta Part A* **26**, 859-869 (1970).
5. A. Sekiguchi, T. Tanaka, M. Ichinohe, K. Akiyama, S. Tero-Kubota, Bis(tri-*tert*-butylsilyl)silylene: Triplet Ground State Silylene. *J. Am. Chem. Soc.* **125**, 4962-4963 (2003).
6. *APEX suite of crystallographic software*. (APEX 3 version 2015.5-2; Bruker AXS Inc.: Madison, Wisconsin, USA, 2015).
7. *SAINT*. (Version 7.56a and SADABS Version 2008/1; Bruker AXS Inc.: Madison, Wisconsin, USA, 2008).
8. G. M. Sheldrick, *SHELXL-2014*. (University of Göttingen, Göttingen, Germany, 2014).
9. C. B. Hübschle, G. M. Sheldrick, B. Dittrich, ShelXle: a Qt graphical user interface for SHELXL. *J. Appl. Cryst.* **44**, 1281-1284 (2011).
10. G. M. Sheldrick, *SHELXL-97*. (University of Göttingen, Göttingen, Germany, 1998).
11. A. J. C. Wilson, *International Tables for Crystallography*. (Vol. C, Tables 6.1.1.4 (pp. 500-502), 4.2.6.8 (pp. 219-222), and 4.2.4.2 (pp. 193-199); Kluwer Academic Publishers: Dordrecht, The Netherlands, 1992).
12. C. F. Macrae *et al.*, Mercury 4.0: from visualization to analysis, design and prediction. *J. Appl. Cryst.* **53**, 226-235 (2020).
13. M. J. Frisch, G. W. Trucks, H. B. Schlegel, G. E. Scuseria, M. A. Robb, J. R. Cheeseman, G. Scalmani, V. Barone, B. Mennucci, G. A. Petersson, H. Nakatsuji, M. Caricato, X. Li, H. P. Hratchian, A. F. Izmaylov, J. Bloino, G. Zheng, J. L. Sonnenberg, M. Hada, M. Ehara, K. Toyota, R. Fukuda, J. Hasegawa, M. Ishida, T. Nakajima, Y. Honda, O. Kitao, H. Nakai, T. Vreven, J. A. Montgomery, Jr., J. E. Peralta, F. Ogliaro, M. Bearpark, J. J. Heyd, E. Brothers, K. N. Kudin, V. N. Staroverov, R. Kobayashi, J. Normand, K. Raghavachari, A. Rendell, J. C. Burant, S. S. Iyengar, J. Tomasi, M. Cossi, N. Rega, J. M. Millam, M. Klene, J. E. Knox, J. B. Cross, V. Bakken, C. Adamo, J. Jaramillo, R. Gomperts, R. E. Stratmann, O. Yazyev, A. J. Austin, R. Cammi, C. Pomelli, J. W. Ochterski, R. L. Martin, K. Morokuma, V. G. Zakrzewski, G. A. Voth, P. Salvador, J. J. Dannenberg, S. Dapprich, A. D. Daniels, Ö. Farkas, J. B. Foresman, J. V. Ortiz, J. Cioslowski, D. J. Fox., *Gaussian 09, Revision D.01*. (Gaussian, Inc., Wallingford, CT, 2009).
14. R. Ditchfield, W. J. Hehre, J. A. Pople, Self-Consistent Molecular-Orbital Methods. IX. An Extended Gaussian-Type Basis for Molecular-Orbital Studies of Organic Molecules. *J. Chem. Phys.* **54**, 724-728 (1971).
15. W. J. Hehre, R. Ditchfield, J. A. Pople, Self—Consistent Molecular Orbital Methods. XII. Further Extensions of Gaussian—Type Basis Sets for Use in Molecular Orbital Studies of Organic Molecules. *J. Chem. Phys.* **56**, 2257-2261 (1972).
16. Y. Zhao, D. G. Truhlar, The M06 suite of density functionals for main group thermochemistry, thermochemical kinetics, noncovalent interactions, excited states, and

transition elements: two new functionals and systematic testing of four M06-class functionals and 12 other functionals. *Theor. Chem. Acc.* **120**, 215-241 (2008).
17. A. V. Marenich, C. J. Cramer, D. G. Truhlar, Universal Solvation Model Based on Solute Electron Density and on a Continuum Model of the Solvent Defined by the Bulk Dielectric Constant and Atomic Surface Tensions. *J. Phys. Chem. B* **113**, 6378-6396 (2009).
18. S. E. Wheeler, K. N. Houk, Integration Grid Errors for Meta-GGA-Predicted Reaction Energies: Origin of Grid Errors for the M06 Suite of Functionals. *J. Chem. Theory Comput.* **6**, 395-404 (2010).
19. K. Fukui, The path of chemical reactions - the IRC approach. *Acc. Chem. Res.* **14**, 363-368 (1981).
20. R. Krishnan, J. S. Binkley, R. Seeger, J. A. Pople, Self‐consistent molecular orbital methods. XX. A basis set for correlated wave functions. *J. Chem. Phys.* **72**, 650-654 (1980).
21. A. D. McLean, G. S. Chandler, Contracted Gaussian basis sets for molecular calculations. I. Second row atoms, Z=11–18. *J. Chem. Phys.* **72**, 5639-5648 (1980).
22. E. D. Glendening *et al.*, *NBO 6.0*, Theoretical Chemistry Institute, University of Wisconsin: Madison, WI, 2013.
23. E. D. Glendening, C. R. Landis, F. Weinhold, Natural bond orbital methods. *Wiley Interdiscip. Rev. Comput. Mol. Sci.* **2**, 1-42 (2011).
24. E. D. Glendening, C. R. Landis, F. Weinhold, NBO 6.0: Natural bond orbital analysis program. *J. Comput. Chem.* **34**, 1429-1437 (2013).
25. T. A. Keith. *AIMAll (Version 19.10.12)*, TK Gristmill Software, Overland Park KS, 2019.
26. T. Lu, *Multiwfn 3.5 - A Multifunctional Wavefunction Analyzer*, School of Chemical and Biological Engineering, University of Science and Technology, Beijing, 2018.
27. T. Lu, F. Chen, Multiwfn: A multifunctional wavefunction analyzer. *J. Comput. Chem.* **33**, 580-592 (2012).
28. R. F. W. Bader, *Atoms in Molecules: A Quantum Theory*. (Oxford University Press, Oxford, 1990).
29. P. Macchi, A. Sironi, *Interactions Involving Metals: From "Chemical Categories" to QTAIM and Backwards*. C. F. Matta, R. J. Boyd, Eds., The Quantum Theory of Atoms in Molecules: From Solid State to DNA and Drug Design (Wiley-VCH, Weinheim, 2007).
30. Y. Zhao, D. G. Truhlar, A new local density functional for main-group thermochemistry, transition metal bonding, thermochemical kinetics, and noncovalent interactions. *J. Chem. Phys.* **125**, 194101 (2006).
31. G. A. Andrienko, *http://www.chemcraftprog.com*, 2015.
32. C. Y. Legault, *Université de Sherbrooke http://www.cylview.org*, 2009.
33. R. Dennington, T. A. Keith, J. M. Millam, GaussView. *Version 5 ed., Semichem Inc., Shawnee Mission, KS*, (2009).
34. K. P. Huber, G. Herzberg, *Molecular Spectra and Molecular Structure IV. Constants of Diatomic Molecules*. (Van Nostrand Reinhold Company, New York, 1979), vol. 4.
35. G. Maier, H. P. Reisenauer, H. Egenolf, Quest for Silaketene: A Matrix-Spectroscopic and Theoretical Study. *Organometallics* **18**, 2155-2161 (1999).
36. C. A. Arrington, J. T. Petty, S. E. Payne, W. C. K. Haskins, The reaction of dimethylsilylene with carbon monoxide in low-temperature matrices. *J. Am. Chem. Soc.* **110**, 6240-6241 (1988).
37. H. Bornemann, W. Sander, Reactions of methyl(phenyl)silylene with CO and PH_3—the formation of acid–base complexes. *J. Organomet. Chem.* **641**, 156-164 (2002).
38. A. Schulz, A. Villinger, Pseudohalonium Ions: $[Me_3Si–X–SiMe_3]+$ (X=CN, OCN, SCN, and NNN). *Chem. Eur. J.* **16**, 7276-7281 (2010).

13.4 Supporting Information Chapter 7

Supporting Information

Oxidation Reactions of a Versatile, Two-Coordinate, Acyclic Iminosiloxysilylene

Dominik Reiter, Philipp Frisch, Daniel Wendel, Fabian M. Hörmann, and Shigeyoshi Inoue[*]

Table of Contents

1. Experimental Section S2
1.1 General Methods and Instrumentation S2
1.2 Synthesis of Iminosiloxysilepin **2** S3
1.3 Synthesis of (IDippN)(^{t}Bu$_3$SiO)Si(P$_4$) (**3**) S6
1.4 Synthesis of (IDippN)(^{t}Bu$_3$SiO)Si(H)(NH$_2$) (**4**) S9
1.5 Synthesis of (IDippN)(^{t}Bu$_3$SiO)Si(NTMSN)$_2$ (**5**) S12
1.6 Synthesis of (IDippN)(^{t}Bu$_3$SiO)Si=NSi^{t}Bu$_2$Me (**6**) S15
1.7 Synthesis of Azaoxasiletane (**7**) S20
1.8 Synthesis of Oxatriazasilole (**8**) S23
1.9 Synthesis of (IDippN)(^{t}Bu$_3$SiO)Si(O$_2$C=O) (**9**) S26
1.10 Synthesis of *trans*-Cyclodisiloxane [(IDippN)(^{t}Bu$_3$SiO)Si=O]$_2$ (**10a**) S31
1.11 Synthesis of Silicon Diselenide [(IDippN)(^{t}Bu$_3$SiO)Si=Se]$_2$ (**10b**) S33
1.12 Synthesis of Silicon Ditelluride (IDippN)(^{t}Bu$_3$SiO)Si=Te (**10c**) S36
1.13 Synthesis of *cis*/*trans*-Cyclodisiloxane [(IDippNO)(^{t}Bu$_3$SiO)Si=O]$_2$ (**11**) S38
1.14 Synthesis of (IDippN)(^{t}Bu$_3$SiO)Si(B(C$_6$F$_5$)$_3$) (**12a**) S41
1.15 Synthesis of (IDippN)(^{t}Bu$_3$SiO)Si=O(IMe$_4$) (**13a**) S43
1.16 Synthesis and Reactivity of (IDippN)(^{t}Bu$_3$SiO)Si=O(I^{i}Pr$_2$Me$_2$) (**13b**) S46
1.17 Synthesis of (IDippN)(^{t}Bu$_3$SiO)Si=O(DMAP) (**13c**) S53
1.18 Synthesis of Aryl(boryloxy)silane **14** S56
2. X-ray Crystallographic Data S59
3. References S75

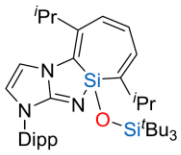
1. Experimental Section

1.1 General Methods and Instrumentation

All manipulations were carried out under exclusion of H_2O and O_2 under an atmosphere of argon 4.6 (≥99.996%; *Westfalen AG*) using standard *Schlenk* techniques or in a *LABstar* glovebox from *MBraun Inertgas-Systeme GmbH* with H_2O and O_2 levels below 0.5 ppm. The glassware used was heat dried under fine vacuum prior to use with *Triboflon III* grease (mixture of polytetrafluoroethylene (PTFE) and perfluoropolyether (PFPE)) from *Freudenberg & Co. KG* as sealant. All solvents were refluxed over sodium/benzophenone, freshly distilled under argon and deoxygenated before use. Deuterated benzene was obtained from *Sigma-Aldrich Chemie GmbH*, dried over Na/K alloy, flask-to-flask condensed, deoxygenated by three freeze-pump-thaw cycles and stored over 3 Å molecular sieves in the glovebox. All NMR samples were prepared under argon in *J. Young* PTFE valve NMR tubes. The NMR spectra were recorded on *Bruker AV400US* (^{1}H: 400.13 MHz, ^{11}B 128.38 MHz), *Avance Neo 400* (^{1}H: 400.23 MHz, ^{13}C: 100.65 MHz, ^{31}P: 162.01 MHz), *AV500* (^{1}H: 500.13 MHz) or *AV500C* (^{1}H: 500.36 MHz, ^{13}C: 125.83 MHz, ^{19}F: 470.77 MHz, ^{29}Si: 99.41 MHz, ^{31}P: 202.57 MHz) spectrometers at ambient temperature (300 K). The ^{1}H, ^{13}C{^{1}H} and ^{29}Si{^{1}H} NMR spectroscopic chemical shifts δ are reported in ppm relative to tetramethylsilane. ^{1}H and ^{13}C{^{1}H} NMR spectra are calibrated against the residual proton and natural abundance carbon resonances of the deuterated solvent as internal standard (C_6D_6: δ(^{1}H) = 7.16 ppm and δ(^{13}C) = 128.1 ppm).[S1] The following abbreviations are used to describe signal multiplicities: s = singlet, d = doublet, t = triplet, sept = septet, m = multiplet, br = broad and combinations thereof (*e.g.* dd = doublet of doublets). Some NMR spectra include resonances for silicone grease (C_6D_6: δ(^{1}H) = 0.29 ppm, δ(^{13}C) = 1.4 ppm and δ(^{29}Si) = –21.8 ppm) derived from *B. Braun Melsungen AG Sterican®* cannulas. Quantitative elemental analyses (EA) were carried out using a *EURO EA* (*HEKAtech*) instrument equipped with a CHNS combustion analyzer at the *Laboratory for Microanalysis* at the *TUM Catalysis Research Center*. Elemental analyses provided partially and reproducibly low carbon percentages (~1% deviation), presumably due to the formation of incombustible SiC compounds. Melting Points (m.p.) were determined in sealed glass capillaries under inert gas by a *Büchi M-565* melting point apparatus. Mass spectra (Liquid Injection Field Desorption Ionization (LIFDI)-MS) were recorded on a *Waters Micromass LCT TOF* mass spectrometer equipped with a LIFDI-ion source (*LIFDI-700*) from *Linden CMS GmbH*. The samples were provided as filtered solution in toluene. Photochemical experiments were carried out using an *Asahi Spectra Co., Ltd. MAX-302* Xenon

Light Source at λ_{max} = 340 nm. Unless otherwise stated, all commercially available reagents were purchased from *abcr GmbH* or *Sigma-Aldrich Chemie GmbH* and used without further purification. Carbon dioxide (CO_2) 5.0 (≥99.999%), dinitrogen monoxide (N_2O) 5.0 (≥99.999%) and oxygen (O_2) 5.0 (≥99.999%) were purchased from *Westfalen AG* and used as received. The compounds iminosiloxysilylene (IDippN)(^{t}Bu$_3$SiO)Si: (**1**)[S2], 1,3,4,5-tetramethylimidazolin-2-ylidene (IMe_4)[S3] and 1,3-diisopropyl-4,5-dimethylimidazolin-2-ylidene ($I^iPr_2Me_2$)[S3] were prepared as described in the corresponding references. Azido(di-*tert*-butylmethyl)silane (^{t}Bu$_2$MeSiN$_3$) was synthesized *via* a modified literature procedure (*vide infra*).[S4] White phosphorus (P_4) was sublimed and stored at –35 °C in the dark in the glovebox.

1.2 Synthesis of Iminosiloxysilepin 2



2
$C_{39}H_{63}N_3OSi_2$
646.12 g/mol

A *J. Young* PTFE valve NMR tube was charged with a solution of silylene **1** (50.0 mg, 77.4 µmol) in C_6D_6 (0.5 mL). After irradiation (λ_{max} = 340 nm) at room temperature for 4 h, quantitative conversion was detected by ^{1}H NMR spectroscopy. Removal of the solvent *in vacuo* provided iminosiloxysilepin **2** as a pale yellow solid (50.0 mg, 77.4 µmol, quantitative yield). Compound **2** is completely stable as a solid and in solution at ambient and elevated temperatures (≤130 °C).

m.p.: 181-182 °C.

^{1}H NMR (500 MHz, C_6D_6, 300 K): δ [ppm] = 7.20–7.14 (m, 2H, *m*-/*p*-$C_{Dipp}\underline{H}$, overlapping with solvent signal), 7.07 (dd, ^4J = 1.9 Hz, ^3J = 7.3 Hz, 1H, *m*-$C_{Dipp}\underline{H}$), 6.83 (d, ^3J = 7.2 Hz, 1H, $C_{silepin}\underline{H}$), 6.70 (d, ^3J = 2.9 Hz, 1H, NC$\underline{H}$), 6.55 (d, ^3J = 13.2 Hz, 1H, $C_{silepin}\underline{H}$), 6.42 (dd, ^3J = 13.2 Hz, ^3J = 6.9 Hz, 1H, $C_{silepin}\underline{H}$), 5.87 (d, ^3J = 2.9 Hz, 1H, NC$\underline{H}$), 3.34 (sept, ^3J = 6.9 Hz, 1H, C$\underline{H}$(CH$_3$)$_2$), 3.06 (sept, ^3J = 7.1 Hz, 1H, C$\underline{H}$(CH$_3$)$_2$), 2.97 (sept, ^3J = 6.7 Hz, 1H, C$\underline{H}$(CH$_3$)$_2$), 2.87 (sept, ^3J = 6.9 Hz, 1H, C$\underline{H}$(CH$_3$)$_2$), 1.40 (d, ^3J = 6.9 Hz, 3H, CH(C$\underline{H}_3$)$_2$), 1.37 (d, ^3J = 7.0 Hz, 3H, CH(C$\underline{H}_3$)$_2$), 1.36 (d, ^3J = 6.7 Hz, 3H, CH(C$\underline{H}_3$)$_2$), 1.25 (d, ^3J = 6.9 Hz, 3H, CH(C$\underline{H}_3$)$_2$), 1.22 (d, ^3J = 6.9 Hz, 3H, CH(C$\underline{H}_3$)$_2$), 1.20 (d, ^3J = 6.9 Hz, 3H, CH(C$\underline{H}_3$)$_2$), 1.13 (s, 27H, C(C$\underline{H}_3$)$_3$), 1.07 (d, ^3J = 6.9 Hz, 3H, CH(C$\underline{H}_3$)$_2$), 0.93 (d, ^3J = 6.9 Hz, 3H, CH(C$\underline{H}_3$)$_2$).

^{13}C{^{1}H} NMR (126 MHz, C_6D_6, 300 K): δ [ppm] = 157.6 (C), 151.1 (C), 148.0 (C), 147.5 (C), 133.9 (C), 133.8 (C), 132.1 (CH), 132.0 (C), 129.7 (CH), 128.6 (CH), 126.6 (CH), 124.3 (CH), 123.9 (CH), 117.1 (NCH), 110.5 (NCH), 36.1 (CH(CH$_3$)$_2$), 30.2 (C(CH$_3$)$_3$), 29.5 (CH(CH$_3$)$_2$), 28.9 (CH(CH$_3$)$_2$), 28.7 (CH(CH$_3$)$_2$), 25.5 (CH(CH$_3$)$_2$), 25.1 (CH(CH$_3$)$_2$), 24.7 (CH(CH$_3$)$_2$), 23.9

($CH(\underline{C}H_3)_2$), 23.7 ($CH(\underline{C}H_3)_2$), 23.2 ($\underline{C}(CH_3)_3$), 23.2 ($CH(\underline{C}H_3)_2$), 22.1 ($CH(\underline{C}H_3)_2$), 22.0 ($CH(\underline{C}H_3)_2$).

$^{29}Si\{^1H\}$ NMR (99 MHz, C_6D_6, 300 K): δ [ppm] = 4.7 (*$\underline{Si}$*^{t}Bu$_3$), –15.5 (*$\underline{silepin\ Si}$*).

Anal. Calcd. [%] for $C_{39}H_{63}N_3OSi_2$: C, 72.50; H, 9.83; N, 6.50. Found [%]: C, 72.25; H, 9.80; N, 6.49.

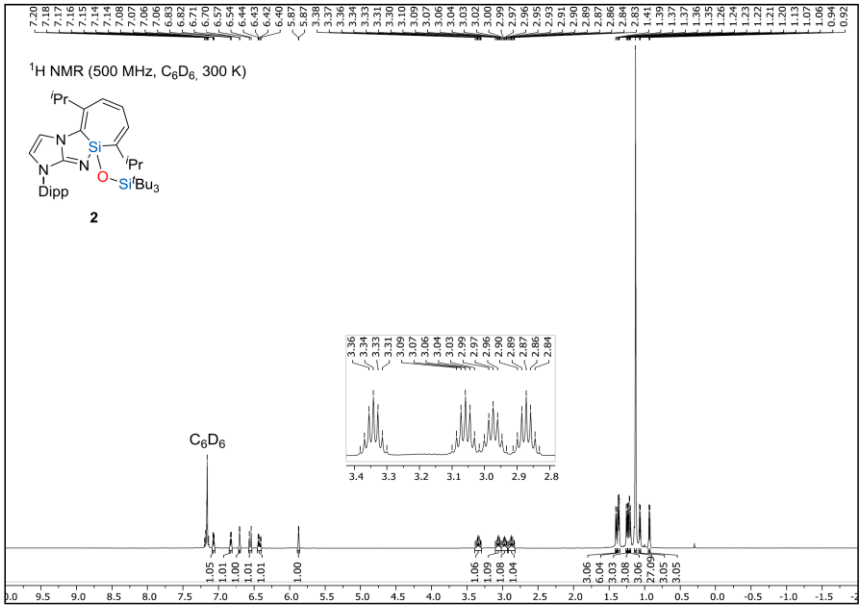


Figure S1. ^{1}H NMR spectrum of iminosiloxysilepin **2** in C_6D_6 at 300 K.

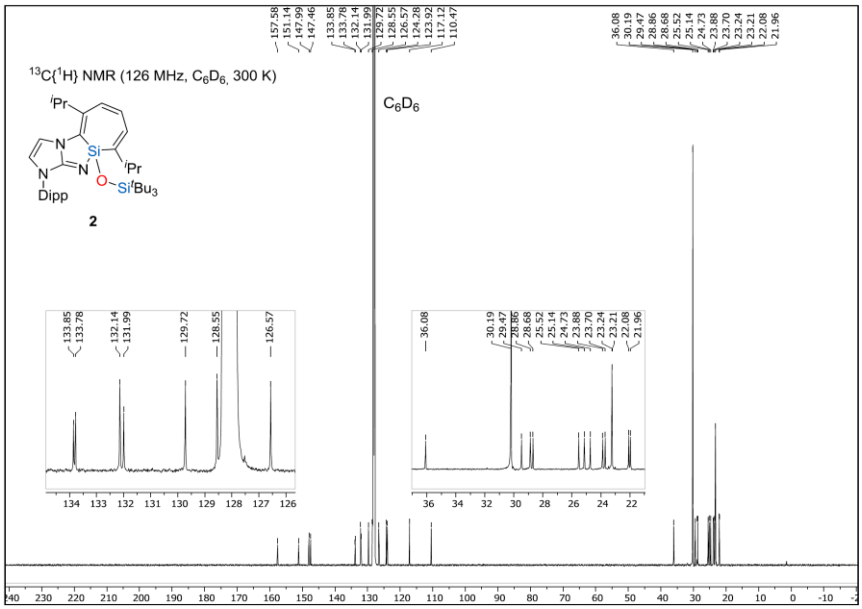


Figure S2. $^{13}C\{^1H\}$ NMR spectrum of iminosiloxysilepin **2** in C_6D_6 at 300 K.

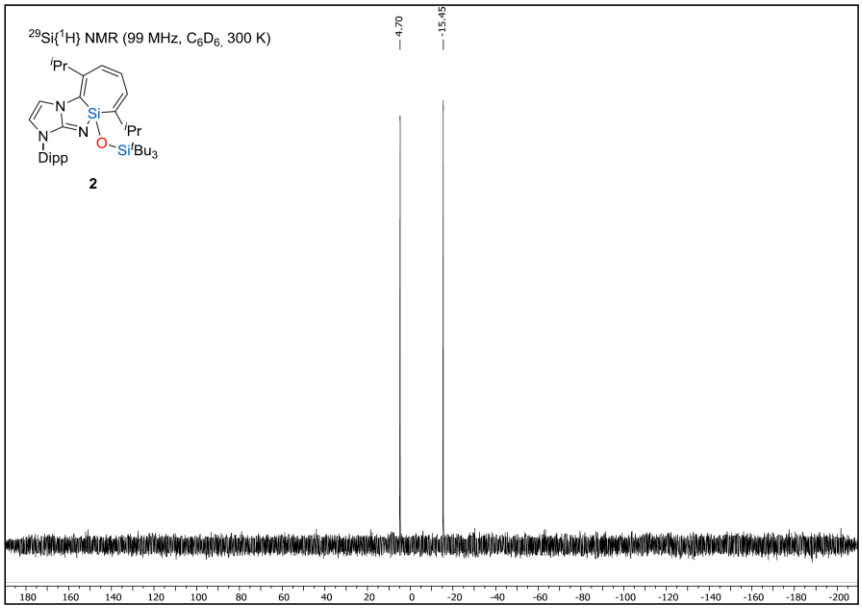


Figure S3. $^{29}Si\{^1H\}$ NMR spectrum of iminosiloxysilepin **2** in C_6D_6 at 300 K.

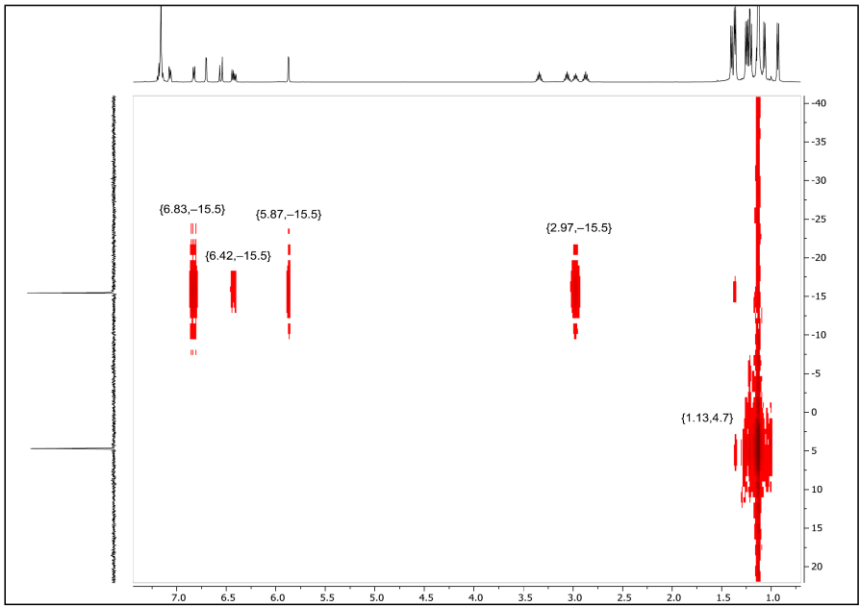


Figure S4. $^{1}H/^{29}Si$ HMBC NMR spectrum of iminosiloxysilepin **2** in C_6D_6 at 300 K.

1.3 Synthesis of (IDippN)(^{t}Bu$_3$SiO)Si(P$_4$) (3)



3
$C_{39}H_{63}N_3OP_4Si_2$
770.02 g/mol

To a mixture of silylene **1** (100 mg, 155 µmol, 1.0 eq.) and P$_4$ (19.2 mg, 155 µmol, 1.0 eq.) was added benzene (3 mL). The Reaction mixture was stirred for 3 h whereby a color change from colorless to orange was observed. After removal of the solvent *in vacuo*, (IDippN)(^{t}Bu$_3$SiO)Si(P$_4$) (**3**) was obtained as a pale orange solid (119 mg, 155 µmol, quantitative yield). Colorless crystals, suitable for single-crystal X-ray diffraction (SC-XRD) analysis, were obtained by cooling a saturated *n*-hexane solution of **3** to –35 °C for several days. Compound **3** is completely stable as a solid and in solution at ambient temperature.

Note: Compound **3** reacts selectively with an equimolar amount of silylene **1** to form a new product, which is most likely ((IDippN)(^{t}Bu$_3$SiO)Si)$_2$(P$_4$), but the reaction is extremely slow (only ~10% conversion after 10 days at 110 °C in benzene detected) and thus was not further studied. A similar reaction between an R$_2$Si(P$_4$) cage compound and a silylene R$_2$Si: was reported previously.[S5]

m.p.: 120-121 °C (decomposition; color change from pale orange to orange).

^{1}H NMR (500 MHz, C$_6$D$_6$, 300 K): δ [ppm] = 7.23–7.18 (m, 6H, C$_{ar}$*H*), 6.01 (s, 2H, NC*H*), 3.25 (sept, ^3J = 6.9 Hz, 4H, C*H*(CH$_3$)$_2$), 1.49 (d, ^3J = 6.9 Hz, 12H, CH(C*H*$_3$)$_2$), 1.17 (s, 27H, C(C*H*$_3$)$_3$), 1.14 (d, ^3J = 6.9 Hz, 12H, CH(C*H*$_3$)$_2$).

$^{13}C\{^1H\}$ NMR (126 MHz, C_6D_6, 300 K): δ [ppm] = 146.5 (*o*-$\underline{C}_{ar}$), 141.7 (N$\underline{C}$N), 134.7 (*ipso*-$\underline{C}_{ar}$), 130.1 (*p*-$\underline{C}_{ar}$H), 125.5 (*m*-$\underline{C}_{ar}$H), 115.5 (N$\underline{C}$H), 30.7 (C($\underline{C}$H$_3$)$_3$), 29.1 ($\underline{C}$H(CH$_3$)$_2$), 24.9 (CH($\underline{C}$H$_3$)$_2$), 23.5 (CH($\underline{C}$H$_3$)$_2$), 23.4 (CH($\underline{C}$H$_3$)$_2$), 23.0 ($\underline{C}$(CH$_3$)$_3$).

$^{29}Si\{^1H\}$ NMR (99 MHz, C_6D_6, 300 K): δ [ppm] = 5.1 ($\underline{Si}$^{t}Bu$_3$), –87.9 (broad s, $\underline{Si}$P$_4$).

$^{31}P\{^1H\}$ NMR (203 MHz, C_6D_6, 300 K): δ [ppm] = 152.1 (dd, $^1J(P_2P_1)$ = 157.6 Hz, $^1J(P_3P_1)$ = 149.6 Hz, 2P, Si$\underline{P}_1$), –327.7 (dt, $^1J(P_2P_3)$ = 181.6 Hz, $^1J(P_1P_3)$ = 149.6 Hz, 1P, $\underline{P}_3$), –337.0 (dt, $^1J(P_3P_2)$ = 181.6 Hz, $^1J(P_1P_2)$ = 157.6 Hz, 1P, $\underline{P}_2$). The assignment of the observed resonances to the respective ^{31}P nuclei can be found in **Figure S8** (*vide infra*).

Anal. Calcd. [%] for $C_{39}H_{63}N_3OP_4Si_2$: C, 60.83; H, 8.25; N, 5.46. Found [%]: C, 60.53; H, 8.24; N, 5.30.

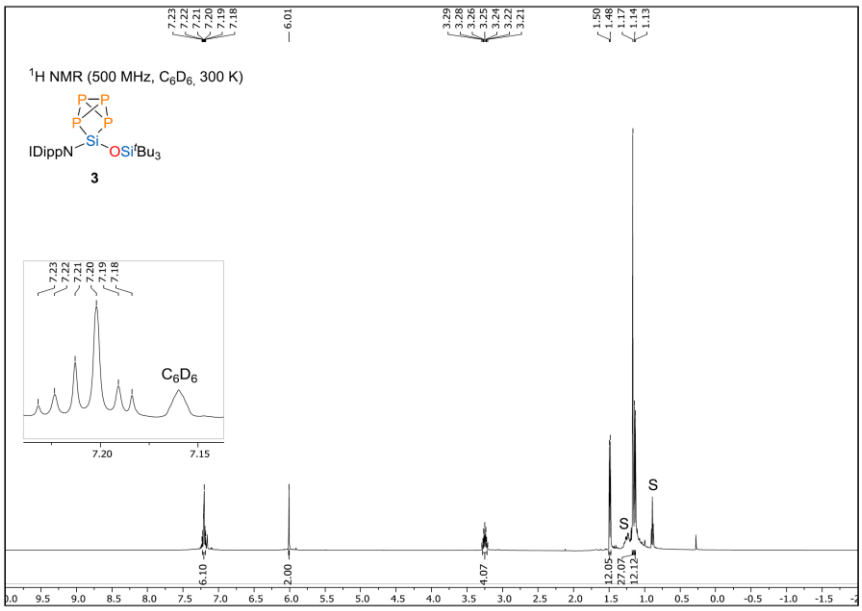


Figure S5. ^{1}H NMR spectrum of (IDippN)(^{t}Bu$_3$SiO)Si(P$_4$) (**3**) in C_6D_6 at 300 K. Residual *n*-hexane (from starting material) is labeled with S.

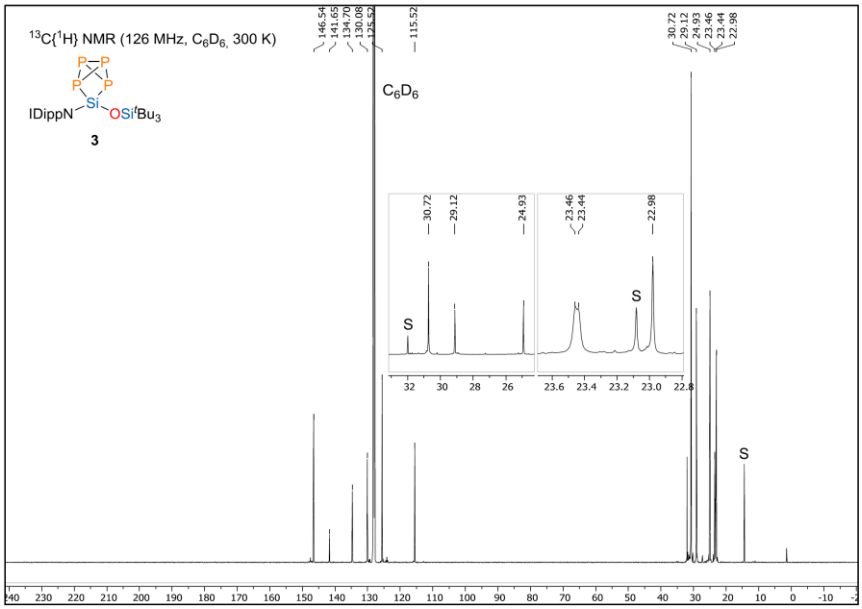


Figure S6. $^{13}C\{^1H\}$ NMR spectrum of (IDippN)(^{t}Bu$_3$SiO)Si(P$_4$) (**3**) in C_6D_6 at 300 K. Residual *n*-hexane (from starting material) is labeled with S.

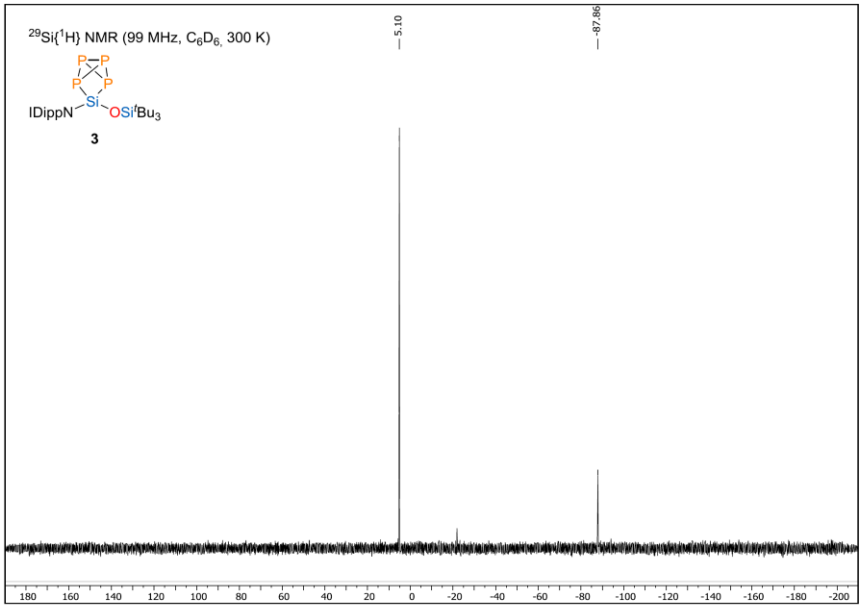


Figure S7. $^{29}Si\{^1H\}$ NMR spectrum of (IDippN)(^{t}Bu$_3$SiO)Si(P$_4$) (**3**) in C_6D_6 at 300 K.

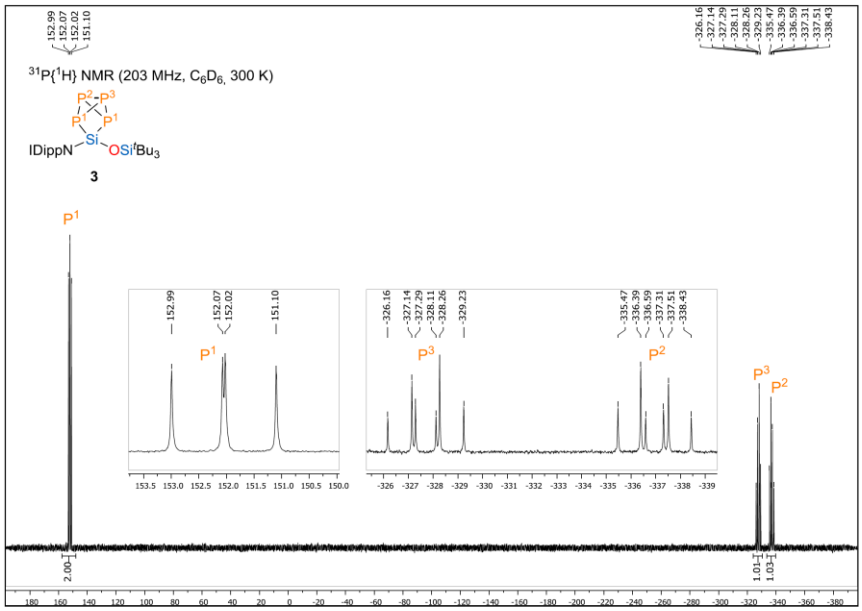
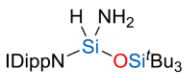


Figure S8. $^{31}P\{^{1}H\}$ NMR spectrum of (IDippN)(^{t}Bu$_3$SiO)Si(P$_4$) (**3**) in C_6D_6 at 300 K.

1.4 Synthesis of (IDippN)(^{t}Bu$_3$SiO)Si(H)(NH$_2$) (4)



4
$C_{39}H_{66}N_4OSi_2$
663.15 g/mol

To a cooled (–80 °C) solution of silylene **1** (300 mg, 464 µmol, 1.0 eq.) in *n*-hexane (10 mL) was added a 0.4 M NH_3 solution in 1,4-dioxane (1.16 mL, 7.91 mg, 464 µmol, 1.0 eq.) under vigorous stirring. An immediate precipitation (1,4-dioxane) was observed. After stirring was continued at –80 °C for one hour, the solution was warmed to ambient temperature. All volatiles were removed *in vacuo*, affording crude aminosilane **4** as a colorless solid. Multinuclear and 2D NMR analysis clearly revealed **4** as the major product. However, all further purification attempts via crystallization, sublimation or washing were unsuccessful so far.

Note: Since the central silicon atom is chiral, the small by-product could be a stereoisomer of **4**. In addition, (IDippN)(^{t}Bu$_3$SiO)Si(H)(NH$_2$) (**4**) reacts with excessive amounts of ammonia to an unidentified mixture of products, presumably also including elimination of the imino ligand under formation of IDippNH and (H$_2$N)(^{t}Bu$_3$SiO)Si(H)(NH$_2$). A similar σ-bond metathesis reaction between an Si–N bond and ammonia was previously observed.[S6]

^{1}H NMR (500 MHz, C$_6$D$_6$, 300 K): δ [ppm] = 7.24–7.21 (m, 2H, *p*-C$_{ar}$*H*), 7.14–7.11 (m, 4H, *m*-C$_{ar}$*H*), 5.95 (s, 2H, NC*H*), 4.81 (s, 1H, Si*H*, $^{1}J_{SiH}$ = 243.8 Hz), 3.20 (sept, ^{3}J = 6.9 Hz, 2H, C*H*(CH$_3$)$_2$), 3.09 (sept, ^{3}J = 6.9 Hz, 2H, C*H*(CH$_3$)$_2$), 1.42 (d, ^{3}J = 6.9 Hz, 6H, CH(C*H*$_3$)$_2$), 1.41 (d,

^3J = 6.9 Hz, 6H, CH(C$\underline{H}_3$)$_2$), 1.18 (d, ^3J = 6.9 Hz, 6H, CH(C$\underline{H}_3$)$_2$), 1.17 (d, ^3J = 6.9 Hz, 6H, CH(C$\underline{H}_3$)$_2$), 1.06 (s, 27H, C(C$\underline{H}_3$)$_3$), –0.14 (br s, 2H. N$\underline{H}_2$).

^{13}C{^{1}H} NMR (126 MHz, C$_6$D$_6$, 300 K): δ [ppm] = 148.2 (*o*-$\underline{C}_{ar}$), 148.0 (*o*-$\underline{C}_{ar}$), 143.7 (N$\underline{C}$N), 134.6 (*ipso*-$\underline{C}_{ar}$), 130.0 (*p*-$\underline{C}_{ar}$H), 124.2 (*m*-$\underline{C}_{ar}$H), 124.0 (*m*-$\underline{C}_{ar}$H), 114.2 (N$\underline{C}$H), 30.2 (C($\underline{C}$H$_3$)$_3$), 29.1 ($\underline{C}$H(CH$_3$)$_2$), 25.5 (CH($\underline{C}$H$_3$)$_2$), 24.0 (CH($\underline{C}$H$_3$)$_2$), 23.2 ($\underline{C}$(CH$_3$)$_3$).

^{29}Si{^{1}H} NMR (99 MHz, C$_6$D$_6$, 300 K): δ [ppm] = 1.3 ($\underline{Si}$^{t}Bu$_3$), –66.5 ($\underline{Si}$NH$_2$).

^{29}Si INEPT NMR (99 MHz, C$_6$D$_6$, 300 K): δ [ppm] = 1.3 ($\underline{Si}$^{t}Bu$_3$), –66.5 (d, $^1J_{HSi}$ = 243.8 Hz, $\underline{Si}$NH$_2$).

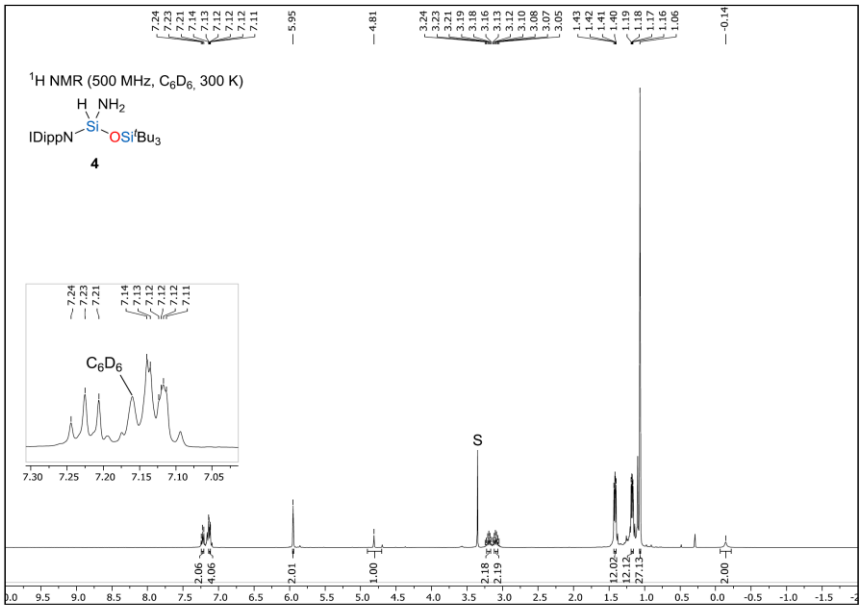


Figure S9. ^{1}H NMR spectrum of (IDippN)(^{t}Bu$_3$SiO)Si(H)(NH$_2$) (**4**) in C$_6$D$_6$ at 300 K. Residual 1,4-dioxane is marked with an S.

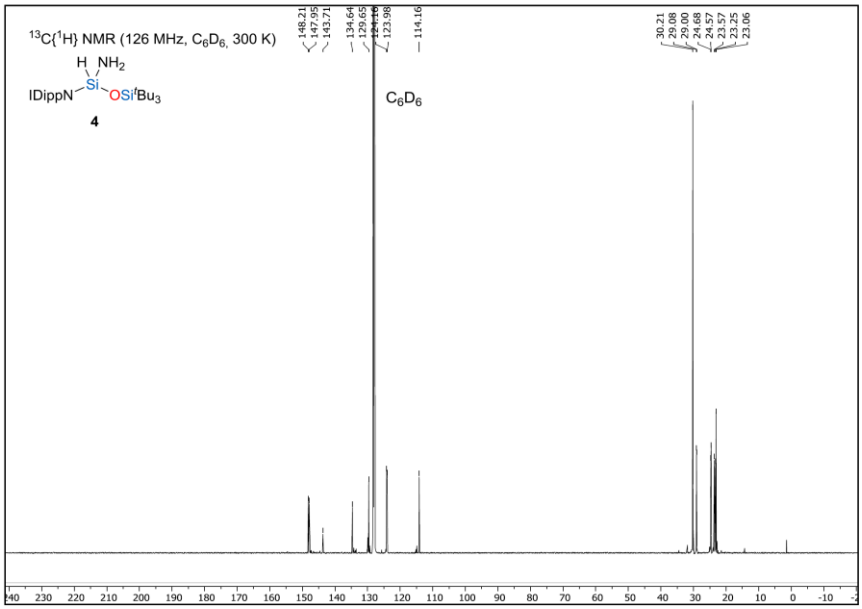


Figure S10. $^{13}C\{^1H\}$ NMR spectrum of (IDippN)(^{t}Bu$_3$SiO)Si(H)(NH$_2$) (**4**) in C_6D_6 at 300 K.

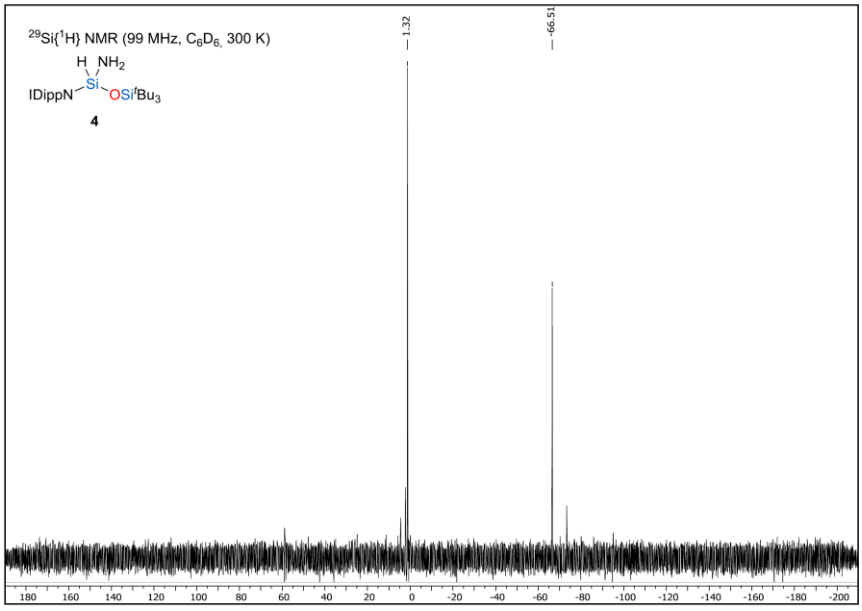


Figure S11. $^{29}Si\{^1H\}$ NMR spectrum of (IDippN)(^{t}Bu$_3$SiO)Si(H)(NH$_2$) (**4**) in C_6D_6 at 300 K.

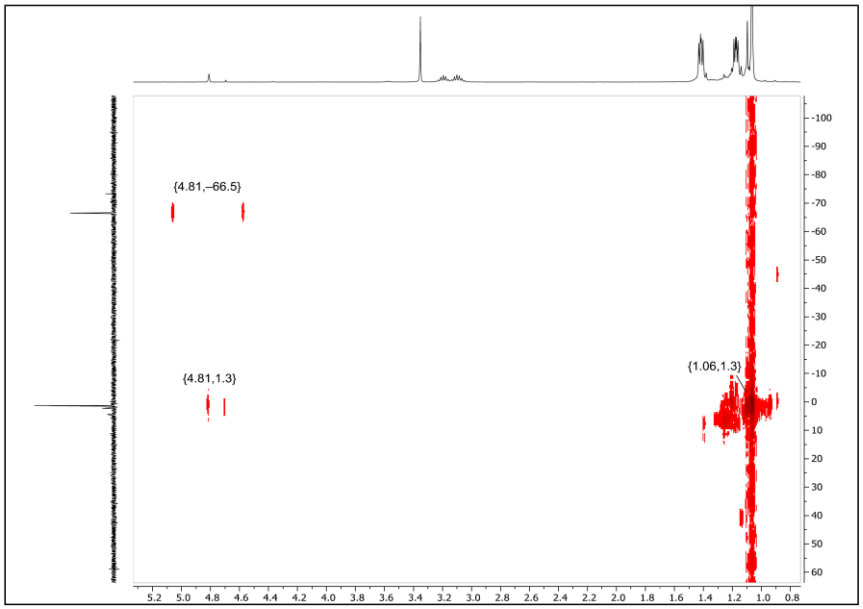


Figure S12. $^{1}H/^{29}Si$ HMBC NMR spectrum of (IDippN)(^{t}Bu$_3$SiO)Si(H)(NH$_2$) (**4**) in C_6D_6 at 300 K.

1.5 Synthesis of (IDippN)(^{t}Bu$_3$SiO)Si(NTMSN)$_2$ (5)



5

$C_{45}H_{81}N_7OSi_4$

848.53 g/mol

To a stirred solution of silylene **1** (50.0 mg, 77.4 µmol, 1.0 eq.) in benzene (2 mL) was added $TMSN_3$ (20.5 µL, 17.8 mg, 155 µmol, 2.0 eq.). After an immediately observed gas evolution (N_2), the reaction mixture was stirred for further 30 min. Removal of all volatiles *in vacuo* provided silatetrazoline **5** as a colorless solid (65.7 mg, 77.4 µmol, quantitative yield).

m.p.: 263-264 °C (decomposition; color change from colorless to yellow).

^{1}H NMR (500 MHz, C_6D_6, 300 K): δ [ppm] = 7.22–7.19 (m, 2H, *p*-C$_{ar}$*H*), 7.16–7.13 (m, 4H, *m*-C$_{ar}$*H*, overlapping with solvent signal), 5.89 (s, 2H, NC*H*), 3.30 (sept, ^{3}J = 6.9 Hz, 2H, C*H*(CH$_3$)$_2$), 3.18 (sept, ^{3}J = 6.9 Hz, 2H, C*H*(CH$_3$)$_2$), 1.46 (d, ^{3}J = 6.9 Hz, 6H, CH(C*H*$_3$)$_2$), 1.43 (d, ^{3}J = 6.9 Hz, 6H, CH(C*H*$_3$)$_2$), 1.16 (s, 27H, C(C*H*$_3$)$_3$), 1.09 (pseudo t, ^{3}J = 6.9 Hz, 12H, CH(C*H*$_3$)$_2$), 0.28 (s, 9H, *TMS*), 0.24 (s, 9H, *TMS*).

^{13}C{^{1}H} NMR (126 MHz, C_6D_6, 300 K): δ [ppm] = 147.4 (*o*-C$_{ar}$), 147.4 (*o*-C$_{ar}$), 141.9 (NCN), 135.8 (*ipso*-C$_{ar}$), 129.7 (*p*-C$_{ar}$H), 125.0 (*m*-C$_{ar}$H), 124.7 (*m*-C$_{ar}$H), 116.5 (NCH), 31.0 (C(CH$_3$)$_3$), 29.5 (CH(CH$_3$)$_2$), 29.1 (CH(CH$_3$)$_2$), 26.3 (CH(CH$_3$)$_2$), 25.8 (CH(CH$_3$)$_2$), 23.2 (CH(CH$_3$)$_2$), 23.1 (C(CH$_3$)$_3$), 23.1 (CH(CH$_3$)$_2$), 6.6 (*TMS*), 6.4 (*TMS*).

^{29}Si{^{1}H} NMR (99 MHz, C_6D_6, 300 K): δ [ppm] = 4.7 (*Si*^{t}Bu$_3$), 2.3 (*TMS*), 0.7 (*TMS*), –90.6 (*Si*(NTMSN)$_2$).

Anal. Calcd. [%] for $C_{45}H_{81}N_7OSi_4$: C, 63.70; H, 9.62; N, 11.56. Found [%]: C, 63.86; H, 9.86; N, 11.29.

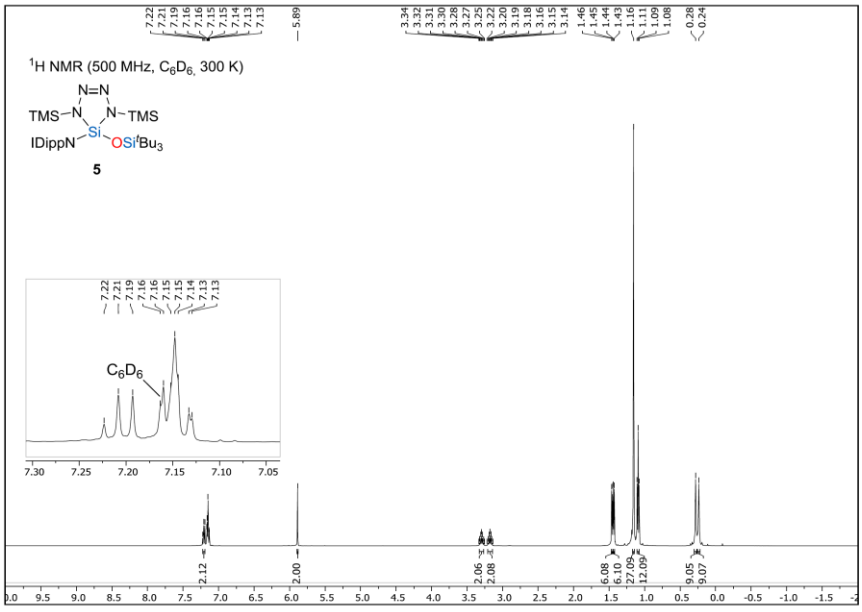


Figure S13. ^{1}H NMR spectrum of (IDippN)(^{t}Bu$_3$SiO)Si(NTMSN)$_2$ (**10**) in C_6D_6 at 300 K.

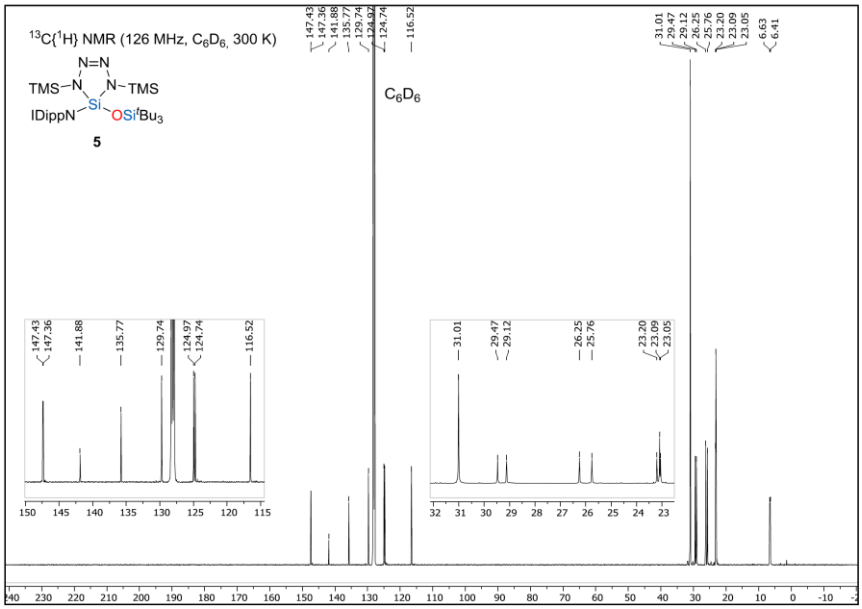


Figure S14. $^{13}C\{^1H\}$ NMR spectrum of (IDippN)(^{t}Bu$_3$SiO)Si(NTMSN)$_2$ (**5**) in C_6D_6 at 300 K.

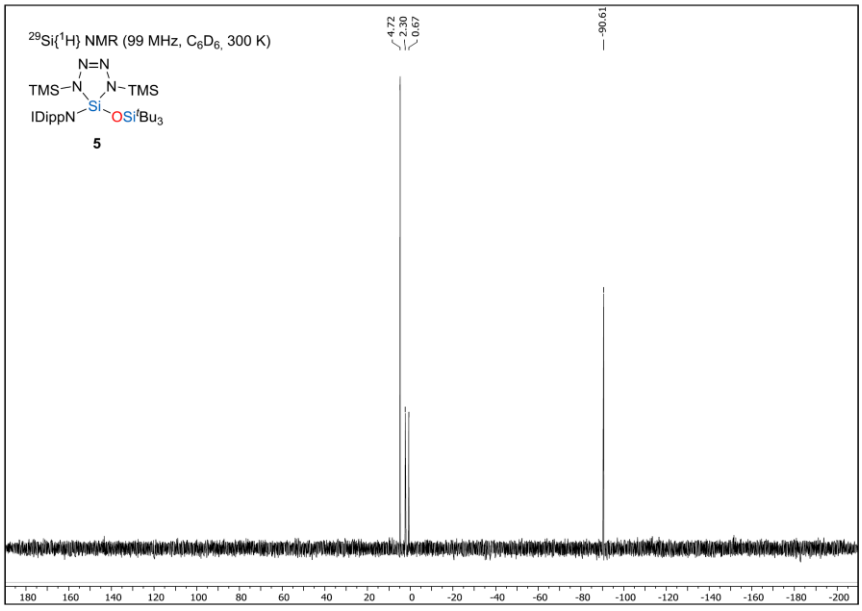


Figure S15. $^{29}Si\{^1H\}$ NMR spectrum of (IDippN)(^{t}Bu$_3$SiO)Si(NTMSN)$_2$ (**5**) in C_6D_6 at 300 K.

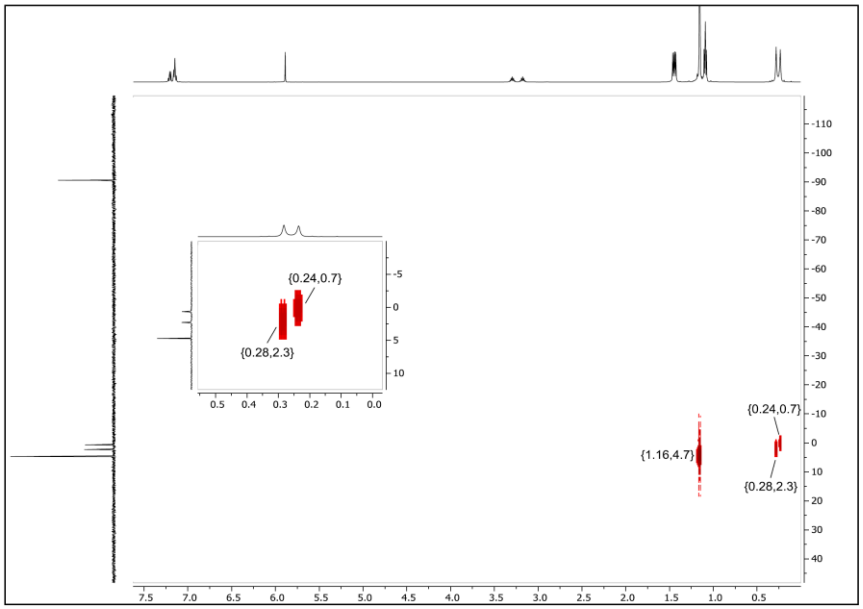
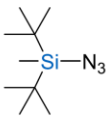


Figure S16. $^{1}H/^{29}Si$ HMBC NMR spectrum of (IDippN)($^{t}Bu_3SiO$)Si(NTMSN)$_2$ (**5**) in C_6D_6 at 300 K.

1.6 Synthesis of (IDippN)($^{t}Bu_3SiO$)Si=NSi$^{t}Bu_2$Me (6)

Synthesis of Azido(di-*tert*-butylmethyl)silane $^{t}Bu_2MeSiN_3$

The following procedure represents a modified version of a method that has already been reported.[S4]



$C_9H_{21}N_3Si$
199.37 g/mol

To a mixture of $^{t}Bu_2MeSiBr$ (3.00 g, 12.6 mmol, 1.0 eq.) and NaN_3 (2.47 g, 37.9 mmol, 3.0 eq) was added THF (20 mL). The resulting colorless suspension was heated under reflux for 48 h. Subsequently, the product solution was flask-to-flask condensed (50 °C / 5.0 × 10^{-3} mbar) to remove excess sodium azide. Removal of THF *in vacuo* at 0 °C provided analytically pure $^{t}Bu_2MeSiN_3$ as a colorless liquid (2.14 g, 10.7 mmol, 85%).

^{1}H NMR (500 MHz, C_6D_6, 300 K): δ [ppm] = 0.90 (s, 18H, C(C$\underline{H}_3$)$_3$), –0.01 (s, 3H, SiC$\underline{H}_3$).

^{13}C{^{1}H} NMR (126 MHz, C_6D_6, 300 K): δ [ppm] = 27.4 (C($\underline{C}$H$_3$)$_3$), 21.0 ($\underline{C}$(CH$_3$)$_3$), –9.0 (Si$\underline{C}$H$_3$).

^{29}Si{^{1}H} NMR (99 MHz, C_6D_6, 300 K): δ [ppm] = 17.7 ($\underline{Si}$CH$_3$).

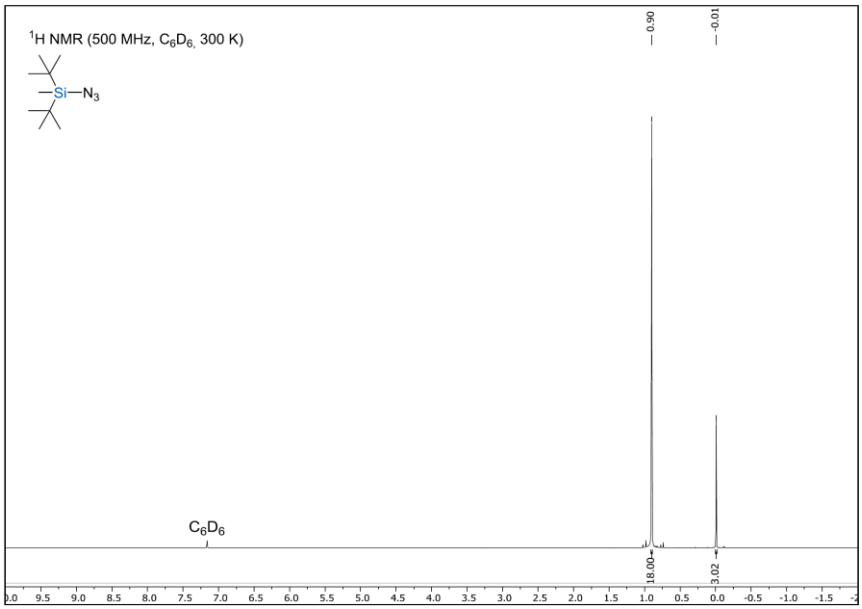


Figure S17. ^{1}H NMR spectrum of ^{t}Bu$_2$MeSiN$_3$ in C_6D_6 at 300 K.

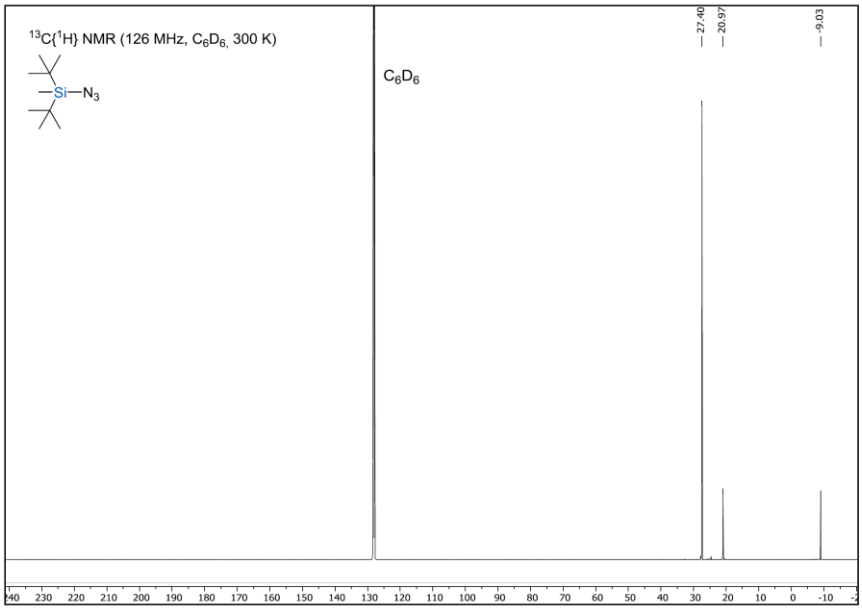


Figure S18. ^{13}C{^{1}H} NMR spectrum of ^{t}Bu$_2$MeSiN$_3$ in C_6D_6 at 300 K.

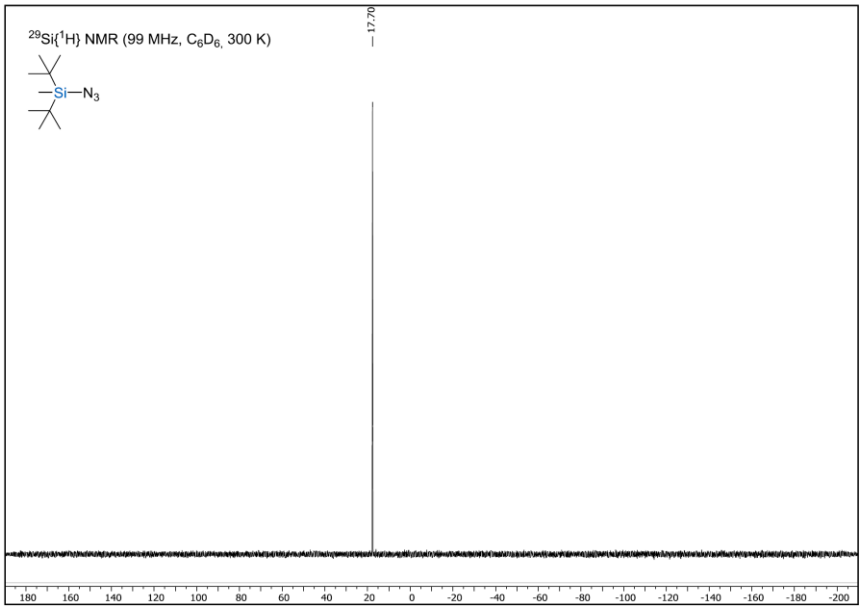
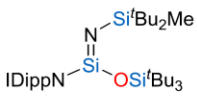


Figure S19. $^{29}Si\{^{1}H\}$ NMR spectrum of $^{t}Bu_2MeSiN_3$ in C_6D_6 at 300 K.

Synthesis of (IDippN)(^{t}Bu$_3$SiO)Si=NSi^{t}Bu$_2$Me (6)



6

$C_{48}H_{84}N_4OSi_3$

817.48 g/mol

To a stirred solution of silylene **1** (300 mg, 464 µmol, 1.0 eq.) in benzene (10 mL) was added a solution of $^{t}Bu_2MeSiN_3$ (92.6 mg, 464 µmol, 1.0 eq.) in benzene (1 mL). After an immediately observed gas evolution (N_2), the reaction mixture was stirred for an additional hour. Removal of all volatiles *in vacuo* afforded silaimine **6** as a colorless solid (380 mg, 464 µmol, quantitative yield). Crystals, suitable for SC-XRD analysis were obtained by cooling a concentrated *n*-hexane solution of **6** to –35 °C for several days. Silaimine **6** is completely stable as a solid and in solution at ambient temperature.

Note: At high temperatures a very slow decomposition to an unidentified mixture of products was observed (~5% decomposition after 24 h at 130 °C).

m.p.: 302-303 °C (decomposition; color change from colorless to yellow).

^{1}H NMR (500 MHz, C$_6$D$_6$, 300 K): δ [ppm] = 7.21–7.18 (m, 2H, *p*-C$_{ar}$*H*), 7.13–7.11 (m, 4H, *m*-C$_{ar}$*H*), 6.01 (s, 2H, NC*H*), 3.15 (sept, ^{3}J = 6.9 Hz, 4H, C*H*(CH$_3$)$_2$), 1.40 (d, ^{3}J = 6.9 Hz, 12H, CH(C*H*$_3$)$_2$), 1.14 (s, 18H, Si^{t}*Bu*$_2$Me), 1.11 (s, 27H, Si^{t}*Bu*$_3$), 1.08 (d, ^{3}J = 6.9 Hz, 12H, CH(C*H*$_3$)$_2$), 0.16 (s, 3H, Si^{t}Bu$_2$*Me*).

$^{13}C\{^1H\}$ NMR (126 MHz, C_6D_6, 300 K): δ [ppm] = 146.5 (*o*-$\underline{C}_{ar}$), 141.1 (N$\underline{C}$N), 133.5 (*ipso*-$\underline{C}_{ar}$), 129.9 (*p*-$\underline{C}_{ar}$H), 125.0 (*m*-$\underline{C}_{ar}$H), 115.5 (N$\underline{C}$H), 30.3 (Si(C($\underline{C}$H$_3$)$_3$)$_3$), 29.7 (Si(C($\underline{C}$H$_3$)$_3$)$_2$Me), 29.0 ($\underline{C}$H(CH$_3$)$_2$), 25.2 (CH($\underline{C}$H$_3$)$_2$), 23.5 (CH($\underline{C}$H$_3$)$_2$), 23.2 (Si($\underline{C}$(CH$_3$)$_3$)$_3$), 21.2 (Si($\underline{C}$(CH$_3$)$_3$)$_2$Me), –6.6 (Si(C(CH$_3$)$_3$)$_2$$\underline{Me}$).

$^{29}Si\{^1H\}$ NMR (99 MHz, C_6D_6, 300 K): δ [ppm] = 6.8 ($\underline{Si}$^{t}Bu$_3$), –6.7 ($\underline{Si}$^{t}Bu$_2$Me), –50.1 ($\underline{Si}$=N).

Anal. Calcd. [%] for $C_{48}H_{84}N_4OSi_3$: C, 70.52; H, 10.36; N, 6.85. Found [%]: C, 70.35; H, 10.17; N, 6.84.

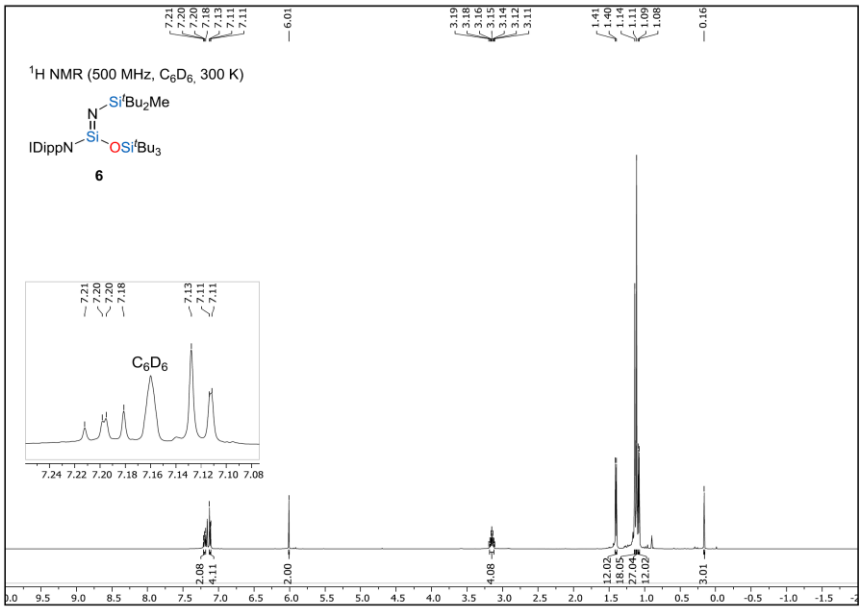


Figure S20. ^{1}H NMR spectrum of (IDippN)(^{t}Bu$_3$SiO)Si=NSi^{t}Bu$_2$Me (**6**) in C_6D_6 at 300 K.

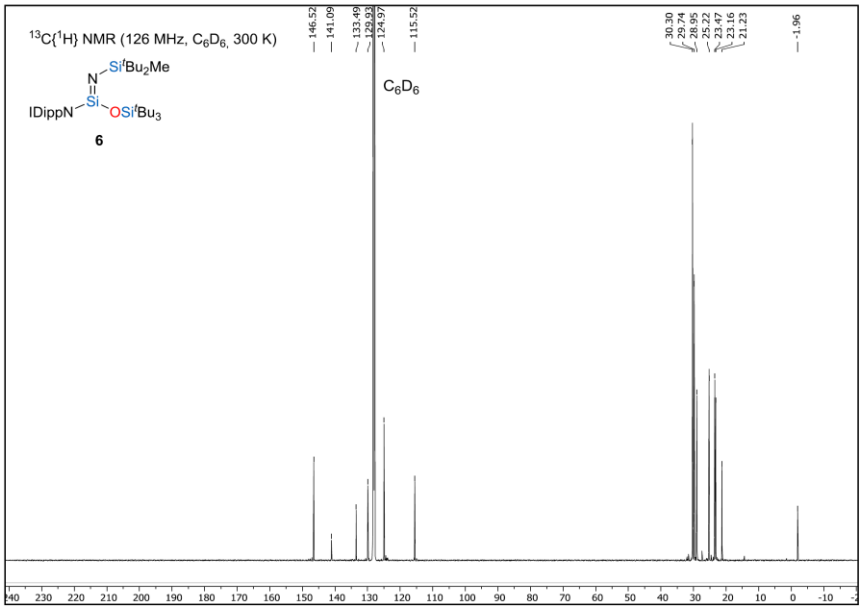


Figure S21. $^{13}C\{^{1}H\}$ NMR spectrum of (IDippN)(^{t}Bu$_3$SiO)Si=NSi^{t}Bu$_2$Me (**6**) in C_6D_6 at 300 K.

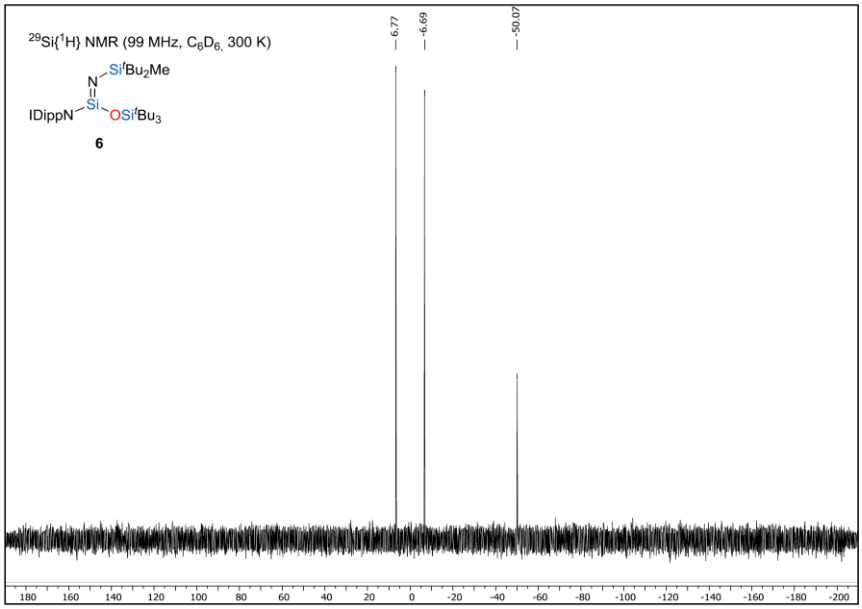


Figure S22. $^{29}Si\{^{1}H\}$ NMR spectrum of (IDippN)(^{t}Bu$_3$SiO)Si=NSi^{t}Bu$_2$Me (**6**) in C_6D_6 at 300 K.

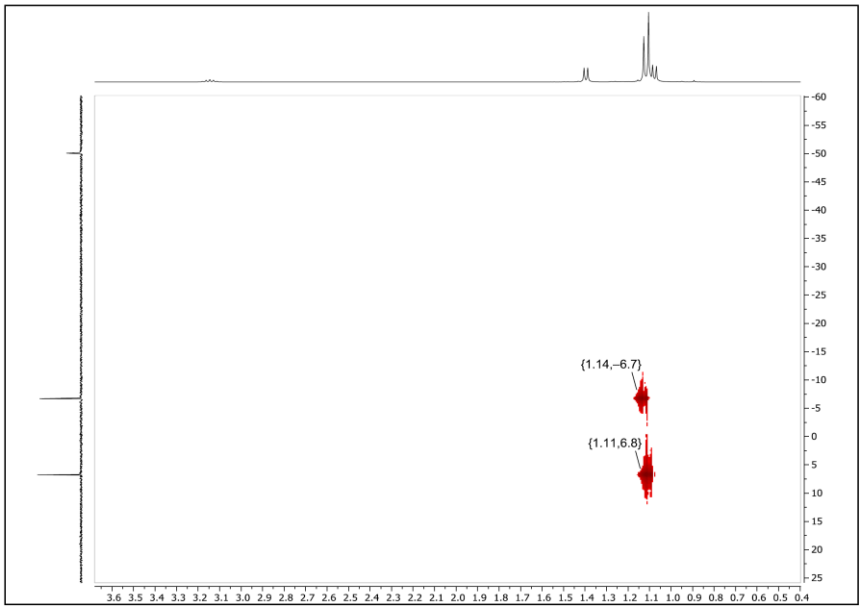
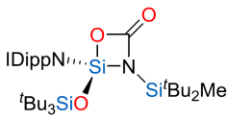


Figure S23. $^{1}H/^{29}Si$ HMBC NMR spectrum of (IDippN)($^{t}Bu_3SiO$)Si=NSi$^{t}Bu_2Me$ (**6**) in C_6D_6 at 300 K.

1.7 Synthesis of Azaoxasiletane (7)



7
$C_{49}H_{84}N_4O_3Si_3$
861.49 g/mol

A solution of silaimine **6** (75.0 mg, 91.8 µmol) in benzene (3 mL) was degassed and subsequently exposed to CO_2 (1 bar) under vigorous stirring at room-temperature. After stirring for additional 30 min, all volatiles were removed *in vacuo*. Azaoxasiletane **7** was afforded as a colorless solid (79.0 mg, 91.8 µmol, quantitative yield). Suitable crystals for SC-XRD analysis were obtained by cooling a saturated toluene solution of **7** to –35 °C for several days. Azaoxasiletane **7** is completely stable as a solid and in solution at room-temperature.

Note: At high temperatures a very slow decomposition to an unidentified mixture of products was observed (~10% decomposition after 24 h at 130 °C).

m.p.: 202-203 °C (decomposition; color change from colorless to yellow).

^{1}H NMR (500 MHz, C_6D_6, 300 K): δ [ppm] = 7.26–7.23 (m, 2H, *p*-$C_{ar}H$), 7.19–7.11 (m, 4H, *m*-$C_{ar}H$, overlapping with solvent signal), 6.05 (s, 2H, NCH), 3.21 (sept, ^{3}J = 6.9 Hz, 2H, CH(CH_3)$_2$), 3.09 (sept, ^{3}J = 6.9 Hz, 2H, CH(CH_3)$_2$), 1.50 (d, ^{3}J = 6.9 Hz, 6H, CH(CH_3)$_2$), 1.41 (d, ^{3}J = 6.9 Hz, 6H, CH(CH_3)$_2$), 1.20 (s, 9H, Si$^{t}Bu_2$Me), 1.08 (s, 36H, Si$^{t}Bu_3$ + Si$^{t}Bu_2$Me), 1.06 (d, ^{3}J = 6.9 Hz, 6H, CH(CH_3)$_2$), 1.05 (d, ^{3}J = 6.9 Hz, 6H, CH(CH_3)$_2$), 0.09 (s, 3H, Si^{t}Bu$_2$*Me*).

$^{13}C\{^1H\}$ NMR (126 MHz, C_6D_6, 300 K): δ [ppm] = 156.7 (*C*=O), 146.9 (*o*-*C*$_{ar}$), 146.6 (*o*-*C*$_{ar}$), 143.0 (N*C*N), 134.0 (*ipso*-*C*$_{ar}$), 130.1 (*p*-*C*$_{ar}$H), 124.9 (*m*-*C*$_{ar}$H), 124.7 (*m*-*C*$_{ar}$H), 116.3 (N*C*H), 30.3 (Si(C(*C*H$_3$)$_3$)$_3$), 29.2 (Si(C(*C*H$_3$)$_3$)$_2$Me), 29.1 (*C*H(CH$_3$)$_2$), 29.0 (*C*H(CH$_3$)$_2$), 25.8 (CH(*C*H$_3$)$_2$), 25.7 (CH(*C*H$_3$)$_2$), 23.3 (CH(*C*H$_3$)$_2$), 23.0 (Si(*C*(CH$_3$)$_3$)$_3$), 22.9 (CH(*C*H$_3$)$_2$), 20.3 (Si(*C*(CH$_3$)$_3$)$_2$Me), 20.3 (Si(*C*(CH$_3$)$_3$)$_2$Me), –5.9 (Si(C(CH$_3$)$_3$)$_2$*Me*).

$^{29}Si\{^1H\}$ NMR (99 MHz, C_6D_6, 300 K): δ [ppm] = 8.4 (*Si*^{t}Bu$_2$Me), 7.7 (*Si*^{t}Bu$_3$), –89.6 (*Si*OC=O).

Anal. Calcd. [%] for $C_{49}H_{84}N_4O_3Si_3$: C, 68.32; H, 9.83; N, 6.50. Found [%]: C, 67.71; H, 9.70; N, 6.73.

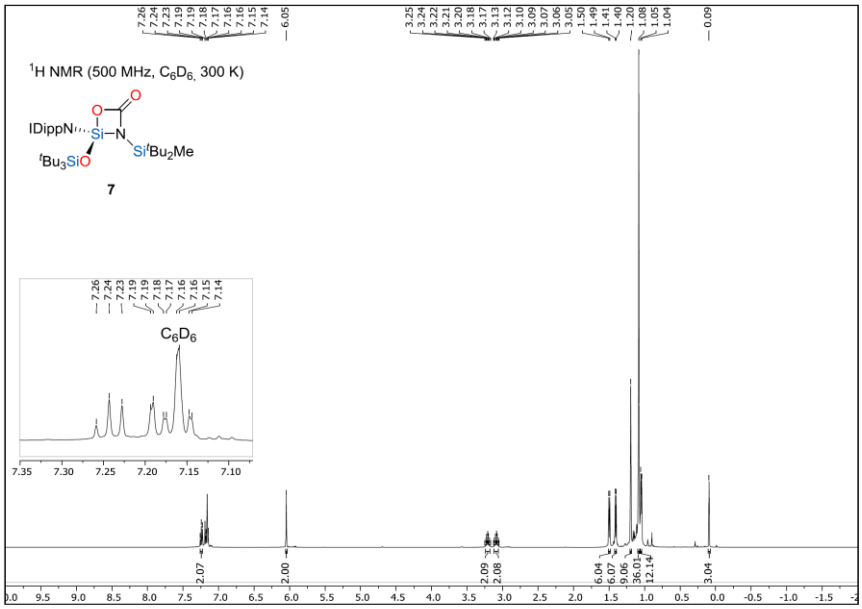


Figure S24. ^{1}H NMR spectrum of azaoxasiletane **7** in C_6D_6 at 300 K.

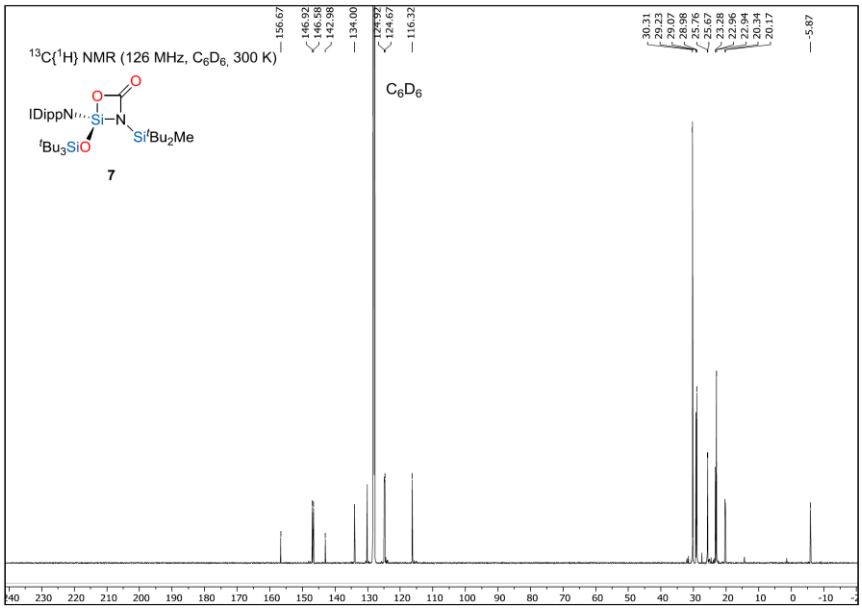


Figure S25. $^{13}C\{^{1}H\}$ NMR spectrum of azaoxasiletane **7** in C_6D_6 at 300 K.

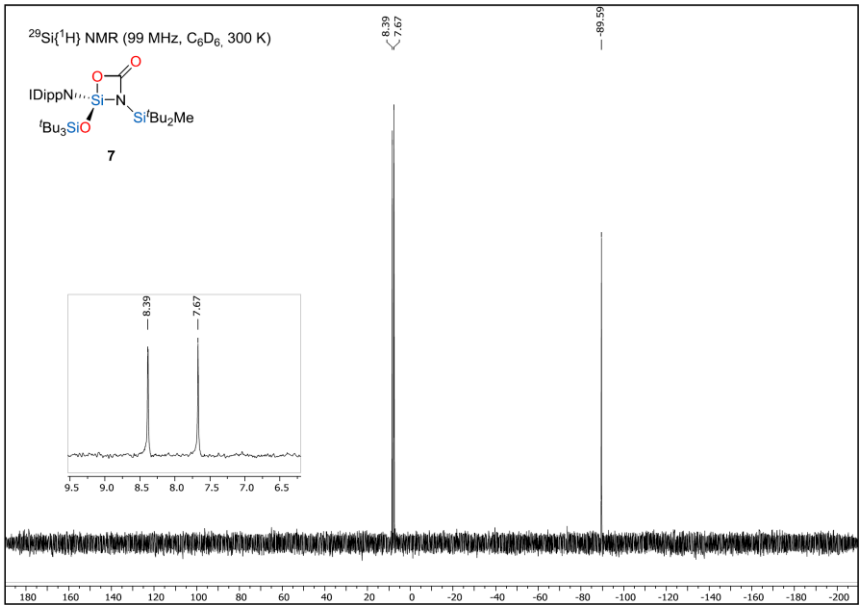


Figure S26. $^{29}Si\{^{1}H\}$ NMR spectrum of azaoxasiletane **7** in C_6D_6 at 300 K.

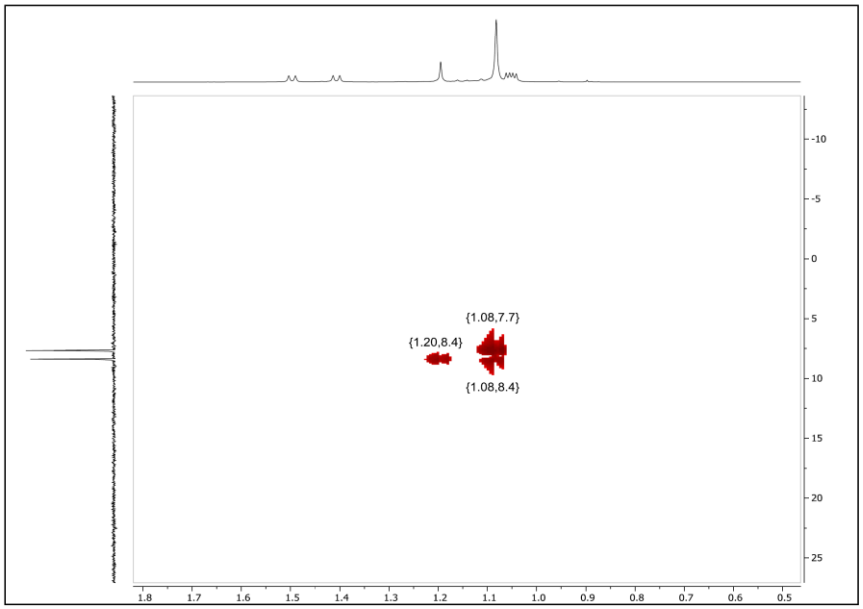
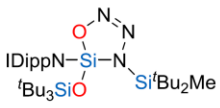


Figure S27. $^{1}H/^{29}Si$ HMBC NMR spectrum of azaoxasiletane **7** in C_6D_6 at 300 K.

1.8 Synthesis of Oxatriazasilole (8)



8
$C_{48}H_{84}N_6O_2Si_3$
861.50 g/mol

A solution of silaimine **6** (75.0 mg, 91.8 µmol) in benzene (3 mL) was degassed and subsequently exposed to N_2O (1 bar) under vigorous stirring at ambient temperature. After an additional hour of stirring, all volatiles were removed *in vacuo*. Oxatriazasilole **8** was provided as a colorless solid (79.0 mg, 91.8 µmol, quantitative yield). Heterocycle **8** is completely stable as a solid and in solution at ambient and elevated temperatures (≤130 °C).

m.p.: 350-351 °C (decomposition; color change from colorless to yellow).

^{1}H NMR (500 MHz, C_6D_6, 300 K): δ [ppm] = 7.24–7.19 (m, 4H, *m*-$C_{ar}\underline{H}$), 7.13–7.11 (m, 2H, *p*-$C_{ar}\underline{H}$), 5.98 (s, 2H, NC$\underline{H}$), 3.36 (sept, ^{3}J = 6.9 Hz, 2H, C$\underline{H}(CH_3)_2$), 3.04 (sept, ^{3}J = 6.9 Hz, 2H, C$\underline{H}(CH_3)_2$), 1.47 (d, ^{3}J = 6.9 Hz, 6H, CH(C$\underline{H}_3)_2$), 1.39 (d, ^{3}J = 6.9 Hz, 6H, CH(C$\underline{H}_3)_2$), 1.13 (s, 27H, Si$^{t}\underline{Bu}_3$), 1.12–1.09 (m, 21H, Si$^{t}\underline{Bu}_2$Me + CH(C$\underline{H}_3)_2$), 1.05 (s, 9H, Si$^{t}\underline{Bu}_2$Me), 0.18 (s, 3H, Si^{t}Bu$_2\underline{Me}$).

^{13}C{^{1}H} NMR (126 MHz, C_6D_6, 300 K): δ [ppm] = 147.8 (*o*-$\underline{C}_{ar}$), 146.8 (*o*-$\underline{C}_{ar}$), 142.1 (N$\underline{C}$N), 134.9 (*ipso*-$\underline{C}_{ar}$), 129.8 (*p*-$\underline{C}_{ar}$H), 125.0 (*m*-$\underline{C}_{ar}$H), 124.1 (*m*-$\underline{C}_{ar}$H), 116.0 (N$\underline{C}$H), 30.4 (Si(C($\underline{C}H_3)_3)_3$), 29.3 ($\underline{C}H(CH_3)_2$), 29.2 ($\underline{C}H(CH_3)_2$), 28.6 (Si(C($\underline{C}H_3)_3)_2$Me), 28.4

(Si(C(<u>C</u>H$_3$)$_3$)$_2$Me), 25.9 (CH(<u>C</u>H$_3$)$_2$), 25.3 (CH(<u>C</u>H$_3$)$_2$), 23.9 (CH(<u>C</u>H$_3$)$_2$), 23.0 (Si(<u>C</u>(CH$_3$)$_3$)$_3$), 22.8 (CH(<u>C</u>H$_3$)$_2$), 20.6 (Si(<u>C</u>(CH$_3$)$_3$)$_2$Me), 20.5 (Si(<u>C</u>(CH$_3$)$_3$)$_2$Me), –4.3 (Si(C(CH$_3$)$_3$)$_2$<u>*Me*</u>).

^{29}Si{^{1}H} NMR (99 MHz, C$_6$D$_6$, 300 K): δ [ppm] = 9.8 (<u>*Si*</u>^{t}Bu$_3$), 3.7 (<u>*Si*</u>^{t}Bu$_2$Me), –103.7 (<u>*Si*</u>ON$_3$).

Anal. Calcd. [%] for C$_{48}$H$_{84}$N$_6$O$_2$Si$_3$: C, 66.92; H, 9.83; N, 9.76. Found [%]: C, 67.56; H, 9.74; N, 9.52.

LIFDI-MS: calculated for **8** (C$_{48}$H$_{84}$N$_6$O$_2$Si$_3$): 860.5964
observed: 860.5765

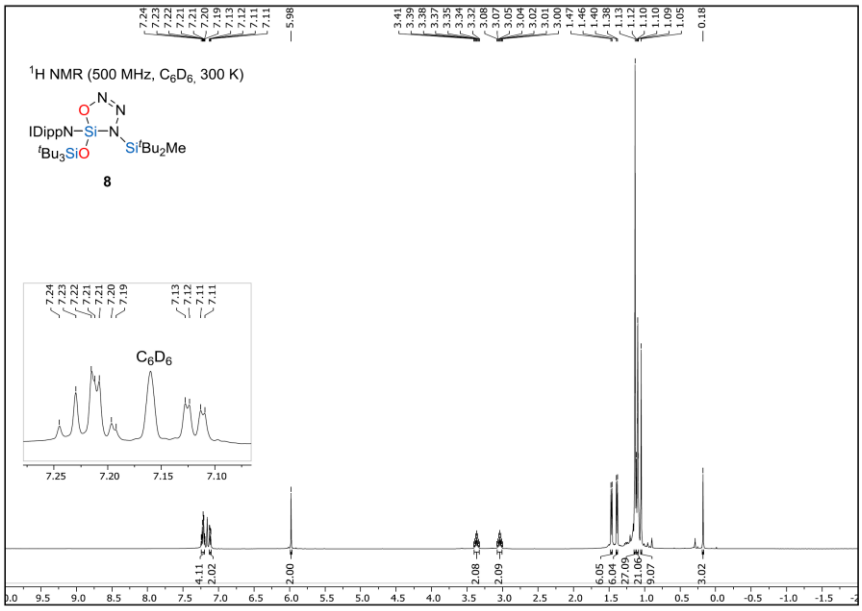


Figure S28. ^{1}H NMR spectrum of oxatriazasilole **8** in C$_6$D$_6$ at 300 K.

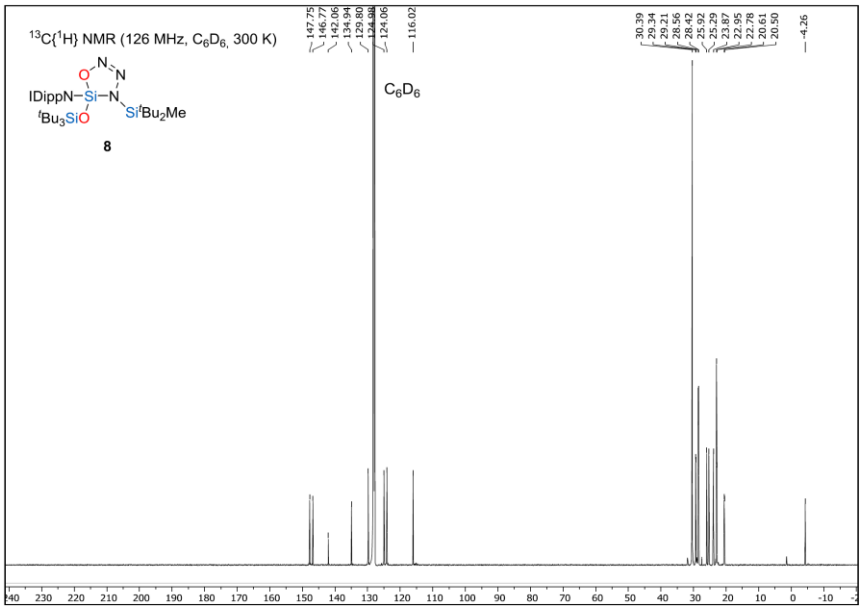


Figure S29. $^{13}C\{^{1}H\}$ NMR spectrum of oxatriazasilole **8** in C_6D_6 at 300 K.

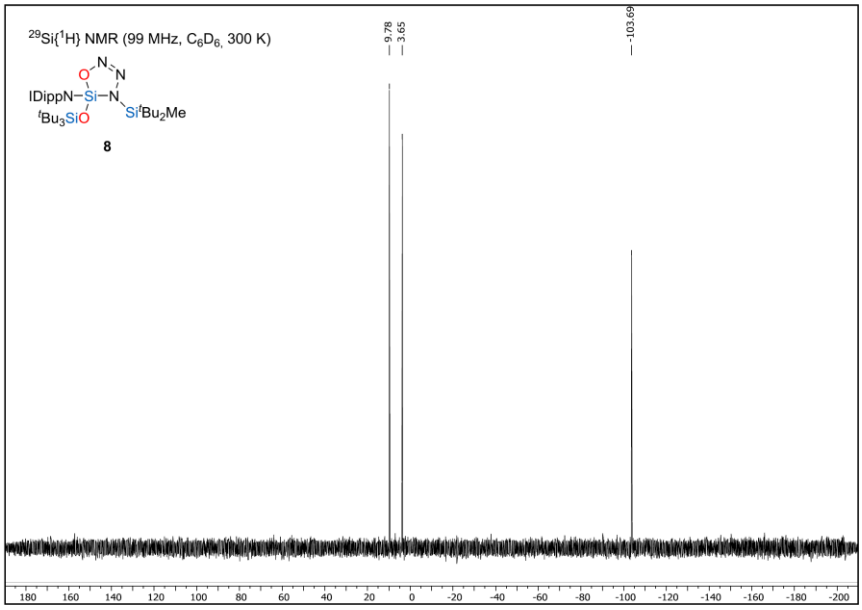


Figure S30. $^{29}Si\{^{1}H\}$ NMR spectrum of oxatriazasilole **8** in C_6D_6 at 300 K.

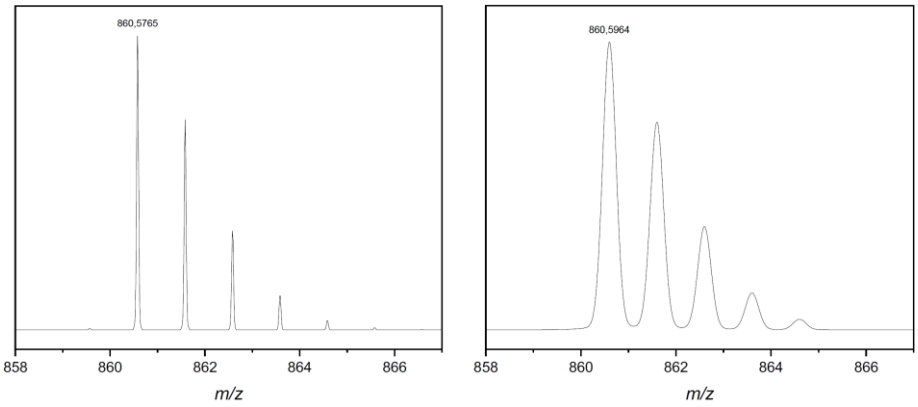
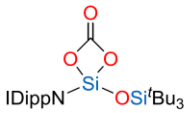


Figure S31. LIFDI-MS spectrometry (detail view with isotope pattern) of oxatriazasilole **8**. Measured (left; m/z = 860.5765) and simulated (right; m/z = 860.5964) mass spectrum.

1.9 Synthesis of (IDippN)(′Bu$_3$SiO)Si(O$_2$C=O) (9)



9
$C_{40}H_{63}N_3O_4Si_2$
706.13 g/mol

A solution of silylene **1** (100 mg, 155 µmol) in toluene (3 mL) was frozen in liquid nitrogen and degassed. The solution was cooled to –80 °C and exposed to CO_2 (1 bar) under vigorous stirring. Subsequently, the reaction mixture was warmed to ambient temperature and the excess of CO_2 and the solvent were removed *in vacuo*. Crystallization of the residue from *n*-hexane at –35 °C provided silicon carbonate complex **9** as colorless crystals (91.5 mg, 130 µmol, 84%), which were suitable for SC-XRD analysis. Compound **9** is completely stable as a solid and in solution at room temperature.

Note: Silicon carbonate complex **9** reacts with another equivalent of CO_2 in a slow equilibrium reaction after several days to compound **9′**. Unfortunately, complete conversion and isolation of **9′** was not possible, as heating of the reaction mixture or removal of CO_2 selectively regenerates **9**. Presumably CO_2 inserts into the Si–N bond; for NMR characterization of **9′** see below.

m.p.: 177-178 °C (gas formation, sticky colorless oil).

^{1}H NMR (500 MHz, C$_6$D$_6$, 300 K): δ [ppm] = 7.30 (t, ^3J = 7.8 Hz, 2H, *p*-C$_{ar}$H), 7.16 (d, ^3J = 7.8 Hz, 4H, *m*-C$_{ar}$H, overlapping with solvent signal), 5.93 (s, 2H, NCH), 2.88 (sept, ^3J = 6.9 Hz, 4H, CH(CH$_3$)$_2$), 1.41 (d, ^3J = 6.9 Hz, 12H, CH(CH$_3$)$_2$), 1.10 (d, ^3J = 6.9 Hz, 12H, CH(CH$_3$)$_2$), 0.97 (s, 27H, C(CH$_3$)$_3$).

^{13}C{^{1}H} NMR (126 MHz, C$_6$D$_6$, 300 K): δ [ppm] = 149.5 (O$_2$C=O), 146.7 (*o*-C$_{ar}$), 146.2 (NCN), 132.4 (*ipso*-C$_{ar}$), 130.8 (*p*-C$_{ar}$H), 124.7 (*m*-C$_{ar}$H), 115.5 (NCH), 29.7 (C(CH$_3$)$_3$), 29.2 (CH(CH$_3$)$_2$), 24.6 (CH(CH$_3$)$_2$), 23.2 (CH(CH$_3$)$_2$), 22.9 (C(CH$_3$)$_3$).

^{29}Si{^{1}H} NMR (99 MHz, C_6D_6, 300 K): δ [ppm] = 7.4 (*Si*^{t}Bu$_3$), –90.9 (*Si*O$_2$C=O).

Anal. Calcd. [%] for $C_{40}H_{63}N_3O_4Si_2$: C, 68.04; H, 8.99; N, 5.95. Found [%]: C, 68.01; H, 9.13; N, 5.94.

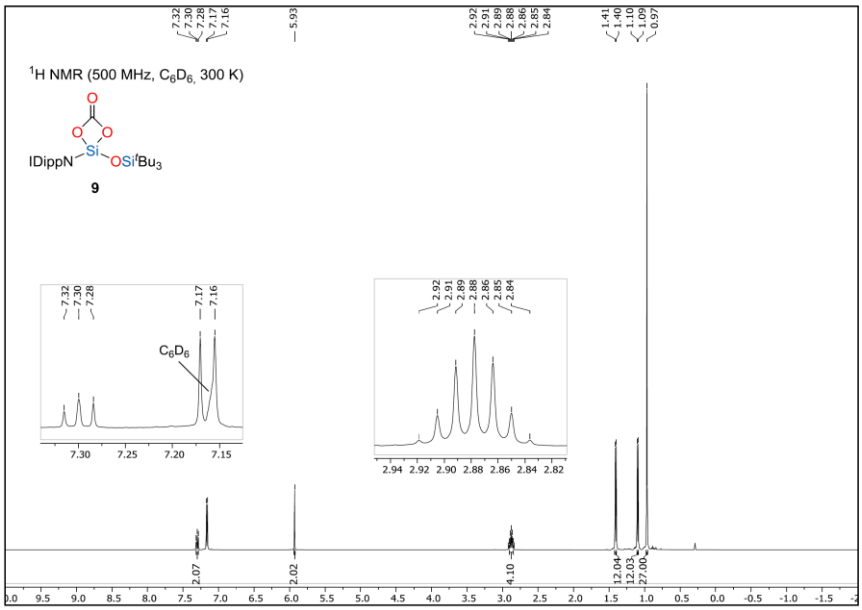


Figure S32. ^{1}H NMR spectrum of (IDippN)(^{t}Bu$_3$SiO)Si(O$_2$C=O) (**9**) in C_6D_6 at 300 K.

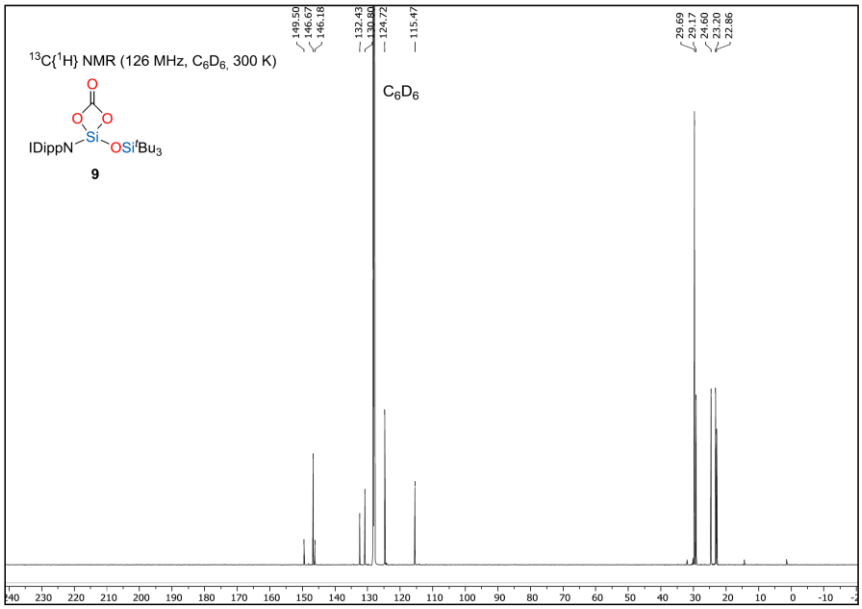


Figure S33. $^{13}C\{^1H\}$ NMR spectrum of (IDippN)(^{t}Bu$_3$SiO)Si(O_2C=O) (**9**) in C_6D_6 at 300 K.

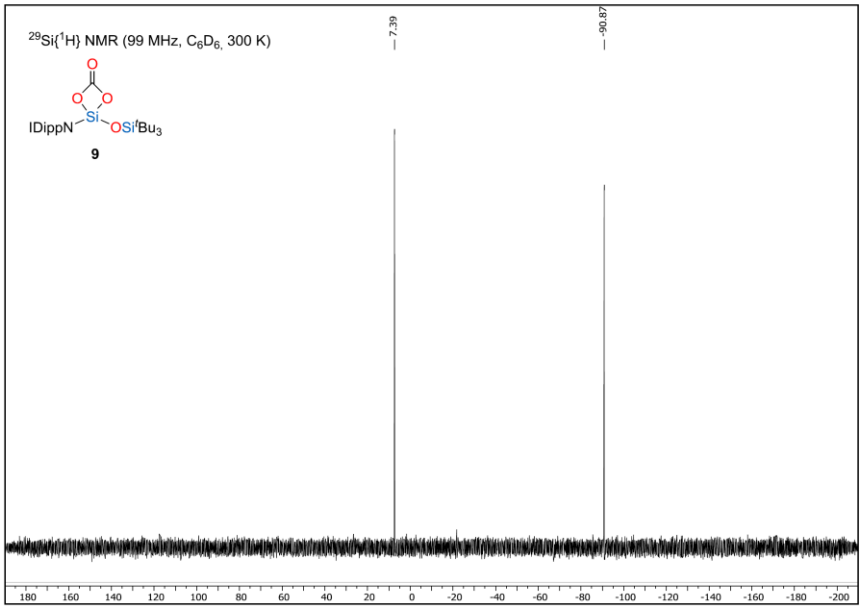


Figure S34. $^{29}Si\{^1H\}$ NMR spectrum of (IDippN)(^{t}Bu$_3$SiO)Si(O_2C=O) (**9**) in C_6D_6 at 300 K.

Multinuclear NMR Characterization of Compound 9′:

^{1}H NMR (500 MHz, C_6D_6, 300 K): δ [ppm] = 7.26 (t, ^{3}J = 7.8 Hz, 2H, *p*-$C_{ar}\underline{H}$), 7.04 (d, ^{3}J = 7.8 Hz, 4H, *m*-$C_{ar}\underline{H}$), 6.05 (s, 2H, NC$\underline{H}$), 2.58 (sept, ^{3}J = 6.9 Hz, 4H, C$\underline{H}(CH_3)_2$), 1.33 (d, ^{3}J = 6.9 Hz, 12H, CH(C$\underline{H}_3)_2$), 1.09 (s, 27H, C(C$\underline{H}_3)_3$) 0.97 (d, ^{3}J = 6.7 Hz, 12H, CH(C$\underline{H}_3)_2$, overlapping with C(C$\underline{H}_3)_3$ resonance of **9**).

^{13}C{^{1}H} NMR (126 MHz, C_6D_6, 300 K): δ [ppm] = 163.1 ($\underline{C}$=O), 152.5 ($O_2\underline{C}$=O), 148.8 (N$\underline{C}$N), 145.7 (*o*-$\underline{C}_{ar}$), 131.9 (*p*-$\underline{C}_{ar}$H), 130.2 (*ipso*-$\underline{C}_{ar}$), 124.8 (*m*-$\underline{C}_{ar}$H), 119.2 (N$\underline{C}$H), 29.9 (C($\underline{C}H_3)_3$), 29.4 ($\underline{C}$H$(CH_3)_2$), 24.8 (CH($\underline{C}H_3)_2$), 23.3 (CH($\underline{C}H_3)_2$), 23.1 ($\underline{C}(CH_3)_3$).

^{29}Si{^{1}H} NMR (99 MHz, C_6D_6, 300 K): δ [ppm] = 7.1 ($\underline{Si}$^{t}Bu$_3$), –126.9 ($\underline{Si}O_2$C=O).

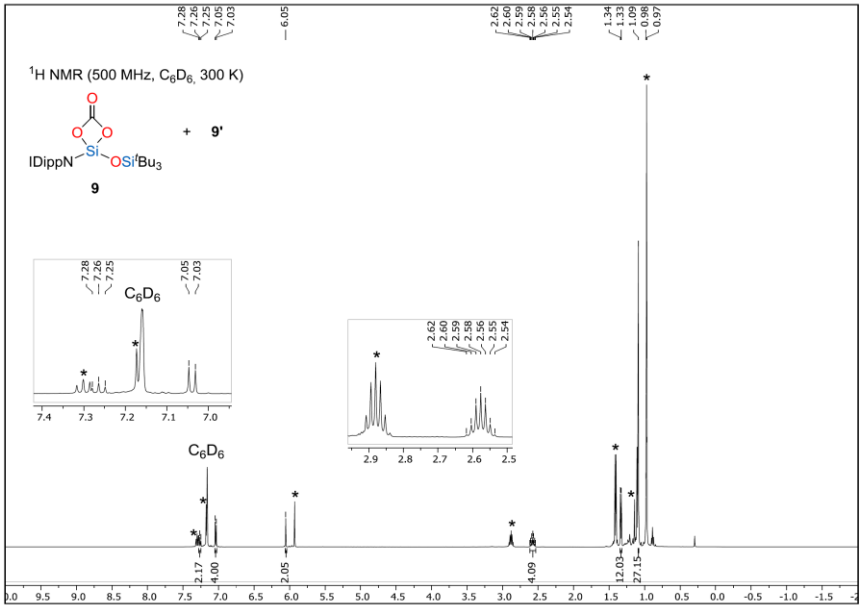


Figure S35. ^{1}H NMR spectrum of (IDippN)(^{t}Bu$_3$SiO)Si(O_2C=O) (**9**) and **9′** in C_6D_6 at 300 K. The respective resonances of compound **9** are marked with asterisks *.

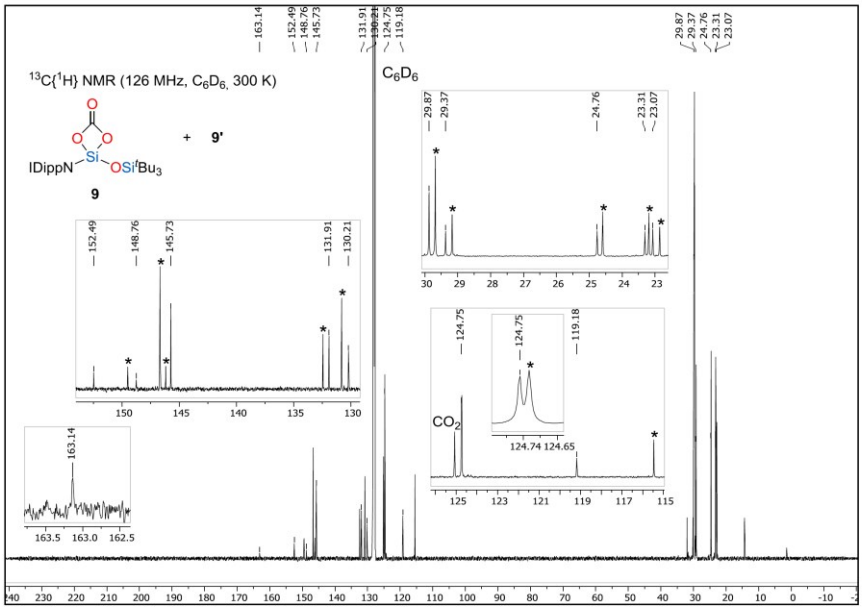


Figure S36. $^{13}C\{^1H\}$ NMR spectrum of (IDippN)(^{t}Bu$_3$SiO)Si(O_2C=O) (**9**) and **9′** in C_6D_6 at 300 K. The respective resonances of compound **9** are marked with asterisks *.

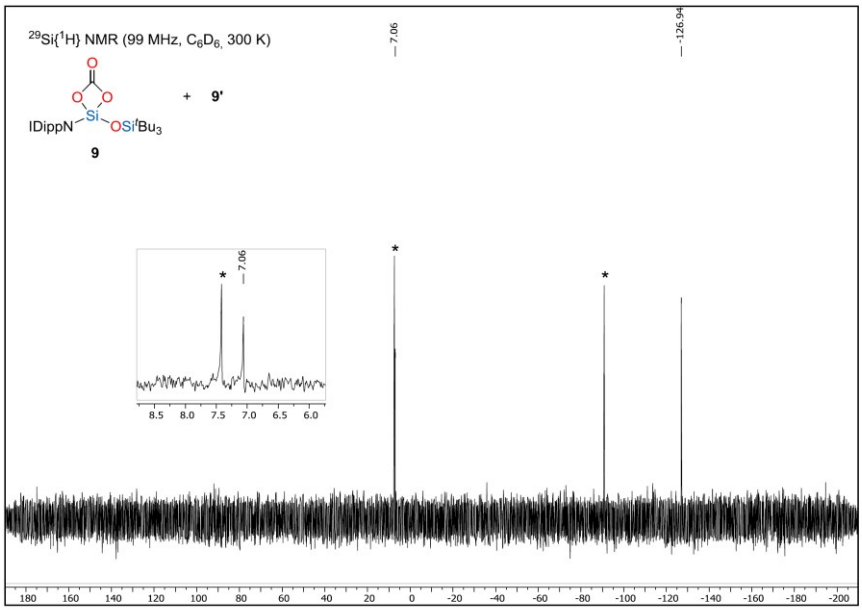
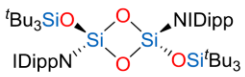


Figure S37. $^{29}Si\{^1H\}$ NMR spectrum of (IDippN)(^{t}Bu$_3$SiO)Si(O_2C=O) (**9**) and **9′** in C_6D_6 at 300 K. The respective resonances of compound **9** are marked with asterisks *.

1.10 Synthesis of *trans*-Cyclodisiloxane [(IDippN)(^{t}Bu$_3$SiO)Si=O]$_2$ (10a)



10a
$C_{78}H_{126}N_6O_4Si_4$
1324.24 g/mol

A solution of silylene **1** (300 mg, 464 µmol) in *n*-hexane (6 mL) was frozen in liquid nitrogen and degassed. The solution was cooled to –80 °C and exposed to N_2O (1 bar) under vigorous stirring. Subsequently, the reaction mixture was warmed to ambient temperature with concomitant formation of a fine white precipitate. The solid was separated *via* filtration, washed with *n*-hexane and dried *in vacuo* to give pure *trans*-cyclodisiloxane **10a** as a white powder (247 mg, 187 µmol, 81%). Suitable crystals for SC-XRD analysis were obtained by cooling an *n*-hexane/toluene solution of **10a** to –35 °C for several days. Compound **10a** is completely stable as a solid and in solution even under air and moisture.

m.p.: 335-336 °C (decomposition; color change from colorless to yellow).

^{1}H NMR (500 MHz, C$_6$D$_6$, 300 K): δ [ppm] = 7.27 (*pseudo* t, ^3J = 7.6 Hz, 4H, *p*-C$_{ar}$H), 7.17 (dd, ^4J = 1.6 Hz, ^3J = 7.6 Hz, 4H, *m*-C$_{ar}$H), 7.02 (dd, ^4J = 1.6 Hz, ^3J = 7.6 Hz, 4H, *m*-C$_{ar}$H), 5.83 (s, 4H, NCH), 3.48 (sept, ^3J = 6.7 Hz, 4H, CH(CH$_3$)$_2$), 2.90 (sept, ^3J = 6.7 Hz, 4H, CH(CH$_3$)$_2$), 1.43 (d, ^3J = 6.7 Hz, 12H, CH(CH$_3$)$_2$), 1.20 (s, 54H, C(CH$_3$)$_3$), 1.15 (d, ^3J = 6.7 Hz, 12H, CH(CH$_3$)$_2$), 1.13 (d, ^3J = 6.7 Hz, 12H, CH(CH$_3$)$_2$), 1.10 (d, ^3J = 6.7 Hz, 12H, CH(CH$_3$)$_2$).

^{13}C{^{1}H} NMR (126 MHz, C$_6$D$_6$, 300 K): δ [ppm] = 148.8 (*o*-C$_{ar}$), 147.3 (*o*-C$_{ar}$), 145.1 (NCN), 136.1 (*ipso*-C$_{ar}$), 129.5 (*p*-C$_{ar}$H), 125.2 (*m*-C$_{ar}$H), 124.2 (*m*-C$_{ar}$H), 116.5 (NCH), 31.1 (C(CH$_3$)$_3$), 29.1 (CH(CH$_3$)$_2$), 28.2 (CH(CH$_3$)$_2$), 27.5 (CH(CH$_3$)$_2$), 26.1 (CH(CH$_3$)$_2$), 23.9 (CH(CH$_3$)$_2$), 23.2 (C(CH$_3$)$_3$), 22.6 (CH(CH$_3$)$_2$).

^{29}Si{^{1}H} NMR (99 MHz, C$_6$D$_6$, 300 K): δ [ppm] = 5.6 (Si^{t}Bu$_3$), –83.5 (Si$_2$O$_2$).

Anal. Calcd. [%] for C$_{78}$H$_{126}$N$_6$O$_4$Si$_4$: C, 70.75; H, 9.59; N, 6.35. Found [%]: C, 70.99; H, 9.90; N, 6.16.

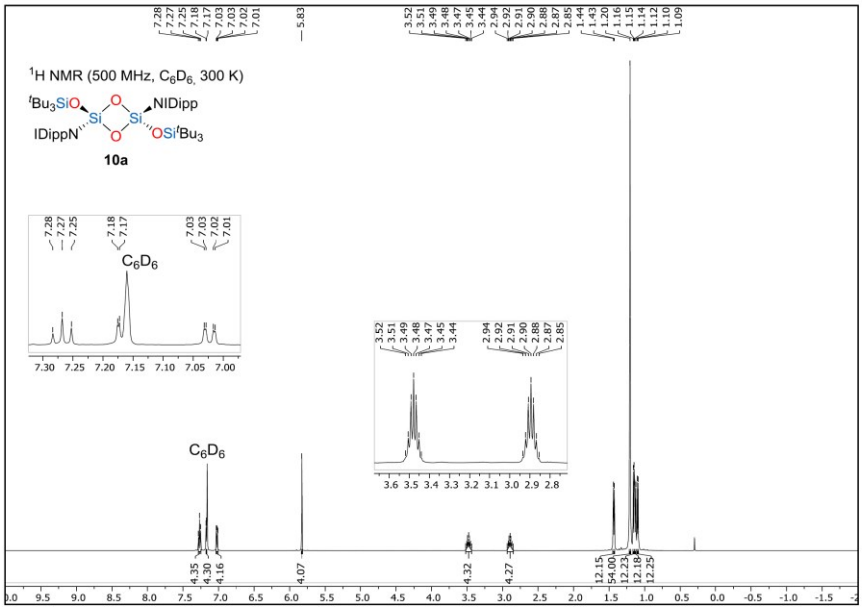


Figure S38. ^{1}H NMR spectrum of [(IDippN)(^{t}Bu$_3$SiO)Si=O]$_2$ (**10a**) in C_6D_6 at 300 K.

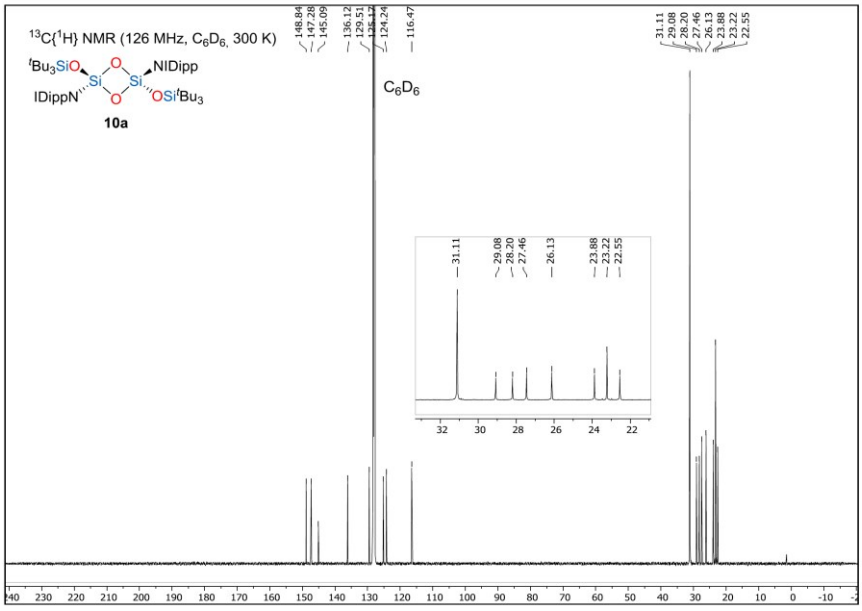


Figure S39. ^{13}C{^{1}H} NMR spectrum of [(IDippN)(^{t}Bu$_3$SiO)Si=O]$_2$ (**10a**) in C_6D_6 at 300 K.

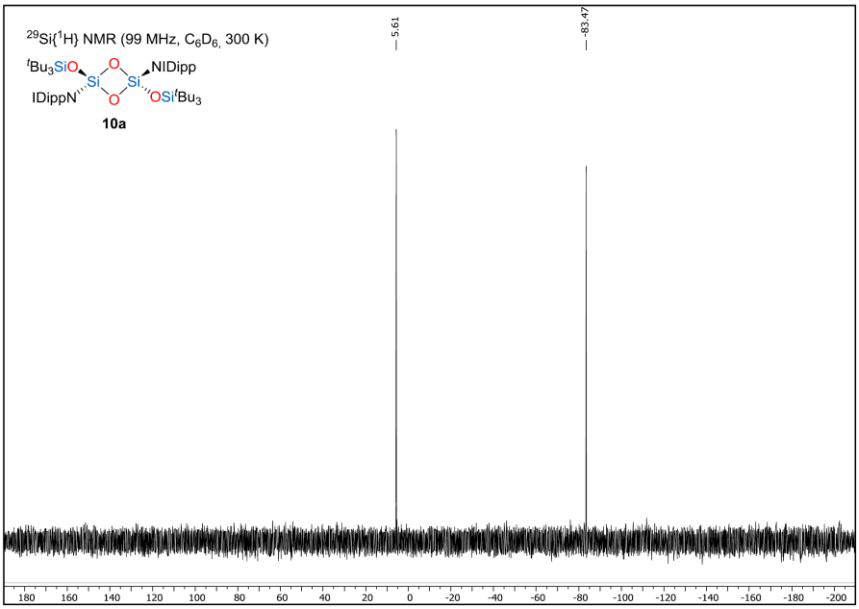
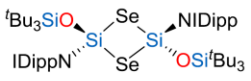


Figure S40. $^{29}Si\{^{1}H\}$ NMR spectrum of [(IDippN)(ᵗBu₃SiO)Si=O]₂ (**10a**) in C_6D_6 at 300 K.

1.11 Synthesis of Silicon Diselenide [(IDippN)(ᵗBu₃SiO)Si=Se]₂ (10b)



10b

$C_{78}H_{126}N_6O_2Se_2Si_4$

1450.17 g/mol

To a solution of silylene **1** (100 mg, 155 µmol, 1.0 eq.) in toluene (3 mL) was added gray selenium powder (12.2 mg, 155 µmol, 1.0 eq.) at room temperature. Quantitative conversion of **1** to silicon diselenide **10b** was detected by ^{1}H NMR spectroscopy after stirring the reaction mixture for 3 days. Subsequently, the solvent was removed *in vacuo* and the residue recrystallized from *n*-hexane/toluene at –35 °C providing **10b** as colorless crystals (95.7 mg, 66.0 mmol, 85%) suitable for SC-XRD analysis. Compound **10b** is completely stable as a solid, but decomposes (or dimerizes) extremely slowly in solution to an unidentified species, which thus was not investigated in more detail.

Note: The NMR data obtained indicate that **10b** presumably exists as monomer **10b′** in solution. The significantly downfield-shifted ^{29}Si NMR resonance for the SiSe moiety compared to that observed for the SiO moiety in **10a** (δ = –83.5 ppm) along with the decreased signal splitting in the ^{1}H NMR suggest a monomer with a three-coordinate Si nucleus.

m.p.: 100-101 °C (decomposition; color change from colorless to red).

^{1}H NMR (500 MHz, C_6D_6, 300 K): δ [ppm] = 7.20–7.17 (m, 2H, *p*-$C_{ar}\underline{H}$), 7.13–7.11 (m, 4H, *m*-$C_{ar}\underline{H}$), 6.08 (s, 2H, NC$\underline{H}$), 3.15 (sept, ^{3}J = 6.9 Hz, 4H, C$\underline{H}(CH_3)_2$), 1.49 (d, ^{3}J = 6.9 Hz, 12H, CH(C$\underline{H}_3)_2$), 1.10 (d, ^{3}J = 6.9 Hz, 12H, CH(C$\underline{H}_3)_2$), 1.06 (s, 27H, C(C$\underline{H}_3)_3$).

^{13}C{^{1}H} NMR (126 MHz, C_6D_6, 300 K): δ [ppm] = 147.7 (N$\underline{C}$N), 147.3 (*o*-$\underline{C}_{ar}$), 132.7 (*ipso*-$\underline{C}_{ar}$), 130.5 (*p*-$\underline{C}_{ar}$H), 124.4 (*m*-$\underline{C}_{ar}$H), 116.3 (N$\underline{C}$H), 30.0 (C($\underline{C}H_3)_3$), 29.1 ($\underline{C}$H($CH_3)_2$), 25.4 (CH($\underline{C}H_3)_2$), 23.8 (CH($\underline{C}H_3)_2$), 23.2 ($\underline{C}(CH_3)_3$).

^{29}Si{^{1}H} NMR (99 MHz, C_6D_6, 300 K): δ [ppm] = 8.8 (*Si*^{t}Bu$_3$), 6.2 (*Si*Se).

Anal. Calcd. [%] for $C_{78}H_{126}N_6O_2Se_2Si_4$: C, 64.60; H, 8.76; N, 5.80. Found [%]: C, 66.42; H, 8.82; N, 5.59.

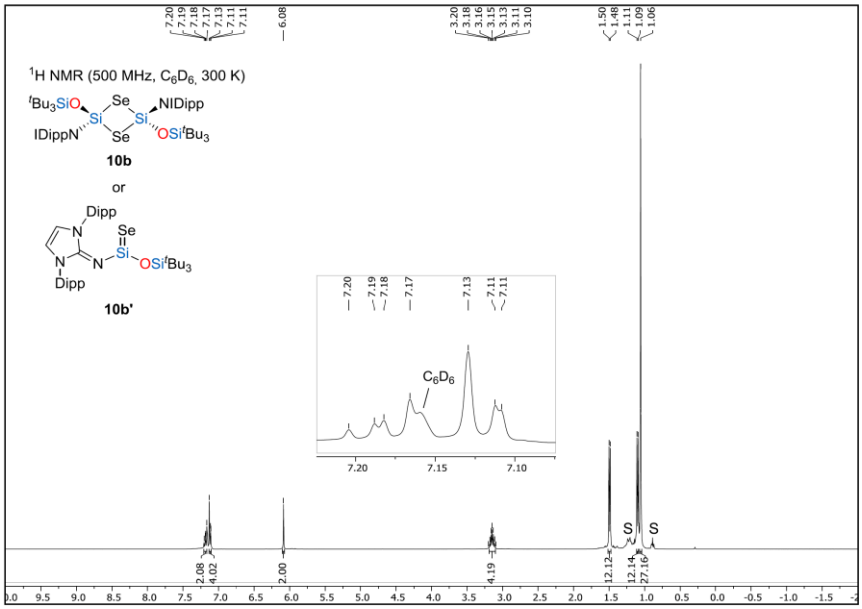


Figure S41. ^{1}H NMR spectrum of [(IDippN)(^{t}Bu$_3$SiO)Si=Se]$_2$ (**10b**) in C_6D_6 at 300 K. Residual *n*-hexane (from starting material) is labeled with S.

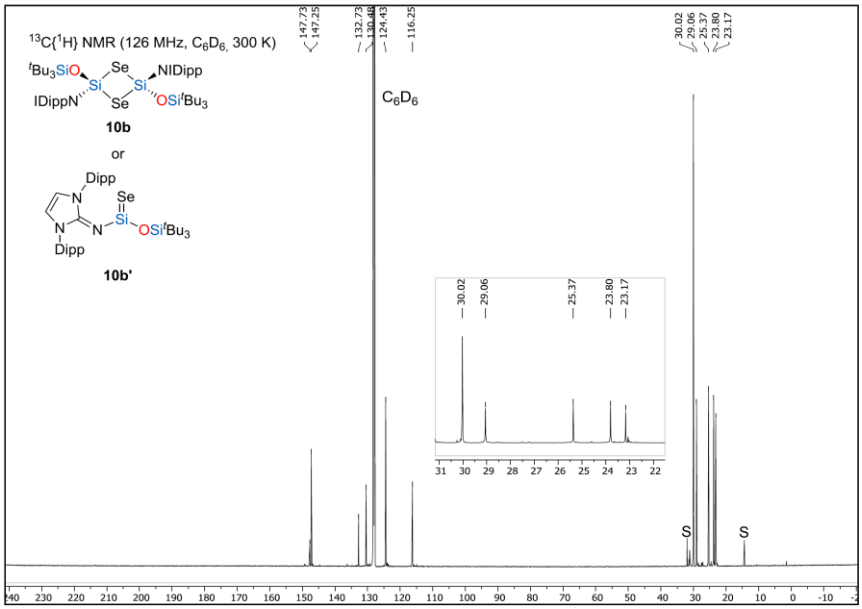


Figure S42. $^{13}C\{^1H\}$ NMR spectrum of [(IDippN)(^{t}Bu$_3$SiO)Si=Se]$_2$ (**10b**) in C_6D_6 at 300 K. Residual *n*-hexane (from starting material) is labeled with S.

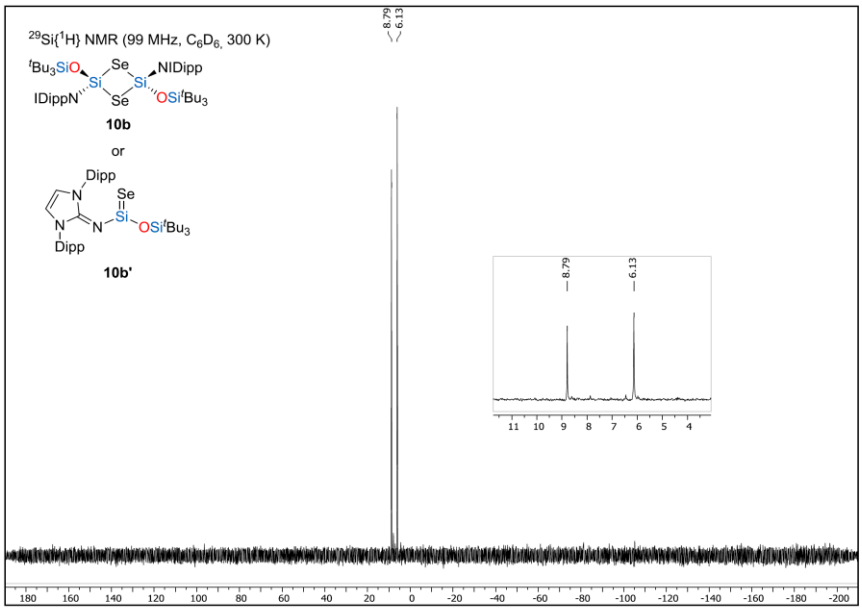
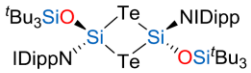


Figure S43. $^{29}Si\{^1H\}$ NMR spectrum of [(IDippN)(^{t}Bu$_3$SiO)Si=Se]$_2$ (**10b**) in C_6D_6 at 300 K.

1.12 Synthesis of Silicon Ditelluride (IDippN)(ᵗBu₃SiO)Si=Te (10c)



10c
$C_{78}H_{126}N_6O_2Te_2Si_4$
1547.45 g/mol

To a solution of silylene **1** (100 mg, 155 µmol, 1.0 eq.) in toluene (3 mL) was added crystalline tellurium (19.8 mg, 155 µmol, 1.0 eq.) at ambient temperature. Quantitative conversion of **1** to silicon ditelluride **10c** was detected by ^{1}H NMR spectroscopy after stirring the reaction mixture for 2 weeks (The reaction time can be significantly shortened by carrying out the reaction at elevated temperatures, so that after heating the reaction mixture to 50 °C for 3 d quantitative conversion was already achieved). Subsequent removal of the solvent afforded **10c** as an off-white solid (119.8 mg, 155 µmol, quantitative yield). Compound **10c** is completely stable as a solid and in solution at ambient temperature.

Note: The NMR data obtained indicate that **10c** presumably exists as monomer **10c′** in solution. The significantly downfield-shifted ^{29}Si NMR resonance for the SiTe moiety compared to that observed for the SiO moiety in **10a** (δ = –83.5 ppm) along with the decreased signal splitting in the ^{1}H NMR suggest a monomer with a three-coordinate Si nucleus.

m.p.: 220-221 °C (decomposition; color change from colorless to black).

^{1}H NMR (500 MHz, C_6D_6, 300 K): δ [ppm] = 7.21–7.17 (m, 2H, *p*-$C_{ar}H$), 7.14–7.11 (m, 4H, *m*-$C_{ar}H$), 6.09 (s, 2H, NC*H*), 3.16 (sept, ^3J = 6.9 Hz, 4H, C*H*$(CH_3)_2$), 1.50 (d, ^3J = 6.9 Hz, 12H, CH(C*H*$_3)_2$), 1.08 (d, ^3J = 6.9 Hz, 12H, CH(C*H*$_3)_2$), 1.06 (s, 27H, C(C*H*$_3)_3$).

^{13}C{^{1}H} NMR (126 MHz, C_6D_6, 300 K): δ [ppm] = 147.1 (*o*-C_{ar}), 146.9 (N*C*N), 132.8 (*ipso*-C_{ar}), 130.5 (*p*-C_{ar}H), 124.5 (*m*-C_{ar}H), 116.5 (N*C*H), 30.2 (C(*C*H$_3)_3$), 29.1 (*C*H$(CH_3)_2$), 25.5 (CH(*C*H$_3)_2$), 24.0 (CH(*C*H$_3)_2$), 23.2 (*C*$(CH_3)_3$).

^{29}Si{^{1}H} NMR (99 MHz, C_6D_6, 300 K): δ [ppm] = 10.1 (*Si*ᵗBu$_3$), –14.6 (*Si*Te).

Anal. Calcd. [%] for $C_{78}H_{126}N_6O_2Te_2Si_4$: C, 60.54; H, 8.21; N, 5.43. Found [%]: C, 60.46; H, 8.27; N, 5.41.

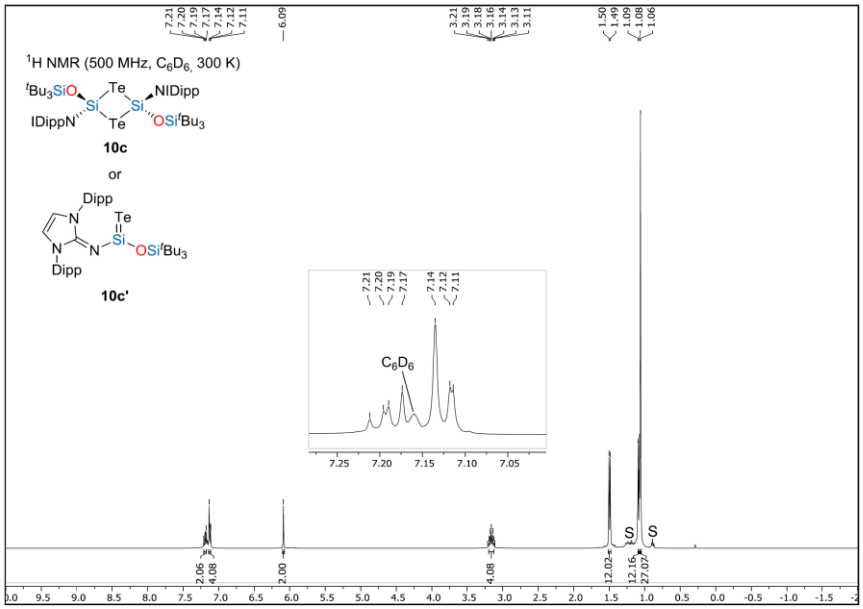


Figure S44. ^{1}H NMR spectrum of [(IDippN)(^{t}Bu$_3$SiO)Si=Te]$_2$ (**10c**) in C_6D_6 at 300 K. Residual *n*-hexane (from starting material) is labeled with S.

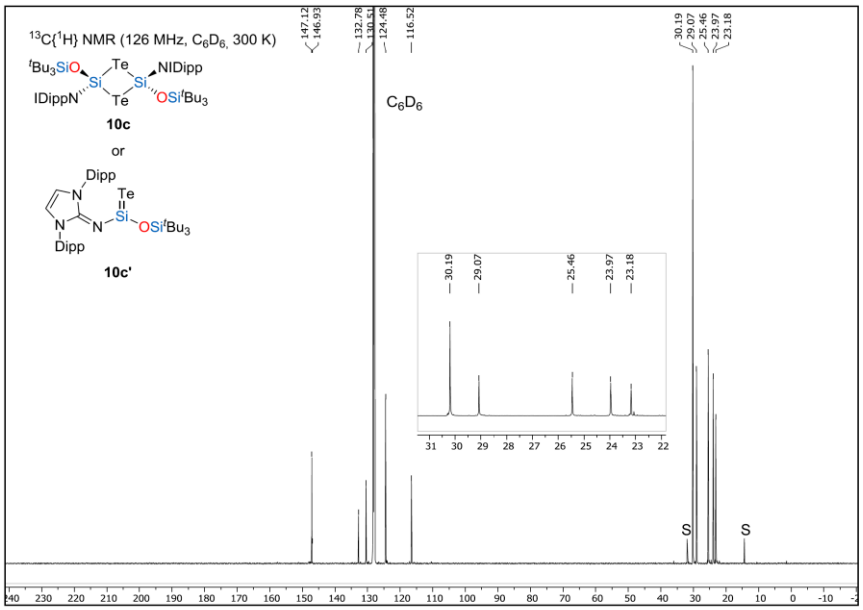


Figure S45. ^{13}C{^{1}H} NMR spectrum of [(IDippN)(^{t}Bu$_3$SiO)Si=Te]$_2$ (**10c**) in C_6D_6 at 300 K. Residual *n*-hexane (from starting material) is labeled with S.

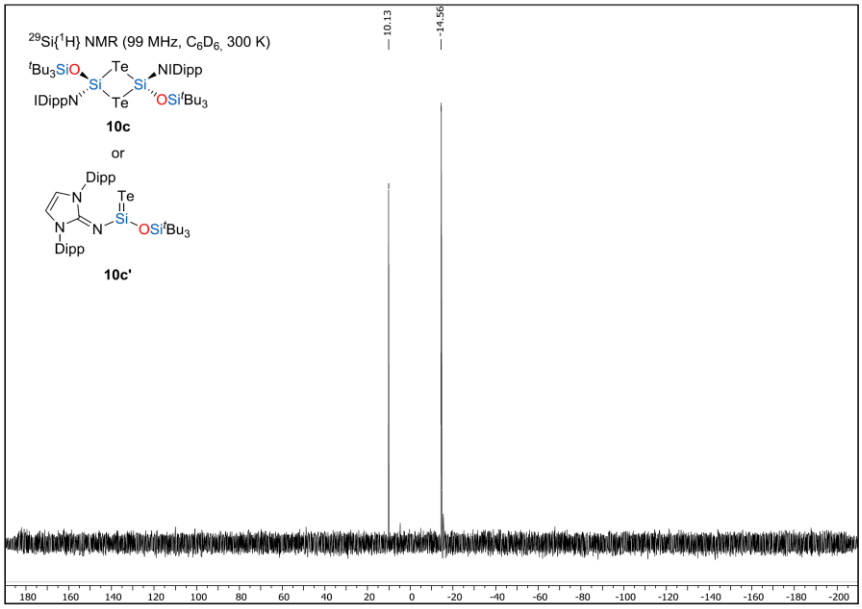
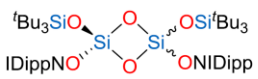


Figure S46. $^{29}Si\{^{1}H\}$ NMR spectrum of $[(IDippN)(^{t}Bu_3SiO)Si{=}Te]_2$ (**10c**) in C_6D_6 at 300 K.

1.13 Synthesis of *cis*/*trans*-Cyclodisiloxane [(IDippNO)(ᵗBu₃SiO)Si=O]₂ (11)



cis/*trans*-**11**
$C_{78}H_{126}N_6O_6Si_4$
1356.24 g/mol

A solution of silylene **1** (100 mg, 155 µmol) in toluene (3 mL) was frozen in liquid nitrogen and degassed. The solution was cooled to –80 °C and exposed to O_2 (1 bar) under vigorous stirring. Subsequently, the reaction mixture was warmed to ambient temperature and the excess of O_2 and the solvent were removed *in vacuo*. Crystallization of the residue from *n*-hexane/toluene at –35 °C provided *cis*/*trans*-cyclodisiloxane **11** as colorless crystals (73.2 mg, 54.0 µmol, 70%), which were suitable for SC-XRD analysis (*cis*-**11**). Compound **11** is completely stable as a solid and in solution even under air and moisture.

Note: *cis*/*trans*-Cyclodisiloxane **11** is insoluble in *n*-hexane and sparingly soluble in benzene. Based on the results of SC-XRD analyses, we assume that the main product of the reaction is the *cis*-isomer formed under kinetic control. The *cis*/*trans*-ratio of **11** was calculated by ^{1}H NMR spectroscopy to about 71/29. The assignment of the resonances in the ^{1}H and ^{13}C NMR spectra proved to be difficult/impossible because many of them superimpose. Hence, in the following only

those signals are given that could be clearly assigned. Carrying out the reaction at higher temperatures leads to a less selective oxygenation and formation of by-products.

m.p.: 298-299 °C (decomposition; color change from colorless to yellow).

Major isomer *cis*-cyclodisiloxane 11 (~71%):

^{1}H NMR (500 MHz, C_6D_6, 300 K): δ [ppm] = 6.13 (d, ^{3}J = 2.6 Hz, 1H, NC*H*), 5.59 (d, ^{3}J = 2.6 Hz, 1H, NC*H*), 1.48 (d, ^{3}J = 6.9 Hz, 6H, CH(CH_3)$_2$), 1.48 (d, ^{3}J = 6.9 Hz, 6H, CH(CH_3)$_2$), 1.08 (s, 27H, C(CH_3)$_3$).

^{29}Si{^{1}H} NMR (99 MHz, C_6D_6, 300 K): δ [ppm] = 6.9 (*Si*^{t}Bu$_3$), –84.5 (*Si*$_2$O$_2$).

Minor isomer *trans*-cyclodisiloxane 11 (~29%):

^{1}H NMR (500 MHz, C_6D_6, 300 K): δ [ppm] = 5.79 (d, ^{3}J = 2.6 Hz, 1H, NC*H*), 5.66 (d, ^{3}J = 2.6 Hz, 1H, NC*H*), 1.02 (s, 27H, C(CH_3)$_3$).

^{29}Si{^{1}H} NMR (99 MHz, C_6D_6, 300 K): δ [ppm] = 3.9 (*Si*^{t}Bu$_3$).

Anal. Calcd. [%] for $C_{78}H_{126}N_6O_6Si_4$: C, 69.08; H, 9.36; N, 6.20. Found [%]: C, 68.12; H, 9.55; N, 6.05.

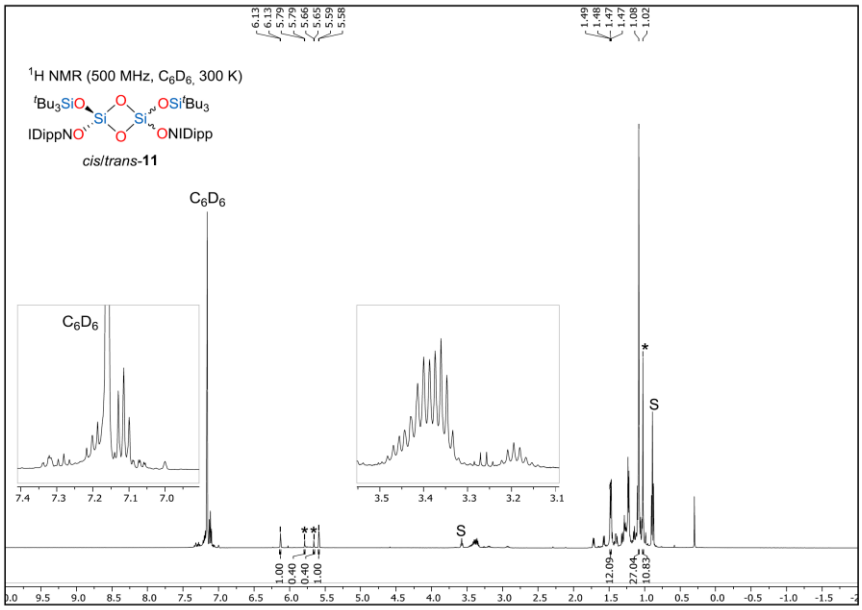


Figure S47. ^{1}H NMR spectrum of [(IDippNO)(^{t}Bu$_3$SiO)Si=O]$_2$ (**11**) in C_6D_6 at 300 K. Unambiguously assigned resonances for the minor *trans*-product and residual solvent are labeled with asterisks * and S, respectively.

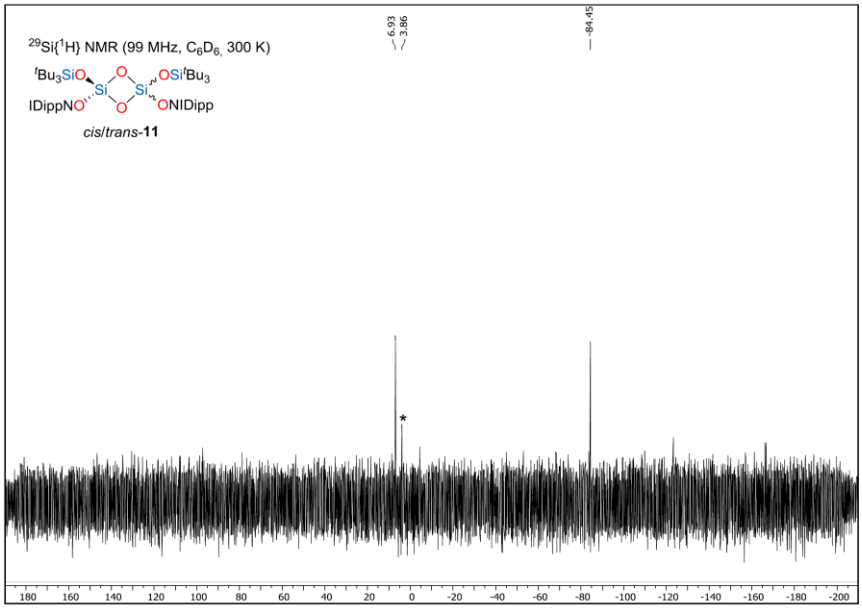


Figure S48. ^{29}Si{^{1}H} NMR spectrum of [(IDippNO)(^{t}Bu$_3$SiO)Si=O]$_2$ (**11**) in C_6D_6 at 300 K. The unambiguously assigned resonance for the minor *trans*-product is labeled with an asterisk *.

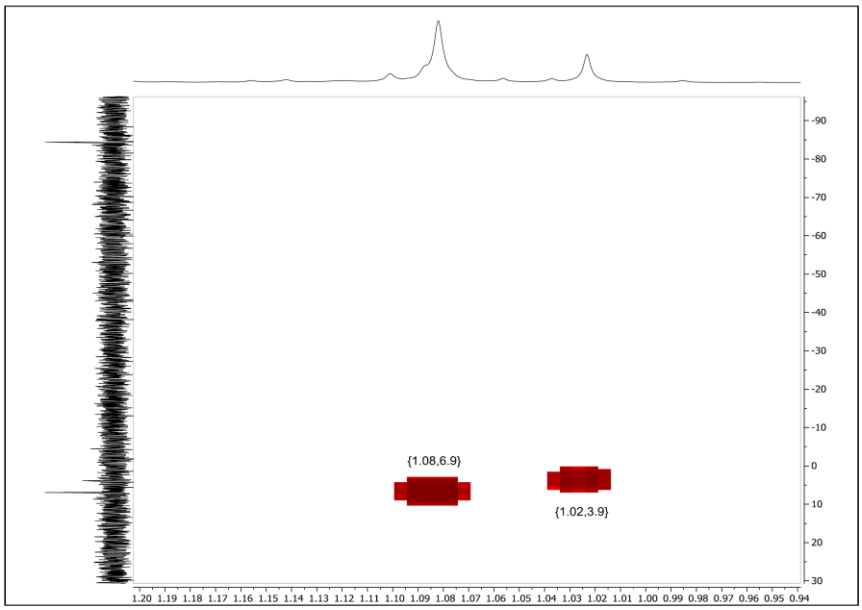
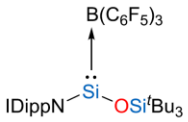


Figure S49. ^{1}H/^{29}Si HMBC NMR spectrum of [(IDippNO)(^{t}Bu$_3$SiO)Si=O]$_2$ (**11**) in C_6D_6 at 300 K.

1.14 Synthesis of (IDippN)(^{t}Bu$_3$SiO)Si(B(C$_6$F$_5$)$_3$) (12a)



12a
$C_{57}H_{63}BF_{15}N_3OSi_2$
1158.11 g/mol

To a solution of silylene **1** (100 mg, 155 µmol, 1.0 eq.) in *n*-hexane (3 mL) was added a solution of B(C$_6$F$_5$)$_3$ (BCF) (79.2 mg, 155 µmol, 1.0 eq.) in *n*-hexane (1 mL) at room temperature. After stirring the resulting colorless solution for 30 min, the solvent was removed *in vacuo*. Crystallization of the residue from *n*-hexane at –35 °C afforded silylene-BCF adduct **12a** as colorless crystals (149 mg, 129 µmol, 83%), which were suitable for SC-XRD analysis. Compound **12a** is completely stable as a solid and in solution at room-temperature.

Note: Due to coupling with the ^{11}B nucleus (high quadrupole moment and spin ^{11}B = 3/2), several resonances are broadened in the NMR spectra or were not observable at all.

m.p.: 200-201 °C (decomposition; color change from colorless to orange).

^{1}H NMR (500 MHz, C$_6$D$_6$, 300 K): δ [ppm] = 7.16–7.11 (m, 4H, *m*-C$_{ar}$*H*, overlapping with solvent signal), 6.80 (br s, 2H, *p*-C$_{ar}$*H*), 5.98 (s, 2H, NC*H*), 3.15–3.09 (m, 2H, C*H*(CH$_3$)$_2$), 2.96–2.85 (m, 2H, C*H*(CH$_3$)$_2$), 1.31–1.12 (m, 12H, CH(C*H*$_3$)$_2$), 0.91–0.87 (m, 12H, CH(C*H*$_3$)$_2$), 0.81 (s, 27H, C(C*H*$_3$)$_3$).

^{11}B{^{1}H} NMR (128 MHz, C$_6$D$_6$, 300 K): δ [ppm] = –20.3.

^{13}C{^{1}H} NMR (126 MHz, C$_6$D$_6$, 300 K): δ [ppm] = 149.6 (*C*F), 148.9 (*o*-*C*$_{ar}$), 147.7 (*C*F), 147.5 (*o*-*C*$_{ar}$), 147.0 (*C*F), 146.0 (*C*F), 145.4 (N*C*N), 138.8 (*C*F), 136.7 (*C*F), 132.8 (*ipso*-*C*$_{ar}$), 130.4 (*p*-*C*$_{ar}$H), 124.7 (*m*-*C*$_{ar}$H), 124.5 (*m*-*C*$_{ar}$H), 117.2 (N*C*H), 30.1 (*C*H(CH$_3$)$_2$), 29.7 (C(*C*H$_3$)$_3$), 28.5 (*C*H(CH$_3$)$_2$), 26.1 (CH(*C*H$_3$)$_2$), 25.9 (CH(*C*H$_3$)$_2$), 22.7 (CH(*C*H$_3$)$_2$), 22.6 (CH(*C*H$_3$)$_2$), 22.4 (*C*(CH$_3$)$_3$).

^{19}F{^{1}H} NMR (471 MHz, C$_6$D$_6$, 300 K): δ [ppm] = –127.6, –157.7, –162.1.

^{29}Si{^{1}H} NMR (99 MHz, C$_6$D$_6$, 300 K): δ [ppm] = 11.4 (*Si*^{t}Bu$_3$)

The resonance for the low-valent Si atom (*silylene Si*) was not observed.

Anal. Calcd. [%] for C$_{57}$H$_{63}$BF$_{15}$N$_3$OSi$_2$: C, 59.12; H, 5.48; N, 3.63. Found [%]: C, 58.19; H, 5.72; N, 3.58.

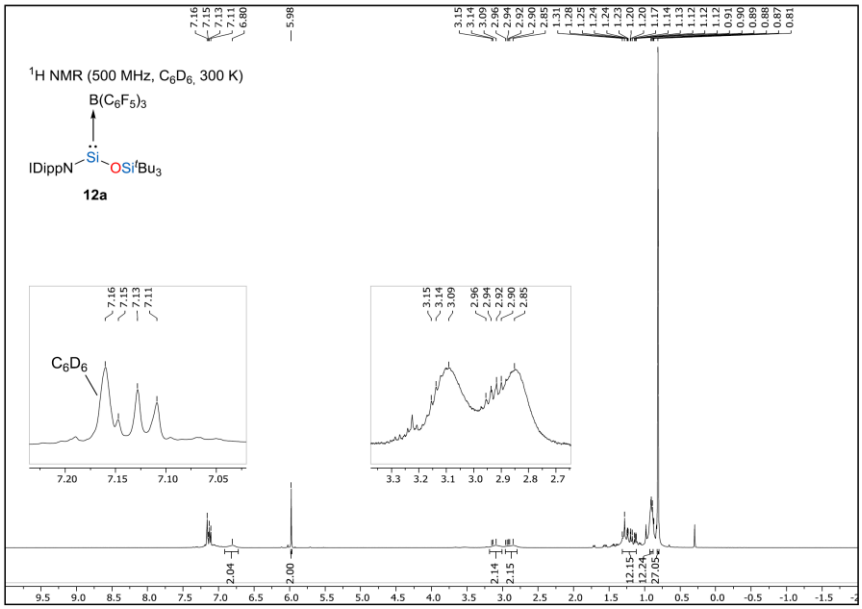


Figure S50. ^{1}H NMR spectrum of (IDippN)(^{t}Bu$_3$SiO)Si(B(C$_6$F$_5$)$_3$) (**12a**) in C$_6$D$_6$ at 300 K.

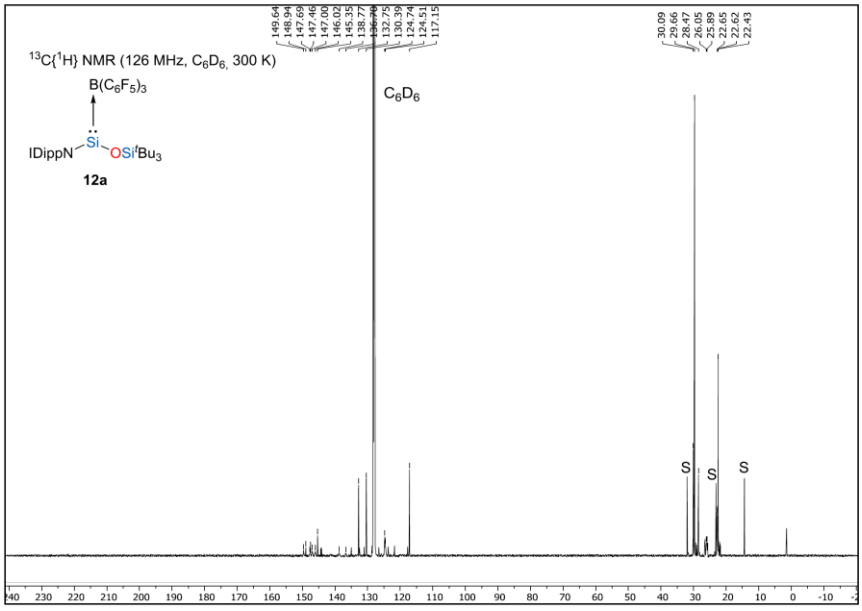


Figure S51. ^{13}C{^{1}H} NMR spectrum of (IDippN)(^{t}Bu$_3$SiO)Si(B(C$_6$F$_5$)$_3$) (**12a**) in C$_6$D$_6$ at 300 K. Residual *n*-hexane is labeled with S.

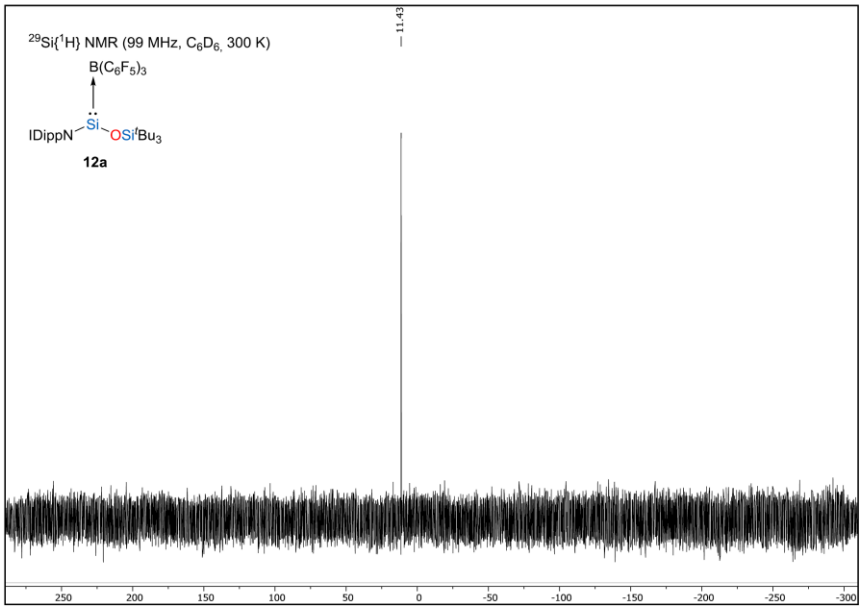
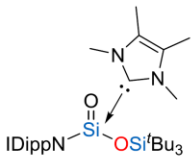


Figure S52. ^{29}Si{^{1}H} NMR spectrum of (IDippN)(^{t}Bu$_3$SiO)Si(B(C_6F_5)$_3$) (**12a**) in C_6D_6 at 300 K.

1.15 Synthesis of (IDippN)(^{t}Bu$_3$SiO)Si=O(IMe$_4$) (13a)



13a
$C_{46}H_{75}N_5O_2Si_2$
786.31 g/mol

A thick-walled, pressurizeable Schlenk flask with a rubber septum, containing a solution of silylene **1** (150 mg, 232 µmol, 1.0 eq.) in *n*-pentane (10 mL) was cooled to –130 °C. A precooled (–80 °C) solution of IMe$_4$ (28.8 mg, 232 µmol, 1.0 eq.) in toluene (0.5 mL) was added under vigorous stirring. A color change from colorless to yellow indicated formation of the NHC-stabilized silylene ((IDippN)(^{t}Bu$_3$SiO)Si(IMe$_4$)). Subsequently, the rubber septum was replaced by a PTFE-sealed screw cap and the reaction mixture was stirred for 30 min at –130 °C. The mixture was then frozen in liquid nitrogen, degassed and warmed to –130 °C. The solution was carefully exposed to N_2O (1 bar; **DANGER**: possible condensation of N_2O) and warmed to room-temperature, whereby a color change from yellow to colorless was observed. After removal of all volatiles *in vacuo*, the residue was washed with *n*-hexane. The IMe$_4$-stabilized silanoic ester derivative **13a** was afforded as a colorless solid (165 mg, 210 µmol, 90%). Colorless crystals, suitable for SC-XRD analysis, were obtained by cooling a saturated toluene solution of **13a** to –35 °C for several days. NHC adduct **13a** is completely stable as a solid and in solution at ambient and elevated temperatures (≤130 °C).

Note: The observed unusual broad splitting of the NHC wingtip methyl protons ($\Delta\delta$ = 1.03 ppm) in the ^{1}H NMR spectrum presumably originates from hydrogen bonding of one methyl C–H proton to the oxygen atom of the Si=O bond. This assumption is supported by the solid-state structure of **13a** (*vide infra*), which revealed a close O···H distance of 2.153 Å, being much shorter than the sum of the van der Waals radii of hydrogen and oxygen (2.72 Å).[S7]

m.p.: 209-210 °C (decomposition; color change from colorless to yellow).

^{1}H NMR (500 MHz, C_6D_6, 300 K): δ [ppm] = 7.21 (t, ^{3}J = 7.8 Hz, 2H, *p*-$C_{ar}H$), 7.12–7.09 (m, 4H, *m*-$C_{ar}H$), 6.03 (s, 2H, NCH), 4.22 (s, 3H, $N_{NHC}CH_3$), 3.38 (sept, ^{3}J = 6.9 Hz, 2H, CH(CH_3)$_2$), 3.29 (sept, ^{3}J = 6.9 Hz, 2H, CH(CH_3)$_2$), 3.19 (s, 3H, $N_{NHC}CH_3$), 1.40 (d, ^{3}J = 6.9 Hz, 6H, CH(CH_3)$_2$), 1.37–1.34 (m, 12H, CH(CH_3)$_2$ + $C_{NHC}CH_3$), 1.22 (d, ^{3}J = 6.9 Hz, 6H, CH(CH_3)$_2$), 1.22 (d, ^{3}J = 6.9 Hz, 6H, CH(CH_3)$_2$), 1.17 (s, 27H, C(CH_3)$_3$).

^{13}C{^{1}H} NMR (126 MHz, C_6D_6, 300 K): δ [ppm] = 159.6 (*carbene C*), 148.6 (*o*-C_{ar}), 148.5 (*o*-C_{ar}), 144.1 (NCN), 136.0 (*ipso*-C_{ar}), 128.8 (*p*-C_{ar}H), 124.7 ($C_{NHC}CH_3$), 123.6 (*m*-C_{ar}H), 123.5 (*m*-C_{ar}H + $C_{NHC}CH_3$), 114.7 (NCH), 33.8 ($N_{NHC}CH_3$), 33.4 ($N_{NHC}CH_3$), 30.7 (C(CH$_3$)$_3$), 29.2 (CH(CH_3)$_2$), 29.1 (CH(CH_3)$_2$), 25.2 (CH(CH$_3$)$_2$), 25.1 (CH(CH$_3$)$_2$), 23.4 (C(CH_3)$_3$), 23.3 (CH(CH$_3$)$_2$), 22.9 (CH(CH$_3$)$_2$), 7.8 ($C_{NHC}CH_3$), 7.8 ($C_{NHC}CH_3$).

^{29}Si{^{1}H} NMR (99 MHz, C_6D_6, 300 K): δ [ppm] = 1.3 (*Si*^{t}Bu$_3$), –88.5 (*central Si*).

Anal. Calcd. [%] for $C_{46}H_{75}N_5O_2Si_2$: C, 70.27; H, 9.61; N, 8.91. Found [%]: C, 69.13; H, 9.78; N, 8.98.

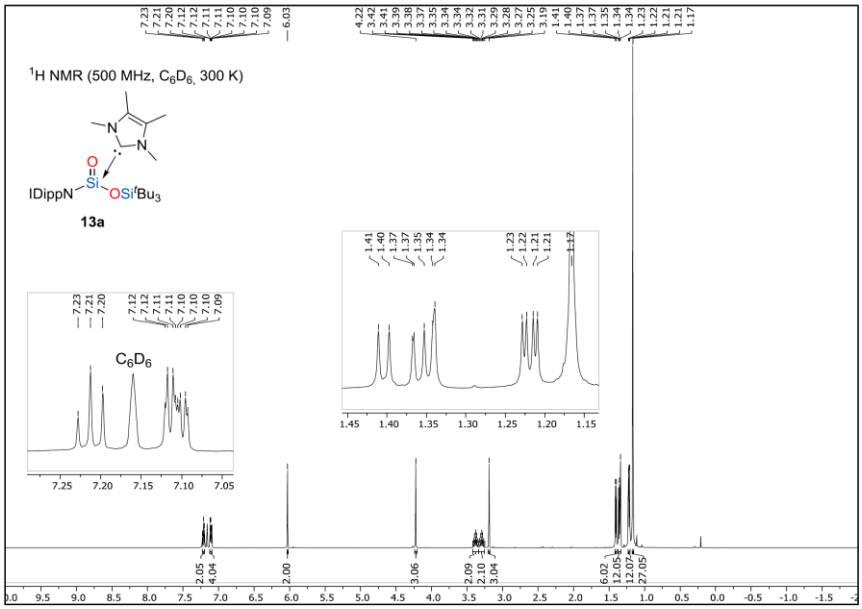


Figure S53. ^{1}H NMR spectrum of (IDippN)(^{t}Bu$_3$SiO)Si=O(IMe$_4$) (**13a**) in C_6D_6 at 300 K.

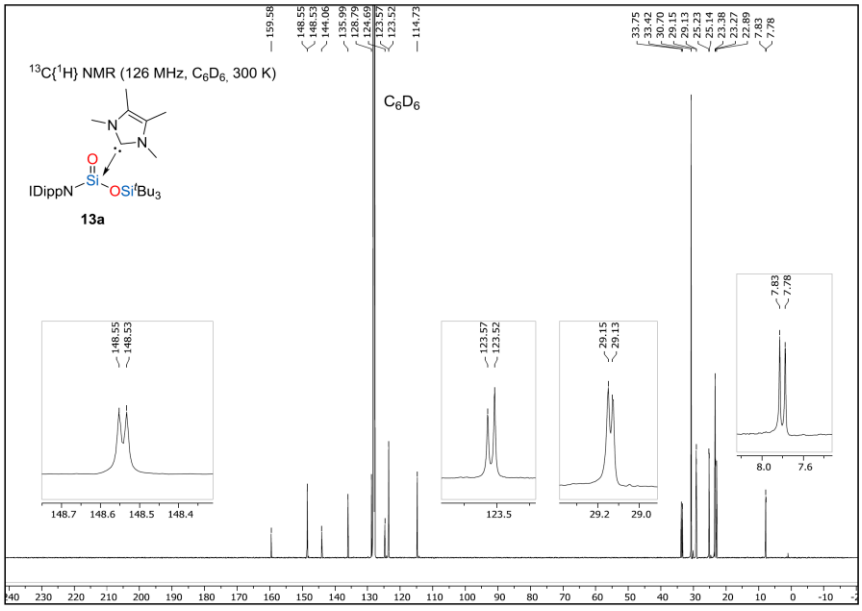


Figure S54. ^{13}C{^{1}H} NMR spectrum of (IDippN)(^{t}Bu$_3$SiO)Si=O(IMe$_4$) (**13a**) in C_6D_6 at 300 K.

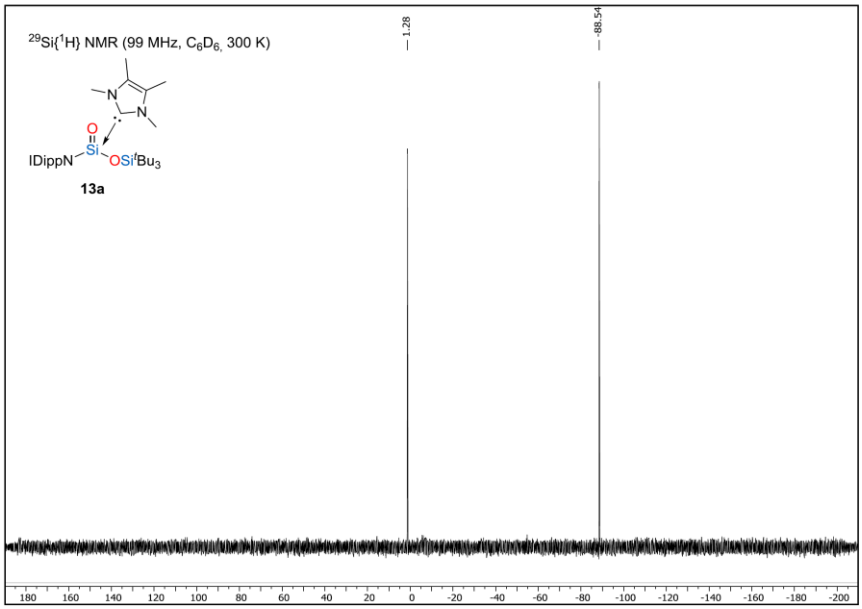
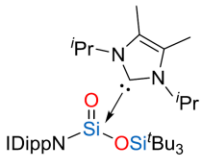


Figure S55. $^{29}Si\{^{1}H\}$ NMR spectrum of (IDippN)(^{t}Bu$_3$SiO)Si=O(IMe$_4$) (**13a**) in C_6D_6 at 300 K.

1.16 Synthesis and Reactivity of (IDippN)(^{t}Bu$_3$SiO)Si=O(I^{i}Pr$_2$Me$_2$) (13b)



13b
$C_{50}H_{83}N_5O_2Si_2$
842.42 g/mol

Benzene (5 mL) was added to a mixture of silylene **1** (100 mg, 155 µmol, 1.0 eq.) and I^{i}Pr$_2$Me$_2$ (27.9 mg, 155 µmol, 1.0 eq.) in a thick-walled, pressurizeable Schlenk flask. The solution was then frozen in liquid nitrogen, degassed and exposed to N_2O (1 bar) at room-temperature. Subsequently, the reaction mixture was stirred for 30 min. Removal of all volatiles *in vacuo* provided the I^{i}Pr$_2$Me$_2$-stabilized silanoic ester derivative **13b** as a colorless solid (130 mg, 155 µmol, quantitative yield). NHC adduct **13b** is completely stable as a solid and in solution at ambient and elevated temperatures (≤130 °C).

Note: The observed unusual broad splitting of the NHC wingtip methine protons (Δδ = 2.74 ppm) in the ^{1}H NMR spectrum presumably originates from hydrogen bonding of one isopropyl C–H proton to the oxygen atom of the Si=O bond.

m.p.: 242-243 °C (decomposition; color change from colorless to yellow).

^{1}H NMR (500 MHz, C_6D_6, 300 K): δ [ppm] = 8.53 (sept, ^{3}J = 6.9 Hz, 1H, $N_{NHC}C\underline{H}(CH_3)_2$), 7.32–7.26 (m, 4H, $C_{ar}\underline{H}$), 7.07–7.05 (m, 2H, $C_{ar}\underline{H}$), 5.89 (s, 2H, NC$\underline{H}$), 5.79 (sept, ^{3}J = 6.9 Hz, 1H, $N_{NHC}C\underline{H}(CH_3)_2$), 3.54 (sept, ^{3}J = 6.9 Hz, 2H, C$\underline{H}(CH_3)_2$), 3.10 (sept, ^{3}J = 6.9 Hz, 2H, C$\underline{H}(CH_3)_2$), 1.71 (br s, 6H, CH(C$\underline{H}_3)_2$), 1.63 (s, 3H, $C_{NHC}C\underline{H}_3$), 1.60 (s, 3H, $C_{NHC}C\underline{H}_3$), 1.40 (d, ^{3}J = 6.9 Hz,

3H, $N_{NHC}CH(C\underline{H}_3)_2$), 1.34 (d, ^3J = 6.9 Hz, 3H, $N_{NHC}CH(C\underline{H}_3)_2$), 1.23 (s, 27H, $C(C\underline{H}_3)_3$), 1.22 (d, ^3J = 6.9 Hz, 6H, $CH(C\underline{H}_3)_2$), 1.16 (d, ^3J = 6.9 Hz, 6H, $CH(C\underline{H}_3)_2$), 1.13 (d, ^3J = 6.9 Hz, 3H, $N_{NHC}CH(C\underline{H}_3)_2$), 1.05 (br s, 6H, $CH(C\underline{H}_3)_2$), 0.81 (d, ^3J = 6.9 Hz, 3H, $N_{NHC}CH(C\underline{H}_3)_2$).

$^{13}C\{^1H\}$ NMR (126 MHz, C_6D_6, 300 K): δ [ppm] = 158.5 (*carbene C*), 149.4 (*o*-$\underline{C}_{ar}$), 147.4 (*o*-$\underline{C}_{ar}$), 144.5 (N$\underline{C}$N), 136.5 (*ipso*-$\underline{C}_{ar}$), 129.2 (*p*-$\underline{C}_{ar}H$), 126.8 ($\underline{C}_{NHC}CH_3$), 124.5 ($\underline{C}_{NHC}CH_3$), 123.9 (*m*-$\underline{C}_{ar}H$), 115.7 (N$\underline{C}$H), 50.4 ($N_{NHC}\underline{C}H(CH_3)_2$), 48.7 ($N_{NHC}\underline{C}H(CH_3)_2$), 30.9 ($C(\underline{C}H_3)_3$), 29.5 ($\underline{C}H(CH_3)_2$), 28.5 ($\underline{C}H(CH_3)_2$), 26.0 ($CH(\underline{C}H_3)_2$), 25.7 ($CH(\underline{C}H_3)_2$), 23.6 ($CH(\underline{C}H_3)_2$), 23.4 ($\underline{C}(CH_3)_3$), 23.1 ($CH(\underline{C}H_3)_2$), 22.8 ($N_{NHC}CH(\underline{C}H_3)_2$), 22.6 ($N_{NHC}CH(\underline{C}H_3)_2$), 21.8 ($N_{NHC}CH(\underline{C}H_3)_2$), 21.7 ($N_{NHC}CH(\underline{C}H_3)_2$), 10.4 ($C_{NHC}\underline{C}H_3$), 10.3 ($C_{NHC}\underline{C}H_3$).

$^{29}Si\{^1H\}$ NMR (99 MHz, C_6D_6, 300 K): δ [ppm] = 1.6 (*Si*^{t}Bu$_3$), –86.7 (*central Si*).

Anal. Calcd. [%] for $C_{50}H_{83}N_5O_2Si_2$: C, 71.29; H, 9.93; N, 8.31. Found [%]: C, 70.40; H, 9.94; N, 8.26.

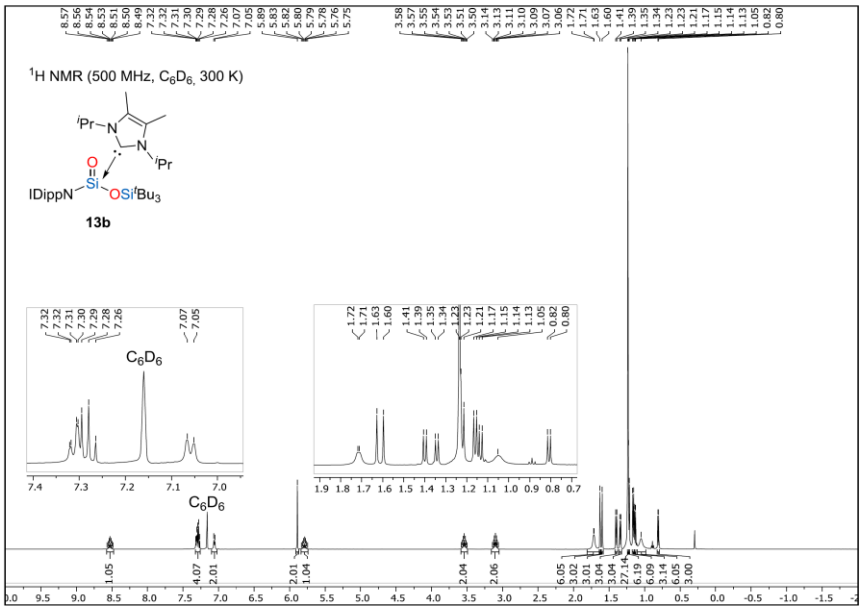


Figure S56. ^{1}H NMR spectrum of (IDippN)(^{t}Bu$_3$SiO)Si=O(I^{i}Pr$_2$Me$_2$) (**13b**) in C_6D_6 at 300 K.

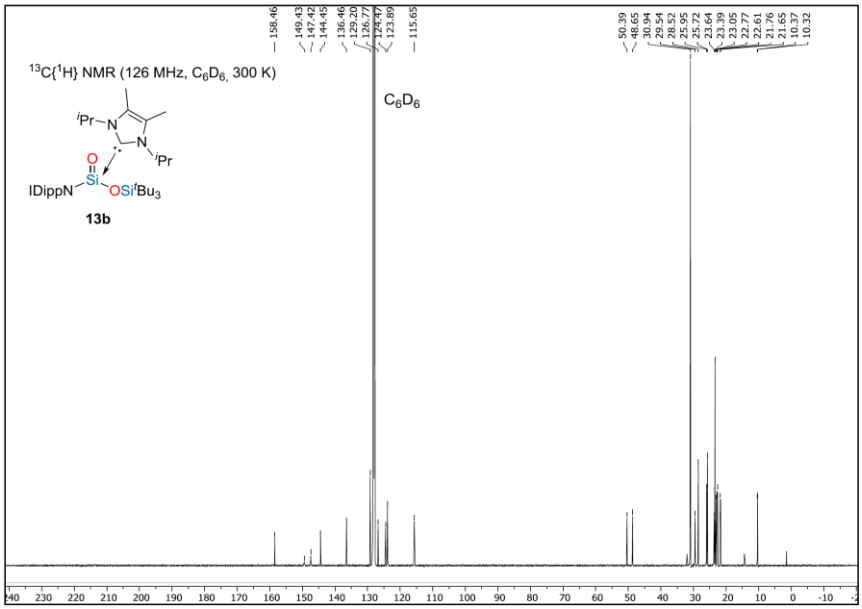


Figure S57. $^{13}C\{^{1}H\}$ NMR spectrum of (IDippN)(^{t}Bu$_3$SiO)Si=O(I^{i}Pr$_2$Me$_2$) (**13b**) in C_6D_6 at 300 K.

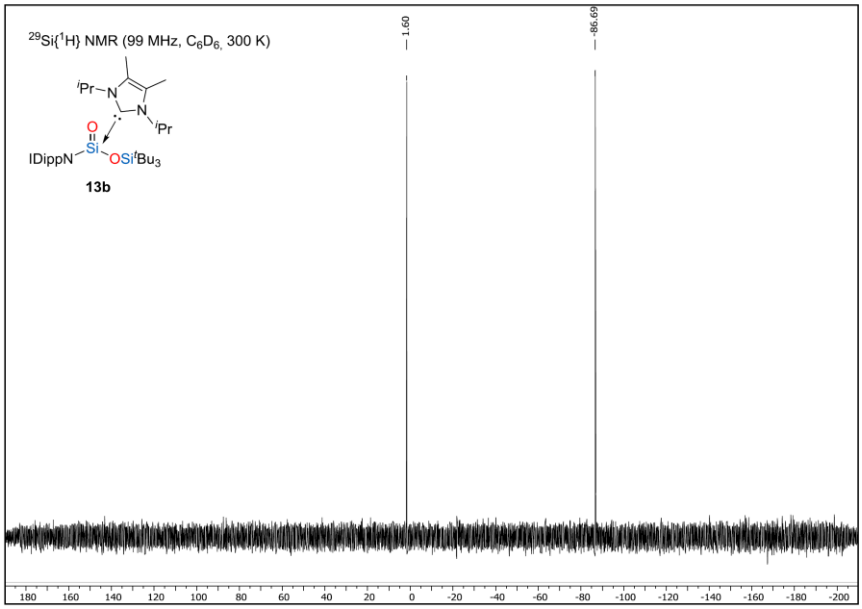


Figure S58. $^{29}Si\{^{1}H\}$ NMR spectrum of (IDippN)(^{t}Bu$_3$SiO)Si=O(I^{i}Pr$_2$Me$_2$) (**13b**) in C_6D_6 at 300 K.

Reactivity Investigations

Due to the convenient access to (IDippN)(^{t}Bu$_3$SiO)Si=O(I^{i}Pr$_2$Me$_2$) (**13b**), this NHC-stabilized silanoic ester derivative was subjected to some subsequent reactions.

Ligand Substitution (NHC Exchange Reaction)

A substitution of a weaker σ-donor by a stronger Lewis base is often observed for NHC-supported organosilicon compounds.[S8] Therefore, a possible ligand exchange reaction was investigated:

A *J. Young* PTFE valve NMR tube was charged with a mixture of (IDippN)(^{t}Bu$_3$SiO)Si=O(I^{i}Pr$_2$Me$_2$) (**13b**) (20.0 mg, 23.7 µmol, 1.0 eq.) and IMe$_4$ (2.95 mg, 23.7 µmol, 1.0 eq.) in C_6D_6 (0.5 mL). Since no reaction was detected after 1 d at room-temperature *via* ^{1}H NMR spectroscopy, we exposed the sample to elevated temperatures. Full conversion of **13b** to the IMe$_4$-stabilized silanoic ester derivative (IDippN)(^{t}Bu$_3$SiO)Si=O(IMe$_4$) (**13a**) with concomitant formation of free I^{i}Pr$_2$Me$_2$ was observed after 1 d at 110 °C.
Note: NHC adduct **13a** can be separated from I^{i}Pr$_2$Me$_2$ and isolated after removing the solvent *in vacuo* and washing the residue with cold *n*-hexane.

NHC Abstraction Reactions

To prove the intermediary formation of (IDippN)(^{t}Bu$_3$SiO)Si=O (**10a′**) during the synthesis of *trans*-cyclodisiloxane [(IDippN)(^{t}Bu$_3$SiO)Si=O]$_2$ (**10a**), we wanted to abstract the NHC and observe subsequent dimerization affording **10a**. For this purpose, the reaction of **13b** toward common NHC abstraction reagents, such as CO_2 or BR_3 compounds, was studied:

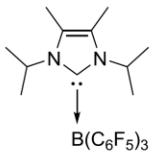
A *J. Young* PTFE valve NMR tube was charged with a solution of (IDippN)(^{t}Bu$_3$SiO)Si=O(I^{i}Pr$_2$Me$_2$) (**13b**) (20.0 mg, 23.7 µmol) in C_6D_6 (0.5 mL), degassed and exposed to CO_2 (1 bar). Immediate full conversion of **13b** to silicon carbonate complex (IDippN)(^{t}Bu$_3$SiO)Si(O_2C=O) (**9**) with simultaneous formation of the NHC-CO_2 adduct I^{i}Pr$_2$Me$_2$·CO_2 was detected by ^{1}H NMR spectroscopy.

Since NHC abstraction with CO_2 worked, but not the dimerization to **10a**, but the [2+2] cycloaddition reaction providing **9** was observed, we turned to the Lewis acids B(C_6F_5)$_3$ and BPh$_3$.

Interestingly, addition of an equimolar amount of BCF to **13b** at room temperature resulted in the unselective formation of novel silicon-containing products, but only a conversion of 50% was detected. The addition of a second equivalent of BCF then led to full conversion. The formation of a mixture of products, containing the desired NHC-borane adduct $I^iPr_2Me_2{\cdot}B(C_6F_5)_3$ and a compound bearing a Si–F bond, was identified by multinuclear and 2D NMR spectroscopy. However, purification and isolation was not possible so far. The reaction most likely proceeds via NHC-abstraction and simultaneous formation of $I^iPr_2Me_2{\cdot}B(C_6F_5)_3$ and the Lewis acid-stabilized silanoic ester derivative (IDippN)(^{t}Bu$_3$SiO)Si=O(B(C_6F_5)$_3$), which undergoes subsequent bond activation and rearrangement reactions.

By-product NHC-borane adduct $I^iPr_2Me_2{\cdot}B(C_6F_5)_3$:

For the sake of comparison, the Lewis acid/base-complex $I^iPr_2Me_2{\cdot}B(C_6F_5)_3$ was separately synthesized and characterized *via* multinuclear NMR spectroscopy:



$I^iPr_2Me_2{\cdot}B(C_6F_5)_3$
$C_{29}H_{20}BF_{15}N_2$
692.28 g/mol

To a solution of BCF (28.4 mg, 55.5 µmol, 1.0 eq.) in benzene (0.5 mL) was added a solution of $I^iPr_2Me_2$ (10.0 mg, 55.5 µmol, 1.0 eq.) in benzene (0.5 mL). Subsequently, the reaction mixture was stirred for 30 min. Removal of the solvent *in vacuo* afforded the NHC-borane adduct $I^iPr_2Me_2{\cdot}B(C_6F_5)_3$ as a colorless solid (38.4 mg, 55.5 µmol, quantitative yield).

Note: Due to coupling with the ^{11}B nucleus (high quadrupole moment and spin ^{11}B = 3/2) and the ^{19}F atoms, several resonances are broadened in the NMR spectra.

^{1}H NMR (500 MHz, C_6D_6, 300 K): δ [ppm] = 4.69 (sept, ^3J = 6.9 Hz, 2H, C*H*(CH$_3$)$_2$), 1.42 (s, 6H, C*H*$_3$), 1.02 (d, ^3J = 6.9 Hz, 6H, CH(C*H*$_3$)$_2$), 0.52 (d, ^3J = 6.9 Hz, 6H, CH(C*H*$_3$)$_2$).

^{11}B{^{1}H} NMR (128 MHz, C_6D_6, 300 K): δ [ppm] = –16.5.

^{13}C{^{1}H} NMR (126 MHz, C_6D_6, 300 K): δ [ppm] = 158.6–157.0 (m, *carbene C*), 150.2–146.6 (m, *C*$_{ar}$), 141.1–140.8 (m, *C*$_{ar}$), 139.1–138.3 (m, *C*$_{ar}$), 137.0–136.2 (m, *C*$_{ar}$), 126.6 (*C*CH$_3$), 49.9 (*C*H(CH$_3$)$_2$), 49.9 (*C*H(CH$_3$)$_2$), 21.3 (CH(*C*H$_3$)$_2$), 21.3 (CH(*C*H$_3$)$_2$), 20.3 (br s, CH(*C*H$_3$)$_2$), 10.2 (C*C*H$_3$).

^{19}F{^{1}H} NMR (471 MHz, C_6D_6, 300 K): δ [ppm] = –126.4 to –126.4 (m, 2F, *o*-C$_{ar}$*F*), –130.3 to –130.4 (m, 2F, *o*-C$_{ar}$*F*), –132.3 to –132.3 (m, 2F, *o*-C$_{ar}$*F*), –157.6 (t, $^3J_{FF}$ = 21.7 Hz, 1F, *p*-C$_{ar}$*F*), –158.2 (t, $^3J_{FF}$ = 21.7 Hz, 2F, *p*-C$_{ar}$*F*), –162.7 (t, $^3J_{FF}$ = 21.7 Hz, 2F, *m*-C$_{ar}$*F*), –164.4 (dt, $^3J_{FF}$ = 21.7 Hz, $^4J_{FF}$ = 7.8 Hz, 2F, *m*-C$_{ar}$*F*), –165.1 to –165.2 (m, 2F, *m*-C$_{ar}$*F*).

The spectroscopic data are consistent with those previously reported.[S9]

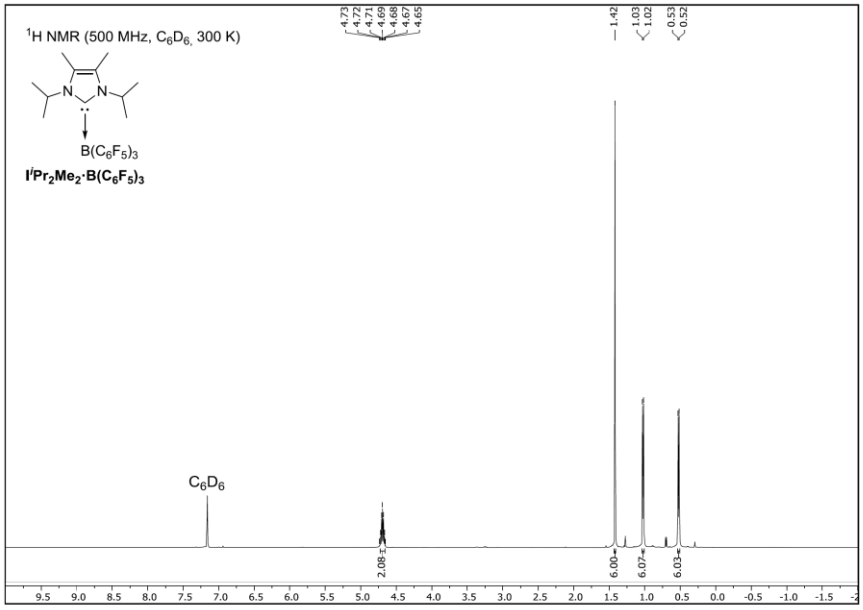


Figure S59. ^{1}H NMR spectrum of $I^iPr_2Me_2{\cdot}B(C_6F_5)_3$ in C_6D_6 at 300 K.

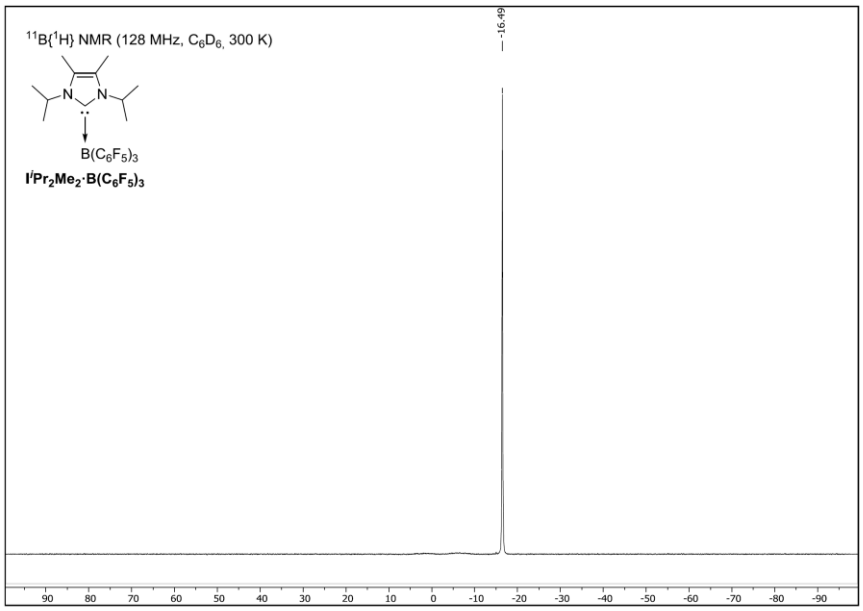


Figure S60. $^{11}B\{^1H\}$ NMR spectrum of $I^iPr_2Me_2{\cdot}B(C_6F_5)_3$ in C_6D_6 at 300 K.

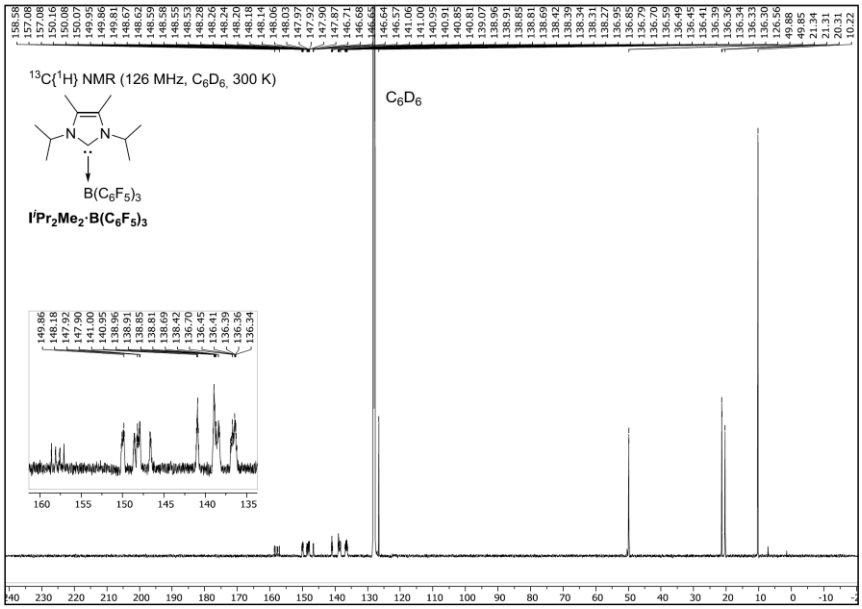


Figure S61. $^{13}C\{^{1}H\}$ NMR spectrum of $I^iPr_2Me_2{\cdot}B(C_6F_5)_3$ in C_6D_6 at 300 K.

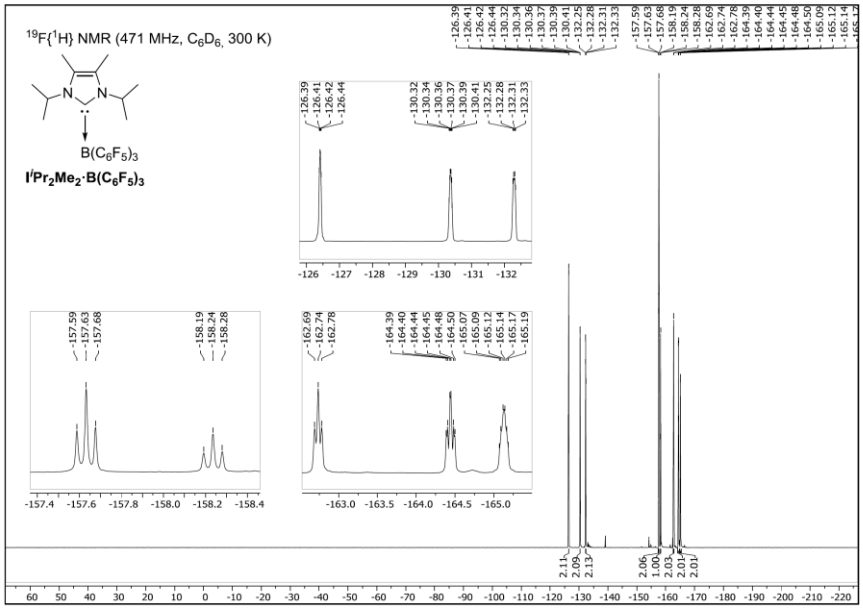


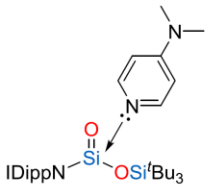
Figure S62. $^{19}F\{^{1}H\}$ NMR spectrum of $I^iPr_2Me_2{\cdot}B(C_6F_5)_3$ in C_6D_6 at 300 K.

In contrast to the reaction of **13b** with BCF, treatment of **13b** with BPh_3 resulted in the clean formation of a sole product, but again two equivalents and additionally elevated temperatures were required to achieve full conversion. In analogy to a recent report by Iwamoto *et al.* on the rearrangement of a BCF-stabilized silanone to an aryl(boryloxy)silane, the intermediary formed Lewis acid-stabilized silanoic ester derivative (IDippN)(^{t}Bu$_3$SiO)Si=O(BPh_3) isomerized to aryl(boryloxy)silane **14**.[S10]

A *J. Young* PTFE valve NMR tube was charged with a mixture of (IDippN)(^{t}Bu$_3$SiO)Si=O(I^{i}Pr$_2$Me$_2$) (**13b**) (20.0 mg, 23.7 µmol, 1.0 eq.) and BPh_3 (11.5 mg, 47.5 µmol, 2.0 eq.) in C_6D_6 (0.5 mL). Since no reaction was detected after 1 d at room-temperature *via* ^{1}H NMR spectroscopy, we exposed the sample to elevated temperatures. Full conversion of **13b** to aryl(boryloxy)silane **14** with concomitant formation of I^{i}Pr$_2$Me$_2$·BPh_3 was observed after 2 h at 130 °C.

Note: It was not possible to separate aryl(boryloxy)silane **14** from the I^{i}Pr$_2$Me$_2$·BPh_3 adduct, however pure **14** can be obtained *via* exposure of the *in-situ* generated (IDippN)(^{t}Bu$_3$SiO)Si(BPh_3) (**12b**) to N_2O (*vide infra*).

1.17 Synthesis of (IDippN)(^{t}Bu$_3$SiO)Si=O(DMAP) (13c)



13c
$C_{46}H_{73}N_5O_2Si_2$
784.29 g/mol

Benzene (5 mL) was added to a mixture of silylene **1** (100 mg, 155 µmol, 1.0 eq.) and DMAP (18.9 mg, 155 µmol, 1.0 eq.) in a thick-walled, pressurizeable Schlenk flask. The solution was then frozen in liquid nitrogen, degassed and exposed to N_2O (1 bar) at room-temperature. Subsequently, the reaction mixture was stirred for 30 min. Removal of all volatiles *in vacuo* provided the DMAP-stabilized silanoic ester derivative **13c** as a colorless solid (121 mg, 155 µmol, quantitative yield). DMAP adduct **13c** is completely stable as a solid and in solution at ambient temperature.

Note: At high temperatures isomerization to an unidentified product was observed, but the reaction is extremely slow (only ~10% conversion after 10 days at 135 °C) and thus was not further studied. However, ^{1}H NMR spectroscopy indicated aromatic C–H bond activation of DMAP.

m.p.: 253-254 °C (decomposition; color change from colorless to yellow).

^{1}H NMR (500 MHz, C_6D_6, 300 K): δ [ppm] = 8.37 (d, ^3J = 6.8 Hz, 2H, *o*-C$_{DMAP}$*H*), 7.20–7.17 (m, 3H, C$_{ar}$*H*), 7.15–7.14 (m, 2H, C$_{ar}$*H*), 7.14–7.13 (m, 1H, C$_{ar}$*H*), 6.48 (d, ^3J = 6.8 Hz, 2H, *m*-C$_{DMAP}$*H*), 6.02 (s, 2H, NC*H*), 3.48 (sept, ^3J = 6.9 Hz, 2H, C*H*(CH$_3$)$_2$), 3.36 (sept, ^3J = 6.9 Hz,

2H, C*H*(CH$_3$)$_2$), 2.59 (s, 6H, N(C*H*$_3$)$_2$), 1.55 (d, ^3J = 6.9 Hz, 6H, CH(C*H*$_3$)$_2$), 1.52 (d, ^3J = 6.9 Hz, 6H, CH(C*H*$_3$)$_2$), 1.25 (d, ^3J = 6.9 Hz, 6H, CH(C*H*$_3$)$_2$), 1.25 (d, ^3J = 6.9 Hz, 6H, CH(C*H*$_3$)$_2$), 1.17 (s, 27H, C(C*H*$_3$)$_3$).

^{13}C{^{1}H} NMR (126 MHz, C$_6$D$_6$, 300 K): δ [ppm] = 156.0 (*p*-*C*$_{DMAP}$), 148.2 (*o*-*C*$_{ar}$), 148.1 (*o*-*C*$_{ar}$), 145.7 (*o*-*C*$_{DMAP}$H), 143.2 (N*C*N), 135.7 (*ipso*-*C*$_{ar}$), 129.2 (*p*-*C*$_{ar}$H), 124.0 (*m*-*C*$_{ar}$H), 123.8 (*m*-*C*$_{ar}$H), 114.5 (N*C*H), 106.3 (*m*-*C*$_{DMAP}$H), 39.4 (N(*C*H$_3$)$_2$), 30.7 (C(*C*H$_3$)$_3$), 29.2 (*C*H(CH$_3$)$_2$), 29.0 (*C*H(CH$_3$)$_2$), 25.1 (CH(*C*H$_3$)$_2$), 24.8 (CH(*C*H$_3$)$_2$), 24.0 (CH(*C*H$_3$)$_2$), 23.5 (CH(*C*H$_3$)$_2$), 23.4 (*C*(CH$_3$)$_3$).

^{29}Si{^{1}H} NMR (99 MHz, C$_6$D$_6$, 300 K): δ [ppm] = 0.6 (*Si*^{t}Bu$_3$), –87.8 (*central Si*).

Anal. Calcd. [%] for C$_{46}$H$_{73}$N$_5$O$_2$Si$_2$: C, 70.45; H, 9.38; N, 8.93. Found [%]: C, 70.14; H, 9.55; N, 8.66.

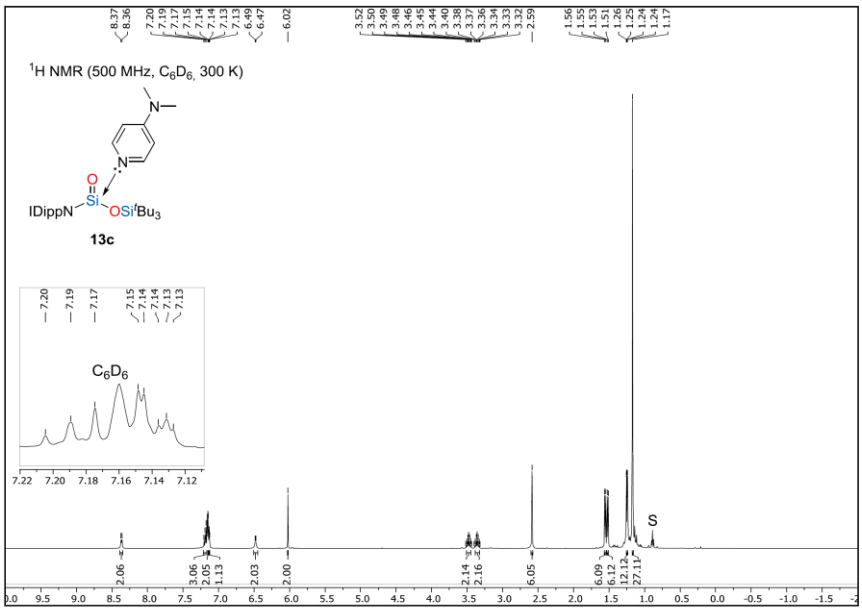


Figure S63. ^{1}H NMR spectrum of (IDippN)(*t*Bu$_3$SiO)Si=O(DMAP) (**13c**) in C$_6$D$_6$ at 300 K. Residual *n*-hexane (from starting material) is labeled with S.

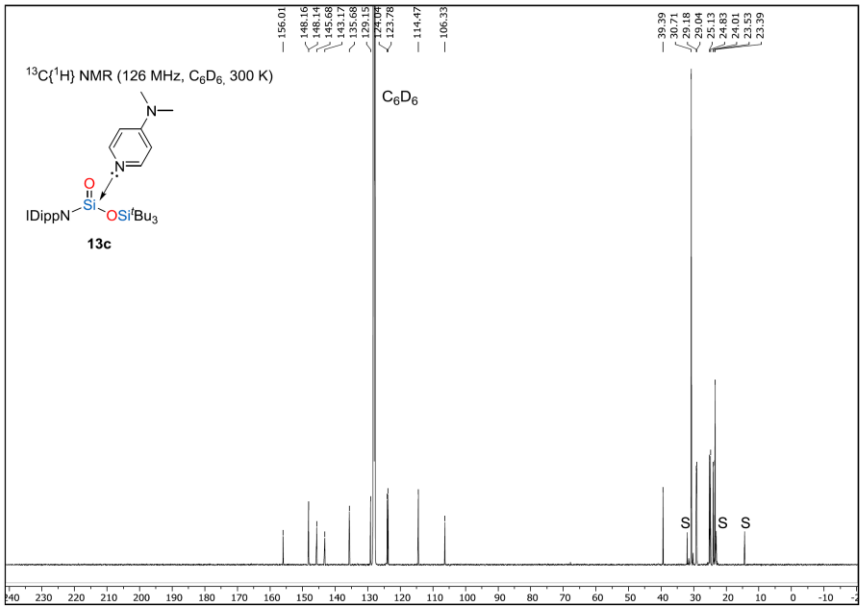


Figure S64. $^{13}C\{^{1}H\}$ NMR spectrum of (IDippN)(^{t}Bu$_3$SiO)Si=O(DMAP) (**13c**) in C_6D_6 at 300 K. Residual *n*-hexane is labeled with S.

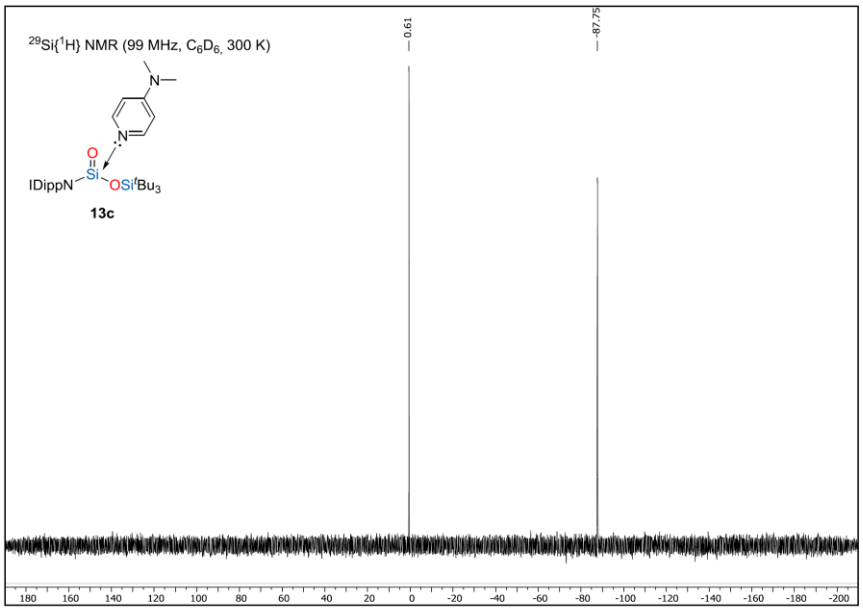


Figure S65. $^{29}Si\{^{1}H\}$ NMR spectrum of (IDippN)(^{t}Bu$_3$SiO)Si=O(DMAP) (**13c**) in C_6D_6 at 300 K.

1.18 Synthesis of Aryl(boryloxy)silane 14



14
$C_{57}H_{78}BN_3O_2Si_2$
904.25 g/mol

Benzene (5 mL) was added to a mixture of silylene **1** (100 mg, 155 µmol, 1.0 eq.) and BPh_3 (37.5 mg, 155 µmol, 1.0 eq.) in a thick-walled, pressurizeable Schlenk flask. The resulting reaction mixture was stirred for 30 min. An observed color change to yellow indicated formation of the silylene-borane adduct (IDippN)(^{t}Bu$_3$SiO)Si(BPh_3) (**12b**). The solution was then frozen in liquid nitrogen, degassed and exposed to N_2O (1 bar) at room-temperature. Subsequently, the reaction mixture was stirred for 30 min. Removal of all volatiles *in vacuo* provided aryl(boryloxy)silane **14** as a colorless solid (140 mg, 155 µmol, quantitative yield). Compound **14** is completely stable as a solid and in solution at ambient and elevated temperatures (≤130 °C).

m.p.: 188-189 °C (decomposition; color change from colorless to yellow).

^{1}H NMR (500 MHz, C_6D_6, 300 K): δ [ppm] = 7.86–7.84 (m, 4H, $C_{ar}\underline{H}$), 7.66–7.64 (m, 2H, $C_{ar}\underline{H}$), 7.34–7.23 (m, 8H, $C_{ar}\underline{H}$), 7.14–7.12 (m, 2H, $C_{ar}\underline{H}$), 7.00–6.99 (m, 3H, $C_{ar}\underline{H}$), 6.92–6.90 (m, 2H, $C_{ar}\underline{H}$), 6.04 (s, 2H, NC$\underline{H}$), 3.29 (sept, ^3J = 6.9 Hz, 2H, C$\underline{H}$(CH$_3$)$_2$), 3.19 (sept, ^3J = 6.9 Hz, 2H, C$\underline{H}$(CH$_3$)$_2$), 1.21 (d, ^3J = 6.9 Hz, 6H, CH(C$\underline{H}_3$)$_2$), 1.12 (d, ^3J = 6.9 Hz, 6H, CH(C$\underline{H}_3$)$_2$), 1.09 (d, ^3J = 6.9 Hz, 6H, CH(C$\underline{H}_3$)$_2$), 1.09 (d, ^3J = 6.9 Hz, 6H, CH(C$\underline{H}_3$)$_2$), 0.88 (s, 27H, C(C$\underline{H}_3$)$_3$).

^{11}B{^{1}H} NMR (128 MHz, C_6D_6, 300 K): In an inexplicable way no ^{11}B NMR resonance could be detected for compound **14**.

^{13}C{^{1}H} NMR (126 MHz, C_6D_6, 300 K): δ [ppm] = 147.3 (*o*-$\underline{C}_{Dipp}$), 147.2 (*o*-$\underline{C}_{Dipp}$), 144.8 (N$\underline{C}$N), 139.4 ($\underline{C}_{ar}$), 137.1 ($\underline{C}_{ar}$H), 135.7 ($\underline{C}_{ar}$H), 134.7 (*ipso*-$\underline{C}_{Dipp}$), 130.4 ($\underline{C}_{ar}$H), 129.8 ($\underline{C}_{ar}$H), 128.9 (*p*-$\underline{C}_{Dipp}$H), 127.3 ($\underline{C}_{ar}$H), 127.1 ($\underline{C}_{ar}$H), 124.4 (*m*-$\underline{C}_{Dipp}$H), 124.3 (*m*-$\underline{C}_{Dipp}$H), 115.6 (N$\underline{C}$H), 30.4 (C($\underline{C}$H$_3$)$_3$), 29.1 ($\underline{C}$H(CH$_3$)$_2$), 29.0 ($\underline{C}$H(CH$_3$)$_2$), 26.1 (CH($\underline{C}$H$_3$)$_2$), 26.1 (CH($\underline{C}$H$_3$)$_2$), 22.9 ($\underline{C}$(CH$_3$)$_3$), 22.8 (CH($\underline{C}$H$_3$)$_2$), 22.3 (CH($\underline{C}$H$_3$)$_2$).

^{29}Si{^{1}H} NMR (99 MHz, C_6D_6, 300 K): δ [ppm] = 2.5 (*Si*^{t}Bu$_3$), –81.4 ($\underline{Si}$O).

Anal. Calcd. [%] for $C_{57}H_{78}BN_3O_2Si_2$: C, 75.71; H, 8.69; N, 4.65. Found [%]: C, 75.62; H, 8.63; N, 4.67.

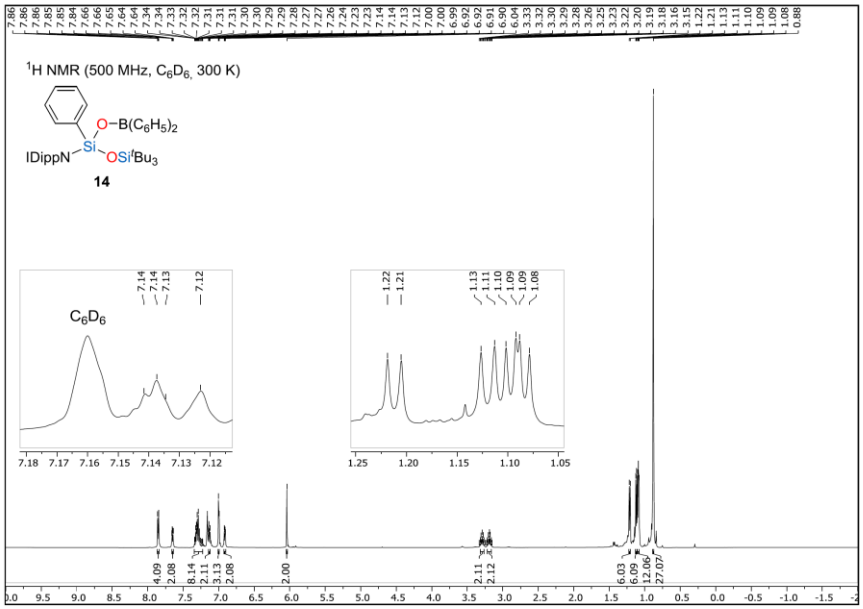


Figure S66. ^{1}H NMR spectrum of aryl(boryloxy)silane **14** in C_6D_6 at 300 K.

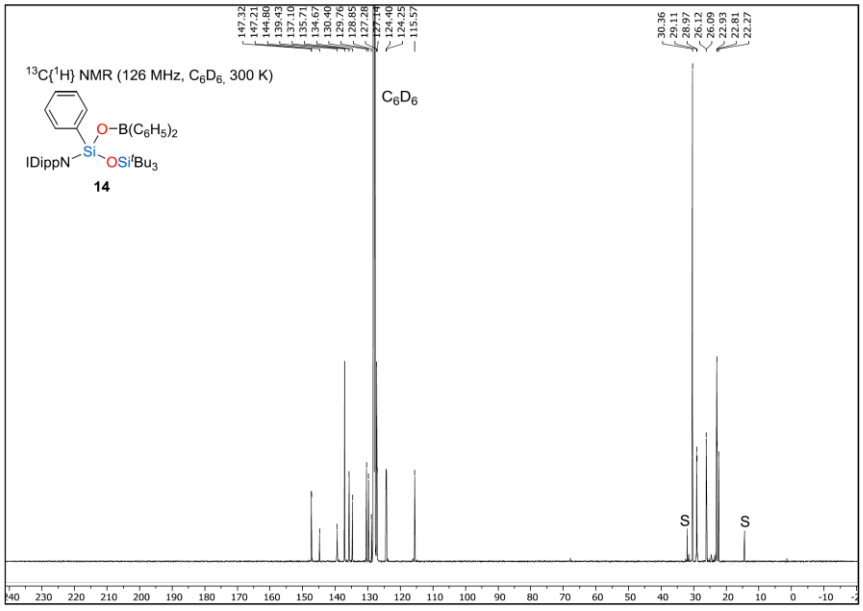


Figure S67. ^{13}C{^{1}H} NMR spectrum of aryl(boryloxy)silane **14** in C_6D_6 at 300 K. Residual *n*-hexane is labeled with S.

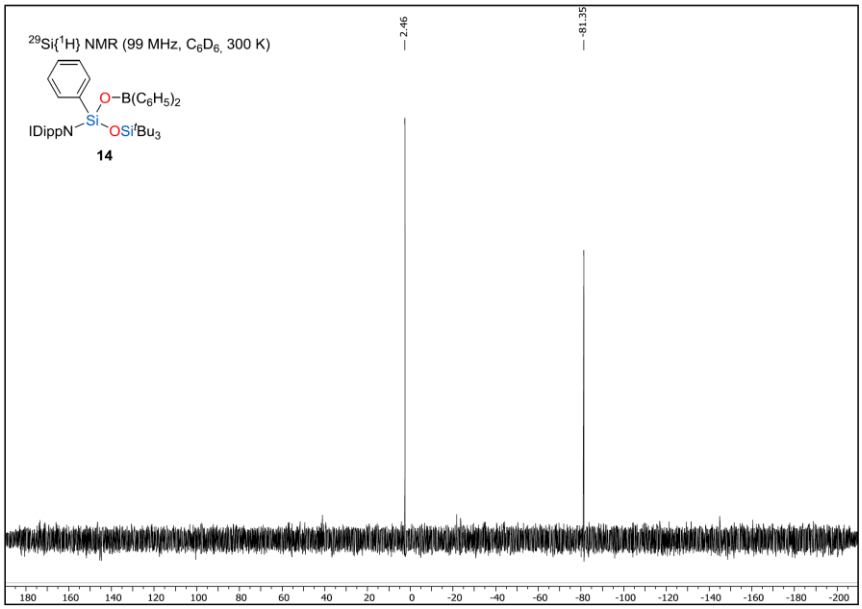


Figure S68. $^{29}Si\{^{1}H\}$ NMR spectrum of aryl(boryloxy)silane **14** in C_6D_6 at 300 K.

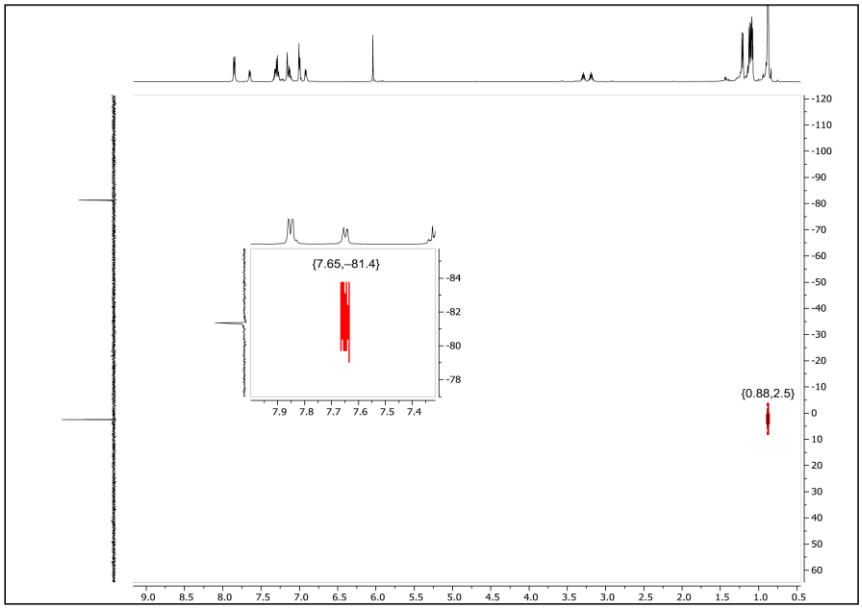


Figure S69. $^{1}H/^{29}Si$ HMBC NMR spectrum of aryl(boryloxy)silane **14** in C_6D_6 at 300 K.

2. X-ray Crystallographic Data

General Information

The X-ray intensity data of **3** was collected on an X-ray single crystal diffractometer equipped with a CMOS detector (*Bruker Photon-100*), a rotating anode (*Bruker TXS*) with MoKα radiation (λ = 0.71073 Å) and a *Helios* mirror optic by using the *APEX III* software package.[S11] The X-ray intensity data of **6**, **7**, **9**, **11**, **12a** and **13a** were collected on an X-ray single crystal diffractometer equipped with a CMOS detector (*Bruker Photon-100*), an IMS microsource with MoKα radiation (λ = 0.71073 Å) and a *Helios* mirror optic by using the *APEX III* software package.[S11] The measurements were performed on single crystals coated with the perfluorinated ether *Fomblin® Y*. The crystals were fixed on the top of a microsampler, transferred to the diffractometer and frozen under a stream of cold nitrogen. A matrix scan was used to determine the initial lattice parameters. Reflections were merged and corrected for Lorenz and polarization effects, scan speed, and background using *SAINT*.[S12] Absorption corrections, including odd and even ordered spherical harmonics were performed using *SADABS*.[S12] Space group assignments were based upon systematic absences, E statistics, and successful refinement of the structures. Structures were solved by direct methods with the aid of successive difference Fourier maps, and were refined against all data using the *APEX III* software in conjunction with *SHELXL-2014*[S13] and *SHELXLE*.[S14] All H atoms were placed in calculated positions and refined using a riding model, with methylene and aromatic C–H distances of 0.99 and 0.95 Å, respectively, and $U_{iso}(H) = 1.2 \cdot U_{eq}(C)$. Full-matrix least-squares refinements were carried out by minimizing $\Delta w(F_o^2 - F_c^2)^2$ with *SHELXL-97*[S15] weighting scheme. Neutral atom scattering factors for all atoms and anomalous dispersion corrections for the non-hydrogen atoms were taken from International Tables for Crystallography.[S16] The images of the crystal structures were generated by *Mercury*.[S17] The CCDC numbers CCDC-1983560 (**13a**), CCDC-1983561 (**3**), CCDC-1983562 (**12a**), CCDC-1983563 (**11**), CCDC-1983564 (**7**), CCDC-1983565 (**6**), and CCDC-1983579 (**9**) contain the supplementary crystallographic data for the structures. These data can be obtained free of charge from the *Cambridge Crystallographic Data Centre via* https://www.ccdc.cam.ac.uk/structures/.

Single Crystal X-ray Structure Determinations

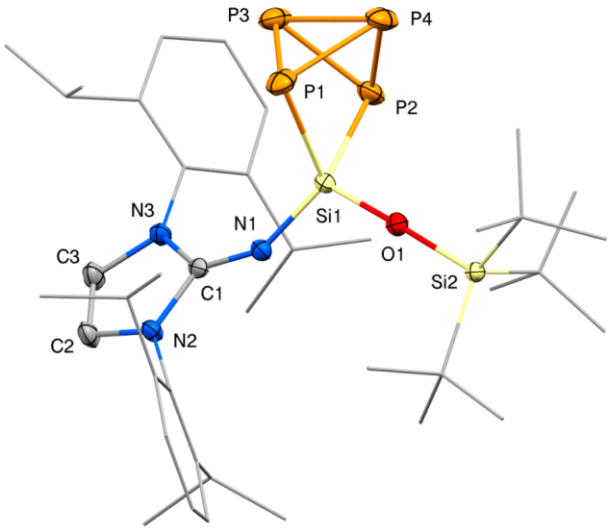


Figure S70. Molecular structure of **3** with ellipsoids set at 50% probability. Hydrogen atoms are omitted for clarity. Selected bond lengths [Å] and angles [°]: Si1–O1 1.617(1), Si1–P1 2.256(1), Si1–P2 2.270(1), Si1–N1 1.657(1), N1–C1 1.280(2), Si2–O1 1.639(1), P1–P3 2.241(1), P1–P4 2.227(1), P2–P3 2.222(1), P2–P4 2.360(1), P3–P4 2.162(1); N1–Si1–O1 109.1(1), Si1–N1–C1 149.0(1), Si1–O1–Si2 166.7(1), P1–Si1–P2 86.7(1).

Table S1. Crystal data and structure refinement for compound **3**.

Chemical formula	$C_{39}H_{63}N_3OP_4Si_2$	
Formula weight	770.02 g/mol	
Temperature	123(2) K	
Wavelength	0.71073 Å	
Crystal size	0.112 × 0.179 × 0.242 mm	
Crystal habit	clear colorless fragment	
Crystal system	monoclinic	
Space group	P 21/c	
Unit cell dimensions	a = 18.2755(11) Å	α = 90(5)°
	b = 10.7417(7) Å	β = 90.804(2)°
	c = 22.0169(15) Å	γ = 90(5)°
Volume	4321.7(5) $Å^3$	
Z	4	
Density (calculated)	1.183 g/cm^3	
Absorption coefficient	0.263 mm^{-1}	
F(000)	1656	
Diffractometer	Bruker D8 Venture	
Radiation source	TXS rotating anode, Mo	
Theta range for data collection	2.23 to 25.35°	
Index ranges	–22<=h<=22, –12<=k<=12, –26<=l<=26	
Reflections collected	79231	
Independent reflections	7897 [R(int) = 0.0367]	
Coverage of independent reflections	99.9%	
Absorption correction	Multi-Scan	
Max. and min. transmission	0.7260 and 0.7452	
Refinement method	Full-matrix least-squares on F^2	
Refinement program	SHELXL-2014 (Sheldrick, 2014)	
Function minimized	$\Sigma\, w(F_o^2 - F_c^2)^2$	
Data / restraints / parameters	7897 / 489 / 39	
Goodness-of-fit on F^2	1.040	
Final R indices	6837 data; I>2σ(I)	R1 = 0.0348, wR2 = 0.0866
	all data	R1 = 0.0427, wR2 = 0.0917
Weighting scheme	$w = 1/[\sigma^2(F_o^2) + (0.0398P)^2 + 4.0672P]$	
	where $P = (F_o^2 + 2F_c^2)/3$	
Largest diff. peak and hole	0.646 and –0.457 $eÅ^{-3}$	
R.M.S. deviation from mean	0.052 $eÅ^{-3}$	

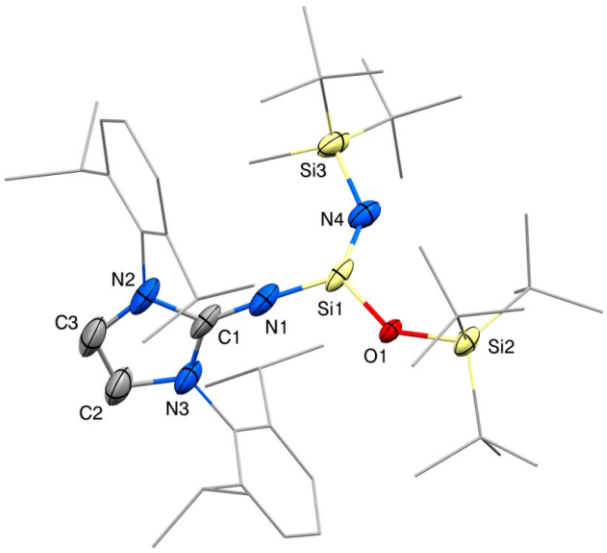


Figure S71. Molecular structure of **6** with ellipsoids set at 50% probability. Hydrogen atoms are omitted for clarity. Selected bond lengths [Å] and angles [°]: Si1–O1 1.618(3), Si1–N1 1.623(2), Si1–N4 1.573(2), N1–C1 1.275(4), Si2–O1 1.651(5), N4–Si3 1.693(2); N1–Si1–O1 107.0(1), N1–Si1–N4 130.7(1), N4–Si1–O1 122.2(1), Si1–N1–C1 153.9(2), Si1–O1–Si2 143.6(3), Si1–N4–Si3 139.4(1).

Table S2. Crystal data and structure refinement for compound **6**.

Chemical formula	$C_{48}H_{84}N_4OSi_3$	
Formula weight	817.48 g/mol	
Temperature	100(2) K	
Wavelength	0.71073 Å	
Crystal size	0.070 × 0.181 × 0.290 mm	
Crystal habit	clear colorless fragment	
Crystal system	monoclinic	
Space group	P 21/n	
Unit cell dimensions	a = 13.2094(8) Å	α = 90°
	b = 18.7067(12) Å	β = 91.315(2)°
	c = 20.3570(13) Å	γ = 90°
Volume	5029.0(5) $Å^3$	
Z	4	
Density (calculated)	1.080 g/cm^3	
Absorption coefficient	0.131 mm^{-1}	
F(000)	1800	
Diffractometer	Bruker D8 Venture Duo IMS	
Radiation source	IMS microsource, Mo	
Theta range for data collection	2.18 to 25.35°	
Index ranges	–15<=h<=15, –22<=k<=22, –24<=l<=24	
Reflections collected	182252	
Independent reflections	9197 [R(int) = 0.0728]	
Coverage of independent reflections	99.8%	
Absorption correction	Multi-Scan	
Max. and min. transmission	0.7209 and 0.7450	
Refinement method	Full-matrix least-squares on F^2	
Refinement program	SHELXL-2014 (Sheldrick, 2014)	
Function minimized	$\Sigma\, w(F_o^2 - F_c^2)^2$	
Data / restraints / parameters	9197 / 818 / 549	
Goodness-of-fit on F^2	1.125	
Final R indices	8326 data; I>2σ(I)	R1 = 0.0662, wR2 = 0.1423
	all data	R1 = 0.0730, wR2 = 0.1462
Weighting scheme	$w = 1/[\sigma^2(F_o^2) + (0.0414P)^2 + 5.7268P]$	
	where $P = (F_o^2 + 2F_c^2)/3$	
Largest diff. peak and hole	0.379 and –0.381 $eÅ^{-3}$	
R.M.S. deviation from mean	0.044 $eÅ^{-3}$	

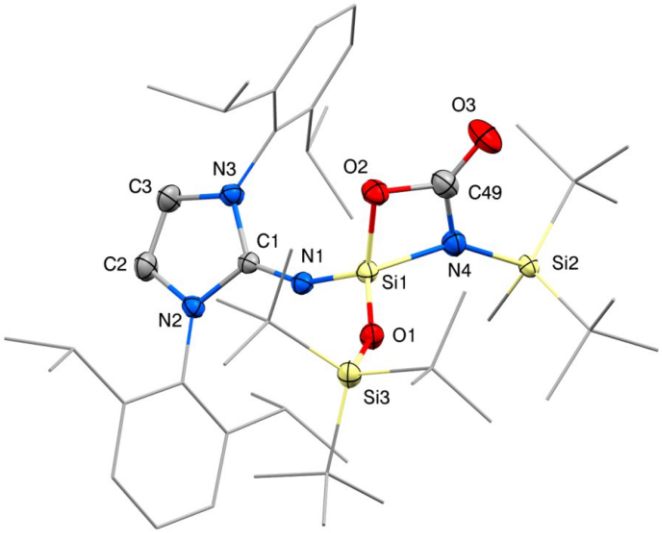


Figure S72. Molecular structure of **7** with ellipsoids set at 50% probability. Hydrogen atoms are omitted for clarity. Selected bond lengths [Å] and angles [°]: Si1–O1 1.613(1), Si1–O2 1.699(1), Si1–N1 1.620(1), Si1–N4 1.764(2), N1–C1 1.286(2), Si2–N4 1.787(2), Si3–O1 1.656(1), N4–C49 1.399(3), O2–C49 1.387(2), C49–O3 1.195(2); N1–Si1–O1 112.7(1), Si1–N1–C1 154.8(1), Si1–O1–Si3 152.5(1), O2–Si1–N4 78.6(1), Si1–O2–C49 90.2(1), Si1–N4–C49 87.2(1), O2–C49–N4 103.9(2).

Table S3. Crystal data and structure refinement for compound **7**.

Chemical formula	$C_{49}H_{84}N_4O_3Si_3$	
Formula weight	861.49 g/mol	
Temperature	100(2) K	
Wavelength	0.71073 Å	
Crystal size	0.236 × 0.297 × 0.373 mm	
Crystal habit	clear colorless fragment	
Crystal system	monoclinic	
Space group	P 21/n	
Unit cell dimensions	a = 13.5215(6) Å	α = 90°
	b = 17.5358(8) Å	β = 93.012(2)°
	c = 22.5862(10) Å	γ = 90°
Volume	5348.0(4) $Å^3$	
Z	4	
Density (calculated)	1.070 g/cm^3	
Absorption coefficient	0.129 mm^{-1}	
F(000)	1888	
Diffractometer	Bruker D8 Venture Duo IMS	
Radiation source	IMS microsource, Mo	
Theta range for data collection	2.14 to 25.35°	
Index ranges	–16<=h<=16, –21<=k<=21, –27<=l<=27	
Reflections collected	102378	
Independent reflections	9793 [R(int) = 0.0444]	
Coverage of independent reflections	99.9%	
Absorption correction	Multi-Scan	
Max. and min. transmission	0.6620 and 0.7453	
Refinement method	Full-matrix least-squares on F^2	
Refinement program	SHELXL-2014 (Sheldrick, 2014)	
Function minimized	$\Sigma\, w(F_o^2 - F_c^2)^2$	
Data / restraints / parameters	9197 / 654 / 102	
Goodness-of-fit on F^2	1.055	
Final R indices	8633 data; I>2σ(I)	R1 = 0.0452, wR2 = 0.1149
	all data	R1 = 0.0523, wR2 = 0.1208
Weighting scheme	$w = 1/[\sigma^2(F_o^2) + (0.0530P)^2 + 4.5428P]$	
	where $P = (F_o^2 + 2F_c^2)/3$	
Largest diff. peak and hole	1.091 and –0.396 $eÅ^{-3}$	
R.M.S. deviation from mean	0.046 $eÅ^{-3}$	

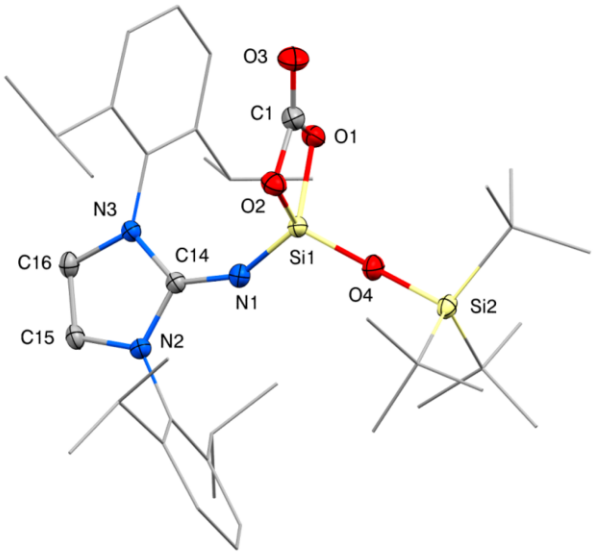


Figure S73. Molecular structure of **9** with ellipsoids set at 50% probability (one out of two independent molecules in the asymmetric unit). Hydrogen atoms are omitted for clarity. Selected bond lengths [Å] and angles [°]: Si1–O1 1.712(2), Si1–O2 1.712(2), Si1–O4 1.585(2), Si1–N1 1.609(2), N1–C14 1.299(3), Si2–O4 1.648(2), O1–C1 1.360(3), O2–C1 1.362(3), C1–O3 1.196(3); N1–Si1–O4 112.5(1), O1–Si1–O2 78.0(1), Si1–N1–C14 150.0(2), Si1–O4–Si2 165.1(1), O1–C1–O2 104.6(2).

Table S4. Crystal data and structure refinement for compound **9**.

Chemical formula	$C_{40}H_{63}N_3O_4Si_2$	
Formula weight	706.13 g/mol	
Temperature	100(2) K	
Wavelength	0.71073 Å	
Crystal size	0.466 × 0.495 × 0.585 mm	
Crystal habit	clear colorless fragment	
Crystal system	orthorhombic	
Space group	P c a 21	
Unit cell dimensions	a = 16.804(2) Å	α = 90°
	b = 14.1855(18) Å	β = 90°
	c = 34.372(4) Å	γ = 90°
Volume	8193.4(17) $Å^3$	
Z	8	
Density (calculated)	1.145 g/cm^3	
Absorption coefficient	0.128 mm^{-1}	
F(000)	3072	
Diffractometer	Bruker D8 Venture Duo IMS	
Radiation source	IMS microsource, Mo	
Theta range for data collection	1.97 to 25.70°	
Index ranges	–20<=h<=20, –17<=k<=17, –41<=l<=41	
Reflections collected	323173	
Independent reflections	15568 [R(int) = 0.0428]	
Coverage of independent reflections	99.9%	
Absorption correction	Multi-Scan	
Max. and min. transmission	0.7017 and 0.7460	
Refinement method	Full-matrix least-squares on F^2	
Refinement program	SHELXL-2014 (Sheldrick, 2014)	
Function minimized	$\Sigma\, w(F_o^2 - F_c^2)^2$	
Data / restraints / parameters	15568 / 918 / 1	
Goodness-of-fit on F^2	1.084	
Final R indices	15207 data; I>2σ(I)	R1 = 0.0290, wR2 = 0.0722
	all data	R1 = 0.0301, wR2 = 0.0729
Weighting scheme	$w = 1/[\sigma^2(F_o^2) + (0.0329P)^2 + 2.9609P]$	
	where $P = (F_o^2 + 2F_c^2)/3$	
Largest diff. peak and hole	0.258 and –0.220 $eÅ^{-3}$	
R.M.S. deviation from mean	0.035 $eÅ^{-3}$	

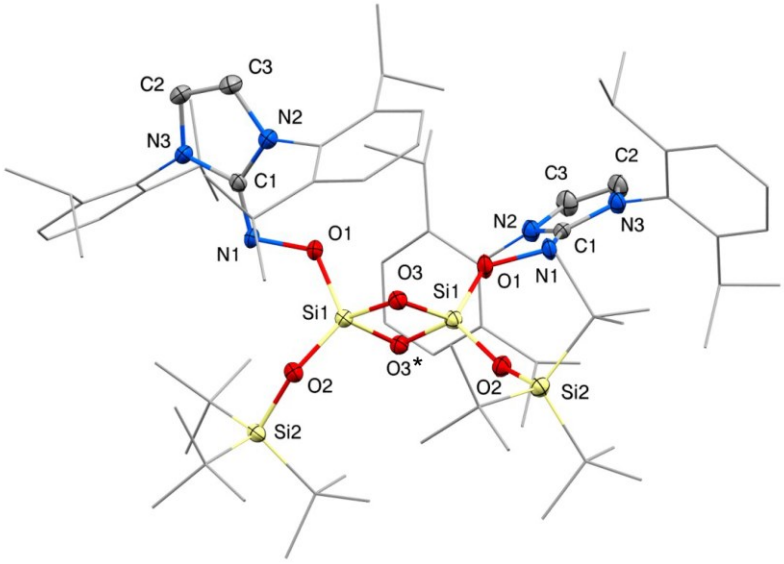


Figure S74. Molecular structure of **11** with ellipsoids set at 50% probability. Hydrogen atoms are omitted for clarity. Selected bond lengths [Å] and angles [°]: Si1–O1 1.623(2), Si1–O2 1.601(2), Si1–O3 1.659(2), Si1–O3* 1.673(2), N1–O1 1.449(3), N1–C1 1.305(2), Si2–O2 1.682(2); O1–Si1–O2 114.5(1), O3–Si1–O3* 88.8(1), Si1–O2–Si2 146.7(1), Si1–O1–N1 125.3(1), O1–N1–C1 106.7(1).

Table S5. Crystal data and structure refinement for compound **11**.

Chemical formula	$C_{78}H_{126}N_6O_6Si_4$	
Formula weight	1356.24 g/mol	
Temperature	100(2) K	
Wavelength	0.71073 Å	
Crystal size	0.331 × 0.394 × 0.411 mm	
Crystal habit	clear colorless fragment	
Crystal system	monoclinic	
Space group	C 2/c	
Unit cell dimensions	a = 26.09(2) Å	α = 90°
	b = 13.509(11) Å	β = 107.52(4)°
	c = 27.21(3) Å	γ = 90°
Volume	9148(14) $Å^3$	
Z	4	
Density (calculated)	0.985 g/cm^3	
Absorption coefficient	0.111 mm^{-1}	
F(000)	2960	
Diffractometer	Bruker D8 Venture Duo IMS	
Radiation source	IMS microsource, Mo	
Theta range for data collection	2.49 to 25.39°	
Index ranges	–31<=h<=31, –16<=k<=16, –32<=l<=32	
Reflections collected	156212	
Independent reflections	8320 [R(int) = 0.0668]	
Coverage of independent reflections	98.9%	
Absorption correction	Multi-Scan	
Max. and min. transmission	0.6421 and 0.7831	
Refinement method	Full-matrix least-squares on F^2	
Refinement program	SHELXL-2016/6 (Sheldrick, 2016)	
Function minimized	$\Sigma\, w(F_o^2 - F_c^2)^2$	
Data / restraints / parameters	8320 / 0 / 441	
Goodness-of-fit on F^2	1.054	
Final R indices	7002 data; I>2σ(I)	R1 = 0.0484, wR2 = 0.1120
	all data	R1 = 0.0606, wR2 = 0.1177
Weighting scheme	$w = 1/[\sigma^2(F_o^2) + (0.0482P)^2 + 14.5084P]$	
	where $P = (F_o^2 + 2F_c^2)/3$	
Largest diff. peak and hole	0.387 and –0.340 $eÅ^{-3}$	
R.M.S. deviation from mean	0.045 $eÅ^{-3}$	

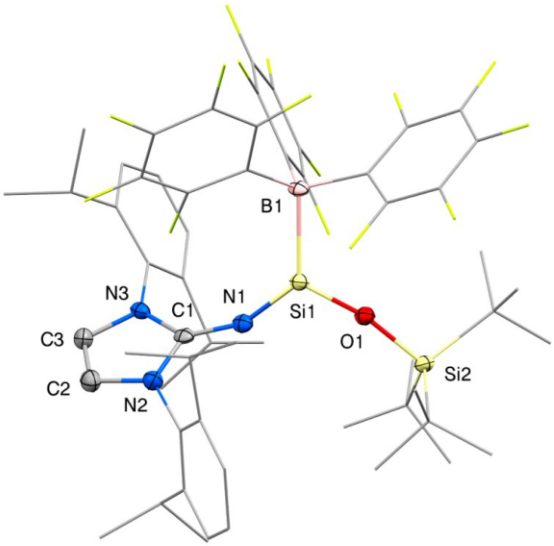


Figure S75. Molecular structure of **12a** with ellipsoids set at 50% probability. Hydrogen atoms and cocrystallized toluene are omitted for clarity. Selected bond lengths [Å] and angles [°]: Si1–B1 2.086(3), Si1–O1 1.598(2), Si1–N1 1.621(2), N1–C1 1.296(4), Si2–O1 1.676(2); B1–Si1–O1 116.5(1), B1–Si1–N1 128.9(1) N1–Si1–O1 114.2(1), Si1–N1–C1 150.8(3), Si1–O1–Si2 164.7(2).

Table S6. Crystal data and structure refinement for compound **12a**.

Chemical formula	$C_{57}H_{63}BF_{15}N_3OSi_2$	
Formula weight	1158.11 g/mol	
Temperature	100(2) K	
Wavelength	0.71073 Å	
Crystal size	0.184 × 0.200 × 0.254 mm	
Crystal habit	clear colorless fragment	
Crystal system	hexagonal	
Space group	P 65	
Unit cell dimensions	a = 21.6490(15) Å	α = 90°
	b = 21.6490(15) Å	β = 90°
	c = 24.0739(18) Å	γ = 120°
Volume	9771.3(18) $Å^3$	
Z	6	
Density (calculated)	1.275 g/cm^3	
Absorption coefficient	0.139 mm^{-1}	
F(000)	3912	
Diffractometer	Bruker D8 Venture Duo IMS	
Radiation source	IMS microsource, Mo	
Theta range for data collection	1.88 to 25.68°	
Index ranges	–26<=h<=26, –26<=k<=26, –29<=l<=29	
Reflections collected	482120	
Independent reflections	12388 [R(int) = 0.0715]	
Coverage of independent reflections	100%	
Absorption correction	Multi-Scan	
Max. and min. transmission	0.8224 and 0.7438	
Refinement method	Full-matrix least-squares on F^2	
Refinement program	SHELXL-2014/5 (Sheldrick, 2016)	
Function minimized	$\Sigma\, w(F_o^2 - F_c^2)^2$	
Data / restraints / parameters	12388 / 911 / 208	
Goodness-of-fit on F^2	1.096	
Final R indices	12202 data; I>2σ(I)	R1 = 0.0387, wR2 = 0.0983
	all data	R1 = 0.0393, wR2 = 0.0987
Weighting scheme	$w = 1/[\sigma^2(F_o^2) + (0.0513P)^2 + 4.9609P]$	
	where $P = (F_o^2 + 2F_c^2)/3$	
Largest diff. peak and hole	0.363 and –0.315 $eÅ^{-3}$	
R.M.S. deviation from mean	0.045 $eÅ^{-3}$	

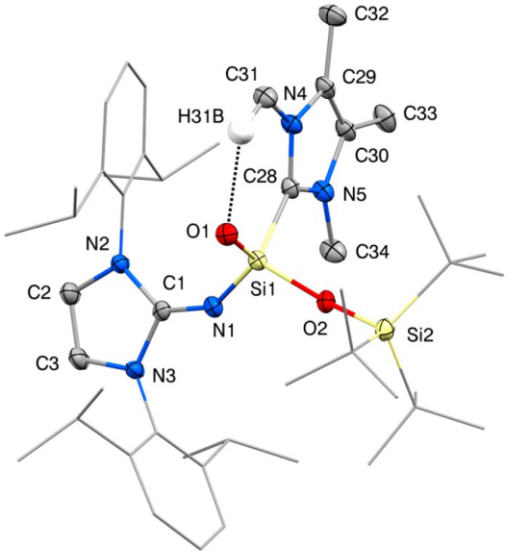


Figure S76. Molecular structure of **13a** with ellipsoids set at 50% probability. Hydrogen atoms, except for H31B involved in hydrogen bonding (visualized by the dashed line), and cocrystallized toluene are omitted for clarity. Selected bond lengths [Å] and angles [°]: Si1–O1 1.554(2), Si1–O2 1.653(2), Si1–C28 1.935(3), Si1–N1 1.684(2), N1–C1 1.271(3), Si2–O2 1.626(2); N1–Si1–O2 104.2(1), O1–Si1–O2 115.5(1), Si1–N1–C1 146.1(2), Si1–O2–Si2 151.6(1).

Table S7. Crystal data and structure refinement for compound **13a**.

Chemical formula	$C_{46}H_{75}N_5O_2Si_2$	
Formula weight	786.31 g/mol	
Temperature	100(2) K	
Wavelength	0.71073 Å	
Crystal size	0.103 × 0.127 × 0.274 mm	
Crystal habit	clear colorless fragment	
Crystal system	orthorhombic	
Space group	P 21 21 21	
Unit cell dimensions	a = 12.3466(7) Å	α = 90°
	b = 16.0952(9) Å	β = 90°
	c = 26.4133(15) Å	γ = 90°
Volume	5248.9(5) $Å^3$	
Z	4	
Density (calculated)	1.112 g/cm^3	
Absorption coefficient	0.110 mm^{-1}	
F(000)	1920	
Diffractometer	Bruker D8 Venture Duo IMS	
Radiation source	IMS microsource, Mo	
Theta range for data collection	2.217 to 25.349°	
Index ranges	–14<=h<=14, –19<=k<=19, –31<=l<=31	
Reflections collected	55732	
Independent reflections	9603 [R(int) = 0.0416]	
Coverage of independent reflections	99.9%	
Absorption correction	Multi-Scan	
Max. and min. transmission	0.7153 and 0.7450	
Refinement method	Full-matrix least-squares on F^2	
Refinement program	SHELXL-2016/6 (Sheldrick, 2016)	
Function minimized	$\Sigma\, w(F_o^2 - F_c^2)^2$	
Data / restraints / parameters	9603 / 581 / 0	
Goodness-of-fit on F^2	1.066	
Final R indices	8376 data; I>2σ(I)	R1 = 0.0366, wR2 = 0.0814
	all data	R1 = 0.0493, wR2 = 0.0896
Weighting scheme	$w = 1/[\sigma^2(F_o^2) + (0.0386P)^2 + 1.2905P]$	
	where $P = (F_o^2 + 2F_c^2)/3$	
Largest diff. peak and hole	0.210 and –0.218 $eÅ^{-3}$	
R.M.S. deviation from mean	0.041 $eÅ^{-3}$	

Preliminary Measurement Results as Structural Evidence

For the following two cases the crystal quality was unfortunately not sufficient for a complete refinement process and subsequent analysis of the structural data. Nevertheless, the preliminary structures obtained serve as evidence for the respective molecular structures in the solid state.

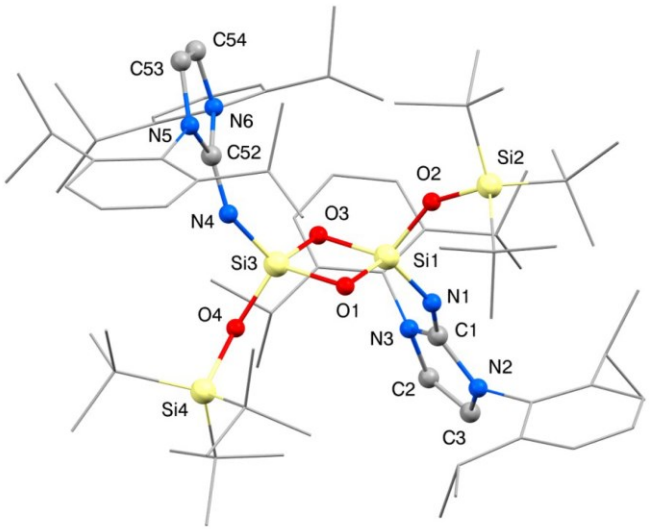


Figure S77. Molecular structure of *trans*-Cyclodisiloxane [(IDippN)(^{t}Bu$_3$SiO)Si=O]$_2$ (**10a**) in the ball-and-stick representation. Hydrogen atoms are omitted for clarity.

Table S8. Structural information for compound **10a**.

Chemical formula	$C_{78}H_{126}N_6O_4Si_4$	
Formula weight	1324.24 g/mol	
Crystal habit	clear colorless fragment	
Crystal system	triclinic	
Space group	P $\bar{1}$	
Unit cell dimensions	a = 14.221(8) Å	α = 89.052(6)°
	b = 14.221(8) Å	β = 89.052(6)°
	c = 45.50(2) Å	γ = 68.589°
Volume	8563.96 Å^3	

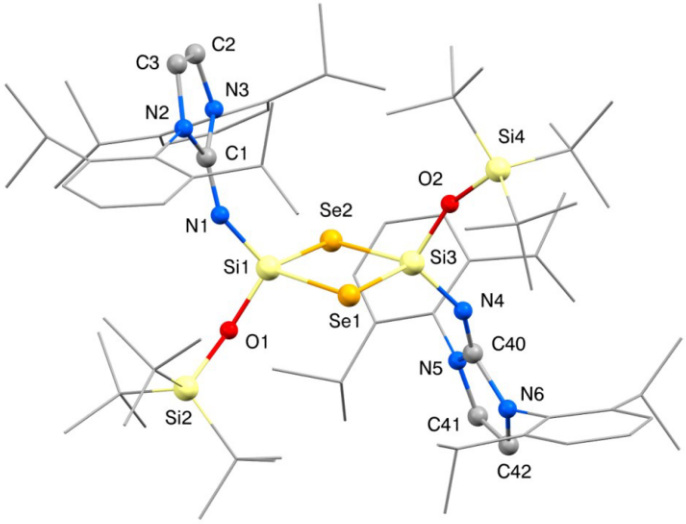


Figure S78. Molecular structure of Silicon Diselenide [(IDippN)(^{t}Bu$_3$SiO)Si=Se]$_2$ (**10b**) in the ball-and-stick representation. Hydrogen atoms are omitted for clarity.

Table S9. Structural information for compound **10b**.

Chemical formula	$C_{78}H_{126}N_6O_2Se_2Si_4$	
Formula weight	1450.17 g/mol	
Crystal habit	clear colorless fragment	
Crystal system	triclinic	
Space group	P $\bar{1}$	
Unit cell dimensions	a = 13.118(13) Å	α = 72.28(3)°
	b = 16.152(16) Å	β = 75.65(3)°
	c = 20.61(2) Å	γ = 76.26(3)°
Volume	3967.27 Å^3	

3. References

[S1] G. R. Fulmer, A. J. M. Miller, N. H. Sherden, H. E. Gottlieb, A. Nudelman, B. M. Stoltz, J. E. Bercaw, K. I. Goldberg, *Organometallics* **2010**, *29*, 2176-2179.
[S2] D. Wendel, D. Reiter, A. Porzelt, P. J. Altmann, S. Inoue, B. Rieger, *J. Am. Chem. Soc.* **2017**, *139*, 17193-17198.
[S3] N. Kuhn, T. Kratz, *Synthesis* **1993**, 561-562.
[S4] N. Wiberg, C.-K. Kim, *Eur. J. Inorg. Chem.* **1986**, *119*, 2980-2994.
[S5] Y. Xiong, S. Yao, M. Brym, M. Driess, *Angew. Chem. Int. Ed.* **2007**, *46*, 4511-4513.

[S6] T. J. Hadlington, J. A. B. Abdalla, R. Tirfoin, S. Aldridge, C. Jones, *Chem. Commun.* **2016**, *52*, 1717-1720.
[S7] A. Bondi, *J. Phys. Chem.* **1964**, *68*, 441-451.
[S8] V. Nesterov, D. Reiter, P. Bag, P. Frisch, R. Holzner, A. Porzelt, S. Inoue, *Chem. Rev.* **2018**, *118*, 9678-9842.
[S9] J. Chen, E. Y.-X. Chen, *Isr. J. Chem.* **2015**, *55*, 216-225.
[S10] R. Kobayashi, S. Ishida, T. Iwamoto, *Angew. Chem. Int. Ed.* **2019**, *58*, 9425-9428.
[S11] *APEX suite of crystallographic software*, APEX 3 version 2015.5-2; Bruker AXS Inc.: Madison, Wisconsin, USA, **2015**.
[S12] *SAINT*, Version 7.56a and SADABS Version 2008/1; Bruker AXS Inc.: Madison, Wisconsin, USA, **2008**.
[S13] G. M. Sheldrick, *SHELXL-2014*, University of Göttingen, Göttingen, Germany, **2014**.
[S14] C. B. Hübschle, G. M. Sheldrick, B. Dittrich, *J. Appl. Cryst.* **2011**, *44*, 1281-1284.
[S15] G. M. Sheldrick, *SHELXL-97*, University of Göttingen, Göttingen, Germany, **1998**.
[S16] A. J. C. Wilson, *International Tables for Crystallography*, Vol. C, Tables 6.1.1.4 (pp. 500-502), 4.2.6.8 (pp. 219-222), and 4.2.4.2 (pp. 193-199); Kluwer Academic Publishers: Dordrecht, The Netherlands, **1992**.
[S17] C. F. Macrae, I. Sovago, S. J. Cottrell, P. T. A. Galek, P. McCabe, E. Pidcock, M. Platings, G. P. Shields, J. S. Stevens, M. Towler, P. A. Wood, *J. Appl. Cryst.* **2020**, *53*, 226-235.

13.5 Supporting Information Chapter 8

Silicon and Oxygen's Bond of Affection: An Acyclic Three-Coordinate Silanone and Its Transformation to an Iminosiloxysilylene

Daniel Wendel,[†,‡] Dominik Reiter,[†,§] Amelie Porzelt,[§] Philipp J. Altmann,[⊥] Shigeyoshi Inoue[*,§] and Bernhard Rieger[*,‡]

[‡]WACKER-Chair of Macromolecular Chemistry, [§]WACKER-Institute of Silicon Chemistry, [⊥]Catalysis Research Center, Technische Universität München, Lichtenbergstraße 4, 85748 Garching bei München, Germany

*s.inoue@tum.de; rieger@tum.de

Supporting Information

1. Experimental Procedures S2
2. X-ray Crystallographic Data S41
3. Computational Calculations S49
4. References S65

Total: S65 pages

1. Experimental Procedures

A) General Methods and Instrumentation

All manipulations were carried out under argon atmosphere using standard Schlenk or glovebox techniques. Glassware was heat-dried under vacuum prior to use. Unless otherwise stated, all chemicals were purchased from Sigma-Aldrich or ABCR and used as received. Benzene, Et_2O, *n*-hexane, THF and toluene were refluxed over sodium/benzophenone, acetonitrile over CaH_2 and methanol over magnesium, distilled and deoxygenated prior to use. Deuterated benzene (C_6D_6), THF (THF-d_8) and acetonitrile (CD_3CN) were obtained from Deutero Deutschland GmbH and were dried over 3 Å molecular sieves. All NMR samples were prepared under argon in J. Young PTFE tubes. Silepin **1a**, IPrNSiBr$_3$, IMe$_4$ and NaSi*t*-Bu$_3$(THF$_2$) were synthesized according to procedures described in literature.[S1-4] Dinitrogen monoxide (5.0), carbon dioxide (5.0), hydrogen (5.0) and ethylene (3.5) were purchased from Westfalen AG and used as received. NMR spectra were recorded on Bruker AV-500C, AV-500 or DRX-400 spectrometers at ambient temperature (300 K), unless otherwise stated. ^{1}H, ^{13}C and ^{29}Si NMR spectroscopic chemical shifts δ are reported in ppm relative to tetramethylsilane. δ(^{1}H) and δ(^{13}C) were referenced internally to the relevant residual solvent resonances. δ(^{29}Si) was referenced to the signal of tetramethylsilane (TMS) (δ = 0 ppm) as external standard. Elemental analyses (EA) were conducted with a EURO EA (HEKA tech) instrument equipped with a CHNS combustion analyzer. Mass spectra (MS-CI) were recorded on a double focusing Finnigan MAT 90 mass spectrometer (isobutene, 150 eV). UV-Vis spectra were taken on an Agilent Cary 60 spectrophotometer. ATR-FTIR spectra were recorded on a Perkin Elmer FTIR spectrometer (diamond ATR, Spectrum Two; located inside an argon-filled glovebox) in a range of 400 – 4000 cm^{-1}. Melting Points (M_p) were determined in sealed glass capillaries under inert gas by a Büchi M-565 melting point apparatus.

B) Synthesis and Characterization of New Compounds

Synthesis of Silepin (Si*t*-Bu$_3$ Substituted) (1b)

An analogue procedure as for the preparation of SiTMS$_3$ substituted silepin **1a** was applied.[S1] A solution of NaSi*t*-Bu$_3$(THF$_2$) (134 mg, 0.18 mmol, 2.00 eq) in toluene (2 mL) was added to IPrNSiBr$_3$ (123 mg, 0.36 mmol, 1.00 eq) in toluene (2 mL) at room temperature. The color rapidly changed to light green (approx. 1 sec) and then immediately to yellow with formation of a white precipitate. After stirring the solution for 20 min, the solvent was removed *in vacuo*. The obtained residue was extracted with *n*-hexane (3 × 5 mL) and filtered through a microfiber glass filter. For further studies, mixtures of **1b**/*t*-Bu$_3$SiBr were prepared in analogue fashion, since attempts to separate both products by fractional crystallization or sublimation were unsuccessful.

^{1}H NMR (500 MHz, C$_6$D$_6$, r.t.): δ = 7.19 – 7.00 (m, 3H, *p*-/*m*-C*H*-Ar), 6.70 (d, *J* = 2.9 Hz, 1H, C*H*-N), 6.63 (d, *J* = 6.5 Hz, 1H, C*H*-Ar), 6.49 (d, *J* = 12.9 Hz, 1H, C*H*-Ar), 6.37 (dd, *J* = 12.9, 6.5 Hz, 1H, C*H*-Ar), 5.88 (d, *J* = 2.9 Hz, 1H, C*H*-N), 3.39 (hept, *J* = 6.8 Hz, 1H, C*H*), 3.22 (hept, *J* = 6.8 Hz, 1H, C*H*), 3.12 (hept, *J* = 6.8 Hz, 1H, C*H*), 3.05 (hept, *J* = 6.8 Hz, 1H, C*H*) 1.35 (d, *J* = 6.8 Hz, 6H, C*H*$_3$), 1.31 (d, *J* = 6.8 Hz, 6H, C*H*$_3$), 1.25 (s, 27H, Si*t*-*Bu*$_3$), 1.21 (d, *J* = 6.8 Hz, 3H, C*H*$_3$), 1.20 (d, *J* = 6.8 Hz, 3H, C*H*$_3$), 1.09 (d, *J* = 6.8 Hz, 3H, C*H*$_3$), 0.93 (d, *J* = 6.8 Hz, 3H, C*H*$_3$).

^{29}Si NMR (99 MHz, C$_6$D$_6$, r.t.): δ = 11.6 (*central Si*), 7.8 (*Si*t-Bu$_3$).

The obtained NMR and UV-VIS data of **1b** are in accordance with the one of SiTMS$_3$ substituted silepin **1a**.[S1]

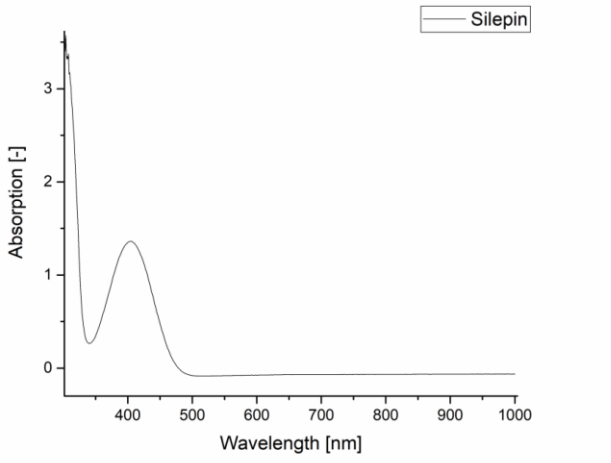


Figure S1. UV-Vis spectrum of silepin **1b**/*t*-Bu$_3$SiBr mixture λ_{max} (r.t., hexane, 8.0×10^{-4} M) = 405 nm.

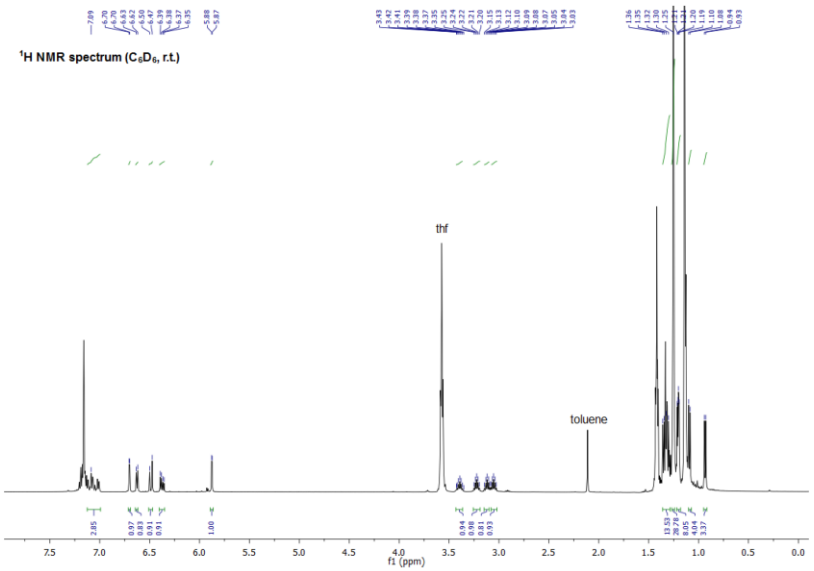


Figure S2: ^{1}H NMR spectrum of silepin **1b**/*t*-Bu_3SiBr mixture (C_6D_6, r.t.).

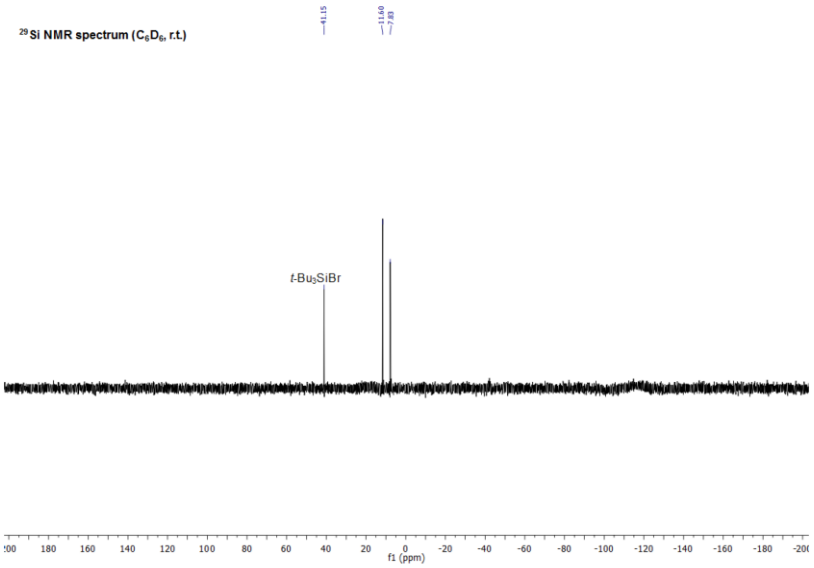


Figure S3: ^{29}Si NMR spectrum of silepin **1b**/*t*-Bu_3SiBr mixture (C_6D_6, r.t.).

Synthesis of Silanone ($SiTMS_3$ Substituted) (2a)

A solution of $KSiTMS_3$ (726 mg, 2.53 mmol, 2.00 eq) in toluene (20 mL) was added to $IPrNSiBr_3$ (849 mg, 1.27 mmol, 1.00 eq) in toluene (20 mL) at room temperature. The color rapidly changed to light green (approx. 1 sec) and then immediately to yellow with formation of a white precipitate. After stirring the solution for 20 min, the solvent was removed *in vacuo*. The obtained residue was extracted with *n*-hexane (3 × 15 mL) and filtered through a microfiber glass filter. The yellow solution was concentrated, cooled to –78 °C and exposed to N_2O (1 bar). While warming up the solution to room temperature, a fine white precipitate forms, which is immediately separated *via* filtration, washed with *n*-hexane and dried *in vacuo* to give pure silanone **2a** (484 mg, 0.51 mmol, 41%) as a white powder. Attempts to crystallize the donor-free silanone **2a** failed in several solvents (e.g. toluene, monofluorobenzene, difluorobenzene or diethylether), however crystallization in acetonitrile at –35 °C yielded single crystals of tetra-coordinate acetonitrile-stabilized silanone **2a** × CD_3CN. The coordination of one acetonitrile molecule to the silicon center of **2a** was additionally verified *via* NMR spectroscopy (see below). Silanone **2a** is indefinitely stable as a solid at –35 °C, but decomposes in C_6D_6 at room temperature within 14 h ($t_{1/2}$ = 7 h). Still, the half-life time of silanone **2a** can be extended considerably by using **2a** × CD_3CN solutions ($t_{1/2}$ = 4 d).

Compound 2a:

^{1}H NMR (500 MHz, C_6D_6, r.t.): δ = 7.34 – 7.05 (m, 6H, C*H*-Ar), 6.08 (s, 2H, C*H*-N), 3.19 (hept, *J* = 6.8 Hz, 4H, C*H*), 1.51 (d, *J* = 6.8 Hz, 12H, CH_3), 1.12 (d, *J* = 6.8 Hz, 12H, CH_3), 0.22 (s, 27H, Si*TMS*$_3$).

^{13}C NMR (126 MHz, C_6D_6, r.t.): δ = 148.8 (N-*C*-N), 147.7 (*C*-Ar), 133.1 (*C*-Ar), 130.2 (*C*H-Ar), 124.3 (*C*H-Ar), 115.7 (*C*H-N), 29.1 (*C*H), 25.4 (*C*H$_3$), 23.8 (*C*H$_3$), 2.5 (Si*TMS*$_3$).

^{29}Si NMR (99 MHz, C_6D_6, r.t.): δ = 33.7 (*central Si*), -9.6 (*TMS*$_3$), -130.6 (*Si*TMS$_3$).

MS-CI (150 eV): m/z (%) = 693 $[M]^+$ (8), 711 $[M+H_2O]^+$ (5).

Reproducible EA could not be obtained for compound **2a** due to its extreme air and moisture sensitivity.

M_p: 111.0 °C (decomposition, color change from colorless to yellow).

Compound 2a × CD_3CN:

^{1}H NMR (500 MHz, CD_3CN, r.t.): δ = 7.46 – 7.38 (m, 2H, *p*-C*H*-Ar), 7.38 – 7.23 (m, 4H, *m*-C*H*-Ar), 6.56 (s, 2H, C*H*-N), 3.01 (overlapping hept, *J* = 6.8 Hz, 4H, C*H*), 1.35 (d, *J* = 6.8 Hz, 6H, CH_3), 1.32 (d, *J* = 6.8 Hz, 6H, CH_3) 1.18 (d, *J* = 6.8 Hz, 6H, CH_3) 1.14 (d, *J* = 6.8 Hz, 6H, CH_3), -0.04 (s, 27H, Si*TMS*$_3$).

^{29}Si NMR (99 MHz, CD_3CN, r.t.): δ = -10.9 (*TMS*$_3$), -48.3 (*central Si*), -133.6 (*Si*TMS$_3$).

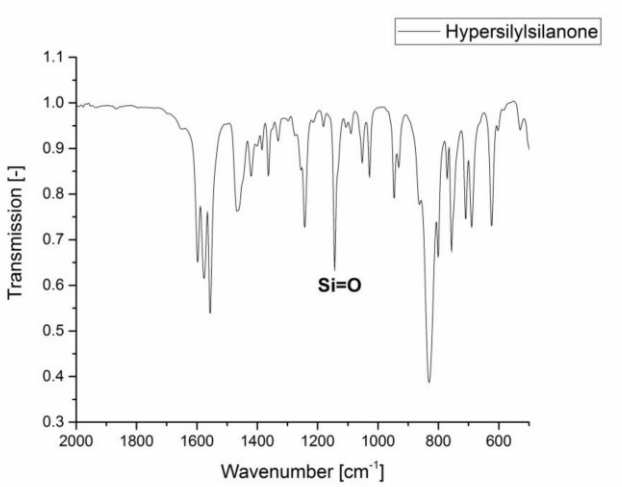


Figure S4: IR spectrum of silanone **2a** (cm^{-1}): 1598 (m), 1577 (m), 1552 (s), 1456 (m), 1420 (w), 1244 (m), 1144 (m, Si=O), 1053 (w), 1023 (w), 944 (w), 825 (s), 751 (m), 721 (m), 685 (m), 622 (m).

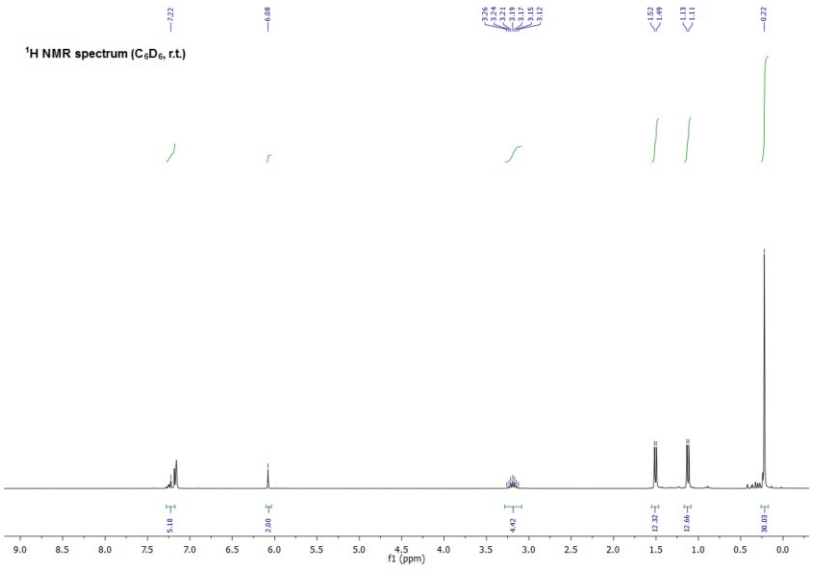


Figure S5: ^1H NMR spectrum of silanone **2a** (C_6D_6, r.t.).

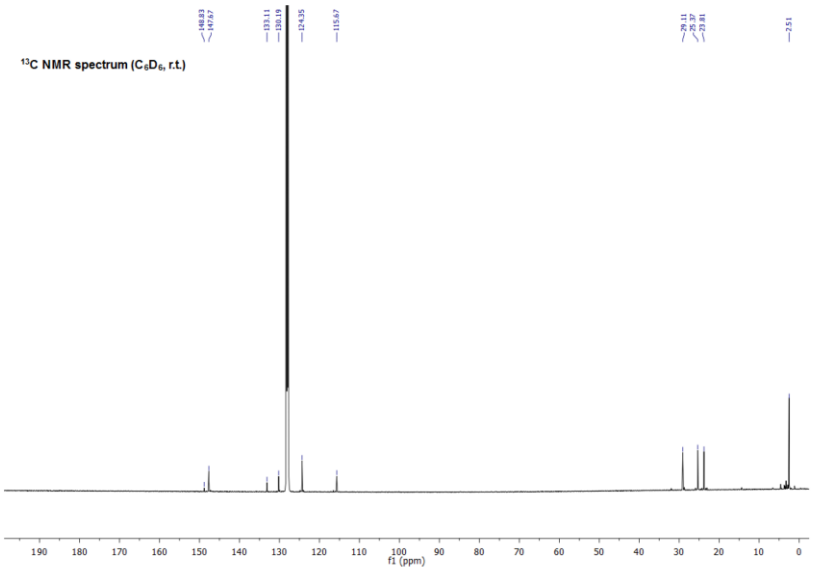


Figure S6: ^{13}C NMR spectrum of silanone **2a** (C_6D_6, r.t.).

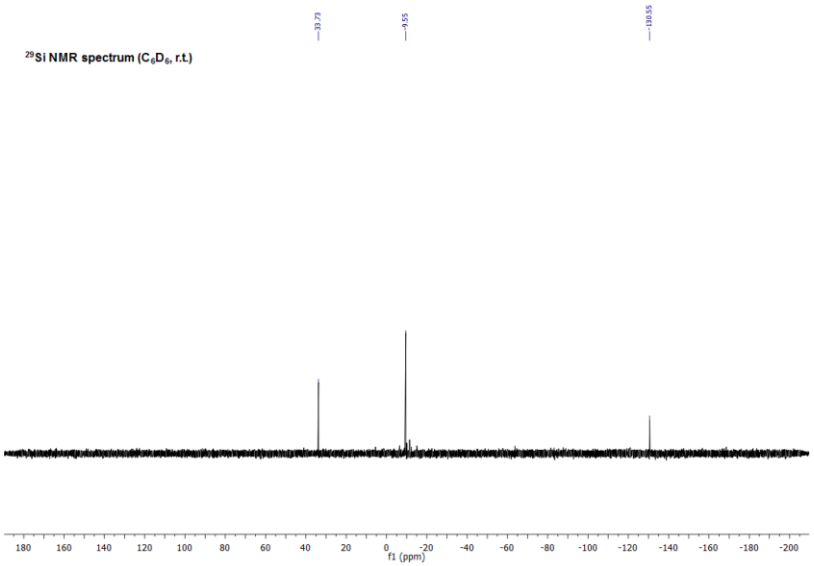


Figure S7: ^{29}Si NMR spectrum of silanone **2a** (C_6D_6, r.t.).

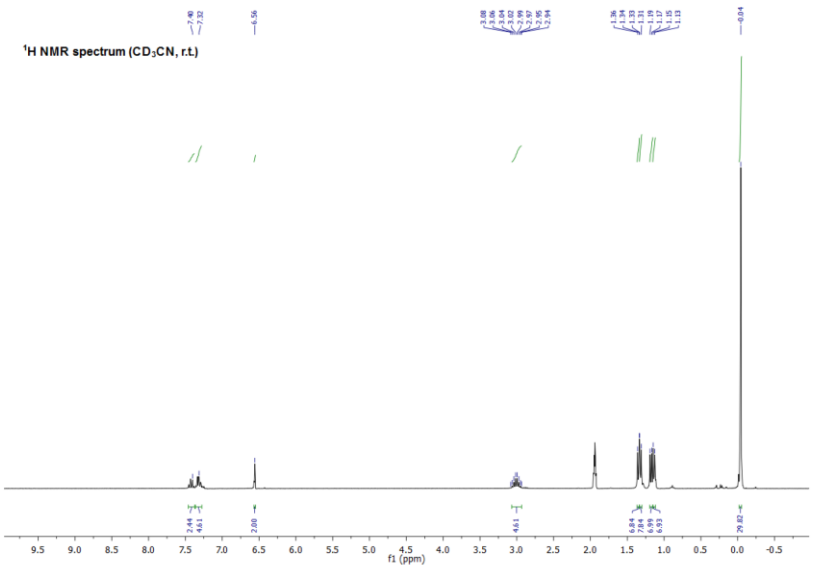


Figure S8: ^{1}H NMR spectrum of tetra-coordinate silanone **2a** × CD$_3$CN (CD$_3$CN, r.t.).

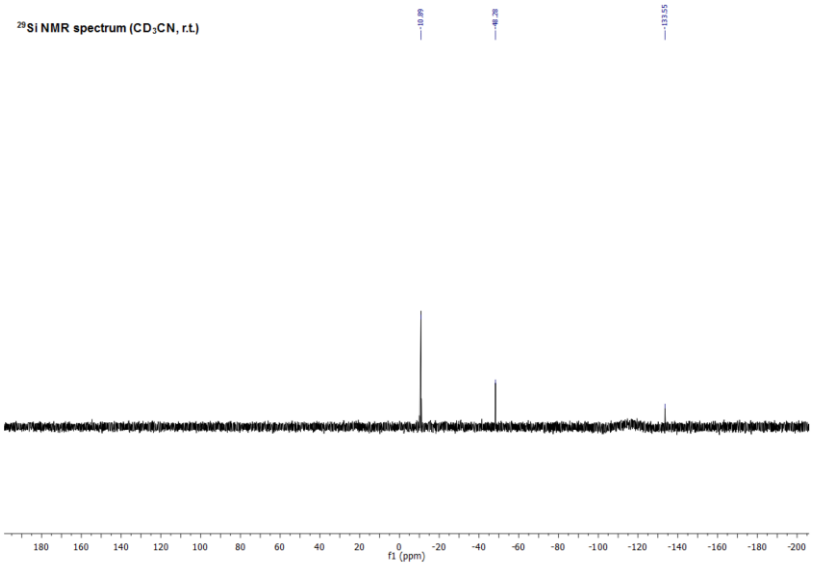


Figure S9: ^{29}Si NMR spectrum of tetra-coordinate silanone **2a** × CD$_3$CN (CD$_3$CN, r.t.).

Decomposition of Silanone 2a

In general, the decomposition process of **2a** in C_6D_6 is rather unspecific and led to several unidentified compounds within 14 h. However, according to the obtained ^{1}H, ^{29}Si and $^{1}H/^{29}Si$ HMBC NMR data one major asymmetric product was identified, presumably formed by TMS migration from the hypersilyl group to the Si=O center and subsequent activation of the NHI ligand (see Figure S11 and Figure S12). A comparable 1,3-silyl migration has been reported for Kira's transient cyclic dialkylsilanone to form an intermediary silene.[S5] For silanone **2a** the identical decomposition pathway leads to transient disilene **INT** (see Figure S10), which probably due to the strong donation of NHI and OTMS group possesses a highly polarized Si=Si bond. Therefore also a zwitterionic resonance form **INT'** should be considered. We propose, that this highly reactive intermediate is capable to intra- or intermolecularly activate the NHI ligand. Although currently specific details are unclear, this reaction seems very likely, since a similar NHI activation has been observed in literature.[S2]

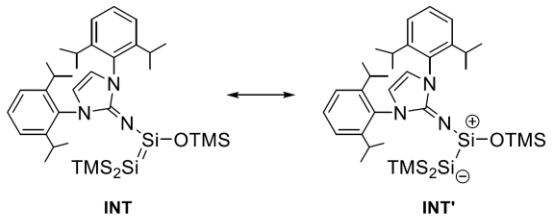


Figure S10: Proposed intermediate **INT** in the decomposition process of silanone **2a** formed by 1,3-silyl migration to the Si=O center.

Moreover, we figured out that the same 1,3-silyl migration can be instantly induced by addition of THF-d_8 to solid **2a**, resulting in a strongly yellow colored solution. Subsequent NMR analysis indicated the quantitative formation of the proposed transient disilene **INT** (NMR data see below). By comparing the NMR shifts of **INT** with the theoretical data (Table S13), exclusively the ^{29}Si NMR shift of the positively polarized Si^{+} atom showed a strong deviation (Δ67.5 ppm). We therefore believe that (very similar to compound **6**) a THF molecule can act as potential donor and coordinate to the silicon center, forming **INT** × THF. This species is highly reactive and decomposed in analogue fashion to **2a** in C_6D_6 within a few hours. All attempts to isolate and crystallize **INT** × THF failed, however trapping experiments with ethylene led to the corresponding [2+2]-cycloaddition product **5**. Further, by using a stronger external NHC donor the IMe_4 stabilized zwitterionic disilene **6** was isolated (for details see compound **5** and **6**).

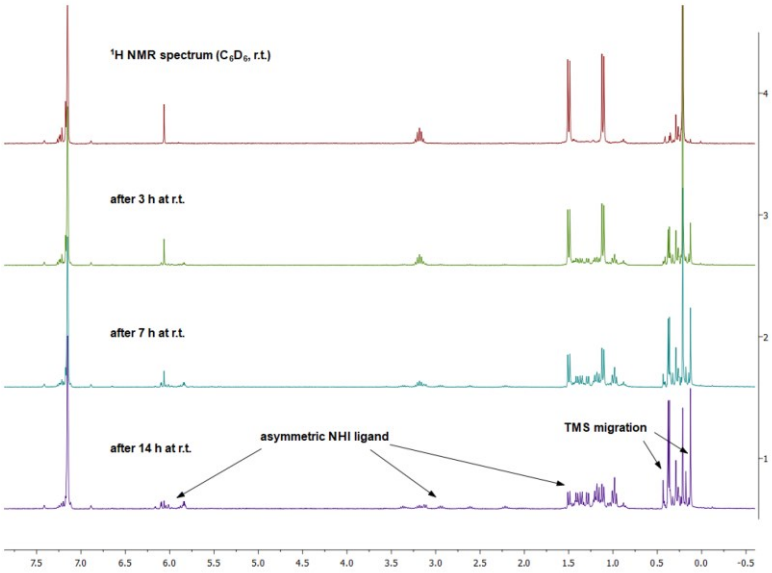


Figure S11: ^{1}H NMR spectra of the decomposition process of silanone **2a** after 3, 7 and 14 h in solution (C_6D_6, r.t.).

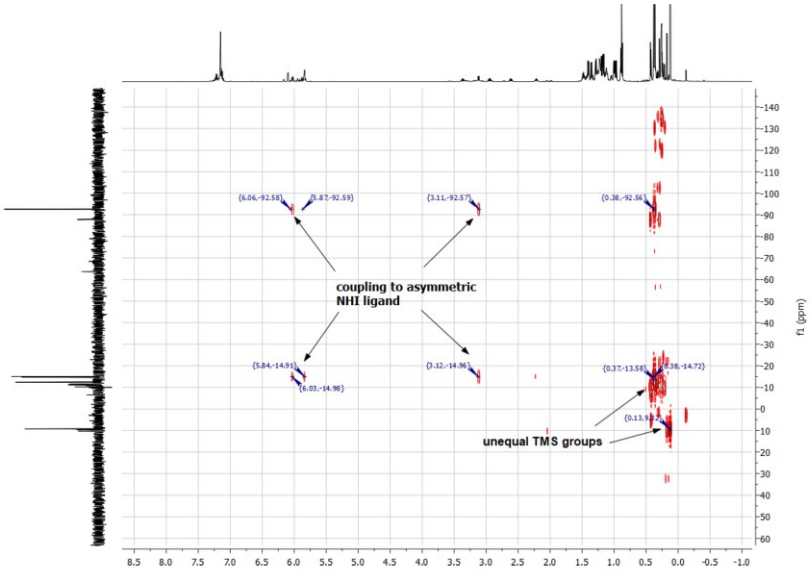


Figure S12: ^{1}H/^{29}Si HMBC NMR spectrum of the decomposition mixture of silanone **2a** after 14 h in solution (C_6D_6, r.t.).

NMR data of transient disilene INT (THF-d_8 induced TMS migration):

^{1}H NMR (500 MHz, THF-d_8, r.t.): δ = 7.39 – 7.35 (m, 4H, *m*-C*H*-Ar), 7.30 – 7.27 (m, 2H, *o*-C*H*-Ar), 6.56 (s, 2H, C*H*-N), 3.16 (hept, *J* = 6.8 Hz, 4H, C*H*), 1.41 (d, *J* = 6.8 Hz, 12H, CH_3), 1.16 (d, *J* = 6.8 Hz, 12H, CH_3), 0.01 (s, 18H, Si*TMS*$_2$), -0.11 (s, 9H, O*TMS*).

^{13}C NMR (126 MHz, THF-d_8, r.t.): δ =, 148.7 (*C*-Ar), 143.0 (N-*C*-N), 136.1 (*C*-Ar), 130.3 (*C*H-Ar), 125.1 (*C*H-Ar), 117.0 (*C*H-N), 29.4 (*C*H), 25.9 (*C*H$_3$), 24.4 (*C*H$_3$), 7.4 (Si*TMS*$_2$), 3.4 (O*TMS*).

^{29}Si NMR (99 MHz, THF-d_8, r.t.): δ = 4.3 (O*TMS*), -7.2 (Si*TMS*$_2$), -8.0 (*Si*OTMS), -196.6 (*Si*TMS$_2$).

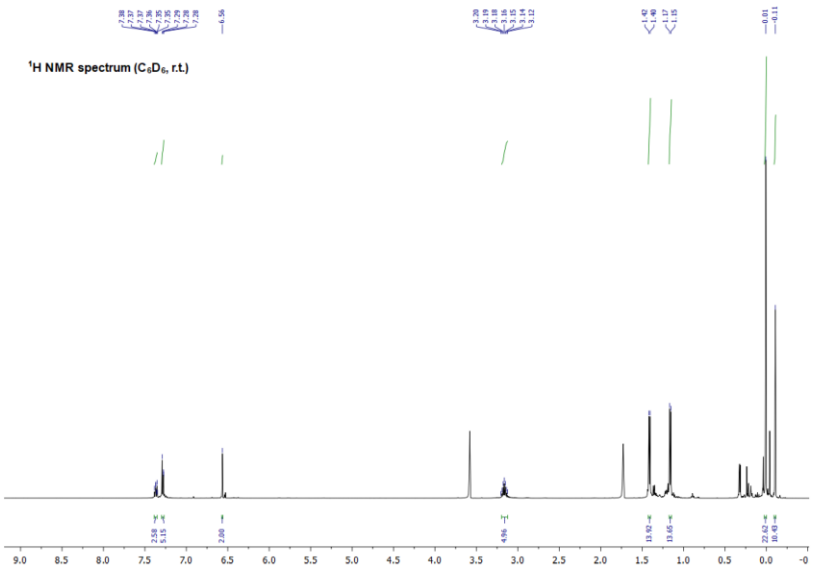


Figure S13: ^{1}H NMR spectrum of transient disilene **INT** (THF-d_8, r.t.).

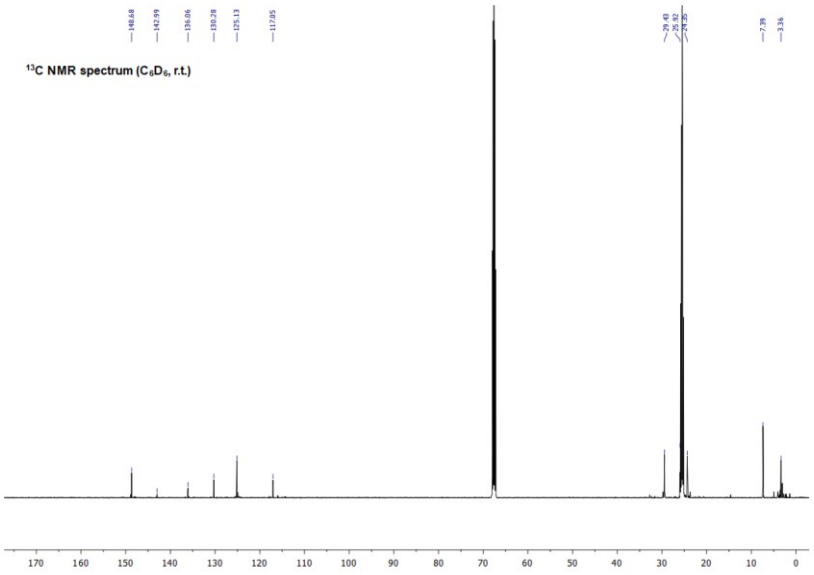


Figure S14: ^{13}C NMR spectrum of transient disilene **INT** (THF-d_8, r.t.).

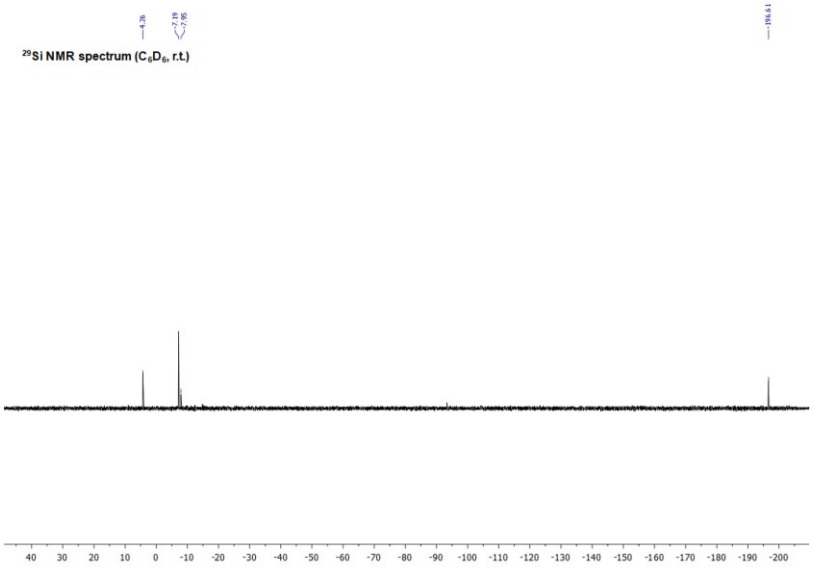


Figure S15: ^{29}Si NMR spectrum of transient disilene **INT** (THF-d_8, r.t.).

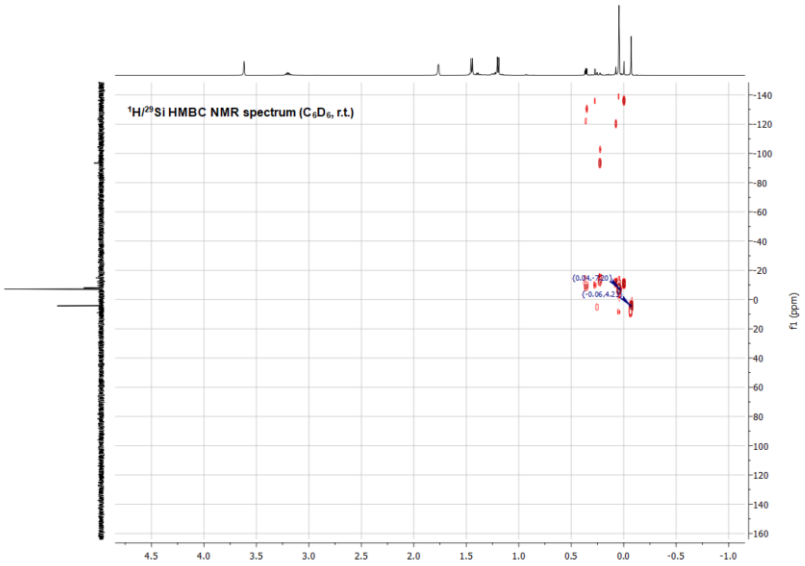


Figure S16: $^{1}H/^{29}Si$ HMBC NMR spectrum of transient disilene **INT** (THF-d_8, r.t.).

Synthesis of Silanone (Si*t*-Bu$_3$ Substituted) (2b)

A solution of NaSi*t*-Bu$_3$(THF$_2$) (1.09 g, 2.98 mmol, 2.00 eq) in benzene (20 mL) was added to IPrNSiBr$_3$ (1.00 g, 1.49 mmol, 1.00 eq) in benzene (20 mL) at room temperature. The color rapidly changed to light green (approx. 1 sec) and then immediately to yellow with formation of a white precipitate. After stirring the solution for 20 min, the solvent was removed *in vacuo*. The obtained residue was extracted with *n*-hexane (3 × 20 mL) and filtered through a microfiber glass filter. The yellow solution was concentrated, cooled to –78 °C and exposed to N_2O (1 bar). While warming up the solution to room temperature, a fine white precipitate forms, which is immediately separated *via* filtration, washed with *n*-hexane and dried *in vacuo* to give pure silanone **2b** (521 mg, 0.81 mmol, 54%) as a white powder. Colorless crystals of **2b** suitable for single crystal X-ray analysis were obtained by slow diffusion of Et_2O into a saturated THF solution at –35 °C for several days. Compound **2b** is indefinitely stable as a solid at r.t. (no changes after 1 month), but quantitatively forms *N*,*O*-silylene **7** in C_6D_6 or THF-d_8 at room temperature within 48 h ($t_{1/2}$ = 24 h).

Compound 2b:

^{1}H NMR (500 MHz, C_6D_6, r.t.): δ = 7.25 – 7.19 (m, 2H, *p*-C*H*-Ar), 7.16 – 7.11 (m, 4H, *m*-C*H*-Ar), 6.11 (s, 2H, C*H*-N), 3.17 (hept, *J* = 6.8 Hz, 4H, C*H*), 1.49 (d, *J* = 6.8 Hz, 12H, CH_3), 1.13 (s, 27H, Si*t*-*Bu*$_3$), 1.12 (d, *J* = 6.8 Hz, 12H, CH_3).

^{13}C NMR (126 MHz, C_6D_6, r.t.): δ = 148.4 (N-*C*-N), 147.6 (*C*-Ar), 133.2 (*C*-Ar), 130.2 (*C*H-Ar), 124.3 (*C*H-Ar), 115.7 (*C*H-N), 31.8 (C(*C*H$_3$)$_3$), 29.1 (*C*H), 25.5 (*C*H$_3$), 23.4 (*C*H$_3$), 23.1 (*C*(CH$_3$)$_3$).

^{29}Si NMR (99 MHz, C_6D_6, r.t.): δ = 28.8 (*central Si*), 13.7 (Si*t*-Bu$_3$).

^{29}Si NMR (99 MHz, THF-d_8, r.t.): δ = 26.2 (*central Si*), 13.0 (Si*t*-Bu$_3$).

EA experimental (calculated): C 72.32 (72.50), H 9.97 (9.83), N 6.45 (6.50) %.

M_p: 126.5 °C (decomposition, color change from colorless to yellowish).

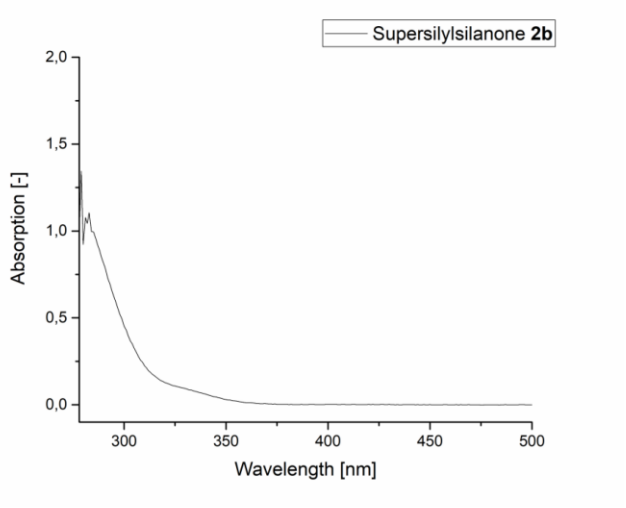


Figure S17. UV-Vis spectrum of silanone **2b** λ_{max} (r.t., toluene, 4.0×10^{-4} M) = 282 nm.

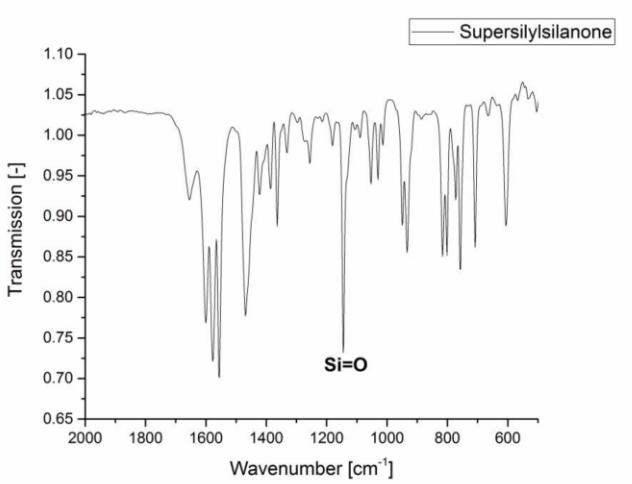


Figure S18: IR spectrum of silanone **2b** (cm^{-1}): 1649 (w), 1599 (m), 1577 (m), 1550 (s), 1463 (m), 1359 (w), 1144 (s, Si=O), 1051 (w), 1029 (w), 945 (w), 936 (m), 808 (m), 755 (m), 705 (m), 606 (m).

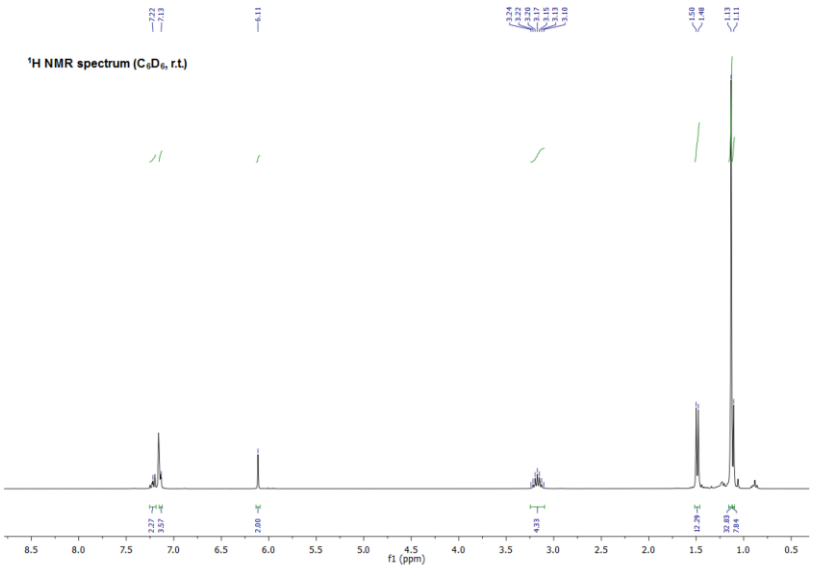


Figure S19: ^{1}H NMR spectrum of silanone **2b** (C_6D_6, r.t.).

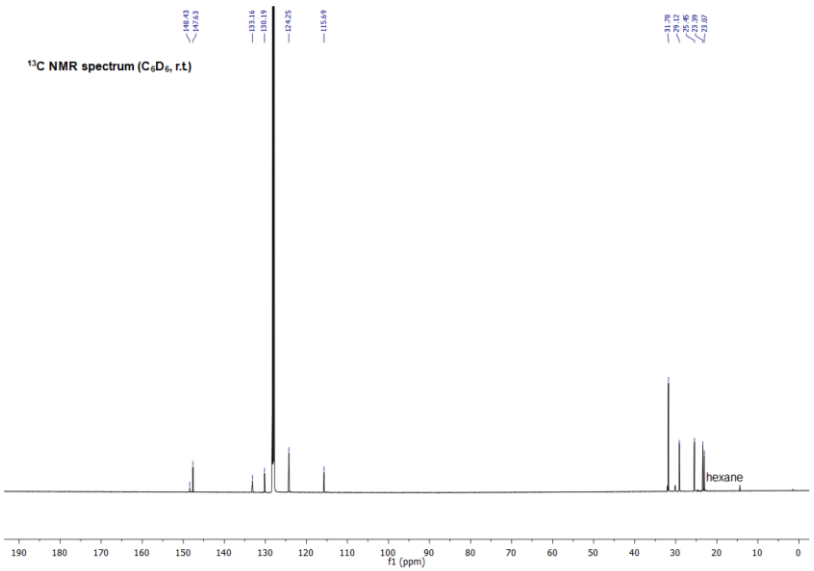


Figure S20: ^{13}C NMR spectrum of silanone **2b** (C_6D_6, r.t.).

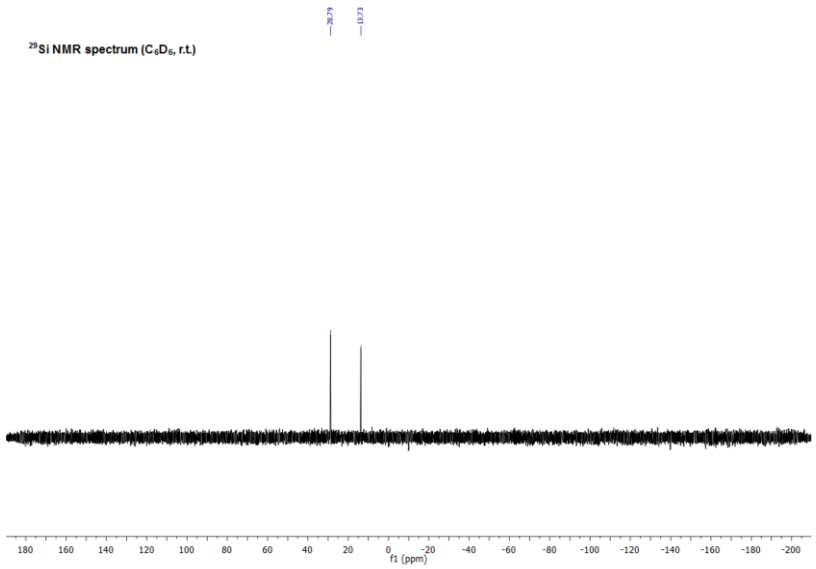


Figure S21: ^{29}Si NMR spectrum of silanone **2b** (C_6D_6, r.t.).

Synthesis of IPrNSi(O_2C=O)SiR_3 (R = TMS 3a, R = *t*-Bu 3b)

Similarly to the reaction of silepin **1a** with CO_2[S1], both silanones **2** can be directly converted with CO_2 to the respective silicon carbonate complexes **3**. Generally, a solution of **2** in C_6D_6 (0.5 mL) was exposed to CO_2 gas (1 bar) at room temperature in a J. Young PTFE tube. Monitoring the reaction *via* NMR spectroscopy showed the direct and quantitative formation of silicon carbonate complexes **3**.

Compound 3a:

The NMR shifts of this reaction product are identical to the published data.[S1]

^{1}H NMR (500 MHz, C_6D_6, r.t.): δ = 7.30 – 7.26 (m, 2H, *p*-C*H*-Ar), 7.19 – 7.16 (m, 4H, *m*-C*H*-Ar), 5.93 (s, 2H, C*H*-N), 2.95 (hept, *J* = 6.9 Hz, 4H, C*H*), 1.47 (d, *J* = 6.9 Hz, 12H, CH_3), 1.08 (d, *J* = 6.9 Hz, 12H, CH_3), 0.18 (s, 27H, Si*TMS*$_3$).

^{13}C NMR (126 MHz, C_6D_6, r.t.): δ = 150.4 (O_2C=O), 146.7 (*C*-Ar), 145.6 (N-*C*-N), 133.2 (*C*-Ar), 130.7 (*C*H-Ar), 124.8 (*C*H-Ar), 116.0 (*C*H-N), 29.2 (*C*H), 25.2 (*C*H_3), 23.2 (*C*H_3), 2.5 (Si*TMS*$_3$).

^{29}Si NMR (99 MHz, C_6D_6, r.t.): δ = -9.8 (*TMS*$_3$), -35.0 (*central Si*), -134.3 (*Si*TMS$_3$).

Compound 3b:

^{1}H NMR (500 MHz, C_6D_6, r.t.): δ = 7.33 – 7.26 (m, 2H, *p*-C*H*-Ar), 7.22 – 7.16 (m, 4H, *m*-C*H*-Ar), 5.97 (s, 2H, C*H*-N), 2.96 (hept, *J* = 6.9 Hz, 4H, C*H*), 1.45 (d, *J* = 6.9 Hz, 12H, CH_3), 1.08 (d, *J* = 6.9 Hz, 12H, CH_3), 1.05 (s, 27H, Si*t*-*Bu*$_3$).

^{13}C NMR (126 MHz, C_6D_6, r.t.): δ = 150.7 (O_2C=O), 146.8 (*C*-Ar), 145.5 (N-*C*-N), 133.3 (*C*-Ar), 130.6 (*C*H-Ar), 124.7 (*C*H-Ar), 116.2 (*C*H-N), 31.4 (C(*C*H_3)$_3$), 29.2 (*C*H), 25.4 (*C*H_3), 22.7 (*C*(CH$_3$)$_3$), 22.6 (*C*H_3).

^{29}Si NMR (99 MHz, C_6D_6, r.t.): δ = 5.5 (Si*t*-Bu$_3$), -43.0 (*central Si*).

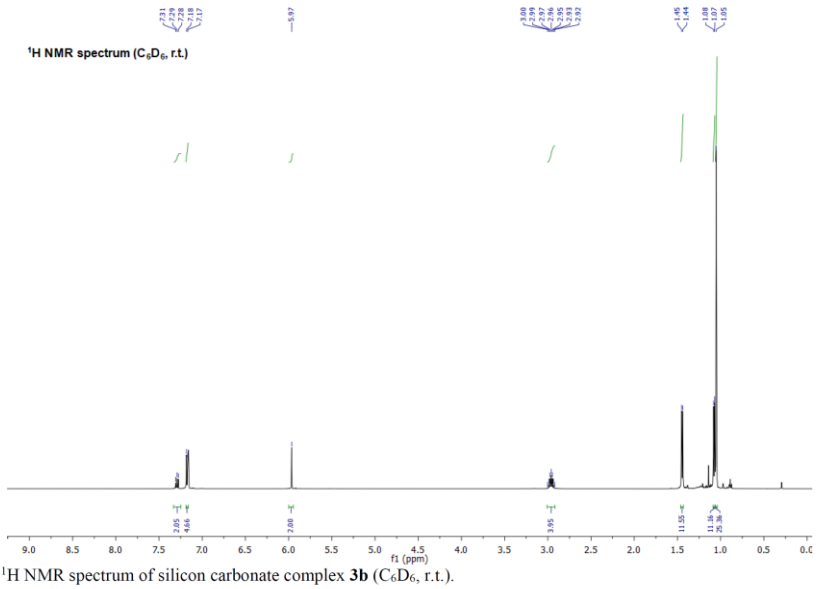


Figure S22: ^{1}H NMR spectrum of silicon carbonate complex **3b** (C_6D_6, r.t.).

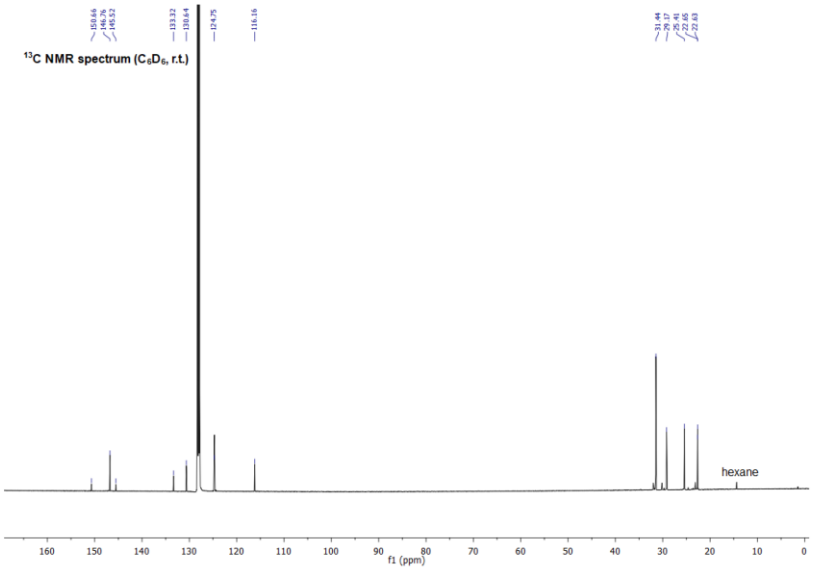


Figure S23: ^{13}C NMR spectrum of silicon carbonate complex **3b** (C_6D_6, r.t.).

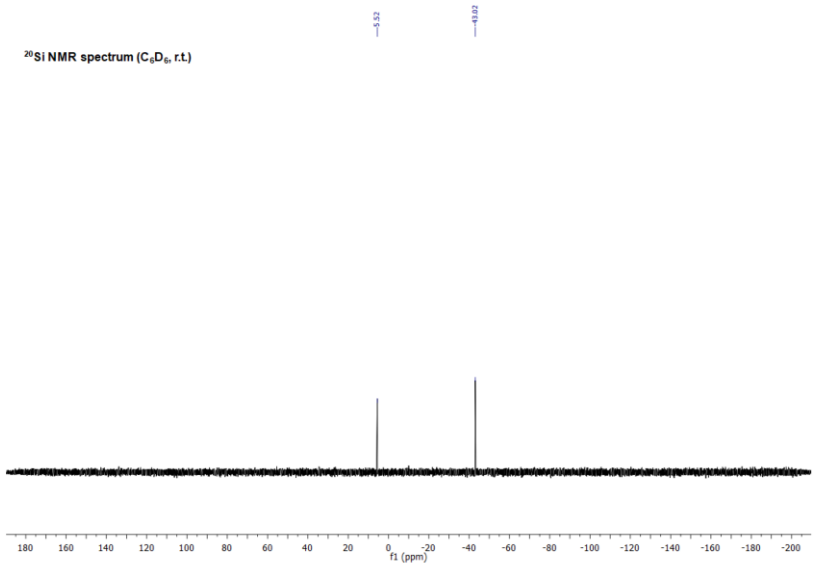


Figure S24: ^{29}Si NMR spectrum of silicon carbonate complex **3b** (C_6D_6, r.t.).

Synthesis of IPrNSi(OMe)(OH)SiR$_3$ (R = TMS 4a, R = *t*-Bu 4b)

To a yellowish solution of **2a** (35 mg, 50.4 µmol, 1.00 eq) in toluene (2 mL) were added a few drops of methanol (dried and degassed). The solution immediately turned colorless and was stirred for additional 20 min. Removal of all volatiles and crystallization in toluene/*n*-hexane at -35 °C for 2 days gave compound **4a** (26 mg, 35.7 µmol, 71%) as colorless crystals suitable for single crystal X-ray analysis. The analogue procedure was repeated for the preparation of compound **4b** (69%). For the synthesis of **4a**, also acetonitrile solutions of tetra-coordinate silanone **2a** × CD_3CN were used successfully.

Compound 4a:

^{1}H NMR (500 MHz, C_6D_6, r.t.): δ = 7.15 – 7.09 (m, 6H, C*H*-Ar), 5.94 (s, 2H, C*H*-N), 3.41 (s, 3H, OMe), 3.17 (overlapping hept, *J* = 6.9 Hz, 4H, C*H*), 1.45 (d, *J* = 6.9 Hz, 6H, CH_3), 1.42 (d, *J* = 6.9 Hz, 6H, CH_3) 1.13 (d, *J* = 6.9 Hz, 6H, CH_3), 1.11 (d, *J* = 6.9 Hz, 6H, CH_3), 0.28 (s, 27H, Si*TMS*$_3$).

^{13}C NMR (126 MHz, C_6D_6, r.t.): δ = 148.1 (*C*-Ar), 148.1 (*C*-Ar), 143.7 (N-*C*-N), 134.8 (*C*-Ar), 129.9 (*C*H-Ar), 124.4 (*C*H-Ar), 124.1 (*C*H-Ar), 114.9 (*C*H-N), 49.6 (O*C*H$_3$), 29.2 (*C*H), 28.9 (*C*H), 25.5 (*C*H$_3$), 25.2 (*C*H$_3$), 23.1 (*C*H$_3$), 23.0 (*C*H$_3$), 3.1 (Si*TMS*$_3$).

^{29}Si NMR (99 MHz, C_6D_6, r.t.): δ = -10.6 (*TMS*$_3$), -38.6 (*central Si*), -137.6 (*Si*TMS$_3$).

EA experimental (calculated): C 60.07 (61.18), H 9.21 (9.30), N 5.64 (5.78) %.

Compound 4b:

^{1}H NMR (500 MHz, C_6D_6, r.t.): δ = 7.18 – 7.14 (m, 2H, *m*-C*H*-Ar), 7.12 – 7.07 (m, 4H, *p*-C*H*-Ar) 5.96 (s, 2H, C*H*-N), 3.45 (s, 3H, OMe), 3.22 (hept, *J* = 6.9 Hz, 2H, C*H*), 3.11 (hept, *J* = 6.9 Hz, 2H, C*H*) 1.38 (d, *J* = 6.9 Hz, 12H, CH_3), 1.23 (s, 27H, Si*t-Bu*$_3$). 1.11 (d, *J* = 6.9 Hz, 6H, CH_3) 1.10 (d, *J* = 6.9 Hz, 6H, CH_3).

^{13}C NMR (126 MHz, C_6D_6, r.t.): δ = 148.0 (*C*-Ar), 147.9 (*C*-Ar), 143.2 (N-*C*-N), 134.9 (*C*-Ar), 129.9 (*C*H-Ar), 124.3 (*C*H-Ar), 124.1 (*C*H-Ar), 115.0 (*C*H-N), 49.7 (O*C*H$_3$), 31.9 (C(*C*H$_3$)$_3$), 28.9 (*C*H), 28.8 (*C*H), 25.7 (*C*H$_3$), 25.5 (*C*H$_3$), 22.7 (*C*H$_3$), 22.5 (*C*(CH$_3$)$_3$), 22.4 (*C*H$_3$).

^{29}Si NMR (99 MHz, C_6D_6, r.t.): δ = 1.2 (Si*t*-Bu$_3$), -46.6 (*central Si*).

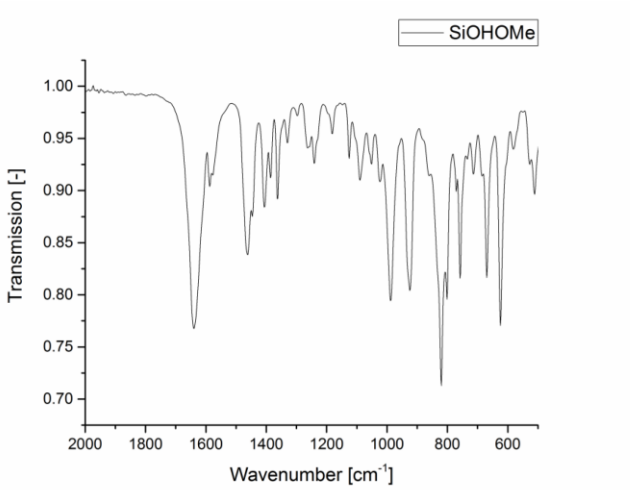


Figure S25: IR spectrum of compound **4a** (cm^{-1}): 1635 (s), 1584 (w), 1463 (m), 1403 (w), 1361 (w), 1237 (w), 1093 (w), 985 (s), 925 (s), 824 (s), 757 (m), 666 (m), 624 (s).

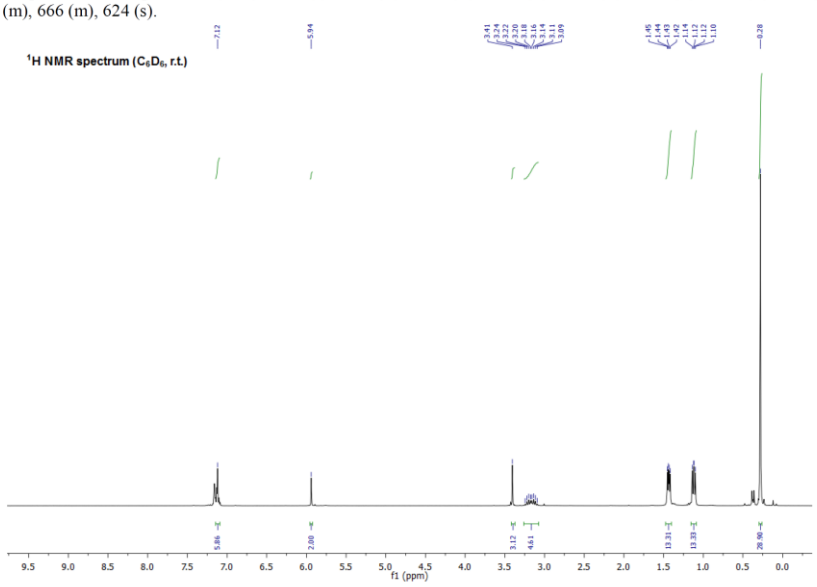


Figure S26: ^{1}H NMR spectrum of compound **4a** (C_6D_6, r.t.).

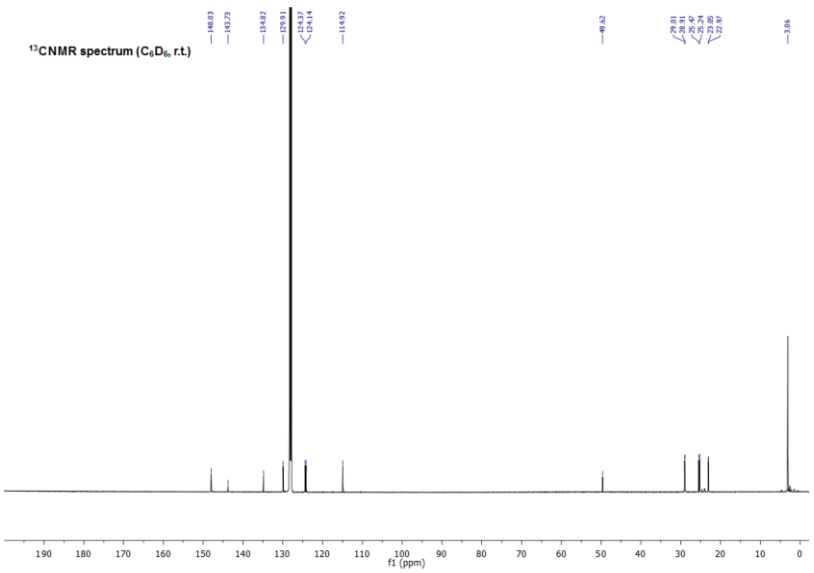


Figure S27: ^{13}C NMR spectrum of compound **4a** (C_6D_6, r.t.).

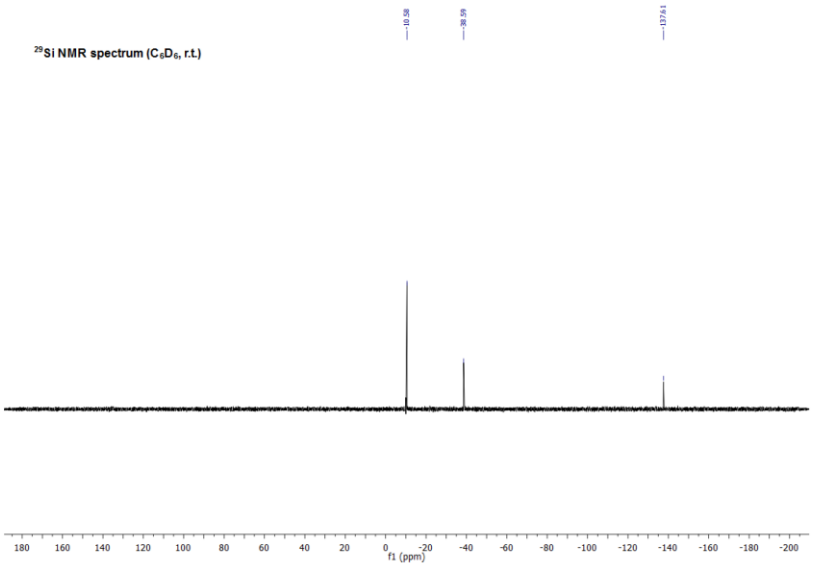


Figure S28: ^{29}Si NMR spectrum of compound **4a** (C_6D_6, r.t.).

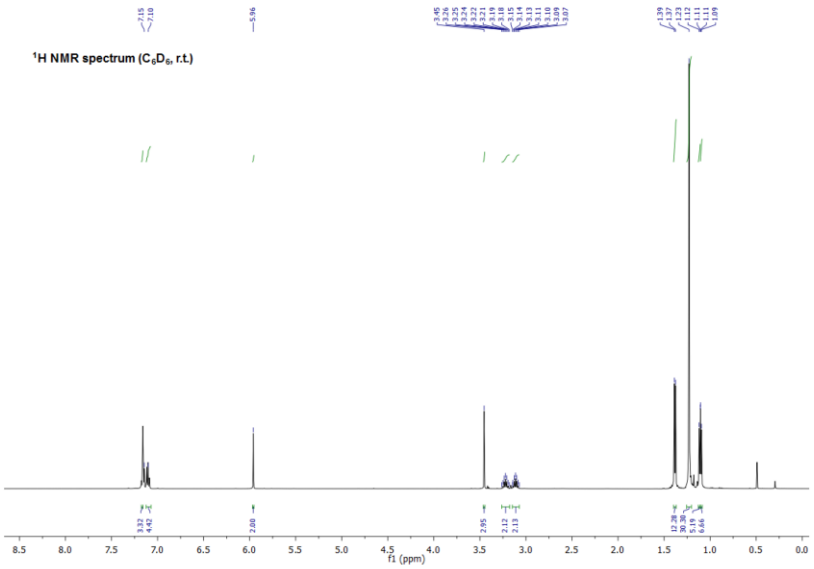


Figure S29: ^{1}H NMR spectrum of compound **4b** (C_6D_6, r.t.).

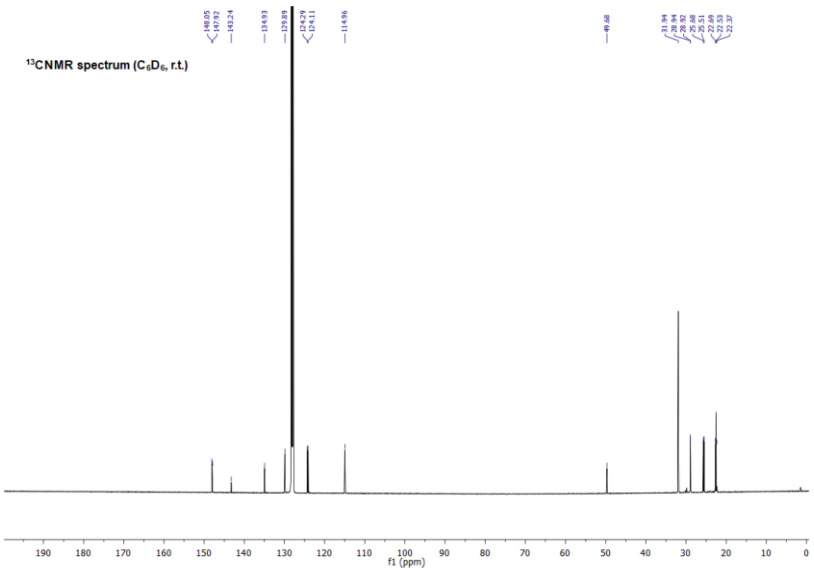


Figure S30: ^{13}C NMR spectrum of compound **4b** (C_6D_6, r.t.).

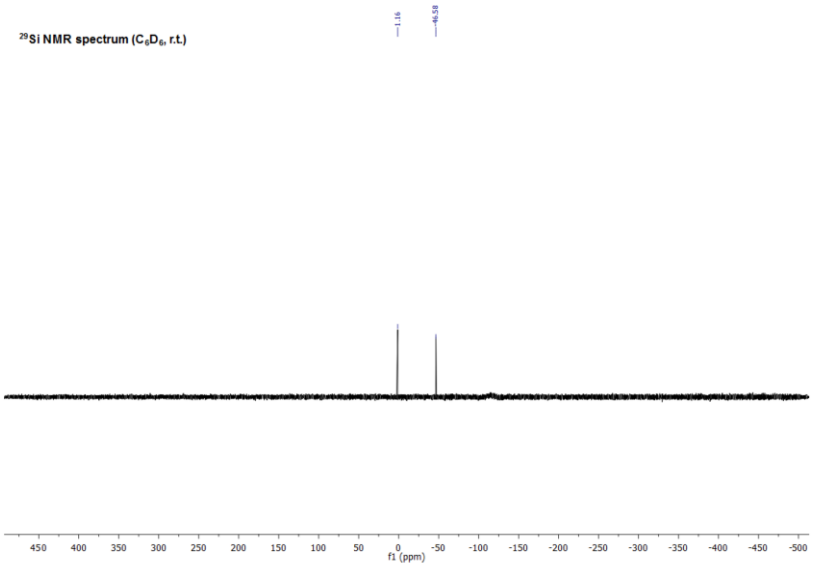


Figure S31: ^{29}Si NMR spectrum of compound **4b** (C_6D_6, r.t.).

Trapping Experiments of Transient Disilene INT with Ethylene and IMe_4

Synthesis of IPrNTMSOSi(CH_2CH_2)SiTMS_2 (5)

A J. Young PTFE tube was loaded with solid silanone **2a** (14 mg, 20.2 µmol, 1.00 eq), addition of THF-d_8 (0.5 mL) instantly formed a strongly yellow colored solution of transient disilene **INT** (NMR data see above). Subsequently, the solution was exposed to ethylene gas (1 bar) and monitored *via* NMR spectroscopy. After 10 min the yellow color faded completely and full conversion to 1,2-disilacyclobutane **5** was detected (structure verified *via* 2D NMR experiments and matching theoretical NMR shifts). In a second experiment, the slow decomposition of **2a** in C_6D_6 was repeated in ethylene atmosphere, here as well the formation of 1,2-disiletane **5** was observed.

^{1}H NMR (500 MHz, THF-d_8, r.t.): δ = 7.35 – 7.30 (m, 2H, *m*-C*H*-Ar), 7.27 – 7.23 (m, 4H, *m*-C*H*-Ar), 6.55 (s, 2H, C*H*-N), 3.20 (hept, *J* = 6.9 Hz, 2H, C*H*), 3.12 (hept, *J* = 6.9 Hz, 2H, C*H*), 1.32 (d, *J* = 6.9 Hz, 12H, CH_3), 1.30 (d, *J* = 6.9 Hz, 6H, CH_3) 1.21 (d, *J* = 6.9 Hz, 6H, CH_3), 1.15 (d, *J* = 6.9 Hz, 6H, CH_3), 0.99 – 0.94 (m, 2H, Si(CH_2CH$_2$)Si), 0.50 – 0.41 (m, 2H, Si(CH$_2$CH_2)Si), 0.39 – 0.36 (m, 1H, Si(CH_2CH$_2$)Si), 0.06 (s, 9H, Si*TMS*$_2$), -0.07 (s, 9H, Si*TMS*$_2$) -0.11 (s, 9H, O*TMS*).

^{13}C NMR (126 MHz, THF-d_8, r.t.): δ = 148.3 (*C*-Ar), 148.1 (*C*-Ar), 143.1 (N-*C*-N), 135.7 (*C*-Ar), 130.0 (*C*H-Ar), 125.0 (*C*H-Ar), 124.9 (*C*H-Ar), 116.1 (*C*H-N), 31.1 (Si(*C*H$_2$CH$_2$)Si), 29.5 (*C*H), 24.5 (*C*H$_3$), 24.0 (*C*H$_3$), 3.2 (O*TMS*), 1.6 (Si*TMS*$_2$), 1.5 (Si*TMS*$_2$),-0.3 (Si(CH$_2$*C*H$_2$)Si).

^{29}Si NMR (99 MHz, THF-d_8, r.t.): δ = 4.3 (O*TMS*), -14.6 (Si*TMS*$_2$), -14.8 (Si*TMS*$_2$), -35.7 (*Si*OTMS), -39.8 (*Si*TMS$_2$).

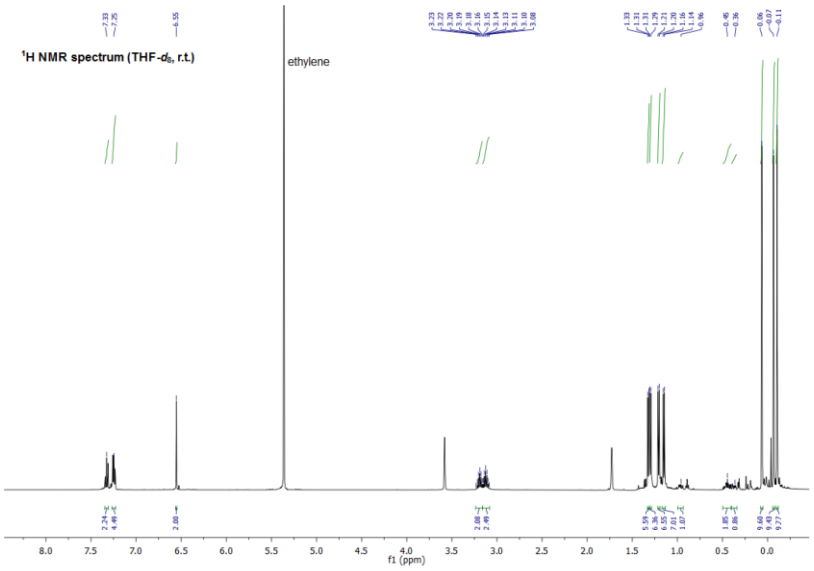


Figure S32: ^{1}H NMR spectrum of 1,2-disiletane **5** (THF-d_8, r.t.).

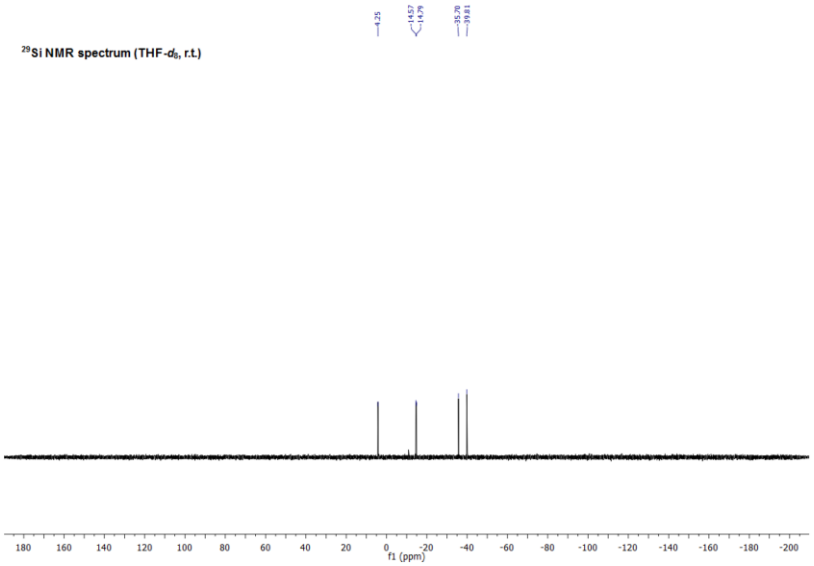


Figure S33: ^{29}Si NMR spectrum of 1,2-disiletane **5** (THF-d_8, r.t.)

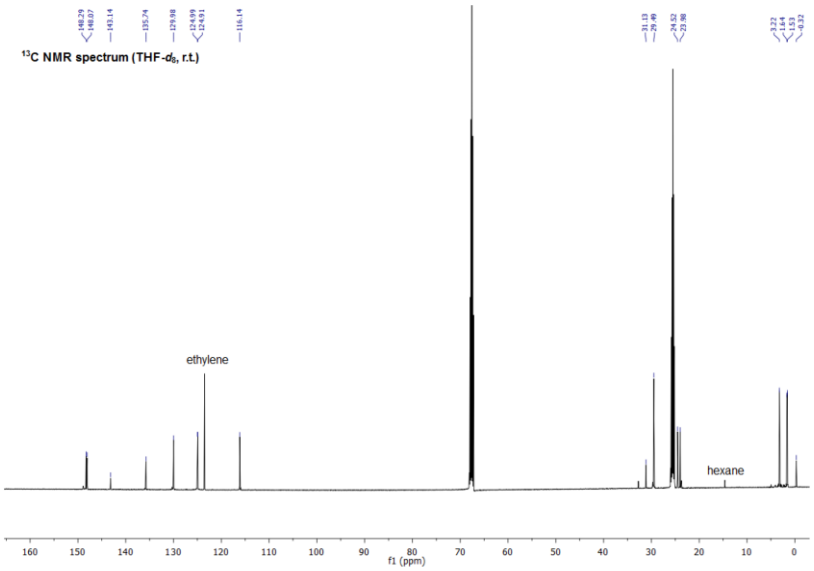


Figure S34: ^{13}C NMR spectrum of 1,2-disiletane **5** (THF-d_8, r.t.)

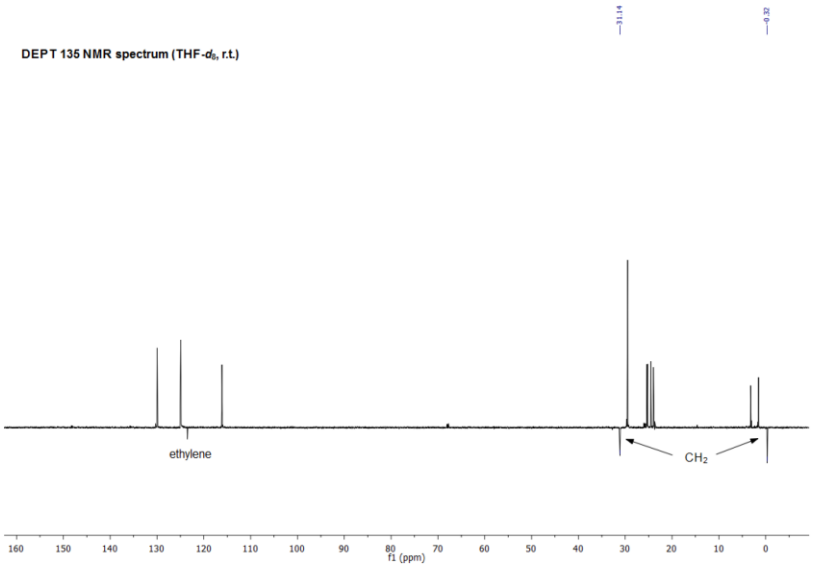


Figure S35: DEPT 135 NMR spectrum of 1,2-disiletane **5** (THF-d_8, r.t.)

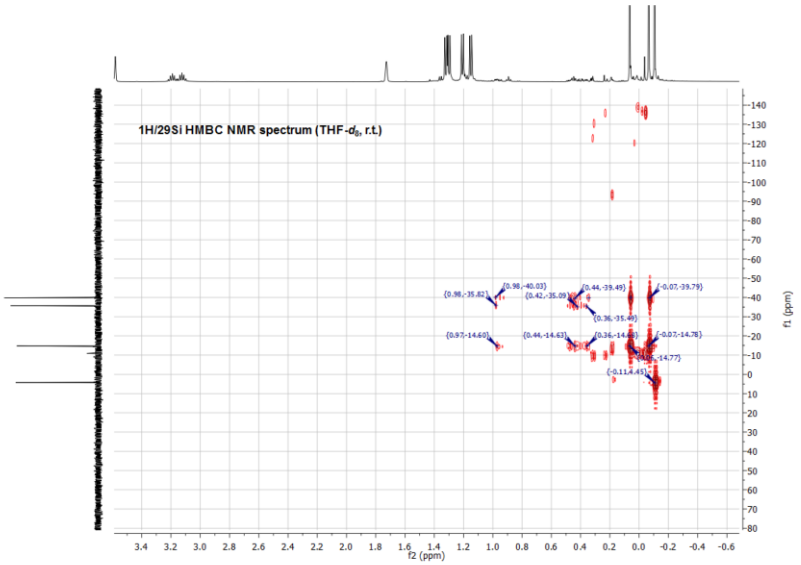


Figure S36: $^{1}H/^{29}Si$ HMBC NMR spectrum of 1,2-disiletane **5** (THF-d_8, r.t.)

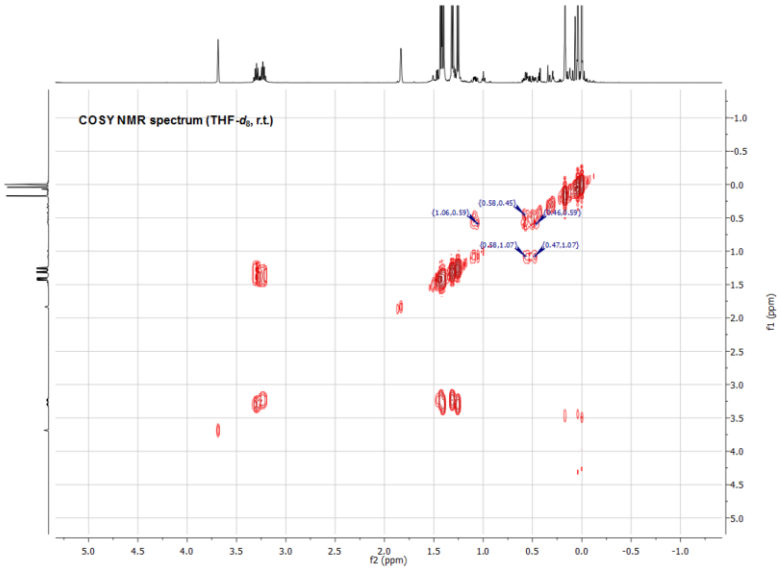


Figure S37: COSY NMR spectrum of 1,2-disiletane **5** (THF-d_8, r.t.)

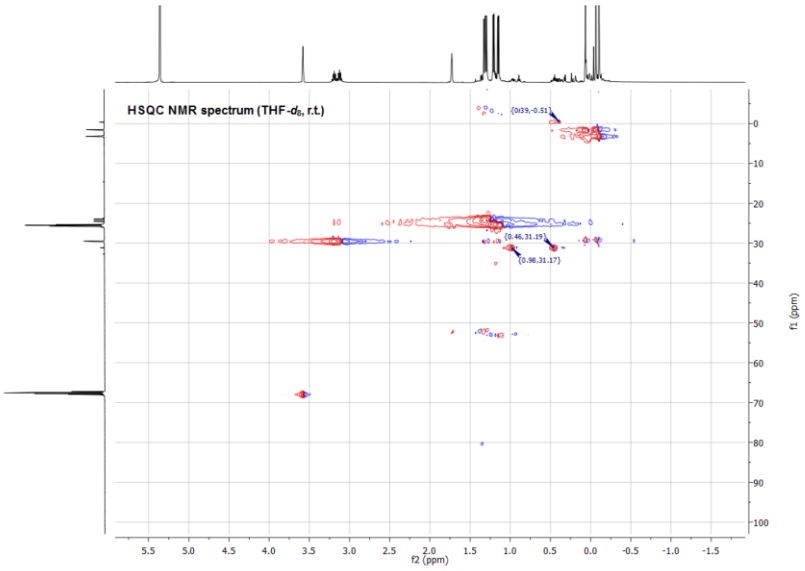


Figure S38: HSQC NMR spectrum of 1,2-disiletane **5** (THF-d_8, r.t.)

Synthesis of IMe_4 Stabilized Zwitterionic Disilene (6)

To a yellowish toluene (2 mL) solution of **2a** (29 mg, 41.9 µmol, 1.00 eq) was added IMe_4 (5.2 mg, 41.9 µmol, 1.00 eq) in toluene (1 mL). The solution immediately turned orange-red and was stirred additional 20 min. Removal of all volatiles and crystallization from *n*-hexane at -35 °C for 1 day gave IMe_4 stabilized zwitterionic disilene **6** (20 mg, 24.4 µmol, 58%) as orange-red crystals suitable for single crystal X-ray analysis. Compound **6** is permanently stable as a solid and in C_6D_6 solution at room temperature. Alternatively, intermediary disilene **INT** can also be trapped, by first inducing the 1,3-silyl migration of silanone **2a** with THF, followed by the addition of IMe_4.

^{1}H NMR (500 MHz, C_6D_6, r.t.): δ = 7.22 – 7.13 (m, 4H, *m*-C*H*-Ar), 6.98 – 6.93 (m, 2H, *p*-C*H*-Ar), 5.91 (s, 2H, C*H*-N), 3.44 (hept, *J* = 6.9 Hz, 2H, C*H*), 3.13 (s, 6H, IMe_4-NC*H*$_3$), 3.09 (hept, *J* = 6.9 Hz, 2H, C*H*), 1.40 (d, *J* = 6.9 Hz, 12H, C*H*$_3$), 1.34 (s, 6H, IMe_4-C*H*$_3$), 1.12 (d, *J* = 6.9 Hz, 6H, C*H*$_3$), 1.08 (d, *J* = 6.9 Hz, 6H, C*H*$_3$), 0.42 (s, 18H, Si*TMS*$_2$), 0.28 (s, 9H, O*TMS*).

^{13}C NMR (126 MHz, C_6D_6, r.t.): δ = 156.3 (IMe_4-N-*C*-N), 148.3 (*C*-Ar), 148.2 (*C*-Ar), 140.2 (N-*C*-N), 135.9 (*C*-Ar), 129.2 (*C*H-Ar), 124.8 (*C*H-Ar), 124.3 (*C*H-Ar), 124.2 (IMe_4-*C*=*C*), 115.3 (*C*H-N), 33.2 (IMe_4-NCH$_3$), 28.7 (*C*H), 28.4 (*C*H), 25.7 (*C*H$_3$), 24.5 (*C*H$_3$), 22.0 (*C*H$_3$), 7.9 (IMe_4-C*C*H$_3$), 7.2 (Si*TMS*$_2$), 4.8 (O*TMS*).

^{29}Si NMR (99 MHz, C_6D_6, r.t.): δ = 6.1 (O*TMS*), -7.1 (Si*TMS*$_2$), -35.2 (*Si*OTMS), -174.6 (*Si*TMS$_2$).

EA experimental (calculated): C 62.37 (63.10), H 9.16 (9.24), N 8.06 (8.56) %.

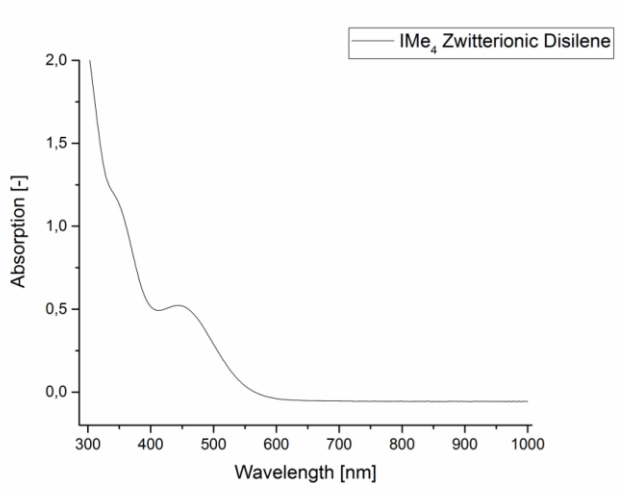


Figure S39. UV-Vis spectrum of IMe_4 stabilized zwitterionic disilene **6** λ_{max} (r.t., toluene, 4.0×10^{-4} M) = 342, 449 nm.

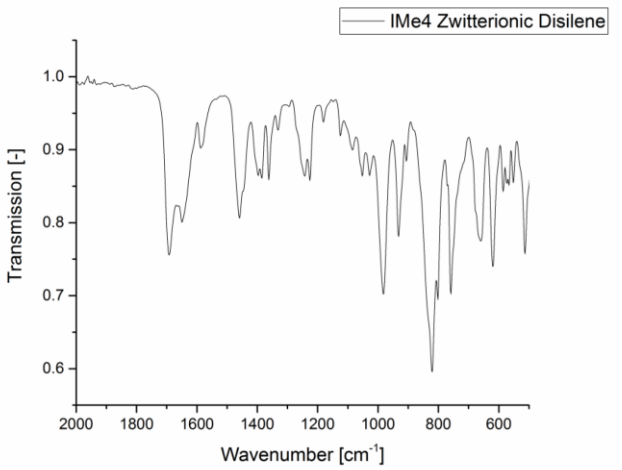


Figure S40: IR spectrum of IMe_4 stabilized zwitterionic disilene **6** (cm^{-1}): 1690 (m), 1641 (m), 1586 (s), 1454 (m), 1401 (s), 1229 (s), 978 (m), 929 (m), 832 (s), 751 (m), 662 (m), 615 (m).

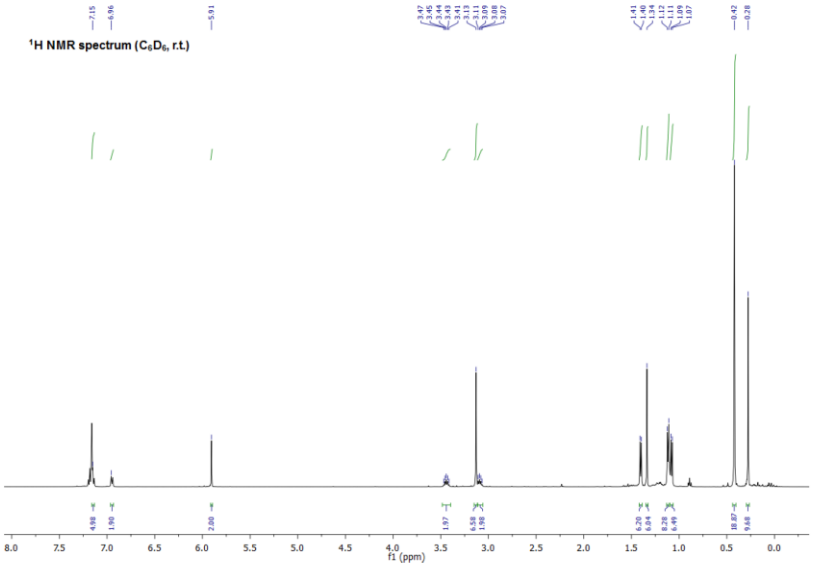


Figure S41: ^1H NMR spectrum of IMe_4 stabilized zwitterionic disilene **6** (C_6D_6, r.t.).

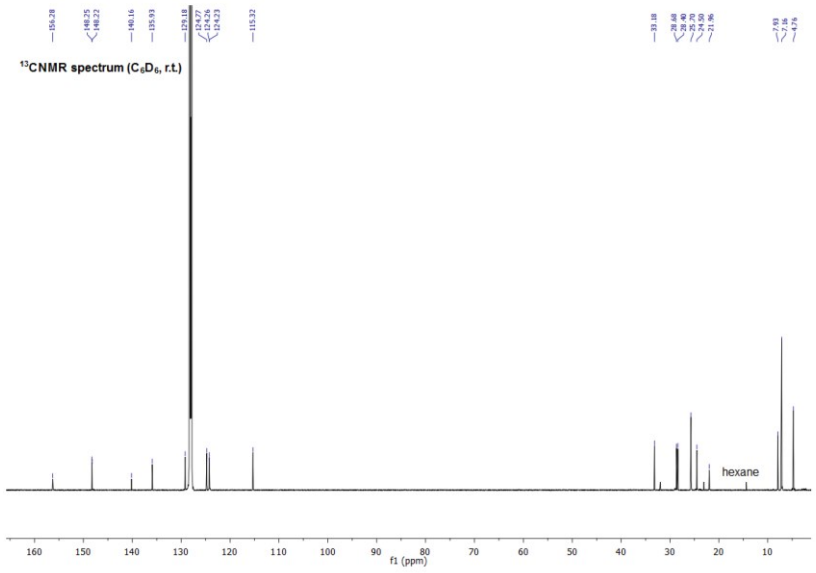


Figure S42: ^{13}C NMR spectrum of IMe_4 stabilized zwitterionic disilene **6** (C_6D_6, r.t.).

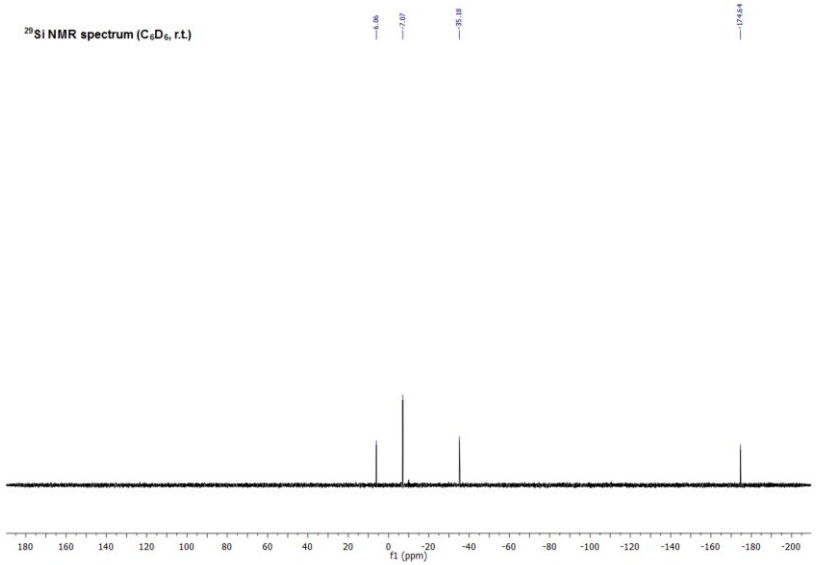


Figure S43: ^{29}Si NMR spectrum of IMe_4 stabilized zwitterionic disilene **6** (C_6D_6, r.t.).

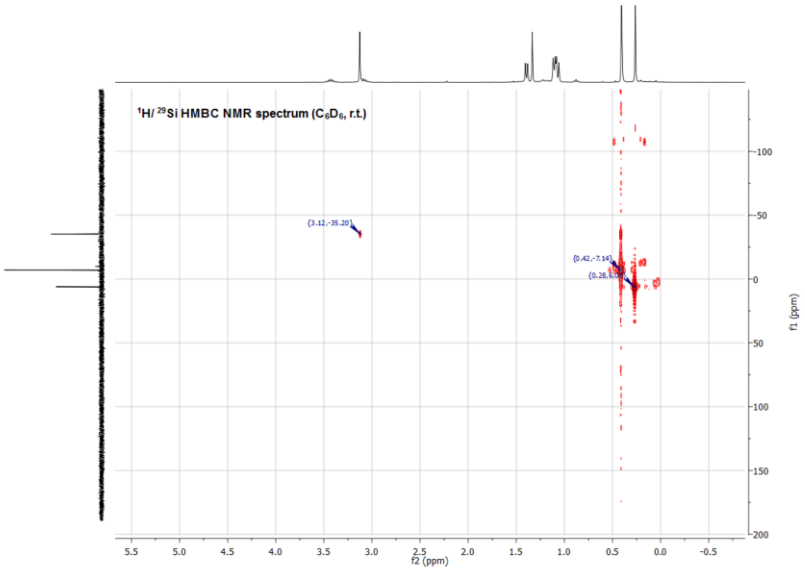


Figure S44: ^{1}H/^{29}Si HMBC NMR spectrum of IMe$_4$ stabilized zwitterionic disilene **6** (C_6D_6, r.t.).

Synthesis of IPrNSi(II)OSi*t*-Bu$_3$ (7)

As already stated, silanone **2b** quantitatively forms *N*,*O*-silylene **7** in C_6D_6 or THF-d_8 at room temperature within 48 h ($t_{1/2}$ = 24 h). By heating the solution to 60 °C, this transformation can be accelerated and full conversion was detected by NMR spectroscopy in less than 1 h. Hence, a solution of **2b** (100 mg, 155 µmol, 1.00 eq) in toluene (5 mL) was heated to 60 °C for 1 h. Removal of all volatiles gave *N*,*O*-silylene **7** as colorless solid (100 mg, 155 µmol, quantitative yield). Crystals suitable for single crystal X-ray analysis were obtained by cooling a concentrated *n*-hexane solution of **7** at -35 °C for several days. *N*,*O*-Silylene **7** is completely stable as a solid and in solution at room temperature.

^{1}H NMR (500 MHz, C_6D_6, r.t.): δ = 7.24 – 7.17 (m, 2H, *p*-C*H*-Ar), 7.15 – 7.09 (m, 4H, *m*-C*H*-Ar), 5.99 (s, 2H, C*H*-N), 3.10 (hept, *J* = 6.8 Hz, 4H, C*H*), 1.46 (d, *J* = 6.8 Hz, 12H, CH_3), 1.17 (d, *J* = 6.8 Hz, 12H, CH_3), 1.07 (s, 27H, Si*t*-*Bu*$_3$).

^{13}C NMR (126 MHz, C_6D_6, r.t.): δ =, 147.7 (*C*-Ar), 146.6 (N-*C*-N) 133.5 (*C*-Ar), 129.9 (*C*H-Ar), 124.0 (*C*H-Ar), 114.9 (*C*H-N), 30.3 (C(*C*H$_3$)$_3$), 29.1 (*C*H), 24.6 (*C*H$_3$), 23.8 (*C*H$_3$), 22.8 (*C*(CH$_3$)$_3$).

^{29}Si NMR (99 MHz, C_6D_6, r.t.): δ = 58.9 (*central Si*), 4.4 (Si*t*-Bu$_3$).

EA experimental (calculated): C 71.92 (72.50), H 10.02 (9.83), N 6.31 (6.50) %.

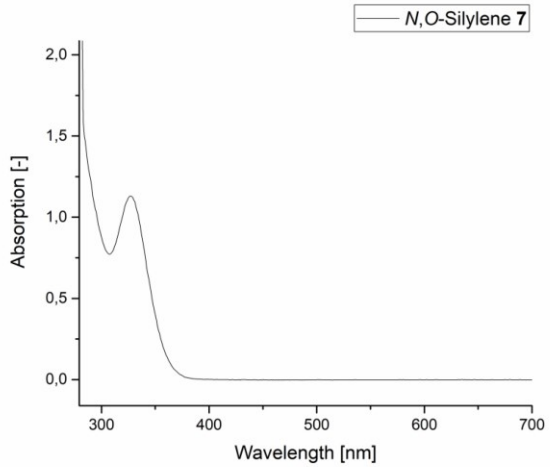


Figure S45. UV-Vis spectrum of *N*,*O*-silylene **7** λ_{max} (r.t., toluene, 8.0×10^{-4} M) = 328 nm.

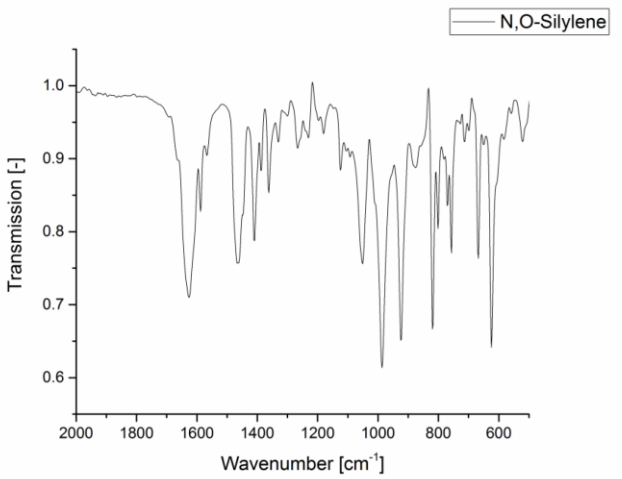


Figure S46: IR spectrum of *N*,*O*-silylene **7** (cm^{-1}): 1624 (s), 1459 (m), 1405 (m), 1365 (s), 1049 (m), 980 (s), 917 (s), 819 (s), 758 (m), 666 (m), 621 (s).

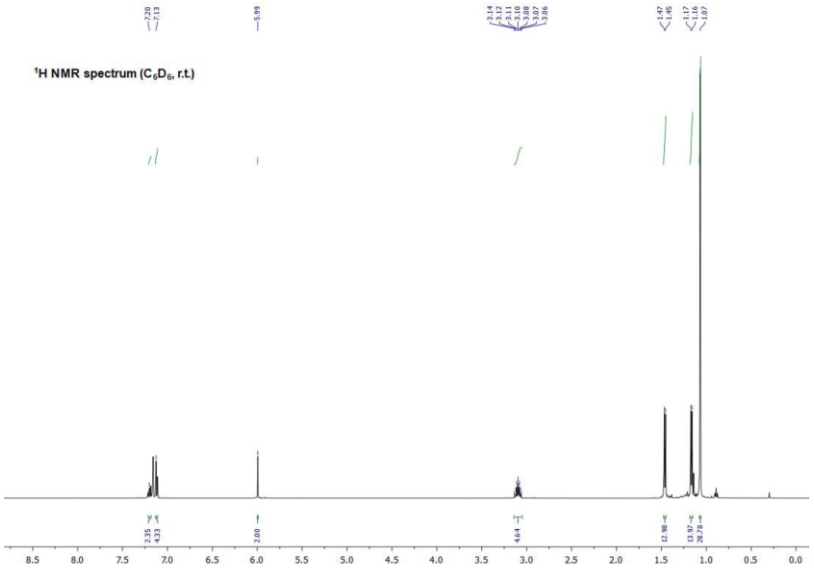


Figure S47: ^{1}H NMR spectrum of *N*,*O*-silylene **7** (C_6D_6, r.t.).

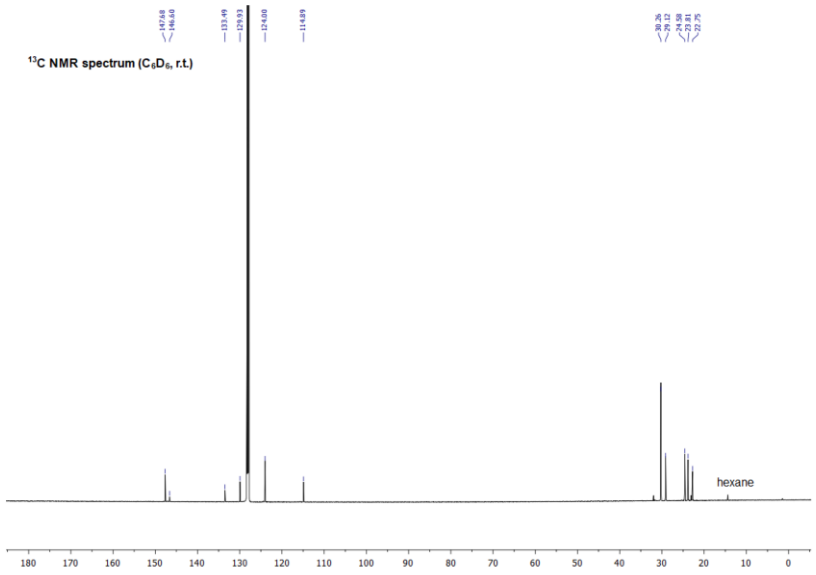


Figure S48: ^{13}C NMR spectrum of *N,O*-silylene **7** (C_6D_6, r.t.).

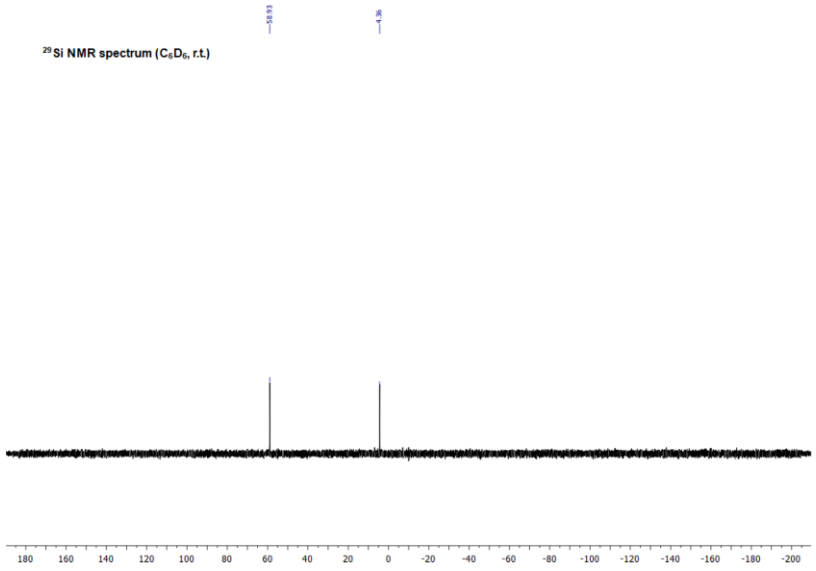


Figure S49: ^{29}Si NMR spectrum of *N,O*-silylene **7** (C_6D_6, r.t.).

NMR Studies on the Reactivity of *N,O*-Silylene 7 towards Ethylene and Hydrogen

Synthesis of IPrNSi(CH$_2$CH$_2$)OSi*t*-Bu$_3$ (8)

A C_6D_6 (0.5 mL) solution of *N,O*-silylene **7** (15 mg, 23.2 µmol, 1.00 eq) in a J. Young PTFE tube was exposed to ethylene or hydrogen gas (1 bar), respectively. With ethylene, monitoring the reaction at room temperature showed silirane **8** as sole product after 20 min reaction time. Removal of all volatiles gave compound **8** as a colorless sticky solid (15.7 mg, 23.2 µmol, quantitative yield). Compound **8** is completely stable as a solid and in solution at room temperature. For hydrogen, no activation was observed even after heating the reaction solution to 60 °C for several days.

^{1}H NMR (500 MHz, C_6D_6, r.t.): δ = 7.26 – 7.21 (m, 2H, *p*-C*H*-Ar), 7.14 – 7.11 (m, 4H, *m*-C*H*-Ar), 5.94 (s, 2H, C*H*-N), 3.15 (hept, *J* = 6.8 Hz, 4H, C*H*), 1.40 (d, *J* = 6.8 Hz, 12H, CH_3), 1.15 (d, *J* = 6.8 Hz, 12H, CH_3), 1.07 (s, 27H, Si*t*-*Bu*$_3$), 0.91 – 0.85 (m, 2H, Si*(*CH_2-CH_2), 0.03 – -0.03 (m, 2H, Si*(*CH_2-CH_2).

^{13}C NMR (126 MHz, C_6D_6, r.t.): δ = 147.5 (*C*-Ar), 142.7 (N-*C*-N), 134.5 (*C*-Ar), 129.8 (*C*H-Ar), 123.0 (*C*H-Ar), 114.6 (*C*H-N), 30.2 (C(*C*H$_3$)$_3$), 29.0 (*C*H), 24.7 (*C*H$_3$), 23.4 (*C*H$_3$), 23.1 (*C*(CH$_3$)$_3$), 4.8 (*C*H$_2$*C*H$_2$).

^{29}Si NMR (99 MHz, C_6D_6, r.t.): δ = 3.4 (Si*t*-Bu$_3$), -75.0 (*central Si*).

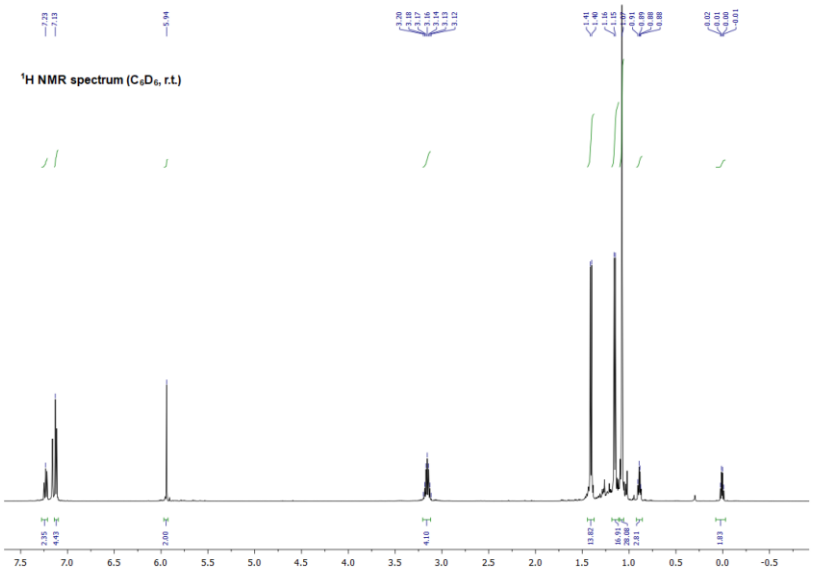


Figure S50: ^{1}H NMR spectrum of silirane **8** (C_6D_6, r.t.).

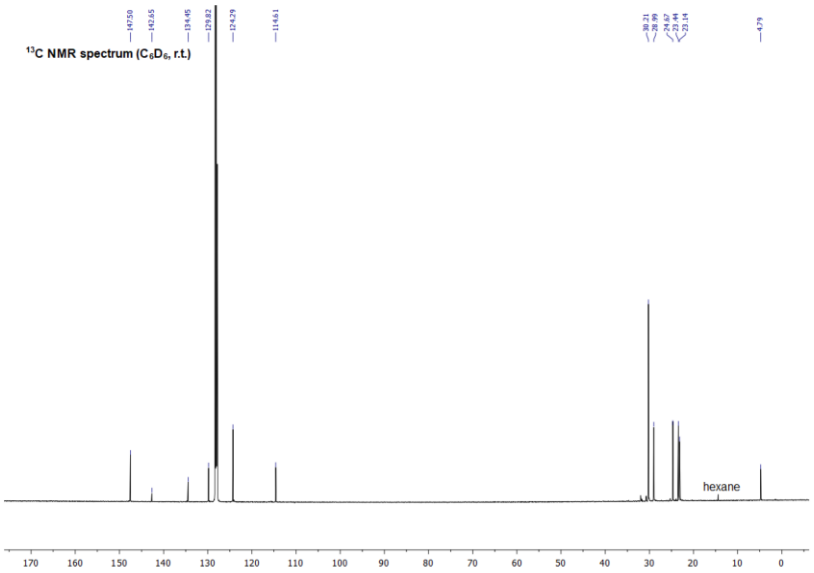


Figure S51: ^{13}C NMR spectrum of silirane **8** (C_6D_6, r.t.).

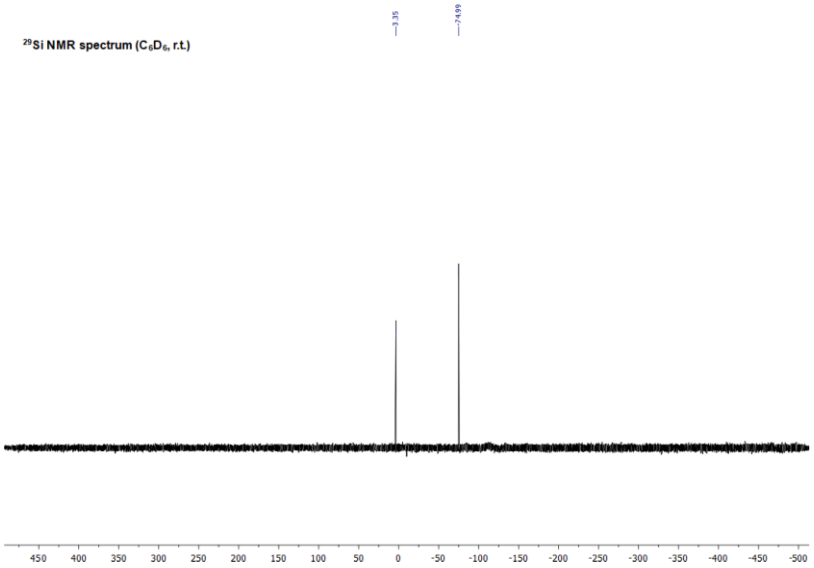


Figure S52: ^{29}Si NMR spectrum of silirane **8** (C_6D_6, r.t.).



Figure S53: $^{1}H/^{29}Si$ HMBC NMR spectrum of silirane **8** (C_6D_6, r.t.).

2. X-ray Crystallographic Data

A) General information

The X-ray intensity data of **2a** × **CD3CN**, **4a**, **6** and **7** were collected on an X-ray single crystal diffractometer equipped with a CMOS detector (Bruker Photon-100), an IMS microsource with MoKα radiation (λ = 0.71073 Å) and a Helios mirror optic by using the APEX III software package.[S6] The X-ray intensity data of **2b** were collected on an X-ray single crystal diffractometer equipped with a CMOS detector (Bruker Photon-100), a rotating anode (Bruker TXS) with MoKα radiation (λ = 0.71073 Å) and a Helios mirror optic by using the APEX III software package.[S6] The measurements were performed on single crystals coated with perfluorinated ether. The crystals were fixed on the top of a microsampler, transferred to the diffractometer and frozen under a stream of cold nitrogen. A matrix scan was used to determine the initial lattice parameters. Reflections were merged and corrected for Lorenz and polarization effects, scan speed, and background using SAINT.[S7] Absorption corrections, including odd and even ordered spherical harmonics were performed using SADABS.[S7] Space group assignments were based upon systematic absences, E statistics, and successful refinement of the structures. Structures were solved by direct methods with the aid of successive difference Fourier maps, and were refined against all data using the APEX III software in conjunction with SHELXL-2014[S8] and SHELXLE[S9]. H atoms bound to aluminium atoms were allowed to refine freely. Other H atoms were placed in calculated positions and refined using a riding model, with methylene and aromatic C–H distances of 0.99 and 0.95 Å, respectively, and $U_{iso}(H) = 1.2 \cdot U_{eq}(C)$. Full-matrix least-squares refinements were carried out by minimizing $\Delta w(F_o^2 - F_c^2)^2$ with SHELXL-97[S10] weighting scheme. Neutral atom scattering factors for all atoms and anomalous dispersion corrections for the non-hydrogen atoms were taken from International Tables for Crystallography.[S11] The image of the crystal structure was generated by Mercury.[S12] CCDC 1577580-1577584 contain the supplementary data for the structures. These data can be obtained free of charge from the Cambridge Crystallographic Data Centre.

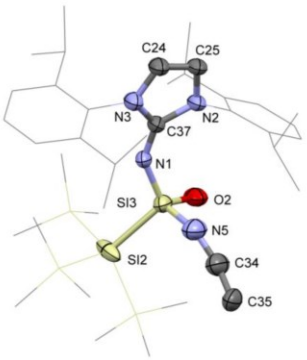


Figure S54: Molecular structure of silanone **2a** × **CD_3CN** in the solid state with ellipsoids set at the 50% probability level. For clarity, hydrogen atoms and co-crystallized solvent molecules are omitted and TMS as well as Dipp groups are simplified as wireframes. Selected bond lengths (Å) and angles (deg): Si3–O2 1.632(6), Si3–N5 1.749(7), Si3–N1 1.670(5), N1–C37 1.277(7), C37–N2 1.390(8), C37–N3 1.397(9), N1–Si3–Si2 114.1(4), C37–N1–Si3 142.1(9).

Table S1: Sample and crystal data for **2a** × **CD_3CN**.

Identification code	WenDa48	
Chemical formula	$C_{38}H_{66}N_4OSi_5$	
Formula weight	735.39	
Temperature	100(2) K	
Wavelength	0.71073 Å	
Crystal size	0.133 mm x 0.276 mm x 0.278 mm	
Crystal habit	clear colorless fragment	
Crystal system	monoclinic	
Space group	*P* 1 $2_1/n$ 1	
Unit cell dimensions	a = 10.3704(11) Å	α = 90°
	b = 33.835(3) Å	β = 97.371(3)°
	c = 12.9525(12) Å	γ = 90°
Volume	4507.2(8) $Å^3$	
Z	4	
Density (calculated)	1.084 g/cm^3	
Absorption coefficient	0.190 mm^{-1}	
F(000)	1600	

Table S2: Data collection and structure refinement for **2a** × **CD_3CN**.

Diffractometer	Bruker D8 Venture, CMOS detector (Bruker Photon-100)	
Radiation source	IMS microsource, Mo	
Theta range for data collection	2.32 to 25.03°	
Index ranges	-12<=h<=12, -40<=k<=40, -15<=l<=15	
Reflections collected	48889	
Independent reflections	7974 [R(int) = 0.0423]	
Coverage of independent reflections	99.9%	
Absorption correction	multi-scan	
Min. and max. transmission	0.6905 and 0.7453	
Refinement method	Full-matrix least-squares on F^2	
Refinement program	SHELXL-2014/7 (Sheldrick, 2014)	
Function minimized	$\Sigma\, w(F_o^2 - F_c^2)^2$	
Data / restraints / parameters	7974 / 682 / 902	
Goodness-of-fit on F^2	1.217	
Δ/σ_{max}	0.011	
Final R indices	5222 data; I>2σ(I)	R1 = 0.0941, wR2 = 0.2488
	all data	R1 = 0.1366, wR2 = 0.2777
Weighting scheme	$w=1/[\sigma^2(F_o^2)+(0.1137P)^2+6.2488P]$ where $P=(F_o^2+2F_c^2)/3$	
Largest diff. peak and hole	1.312 and -0.629 eÅ^{-3}	
R.M.S. deviation from mean	0.073 eÅ^{-3}	

Table S3: Sample and crystal data for **2b**.

Identification code	ReiDo8	
Chemical formula	$C_{30}H_{63}N_3OSi_3$	
Formula weight	646.10	
Temperature	100(2) K	
Wavelength	0.71073 Å	
Crystal size	0.138 mm x 0.144 mm x 0.517 mm	
Crystal habit	clear colorless fragment	
Crystal system	monoclinic	
Space group	$P\ 1\ 2_1/c\ 1$	
Unit cell dimensions	a = 13.987(10) Å	α = 90°
	b = 21.397(15) Å	β = 92.58(2)°
	c = 27.532(12) Å	γ = 90°
Volume	8231(10) $Å^3$	
Z	8	
Density (calculated)	1.043 g/cm^3	
Absorption coefficient	0.117 mm^{-1}	
F(000)	2832	

Table S4: Data collection and structure refinement for **2b**.

Diffractometer	Bruker D8 Venture, CMOS detector (Bruker Photon-100)	
Radiation source	TXS rotating anode, Mo	
Theta range for data collection	1.92 to 25.03°	
Index ranges	-16<=h<=16, -25<=k<=25, -32<=l<=32	
Reflections collected	193064	
Independent reflections	14326 [R(int) = 0.0786]	
Coverage of independent reflections	98.4%	
Absorption correction	multi-scan	
Min. and max. transmission	0.6460 and 0.7453	
Refinement method	Full-matrix least-squares on F^2	
Refinement program	SHELXL-2014/7 (Sheldrick, 2014)	
Function minimized	$\Sigma\ w(F_o^2 - F_c^2)^2$	
Data / restraints / parameters	14326 / 557 / 1300	
Goodness-of-fit on F^2	1.108	
Δ/σ_{max}	0.001	
Final R indices	11065 data; I>2σ(I)	R1 = 0.0788, wR2 = 0.1647
	all data	R1 = 0.1059, wR2 = 0.1786
Weighting scheme	$w=1/[\sigma^2(F_o^2)+(0.0344P)^2+20.6132P]$ where $P=(F_o^2+2F_c^2)/3$	
Largest diff. peak and hole	0.533 and -0.469 $eÅ^{-3}$	
R.M.S. deviation from mean	0.062 $eÅ^{-3}$	

Table S5: Sample and crystal data for **4a**.

Identification code	WenDa39	
Chemical formula	$C_{37}H_{67}N_3O_2Si_5$	
Formula weight	726.38	
Temperature	100(2) K	
Wavelength	0.71073 Å	
Crystal size	0.134 mm x 0.180 mm x 0.509 mm	
Crystal habit	clear colorless fragment	
Crystal system	monoclinic	
Space group	$P\ 1\ 2_1/n\ 1$	
Unit cell dimensions	a = 13.2302(14) Å	α = 90°
	b = 11.9923(13) Å	β = 96.613(3)°
	c = 28.620(3) Å	γ = 90°
Volume	4510.7(8) Å^3	
Z	4	
Density (calculated)	1.070 g/cm^3	
Absorption coefficient	0.190 mm^{-1}	
F(000)	1584	

Table S6: Data collection and structure refinement for **4a**.

Diffractometer	Bruker D8 Venture, CMOS detector (Bruker Photon-100)	
Radiation source	IMS microsource, Mo	
Theta range for data collection	2.22 to 25.03°	
Index ranges	-15<=h<=15, -11<=k<=11, -34<=l<=34	
Reflections collected	39229	
Independent reflections	7963 [R(int) = 0.0595]	
Coverage of independent reflections	99.9%	
Absorption correction	multi-scan	
Min. and max. transmission	0.5815 and 0.7453	
Refinement method	Full-matrix least-squares on F^2	
Refinement program	SHELXL-2014/7 (Sheldrick, 2014)	
Function minimized	$\Sigma\, w(F_o^2 - F_c^2)^2$	
Data / restraints / parameters	7963 / 0 / 446	
Goodness-of-fit on F^2	1.082	
Δ/σ_{max}	0.001	
Final R indices	5981 data; I>2σ(I)	R1 = 0.0563, wR2 = 0.1234
	all data	R1 = 0.0832, wR2 = 0.1342
Weighting scheme	$w=1/[\sigma^2(F_o^2)+(0.0351P)^2+9.0134P]$ where $P=(F_o^2+2F_c^2)/3$	
Largest diff. peak and hole	0.483 and -0.402 eÅ^{-3}	
R.M.S. deviation from mean	0.065 eÅ^{-3}	

Table S7: Sample and crystal data for **6**.

Identification code	WenDa40	
Chemical formula	$C_{43}H_{75}N_5OSi_5$	
Formula weight	818.53	
Temperature	100(2) K	
Wavelength	0.71073 Å	
Crystal size	0.133 mm x 0.148 mm x 0.167 mm	
Crystal habit	clear orange fragment	
Crystal system	triclinic	
Space group	*P* -1	
Unit cell dimensions	a = 12.4388(5) Å	α = 103.4770(10)°
	b = 20.3429(7) Å	β = 99.6220(10)°
	c = 20.7659(8) Å	γ = 94.4910(10)°
Volume	5000.2(3) $Å^3$	
Z	2	
Density (calculated)	1.087 g/cm^3	
Absorption coefficient	0.178 mm^{-1}	
F(000)	1784	

Table S8: Data collection and structure refinement for **6**.

Diffractometer	Bruker D8 Venture, CMOS detector (Bruker Photon-100)	
Radiation source	IMS microsource, Mo	
Theta range for data collection	1.39 to 25.03°	
Index ranges	-14<=h<=14, -24<=k<=24, -24<=l<=24	
Reflections collected	93632	
Independent reflections	17649 [R(int) = 0.0682]	
Coverage of independent reflections	99.9%	
Absorption correction	multi-scan	
Min. and max. transmission	0.7185 and 0.7453	
Refinement method	Full-matrix least-squares on F^2	
Refinement program	SHELXL-2014/7 (Sheldrick, 2014)	
Function minimized	$\Sigma\, w(F_o^2 - F_c^2)^2$	
Data / restraints / parameters	17649 / 84 / 1095	
Goodness-of-fit on F^2	1.025	
Δ/σ_{max}	0.001	
Final R indices	13203 data; I>2σ(I)	R1 = 0.0476, wR2 = 0.0957
	all data	R1 = 0.0748, wR2 = 0.1063
Weighting scheme	$w=1/[\sigma^2(F_o^2)+(0.0327P)^2+5.0730P]$ where $P=(F_o^2+2F_c^2)/3$	
Largest diff. peak and hole	0.469 and -0.419 $eÅ^{-3}$	
R.M.S. deviation from mean	0.051 $eÅ^{-3}$	

Table S9: Sample and crystal data for **7**.

Identification code	WenDa47	
Chemical formula	$C_{39}H_{63}N_3OSi_3$	
Formula weight	646.10	
Temperature	100(2) K	
Wavelength	0.71073 Å	
Crystal size	0.176 mm x 0.179 mm x 0.217 mm	
Crystal habit	clear colorless fragment	
Crystal system	monoclinic	
Space group	$P\ 1\ 2_1/c\ 1$	
Unit cell dimensions	a = 34.475(3) Å	α = 90°
	b = 10.6878(9) Å	β = 107.847(3)°
	c = 22.1910(19) Å	γ = 90°
Volume	7783.1(12) $Å^3$	
Z	4	
Density (calculated)	1.103 g/cm^3	
Absorption coefficient	0.123 mm^{-1}	
F(000)	2832	

Table S10: Data collection and structure refinement for **7**.

Diffractometer	Bruker D8 Venture, CMOS detector (Bruker Photon-100)	
Radiation source	IMS microsource, Mo	
Theta range for data collection	2.20 to 25.03°	
Index ranges	-41<=h<=41, -12<=k<=12, -26<=l<=26	
Reflections collected	152111	
Independent reflections	13754 [R(int) = 0.0652]	
Coverage of independent reflections	99.9%	
Absorption correction	multi-scan	
Min. and max. transmission	0.7188 and 0.7452	
Refinement method	Full-matrix least-squares on F^2	
Refinement program	SHELXL-2014/7 (Sheldrick, 2014)	
Function minimized	$\Sigma\ w(F_o^2 - F_c^2)^2$	
Data / restraints / parameters	13754 / 54 / 905	
Goodness-of-fit on F^2	1.081	
Δ/σ_{max}	0.001	
Final R indices	10907 data; I>2σ(I)	R1 = 0.0491, wR2 = 0.1006
	all data	R1 = 0.0704, wR2 = 0.1084
Weighting scheme	$w=1/[\sigma^2(F_o^2)+(0.0377P)^2+6.6255P]$ where $P=(F_o^2+2F_c^2)/3$	
Largest diff. peak and hole	0.378 and -0.326 $eÅ^{-3}$	
R.M.S. deviation from mean	0.049 $eÅ^{-3}$	

3. Computational Calculations

A) General

All calculations were performed at the B3LYP[S13-S15]/6-311+G(d) level of theory using Gaussian 09[S16]. The geometry of compounds **2b**, **6** and **7** were optimized starting from the solid state structures. The nature of stationary points found was assessed by frequency calculations, excluding **6**, where due to the size of the system, frequency calculations where only performed on the reduced system (Dipp groups replaced by 2,6-dimethyl-phenyl groups). Natural bond orbital (NBO)[S17] analyses were performed using the NBO 3.1 program implemented in Gaussian.

B) Theoretical Investigations

Influences on Si=O bonds and Related Structures

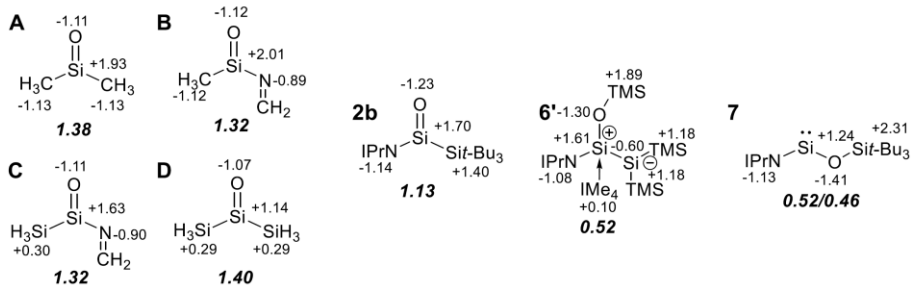


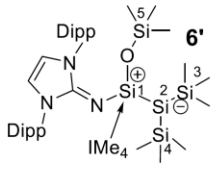
Figure S55: NPA charges and WBIs (bold & italic) of the corresponding Si-O bond of **2b**, **6**, **7** and comparable smaller silanones **A**-**D**.

By comparing smaller silanones **A**, **B**, **C** and **D**, the influence of silyl and imino groups on the Si=O moiety were investigated. As expected implementation of a π-donating imino function increases the polarization of the Si=O bond (see NPA charges O/Si of **A**: -1.11/+1.93 and **B**: -1.12/+2.01). However, addition of silyl moieties effectively reduces the positive charge at the silicon center (**B** (+2.01) and **C** (+1.63) or **A** (+1.93) and **D** (+1.14)). Most likely this is a result of inductive σ-donation of the silyl group to the electron deficient silicon center. Further, hyperconjugation of Si-C σ-orbitals with the π*-orbital of the Si=O moiety may also have a similar effect.

For compound **6** the obtained crystallographic and theoretical data point to resonance form **6'** with a zwitterionic Si1-Si2 bond (WBI 1.04) and a dative Si-NHC bond (WBI 0.60) as most fitting representation (Table S11). Still, we would like to note, that several more, but less likely, canonical forms (e.g. delocalization of the positive charge inside the NHI or NHC moiety) are generally imaginable.

Table S11: Selected WBI and NPA charges of **6**.

Bond	WBI	NPA charges
Si1Si2	1.04	1.61/-0.60
Si2Si3	0.99	-0.60/1.18
Si2Si4	0.98	-0.60/1.18
Si1O	0.52	1.61/-1.30
$Si1C^{IMe4}$	0.60	1.61/0.10
Si1N	0.73	1.61/-1.08
NC^{Imin}	1.60	-1.08/0.67



Calculated IR Stretching Frequencies of 2b, 6 and 7

Table S12: Experimental and calculated IR frequencies B3LYP/6-311+G(2d,2p)).

Compound	Mode	Exp. ν [cm^{-1}]	Calc. ν [cm^{-1}]
2b	stretch. Si=O	1144	1155
	stretch. C=N	1649	1647
6	asym. stretch. Si-O-Si	978	967
	stretch. C=N	1690	1751
7	asym. stretch. Si-O-Si	980	992
	stretch. C=N	1624	1684

asym. stretch.: asymmetric stretching

Calculated NMR Values

NMR chemical shifts were calculated at the SMD-B3LYP/6-311+G(2d,2p) level of theory based on the optimized geometries and referenced to tetramethylsilane. In the case of **5** and **6** the NMR shifts on this level where not satisfying (only the *Si*TMS_2 moiety showed a huge variance compared to experiment, indicating an incorrect representation of this moiety), inclusion of Grimme's dispersion[S18] improved the results in these cases, whereas only negligible effects occurred for **2b** and **7**.

Table S13: Experimental and calculated NMR chemical shifts(δ(TMS) = 0; SMD-B3LYP/6-311+G(2d,2p)).

Compound	Si	Exp. δ(^{29}Si) [ppm]	Calc. δ(^{29}Si) [ppm]	Δ [ppm]
2b	*central Si*	28.8	33.3[a]	-4.5
	Sit-Bu_3	13.7	18.6[a]	-4.9
5	O*TMS*	4.3	2.0[b,c]	2.3
	Si*TMS*$_2$	-14.6	-19.8[b,c]	5.2
	Si*TMS*$_2$	-14.8	-20.1[b,c]	5.3
	*Si*OTMS	-35.7	-37.6[b,c]	1.9
	SiTMS_2	-39.8	-41.4[b,c]	1.6

6	O*TMS*	6.1	11.7 [a,c]	-5.6
	Si*TMS*$_2$	-7.1	-3.4 [a,c]	-3.7
	*Si*OTMS	-35.2	-32.8 [a,c]	-2.4
	*Si*TMS$_2$	-174.6	-170.5 [a,c]	-4.1
7	*central Si*	58.9	54.4 [a]	4.5
	Sit-Bu$_3$	4.4	5.5 [a]	-1.1
INT	O*TMS*	4.3	17.1 [b,c]	-12.8
	Si*TMS*$_2$	-7.2	-3.0 [b,c]	-4.2
	*Si*OTMS	-8.0	59.5 [b,c]	-67.5
	*Si*TMS$_2$	-196.6	-198.2 [b,c]	1.6

[a] solvent benzene, [b] solvent tetrahydrofuran, [c] calculated including Grimme's dispersion[S18]

Calculated UV-VIS Values

Table S14: Excerpt of the TD-DFT calculation of **2b**.

Wavelength [nm]	MO contributions	f	Contributions
285.07	HOMO→LUMO	0.0019	92.97%
	HOMO→LUMO+4		3.83%
283.97	HOMO-1→LUMO+4	0.0035	6.10%
	HOMO→LUMO		5.23%
	HOMO→LUMO+1		30.30%
	HOMO→LUMO+4		53.32%
273.99	HOMO→LUMO+1	0.0046	45.36%
	HOMO→LUMO+2		7.75%
	HOMO→LUMO+3		17.04%
	HOMO→LUMO+4		25.10%
272.50	HOMO→LUMO+1	0.0030	21.56%
	HOMO→LUMO+2		45.32%
	HOMO→LUMO+3		28.56%
	HOMO→LUMO+4		3.05%
269.98	HOMO→LUMO+2	0.0004	44.09%
	HOMO→LUMO+3		52.74%
273.99	HOMO-1→LUMO+1	0.0046	15.04%
	HOMO-1→LUMO+4		70.11%
	HOMO→LUMO+4		10.86%

Table S15: Excerpt of the TD-DFT calculation of **7**

Wavelength [nm]	MO contributions	f	Contributions
340.57	HOMO→LUMO	0.0262	94.98%
	HOMO→LUMO+3		2.16%
335.05	HOMO→LUMO+1	0.0001	98.87%
320.66	HOMO→LUMO+2	0.0007	6.52%
	HOMO→LUMO+3		81.48%
	HOMO→LUMO+4		9.88%
319.73	HOMO→LUMO+2	0.0006	92.63%
	HOMO→LUMO+3		4.90%
318.47	HOMO→LUMO	0.0010	2.14%
	HOMO→LUMO+3		10.14%
	HOMO→LUMO+4		85.79%
291.46	HOMO→LUMO+5	0.0026	93.82%
	HOMO→LUMO+6		2.69%

Energy Difference between 2b and 7

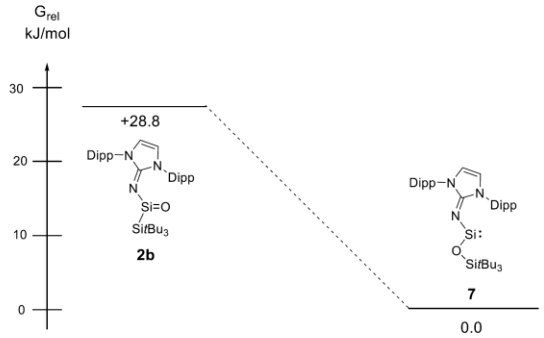


Figure S56: Energy difference between **2b** and **7**.

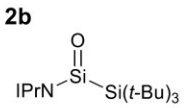
Orbitals of Calculated Species

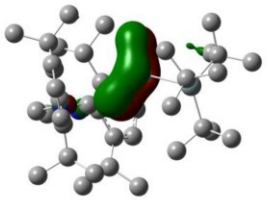
Silanone 2b and Comparable Smaller Silanones

To illustrate the electronic influences of NHI and silyl ligands on the Si=O orbitals, the energy and shape of π and π* orbitals of silanone **2b** and analogue orbitals of smaller silanones **A**, **B**, **C** and **D** were compared. In general, both orbitals of **2b** look similar to structure **C**, but are significantly higher in energy than those of Me_2Si=O **A**. Furthermore, the π/π*-energy splitting is increased (ΔE in **2b** 7.37 eV vs. **A** 6.92 eV), illustrating its total stabilization, which can mainly be attributed to the NHI ligand by general decreasing the energy of the π-orbital and increasing the energy of the π*-orbital (see orbitals of **A** and **B**

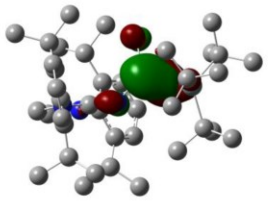
for comparison) by mixing with the corresponding orbital of the imino group. By comparing the orbitals of structure **A** and **D** as well as **B** and **C**, it becomes evident that silyl groups not only decrease π/π*-orbitals in energy, but also lower the energy difference between these Si=O orbitals. On the first sight this observation may be considered as counteracting stabilization effect. However, we believe that hyperconjugation of the Si-C σ-orbitals of the silyl group with the π*-orbital of the Si=O moiety (see LUMO of **D**) is far more relevant to preserve the Si=O double bond nature and to effectively reduce the positive charge at the silicon center (already seen at the WBI and NPA charges of **A** and **D**).

Table S16: Representation of the most important orbitals of **2b**.

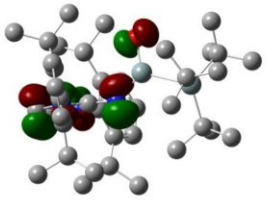




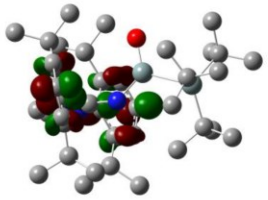
π (Si=O)
HOMO-10 (-7.78 eV)



π* (Si=O)
LUMO+4 (-0.41 eV)

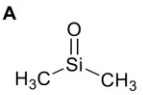
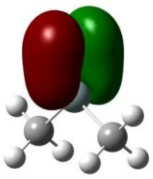
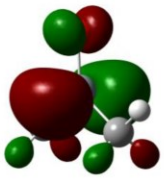
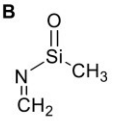
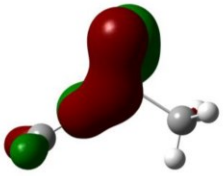
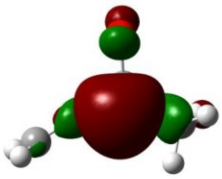
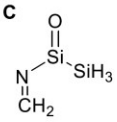
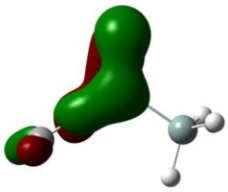
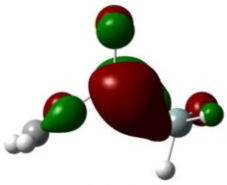
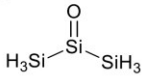
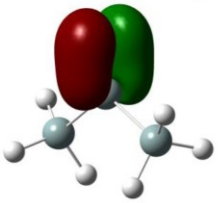
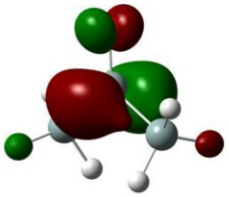


HOMO (-5.82 eV)



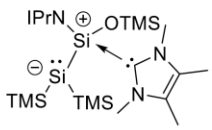
LUMO (-0.73 eV)

Table S17: Representation of π and π* orbitals of **A**, **B**, **C** and **D**.

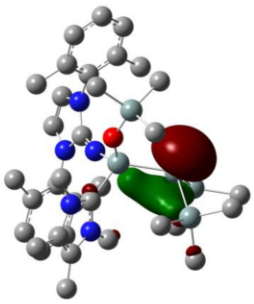
A 			**π (Si=O)** **HOMO-1 (-8.18 eV)** **π* (Si=O)** **LUMO (-1.26 eV)**
B 			**π (Si=O)** **HOMO-2 (-8.44 eV)** **π* (Si=O)** **LUMO+1 (-1.00 eV)**
C 			**π (Si=O)** **HOMO-2 (-8.61 eV)** **π* (Si=O)** **LUMO+1 (-1.53 eV)**
D 			**π (Si=O)** **HOMO-1 (-8.65 eV)** **π* (Si=O)** **LUMO (-2.76 eV)**

IMe$_4$ Zwitterionic Disilene 6

Table S18: Representation of the most important orbitals of **6**.

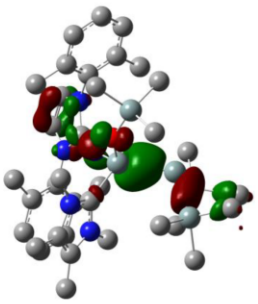


6'



mainly lone pair of Si(2)

HOMO (-3.54 eV)



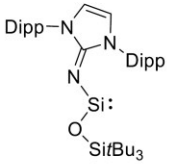
σ-bond (Si1Si2)

HOMO-3 (-6.11 eV)

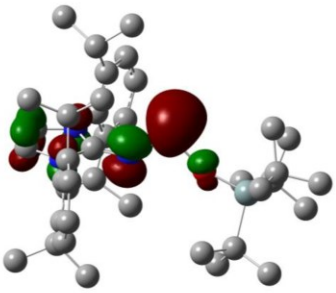
***N,O*-Silylene 7**

The HOMO of *N,O*-silylene **7** exhibits mainly lone pair character (Si_n), the LUMO resembles the empty Si_{3p} orbital with a HOMO-LUMO gap of 4.33 eV. Both orbitals show only minor contributions from donating N or O atoms. For orbitals lower in energy some interactions of silicon with nitrogen, and even lower, minor interactions with oxygen can be found. HOMO-6 represents the lone pair on nitrogen atom N_n with obvious mixing with the empty Si_{3p} orbital, illustrating partial Si-N double bond character (similarly to HOMO-10 of silanone **2b**). For oxygen, the related lone pair orbital O_n (seen in HOMO-2, HOMO-15 and even HOMO-21) shows almost no extent towards the silicon center. Similar low-lying orbital interactions (Si-S) have been found for related dithiolato silylene by Power *et al.*.[S19]

Table S19: Representation of the most important orbitals of **7**.

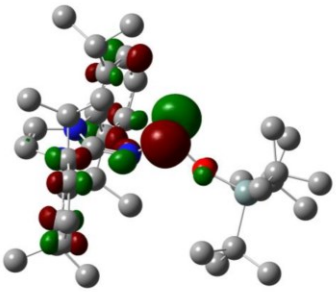


7



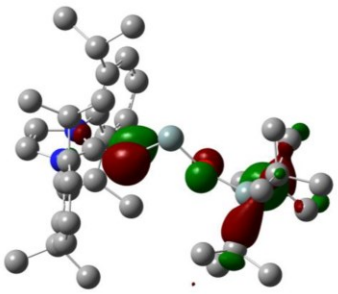
lone pair Si_n

HOMO (-5.04 eV)

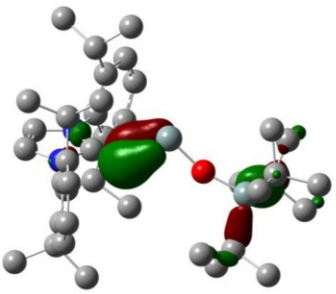


empty Si_{3p}

LUMO (-0.71 eV)

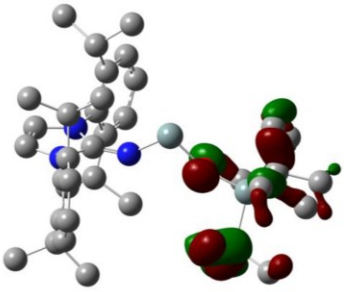


HOMO-2 (-6.56 eV)

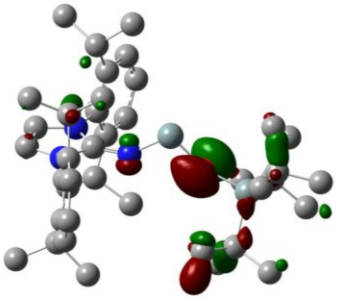


Mixing of N_n and Si_{3p} orbital

HOMO-6 (-6.96 eV)



HOMO-15 (-8.82 eV)



HOMO-21 (-9.09 eV)

C) Calculated Structures

Table S20: Cartesian coordinated (x,y,z) for the optimized structure of **INT**.

Si	-0.084421	-0.990804	0.065906
Si	1.274059	-2.268833	1.364051
Si	2.346298	-0.452781	2.483878
Si	2.852935	-2.657372	-0.398189
Si	-2.168470	-3.078355	-0.992106
O	-1.166992	-1.718455	-0.953212
N	-0.263453	0.641853	0.024790
N	-0.139748	2.886932	-0.742623
N	-2.051480	2.248578	0.121667
C	-0.780905	1.793941	-0.186205
C	-1.002909	3.982143	-0.776884
H	-0.688692	4.930580	-1.178073
C	-2.179025	3.591257	-0.245045
H	-3.100265	4.127509	-0.092472
C	1.208927	2.871299	-1.227811
C	1.480348	2.234532	-2.446581
C	2.801123	2.238573	-2.900102
H	3.043414	1.739947	-3.832888
C	3.805031	2.862379	-2.165892
H	4.826627	2.851979	-2.531625
C	3.508859	3.480968	-0.955336
H	4.301544	3.938381	-0.372316
C	2.204317	3.486451	-0.457133
C	0.389096	1.550400	-3.228427
H	0.063743	0.634787	-2.727066
C	1.884310	4.072300	0.894195
H	1.447848	3.313701	1.549876
C	-3.138633	1.413362	0.542799
C	-3.447469	1.335350	1.906624
C	-4.541212	0.549429	2.279913
H	-4.802532	0.466481	3.330022
C	-5.296142	-0.120321	1.321475
H	-6.145130	-0.722876	1.627960
C	-4.964000	-0.028502	-0.027230
H	-5.556664	-0.557825	-0.766246
C	-3.870362	0.734727	-0.442360
C	-2.622306	2.072109	2.929501
H	-1.598706	1.692532	2.958384
C	-3.463947	0.809586	-1.891178
H	-3.226914	1.831632	-2.195826
C	3.435590	-1.208523	3.846724
H	2.842505	-1.809854	4.542563
H	3.941353	-0.427627	4.426467
H	4.206306	-1.862690	3.427937
C	3.453141	0.709893	1.468831
H	4.318310	0.196191	1.042263
H	3.835004	1.523145	2.098274
H	2.900571	1.160789	0.643179
C	1.066601	0.666847	3.336057
H	0.493999	1.214844	2.583817
H	1.555033	1.398043	3.990616
H	0.359908	0.093458	3.943634
C	3.125448	-1.278461	-1.682519
H	2.247870	-1.166487	-2.329016
H	3.977513	-1.516426	-2.331688
H	3.315486	-0.306469	-1.224535
C	4.523665	-2.985296	0.450595
H	4.448977	-3.809985	1.165834
H	4.897983	-2.113377	0.992831
H	5.278553	-3.259923	-0.295415
C	2.460658	-4.214723	-1.409873
H	2.247421	-5.077876	-0.773247
H	3.317419	-4.471147	-2.044349
H	1.600352	-4.068479	-2.066946
C	-3.012333	-3.213442	0.677693
H	-3.550458	-2.296435	0.930900
H	-2.273465	-3.396930	1.463764
H	-3.731045	-4.039505	0.699073

C	-1.162753	-4.619466	-1.338523
H	-1.803986	-5.507320	-1.308780
H	-0.374968	-4.754809	-0.593501
H	-0.689858	-4.591169	-2.323952
C	-3.405903	-2.800585	-2.376771
H	-4.005720	-3.701488	-2.543612
H	-2.901995	-2.563333	-3.318657
H	-4.093895	-1.983452	-2.152158
H	-4.255404	0.437730	-2.543150
H	-2.572464	0.199122	-2.061582
H	0.732999	1.281318	-4.228250
H	-3.047058	1.963795	3.928694
H	-0.494089	2.186417	-3.332283
H	1.163838	4.892546	0.830438
H	2.785017	4.453130	1.377379
H	-2.558499	3.140184	2.703796

Table S21: Cartesian coordinated (x,y,z) for the optimized structure of **2b**.

Si	0.952533	0.098959	0.874213
Si	3.200795	0.116559	0.065987
O	0.790816	0.138393	2.419141
N	-0.313454	0.012973	-0.206669
N	-2.503725	1.010456	-0.213832
N	-2.401561	-1.182610	-0.187088
C	-1.608304	-0.046705	-0.173750
C	-3.811539	0.524225	-0.251152
H	-4.658236	1.188338	-0.279000
C	-3.748748	-0.821903	-0.236314
H	-4.529184	-1.563221	-0.254807
C	-2.141899	2.402534	-0.124265
C	-2.152438	3.023883	1.138595
C	-1.814815	4.381243	1.189912
H	-1.810966	4.893610	2.145682
C	-1.484361	5.084145	0.039672
H	-1.221985	6.135659	0.104526
C	-1.489008	4.447037	-1.197166
H	-1.231787	5.013831	-2.084550
C	-1.818201	3.094381	-1.308820
C	-2.565306	2.300859	2.417425
H	-2.664943	1.237268	2.190156
C	-1.516689	2.417214	3.536813
H	-1.876010	1.901235	4.432537
H	-1.330059	3.458386	3.817164
H	-0.574698	1.947274	3.248574
C	-3.943992	2.799921	2.893718
H	-4.270225	2.236113	3.772581
H	-4.709046	2.688117	2.119790
H	-3.910848	3.857424	3.172629
C	-1.877939	2.416977	-2.674274
H	-1.722684	1.346566	-2.518976
C	-3.268982	2.599756	-3.313936
H	-3.319862	2.085215	-4.278447
H	-3.483449	3.658584	-3.488301
H	-4.064828	2.199564	-2.681461
C	-0.782587	2.891639	-3.640839
H	-0.788465	2.273208	-4.542877
H	0.210243	2.819578	-3.193269
H	-0.935112	3.925617	-3.963352
C	-1.912201	-2.534618	-0.101200
C	-1.581006	-3.208833	-1.292360
C	-1.123877	-4.524838	-1.185911
H	-0.861961	-5.076225	-2.082401
C	-1.001479	-5.142860	0.053474
H	-0.640672	-6.164980	0.114839
C	-1.345259	-4.459110	1.212607
H	-1.253686	-4.958309	2.170945
C	-1.812463	-3.141152	1.166018
C	-1.760300	-2.569163	-2.664437
H	-1.917774	-1.498530	-2.516975
C	-0.521346	-2.719917	-3.561301
H	-0.664984	-2.171411	-4.496841
H	-0.327239	-3.763095	-3.826291

H	0.371346	-2.323314	-3.074683
C	-3.014099	-3.126988	-3.365666
H	-3.914015	-2.977068	-2.763202
H	-3.169948	-2.632192	-4.329224
H	-2.918476	-4.200569	-3.554250
C	-2.251442	-2.447908	2.452486
H	-2.452016	-1.399606	2.221100
C	-3.567546	-3.063860	2.968715
H	-3.918375	-2.524561	3.853445
H	-3.433502	-4.112306	3.251748
H	-4.360146	-3.025015	2.215809
C	-1.169748	-2.461859	3.545563
H	-1.551660	-1.973119	4.446932
H	-0.281023	-1.910546	3.234311
H	-0.883589	-3.479916	3.826567
C	4.118689	1.248458	1.396235
C	3.308436	2.536321	1.682002
H	3.857797	3.152402	2.405860
H	2.339214	2.308224	2.130236
H	3.143251	3.154687	0.799713
C	4.246096	0.521262	2.754350
H	4.690531	1.208470	3.486376
H	4.898016	-0.353121	2.709709
H	3.271077	0.216988	3.140579
C	5.533595	1.660753	0.932631
H	6.023439	2.239162	1.726647
H	5.517968	2.296085	0.044181
H	6.177690	0.804504	0.718103
C	3.297078	0.859296	-1.754243
C	4.674205	0.621429	-2.412073
H	4.690973	1.081570	-3.408844
H	4.893047	-0.439529	-2.549355
H	5.497338	1.058441	-1.843052
C	2.215773	0.236567	-2.666361
H	2.246179	0.724742	-3.649665
H	1.209538	0.363014	-2.262364
H	2.371448	-0.827915	-2.837385
C	3.036427	2.380157	-1.733377
H	3.004982	2.759178	-2.763158
H	3.819315	2.935212	-1.215221
H	2.079472	2.633145	-1.267964
C	3.782392	-1.768690	0.147942
C	3.287861	-2.572870	-1.073695
H	3.545384	-3.631200	-0.937418
H	3.750932	-2.253055	-2.008816
H	2.202703	-2.522454	-1.195926
C	5.321759	-1.894627	0.198144
H	5.603743	-2.955728	0.196058
H	5.750000	-1.455188	1.100201
H	5.812194	-1.432419	-0.662045
C	3.196173	-2.470250	1.394732
H	3.585010	-3.495665	1.450074
H	2.106181	-2.547986	1.348785
H	3.443046	-1.974741	2.332102

Table S22: Cartesian coordinated (x,y,z) for the optimized structure of **5**.

Si	0.487020	-0.382597	-0.994271
Si	2.243979	-0.869050	0.495466
Si	2.126946	-0.264207	2.766412
Si	4.347904	-0.401921	-0.451662
Si	0.922848	2.295854	-2.516061
O	0.788461	0.653571	-2.259057
N	-1.008265	0.046967	-0.333072
N	-2.879017	0.667591	0.983225
N	-2.765781	-1.458687	0.415542
C	0.886913	-2.197802	-1.435233
H	0.073288	-2.870592	-1.711539
H	1.598119	-2.188391	-2.269097
C	1.617779	-2.613724	-0.112049
H	0.899227	-3.029162	0.600911
H	2.387354	-3.376340	-0.266577
C	-2.079312	-0.243852	0.282344

C	-4.003360	0.029375	1.506776
H	-4.740202	0.566693	2.079802
C	-3.936035	-1.271445	1.160996
H	-4.604390	-2.089826	1.368929
C	-2.632898	2.077270	0.992774
C	-2.969580	2.821272	-0.147625
C	-2.701681	4.191385	-0.140922
H	-2.943771	4.784994	-1.016950
C	-2.123733	4.796835	0.971508
H	-1.912936	5.861410	0.959522
C	-1.810590	4.041083	2.096909
H	-1.357059	4.517492	2.960418
C	-2.061153	2.666263	2.127539
C	-3.593081	2.146599	-1.340185
H	-2.895634	1.435465	-1.787407
C	-1.733143	1.837763	3.341284
H	-1.150126	0.957632	3.073264
C	-2.459541	-2.655254	-0.307658
C	-1.942995	-3.756701	0.389669
C	-1.670878	-4.922809	-0.329479
H	-1.258271	-5.782396	0.189256
C	-1.908926	-4.986900	-1.698725
H	-1.685156	-5.897388	-2.245257
C	-2.426257	-3.883440	-2.370234
H	-2.606795	-3.936454	-3.439340
C	-2.711771	-2.698311	-1.688447
C	-1.686713	-3.683189	1.872259
H	-1.143590	-2.776825	2.138842
C	-3.243900	-1.496586	-2.422968
H	-4.046931	-1.004908	-1.869072
C	3.696542	-0.681445	3.747055
H	3.925730	-1.750775	3.712575
H	3.587904	-0.399992	4.800639
H	4.567380	-0.147787	3.354332
C	1.872840	1.615245	2.826730
H	2.750601	2.143459	2.441171
H	1.706981	1.960119	3.853434
H	1.016479	1.927510	2.223873
C	0.660924	-1.127347	3.603643
H	-0.258876	-0.991337	3.029961
H	0.486575	-0.733564	4.610848
H	0.835522	-2.203471	3.694836
C	4.799391	1.417951	-0.155283
H	4.024855	2.096320	-0.522400
H	5.733879	1.678271	-0.664484
H	4.939018	1.628151	0.909831
C	5.708425	-1.480005	0.315774
H	5.498034	-2.545385	0.179593
H	5.811718	-1.301636	1.390060
H	6.679530	-1.275221	-0.149288
C	4.307379	-0.743996	-2.315037
H	4.179323	-1.812490	-2.514651
H	5.243829	-0.432099	-2.791114
H	3.486473	-0.217834	-2.807339
C	0.912243	3.195283	-0.864719
H	1.733918	2.866802	-0.221453
H	-0.019950	3.010315	-0.325248
H	1.010543	4.278170	-0.994824
C	-0.516232	2.866540	-3.582486
H	-0.404311	3.917472	-3.870486
H	-1.467122	2.769378	-3.054110
H	-0.584123	2.277746	-4.502556
C	2.534522	2.600800	-3.435018
H	2.655323	3.661219	-3.681406
H	2.566072	2.039297	-4.374016
H	3.403865	2.299249	-2.845064
H	-4.486214	1.582300	-1.057283
H	-3.627225	-1.775356	-3.406055
H	-2.454284	-0.753192	-2.566061
H	-1.104487	-4.541077	2.213025
H	-2.620704	-3.667719	2.443015
H	-1.159481	2.413316	4.069138
H	-2.640010	1.477256	3.837146

H	-3.878970	2.873273	-2.102269

Table S23: Cartesian coordinated (x,y,z) for the optimized structure of **6**

Si	0.086278	-0.710726	-0.233549
Si	0.857753	-1.816848	1.685182
Si	1.292703	-0.415120	3.544640
Si	2.971021	-2.790628	1.156254
Si	-1.513532	-3.342955	-1.142879
O	-0.753305	-1.848222	-1.151440
N	-0.775799	0.743805	-0.116799
N	-1.361508	3.039605	0.220431
N	-3.022876	1.585108	0.290070
N	1.575395	-0.501708	-2.915418
N	2.533302	0.576306	-1.318040
C	-1.625136	1.653600	0.107563
C	-2.541006	3.748040	0.458870
H	-2.543449	4.819465	0.569492
C	-3.550904	2.863072	0.499510
H	-4.606690	3.011967	0.653059
C	-0.104546	3.687885	0.007272
C	0.380273	3.828724	-1.305303
C	1.571306	4.533853	-1.498003
H	1.953978	4.660455	-2.506520
C	2.254569	5.092307	-0.421036
H	3.173646	5.645557	-0.587762
C	1.755438	4.947719	0.869055
H	2.290689	5.381774	1.707854
C	0.568628	4.246223	1.107614
C	-0.373548	3.258857	-2.478852
H	-0.400191	2.167184	-2.436331
C	0.029179	4.116965	2.509779
H	-0.317549	3.104787	2.720616
C	-3.894705	0.454623	0.134331
C	-4.431964	-0.150469	1.281796
C	-5.409943	-1.134786	1.108854
H	-5.836344	-1.615575	1.983656
C	-5.834737	-1.506290	-0.161987
H	-6.597091	-2.270254	-0.277207
C	-5.277429	-0.905170	-1.285994
H	-5.612355	-1.196380	-2.276816
C	-4.301293	0.086492	-1.158856
C	-3.973284	0.239908	2.662916
H	-2.909346	0.034837	2.797908
C	-3.718365	0.754839	-2.377511
H	-3.852209	1.840064	-2.345712
C	1.438406	-0.174066	-1.601841
C	2.751649	0.028429	-3.442805
C	3.353663	0.715786	-2.431954
C	0.628742	-1.256738	-3.731625
H	-0.254034	-1.459644	-3.138504
H	1.074931	-2.201626	-4.048767
H	0.361509	-0.674854	-4.615714
C	3.169134	-0.191777	-4.857443
H	3.284268	-1.255450	-5.086880
H	4.128933	0.287858	-5.050213
H	2.448150	0.219794	-5.571013
C	4.628744	1.489005	-2.407627
H	5.067731	1.528668	-3.404811
H	5.370860	1.037216	-1.742167
H	4.470374	2.518360	-2.073204
C	2.811797	1.189953	-0.022840
H	2.380669	2.188010	0.026777
H	3.888400	1.249057	0.124892
H	2.382000	0.564503	0.757165
C	1.975556	-1.546926	4.920829
H	1.305372	-2.391313	5.107520
H	2.082360	-0.993785	5.861667
H	2.958039	-1.961509	4.675408
C	2.497583	1.073769	3.485044
H	3.498529	0.780305	3.155520
H	2.600369	1.510308	4.486473

H	2.148550	1.869836	2.820653
C	-0.334970	0.297753	4.238192
H	-0.835295	0.959110	3.524501
H	-0.154286	0.875697	5.152565
H	-1.036073	-0.504501	4.486612
C	4.552528	-1.866518	1.714328
H	4.695410	-0.925764	1.173879
H	5.439703	-2.485917	1.532212
H	4.537690	-1.628023	2.781274
C	3.060508	-4.481290	2.032696
H	2.276007	-5.155724	1.675975
H	2.922355	-4.378241	3.113599
H	4.027017	-4.972453	1.866217
C	3.268306	-3.146066	-0.698241
H	2.447889	-3.705061	-1.153904
H	4.179326	-3.744190	-0.821911
H	3.403794	-2.224548	-1.272819
C	-2.561612	-3.613909	0.386964
H	-3.313508	-2.832566	0.514262
H	-1.935482	-3.625641	1.282273
H	-3.088248	-4.573553	0.324602
C	-0.256178	-4.738034	-1.291056
H	-0.772181	-5.700139	-1.387959
H	0.383281	-4.798563	-0.407407
H	0.389993	-4.629838	-2.167907
C	-2.594635	-3.375714	-2.692748
H	-3.168752	-4.307212	-2.746506
H	-2.002217	-3.313801	-3.611942
H	-3.311660	-2.550739	-2.701501
H	-4.519629	-0.319028	3.424520
H	-4.119451	1.305599	2.860128
H	-2.644614	0.564773	-2.452939
H	-4.193793	0.385366	-3.288042
H	0.794112	4.373007	3.244448
H	-0.822493	4.784804	2.675909
H	-1.411895	3.601544	-2.490702
H	0.090119	3.557532	-3.421063

Table S24: Cartesian coordinated (x,y,z) for the optimized structure of **7**.

Si	0.569249	-0.060922	-1.326705
Si	3.658416	-0.017648	-0.193874
O	2.014103	-0.071847	-0.482027
N	-0.627171	-0.019280	-0.128190
N	-2.752876	-1.095913	0.214470
N	-2.731785	1.107181	0.186488
C	-1.896951	-0.004575	0.052983
C	-4.055726	-0.652522	0.454880
H	-4.864905	-1.344555	0.615600
C	-4.042954	0.694296	0.436847
H	-4.839839	1.404970	0.576050
C	-2.349662	-2.474814	0.176248
C	-1.893300	-3.080636	1.362633
C	-1.521098	-4.426602	1.304179
H	-1.160015	-4.921323	2.199817
C	-1.607029	-5.144462	0.117448
H	-1.313179	-6.189342	0.093777
C	-2.068869	-4.527508	-1.038891
H	-2.133688	-5.101086	-1.957440
C	-2.446254	-3.181193	-1.038199
C	-1.797196	-2.324423	2.682365
H	-2.176501	-1.313777	2.518297
C	-0.337560	-2.190790	3.148751
H	0.269631	-1.692232	2.391362
H	0.110941	-3.167500	3.353596
H	-0.283383	-1.603664	4.070768
C	-2.676112	-2.964740	3.771821
H	-2.644529	-2.365597	4.686864
H	-2.337037	-3.972322	4.029402
H	-3.720151	-3.038267	3.454773
C	-2.968727	-2.539286	-2.318629
H	-3.087384	-1.469620	-2.131945
C	-1.985472	-2.687746	-3.492068

H	-2.367691	-2.164042	-4.373484
H	-1.839861	-3.734488	-3.774096
H	-1.008710	-2.262915	-3.249922
C	-4.356969	-3.094943	-2.689574
H	-5.077784	-2.954482	-1.879402
H	-4.313111	-4.165834	-2.909980
H	-4.748486	-2.589914	-3.577834
C	-2.303947	2.477435	0.110674
C	-2.304772	3.125491	-1.139841
C	-1.914573	4.467565	-1.176138
H	-1.904984	4.997397	-2.122430
C	-1.538972	5.137999	-0.018396
H	-1.237421	6.179715	-0.069462
C	-1.549272	4.478398	1.204582
H	-1.256171	5.016017	2.100099
C	-1.930298	3.136726	1.297798
C	-2.760484	2.429989	-2.417943
H	-2.829221	1.360128	-2.208586
C	-4.166610	2.909511	-2.827675
H	-4.896991	2.747633	-2.030415
H	-4.513474	2.370978	-3.714808
H	-4.168021	3.977687	-3.065233
C	-1.765941	2.599192	-3.578079
H	-1.674420	3.642413	-3.893556
H	-2.103187	2.027286	-4.447585
H	-0.772017	2.236015	-3.308237
C	-1.969251	2.449825	2.658388
H	-2.138163	1.384086	2.491142
C	-0.641957	2.579564	3.423063
H	-0.420831	3.617201	3.689271
H	0.194990	2.197971	2.835868
H	-0.686991	2.009537	4.355936
C	-3.144056	2.974280	3.506039
H	-3.033487	4.040882	3.723815
H	-3.196017	2.443904	4.461773
H	-4.101735	2.839473	2.996137
C	4.524188	0.710879	-1.794988
C	4.291957	2.233036	-1.925476
H	3.230299	2.494285	-1.925221
H	4.708550	2.584247	-2.878547
H	4.780891	2.806283	-1.136008
C	3.928914	0.077337	-3.074505
H	4.076000	-1.000710	-3.131834
H	4.414158	0.515975	-3.956562
H	2.857360	0.268611	-3.167278
C	6.049708	0.468107	-1.797992
H	6.550302	0.902604	-0.929048
H	6.497468	0.928451	-2.688439
H	6.305904	-0.592910	-1.828841
C	4.186878	-1.867677	0.167592
C	4.270418	-2.702958	-1.129503
H	4.465639	-3.752289	-0.873043
H	5.076606	-2.384381	-1.792392
H	3.336198	-2.681282	-1.697572
C	5.552128	-1.967210	0.883254
H	5.546877	-1.490047	1.865629
H	6.366411	-1.522160	0.305438
H	5.812784	-3.021765	1.043383
C	3.119787	-2.558280	1.048905
H	3.010298	-2.101207	2.031811
H	3.404233	-3.606462	1.210891
H	2.137418	-2.555594	0.572757
C	3.849482	1.155924	1.359912
C	2.943815	2.396640	1.180909
H	1.902902	2.113783	1.012234
H	3.250061	3.037795	0.354759
H	2.977785	3.009261	2.091515
C	5.298673	1.630421	1.598322
H	5.342753	2.255905	2.499715
H	5.685799	2.235799	0.775690
H	5.993613	0.800598	1.752720
C	3.363372	0.453357	2.647077
H	3.377183	1.168290	3.480247

H	3.998572	-0.384681	2.940021
H	2.338592	0.086461	2.552354

Table S25: Cartesian coordinated (x,y,z) for the optimized structure of **A**.

C	1.555676	-0.860994	-0.000244
Si	-0.000008	0.176612	0.000224
O	-0.000102	1.711546	-0.000060
H	1.603002	-1.501429	0.886858
H	1.587871	-1.526051	-0.869628
H	2.441798	-0.225061	-0.015973
C	-1.555565	-0.861185	0.000294
H	-2.441770	-0.225360	0.015680
H	-1.602558	-1.501749	-0.886735
H	-1.587925	-1.526126	0.869759

Table S26: Cartesian coordinated (x,y,z) for the optimized structure of **B**.

Si	-0.029949	0.021074	-0.182146
O	0.155622	1.508267	0.139147
N	1.234258	-1.031106	-0.553655
C	2.122670	-1.533476	-1.280612
H	2.216039	-1.316564	-2.353530
H	2.861648	-2.230743	-0.867536
C	-1.609286	-0.953318	-0.044707
H	-1.606945	-1.836226	-0.687240
H	-1.753132	-1.290187	0.986170
H	-2.461251	-0.321388	-0.302827

Table S27: Cartesian coordinated (x,y,z) for the optimized structure of **C**.

Si	0.008395	0.021673	-0.107122
O	0.173786	1.466324	0.388174
N	1.255903	-0.958284	-0.659438
Si	-1.993293	-1.205993	-0.038167
H	-1.814195	-2.517085	-0.711124
H	-2.373633	-1.417512	1.379627
H	-3.048688	-0.425728	-0.727415
C	2.143621	-1.511541	-1.347026
H	2.269016	-1.315517	-2.420120
H	2.844360	-2.228951	-0.902551

Table S28: Cartesian coordinated (x,y,z) for the optimized structure of **D.**

Si	-0.000758	0.115697	-0.018421
O	0.000000	1.658096	-0.049417
Si	-2.047135	-1.094679	0.094921
H	-1.930788	-2.337928	-0.712299
H	-2.291555	-1.472906	1.511728
H	-3.159314	-0.255816	-0.409784
Si	2.046507	-1.096834	-0.084908
H	1.912266	-2.340907	0.718178
H	2.324183	-1.472213	-1.496205
H	3.146587	-0.258449	0.446705

4. References

(S1) Wendel, D.; Porzelt, A.; Herz, F. A. D.; Sarkar, D.; Jandl, C.; Inoue, S.; Rieger, B., *J. Am. Chem. Soc.* **2017**, *139*, 8134-8137.

(S2) Lui, M. W.; Merten, C.; Ferguson, M. J.; McDonald, R.; Xu, Y.; Rivard, E., *Inorg. Chem.* **2015**, *54*, 2040-2049.

(S3) Kuhn, N.; Kratz, T., *Synthesis* **1993**, *1993*, 561-562.

(S4) Wiberg, N.; Amelunxen, K.; Lerner, H. W.; Schuster, H.; Nöth, H.; Krossing, I.; Schmidt-Amelunxen, M.; Seifert, T., *J. Organomet. Chem.* **1997**, *542*, 1-18.

(S5) Ishida, S.; Abe, T.; Hirakawa, F.; Kosai, T.; Sato, K.; Kira, M.; Iwamoto, T., *Chem. Eur. J.* **2015**, *21*, 15100-15103.

(S6) *APEX suite of crystallographic software,* APEX 3 version 2015.5-2; Bruker AXS Inc.: Madison, Wisconsin, USA, **2015**.

(S7) *SAINT*, Version 7.56a and SADABS Version 2008/1; Bruker AXS Inc.: Madison, Wisconsin, USA, **2008**.

(S8) Sheldrick, G. M., *SHELXL-2014*, University of Göttingen, Göttingen, Germany, **2014**.

(S9) Huebschle, C. B.; Sheldrick, G. M.; Dittrich, B., *J. Appl. Cryst.* **2011**, 44, 1281.

(S10) Sheldrick, G. M., *SHELXL-97,* University of Göttingen, Göttingen, Germany, **1998**.

(S11) Wilson, A. J. C. *International Tables for Crystallography*, Vol. C, Tables 6.1.1.4 (pp. 500-502), 4.2.6.8 (pp. 219-222), and 4.2.4.2 (pp. 193-199); Kluwer Academic Publishers: Dordrecht, The Netherlands, **1992**.

(S12) Macrae, C. F., Bruno, I. J., Chisholm, J. A., Edgington, P. R., McCabe, P., Pidcock, E., Rodriguez-Monge, L., Taylor, R., van de Streek, J. & Wood, P. A., *J. Appl. Cryst.* **2008**, *41*, 466–470.

(S13) Becke, A. D., *J. Chem. Phys*. **1993**, *98*, 5648-5652.

(S14) Vosko, S. H.; Wilk, L., Nusair, M., *Can. J. Phys*. **1980**, *58*, 1200-1211.

(S15) Lee, C.; Yang, W.; Parr, R. G., *Phys. Rev. B* **1988**, *37*, 785-789.

(S16) Frisch, M. J.; Trucks, G. W.; Schlegel, H. B.; Scuseria, G. E.; Robb, M. A.; Cheeseman, J. R;.Scalmani, G.; Barone, V.; Petersson, G. A.; Nakatusji, H.; Li, X.; Caricato, M.; Marenich, A.; Bloino, J.; Janesko, B. G.; Gomperts, R.; Mennucci, B.; Hratchian, H. P.; Ortiz, J. V.; Izmaylov, A. F.; Sonnenberg, J. L.; Williams-Young, D.; Ding, F.; Lipparini, F.; Egidi, F.; Goings, J.; Peng, B.; Petrone, A.; Henderson, T.; Ranashinghe, D.; Zakrzewski, V. G.; Gao, J.; Rega, N.; Zheng, G.; Liang, W.; Hada, M.; Ehara, M.; Toyota, K.; Fukuda, R.; Hasekawa, J.; Ishida, M.; Nakajima, T.; Honda, Y; Kitao, O.; Nakao, H.; Vreven, T.; Throssell, K.; Montgomery, Jr., J. A.; Peralta, J. E.; Ogliaro, F.; Bearpark, M.; Heyd, J. J.; Brothers, E.; Kudin, K. N.; Staroverov, V. N.; Keith, T.; Kobayashi, R.; Normand, J.; Raghavachari, K; Rendell, A.; Burant, J. C.; Iyengar, S. S.; Tomasi, J.; Cossi, M.; Millam, J. M.; Klene, M.; Adamo, C.; Cammi, R.; Ochterski, J. W.; Martin, R. L.; Morokuma, K.; Farkas, O.; Forseman, J. B.; Fox, D.J., *Gaussian 09, Revision E.01,* Gaussian, Inc., Wallingford CT, **2016**.

(S17) Reed, A. E.; Curtiss, L. A.; Weinhold, F., *Chem. Rev.* **1988**, *88*, 899-926.

(S18) Grimme, S.; Antony, J.; Ehrlich, S.; Krieg, H., *J. Chem. Phys* **2010**, *132*, 154104-154119.

(S19) Rekken, B. D.; Brown, T. M.; Fettinger, J. C.; Tuononen, H. M.; Power, P. P., *J. Am. Chem. Soc.* **2012**, *134*, 6504-6507.

13.6 Supporting Information Chapter 9

Supporting Information

Heavier Carbonyl Olefination: The Sila-Wittig Reaction

Dominik Reiter,[†] Philipp Frisch,[†] Tibor Szilvási,[‡] and Shigeyoshi Inoue[,†]

Table of Contents

1. Experimental Section S2
1.1 General Methods and Instrumentation S2
1.2 Syntheses of the Wittig ylides S3
1.3 Spectroscopic data of $Ph_3P{=}O$ S24
1.4 Reactivity of silanone **1** toward stabilized ylides S26
1.4.1 Synthesis of dioxaphosphasiline **3** S26
1.4.2 Synthesis of (IDippN)(^{t}Bu$_3$Si)Si(OH)$_2$ (**4**) S30
1.4.3 Synthesis of (IDippN)(^{t}Bu$_3$Si)Si(OH)(OMe) (**5**) S33
1.4.4 Synthesis of ylide-stabilized silanone **6** S34
1.4.5 Synthesis of silyl-substituted phosphorus ylide **7** S37
1.5 Reactivity of silanone **1** toward semi-stabilized ylides S41
1.5.1 Synthesis of silanoyl-substituted phosphorus ylide **8** S41
1.5.2 Synthesis of silacyclobutene **9** S44
1.6 Reactivity of silanone **1** toward non-stabilized ylides S47
1.6.1 Sila-Wittig reaction S47
1.6.1 Synthesis of silyl-substituted NHC **11** S78
2. X-ray Crystallographic Data S81
3. DFT Calculations S98
4. References S113

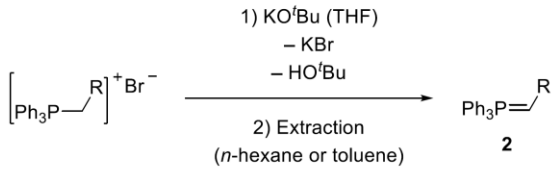
1. Experimental Section

1.1 General Methods and Instrumentation

All manipulations were carried out under exclusion of H_2O and O_2 under an atmosphere of argon 4.6 (≥99.996%; *Westfalen AG*) using standard *Schlenk* techniques or in a *LABstar* glovebox from *MBraun Inertgas-Systeme GmbH* with H_2O and O_2 levels below 0.5 ppm. The glassware used was heat dried under fine vacuum prior to use with *Triboflon III* grease (mixture of polytetrafluoroethylene (PTFE) and perfluoropolyether (PFPE)) from *Freudenberg & Co. KG* as sealant. All solvents were refluxed over sodium/benzophenone, freshly distilled under argon and deoxygenated before use. Deuterated benzene was obtained from *Sigma-Aldrich Chemie GmbH*, dried over Na/K alloy, flask-to-flask condensed, deoxygenated by three freeze-pump-thaw cycles and stored over 3 Å molecular sieves in the glovebox. All NMR samples were prepared under argon in *J. Young* PTFE valve NMR tubes. The NMR spectra were recorded on *Bruker AV400US* (^{1}H: 400.13 MHz), *Avance Neo 400* (^{1}H: 400.23 MHz, ^{13}C: 100.65 MHz, ^{31}P: 162.01 MHz), *AV500* (^{1}H: 500.13 MHz) or *AV500C* (^{1}H: 500.36 MHz, ^{13}C: 125.83 MHz, ^{29}Si: 99.41 MHz, ^{31}P: 202.57 MHz) spectrometers at ambient temperature (300 K). The ^{1}H, ^{13}C{^{1}H} and ^{29}Si{^{1}H} NMR spectroscopic chemical shifts δ are reported in ppm relative to tetramethylsilane. ^{1}H and ^{13}C{^{1}H} NMR spectra are calibrated against the residual proton and natural abundance carbon resonances of the deuterated solvent as internal standard (C_6D_6: δ(^{1}H) = 7.16 ppm and δ(^{13}C) = 128.1 ppm).[S1] The following abbreviations are used to describe signal multiplicities: s = singlet, d = doublet, t = triplet, sept = septet, m = multiplet, br = broad and combinations thereof (*e.g.* dd = doublet of doublets). Some NMR spectra include resonances for silicone grease (C_6D_6: δ(^{1}H) = 0.29 ppm, δ(^{13}C) = 1.4 ppm and δ(^{29}Si) = –21.8 ppm) derived from *B. Braun Melsungen AG Sterican®* cannulas. Quantitative elemental analyses (EA) were carried out using a *EURO EA* (*HEKAtech*) instrument equipped with a CHNS combustion analyzer at the *Laboratory for Microanalysis* at the *TUM Catalysis Research Center*. Melting Points (m.p.) were determined in sealed glass capillaries under inert gas by a *Büchi M-565* melting point apparatus. Mass spectra (Liquid Injection Field Desorption Ionization (LIFDI)-MS) were recorded on a *Waters Micromass LCT TOF* mass spectrometer equipped with a LIFDI-ion source (*LIFDI-700*) from *Linden CMS GmbH*. The samples were provided as filtered solution in toluene. Unless otherwise stated, all commercially available reagents were purchased from *abcr GmbH*, *Alfa Aesar*, *Sigma-Aldrich Chemie GmbH* or *Tokyo Chemical Industry Co., Ltd.* and used without further purification. The

compounds iminosilylsilanone (IDippN)(^{t}Bu$_3$Si)Si=O (**1**)[S2] and 1,3,4,5-tetramethylimidazolin-2-ylidene (IMe$_4$)[S3] were prepared as described in the corresponding references.

1.2 Syntheses of the Wittig ylides

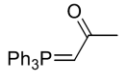


All Wittig reagents, with the exception of those commercially available, have been synthesized and isolated using the following procedure. This general method was adapted from a recently described procedure.[S4]

General procedure

To a mixture of the respective triphenylphosphonium bromide (200 mg, 1.00 eq.) and KO^{t}Bu (1.05 eq) was added THF (5 mL) at ambient temperature. Whereas an immediate color change was observed in the synthesis of non- and semi-stabilized ylides (from colorless to pale yellow, orange or red), the color did not change during the synthesis of stabilized-ylides. The reaction mixture was usually stirred for approximately 30 min to 1 hour. Subsequently, all volatiles were removed *in vacuo* and the residue was extracted with either toluene or *n*-hexane (3 × 2 mL). KBr and any residual starting material were removed *via* filtration. Removal of the solvent *in vacuo* provided the phosphorus ylides in approximately quantitative yield. Crystals suitable for single-crystal X-ray diffraction (SC-XRD) can be easily obtained by crystallization from *n*-hexane or toluene. Thus, the solid-state structures of **2h** and **2m** were acquired as representative examples (*vide infra*).

Spectroscopic data (including commercially available Wittig reagents)



2a
$C_{21}H_{19}OP$
318.36 g/mol

^{1}H NMR (400 MHz, C_6D_6, 300 K): δ [ppm] = 7.73–7.68 (m, 6H, C$_{ar}$*H*), 7.05–6.95 (m, 9H, C$_{ar}$*H*), 3.76 (d, $^2J_{PH}$ = 28.0 Hz, 1H, PC*H*), 2.37 (d, $^4J_{PH}$ = 1.8 Hz, 3H, C*H*$_3$).
^{31}P{^{1}H} NMR (162 MHz, C_6D_6, 300 K): δ [ppm] = 14.9.

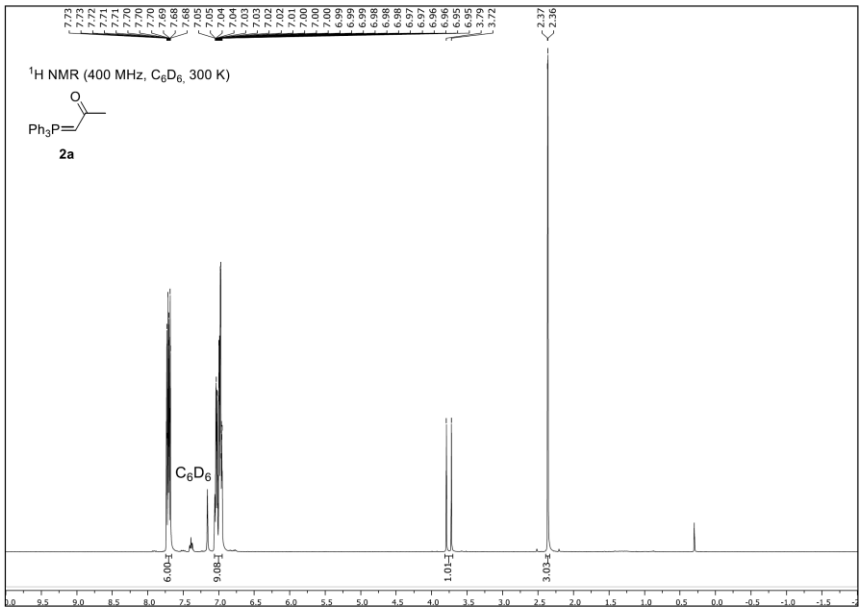


Figure S1. ^{1}H NMR spectrum of phosphorus ylide **2a** in C_6D_6 at 300 K.

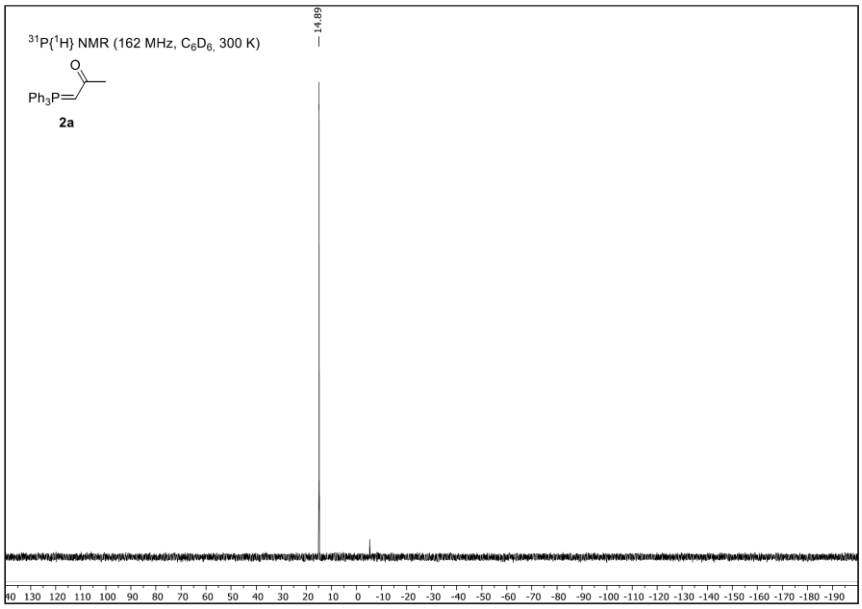
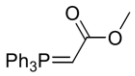


Figure S2. ^{31}P{^{1}H} NMR spectrum of phosphorus ylide **2a** in C_6D_6 at 300 K.



2b
$C_{21}H_{19}O_2P$
334.35 g/mol

Two rotational isomers of **2b** were detected *via* NMR spectroscopy.

Major isomer (~91%):

^{1}H NMR (400 MHz, C_6D_6, 300 K): δ [ppm] = 7.72–7.67 (m, 6H, $C_{ar}\underline{H}$), 7.04–6.92 (m, 9H, $C_{ar}\underline{H}$), 3.79 (s, 1H, $OC\underline{H}_3$), 3.37 (d, $^2J_{PH}$ = 23.8 Hz, 1H, $PC\underline{H}$).

^{31}P{^{1}H} NMR (162 MHz, C_6D_6, 300 K): δ [ppm] = 18.3.

Minor isomer (~9%):

^{1}H NMR (400 MHz, C_6D_6, 300 K): δ [ppm] = 7.61–7.55 (m, 6H, $C_{ar}\underline{H}$), 3.47 (s, 1H, $OC\underline{H}_3$), 3.03 (d, $^2J_{PH}$ = 22.5 Hz, 1H, $PC\underline{H}$). The multiplet resonance for the remaining $C_{ar}\underline{H}$ protons was not observed, due to an overlap with the corresponding multiplet of the major rotational isomer of **2b**.

^{31}P{^{1}H} NMR (162 MHz, C_6D_6, 300 K): δ [ppm] = 16.3.

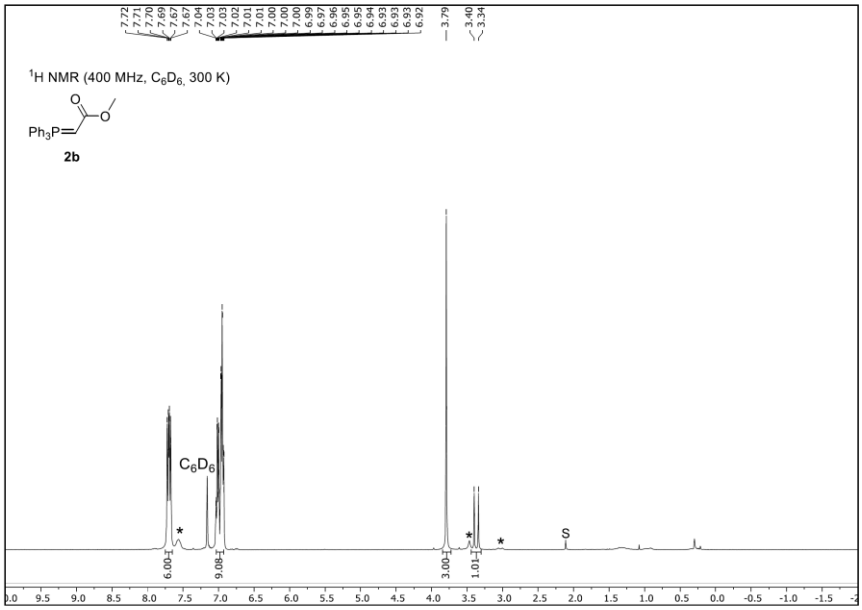


Figure S3. ^{1}H NMR spectrum of phosphorus ylide **2b** in C_6D_6 at 300 K. The respective resonances for the minor rotational isomer of **2b** and residual toluene are marked with asterisks * and an S, respectively.

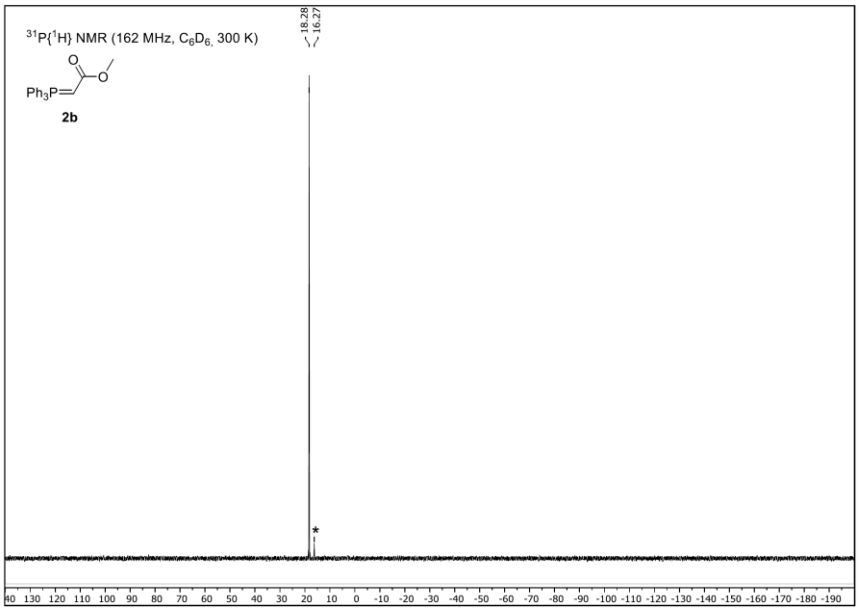
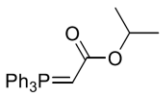


Figure S4. $^{31}P\{^{1}H\}$ NMR spectrum of phosphorus ylide **2b** in C_6D_6 at 300 K. The respective resonance for the minor rotational isomer of **2b** is marked with an asterisk *.



2c

$C_{22}H_{23}O_2P$

362.41 g/mol

Two rotational isomers of **2c** were detected *via* NMR spectroscopy.

Major isomer (~78%):

^{1}H NMR (500 MHz, C_6D_6, 300 K): δ [ppm] = 7.73–7.68 (m, 6H, $C_{ar}\underline{H}$), 7.04–6.93 (m, 9H, $C_{ar}\underline{H}$), 5.41 (sept, ^{3}J = 6.2 Hz, 1H, $OC\underline{H}(CH_3)_2$), 3.32 (d, $^{2}J_{PH}$ = 24.3 Hz, 1H, $PC\underline{H}$), 1.36 (d, ^{3}J = 6.2 Hz, 6H, $OCH(C\underline{H}_3)_2$).

^{13}C{^{1}H} NMR (126 MHz, C_6D_6, 300 K): δ [ppm] = 171.8 (d, $^{2}J_{PC}$ = 15.0 Hz, $\underline{C}$=O), 133.4 (d, $^{3}J_{PC}$ = 10.1 Hz, *m*-$\underline{C}_{ar}H$), 131.7 (d, $^{4}J_{PC}$ = 3.0 Hz, *p*-$\underline{C}_{ar}H$), 129.3 (d, $^{1}J_{PC}$ = 91.2 Hz, *ipso*-$\underline{C}_{ar}$), 128.7 (d, $^{2}J_{PC}$ = 12.1 Hz, *o*-$\underline{C}_{ar}H$), 64.1 (d, $^{4}J_{PC}$ = 2.9 Hz, $\underline{C}H(CH_3)_2$), 30.2 (d, $^{1}J_{PC}$ = 130.0 Hz, P$\underline{C}$H), 23.2 ($CH(\underline{C}H_3)_2$).

^{31}P{^{1}H} NMR (203 MHz, C_6D_6, 300 K): δ [ppm] = 18.3.

Minor isomer (~22%):

^{1}H NMR (500 MHz, C_6D_6, 300 K): δ [ppm] = 7.59–7.55 (m, 6H, $C_{ar}\underline{H}$), 5.31 (sept, ^{3}J = 6.2 Hz, 1H, $OC\underline{H}(CH_3)_2$), 3.02 (d, $^{2}J_{PH}$ = 23.5 Hz, 1H, $PC\underline{H}$), 0.86 (d, ^{3}J = 6.2 Hz, 6H, $OCH(C\underline{H}_3)_2$). The multiplet resonance for the remaining $C_{ar}\underline{H}$ protons was not observed, due to an overlap with the corresponding multiplet of the major rotational isomer of **2c**.

$^{13}C\{^1H\}$ NMR (126 MHz, C_6D_6, 300 K): δ [ppm] = 168.7 (d, $^2J_{PC}$ = 8.0 Hz, C=O), 131.5 (br s, *p*-$C_{ar}H$), 129.9 (d, $^1J_{PC}$ = 91.1 Hz, *ipso*-C_{ar}), 63.6 (br s, $CH(CH_3)_2$), 29.1 (d, $^1J_{PC}$ = 120.5 Hz, PCH), 22.5 ($CH(CH_3)_2$). The resonances for the *m*-$C_{ar}H$ and *o*-$C_{ar}H$ protons were not observed, due to overlaps with the corresponding resonances for the major rotational isomer of **2c**.

$^{31}P\{^1H\}$ NMR (203 MHz, C_6D_6, 300 K): δ [ppm] = 16.4.

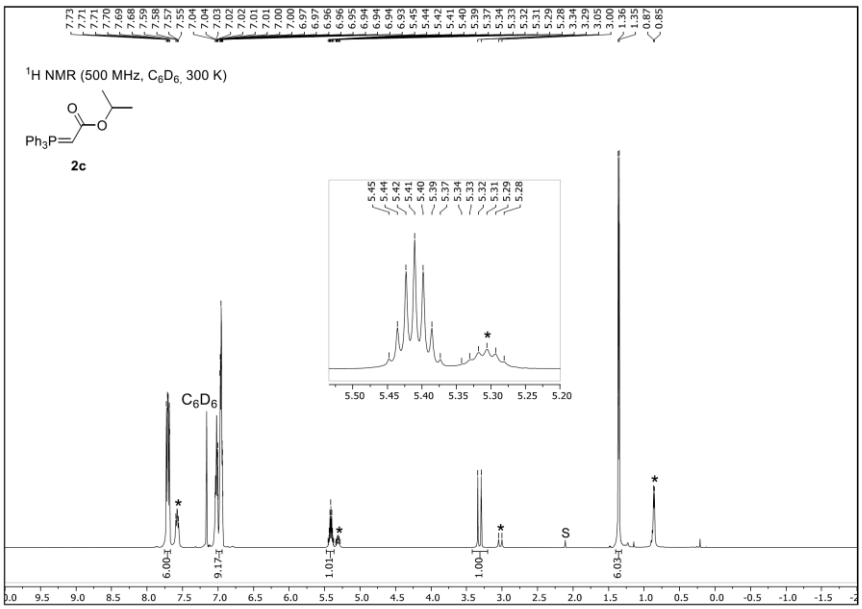


Figure S5. ^{1}H NMR spectrum of phosphorus ylide **2c** in C_6D_6 at 300 K. The respective resonances for the minor rotational isomer of **2c** and residual toluene are marked with asterisks * and an S, respectively.

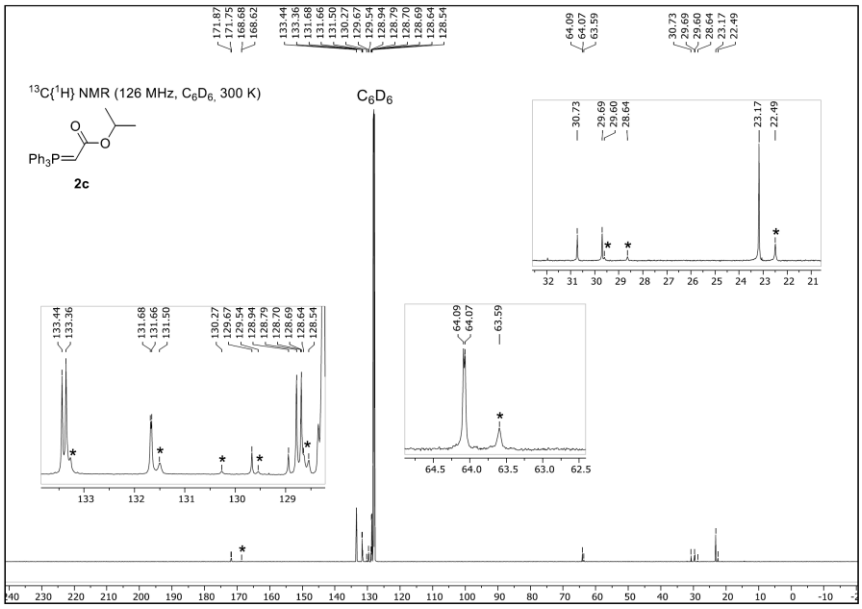


Figure S6. $^{13}C\{^1H\}$ NMR spectrum of phosphorus ylide **2c** in C_6D_6 at 300 K. The respective resonances for the minor rotational isomer of **2c** are marked with asterisks *

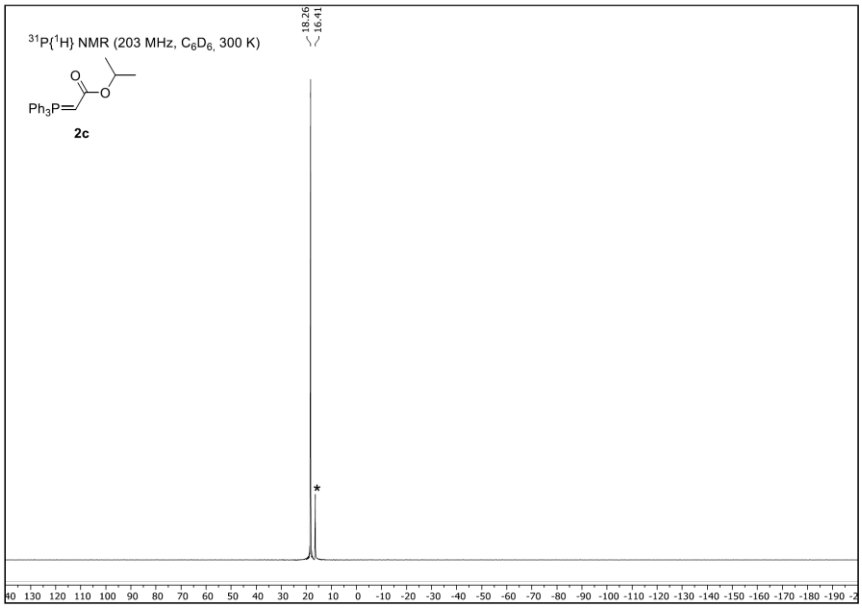
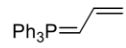


Figure S7. $^{31}P\{^1H\}$ NMR spectrum of phosphorus ylide **2c** in C_6D_6 at 300 K. The respective resonance for the minor rotational isomer of **2c** is marked with an asterisk *.



2d

$C_{21}H_{19}P$

302.36 g/mol

^{1}H NMR (400 MHz, C_6D_6, 300 K): δ [ppm] = 7.63–7.58 (m, 6H, $C_{ar}\underline{H}$), 7.05–6.95 (m, 9H, $C_{ar}\underline{H}$), 6.78–6.63 (m, 1H, $C\underline{H}CH_2$), 4.89 (*pseudo* dd, ^2J = 16.3 Hz, $^4J_{PH}$ = 2.4 Hz, 1H, $CHC\underline{H}_2$), 4.53 (ddd, ^2J = 10.2 Hz, ^3J = 4.0 Hz, $^4J_{PH}$ = 2.4 Hz, 1H, $CHC\underline{H}_2$), 2.90 (dd, $^2J_{PH}$ = 21.0 Hz, ^3J = 11.6 Hz, 1H, $PC\underline{H}$).

^{31}P{^{1}H} NMR (162 MHz, C_6D_6, 300 K): δ [ppm] = 11.4.

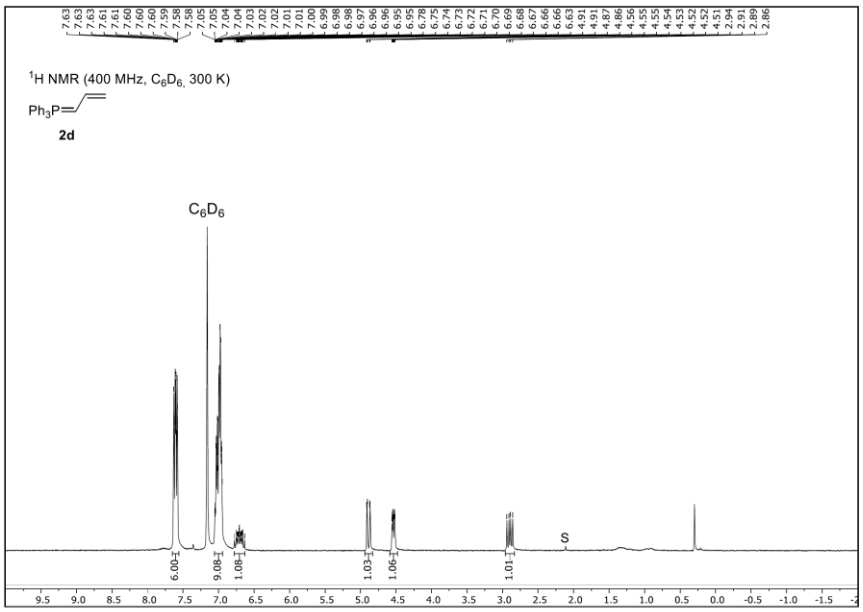


Figure S8. ^{1}H NMR spectrum of phosphorus ylide **2d** in C_6D_6 at 300 K. Residual toluene is marked with an S.

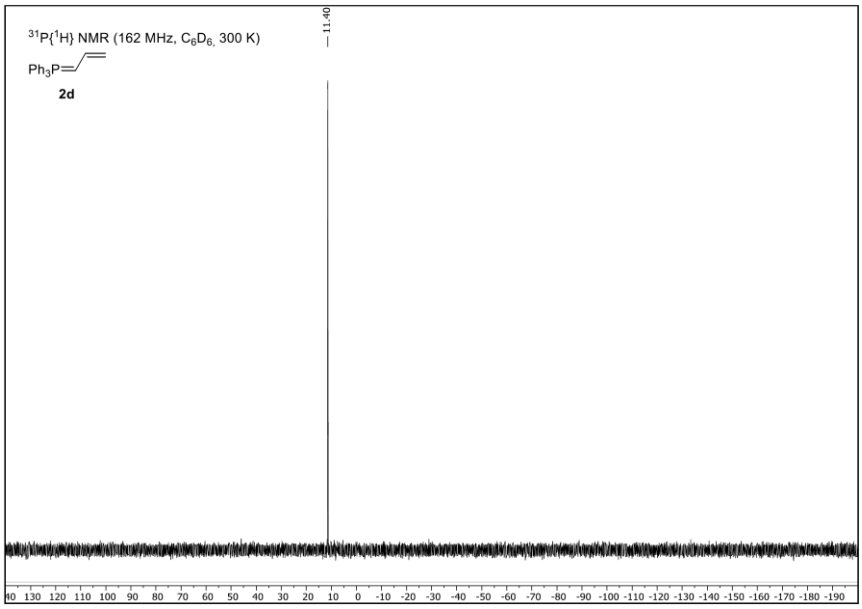
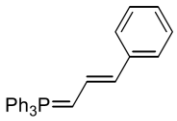


Figure S9. $^{31}P\{^{1}H\}$ NMR spectrum of phosphorus ylide **2d** in C_6D_6 at 300 K.



2e
$C_{27}H_{23}P$
378.45 g/mol

^{1}H NMR (400 MHz, C_6D_6, 300 K): δ [ppm] = 7.57–7.52 (m, 6H, $C_{ar}\underline{H}$), 7.33–7.14 (m, 5H, $C_{ar}\underline{H}$, overlapping with solvent signal), 7.06–6.94 (m, 9H, $C_{ar}\underline{H}$), 6.88 (*pseudo* tt, ^{3}J = 7.2 Hz, $^{3}J_{PH}$ = 1.2 Hz, 1H, PCHC$\underline{H}$), 6.27 (d, ^{3}J = 14.7 Hz, 1H, CHC$\underline{H}$), 3.13 (dd, $^{2}J_{PH}$ = 21.4 Hz, ^{3}J = 12.1 Hz, 1H, PC$\underline{H}$).

^{31}P{^{1}H} NMR (162 MHz, C_6D_6, 300 K): δ [ppm] = 12.5.

Note: multinuclear NMR spectroscopy revealed the presence of an additional species, presumably another rotational isomer or stereoisomer of **2e**.

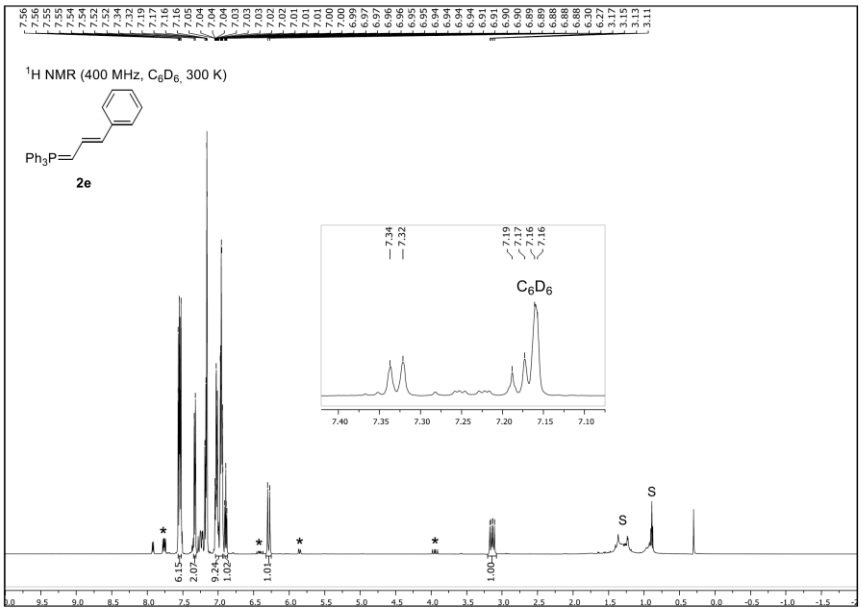


Figure S10. ^{1}H NMR spectrum of phosphorus ylide **2e** in C_6D_6 at 300 K. The respective resonances for the additional species and residual *n*-hexane are marked with asterisks * and an S, respectively.

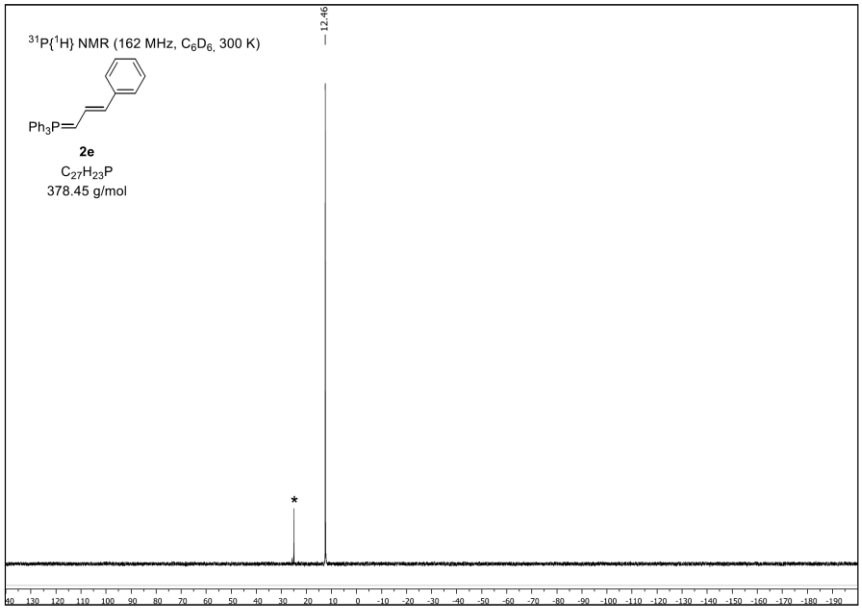


Figure S11. ^{31}P{^{1}H} NMR spectrum of phosphorus ylide **2e** in C_6D_6 at 300 K. The resonance for the additional species is marked with an asterisk *.



2f

$C_{19}H_{17}P$

276.32 g/mol

^{1}H NMR (500 MHz, C_6D_6, 300 K): δ [ppm] = 7.76–7.72 (m, 6H, $C_{ar}\underline{H}$), 7.07–7.00 (m, 9H, $C_{ar}\underline{H}$), 0.81 (d, $^{2}J_{PH}$ = 7.6 Hz, 2H, $PC\underline{H}_2$).

^{31}P{^{1}H} NMR (203 MHz, C_6D_6, 300 K): δ [ppm] = 20.6.

The spectroscopic data match those recently reported.[S4]

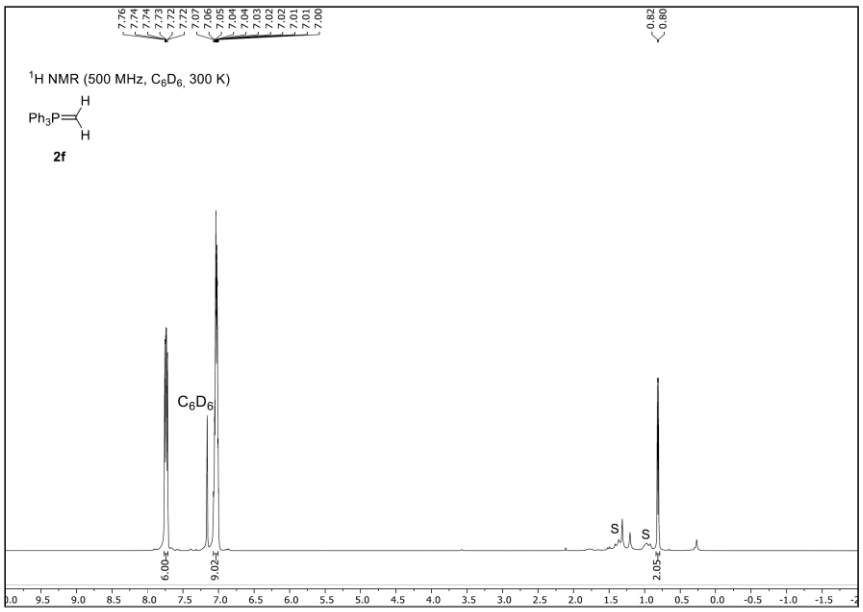


Figure S12. ^{1}H NMR spectrum of phosphorus ylide **2f** in C_6D_6 at 300 K. Residual *n*-hexane is marked with an S.

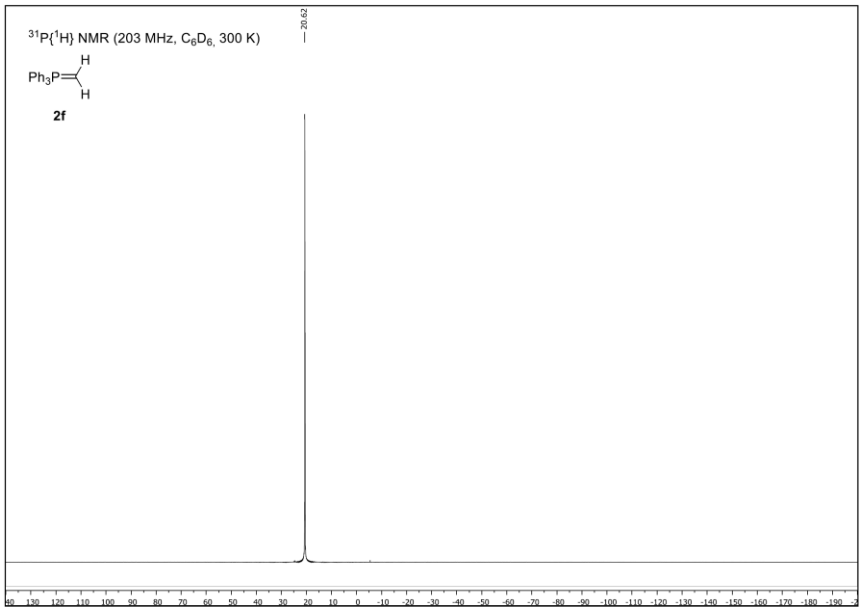


Figure S13. $^{31}P\{^{1}H\}$ NMR spectrum of phosphorus ylide **2f** in C_6D_6 at 300 K.

Ph_3P

2g

$C_{20}H_{19}P$

290.35 g/mol

^{1}H NMR (400 MHz, C_6D_6, 300 K): δ [ppm] = 7.72–7.67 (m, 6H, $C_{ar}\underline{H}$), 7.10–7.02 (m, 9H, $C_{ar}\underline{H}$), 2.16 (*pseudo* d, $^{3}J_{PH}$ = 19.0 Hz, 3H, $C\underline{H}_3$), 1.06 (br s, 1H, $PC\underline{H}$).

$^{31}P\{^{1}H\}$ NMR (162 MHz, C_6D_6, 300 K): δ [ppm] = 14.5.

The spectroscopic data match those recently reported.[S4]

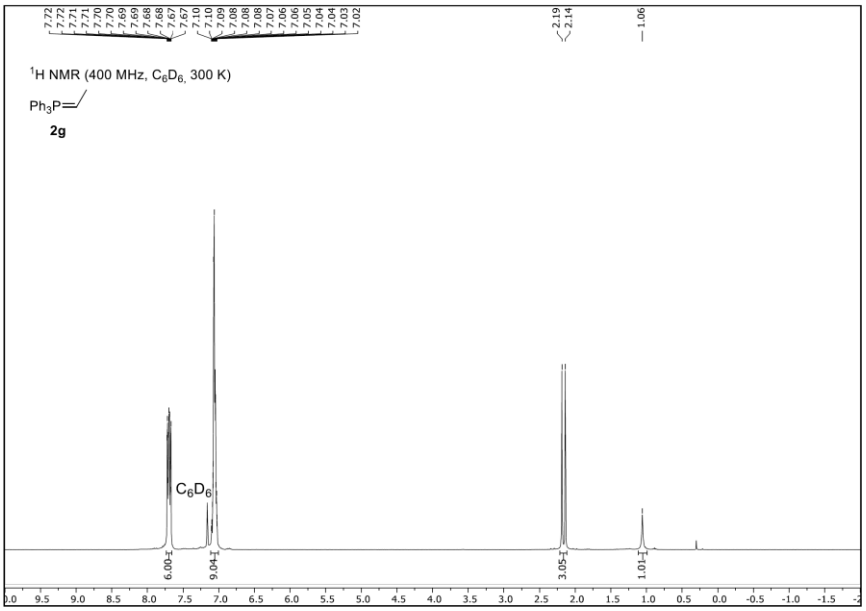


Figure S14. ^{1}H NMR spectrum of phosphorus ylide **2g** in C_6D_6 at 300 K.

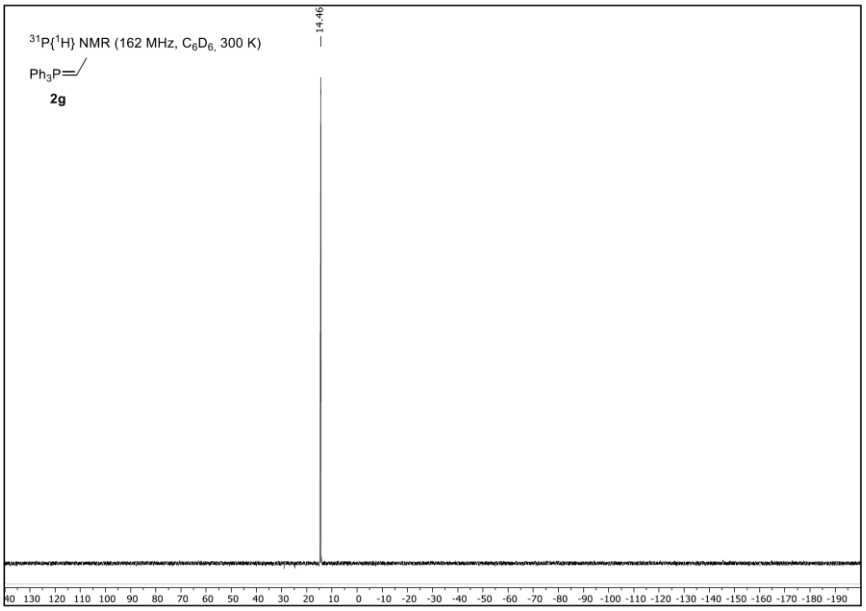
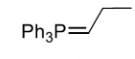


Figure S15. ^{31}P{^{1}H} NMR spectrum of phosphorus ylide **2g** in C_6D_6 at 300 K.



2h

$C_{21}H_{21}P$

304.37 g/mol

^{1}H NMR (400 MHz, C_6D_6, 300 K): δ [ppm] = 7.73–7.68 (m, 6H, $C_{ar}\underline{H}$), 7.10–7.02 (m, 9H, $C_{ar}\underline{H}$), 2.45 (*pseudo* dq, $^3J_{PH}$ = 14.7 Hz, ^3J = 7.2 Hz, 2H, $C\underline{H}_2$), 1.41 (dt, ^3J = 7.2 Hz, $^4J_{PH}$ = 1.4 Hz, 3H, $C\underline{H}_3$), 1.11 (br s, 1H, $PC\underline{H}$).

^{31}P{^{1}H} NMR (162 MHz, C_6D_6, 300 K): δ [ppm] = 12.3.

The spectroscopic data match those recently reported.[S4]

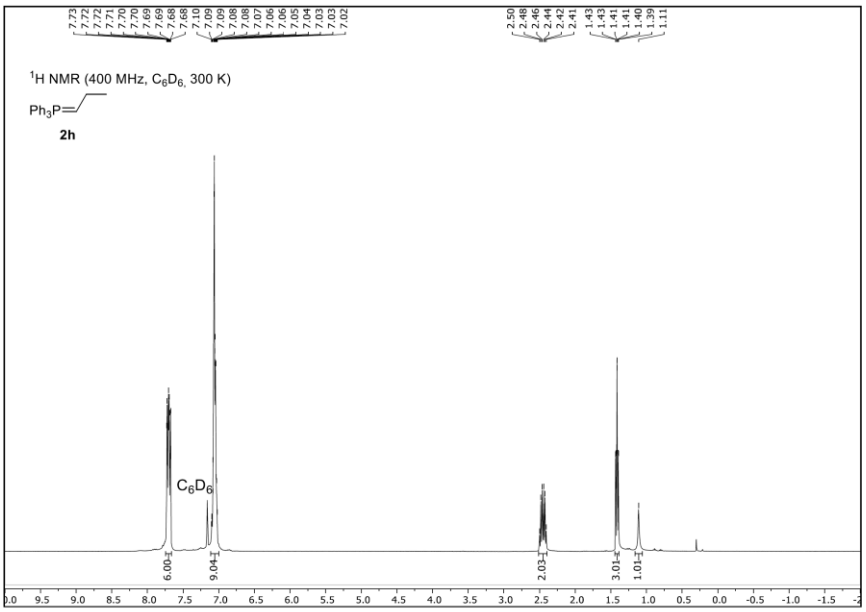


Figure S16. ^{1}H NMR spectrum of phosphorus ylide **2h** in C_6D_6 at 300 K.

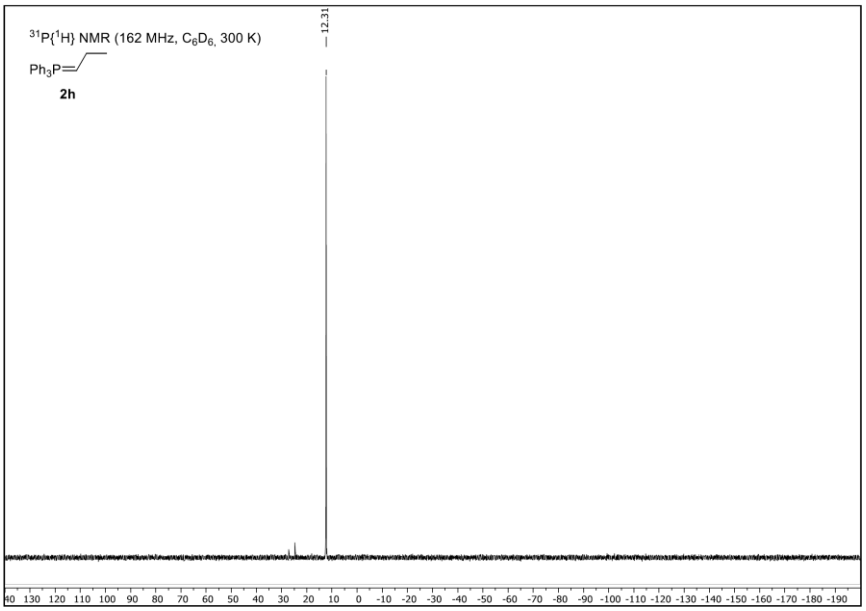


Figure S17. $^{31}P\{^{1}H\}$ NMR spectrum of phosphorus ylide **2h** in C_6D_6 at 300 K.

Ph$_3$P=

2i

$C_{22}H_{23}P$

318.40 g/mol

^{1}H NMR (400 MHz, C$_6$D$_6$, 300 K): δ [ppm] = 7.73–7.68 (m, 6H, C$_{ar}$H), 7.10–7.02 (m, 9H, C$_{ar}$H), 2.40 (*pseudo* dt, $^{3}J_{PH}$ = 15.1 Hz, ^{3}J = 7.2 Hz, 2H, CHCH$_2$), 1.80–1.70 (m, 2H, CH$_2$CH$_3$), 1.12 (t, ^{3}J = 7.2 Hz, 3H, CH$_3$). The resonance for the PCH nucleus was not directly observed, due to an overlap with the CH$_3$ signal.

^{31}P{^{1}H} NMR (162 MHz, C$_6$D$_6$, 300 K): δ [ppm] = 12.7.

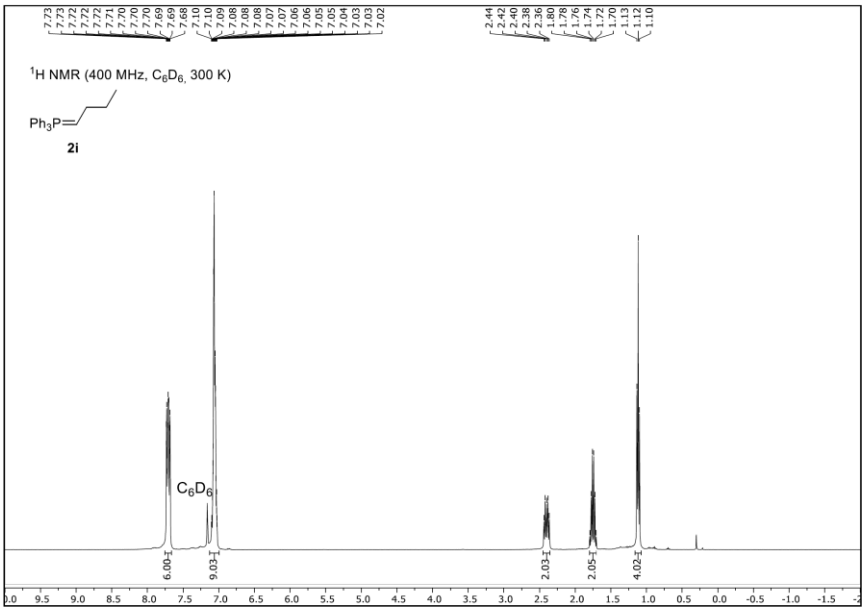


Figure S18. ^{1}H NMR spectrum of phosphorus ylide **2i** in C_6D_6 at 300 K.

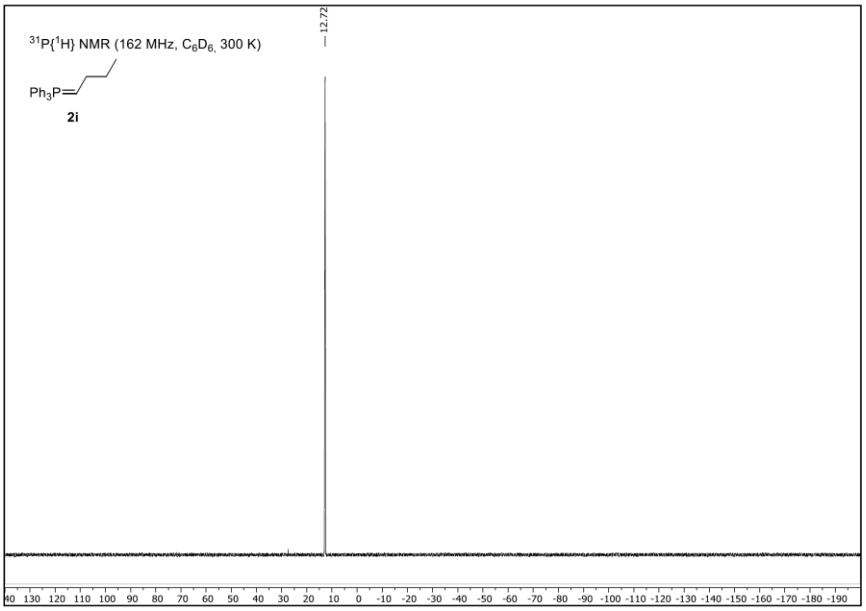
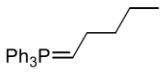


Figure S19. ^{31}P{^{1}H} NMR spectrum of phosphorus ylide **2i** in C_6D_6 at 300 K.



2j
$C_{23}H_{25}P$
332.43 g/mol

^{1}H NMR (400 MHz, C_6D_6, 300 K): δ [ppm] = 7.74–7.69 (m, 6H, $C_{ar}\underline{H}$), 7.11–7.03 (m, 9H, $C_{ar}\underline{H}$), 2.43 (*pseudo* dt, $^3J_{PH}$ = 14.9 Hz, ^3J = 7.2 Hz, 2H, CHC$\underline{H}_2$), 1.77–1.70 (m, 2H, C$\underline{H}_2$CH$_2$CH$_3$), 1.61–1.52 (m, 2H, CH$_2$C$\underline{H}_2$CH$_3$), 1.09 (br s, 1H, PC$\underline{H}$), 0.89 (t, ^3J = 7.3 Hz, 3H, C$\underline{H}_3$).

^{31}P{^{1}H} NMR (162 MHz, C_6D_6, 300 K): δ [ppm] = 12.6.

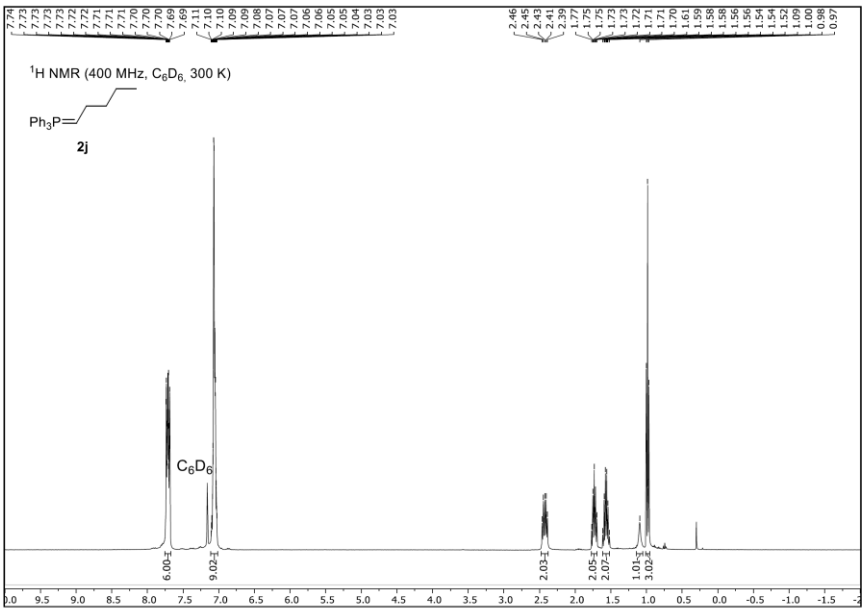


Figure S20. ^{1}H NMR spectrum of phosphorus ylide **2j** in C_6D_6 at 300 K.

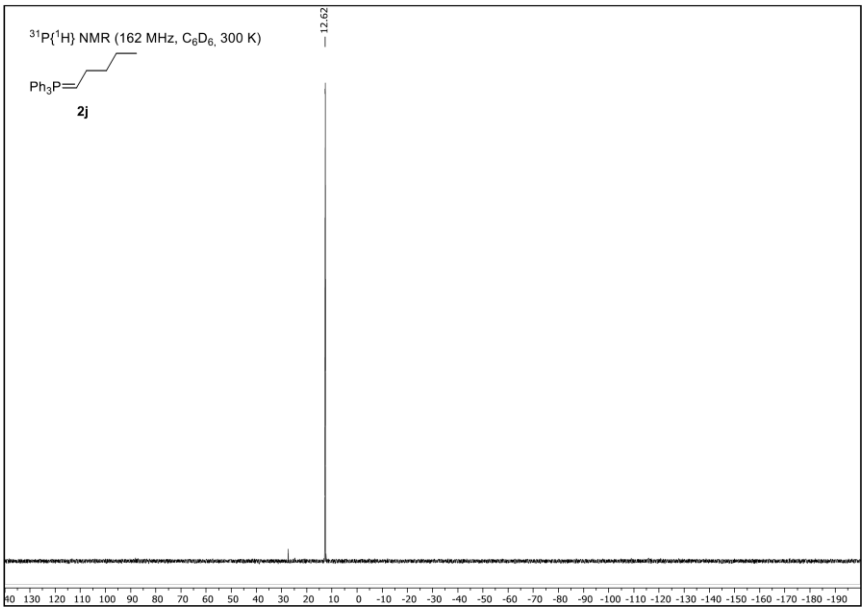
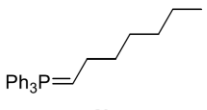


Figure S21. $^{31}P\{^{1}H\}$ NMR spectrum of phosphorus ylide **2j** in C_6D_6 at 300 K.



2k
$C_{25}H_{29}P$
360.48 g/mol

^{1}H NMR (400 MHz, C_6D_6, 300 K): δ [ppm] = 7.75–7.69 (m, 6H, $C_{ar}\underline{H}$), 7.10–7.03 (m, 9H, $C_{ar}\underline{H}$), 2.43 (*pseudo* dt, $^{3}J_{PH}$ = 15.0 Hz, ^{3}J = 7.2 Hz, 2H, $CHC\underline{H}_2CH_2CH_2$), 1.79–1.71 (m, 2H, $CHCH_2C\underline{H}_2CH_2$), 1.58–1.51 (m, 2H, $CHCH_2CH_2C\underline{H}_2$), 1.39–1.27 (m, 4H, $C\underline{H}_2CH_2CH_3$ + $CH_2C\underline{H}_2CH_3$), 1.11 (br s, 1H, $PC\underline{H}$), 0.89 (t, ^{3}J = 7.0 Hz, 3H, $C\underline{H}_3$).

^{31}P{^{1}H} NMR (162 MHz, C_6D_6, 300 K): δ [ppm] = 12.7.

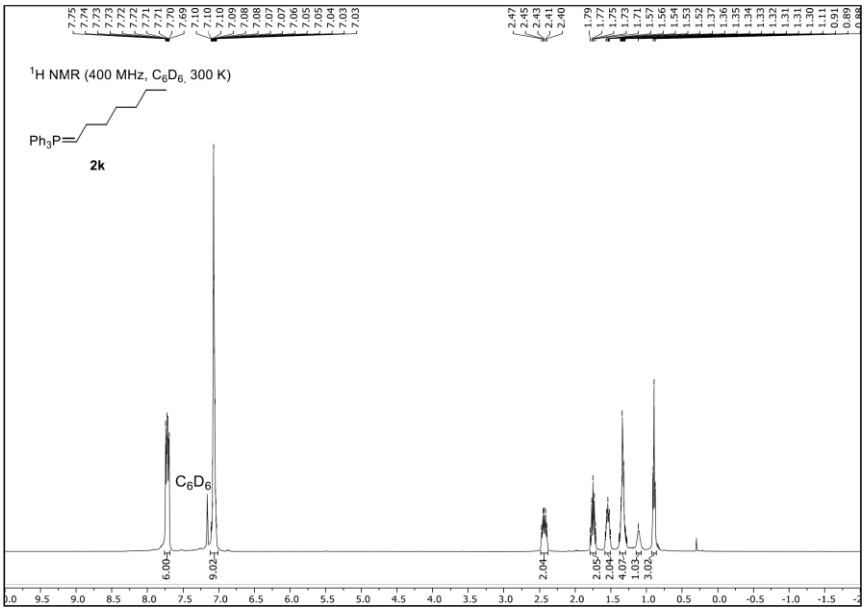


Figure S22. ^{1}H NMR spectrum of phosphorus ylide **2k** in C_6D_6 at 300 K.

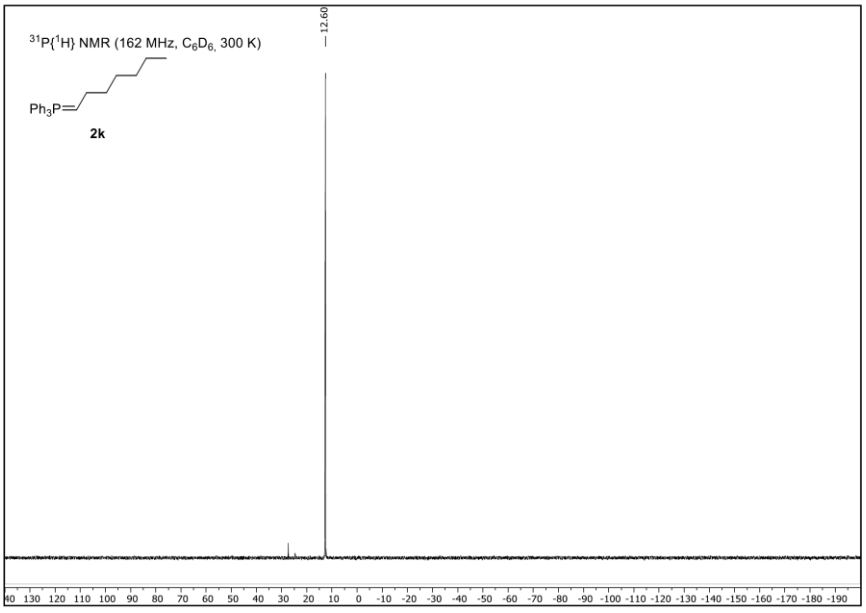
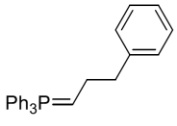


Figure S23. ^{31}P{^{1}H} NMR spectrum of phosphorus ylide **2k** in C_6D_6 at 300 K.



2l
$C_{27}H_{25}P$
380.47 g/mol

^{1}H NMR (400 MHz, C_6D_6, 300 K): δ [ppm] = 7.68–7.62 (m, 6H, $C_{ar}\underline{H}$), 7.24–7.15 (m, 5H, $C_{ar}\underline{H}$, overlapping with solvent signal), 7.10–7.01 (m, 9H, $C_{ar}\underline{H}$), 2.95 (m, 2H, $C\underline{H}_2CH_2$), 2.68 (m, $CH_2C\underline{H}_2$), 1.11 (br s, 1H, $PC\underline{H}$).

^{31}P{^{1}H} NMR (162 MHz, C_6D_6, 300 K): δ [ppm] = 13.0.

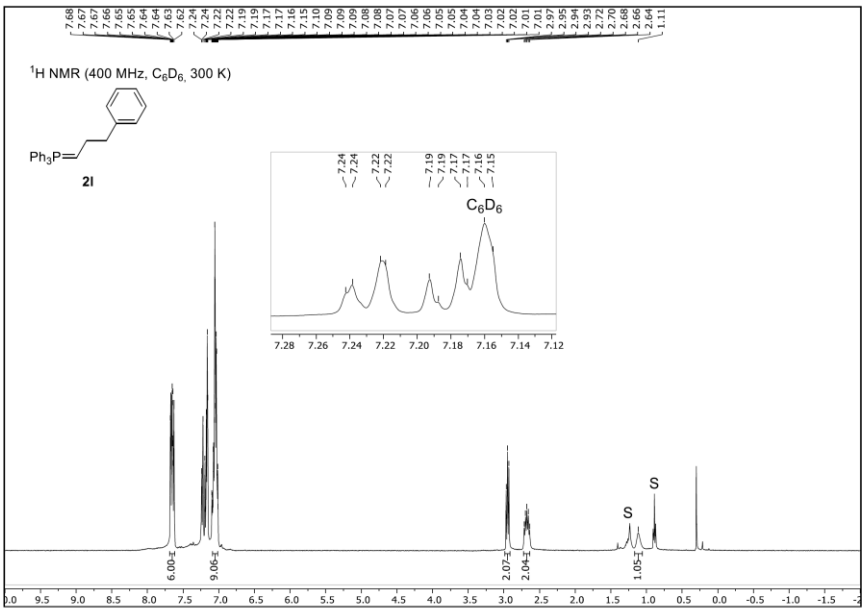


Figure S24. ^{1}H NMR spectrum of phosphorus ylide **2l** in C_6D_6 at 300 K. Residual *n*-hexane is marked with an S.

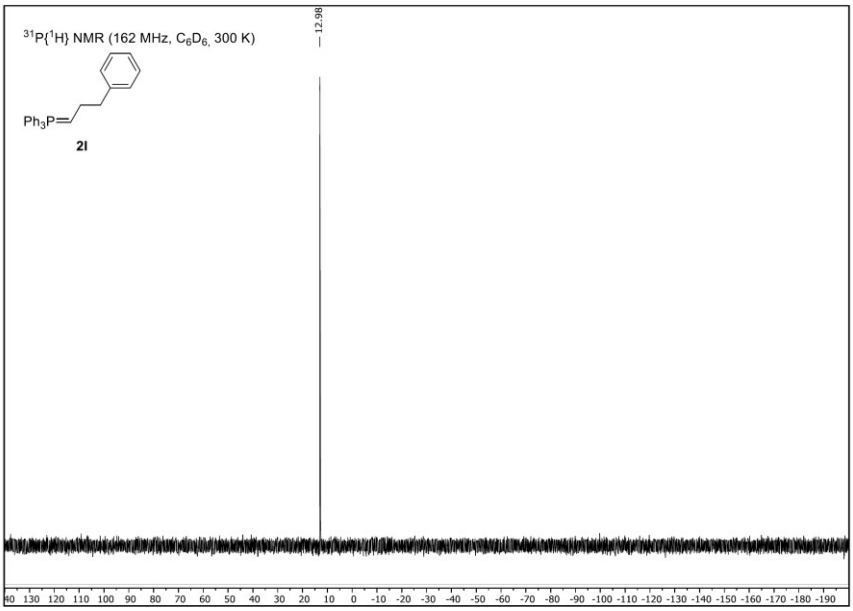
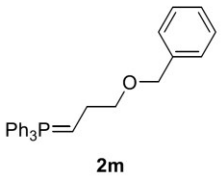


Figure S25. $^{31}P\{^{1}H\}$ NMR spectrum of phosphorus ylide **2l** in C_6D_6 at 300 K.



2m
$C_{28}H_{27}OP$
410.50 g/mol

^{1}H NMR (400 MHz, C_6D_6, 300 K): δ [ppm] = 7.70–7.65 (m, 6H, $C_{ar}\underline{H}$), 7.34–7.33 (m, 2H, $C_{ar}\underline{H}$), 7.18–7.14 (m, 2H, $C_{ar}\underline{H}$, overlapping with solvent signal), 7.11–7.08 (m, 1H, $C_{ar}\underline{H}$), 7.07–7.00 (m, 9H, $C_{ar}\underline{H}$), 4.44 (s, 2H, $C\underline{H}_2Ph$), 3.70 (t, ^{3}J = 7.3 Hz, 2H, $CH_2C\underline{H}_2$), 2.76 (*pseudo* dt, ^{3}J = 16.2 Hz, ^{3}J = 7.3 Hz, 2H, $C\underline{H}_2CH_2$), 1.01 (br s, 1H, $PC\underline{H}$).

^{31}P{^{1}H} NMR (162 MHz, C_6D_6, 300 K): δ [ppm] = 14.6.

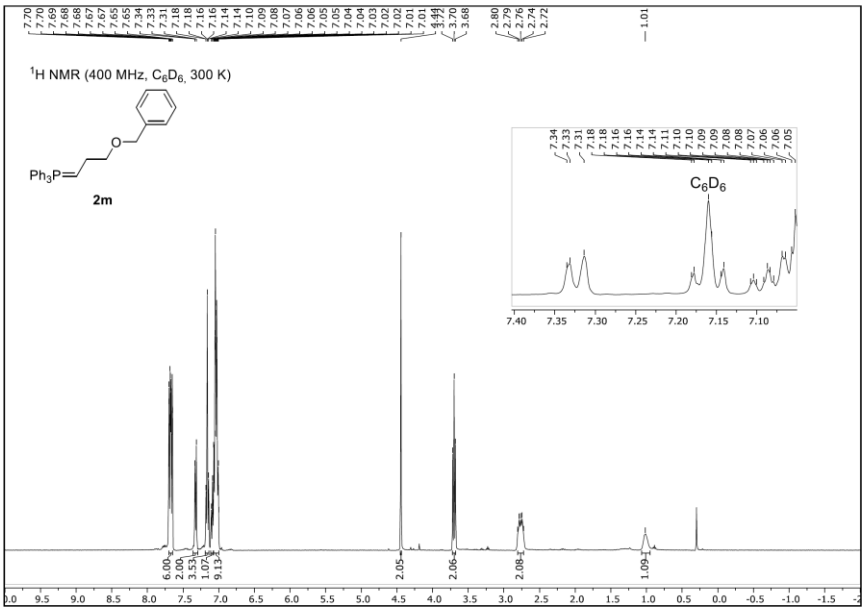


Figure S26. ^{1}H NMR spectrum of phosphorus ylide **2m** in C_6D_6 at 300 K.

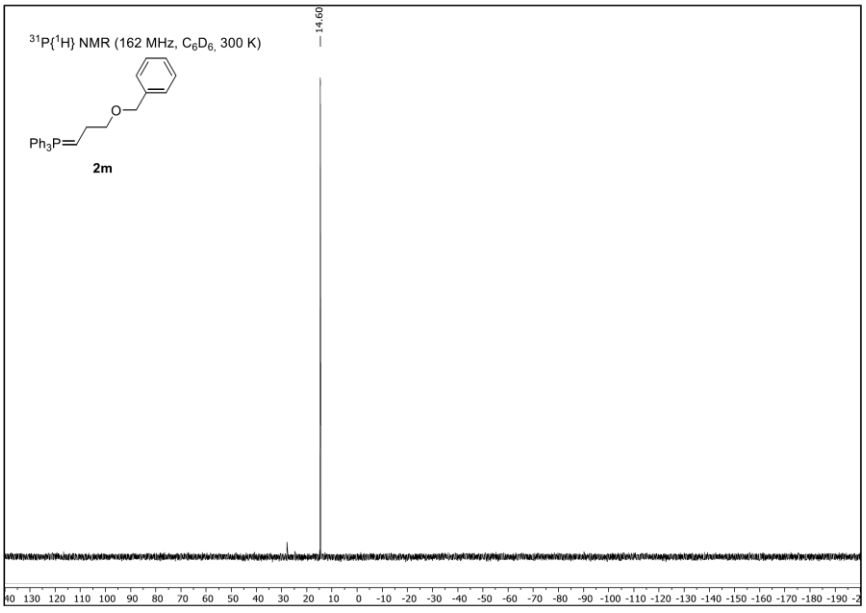
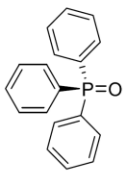


Figure S27. ^{31}P{^{1}H} NMR spectrum of phosphorus ylide **2m** in C_6D_6 at 300 K.

1.3 Spectroscopic data of $Ph_3P{=}O$

For a comparison with the Sila-Wittig reactions, commercially available triphenylphosphine oxide was examined *via* NMR spectroscopy.



$C_{18}H_{15}OP$
278.29 g/mol

^{1}H NMR (500 MHz, C_6D_6, 300 K): δ [ppm] = 7.78–7.73 (m, 6H, $C_{ar}\underline{H}$), 7.08–6.99 (m, 9H, $C_{ar}\underline{H}$).

^{13}C{^{1}H} NMR (126 MHz, C_6D_6, 300 K): δ [ppm] = 134.4 (d, $^{1}J_{PC}$ = 102.5 Hz, *ipso*-$\underline{C}_{ar}$), 132.4 (d, $^{3}J_{PC}$ = 9.7 Hz, *m*-$\underline{C}_{ar}$H), 131.6 (d, $^{4}J_{PC}$ = 2.8 Hz, *p*-$\underline{C}_{ar}$H), 128.6 (d, $^{2}J_{PC}$ = 12.0 Hz, *o*-$\underline{C}_{ar}$H).

^{31}P{^{1}H} NMR (203 MHz, C_6D_6, 300 K): δ [ppm] = 24.9.

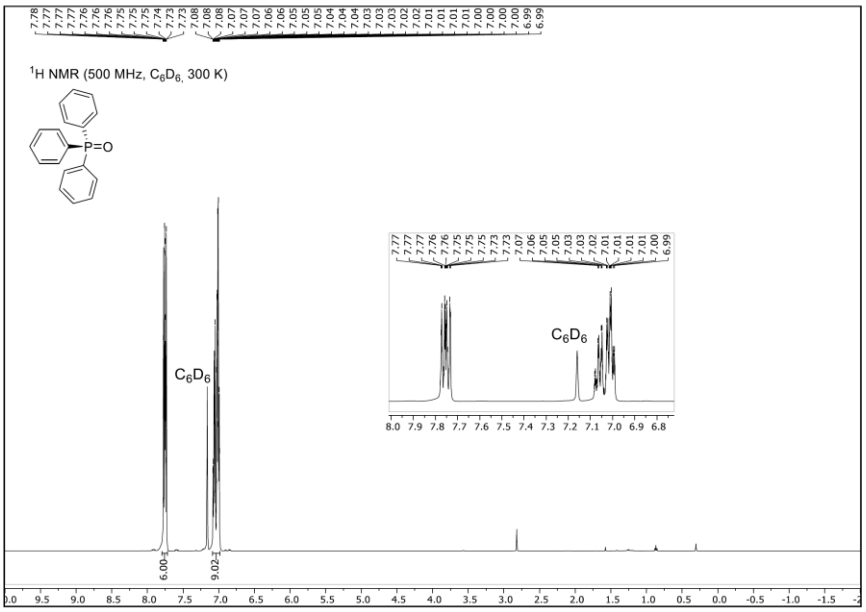


Figure S28. ^{1}H NMR spectrum of $Ph_3P{=}O$ in C_6D_6 at 300 K.

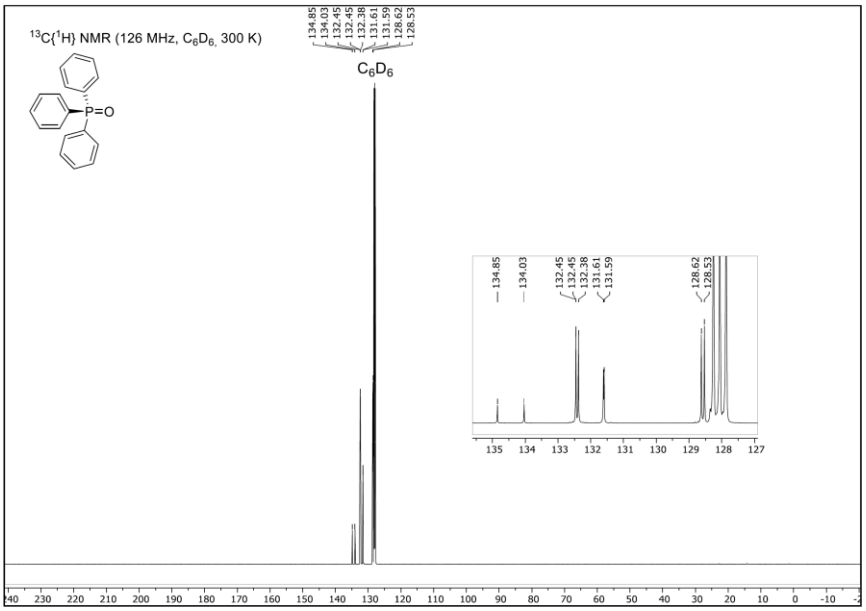


Figure S29. $^{13}C\{^1H\}$ NMR spectrum of $Ph_3P{=}O$ in C_6D_6 at 300 K.

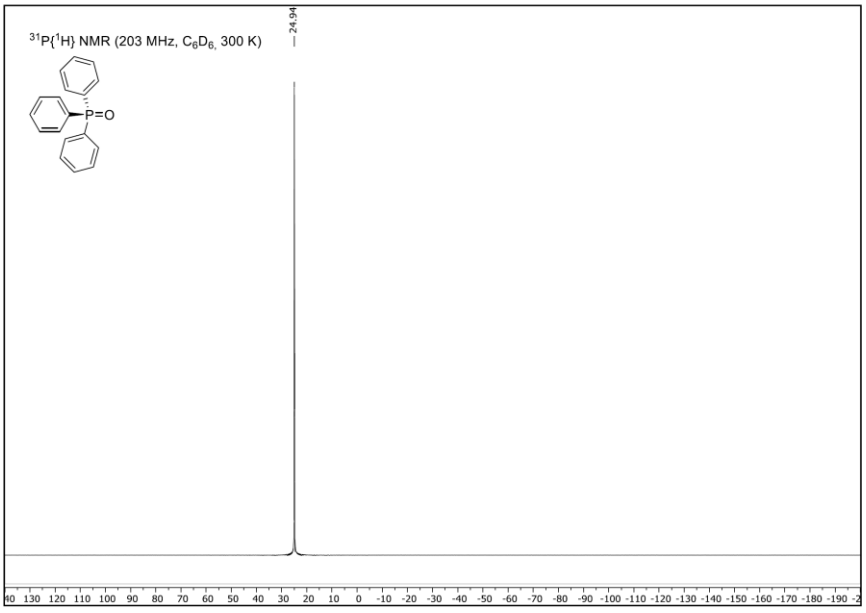
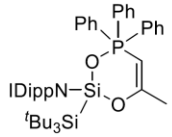


Figure S30. $^{31}P\{^1H\}$ NMR spectrum of $Ph_3P{=}O$ in C_6D_6 at 300 K.

1.4 Reactivity of silanone 1 toward stabilized ylides

1.4.1 Synthesis of dioxaphosphasiline 3



3
$C_{60}H_{82}N_3O_2PSi_2$
964.48 g/mol

To a mixture of silanone **1** (100 mg, 155 µmol, 1.0 eq.) and ketone-substituted ylide **2a** (49.3 mg, 155 µmol, 1.0 eq.) was added benzene (5 mL). An immediate color change from colorless to cherry red was observed. The reaction mixture was stirred for an additional hour. Subsequent removal of the solvent *in vacuo* afforded dioxaphosphasiline **3** as a cherry red waxy solid (149 mg, 155 µmol, quantitative yield).

m.p.: 158-159 °C (decomposition; color change from cherry red to black).

^{1}H NMR (500 MHz, C_6D_6, 300 K): δ [ppm] = 7.80–7.72 (m, 3H, $C_{ar}\underline{H}$), 7.30–7.21 (m, 5H, $C_{ar}\underline{H}$), 7.18–7.15 (m, 2H, $C_{ar}\underline{H}$, overlapping with solvent signal), 7.08–6.93 (m, 11H, $C_{ar}\underline{H}$), 6.19 (d, ^3J = 2.9 Hz, 1H, NC$\underline{H}$), 6.11 (d, ^3J = 2.9 Hz, 1H, NC$\underline{H}$), 4.52 (d, $^2J_{PH}$ = 25.4 Hz, 1H, PC$\underline{H}$), 3.88 (sept, ^3J = 6.7 Hz, 1H, C$\underline{H}$(CH$_3$)$_2$), 3.49 (sept, ^3J = 6.7 Hz, 1H, C$\underline{H}$(CH$_3$)$_2$), 2.94 (sept, ^3J = 6.7 Hz, 1H, C$\underline{H}$(CH$_3$)$_2$), 2.85 (sept, ^3J = 6.7 Hz, 1H, C$\underline{H}$(CH$_3$)$_2$), 1.54 (d, ^3J = 6.7 Hz, 3H, CH(C$\underline{H}_3$)$_2$), 1.45 (s, 3H, C$\underline{H}_3$), 1.44 (d, ^3J = 6.7 Hz, 3H, CH(C$\underline{H}_3$)$_2$), 1.36 (d, ^3J = 6.7 Hz, 3H, CH(C$\underline{H}_3$)$_2$), 1.22 (d, ^3J = 6.7 Hz, 3H, CH(C$\underline{H}_3$)$_2$), 1.13 (d, ^3J = 6.7 Hz, 3H, CH(C$\underline{H}_3$)$_2$), 1.09 (d, ^3J = 6.7 Hz, 3H, CH(C$\underline{H}_3$)$_2$), 0.94 (s, 27H, C(C$\underline{H}_3$)$_3$), 0.88 (d, ^3J = 6.7 Hz, 3H, CH(C$\underline{H}_3$)$_2$), 0.84 (d, ^3J = 6.7 Hz, 3H, CH(C$\underline{H}_3$)$_2$).

^{13}C{^{1}H} NMR (126 MHz, C_6D_6, 300 K): δ [ppm] = 176.3 (d, $^2J_{PC}$ = 1.8 Hz, O$\underline{C}$CH$_3$), 149.1 (*o*-$\underline{C}_{Dipp}$), 147.8 (*o*-$\underline{C}_{Dipp}$, 2 overlapping resonances), 147.6 (*o*-$\underline{C}_{Dipp}$), 141.9 (N$\underline{C}$N), 135.6 (*ipso*-$\underline{C}_{Dipp}$), 135.1 (*ipso*-$\underline{C}_{Dipp}$), 129.7 (*p*-$\underline{C}_{Dipp}$H), 129.5 (*p*-$\underline{C}_{Dipp}$H), 124.8 (*m*-$\underline{C}_{Dipp}$H), 124.2 (*m*-$\underline{C}_{Dipp}$H), 123.9 (*m*-$\underline{C}_{Dipp}$H), 123.8 (*m*-$\underline{C}_{Dipp}$H), 115.8 (N$\underline{C}$H), 115.4 (N$\underline{C}$H), 92.7 (d, $^1J_{PC}$ = 170.3 Hz, P$\underline{C}$H), 32.1 (C($\underline{C}$H$_3$)$_3$), 29.5 ($\underline{C}$H(CH$_3$)$_2$), 28.8 ($\underline{C}$H(CH$_3$)$_2$), 28.4 ($\underline{C}$H(CH$_3$)$_2$), 28.3 ($\underline{C}$H(CH$_3$)$_2$), 27.6 (CH($\underline{C}$H$_3$)$_2$), 27.3 (CH($\underline{C}$H$_3$)$_2$), 27.2 (d, $^3J_{PC}$ = 19.2 Hz, OC$\underline{C}$H$_3$), 27.1 (CH($\underline{C}$H$_3$)$_2$), 26.2 (CH($\underline{C}$H$_3$)$_2$), 25.3 (CH($\underline{C}$H$_3$)$_2$), 23.3 (CH($\underline{C}$H$_3$)$_2$), 22.9 (CH($\underline{C}$H$_3$)$_2$), 22.4 ($\underline{C}$(CH$_3$)$_3$), 21.1 (CH($\underline{C}$H$_3$)$_2$). The resonances for the PPh_3 nuclei could not be unambigously assigned due to non-chemical equivalence, coupling with ^{31}P and signal broadening.

^{29}Si{^{1}H} NMR (99 MHz, C_6D_6, 300 K): δ [ppm] = 0.9 ($\underline{Si}$^{t}Bu$_3$), –61.0 (d, $^2J_{PSi}$ = 20.4 Hz, $\underline{Si}$O$_2$).

^{31}P{^{1}H} NMR (203 MHz, C_6D_6, 300 K): δ [ppm] = –86.9.

Anal. Calcd. [%] for $C_{60}H_{82}N_3O_2PSi_2$: C, 74.72; H, 8.57; N, 4.36. Found [%]: C, 73.78; H, 8.67; N, 4.28.

LIFDI-MS: calculated (for $C_{60}H_{82}N_3O_2PSi_2$): 963.5683
observed: 963.5403

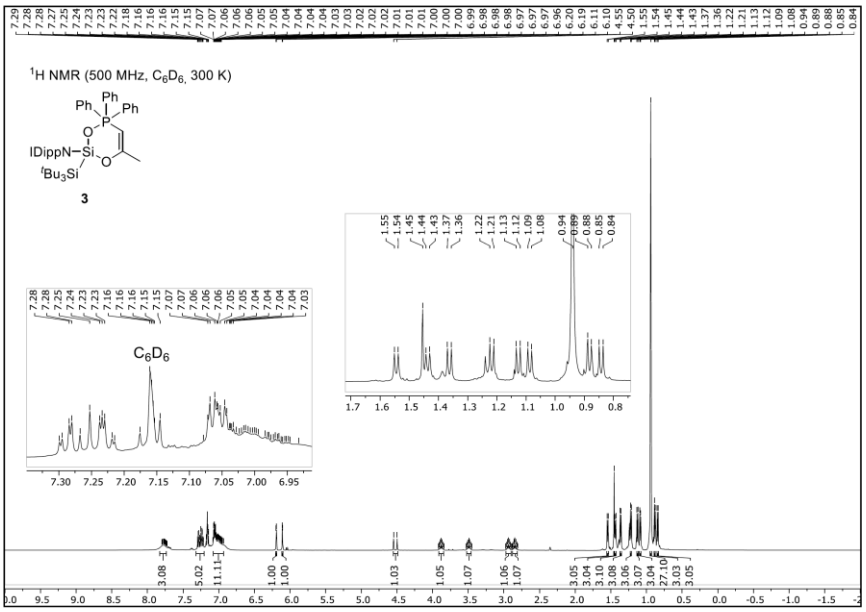


Figure S31. ^{1}H NMR spectrum of dioxaphosphasiline **3** in C_6D_6 at 300 K.

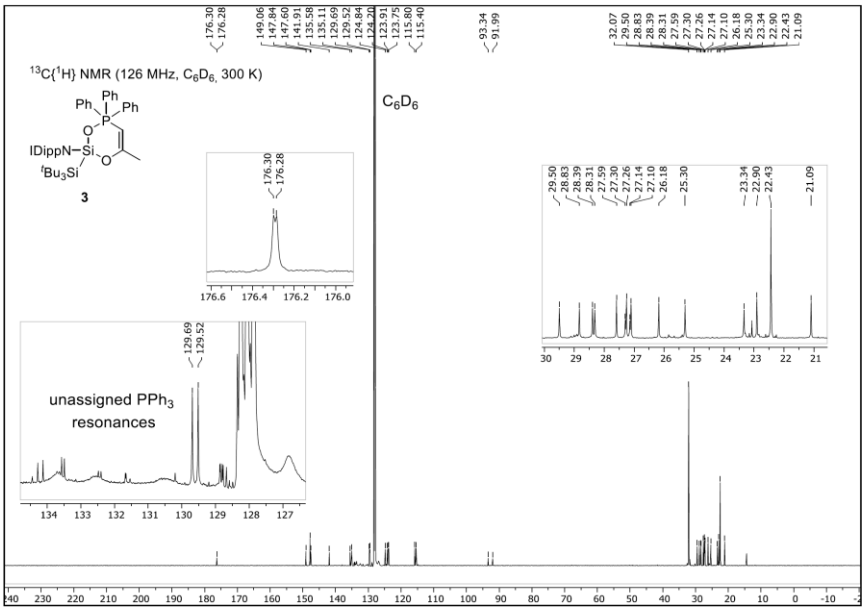


Figure S32. $^{13}C\{^{1}H\}$ NMR spectrum of dioxaphosphasiline **3** in C_6D_6 at 300 K.

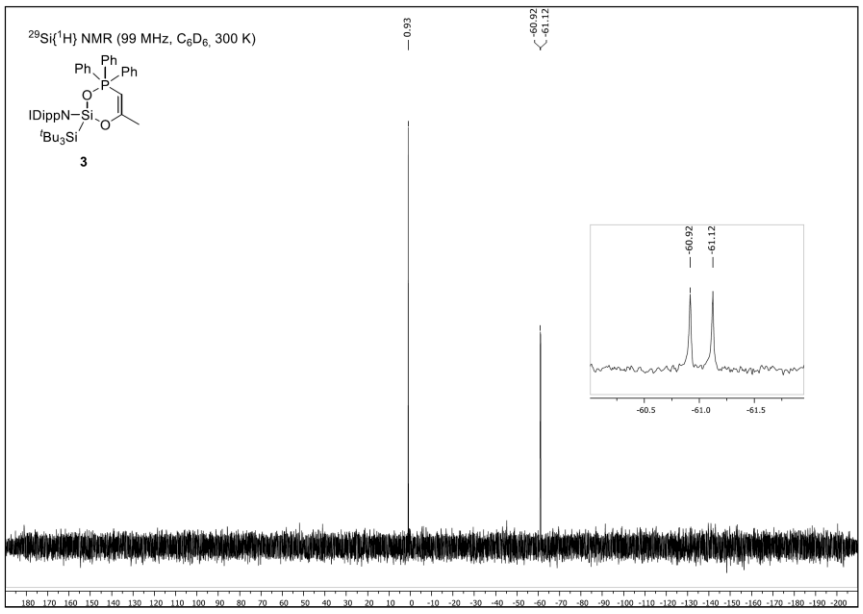


Figure S33. $^{29}Si\{^{1}H\}$ NMR spectrum of dioxaphosphasiline **3** in C_6D_6 at 300 K.

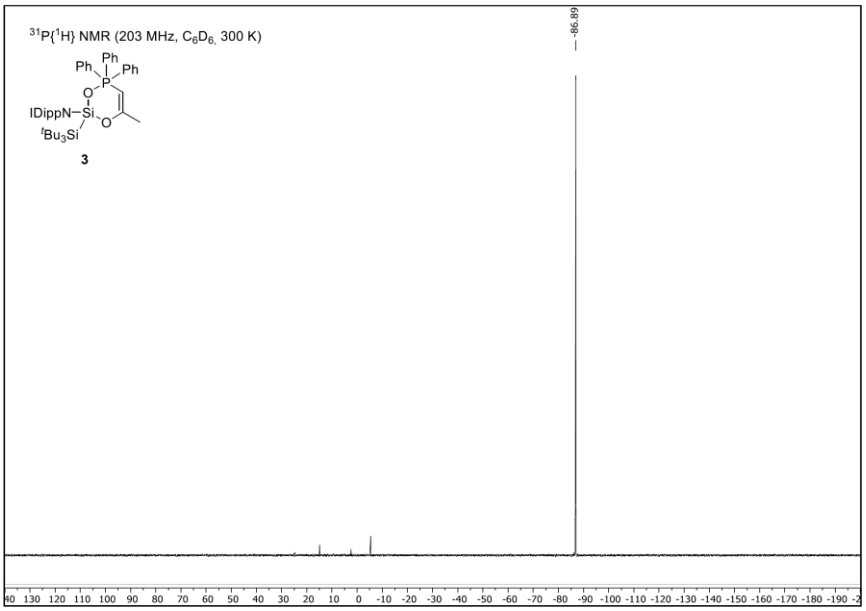


Figure S34. $^{31}P\{^{1}H\}$ NMR spectrum of dioxaphosphasiline **3** in C_6D_6 at 300 K.

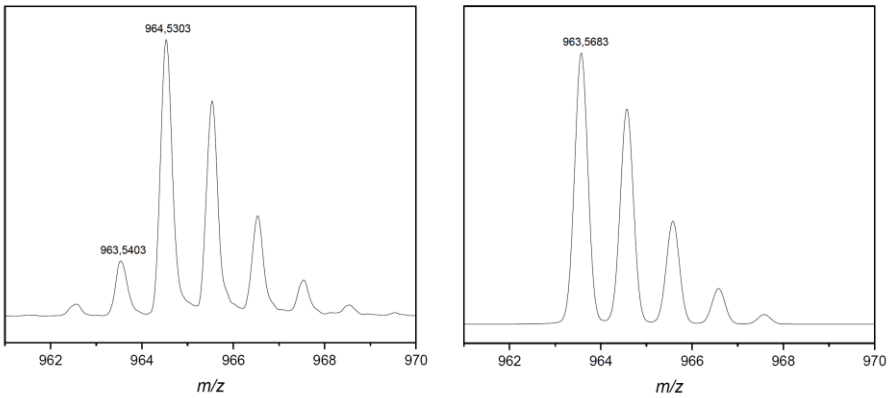
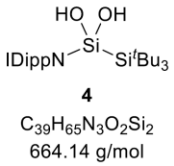


Figure S35. LIFDI-MS spectrometry (detail view with isotope pattern) of dioxaphosphasiline **3**. Measured (left; m/z = 963.5403) and simulated (right; m/z = 963.5683) mass spectrum. Due to an overlap with another mass peak, the observed isotope pattern does not perfectly match the simulated one.

1.4.2 Synthesis of (IDippN)(^{t}Bu$_3$Si)Si(OH)$_2$ (4)



4
$C_{39}H_{65}N_3O_2Si_2$
664.14 g/mol

Silanediol **4** was obtained by two different methods, either by addition of H_2O to dioxaphosphasiline **3** (Method A) or *via* direct exposure of silanone **1** to H_2O (Method B).

Method A:

To a solution of dioxaphosphasiline **3** (30 mg, 31.1 µmol, 1.0 eq.) in benzene (2 mL) was added a 0.02 M H_2O solution in THF (1.56 mL, 560 µg, 31.1 µmol, 1.0 eq.) under vigorous stirring. The observed color change from red to colorless indicated complete conversion. Removal of the solvent *in vacuo* provided a colorless solid identified by NMR spectroscopy as a mixture of silanediol **4** and ketone-substituted ylide **2a**.

Method B:

To a cooled (–80 °C) solution of silanone **1** (50 mg, 77.4 µmol, 1.0 eq.) in THF (2 mL) was added a 0.02 M H_2O solution in THF (3.87 mL, 1.39 mg, 77.4 µmol, 1.0 eq.) under vigorous stirring. Subsequently, the solution was warmed to ambient temperature. Removal of the solvent *in vacuo* provided silanediol **4** as a colorless solid (50 mg, 77.4 µmol, quantitative yield).

m.p.: 190-191 °C (decomposition; color change from colorless to pale yellow).

^{1}H NMR (500 MHz, C_6D_6, 300 K): δ [ppm] = 7.18–7.15 (m, 2H, *p*-$C_{ar}\underline{H}$, overlapping with solvent signal), 7.11–7.09 (m, 4H, *m*-$C_{ar}\underline{H}$), 5.96 (s, 2H, NC$\underline{H}$), 3.15 (sept, ^3J = 6.9 Hz, 4H, C$\underline{H}$(CH$_3$)$_2$), 1.39 (d, ^3J = 6.9 Hz, 12H, CH(C$\underline{H}_3$)$_2$), 1.20 (s, 27H, C(C$\underline{H}_3$)$_3$), 1.12 (d, ^3J = 6.9 Hz, 12H, CH(C$\underline{H}_3$)$_2$), 0.89 (s, 2H, O$\underline{H}$).

^{13}C{^{1}H} NMR (126 MHz, C_6D_6, 300 K): δ [ppm] = 148.0 (*o*-$\underline{C}_{ar}$), 143.4 (N$\underline{C}$N), 134.9 (*ipso*-$\underline{C}_{ar}$), 129.9 (*p*-$\underline{C}_{ar}$H), 124.3 (*m*-$\underline{C}_{ar}$H), 114.7 (N$\underline{C}$H), 31.9 (C($\underline{C}$H$_3$)$_3$), 29.0 ($\underline{C}$H(CH$_3$)$_2$), 25.3 (CH($\underline{C}$H$_3$)$_2$), 22.7 (CH($\underline{C}$H$_3$)$_2$), 22.5 ($\underline{C}$(CH$_3$)$_3$).

^{29}Si{^{1}H} NMR (99 MHz, C_6D_6, 300 K): δ [ppm] = –0.2 ($\underline{Si}$^{t}Bu$_3$), –44.7 ($\underline{Si}$(OH)$_2$).

Anal. Calcd. [%] for $C_{39}H_{65}N_3O_2Si_2$: C, 70.53; H, 9.87; N, 6.33. Found [%]: C, 69.50; H, 10.00; N, 6.23.

LIFDI-MS: calculated (for $C_{39}H_{65}N_3O_2Si_2$): 663.4615
observed: 663.4343

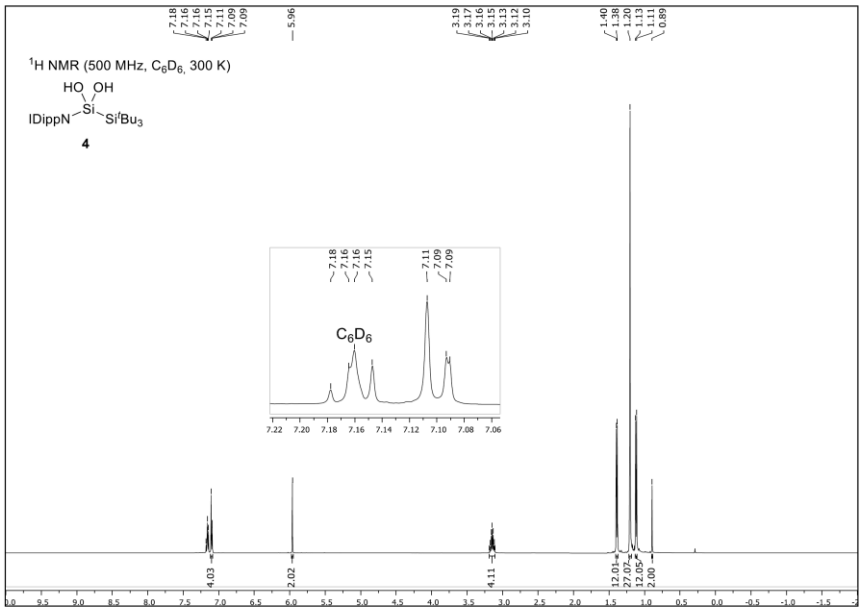


Figure S36. ^{1}H NMR spectrum of (IDippN)(^{t}Bu$_3$Si)Si(OH)$_2$ (**4**) in C_6D_6 at 300 K.

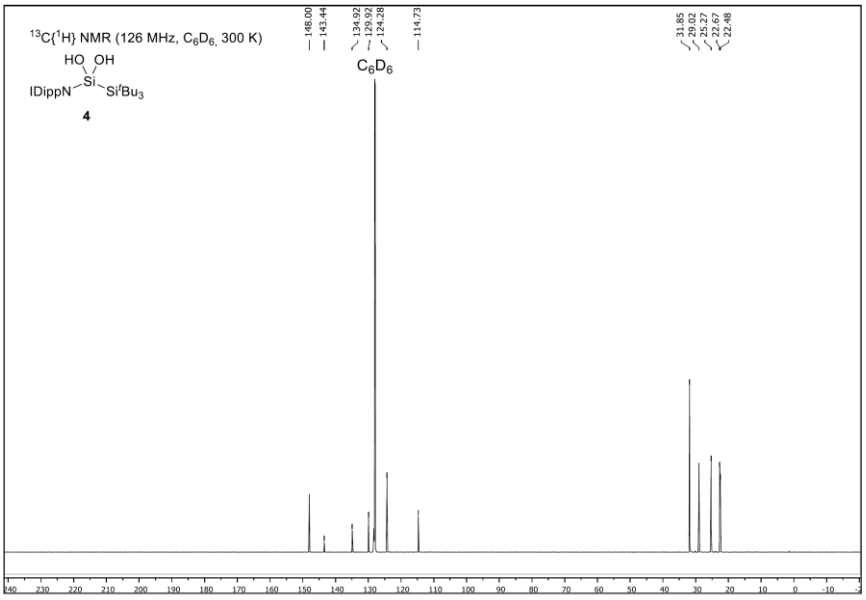


Figure S37. ^{13}C{^{1}H} NMR spectrum of (IDippN)(^{t}Bu$_3$Si)Si(OH)$_2$ (**4**) in C_6D_6 at 300 K.

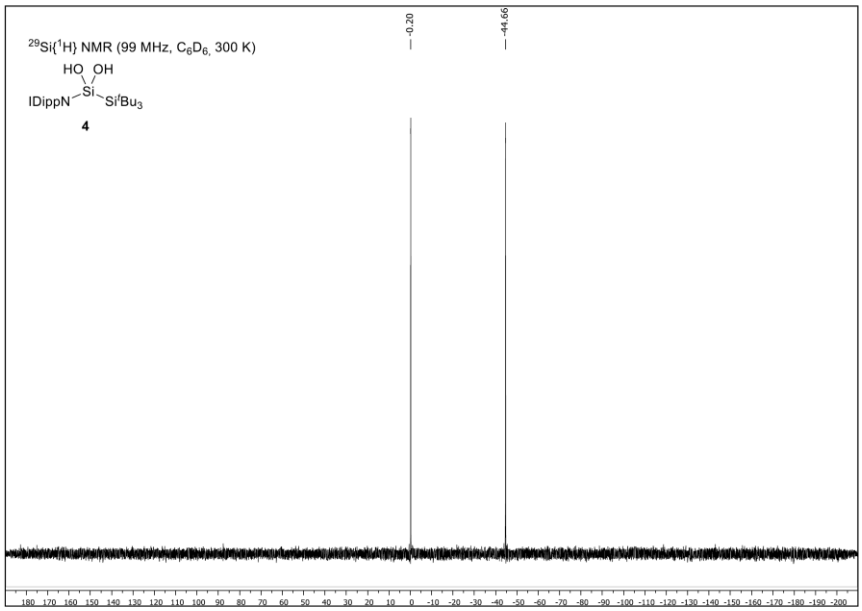


Figure S38. $^{29}Si\{^{1}H\}$ NMR spectrum of (IDippN)(^{t}Bu$_3$Si)Si(OH)$_2$ (**4**) in C_6D_6 at 300 K.

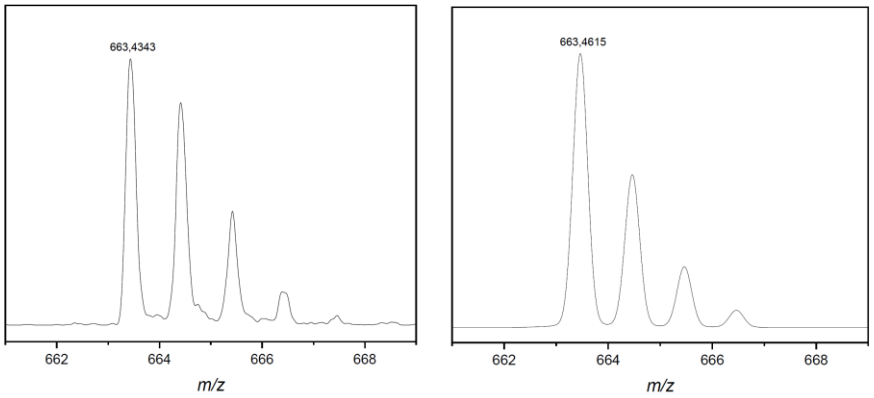
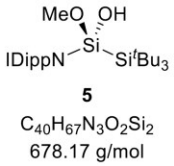


Figure S39. LIFDI-MS spectrometry (detail view with isotope pattern) of (IDippN)(^{t}Bu$_3$Si)Si(OH)$_2$ (**4**). Measured (left; m/z = 663.4343) and simulated (right; m/z = 663.4615) mass spectrum.

1.4.3 Synthesis of (IDippN)(^{t}Bu$_3$Si)Si(OH)(OMe) (5)



5
$C_{40}H_{67}N_3O_2Si_2$
678.17 g/mol

To a mixture of silanone **1** (100 mg, 155 µmol, 1.0 eq.) and ester-substituted ylide **2b** (51.8 mg, 155 µmol, 1.0 eq.) was added benzene (5 mL). The reaction mixture was stirred for one hour and subsequently the solvent removed *in vacuo*. The residue was extracted with *n*-hexane (3 × 2 mL) and filtered. Removal of the solvent of the filtrate *in vacuo* provided methoxysilanol **5** as a colorless solid (98.7 mg, 146 µmol, 94%). Crystals suitable for SC-XRD analysis were obtained by cooling a concentrated toluene solution of **5** to –35 °C for several days. The filter residue was identified as the Bestmann ylide $Ph_3P{=}C{=}C{=}O$[S5] (**5a**) by NMR spectroscopy. Colorless crystals thereof, suitable for SC-XRD analysis, were grown by storing a saturated toluene solution at –35 °C for a few days.

^{1}H NMR (500 MHz, C_6D_6, 300 K): δ [ppm] = 7.18–7.14 (m, 2H, *p*-$C_{ar}\underline{H}$, overlapping with solvent signal), 7.12–7.07 (m, 4H, *m*-$C_{ar}\underline{H}$), 5.96 (s, 2H, NC$\underline{H}$), 3.45 (s, 3H, OC$\underline{H}_3$), 3.22 (sept, ^3J = 6.9 Hz, 2H, C$\underline{H}$(CH$_3$)$_2$), 3.11 (sept, ^3J = 6.9 Hz, 2H, C$\underline{H}$(CH$_3$)$_2$), 1.38 (d, ^3J = 6.9 Hz, 12H, CH(C$\underline{H}_3$)$_2$), 1.23 (s, 27H, C(C$\underline{H}_3$)$_3$), 1.11 (d, ^3J = 6.9 Hz, 6H, CH(C$\underline{H}_3$)$_2$), 1.10 (d, ^3J = 6.9 Hz, 6H, CH(C$\underline{H}_3$)$_2$), 0.50 (s, 1H, O$\underline{H}$).

^{13}C{^{1}H} NMR (126 MHz, C_6D_6, 300 K): δ [ppm] = 148.0 (*o*-$\underline{C}_{ar}$), 147.9 (*o*-$\underline{C}_{ar}$), 143.2 (N$\underline{C}$N), 134.9 (*ipso*-$\underline{C}_{ar}$), 129.9 (*p*-$\underline{C}_{ar}$H), 124.3 (*m*-$\underline{C}_{ar}$H), 124.1 (*m*-$\underline{C}_{ar}$H), 115.0 (N$\underline{C}$H), 49.7 (O$\underline{C}$H$_3$), 31.9 (C($\underline{C}$H$_3$)$_3$), 28.9 ($\underline{C}$H(CH$_3$)$_2$), 28.8 ($\underline{C}$H(CH$_3$)$_2$), 25.7 (CH($\underline{C}$H$_3$)$_2$), 25.5 (CH($\underline{C}$H$_3$)$_2$), 22.7 (CH($\underline{C}$H$_3$)$_2$), 22.5 ($\underline{C}$(CH$_3$)$_3$), 22.4 (CH($\underline{C}$H$_3$)$_2$).

^{29}Si{^{1}H} NMR (99 MHz, C_6D_6, 300 K): δ [ppm] = 1.1 ($\underline{Si}$^{t}Bu$_3$), –46.6 ($\underline{Si}$(OH)(OMe)).

The spectroscopic data match those recently reported.[S2]

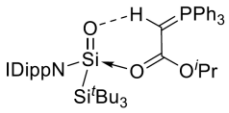
Spectroscopic data for Bestmann ylide $Ph_3P{=}C{=}C{=}O$ (5a):

^{1}H NMR (400 MHz, C_6D_6, 300 K): δ [ppm] = 7.58–7.52 (m, 6H, $C_{ar}\underline{H}$), 7.04–6.91 (m, 9H, $C_{ar}\underline{H}$).

^{31}P{^{1}H} NMR (162 MHz, C_6D_6, 300 K): δ [ppm] = 3.0.

The spectroscopic data are consistent with those previously reported.[S6]

1.4.4 Synthesis of ylide-stabilized silanone 6



6
$C_{62}H_{86}N_3O_3PSi_2$
1008.53 g/mol

To a mixture of silanone **1** (300 mg, 464 µmol, 1.0 eq.) and ester-substituted ylide **2c** (168 mg, 464 µmol, 1.0 eq.) was added benzene (10 mL). The reaction mixture was stirred for one hour, whereby formation of a precipitate was observed. Subsequently, the amount of solvent was reduced *in vacuo* and *n*-hexane (15 mL) was added to ensure complete precipitation. The solid was separated *via* filtration, washed with *n*-hexane and dried *in vacuo* providing ylide-stabilized silanone **6** as a colorless solid (432 mg, 428 µmol, 92%). Crystals suitable for SC-XRD analysis were obtained by cooling a concentrated THF solution of **6** to –35 °C overnight. Adduct **6** isomerizes slowly to compound **7** in solution (*vide infra*).

m.p.: 128-129 °C (decomposition; color change from colorless to amber).

^{1}H NMR (500 MHz, C_6D_6, 300 K): δ [ppm] = 7.63–7.59 (m, 6H, $C_{ar}\underline{H}$), 7.55 (d, $^2J_{PH}$ = 21.7 Hz, 1H, PC$\underline{H}$), 7.32 (d, ^3J = 7.5 Hz, 2H, *m*-$C_{Dipp}\underline{H}$), 7.11–7.00 (m, 11H, $C_{ar}\underline{H}$ + *p*-$C_{Dipp}\underline{H}$), 6.91 (d, ^3J = 7.5 Hz, 2H, *m*-$C_{Dipp}\underline{H}$), 6.12 (s, 2H, NC$\underline{H}$), 5.15 (sept, ^3J = 6.3 Hz, 1H, OC$\underline{H}$(CH$_3$)$_2$), 3.88 (sept, ^3J = 6.9 Hz, 2H, C$\underline{H}$(CH$_3$)$_2$), 3.19 (sept, ^3J = 6.9 Hz, 2H, C$\underline{H}$(CH$_3$)$_2$), 1.87 (d, ^3J = 6.9 Hz, 6H, CH(C$\underline{H}_3$)$_2$), 1.45 (s, 27H, C(C$\underline{H}_3$)$_3$), 1.33 (d, ^3J = 6.9 Hz, 6H, CH(C$\underline{H}_3$)$_2$), 1.28 (d, ^3J = 6.9 Hz, 6H, CH(C$\underline{H}_3$)$_2$), 1.21 (d, ^3J = 6.9 Hz, 6H, CH(C$\underline{H}_3$)$_2$), 0.92 (d, ^3J = 6.3 Hz, 3H, OCH(C$\underline{H}_3$)$_2$), 0.68 (d, ^3J = 6.3 Hz, 3H, OCH(C$\underline{H}_3$)$_2$).

^{13}C{^{1}H} NMR (126 MHz, C_6D_6, 300 K): δ [ppm] = 170.2 (d, $^2J_{PC}$ = 6.9 Hz, $\underline{C}$=O), 150.1 (*o*-$\underline{C}_{Dipp}$), 146.6 (*o*-$\underline{C}_{Dipp}$), 142.6 (N$\underline{C}$N), 136.9 (*ipso*-$\underline{C}_{Dipp}$), 133.8 (d, $^3J_{PC}$ = 10.3 Hz, *m*-$\underline{C}_{ar}$H), 132.5 (d, $^4J_{PC}$ = 3.0 Hz, *p*-$\underline{C}_{ar}$H), 128.9 (d, $^2J_{PC}$ = 12.5 Hz, *o*-$\underline{C}_{ar}$H), 128.4 (*p*-$\underline{C}_{Dipp}$H), 126.4 (d, $^1J_{PC}$ = 91.2 Hz, *ipso*-$\underline{C}_{ar}$), 123.5 (*m*-$\underline{C}_{Dipp}$H), 123.3 (*m*-$\underline{C}_{Dipp}$H), 115.0 (N$\underline{C}$H), 67.6 (O$\underline{C}$H(CH$_3$)$_2$), 42.5 (d, $^1J_{PC}$ = 111.0 Hz, P$\underline{C}$H), 32.7 (C($\underline{C}$H$_3$)$_3$), 29.6 ($\underline{C}$H(CH$_3$)$_2$), 28.5 ($\underline{C}$H(CH$_3$)$_2$), 25.8 (CH($\underline{C}$H$_3$)$_2$), 25.6 (CH($\underline{C}$H$_3$)$_2$), 24.0 (CH($\underline{C}$H$_3$)$_2$), 23.2 ($\underline{C}$(CH$_3$)$_3$ + OCH($\underline{C}$H$_3$)$_2$), 22.6 (CH($\underline{C}$H$_3$)$_2$), 22.2 (OCH($\underline{C}$H$_3$)$_2$).

^{29}Si{^{1}H} NMR (99 MHz, C_6D_6, 300 K): δ [ppm] = –3.2 ($\underline{Si}$^{t}Bu$_3$), –50.2 ($\underline{Si}$=O).

^{31}P{^{1}H} NMR (203 MHz, C_6D_6, 300 K): δ [ppm] = 12.9.

Anal. Calcd. [%] for $C_{62}H_{86}N_3O_3PSi_2$: C, 73.84; H, 8.60; N, 4.17. Found [%]: C, 73.17; H, 8.76; N, 4.19.

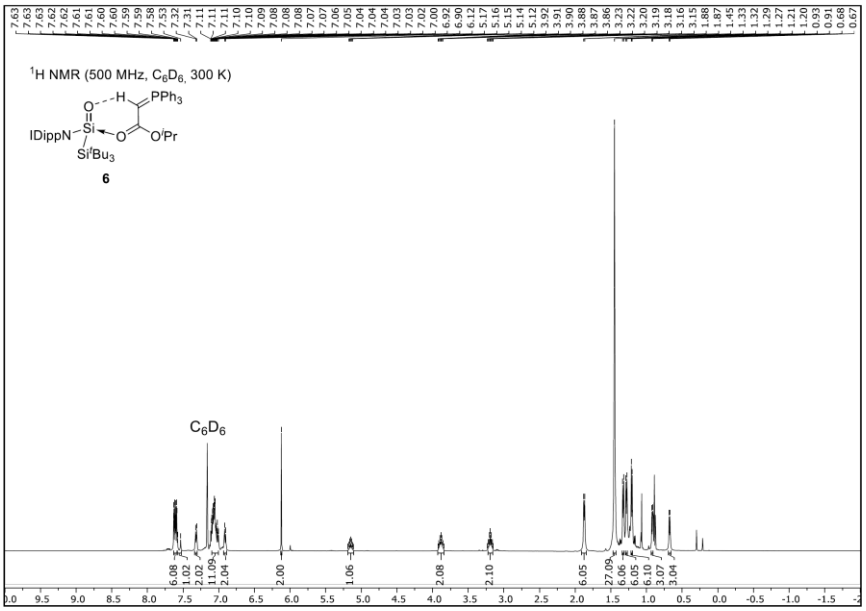


Figure S40. ^{1}H NMR spectrum of ylide-stabilized silanone **6** in C_6D_6 at 300 K.

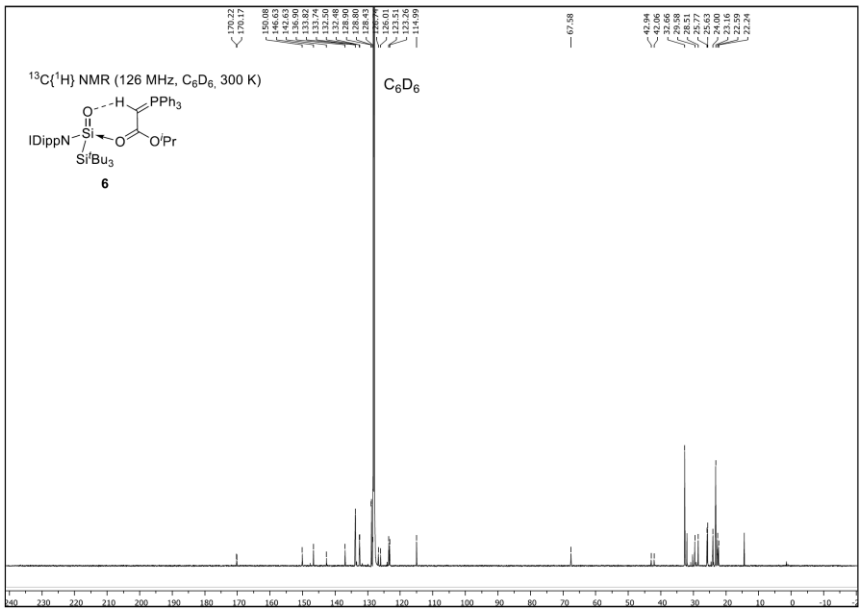


Figure S41. ^{13}C{^{1}H}99.2 NMR spectrum of ylide-stabilized silanone **6** in C_6D_6 at 300 K.

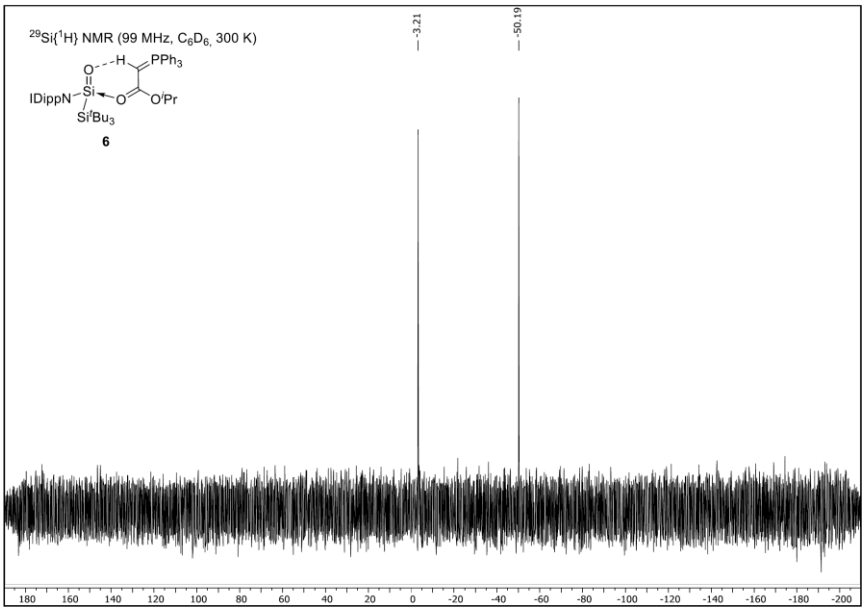


Figure S42. $^{29}Si\{^1H\}$ NMR spectrum of ylide-stabilized silanone **6** in C_6D_6 at 300 K.

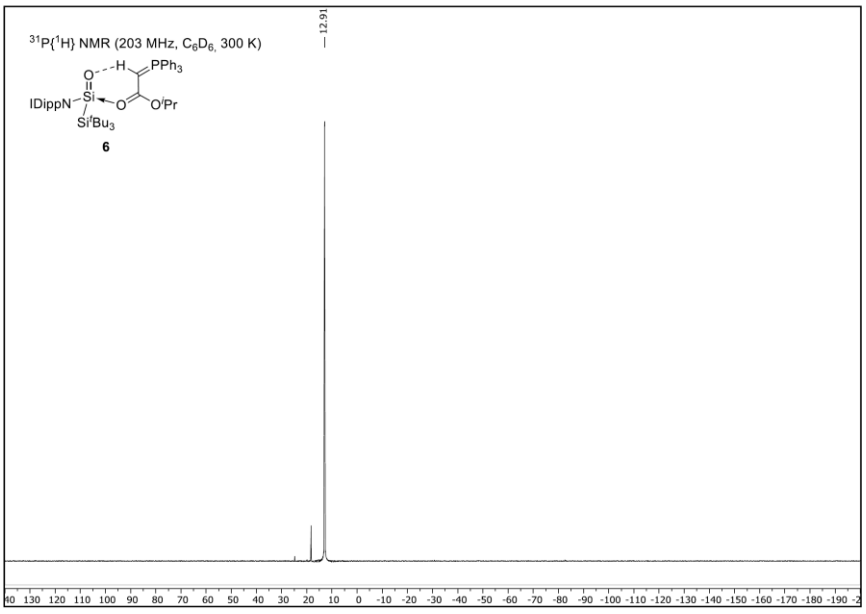
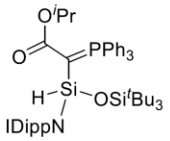


Figure S43. $^{31}P\{^1H\}$ NMR spectrum of ylide-stabilized silanone **6** in C_6D_6 at 300 K.

1.4.5 Synthesis of silyl-substituted phosphorus ylide 7



7
$C_{62}H_{86}N_3O_3PSi_2$
1008.53 g/mol

A solution of ylide-stabilized silanone **6** (100 mg, 99.2 µmol) in benzene (3 mL) was heated to 65 °C for 16 hours. Quantitative conversion was detected by ^{1}H NMR spectroscopy. Removal of the solvent *in vacuo* afforded silyl-substituted phosphorus ylide **7** as a colorless solid (100 mg, 99.2 µmol, quantitative yield).

Note: Compound **7** can also be obtained by stirring a reaction mixture of iminosiloxysilylene (IDippN)(^{t}Bu$_3$SiO)Si: (**1′**)[S2] with an equimolar amount of ylide **2c** in benzene at ambient temperature for 16 h. Subsequent solvent removal provides **7** in quantitative yield.

m.p.: 217-218 °C (decomposition; color change from colorless to black).

^{1}H NMR (500 MHz, C_6D_6, 300 K): δ [ppm] = 7.44–7.40 (m, 6H, C$_{ar}$H), 7.28 (dd, ^4J = 1.5 Hz, ^3J = 7.7 Hz, 2H, *m*-C$_{Dipp}$H), 7.19 (*pseudo* t, ^3J = 7.7 Hz, 2H, *p*-C$_{Dipp}$H), 7.12–7.07 (m, 9H, C$_{ar}$H), 6.99 (dd, ^4J = 1.5 Hz, ^3J = 7.7 Hz, 2H, *m*-C$_{Dipp}$H), 5.99 (s, 2H, NCH), 4.91 (sept, ^3J = 6.3 Hz, 1H, OCH(CH$_3$)$_2$), 4.50 (d, $^3J_{PH}$ = 3.1 Hz, 1H, SiH), 3.99 (br sept, ^3J = 6.9 Hz, 2H, CH(CH$_3$)$_2$), 3.21 (sept, ^3J = 6.9 Hz, 2H, CH(CH$_3$)$_2$), 1.52 (br d, ^3J = 6.9 Hz, 6H, CH(CH$_3$)$_2$), 1.37 (d, ^3J = 6.9 Hz, 6H, CH(CH$_3$)$_2$), 1.30 (d, ^3J = 6.9 Hz, 6H, CH(CH$_3$)$_2$), 1.27 (d, ^3J = 6.9 Hz, 6H, CH(CH$_3$)$_2$), 1.07 (s, 27H, C(CH$_3$)$_3$), 0.96 (d, ^3J = 6.3 Hz, 3H, OCH(CH$_3$)$_2$), 0.66 (d, ^3J = 6.3 Hz, 3H, OCH(CH$_3$)$_2$).

^{13}C{^{1}H} NMR (126 MHz, C_6D_6, 300 K): δ [ppm] = 168.9 (C=O), 148.9 (*o*-C$_{Dipp}$), 147.2 (*o*-C$_{Dipp}$), 139.8 (NCN), 136.8 (*ipso*-C$_{Dipp}$), 135.2 (d, $^3J_{PC}$ = 9.6 Hz, *m*-C$_{ar}$H), 130.9 (d, $^4J_{PC}$ = 2.9 Hz, *p*-C$_{ar}$H), 130.2 (d, $^1J_{PC}$ = 88.0 Hz, *ipso*-C$_{ar}$), 128.6 (*p*-C$_{Dipp}$H), 127.6 (d, $^2J_{PC}$ = 11.9 Hz, *o*-C$_{ar}$H), 125.0 (*m*-C$_{Dipp}$H), 123.8 (*m*-C$_{Dipp}$H), 115.2 (NCH), 64.2 (OCH(CH$_3$)$_2$), 30.8 (C(CH$_3$)$_3$), 29.6 (CH(CH$_3$)$_2$), 28.6 (CH(CH$_3$)$_2$), 25.5 (CH(CH$_3$)$_2$), 24.2 (CH(CH$_3$)$_2$), 24.1 (CH(CH$_3$)$_2$), 23.3 (C(CH$_3$)$_3$), 22.8 (OCH(CH$_3$)$_2$), 22.3 (CH(CH$_3$)$_2$), 21.9 (OCH(CH$_3$)$_2$). The resonance of the P=C nucleus could not be located.

^{29}Si{^{1}H} NMR (99 MHz, C_6D_6, 300 K): δ [ppm] = 0.3 (Si^{t}Bu$_3$), –58.6 (d, $^2J_{PSi}$ = 38.6 Hz, SiH).

^{29}Si INEPT NMR (99 MHz, C_6D_6, 300 K): δ [ppm] = 0.3 (Si^{t}Bu$_3$), –58.7 (dd, $^1J_{HSi}$ = 229.8 Hz, $^2J_{PSi}$ = 38.2 Hz, SiH).

^{31}P{^{1}H} NMR (203 MHz, C_6D_6, 300 K): δ [ppm] = 19.9.

Anal. Calcd. [%] for $C_{62}H_{86}N_3O_3PSi_2$: C, 73.84; H, 8.60; N, 4.17. Found [%]: C, 74.49; H, 8.81; N, 4.12.

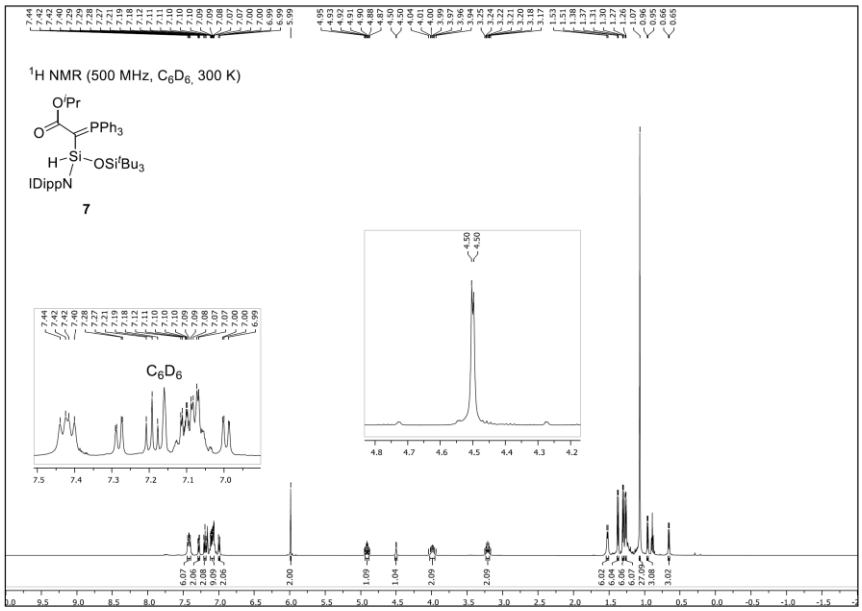


Figure S44. ^{1}H NMR spectrum of silyl-substituted phosphorus ylide **7** in C_6D_6 at 300 K.

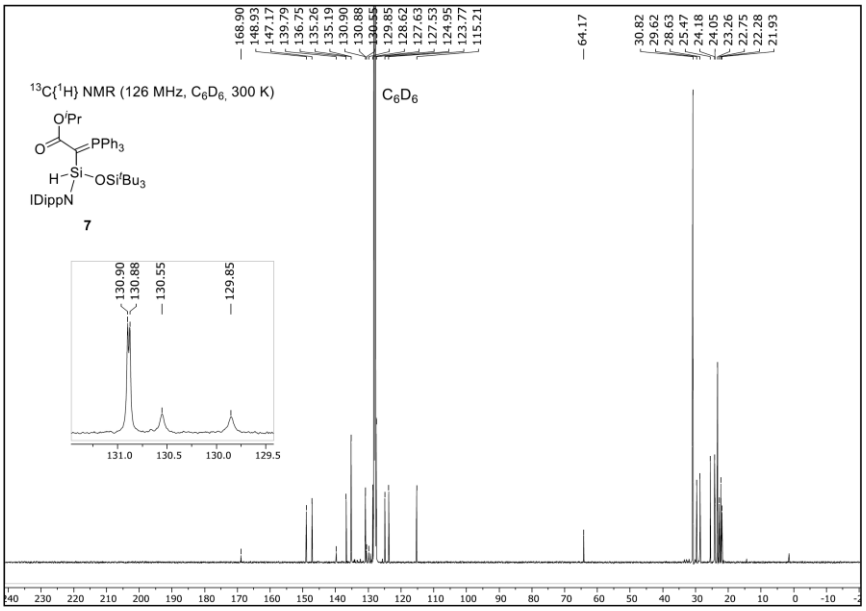


Figure S45. ^{13}C{^{1}H} NMR spectrum of silyl-substituted phosphorus ylide **7** in C_6D_6 at 300 K.

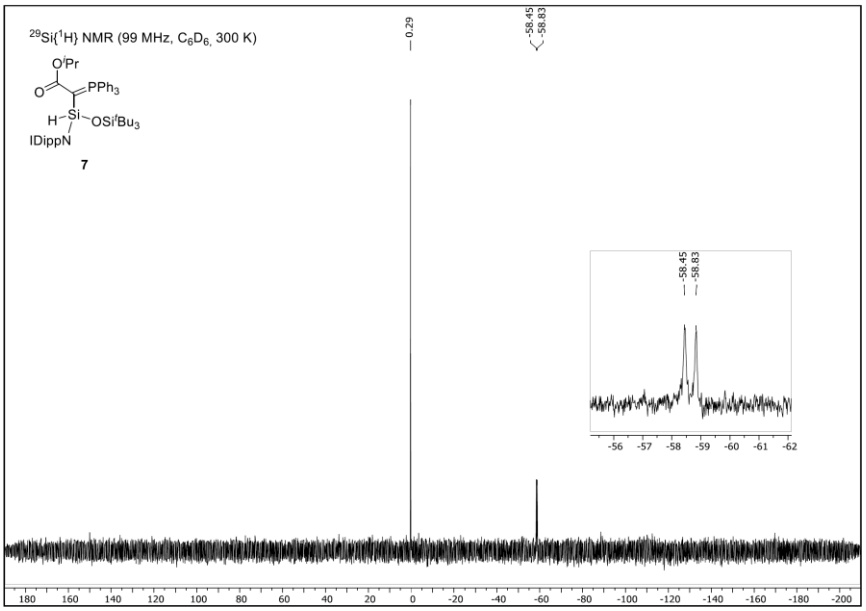


Figure S46. $^{29}Si\{^{1}H\}$ NMR spectrum of silyl-substituted phosphorus ylide **7** in C_6D_6 at 300 K.

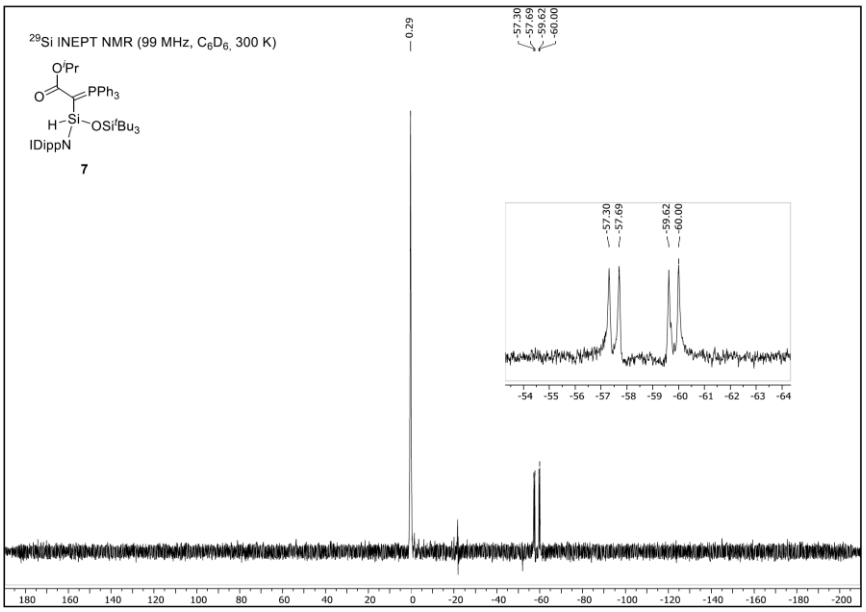


Figure S47. ^{29}Si INEPT NMR spectrum of silyl-substituted phosphorus ylide **7** in C_6D_6 at 300 K.

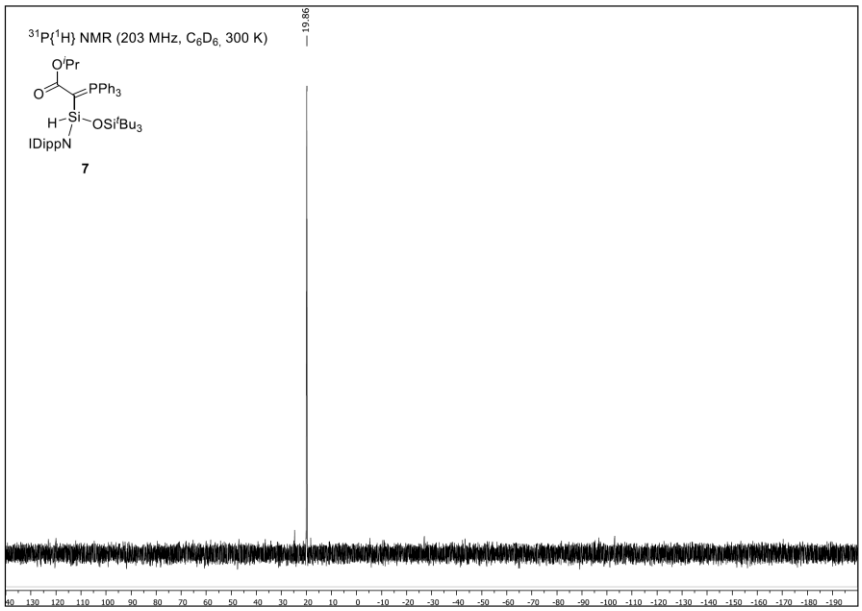


Figure S48. $^{31}P\{^{1}H\}$ NMR spectrum of silyl-substituted phosphorus ylide **7** in C_6D_6 at 300 K.

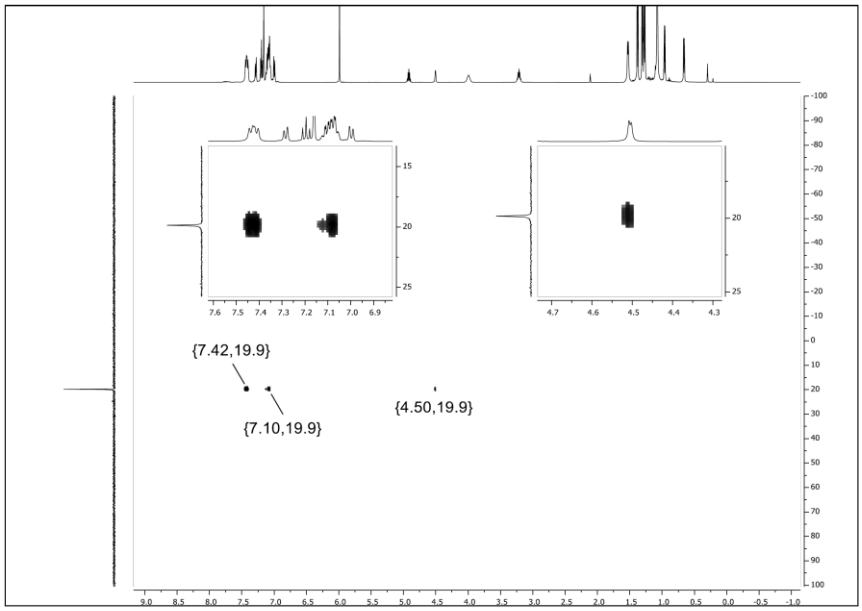
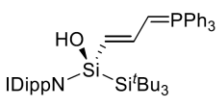


Figure S49. $^{1}H/^{31}P$ HMBC NMR spectrum of silyl-substituted phosphorus ylide **7** in C_6D_6 at 300 K.

1.5 Reactivity of silanone 1 toward semi-stabilized ylides

1.5.1 Synthesis of silanoyl-substituted phosphorus ylide 8



8

$C_{60}H_{82}N_3OPSi_2$

948.48 g/mol

Benzene (3 mL) was added to a mixture of **1** (100 mg, 155 µmol, 1.0 eq.) and **2d** (46.8 g, 155 µmol, 1.0 eq.) at ambient temperature. The resulting solution was stirred for 30 min. Removal of the solvent *in vacuo* afforded silanoyl-substituted phosphorus ylide **8** as an orange powder (146.8 mg, 155 µmol, quantitative yield). Crystals, suitable for SC-XRD analysis, were obtained by storing a saturated C_6D_6 solution of **8** at room temperature overnight.

Note: multinuclear NMR spectroscopy revealed the presence of an additional species ($\delta(^{29}Si)$ = 0.1 & –33.1 ppm), presumably another stereoisomer of **8** or the silacyclobutene analogue to compound **9** (*vide infra*). However, further purification and identification was not possible so far.

^{1}H NMR (500 MHz, C_6D_6, 300 K): δ [ppm] = 7.59–7.55 (m, 6H, $C_{ar}\underline{H}$), 7.19–7.17 (m, 4H, $C_{ar}\underline{H}$), 7.12–7.07 (m, 11H, $C_{ar}\underline{H}$), 6.29 (pseudo dt, ^3J = 17.1 Hz, ^3J = 12.5 Hz, 1H, SiCHC$\underline{H}$), 6.06 (s, 2H, NC$\underline{H}$), 4.95 (d, ^3J = 17.1 Hz, 1H, SiC$\underline{H}$CH), 3.59 (sept, ^3J = 6.9 Hz, 2H, C$\underline{H}(CH_3)_2$), 3.22 (sept, ^3J = 6.9 Hz, 2H, C$\underline{H}(CH_3)_2$), 2.98 (dd, $^2J_{PH}$ = 23.7 Hz, ^3J = 12.5 Hz, 1H, C$\underline{H}$P), 1.51 (d, ^3J = 6.9 Hz, 6H, CH(C$\underline{H}_3)_2$), 1.48 (d, ^3J = 6.9 Hz, 6H, CH(C$\underline{H}_3)_2$), 1.33 (s, 27H, C(C$\underline{H}_3)_3$), 1.20 (d, ^3J = 6.9 Hz, 6H, CH(C$\underline{H}_3)_2$), 1.18 (d, ^3J = 6.9 Hz, 6H, CH(C$\underline{H}_3)_2$), –0.15 (s, 1H, O$\underline{H}$).

^{13}C{^{1}H} NMR (126 MHz, C_6D_6, 300 K): δ [ppm] = 148.7 (*o*-$\underline{C}_{Dipp}$), 148.4 (*o*-$\underline{C}_{Dipp}$), 145.4 (d, $^3J_{PC}$ = 7.5 Hz, Si$\underline{C}$HCH), 142.2 (N$\underline{C}$N), 135.9 (*ipso*-$\underline{C}_{Dipp}$), 133.1 (d, $^3J_{PC}$ = 9.6 Hz, *m*-$\underline{C}_{ar}$H), 131.4 (d, $^1J_{PC}$ = 86.1 Hz, *ipso*-$\underline{C}_{ar}$), 131.3 (d, $^4J_{PC}$ = 2.8 Hz, *p*-$\underline{C}_{ar}$H), 129.2 (*p*-$\underline{C}_{Dipp}$H), 128.7 (d, $^2J_{PC}$ = 11.6 Hz, *o*-$\underline{C}_{ar}$H), 124.2 (*m*-$\underline{C}_{Dipp}$H), 123.6 (*m*-$\underline{C}_{Dipp}$H), 114.8 (N$\underline{C}$H), 109.6 (d, $^2J_{PC}$ = 17.8 Hz, SiCH$\underline{C}$H), 36.0 (d, $^1J_{PC}$ = 121.5 Hz, $\underline{C}$HP), 32.2 (C($\underline{C}H_3)_3$), 29.1 ($\underline{C}H(CH_3)_2$), 29.0 ($\underline{C}H(CH_3)_2$), 26.2 (CH($\underline{C}H_3)_2$), 25.6 (CH($\underline{C}H_3)_2$), 23.3 ($\underline{C}(CH_3)_3$), 23.1 (CH($\underline{C}H_3)_2$), 22.2 (CH($\underline{C}H_3)_2$).

^{29}Si{^{1}H} NMR (99 MHz, C_6D_6, 300 K): δ [ppm] = –2.7 ($\underline{Si}^tBu_3$), –30.4 (d, $^4J_{PSi}$ = 3.4 Hz, $\underline{Si}$OH).

^{31}P{^{1}H} NMR (203 MHz, C_6D_6, 300 K): δ [ppm] = 9.6.

LIFDI-MS: calculated (for $C_{60}H_{82}N_3OPSi_2$): 947.5734
observed: 947.5626

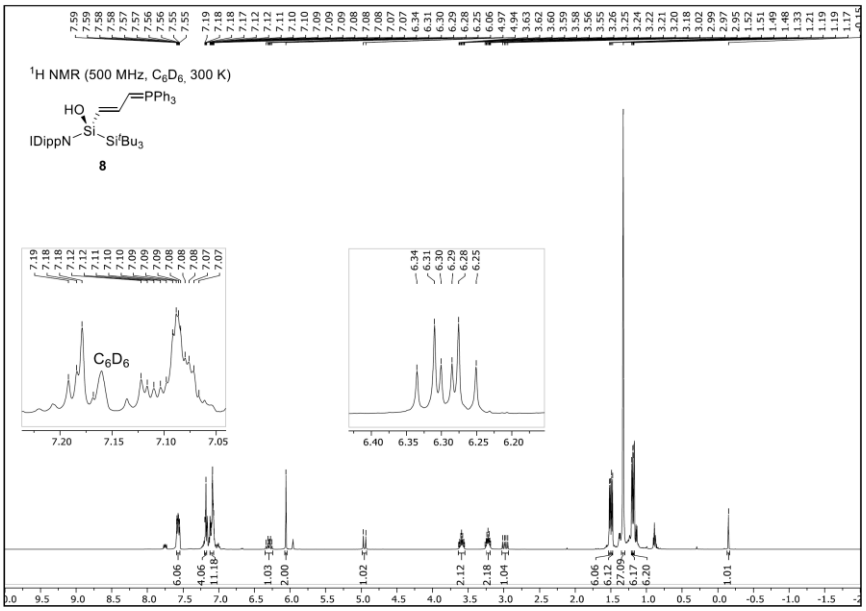


Figure S50. ^{1}H NMR spectrum of silanoyl-substituted phosphorus ylide **8** in C_6D_6 at 300 K.

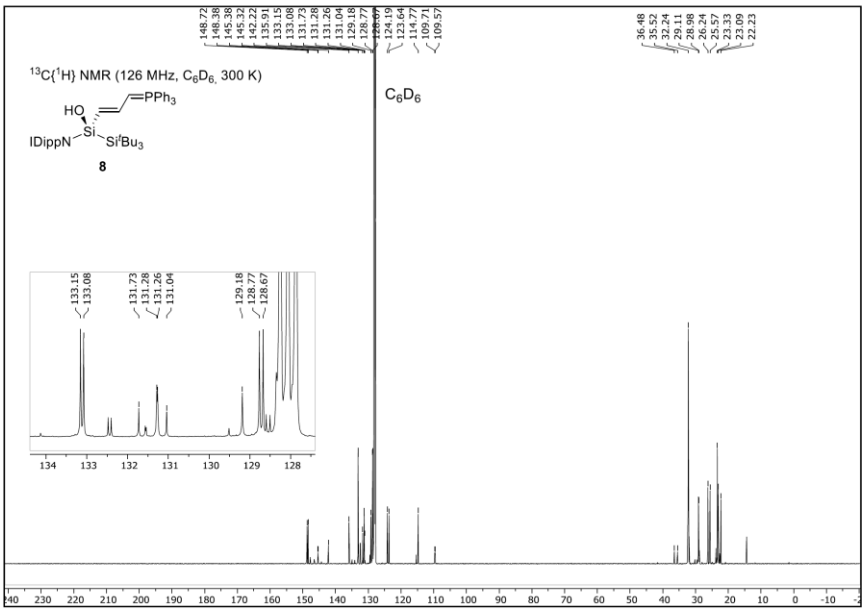


Figure S51. ^{13}C{^{1}H} NMR spectrum of silanoyl-substituted phosphorus ylide **8** in C_6D_6 at 300 K.

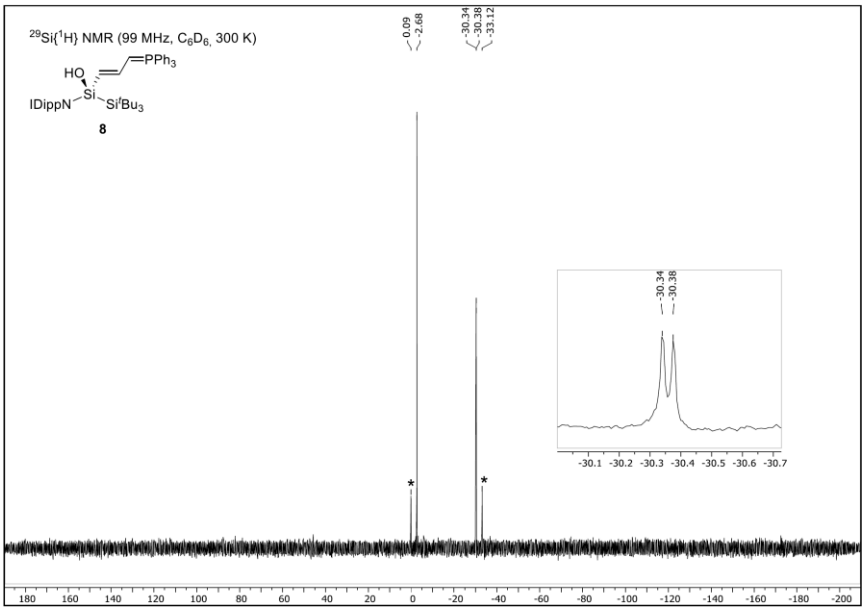


Figure S52. $^{29}Si\{^{1}H\}$ NMR spectrum of silanoyl-substituted phosphorus ylide **8** in C_6D_6 at 300 K. The resonances for the unidentified by-product are marked with asterisks *.

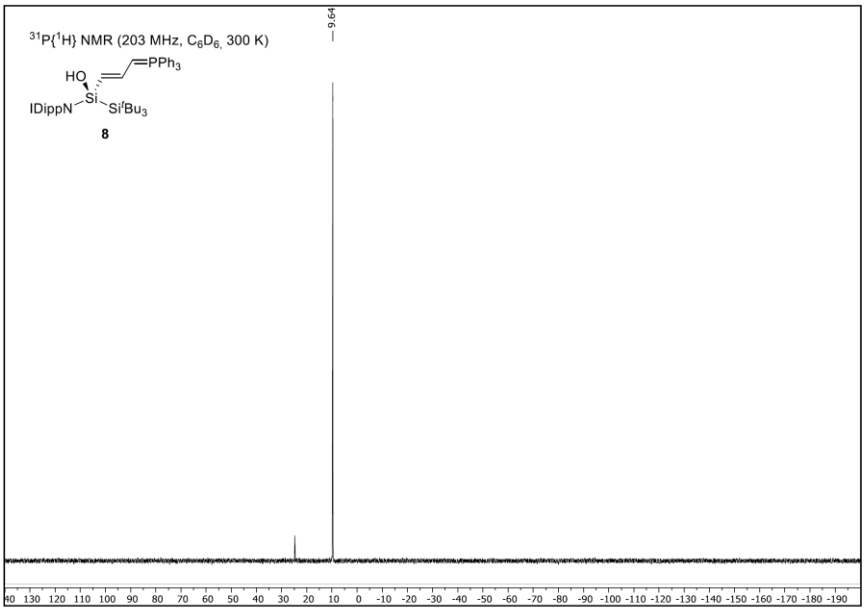


Figure S53. $^{31}P\{^{1}H\}$ NMR spectrum of silanoyl-substituted phosphorus ylide **8** in C_6D_6 at 300 K.

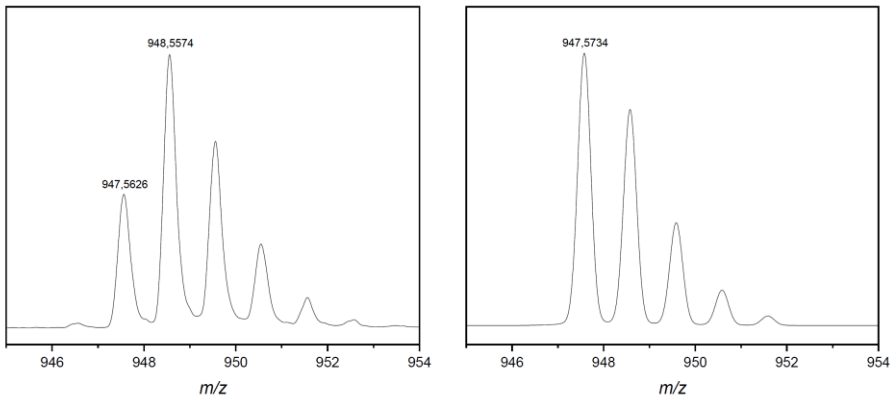
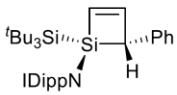


Figure S54. LIFDI-MS spectrometry (detail view with isotope pattern) of silanoyl-substituted phosphorus ylide **8**. Measured (left; m/z = 947.5626) and simulated (right; m/z = 947.5734) mass spectrum. Due to an overlap with another mass peak, the observed isotope pattern does not perfectly match the simulated one.

1.5.2 Synthesis of silacyclobutene 9



9
$C_{48}H_{71}N_3Si_2$
746.29 g/mol

Benzene (5 mL) was added to a mixture of **1** (300 mg, 464 µmol, 1.0 eq.) and **2e** (176 mg, 464 µmol, 1.0 eq.) at ambient temperature. The resulting solution was stirred for 1 h. Subsequently, the solvent was removed *in vacuo* and the residue extracted with cold *n*-hexane (3 × 2 mL). $Ph_3P{=}O$ was separated from the mixture *via* filtration and the solvent of the filtrate was removed under vacuum. Crystallization of the residue from *n*-hexane/toluene at –35 °C provided **9** as colorless crystals (278 mg, 373 µmol, 80%), which were suitable for SC-XRD analysis.

Note: ^{1}H NMR spectroscopy revealed the presence of an additional unidentified species (or stereoisomer of **9**). However, further purification and identification was not possible so far. No satisfying elemental analysis of compound **9** could be obtained, presumably due to the additional species or silicon carbide formation.

^{1}H NMR (500 MHz, C_6D_6, 300 K): δ [ppm] = 7.23–7.20 (m, 4H, $C_{ar}\underline{H}$), 7.17–7.16 (m, 3H, $C_{ar}\underline{H}$, overlapping with solvent signal), 7.14–7.10 (m, 4H, $C_{ar}\underline{H}$), 6.70 (dd, ^3J = 7.3 Hz, ^3J = 1.3 Hz, 1H, SiC$\underline{H}$CH), 5.98 (s, 2H, NC$\underline{H}$), 5.83 (dd, ^3J = 7.3 Hz, ^3J = 2.8 Hz, 1H, SiCHC$\underline{H}$), 3.44 (sept, ^3J = 6.9 Hz, 2H, C$\underline{H}$(CH$_3$)$_2$), 3.38 (br s, 1H, SiC$\underline{H}$Ph), 3.14 (sept, ^3J = 6.9 Hz, 2H, C$\underline{H}$(CH$_3$)$_2$), 1.48 (d, ^3J = 6.9 Hz, 6H, CH(C$\underline{H}_3$)$_2$), 1.32 (d, ^3J = 6.9 Hz, 6H, CH(C$\underline{H}_3$)$_2$), 1.16 (d, ^3J = 6.9 Hz, 6H, CH(C$\underline{H}_3$)$_2$), 1.12 (d, ^3J = 6.9 Hz, 6H, CH(C$\underline{H}_3$)$_2$), 1.01 (s, 27H, C(C$\underline{H}_3$)$_3$).

^{13}C{^{1}H} NMR (126 MHz, C_6D_6, 300 K): δ [ppm] = 147.4 (*o*-$\underline{C}_{Dipp}$), 147.4 (*o*-$\underline{C}_{Dipp}$), 146.1 (SiCH$\underline{C}$H), 144.7 (*ipso*-$\underline{C}_{Ph}$), 144.7 (Si$\underline{C}$HCH), 143.9 (N$\underline{C}$N), 136.0 (*ipso*-$\underline{C}_{Dipp}$), 129.6 (*p*-$\underline{C}_{Dipp}$H),

128.7 (*o*-$\underline{C}_{Ph}H$), 128.6 (*o*-$\underline{C}_{Ph}H$), 128.1 (*m*-$\underline{C}_{Ph}H$, overlapping with solvent signal, but located with DEPT-90/DEPT-135), 127.1 (*m*-$\underline{C}_{Ph}H$), 124.5 (*m*-$\underline{C}_{Dipp}H$), 124.1 (*m*-$\underline{C}_{Dipp}H$), 124.0 (*p*-$\underline{C}_{Ph}H$), 115.8 (N$\underline{C}$H), 49.0 (Si$\underline{C}$HPh), 32.0 (C($\underline{C}H_3$)$_3$), 29.0 ($\underline{C}H(CH_3)_2$), 28.9 ($\underline{C}H(CH_3)_2$), 26.3 (CH($\underline{C}H_3$)$_2$), 25.4 (CH($\underline{C}H_3$)$_2$), 23.3 ($\underline{C}(CH_3)_3$), 22.7 (CH($\underline{C}H_3$)$_2$), 22.5 (CH($\underline{C}H_3$)$_2$).

^{29}Si{^{1}H} NMR (99 MHz, C_6D_6, 300 K): δ [ppm] = 5.3 ($\underline{Si}^t$Bu$_3$), –30.2 ($\underline{Si}$CHCH).

LIFDI-MS: calculated (for $C_{48}H_{71}N_3Si_2$): 745.5187
observed: 745.3865

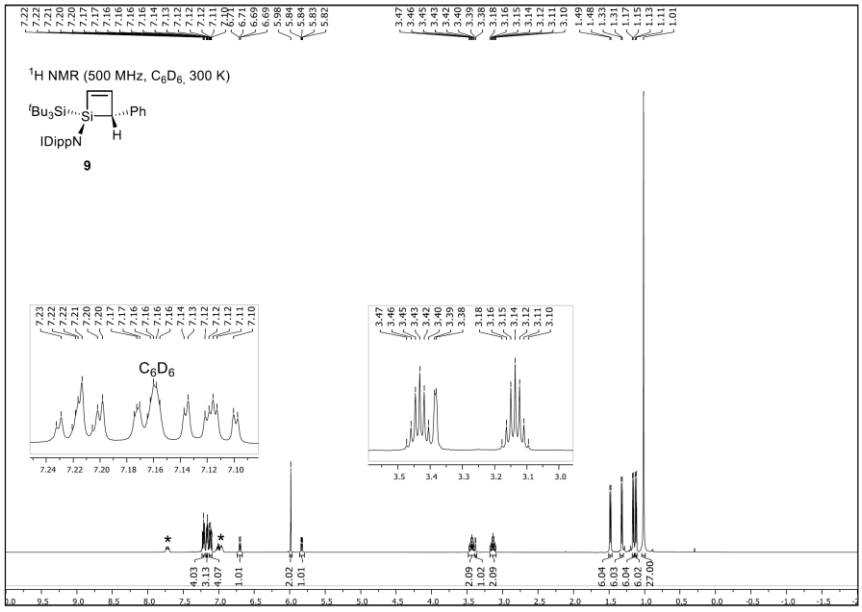


Figure S55. ^{1}H NMR spectrum of silacyclobutene **9** in C_6D_6 at 300 K. The resonances for the additional species are marked with asterisks *.

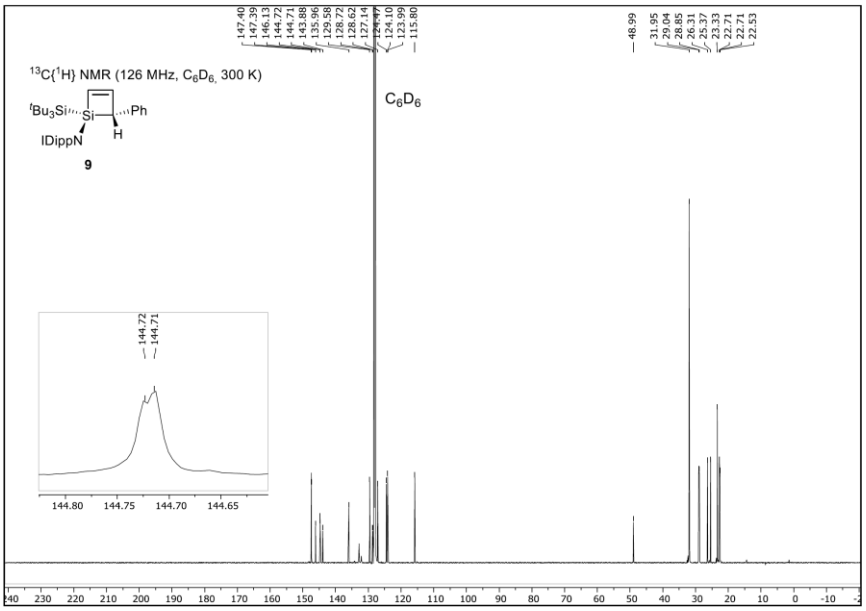


Figure S56. $^{13}C\{^{1}H\}$ NMR spectrum of silacyclobutene **9** in C_6D_6 at 300 K.

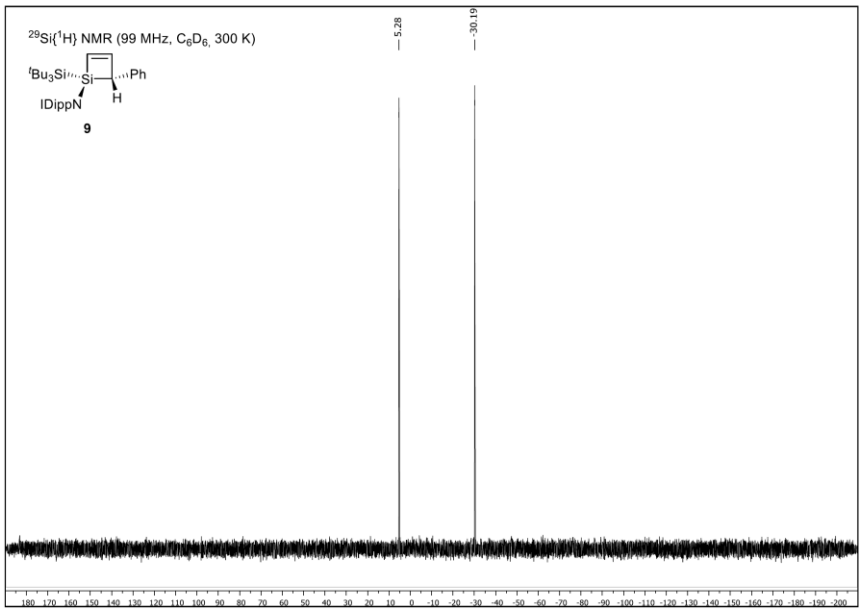


Figure S57. $^{29}Si\{^{1}H\}$ NMR spectrum of silacyclobutene **9** in C_6D_6 at 300 K.

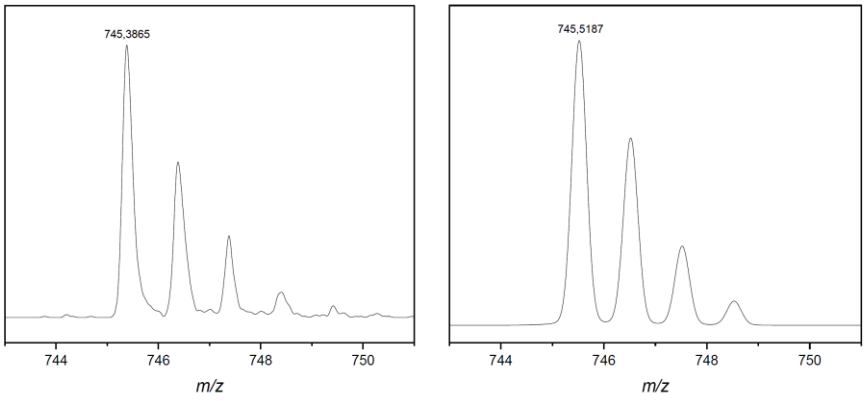
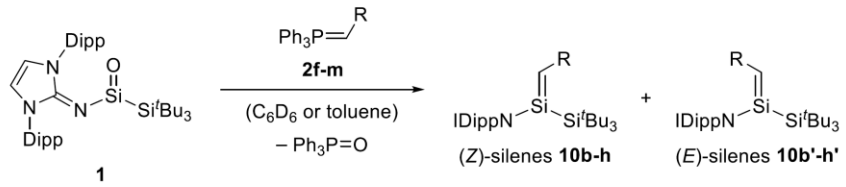


Figure S58. LIFDI-MS spectrometry (detail view with isotope pattern) of silacyclobutene **9**. Measured (left; m/z = 745.3865) and simulated (right; m/z = 745.5187) mass spectrum.

1.6 Reactivity of silanone 1 toward non-stabilized ylides

1.6.1 Sila-Wittig reaction



Reaction of iminosilylsilanone **1** with non-stabilized ylides resulted in silene formation analogous to the "classical" Wittig reaction affording alkenes. However, the isolation of **10** (*via* removal of the by-product $Ph_3P{=}O$) was not possible at all, because during workup (solvent removal and subsequent extraction/filtration with cold Et_2O and/or *n*-hexane) decomposition to unidentified product mixtures occurred. Presumably, the steric encumbrance at the low-coordinate carbon nuclei is not sufficient and subsequent reactions are thermodynamically favored. Nevertheless, the transient silenes were sufficiently characterized by multinuclear and 2D NMR spectroscopy and mass spectrometry. Additionally, the formation of $Ph_3P{=}O$ was unambiguously confirmed by ^{31}P NMR spectroscopy. The following methods were used for the synthesis and characterization of transient iminosilylsilenes **10** *via* the Sila-Wittig reaction.

General procedure for NMR characterization

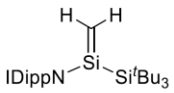
To a mixture of silanone **1** (30.0 mg, 46.4 µmol, 1.0 eq.) and the respective Wittig reagent **2f-m** (46.4 µmol, 1.0 eq.) was added C_6D_6 (0.5 mL) at ambient temperature. Immediate full conversion was detected by ^{1}H NMR spectroscopy. Subsequently, additional multinuclear and 2D NMR spectroscopic measurements were performed.

General procedure for LIFDI-MS characterization

To a mixture of silanone **1** (5.00 mg, 7.74 µmol, 1.0 eq.) and the respective Wittig reagent **2f-m** (7.74 µmol, 1.0 eq.) was added toluene (0.5 mL) at ambient temperature. The resulting solution was filtered *via* a syringe filter and used directly for mass spectrometric analysis.

Analytical data of the transient iminosilylsilenes

Reaction of silanone 1 with phosphorus ylide 2f



10a
$C_{40}H_{65}N_3Si_2$
644.15 g/mol

^{1}H NMR (500 MHz, C_6D_6, 300 K): δ [ppm] = 5.98 (s, 2H, NC*H*), 3.40 (d, ^2J = 9.3 Hz, 1H, Si=C*H*H), 3.16 (sept, ^3J = 6.9 Hz, 4H, C*H*(CH$_3$)$_2$), 2.44 (d, ^2J = 9.3 Hz, 1H, Si=CH*H*), 1.47 (d, ^3J = 6.9 Hz, 12H, CH(C*H*$_3$)$_2$), 1.18 (s, 27H, C(C*H*$_3$)$_3$), 1.14 (d, ^3J = 6.9 Hz, 12H, CH(C*H*$_3$)$_2$). The resonances for the *p*-C$_{ar}$*H* and *m*-C$_{ar}$*H* nuclei could not be unambigously assigned.

^{29}Si{^{1}H} NMR (99 MHz, C_6D_6, 300 K): δ [ppm] = 68.1 (*Si*=C), 11.9 (*Si*^{t}Bu$_3$).

The ^{13}C{^{1}H} NMR spectrum of **10a** was not evaluated more precisely and is not shown here, because many of the signals were superimposed and could not be assigned unambiguously. Nevertheless, the characteristic doublet resonances for Ph_3P=O were observed.

LIFDI-MS: no characteristic peak for **10a** was found.

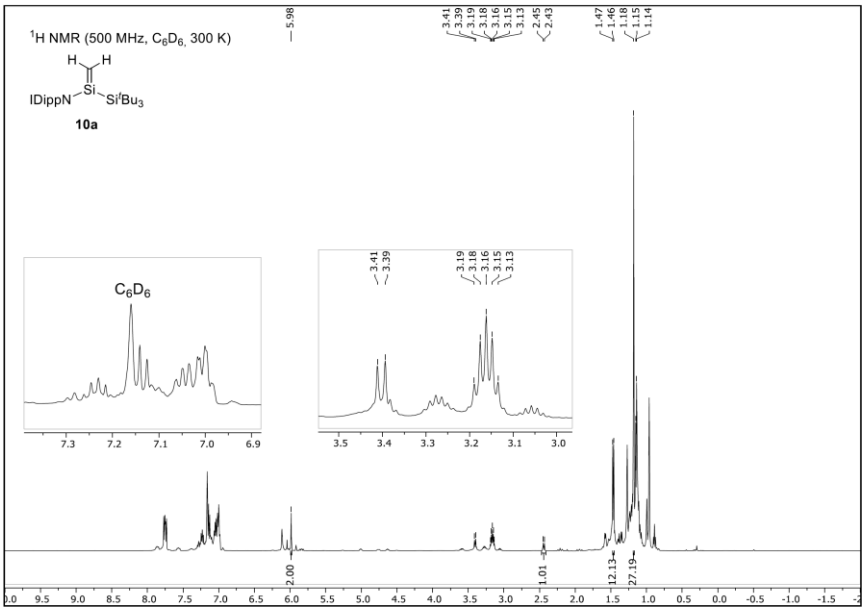


Figure S59. ^{1}H NMR spectrum of half-parent silene **10a** in C_6D_6 at 300 K. A proper integration was partly not possible due to overlapping resonances.

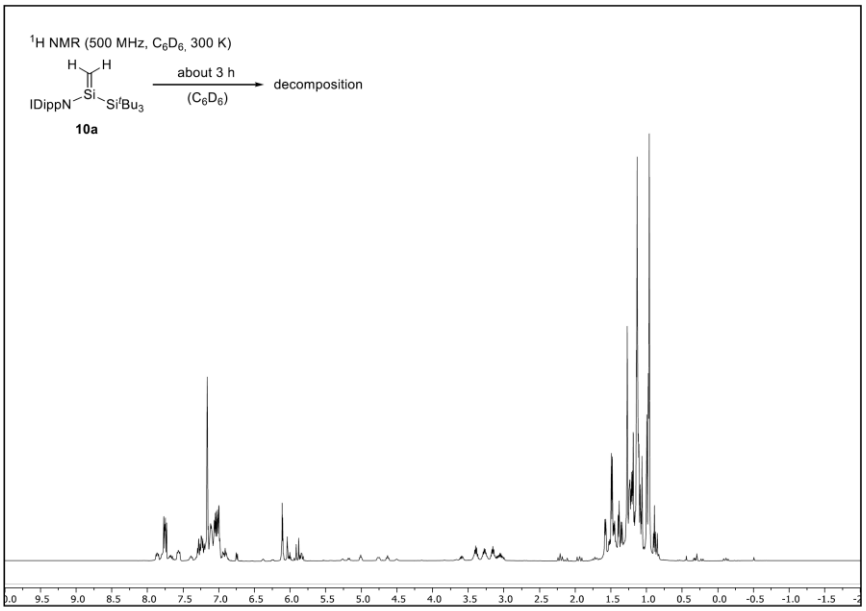


Figure S60. ^{1}H NMR spectrum of the decomposition products of the half-parent silene **10a** in C_6D_6 at 300 K.

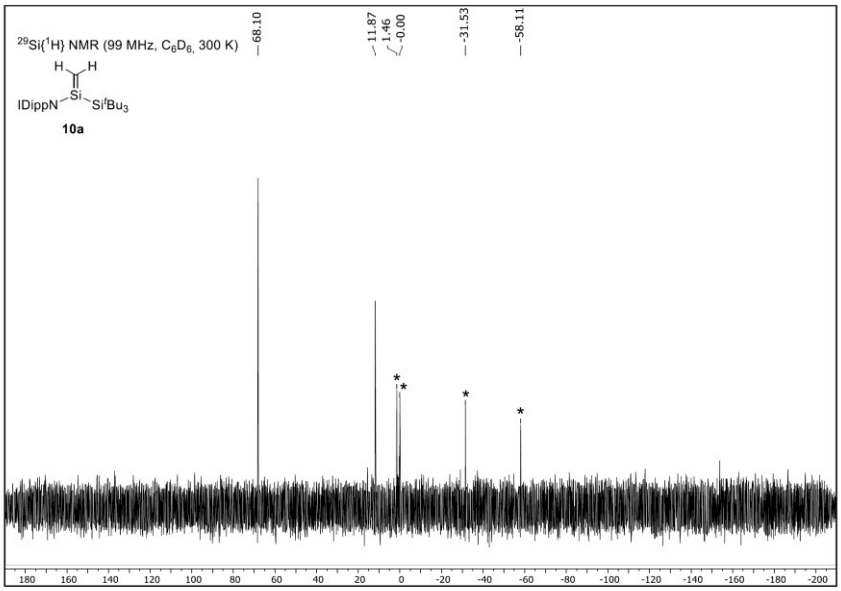


Figure S61. ^{29}Si{^{1}H} NMR spectrum of half-parent silene **10a** in C_6D_6 at 300 K. The resonances for the decomposition products are marked with asterisks *.

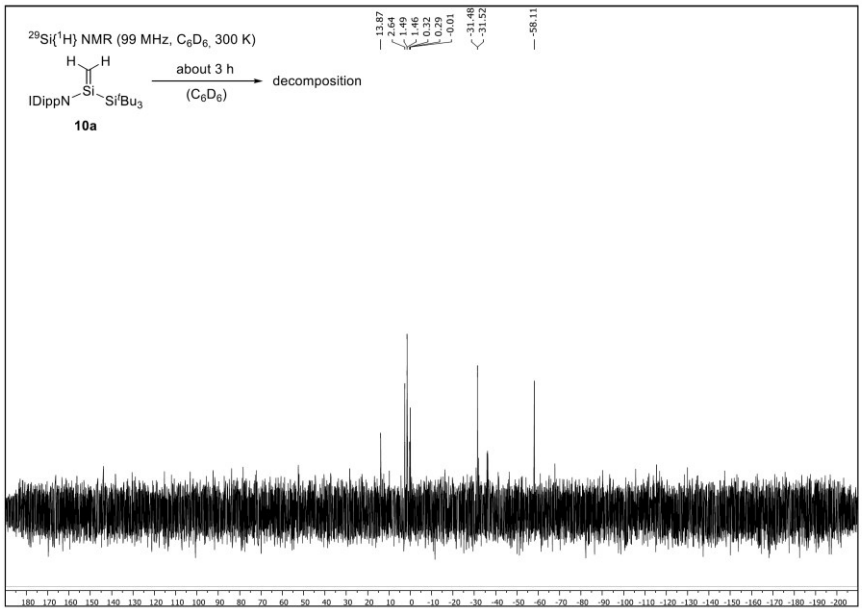


Figure S62. ^{29}Si{^{1}H} NMR spectrum of the decomposition products of the half-parent silene **10a** in C_6D_6 at 300 K.

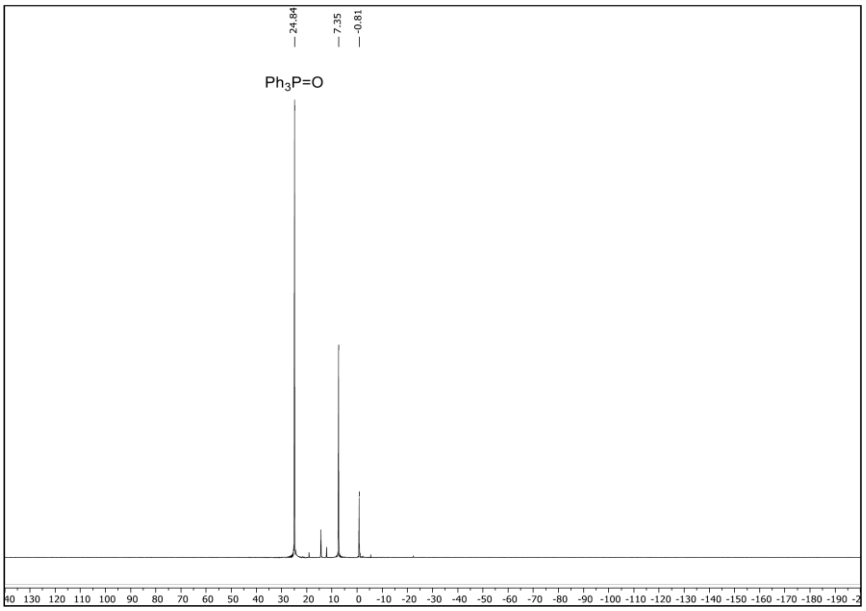
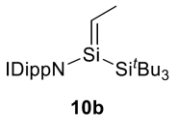


Figure S63. $^{31}P\{^{1}H\}$ NMR spectrum of the reaction of silanone **1** with phosphorus ylide **2f**.

Reaction of silanone 1 with phosphorus ylide 2g

The (*Z*)/(*E*)-ratio between **10b** and **10b′** was calculated by ^{1}H NMR spectroscopy to about 92/8.



10b
$C_{41}H_{67}N_3Si_2$
658.18 g/mol

Major isomer (*Z*)-silene 10b (~92%):

^{1}H NMR (500 MHz, C_6D_6, 300 K): δ [ppm] = 7.22 (t, ^{3}J = 7.7 Hz, 2H, *p*-$C_{ar}\underline{H}$), 7.14 (d, ^{3}J = 7.7 Hz, 4H, *m*-$C_{ar}\underline{H}$), 6.05 (s, 2H, NC$\underline{H}$), 3.98 (q, ^{3}J = 9.0 Hz, 1H, Si=C$\underline{H}$), 3.25 (sept, ^{3}J = 6.9 Hz, 4H, C$\underline{H}(CH_3)_2$), 2.05 (d, ^{3}J = 9.0 Hz, 3H, Si=CC$\underline{H}_3$), 1.45 (d, ^{3}J = 6.9 Hz, 12H, CH(C$\underline{H}_3)_2$), 1.18 (s, 27H, C(C$\underline{H}_3)_3$), 1.14 (d, ^{3}J = 6.9 Hz, 12H, CH(C$\underline{H}_3)_2$).

$^{13}C\{^{1}H\}$ NMR (126 MHz, C_6D_6, 300 K): δ [ppm] = 147.5 (*o*-$\underline{C}_{ar}$), 145.4 (N$\underline{C}$N), 135.0 (*ipso*-$\underline{C}_{ar}$), 129.6 (*p*-$\underline{C}_{ar}$H), 124.1 (*m*-$\underline{C}_{ar}$H), 115.5 (N$\underline{C}$H), 101.3 (Si=$\underline{C}$H), 32.1 (C($\underline{C}H_3)_3$), 29.0 ($\underline{C}H(CH_3)_2$), 25.5 (CH($\underline{C}H_3)_2$), 23.5 ($\underline{C}(CH_3)_3$), 23.1 (CH($\underline{C}H_3)_2$), 15.3 (Si=C$\underline{C}H_3$).

$^{29}Si\{^{1}H\}$ NMR (99 MHz, C_6D_6, 300 K): δ [ppm] = 55.9 ($\underline{Si}$=C), 15.2 ($\underline{Si}^{t}Bu_3$).

Minor isomer (*E*)-silene 10b′ (~8%):

$^{29}Si\{^{1}H\}$ NMR (99 MHz, C_6D_6, 300 K): δ [ppm] = 50.5 ($\underline{Si}$=C), 12.2 ($\underline{Si}^{t}Bu_3$).

LIFDI-MS: no characteristic peak for **10b/10b′** was found.

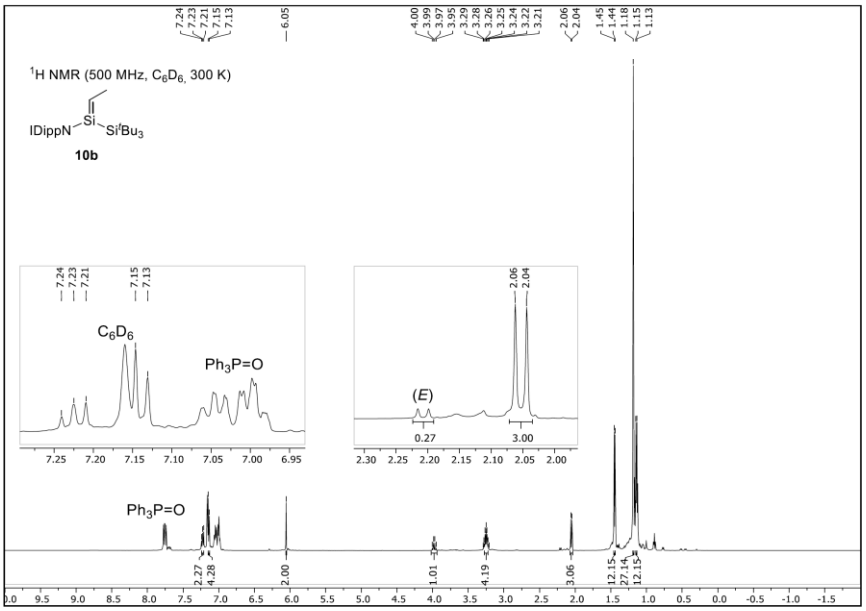


Figure S64. ^{1}H NMR spectrum of (*Z*)-silene **10b** in C_6D_6 at 300 K. The corresponding resonance of (*E*)-silene **10b′** used for the determination of the (*Z*)/(*E*)-ratio is marked with an (*E*).

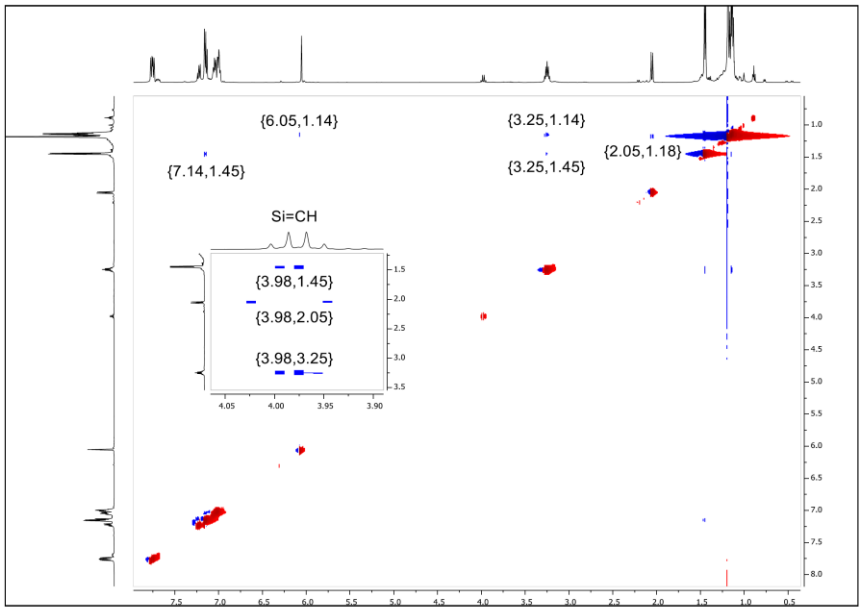


Figure S65. ^{1}H/^{1}H NOESY NMR spectrum of (*Z*)-silene **10b** in C_6D_6 at 300 K.

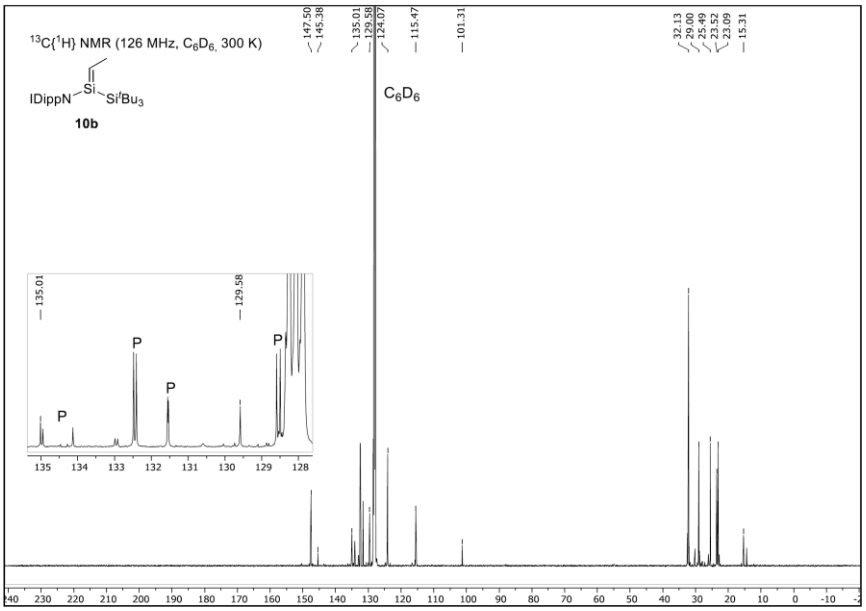


Figure S66. $^{13}C\{^1H\}$ NMR spectrum of (*Z*)-silene **10b** in C_6D_6 at 300 K. The resonances of $Ph_3P{=}O$ are marked with a P.

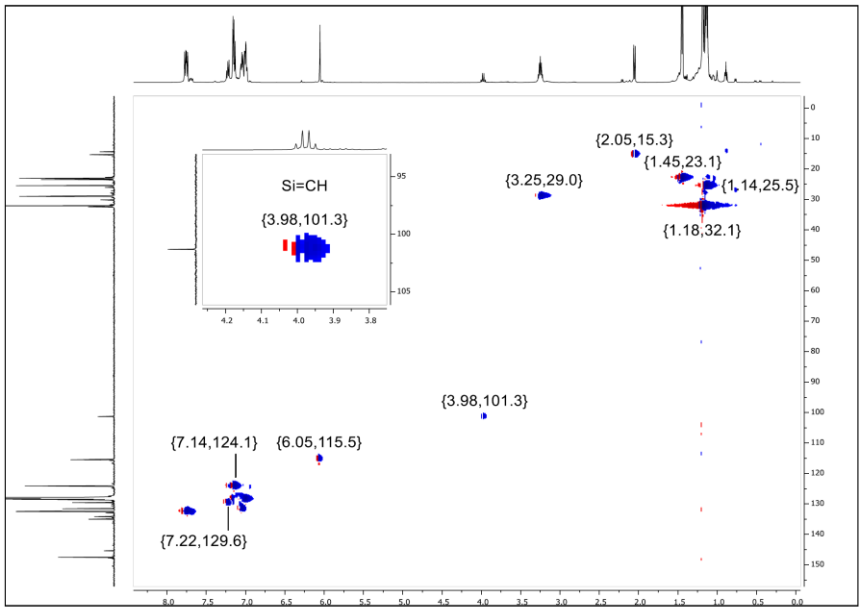


Figure S67. $^1H/^{13}C$ HSQC NMR spectrum of (*Z*)-silene **10b** in C_6D_6 at 300 K.

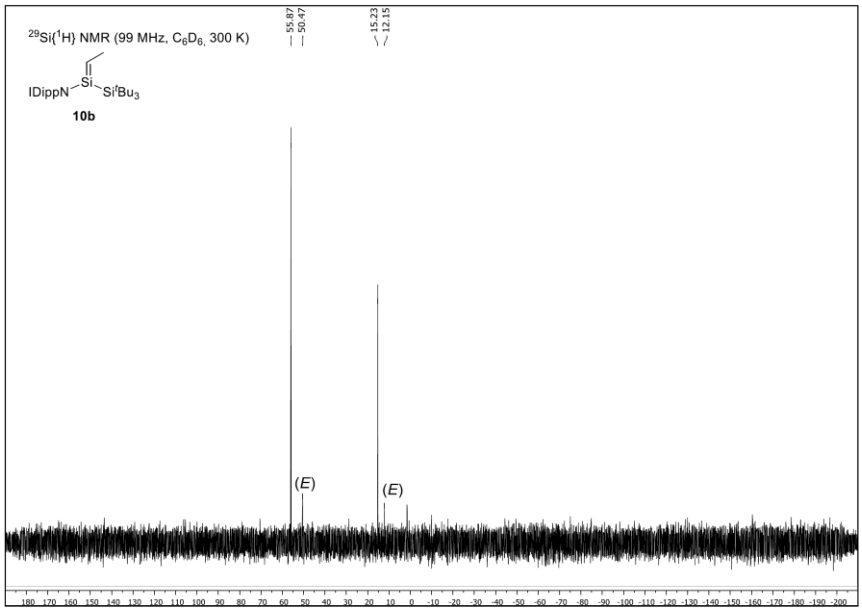


Figure S68. ^{29}Si{^{1}H} NMR spectrum of (*Z*)-silene **10b** in C_6D_6 at 300 K. The resonances of (*E*)-silene **10b′** are labeled with (*E*).

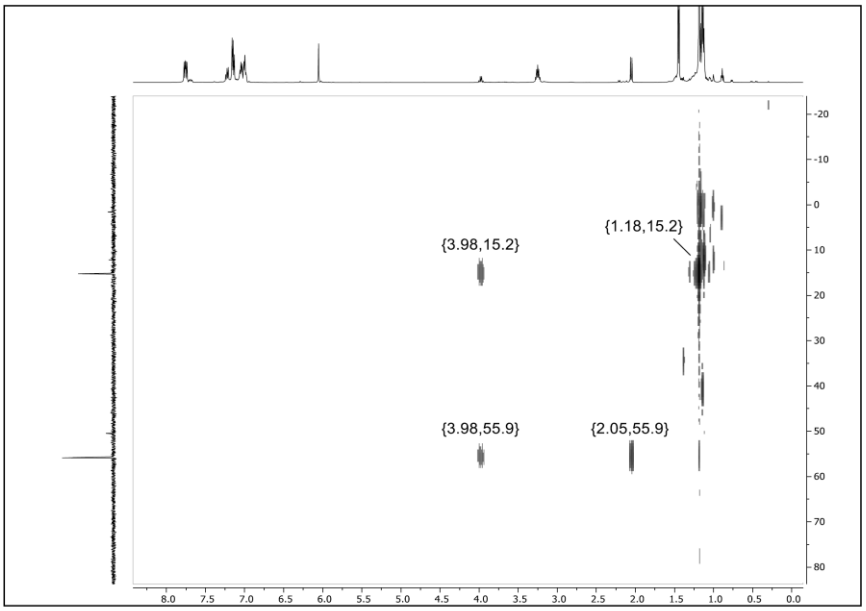


Figure S69. ^{1}H/^{29}Si HMBC NMR spectrum of (*Z*)-silene **10b** in C_6D_6 at 300 K.

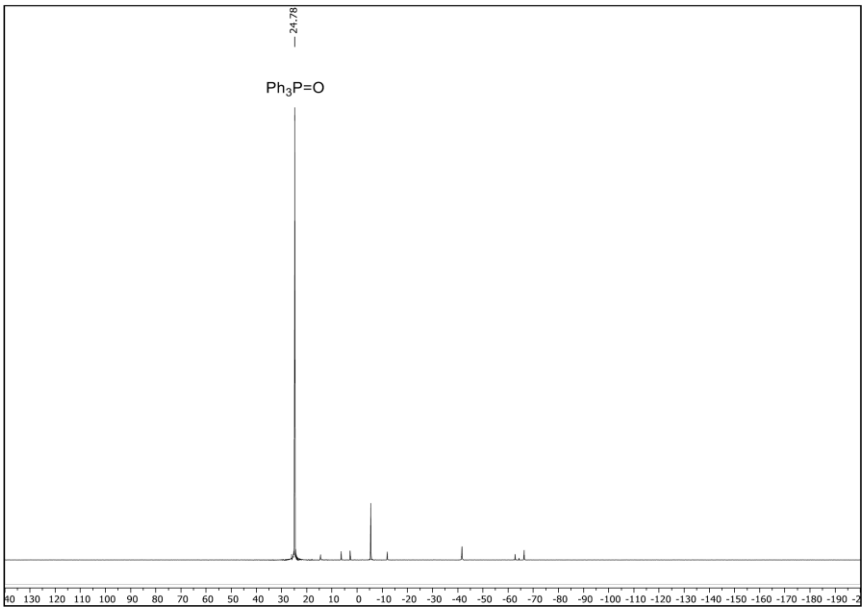
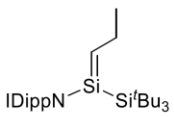


Figure S70. $^{31}P\{^{1}H\}$ NMR spectrum of the reaction of silanone **1** with phosphorus ylide **2g**.

Reaction of silanone 1 with phosphorus ylide 2h

The (*Z*)/(*E*)-ratio between **10c** and **10c′** was calculated by ^{1}H NMR spectroscopy to about 94/6.



10c
$C_{42}H_{69}N_3Si_2$
672.21 g/mol

Major isomer (*Z*)-silene 10c (~94%):

^{1}H NMR (500 MHz, C_6D_6, 300 K): δ [ppm] = 7.23 (t, ^{3}J = 7.7 Hz, 2H, *p*-$C_{ar}\underline{H}$), 7.13 (d, ^{3}J = 7.7 Hz, 4H, *m*-$C_{ar}\underline{H}$), 6.02 (s, 2H, NC$\underline{H}$), 3.82 (t, ^{3}J = 9.8 Hz, 1H, Si=C$\underline{H}$), 3.24 (sept, ^{3}J = 6.9 Hz, 4H, C$\underline{H}$(CH$_3$)$_2$), 2.37 (dq, ^{3}J = 9.8 Hz, ^{3}J = 7.2 Hz, 2H, Si=CC$\underline{H}_2$), 1.45 (d, ^{3}J = 6.9 Hz, 12H, CH(C$\underline{H}_3$)$_2$), 1.19 (s, 27H, C(C$\underline{H}_3$)$_3$), 1.14 (d, ^{3}J = 6.9 Hz, 12H, CH(C$\underline{H}_3$)$_2$), 1.01 (t, ^{3}J = 7.2 Hz, 3H, CH$_2$C$\underline{H}_3$).

$^{13}C\{^{1}H\}$ NMR (126 MHz, C_6D_6, 300 K): δ [ppm] = 147.5 (*o*-$\underline{C}_{ar}$), 144.5 (N$\underline{C}$N), 135.2 (*ipso*-$\underline{C}_{ar}$), 129.6 (*p*-$\underline{C}_{ar}$H), 124.1 (*m*-$\underline{C}_{ar}$H), 115.5 (N$\underline{C}$H), 112.9 (Si=$\underline{C}$H), 32.1 (C($\underline{C}$H$_3$)$_3$), 28.9 ($\underline{C}$H(CH$_3$)$_2$), 25.4 (CH($\underline{C}$H$_3$)$_2$), 23.4 ($\underline{C}$(CH$_3$)$_3$), 23.2 (CH($\underline{C}$H$_3$)$_2$), 22.8 (Si=C$\underline{C}$H$_2$), 20.3 (CH$_2\underline{C}$H$_3$).

$^{29}Si\{^{1}H\}$ NMR (99 MHz, C_6D_6, 300 K): δ [ppm] = 51.3 ($\underline{Si}$=C), 15.3 ($\underline{Si}^{t}$Bu$_3$).

Minor isomer (*E*)-silene 10c′ (~6%):

^{29}Si{^{1}H} NMR (99 MHz, C_6D_6, 300 K): δ [ppm] = 43.1 (*Si*=C). The resonance for the *Si*^{t}Bu$_3$ nucleus was not observed.

LIFDI-MS: calculated (for $C_{42}H_{69}N_3Si_2$): 671.5030
observed: 671.4768

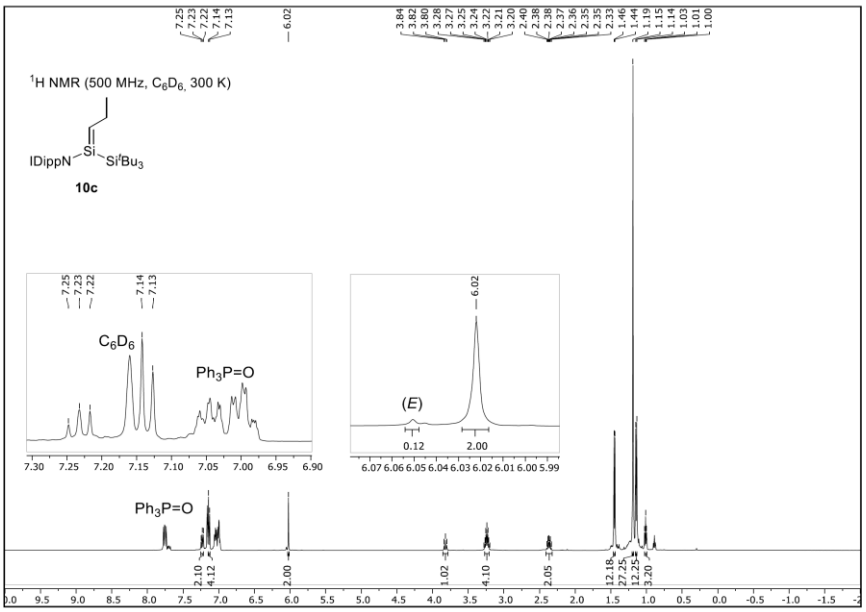


Figure S71. ^{1}H NMR spectrum of (*Z*)-silene **10c** in C_6D_6 at 300 K. The corresponding resonance of (*E*)-silene **10c′** used for the determination of the (*Z*)/(*E*)-ratio is marked with an (*E*).

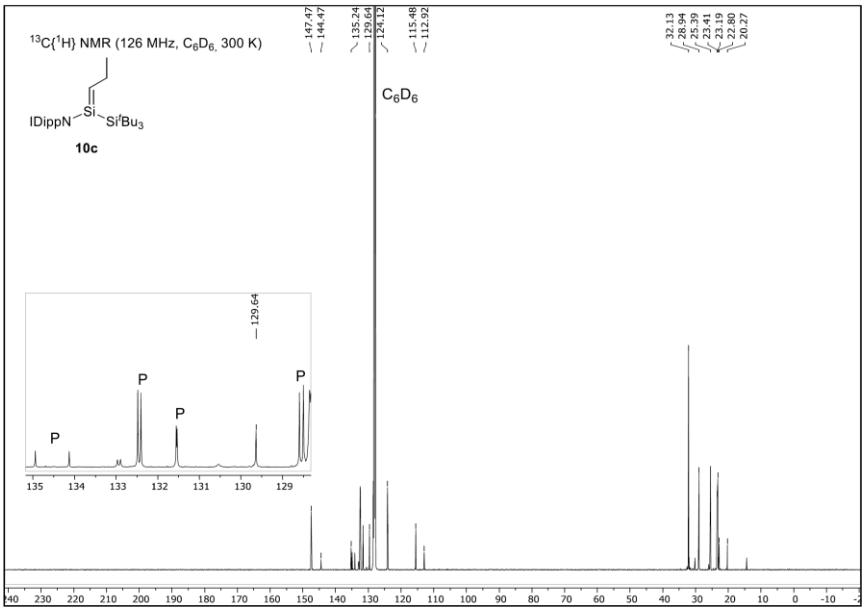


Figure S72. $^{13}C\{^1H\}$ NMR spectrum of (*Z*)-silene **10c** in C_6D_6 at 300 K. The resonances of $Ph_3P{=}O$ are marked with a P.

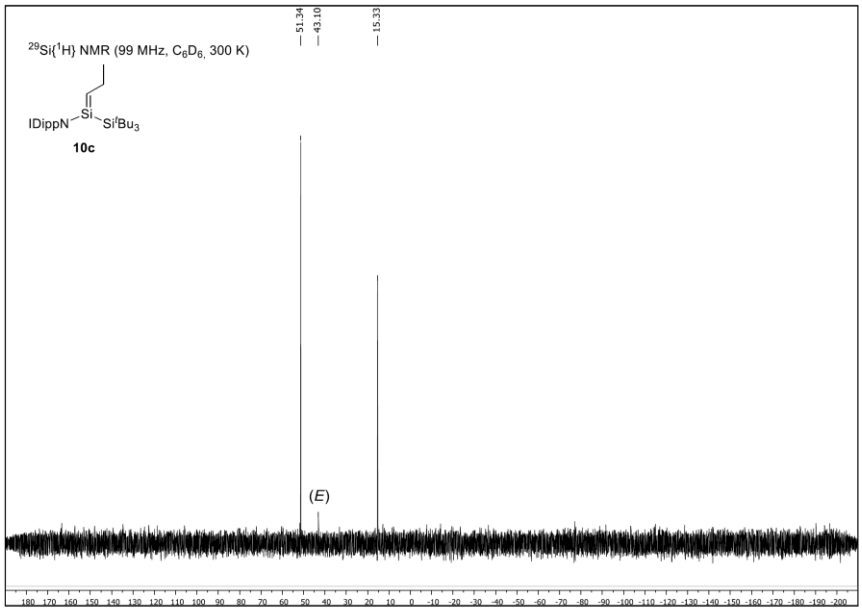


Figure S73. $^{29}Si\{^1H\}$ NMR spectrum of (*Z*)-silene **10c** in C_6D_6 at 300 K. The resonance of (*E*)-silene **10c′** is labeled with an (*E*).

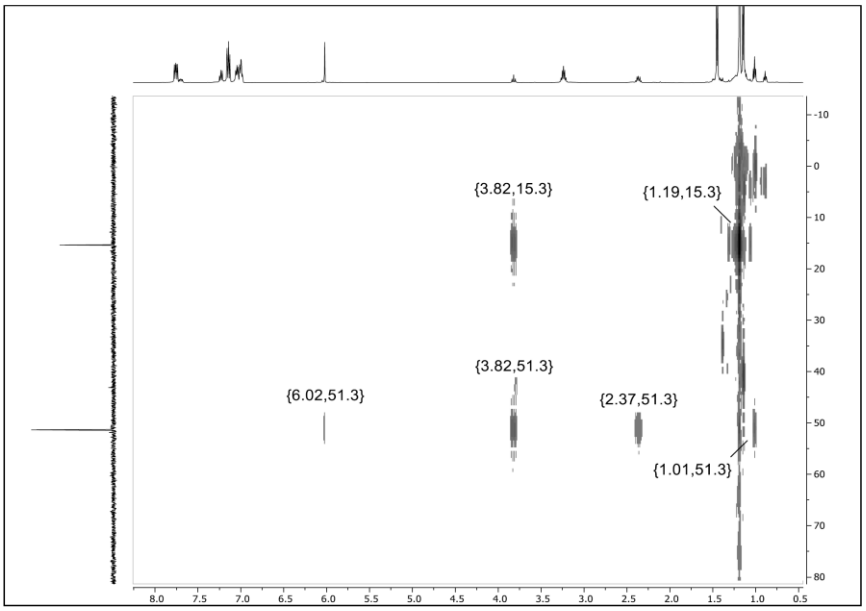


Figure S74. $^{1}H/^{29}Si$ HMBC NMR spectrum of (*Z*)-silene **10c** in C_6D_6 at 300 K.

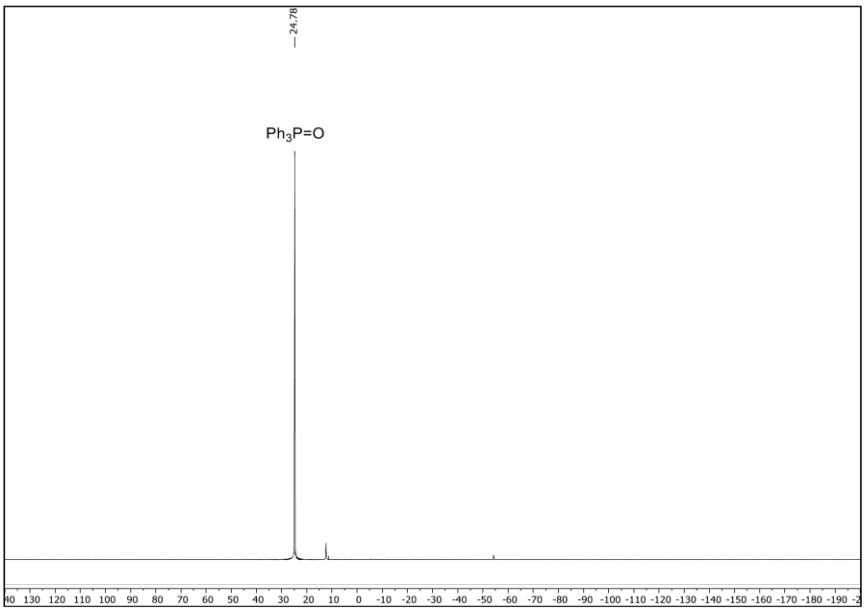


Figure S75. $^{31}P\{^{1}H\}$ NMR spectrum of the reaction of silanone **1** with phosphorus ylide **2h**.

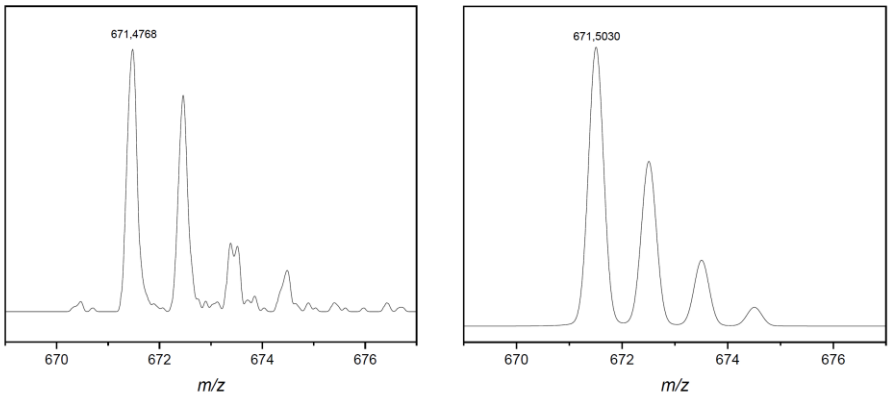
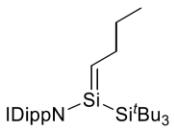


Figure S76. LIFDI-MS spectrometry (detail view with isotope pattern) of (*Z*)/(*E*)-silenes **10c/10c′**. Measured (left; m/z = 671.4768) and simulated (right; m/z = 671.5030) mass spectrum.

Reaction of silanone 1 with phosphorus ylide 2i

The (*Z*)/(*E*)-ratio between **10d** and **10d′** was calculated by ^{1}H NMR spectroscopy to about 94/6.



10d
$C_{43}H_{71}N_3Si_2$
686.23 g/mol

Major isomer (*Z*)-silene 10d (~94%):

^{1}H NMR (500 MHz, C_6D_6, 300 K): δ [ppm] = 7.23 (t, ^{3}J = 7.7 Hz, 2H, *p*-$C_{ar}H$), 7.14 (d, ^{3}J = 7.7 Hz, 4H, *m*-$C_{ar}H$), 6.03 (s, 2H, NC*H*), 3.80 (t, ^{3}J = 9.8 Hz, 1H, Si=C*H*), 3.24 (sept, ^{3}J = 6.9 Hz, 4H, C*H*$(CH_3)_2$), 2.35–2.30 (m, 2H, Si=CCH_2), 1.45 (d, ^{3}J = 6.9 Hz, 12H, CH(CH_3)$_2$), 1.35–1.30 (m, 2H, CH_2CH_2), 1.19 (s, 27H, C(CH_3)$_3$), 1.14 (d, ^{3}J = 6.9 Hz, 12H, CH(CH_3)$_2$), 1.02 (t, ^{3}J = 7.2 Hz, 3H, CH_2CH_3).

^{13}C{^{1}H} NMR (126 MHz, C_6D_6, 300 K): δ [ppm] = 147.4 (*o*-C_{ar}), 144.4 (NCN), 135.2 (*ipso*-C_{ar}), 129.6 (*p*-C_{ar}H), 124.1 (*m*-C_{ar}H), 115.5 (NCH), 110.4 (Si=CH), 32.2 (C(CH_3)$_3$), 32.0 (Si=CCH_2), 28.9 (C$H(CH_3)_2$), 28.9 (CH_2CH_3), 25.4 (CH(CH_3)$_2$), 23.4 (C$(CH_3)_3$), 23.2 (CH(CH_3)$_2$), 14.4 (CH_2CH_3).

^{29}Si{^{1}H} NMR (99 MHz, C_6D_6, 300 K): δ [ppm] = 52.3 (*Si*=C), 15.6 (*Si*^{t}Bu$_3$).

Minor isomer (*E*)-silene 10d′ (~6%):

^{29}Si{^{1}H} NMR (99 MHz, C_6D_6, 300 K): δ [ppm] = 42.8 (*Si*=C), 12.9 (*Si*^{t}Bu$_3$).

LIFDI-MS: calculated (for $C_{43}H_{71}N_3Si_2$): 685.5220
observed: 685.7172

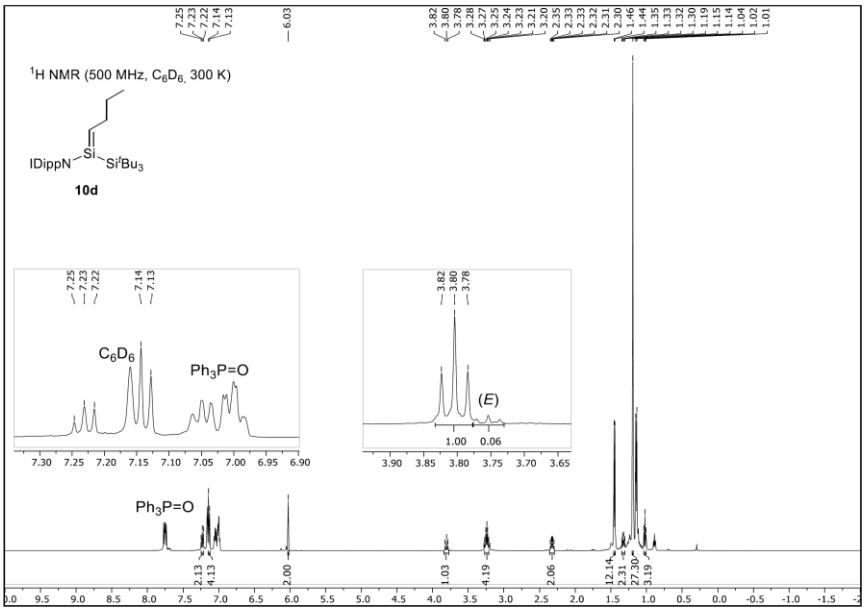


Figure S77. ^{1}H NMR spectrum of (*Z*)-silene **10d** in C_6D_6 at 300 K. The corresponding resonance of (*E*)-silene **10d′** used for the determination of the (*Z*)/(*E*)-ratio is marked with an (*E*).

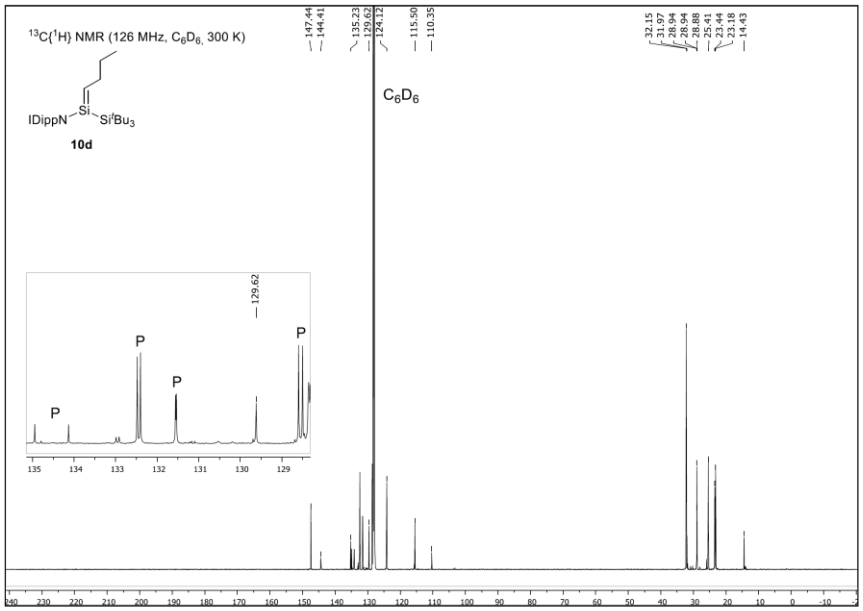


Figure S78. ^{13}C{^{1}H} NMR spectrum of (*Z*)-silene **10d** in C_6D_6 at 300 K. The resonances of Ph_3P=O are marked with a P.

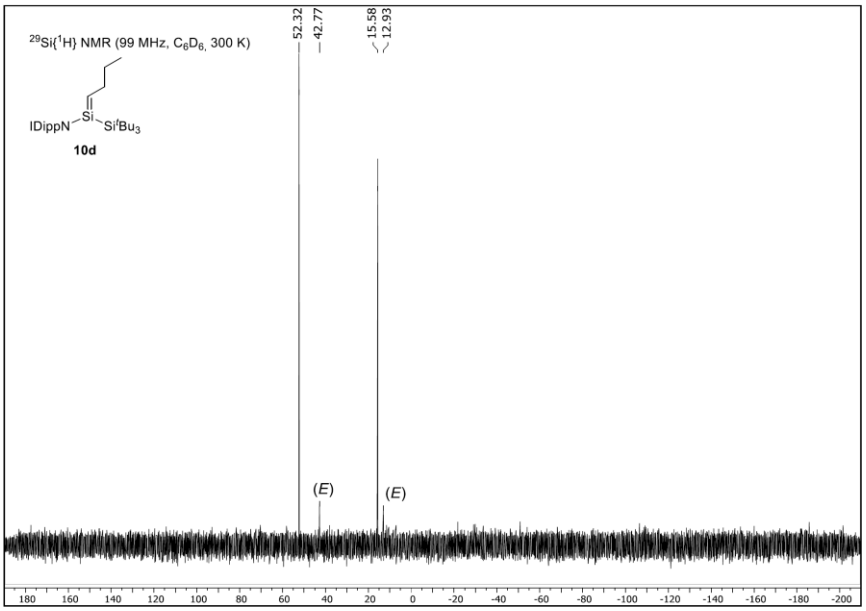


Figure S79. ^{29}Si{^{1}H} NMR spectrum of (*Z*)-silene **10d** in C_6D_6 at 300 K. The resonances of (*E*)-silene **10d′** are labeled with (*E*).

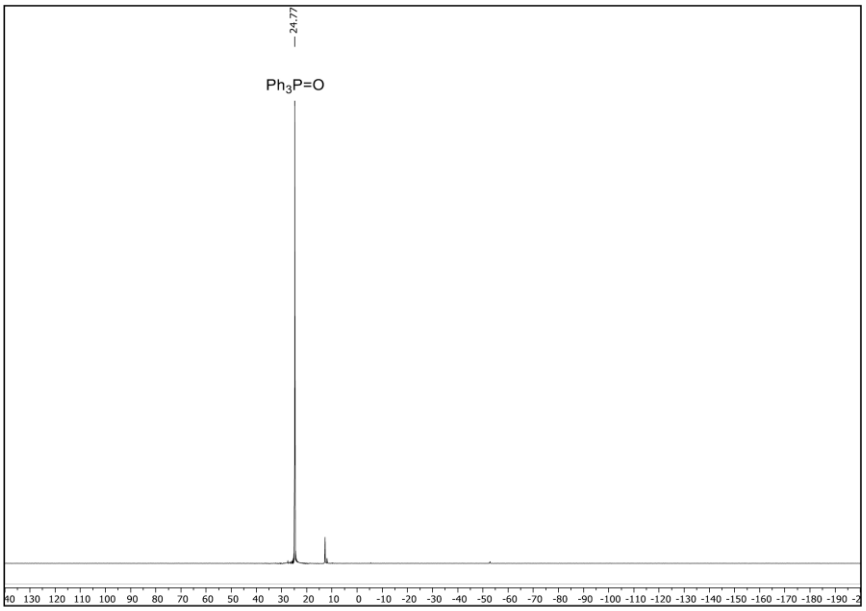


Figure S80. ^{31}P{^{1}H} NMR spectrum of the reaction of silanone **1** with phosphorus ylide **2i**.

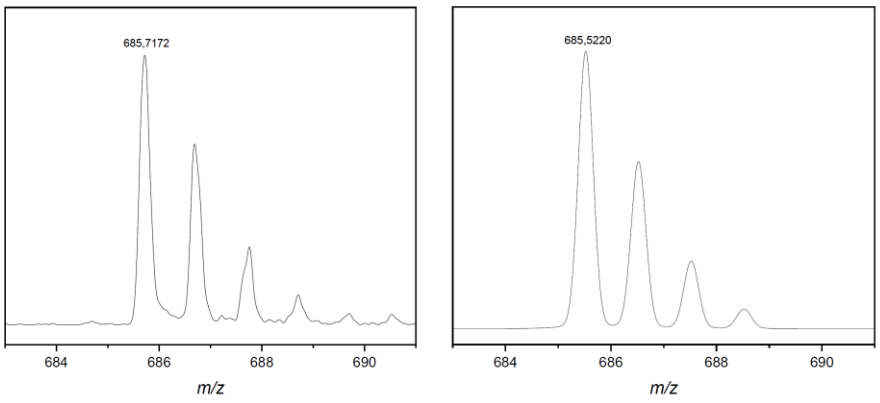
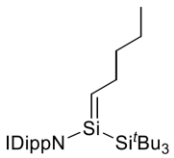


Figure S81. LIFDI-MS spectrometry (detail view with isotope pattern) of (*Z*)/(*E*)-silenes **10d/10d′**. Measured (left; m/z = 685.7172) and simulated (right; m/z = 685.5220) mass spectrum.

Reaction of silanone 1 with phosphorus ylide 2j

The (*Z*)/(*E*)-ratio between **10e** and **10e′** was calculated by ^{1}H NMR spectroscopy to about 89/11.



10e
$C_{44}H_{73}N_3Si_2$
700.26 g/mol

Major isomer (*Z*)-silene 10e (~89%):

^{1}H NMR (500 MHz, C_6D_6, 300 K): δ [ppm] = 7.24 (t, ^{3}J = 7.7 Hz, 2H, *p*-$C_{ar}\underline{H}$), 7.14 (d, ^{3}J = 7.7 Hz, 4H, *m*-$C_{ar}\underline{H}$), 6.03 (s, 2H, NC$\underline{H}$), 3.80 (t, ^{3}J = 9.8 Hz, 1H, Si=C$\underline{H}$), 3.24 (sept, ^{3}J = 6.9 Hz, 4H, C$\underline{H}$(CH_3)$_2$), 2.36–2.31 (m, 2H, Si=CC$\underline{H}_2$), 1.45 (d, ^{3}J = 6.9 Hz, 12H, CH(C$\underline{H}_3$)$_2$), 1.32–1.26 (m, 4H, C$\underline{H}_2$$CH_2CH_3$ + CH_2C$\underline{H}_2$$CH_3$), 1.19 (s, 27H, C(C$\underline{H}_3$)$_3$), 1.14 (d, ^{3}J = 6.9 Hz, 12H, CH(C$\underline{H}_3$)$_2$), 1.02 (t, ^{3}J = 7.2 Hz, 3H, CH_2C$\underline{H}_3$).

^{13}C{^{1}H} NMR (126 MHz, C_6D_6, 300 K): δ [ppm] = 147.5 (*o*-$\underline{C}_{ar}$), 144.4 (N$\underline{C}$N), 135.2 (*ipso*-$\underline{C}_{ar}$), 129.6 (*p*-$\underline{C}_{ar}$H), 124.1 (*m*-$\underline{C}_{ar}$H), 115.5 (N$\underline{C}$H), 110.6 (Si=$\underline{C}$H), 38.3 ($\underline{C}H_2CH_2CH_3$), 32.2 (C($\underline{C}H_3$)$_3$), 29.5 (Si=C$\underline{C}H_2$), 28.9 ($\underline{C}$H(CH_3)$_2$), 25.4 (CH($\underline{C}H_3$)$_2$), 23.5 ($\underline{C}$(CH_3)$_3$), 23.2 (CH($\underline{C}H_3$)$_2$), 23.1 ($\underline{C}H_2CH_3$), 14.8 ($CH_2\underline{C}H_3$).

^{29}Si{^{1}H} NMR (99 MHz, C_6D_6, 300 K): δ [ppm] = 52.0 ($\underline{Si}$=C), 15.5 ($\underline{Si}$^{t}Bu$_3$).

Minor isomer (*E*)-silene 10e′ (~11%):

^{29}Si{^{1}H} NMR (99 MHz, C_6D_6, 300 K): δ [ppm] = 42.6 ($\underline{Si}$=C), 12.8 ($\underline{Si}$^{t}Bu$_3$).

LIFDI-MS: calculated (for $C_{44}H_{73}N_3Si_2$): 699.5343
observed: 699.6519

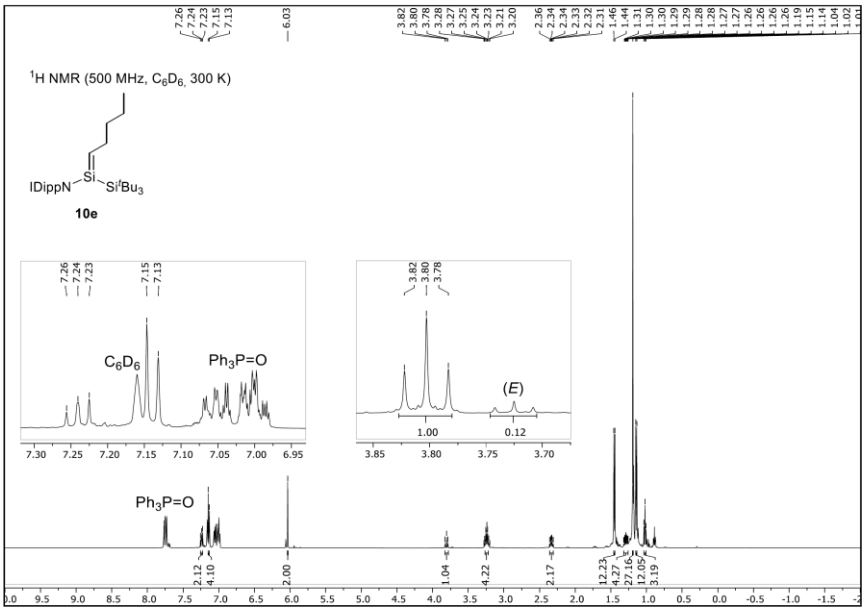


Figure S82. ^{1}H NMR spectrum of (*Z*)-silene **10e** in C_6D_6 at 300 K. The corresponding resonance of (*E*)-silene **10e′** used for the determination of the (*Z*)/(*E*)-ratio is marked with an (*E*).

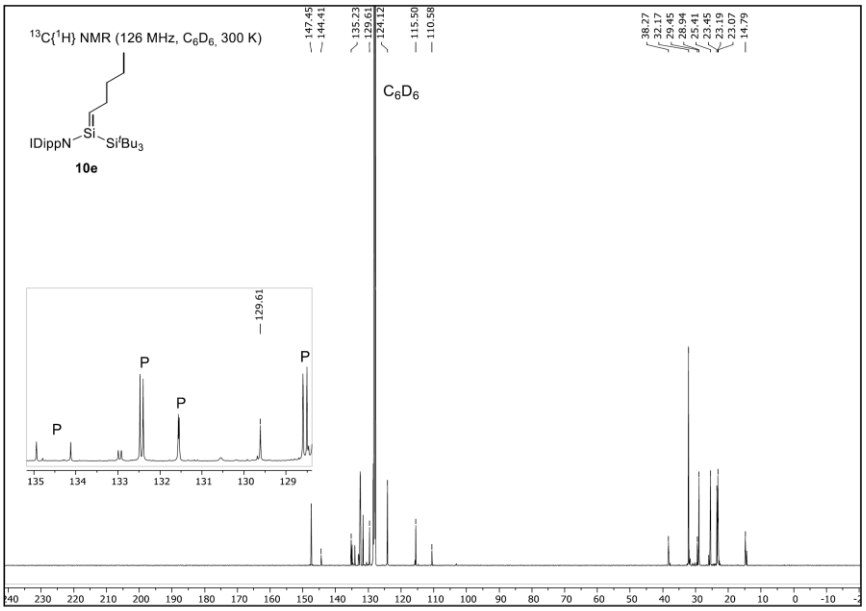


Figure S83. ^{13}C{^{1}H} NMR spectrum of (*Z*)-silene **10e** in C_6D_6 at 300 K. The resonances of $Ph_3P=O$ are marked with a P.

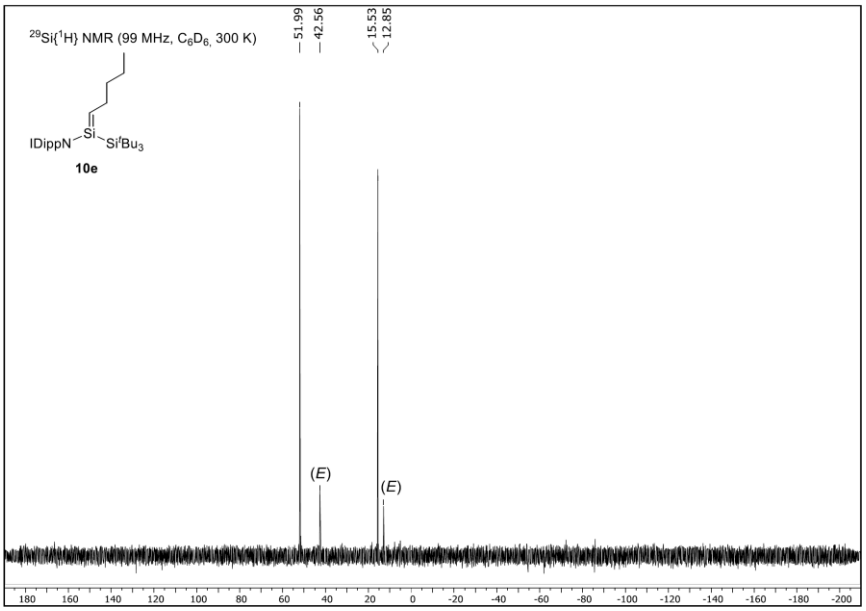


Figure S84. ^{29}Si{^{1}H} NMR spectrum of (*Z*)-silene **10e** in C_6D_6 at 300 K. The resonances of (*E*)-silene **10e′** are labeled with (*E*).

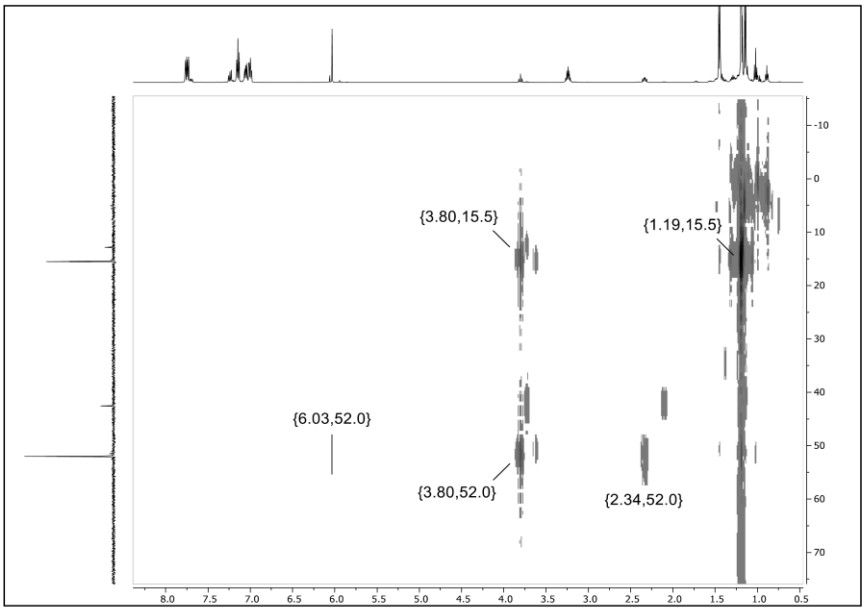


Figure S85. ^{1}H/^{29}Si HMBC NMR spectrum of (*Z*)-silene **10e** in C_6D_6 at 300 K.

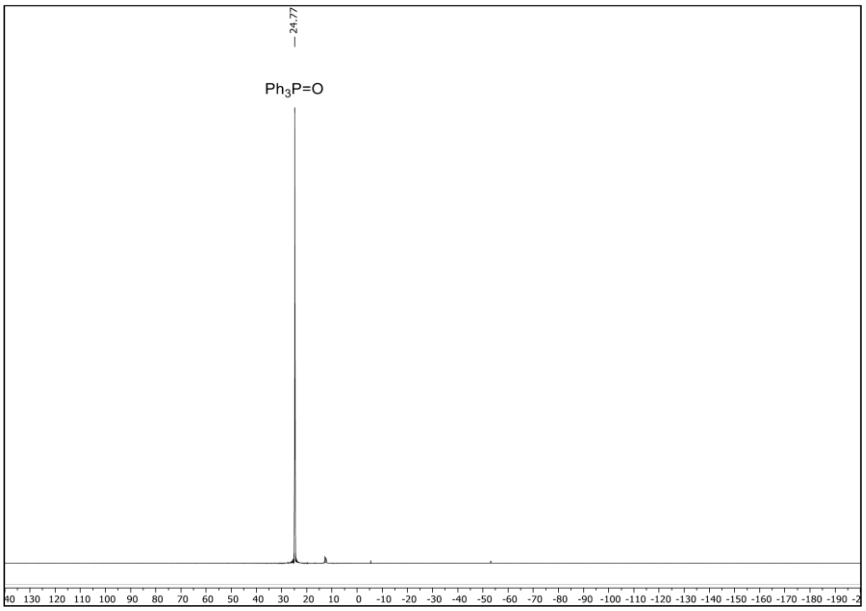


Figure S86. $^{31}P\{^{1}H\}$ NMR spectrum of the reaction of silanone **1** with phosphorus ylide **2j**.

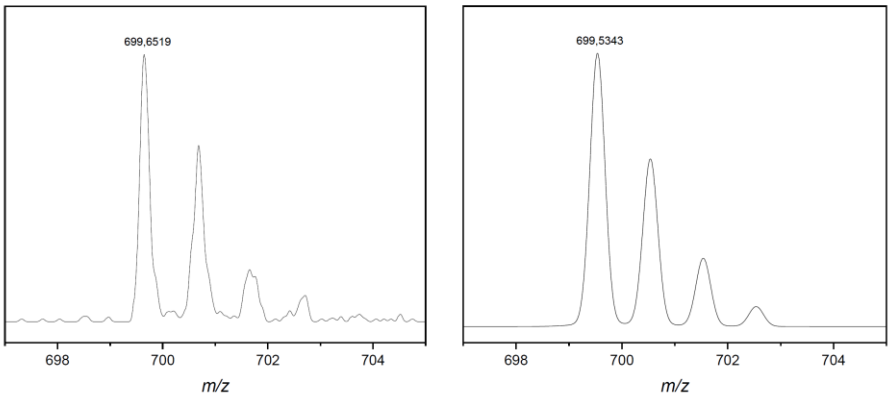
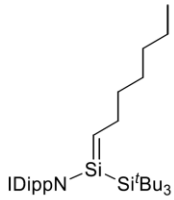


Figure S87. LIFDI-MS spectrometry (detail view with isotope pattern) of (*Z*)/(*E*)-silenes **10e/10e′**. Measured (left; m/z = 699.6519) and simulated (right; m/z = 699.5343) mass spectrum.

Reaction of silanone 1 with phosphorus ylide 2k

The (*Z*)/(*E*)-ratio between **10f** and **10f'** was calculated by ^{1}H NMR spectroscopy to about 85/15.



10f
$C_{46}H_{77}N_3Si_2$
728.31 g/mol

Major isomer (*Z*)-silene 10f (~85%):

^{1}H NMR (500 MHz, C_6D_6, 300 K): δ [ppm] = 7.25 (t, ^{3}J = 7.7 Hz, 2H, *p*-$C_{ar}\underline{H}$), 7.15 (d, ^{3}J = 7.7 Hz, 4H, *m*-$C_{ar}\underline{H}$, overlapping with solvent signal), 6.04 (s, 2H, NC$\underline{H}$), 3.81 (t, ^{3}J = 9.8 Hz, 1H, Si=C$\underline{H}$), 3.24 (sept, ^{3}J = 6.9 Hz, 4H, C$\underline{H}$(CH_3)$_2$), 2.36–2.31 (m, 2H, Si=CC$\underline{H}_2$), 1.46 (d, ^{3}J = 6.9 Hz, 12H, CH(C$\underline{H}_3$)$_2$), 1.33–1.23 (m, 8H, C$\underline{H}_2$$CH_2CH_2CH_2CH_3$ + $CH_2C\underline{H}_2CH_2CH_2CH_3$ + $CH_2CH_2C\underline{H}_2CH_2CH_3$ + $CH_2CH_2CH_2C\underline{H}_2CH_3$), 1.19 (s, 27H, C(C$\underline{H}_3$)$_3$), 1.15 (d, ^{3}J = 6.9 Hz, 12H, CH(C$\underline{H}_3$)$_2$), 0.95 (t, ^{3}J = 7.2 Hz, 3H, $CH_2C\underline{H}_3$).

^{13}C{^{1}H} NMR (126 MHz, C_6D_6, 300 K): δ [ppm] = 147.5 (*o*-$\underline{C}_{ar}$), 144.4 (N$\underline{C}$N), 135.3 (*ipso*-$\underline{C}_{ar}$), 129.6 (*p*-$\underline{C}_{ar}$H), 124.1 (*m*-$\underline{C}_{ar}$H), 115.5 (N$\underline{C}$H), 110.7 (Si=$\underline{C}$H), 36.0 (SiC$H_2\underline{C}H_2$), 32.7 ($\underline{C}H_2CH_2CH_3$), 32.2 (C($\underline{C}H_3$)$_3$), 29.9 ($\underline{C}H_2CH_2CH_2CH_3$), 29.8 (Si=C$\underline{C}H_2$), 28.9 ($\underline{C}$H($CH_3$)$_2$), 25.4 (CH($\underline{C}H_3$)$_2$), 23.5 ($\underline{C}$($CH_3$)$_3$), 23.2 (CH($\underline{C}H_3$)$_2$), 23.4 ($\underline{C}H_2CH_3$), 14.5 ($CH_2\underline{C}H_3$).

^{29}Si{^{1}H} NMR (99 MHz, C_6D_6, 300 K): δ [ppm] = 52.0 ($\underline{Si}$=C), 15.5 ($\underline{Si}$^{t}Bu$_3$).

Minor isomer (*E*)-silene 10f' (~15%):

^{29}Si{^{1}H} NMR (99 MHz, C_6D_6, 300 K): δ [ppm] = 42.6 ($\underline{Si}$=C), 12.9 ($\underline{Si}$^{t}Bu$_3$).

LIFDI-MS: calculated (for $C_{46}H_{77}N_3Si_2$): 727.5656
observed: 727.4438

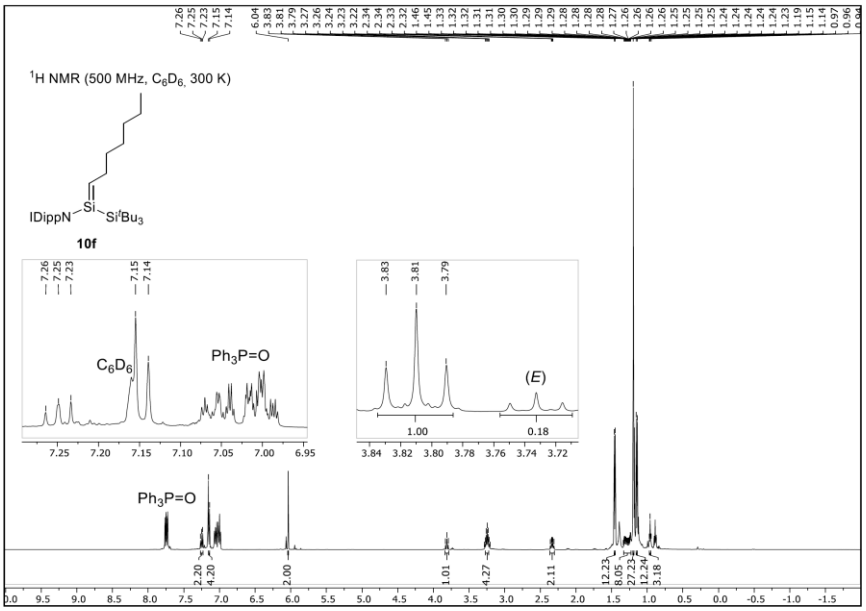


Figure S88. ^{1}H NMR spectrum of (*Z*)-silene **10f** in C_6D_6 at 300 K. The corresponding resonance of (*E*)-silene **10f'** used for the determination of the (*Z*)/(*E*)-ratio is marked with an (*E*).

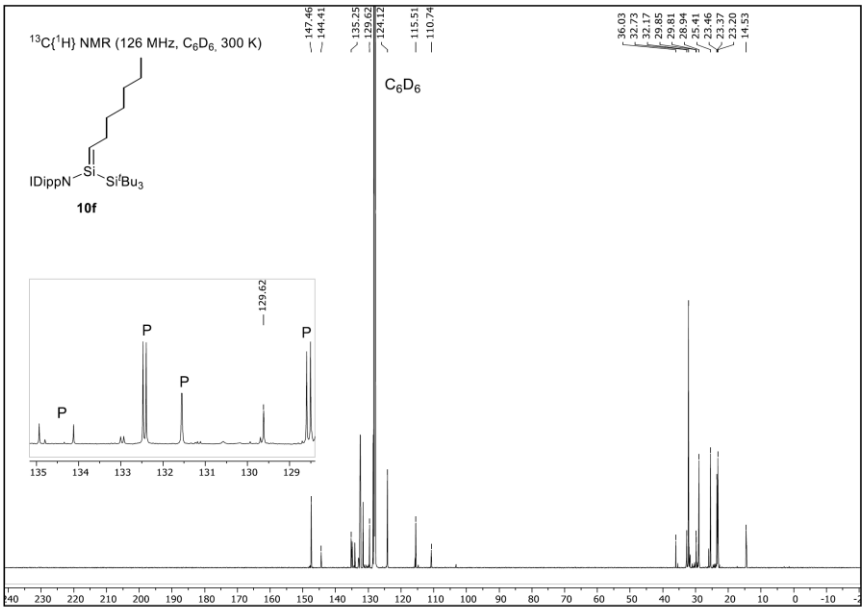


Figure S89. ^{13}C{^{1}H} NMR spectrum of (*Z*)-silene **10f** in C_6D_6 at 300 K. The resonances of Ph_3P=O are marked with a P.

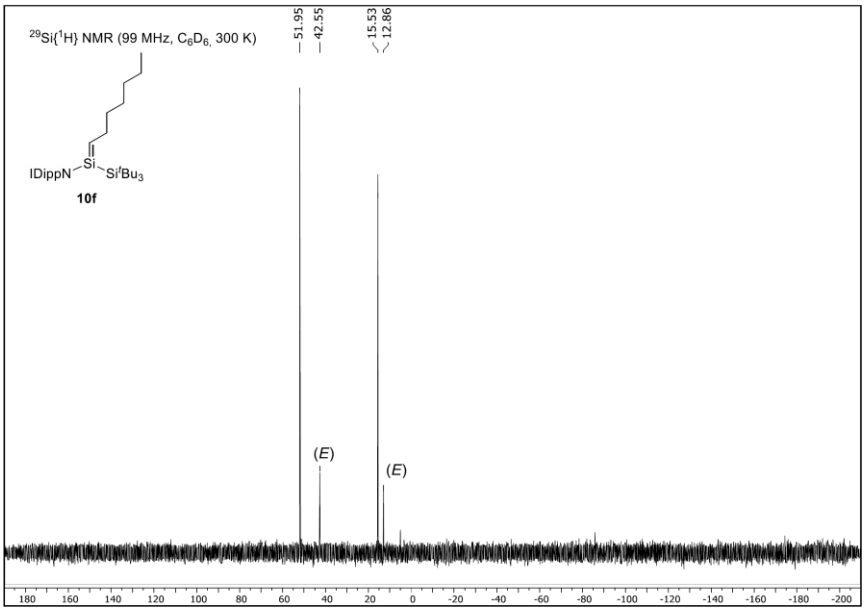


Figure S90. ^{29}Si{^{1}H} NMR spectrum of (*Z*)-silene **10f** in C_6D_6 at 300 K. The resonances of (*E*)-silene **10f′** are labeled with (*E*).

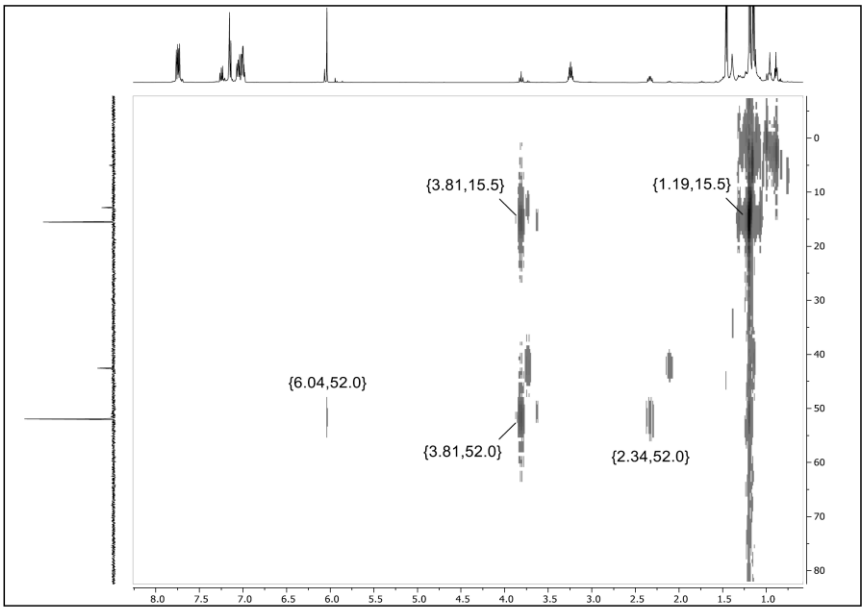


Figure S91. ^{1}H/^{29}Si HMBC NMR spectrum of (*Z*)-silene **10f** in C_6D_6 at 300 K.

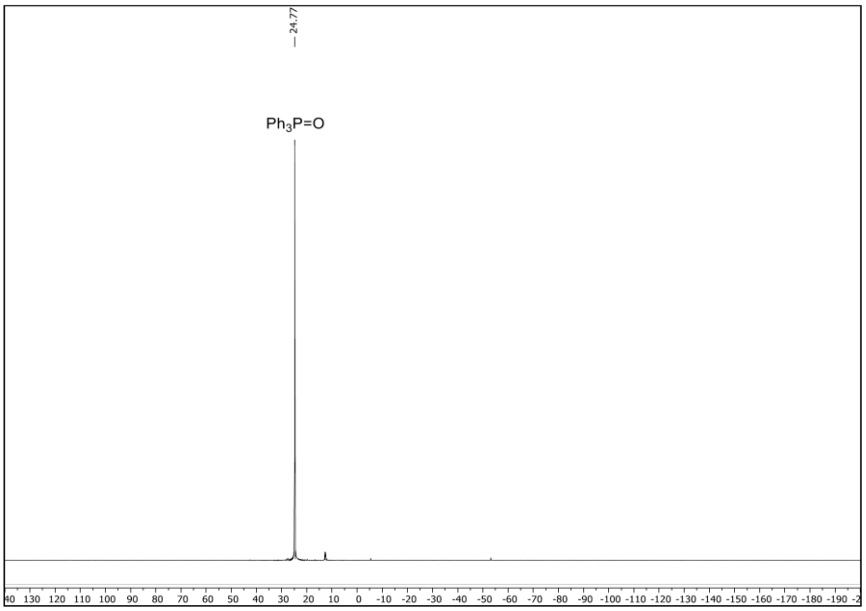


Figure S92. $^{31}P\{^{1}H\}$ NMR spectrum of the reaction of silanone **1** with phosphorus ylide **2k**.

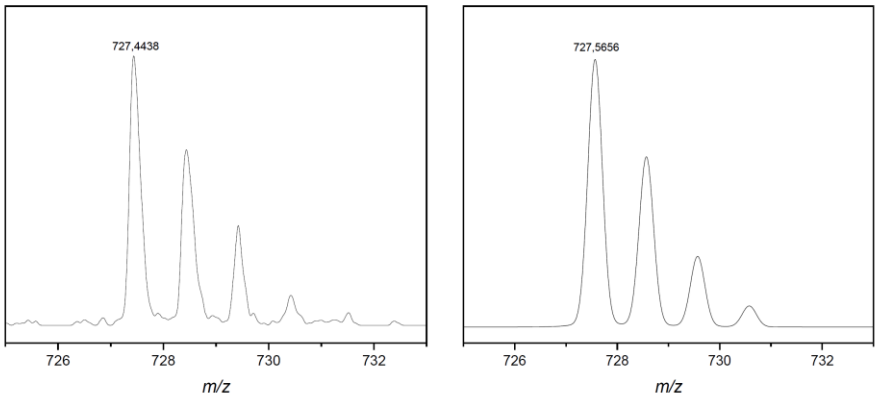
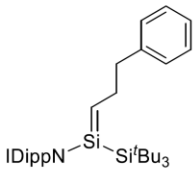


Figure S93. LIFDI-MS spectrometry (detail view with isotope pattern) of (*Z*)/(*E*)-silenes **10f/10f′**. Measured (left; m/z = 727.4438) and simulated (right; m/z = 727.5656) mass spectrum.

Reaction of silanone 1 with phosphorus ylide 2l

The (*Z*)/(*E*)-ratio between **10g** and **10g′** was calculated by ^{1}H NMR spectroscopy to about 76/24.



10g
$C_{48}H_{73}N_3Si_2$
748.30 g/mol

Major isomer (*Z*)-silene 10g (~76%):

^{1}H NMR (500 MHz, C_6D_6, 300 K): δ [ppm] = 7.28 (t, ^{3}J = 7.7 Hz, 2H, *p*-$C_{Dipp}\underline{H}$, overlapping with *p*-$C_{Dipp}\underline{H}$ of **10g′**), 7.25–7.21 (m, 5H, $C_{Ph}\underline{H}$, overlapping with $C_{Ph}\underline{H}$ of **10g′**), 7.14 (d, ^{3}J = 7.7 Hz, 4H, *m*-$C_{Dipp}\underline{H}$, overlapping with *m*-$C_{Dipp}\underline{H}$ of **10g′**), 6.04 (s, 2H, NC$\underline{H}$), 3.87 (t, ^{3}J = 9.8 Hz, 1H, Si=C$\underline{H}$), 3.24 (sept, ^{3}J = 6.9 Hz, 4H, C$\underline{H}$(CH_3)$_2$), 2.64–2.57 (m, 2H, $CH_2C\underline{H}_2$), 2.55–2.50 (m, 2H, C$\underline{H}_2CH_2$), 1.45 (d, ^{3}J = 6.9 Hz, 12H, CH(C$\underline{H}_3$)$_2$), 1.16 (s, 27H, C(C$\underline{H}_3$)$_3$, overlapping with CH(C$\underline{H}_3$)$_2$), 1.15 (d, ^{3}J = 6.9 Hz, 12H, CH(C$\underline{H}_3$)$_2$, overlapping with C(C$\underline{H}_3$)$_3$).

^{13}C{^{1}H} NMR (126 MHz, C_6D_6, 300 K): δ [ppm] = 147.5 (*o*-$\underline{C}_{Dipp}$), 144.7 (N$\underline{C}$N), 144.2 (ipso-$\underline{C}_{ar}$), 135.2 (*ipso*-$\underline{C}_{Dipp}$), 129.7 (*p*-$\underline{C}_{Dipp}$H), 128.8 (*m*-$\underline{C}_{ar}$H), 128.5 (*o*-$\underline{C}_{ar}$H), 125.6 (*p*-$\underline{C}_{ar}$H), 124.2 (*m*-$\underline{C}_{Dipp}$H), 115.6 (N$\underline{C}$H), 109.3 (Si=$\underline{C}$H), 43.1 ($CH_2\underline{C}H_2$Ph), 32.8 (Si=C$\underline{C}H_2$), 32.1 (C($\underline{C}H_3$)$_3$), 29.0 ($\underline{C}$H(CH_3)$_2$), 25.4 (CH($\underline{C}H_3$)$_2$), 23.4 ($\underline{C}$(CH_3)$_3$), 23.2 (CH($\underline{C}H_3$)$_2$).

^{29}Si{^{1}H} NMR (99 MHz, C_6D_6, 300 K): δ [ppm] = 53.0 ($\underline{Si}$=C), 15.7 ($\underline{Si}^{t}Bu_3$).

Minor isomer (*E*)-silene 10g′ (~24%):

^{29}Si{^{1}H} NMR (99 MHz, C_6D_6, 300 K): δ [ppm] = 43.3 ($\underline{Si}$=C), 13.0 ($\underline{Si}^{t}Bu_3$).

LIFDI-MS: calculated (for $C_{48}H_{73}N_3Si_2$): 747.5343
observed: 747.6791

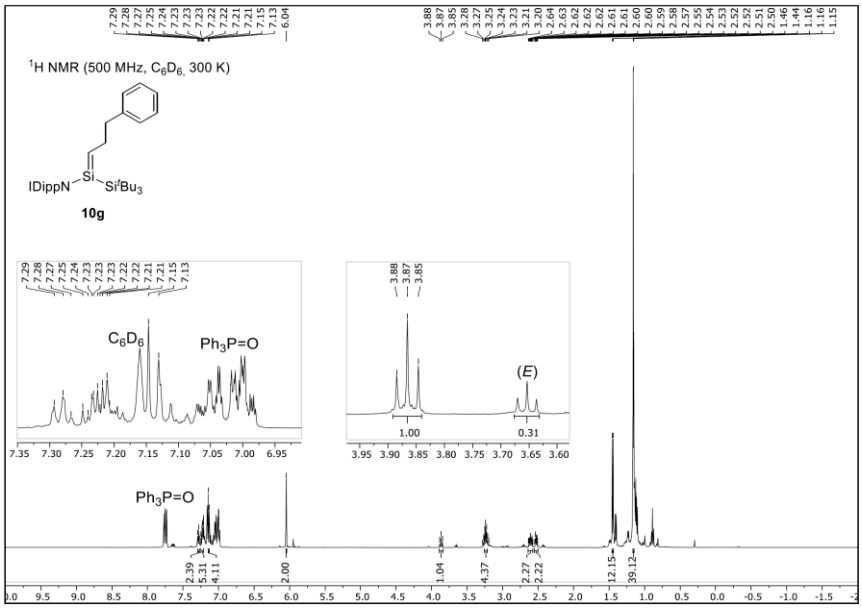


Figure S94. ^{1}H NMR spectrum of (*Z*)-silene **10g** in C_6D_6 at 300 K. The corresponding resonance of (*E*)-silene **10g′** used for the determination of the (*Z*)/(*E*)-ratio is marked with an (*E*).

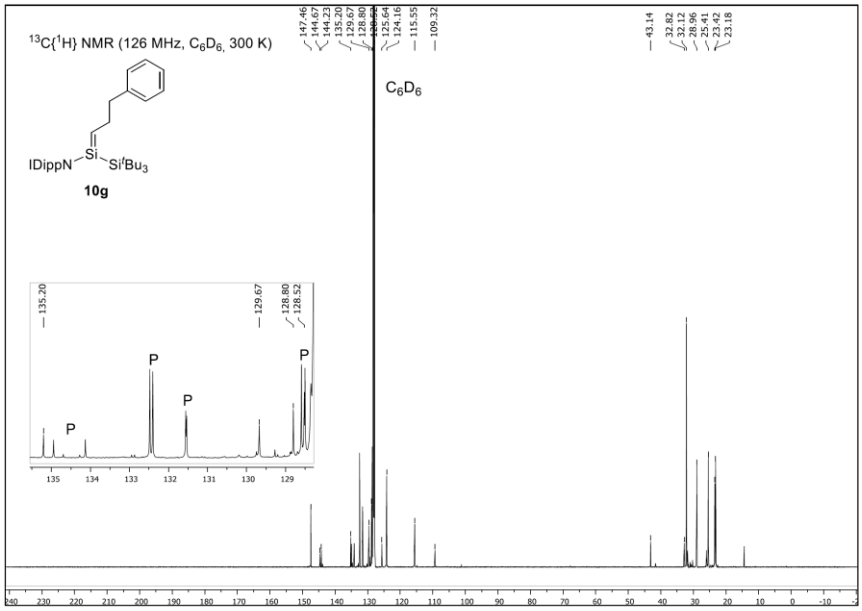


Figure S95. ^{13}C{^{1}H} NMR spectrum of (*Z*)-silene **10g** in C_6D_6 at 300 K. The resonances of Ph_3P=O are marked with a P.

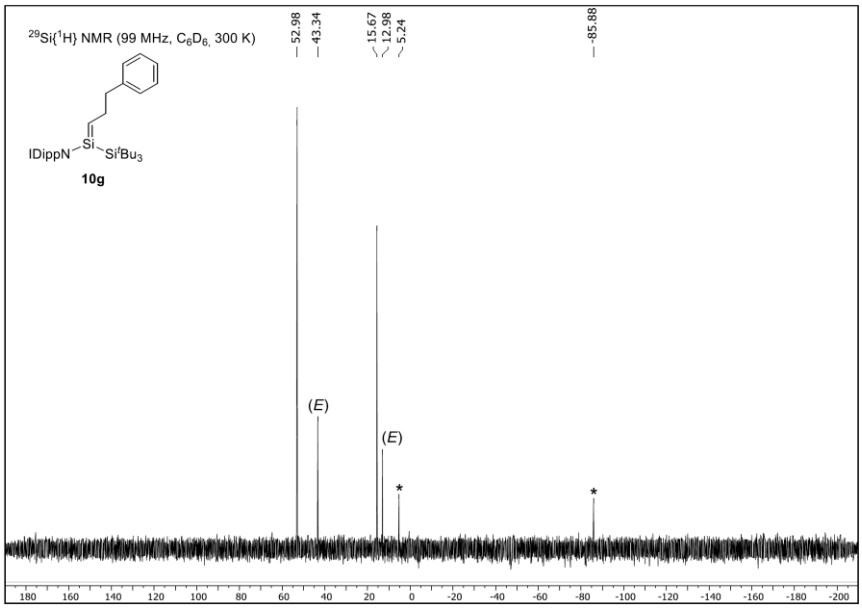


Figure S96. ^{29}Si{^{1}H} NMR spectrum of (*Z*)-silene **10g** in C_6D_6 at 300 K. The resonances of (*E*)-silene **10g′** and an unidentified by-product are labeled with (*E*) and asterisks *, respectively.

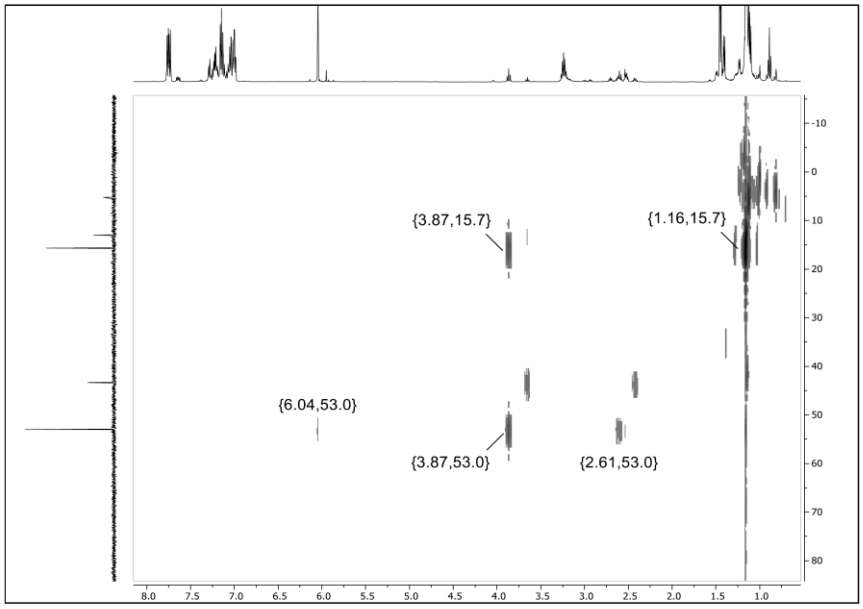


Figure S97. ^{1}H/^{29}Si HMBC NMR spectrum of (*Z*)-silene **10g** in C_6D_6 at 300 K.

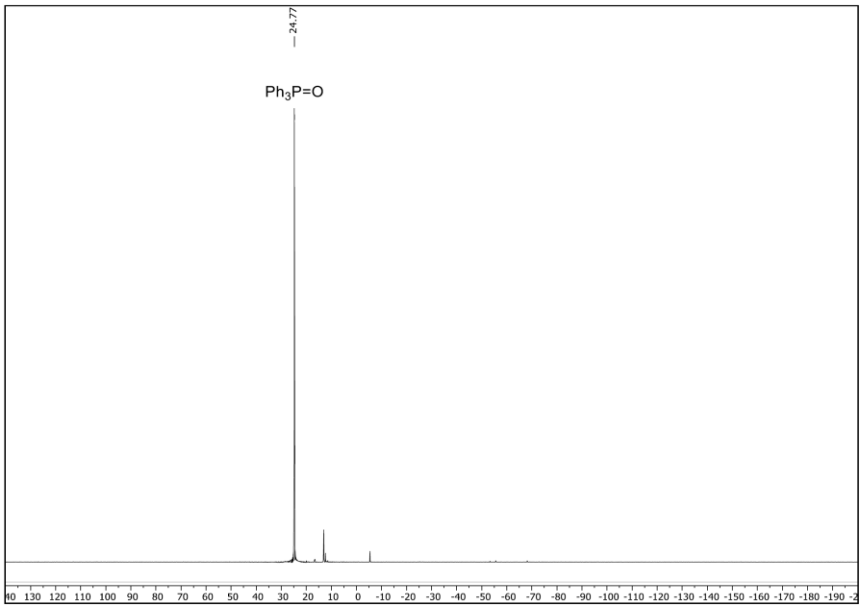


Figure S98. $^{31}P\{^{1}H\}$ NMR spectrum of the reaction of silanone **1** with phosphorus ylide **2l**.

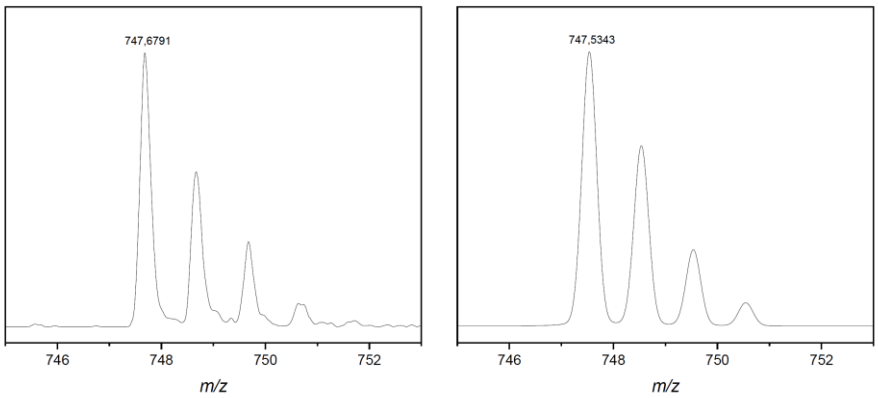
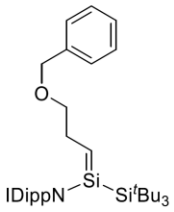


Figure S99. LIFDI-MS spectrometry (detail view with isotope pattern) of (*Z*)/(*E*)-silenes **10g**/**10g′**. Measured (left; m/z = 747.6791) and simulated (right; m/z = 747.5343) mass spectrum.

Reaction of silanone 1 with phosphorus ylide 2m

The (*Z*)/(*E*)-ratio between **10h** and **10h′** was calculated by ^{1}H NMR spectroscopy to about 45/55.

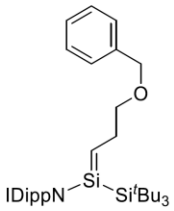


10h'
$C_{49}H_{75}N_3OSi_2$
778.33 g/mol

Major isomer (*E*)-silene 10h′ (~55%):

^{1}H NMR (500 MHz, C_6D_6, 300 K): δ [ppm] = 7.14 (d, ^{3}J = 7.7 Hz, 4H, *m*-$C_{Dipp}\underline{H}$), 6.08 (s, 2H, NC$\underline{H}$), 4.44 (s, 2H, OC$\underline{H}_2$Ph), 3.56–3.51 (m, 1H, Si=C$\underline{H}$, overlapping with Si=C$\underline{H}$ of **10h**), 3.42 (t, ^{3}J = 7.6 Hz, 2H, $CH_2C\underline{H}_2O$), 3.26–3.17 (m, 4H, C$\underline{H}(CH_3)_2$, overlapping with C$\underline{H}(CH_3)_2$ of **10h**), 2.55–2.51 (m, 2H, $C\underline{H}_2CH_2O$), 1.45 (d, ^{3}J = 6.9 Hz, 12H, CH(C$\underline{H}_3)_2$), 1.15 (s, 27H, C(C$\underline{H}_3)_3$), 1.10 (d, ^{3}J = 6.9 Hz, 12H, CH(C$\underline{H}_3)_2$). The resonances for the *p*-$C_{Dipp}\underline{H}$ and $C_{Ph}\underline{H}$ nuclei could not be unambiguously assigned, due to overlapping resonances of **10h** and minor, unidentified by-products.

^{29}Si{^{1}H} NMR (99 MHz, C_6D_6, 300 K): δ [ppm] = 46.5 (*Si*=C), 12.9 (*Si*^{t}Bu$_3$).



10h
$C_{49}H_{75}N_3OSi_2$
778.33 g/mol

Minor isomer (*Z*)-silene 10h (~45%):

^{1}H NMR (500 MHz, C_6D_6, 300 K): δ [ppm] = 7.10 (d, ^{3}J = 7.7 Hz, 4H, *m*-$C_{Dipp}\underline{H}$), 6.04 (s, 2H, NC$\underline{H}$), 4.52 (s, 2H, OC$\underline{H}_2$Ph), 3.56–3.51 (m, 1H, Si=C$\underline{H}$, overlapping with Si=C$\underline{H}$ of **10h′**), 3.26–3.17 (m, 4H, C$\underline{H}(CH_3)_2$, overlapping with C$\underline{H}(CH_3)_2$ of **10h′**), 2.75–2.71 (m, 2H, $C\underline{H}_2CH_2O$), 1.41 (d, ^{3}J = 6.9 Hz, 12H, CH(C$\underline{H}_3)_2$), 1.16 (s, 27H, C(C$\underline{H}_3)_3$), 1.12 (d, ^{3}J = 6.9 Hz, 12H, CH(C$\underline{H}_3)_2$). The resonances for the *p*-$C_{Dipp}\underline{H}$, $C_{Ph}\underline{H}$ and $CH_2C\underline{H}_2O$ nuclei could not be unambiguously assigned, due to overlapping resonances of **10h′** and minor, unidentified by-products.

^{29}Si{^{1}H} NMR (99 MHz, C_6D_6, 300 K): δ [ppm] = 56.3 (*Si*=C), 15.7 (*Si*^{t}Bu$_3$).

LIFDI-MS: calculated (for $C_{49}H_{75}N_3OSi_2$): 777.5449
observed: 777.3004

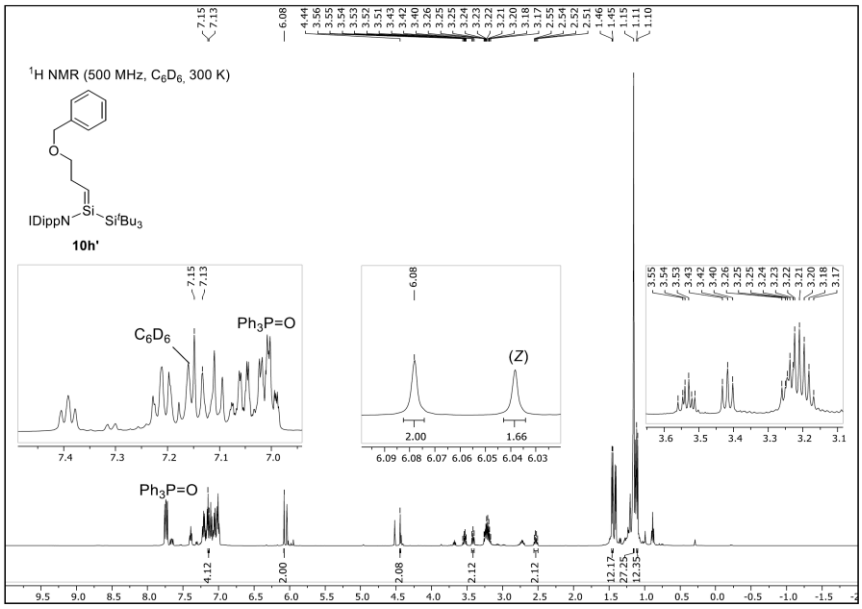


Figure S100. ^{1}H NMR spectrum of (*Z*)-silene **10h** and (*E*)-silene **10h′** in C_6D_6 at 300 K. Here, only the resonances of (*E*)-silene **10h′** are assigned. The corresponding resonance of (*Z*)-silene **10h** used for the determination of the (*Z*)/(*E*)-ratio is marked with an (*Z*).

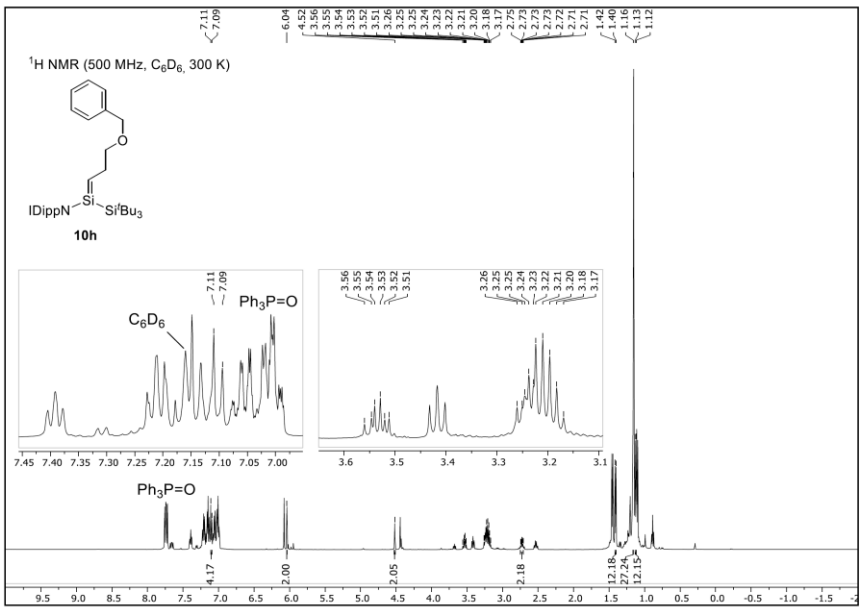


Figure S101. ^{1}H NMR spectrum of (*Z*)-silene **10h** and (*E*)-silene **10h′** in C_6D_6 at 300 K. Here, only the resonances of (*Z*)-silene **10h** are assigned.

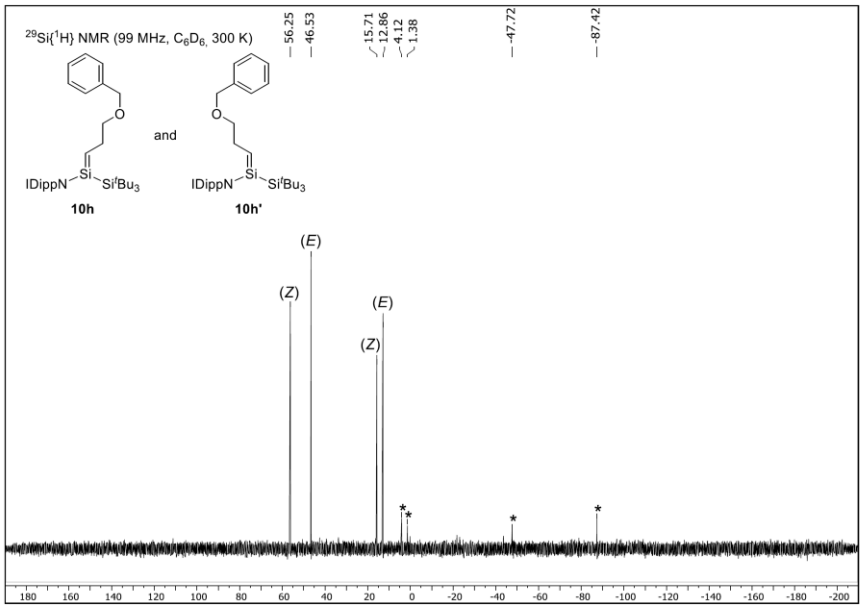


Figure S102. $^{29}Si\{^{1}H\}$ NMR spectrum of (*Z*)-silene **10h** and (*E*)-silene **10h′** in C_6D_6 at 300 K. The resonances of (*Z*)/(*E*)-silene **10h**/**10h′** and an unidentified by-product are labeled with (*Z*)/(*E*) and asterisks *, respectively.

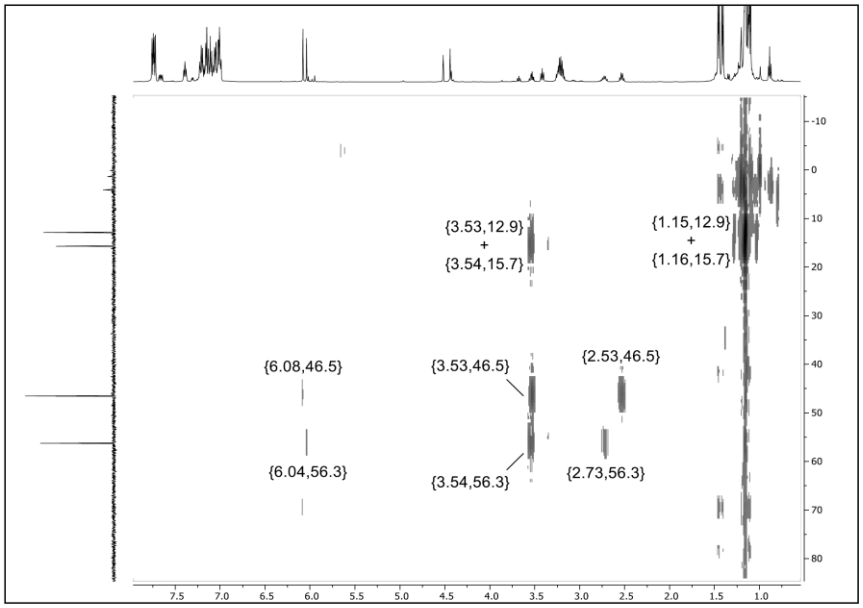


Figure S103. $^{1}H/^{29}Si$ HMBC NMR spectrum of (*Z*)-silene **10h** and (*E*)-silene **10h′** in C_6D_6 at 300 K.

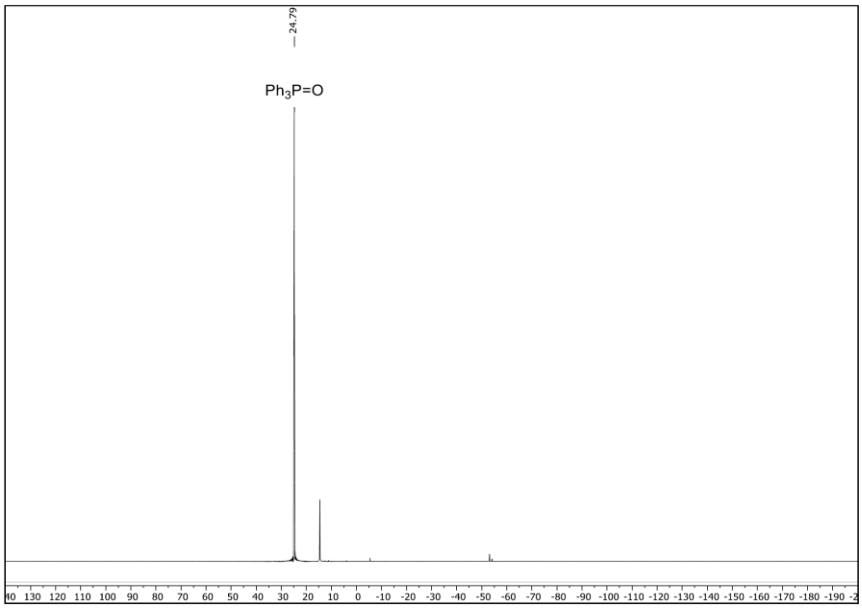


Figure S104. $^{31}P\{^{1}H\}$ NMR spectrum of the reaction of silanone **1** with phosphorus ylide **2m**.

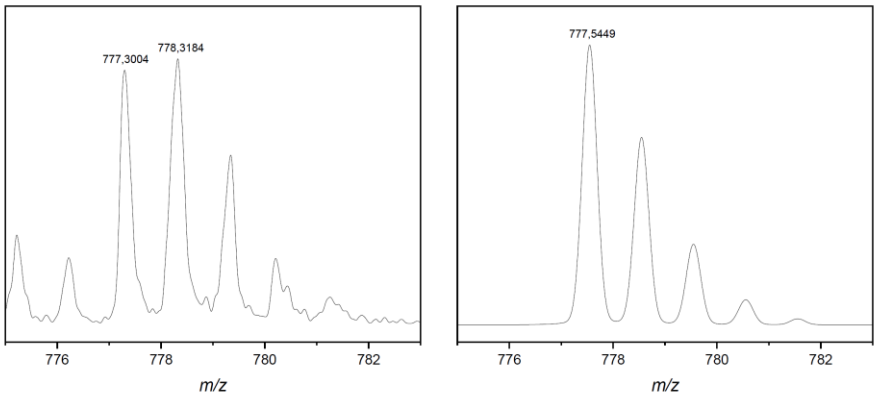
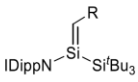
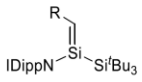


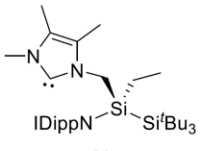
Figure S105. LIFDI-MS spectrometry (detail view with isotope pattern) of (*Z*)/(*E*)-silenes **10h/10h′**. Measured (left; m/z = 777.3004) and simulated (right; m/z = 777.5449) mass spectrum. Due to an overlap with another mass peak, the observed isotope pattern does not perfectly match the simulated one.

Overview of the spectroscopic data for the Sila-Wittig reaction

Table S1. Key spectroscopic features for the Sila-Wittig reaction of silanone **1** with non-stabilized ylides **2f-m**.

	 **2f-m**		 (*Z*)-silenes **10b-h**			 (*E*)-silenes **10b'-h'**			
	Ylide		**(*Z*)-Silene: δ(^{29}Si) [ppm]**			**(*E*)-Silene: δ(^{29}Si) [ppm]**			**Stereoselectivity**
R	**#**	**δ(^{31}P) [ppm]**	**#**	**Si=C**	**Si^{t}Bu$_3$**	**#**	**Si=C**	**Si^{t}Bu$_3$**	**(*Z*)/(*E*) [%]**
H	**2f**	20.6	**10a**	Si=C: 68.1			Si^{t}Bu$_3$: 11.9		–
Me	**2g**	14.5	**10b**	55.9	15.2	**10b′**	50.5	12.2	~92/8
Et	**2h**	12.3	**10c**	51.3	15.3	**10c′**	43.1	–	~94/6
Pr	**2i**	12.7	**10d**	52.3	15.6	**10d′**	42.8	12.9	~94/6
Bu	**2j**	12.6	**10e**	52.0	15.5	**10e′**	42.6	12.8	~89/11
Hex	**2k**	12.7	**10f**	52.0	15.5	**10f′**	42.6	12.9	~85/15
2-PhEt	**2l**	13.0	**10g**	53.0	15.7	**10g′**	43.3	13.0	~76/24
2-BnOEt	**2m**	14.6	**10h**	56.3	15.7	**10h′**	46.5	12.9	~45/55

1.6.1 Synthesis of silyl-substituted NHC 11



11
$C_{48}H_{79}N_5Si_2$
782.37 g/mol

Benzene (3 mL) was added to a mixture of **1** (100 mg, 155 µmol, 1.0 eq.) and **2g** (44.9 g, 155 µmol, 1.0 eq.) at ambient temperature. The resulting solution was stirred for 30 min. Subsequently, a solution of IMe_4 (19.2 mg, 155 µmol, 1.0 eq.) in benzene (0.5 mL) was added. After stirring the reaction mixture for 1 h, the solvent was removed *in vacuo* and the residue was extracted with cold *n*-hexane (3 × 1 mL). $Ph_3P{=}O$ was partially separated from the mixture by filtration (complete removal was not possible) and the solvent was removed under vacuum. Crystallization of the residue from *n*-hexane/toluene at –35 °C provided **11** as colorless crystals (84.8 mg, 129 µmol, 83%), which were suitable for SC-XRD analysis.

m.p.: 170-171 °C (decomposition; color change from colorless to dark brown/black).

^{1}H NMR (500 MHz, C_6D_6, 300 K): δ [ppm] = 7.25–7.19 (m, 4H, $C_{ar}\underline{H}$), 7.12–7.10 (m, 2H, $C_{ar}\underline{H}$), 6.00 (s, 2H, NC$\underline{H}$), 3.58 (sept, ^3J = 6.9 Hz, 2H, C$\underline{H}$(CH$_3$)$_2$), 3.34 (sept, ^3J = 6.9 Hz, 2H, C$\underline{H}$(CH$_3$)$_2$), 3.31 (s, 3H, NC$\underline{H}_3$), 2.86 (d, ^2J = 15.3 Hz, 1H, NC$\underline{H}_2$), 2.66 (d, ^2J = 15.3 Hz, 1H, NC$\underline{H}_2$), 1.78 (s, 3H, NCC$\underline{H}_3$), 1.60 (s, 3H, NCC$\underline{H}_3$), 1.57 (t, ^3J = 7.7 Hz, 3H, SiCH$_2$C$\underline{H}_3$), 1.45 (d, ^3J = 6.9 Hz, 6H, CH(C$\underline{H}_3$)$_2$), 1.33 (d, ^3J = 6.9 Hz, 6H, CH(C$\underline{H}_3$)$_2$), 1.16 (d, ^3J = 6.9 Hz, 6H, CH(C$\underline{H}_3$)$_2$), 1.15 (s,

27H, C(C<u>*H*</u>$_3$)$_3$), 1.10 (d, ^3J = 6.9 Hz, 6H, CH(C<u>*H*</u>$_3$)$_2$). The resonance for the SiC<u>*H*</u>$_2$CH$_3$ nucleus could not be located.

^{13}C{^{1}H} NMR (126 MHz, C$_6$D$_6$, 300 K): δ [ppm] = 213.2 (<u>*carbene C*</u>), 148.3 (*o*-<u>C</u>$_{ar}$), 148.0 (*o*-<u>C</u>$_{ar}$), 144.4 (N<u>C</u>N), 136.6 (*ipso*-<u>C</u>$_{ar}$), 129.5 (*p*-<u>C</u>$_{ar}$H), 124.4 (*m*-<u>C</u>$_{ar}$H), 124.0 (*m*-<u>C</u>$_{ar}$H), 123.7 (N<u>C</u>CH$_3$), 121.2 (N<u>C</u>CH$_3$), 115.6 (N<u>C</u>H), 39.5 (N<u>C</u>H$_2$), 35.0 (N<u>C</u>H$_3$), 32.5 (C(<u>C</u>H$_3$)$_3$), 28.7 (<u>C</u>H(CH$_3$)$_2$), 26.5 (CH(<u>C</u>H$_3$)$_2$), 25.9 (CH(<u>C</u>H$_3$)$_2$), 23.7 (<u>C</u>(CH$_3$)$_3$), 23.1 (CH(<u>C</u>H$_3$)$_2$), 22.6 (CH(<u>C</u>H$_3$)$_2$), 14.8 (Si<u>C</u>H$_2$CH$_3$), 9.9 (NC<u>C</u>H$_3$), 9.1 (SiCH$_2$<u>C</u>H$_3$), 9.1 (NC<u>C</u>H$_3$).

^{29}Si{^{1}H} NMR (99 MHz, C$_6$D$_6$, 300 K): δ [ppm] = 2.4 (<u>*Si*</u>^{t}Bu$_3$), –21.0 (<u>*Si*</u>CH$_2$CH$_3$).

Anal. Calcd. [%] for C$_{48}$H$_{79}$N$_5$Si$_2$: C, 73.69; H, 10.18; N, 8.95. Found [%]: C, 73.04; H, 10.16; N, 8.70.

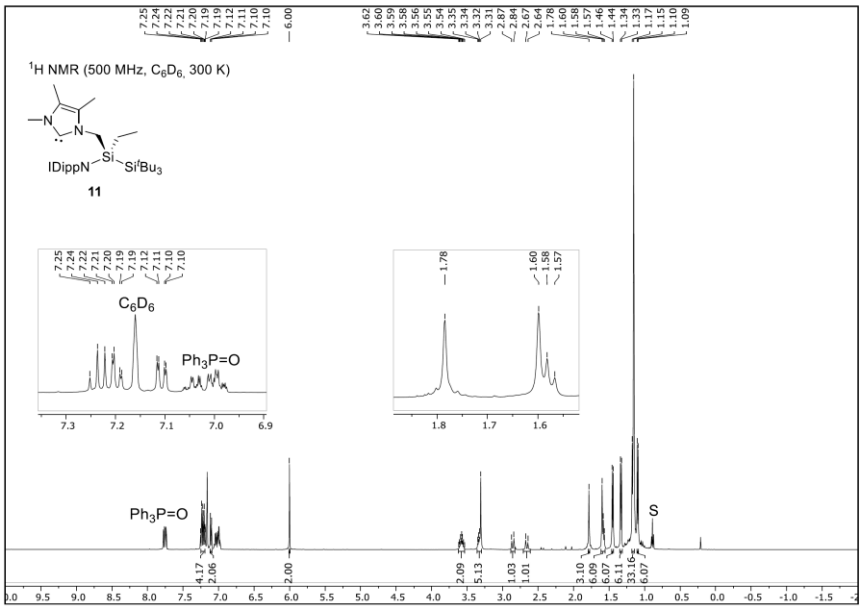


Figure S106. ^{1}H NMR spectrum of silyl-substituted NHC **11** in C$_6$D$_6$ at 300 K. Residual *n*-hexane (S) and Ph$_3$P=O are labeled accordingly.

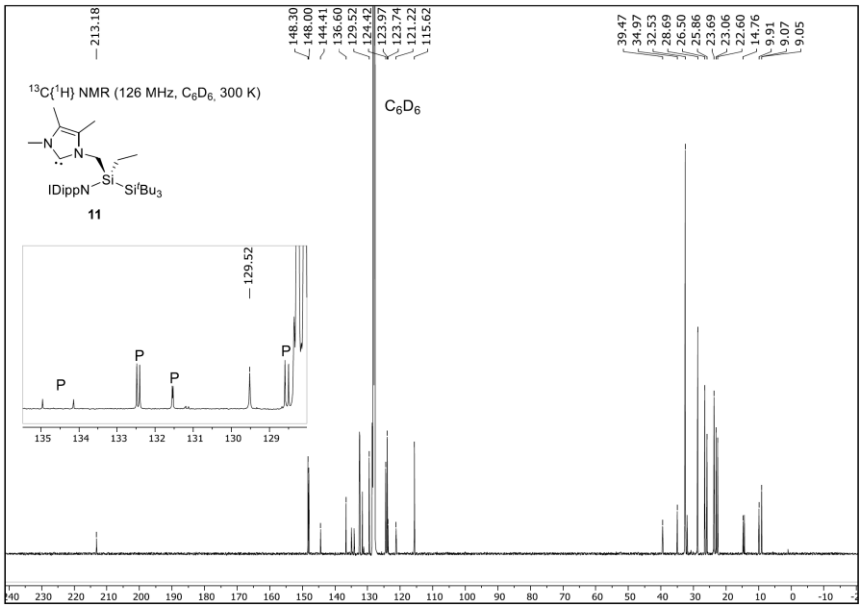


Figure S107. $^{13}C\{^{1}H\}$ NMR spectrum of silyl-substituted NHC **11** in C_6D_6 at 300 K. Residual $Ph_3P{=}O$ is marked with a P.

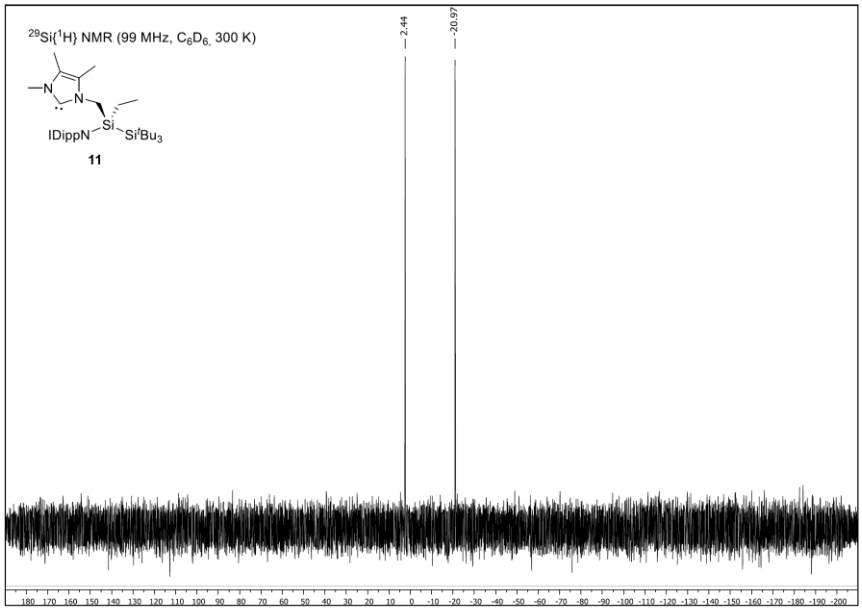


Figure S108. $^{29}Si\{^{1}H\}$ NMR spectrum of silyl-substituted NHC **11** in C_6D_6 at 300 K.

2. X-ray Crystallographic Data

General Information

The X-ray intensity data of **2h** and **6** were collected on an X-ray single crystal diffractometer equipped with a CCD detector (*Apex II CCD*), a fine focus sealed tube with MoKα radiation (λ = 0.71073 Å) and a *Triumph* monochromator by using the *APEX II/III* software package.[S7] The X-ray intensity data of **2m**, **5**, **9** and **11** were collected on an X-ray single crystal diffractometer equipped with a CMOS detector (*Bruker Photon-100*), an IMS microsource with MoKα radiation (λ = 0.71073 Å) and a *Helios* mirror optic by using the *APEX III* software package.[S7] The X-ray intensity data of **5a** and **8** were collected on an X-ray single crystal diffractometer equipped with a CMOS detector (*Bruker Photon-100*), a rotating anode (*Bruker TXS*) with MoKα radiation (λ = 0.71073 Å) and a *Helios* mirror optic by using the *APEX III* software package.[S7] The measurements were performed on single crystals coated with the perfluorinated ether *Fomblin® Y*. The crystals were fixed on the top of a microsampler, transferred to the diffractometer and frozen under a stream of cold nitrogen. A matrix scan was used to determine the initial lattice parameters. Reflections were merged and corrected for Lorenz and polarization effects, scan speed, and background using *SAINT*.[S8] Absorption corrections, including odd and even ordered spherical harmonics were performed using *SADABS*.[S8] Space group assignments were based upon systematic absences, E statistics, and successful refinement of the structures. Structures were solved by direct methods with the aid of successive difference Fourier maps, and were refined against all data using the *APEX III* software in conjunction with *SHELXL-2014*[S9] and *SHELXLE*.[S10] All H atoms were placed in calculated positions and refined using a riding model, with methylene and aromatic C–H distances of 0.99 and 0.95 Å, respectively, and $U_{iso}(H) = 1.2 \cdot U_{eq}(C)$. Full-matrix least-squares refinements were carried out by minimizing $\Delta w(F_o^2 - F_c^2)^2$ with *SHELXL-97*[S11] weighting scheme. Neutral atom scattering factors for all atoms and anomalous dispersion corrections for the non-hydrogen atoms were taken from International Tables for Crystallography.[S12] The images of the crystal structures were generated by *Mercury*.[S13] The CCDC numbers CCDC-1949650 (**2h**), CCDC-1949651 (**2m**), CCDC-1949652 (**5**), CCDC-1949653 (**5a**), CCDC-1949654 (**6**), CCDC-1949655 (**8**), CCDC-1949656 (**9**) and CCDC-1949657 (**11**) contain the supplementary crystallographic data for the structures. These data can be obtained free of charge from the *Cambridge Crystallographic Data Centre via* https://www.ccdc.cam.ac.uk/structures/.

Single Crystal X-ray Structure Determinations

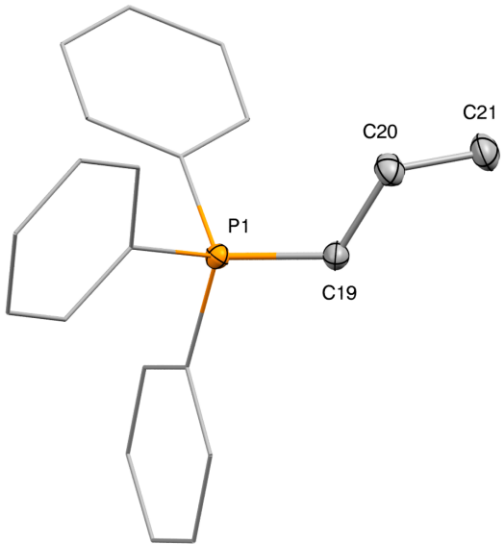


Figure S109. Molecular structure of **2h** with ellipsoids set at 50% probability. Hydrogen atoms are omitted for clarity. Selected bond lengths [Å] and angles [°]: P1–C19 1.674(1), C19–C20 1.511(1), C20–C21 1.528(2); P1–C19–C20 123.4(1), C19–C20–C21 112.1(1).

Table S2. Crystal data and structure refinement for compound **2h**.

Chemical formula	$C_{21}H_{21}P$	
Formula weight	304.37 g/mol	
Temperature	100(2) K	
Wavelength	0.71073 Å	
Crystal size	0.283 × 0.379 × 0.482 mm	
Crystal habit	clear intense orange fragment	
Crystal system	triclinic	
Space group	P $\bar{1}$	
Unit cell dimensions	a = 8.7733(9) Å	α = 66.036(5)°
	b = 9.6719(11) Å	β = 84.097(5)°
	c = 10.8271(12) Å	γ = 80.862(5)°
Volume	882.13(16) $Å^3$	
Z	2	
Density (calculated)	1.221 g/cm^3	
Absorption coefficient	0.161 mm^{-1}	
F(000)	324	
Diffractometer	Bruker D8 Kappa Apex II	
Radiation source	fine-focus sealed tube, Mo	
Theta range for data collection	2.32 to 32.60°	
Index ranges	–12<=h<=12, –14<=k<=13, –16<=l<=15	
Reflections collected	38158	
Independent reflections	5362 [R(int) = 0.0222]	
Coverage of independent reflections	88.9%	
Absorption correction	Multi-Scan	
Max. and min. transmission	0.929 and 0.955	
Refinement method	Full-matrix least-squares on F^2	
Refinement program	SHELXL-2017/1 (Sheldrick, 2017)	
Function minimized	$\Sigma\, w(F_o^2 - F_c^2)^2$	
Data / restraints / parameters	5363 / 0 / 200	
Goodness-of-fit on F^2	1.023	
Final R indices	4633 data; I>2σ(I)	R1 = 0.0395, wR2 = 0.1007
	all data	R1 = 0.0477, wR2 = 0.1058
Weighting scheme	$w = 1/[\sigma^2(F_o^2) + (0.0505P)^2 + 0.4239P]$	
	where $P = (F_o^2 + 2F_c^2)/3$	
Largest diff. peak and hole	0.585 and –0.478 $eÅ^{-3}$	
R.M.S. deviation from mean	0.057 $eÅ^{-3}$	

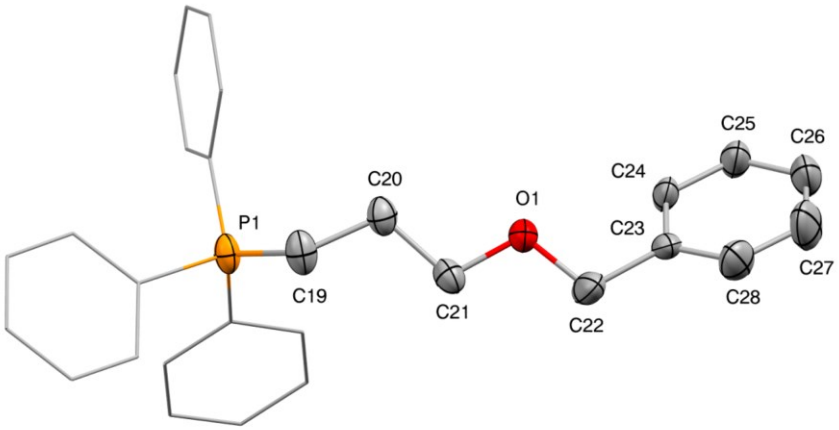


Figure S110. Molecular structure of **2m** with ellipsoids set at 50% probability. Hydrogen atoms are omitted for clarity. Selected bond lengths [Å] and angles [°]: P1–C19 1.670(2), C19–C20 1.503(3), C20–C21 1.512(2), C21–O1 1.422(2), O1–C22 1.419(2), C22–C23 1.52(1); P1–C19–C20 126.3(1), C19–C20–C21 113.7(1), C20–C21–O1 109.5(1), C21–O1–C22 112.2(1), O1–C22–C23 111.3(5).

Table S3. Crystal data and structure refinement for compound **2m**.

Chemical formula	$C_{28}H_{27}OP$	
Formula weight	410.50 g/mol	
Temperature	100(2) K	
Wavelength	0.71073 Å	
Crystal size	0.162 × 0.218 × 0.289 mm	
Crystal habit	clear orange fragment	
Crystal system	triclinic	
Space group	P $\bar{1}$	
Unit cell dimensions	a = 9.1563(12) Å	α = 95.900(5)°
	b = 9.899(2) Å	β = 108.600(7)°
	c = 13.221(3) Å	γ = 95.516(5)°
Volume	1119.1(4) $Å^3$	
Z	2	
Density (calculated)	1.218 g/cm^3	
Absorption coefficient	0.140 mm^{-1}	
F(000)	436	
Diffractometer	Bruker D8 Venture Duo IMS	
Radiation source	IMS microsource, Mo	
Theta range for data collection	2.09 to 25.35°	
Index ranges	–11<=h<=10, –11<=k<=11, –15<=l<=15	
Reflections collected	45471	
Independent reflections	4076 [R(int) = 0.0390]	
Coverage of independent reflections	99.9%	
Absorption correction	Multi-Scan	
Max. and min. transmission	0.964 and 0.978	
Refinement method	Full-matrix least-squares on F^2	
Refinement program	SHELXL-2017/1 (Sheldrick, 2017)	
Function minimized	$\Sigma\, w(F_o^2 - F_c^2)^2$	
Data / restraints / parameters	4076 / 108 / 326	
Goodness-of-fit on F^2	1.049	
Final R indices	3711 data; I>2σ(I)	R1 = 0.0358, wR2 = 0.0876
	all data	R1 = 0.0396, wR2 = 0.0901
Weighting scheme	$w = 1/[\sigma^2(F_o^2) + (0.0363P)^2 + 0.4844P]$	
	where $P = (F_o^2 + 2F_c^2)/3$	
Largest diff. peak and hole	0.372 and –0.266 $eÅ^{-3}$	
R.M.S. deviation from mean	0.034 $eÅ^{-3}$	

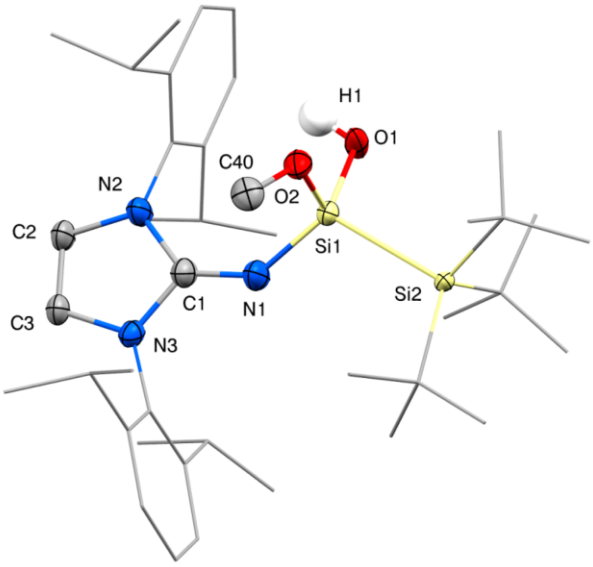


Figure S111. Molecular structure of **5** with ellipsoids set at 50% probability. Hydrogen atoms, except for the O–H nucleus, and cocrystallized toluene are omitted for clarity. Selected bond lengths [Å] and angles [°]: Si1–Si2 2.367(2), Si1–O1 1.659(4), Si1–O2 1.660(2), Si1–N1 1.717(2), N1–C1 1.276(2), O2–C40 1.402(3); Si2–Si1–O1 103.6(2), Si2–Si1–O2 110.7(1), Si2–Si1–N1 111.2(1), O1–Si1–O2 103.2(2), O1–Si1–N1 117.6(2), O2–Si1–N1 110.2(1).

Table S4. Crystal data and structure refinement for compound **5**.

Chemical formula	$C_{40}H_{67}N_3O_2Si_2$	
Formula weight	678.71 g/mol	
Temperature	100(2) K	
Wavelength	0.71073 Å	
Crystal size	0.204 × 0.228 × 0.284 mm	
Crystal habit	clear colourless fragment	
Crystal system	monoclinic	
Space group	P 21/n	
Unit cell dimensions	a = 10.8780(7) Å	α = 90°
	b = 20.5915(14) Å	β = 92.593(2)°
	c = 20.3438(13) Å	γ = 90°
Volume	4552.2(5) $Å^3$	
Z	4	
Density (calculated)	1.124 g/cm^3	
Absorption coefficient	0.117 mm^{-1}	
F(000)	1688	
Diffractometer	Bruker D8 Venture Duo IMS	
Radiation source	IMS microsource, Mo	
Theta range for data collection	1.98 to 25.68°	
Index ranges	–13<=h<=13, –25<=k<=25, –24<=l<=24	
Reflections collected	199873	
Independent reflections	8621 [R(int) = 0.0442]	
Coverage of independent reflections	99.7%	
Absorption correction	Multi-Scan	
Max. and min. transmission	0.968 and 0.976	
Refinement method	Full-matrix least-squares on F^2	
Refinement program	SHELXL-2017/1 (Sheldrick, 2017)	
Function minimized	$\Sigma\, w(F_o^2 - F_c^2)^2$	
Data / restraints / parameters	8621 / 535 / 838	
Goodness-of-fit on F^2	1.054	
Final R indices	7885 data; I>2σ(I)	R1 = 0.0488, wR2 = 0.1149
	all data	R1 = 0.0532, wR2 = 0.1182
Weighting scheme	$w = 1/[\sigma^2(F_o^2) + (0.0432P)^2 + 3.6461P]$	
	where $P = (F_o^2 + 2F_c^2)/3$	
Largest diff. peak and hole	0.592 and –0.295 $eÅ^{-3}$	
R.M.S. deviation from mean	0.040 $eÅ^{-3}$	

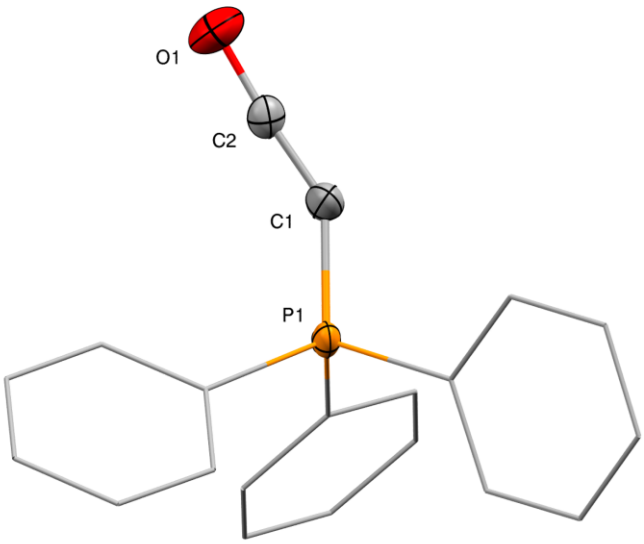


Figure S112. Molecular structure of **5a** with ellipsoids set at 50% probability. Hydrogen atoms are omitted for clarity. Selected bond lengths [Å] and angles [°]: P1–C1 1.667(2), C1–C2 1.238(2), C2–O1 1.192(2); P1–C1–C2 143.0(1), C1–C2–O1 174.5(2).

Table S5. Crystal data and structure refinement for compound **5a**.

Chemical formula	$C_{20}H_{15}OP$	
Formula weight	302.31 g/mol	
Temperature	100(2) K	
Wavelength	0.71073 Å	
Crystal size	0.196 × 0.256 × 0.319 mm	
Crystal habit	clear colourless fragment	
Crystal system	monoclinic	
Space group	P 21/n	
Unit cell dimensions	a = 10.6676(8) Å	α = 90°
	b = 10.1180(9) Å	β = 93.603(3)°
	c = 14.5035(11) Å	γ = 90°
Volume	1562.3(2) $Å^3$	
Z	4	
Density (calculated)	1.285 g/cm^3	
Absorption coefficient	0.175 mm^{-1}	
F(000)	632	
Diffractometer	Bruker D8 Venture	
Radiation source	TXS rotating anode, Mo	
Theta range for data collection	2.30 to 25.68°	
Index ranges	–13<=h<=13, –12<=k<=12, –17<=l<=17	
Reflections collected	65167	
Independent reflections	2964 [R(int) = 0.0298]	
Coverage of independent reflections	99.9%	
Absorption correction	Multi-Scan	
Max. and min. transmission	0.948 and 0.966	
Refinement method	Full-matrix least-squares on F^2	
Refinement program	SHELXL-2016/6 (Sheldrick, 2016)	
Function minimized	$\Sigma\, w(F_o^2 - F_c^2)^2$	
Data / restraints / parameters	2964 / 0 / 199	
Goodness-of-fit on F^2	1.062	
Final R indices	2763 data; I>2σ(I)	R1 = 0.0321, wR2 = 0.0867
	all data	R1 = 0.0342, wR2 = 0.0886
Weighting scheme	$w = 1/[\sigma^2(F_o^2) + (0.0408P)^2 + 0.9652P]$	
	where $P = (F_o^2 + 2F_c^2)/3$	
Largest diff. peak and hole	0.285 and –0.325 $eÅ^{-3}$	
R.M.S. deviation from mean	0.048 $eÅ^{-3}$	

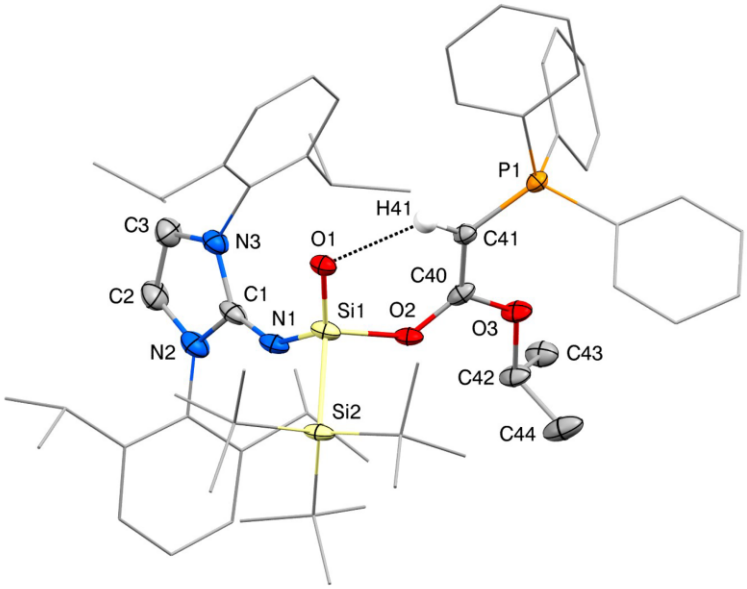


Figure S113. Molecular structure of **6** with ellipsoids set at 30% probability. Hydrogen atoms, except for H41 involved in hydrogen bonding (visualized by the dashed line), are omitted for clarity. Selected bond lengths [Å] and angles [°]: Si1–O1 1.548(3), Si1–O2 1.806(3), Si1–Si2 2.360(5), Si1–N1 1.707(5), N1–C1 1.270(8), O2–C40 1.299(6), C40–C41 1.365(6), C41–P1 1.712(5); Si2–Si1–O1 109.9(2), Si2–Si1–N1 107.2(2), O1–Si1–N1 124.9(2), Si1–O2–C40 128.5(3).

Table S6. Crystal data and structure refinement for compound **6**.

Chemical formula	$C_{62}H_{86}N_3O_3PSi_2$	
Formula weight	1008.53 g/mol	
Temperature	100(2) K	
Wavelength	0.71073 Å	
Crystal size	0.185 × 0.204 × 0.228 mm	
Crystal habit	clear colourless fragment	
Crystal system	trigonal	
Space group	R $\bar{3}$	
Unit cell dimensions	a = 36.225(5) Å	α = 90°
	b = 36.225(5) Å	β = 90°
	c = 34.334(5) Å	γ = 120°
Volume	39019(14) $Å^3$	
Z	18	
Density (calculated)	0.772 g/cm^3	
Absorption coefficient	0.090 mm^{-1}	
F(000)	9828	
Diffractometer	Bruker D8 Kappa Apex II	
Radiation source	fine-focus sealed tube, Mo	
Theta range for data collection	0.88 to 25.35°	
Index ranges	–43<=h<=43, –43<=k<=43, –40<=l<=41	
Reflections collected	133738	
Independent reflections	15883 [R(int) = 0.1189]	
Coverage of independent reflections	99.9%	
Absorption correction	Multi-Scan	
Max. and min. transmission	0.980 and 0.983	
Refinement method	Full-matrix least-squares on F^2	
Refinement program	SHELXL-2016/6 (Sheldrick, 2016)	
Function minimized	$\Sigma\, w(F_o^2 - F_c^2)^2$	
Data / restraints / parameters	15883 / 674 / 1024	
Goodness-of-fit on F^2	1.041	
Final R indices	9053 data; I>2σ(I)	R1 = 0.0813, wR2 = 0.2419
	all data	R1 = 0.1350, wR2 = 0.2755
Weighting scheme	$w = 1/[\sigma^2(F_o^2) + (0.1311P)^2 + 153.5113P]$	
	where $P = (F_o^2 + 2F_c^2)/3$	
Largest diff. peak and hole	0.340 and –0.379 $eÅ^{-3}$	
R.M.S. deviation from mean	0.063 $eÅ^{-3}$	

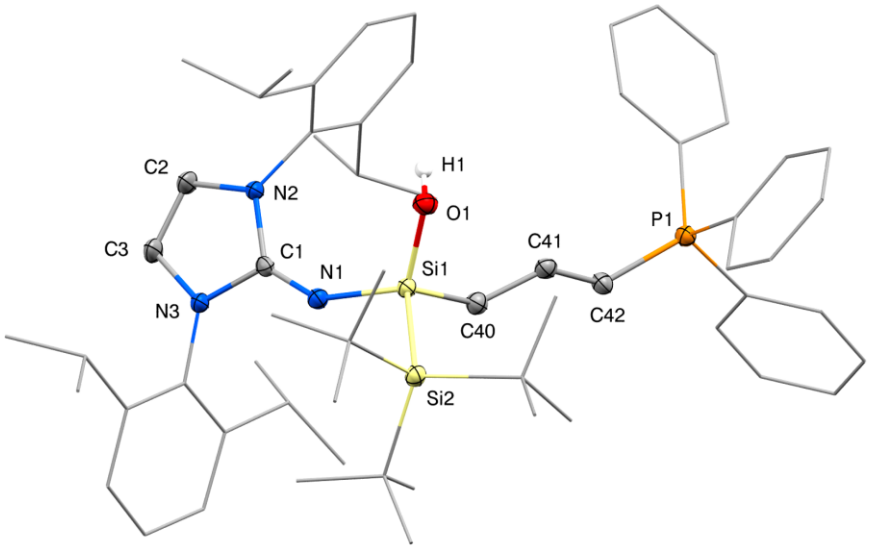


Figure S114. Molecular structure of **8** with ellipsoids set at 50% probability. Hydrogen atoms, except for the O1–H1 nucleus, and cocrystallized benzene are omitted for clarity. Selected bond lengths [Å] and angles [°]: Si1–O1 1.668(1), Si1–Si2 2.373(1), Si1–N1 1.698(2), Si1–C40 1.838(2), N1–C1 1.269(2), C40–C41 1.362(3), C41–C42 1.424(2), P1–C42 1.695(2); Si2–Si1–O1 103.4(1), Si1–C40–C41 126.0(1), C40–C41–C42 126.3(2), C41–C42–P1 126.7(1).

Table S7. Crystal data and structure refinement for compound **8**.

Chemical formula	$C_{60}H_{82}N_3OPSi_2$	
Formula weight	948.48 g/mol	
Temperature	100(2) K	
Wavelength	0.71073 Å	
Crystal size	0.091 × 0.193 × 0.208 mm	
Crystal habit	clear orange fragment	
Crystal system	triclinic	
Space group	P $\bar{1}$	
Unit cell dimensions	a = 12.3115(8) Å	α = 83.152(3)°
	b = 16.7455(12) Å	β = 78.214(3)°
	c = 17.3782(12) Å	γ = 83.253(3)°
Volume	3466.2(4) Å^3	
Z	2	
Density (calculated)	1.133 g/cm^3	
Absorption coefficient	0.120 mm^{-1}	
F(000)	1280	
Diffractometer	Bruker D8 Venture	
Radiation source	TXS rotating anode, Mo	
Theta range for data collection	2.19 to 25.68°	
Index ranges	–14<=h<=15, –20<=k<=20, –21<=l<=21	
Reflections collected	132902	
Independent reflections	13161 [R(int) = 0.0732]	
Coverage of independent reflections	100%	
Absorption correction	Multi-Scan	
Max. and min. transmission	0.975 and 0.989	
Refinement method	Full-matrix least-squares on F^2	
Refinement program	SHELXL-2014/5 (Sheldrick, 2014)	
Function minimized	$\Sigma\, w(F_o^2 - F_c^2)^2$	
Data / restraints / parameters	8829 / 0 / 787	
Goodness-of-fit on F^2	1.042	
Final R indices	10299 data; I>2σ(I)	R1 = 0.0421, wR2 = 0.0948
	all data	R1 = 0.0626, wR2 = 0.1052
Weighting scheme	$w = 1/[\sigma^2(F_o^2) + (0.0406P)^2 + 2.4471P]$	
	where $P = (F_o^2 + 2F_c^2)/3$	
Largest diff. peak and hole	0.664 and –0.526 eÅ^{-3}	
R.M.S. deviation from mean	0.048 eÅ^{-3}	

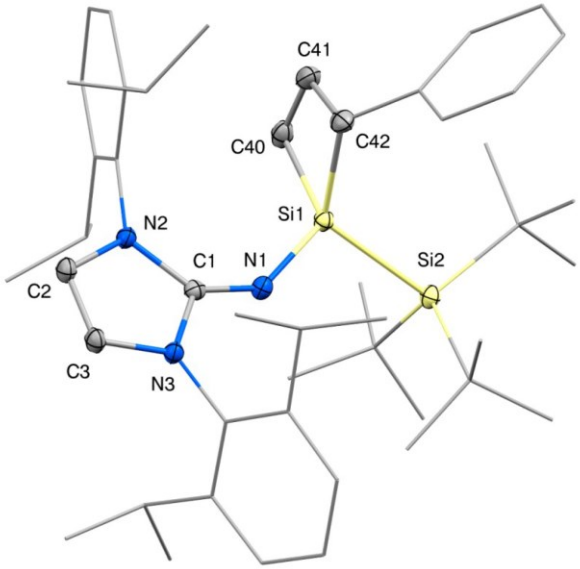


Figure S115. Molecular structure of **9** with ellipsoids set at 50% probability. Hydrogen atoms are omitted for clarity. Selected bond lengths [Å] and angles [°]: Si1–Si2 2.393(1), Si1–N1 1.697(1), Si1–C40 1.874(1), Si1–C42 1.943(1), N1–C1 1.279(1), C40–C41 1.333(2), C41–C42 1.516(2); Si2–Si1–N1 108.4(1), Si2–Si1–C40 112.7(1), Si2–Si1–C42 124.5(1), N1–Si1–C40 122.8(1), N1–Si1–C42 111.2(1), C40–Si1–C42 74.9(1), Si1–C40–C41 91.8(1), C40–C41–C42 109.0(1), Si1–C42–C41 83.9(1).

Table S8. Crystal data and structure refinement for compound **9**.

Chemical formula	$C_{48}H_{71}N_3Si_2$	
Formula weight	746.29 g/mol	
Temperature	100(2) K	
Wavelength	0.71073 Å	
Crystal size	0.219 × 0.263 × 0.349 mm	
Crystal habit	clear colourless plate	
Crystal system	monoclinic	
Space group	P 21/n	
Unit cell dimensions	a = 19.5253(16) Å	α = 90°
	b = 11.8248(9) Å	β = 99.975(3)°
	c = 19.9542(16) Å	γ = 90°
Volume	4537.4(6) $Å^3$	
Z	4	
Density (calculated)	1.092 g/cm^3	
Absorption coefficient	0.112 mm^{-1}	
F(000)	1632	
Diffractometer	Bruker D8 Venture Duo IMS	
Radiation source	IMS microsource, Mo	
Theta range for data collection	2.01 to 25.68°	
Index ranges	–23<=h<=23, –14<=k<=14, –24<=l<=24	
Reflections collected	193575	
Independent reflections	8622 [R(int) = 0.0463]	
Coverage of independent reflections	99.9%	
Absorption correction	Multi-Scan	
Max. and min. transmission	0.965 and 0.976	
Refinement method	Full-matrix least-squares on F^2	
Refinement program	SHELXL-2016/6 (Sheldrick, 2016)	
Function minimized	$\Sigma\, w(F_o^2 - F_c^2)^2$	
Data / restraints / parameters	8622 / 0 / 495	
Goodness-of-fit on F^2	1.054	
Final R indices	7883 data; I>2σ(I)	R1 = 0.0348, wR2 = 0.0847
	all data	R1 = 0.0386, wR2 = 0.0869
Weighting scheme	$w = 1/[\sigma^2(F_o^2) + (0.0357P)^2 + 2.7125P]$	
	where $P = (F_o^2 + 2F_c^2)/3$	
Largest diff. peak and hole	0.329 and –0.282 $eÅ^{-3}$	
R.M.S. deviation from mean	0.038 $eÅ^{-3}$	

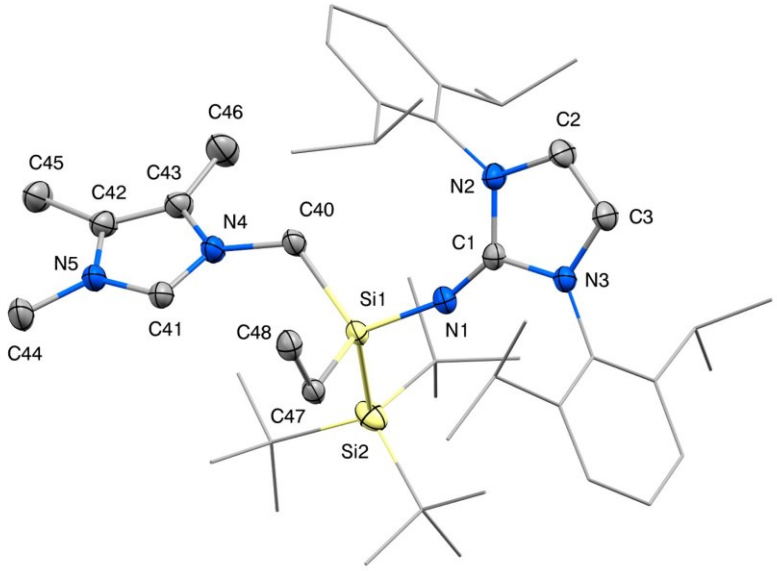


Figure S116. Molecular structure of **11** with ellipsoids set at 50% probability. Hydrogen atoms are omitted for clarity. Selected bond lengths [Å] and angles [°]: Si1–Si2 2.421(1), Si1–N1 1.692(1), Si1–C40 1.917(1), Si1–C47 1.888(1), N1–C1 1.268(2), N4–C40 1.470(2), C47–C48 1.528(2); Si2–Si1–N1 109.8(1), Si2–Si1–C40 115.9(1), Si2–Si1–C47 108.0(1), N1–Si1–C40 106.3(1), N1–Si1–C47 109.0(1).

Table S9. Crystal data and structure refinement for compound **11**.

Chemical formula	$C_{48}H_{79}N_5Si_2$	
Formula weight	782.37 g/mol	
Temperature	100(2) K	
Wavelength	0.71073 Å	
Crystal size	0.253 × 0.326 × 0.335 mm	
Crystal habit	clear colourless fragment	
Crystal system	orthorhombic	
Space group	P b c a	
Unit cell dimensions	a = 23.695(3) Å	α = 90°
	b = 18.5885(19) Å	β = 90°
	c = 25.738(2) Å	γ = 90°
Volume	11336(2) $Å^3$	
Z	8	
Density (calculated)	0.917 g/cm^3	
Absorption coefficient	0.093 mm^{-1}	
F(000)	3440	
Diffractometer	Bruker D8 Venture Duo IMS	
Radiation source	IMS microsource, Mo	
Theta range for data collection	2.04 to 25.35°	
Index ranges	–28<=h<=28, –22<=k<=22, –31<=l<=31	
Reflections collected	488979	
Independent reflections	10380 [R(int) = 0.0533]	
Coverage of independent reflections	100.0%	
Absorption correction	Multi-Scan	
Max. and min. transmission	0.969 and 0.977	
Refinement method	Full-matrix least-squares on F^2	
Refinement program	SHELXL-2016/6 (Sheldrick, 2016)	
Function minimized	$\Sigma\, w(F_o^2 - F_c^2)^2$	
Data / restraints / parameters	10380 / 0 / 517	
Goodness-of-fit on F^2	1.074	
Final R indices	9550 data; I>2σ(I)	R1 = 0.0428, wR2 = 0.1062
	all data	R1 = 0.0466, wR2 = 0.1091
Weighting scheme	$w = 1/[\sigma^2(F_o^2) + (0.0456P)^2 + 6.2777P]$	
	where $P = (F_o^2 + 2F_c^2)/3$	
Largest diff. peak and hole	0.282 and –0.258 $eÅ^{-3}$	
R.M.S. deviation from mean	0.036 $eÅ^{-3}$	

3. DFT Calculations

General Information

All geometry optimizations were carried out at B97-D/def2-SVP level of theory.[S14] Harmonic frequency calculations were used to verify the nature of the calculated structures. NMR shifts were calculated using the optimized geometries at the HCTH407/6-311+G(d)//B97-D/def2-SVP level of theory.[S15] All calculations were executed using Gaussian 09.[S16]

Calculated Structures

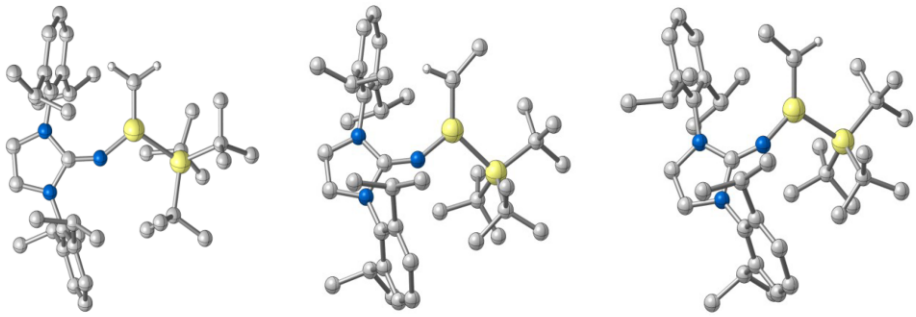


Figure S117. Calculated structures of half-parent silene **10a** (left), (*Z*)-silene **10b** and (*E*)-silene **10b′** at the HCTH407/6-311+G(d)//B97-D/def2-SVP level of theory

Calculated $^{29}Si\{^{1}H\}$ and $^{31}P\{^{1}H\}$ NMR Resonances

Table S10. Comparison of experimental and calculated NMR chemical shifts.

Compound	Nucleus	Exp. δ [ppm]	Calc. δ [ppm]	Δδ [ppm]
3	*Si*O_2	–61.0	–55.9	5.1
	PPh_3	–86.9	–80.5	6.4
7	*Si*H	–58.6	–57.5	1.1
	PPh_3	19.9	17.2	2.7
10a	*Si*=C	68.1	68.9	0.8
10b	*Si*=C	55.9	56.5	0.6
10b′	*Si*=C	50.5	51.2	0.7

Cartesian coordinates (x, y, z) for the optimized structures

Table S11. Cartesian geometry of **3**.

Atomtype	X Coordinate [Å]	Y Coordinate [Å]	Z Coordinate [Å]
C	5.023643	-0.720652	-1.539913
C	3.887224	0.080448	-1.820085
C	3.105049	-0.099205	-2.991461
C	3.497972	-1.108199	-3.890039
C	4.63359	-1.894641	-3.648182
C	5.388162	-1.697683	-2.486345
N	3.530399	1.115408	-0.898141
C	2.375262	1.149401	-0.094771
N	2.511283	2.344075	0.633298
C	3.683662	3.010492	0.264973
C	4.311651	2.252267	-0.672113
C	1.392864	3.017169	1.223453
C	0.49117	3.675374	0.352312
C	-0.607413	4.337206	0.932137
C	-0.776679	4.366895	2.323337
C	0.152597	3.734806	3.163002
C	1.249519	3.032918	2.628912
C	0.706118	3.723347	-1.158193
C	-0.447797	3.051083	-1.919494
C	2.286116	2.377236	3.533669
C	1.662361	1.599126	4.704398
N	1.429591	0.28993	-0.080669
Si	0.011435	-0.378384	0.55568
O	-0.45732	0.331893	2.10598
C	-1.736813	0.503916	2.440349
C	-1.891411	0.867104	3.899111
C	1.935687	0.82955	-3.308658
C	2.472579	2.138261	-3.929758
C	5.859804	-0.547431	-0.272534
C	6.140759	-1.88411	0.444693
C	0.858613	0.191936	-4.202464
C	7.191816	0.16657	-0.594825
Si	0.52938	-2.637817	1.163773
C	1.21987	-3.498285	-0.46131
C	0.314847	-3.120742	-1.659579
O	-1.294346	0.036445	-0.372091
P	-3.132821	0.049127	-0.130783
C	-2.859439	0.337464	1.660702
C	-0.996055	-3.658306	1.875838
C	-1.954977	-4.033503	0.723758
C	1.935958	-2.476617	2.548037

C	2.913252	-1.32184	2.212704
C	-0.532603	-4.960006	2.573365
C	-1.842368	-2.848528	2.887657
C	3.291429	3.435012	4.039821
C	0.918895	5.175772	-1.634149
C	2.753583	-3.78167	2.705145
C	1.310746	-2.135998	3.921176
C	2.624362	-2.951599	-0.783197
C	1.320564	-5.037887	-0.36413
H	3.942734	3.975923	0.69819
H	5.251284	2.400302	-1.201111
H	0.023781	3.780633	4.250965
H	-1.636247	4.893732	2.758352
H	-1.331119	4.837103	0.279647
H	2.849085	1.652159	2.91971
H	3.789297	3.95047	3.196951
H	4.071447	2.9612	4.667684
H	2.773499	4.20127	4.649665
H	1.149453	2.275724	5.415512
H	2.451659	1.062715	5.264434
H	0.932411	0.862039	4.332612
H	1.627265	3.171926	-1.402928
H	1.130705	5.191389	-2.720894
H	1.76671	5.652951	-1.105888
H	0.013008	5.786864	-1.455093
H	-1.387886	3.608101	-1.775164
H	-0.604388	2.017089	-1.570057
H	-0.22758	3.037452	-3.003242
H	6.265901	-2.325868	-2.29395
H	4.924719	-2.67155	-4.366753
H	2.912104	-1.273954	-4.800382
H	5.291144	0.08838	0.429034
H	7.025709	1.146998	-1.077937
H	7.799662	-0.449472	-1.285858
H	7.779253	0.328765	0.329922
H	5.205183	-2.417801	0.682305
H	6.681872	-1.69379	1.391255
H	6.772113	-2.549324	-0.174593
H	1.435141	1.080854	-2.36212
H	-0.013618	0.868328	-4.266884
H	0.520471	-0.772659	-3.782317
H	1.223903	0.016738	-5.233428
H	1.641131	2.840248	-4.129993
H	2.991277	1.930382	-4.886297
H	3.187643	2.637794	-3.250245
H	-0.731419	-3.44458	-1.539959
H	0.711678	-3.591032	-2.585092

H	0.308927	-2.027725	-1.824261
H	2.959634	-3.337473	-1.766979
H	3.376638	-3.256998	-0.03779
H	2.616399	-1.853575	-0.838715
H	0.336524	-5.524944	-0.247814
H	1.961377	-5.354879	0.479331
H	1.776308	-5.430994	-1.298443
H	-2.870301	-4.505959	1.140685
H	-1.513287	-4.748007	0.008373
H	-2.268995	-3.142853	0.156518
H	-1.425832	-5.557566	2.856585
H	0.029715	-4.754216	3.501796
H	0.099731	-5.587515	1.922097
H	-2.343299	-1.996874	2.398922
H	-1.258048	-2.461061	3.737851
H	-2.637327	-3.507961	3.298637
H	3.352512	-1.406691	1.207121
H	3.740614	-1.317401	2.955174
H	2.406052	-0.343947	2.270369
H	2.119364	-4.64124	2.983706
H	3.50846	-3.645432	3.509965
H	3.300341	-4.049731	1.784483
H	0.665992	-1.241579	3.856238
H	2.119657	-1.919089	4.651548
H	0.713811	-2.971145	4.327564
C	-3.36376	1.691934	-0.956501
H	-3.793116	0.497763	2.206959
H	-1.474618	0.0517	4.522232
H	-1.303225	1.777017	4.112546
H	-2.946328	1.033067	4.176297
C	-5.054913	-0.225281	0.209536
C	-3.155328	-1.299484	-1.491804
C	-4.056743	-2.385595	-1.486613
C	-4.062711	-3.327747	-2.530488
C	-3.200843	-3.179711	-3.62742
C	-2.31383	-2.090577	-3.657916
C	-2.273287	-1.178845	-2.593385
H	-4.756977	-2.525828	-0.660057
H	-4.756476	-4.176944	-2.481625
H	-3.216243	-3.908157	-4.448572
H	-1.624752	-1.958923	-4.502111
H	-1.543264	-0.368025	-2.613422
C	-6.071093	0.343912	-0.585436
C	-7.427758	0.044617	-0.361605
C	-7.800906	-0.845038	0.659142
C	-6.803037	-1.430673	1.457314
C	-5.451211	-1.118264	1.233523

H	-5.814362	1.037506	-1.394126
H	-8.196757	0.512633	-0.991063
H	-8.859423	-1.079645	0.832393
H	-7.075713	-2.13261	2.256965
H	-4.685958	-1.591624	1.863929
C	-3.485616	2.836104	-0.143664
C	-3.809503	4.080109	-0.707625
C	-4.007757	4.202139	-2.093594
C	-3.877462	3.066556	-2.909846
C	-3.563097	1.818139	-2.345639
H	-3.323306	2.752556	0.936449
H	-3.906867	4.959857	-0.058045
H	-4.260479	5.175185	-2.533999
H	-4.02739	3.146595	-3.994297
H	-3.495265	0.940073	-2.994568

Table S12. Cartesian geometry of **7**.

Atomtype	X Coordinate [Å]	Y Coordinate [Å]	Z Coordinate [Å]
C	-5.493598	-0.349203	-0.438304
C	-4.318413	-0.873335	-1.033236
C	-4.013455	-0.686741	-2.406457
C	-4.936272	0.04192	-3.180628
C	-6.122416	0.54149	-2.622632
C	-6.397374	0.345819	-1.26423
N	-3.466497	-1.698956	-0.231602
C	-2.180557	-1.386229	0.272841
N	-1.846202	-2.553319	1.004112
C	-2.885787	-3.486999	0.958687
C	-3.878521	-2.959315	0.198568
C	-0.597811	-2.857235	1.624731
C	0.215002	-3.860951	1.031031
C	1.3705	-4.258379	1.731509
C	1.724139	-3.648407	2.94307
C	0.919073	-2.642313	3.49272
C	-0.272629	-2.242364	2.858967
C	-0.151062	-4.447862	-0.335193
C	0.119198	-3.435784	-1.472938
C	-1.23742	-1.252776	3.506528
C	-0.574362	-0.32133	4.53257
N	-1.537308	-0.30128	0.086075
Si	-0.181716	0.719584	0.42213
C	1.404359	0.271922	-0.53334
C	-2.767392	-1.317979	-3.024993
C	-2.980758	-2.838163	-3.216306
C	-5.801843	-0.518379	1.04906

C	-6.137012	0.82331	1.732562
C	-2.337343	-0.685877	-4.358908
C	-6.949152	-1.529224	1.26446
Si	-0.973151	2.993795	0.217173
C	-2.479503	3.092061	-1.035753
C	-2.185973	2.250249	-2.299047
H	0.22616	0.603748	1.864466
C	0.464727	4.203886	-0.375262
C	0.733729	3.957784	-1.880719
C	-1.574644	3.488817	2.03999
C	-2.375121	2.328105	2.679406
C	0.149089	5.7018	-0.160659
C	1.779261	3.892602	0.368499
C	-2.429868	-1.996527	4.151318
C	0.522094	-5.796213	-0.64031
C	-2.451906	4.762395	2.056267
C	-0.364221	3.74229	2.968701
C	-3.732484	2.472571	-0.381621
C	-2.829331	4.533876	-1.471288
H	-2.811826	-4.439672	1.482181
H	-4.852409	-3.356387	-0.082507
H	1.214973	-2.168572	4.433109
H	2.640549	-3.957964	3.461487
H	2.015253	-5.037753	1.31318
H	-1.639857	-0.620845	2.696654
H	-2.971007	-2.617279	3.415387
H	-3.14477	-1.264889	4.576283
H	-2.079106	-2.65339	4.971859
H	-0.231001	-0.881578	5.424433
H	-1.303672	0.436296	4.871909
H	0.292423	0.20096	4.092811
H	-1.240373	-4.634339	-0.333525
H	0.131562	-6.199645	-1.593366
H	0.333978	-6.538895	0.158393
H	1.617714	-5.687838	-0.755065
H	1.202098	-3.309855	-1.638978
H	-0.304853	-2.440295	-1.260341
H	-0.3247	-3.805533	-2.414718
H	-7.316007	0.756152	-0.827409
H	-6.830331	1.097039	-3.25139
H	-4.728129	0.213329	-4.241679
H	-4.898785	-0.919972	1.54294
H	-6.708082	-2.516959	0.830258
H	-7.879127	-1.165806	0.785097
H	-7.149227	-1.66555	2.345305
H	-5.329699	1.558856	1.57966
H	-6.273858	0.669102	2.820423

H	-7.075034	1.255124	1.333644
H	-1.932215	-1.162217	-2.320244
H	-1.368952	-1.118343	-4.666817
H	-2.199881	0.403722	-4.260278
H	-3.074983	-0.887157	-5.161729
H	-2.084534	-3.288456	-3.684172
H	-3.844978	-3.022885	-3.884977
H	-3.163555	-3.357364	-2.258964
H	-1.303841	2.600946	-2.858555
H	-3.065867	2.303934	-2.974191
H	-2.019552	1.192748	-2.043342
H	-4.534628	2.367541	-1.138334
H	-4.131223	3.093837	0.439312
H	-3.513355	1.465728	0.007811
H	-2.030687	4.990806	-2.083391
H	-3.025572	5.19872	-0.610351
H	-3.748392	4.508931	-2.096011
H	1.647247	4.511412	-2.187799
H	-0.09858	4.312785	-2.512583
H	0.891839	2.88508	-2.09967
H	0.97659	6.316407	-0.577882
H	0.067907	5.946837	0.914505
H	-0.785882	6.014379	-0.655826
H	2.038237	2.830766	0.252961
H	1.732214	4.134688	1.442521
H	2.614034	4.478688	-0.069621
H	-3.275216	2.055746	2.107707
H	-2.698161	2.623822	3.70164
H	-1.748392	1.427025	2.779688
H	-1.924178	5.636249	1.635079
H	-2.728473	5.007494	3.105008
H	-3.388965	4.629263	1.489394
H	0.33507	2.886022	2.974242
H	-0.722775	3.886802	4.011261
H	0.19167	4.653315	2.684462
C	1.254874	0.064904	-1.956902
P	3.034168	0.172492	0.089603
O	2.461459	-0.217927	-2.597888
O	0.207196	0.123024	-2.59895
C	2.449192	-0.51167	-4.012119
H	1.726425	0.173607	-4.49699
C	3.866928	-0.240593	-4.514007
C	2.000657	-1.956471	-4.244884
H	3.922009	-0.415913	-5.605192
H	4.165483	0.803668	-4.306208
H	4.585902	-0.915136	-4.011141
H	2.006182	-2.18791	-5.327708

H	2.686366	-2.655058	-3.727988
H	0.978541	-2.100317	-3.856216
C	3.122318	0.126976	1.927202
C	3.983113	-1.307855	-0.474086
C	4.166405	1.575443	-0.352734
C	5.251554	1.902984	0.485811
C	6.122616	2.949107	0.136346
C	5.91607	3.669235	-1.052894
C	4.831652	3.345076	-1.887747
C	3.957899	2.304496	-1.539245
H	5.414295	1.3442	1.415484
H	6.961334	3.203237	0.7972
H	6.594735	4.488056	-1.324508
H	4.656281	3.912967	-2.810266
H	3.0984	2.071893	-2.172279
C	3.359086	-2.560965	-0.351161
C	4.021287	-3.722519	-0.775366
C	5.307376	-3.636581	-1.337126
C	5.930485	-2.382697	-1.46393
C	5.27399	-1.218743	-1.029731
H	2.351984	-2.618616	0.069024
H	3.526528	-4.695927	-0.674705
H	5.821399	-4.544385	-1.678255
H	6.931955	-2.307445	-1.906757
H	5.760364	-0.244088	-1.141805
C	3.728368	-0.948913	2.60537
C	3.854403	-0.921943	4.005366
C	3.376531	0.174337	4.739125
C	2.775323	1.252891	4.066179
C	2.654639	1.233523	2.669792
H	4.104667	-1.812051	2.048236
H	4.325537	-1.768678	4.52032
H	3.473474	0.191919	5.832222
H	2.395826	2.115881	4.626984
H	2.205654	2.088671	2.162015

Table S13. Cartesian geometry of **10a**.

Atomtype	X Coordinate [Å]	Y Coordinate [Å]	Z Coordinate [Å]
C	-0.619916	3.284901	-1.224823
C	-0.93751	2.860978	0.091294
C	-0.430201	3.504562	1.244292
C	0.373829	4.646005	1.057522
C	0.683326	5.101895	-0.229354
C	0.202327	4.418921	-1.357561
N	-1.827051	1.754018	0.267679

C	-1.478139	0.405044	0.108192
N	-2.65977	-0.281168	0.425622
C	-3.669646	0.618505	0.774135
C	-3.152399	1.874578	0.681172
C	-2.874916	-1.691041	0.301206
C	-2.417514	-2.548172	1.329357
C	-2.710243	-3.920133	1.208106
C	-3.415215	-4.411005	0.101194
C	-3.826156	-3.54389	-0.921568
C	-3.560562	-2.163182	-0.846125
N	-0.316294	-0.02114	-0.238552
Si	0.640007	-1.393784	-0.578363
C	0.031746	-2.984651	-0.925183
C	-1.643867	-1.988199	2.521218
C	-0.732932	-3.025544	3.198835
C	-3.899297	-1.219022	-1.999111
C	-2.661436	-1.049214	-2.910541
C	-0.739498	2.99992	2.652143
C	0.531095	2.855047	3.513628
C	-1.179815	2.540488	-2.43749
C	-2.676168	2.865668	-2.652392
Si	2.9295	-0.899677	-0.296603
C	3.318134	-1.387882	1.573549
C	3.382435	-2.927176	1.708219
C	3.160056	1.025716	-0.598444
C	4.646244	1.425525	-0.756048
C	4.007512	-1.954618	-1.559859
C	3.494708	-3.410859	-1.679597
C	-2.599435	-1.347249	3.552566
C	-5.12477	-1.654994	-2.821428
C	-1.77091	3.91533	3.346561
C	-0.403408	2.795432	-3.740849
C	2.380621	1.468546	-1.861248
C	2.568498	1.826049	0.584279
C	3.913513	-1.348074	-2.980727
C	5.496342	-1.987789	-1.13783
C	2.17863	-0.908972	2.506756
C	4.651029	-0.786548	2.076978
H	-4.663754	0.269007	1.051504
H	-3.598647	2.850305	0.867941
H	-2.367889	-4.616801	1.980097
H	-3.629471	-5.484722	0.024047
H	-4.349863	-3.947185	-1.795179
H	-0.987945	-1.187881	2.130632
H	-3.20801	-0.544624	3.098519
H	-2.020076	-0.910106	4.389422
H	-3.284954	-2.111219	3.969372

H	-1.324441	-3.810402	3.70935
H	-0.10672	-2.528939	3.962198
H	-0.068791	-3.508214	2.459078
H	-4.130328	-0.225246	-1.572495
H	-5.375528	-0.87155	-3.561369
H	-6.008292	-1.825126	-2.176784
H	-4.924302	-2.587244	-3.384064
H	-2.390464	-2.017459	-3.372836
H	-1.783802	-0.700372	-2.339561
H	-2.875149	-0.319801	-3.716097
H	0.775878	5.168042	1.934202
H	1.318298	5.98788	-0.358458
H	0.473562	4.774441	-2.357115
H	-1.188718	1.99432	2.563255
H	-2.708909	3.979284	2.763929
H	-1.36723	4.940978	3.455784
H	-2.014435	3.530634	4.356162
H	1.271973	2.202515	3.019658
H	0.272352	2.414711	4.4958
H	1.006407	3.836985	3.700847
H	-1.095205	1.461868	-2.213812
H	-0.790245	2.130567	-4.535837
H	0.675706	2.598904	-3.616571
H	-0.531101	3.839309	-4.089026
H	-3.069955	2.282284	-3.507187
H	-2.806252	3.942009	-2.880138
H	-3.286013	2.622601	-1.765075
H	2.725353	0.967752	-2.78154
H	2.510762	2.562275	-2.000149
H	1.300359	1.281047	-1.735769
H	2.580663	2.907896	0.341396
H	3.15161	1.686889	1.512102
H	1.518687	1.542957	0.770304
H	5.111094	0.971666	-1.64942
H	5.249057	1.138211	0.124919
H	4.717751	2.528712	-0.868287
H	4.449683	-2.008116	-3.695521
H	4.373722	-0.347038	-3.045278
H	2.861602	-1.270581	-3.317786
H	6.087298	-2.520216	-1.91371
H	5.642063	-2.528112	-0.185091
H	5.922943	-0.974872	-1.025322
H	2.483732	-3.43364	-2.122981
H	3.463691	-3.94304	-0.714262
H	4.170919	-3.975995	-2.356551
H	2.059912	0.185683	2.514992
H	2.396738	-1.235949	3.5461

H	1.209201	-1.352607	2.216851
H	5.511647	-1.106692	1.462836
H	4.837854	-1.119544	3.120637
H	4.626254	0.31806	2.080528
H	2.466367	-3.406271	1.31112
H	3.471478	-3.201478	2.781199
H	4.254469	-3.355066	1.182832
H	0.716703	-3.817734	-1.133644
H	-1.037125	-3.226848	-0.99058

Table S14. Cartesian geometry of **10b**.

Atomtype	X Coordinate [Å]	Y Coordinate [Å]	Z Coordinate [Å]
C	-1.189735	3.034013	-1.337423
C	-1.138892	2.827457	0.067419
C	-0.443547	3.704912	0.936617
C	0.172304	4.83848	0.36931
C	0.121261	5.072996	-1.009368
C	-0.545131	4.173387	-1.853262
N	-1.812916	1.688603	0.615902
C	-1.391226	0.35857	0.431474
N	-2.436258	-0.4065	0.978829
C	-3.448523	0.430236	1.460048
C	-3.064626	1.716735	1.235181
C	-2.62341	-1.799715	0.70415
C	-1.974288	-2.759012	1.516915
C	-2.213711	-4.117602	1.242741
C	-3.053944	-4.502785	0.18715
C	-3.644473	-3.534163	-0.634279
C	-3.428138	-2.161168	-0.402994
N	-0.29854	-0.005052	-0.124138
Si	0.704981	-1.308458	-0.592754
C	0.030234	-2.738739	-1.331233
C	-1.05859	-2.306817	2.649091
C	0.043387	-3.323173	2.990073
C	-3.965377	-1.128676	-1.390033
C	-3.266848	-1.288442	-2.758143
C	-0.372311	3.458568	2.441979
C	0.987813	3.851109	3.054728
C	-1.961495	2.08203	-2.250327
C	-3.468647	2.420702	-2.225784
Si	2.930334	-0.580938	-0.323596
C	3.1927	-0.123147	1.573314
C	3.394218	-1.396299	2.427329
C	3.080595	1.015949	-1.470876
C	4.554164	1.384679	-1.762389

C	4.133913	-2.021507	-0.883717
C	3.720826	-3.364562	-0.22201
C	-1.88328	-1.93413	3.900445
C	-5.49833	-1.198088	-1.528658
C	-1.50378	4.212466	3.177826
C	-1.436393	2.045485	-3.695844
C	2.350794	0.778467	-2.815762
C	2.390178	2.230074	-0.807443
C	4.038038	-2.19077	-2.419995
C	5.610556	-1.74446	-0.514865
C	1.944871	0.595754	2.138881
C	4.433629	0.780127	1.775141
H	-4.351148	0.020612	1.912997
H	-3.566268	2.657153	1.456649
H	-1.72451	-4.88603	1.85073
H	-3.226645	-5.568378	-0.011553
H	-4.261574	-3.841923	-1.487406
H	-0.555997	-1.3871	2.299019
H	-2.628276	-1.151243	3.667193
H	-1.219848	-1.553883	4.701854
H	-2.421054	-2.822067	4.287375
H	-0.376116	-4.241583	3.445204
H	0.747293	-2.881383	3.719561
H	0.608527	-3.60728	2.082501
H	-3.715027	-0.122374	-1.017543
H	-5.856503	-0.411856	-2.221052
H	-5.994812	-1.053822	-0.550056
H	-5.818385	-2.177838	-1.933749
H	-3.499953	-2.273255	-3.206975
H	-2.169051	-1.213219	-2.652298
H	-3.612221	-0.501554	-3.455766
H	0.712573	5.537684	1.017495
H	0.616055	5.956346	-1.433191
H	-0.562398	4.360843	-2.932181
H	-0.520513	2.375305	2.606005
H	-2.502134	3.907629	2.819112
H	-1.400714	5.303702	3.018219
H	-1.454725	4.01603	4.266727
H	1.830103	3.414918	2.490842
H	1.044928	3.491854	4.099588
H	1.115412	4.950649	3.074814
H	-1.836922	1.062424	-1.851759
H	-1.944703	1.235893	-4.251598
H	-0.348188	1.853264	-3.719355
H	-1.636238	2.993914	-4.23183
H	-4.031609	1.706789	-2.85695
H	-3.641232	3.442314	-2.617581

H	-3.877852	2.367915	-1.20069
H	2.76504	-0.070709	-3.385144
H	2.441343	1.6891	-3.446164
H	1.272792	0.589479	-2.65197
H	2.414513	3.09105	-1.506632
H	2.89355	2.547581	0.121598
H	1.334231	2.012663	-0.576157
H	5.073081	0.602113	-2.345549
H	5.131133	1.561709	-0.836022
H	4.586464	2.320336	-2.361063
H	4.613314	-3.088884	-2.730335
H	4.461857	-1.322464	-2.955766
H	2.994348	-2.322109	-2.761575
H	6.248746	-2.575455	-0.88494
H	5.749971	-1.682864	0.579924
H	5.985634	-0.807055	-0.962608
H	2.63429	-3.552049	-0.279843
H	4.006258	-3.403687	0.841671
H	4.239623	-4.202251	-0.734892
H	1.656946	1.484076	1.558779
H	2.147158	0.910931	3.184772
H	1.070045	-0.077093	2.148414
H	5.356914	0.298688	1.403941
H	4.570703	0.980422	2.859791
H	4.332798	1.756271	1.269624
H	2.581756	-2.130077	2.274246
H	3.39872	-1.115832	3.502505
H	4.357814	-1.892271	2.214137
C	0.62066	-3.949528	-2.011607
H	-1.0702	-2.751659	-1.297843
H	0.192513	-4.084187	-3.029973
H	1.717418	-3.903437	-2.128202
H	0.38787	-4.887074	-1.457094

Table S15. Cartesian geometry of **10b′**.

Atomtype	X Coordinate [Å]	Y Coordinate [Å]	Z Coordinate [Å]
C	-0.939911	3.078969	-1.234388
C	-0.770487	2.834094	0.155583
C	0.06997	3.640013	0.964903
C	0.734555	4.720144	0.35061
C	0.593703	4.97226	-1.018201
C	-0.232618	4.154716	-1.801569
N	-1.488819	1.744899	0.74664
C	-1.270914	0.38652	0.43567
N	-2.333304	-0.281567	1.074632

C	-3.148033	0.638866	1.743778
C	-2.632075	1.880316	1.538129
C	-2.785905	-1.594049	0.71475
C	-2.178426	-2.73027	1.302978
C	-2.699778	-3.994565	0.972222
C	-3.789275	-4.121701	0.097264
C	-4.350344	-2.986022	-0.49709
C	-3.843536	-1.700644	-0.22245
N	-0.325981	-0.076715	-0.285625
Si	0.681699	-1.345967	-0.801047
C	0.178415	-2.673172	-1.809945
C	-1.028039	-2.560341	2.290062
C	-0.11938	-3.794103	2.400139
C	-4.4053	-0.492331	-0.969745
C	-4.275265	-0.669617	-2.497222
C	0.247839	3.38915	2.460568
C	1.702125	3.593308	2.935302
C	-1.935751	2.276319	-2.069833
C	-3.346214	2.887136	-1.907115
Si	2.945618	-0.855566	-0.399532
C	3.17206	-0.522038	1.527136
C	3.234403	-1.853081	2.310452
C	3.299149	0.776506	-1.448001
C	4.81346	1.035291	-1.62462
C	4.043976	-2.369542	-0.999609
C	3.490203	-3.717832	-0.469133
C	-1.557027	-2.137414	3.678215
C	-5.865873	-0.207104	-0.566144
C	-0.689723	4.301347	3.285466
C	-1.55049	2.15418	-3.554143
C	2.646963	0.683558	-2.851418
C	2.659718	2.005499	-0.761563
C	4.031297	-2.443628	-2.546126
C	5.51243	-2.23586	-0.529253
C	1.954666	0.257818	2.077769
C	4.461847	0.275232	1.835203
H	-4.02592	0.312457	2.300411
H	-2.969397	2.855965	1.882682
H	-2.250163	-4.894395	1.404554
H	-4.186667	-5.117301	-0.138331
H	-5.17483	-3.093294	-1.212427
H	-0.406347	-1.731939	1.905251
H	-2.159328	-1.213042	3.61421
H	-0.71171	-1.952955	4.369669
H	-2.190397	-2.937358	4.109838
H	-0.657136	-4.657898	2.837046
H	0.734862	-3.56843	3.064377

S111

H	0.272298	-4.082429	1.406944
H	-3.809479	0.394532	-0.700538
H	-6.243302	0.689749	-1.094684
H	-5.951521	-0.031135	0.522643
H	-6.521345	-1.061054	-0.82672
H	-4.855437	-1.542601	-2.852376
H	-3.220543	-0.817276	-2.790908
H	-4.662017	0.228023	-3.016094
H	1.387934	5.359936	0.95449
H	1.133965	5.808385	-1.480401
H	-0.337962	4.363828	-2.871556
H	-0.032717	2.33857	2.657649
H	-1.752055	4.151597	3.023678
H	-0.442945	5.365293	3.101747
H	-0.569839	4.101031	4.36816
H	2.419832	3.047485	2.299679
H	1.811781	3.231063	3.974814
H	1.97776	4.665229	2.926148
H	-1.9688	1.24839	-1.678123
H	-2.242669	1.454712	-4.058941
H	-0.520702	1.766335	-3.664361
H	-1.61752	3.125894	-4.081276
H	-4.087953	2.304595	-2.485391
H	-3.360408	3.93222	-2.273246
H	-3.659827	2.887051	-0.846581
H	3.020965	-0.16557	-3.44696
H	2.86541	1.617297	-3.413094
H	1.546551	0.587795	-2.7792
H	2.787317	2.895124	-1.411952
H	3.123036	2.245427	0.210607
H	1.578	1.859275	-0.603871
H	5.299465	0.249709	-2.231578
H	5.340534	1.094144	-0.655289
H	4.963212	2.002419	-2.151118
H	4.573617	-3.356177	-2.87375
H	4.536611	-1.575725	-3.006114
H	3.001219	-2.495734	-2.946814
H	6.104389	-3.09084	-0.920956
H	5.594975	-2.254297	0.572674
H	5.985059	-1.306018	-0.89169
H	2.429877	-3.867087	-0.739195
H	3.573027	-3.804689	0.626479
H	4.078546	-4.54899	-0.91409
H	1.742758	1.179401	1.518579
H	2.139317	0.529423	3.138818
H	1.041011	-0.358811	2.042764
H	5.366409	-0.246617	1.473472

H	4.562428	0.40312	2.934524
H	4.449597	1.282891	1.384971
H	2.375733	-2.50612	2.070528
H	3.205616	-1.640242	3.400939
H	4.163312	-2.415968	2.10985
C	-1.20007	-3.035812	-2.301406
H	0.997222	-3.322888	-2.159828
H	-1.471408	-4.085201	-2.054908
H	-1.975325	-2.392027	-1.852611
H	-1.287765	-2.941832	-3.408002

4. References

[S1] G. R. Fulmer, A. J. M. Miller, N. H. Sherden, H. E. Gottlieb, A. Nudelman, B. M. Stoltz, J. E. Bercaw, K. I. Goldberg, *Organometallics* **2010**, *29*, 2176-2179.

[S2] D. Wendel, D. Reiter, A. Porzelt, P. J. Altmann, S. Inoue, B. Rieger, *J. Am. Chem. Soc.* **2017**, *139*, 17193-17198.

[S3] N. Kuhn, T. Kratz, *Synthesis* **1993**, 561-562.

[S4] W. J. Transue, J. Yang, M. Nava, I. V. Sergeyev, T. J. Barnum, M. C. McCarthy, C. C. Cummins, *J. Am. Chem. Soc.* **2018**, *140*, 17985-17991.

[S5] M. Bartlett, *Synlett* **2013**, *24*, 773-774.

[S6] A. Brar, D. K. Unruh, A. J. Aquino, C. Krempner, *Chem. Commun.* **2019**, *55*, 3513-3516.

[S7] *APEX suite of crystallographic software*, APEX 3 version 2015.5-2; Bruker AXS Inc.: Madison, Wisconsin, USA, **2015**.

[S8] *SAINT*, Version 7.56a and SADABS Version 2008/1; Bruker AXS Inc.: Madison, Wisconsin, USA, **2008**.

[S9] G. M. Sheldrick, *SHELXL-2014*, University of Göttingen, Göttingen, Germany, **2014**.

[S10] C. B. Hübschle, G. M. Sheldrick, B. Dittrich, *J. Appl. Cryst.* **2011**, *44*, 1281-1284.

[S11] G. M. Sheldrick, *SHELXL-97*, University of Göttingen, Göttingen, Germany, **1998**.

[S12] A. J. C. Wilson, *International Tables for Crystallography*, Vol. C, Tables 6.1.1.4 (pp. 500-502), 4.2.6.8 (pp. 219-222), and 4.2.4.2 (pp. 193-199); Kluwer Academic Publishers: Dordrecht, The Netherlands, **1992**.

[S13] C. F. Macrae, I. J. Bruno, J. A. Chisholm, P. R. Edgington, P. McCabe, E. Pidcock, L. Rodriguez-Monge, R. Taylor, J. van de Streek, P. A. Wood, *J. Appl. Cryst.* **2008**, *41*, 466-470.

[S14] a) A. D. Becke, *J. Chem. Phys.* **1997**, *107*, 8554-8560; b) F. Weigend, R. Ahlrichs, *Phys. Chem. Chem. Phys.* **2005**, *7*, 3297-3305; c) S. Grimme, *J. Comput. Chem.* **2006**, *27*, 1787-1799.

[S15] a) M. J. Frisch, J. A. Pople, *J. Chem. Phys.* **1984**, *80*, 3265-3269; b) A. D. Boese, N. C. Handy, *J. Chem. Phys.* **2001**, *114*, 5497-5503.

[S16] M. J. Frisch, G. W. Trucks, H. B. Schlegel, G. E. Scuseria, M. A. Robb, J. R. Cheeseman, G. Scalmani, V. Barone, B. Mennucci, G. A. Petersson, H. Nakatsuji, M. Caricato, X. Li, H. P. Hratchian, A. F. Izmaylov, J. Bloino, G. Zheng, J. L. Sonnenberg, M. Hada, M. Ehara, K. Toyota, R. Fukuda, J. Hasegawa, M. Ishida, T. Nakajima, Y. Honda, O. Kitao, H. Nakai, T. Vreven, J. A. Montgomery, Jr., J. E. Peralta, F. Ogliaro, M. Bearpark, J. J. Heyd, E. Brothers, K. N. Kudin, V. N. Staroverov, R. Kobayashi, J. Normand, K. Raghavachari, A.

Rendell, J. C. Burant, S. S. Iyengar, J. Tomasi, M. Cossi, N. Rega, J. M. Millam, M. Klene, J. E. Knox, J. B. Cross, V. Bakken, C. Adamo, J. Jaramillo, R. Gomperts, R. E. Stratmann, O. Yazyev, A. J. Austin, R. Cammi, C. Pomelli, J. W. Ochterski, R. L. Martin, K. Morokuma, V. G. Zakrzewski, G. A. Voth, P. Salvador, J. J. Dannenberg, S. Dapprich, A. D. Daniels, Ö. Farkas, J. B. Foresman, J. V. Ortiz, J. Cioslowski, D. J. Fox, *Gaussian 09, Revision E.01*, Gaussian, Inc., Wallingford CT, **2009**.

13.7 Licenses for Copyrighted Content

13.7.1 License for Chapter 4



9.10.2019 Rightslink® by Copyright Clearance Center

Copyright Clearance Center RightsLink®

Home | Create Account | Help | LIVE CHAT

ACS Publications
Most Trusted. Most Cited. Most Read.

Title: Disilene–Silylene Interconversion: A Synthetically Accessible Acyclic Bis(silyl)silylene

Author: Dominik Reiter, Richard Holzner, Amelie Porzelt, et al

Publication: Journal of the American Chemical Society

Publisher: American Chemical Society

Date: Aug 1, 2019

Copyright © 2019, American Chemical Society

LOGIN

If you're a copyright.com user, you can login to RightsLink using your copyright.com credentials.

Already **a RightsLink user** or want to learn more?

PERMISSION/LICENSE IS GRANTED FOR YOUR ORDER AT NO CHARGE

This type of permission/license, instead of the standard Terms & Conditions, is sent to you because no fee is being charged for your order. Please note the following:

- Permission is granted for your request in both print and electronic formats, and translations.
- If figures and/or tables were requested, they may be adapted or used in part.
- Please print this page for your records and send a copy of it to your publisher/graduate school.
- Appropriate credit for the requested material should be given as follows: "Reprinted (adapted) with permission from (COMPLETE REFERENCE CITATION). Copyright (YEAR) American Chemical Society." Insert appropriate information in place of the capitalized words.
- One-time permission is granted only for the use specified in your request. No additional uses are granted (such as derivative works or other editions). For any other uses, please submit a new request.

BACK CLOSE WINDOW

Copyright © 2019 Copyright Clearance Center, Inc. All Rights Reserved. Privacy statement. Terms and Conditions.
Comments? We would like to hear from you. E-mail us at customercare@copyright.com

https://s100.copyright.com/AppDispatchServlet 1/1

13.7.2 License for Chapter 5

DMAP-stabilized bis(silyl)silylenes as versatile synthons for organosilicon compounds

R. Holzner, D. Reiter, P. Frisch and S. Inoue, *RSC Adv.*, 2020, **10**, 3402
DOI: 10.1039/C9RA10628F

This article is licensed under a Creative Commons Attribution 3.0 Unported Licence. Material from this article can be used in other publications provided that the correct acknowledgement is given with the reproduced material.

Reproduced material should be attributed as follows:

- For reproduction of material from NJC:
  [Original citation] - Published by The Royal Society of Chemistry (RSC) on behalf of the Centre National de la Recherche Scientifique (CNRS) and the RSC.
- For reproduction of material from PCCP:
  [Original citation] - Published by the PCCP Owner Societies.
- For reproduction of material from PPS:
  [Original citation] - Published by The Royal Society of Chemistry (RSC) on behalf of the European Society for Photobiology, the European Photochemistry Association, and RSC.
- For reproduction of material from all other RSC journals:
  [Original citation] - Published by The Royal Society of Chemistry.

Information about reproducing material from RSC articles with different licences is available on our Permission Requests page.

13.7.3 License for Chapter 7

Oxidation reactions of a versatile, two-coordinate, acyclic iminosiloxysilylene

D. Reiter, P. Frisch, D. Wendel, F. M. Hörmann and S. Inoue, *Dalton Trans.*, 2020, **49**, 7060
DOI: 10.1039/D0DT01522A

If you are not the author of this article and you wish to reproduce material from it in a third party non-RSC publication you must formally request permission using Copyright Clearance Center. Go to our Instructions for using Copyright Clearance Center page for details.

Authors contributing to RSC publications (journal articles, books or book chapters) do not need to formally request permission to reproduce material contained in this article provided that the correct acknowledgement is given with the reproduced material.

Reproduced material should be attributed as follows:

- For reproduction of material from NJC:
  Reproduced from Ref. XX with permission from the Centre National de la Recherche Scientifique (CNRS) and The Royal Society of Chemistry.
- For reproduction of material from PCCP:
  Reproduced from Ref. XX with permission from the PCCP Owner Societies.
- For reproduction of material from PPS:
  Reproduced from Ref. XX with permission from the European Society for Photobiology, the European Photochemistry Association, and The Royal Society of Chemistry.
- For reproduction of material from all other RSC journals and books:
  Reproduced from Ref. XX with permission from The Royal Society of Chemistry.

If the material has been adapted instead of reproduced from the original RSC publication "Reproduced from" can be substituted with "Adapted from".

In all cases the Ref. XX is the XXth reference in the list of references.

If you are the author of this article you do not need to formally request permission to reproduce figures, diagrams etc. contained in this article in third party publications or in a thesis or dissertation provided that the correct acknowledgement is given with the reproduced material.

Reproduced material should be attributed as follows:

- For reproduction of material from NJC:
  [Original citation] - Reproduced by permission of The Royal Society of Chemistry (RSC) on behalf of the Centre National de la Recherche Scientifique (CNRS) and the RSC
- For reproduction of material from PCCP:
  [Original citation] - Reproduced by permission of the PCCP Owner Societies
- For reproduction of material from PPS:
  [Original citation] - Reproduced by permission of The Royal Society of Chemistry (RSC) on behalf of the European Society for Photobiology, the European Photochemistry Association, and RSC
- For reproduction of material from all other RSC journals:
  [Original citation] - Reproduced by permission of The Royal Society of Chemistry

If you are the author of this article you still need to obtain permission to reproduce the whole article in a third party publication with the exception of reproduction of the whole article in a thesis or dissertation.

Information about reproducing material from RSC articles with different licences is available on our Permission Requests page.

13.7.4 License for Chapter 8

9.10.2019 Rightslink® by Copyright Clearance Center

Copyright Clearance Center RightsLink® Home Create Account Help LIVE CHAT

ACS Publications Most Trusted. Most Cited. Most Read.

Title: Silicon and Oxygen's Bond of Affection: An Acyclic Three-Coordinate Silanone and Its Transformation to an Iminosiloxysilylene

Author: Daniel Wendel, Dominik Reiter, Amelie Porzelt, et al

Publication: Journal of the American Chemical Society

Publisher: American Chemical Society

Date: Nov 1, 2017

Copyright © 2017, American Chemical Society

LOGIN

If you're a copyright.com user, you can login to RightsLink using your copyright.com credentials.

Already **a RightsLink user** or want to learn more?

PERMISSION/LICENSE IS GRANTED FOR YOUR ORDER AT NO CHARGE

This type of permission/license, instead of the standard Terms & Conditions, is sent to you because no fee is being charged for your order. Please note the following:

- Permission is granted for your request in both print and electronic formats, and translations.
- If figures and/or tables were requested, they may be adapted or used in part.
- Please print this page for your records and send a copy of it to your publisher/graduate school.
- Appropriate credit for the requested material should be given as follows: "Reprinted (adapted) with permission from (COMPLETE REFERENCE CITATION). Copyright (YEAR) American Chemical Society." Insert appropriate information in place of the capitalized words.
- One-time permission is granted only for the use specified in your request. No additional uses are granted (such as derivative works or other editions). For any other uses, please submit a new request.

BACK CLOSE WINDOW

Copyright © 2019 Copyright Clearance Center, Inc. All Rights Reserved. Privacy statement. Terms and Conditions.
Comments? We would like to hear from you. E-mail us at customercare@copyright.com

https://s100.copyright.com/AppDispatchServlet 1/1

13.7.5 License for Chapter 9

9.10.2019 Rightslink® by Copyright Clearance Center

Copyright Clearance Center RightsLink® Home Create Account Help LIVE CHAT

ACS Publications Most Trusted. Most Cited. Most Read.

Title: Heavier Carbonyl Olefination: The Sila-Wittig Reaction
Author: Dominik Reiter, Philipp Frisch, Tibor Szilvási, et al
Publication: Journal of the American Chemical Society
Publisher: American Chemical Society
Date: Oct 1, 2019
Copyright © 2019, American Chemical Society

LOGIN

If you're a copyright.com user, you can login to RightsLink using your copyright.com credentials.

Already a RightsLink user or want to learn more?

PERMISSION/LICENSE IS GRANTED FOR YOUR ORDER AT NO CHARGE

This type of permission/license, instead of the standard Terms & Conditions, is sent to you because no fee is being charged for your order. Please note the following:

- Permission is granted for your request in both print and electronic formats, and translations.
- If figures and/or tables were requested, they may be adapted or used in part.
- Please print this page for your records and send a copy of it to your publisher/graduate school.
- Appropriate credit for the requested material should be given as follows: "Reprinted (adapted) with permission from (COMPLETE REFERENCE CITATION). Copyright (YEAR) American Chemical Society." Insert appropriate information in place of the capitalized words.
- One-time permission is granted only for the use specified in your request. No additional uses are granted (such as derivative works or other editions). For any other uses, please submit a new request.

BACK CLOSE WINDOW

Copyright © 2019 Copyright Clearance Center, Inc. All Rights Reserved. Privacy statement. Terms and Conditions.
Comments? We would like to hear from you. E-mail us at customercare@copyright.com

https://s100.copyright.com/AppDispatchServlet 1/1

Oath of Compliance with the Principles of Scientific Integrity

I hereby declare that the enclosed PhD thesis was prepared independently at the Fakultät für Chemie of the Technische Universität München under the supervision of Prof. Dr. Shigeyoshi Inoue. All references and additional sources used have been cited appropriately.

Geiselfing, 01.07.2020

Place, Date

Dominik Reiter